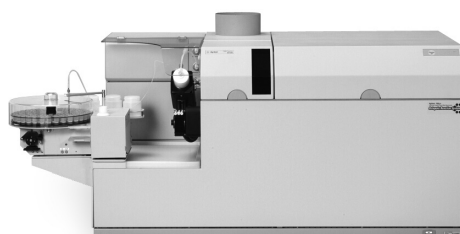
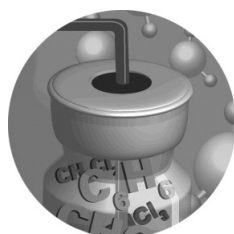
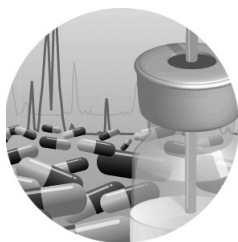


Analysis of pharmaceuticals and drug related impurities using Agilent instrumentation

Application Compendium



Agilent Technologies

Introduction

The analysis of impurities in drug substances, from initial screening to the use of validated methods in routine quality control and quality assurance, is becoming an increasingly challenging task along the pharmaceutical value delivery chain.

In general, impurities in drug substances are addressed from two perspectives:

- The chemical aspects, which include classification and identification of impurities, denote how to generate reports, set appropriate specifications, and describe analytical procedures.
- The safety aspects, more importantly, for the patients using the final product when a new drug is brought to the market.

Comparative studies and genotoxicity testing are of increasing importance in this context. Impurities can be classified in three groups, according to regulatory bodies, such as the US FDA, or EMEA:

- Organic impurities (process and drug related)
- Inorganic impurities
- Residual solvents

During the past years, Agilent Technologies has broadened its applications and product portfolio in impurity analysis to help solve any critical issues encountered during this procedure.

This Application Compendium offers guidance on improving overall workflow for analyzing and identifying impurities in drug substances with Agilent products and applications. This applies to small molecules as well as biologics.

The compendium is a comprehensive collection of Application Notes on:

- Analysis of organic impurities with the Agilent 1120 Compact LC, the Agilent 1200 Series LC, and the Agilent 1290 Infinity LC system
- Analysis of organic impurities with the Agilent 7100 Capillary Electrophoresis system
- Analysis of residual solvents with the Agilent 6890 and 7890 Series GCs as well as the Agilent 5975 Series GC/MS
- Analysis of inorganic impurities with the Agilent 7700ICP-MS
- Determination of impurities with Agilent 6000 Series LC/MS portfolio offering

The combination of Agilent's reliable instrumentation and unique services portfolio, including instrument qualification and sophisticated diagnostic programs, ensures accurate and dependable impurity analysis.

Table of Contents

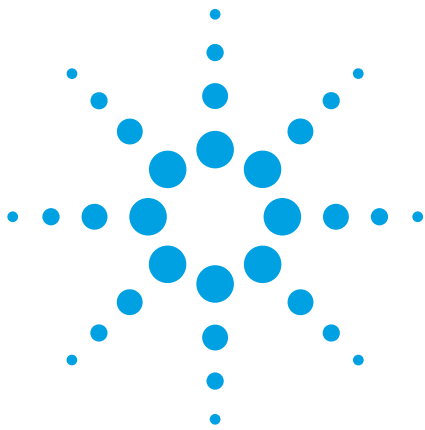
| | |
|---|-----|
| Stepwise upgrade to high speed separation of anesthetics on the Agilent 1290 Infinity LC system with different columns | 11 |
| Analytical instrument qualification and system validation according to USP Chapter <1058> for the Agilent 1290 Infinity LC system | 19 |
| Determination of water soluble vitamins with the Agilent 1120 Compact LC after method development with the Agilent 1200 Series Rapid Resolution LC system and back transfer | 27 |
| Determination of degradation products of Metoprolol tablets with the Agilent 1120 Compact LC after method development with the Agilent 1200 Series Rapid Resolution LC system | 35 |
| Screening impurities in fine chemicals using the Agilent 1290 Infinity LC system | 43 |
| Increasing productivity in the analysis of impurities in metoclopramide hydrochloride formulations using the Agilent 1290 Infinity LC system | 53 |
| Development, validation, and comparison of an HPLC method to analyze paracetamol and related impurities according to the European Pharmacopoeia (EP) and USP using the Agilent 1120 Compact LC and the Agilent 1200 Series LC system | 61 |
| More chromatographic power for the Agilent 1200 Series LC: How the Agilent 1200 Series VWD SL Plus and ZORBAX RRHT 1.8 µm columns can boost speed and sensitivity, and cut solvent consumption | 69 |
| Software-assisted, high-throughput identification of main metabolites of pharmaceutical drugs: Rapid data acquisition by Agilent 1290 Infinity LC, TOF and Q-TOF instrumentation, and subsequent identification of metabolites by Agilent MassHunter Metabolite Identification software | 73 |
| Separation of salicylic acid impurities with different acid mobile-phase modifiers | 81 |
| The high-resolution reversed-phase HPLC separation of licorice root extracts using long rapid resolution HT 1.8-µm columns | 85 |
| Analysis of beta-blocking drugs on Agilent 1100 Series LC systems using UV, fluorescence and mass spectrometry | 91 |
| Sensitive analysis of beta-blocking drugs on the Agilent 1100 Series capillary LC system | 99 |
| Screening and qualitative identification of antioxidant polymer additives by HPLC with UV/VIS and APCI-MS detection | 107 |

| | |
|--|-----|
| Separation of ceftibuten stereo isomers with 100% aqueous mobile phase using ZORBAX SB-Aq | 127 |
| Extraction and HPLC analysis of alkaloids in goldenseal | 129 |
| Lot-to-lot reproducibility amphetamines | 135 |
| Effect of silica-support type reversed-phase separation of 137 tricyclic antidepressants | 137 |
| Tricyclic antidepressants separation with excellent peak shape using XDB-C8 and THF-containing mobile phase | 139 |
| Narrow-bore (2.1 mm) separation of nonsteroidal anti-inflammatory drugs | 141 |
| Separation of tricyclic antidepressants and metabolites | 143 |
| Saponification of procaine: Kinetic measurements with the Agilent high-throughput analysis system | 145 |
| Peptide mapping of a monoclonal antibody using a microfluidic-based HPLC-chip coupled to an Agilent accurate mass Q-TOF LC/MS | 153 |
| Tryptic digest analysis using the Agilent 1290 Infinity LC system | 159 |
| Converting the USP insulin assay method for use on the Agilent 1200 Series Rapid Resolution LC system | 163 |
| Using the high-pH stability of ZORBAX Poroshell 300 Extend-C18 to increase signal-to-noise in LC/MS | 171 |
| Using ZORBAX Poroshell 300 Extend-C18 to achieve unique selectivity at pH 2 and 10: Angiotensins | 173 |
| Comparison of ZORBAX Poroshell 300 Extend-C18 and totally porous packing in achieving very rapid, high-pH separation of peptides | 175 |
| High speed and ultra high speed peptide mapping of human monoclonal IgG on ZORBAX Poroshell 300 SB-C18, C8, and C3 | 177 |
| Use of temperature to increase resolution in the ultrafast HPLC separation of proteins with ZORBAX Poroshell 300 SB-C8 HPLC columns | 181 |
| Computer assisted identification of metabolites from pharmaceutical drugs part 2: Identification of non-expected metabolites of nefazodone identification of metabolites by the MassHunter metabolite ID software from RRLC – QTOF MS data | 185 |
| Computer assisted identification of metabolites from pharmaceutical drugs Part 1: Identification of expected metabolites of nefazodone identification of metabolites by the MassHunter metabolite ID software from RRLC – QTOF MS data | 201 |

| | |
|---|-----|
| Detection and identification of impurities in pharmaceutical drugs: Computer-assisted extraction, profiling and analysis of Q-TOF data for determination of impurities using Agilent MassHunter software | 213 |
| Fast, computer-assisted detection of degradation products and impurities in pharmaceutical products identification of minor components in drug substances using the Agilent 6210 accurate-mass, time-of-flight mass spectrometer and MassHunter Profiling software | 221 |
| High throughput LC/MS TOF analysis of drug degradation products Agilent 1200 Series Rapid Resolution LC and Agilent 6210 Time-of-Flight MS with alternating column regeneration | 229 |
| Impurity profiling with the Agilent 1200 Series LC system Part 1: Structure elucidation of impurities with LC/MS | 237 |
| Impurity profiling with the Agilent 1200 Series LC system Part 2: Isolation of impurities with preparative HPLC | 245 |
| Impurity profiling with the Agilent 1200 Series LC system Part 3: Rapid condition scouting for method development | 253 |
| Impurity profiling with the Agilent 1200 Series LC system Part 4: Method validation of a fast LC method | 261 |
| Impurity profiling with the Agilent 1200 Series LC system Part 5: QA/QC application example using a fast LC method for higher sample throughput | 269 |
| Analysis of a complex natural product extract from ginseng – Part I: Structure elucidation of ginsenosides by rapid resolution LC–ESI TOF with accurate mass measurement | 277 |
| Analysis of a complex natural product extract from ginseng – Part II: Structure elucidation of ginsenosides by high resolution ion trap LC/MS | 285 |
| Hydrophilic interaction chromatography (HILIC) separation of basic drugs using MS/MS detection | 293 |
| Statistic evaluation of mass accuracy measurements by ESI TOF with a sample of degradation products from the antibiotic drug amoxicillin | 301 |
| Structure elucidation of degradation products of the antibiotic drug amoxicillin Part I | 309 |
| Structure elucidation of degradation products of the antibiotic drug amoxicillin Part II | 317 |
| Structure elucidation of degradation products of the antibiotic drug amoxicillin Part III: Identification of minor byproducts in a formulation trial with accurate mass measurement using ESI TOF and ion trap MRM | 329 |
| Therapeutic drug monitoring by LC/MSD - Clozapine, an example | 337 |

| | |
|---|-----|
| High efficiency, high throughput LC and LC/MS applications using ZORBAX Rapid Resolution HT columns | 345 |
| Analysis of ephedrine isomers using the LC/MSD Quadrupole system | 349 |
| Structural determination of ginsenosides using MSn analysis | 355 |
| Simultaneous dual capillary column headspace GC with flame ionization confirmation and quantification according to USP <467> | 361 |
| Fast analysis of USP 467 residual solvents using the Agilent 7890A GC and Low Thermal Mass (LTM) system | 369 |
| Improved retention time, area repeatability, and sensitivity for analysis of residual solvents | 381 |
| Better precision, sensitivity, and higher sample throughput for the analysis of residual solvents in pharmaceuticals using the Agilent 7890A GC system with G1888 headspace sampler in drug quality control | 385 |
| Headspace analysis of organic volatile impurities by USP <467> using the DB-624 and the HP-Fast GC residual solvent column | 393 |
| A unified gas chromatography method for aromatic solvent analysis | 401 |
| Retention time locking using USP 467 standard sample and automated headspace sampling | 417 |
| Headspace analysis of residual ethylene oxide in sterilized medical devices | 423 |
| The determination of residual solvents in pharmaceuticals using the Agilent G1888 headspace/6890N GC/5975 inert MSD system | 431 |
| The determination of residual solvents in pharmaceuticals using the Agilent G1888 network headspace sampler | 439 |
| A new approach to the analysis of phthalate esters by GC/MS | 451 |
| Determination of the vasodilator isosorbide-5-mononitrate in human plasma using GC/MS with electron capture negative ion chemical ionization | 461 |
| Fast determination of five toxic elements in traditional Chinese medicine (TCM) by ICP-MS | 465 |
| Determination of toxic elements in traditional Chinese medicine using inductively coupled plasma mass spectrometry | 469 |
| The use of collision/reaction cell ICP-MS for the simultaneous determination of 18 elements in blood and serum samples | 477 |
| Evaluation of conventional ICP-MS and ORS-ICP-MS for analysis of traditional Chinese medicines | 485 |

| | |
|---|------|
| Rapid and reliable routine analysis of urine by octopole reaction cell ICP-MS | .491 |
| Ion chromatography (IC) ICP-MS for chromium speciation in natural samples | .497 |
| A comparison of the relative cost and productivity of traditional metals analysis techniques versus ICP-MS in high throughput commercial laboratories | .505 |
| Determination of platinum compounds by LC-ICP-MS | .511 |
| Speciation of arsenic compounds in urine of dimethylarsinic acid orally exposed rat by using IC-ICP-MS | .515 |
| Practical benefits of abundance sensitivity in ICP-MS | .521 |
| Ultra-low level impurity analysis by capillary zone electrophoresis | .527 |
| Analysis of chlorogenic acid in traditional Chinese medicines by capillary electrophoresis | .529 |
| Analysis of fangchinoline and tetrandrine in Chinese traditional medicine by capillary electrophoresis | .531 |
| Development of a method for separation of the four stereoisomers of troglitazone using capillary electrophoresis | .533 |
| Oligonucleotide analysis by capillary gel electrophoresis | .541 |
| High sensitivity SDS-protein separations by capillary electrophoresis | .543 |
| Ultra-low level impurity analysis by capillary zone electrophoresis | .545 |
| Analysis of steroid isomers by capillary electrochromatography | .547 |
| The Agilent 2100 Bioanalyzer System - A compliant tool in life sciences IQ OQ/PV 21CFR Part 11 | .549 |
| Quality Control for the Agilent 2100 Bioanalyzer Protein 200 Plus LabChip kits | .555 |
| Using the Agilent 2100 Bioanalyzer for quality control of protein samples prior to MS-analysis | .563 |
| Glycoprotein sizing on the Agilent 2100 Bioanalyzer | .567 |
| Analysis of bispecific antibodies using the Agilent 2100 Bioanalyzer and the Protein 200 Plus assay | .575 |
| Quality control of antibodies using the 2100 Bioanalyzer and the Protein 200 Plus assay | .577 |



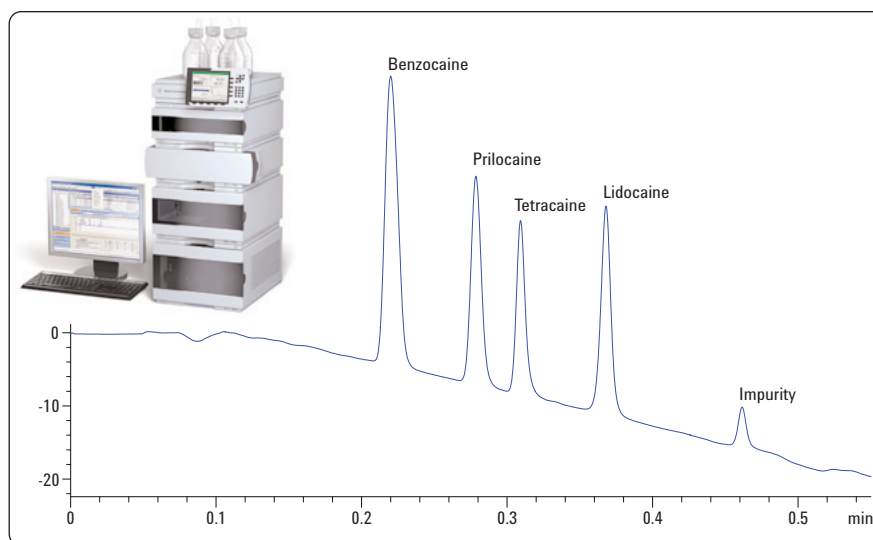
Stepwise upgrade to high speed separation of anesthetics on the Agilent 1290 Infinity LC system with different columns

Application Note

Authors

Detlef Wilhelm
ANATOX GmbH & Co. KG
Fuerstenwalde
Germany

Edgar Naegele
Agilent Technologies GmbH
Hewlett-Packard St. 8
76337 Waldbronn
Germany



Abstract

The limits of resolution, peak capacity and pressure can be explicitly reduced when analyzing with the Agilent 1290 Infinity LC system. The power and flow design of the Agilent 1290 Infinity Binary Pump allows the use of various eluent compositions with any column type, and provides the high sensitivity of the new UV detection system.

The need to convert existing methods to fast or high resolution methods, causes difficulties such as the adaptation of delay volumes of the former HPLC system or the back pressure of the required column type to the new setup.

This Application Note shows the separation of local anesthetics with different column types. It demonstrates the transfer of parameters from a 5 μm column to columns with particles < 2 μm . The results show high resolution even under high throughput conditions. The best separation results (0.4 min) were achieved with the Agilent ZORBAX RRHD Eclipse Plus C18 HD 50 mm \times 2.1 mm, 1 μm column with an overall runtime of 1 min, including regeneration. The results for the determination of the precision of areas and retention times (< 0.5 %) show that all criteria for qualified instruments are fulfilled. The correlation coefficients for linearity for all components are better than 0.999. No carryover was detected.



Agilent Technologies

Introduction

The development of the Agilent 1290 Infinity LC system resolved many issues around ultra-high performance, ultra-high pressure liquid chromatography. In addition, it has extended the limits of resolution, peak capacity, and pressure.

The power and flow design of the pump with reduced delay volumes, the elimination of an extra mechanical pulsation damper, and the new Jet Weaver for gradient mixing allows the use of any eluent composition, and any column type while still producing the highest sensitivity.

Many other HPLC systems need to be optimized to special column types, (such as columns with 4.6 mm diameter) because of their flow design. The Agilent 1290 Infinity LC system uses a small system volume, which has very little influence on dispersion and peak width. This allows the use of any column, with any diameter, or length, filled with any particle size packing, and still provides good results. This is especially true with 2.1 mm columns.

The recent trend to improve resolution, save time, and reduce solvent costs was to transfer methods from 4.6 mm columns with 5 μm particles to columns with smaller diameters and smaller particles. This also lowered the cost per analysis by shortening the analysis time. The transfer of methods by calculation to fast or high resolution methods provides the challenges of adapting delay volumes of the former HPLC system, and adjusting the back pressure of the required column type to the new setup.

This Application Note describes the separation of four local anesthetics using different column types from different vendors. It will also describe the transfer of parameters from a 5- μm column to columns with particles < 2 μm from

different vendors. The results show high resolution even under the high throughput conditions. The best results were achieved with the Agilent ZORBAX RRHD Eclipse Plus C18 HD 50 mm \times 2.1 mm, 1 μm column. The criteria for precision of retention times and areas are fulfilled, and demonstrate the versatility of high speed applications.

Experimental

Instrumentation

An Agilent 1290 Infinity LC system with the following configuration was used:

| | |
|-----------|--|
| G4220A | 1290 Infinity Binary pump with integrated vacuum degasser and 35 μL Jet Weaver as mixing device |
| G4226A | 1290 Infinity Autosampler |
| G1316C | 1290 Infinity Thermostatted Column Compartment |
| G4212A | 1290 Infinity Diode Array Detector |
| Software: | ChemStation B.04.02 |

Configuration of the Agilent 1290 Infinity LC system

Preparation of samples

Reference samples

The stock solution of each anesthetic was prepared by dissolving 10 mg of each compound in water in a 100 mL volumetric flask yielding a concentration of 100 $\mu\text{g}/\text{mL}$ (Figure 1). Samples were prepared by mixing aliquots of each component to yield the final concentration. The reference sample used to check the separation was prepared by mixing 2.5 mL of each stock solution in a 10-mL flask to yield a ready-to-use solution. As an example for the calibration samples: the solution used for calibration of the 10 $\mu\text{g}/\text{mL}$ point was prepared by mixing 1 mL of each stock solution in a 10-mL volumetric flask and diluting it to the final volume with water. Calibration points used to evaluate the correlation were: 1, 2.5, 10, 25, 50, 100 $\mu\text{g}/\text{mL}$ with the Agilent ZORBAX RRHD Eclipse Plus C18 50 mm \times 2.1 mm, 1 μm column at 1.9 mL/min.

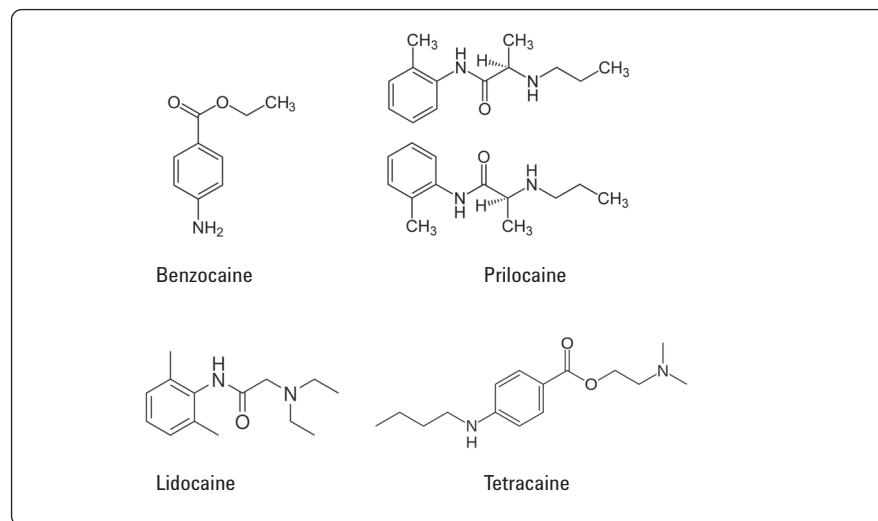


Figure 1
Chemical structures.

Chromatographic conditions

| | |
|--------------|--|
| Columns | Agilent ZORBAX Eclipse Plus C18, 150 × 2.1 mm, 5 µm Agilent ZORBAX Eclipse Plus C18, 50 × 2.1mm, 3.5 µm Agilent ZORBAX RRHD Eclipse Plus C18, 50 × 2.1 mm, 1 µm Waters BEH C18, 50 × 2.1 mm, 1.7 µm |
| Mobile Phase | A: 50 mM Ammonium formate, pH=8.2 B: Acetonitrile |

Detailed chromatographic conditions are listed in Table 1.

| | Agilent ZORBAX Eclipse Plus C18, 150 × 2.1 mm, 5 µm | Agilent ZORBAX Eclipse Plus C18, 50 × 2.1 mm, 3.5 µm | Agilent ZORBAX RRHD Eclipse Plus C18, 50 × 2.1 mm, 1 µm | Waters BEH C18, 50 × 2.1 mm, 1.7 µm |
|------------------|--|--|---|-------------------------------------|
| Flow rate | 0.8 ml/min | 0.5 ml/min | 1.9 ml/min | 1.5 ml/min |
| Gradient | 0-1 min 0-28% B 1-7 min 28-70% B | 0-4 min 0-70% B | 0-0.45 min 0-70% B | 0-0.45 min 0-70% B |
| Temperature | 40 °C | 40 °C | 40 °C | 40 °C |
| Injection volume | 5 µl | 5 µl | 1 µl | 1 µl |
| Detection | DAD, Signal 225/4, Reference 400/80, standard Cell (1 µl, 10 mm) | | | |
| Data rate | 2 Hz | 10 Hz | 80 Hz | 80 Hz |
| Maximum pressure | 98 bar | 65 bar | 945 bar | 865 bar |

Table 1
Instrument conditions.

| Sample | Purpose | Number of injections |
|--|--|----------------------|
| Blanc solution | Verify baseline stability and identify artifacts | 3 |
| Reference sample | Verify precision of areas and retention times for reference solution | 10 |
| Calibration | Verify linearity | 3 for each level |
| Highest concentration and Blanc solution | Verify carryover | 3 of each sample |

Table 2
Sample setup for testing.

Setup for testing

With the following setup for the reference sample the transferred methods can be checked:

- Establishment of a chromatographic separation to compare the performance of different column types (Resolution > 2)
- Precision of areas must be < 1 % RSD.
- Precision of retention times must be < 0.5 % RSD.
- Linearity should be given at least with $R^2 > 0.999$
- With these limits and settings for testing the following samples were prepared and analyzed (Table 2).

Results and discussion

Due to the varied pharmacological properties of local anesthetics, they are used in many different anesthesia applications.

The chromatographic properties result from the chemical structure; many of them are aminoesters or aminoamides. These primary or secondary amines (Figure 1) tend to tail on RP-columns at low pH-values. Separations in the mid or high pH-range (pH=8-10) are preferred to avoid asymmetric peaks. Therefore, RP

materials with high stability such as the ZORBAX Eclipse Plus C18 are needed. A typical chromatogram for a separation of four local anesthetics, with the impurity originated from tetracaine, at pH = 8.2 is shown in Figure 2. The instrument conditions are listed in Table 1. A simple mixture for the eluents without attention to the baseline was chosen.

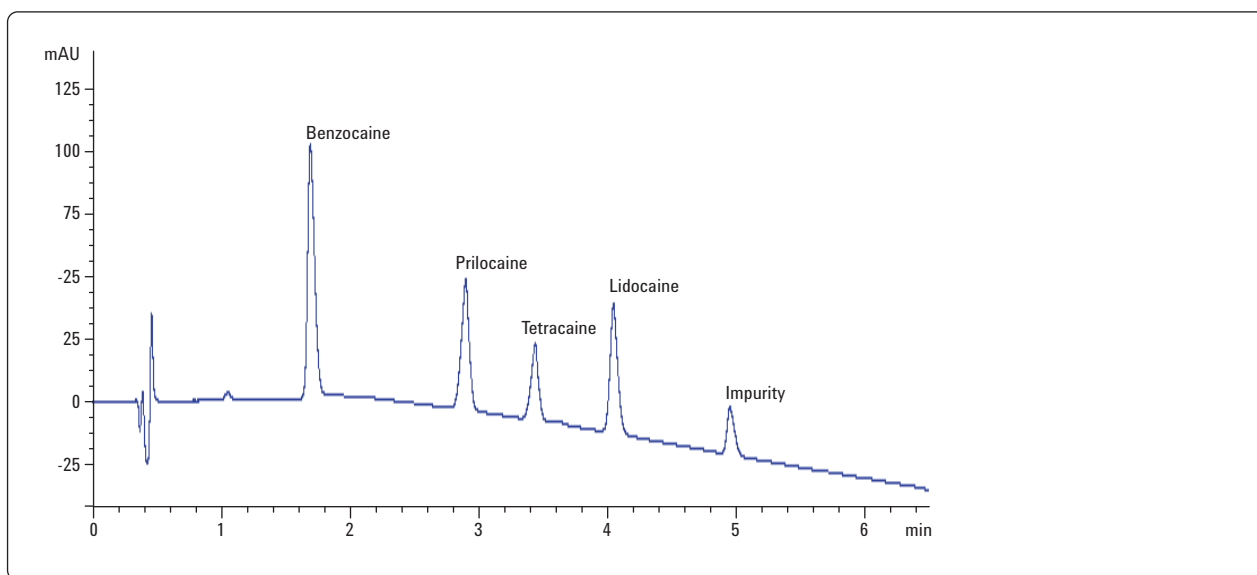


Figure 2
Separation of local anesthetics on Agilent ZORBAX Eclipse Plus C18, 150 × 2.1 mm, 5 µm.

When using 3.5 μm material to shorten analysis time, the parameters of the separation with the ZORBAX Eclipse Plus C18, 150 \times 2.1 mm column with 5 μm -material can be used. With the Method Translator the new parameters can easily be calculated (Figures 3 and 4).

Original Method

System Info
Conventional LC

Column Info
Column ID (mm): 2.1
Column length (mm): 150
Particle Size (μm): 5

Method Info
Flow Rate (mL/min): 0.8
Injection Vol. (μL): 5
Pressure (bar): 156
Solvent: Water / Acetonitrile
Temperature ($^{\circ}\text{C}$): 40
Max. Solvent Visc. (cP): 0.75

| | Time | %B | Flow |
|---------------|------|----|------|
| Initial: | 0.00 | 0 | 0.80 |
| Initial Hold: | 1 | 28 | 0.80 |
| Gradient: | 7 | 70 | 0.80 |
| Hold to: | 7 | 70 | 0.80 |
| Return by: | 7.01 | 0 | 0.80 |
| End of Run: | 7.01 | 0 | 0.80 |

New Method

System Info
Agilent 1200 Series RRLC System

Column Info
Column ID (mm): 2.1
Column length (mm): 50
Particle Size (μm): 3.5

Method Info
Flow Rate (mL/min): 0.80
Injection Vol. (μL): 1.7
Pressure (bar): 106
Detector Settings: (0.5 sec)

| | Time | %B | Flow |
|---------------|------|----|------|
| Initial: | 0.00 | 0 | 0.80 |
| Initial Hold: | 0.33 | 28 | 0.80 |
| Gradient: | 2.33 | 70 | 0.80 |
| Hold to: | 2.33 | 70 | 0.80 |
| Return by: | 2.34 | 0 | 0.80 |
| End of Run: | 2.34 | 0 | 0.80 |

Time Saving Factor
3.0

fast ————— ultra-fast

Simple Conversion
 Speed Optimized
 Resolution Optimized

Figure 3
Calculating the new parameters for the 3.5 μm column with the Method Translator Software.

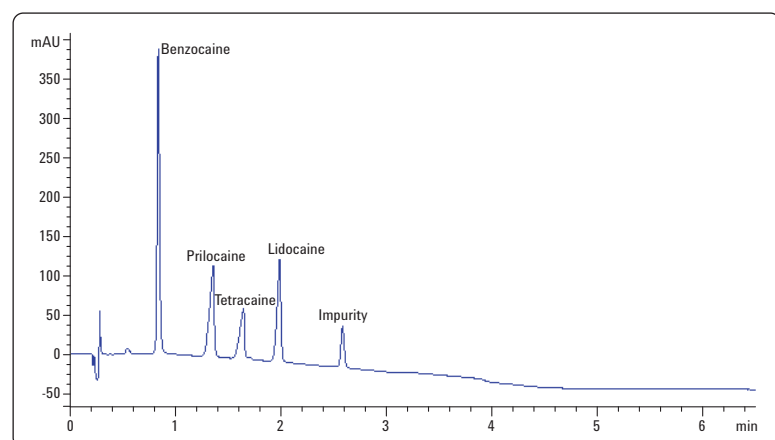


Figure 4
Separation of local anesthetics on Agilent ZORBAX Eclipse Plus C18, 50 \times 2.1 mm, 3.5 μm .

To further reduce the analysis time the parameters can be transferred to columns with particles < 2 µm. Leaving the column dimension constant (50 mm × 2.1 mm) will improve the separation power because of the increased number of plates. When the system is independent of back pressure like the 1290 Infinity LC system the flow and the gradient shape can be increased, which dramatically decreases the run time. The results can be seen with separations in Figures 5 and 6. Both the Waters BEH C18 and the Agilent ZORBAX RRHD Eclipse Plus columns with particles < 2 µm provide a full separation of all peaks.

Table 3 lists the results of resolution calculations for all anesthetics separated with the different columns. For all peaks the resolution is greater than 2.5, even at highest flows and highest back pressures. With the BEH column the back pressure is remarkably higher resulting in lower flow rates and the peak shape shows some tailing, which is probably reduced at higher pH values. With the ZORBAX RRHD Eclipse Plus column no peak tailing at pH = 8.2 is seen as a result of good endcapping. An overall run time of 1.00 min is achieved with a flow of 1.9 mL/min. This is because reequilibration is done in 30 s, due to the small system and delay volume of the column.

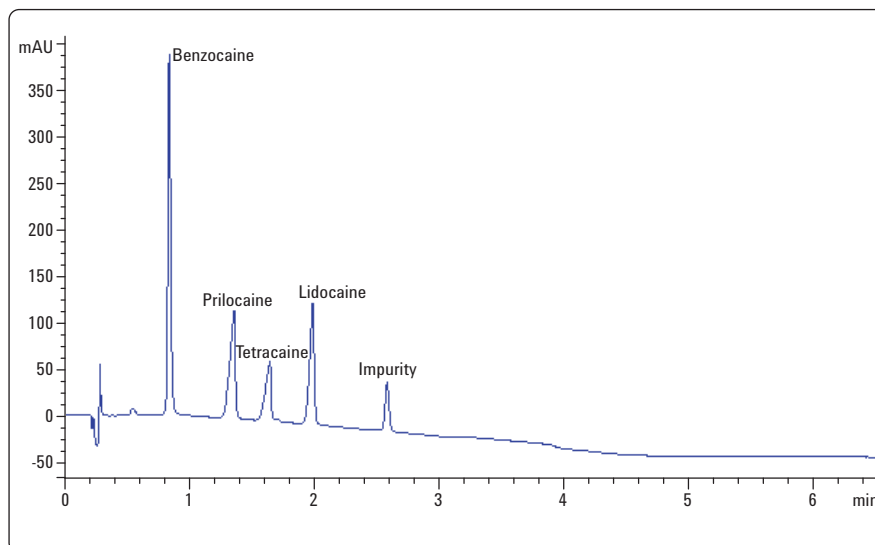


Figure 5
Separation of local anesthetics on Water BEH C18, 50 × 2.1 mm, 1.7 µm, Flow: 1.5 ml/min.

| Compound | Agilent ZORBAX Eclipse Plus, 150 × 2.1 mm, 5 µm, 0.8 ml/min | Agilent ZORBAX Eclipse Plus, 50 × 2.1 mm, 3.5 µm, 0.5 ml/min | Agilent ZORBAX RRHD Eclipse Plus, 50 × 2.1 mm, 1 µm, 1.9 ml/min | Water BEH C18, 50 × 2.1 mm, 1.7 µm, 1.3 ml/min |
|------------|---|--|---|--|
| Benzocaine | - | - | - | - |
| Prilocaine | 11.57 | 8.52 | 3.91 | 4.23 |
| Tetracaine | 5.15 | 3.57 | 2.56 | 2.64 |
| Lidocaine | 5.94 | 4.65 | 5.13 | 3.88 |
| Stop time | 6 min | 3 min | 0.5 min | 0.6 min |

Table 3
Resolution of the anesthetics depending on column types (see Figures 2, 4-6).

Table 4 shows the data for the precision of the method applied to the separation with the Agilent ZORBAX RRHD Eclipse Plus C18, 50 mm × 2.1 mm column, and the high flow rate of 1.9 mL/min (Figure 6).

The data for precision of the retention times prove the high precision and stability of the flow, even at high pressure

and high flow rates. The data also reflect the high efficiency of the new low volume jet weaver as a gradient mixing tool. The data for precision of areas show the good performance of the Autosampler. This is also illustrated by correlation coefficients for all components greater than 0.999 (Figure 7) with lidocaine as a reference.

| | Retention times | | Areas | | Linearity |
|------------|-----------------|-------|--------------|-------|----------------|
| | Mean | RSD | Mean | RSD | R ² |
| Benzocaine | 0.214 | 0.214 | 2,885,499.30 | 0.485 | 0.9998 |
| Prilocaine | 0.286 | 0.289 | 1,930,676.50 | 0.366 | 0.9999 |
| Tetracaine | 0.318 | 0.207 | 1,424,720.20 | 0.451 | 0.9998 |
| Lidocaine | 0.373 | 0.144 | 1,882,887.60 | 0.371 | 1.0000 |

Table 4

Determination of the precision of areas and retention times for the reference sample (chromatogram see Figure 6), linearity for 1-100 µg/ml calibration.

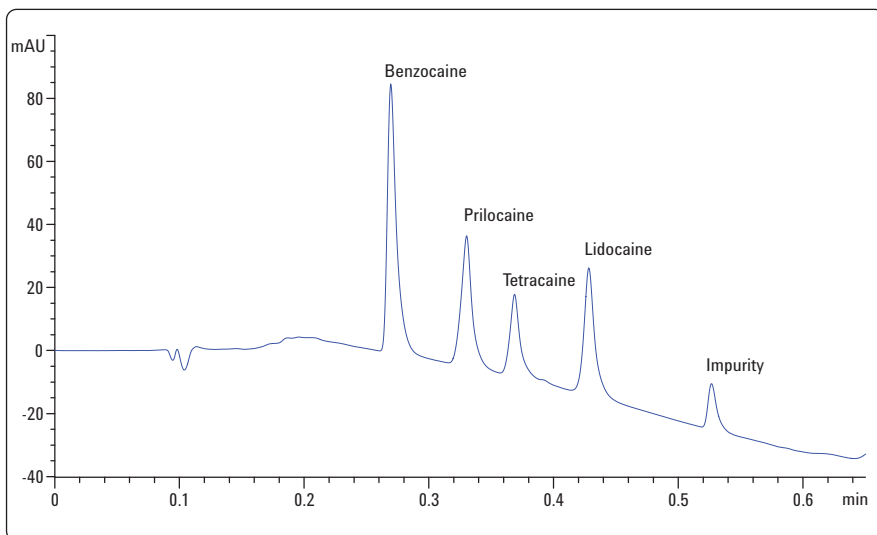


Figure 6

Separation of local anesthetics on Agilent ZORBAX Eclipse Plus RRHD C18, 50 × 2.1 mm, 1 µm, Flow: 1.9 ml/min.

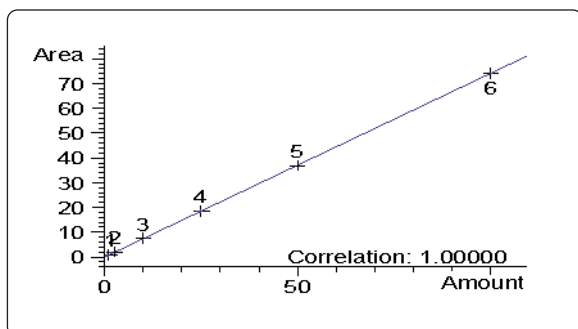


Figure 7

Calibration curve for lidocaine as example for all anesthetics.

A further test to evaluate the sampler performance is the determination of carryover. Figure 8 shows the chromatogram after an injection of the mixture. No carryover can be seen.

Conclusion

The new Agilent 1290 Infinity LC is designed to provide the highest speed, resolution and sensitivity. A new power range allows you to operate with columns filled with any particle type, any column dimensions, or any mobile and stationary phase. The 1290 Infinity LC is the first system to allow method transfer from any Agilent HPLC System to a new system.

The example separation of four local anesthetics has also shown that applications with conventional columns will run with high performance. The Method Translator is a helpful tool to make these methods faster. The good results of method transfer show that the selectivity and performance of the Agilent ZORBAX Eclipse Plus C18 material is independent of the particle size. The overall run time of the final method of 1.00 min, including reequilibration shows the infinite number of opportunities for establishing high resolution and ultrafast liquid chromatography.

With the new low volume jet weaver, effective gradient mixing provides high precision of gradient times.

The results shown in Tables 3 and 4 illustrate that all criteria for the precision of determination: areas, retention times, and resolution are fulfilled. Also the coefficients for linearity for all components are better than 0.999. All results explicitly show the applicability of the 1290 Infinity LC system for quality control testing as well as for high resolution and ultrafast liquid chromatography.

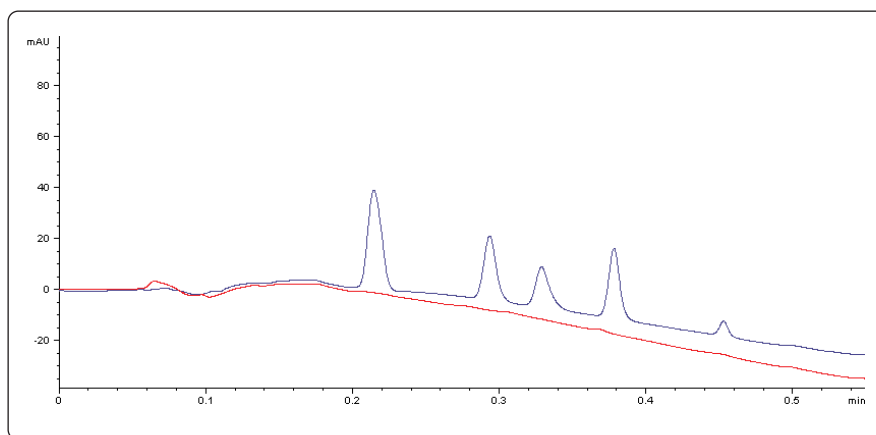


Figure 8
Blank injection to detect any carryover (blue-mixture, red-blank).

The infinite possibilities of the system are best shown by the overall run time including reequilibration of 1.00 min. The good flow design of the 1290 Infinity LC system assures the user that no band broadening or peak distortion will occur to hinder the separation power. In addition the “system pressure” will not limit the possible high operating flow rates.

In summary, the data obtained in this Application Note demonstrates the versatility and reliability of the Agilent 1290 Infinity LC system. It shows fast method transfer from or to any column and particle size and therefore, is applicable for any desired application. The Agilent 1290 Infinity LC system meets highest requirements for every LC function.

References

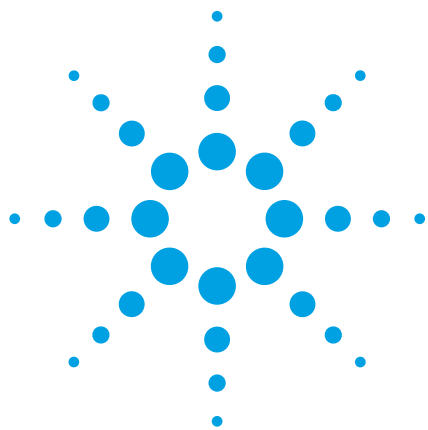
R. Ricker, “Bonded-phase selectivity, separation of local anesthetics”, Agilent Publication 5988-6424EN, 2002

www.agilent.com/chem/1290

© Agilent Technologies, Inc., 2009
December 1, 2009
Publication Number 5990-4994EN



Agilent Technologies



Analytical instrument qualification and system validation according to USP Chapter <1058> for the Agilent 1290 Infinity LC system

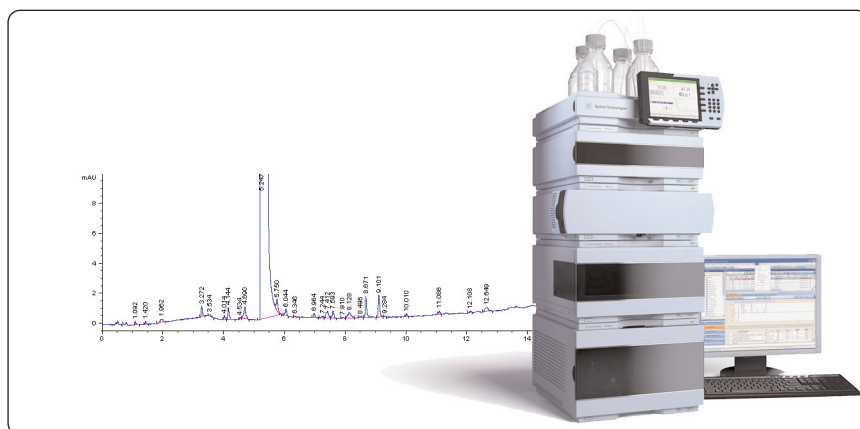
Application Note

Pharmaceutical QA/QC

Authors

Detlef Wilhelm
ANATOX GmbH & Co. KG
Fuerstenwalde
Germany

Edgar Naegele
Agilent Technologies
Waldbronn, Germany



Abstract

According to USP Chapter <1058> analytical instruments must be qualified before use. This Application Note will show a setup for testing the Agilent 1290 Infinity LC System. Metoclopramide was chosen as example substance to acquire data for testing accuracy, precision, and linearity and the results are presented.

The results of independent gradient testing with the Jet Weaver show steep gradient shapes and high plateau accuracy. The setup for different columns to achieve comparable separations starting with 5 μ m material (250 mm \times 4.6 mm), 3.5 μ m material and columns with sub-2 μ m materials of different vendors are shown. This versatility makes the system applicable for standard LC methodology as well as where highest separation power is needed.

The results for the determination of the precision of areas (<2% required), and retention times (<0.05% required) show that all criteria for qualified instruments are fulfilled. The coefficients for linearity for all components are better than 0.999. No carry-over was detected.



Agilent Technologies

Introduction

USP Chapter <1058>¹ describes the relevant guidelines for analytical instrument qualification. These guidelines are not mandatory and allow different approaches. If analytical instruments are used in FDA regulated environments, related procedures are recommended. USP guidelines are mandatory only if any USP monographs require qualified instruments for a specific analysis, or if any regulated testing is applied.

The USP Chapter <1058> divides laboratory tools and instruments into three categories (A, B, C). Group A includes tools such as magnetic stirrers, Group B lists balances and pH-meters and Group C contains complex instruments like HPLCs or mass spectrometers. Depending on the complexity of the instrument and its application, the effort for qualification increases. The 4Q-model (design qualification, installation qualification, operational qualification, performance qualification) supports the guidelines of the instrument qualification for Group C instruments. Since it has been in use for 10 years, many users are familiar with the model.²

This model is applicable to all types of instruments because it is flexible and allows all laboratories to define test procedures and acceptance criteria.

The Agilent 1290 Infinity LC System belongs to category C, where testing according USP Chapter <1058> is necessary. This Application Note will show a setup for testing the instrument. Metoclopramide was chosen as an example substance to acquire data for testing of accuracy, precision and linearity. For setup of the method, the results of previous method developments were used.³

Experimental

Instrumentation

Table 1 shows the configuration of the Agilent 1290 Infinity LC system that was used. Several columns were used to show the performance.

| Part No | Module |
|-----------|--|
| G4220A | 1290 Infinity Binary pump with integrated vacuum degasser and different solvent mixers |
| G4226A | 1290 Infinity Autosampler |
| G1316C | 1290 Infinity Column Compartment |
| G4212A | 1290 Infinity Diode Array Detector |
| Software: | Chemstation B.04.02 |

Table 1
Configuration of the Agilent 1290 Infinity LC system

Preparation of samples

Reference samples

The stock solution was prepared by mixing two different liquid formulations of metoclopramide hydrochloride (each 5 mg/mL, each 1 mL). One millilitre of the mixture was diluted with 4 mL of methanol to yield a concentration of 1 mg/mL for the main component. The resulting solution was diluted to the 0.01% concentration of the impurities.³ Figure 1 shows the structure of metoclopramide.

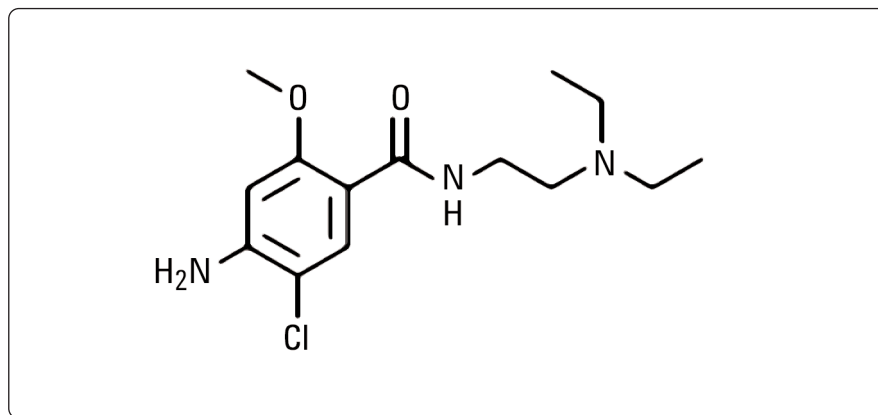


Figure 1
Structure of metoclopramide.

Chromatographic conditions

Columns:

- Agilent TC C18(2), 250 mm × 4.6 mm, 5 μm
- ZORBAX Eclipse Plus C18, 150 mm × 2.1 mm, 3.5 μm
- ZORBAX RRHD Eclipse Plus C18, 150 mm × 2.1 mm, 1.8 μm
- Waters BEH C18, 150 mm × 2.1 mm, 1.7 μm

Mobile phases: Gradient testing

- Mobile phase A: water
- Mobile phase B: water + 0.5% acetone (v/v)

| Time | % A | % B |
|-------|--------|--------|
| 0.00 | 100.00 | 0.00 |
| 3.00 | 100.00 | 0.00 |
| 3.01 | 90.00 | 10.00 |
| 6.00 | 90.00 | 10.00 |
| 6.01 | 52.00 | 48.00 |
| 9.00 | 52.00 | 48.00 |
| 9.01 | 48.00 | 52.00 |
| 12.00 | 48.00 | 52.00 |
| 12.01 | 10.00 | 90.00 |
| 15.00 | 10.00 | 90.00 |
| 15.01 | 0.00 | 100.00 |
| 18.00 | 0.00 | 100.00 |
| 18.01 | 48.00 | 52.00 |
| 21.00 | 48.00 | 52.00 |
| 21.01 | 52.00 | 48.00 |
| 24.00 | 52.00 | 48.00 |
| 24.01 | 100.00 | 0.00 |
| 27.00 | 100.00 | 0.00 |

Table 2
Gradient.

Gradient for separation of metoclopramide and impurities

- Mobile phase A : 0.25% w/w ammonium acetate in water
- Mobile phase B : acetonitrile

The setup for all columns was found by using the parameters determined in Agilent publication number 5990-3981EN for the BEH column for starting conditions, converting them with the Method Translator Software⁴. (Instrument conditions are shown in Table 3.)

Setup for testing

USP Chapter <1058> defines tests and limits for the evaluation of HPLC systems. Typically, tests are used to evaluate pump performance, autosampler performance, the stability of temperatures, or the accuracy of optical detectors.

The chromatographic performance of the pump is shown by plotting and evaluating gradient mixing capabilities with a tracer and retention time precision. The autosampler can be validated by calculating the area precision of equal injection volumes, the correlation of

calibration curves or the determination of the carryover. These results are only valid, if the detection system is stable enough to deliver reproducible data with sufficient sensitivity and high signal-to-noise values.

The following setup is the selection from a typical assortment of tests for system suitability with a reference sample :

- Determination of pump performance depending on dwell volumes by gradient tests
- Establishment of a chromatographic separation to achieve data for long time evaluations
- Similar peak pattern and resolution according to selected column with respect to particle size and column dimension and adapted to gradient shape and flow
- Precision of areas must be < 2 % RSD.
- Precision of retention times must be < 0.5 % RSD.
- Linearity should be $R^2 > 0.999$

| | Agilent TC C18(2), 250×4.6mm, 5μm, | Eclipse Plus C18, 150×2.1mm, 3.5μm | RRHD Eclipse Plus C18, 150×2.1mm, 1.8μm | Waters BEH C18, 150×2.1mm, 1.7μm |
|------------------|---------------------------------------|---------------------------------------|---|--------------------------------------|
| Flow rate | 1.058 mL/min | 1.058 mL/min | 0.221 mL/min | 0.221 mL/min |
| Gradient | 0-25 min 5-57% B | 0-15 min 5-57% B | 0-15 min 5-57% B | 0-15 min 5-57% B |
| Temperature | 37 °C | 37 °C | 37 °C | 37 °C |
| Injection volume | 8 μl | 2 μl | 1 μl | 1 μl |
| Detection | DAD, Signal | 275/4, Reference | 400/60 | standard cell (10 mm path length) |
| Data rate | 2 Hz | 2 Hz | 40 Hz | 40 Hz |
| Maximum pressure | 138 bar | 145 bar | 310 bar | 435 bar |

Table 3
Instrument conditions.

There are more tests available to evaluate the accuracy of the optical unit of the detector. These tests can be established in addition to those mentioned, but are often part of a special setup available during diagnosis, and are not evaluated with a chromatographic test.

The samples in Table 4 were prepared and analyzed with these limits and settings for testing.

Results and discussion

USP Chapter <1058> defines tests and limits for the evaluation of HPLC modules and HPLC systems. The results shown here illustrate this process.

The accuracy of gradient mixing, as well as flow accuracy, are the main tests for evaluating a gradient pump. Gradient mixing becomes more and more influenced by the dwell volume. The testing setup must be variable to eliminate the effects of the mixer used.

The Agilent Jet Weavers for high efficiency mixing allow the use of different mixing volumes. The delay and dwell volume of the pumps have an influence on the separation for narrow bore applications combined with fast gradients. Enlarging the dwell volumes, thereby increasing retention times, could affect the resolution, and the gradient shape because of dispersion effects and different flush-out behavior. Chromatograms can appear different due to different mixers and mixing volumes. Figure 2 shows the different but steep gradient shapes, resulting in very short response times depending on the mixer. It also shows high accuracy of the gradient steps independent of the mixer used.

| Sample | Purpose | Number of injections |
|--|--|----------------------|
| Blanc solution | Verify baseline stability and identify artifacts | 3 |
| Suitability sample | Verify precision of areas and retention times for reference solution | 10 |
| Calibration | Verify linearity | 3 for each level |
| Highest concentration and Blanc solution | Verify carryover | 3 of each sample |

Table 4
Setup for testing.

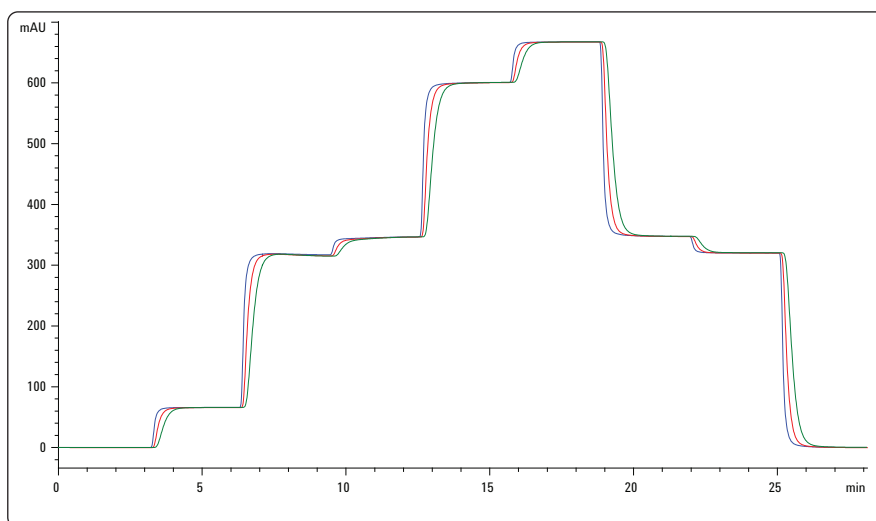


Figure 2
Gradient test depending on the volume of the mixers (blue-35 µL, red-135 µL, green-300 µL).

The next test evaluates the functionality of the system with different columns. For that purpose, four different columns with different particle sizes were tested (Figure 3).

In addition, the flow precision was evaluated using the retention time stability of some selected components in the mixture. With the same setup, the precision of the autosampler can be calculated, if the test sample is injected a minimum of 10 times and the relative standard deviation (RSD) of the areas is calculated. The data in Table 5 show high stability of retention times and high precision of areas even at low levels of impurities.

The accuracy of retention times is not only influenced by the flow precision but also by the temperature. The remarkable high stability is also a demonstration of excellent temperature stability in the column compartment.

The test for linearity shows correlation coefficients for all components greater than 0.999 which prove the high performance of the autosampler.

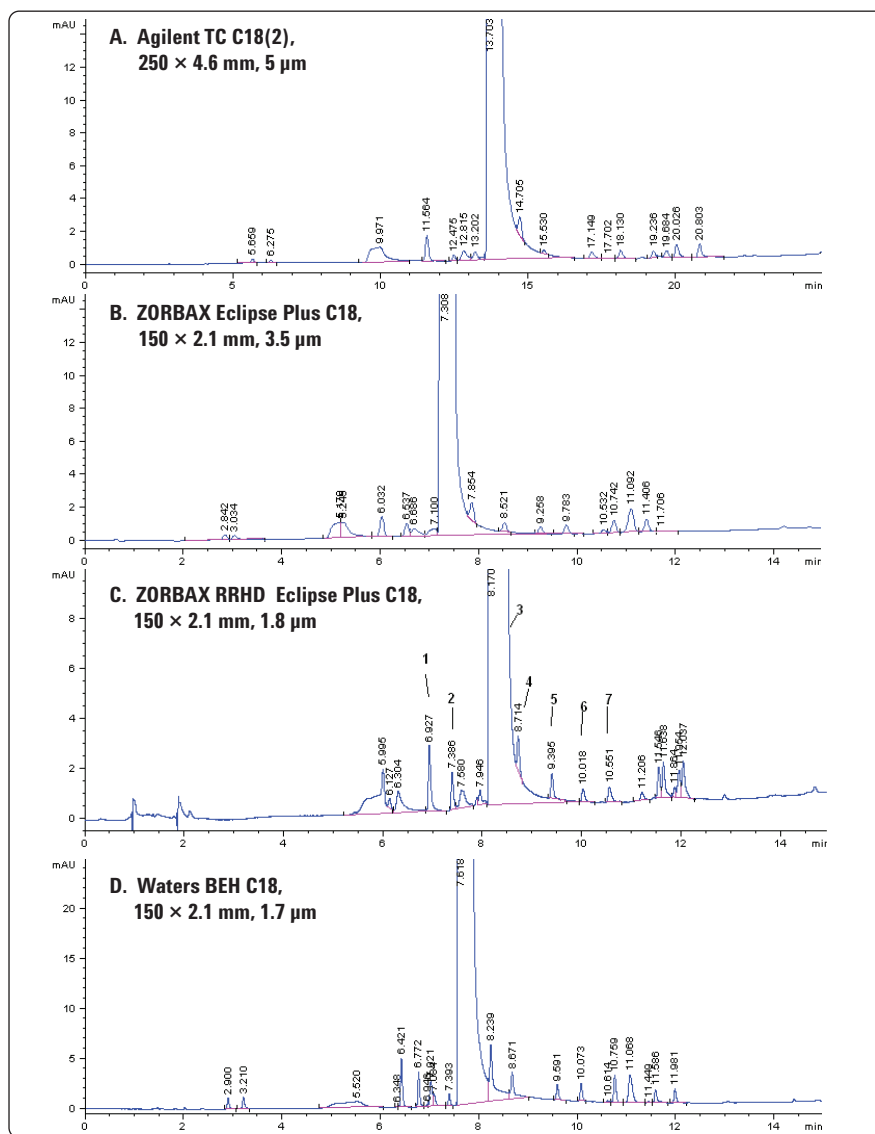


Figure 3
Separation of metoclopramide and its impurities.

| | Retention times | | Areas | | Linearity R ² |
|------------------|-----------------|-------|-----------|------|--------------------------|
| | Mean | RSD | Mean | RSD | |
| Impurity 1 | 6.927 | 0.030 | 3.765 | 1.36 | 0.9994 |
| Impurity 2 | 7.386 | 0.025 | 2.170 | 1.49 | 0.9997 |
| Metoclopramide 3 | 8.170 | 0.039 | 10190.182 | 0.58 | 0.9998 |
| Impurity 4 | 8.714 | 0.035 | 1.707 | 1.48 | 0.9993 |
| Impurity 5 | 9.395 | 0.013 | 1.496 | 1.58 | 0.9993 |
| Impurity 6 | 10.018 | 0.039 | 1.023 | 1.55 | 0.9990 |
| Impurity 7 | 10.551 | 0.039 | 1.971 | 1.46 | 0.9993 |

Table 5
Determination of the precision of areas and retention times in Figure 3C.

A further test to evaluate sampler performance is the determination of carryover. Figure 4A shows the chromatogram after an injection of the highest concentration of metoclopramide. No carryover can be seen (Figure 4B).

The chromatogram in Figure 5 shows further method optimization, where the analysis time was shortened to improve the capacity of the system. It can be seen that all peaks are eluted within 10 minutes.

Conclusion

The Agilent 1290 Infinity LC system is designed to provide highest speed, resolution and sensitivity. A new power range allows operation with any particle type, any column dimension, or any mobile and stationary phase. The 1290 Infinity LC is the first system that allows method transfer from any Agilent HPLC System.

To use this system for quality control testing and development, as well as in an FDA regulated environment, it is necessary to meet the criteria of the new USP Chapter <1058>. These new regulations enforce procedures for testing and evaluating the applicability and versatility of the equipment before use.

This Application Note shows a selection of tests that can be established to evaluate an LC system.

Figure 2 shows the results of gradient testing. Independent of the Jet Weavers used and mixing volumes, the gradient shapes are steep and show high accuracy of each plateau.

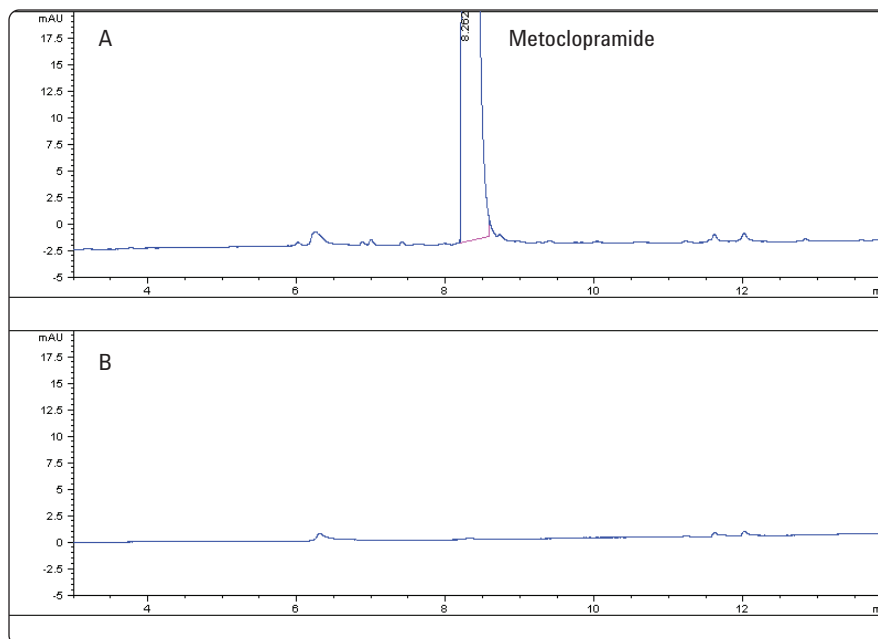


Figure 4
Determination of carryover. A. Injection of sample with highest concentration of metoclopramide. B. Injection of a blank solvent sample.

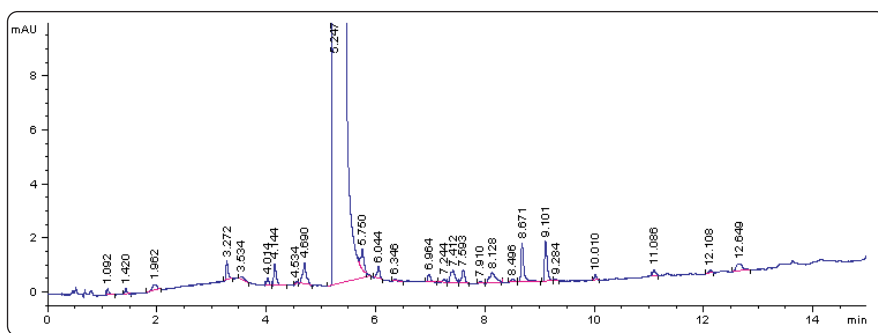


Figure 5
Separation of metoclopramide and its impurities on a ZORBAX RRHD Eclipse Plus C18, 150 × 2.1 mm, 1.8 μm, speed optimized (flow: 0.44 ml/min).

One of the great benefits of the system is the use of any column dimension or particle size. This was proven by the comparison of the separation power of a developed method with different column sizes. Figure 3 shows very similar chromatograms achieved from a column with 5 μm material (250 mm \times 4.6 mm), a column with 3.5 μm material, and columns with sub-2 μm materials from different vendors. This versatility allows the use of the system for standard LC methodology as well as methods in which the highest separation power is needed.

The results shown in Table 5 show that all criteria for the precision of the determination (areas, retention times) are fulfilled. The coefficients of linearity for all components are better than 0.999. This is not only proven for the main component but also for the impurities at the 0.01%-level. No carryover was detected (Figure 4).

All results explicitly show the applicability of the 1290 Infinity LC system for quality control testing and development as well as in an FDA regulated environment.

In addition, the speed optimization test confirms that the system provides excellent separation possibilities (Figure 5).

The results of method transfer show that the selectivity and performance of the Agilent ZORBAX Eclipse Plus C18 material is independent of the particle size. The data also show the excellent flow design of the Agilent 1290 Infinity LC system, assuring the user that no band broadening or peak distortion will occur, hindering the separation power.

In summary, the data presented in this Application Note has illustrated the versatility and reliability of the Agilent 1290 Infinity LC system. This system allows fast method transfer to and from any column or particle size, allowing its use for almost any applications.

The Agilent 1290 Infinity LC system is qualified for the criteria of USP Chapter <1058> and will meet the highest requirements for every LC application.

References

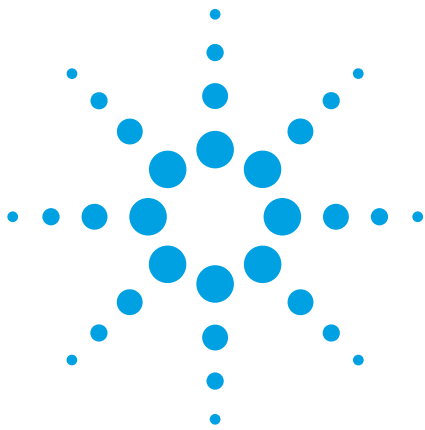
1. United States Pharmacopeia, Chapter <1058>, Analytical Instrument Qualification, USA, 2008.
2. Analytical Instrument Qualification and System Validation, January 1, 2009, Agilent Technologies publication number 5990-3288EN.
3. Increasing productivity in the analysis of impurities in metoclopramide hydrochloride formulations using the Agilent 1290 Infinity LC system, Agilent Technologies publication number 5990-3981EN.
4. <http://www.agilent.com/chem/hplc2uhplc>

www.agilent.com/chem/1290

© Agilent Technologies, Inc., 2009
December 7, 2009
Publication Number 5990-4781EN



Agilent Technologies



Determination of water soluble vitamins with the Agilent 1120 Compact LC after method development with the Agilent 1200 Series Rapid Resolution LC system and back transfer

Application Note

Food

Authors

Detlef Wilhelm
ANATOX GmbH & Co. KG
Fuerstenwalde
Germany



Abstract

Quality control to characterize products is often done with standardized liquid chromatography (LC) methods. The needed analytical instrumentation requires optimal cost-of-ownership instruments with high reliability, high flexibility, and ease of use.

The analysis of several water soluble vitamins with the Agilent 1120 Compact LC is described. The preceding method development was done with Agilent 1200 Series Rapid Resolution (RR). This Application Note starts with the final results of that method development. The transfer of those results by the Method Translator Software to conventional LC parameters and columns shows that this method can be used with standard LC equipment.

This Application Note shows that the Agilent 1120 Compact LC works as a reliable and highly robust instrument for routine LC analyses and everyday quality control testing. Full separation was achieved by using an ion pairing eluent and Agilent ZORBAX Eclipse Plus material. The analysis of a typical nutritional mixture of vitamins shows no disturbances by other peaks. The results for reliability and quality testing, system suitability, and performance are shown.



Agilent Technologies

Introduction

Quality control is a main consideration in the field of standard LC product analyses. The analytical instrumentation has several requirements, such as optimal cost-of-ownership, high reliability, high flexibility, and ease of use.

This Application Note targets routine quality control testing, and shows that the Agilent 1120 Compact LC is a reliable and highly robust instrument for standard methodology. The Agilent 1120 Compact LC can also be used for determinations after method development with an Agilent 1200 Series RRLLC system. Back transfer from the RR separation to conventional columns can be achieved by the Method Translator Software, and the results of reliability, quality, system suitability, and performance testing are shown.

Instrumentation

An Agilent 1200 Series Rapid Resolution LC system and an Agilent 1120 Compact LC were used for the method development. Table 1 lists the configurations used for each instrument.

| Configuration of the Agilent 1200 LC Series | Configuration of the Agilent 1120 Compact LC |
|---|--|
| Binary pump and vacuum degasser | Gradient pump and vacuum degasser |
| Well-plate autosampler | Autosampler |
| Column compartment | Column oven |
| Diode array detector | Variable wavelength Detector |
| Software: Chemstation B.04.01 | Software: EZ-Chrom Elite Compact 3.3 |

Table 1
Instrumentation configurations used for method development

Preparation of samples

Reference samples

Dissolve 10 mg of each vitamin in water and dilute to 100 mL with the same solvent. Dilute 1 mL of the solution to 20 mL with the mobile phase. Figure 1 illustrates the substances to check.

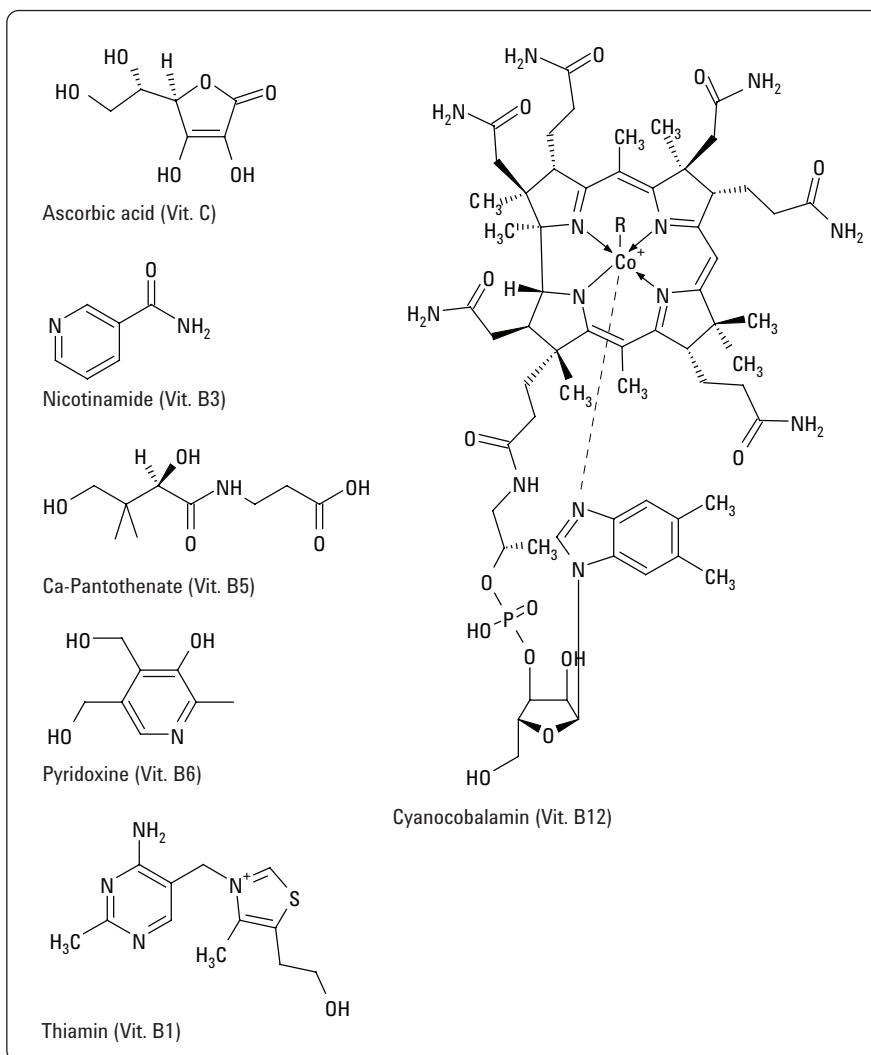


Figure 1
Substances to check.

Chromatographic conditions

Column

For method development: ZORBAX Eclipse Plus C18, 50 mm × 2.1 mm, 1.8 µm
For routine testing: ZORBAX Eclipse Plus C18, 150 mm × 4.6 mm, 5 µm

Mobile phases

Phase A: Dissolve 1.03 g hexane sulfonic acid and 6.8 g potassium dihydrogen phosphate in 1000 mL water. The pH value should be adjusted to pH = 2.3 with phosphoric acid.
Phase B: Acetonitrile

Gradient (linear):

| Time (min) | |
|------------|-------------|
| 0 | 100% A/0% B |
| 6 | 80% A/20% B |
| 9 | 50% A/50% B |
| 10 | 100% A/0% B |

Pump settings

Stop time: 10 min
Post time: 5 min
Flow rate: 1.0 mL/min

Autosampler

Injection volume: 30 µL

Thermostatted column compartment

Temperature: 40 °C

Detector

14-µL cell for the Agilent 1120 LC system,
Peak width: >0.05 min, 1 s response time (10Hz),
Signal: 220 nm
13-µL cell for the Agilent 1200 LC system,
Peak width: >0.05 min, 1 s response time (10Hz),
Signal: 220 nm

System suitability and performance test:

For system suitability testing the reference solution with the following limits was used:

- Resolution: minimum 1.5 between peaks.

- Precision of areas must be < 2 % RSD.
- Precision of retention times must be < 0.5 % RSD.

With these limits and settings for testing, the samples in Table 2 were prepared and analyzed.

| Sample | Purpose | Number of injections |
|---------------------|--|----------------------|
| Blanc solution | Verify baseline stability and identify artifacts | 2 |
| Calibration samples | Verify linearity | 3 of each level |
| Control sample | Verify sensitivity and resolution for reference solution | 6 |
| Suitability sample | Verify precision of areas and retention times for reference solution | 10 |

Table 2
Setup for testing

Results and discussion

Hexanesulfonic acid was chosen as the ion-pairing agent to achieve the best separations for all peaks. The results in Figure 2 show good separation of all vitamins with the ZORBAX Eclipse Plus C18 material on an Agilent 1200 Series RRLC system.

The parameters found during method development with the Agilent 1200 Series RRLC system were transferred to parameters suitable for using 5- μm columns with conventional HPLC systems with the Agilent Method Translator Software (see Figure 3).

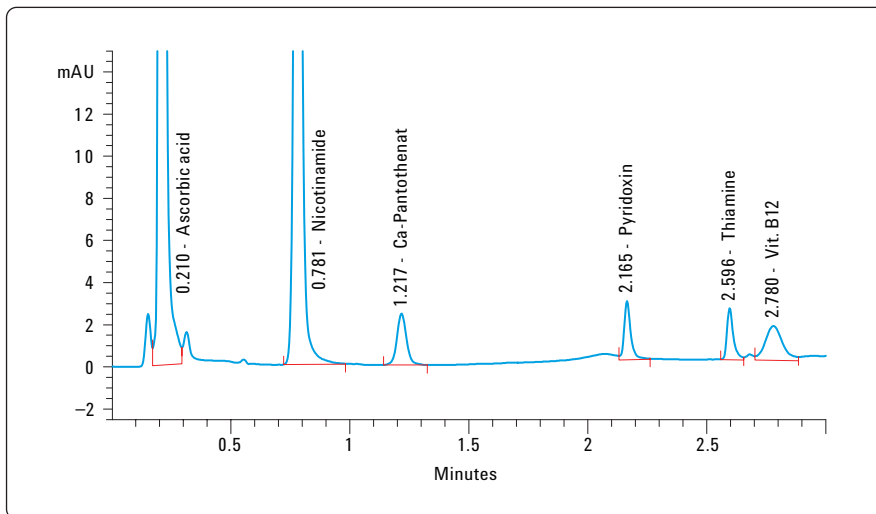


Figure 2
Example chromatogram of water soluble vitamins with the Agilent 1200 Series RRLC system.

Original Method

System Info

- Agilent 1100/1200 Series Binary Pump
- Agilent 1100/1200 Series Quat. Pump

Column Info

Column ID [mm] 2,1

Column Length [mm] 50

Particle Size [μm] 1,8

Method Info

Flow Rate [mL/min] 0,75

Injection Vol. [μL] 2,00

Pressure [bar] 375,93

Solvent Water / Acetonitrile

Temperature [°C] 40,00

max. Solvent Visc. [cP] 0,75

| | Time [min] | %B | Flow [ml/min] |
|-----------|------------|------|---------------|
| Initial | 0,250 | 0,0 | 0,750 |
| Gradient | 2,000 | 20,0 | 0,750 |
| Hold to | 3,000 | 50,0 | 0,750 |
| Return to | 3,010 | 0,0 | 0,750 |
| Stop | 5,000 | 0,0 | 0,750 |

New Method

System Info

Agilent 1200 Series RRLC

Column Info

Column ID [mm] 4,6

Column Length [mm] 150

Particle Size [μm] 5,0

Method Info

Flow Rate [mL/min] 3,599

Injection Vol. [μL] 28,79

Pressure [bar] 146,16

Detector Settings >0,10 min (2 s)

Time-Saving Factor: 0,3

fast ultra-fast

- Simple Conversion
- Speed Optimized
- Resolution Optimized

| | Time [min] | %B | Flow [ml/min] |
|-----------|------------|------|---------------|
| Initial | 0,750 | 0,0 | 3,599 |
| Gradient | 6,000 | 20,0 | 3,599 |
| Hold to | 9,000 | 50,0 | 3,599 |
| Return to | 9,030 | 0,0 | 3,599 |
| Stop | 15,000 | 0,0 | 3,599 |

Figure 3
Conversion of LC parameters found by Rapid Resolution to parameters suitable for conventional HPLC with the Method Translator software.

Because Ca-pantothenate has no significant absorbance at wavelengths >230 nm, a 220 nm setting on the Agilent 1120 Compact LC wavelength detector was selected to detect all components. Figure 4 shows a chromatogram, achieved after transfer of the parameters from the 50 mm × 2.1 mm Rapid Resolution column to a 150 mm × 4.6 mm (5-µm material) column with the Agilent 1120 Compact LC and EZ-Chrom Elite Compact Software.

As Figure 4 shows, the elution order is the same, which proves that the selectivity does not change with the particle size. Only small differences can be seen in the resolution between nicotinamide and Ca-pantothenate, but full baseline separation still exists. Detailed data are listed in Table 3. As a main result it can be emphasized that it is possible to transfer LC parameters from Rapid Resolution to conventional LC systems and columns with 5-µm particles.

The only difference in parameters between the Agilent 1200 Series binary system and the Agilent 1120 Compact LC is that the 1120 LC separation resulted in slightly later eluting peaks, as seen in Figures 2 and 3. The reason can be found in the difference of gradient mixing. With the Agilent 1120 Compact LC, the gradient is mixed at the low pressure site whereas with the Agilent 1200 binary system the mixing is done at the high pressure site. The different mixing volumes (delay volumes) are responsible for the different raise of the gradients in the columns.

However, as seen in Figure 3 the resolution of all peaks is unaffected by the different gradient mixing. In addition, all other impurities in the fine chemicals are separated.

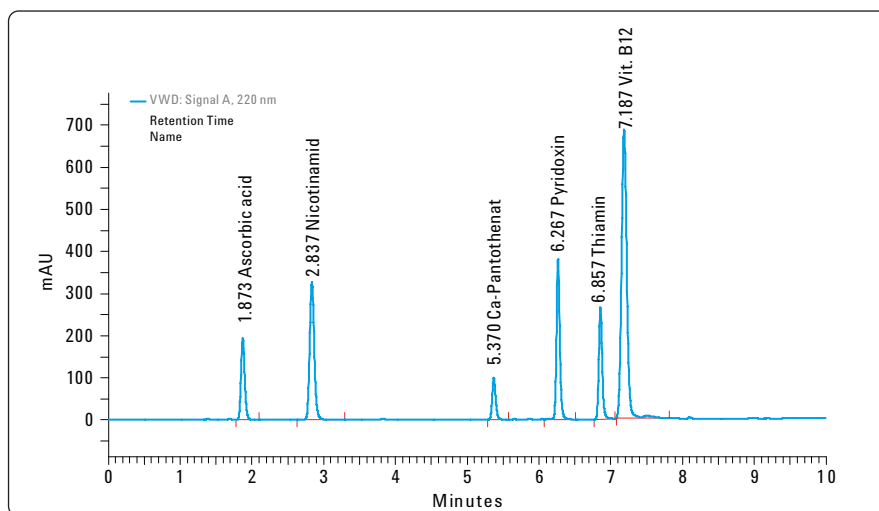


Figure 4
Example chromatogram of water soluble vitamins with the Agilent 1120 Compact LC.

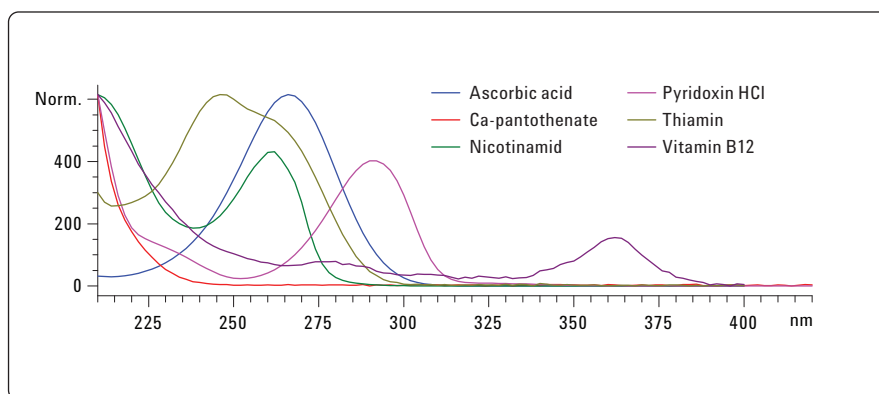


Figure 5
UV spectra of all vitamins acquired by the Agilent 1200 Series Diode Array Detector.

| Compound | Retention time 1200er (min) | Retention time 1120 (min) | Resolution 1200er | Resolution 1120 |
|-----------------|-----------------------------|---------------------------|-------------------|-----------------|
| Ascorbic acid | 0.210 | 1.873 | – | – |
| Nicotinamide | 0.781 | 2.837 | 12.78 | 9.24 |
| Ca-Pantothenate | 1.217 | 5.370 | 7.27 | 23.18 |
| Pyridoxine | 2.165 | 6.267 | 16.68 | 10.10 |
| Thiamine | 2.596 | 6.857 | 9.76 | 6.83 |
| Vitamin B12 | 2.780 | 7.187 | 2.24 | 3.38 |

Table 3
Results for control sample: Retention times and resolution.

The results shown in Table 3 illustrate good separation achieved with the ZORBAX Eclipse Plus C18 material. The high resolution (every peak >2) for both systems shows that this column material is highly suitable for this determination, because of its good performance (see data for asymmetry in Table 4).

Table 4 shows the areas and retention time precision results of all compounds in the suitability sample. The reliability and precision of the Agilent 1120 Compact LC is demonstrated. The criteria (see "System suitability and performance tests") of precision of retention times and areas are fulfilled for all compounds. This shows that the system can be used for QC methods.

The high precision and reliability of the autosampler is best shown by the data in Tables 4 and 5. The correlation coefficient for each calibration curve is very close to 1.0 showing high versatility and quality for QC testing.

The chromatogram in Figure 6, shows the determination of a nutritional mixture of vitamins with great differences in concentration of each vitamin, which illustrates the capabilities of the method.

| Compound | Retention time (min) | RSD RT n = 10 | RSD Area n = 10 | Asymmetry 1120 |
|-----------------|----------------------|---------------|-----------------|----------------|
| Ascorbic acid | 1.873 | 0.225 | 0.234 | 1.186 |
| Nicotinamide | 2.837 | 0.398 | 0.236 | 1.185 |
| Ca-Pantothenate | 5.370 | 0.277 | 0.508 | 1.238 |
| Pyridoxine | 6.267 | 0.323 | 0.325 | 1.178 |
| Thiamine | 6.857 | 0.407 | 0.374 | 1.193 |
| Vitamin B12 | 7.187 | 0.145 | 0.652 | 1.116 |

Table 4
Suitability sample: Precision of Retention times and areas for the Agilent 1120 Compact LC.

| Compound | m | b | r |
|-----------------|-------------|---------|-------|
| Ascorbic acid | 1601035.9 | 48890.7 | 0.999 |
| Nicotinamide | 17812069.2 | 17303.5 | 1.0 |
| Ca-Pantothenate | 2231477.8 | 3546.1 | 1.0 |
| Pyridoxine | 35097452.7 | 75231.6 | 0.999 |
| Thiamine | 26988637.8 | 40978.7 | 0.999 |
| Vitamin B12 | 104653435.3 | 19666.3 | 0.999 |

Table 5
Calibration data of the Agilent 1120 Compact LC (Setting "Ignore Origin", $Y = mx + b$, 1.6–16.1 µg/mL for ascorbic acid and 0.11–1.12 mg/L for the other vitamins).

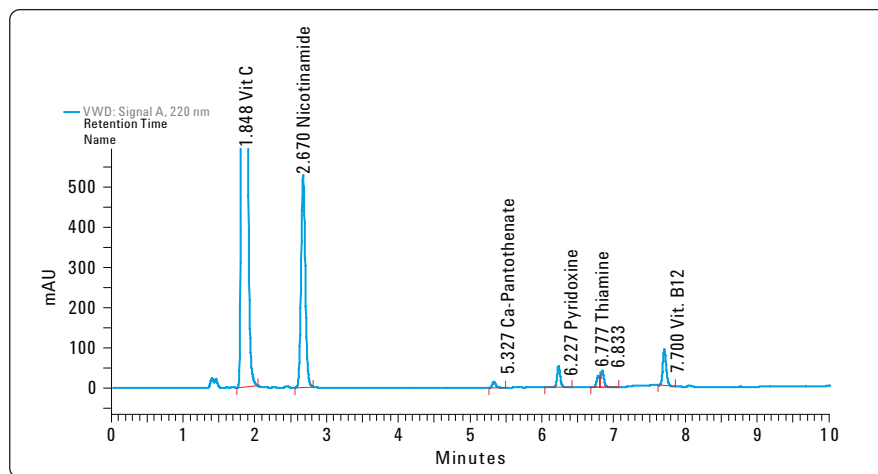


Figure 6
Chromatogram of a typical nutritional mixture of vitamins.

Conclusion

The Agilent 1120 Compact LC is a good choice for medium to small sized company users who need high reliability, ease-of-use, and lowest cost-of-ownership for standard QA/QC LC methodology.

This Application Note shows the setup for the determination of water soluble vitamins after method development with rapid resolution. This reliable approach is proven with precision of areas and retention time data, as well as chromatographic parameters such as resolution and asymmetry. The results from a system optimized for everyday productivity and calibration meet the requirements for routine analysis.

As shown in Table 3 the resolution of all peaks was found to be greater than 3.0 with values near 1.0 for the asymmetry of all main peaks. It is concluded from the calibration data that the instrument can be operated in a quality control environment.

The results in Table 4 show that all criteria for the determination of precision (areas, retention times) are fulfilled. From these results, it can be concluded that the Agilent 1120 Compact LC can be used in QA/QC laboratories to determine water soluble vitamins in samples for nutritional purposes.

All results show the applicability of the Agilent 1120 Compact LC for quality control testing by reduced costs per system and improved simplicity of use. In addition to the instrument capabilities, the new version of the EZChrom Elite compact software allows full control of the Agilent 1120 Compact LC with a wide range of features for data analysis and results reporting.

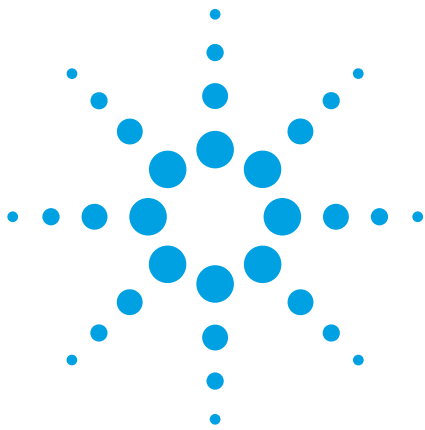
The results for resolution and asymmetry show good selectivity and performance of the ZORBAX Eclipse Plus material, independent of the particle size. The data also show good flow design of the LC systems ensuring that no band broadening and peak distortion will occur during method transfer. In summary, this Application Note shows that fast method development can be achieved with an Agilent 1200 Series Rapid Resolution LC system and the results can be back transferred to a conventional HPLC such as the Agilent 1120 Compact LC. This approach will meet the highest requirements for everyday productivity.

www.agilent.com/chem/1120

© Agilent Technologies, Inc., 2009
July 31, 2009
Publication Number 5990-4379EN



Agilent Technologies



Determination of degradation products of Metoprolol tablets with the Agilent 1120 Compact LC after method development with the Agilent 1200 Series Rapid Resolution LC system

Application Note

Pharmaceuticals

Authors

Detlef Wilhelm
ANATOX GmbH & Co. KG
Fuerstenwalde
Germany



Abstract

Conventional LC methods used in routine analyses to characterize or monitor chemicals are often standardized for quality control of pharmaceutical products. This Application Note describes the analysis of several degradation products of metoprolol with the Agilent 1120 Compact LC. The preceding method development was done with the Agilent 1200 Series Rapid Resolution LC (RRLC) system.

This Application Note starts with the final result of method development, to prove that no further development is necessary.¹ It shows that the Agilent 1120 Compact LC works as a reliable and highly robust instrument for standard LC methodology. The transfer from rapid resolution separation material to conventional columns by the Method Translator Software is shown. The results of system suitability and performance tests prove the reliability and quality of the Agilent 1120 Compact LC system for everyday quality control testing.



Agilent Technologies

Introduction

The Agilent 1120 Compact LC was designed to meet the highest requirements for analytical instrumentation used in routine analysis. In the field of quality control testing, products are often characterized with standard LC methods. Therefore, instruments used for these purposes need optimal cost-of-ownership, high reliability, high flexibility, and ease of use.

In the last few years the method development of new tests with a high-end Agilent 1200 Series RRLC system became familiar. In the Application Note "Agilent 1200 Series LC Method Development Solution for the analysis of degradation products of metoprolol tablets, Agilent Technologies publication 5989-9339EN" the results of the Agilent method development solution are shown.

This Application Note starts with the final results of method development, to prove that no further enhancement is necessary. It then shows that the Agilent 1120 Compact LC works as a reliable and highly robust instrument for standard LC methodology. It also shows that the Agilent 1120 Compact LC can be used for determinations after back transfer from rapid resolution separation material to conventional columns by the Agilent Method Translator Software. The results of system suitability and performance tests in this Application Note prove the reliability and quality of Agilent 1120 Compact LC for everyday quality control testing.

Instrumentation

For method development an Agilent 1200 Series RRLC system and an Agilent 1120 Compact LC with the following configurations were used:

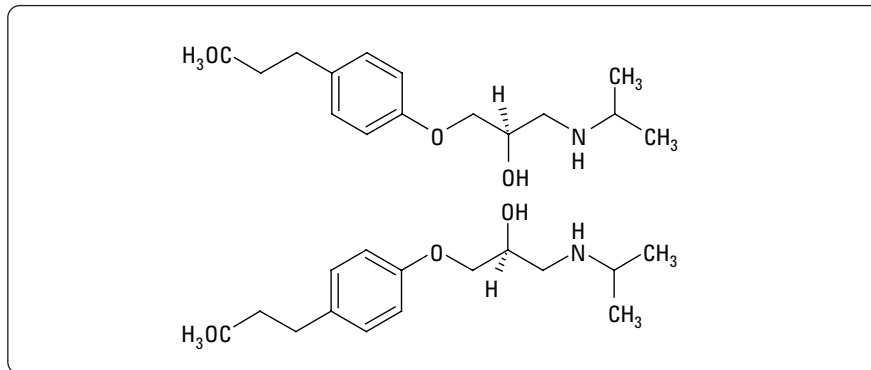
| Configuration of the Agilent 1200 Series Rapid Resolution LC System | Configuration of the Agilent 1120 Compact LC |
|---|--|
| Binary pump (low delay configuration) and vacuum degasser | Gradient pump and vacuum degasser |
| Wellplate autosampler | Auto sampler |
| 2 Column compartments | Column oven |
| Diode array detector | Variable wavelength detector |
| Software: ChemStation B.04.01 | Software: EZ-Chrom Elite Compact 3.3 |

Preparation of samples

Reference samples

Samples were prepared in the same manner as those described in another Application Note.¹ Two 50-mg metoprolol tablets were powdered. One of the samples was dissolved in water. The other tablet was heated to 80 °C for 3 hours, and the residue also dis-

solved in water. Both solutions were two step filtered by syringe filters: first by an Agilent p/n 5064-8222, 2- μ m filter followed by an Agilent p/n 5064-8221, 0.45- μ m filter. Five microliters of the resulting liquids were injected.



Structure of Metoprolol (both isomers)

Chromatographic conditions

Column

For method development: Agilent ZORBAX StableBond C18, 50 mm × 2.1 mm, 1.8 µm
For routine testing: Agilent ZORBAX StableBond C18, 150 mm × 4.6 mm, 5 µm

Mobile Phase A: Water + 0.2% TFA
Mobile Phase B: Acetonitrile + 0.16% TFA

| | | |
|--------------------|------------|-----|
| Gradient (linear): | Time (min) | % B |
| | 0 | 5 |
| | 45 | 50 |

Pump settings

| | |
|------------|------------|
| Stop time: | 45 min |
| Post time: | 5 min |
| Flow rate: | 2.0 mL/min |

Autosampler

| | |
|-------------------|-------|
| Injection volume: | 15 µL |
|-------------------|-------|

Thermostatted column compartment

| | |
|--------------|-------|
| Temperature: | 30 °C |
|--------------|-------|

Detector

| |
|---|
| 14 µL cell, Peak width: >0.05 min, 1 s response time (10 Hz), Signal: 210 nm |
|---|

System suitability and performance test

The following limits were used for system suitability testing the reference samples (see Reference Sample Preparation):

Precision of areas must be < 2 % RSD.

Precision of retention times must be < 0.5 % RSD.

Similar peak pattern according to separation with rapid resolution

The following samples were prepared and analyzed, using the limits and settings recorded in Table 1.

| Sample | Purpose | Number of injections |
|--------------------|--|----------------------|
| Blanc solution | Verify baseline stability and identify artifacts | 2 |
| Suitability sample | Verify precision of areas and retention times for reference solution | 10 |

Table 1
Setup for testing.

Results and discussion

Conditions for the method transfer were chosen from the Agilent 1200 Series RRLC method development system (see Preparation of samples).

The first step was to select the same column selectivity and column efficiency. The efficiency for the 50 mm × 2.1 mm, 1.8 μm rapid resolution high throughput (RRHT) column was estimated to nearly 12000 plates whereas for the 150 mm × 4.6 mm, 5 μm conventional column, 10700 plates were calcu-

lated. Agilent provides materials with the same selectivity independent of the particle size. As a final result of method development, the Agilent ZORBAX StableBond C18 material was found to separate all compounds.

According to these data, the RRLC parameters were transferred into the Agilent Method Translator to transform them to parameters suitable for conventional HPLC systems by selecting the simple conversion option (see Figure 1).

The Agilent Method Translator software calculates the new LC parameters, which should be used as starting conditions. Some parameters such as the different delay volumes of the pumps and different types of gradient mixing (high pressure versus low pressure) could not be converted satisfactorily. Sometimes these parameters must be adapted by experimentally optimizing the gradient steps.

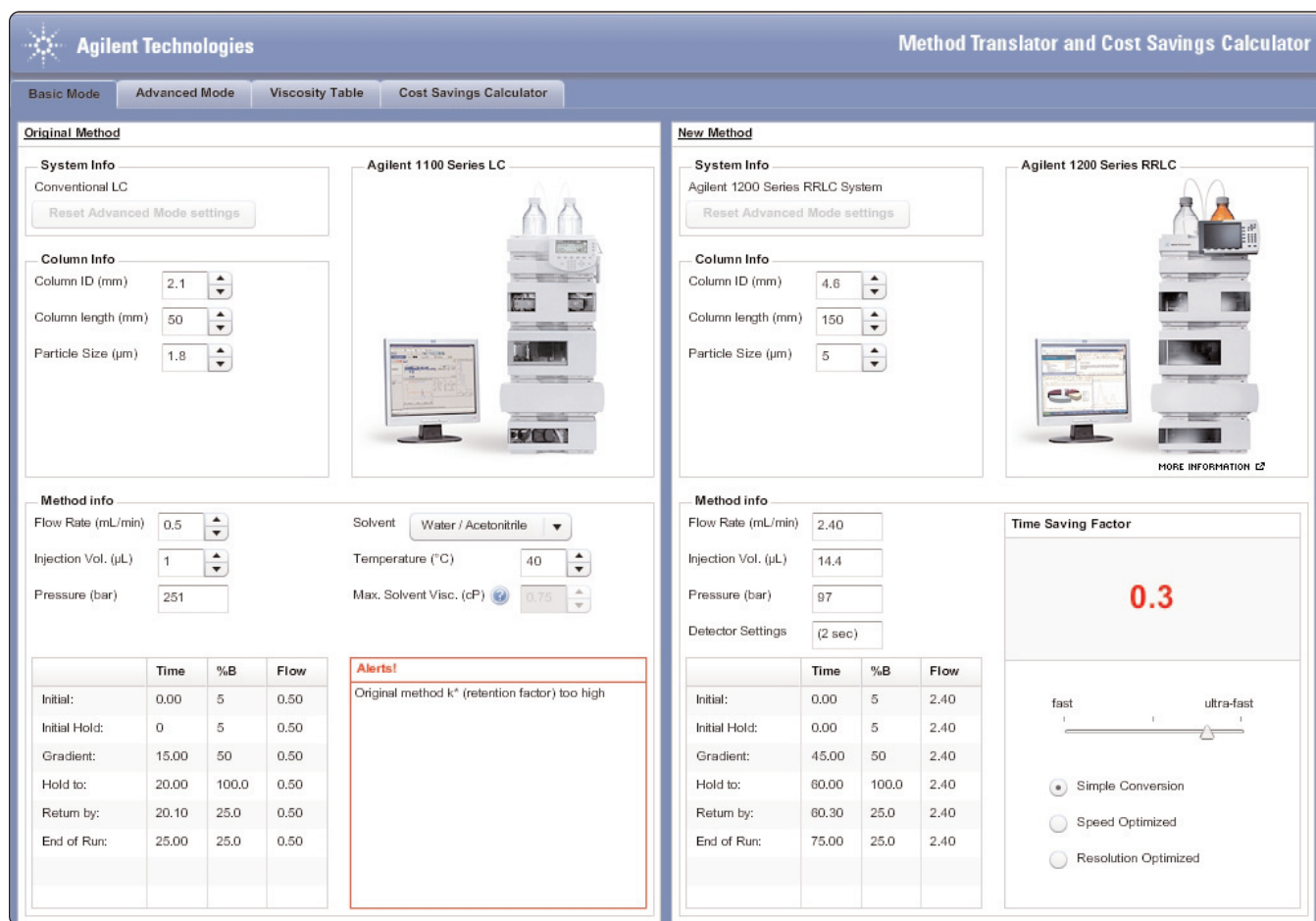


Figure 1
Conversion of LC parameters found by rapid resolution to parameters suitable for conventional HPLC with Method Translator software.

After transferring the parameters from the 50 mm × 2.1mm, 1.8 μm RRHT column to the 150 mm × 4.6 mm, 5 μm column, the analysis of pure metoprolol tablets with the Agilent 1120 Compact LC system and EZ-Chrom Elite Compact Software obtained chromatograms similar to those in Figure 2. As a result of the Method Translator, the flow was set to 2 mL/min, which prolonged the analysis time without any influence on the resolution.

The chromatogram in Figure 3 shows the appropriate separation of the degradation products from the Metoprolol peak. With the variable wavelength detector, several peaks at 210 nm are detected. The pattern looks very similar to the pattern obtained after separation with the Agilent 1200 Series RRLC system (see "Preparation of samples").

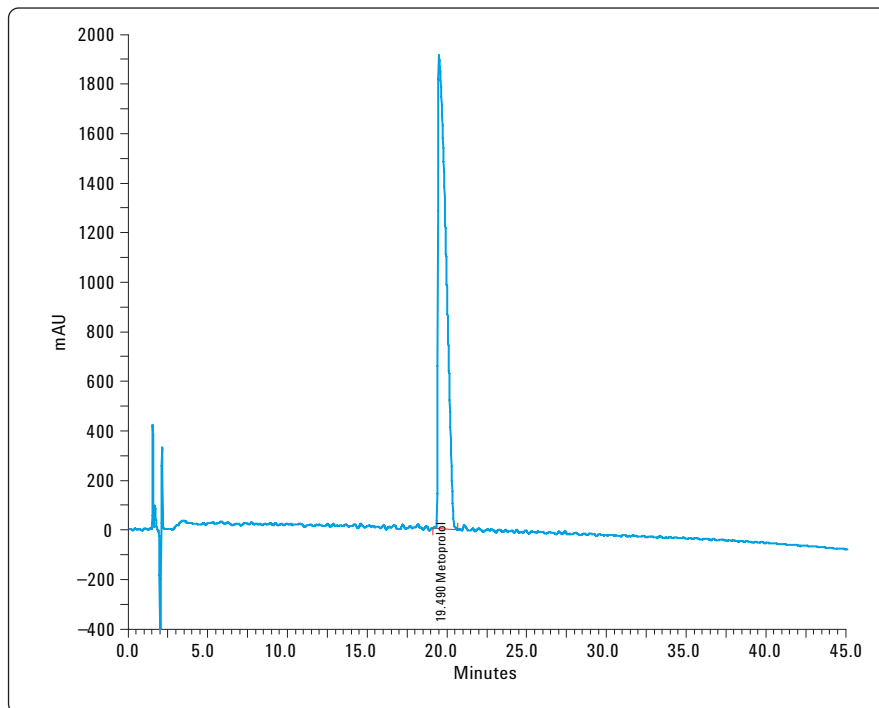


Figure 2
Analysis of metoprolol tablet after powdering, dissolving in water and filtering.

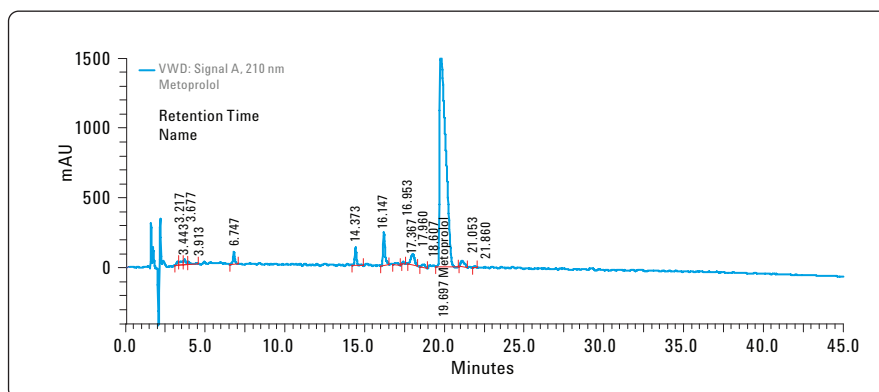


Figure 3
Analysis of a "stressed" metoprolol tablet after powdering, dissolving in water and filtering.

Compared to the results obtained with the Agilent 1200 Series RRLC system (see Table 2) the chromatogram in Figure 3 shows that the elution order has not changed. It shows that the selectivity does not change with the particle size. Detailed data for some selected peaks (see Figure 4) are listed in Table 3. As a main result it can be emphasized that it is possible to transfer LC parameters from rapid resolution by the Method Translator to conventional LC systems and columns with 5- μ m particles.

The adaptation of method development results with rapid resolution to the Agilent 1120 Compact LC was successful. The appropriate separation with the Agilent ZORBAX StableBond C18 material is proven by the data shown in Table 3. High resolution for every peak > 2 shows that this column material is highly suitable for the determination of the degradation peaks of Metoprolol.

To demonstrate the reliability and precision of the Agilent 1120 Compact LC the suitability sample was analyzed 10 times. The data presented in Table 4 show the areas and retention time precision results of all compounds.

To use the system for QC methods the criteria (see System suitability and performance test) must be fulfilled for all compounds due to strong limits. The data for precision of retention times and areas show that all data are within the limits.

The high precision of retention times for all components is also a result of performance and reliability of the pumping system. The high reproducibility of the autosampler is best shown by the data for area precision. These data allocate the Agilent 1120 Compact LC to be used for QC testing.

| Parameter | Agilent 1200 SL System | Agilent 1120 Compact LC System |
|-------------------|-------------------------|--------------------------------|
| Column-dimensions | 50 mm \times 2.1 mm | 150 mm \times 4.6 mm |
| Particle-size | 1.8 μ m | 5 μ m |
| Flow | 0.50 mL/min | 2.0 mL/min |
| Temperature | 30 $^{\circ}$ C | 30 $^{\circ}$ C |
| Gradient time | 0-15 min | 0-45 min |
| Composition | 5% to 50% | 5% to 50% |
| Delay volume | Low delay (120 μ L) | Normal delay (approx. 1 mL) |

Table 2
Detailed parameters for instrument setup.

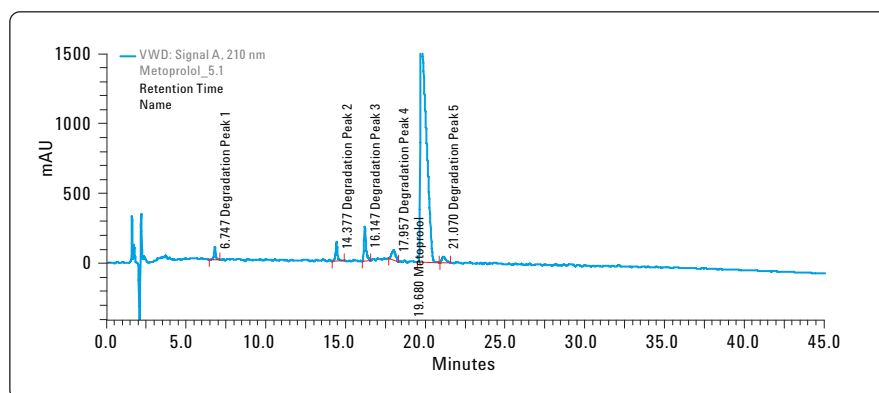


Figure 4
Selection of some representative peaks of a “stressed” metoprolol tablet for evaluating the stability of the separation.

| Compound | Retention-time (min) | Resolution |
|--------------------|----------------------|------------|
| Degradation peak 1 | 6.747 | – |
| Degradation peak 2 | 14.377 | 37.84 |
| Degradation peak 3 | 16.147 | 8.02 |
| Degradation peak 4 | 17.957 | 5.23 |
| Metoprolol | 19.680 | 2.78 |
| Degradation peak 5 | 21.070 | 2.25 |

Table 3
Results for retention times and resolution.

| Compound | Retention-time (min) | RSD RT n=10 | RSD Area n=10 |
|--------------------|----------------------|-------------|---------------|
| Degradation peak 1 | 6.747 | 0 | 0.633 |
| Degradation peak 2 | 14.377 | 0.023 | 0.747 |
| Degradation peak 3 | 16.147 | 0.016 | 0.702 |
| Degradation peak 4 | 17.957 | 0.048 | 0.601 |
| Metoprolol | 19.680 | 0.063 | 0.664 |
| Degradation peak 5 | 21.070 | 0.048 | 0.895 |

Table 4
Suitability sample: Precision of retention times and areas.

Conclusion

The Agilent 1120 Compact LC was designed for conventional chromatography. Users from medium to small size companies, who have high requirements of reliability, ease-of-use and lowest cost-of-ownership for standard LC methodology in a QA/QC environment should be supported with this compact nonmodular LC system.

This Application Note shows the easy transfer of parameters determined by method development with Rapid Resolution (see Table 2). This approach is reliable and provides precision of areas and retention times, and high chromatographic resolution. The results show a system optimized for everyday productivity, which meets the highest requirements for routine analysis.

With the results shown in Table 3 the resolution of all main peaks was found to be greater than 2. The results in Table 4 show that all criteria for the precision of determination, such as area and retention times are fulfilled. The results allow the use of the Agilent 1120 Compact LC in QA/QC laboratories to determine degradation products of Metoprolol tablets.

All results show the applicability of the Agilent 1120 Compact LC for quality control testing with reduced costs per system and improved simplicity of use. In addition to the instrument capabili-

ties, the new version of the EZChrom Elite compact software allows the full control of the Agilent 1120 Compact LC with a wide range of features for data analysis and reporting of results.

The high resolution results show that selectivity and performance of the Agilent ZORBAX StableBond material is independent of the particle size. The data also show that the design of the LC systems eliminates band broadening and peak distortion, and enhances the method transfer. In summary, an Agilent 1200 Series RRLC system provides fast method development and back transfer of results to conventional HPLC. The Agilent 1120 Compact LC is qualified for such an approach and meets the highest requirements for ordinary productivity.

References

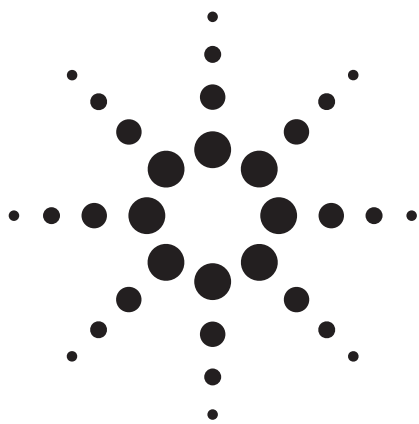
1. Agilent 1200 Series LC Method Development Solution for the analysis of degradation products of Metoprolol tablets, Agilent Technologies publication 5989-9339EN, **2009**

www.agilent.com/chem/1120

© Agilent Technologies, Inc., 2009
July 1, 2009
Publication Number 5990-4322EN



Agilent Technologies



Screening Impurities in Fine Chemicals Using the Agilent 1290 Infinity LC System

Application Note

Fine Chemical

Authors

Michael Woodman
Agilent Technologies, Inc.
2850 Centerville Road
Wilmington, DE 19808
USA

Abstract

The Agilent 1290 Infinity LC System with ultra violet/visible (UV/VIS) Diode Array detection (DAD) is used to analyze octyl-dimethyl-p-aminobenzoic acid for the presence of impurities. The system is used for the chromatographic separation of the compound from its impurities on 3.0 and 2.1 mm id C18 columns, of various lengths, with 1.8-um packing materials prepared in 600-bar (9000 psi) or special 1200-bar (18,000 psi) configurations. The ability of the 1290 Infinity LC System to operate with long, high resolution columns under conditions of rapid analysis is demonstrated with low viscosity acetonitrile (ACN) and higher viscosity methanol (MeOH) solvent conditions.



Agilent Technologies

Introduction

The analysis of impurities in starting materials, intermediates and finished products intended for a wide range of final uses is essential for ensuring product quality, performance, and consumer safety. The general conditions for successful analysis of impurities by high-performance liquid chromatography (HPLC) include gradient elution and multi-wavelength monitoring of the overall separation and may benefit from other detectors including evaporative light scattering (ELSD) and mass spectrometers (MS). Because impurity determination is the primary goal, one needs to ensure that mobile phase, vials, and HPLC components are free of minor impurities that might lead to confusing results during the analysis. Careful preparation of diluent blanks and blanks that might represent contamination sources due to additional sample preparation, such as filtration, are also appropriate. The analysis sequence is likely to include runs of the production material, solvent or diluent blank runs. It is also typical to include limit standards prepared by diluting the primary component to the lowest level where detection of impurities might be required. Finally, it is generally essential to include an authentic high purity reference standard.

Para-aminobenzoic acid (PABA) has historically been used as an ultra-violet filter ingredient in sunscreen formulations. As its use can increase the risk of skin cancer a derivative in the form of octyl-dimethyl-p-aminobenzoic acid (OD-PABA), is currently and more commonly used. However, PABA may be formed as a degradate of OD-PABA, so it is important to monitor its potential presence in samples of OD-PABA. As a commercial product, the purity of OD-PABA is important to manufacturers, for the purposes of safety and economics. In this work we investigate the capability of the Agilent 1290 Infinity LC system (UHPLC system with 1200 bar pressure limit) to detect impurities in OD-PABA samples with UV/VIS Diode Array detection.

The structure of the OD-PABA compound analyzed in this work is shown in Figure 1.

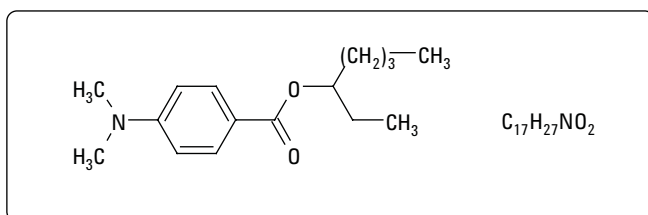


Figure 1. Octyl-dimethyl-p-aminobenzoic acid (OD-PABA).

Experimental

Sample Preparation

The primary OD-PABA solution was prepared at a concentration of 1 mg/mL in 2-propanol and subsequently diluted to lower concentrations as needed. Injection volumes of 0.2–2 μ L were made into the LC/DAD system.

LC Method Details

LC Conditions

Agilent 1290 Infinity LC system binary pump G4220A,
Agilent 1290 Infinity LC system autosampler G4226A
Agilent Thermostatted Column Compartment G1316C with switching valve
Agilent 1290 Infinity system diode array UV/VIS detector G4212A with 10 mm path fiber optic flow cell

Columns: (See individual figures for specific usage)
Agilent ZORBAX SB-C18 RRHT, 3 mm \times 50 mm, 1.8 μ m
600 bar p/n 827975-302
Agilent ZORBAX SB-C18 RRHD, 2.1 mm \times 100 mm, 1.8 μ m
1200 bar, p/n 858700-902
Agilent ZORBAX SB-C18 RRHD, 2.1 mm \times 150 mm, 1.8 μ m
1200 bar, p/n 859700-902

Column temp: 40 $^{\circ}$ C

Mobile phase: A = HPLC grade water
B = Acetonitrile (ACN) or methanol (MeOH)
(See individual figures)

Flow rate: See individual figures

Gradient: Gradient: the gradient conditions were either 40% to 90% ACN or 50% to 100% MeOH. The gradient slope was maintained at 3.5% organic phase increase per column volume, altering gradient time and flow rate accordingly. This is based on calculations using a modification of the Agilent Method Translator. [1]

UV Conditions

Monitoring 210, 254, 280 and 320 nm, bandwidth 4 nm, reference wavelength off

Results and Discussion

The UV response of OD-PABA, with four wavelengths monitored, is shown at a retention time of 2 min in Figure 2. Multi-wavelength monitoring of the separation provides a simple way to account for multiple impurities and assist in the selection of a final wavelength condition that can maximize sensitivity for all detected analytes.

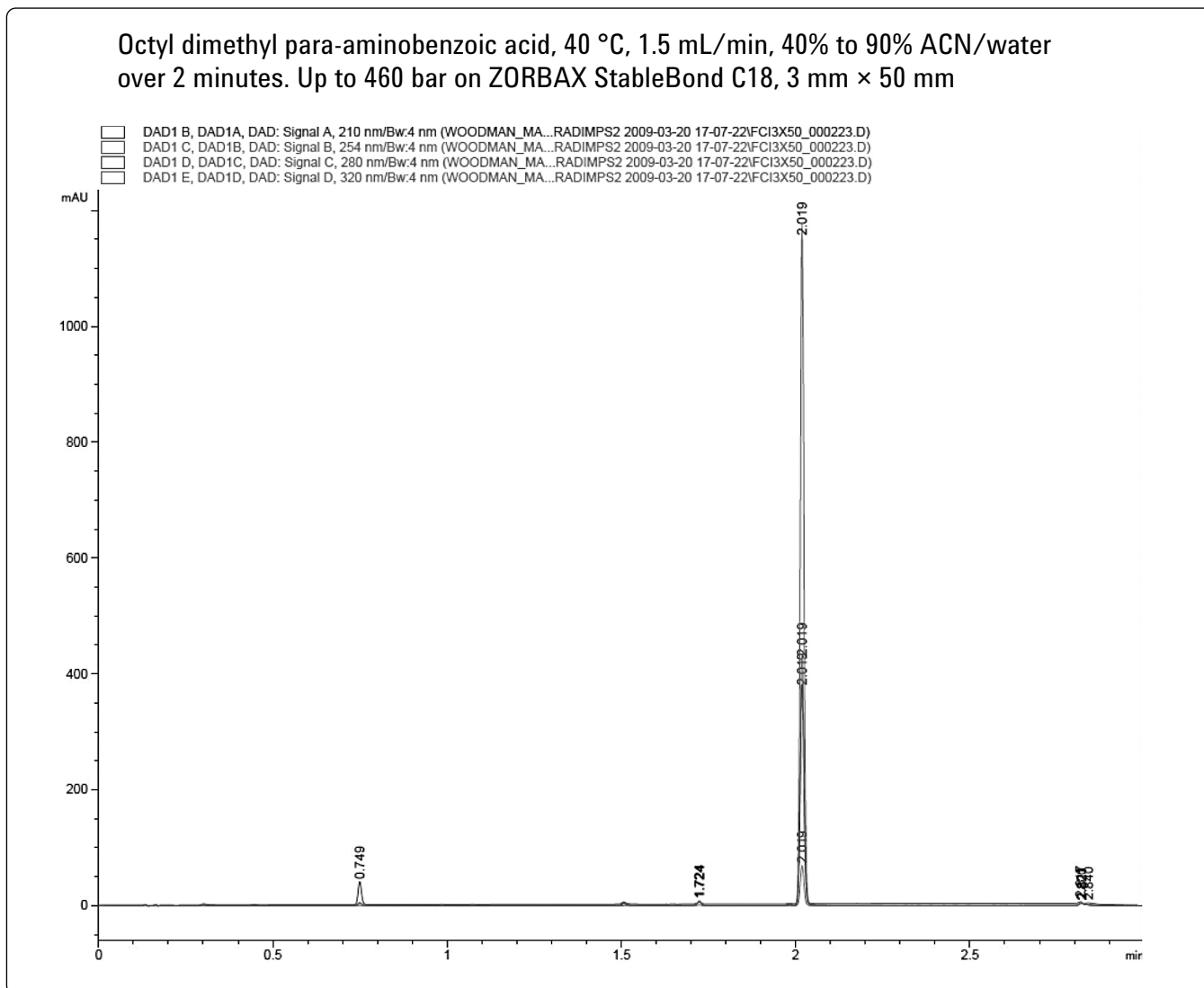


Figure 2. Multi-wavelength UV chromatogram of OD-PABA production material on a 3 mm × 50 mm ZORBAX Rapid Resolution High Throughput (RRHT) column. The chromatogram demonstrates the typical difficulties encountered with this type of separation, which are a need for wide dynamic range detection and sensitive impurity measurement. The peak at 0.75 minutes is confirmed by retention time matching and UV spectra to be PABA, the primary impurity in the mixture.

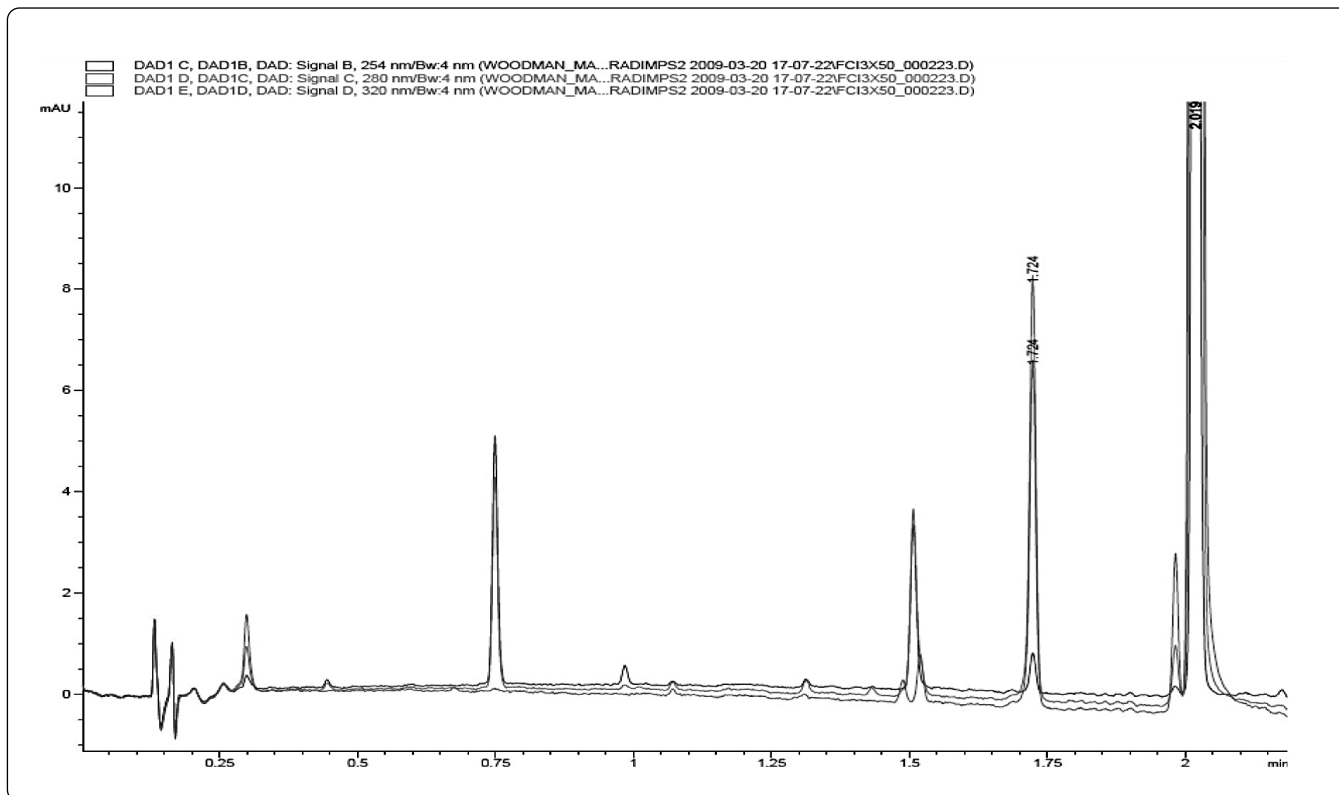


Figure 3. An expanded presentation of the chromatogram shown in Figure 2 based on the 3 mm × 50 mm gradient separation.

In Figure 3 the expanded multi-wavelength chromatogram allows us to see close detail and shows the number of impurities, as well as several areas where chromatographic resolution is clearly inadequate for individual component measurement. Despite the small particle size used in this column, the relatively short length limits the total resolution. As we move to longer column dimensions we will often reduce column diameter to reduce overall solvent consumption at the same time.

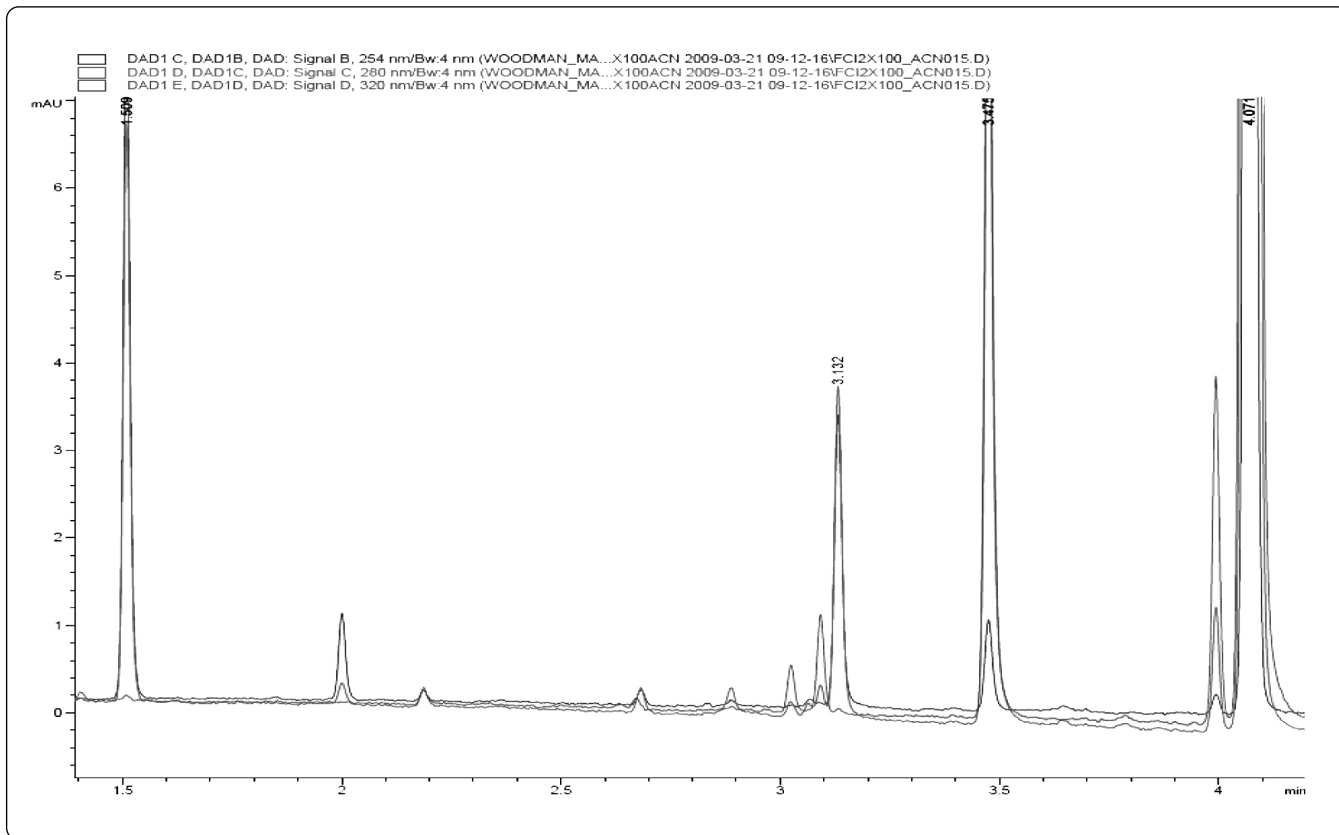


Figure 4. Analysis of the standard material on a 2.1 mm × 100 mm Agilent ZORBAX StableBond C18 column prepared for operation at 1200 bar pressure limit. Acetonitrile water gradient, 0.74 mL per minute, gradient time 4.0 minutes.

In Figure 4, we see that increasing the length of the column has resulted in a significant increase in the resolution of some of the observed components. To further increase resolution it would be practical to explore longer columns or explore alternative mobile phase or column chemistries.

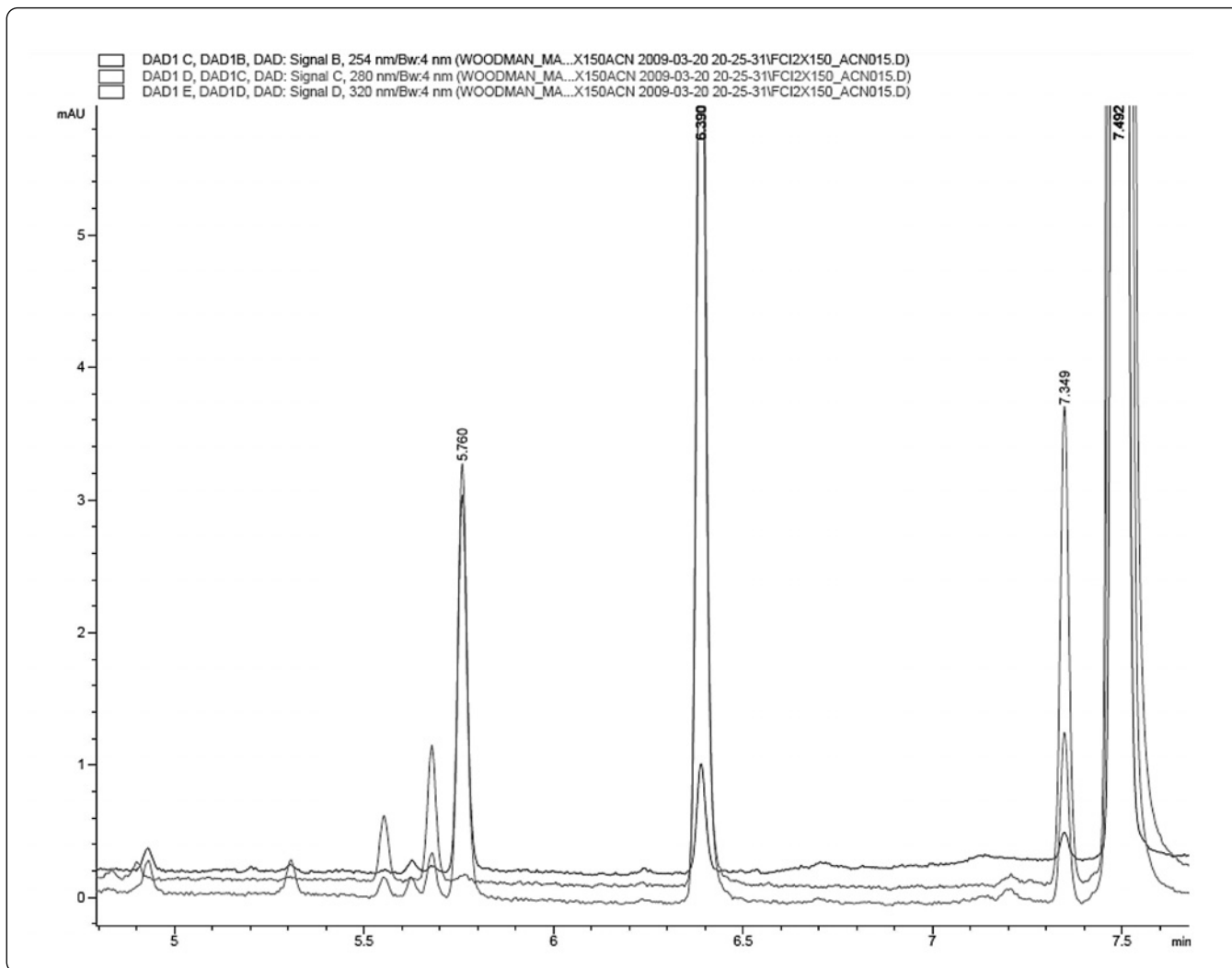


Figure 5. An expanded view of the acetonitrile separation using the same gradient slope on a 2.1 mm × 150 mm column rated for 1200 bar operating pressure. Agilent ZORBAX StableBond C18, 1.8 μm.

The increased column length clearly gives more resolution, however the increased back pressure also limits the flow rate if one is to operate in a conservative range of operating pressure. The Agilent 1290 Infinity LC system and associated ZORBAX Rapid Resolution High Definition (RRHD) chemistries are capable of operating pressures up to 1200 bar, approximately 18,000 psi. To ensure robust and rugged system operation many users typically specify the upper pressure limit for a method at a value less than 80% of the rated operating pressure.

Octyl dimethyl para-aminobenzoic acid, 0.52 mL/min, 50% to 100% MeOH/water over 5.7 minutes. Up to 845 bar on Agilent ZORBAX StableBond C18, 2.1 mm × 100 mm, 1.8 μm.

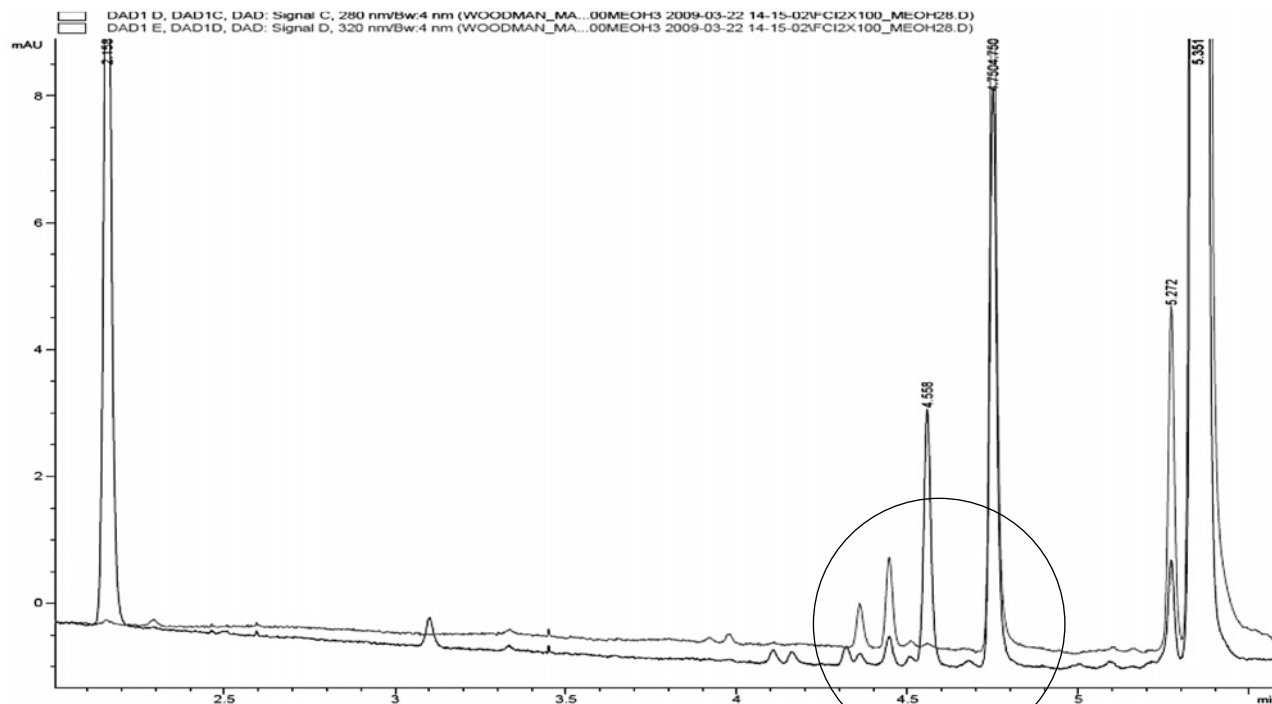


Figure 6. Separation of the sample mixture on a 2.1 mm × 100 mm Agilent ZORBAX StableBond C18, using methanol as the organic phase. Flow rate 0.52 mL/min gradient time 5.7 min, for a gradient of 5% to 100% methanol

When considering the fundamental components of the resolution equation we are all quite familiar with the concepts of capacity, selectivity, and efficiency. Increasing the column length, like decreasing the particle size of the packing material, will increase the efficiency of the overall separation. Because the increase in efficiency yields a relatively low return in terms of resolution, users often need to ensure that the capacity factor is optimized by exploring alternative chemical variables that could promote increased selectivity in the separation.

In Figure 6 we see the dramatic results achieved by changing the separation conditions from using acetonitrile as the

organic phase to methanol. If this separation was highly dependent on monitoring the separation at very low wavelengths one might find the UV cutoff of the methanol, 205 nm, to be problematic. In this example, however, the highly conjugated structures of the parents and related impurity structures allow sensitive detection at wavelengths well above the UV cutoff of common organic solvents used in reversed phase chromatography. In about the same amount of analysis time as the example in Figure 5, we achieve significantly higher selectivity leading to more resolved impurities while reducing overall solvent consumption and eliminating the need for expensive acetonitrile as the organic phase.

Octyl dimethyl para-aminobenzoic acid, 0.52 mL/min, 50% to 100% MeOH/water over 5.7 minutes.
Up to 845 bar on Agilent ZORBAX StableBond C18, 2.1 mm × 100 mm, 1.8 μm, 40 °C.

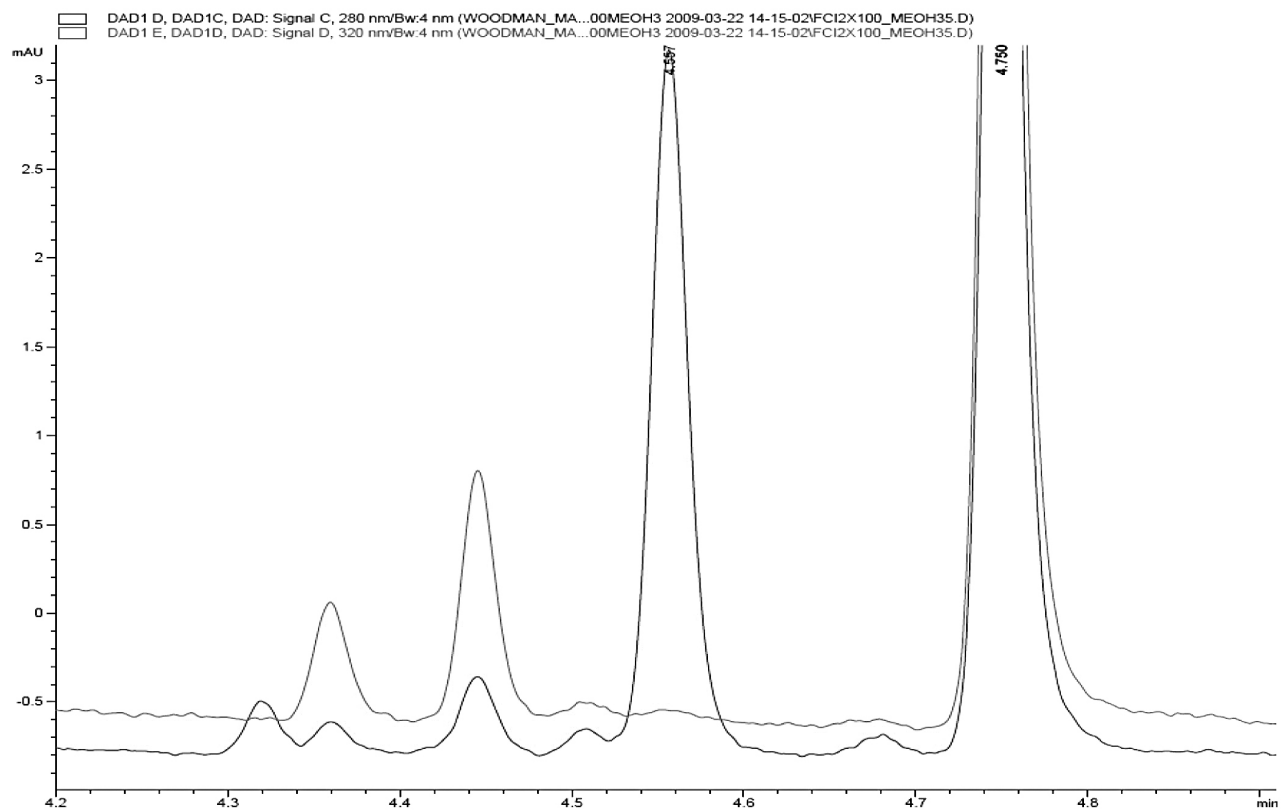


Figure 7. An expanded view of the small region of the chromatogram in Figure 6 showing a significant number of low concentration impurities. Conditions as in Figure 6. Estimated impurity concentrations for the smallest peaks in this figure are less than 0.02%.

Conclusions

The detection of low-level impurities in synthetic materials and highly refined natural products is of critical importance to the ultimate utility of these substances. Rapid analysis by HPLC using high-resolution columns and appropriately chosen organic phases ensures consistent results with rapid analysis turnaround time. Using the Agilent 1290 Infinity LC system, we were able to easily demonstrate UHPLC capabilities well within the operating range of the designed system. Higher throughput could still be achieved with this system by increasing flow rate and simultaneously reducing the gradient segment time to reproduce the gradient slope in a shorter total analysis time.

For More Information

For more information on our products and services, visit our Web site at www.agilent.com/chem.

References

1. <http://www.chem.agilent.com/en-US/products/instruments/lc/pages/gp60931.aspx>

www.agilent.com/chem

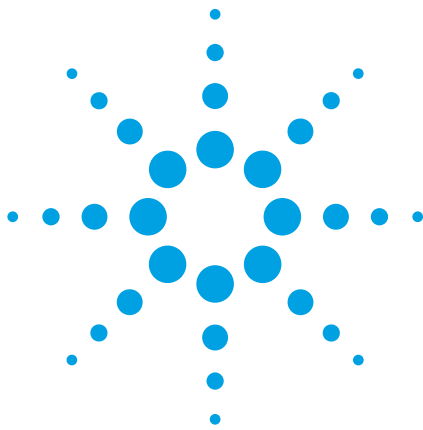
Agilent shall not be liable for errors contained herein or for incidental or consequential damages in connection with the furnishing, performance, or use of this material.

Information, descriptions, and specifications in this publication are subject to change without notice.

© Agilent Technologies, Inc., 2009
Printed in the USA
August 3, 2009
5990-4293EN



Agilent Technologies



Increasing productivity in the analysis of impurities in metoclopramide hydrochloride formulations using the Agilent 1290 Infinity LC system

Application Note

Pharmaceuticals

Authors

Gerd Vanhoenacker, Frank David,
Pat Sandra
Research Institute for Chromatography
Kennedypark 26
B-8500 Kortrijk
Belgium

Bernd Glatz and Edgar Naegele
Agilent Technologies
R&D and Marketing GmbH & Co. KG
Hewlett-Packard-Str. 8
76337 Waldbronn
Germany

Abstract

This Application Note evaluates the performance of the Agilent 1290 Infinity LC system for the determination of impurities and related substances of metoclopramide hydrochloride in a pharmaceutical formulation. The translation of a conventional liquid chromatography (LC) method on a 1200 Series HPLC system to an ultra high pressure method on an Agilent 1290 Infinity LC system is discussed. Method translation is relatively easy and temperature fine-tuning is the most important parameter to obtain the same selectivity for the different impurities. Pressures as high as 1070 bar were applied during method development.

The final high productivity method is carried out at 880 bar in an analysis time of 3.5 min which is approximately 4 times faster than the original HPLC method but with the same accuracy. A validation study was carried out to demonstrate the performance of the Agilent 1290 Infinity LC system. Limits of detection for the impurities were as low as 0.001 % w/w relative to the main compound using the new diode array detector (DAD). This is more than one order of magnitude lower than required.



Agilent Technologies

Introduction

In pharmaceutical analysis present key words are high throughput, high productivity and high resolution. In high productivity, the goal is to develop analytical methods that are approximately 4–5 times faster than those presently used with the prerequisite that accuracy, precision, and repeatability of developed and validated methods are kept intact.

In liquid chromatography (LC), ways to speed up analysis include the use of particles less than 2 μm and/or operation at elevated temperature. Columns packed with particles less than 2 μm can be operated at much higher velocities compared to conventional columns but dedicated LC instrumentation is required.

The Agilent 1290 Infinity LC system was applied for the determination of impurities in a metoclopramide hydrochloride formulation. The system was equipped with a high pressure pump capable of delivering up to 1200 bar and a new fast and sensitive diode array detector (DAD). Method develop-

ment consisted of the translation of conditions from a conventional instrument (Agilent 1200 Series LC system) equipped with a column packed with 3.5- μm particles to an UHPLC system (Agilent 1290 Infinity LC system) equipped with columns packed with 1.7- μm particles. The data from the two systems were compared and evaluated in terms of accuracy, precision, and repeatability.

Experimental

Instrumentation

A standard Agilent 1200 Series HPLC system and an Agilent 1290 Infinity LC system with the following configurations were used:

| 1200 Series HPLC | | Agilent 1290 Infinity LC system | |
|------------------|----------------------------------|---------------------------------|---|
| G1322A | Vacuum degasser | G4220A | 1290 Infinity Binary Pump with integrated vacuum degasser |
| G1311A | Quaternary pump | | |
| G1313A | Automated liquid sampler | G4226A | 1290 Infinity Autosampler |
| G1316A | Thermostatted column compartment | G1316C | 1290 Infinity Thermostatted Column Compartment |
| G1315B | Diode Array Detector | G4212A | 1290 Infinity Diode Array Detector |

Solutions

Stock solutions of the impurities and related substances were prepared in methanol. The structures of the compounds together with their EP-code are listed in Table 1. The peak numbering is used throughout the text. The stock solutions were mixed and diluted at the appropriate concentrations with water. The formulation was a solution in water for injection of metoclopramide hydrochloride (5 mg/mL) together with some other substances (confidential composition).

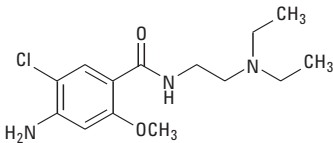
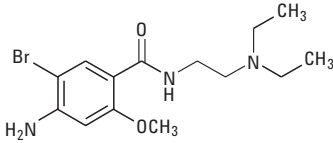
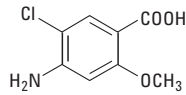
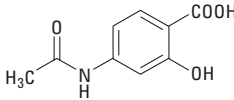
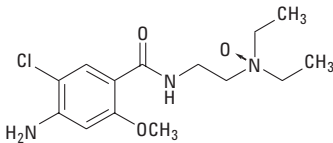
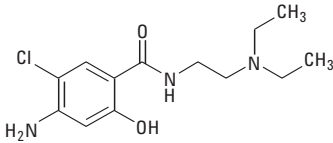
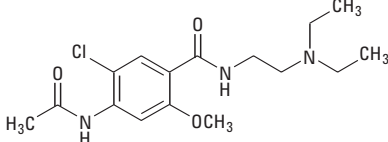
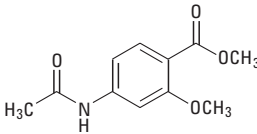
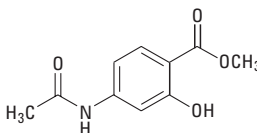
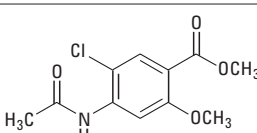
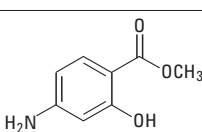
| Peak | Name (European Pharmacopoeia code, EP) | Structure |
|------|--|---|
| Main | Metoclopramide |  |
| X | Bromated metoclopramide |  |
| 1 | 4-Amino-5-chloro-2-methoxybenzoic acid (EP C) |  |
| 2 | 4-(Acetylamino)-2-hydroxybenzoic acid (EP H) |  |
| 3 | 4-Amino-5-chloro-N-2-(diethylaminoethyl)-2-methoxybenzamide N-oxide (EP G) |  |
| 4 | 4-Amino-5-chloro-N-2-(diethylaminoethyl)-2-hydroxybenzamide (EP F) |  |
| 5 | 4-(Acetylamino)-5-chloro-N-2-(diethylaminoethyl)-2-methoxybenzamide (EP A) |  |
| 6 | Methyl 4-(acetylamino)-2-methoxybenzoate (EP D) |  |
| 7 | Methyl 4-(acetylamino)-2-hydroxybenzoate |  |
| 8 | Methyl 4-(acetylamino)-5-chloro-2-methoxybenzoate (EP B) |  |
| 9 | Methyl 4-amino-2-methoxybenzoate |  |

Table 1
Compounds under investigation.

Results and Discussion

1. Method translation from a 1200 Series LC to a 1290 LC Infinity System

The original method was developed on a 1200 Series HPLC with a linear gradient using a quaternary pump. A chromatogram for a spiked formulation at 0.5% w/w level is shown in Figure 1A. The column used was an XBridge C-18 column packed with 3.5- μm particles. The initial pressure was 140 bar. The method was easily transferred to the 1290 Infinity LC as long as some instrumental differences were taken into account. When the method parameters were copied to the 1290 Infinity LC system retention times were significantly shorter. Selectivity changes were noted and attributed to the difference in delay volume for the two systems. A quaternary pump has a delay volume of 950 μL , while the 1290 Infinity Binary Pump has a reduced volume of 10 μL . An initial isocratic hold time was introduced into the 1290 Infinity LC method to compensate for this difference. After this straightforward correction, the retention times and selectivity were very similar for both systems, while the efficiency for the 1290 Infinity LC was higher than that of the 1200 Series (Chromatogram not shown).

The method was then translated to a 2.1 mm id BEH C18 column packed with 1.7- μm particles. The flow rate was reduced to 0.22 mL/min to maintain the same linear velocity in both columns while the injection volume was decreased from 2 μL to 0.8 μL . The pressure was 380 bar. An initial 0.5 min hold time on the gradient was introduced to compensate for differences in delay volume. Under these conditions the result was very similar (Figure 1B) but slightly faster compared to the result obtained by the column with 3.5- μm particles (Figure 1A).

Efficiency and resolution were improved significantly with the 1290 Infinity setup. The theoretical efficiency can roughly be calculated as the ratio between column length and two times the particle diameter. Therefore, the efficiency of the 1.7- μm particle column should be about double the efficiency of the 3.5- μm column. Consequently, resolution should increase by a factor of 1.4

on the same system since resolution is related to the square root of the efficiency. In this particular case, the resolution enhancement is much higher than theoretically predicted (for example, from 2.6 to 5.9 for peaks 1 and 2). This is due to the lower dead volume and the superior pump drives of the Agilent 1290 Infinity LC system.

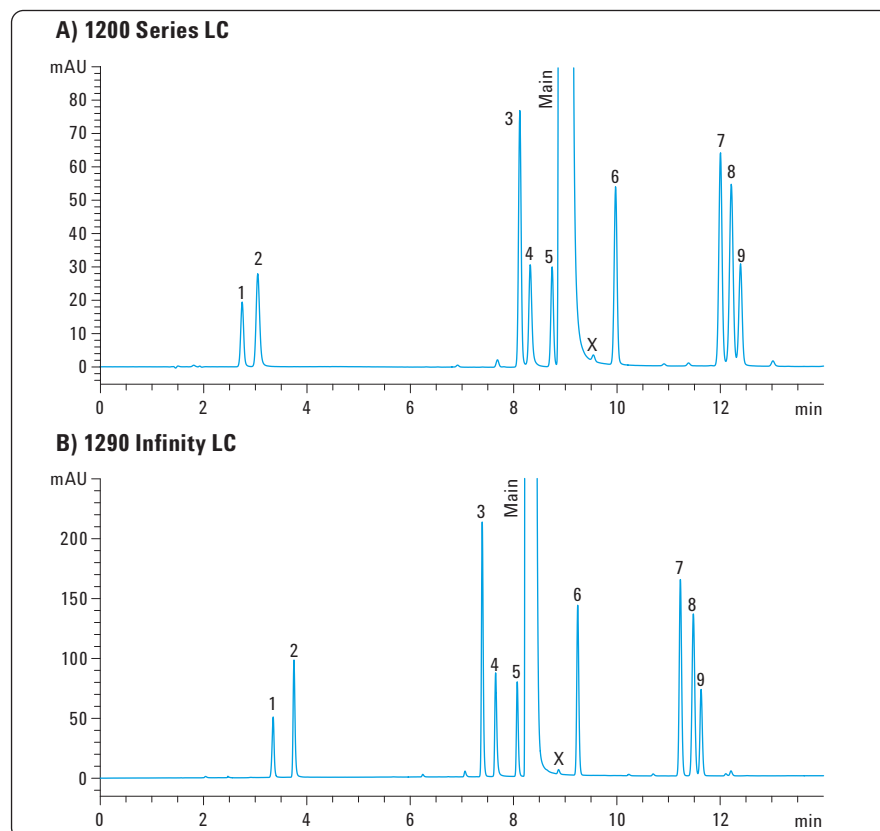


Figure 1. Method transfer from an Agilent 1200 Series LC system to an Agilent 1290 Infinity system. Sample: formulation spiked at 0.5% w/w level with impurities 1 to 9.

| Conditions | Figure 1 A | B |
|------------------|---|--|
| Column | XBridge C-18, 150 mm \times 3.0 mm, 3.5 μm | BEH C18, 150 mm \times 2.1 mm, 1.7 μm |
| Mobile phase | A = 0.25% w/w ammonium acetate in water B = acetonitrile | |
| Flow rate | 0.45 mL/min | 0.22 mL/min |
| Gradient | 0-15 min: 5–57.5% B | 0-0.5 min: 5% B isocratic 0.5–15.5 min: 5–57.5% B |
| Temperature | 37 $^{\circ}\text{C}$ | 37 $^{\circ}\text{C}$ |
| Injection volume | 2 μL | 0.8 μL |
| Detection | DAD, Signal 275/4 nm, Reference 400/60 nm | |
| Maximum pressure | 140 bar | 380 bar |

2. Increasing speed with the Agilent 1290 Infinity LC system

The analysis on the 1.7- μm particle column was performed at 380 bar which is far below the 1200 bar upper pressure limit of the 1290 Infinity LC system pump. Therefore, the flow rate could be increased to shorten the analysis time. When doing this, the gradient time should be reduced in proportion to the flow rate increase in order to maintain the same elution profile.

The operating pressure increased from 380 bar to 1020 bar when the flow rate was changed from 0.22 to 0.66 mL/min. As expected, at very high pressure, or high mobile phase velocity in the column, frictional heat is generated [1,2]. Since retention of some of the analytes is temperature dependent, the selectivity differences at high flow rates were noted. It can be seen that the resolution between compound 5 and the main compound, and of compounds 7 and 8 were especially affected by this temperature change. (Figure 2A).

The heat effect could be counteracted by reducing the temperature of the column from 37 to 32 °C (Figure 2B). Under these conditions good separation was achieved in 4.5–5 min which is about 3 times lower than the original LC method. However, the pressure increased to 1070 bar while the columns are only rated at 1000 bar. Using the column at higher pressures than the maximum rated pressure for a longer time will definitely reduce the column's lifetime and the robustness of the method.

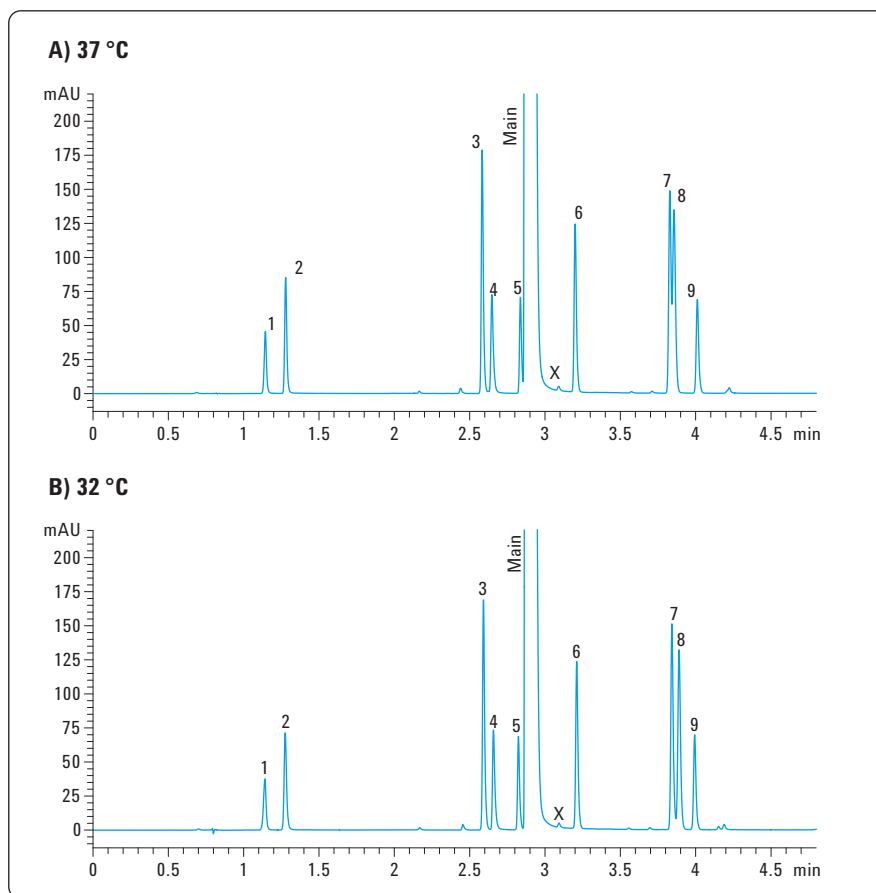


Figure 2. Influence of frictional heat generation on selectivity and effect of lowering column temperature. Sample: formulation spiked at 0.5% w/w level with impurities 1 to 9.

| Conditions Figure 2 | A | B |
|---------------------|--|------------------|
| Column | BEH C18, 150 mm \times 2.1 mm, 1.7 μm | |
| Mobile phase | A = 0.25% w/w ammonium acetate in water | B = acetonitrile |
| Flow rate | 0.66 mL/min | |
| Gradient | 0-16 min: 5% B isocratic 0.16-5.16 min: 5–57.5% B | |
| Temperature | 37 °C | 32 °C |
| Injection volume | 0.8 μL | |
| Detection | DAD, Signal 275/4 nm, Reference 400/60 nm | |
| Maximum pressure | 1020 bar | 1070 bar |

Therefore, for routine application, the column length was decreased from 150 mm to 100 mm to provide a maximum backpressure of 880 bar, at 0.66 ml/min. The gradient hold time and gradient time were reduced further to preserve the selectivity of the original method. The total analysis time was 3.5 min compared to 15.5 min with the original 3.5- μ m particle column (Figure 3). The resolution for the initial peaks is 3.8 which is higher than the value obtained with the 1200 Series LC.

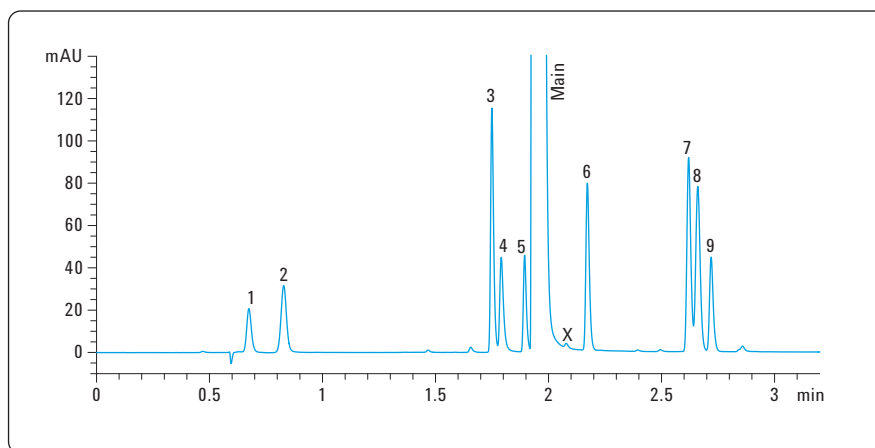


Figure 3.
Result with the final Agilent 1290 Infinity LC system method. Sample: formulation spiked at 0.5% w/w level with impurities 1 to 9.

| Conditions Figure 3 Final Agilent 1290 Infinity LC system method | |
|---|---|
| Column | BEH C18, 100 mm \times 2.1 mm, 1.7 μ m |
| Mobile phase | A = 0.25% w/w ammonium acetate in water B = acetonitrile |
| Flow rate | 0.66 mL/min |
| Gradient | 0–0.1 min: 5% B isocratic 0.1–3.45 min: 5–57.5% B |
| Temperature | 32 $^{\circ}$ C |
| Injection volume | 1 μ L |
| Detection | DAD, Signal 275/4 nm, Reference 400/60 nm |
| Maximum pressure | 880 bar |

3. Method validation

Using the conditions of Figure 3, an analysis was performed on the parameters of linearity, repeatability of injection, and detection limit (Table 2). It was determined that good linearity (>0.999 for all compounds) and injection precision were obtained. RSDs at the 0.005% level, which is close to the limit of detection (LOD) for some compounds was below 8% for all and below 3.5% for most compounds. This is more than acceptable at this level. The chromatograms for analysis at the LOD are shown in Figure 4. The LOD varies between 0.001 and 0.005% w/w relative to the main compound (50–250 pg on-column). This means that the impurities are detected at levels which are 10 to 50 times lower than the reporting threshold.

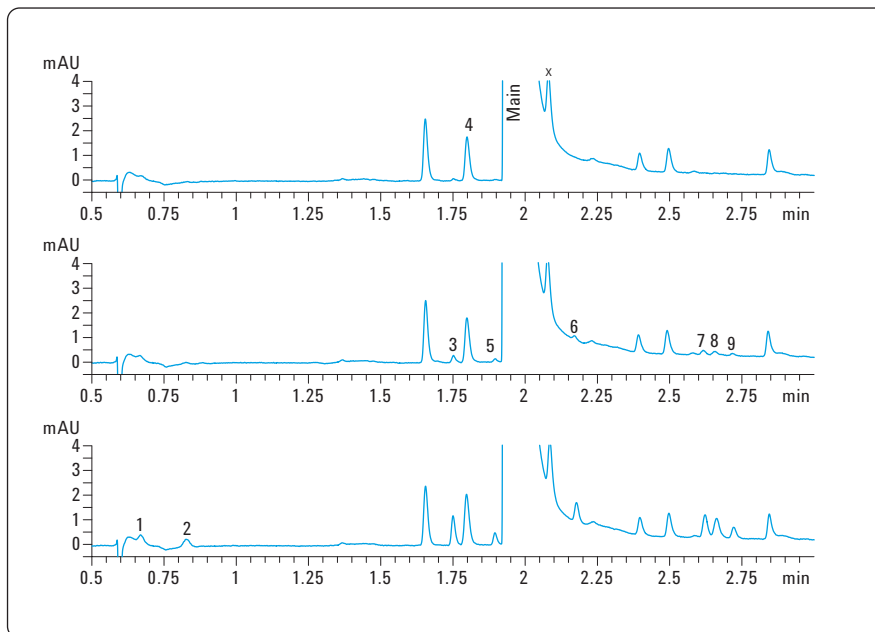


Figure 4. Analysis of formulation (top chromatogram) and spiked formulations with impurities 1 to 9 at LOD level (middle chromatogram: 0.001% w/w, bottom chromatogram: 0.005% w/w). Conditions: see Figure 3.

| Compound | Linearity, R^2 ⁽¹⁾ | Repeatability of injection, % RSD ⁽²⁾ | | LOD | | |
|----------|---------------------------------|--|-------------|-------------------|-------------------|--------------------|
| | | Area, 0.005% | Area, 0.05% | % w/w | On-column (pg) | S/N ⁽³⁾ |
| 1 | 1.0000 | 4.50 | 2.65 | 0.005 | 250 | 7.3 |
| 2 | 0.9999 | 7.54 | 1.72 | 0.005 | 250 | 8.6 |
| 3 | 1.0000 | 1.35 | 0.95 | 0.001 | 50 | 7.9 |
| 4 | 0.9994 | 1.77 | 1.74 | NA ⁽⁴⁾ | NA ⁽⁴⁾ | NA ⁽⁴⁾ |
| 5 | 1.0000 | 2.35 | 2.24 | 0.001 | 50 | 3.6 |
| 6 | 0.9997 | 3.32 | 0.93 | 0.001 | 50 | 4.3 |
| 7 | 1.0000 | 2.42 | 0.49 | 0.001 | 50 | 5.3 |
| 8 | 1.0000 | 1.92 | 0.81 | 0.001 | 50 | 4.5 |
| 9 | 1.0000 | 3.61 | 1.42 | 0.001 | 50 | 3.0 |

⁽¹⁾ 0.01, 0.02, 0.05, 0.1, 0.2, 0.5%, 1 injection/level

⁽²⁾ 6 consecutive injections/level

⁽³⁾ Signal-to-noise ratio, noise was taken from approximately 1–1.25 minutes

⁽⁴⁾ No data available, impurity already present in formulation

Conclusion

This application note demonstrates the feasibility of translating existing HPLC methods to fast Agilent 1290 Infinity LC system methods.

Initially, the HPLC analysis developed on a 1200 Series LC was simply transferred to a 1290 Infinity LC System instrument. The method transfer was relatively straightforward if some instrumental characteristics were taken into account. The original column (150 mm × 3.0 mm, 3.5- μ m particle size) was then changed to a narrow bore 2.1-mm column with smaller 1.7- μ m particles. This significantly increased the resolution between the compounds.

The use of particles less than 2 μ m allowed an increase of velocity in the mobile phase to reduce the analysis time without hampering resolution. Frictional heat generation at high pressure and mobile phase velocity changed

the selectivity of the method. The column temperature setting was lowered in order to maintain the original selectivity.

The final Agilent 1290 Infinity LC system analysis was carried out on a 100-mm column at 880 bar and was four times faster than the original HPLC method. This Agilent 1290 Infinity LC system method was successfully validated. Limit of detection varied between 0.001 and 0.005% w/w relative to the main compound corresponding to 50–250 pg on-column, which is 10 to 50 times lower than the required reporting level.

References

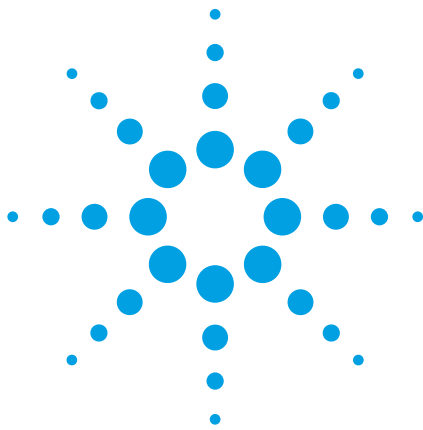
1. de Villiers A., Lauer H., Szucs R., Goodall S., Sandra P., *J. Chromatogr. A*, 1113 84–91. **2006**
2. Gritti F., Guiochon G., *J. Chromatogr. A*, 1187 165–179. **2008**

www.agilent.com/chem/1290

© Agilent Technologies, Inc., 2009
May 15, 2009
Publication Number 5990-3981EN



Agilent Technologies



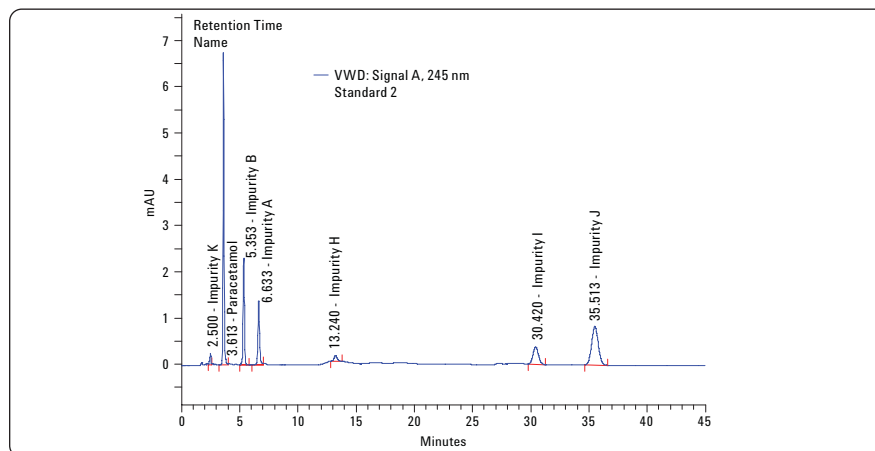
Development, validation, and comparison of an HPLC method to analyze paracetamol and related impurities according to the European Pharmacopoeia (EP) and USP using the Agilent 1120 Compact LC and the Agilent 1200 Series LC system

Application Note

Pharmaceuticals

Author

Detlef Wilhelm
ANATOX GmbH & Co. KG
Fuerstenwalde, Germany



Abstract

This Application Note compares the results of the development of an accurate and reproducible method to analyze paracetamol and related impurities according to European Pharmacopoeia (EP) and USP regulations¹, using an Agilent 1120 Compact LC and a 1200 Series LC system. The experiments described in this Application Note include the determination of the precision of areas and retention times, as well as chromatographic parameters such as resolution and signal-to-noise ratios. The well-suited Agilent ZORBAX StableBond RP8 column shows good selectivity for this application.

The results of these experiments prove that the Agilent 1120 Compact LC is a reliable instrument for routine testing that is able to fulfill the requirements of the European and U.S. regulations and can produce results comparable to those of a standard Agilent 1200 Series LC system.



Agilent Technologies

Introduction

The analytical instrumentation for routine analysis of samples with standardized LC methods, especially for quality control testing, have several requirements. Foremost are high reliability, ease of use, and an optimal cost of ownership.

This Application Note shows how the Agilent 1120 Compact LC, in comparison with a standard Agilent 1200 Series LC system, works as a highly robust and reliable instrument for standard LC methodology and can be used effectively in a routine environment to efficiently measure pharmaceutical compounds, such as paracetamol and related impurities.

According to the EP regulations, paracetamol impurities A, B, F, H, I, J, and K were analyzed on both LC systems, and system suitability and performance tests were executed.

Experimental

Instrumentation

An Agilent 1120 Compact LC system and a standard Agilent 1200 Series LC system with the following configurations were used:

| Configuration of the 1120 Compact LC | Configuration of the 1200 Series system |
|--------------------------------------|---|
| Gradient pump and vacuum degasser | Quaternary pump and vacuum degasser |
| Auto sampler | Standard autosampler |
| Column oven | Column compartment |
| Variable wavelength detector | Diode array detector |
| Software: EZChrom Elite Compact 3.3 | Software: ChemStation B.04.01 |

Preparation of samples

The reference solution was prepared as follows, in accordance with EP regulations. 5 mg of paracetamol and 5 mg of each impurity were dissolved in methanol and diluted to 20 mL with the same solvent. 1 mL of the solution was diluted to 250 mL with mobile phase. The substances to be checked were paracetamol and impurities K, A, B, H, I, J, and F.

Chromatographic conditions

| | |
|--------------------------|--|
| Column | Agilent ZORBAX StableBond-C8, 4.6 x 250 mm, 5 µm |
| Mobile phase | Mix together 375 mL of a 17.9 g/L solution of disodium hydrogen phosphate, 375 mL of a 7.8 g/L solution of sodium dihydrogen phosphate, and 250 mL of methanol containing 6 mL of a 400 g/L solution of tetrabutylammonium hydroxide in methanol |
| Pump settings | No gradient (in accordance with EP regulations) |
| Stop time | 45 min |
| Flow rate | 1.5 mL/min, isocratic |
| Injection volume | 20 µL |
| Column compartment temp. | 35 °C |
| Detector | |
| 1120 LC system | 14 µL |
| 1200 Series system | 13 µL |
| Peak width | 0.1 min (5 Hz) |
| Signal | 245 nm |

System suitability and performance test

The EP regulations for paracetamol require system suitability testing with a reference solution, as described in Preparation of samples, above. The testing included the following limits:

| | |
|-----------------------------------|--|
| Resolution | 4.0 minimum between peaks to impurity K and to paracetamol |
| Signal-to-noise ratio | 50 minimum for the peak due to impurity J |
| Relative retentions (paracetamol) | Impurity K = 0.8 Impurity F = 3 Impurity J = 7 |

No special regulations for paracetamol come from the USP. However, according to USPC Official 8/1/08, General Chapter <621> (Chromatography, System Suitability, p. 28) if there are no special requirements in the monographs, the data of five replicate injections should have a relative standard deviation of less than 2% for each calculated parameter.

From these above-mentioned requirements and to check and compare the chromatographic performance of both LC systems, the following parameters were tested and the limit settings below were fulfilled:

- Precision of areas must be < 2% RSD
- Precision of retention times must be < 0.5% RSD
- Resolution must be > 4 for impurity K and Paracetamol
- Signal-to-noise ratio must be > 50 for impurity J

With these limits and settings for testing, the samples in Table 1 were prepared and analyzed.

| Sample | Purpose | Number of injections |
|--------------------|--|----------------------|
| Blank solution | Verify baseline stability and identify artifacts | 2 |
| Control sample | Verify sensitivity and resolution for reference solution | 6 |
| Suitability sample | Verify precision of areas and retention times for reference solution | 10 |

Table 1
Setup for testing.

Results and discussion

Figure 1 shows a chromatogram achieved with the 1200 Series system and ChemStation, whereas Figure 2 shows the chromatogram yielded with the 1120 Compact LC and EZChrom Elite Compact. The data for both chromatograms, shown in Tables 2 and 3, are very similar.

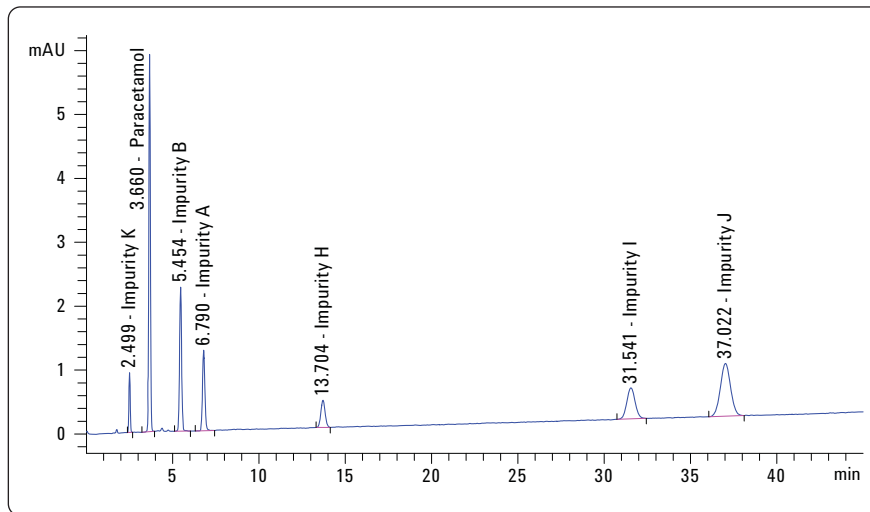


Figure 1
Example chromatogram of paracetamol and impurities with the Agilent 1200 Series system.

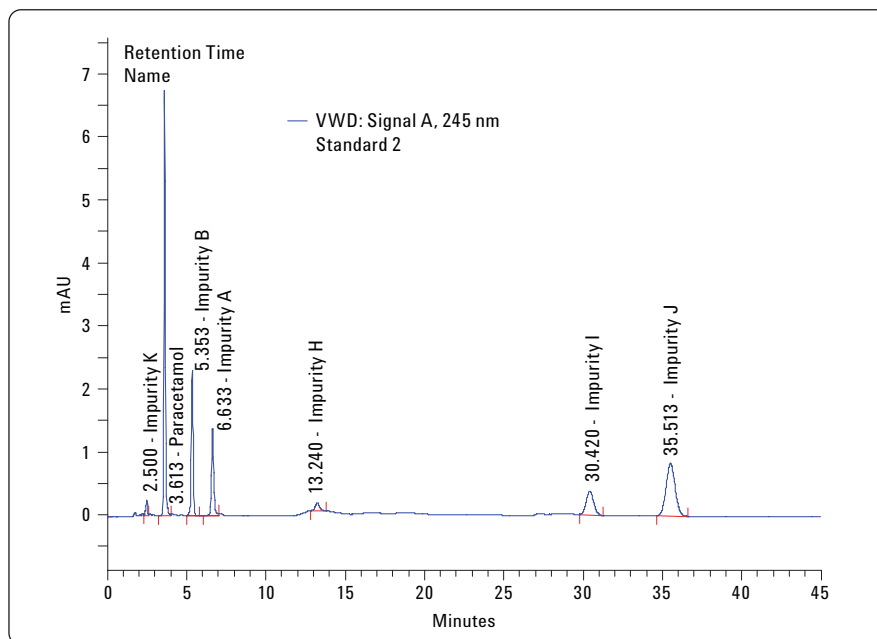


Figure 2
Example chromatogram of paracetamol and impurities with the Agilent 1120 Compact LC.

As shown in Figures 1, 2, and 3, the resolution and relative retention meet the EP requirement for both paracetamol and impurity F.

The results of the control sample, shown in Table 2, fulfill all criteria. The sensitivity was given for all peaks and resolution was achieved for all relevant compounds of the mixture. Not only for impurity K and paracetamol, but for all other relevant peaks the resolution was greater than 4, showing very good selectivity for the ZORBAX StableBond RP8 material and the good performance of the system. The data for peak symmetry (not shown) for all peaks ranged from 0.88–1.02.

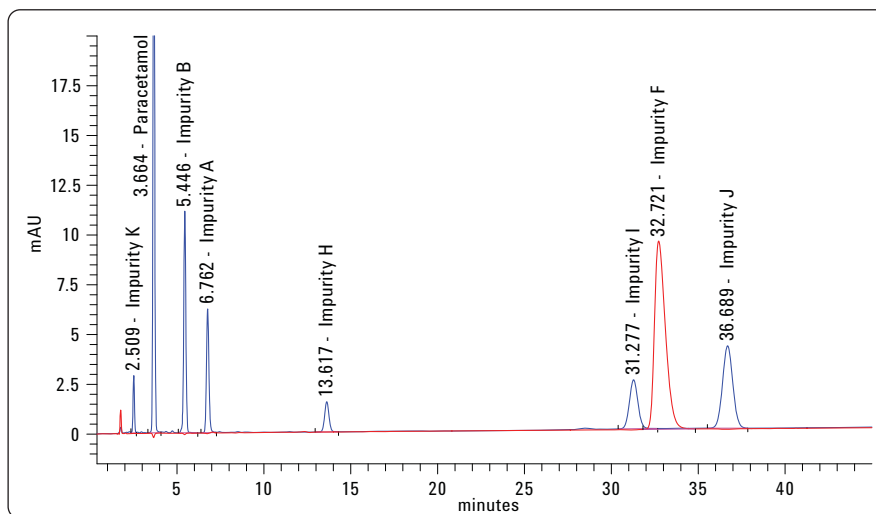


Figure 3
Chromatogram with all relevant impurities.

| Compound | Retention time (minutes) | | Resolution | |
|-------------|-------------------------------|-------------------------|-------------------------------|-------------------------|
| | Agilent 1200 Series LC system | Agilent 1120 Compact LC | Agilent 1200 Series LC system | Agilent 1120 Compact LC |
| Impurity K | 2.498 | 2.507 | – | – |
| Paracetamol | 3.659 | 3.620 | 7.19 | 7.03 |
| Impurity B | 5.454 | 5.353 | 9.22 | 9.04 |
| Impurity A | 6.792 | 6.633 | 5.75 | 5.51 |
| Impurity H | 13.716 | 13.240 | 19.52 | 18.35 |
| Impurity I | 31.562 | 30.387 | 26.25 | 24.89 |
| Impurity J | 37.066 | 35.480 | 5.47 | 5.03 |

Table 2
Results for control sample: retention times and resolution.

The criterion for the signal-to-noise ratio for impurity J was fulfilled for both systems. With the Agilent 1200 Series system the average value was found to be 61.4 and with the Agilent 1120 Compact LC system, it was 63.9 for the reference solution.

Table 3 shows the areas and retention time precision results of the main compound and the impurities of the suitability sample. The reliability and precision of the Agilent 1200 Series and the Agilent 1120 Compact LC system were proven. For all components the criteria for precision of retention times and areas were fulfilled, so that both systems can be used for QC methods.

Comparing the results for the suitability sample, it was found that the precision of retention times was nearly the same. Only few deviations were observed. The same was seen with the precision of areas. Both systems provide for the same injector and detector performance, independent of the hardware.

| Compound | Agilent 1200 Series LC system | | | Agilent 1120 Compact LC | | |
|-------------|-------------------------------|---------------|-----------------|-------------------------|---------------|-----------------|
| | Retention time (min) | RSD RT n = 25 | RSD Area n = 10 | Retention time (min) | RSD RT n = 25 | RSD Area n = 10 |
| Impurity K | 2.498 | 0.127 | 0.656 | 2.507 | 0.177 | 0.690 |
| Paracetamol | 3.659 | 0.048 | 0.545 | 3.620 | 0.111 | 0.342 |
| Impurity B | 5.454 | 0.061 | 0.263 | 5.353 | 0.135 | 0.352 |
| Impurity A | 6.792 | 0.154 | 0.215 | 6.633 | 0.206 | 0.348 |
| Impurity H | 13.716 | 0.22 | 0.831 | 13.240 | 0.311 | 0.636 |
| Impurity I | 31.562 | 0.278 | 0.599 | 30.387 | 0.371 | 0.681 |
| Impurity J | 37.066 | 0.324 | 0.404 | 35.480 | 0.386 | 0.258 |

Table 3
Suitability sample: precision of retention times and areas.

Conclusion

The Agilent 1120 Compact LC is designed for users who need the highest reliability, ease of use, and lowest cost of ownership for standard LC methodology in a QA/QC environment in medium to small companies. The comparison with the standard 1200 Series LC system shows very similar results for these applications.

To prove precise results from a system optimized for everyday productivity and to fulfill regulatory compliance, the experiments in this Application Note included determination of precision of areas and retention times, as well as chromatographic parameters like resolution and signal-to-noise ratios.

As shown in Table 2, the resolution of all peaks was found to be greater than 4.0, with a signal-to-noise ratio of more than 60 (> 50 required) with both systems for the relevant compound. The calculated signal-to-noise ratios prove the sensitivity of the system and show that the instrument can be operated according to the requirements in a quality control environment.

The results of Table 3 show that all criteria for the precision of the determination (areas and retention times) are fulfilled. All criteria related to EP and USP requirements are fulfilled, and the determination of paracetamol and its impurities can also be done with the reliable Agilent 1120 Compact LC system.

All results explicitly show the applicability of the 1120 Compact LC system for drug testing in QA/QC departments

due to reduced costs per system and improved simplicity of use. In addition to the instrument capabilities, the new version of the EZChrom Elite Compact software allows full control of the Agilent 1120 Compact LC, with a wide range of features for data analysis and reporting of the results.

The high performance of the new pump is strongly demonstrated by the good results for the precision of the retention times. Also the high S/N ratios (> 50 for the relevant components with the reference sample) are a result of the low pump pulsation. The high precision of the injector is shown with very similar results for area precision compared to the standard LC system.

The results for peak symmetry show the good selectivity and performance of Agilent column technology as well as the very good flow design of the LC systems, with no band broadening or peak distortion.

Reference

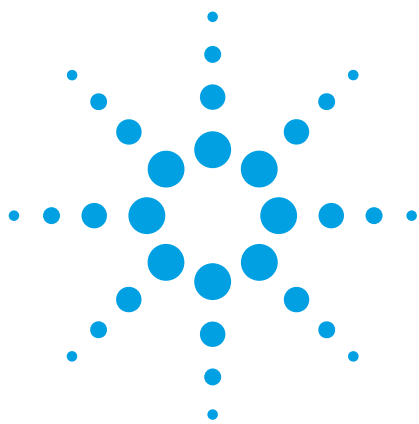
1. European Pharmacopoeia 5.0, 2184–5

www.agilent.com/chem/1200

© Agilent Technologies, Inc., 2009
March 15, 2009
Publication Number 5990-3739EN



Agilent Technologies



More Chromatographic Power for the Agilent 1200 Series LC

How the Agilent 1200 Series VWD SL Plus and ZORBAX RRHT 1.8 μm columns can boost speed and sensitivity, and cut solvent consumption

Technical Note



Introduction

The Agilent 1200 Series LC is a robust and reliable workhorse for conventional HPLC methodologies and is deployed worldwide in chemical, environmental, food and pharmaceutical laboratories for a vast range of applications in routine analysis through new product research and development. Significant performance gains in terms of detection limits, analysis speed and solvent consumption can be attained through simple addition of the new Agilent 1200 Series Variable Wavelength Detector (VWD) SL Plus and Agilent ZORBAX RRHT 1.8 μm columns with sub-2-micron particles. These include:

- 5 times shorter run and cycle times for increased productivity
- Simultaneous 3 times improved signal-to-noise ratio using the new Agilent 1200 Series VWD and fast analysis with sub-2-micron particle columns
- 50 percent less solvent consumption



Agilent Technologies

Overview

Significant hardware improvements in the Agilent 1200 Series VWD SL Plus facilitate lowest baseline noise and drift for highest sensitivity and lowest limits of detection.

- 160 Hz data acquisition rate gives up to 100 percent gains in resolution for ultra-fast LC, making the 1200 Series VWD SL Plus future proof for fastest separations
- Electronic Temperature Control (ETC) for maximum baseline stability and practical sensitivity under fluctuating ambient temperature and humidity conditions
- Latest electronics with built-in LAN ensure highest up-time and a secure investment
- Data Recovery Card (DRC) and radio frequency identification (RFID) technology for flow cells and lamps provide for a new level of data security and traceability
- A wide linear range facilitates reliable, simultaneous quantification of primary compounds, by-products and impurities
- Programmable wavelength switching enables sensitivity and selectivity to be optimized for the elution of each analyte
- Extensive diagnostics, error detection and display through the Agilent 1200 Series Instant Pilot or Agilent ChemStation make the VWD SL Plus easy to use and maintain
- Wavelength accuracy verification helps you to comply with GLP – an automatic holmium oxide filter can be programmed at the beginning of your chromatography to verify the accuracy of the set wavelength
- Early Maintenance Feedback (EMF) continuously tracks instrument usage such as lamp burn-time – user-settable limits and feedback messages inform you of problems before they happen.

In addition to the 1200 Series VWD SL Plus, deploying ZORBAX RRHT 1.8 μm columns with sub-2-micron particles gives further performance improvements. For example, 50 mm columns

packed with 1.8 μm particles give the same resolution as 150 mm columns packed with 5 μm particles but in considerably shorter analysis times. Table 1 shows that shorter columns with small particles achieve the chromatographic efficiency of longer columns with large particles.

Experimental

Equipment

Initial configuration:

- Agilent 1200 Series LC system, including quaternary pump and standard autosampler
- Agilent 1200 Series VWD ("B" model) with 13 μL flow cell
- Agilent ZORBAX SB-C18 column, 150 x 4.6 mm, 5 μm (PN 883975-902)

Configuration for detector upgrade:

- Agilent 1200 Series LC system,

including quaternary pump and standard autosampler

- Agilent 1200 Series VWD SL Plus
- Agilent ZORBAX SB-C18 column, 150 x 4.6 mm, 5 μm (PN 883975-902)

Third configuration for deployment of sub-2-micron column technology:

- Agilent 1200 Series LC system, including quaternary pump and standard autosampler
- Agilent 1200 Series VWD SL Plus
- Agilent ZORBAX SB-C18 column, 50 x 4.6 mm, 1.8 μm (PN 827975-902)

Chromatographic conditions

- Sample: Tramadol with 4 impurities in the range 0.7 to 1.25 %
- Mobile phase: Water with 0.1 % TFA and Acetonitrile with 0.650 % TFA

| Column Length [mm] | Column Efficiency [N] | | | Reduction in Analysis Time [%] |
|--------------------|---------------------------|-----------------------------|-----------------------------|--------------------------------|
| | 5 μm Particles | 3.5 μm Particles | 1.8 μm Particles | |
| 150 | 12.500 | 21.000 | 35.000 | |
| 100 | 8.500 | 14.000 | 23.250 | 33 % |
| 75 | 6.000 | 10.500 | 17.500 | 50 % |
| 50 | 4.200 | 7.000 | 12.000 | 67 % |
| 30 | n.a. | 4.200 | 6.500 | 80 % |
| 15 | n.a. | 2.100 | 2.500 | 90 % |

Table 1
Comparison of columns with different lengths and particle sizes, showing reduction in analysis times (all columns with of 4.6 mm inside diameter).

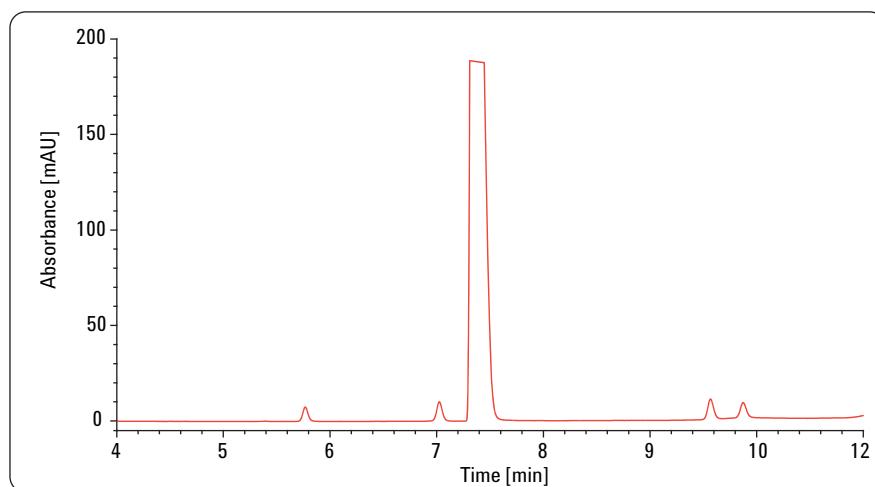


Figure 1
Chromatogram of analysis using VWD "B" model and column packed with 5 μm particles.

Chromatographic conditions

Flow rate: 1 mL/min
 Gradient: 0 min, 10 %B; 8 min, 45 %B; 10.5 min, 45 %B; 11min, 10 %B; 15 min, 10 %B
 Column temp.: 30 °C
 Injection vol.: 5 μL
 Detection: 270 nm, response time 0.25 s (equivalent to 14 Hz)

Results and discussion

Three steps were performed to evaluate the gain in performance through deployment of the new detector and columns with sub-2-micron technology.

In the first step the Agilent 1200 Series LC system was equipped with an earlier “B” model of the VWD and a 150 mm ZORBAX column packed with 5 μ m particles. Figure 1 shows the chromatogram from the analysis of the Tramadol impurity mixture.

In the second step the old VWD “B” model was replaced by the new VWD SL Plus. Figure 2 shows the chromatogram from the analysis of the Tramadol impurity mixture. The lower noise level of the VWD SL Plus as well as a two-fold increase in the signal-to-noise ratio can be seen clearly (table 2). Figure 3 shows the noise levels of both detectors. Even at a data acquisition rate of 40 Hz the noise level of the VWD SL Plus is a factor 1.8 lower.

In a final step the 150 mm column packed with 5 μ m particles was replaced by a 50 mm column packed with 1.8 μ m particles. Figure 4 shows the chromatogram from the analysis of the Tramadol impurity mixture. The signal-to-noise ratio increased by a factor of three. The run time was shortened from 15 min to 3 min, representing a fivefold increase in analysis speed. Comparing the chromatograms obtained in all three steps clearly shows that upgrading to the new VWD SL Plus and ZORBAX RRHT 1.8 μ m columns with sub-2-micron particles increases chromatographic performance in terms of signal-to-noise ratio, analysis speed and solvent consumption. This is summarized in table 2.

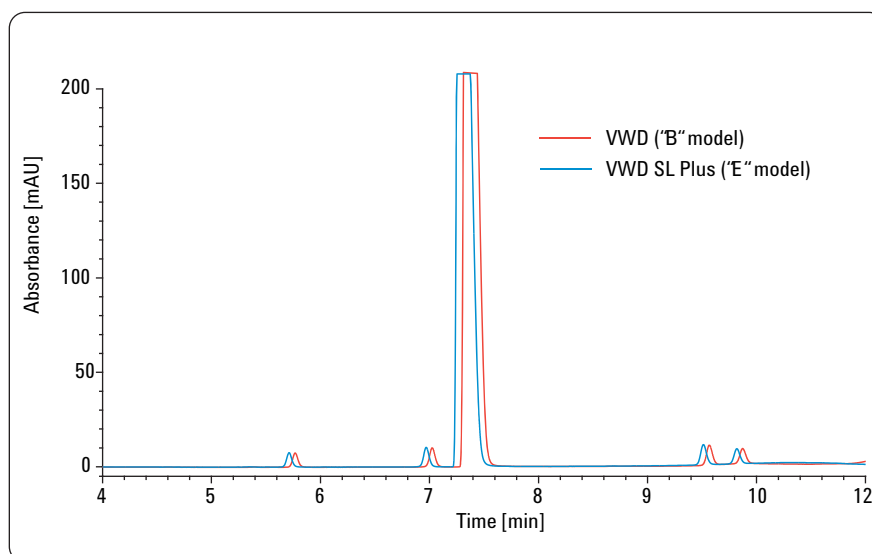


Figure 2
Comparison of chromatograms obtained with the VWD “B” model and the new VWD SL Plus and using a column packed with 5 μ m particles.

Chromatographic conditions

Flow rate: 1 mL/min
 Gradient: 0 min, 10 %B; 8 min, 45 %B; 10.5 min, 45 %B; 11min, 10 %B; 15 min, 10 %B
 Column temp.: 30 °C
 Injection vol.: 5 μ L
 Detection: 270 nm, response time 0.25 s (equivalent to 40 Hz)

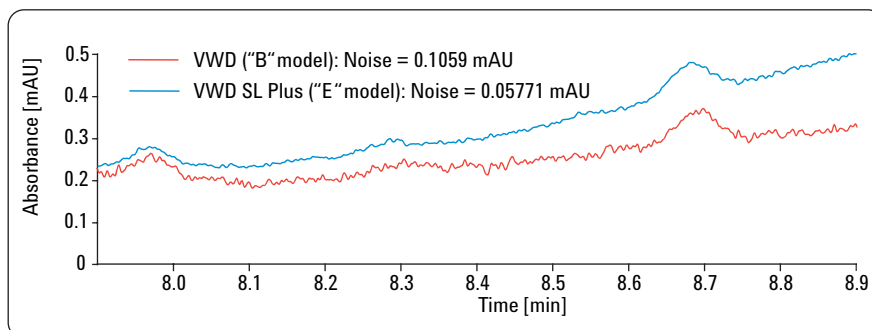


Figure 3
Comparison of the noise levels of the VWD “B” model and the new VWD SL Plus.

| Parameter | VWD SL Plus with 50 x 4.6 mm, 1.8 μ m ZORBAX column | VWD SL Plus with 150 x 4.6, 5 μ m column | VWD “B” model with 150 x 4.6, 5 μ m column |
|---|---|--|--|
| S/N impurity 1 | 275.8 | 149.8 | 63.0 |
| S/N impurity 1 | 314.2 | 203.4 | 84.9 |
| S/N impurity 1 | 337.7 | 210.9 | 89.5 |
| S/N impurity 1 | 254.0 | 157.3 | 71.2 |
| Noise level | 0.03063 mAU | 0.05771 mAU | 0.1059 mAU |
| Run time | 3 min including equilibration time | 15 min including equilibration time | 15 min including equilibration time |
| Solvent consumption/run, including run and equilibration time | ~8 mL | ~16 mL | ~16 mL |

Table 2
Comparison of chromatographic performance.

Conclusion

The chromatographic performance of a standard Agilent 1200 Series LC system can be significantly improved through addition of the new Agilent 1200 Series Variable Wavelength Detector SL Plus and deployment of Agilent ZORBAX RRHT 1.8 μm columns with sub-2-micron particles. The signal-to-noise ratio can be increased by a factor of three and analysis speed can be increased by a factor of five. A further benefit is reduced solvent consumption, which can be cut by 50 %.

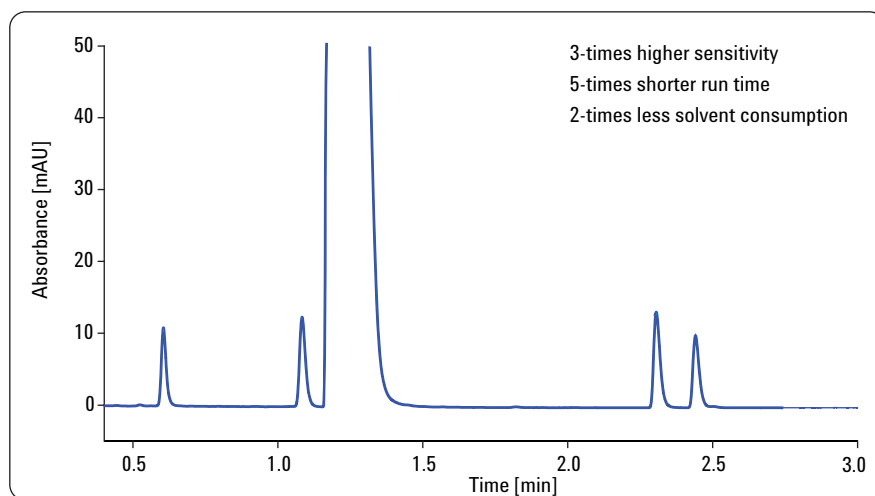


Figure 4

Final chromatogram from the analysis of the Tramadol impurity mixture using the Agilent 1200 Series VWD SL Plus and ZORBAX RRHT 1.8 μm columns with sub-2-micron particles.

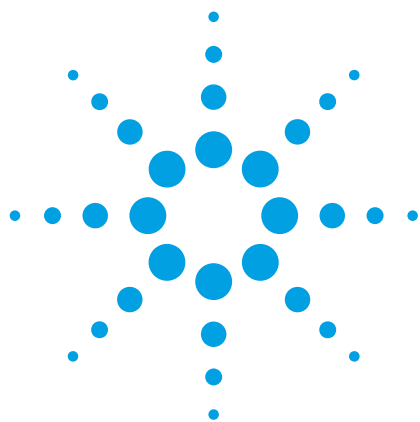
Chromatographic conditions

Flow rate: 2 mL/min
Gradient: 0 min, 20 %B; 2.7 min, 45 %B; 3 min, 45 %B; 3.1 min, 20 %B; 4.2 min, 20 %B
Column temp.: 30 °C
Injection vol.: 5 μL
Detection: 270 nm, response time 0.25 s (equivalent to 40 Hz)

www.agilent.com/chem/1200

© Agilent Technologies, Inc., 2009
Published February 1, 2009
Publication Number 5990-3471EN





Software-assisted, high-throughput identification of main metabolites of pharmaceutical drugs

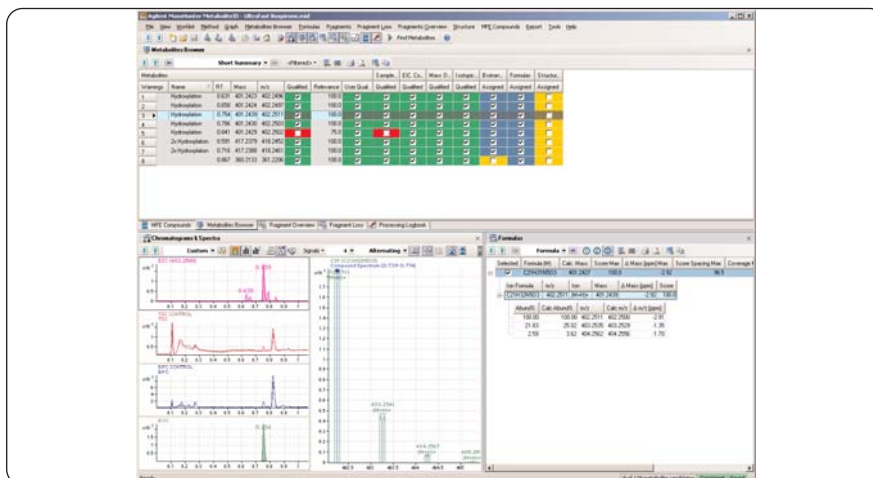
Rapid data acquisition by Agilent 1290 Infinity LC, TOF and Q-TOF instrumentation, and subsequent identification of metabolites by Agilent MassHunter Metabolite Identification software

Application Note

Metabolite identification in drug discovery and drug development

Author

Edgar Naegele
Agilent Technologies
Waldbronn, Germany



Abstract

This Application Note describes:

- Rapid separation of metabolites generated from in-vitro experiments using the Agilent 1290 Infinity LC, system
- Fast acquisition of TOF mass spectra using Agilent 6530 Accurate-Mass Quadrupole Time-of-Flight LC/MS systems
- Fast, software-assisted identification of main metabolites from in-vitro experiments using Agilent MassHunter Metabolite Identification software
- Generation of reports for the identified metabolites using Agilent MassHunter software



Agilent Technologies

Introduction

In modern pharmaceutical drug development it is of crucial importance to analyze the adsorption, distribution, metabolism and excretion (ADME) properties of possible new drug candidates as quickly as possible in order to make decisions about further investments in the development of a special compound. To find compounds with the correct properties it is essential to screen a large number of compounds for their ADME properties, which requires to work in a high-throughput environment. This Application Note describes the application of the Agilent 1290 Infinity LC system, the Agilent 6530 Q-TOF MS system and the MassHunter Metabolite Identification software for fast, high-throughput identification of main metabolites of new pharmaceutical drug candidate compounds.

Experimental

Equipment

- Agilent 1290 Infinity LC system consisting of 1290 Infinity Binary Pump with integrated degasser, 1290 High Performance Autosampler with thermostat, and 1290 Infinity Thermostatted Column compartment
- Agilent 6530 Accurate-Mass Q-TOF LC/MS system
- Agilent MassHunter Metabolite Identification (MetID) software
- Column: ZORBAX SB-C18, 2.1 x 50 mm, 1.8 μ m

Sample preparation

The following stock solutions were used:

- 20 mg/mL microsomal S9 preparation
- 0.1 mg/mL buspirone in water
- 1.6 mg NADP in 1.6 mL 0.1 M phosphate buffer, pH 7.4

- 50 mM isocitrate/MgCl₂ (203 mg MgCl₂·6H₂O + 258.1 mg isocitrate in 20 mL H₂O)
- Isocitrate dehydrogenase 0.33 unit/ μ L

NADPH regeneration system: 1.6 mL NADP solution + 1.6 mL Isocitrate solution + 100 μ L IDH solution.

Incubation mixture: 3.85 μ L substrate + 200 μ L NADPH regeneration system + 746.15 μ L phosphate buffer + 50 μ L S9.

Incubation was carried out at 37 °C for 60 minutes. A 100 μ L aliquot was taken at the beginning (t=0) and at t=60 min. The reaction was stopped by adding 6 μ L perchloric acid and 100 μ L acetonitrile followed by centrifugation for 15 min at 14,000 rpm. The supernatant was evaporated to dryness using a SpeedVac concentrator and reconstituted with water containing 0.1 % formic acid for LC/MS analysis. The incubation sample stopped at 0 min was used as control.

LC method

Solvent A: Water + 0.1 % formic acid
Solvent B: ACN + 0.1 % formic acid
Flow: 0.8 mL/min
Gradient 0 min, 5 %B; 0.10 min, 5 %B; 1.10 min, 75 %B;
Stop time: 1.1.0 min
Post time: 1 min.
Injection: Volume 5 μ L, sample cooler at 4 °C, needle wash in 50 % methanol for 5 s, injection loop to bypass at 0.1 min with flush out factor 16
Column: Temperature 60 °C

TOF MS method

Source: ESI positive
Capillary: 3500 V
Dry gas: 12 L/min
Nebulizer: 55 psi
Gas temp.: 350 °C

Skimmer: 65 V
Fragmentor: 200 V
Mass range: 100-1000 m/z
Acquisition rate: 5 spectra/s
Reference masses: 121.0508 and 922.0080

Data analysis method in the MetID software

The first step in the analysis comprised a comparison between the data file that contained the metabolite compounds (metabolite sample) and the data file that contained only the parent drug (control sample). All detectable mass signals were extracted from the MS level data using the Molecular Feature Extraction (MFE) algorithm. Related compound isotope masses and adduct masses were grouped together into discrete molecular features, and chemical noise was removed. The compounds lists of the metabolized sample and the control were then compared.

All new compounds or those that increased twofold in the metabolized sample were considered potential metabolites and were subjected to further analysis by different algorithms. The algorithms can identify and qualify new metabolites, or just qualify metabolites found by another algorithm. In this high-throughput experiment all algorithms' results were weighted equally and combined into a final identification relevance score. Metabolites were qualified when their final score was above the stringently defined relevance threshold. The results from all algorithms were collated in a results table, which could be inspected at-a-glance and reported¹.

Results and discussion

To achieve fast separation of the metabolites on a 50 mm, 1.8 µm particle size column, a 1 minute gradient was applied by the Agilent 1290 Infinity LC system. The metabolites were generated from the pharmaceutical test compound buspirone in an in-vitro assay. For adequate detection with the time-of-flight mass spectrometer the instrument was operated at a data rate of 5 Hz.

After generation the data was loaded into the MetID software and analyzed using a common method. The result was displayed by the MetID software in an at-a-glance table, in which the result for each metabolite could be examined in more detail (figure 1). From the results table a summary report was generated, which showed the available information for each metabolite (figure 2). The more extensive report contained the detailed results for each metabolite. As example the result for a mono-hydroxyl metabolite (figures 3 to 5) and a dihydroxy metabolite (figures 6 to 8) of buspirone are discussed here.

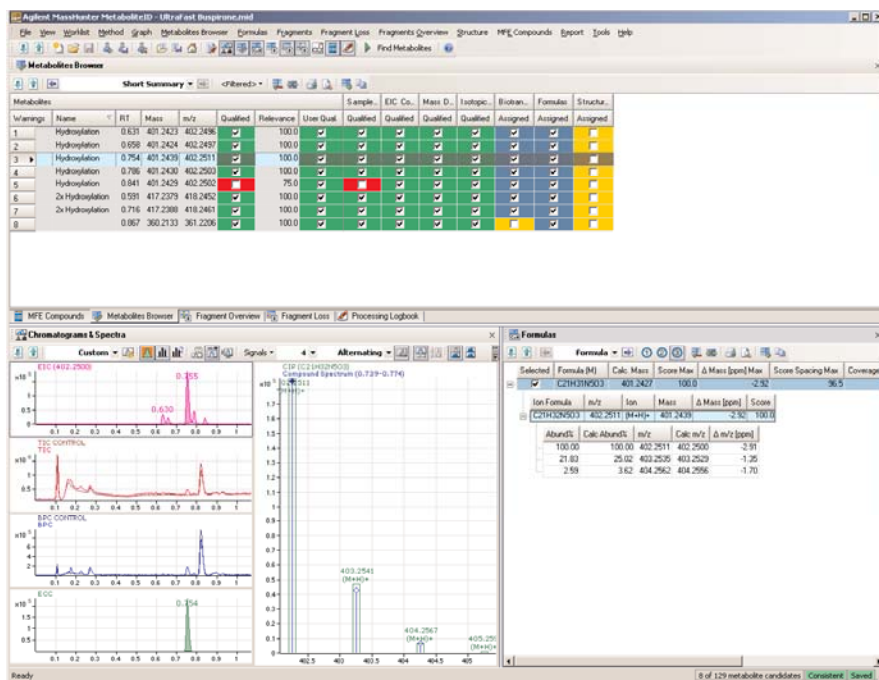


Figure 1
Result table showing an at-a-glance summary of buspirone metabolite analysis with overall identified metabolites, extracted ion chromatograms (EIC), extracted compound chromatograms (ECC), isotopic pattern analysis and calculated formulas.

| Name | Mass | RT | Rel. | Qual. | User | SC | IPM | EIC | MDF | Form. | BioXF |
|------------------|----------|------|--------|-------|------|----|-----|-----|-----|-------|-------|
| 2x Hydroxylation | 417.2379 | 0.59 | 100.00 | ✓ | ✓ | ✓ | ✓ | ✓ | ✓ | ✓ | ✓ |
| Hydroxylation | 401.2423 | 0.63 | 100.00 | ✓ | ✓ | ✓ | ✓ | ✓ | ✓ | ✓ | ✓ |
| Hydroxylation | 401.2424 | 0.66 | 100.00 | ✓ | ✓ | ✓ | ✓ | ✓ | ✓ | ✓ | ✓ |
| 2x Hydroxylation | 417.2388 | 0.72 | 100.00 | ✓ | ✓ | ✓ | ✓ | ✓ | ✓ | ✓ | ✓ |
| Hydroxylation | 401.2439 | 0.75 | 100.00 | ✓ | ✓ | ✓ | ✓ | ✓ | ✓ | ✓ | ✓ |
| Hydroxylation | 401.2430 | 0.79 | 100.00 | ✓ | ✓ | ✓ | ✓ | ✓ | ✓ | ✓ | ✓ |
| Buspirone | 385.2478 | 0.82 | — | — | — | — | ✓ | ✓ | ✓ | ✓ | — |
| Hydroxylation | 401.2429 | 0.84 | 75.00 | × | ✓ | × | ✓ | ✓ | ✓ | ✓ | ✓ |

Figure 2
Summary result report, including qualified metabolites sorted by their retention times (RT), with their metabolite names and relative score, molecular mass and the passed flag for individual algorithm results. SC=Sample-control comparison, IPM = Isotopic Pattern Matching, EIC = Extracted Ion Chromatogram, MDF = Mass Defect Filter, Form. = Calculated Formula, BioXF = Assigned Biotransformation, Qual. = Qualified by Score, User = Qualified by User.

The extensive report for the mono-hydroxyl metabolite, which eluted after 0.75 minutes at m/z 402.2511, showed the detailed information about the metabolite itself such as measured accurate mass, calculated formula, assigned biotransformation and ion species. Further, the report showed more detailed information about the result of each individual algorithm, for example, Molecular Feature Extraction (MFE), Extracted Ion Chromatogram (EIC) compound search and Mass Defect Filter Result (figure 3). For the hydroxyl metabolite the possible formula was calculated based not only on a defined mass error window but also on the measured isotopic pattern, which increased the quality of the calculated formula and limited the possible number of hits significantly. These results were also displayed in the detailed metabolite result report for the formula (figure 4).

| <u>Metabolite Information</u> | | | | | | | |
|--|------------------|-------------|------------------|-------------------|-----------------------|------------|--------|
| Name | Hydroxylation | BioXF Name | Hydroxylation | | | | |
| Formula | C21H31N5O3 | Mass | 401.2439 | | | | |
| m/z | 402.2511 | Species | (M+H)+ | | | | |
| RT | 0.754 | Sample Type | MetaboliteSample | | | | |
| <u>MFE Compound Search</u> | | | | | | | |
| Mass | m/z | Species | RT | Start Time | End Time | Volume | Height |
| 401.2439 | 402.2511 | (M+H)+ | 0.754 | 0.739 | 0.774 | 192448 | 187344 |
| <u>EIC Compound Search</u> | | | | | | | |
| Mass | m/z | Species | RT | Start Time | End Time | Area | Area % |
| 401.2427 | 402.2500 | (M+H)+ | 0.755 | 0.739 | 0.774 | 149323 | 100.00 |
| <u>Sample Comparison Results</u> | | | | | | | |
| Qualified | Changed | Resp. Ratio | Corr. RT | Normalized Height | | | |
| <input checked="" type="checkbox"/> | New | | | | | | |
| <u>Isotopic Pattern Matching Results</u> | | | | | | | |
| Qualified | Score | Delta m/z | | | | | |
| <input checked="" type="checkbox"/> | 95.91 | 0.00 | | | | | |
| <u>Mass Defect Filter Results</u> | | | | | | | |
| Qualified | Delta Mass [mDa] | | | | | | |
| <input checked="" type="checkbox"/> | -3.91 | | | | | | |
| <u>Formula Results</u> | | | | | | | |
| Assigned | Neutral Formula | Calc. Mass | Delta Mass [mDa] | Delta Mass [ppm] | Calculation Base | | |
| <input checked="" type="checkbox"/> | C21H31N5O3 | 401.2427 | -1.17 | -2.92 | MfeCompoundMsSpectrum | | |
| <u>Biotransformation Results</u> | | | | | | | |
| Assigned | Name | Phase | Offset Formula | Delta Mass [mDa] | Delta Mass [ppm] | Calc. Mass | |
| <input checked="" type="checkbox"/> | Hydroxylation | I | +O | 1.17 | 2.92 | 401.2427 | |

Figure 3 Detailed metabolite report for the buspirone hydroxy metabolite at retention time 0.75 min. This part of the report gives detailed information about the identified metabolite and the identifying algorithms. Other detailed information about formula (figure 4), chromatograms and isotopic pattern (figure 5) are also available.

| <u>Metabolite Information</u> | | | | | | |
|----------------------------------|---------------|------------|---------------|--------------|------------|--------------|
| Name | Hydroxylation | BioXF Name | Hydroxylation | | | |
| Formula | C21H31N5O3 | Mass | 401.2439 | | | |
| m/z | 402.2511 | RT | 0.754 | | | |
| <u>Formula Summary</u> | | | | | | |
| Selected | Score | Formula | Ion Formula | Mass | Calc. Mass | Δ Mass [ppm] |
| TRUE | 100.0 | C21H31N5O3 | C21H32N5O3 | 401.2439 | 401.2427 | -2.92 |
| <u>Formula Details</u> | | | | | | |
| Formula (M) | Selected | | | | | |
| C21H31N5O3 | TRUE | | | | | |
| Species | m/z | | | | | |
| (M+H)+ | 402.2511 | | | | | |
| <u>Formula Results</u> | | | | | | |
| Ion Formula | Score | Mass | Δ Mass [mDa] | Δ Mass [ppm] | DBE | |
| C21H32N5O3 | 100.0 | 401.2439 | -1.17 | -2.92 | 9 | |
| <u>Isotopic Peak Information</u> | | | | | | |
| Abund % | Calc Abund% | m/z | Calc m/z | Δ m/z [ppm] | | |
| 100.00 | 100.00 | 402.2511 | 402.2500 | -2.91 | | |
| 21.83 | 25.02 | 403.2535 | 403.2529 | -1.35 | | |
| 2.59 | 3.62 | 404.2562 | 404.2556 | -1.70 | | |

Figure 4 Detailed metabolite report about the formula including isotopic pattern, calculated for the buspirone hydroxy metabolite at retention time 0.75 min.

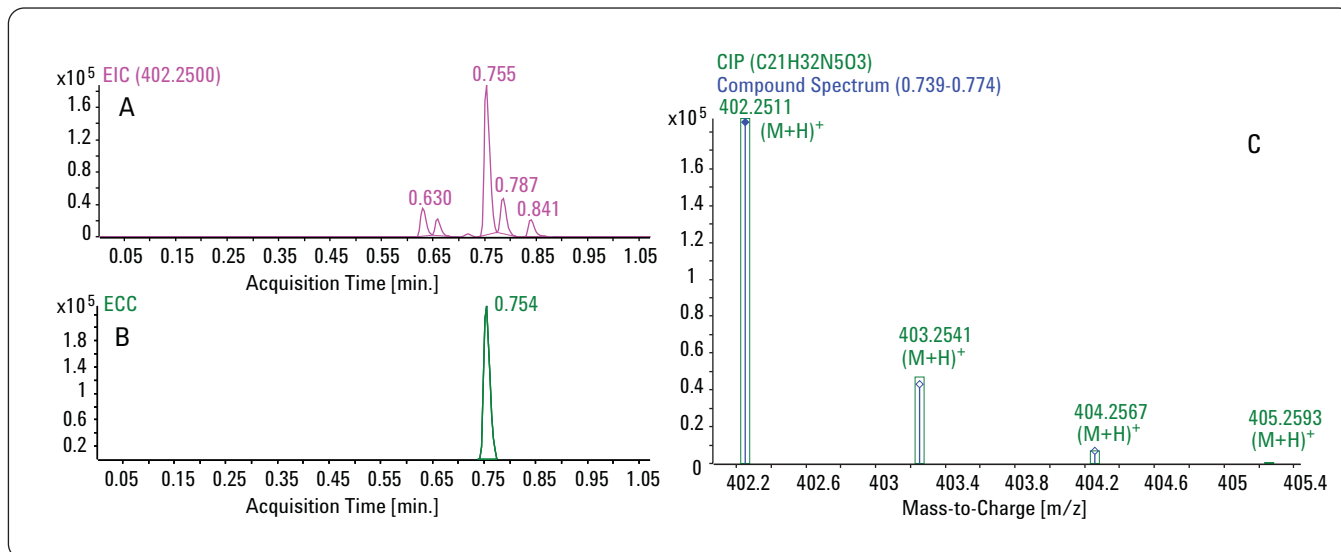


Figure 5
Detailed metabolite report for buspirone hydroxy metabolite at retention time 0.75 min:
A) Extracted Ion Chromatograms (EIC) of compounds with mass 402.25
B) Extracted Compound Chromatogram (ECC) of buspirone hydroxy metabolite at retention time 0.75 min
C) Measured isotopic pattern of buspirone hydroxy metabolite at retention time 0.75 min (blue lines) and calculated isotopic pattern (CIP, green box).

Finally, the EIC, ECC and isotopic pattern were displayed (figure 5). The EIC of m/z 402.25 showed 5 peaks for possible hydroxyl metabolites of buspirone with the selected one at retention time 0.75 minutes (figure 5A). The ECC showed the extracted MFE compound for the molecular mass of 401.2439 at retention time 0.75 minutes identical to the EIC (figure 5B). The measured isotopic pattern of this compound showed an excellent fit to the calculated isotopic pattern as a basis for the formula calculation (figure 5C).

Within the same data analysis the dihydroxy metabolites at a level of two orders of magnitude below the mono-hydroxy metabolites were also identified. The extensive report showed detailed information about the dihydroxy metabolite, which elutes after 0.71 minutes at m/z 418.2461 and the detailed information about each algorithm (figure 6).

| <u>Metabolite Information</u> | | BioXF Name | | | | | |
|--|------------------|--------------------|--------------------|-------------------|-----------------------|------------|--------|
| Name | 2x Hydroxylation | BioXF Name | 2x Hydroxylation | | | | |
| Formula | C21H31N5O4 | Mass | 417.2388 | | | | |
| m/z | 418.2461 | Species | (M+H) ⁺ | | | | |
| RT | 0.716 | Sample Type | MetaboliteSample | | | | |
| <u>MFE Compound Search</u> | | | | | | | |
| Mass | m/z | Species | RT | Start Time | End Time | Volume | Height |
| 417.2388 | 418.2461 | (M+H) ⁺ | 0.716 | 0.700 | 0.726 | 3865 | 3889 |
| <u>EIC Compound Search</u> | | | | | | | |
| Mass | m/z | Species | RT | Start Time | End Time | Area | Area % |
| 417.2376 | 418.2449 | (M+H) ⁺ | 0.713 | 0.703 | 0.739 | 3483 | 100.00 |
| <u>Sample Comparison Results</u> | | | | | | | |
| Qualified | Changed | Resp. Ratio | Corr. RT | Normalized Height | | | |
| <input checked="" type="checkbox"/> | New | | | | | | |
| <u>Isotopic Pattern Matching Results</u> | | | | | | | |
| Qualified | Score | Delta | m/z | | | | |
| <input checked="" type="checkbox"/> | 91.50 | | 0.00 | | | | |
| <u>Mass Defect Filter Results</u> | | | | | | | |
| Qualified | Delta Mass [mDa] | | | | | | |
| <input checked="" type="checkbox"/> | -8.97 | | | | | | |
| <u>Formula Results</u> | | | | | | | |
| Assigned | Neutral Formula | Calc. Mass | Delta Mass [mDa] | Delta Mass [ppm] | Calculation Base | | |
| <input checked="" type="checkbox"/> | C21H31N5O4 | 417.2376 | -1.20 | -2.87 | MfeCompoundMsSpectrum | | |
| <u>Biotransformation Results</u> | | | | | | | |
| Assigned | Name | Phase | Offset Formula | Delta Mass [mDa] | Delta Mass [ppm] | Calc. Mass | |
| <input checked="" type="checkbox"/> | 2x Hydroxylation | I | +O2 | 1.20 | 2.87 | 417.2376 | |

Figure 6
Detailed metabolite report for dihydroxy metabolite of buspirone at retention time 0.71 min. This part of the report gives detailed information about the identified metabolite and the identifying algorithms. Other detailed information about formula (see figure 7), chromatograms and isotopic pattern (see figure 8) are also available.

The calculation of the formula was outlined in the detailed formula report (figure 7).

The EIC of m/z 418.24 showed about five significant peaks for possible dihydroxylated metabolites of buspirone with the selected peak at 0.71 minutes (figure 7A). The ECC showed the extracted MFE compound for the molecular mass of 417.2388 at retention time 0.71 identical to the EIC (figure 7B). The measured and calculated isotopic pattern of this compound is shown in figure 7C.

| Metabolite Information | | | | | | |
|---|---|---|---|--------------|-------------|--------------|
| Name | 2x Hydroxylation | BioXF Name | 2x Hydroxylation | | | |
| Formula | C ₂₁ H ₃₁ N ₅ O ₄ | Mass | 417.2388 | | | |
| m/z | 418.2461 | RT | 0.716 | | | |
| Formula Summary | | | | | | |
| Selected | Score | Formula | Ion Formula | Mass | Calc. Mass | Δ Mass [ppm] |
| TRUE | 100.0 | C ₂₁ H ₃₁ N ₅ O ₄ | C ₂₁ H ₃₂ N ₅ O ₄ | 417.2388 | 417.2376 | -2.87 |
| Formula Details | | | | | | |
| Formula (M) | Selected | | | | | |
| C ₂₁ H ₃₁ N ₅ O ₄ | TRUE | | | | | |
| Species | m/z | | | | | |
| (M+H) ⁺ | 418.2461 | | | | | |
| Formula Results | | | | | | |
| Ion Formula | Score | Mass | Δ Mass [mDa] | Δ Mass [ppm] | DBE | |
| C ₂₁ H ₃₂ N ₅ O ₄ | 100.0 | 417.2388 | -1.20 | -2.87 | 9 | |
| Isotopic Peak Information | | | | | | |
| Abund % | Calc | Abund% | m/z | Calc m/z | Δ m/z [ppm] | |
| 100.00 | | 100.00 | 418.2461 | 418.2449 | -2.86 | |
| 23.90 | | 25.06 | 419.2488 | 419.2478 | -2.35 | |

Figure 7
Detailed metabolite report about the formula, including isotopic pattern, calculated for dihydroxy metabolite of buspirone at retention time 0.71 min.

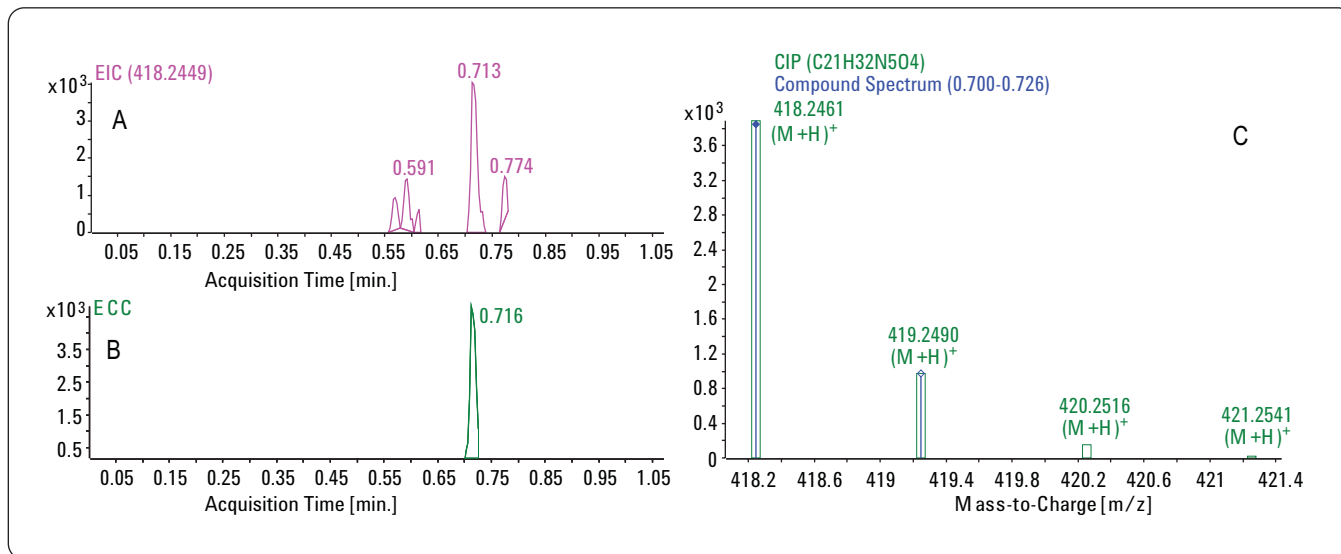


Figure 8
Detailed metabolite report for dihydroxy metabolite buspirone at retention time 0.71 min:
A) Extracted Ion Chromatograms (EIC) of compounds with mass 418.24
B) Extracted Compound Chromatogram (ECC) of dihydroxy metabolite of buspirone at retention time 0.71 min
C) Measured and calculated isotopic pattern of dihydroxy buspirone metabolite at retention time 0.71 min.

Conclusion

This Application Note demonstrated the use of the Agilent 1290 Infinity LC system with an Agilent Q-TOF LC/MS system for fast separation and accurate mass measurement of compounds in an in-vitro metabolite sample under high-throughput conditions. The metabolite compounds were separated in a run time below one minute and the width of the peaks extracted by the Metabolite ID software were below one second (FWHH). The major metabolites were identified quickly by means of the Agilent Metabolite Identification software.

A summary report as well as detailed reports for each metabolite were generated.

References

1. E. Naegele, F. Wolf, U. Nassal, R. Jäger, H. Lehmann, F. Kuhlmann, K. Subramanian, "An interwoven, multi-algorithm approach for computerassisted identification of drug metabolites", *Agilent Technologies Application Note, publication number 5989-7375EN, 2007*.

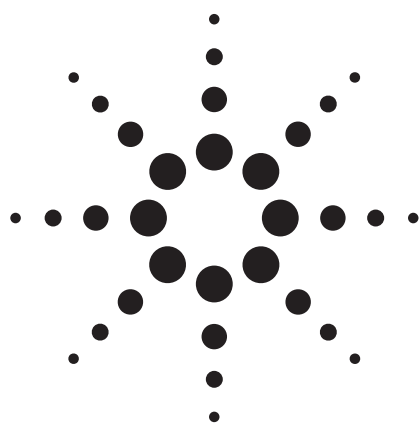
www.agilent.com/chem/metid

© Agilent Technologies, Inc., 2009
Published May 1, 2009
Publication Number 5989-9924EN



Agilent Technologies

Separation of Salicylic Acid Impurities with Different Acid Mobile-Phase Modifiers



Application

Pharmaceuticals

Authors

William J. Long and John W. Henderson Jr.
Agilent Technologies, Inc.
2850 Centerville Road
Wilmington, DE 19808-1610
USA

Abstract

Optimization of chromatographic separations can best be accomplished using the selectivity tools of bonded-phase and mobile-phase choice. In this application, mobile-phase additives such as trifluoroacetic acid (TFA) and acetic acid change the selectivity of the separation of salicylic acid and several of its documented side products. The rapid sample throughput allowed by short 1.8- μ m columns, and a rugged low-pH stationary phase, enabled quick evaluation of this important method-development parameter.

Introduction

Benefits of Low-pH HPLC

When analyzing organic acids, the ZORBAX StableBond SB-Aq becomes a frequent choice for bonded phase. It is durable at low pH conditions, and can be used with little or no organic solvent. Its patented bonded-phase chemistry includes diisopropyl side chain groups that sterically protect the key siloxane bond to the silica surface from hydrolytic attack at low pH. This ensures long column lifetime and reproducibility at low pH. Recent StableBond SB-Aq examples include organic acids found in fruit juices [1], water-soluble vitamins [2], and isomers of the pharmaceutical compound cefitibuten [3].

In method optimization, two key parameters that can be changed are the organic solvent and the mobile-phase pH. Examples of selectivity derived from changing from acetonitrile to methanol can be found in Reference 4.

An ionizable compound will exist as a charged species in certain pH environments. For the ionizable compound benzoic acid, its retention and therefore its chromatographic interaction is very different at pH 3 and pH 7. At pH 3, benzoic acid is well retained (protonated), and at pH 7, it elutes near the void volume (ionized). Polar compounds, like benzyl alcohol and nitrobenzene, which are not ionizable but are polar, show much fewer shifts in retention with changes in pH.

Salicylic Acid Analysis

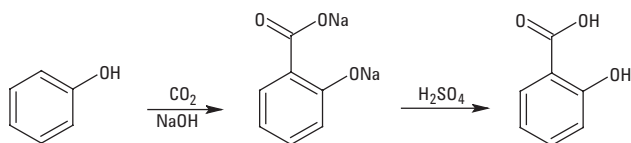
Salicylic acid, also known as 2-hydroxybenzoic acid is one of several beta hydroxy acids. It is the key additive in many skin-care products for the treatment of acne, psoriasis, calluses, corns, and warts. It treats acne by causing skin cells to slough off more readily, preventing pores from becoming clogged. This effect on skin cells makes salicylic acid an active ingredient in several shampoos to treat dandruff. Salicylic acid is also an active ingredient in gels that remove warts. The medicinal properties of salicylate (mainly for fever relief) have been known since ancient times. This colorless crystalline organic acid is also widely used in organic synthesis and functions as a plant hormone. The substance occurs in the bark of willow trees; the name *salicylic acid* is derived from *salix*, the Latin name for the willow tree [5].

Sodium salicylate is commercially prepared from sodium phenoxide and carbon dioxide at high



Agilent Technologies

pressure and temperature in the Kolbe-Schmitt reaction. It is acidified to give the desired salicylic acid. The main reaction is shown in Figure 1; however, several additional materials are also formed in this reaction, including 2,5-dihydroxybenzoic acid, 5-hydroxy-1,3-benzenedicarboxylic acid, 4-hydroxybenzoic acid, phenol, and salicylglycine. These compounds are listed with their common names, structures, and pKa values in Figure 2.



Introduction to Organic Chemistry, Streitweiser and Heathcock, MacMillan, NY (1981). (Reference 6)

Figure 1. Synthesis of salicylic acid using the Kolbe-Schmitt reaction.

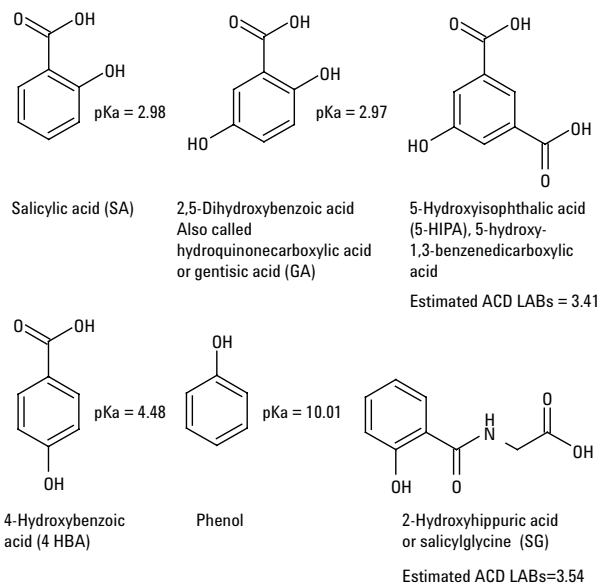


Figure 2. Structures of major salicylic acid impurities.

Purity was tested typically using a 5-micron C-18 column with an acidic mobile phase of water, methanol, and glacial acetic acid (60:40:1). This, however, only addresses three of the major impurities (4-hydroxybenzoic acid, 4-hydroxyisophthalic acid, and phenol). The compendial method also states that changes to the composition of the mobile phase could result in changes of elution order [7]. A reason these peaks may change elution order is that those compounds are all ionizable. As the mobile-phase constitution changes, so does the pH of the mobile phase.

In this work, changes in chromatography are made by changing the mobile-phase additives used. Commonly used concentrations of TFA, phosphoric acid, acetic acid, and formic acid are used to help resolve salicylic acid and five impurities.

Experimental

LC System

An Agilent 1200 Rapid Resolution liquid chromatograph (RRLC) (degasser, binary pump, well-plate autosampler, and diode-array detector set at 220 nm) was used with a StableBond SB-Aq, 1.8 μ m, 4.6 mm \times 50 mm column (part number 827975-914). The binary gradient was 5% to 30% methanol (channel B) over 10 minutes. Methanol was from Burdick and Jackson (HPLC grade).

Analytes:

- Salicylic acid (SA)
- Phenol (Phe)
- 4-Hydroxybenzoic acid (4-HBA)
- Gentisic acid (GA)
- 5-Hydroxyisophthalic (5-HIPA)
- 2-Hydroxyhippuric acid (SG)

All were obtained from Sigma Aldrich or ARCOS.

Modifiers added to channel A:

- Trifluoroacetic acid (TFA), 99 % purity, (pKa=0.23)
- Phosphoric acid ACS grade (85 % purity) (pKa= 2.12)
- Acetic acid, glacial 99% (pKa=3.8)
- Formic acid ACS grade 99 % (pKa= 4.8)

Phosphoric, formic, and acetic acids were obtained from EM Science. TFA was from Sigma Aldrich.

Results and Discussion

Phosphoric acid, trifluoroacetic acid, acetic acid, and formic acid are commonly used to control the pH of HPLC mobile phases. The addition of an acid to the aqueous component of a mobile phase is a simple and sometimes effective alternative to buffers. In addition, in rapid gradients using low-volume columns, the small volume of the rapid resolution high throughput (RRHT) column allows equilibration in only a few minutes. Figure 3 shows the gradient described previously, using those four different acid modifiers in commonly used concentrations. While the initial separation was developed using nonvolatile phosphoric acid, it is generally not considered compatible with MS detectors. TFA is also sometimes excluded from LCMS because TFA can cause ion suppression by ion pairing to the analyte. However, in some cases

TFA can be displaced from the ion-pair complex by exposing the effluent to a higher concentration of a different acid post-column and before the MS detector. One acid that works well for this approach is acetic acid. Another ion pair displacer is a solution of 75% propionic acid:25% isopropanol. TFA and phosphoric acids yield the best separations as shown in Figure 3, while commonly used formic acid and acetic acid concentrations resolve only at best five of six components. Furthermore, in the examples using formic acid and acetic acid, 4-HBA and GA switch elution order compared to the TFA and phosphoric acid examples. This may be due to changes in pH; however, additional work is needed

to determine the actual mechanism. For the scope of this work, observing elution order change is sufficient.

Figure 4 shows the effect of higher acid concentration on the separation. In almost all cases there are sharper peaks, the SG peak showing the greatest improvement. In Figure 3, the mobile-phase pH was near the pKa values of all compounds except phenol, so the addition of more acid would be expected to lower the solution pH to a point where the compounds are more completely uncharged, causing better peak shape.

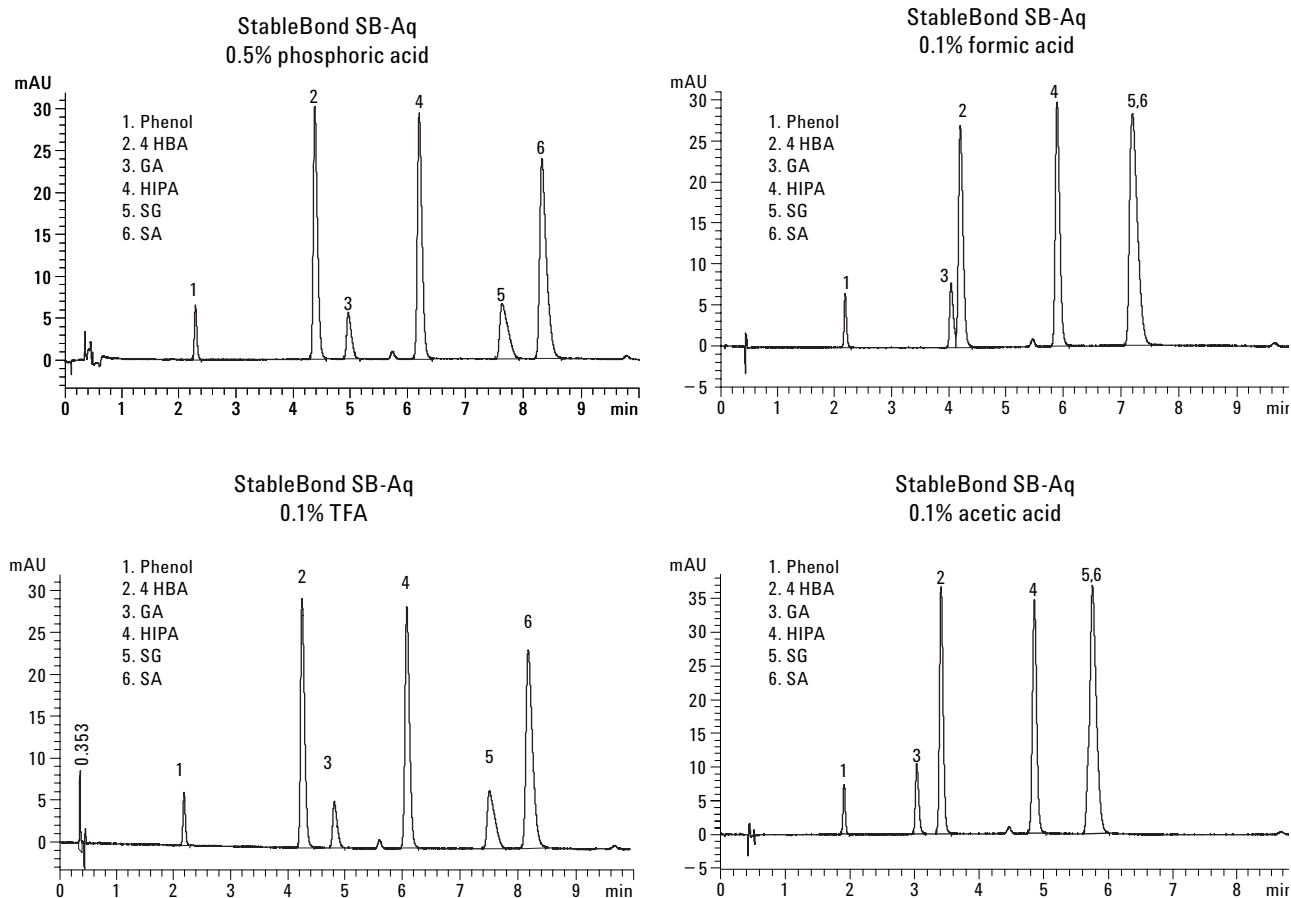


Figure 3. Effect of different acid modifiers on the separation of salicylic acid and its impurities.

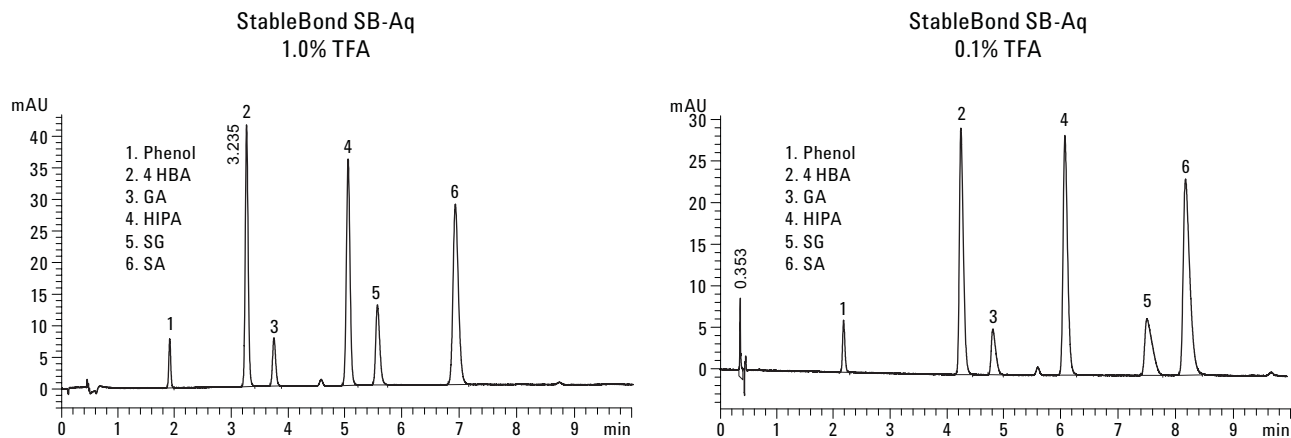


Figure 4. Effect of acid modifier concentration on separation and peak shape.

Conclusions

Evaluating several aqueous mobile-phase modifiers in method development has become more practical due to the short equilibration and analysis times afforded by RRHT 50-mm columns. Better peak shape and resolution may be achieved by simply substituting one acid modifier for another. Additionally, lowering pH (increasing acid strength) away from the pKa of the analytes can improve peak shape. This extra method development takes significantly little time when short, low-volume columns such as RRHT SB-Aq columns are used. In these cases, simple acids were used to control pH, but this concept can be extended to the evaluation of different mobile-phase buffers and optimization of buffer concentration.

StableBond columns are ideal for low-pH applications. Their unique column chemistry and variety of bonded phases, such as SB-Aq, provide broad selectivity, long lifetime, and reproducibility at low pH.

References

1. M.A. Van Straten, H A. Claessens A. Dams, "Analysis of Organic Acids in Aqueous Solutions," Agilent publication 5989-1265EN, 2006.
2. "Quick Screening and Quantification of Water-Soluble Vitamins Using Rapid Resolution LC/MS/MS" S. Mosin Poster THPH 115 ASMS 2007.

3. Adebayo O. Onigbinde, "Separation of Ceftibuten Stereo Isomers with 100% Aqueous Mobile Phase Using Zorbax SB-Aq," Agilent publication 5988-7625EN, 2002.
4. William J. Long and John W. Henderson Jr., "Unique Selectivity and High-Throughput Applications of SB-Phenyl RRHT," Agilent publication 5989-5057EN, 2007.
5. A Brief History of Antipyretic Therapy, P. Mackowiak, *Clinical Therapeutic Disease*, 31,154-156, 2000.
6. Introduction to Organic Chemistry, Streitweiser and Heathcock, MacMillan, NY (1981).
7. Salicylic Acid, USP 23 (1995) 1395.

For More Information

For more information on our products and services, visit our Web site at www.agilent.com/chem.

Agilent shall not be liable for errors contained herein or for incidental or consequential damages in connection with the furnishing, performance, or use of this material.

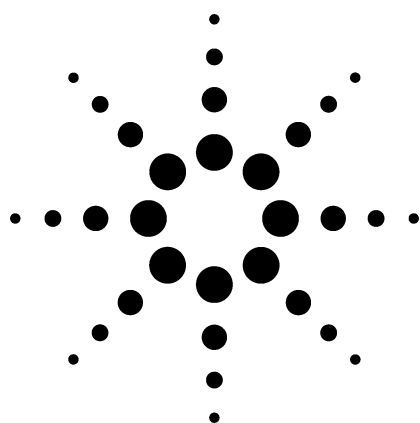
Information, descriptions, and specifications in this publication are subject to change without notice.

© Agilent Technologies, Inc. 2009

Printed in the USA
July 24, 2009
5989-7731EN



Agilent Technologies



The High-Resolution Reversed-Phase HPLC Separation of Licorice Root Extracts Using Long Rapid Resolution HT 1.8- μm Columns

Application

Food Additive, Natural Products, and Pharmaceuticals

Author

Bernard Permar and Ronald E. Majors
Agilent Technologies, Inc.
2850 Centerville Road
Wilmington, DE 19808-1610
USA

Abstract

High-resolution reversed-phase HPLC analytical studies using licorice, a licorice hydrolysis product, and commercial licorice samples, showed that resolution and throughput using a ZORBAX 1.8- μm column greatly exceeded that obtained using the conventional 5.0- μm column.

Introduction

Licorice is derived from the root of the *Glycyrrhiza glabra* plant, a 4- to 5-foot woody shrub that grows in Europe, the Middle East and Western Asia. The root of the plant is known to contain about 4% glycyrrhizin, the potassium or calcium salt of glycyrrhizinic acid. The latter is a glycoside of a pentacyclic triterpene carboxylic acid (18- β -glycyrrhetic acid) with two molecules of glucuronic acid (Figure 1).

Glycyrrhizin is about 50 times sweeter than sucrose (cane sugar) but at high dosage is known to have toxicity. Upon hydrolysis, the glycoside loses its sweet taste and is converted to the aglycone glycyrrhetic acid plus two molecules of glucuronic acid.

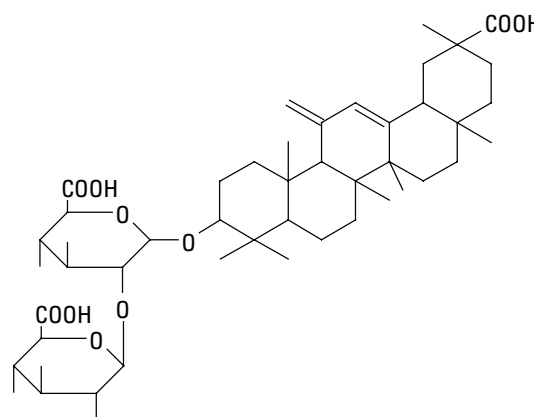


Figure 1. Structure of glycyrrhizinic acid.

Extractions from any of the many species of this plant will yield a complex mixture containing more than 100 compounds. Several of these compounds are used as additives in candy as sweeteners, in cough syrup as flavoring agents, and in drugs to mask a bitter taste, or for their therapeutic qualities, mainly in Traditional Chinese Medicines (TCMs). The medicinal properties of licorice have been known for several centuries in China, as well as India, Egypt, Greece, and Rome. Uses included cough suppressant, laxative, and treatments for gastric ulcer, early Addison disease, and liver disease. Most recently, glycyrrhizin has been shown to have antiviral activity against DNA and RNA viruses (influenza A and B, HIV, VZV, Hepatitis B and C) [1]. Licorice has also been used in topical cosmetic applications.



Agilent Technologies

The abundance of certain compounds of interest will vary greatly according to the species of the plant, the time of harvest, and the method of extraction. Thus, analytical methods to follow the active ingredients are required. Gradient elution reversed-phase HPLC has been found to be an effective method for separating some of the important compounds in licorice [2]. This application note compares the traditional HPLC methodology and the newer Rapid Resolution high-throughput (RRHT) columns. We will apply these HPLC techniques to investigate the differences between two commercially available licorice root extracts.

Experimental

Two reversed-phase (RP) columns were used in this study:

- Conventional ZORBAX StableBond (SB)-C18, 4.6 mm × 250 mm, 5 μm
- ZORBAX SB-C18 RRHT, 4.6 mm × 150 mm, 1.8 μm

The smaller particle size of the RRHT column allows use of a shorter column to achieve the same resolution as the longer conventional column, and also allows more rapid separations.

HPLC conditions

| | |
|--|---|
| Instrument: | Agilent 1200 Series Rapid Resolution System |
| Detector: | Multiple wavelength detector (MWD), 254 nm/100 BW, 450 nm reference |
| Mobile phase: | A = 1% Acetic acid in water B = 1% Acetic acid in acetonitrile |
| Gradient conditions for ZORBAX SB-C18 columns: | |
| Conventional: | 4.6 mm × 250 mm, 5 μm 5% to 100% B in 50 minutes |
| RRHT: | 4.6 mm × 150 mm, 1.8 μm 5% to 100% B in 30 minutes |
| Flow: | 1.0 mL/min |
| Temperature: | Ambient |

Standards: Purchased from Sigma Aldrich

- (G) 0.1-mg glycyrrhizic acid ammonium salt, ~75 %, dissolved in 0.5-mL mobile phase B, then brought to 1.0 mL by adding 0.5-mL mobile phase A
- (GA) 0.1-mg 18-beta-glycyrrhetic acid, 97%, dissolved in 0.5-mL mobile phase B, then brought to 1.0 mL by adding 0.5-mL mobile phase A

Samples:

- Licorice root extract A (HERB FARM brand)
- Licorice root extract B (Newark Natural Foods)

Both extracts should be vortexed, then filtered (0.2 micron) prior to injection.

Injection volume: 5 μL of extract

Results

The most important compound found in a typical licorice extract is G and to a lesser extent, its hydrolysis product, GA. These substances can be purchased commercially. Although some of the other components of licorice have been identified and are available commercially, they are quite expensive. Since our main objective was to demonstrate the advantage of using shorter, high-resolution HPLC columns, we used only two standards (G and GA) to develop the initial method. Figure 2a shows the gradient separation of G and GA on the conventional column (ZORBAX SB-C18, 4.6 mm × 250 mm, 5 μm) using gradient elution. Since the licorice extract to be examined was quite complex, isocratic conditions were not usable to separate all of the components. The G being more polar by virtue of the additional sugar moieties eluted first while the GA came off the column much later. Using this gradient, the GA eluted in just under 42 minutes. By switching to the shorter ZORBAX SB-C18 RRHT column (4.6 × 150 mm, 1.8 μm), the separation was virtually the same, as can be seen in Figure 2b. However, the separation time was now just over 25 min, a savings of about 40% in time.

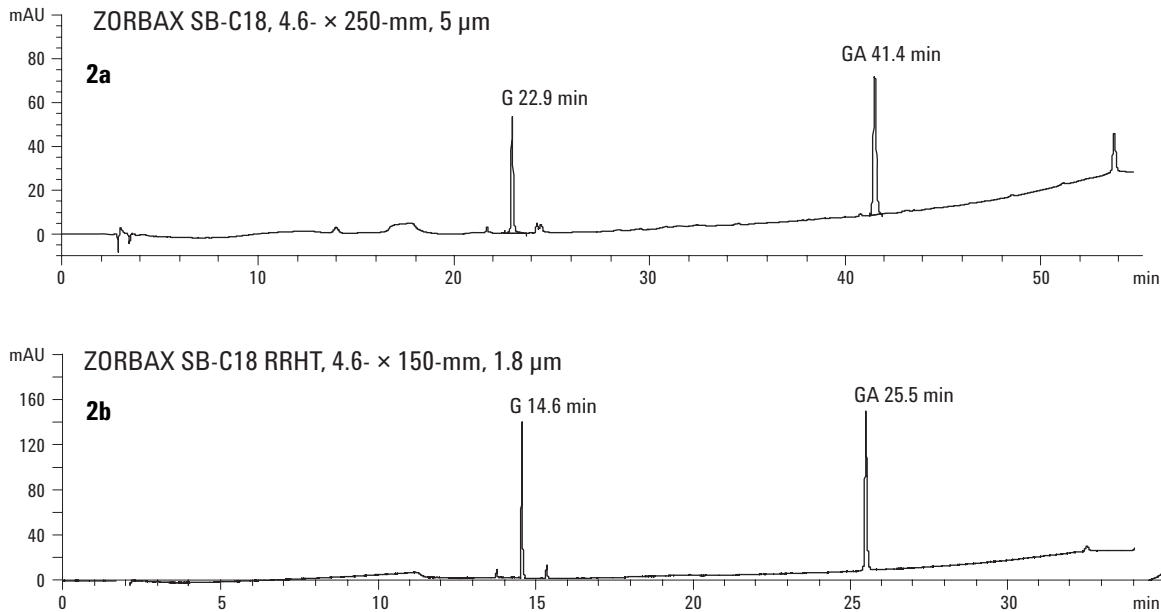


Figure 2. Gradient reversed-phase separation of G and GA on the test 5.0- and 1.8- μ m columns.

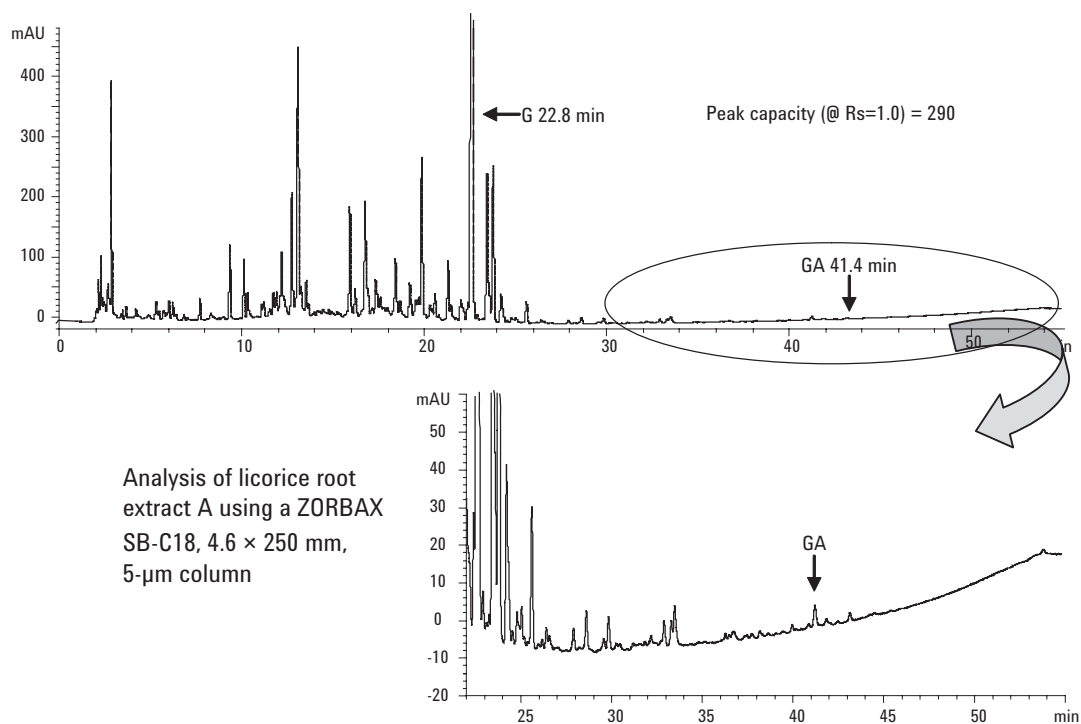
To investigate the use of these columns for the separation of actual licorice root extracts, Figures 3 and 4 depict the complex chromatograms observed by injection of filtered extracts, identified in the Experimental section. Figure 3a shows the complex chromatogram obtained using the 5- μ m 250-mm column. The cut-away shows the small amount of GA that was present in the extract. Since GA is a hydrolysis product of G, it should be at a much lower concentration in a licorice extract, unless the extract was treated to enhance the concentration of the hydrolyzed product. Based on the area count, the GA concentration was less than 0.5% of the G concentration in extract A.

Although the actual peaks were not counted, the calculated peak capacity (3) for the 5- μ m column was determined to be 290 (resolution: 1.0). Running the same extract A on the 1.8- μ m 150-mm column, one can see the finer structured (that is, higher resolution) chromatogram that results

(Figure 3b). The calculated peak capacity for this higher efficiency column was determined to be 442, over 50% higher than by using the longer 5- μ m column. Thus, it would be easier to determine minor components on this shorter rapid resolution column. The peaks per unit time (Resolution = 1.0) was calculated to be 17.7 peaks/min for the 1.8- μ m column versus 7.1 for the 5- μ m column.

Figures 4a and 4b show similar runs using extract B. This extract was even more complex than extract A which is borne out by comparing the high resolution chromatograms of Figure 3b versus Figure 4b. Again, the calculated peaks per minute for the 1.8- μ m column greatly exceeded that of the 5- μ m column (17 versus 7.5 respectively). Based on the peak area counts for GA, it was roughly 1% of the concentration of G in extract B.

(A)



(B)

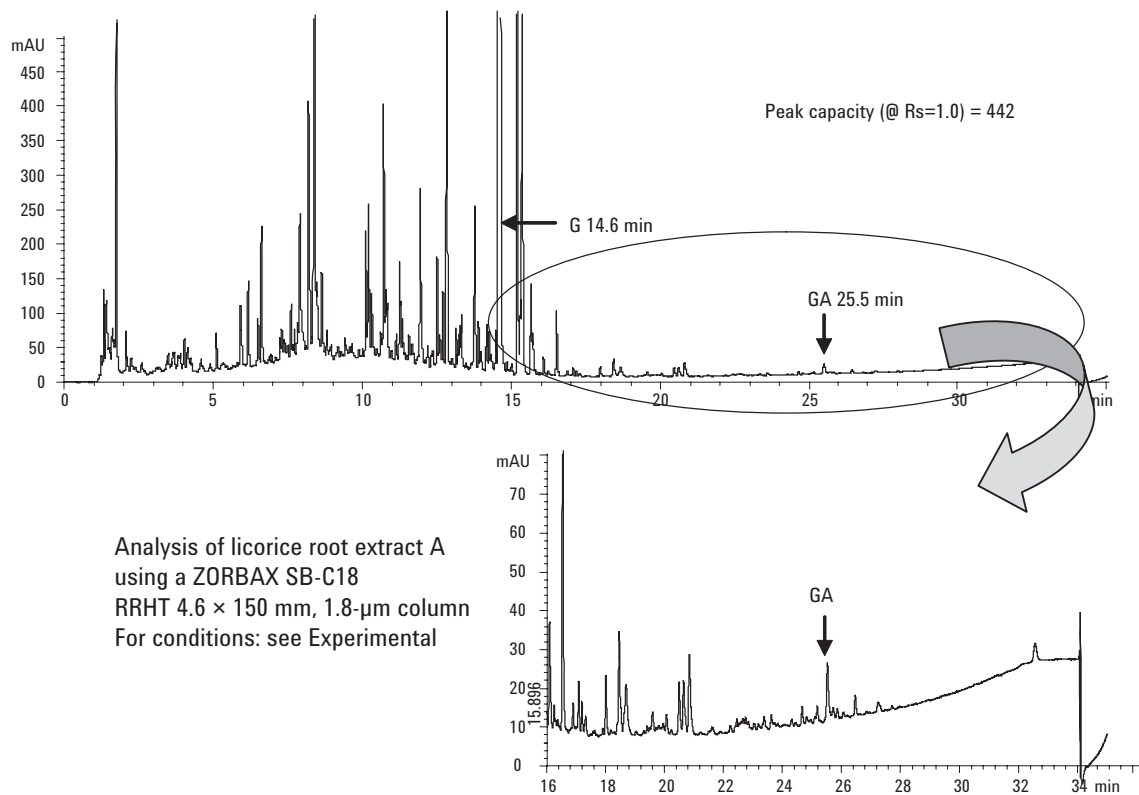
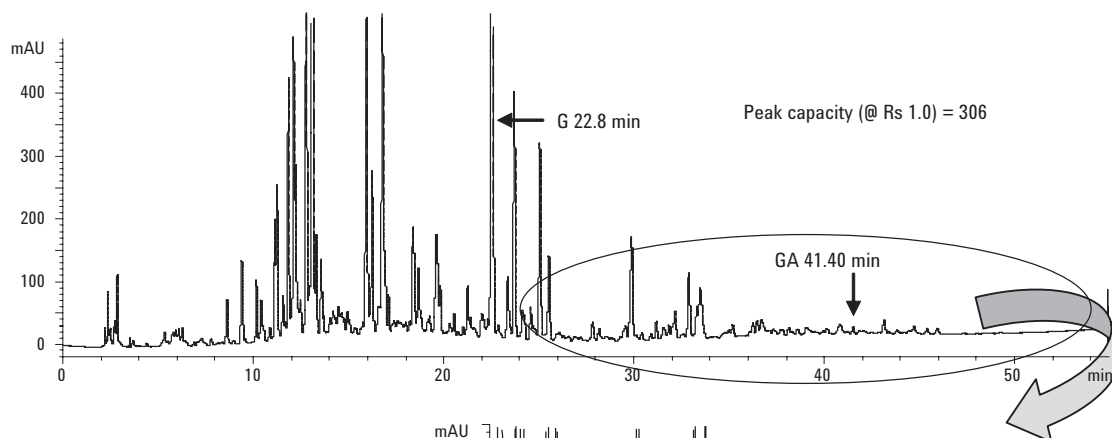
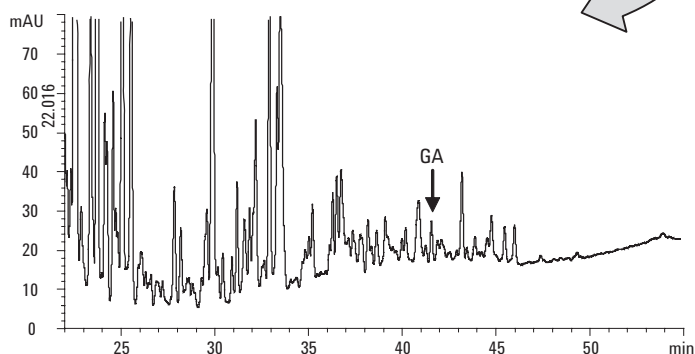


Figure 3a and 3b. The gradient reversed-phase separation of licorice root extract A on the 5.0-µm column (A) and on the 1.8-µm column (B).

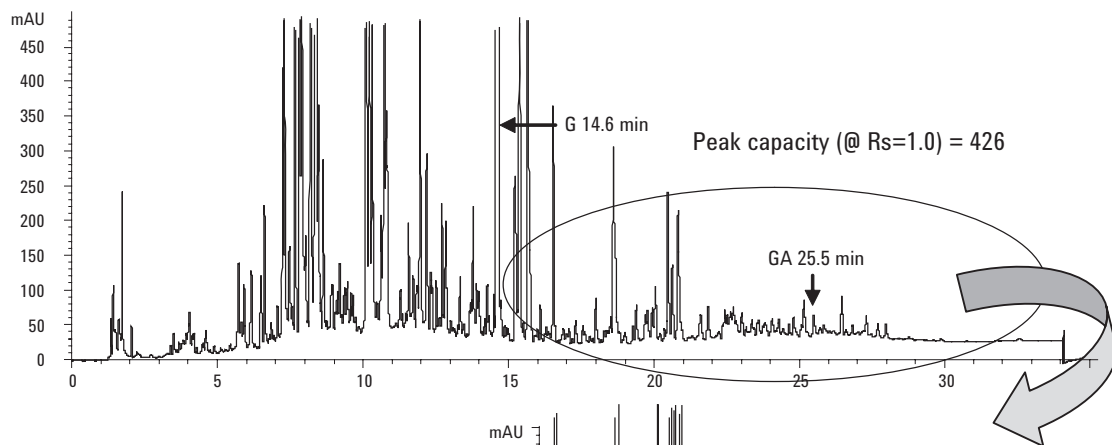
(A)



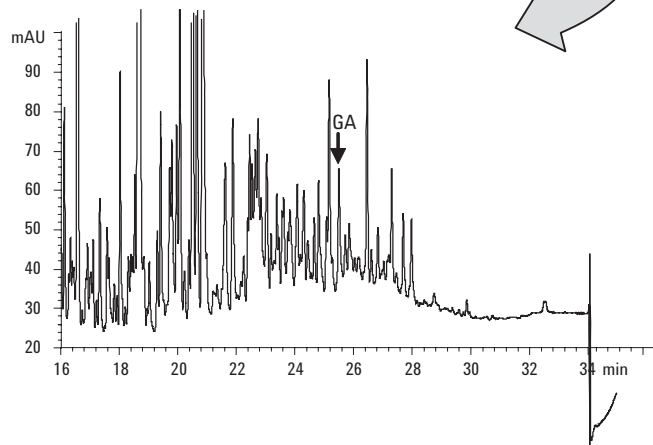
Analysis of licorice root extract B using a ZORBAX SB-C18 4.6 × 250-mm column, 5 µm



(B)



Analysis of licorice root extract B using a ZORBAX SB-C18 RRHT 4.6 × 150-mm column



Figures 4a and 4b. Gradient reversed-phase separation of licorice root extract B on the 5.0-µm column (A) and on the 1.8-µm column (B).

Conclusions

No attempt was made to perform quantitative analysis on the components of the licorice extracts. From our studies, it was obvious that resolution and throughput using the 1.8- μm column greatly exceeded that obtained using the 5.0- μm conventional column. As more complex samples of natural products are encountered and researchers require more detailed component analyses, the use of high resolution, small particle columns should grow. In the investigation of licorice root, other natural products, and TCMs, it is necessary to have gradient capability and sensitive detection.

References

1. S. Fanali, Z. Aturki, G. D'Orazio, M. A. Raggi, M. G. Quaglia, C. Sabbioni, and A. Rocco, (2005) *J. Sep. Sci.*, **28**, 982–986.
2. I. Kitagawa, (2002) *Pure Appl. Chem.* **74** (7), 1189–1198.

For More Information

For more information on our products and services, visit our Web site at www.agilent.com/chem.

Agilent shall not be liable for errors contained herein or for incidental or consequential damages in connection with the furnishing, performance, or use of this material.

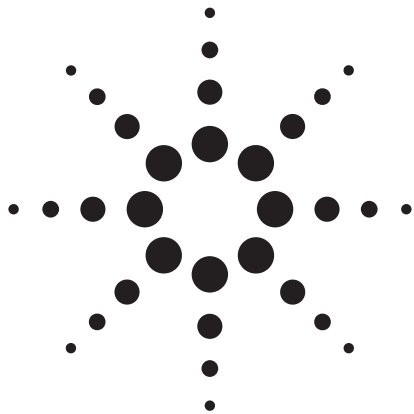
Information, descriptions, and specifications in this publication are subject to change without notice.

© Agilent Technologies, Inc. 2006

Printed in the USA
March 14, 2006
5989-4907EN



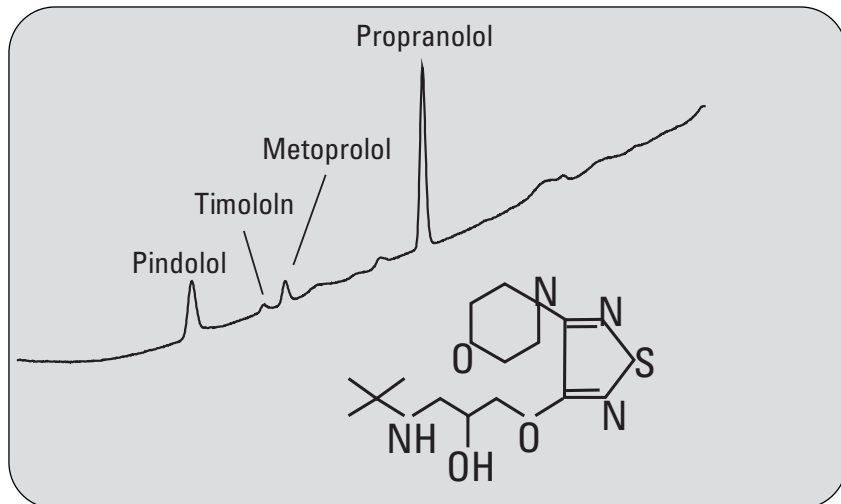
Agilent Technologies



Analysis of beta-blocking drugs on Agilent 1100 Series LC systems using UV, fluorescence and mass spectrometry

Application

Angelika Gratzfeld-Huesgen
Mark Stahl



Abstract

This Application Note compares the detection techniques UV, fluorescence and mass spectrometry in combination with standard and capillary LC systems, and columns with different internal diameters. Advantages and disadvantages of the different detector/column/LC system combinations are discussed.



Agilent Technologies

Introduction

Beta-blocking drugs are widely used in the treatment of hypertension and glaucoma. The determination of these drugs in biological fluids is nowadays done by fluorescence or mass spectrometry in combination with standard bore or narrow bore columns¹⁻³.

With fluorescence detection beta blocking drugs are analyzed in the low ng range. The disadvantage is that not all beta-blocking drugs fluoresce. These compounds can be analyzed using UV detection. The disadvantage of using UV detection is that it is typically less sensitive than fluorescence detection. Recently mass spectrometry is also being used to identify beta-blocking drugs and their metabolites in the low pg range.

The following Agilent 1100 Series LC system combinations were evaluated:

- Agilent 1100 Series standard LC system with standard bore and narrow bore columns using UV, fluorescence and mass spectrometry detection
- Agilent 1100 Series capillary LC system with capillary columns using UV and MS detection

For all system combinations the limit of detection was determined using Pindolol, Timolol, Metoprolol and Propranolol as beta-blocking drugs.

Experimental

A standard Agilent 1100 Series LC system was used in combination with UV detection, fluorescence detection and mass spectrometry. This modular system consists of:

- Agilent 1100 Series binary pump for precise flow rates and a micro degasser with an internal volume of 1 mL
- Agilent 1100 Series well-plate sampler for precise injection in the μ L range with cooling option for the samples
- A column thermostat for precise retention times at above or below room temperature
- Agilent 1100 Series diode-array detector equipped with a 8- μ L cell for highly precise quantitation
- Agilent 1100 Series LC/MSD Quadrupole SL with an ESI source for identification and highly selective and sensitive analysis. For the Agilent 1100 Series capillary system the ESI source with microspray nebulizer was used.
- Agilent 1100 Series fluorescence detector for multi signal and sensitive analysis of all compounds showing fluorescence activities.

The Agilent 1100 Series capillary LC system was used for experiments using capillary columns with an internal diameter of 0.3 mm. This modular system consists of:

- Agilent 1100 Series capillary pump with electronic flow con-

trol for precise flow rates even at changing back-pressure.

The capillary pump was also equipped with a micro degasser with an internal volume of 1 mL

- Agilent 1100 Series micro well-plate sampler for precise injection in the nl and μ L range with cooling option for the samples
- A column thermostat for precise retention times at room temperature, above or below room temperature
- Agilent 1100 Series diode-array detector equipped with a 500 nl cell for sensitive analysis of small peak volumes
- Agilent 1100 Series LC/MSD Quadrupole with a capillary ESI source for identification and highly selective and sensitive analysis.

Three capillary columns of the same type but of different length were tested:

- 150 x 0.3 mm Zorbax SB C-8, 3.5 μ m
- 75 x 0.3 mm Zorbax SB C-8, 3.5 μ m
- 50 x 0.3 mm Zorbax SB C-8, 3.5 μ m

One narrow bore column was used:

- 30 x 2.1 mm Zorbax SB C-8, 3.5 μ m

One standard bore column was used:

- 150 x 4.6 mm Zorbax Eclipse C-8, 5 μ m

Beta-blocking drugs Pindolol, Timolol, Metoprolol and Propranolol were purchased from Sigma Aldrich.

Results and discussion

Limit of detection using UV detection

To evaluate optimum performance using UV detection three different combinations were tested:

1. The standard 1100 Series LC system with standard bore column with an internal diameter (id) of 4.6 mm
2. The standard 1100 Series LC system with narrow bore column with an id of 2.1 mm
3. The 1100 Series capillary LC system with a capillary column of 0.3 mm id⁴

Table 1 summarizes the results for all three combinations:

The 1100 Series capillary LC system in combination with a 0.3-mm id column delivers the best limits of detection. Figure 1 shows a chromatogram representing the injection of beta-blocking drugs in the low ng range. Typically, UV detection cannot compete with fluorescence detection regarding sensitivity (figure 2). However, using capillary columns in combination with a capillary LC system instead of standard bore or narrow bore columns, comparable

limits of detection can be achieved with UV detection (table 5). A significant advantage of the UV LC system is, that all beta-blocking drug can be detected.

Limit of detection (LOD) using fluorescence detection

Fluorescence detection is a very sensitive method for the analysis of beta-blocking drugs compared to UV detection under the same chromatographic conditions, (figure 2). To evaluate this detector the following combination was tested:

| Compound | Standard 1100 Series LC system | | | 1100 Series capillary LC system | |
|-------------|--------------------------------|----------------|----------------|---------------------------------|----------------|
| | LOD DAD 220 nm | LOD DAD 220 nm | LOD DAD 290 nm | LOD DAD 220 nm | LOD DAD 290 nm |
| Pindolol | 13.49 ng | 3.12 ng | | 0.960 ng | |
| Timolol | 243.99 ng | 65.9 ng | 4.55 ng | 10.16 ng | 0.830 ng |
| Metoprolol | 61.99 ng | 16.7 ng | | 2.910 ng | |
| Propranolol | 11.89 ng | 3.1 ng | | 0.12 ng | |
| Column id | 4.6 mm | 2.1 mm | 2.1 mm | 0.3 mm | 0.3 mm |

Table 1
Limit of detection for different instrument combinations using UV detection

Chromatographic conditions:
 Column: 150 x 0.3 mm Zorbax SB C-8:
 gradient from 10 % ACN to
 80 % ACN in 20min
 Flow rate: 5 µL/min
 Column oven: 20 °C
 Detection
 wavelength: 220/10 nm with a reference
 wavelength at 500/100 nm.
 Mobile phase: water + 0.05 % TFA and
 acetonitrile + 0.045 % TFA
 was used for UV detection.

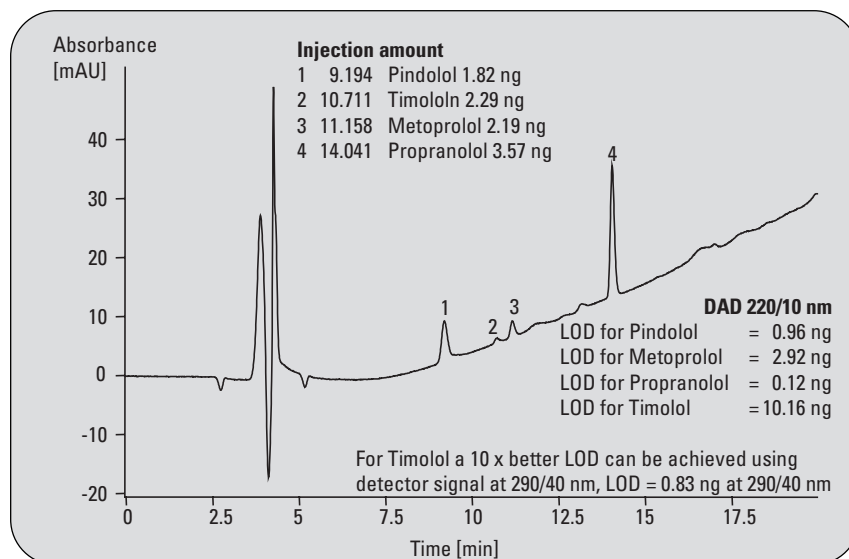


Figure 1
Limit of detection for four beta-blocking drugs, analyzed using a capillary column and diode-array UV detector

- The standard 1100 Series LC system with narrow bore column with an id of 2.1 mm

The advantage is that compounds, which have good fluorescent behavior, can be detected very sensitively and selectively. The disadvantage is that some beta-blocking drugs show only weak fluorescence, for example, Pindolol. Timolol does not fluoresce at all. Both detectors were switched in series and the signal-to-noise ratio were evaluated and compared. Except for Timolol the signal-to-noise ratios for fluorescence detection was significantly better, especially for Propranolol. The limit of detection using the fluorescence detection is in the high pg range for Pindolol and Metoprolol. For Propranolol the limit of detection is about 120 pg. Figure 3 shows a chromatogram with injected amounts in the low ng range. It is quite obvious that Propranolol shows the best limit of detection due to its very good fluorescence.

Chromatographic conditions:

Column: 30 x 2.1 mm Zorbax SB C-8;
 Gradient: 10 % ACN to 80 % ACN in 10 min
 Flow rate: 0.4 mL/min
 Column oven: 20 °C
 FLD
 wavelength: Multi signal mode Ex/EM
 = 220/320 nm and 265/320 nm
 Mobile phase: water + 0.05 % TFA and acetonitrile
 + 0.045 % TFA was used for
 FLD detection.

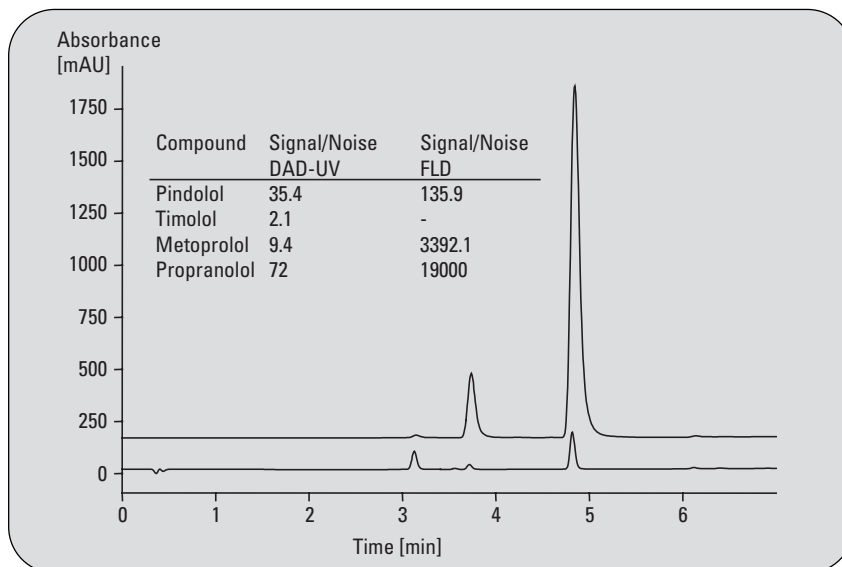


Figure 2
 Analysis of beta-blocking drugs with DAD-UV and fluorescence detection using a 2.1-mm id column

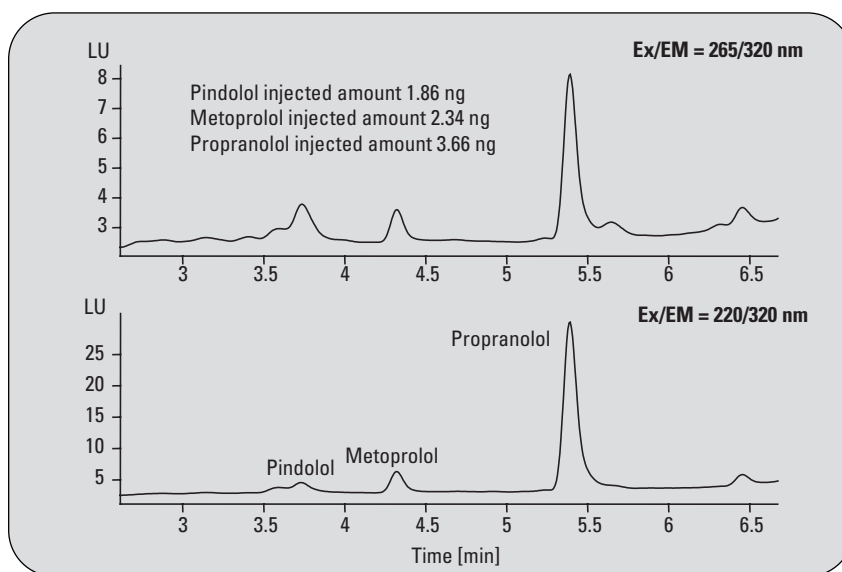


Figure 3
 Analysis of beta-blocking drugs with fluorescence detection and 2.1-mm id column in the low ng range

The limit of detection for the three compounds using fluorescence detection is summarized in table 2. The advantage of fluorescence detection is, that strongly fluorescent compounds can be detected with high sensitivity using standard 1100 LC equipment and narrow bore columns.

Limit of detection using MSD Quadrupole

To evaluate optimum performance using MS detection two different combinations were tested:

- The standard 1100 Series LC system with narrow bore column with an internal diameter of 2.1 mm
- The 1100 Series capillary LC system with a capillary column of 0.3 mm internal diameter

Using the selected ion mode (SIM) beta-blocking drugs can be detected with high sensitivity in the low pg range. (figure 4). A very powerful

Chromatographic conditions:

Column: 50 x 0.3 mm Zorbax SB C-8
 Mobile phase: Water+ 0.05 %FA, Acetonirile + 0.045 % FA
 Flow rate: 0.01 mL/min
 Gradient: at 0 min 10 % ACN, at 10 min 90 % ACN with fast reconditioning
 Injection volume: 1 µL with needle wash in flush port

MS conditions:

Source: ESI
 Peak width: 0.1 min
 Time filter: On
 SIM mode: SIM ions 249, 260, 268, 317, Fragmentor 60V, Gain 10, Actual dwell 144
 Gas temperature: 350 °C
 Drying gas: 5L/min
 Nebulizer pressure: 15 psig
 Vcap: 4000V positive
 Scan: m/z 120-450

| Compound | FLD EX/Em 220/320 | FLD EX/Em 265/320 |
|----------------------------|--|-------------------|
| Pindolol | - | 430 pg |
| Timolol | - | - |
| Metoprolol | 600 pg | - |
| Propranolol | 120 pg | - |
| Column id/LC system | 2.1 mm / Standard 1100 Series LC system | |

Table 2
Limit of detection for fluorescence detection in combination with a column of 2.1 mm id

| Compound | LOD MSD SIM | |
|----------------------------|--|---|
| Pindolol | 9.00 pg | 2.04 pg |
| Timolol | 7.70 pg | 1.86 pg |
| Metoprolol | 7.40 pg | 0.85 pg |
| Propranolol | 16.80 pg | 1.64 pg |
| Column id/LC system | 2.1 mm standard 1100 Series LC system | 0.3 mm 1100 Series capillary LC system |

Table 3
Limit of detection for Agilent 1100 Series MSD in selected ion mode using 2.1- and 0.3-mm id columns

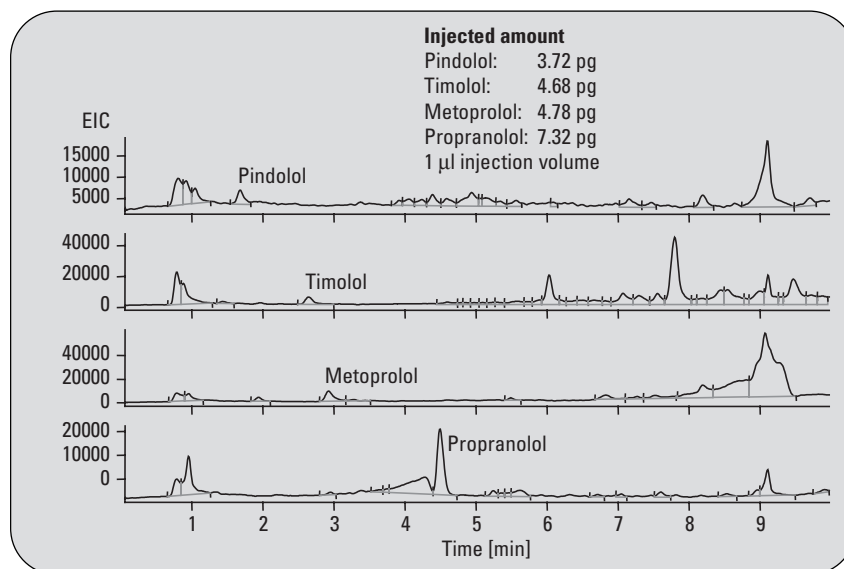


Figure 4
Limit of detection for MS quadrupole using a capillary column with 0.3-mm id

combination regarding speed and sensitivity is the combination of short capillaries with a mass spectrometer. In table 3 the results for the two combinations are summarized. The advantage of MSD quadrupole in combination with capillary columns is that the best limits of detection can be achieved. MS detection is the best choice, if beta-blocking drugs should be identified at trace levels. The advantage of the other, less sensitive detectors, is that they provide improved quantitative results. In table 4 precisions of areas are compared for all three detectors using 2.1-mm id columns.

Conclusion

The limits of detections were evaluated for different Agilent 1100 Series LC/detector systems using standard bore, narrow bore and capillary columns. For standard and narrow bore columns the standard 1100 Series LC system using DAD-UV, fluorescence and mass spectrometer were used. For capillary columns the 1100 Series capillary LC system was used with DAD-UV and mass spectrometer. The results are summarized in table 5 for a signal-to-noise ratio of 2. From this table it is obvious that the combination 1100 capillary LC/MSD is a very powerful

solution, if lowest limits of detection should be achieved.

Best quantitative data are provided if the LC/DAD-UV combination is used. For these combinations precision for areas between 0.16 and 1.02 RSD can be expected.

| Compounds | DAD RSD area (%) | FLD RSD area (%) | MSD RSD area (%) | RSD RT (%) |
|----------------------|------------------|------------------|------------------|------------|
| Pindolol (186 ng) | 0.16 | 2.70 | 2.94 | 0.11 |
| Timolol (234 ng) | 1.02 | n.a. | 1.59 | 0.06 |
| Metoprolol (239 ng) | 0.20 | 0.37 | 2.05 | 0.06 |
| Propranolol (366 ng) | 0.18 | 0.59 | 2.00 | 0.04 |

Table 4
Precision results for DAD, FLD and MSD

| Compound | LOD DAD-UV | | LOD FLD | LOD MS Quadrupole SIM mode | | |
|------------------|---------------|---------------|---------------|----------------------------|---------------|---------------|
| Pindolol | 13.49 ng | 3.12 ng | 0.96 ng | 0.43 ng | 9 µg | 2.04 µg |
| Timolol | 243.90 ng | 4.55 ng | 0.83 ng | - | 7.70 µg | 1.86 µg |
| Metoprolol | 61.99 ng | 16.70 ng | 2.91 ng | 0.60 ng | 7.40 µg | 0.85 µg |
| Propranolol | 11.89 ng | 3.10 ng | 0.12 ng | 0.12 ng | 16.80 µg | 1.64 µg |
| Column id | 4.6 mm | 2.1 mm | 0.3 mm | 2.1 mm | 2.1 mm | 0.3 mm |

Table 5
LODs for different LC/detector systems using columns with different internal diameter

References

1.

“Simultaneous determination of eight beta-blockers by gradient high-performance liquid chromatography with combined ultraviolet fluorescence detection in corneal permeability studies in vitro”, *Veli-Pekka Ranta et al., Journal of Chromatography B*, 772, pp81-87, **2002**.

2.

“Chiral separation of the enantiomers of metoprolol and its metabolites by high performance liquid chromatography”, *Kyeong HO Kim et al., Arch Pharm Res Vol 23, No 3, pp 230-236, 2000*.

3.

“Influence of various biological matrices (plasma, blood microdialysate) on chromatographic performance in the determination of beta-blockers using alkyl-diol silica precolumn for sample clean-up”, *Csilla Misl'anovanet al., Journal of Chromatography B*, 765, pp 167-177, **2001**.

4.

“Sensitive Analysis of beta blocking drugs on Agilent 1100 Capillary LC system”, *A.Gratzfeld-Huesgen, Agilent application note, Pub.No. 5988-9915EN, 2003*.

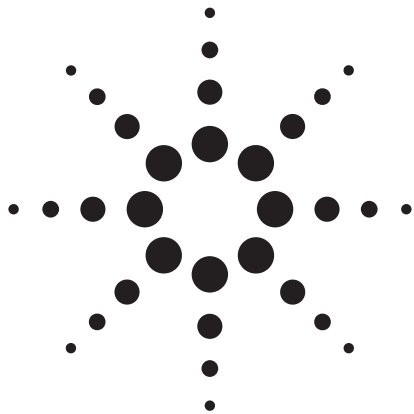
*Angelika Gratzfeld-Huesgen and
Mark Stahl are Application
Chemists at Agilent Technologies,
Waldbronn, Germany.*

www.agilent.com/chem/1100

Copyright © 2003 Agilent Technologies
All Rights Reserved. Reproduction, adaptation
or translation without prior written permission
is prohibited, except as allowed under the
copyright laws.

Published September 1, 2003
Publication number: 5988-9916EN

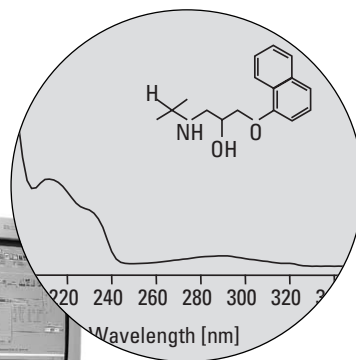
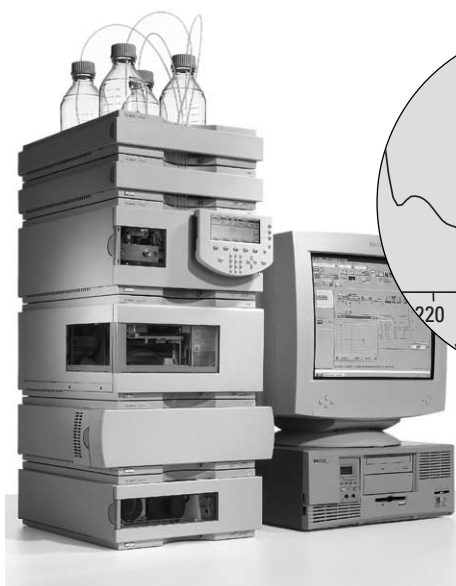




Sensitive analysis of beta-blocking drugs on the Agilent 1100 Series capillary LC system

Application

Angelika Gratzfeld-Huesgen
Mark Stahl



Abstract

This Application Note demonstrates that using capillary columns with an internal diameter of 0.3 mm and the Agilent 1100 Series capillary LC system, detection limits with good quantitative results can be achieved in the low ng range with UV detection. Further, it is demonstrated that Agilent 1100 Series capillary LC in combination with mass spectrometry provides limits of detection in the low pg range as well as safe identification.



Agilent Technologies

Introduction

Beta-blocking drugs are widely used in the treatment of hypertension and glaucoma. The determination of these compounds in biological fluids requires high standards in sensitivity and identification. The determination of the compounds in pharmaceutical formulations demands high standards regarding precision of quantitation. Typically, capillary LC provides better limits of detection compared to results obtained from columns with wider internal diameter, for the same sample amounts and comparable chromatographic conditions.

To show the performance of the Agilent 1100 capillary LC systems four beta-blocking drugs were used to determine the limit of detection and precision of the complete system. In addition, reduction of cycle time (time needed from injection to injection) and reduction of carry-over is discussed and solutions are described.

Experimental

The Agilent 1100 capillary LC system was used for all experiments. The modular system consists of:

- Agilent 1100 Series capillary pump with electronic flow control for precise flow rates even at changing back-pressure, the capillary pump was also equipped with a micro degasser with an internal volume of 1 mL
- Agilent 1100 Series micro well-plate autosampler for precise injection in the nL and μ L range with cooling option for the samples
- Agilent 1100 Series column thermostat for precise retention times at room temperature, and above or below room temperature
- Agilent 1100 Series diode-array detector equipped with a 500-nL cell for sensitive analysis of small peak volumes
- Agilent 1100 Series LC/MSD Quadrupole SL using ESI source with microspray nebulizer for identification and highly selective and sensitive analysis

Three capillary columns of the same type but of different length were selected:

- 150 x 0.3 mm Zorbax SB C-8, 3.5 μ m
- 75 x 0.3 mm Zorbax SB C-8, 3.5 μ m
- 50 x 0.3 mm Zorbax SB C-8, 3.5 μ m

Beta-blocking drugs Pindolol, Timolol, Metoprolol and Propranolol were purchased from Sigma Aldrich.

Results and discussion

Method development

Method development starts with the evaluation of the best-suited column material for the compounds of interest. Two capillary columns of different polarities were tested. In figure 1 an overlay is shown representing the analysis of four beta-blocking drugs on these two different column materials.

Considering the chemical structure of the selected beta-blocking drugs (figure 2) it is quite obvious that the pH of the mobile phase has a significant influence on peak shape and elution. Acidic conditions are preferred and as mobile phases water and acetonitrile were chosen, modified with Trifluoroacetic acid (TFA). TFA is used to improve peak shape and consequently to improve separation and the limit of detection and quantitation. For mass spectrometers TFA was replaced by formic acid (FA) to reduce ion suppression. It is quite obvious that the Zorbax SB C-8 material is better suited for this application. Separation is near baseline and peak shape is close to Gaussian peak shape because the Zorbax SB material sterically protects the siloxane bonds from hydrolytic attack at low pHs.

Chromatographic conditions:

Columns:

150 x 0.3 mm Zorbax SB C-8:

Gradient from 10 % ACN to 80 % ACN in 20 min

150 x 0.3mm ODS Hypersil C-18:

Gradient from 10 % ACN to 80 % ACN in 20 min

Column oven: 20 °C

DAD wavelength: 220/10 nm, reference wavelength at 500/100 nm.

Mobile phase: Water + 0.05 % TFA (pH = 2.2) and acetonitrile + 0.045 % TFA was used for UV detection.

For MS detection TFA was replaced by the same concentration of formic acid (FA)

Flow rate: 5 µL/min

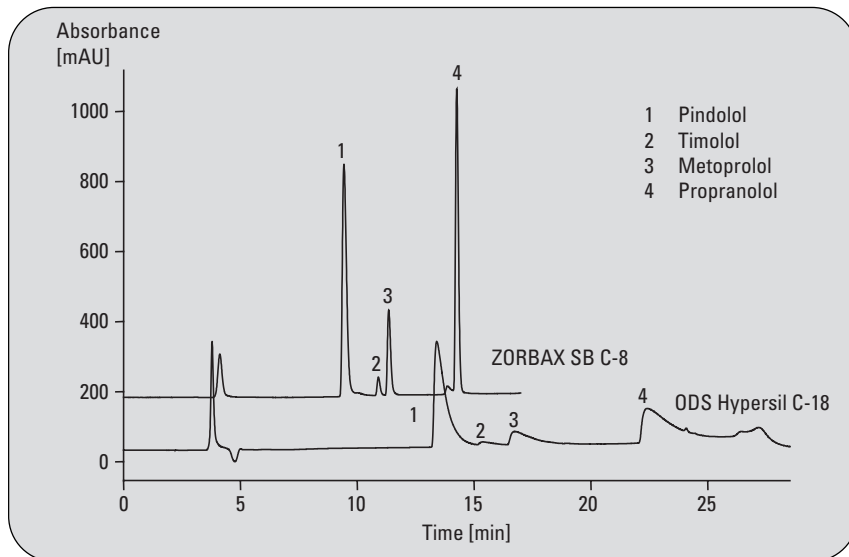


Figure 1

Analysis of four beta-blocking drugs on 23 different column materials

Hypersil is a material, which is endcapped to reduce silanol interaction. But for this application at this low pH the material shows long retention and bad peak shape due to strong interaction with the stationary phase. To find the optimum UV detection wavelength spectra for all peaks were evaluated (figure 2) and two detection wavelengths were selected. For Pindolol, Propranolol and Metoprolol the best compromise UV detection wavelength was found to be 220 nm with a bandwidth of 10 nm with a reference wavelength of 500/100 nm. Although 220 nm is not in the absolute maximum it is recommended to use a sampling wavelength, which avoids too many interferences with background noise. 220 nm are an acceptable compromise to obtain a good signal-to-noise ratio. For Timolol the best wavelength was found to be 290/40 nm with a reference at 500/80 nm.

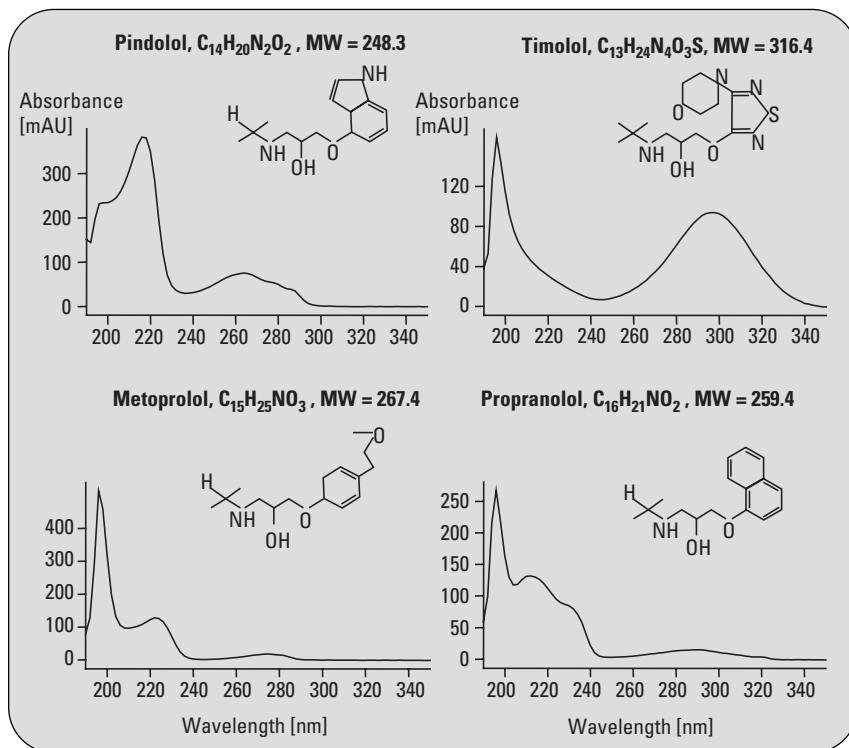


Figure 2

Evaluation of UV spectra

Especially for Timolol and Metoprolol selection of detection wavelength can significantly contribute to selectivity (figure 3). At 300 nm detection wavelength only Timolol is visible, whereas at 220 nm Metoprolol can be detected best.

Limit of detection (LOD) for UV detection

Using the evaluated instrumental and chromatographic parameters the limit of detection was determined (figure 4). For all beta-blocking drugs 220 nm was selected as detection wavelength except for Timolol. Timolol was best detected at 290 nm. The limit of detection, using 220 nm and 290 nm as detection signal, is in the range between 0.12 and 2.92 ng with a signal-to-noise ratio of two for all compounds. Nowadays, beta-blocking drugs are frequently determined using HPLC and fluorescence detection (FLD). With this instrument combination and a short 2.1-mm id column the limit of detection is less than 1 ng injected amount. A disadvantage of this method is, for example, that Timolol cannot be detected with fluorescence detection. (More information about limit of detection using different detectors and columns can be obtained from reference 1).

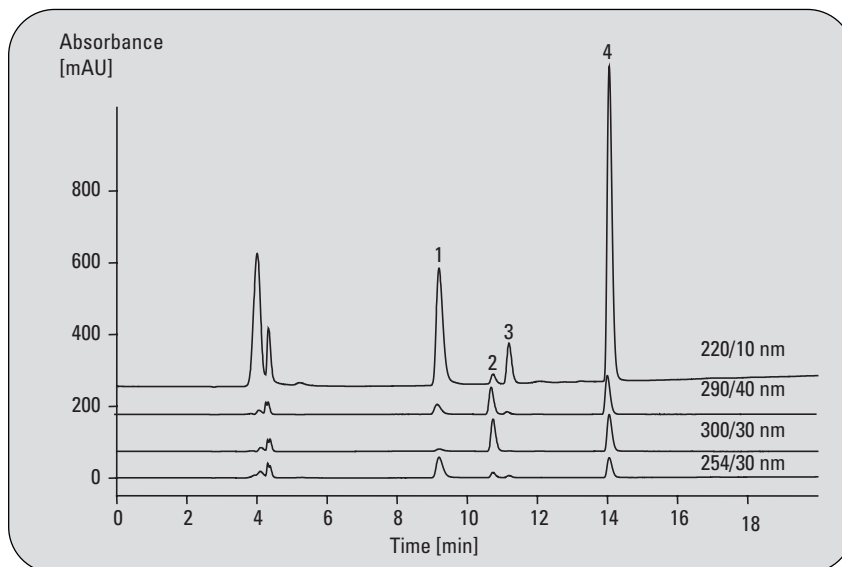


Figure 3
Analysis of beta-blocking drug at different detection wavelength

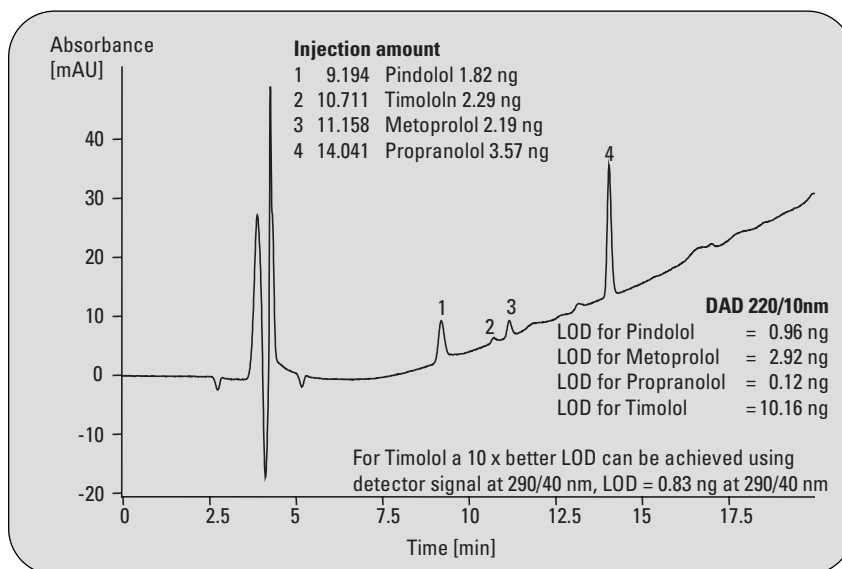


Figure 4
Limit of detection for four beta-blocking drugs, analyzed using a capillary column and diode-array UV detector

Limit of detection using MSD

Quadrupole

A very powerful combination regarding speed and sensitivity is the combination of short capillaries with a mass spectrometer. First, a higher concentration of the standards in scan mode was analyzed to determine the predominant ion formed for each analyte (figure 5), which are then used for the sensitive selected ion mode (SIM) analysis. The selected ion mode enables the detection of beta-blocking drugs in the low pg range. Figure 6 shows a chromatogram which represents the injections of beta-blocking drugs in the low pg range.

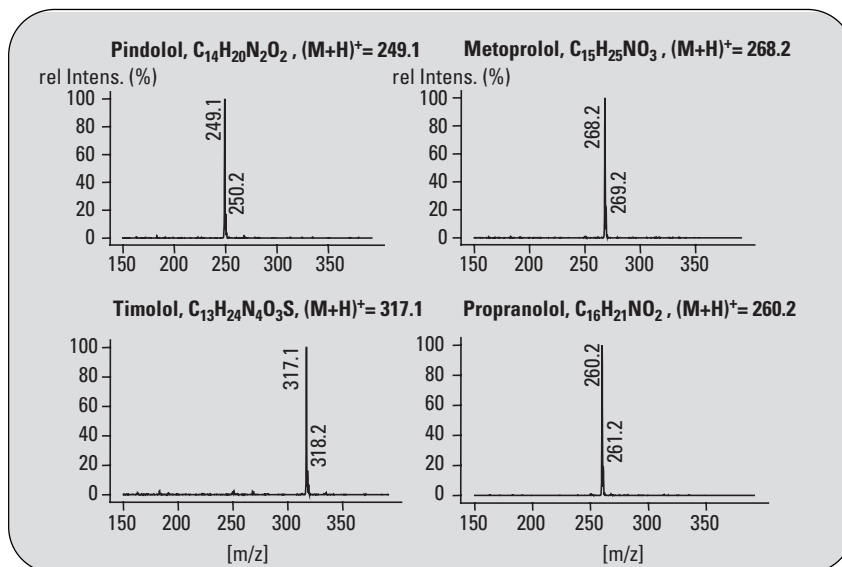


Figure 5
MS spectra of beta-blocking drugs, positive scan

Chromatographic conditions:

Column: 50 x 0.3 mm Zorbax SB C-8
Mobile phase: water+ 0.05%FA,
acetonitrile + 0.045% FA
Flow rate: 0.01 mL/min
Gradient: at 0 min 10 % ACN, at 10 min 90 %
ACN with fast reconditioning
Injection volume: 1 µL with needle wash
in flush port

MS conditions:

Source: ESI
Peak width: 0.1 min
Time filter: On
SIM mode: SIM ions 249, 260, 268, 317,
Fragmentor 60, Gain 10,
Actual dwell 144
Gas temperature: 350 °C
Drying gas: 5 L/min
Nebulizer
pressure: 15 psig
Vcap: 4000V positive
Scan: m/z 120-450
Fragmentor: 60 V

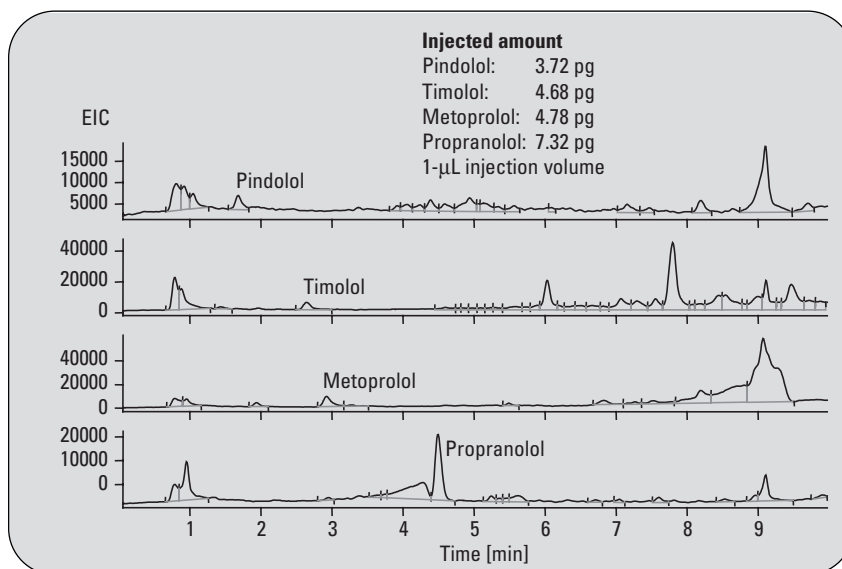


Figure 6
Limit of detection for MS quadrupole using a capillary column with 0.3-mm id

Precision of Agilent 1100 Series capillary LC systems

Typically the following precision results can be obtained for UV detection:

- Relative standard deviation for retention times < 0.1 %
- Relative standard deviation for areas between 0.5 % and 1 %

Typically for mass spectrometers the following precision can be obtained for quantitative results

- 3 % to 5 % for the relative standard deviation for areas for a well developed ESTD method

For more information about the performance of the Agilent 1100 Series capillary system see reference 2. Which LC/detection system is appropriate depends on the application area. For trace analysis in biological fluids capillary LC with short capillary columns and MS detection with selected ion mode is a powerful solution. If concentrations in pharmaceutical formulations should be determined capillary LC with 150-mm capillary columns and DAD-UV detection is a solution which provides precise quantitation and high peak resolution.

Cycle times (injection to injection)

It is obvious that the capillary column with 150 mm length shows the longest cycle times with 35 minutes. Figure 7 shows a chromatogram obtained from a short capillary column applying a high

0.3 x 50 mm column, MS detection
Flow rate: 0.01 mL/min
Gradient: 10 % B to 90 % B in 10 min
Automatic delay volume reduction
Fast reconditioning

flow rate. For the application described here cycle times of 10 to 15 minutes, depending on the needed cleaning and equilibration time, can be obtained when using a 50-mm capillary. Decreasing the column length and increasing the flow rate and gradient steepness are the most important parameters to reduce cycle times. This can also help to further increase the signal-to-noise ratio and therefore helps to improve the limit of detection. On the other hand, resolution may suffer. For exact quantitation with UV detection baseline separation of all peaks is desirable, whereas exact identifi-

cation using a mass spectrometer is also possible for co-eluting peaks. Which system is best suited depends on whether the exact concentration in a pharmaceutical formulation should be determined or whether compounds should be identified in a biological sample where quantitation is of second priority. In addition, the Agilent 1100 Series capillary LC system offers two instrument parameters to reduce cycle times

- Automatic delay volume reduction in the autosampler set up screen
- Fast reconditioning in the pump set up screen

| Compounds | LOD MSD SIM | LOD DAD at 220 and 290nm |
|-------------|-------------|--------------------------|
| Pindolol | 2.04 pg | 0.96 ng |
| Timolol | 1.86 pg | 0.83 ng |
| Metoprolol | 0.85 pg | 2.91 ng |
| Propranolol | 1.64 pg | 0.12 ng |

Table 1
Limit of detection for detection of beta-blocking drugs with MS quadrupole and diode-array UV detection and 0.3-mm id capillary column

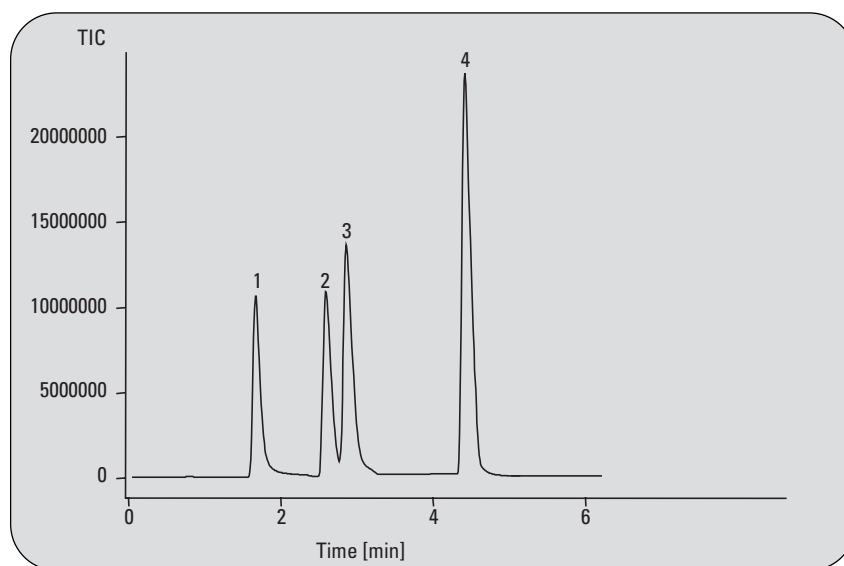


Figure 7
Reduction of cycle time using shorter capillary columns, higher flow rates and steep gradients

Automatic delay volume reduction means that the auto sampler delay volume is switched out of the flow path after the injected compounds have reached the top of the column. This ensures that gradient changes can reach the column without passing the autosampler delay volume.

Fast reconditioning means that the volume in front of the column is flushed after the run with a high flow rate (highest possible flow is set based on pressure) for fast equilibration. For this time the column is out of the flow path and is then equilibrated with the original column flow rate.

Carry over

When highly concentrated samples are injected, it is recommended to:

- clean the needle exterior using the flush port, where the needle is cleaned with fresh solvent. This also ensures that the needle seat is not contaminated with residues remaining at the outside of the needle
- perform fast reconditioning to rapidly clean with high flow rate the interior of the needle and all other autosampler parts, which can come in contact with the sample.

It is not recommended to only use the automatic delay volume reduction (table 2). Activating only the fast reconditioning parameter will reduce carry-over, but cycle time will increase, because the autosampler delay volume is not switched out of the flow path and gradient changes will therefore reach the column later. A good compromise is to activate fast

reconditioning and to set up an appropriate injector program. This will minimize carry-over and keeps cycle times in a reasonable time range. In table 2 results are shown using different set-ups for the injector and the pump. Based on these experiments the following was evaluated:

- Influence on carry-over and cycle time, if *Automatic delay volume reduction* is used
- Influence on carry over and cycle time, if *Fast reconditioning* is used and no *Automatic delay volume reduction*
- Influence on carry-over and cycle time, if *Fast reconditioning* with injector program is used

The injector program does two things:

- first, it switches the autosampler delay volume out of the flow pass (bypass) to save cycle time
- secondly, it cleans with additional valve switching events the injector rotor seal grooves and flow lines, which are without flow during bypass of the autosampler. This ensures that residues are swept out and carry over is reduced.

The combination of fast reconditioning and this injector program is ideally suited to keep cycle time and carry over in acceptable ranges. Propranolol is one of the critical compounds for carry-over where-

| Compounds | Automatic delay volume reduction only | Fast reconditioning only** | Fast reconditioning and injector program* |
|-------------------|---------------------------------------|----------------------------|---|
| Pindolol | Carry over=0.51 % | Not measurable | Not measurable |
| Timolol | Carry over=0.44 % | Not measurable | Not measurable |
| Metoprolol | Carry over=0.44 % | Not measurable | Not measurable |
| Propranolol | Carry over=1.34 % | Carry over=0.058 % | Carry over=0.051 % |
| Cycle time | 35 min | 40 min | 35 min |

Chromatographic conditions:

Column: 150 x 0.3 Zorbax SB C-8

**Pump control:

Column Flow: 5.000 µL/min

Stoptime: 20.00 min

Fast Reconditioning: On (*All flow lines are flushed in front of the column to reduce carry over*)

Posttime: 15.00 min

*Injector program table

- 1 DRAW 1.000 µL from sample, def. speed, def. offset
 - 2 NEEDLE wash as method
 - 3 INJECT
 - 4 WAIT 1.50 min
 - 5 VALVE bypass (*Auto sampler delay volume is switched out of the flow path to reduce cycle time*)
 - 6 WAIT 15.00 min
 - 7 VALVE mainpass
 - 8 WAIT 1.00 min
 - 9 VALVE bypass
 - 10 VALVE mainpass
- } (*Cleaning of the injection valve to reduce carry over*)

Table 2
Cycle times and carry over data with different instrument set up

as all other compounds do not show any carry-over if fast reconditioning only or in combination with the above mentioned injector program is used. Carry over is as low as 0.051 % for propranolol if optimum conditions are applied.

Conclusion

The Agilent 1100 Series capillary LC/UV/MSD system provides highly sensitive analysis of beta-blocking drugs. Whereas mass spectrometry allows the identification and detection in the low pg range, DAD UV detection using a 500-nL cell allows the detection of beta-blocking drugs in the low ng range with good quantitative results. The precision for retention times is typically below 0.1 % relative standard deviation for both detection systems. UV detection in the low ng range shows a precision for areas of below 0.5 % relative standard deviation. Using the mass spectrometer the relative standard deviation for areas in the low ng range is around 3 % relative standard deviation. Optimizing column length, flow rate and instrument parameters cycle times can be as low as 10 to 15 minutes even for capillary columns. If highly concentrated samples are injected the instrument set up should include an appropriate injector program. This helps to keep carry-over to nearly zero for Pindolol, Timolol and Metoprolol. Propranolol shows a carry-over in the 0.05 % range under the conditions used, which is still very low.

References

1. "Analysis of beta blocking drugs on Agilent 1100 Series LC systems using UV, fluorescence and mass spectrometer detection", *Agilent Application Note, publication number 5988-9916EN, 2003.*
2. "Performance characteristics of the Agilent 1100 Series capillary LC system using diode-array and MS for detection", *Agilent Technical Note, Publication number 5988-7511EN, 2002.*

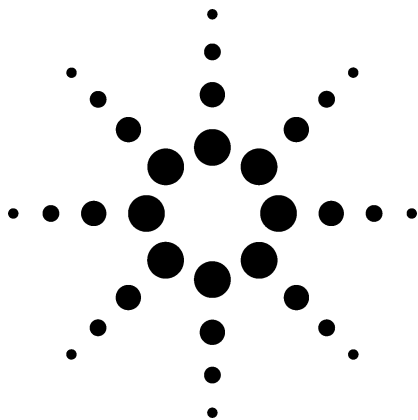
Angelika Gratzfeld-Huesgen and Mark Stahl are Application Chemists at Agilent Technologies, Waldbronn, Germany.

www.agilent.com/chem/1100

Copyright © 2003 Agilent Technologies
All Rights Reserved. Reproduction, adaptation or translation without prior written permission is prohibited, except as allowed under the copyright laws.

Published September 1, 2003
Publication number: 5988-9915EN





Screening and Qualitative Identification of Antioxidant Polymer Additives by HPLC with UV/VIS and APCI-MS Detection

Application

Consumer Products

Author

Michael Woodman
Agilent Chemical Analysis Solutions
Wilmington, DE
USA

Abstract

Liquid chromatography with ultraviolet/visible spectroscopy and mass selective detection is a powerful approach to antioxidant analysis and identification. Examples illustrate that mobile-phase conditions affect the quality and usability of the acquired data. Unknown compounds can be identified with sufficient MS data and additive degradation can be quickly evaluated.

Introduction

Plastic products are an essential part of our lives today. Whether they are used for automotive components, CDs, toys, or biocompatible replacement parts for humans, they are the subjects of intense research into new and improved polymers and blends. Equally important is the selection and quantity of chemical additives which are used to provide color, density, opacity, stiffness, flexibility, resistance to heat, light and air, flame retardance, and to improve processing properties during pellet creation and final product fabrication.

This application note examines several antioxidant (AO) types, their chemical composition, and suitable high-performance liquid chromatography (HPLC) conditions for assessing their concentration and identity, as well as their degradation products.

AOs arise from various compound classes including small hindered phenols, large hydrophobic hindered phenols, and phosphite or phosphonate linked aromatics. Examples appear in Tables 1 and 2.



Agilent Technologies

Table 1. AO Studied with Structures

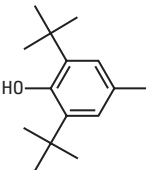
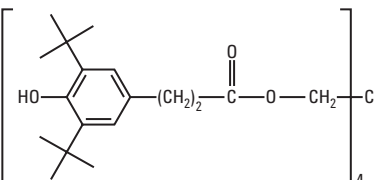
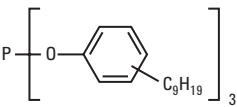
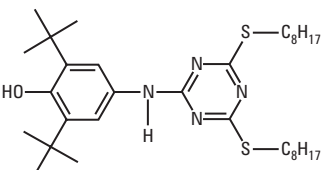
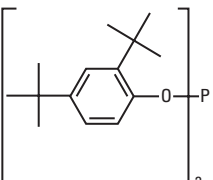
| | | |
|---------------------------|-----------------------------|---|
| Name: | BHT | Butylated hydroxytoluene |
| Formula: | $C_{15}H_{24}O$ |  |
| Molecular Weight: (MW) | 220.2 | |
| Trade name: | Irganox 1010 (CibaGeigy) | Pentaerythritol tetrakis(3-(3,5-di-tert-butyl-4-hydroxyphenyl) propionate) |
| Formula: | $C_{73}H_{108}O_{12}$ |  |
| Molecular Weight: (MW) | 1176.8 | |
| Trade name: | Naugard P (Uniroyal) | Tris nonylphenyl phosphite |
| Formula: | $(C_{15}H_{23}O)_3P$ |  |
| Molecular Weight: (MW) | 688.5 | |
| Trade name: | Irganox 565 (CibaGeigy) | |
| Formula: | $C_{33}H_{56}N_4OS_2$ |  |
| Molecular Weight: (MW) | 588.4 | |
| Trade name: | Irgafos 168 | |
| Formula: | $C_{42}H_{63}O_3P$ |  |
| Molecular Weight: (MW) | 646.5 | |

Table 2. Other Common AOs

| Name | Formula | MW |
|-----------------|----------------------|--------|
| BHA | $C_{11}H_{16}O_2$ | 180.1 |
| t-BHQ | $C_{10}H_{14}O_2$ | 166.1 |
| Cyanox 1790 | $C_{42}H_{57}N_3O_6$ | 699.4 |
| Ethanox 330 | $C_{54}H_{76}O_3$ | 772.6 |
| Irganox 1076 | $C_{35}H_{62}O_3$ | 530.5 |
| Sandostab P-EPO | $C_{68}H_{92}O_4P_2$ | 1034.6 |

Gas chromatographs with conventional detectors or mass spectrometers (MS) can readily analyze many small molecules; however, the increased molecular weight (MW) and decreased volatility of many AOs makes gas chromatography (GC) generally unsuitable. Liquid chromatography (LC) is a common choice because it can analyze materials exhibiting a wide MW range and varied solubility. Since LC is generally a nondestructive technique, it offers the possibility of compound isolation and recovery.

Many AOs contain functionalized aromatic groups and offer distinctive ultraviolet/visible spectroscopy (UV/VIS) spectral opportunities. This detector type is an essential part of an additive analysis system. Since UV/VIS detectors are relatively insensitive to the chromatographic mobile phase, they are readily compatible with gradient-elution separation methods.

The presence of functionalized aromatic rings, oxygen, nitrogen, phosphorous, and sulfur in many of the AOs also makes them ideal candidates for investigation by atmospheric pressure ionization mass spectrometry (API-MS). Compound identity can be supported by matching retention data, UV/VIS spectra, and from the MS, a molecular ion (essentially giving the molecular weight of the compound). Depending on the type of ionization and MS chosen, further identification can be made where higher energy is employed, causing fragmentation of the molecules. These fragments help experienced users propose chemical structures.

Instrumentation and General Method

Agilent 1100 LC system:

- Quaternary gradient pump with low volume degasser
- Binary gradient pump with degasser, for pre-MSD reagent addition
- ALS automatic sampler with 2-mL vial tray
- Thermostatted column compartment with automated 6-port, 2-position switching valve
- Diode array UV/VIS spectrophotometer

General chromatographic conditions:

- Gradient elution of increasing organic-solvent strength with combinations of:
 - Water/Acetonitrile (ACN)
 - Water/Methanol (MeOH)
 - Water/Methanol/Tetrahydrofuran (THF), HPLC grade
- UV/VIS spectral-data collection from 200–400 nm, 1-nm slit, 4 nm resolution
- UV/VIS single-wavelength collection for 210 and 280 nm, at 4 nm resolution

ChemStation PC Data and Control System

Mass selective detector (MSD) SL single quadrupole MS with APCI interface

Fragmentor: 100 V, positive and negative ionization

Vaporizer: 400 °C

Nebulizer: 50 psi nitrogen

Drying gas: 6 LPM Nitrogen

Column: Zorbax XDB-C8, 4.6 mm id × 50 mm L, 3.5 μm particles

Gradients:

Method 1. "MeOH/THF", Column 30 °C, 25 min cycle

| Flow | Time | % Water | % MeOH | % ACN | % THF |
|------|------|---------|--------|-------|-------|
| 1 | 0 | 40 | 50 | 0 | 10 |
| 1 | 15 | 0 | 90 | 0 | 10 |
| 1 | 20 | 0 | 90 | 0 | 10 |
| 1 | 21 | 40 | 50 | 0 | 10 |

Method 2. "MeOH", Column 40 °C, 20 min cycle

| Flow | Time | % Water | % MeOH | % ACN | % THF |
|------|------|---------|--------|-------|-------|
| 1 | 0 | 40 | 60 | 0 | 0 |
| 1 | 10 | 0 | 100 | 0 | 0 |
| 1 | 15 | 0 | 100 | 0 | 0 |
| 1 | 16 | 40 | 60 | 0 | 0 |

Method 3. "ACN", column 50 °C, 20 min cycle

| Flow | Time | % Water | % MeOH | % ACN | % THF |
|------|------|---------|--------|-------|-------|
| 1 | 0 | 40 | 0 | 60 | 0 |
| 1 | 10 | 0 | 0 | 100 | 0 |
| 1 | 15 | 0 | 0 | 100 | 0 |
| 1 | 16 | 40 | 0 | 60 | 0 |

Experimental Results

Figures 1 through 3 are overlaid UV chromatograms for nine AOs, using three different gradients.

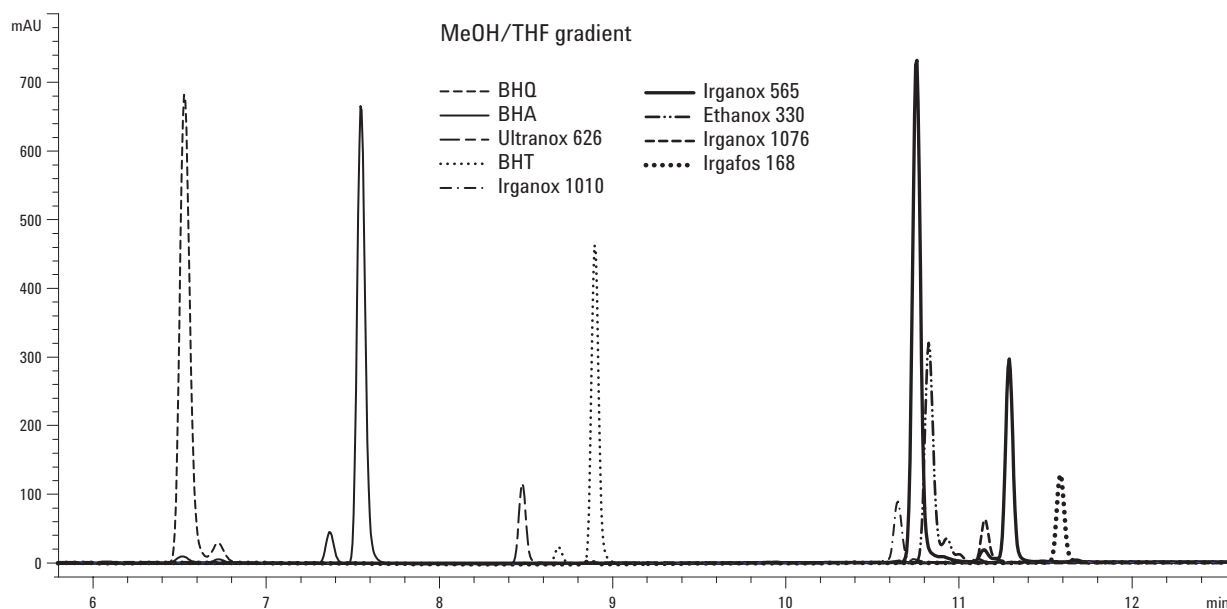


Figure 1. Overlaid UV chromatograms for the selected AOs using the methanol/THF gradient.

Many samples have minor peaks originating from impurities or degradation products having structures similar to the parent molecules. For the smaller molecules like BHA, BHQ, and BHT, there is no problem with resolution. For larger

molecules, there is reduced resolution in the 10- to 12-minute region. These molecules have unique MWs, though, and can be analyzed using selective MS detection.

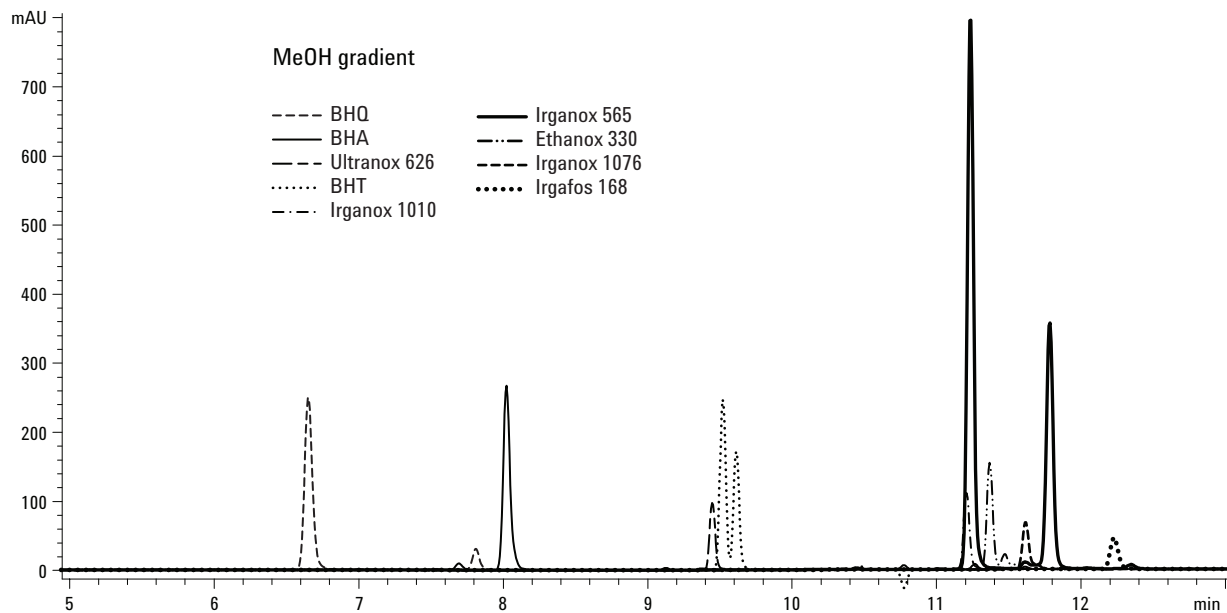


Figure 2. Separation of AOs using the MeOH gradient.

Using the MeOH gradient, relative separation is somewhat different, and as before, the smaller molecules are well resolved. The larger molecules in the 11- to 12-minute region exhibit reduced resolution, but can be analyzed using selective MS detection.

Figure 3 shows the separation of the same AOs using the ACN gradient.

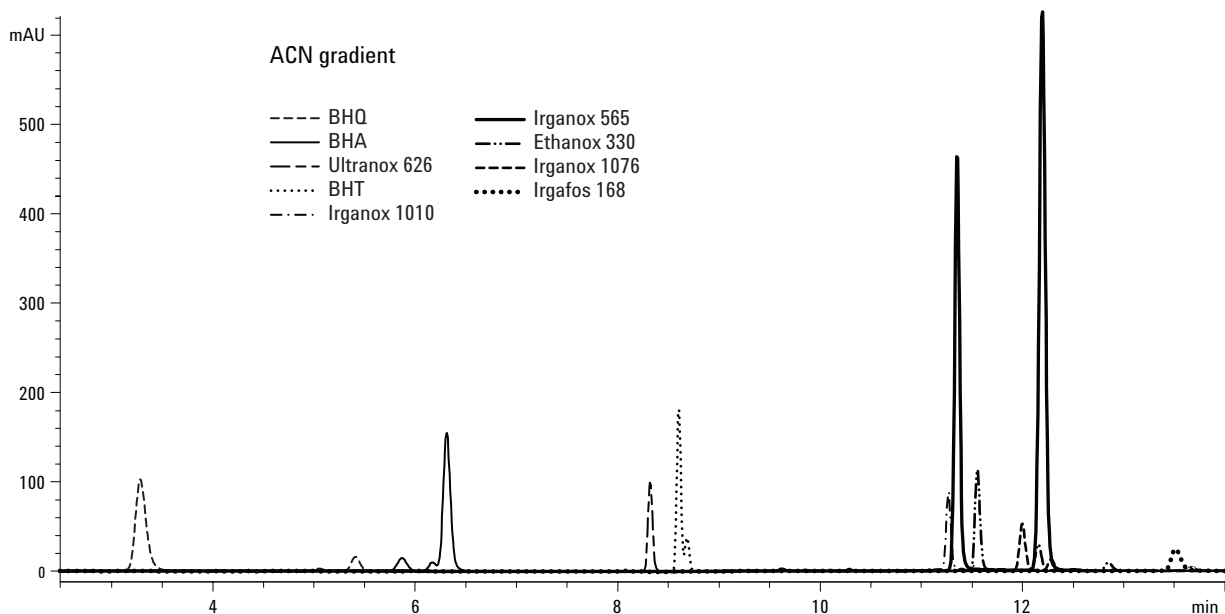


Figure 3. Separation of AOs using the ACN gradient.

Once again, no problem exists with resolution of the smaller molecules. For larger molecules in the 11- to 12-minute region there is somewhat better resolution. ACN has the best UV transparency at low wavelengths, maximizing baseline stability in the wavelength range where UV response would be observed for the AOs.

It is often attractive to use UV/VIS libraries to tentatively identify components in the sample

mixture. This approach is especially useful when the various analytes have distinct spectra. Where many AOs have phenolic rings with characteristic UV/VIS spectra, distinguishing analytes by this approach is difficult and the user must rely on retention time data to support any identification attempt.

As we investigate various AO molecules, it is useful to note the general mass range for single- and multiple-ring structures. See Figure 4.

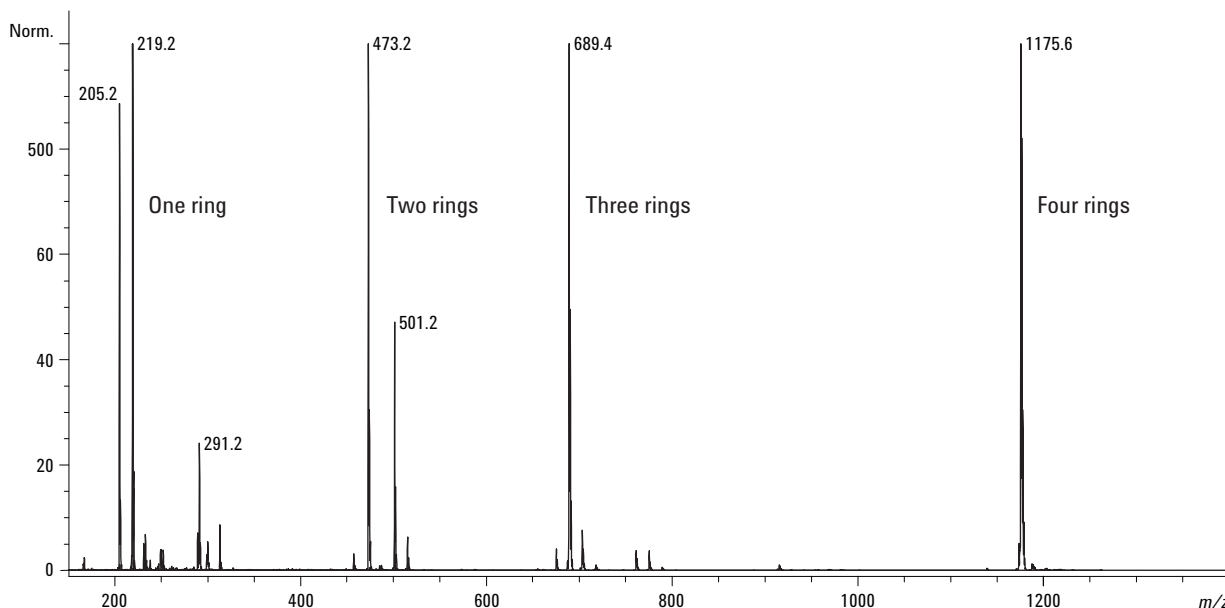


Figure 4. Overlaid AO mass spectra, illustrating effect of ring number on observed mass range.

In Figure 4 we see intact and fragmentation ions representing structures from one to four aromatic rings. The m/z 219 is $[M-H]^-$ for BHT while m/z 205, less one CH_2 , is a fragmentation ion of a larger molecule having the hindered phenolic feature. The m/z 473 and m/z 501 are fragments discussed later in this text. The m/z 689 is Naugard P, $(C_{15}H_{23}O)_3P$. The m/z 1176, Irganox 1010, $(C_{73}H_{108}O_{12})$ has four rings and long alkyl chains that increase the mass and remind us that it is important to acquire mass data well over 1000 Da for general AO screening and analysis.

The mobile phase absorbance background invariably affects UV/VIS spectra. See Figure 5. In this example, the UV/VIS spectra for Irgafos 168 are shown for the three previously described solvent conditions.

Significant differences in response, especially in the important low UV range, are generally observed. This interference is also found with many ionic modifiers added to the mobile phase to control ionization of analytes, possibly improving the separation or enhancing ionization of the compounds in the MS.

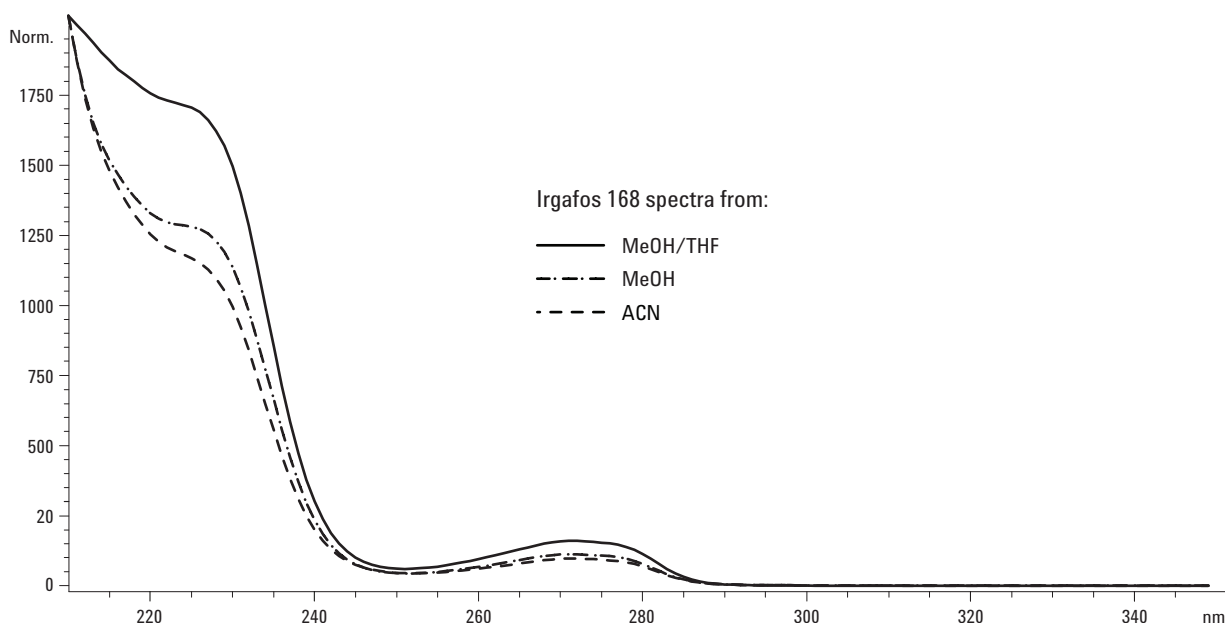


Figure 5. Solvent effects on UV/VIS spectra for Irgafos 168.

Ionization, and thus ion abundance in the MS, may also be affected by the mobile phase composition.

In Figure 6, the extracted positive-ion spectra for Irgafos 168 (molecular weight 646.5, detected as the $[M+H]^+$ ion) appear in the three previously described solvent conditions, where it elutes in high organic concentrations. Observe the significant differences in response, with the lowest response in ACN. Reduced response from the molecular ion may be from decreased ionization or increased fragmentation. It may be possible to add

modifiers after the UV, and prior to the MSD inlet, to enhance MS response in circumstances where the solvent offers chromatographic or UV/VIS advantages but negatively impacts ionization in the MS.

The degree of fragmentation in the MS may also be affected by the mobile-phase composition. In Figure 7, the extracted negative-ion spectra for Irgafos 168 appear in the three previously described solvent conditions.

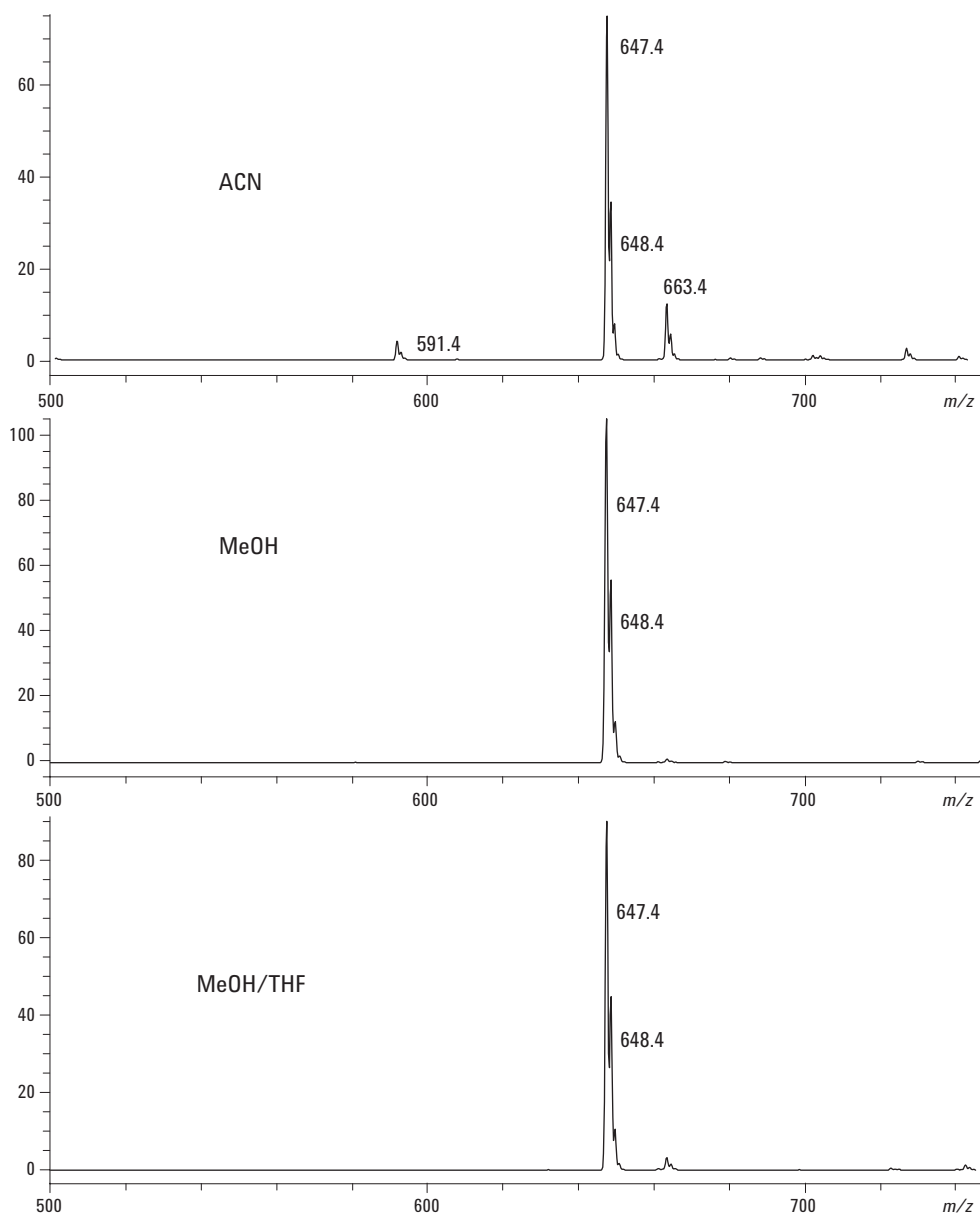


Figure 6. Solvent effects on positive-ion MSD spectra for Irgafos 168.

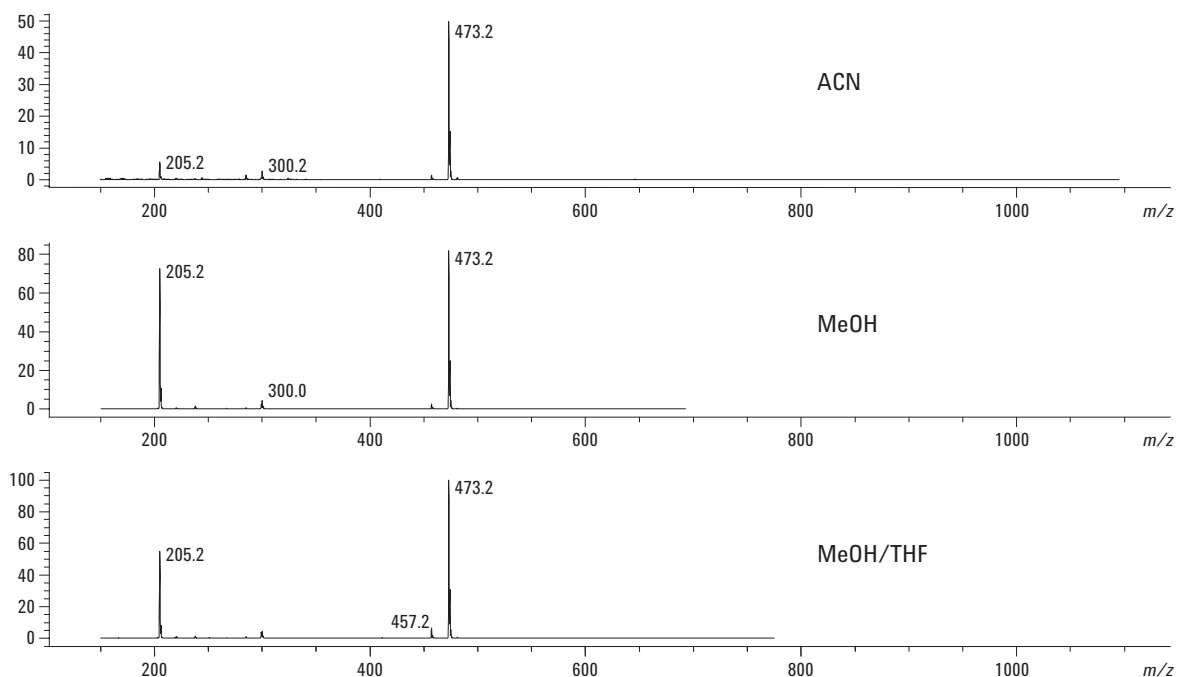


Figure 7. Solvent effects on negative-ion MSD spectra for Irgafos 168.

Note the significant differences in response with the lowest response in ACN. Reduced response for the molecular ion and fragment ions suggests that the ACN response is simply reduced ionization. Based on known degradation chemistry of Irgafos 168 and similar compounds, the m/z 473 fragment is likely $[C_{28}H_{42}O_4P]^-$ where an “arm” is lost (m/z 205) and an oxygen remains on phosphorous as $P=O$.

Identification of Unknowns

Retention data may allow experienced chromatographers to suggest how an unknown peak might differ structurally from a group of knowns run under the same conditions, but identification invariably takes far more resources than simple elution patterns provide. From UV/VIS data, we

can often suggest molecule class, especially so in our discussion of compounds commonly having the phenoxy group in the chemical structure. UV/VIS spectra may be suggestive but, when used without significant prior knowledge, lack sufficient resolution to confirm identity. MS data, on the other hand, have the spectral resolution necessary to infer structural details leading to actual chemical identification. The following examples describe several situations in which either detector would be helpful.

In the simple case of an unknown containing either BHA or BHT, the UV spectra (Figure 8) are sufficiently unique to allow a reasonable identification along with characteristic retention data. Nearly 1.5 minutes separate these two peaks in the conditions above and little doubt would remain.

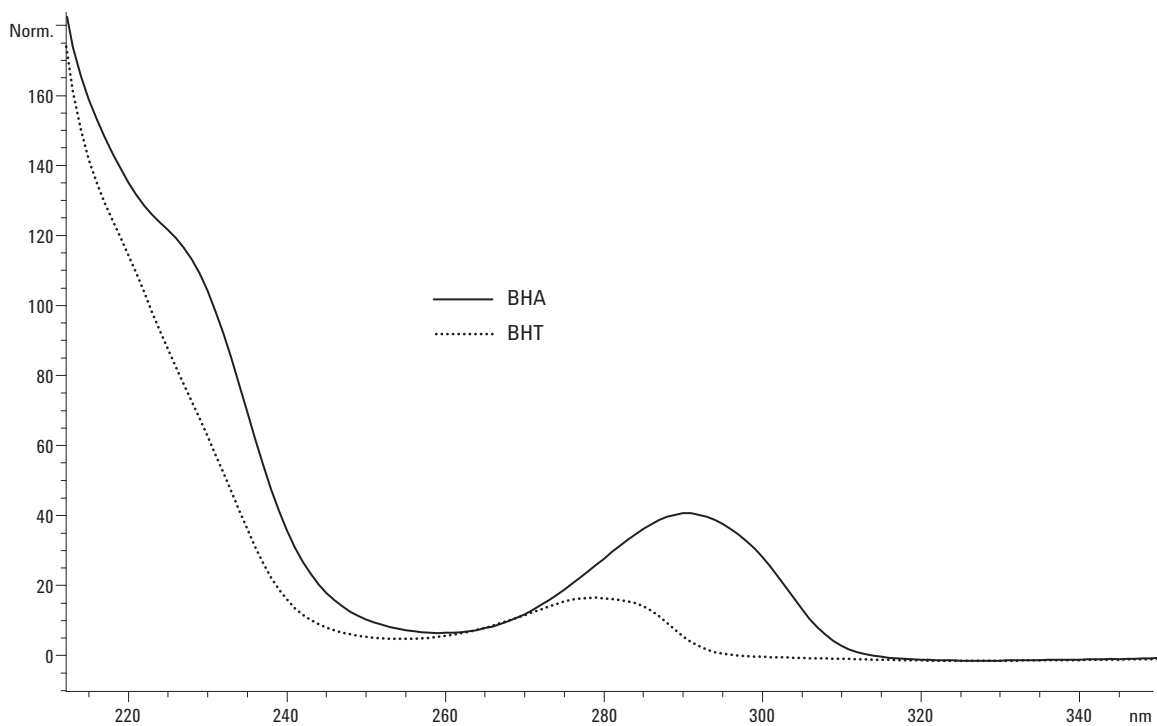


Figure 8. Extracted UV spectra from mixture containing only BHA and BHT.

Using MS data for the same sample, we would reach similar conclusions. See Figure 9.

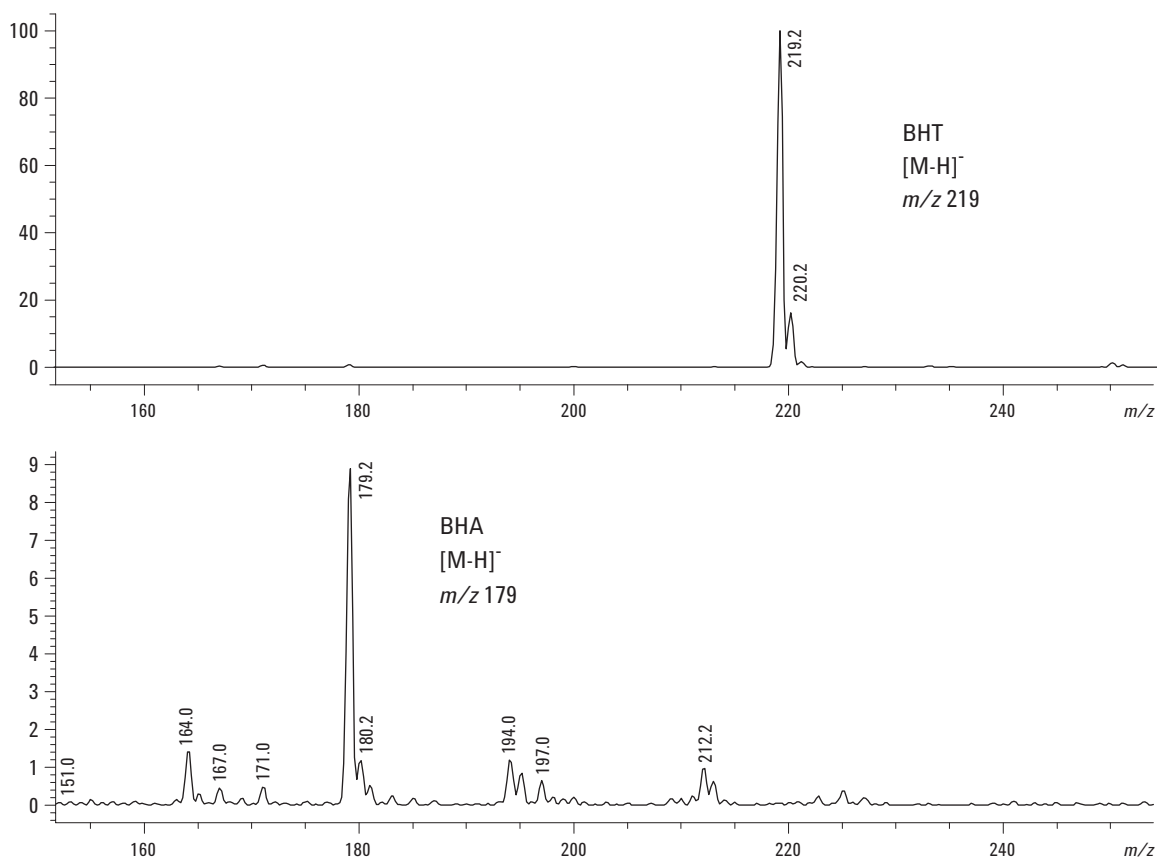


Figure 9. Extracted negative-ion MS spectra from mixture containing only BHA and BHT.

Retention data suggests two distinct molecules leading to an unambiguous identification without any need for MS fragmentation data.

When examining MS data, we generally expect to see classic molecular ions, either molecular mass+1 in positive-ion mode or mass-1 in negative-ion mode. These conditions, in the absence of significant adduct or fragment ion formation, often yield the best sensitivity and quantitative result. Such is the case in the Irganox 565 example shown in Figure 10.

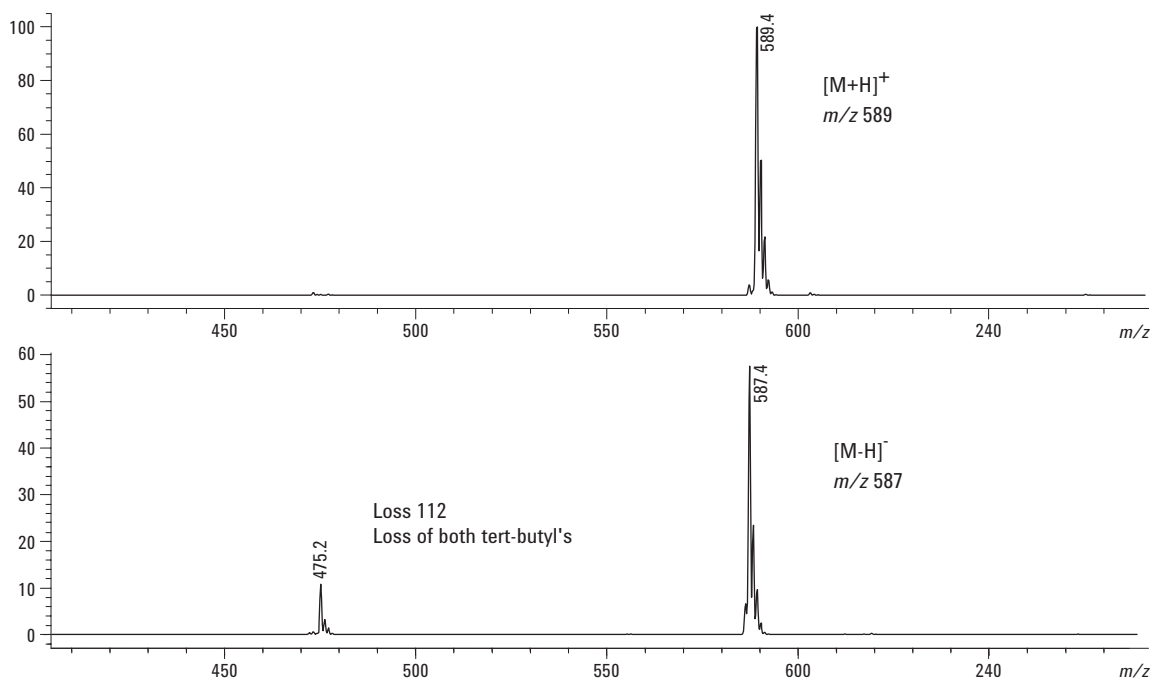


Figure 10. Positive- (upper) and negative- (lower) ion spectra for Irganox 565, using MeOH/THF gradient.

Only minor amounts of fragmentation are seen in the negative-ion spectrum, corresponding to the loss of both tert-butyl groups. In some cases, a radical ion is formed and the MS ion observed will correspond to the mass of the parent molecule. It is difficult to predict when this may occur, but the user must be prepared to interpret the spectral data with this situation in mind.

Irganox 1010 was run under the same conditions and produced minimal fragmentation in the negative-ion spectrum. An $[M-H]^-$ ion at m/z 1175.6 is detected for the expected MW 1176.8. See Figure 11.

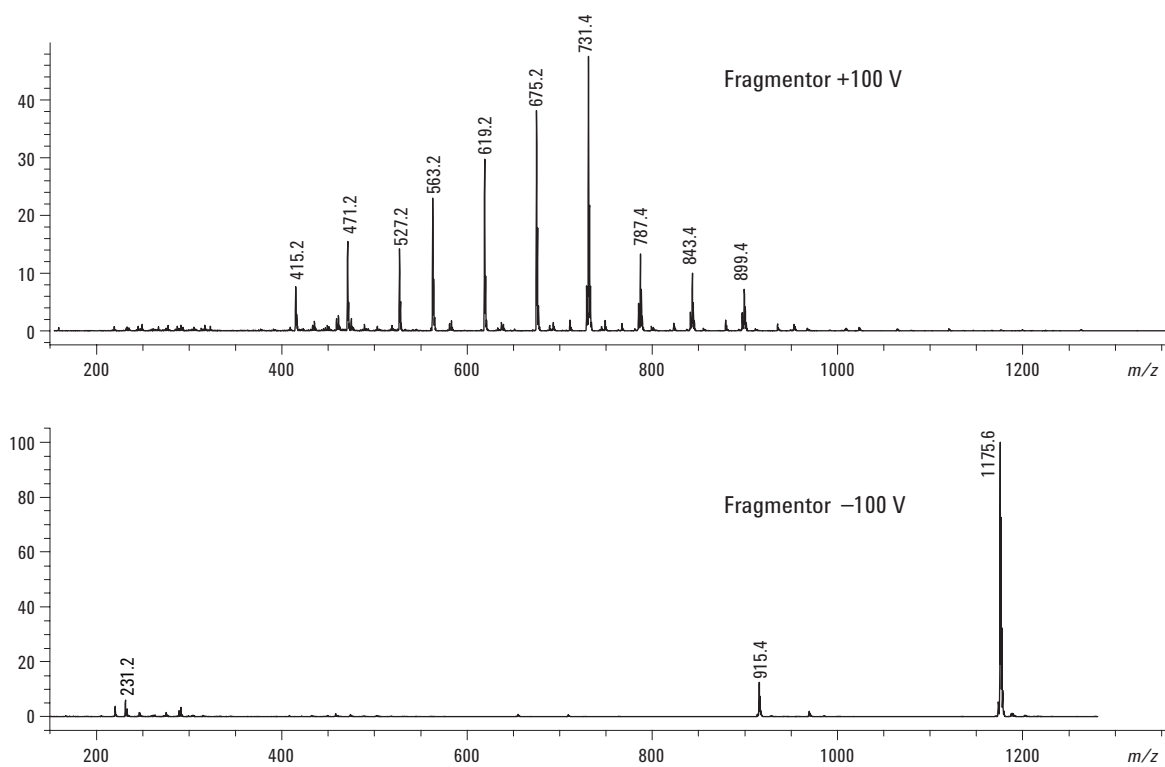


Figure 11. Positive- (upper) and negative- (lower) ion spectra for Irganox 1010, using MeOH/THF gradient.

The positive-ion spectrum, however, is devoid of any useful amount of the molecular ion. The resulting fragmentation pattern suggests a molecule with a significant number of tert-butyl structures which, with the molecular ion from negative ionization, is consistent for a tentative identification for the named compound.

Little change is observed in the fragmentation pattern by reducing the fragmentor voltage to 25 V, though overall ion production is reduced from the 100 V experiments. See Figure 12.

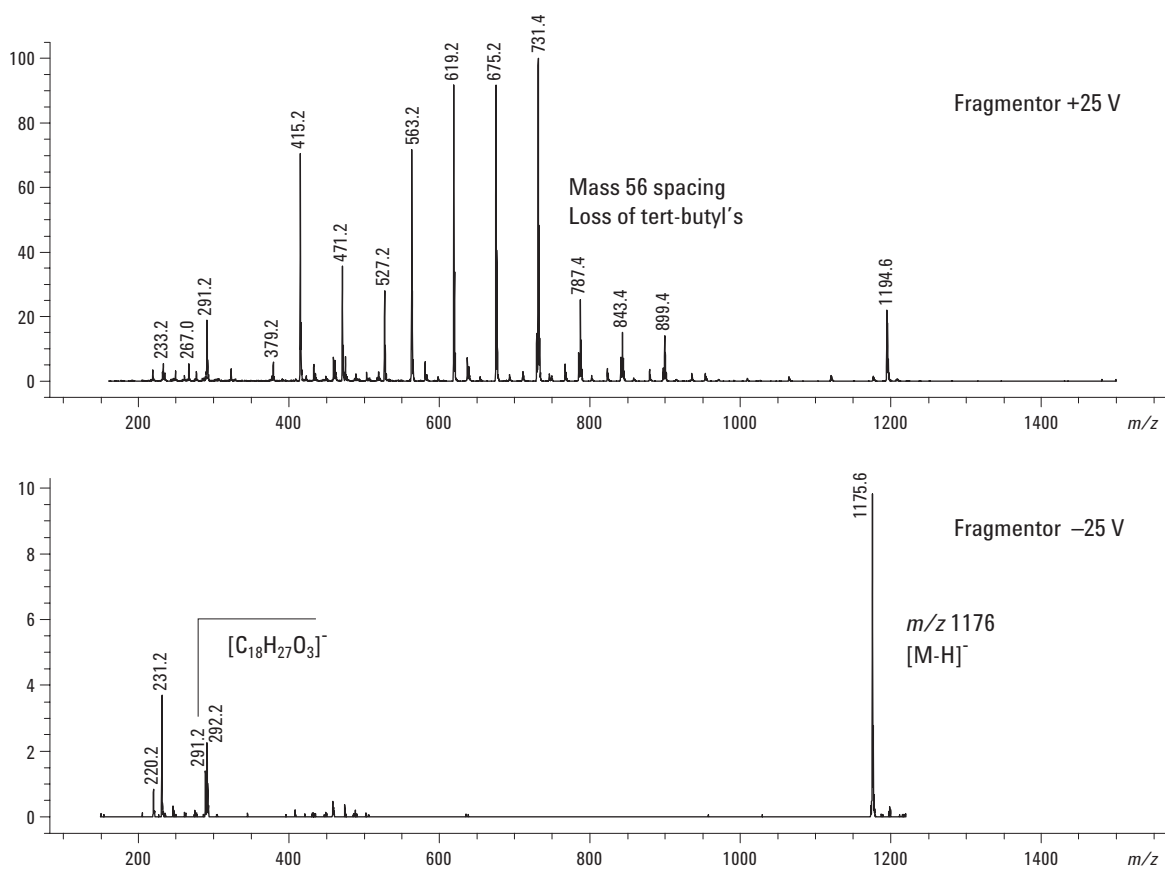


Figure 12. Positive- (upper) and negative- (lower) ion spectra for Irganox 1010, using MeOH gradient.

An m/z 291 fragment ion can be observed, which corresponds to one of the symmetrical "arms" of the molecule.

The positive- and negative-ion spectra extracted from the main peak in a degraded standard of Naugard P appear in Figure 13. Naugard P responds comparably to the Irganox 1010 in positive-ion mode, yielding an easily observed molecular ion.

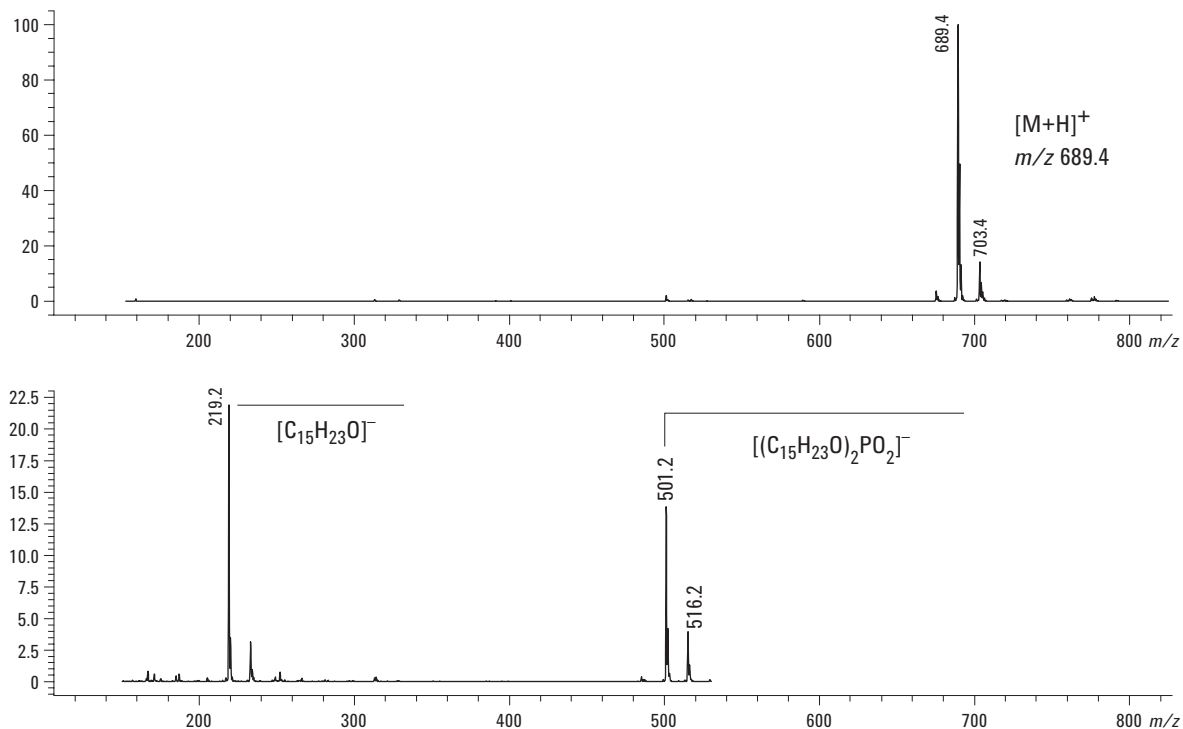


Figure 13. Extracted positive- (upper) and negative- (lower) ion spectra from the main peak in a degraded Naugard P standard.

Poor response in negative-ion mode is presumably due to excessive fragmentation, and no molecular ion is observed. Fragments and minor rearrangements found under these conditions are excellent markers for this sample type and would be good indicators if unknown samples were analyzed.

Peaks in the degraded Naugard P analysis have characteristic positive- and negative-ion spectra which could be studied to confirm typical or propose unknown degradation products. All the peaks seem to have the alkyl side chain present. The other variations presumably lie with the number of oxygen atoms attached to the phosphorous, as proposed in the spectra of the peak at 11.6 min in Figure 14.

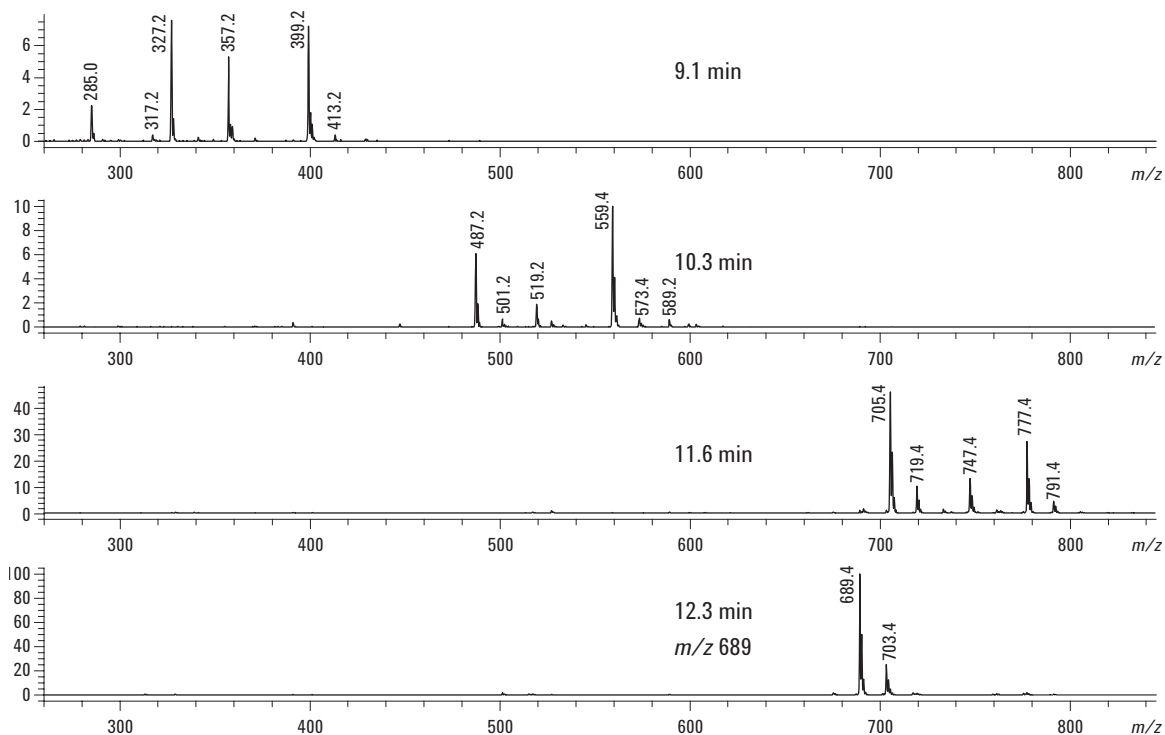


Figure 14. Extracted positive-ion spectra for Naugard P.

Likewise, the negative-ion fragmentation patterns shown in Figure 15 help simplify the investigation by showing differences in the alkyl chain or P-O bonds.

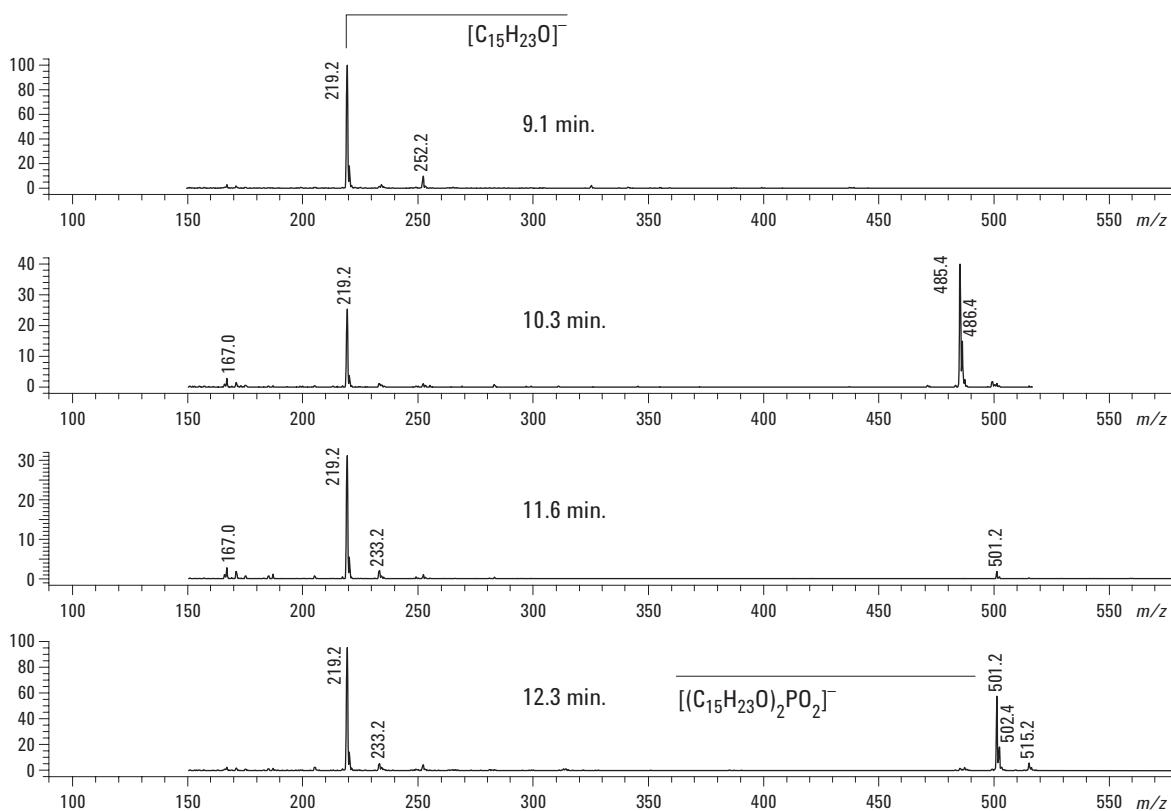


Figure 15. Extracted negative-ion spectra for Naugard P.

We received several unknown samples containing polymer additives. The prepared solutions were analyzed with a wide variety of known standards of AOs and other additive classes. Of all the analyzed standards, Naugard P chromatographic patterns, as shown in Figure 16, most closely matched the unknown samples. Additional spectral investigations followed.

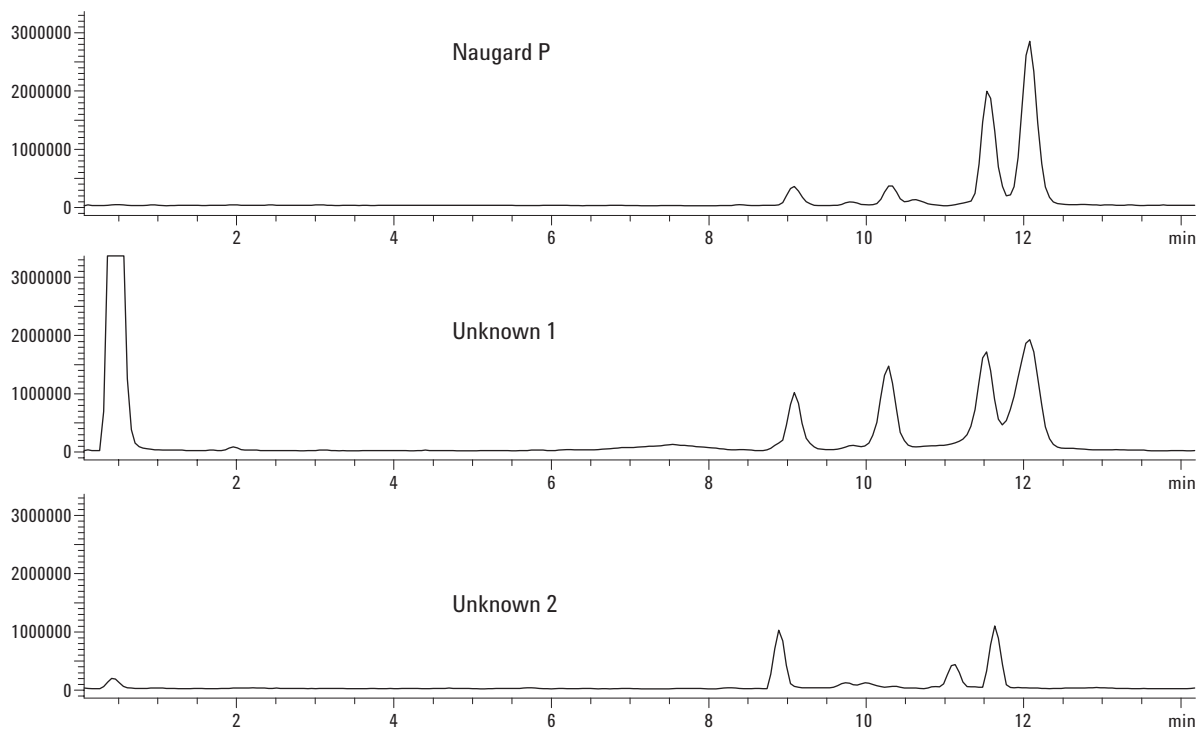


Figure 16. Total positive-ion chromatograms of Naugard P and two unknowns are compared.

The UV spectra for these same samples shown in Figure 17 are similar, though still generally characteristic of many aromatic compounds having minimal ring substitution. These data are interesting, but not conclusive.

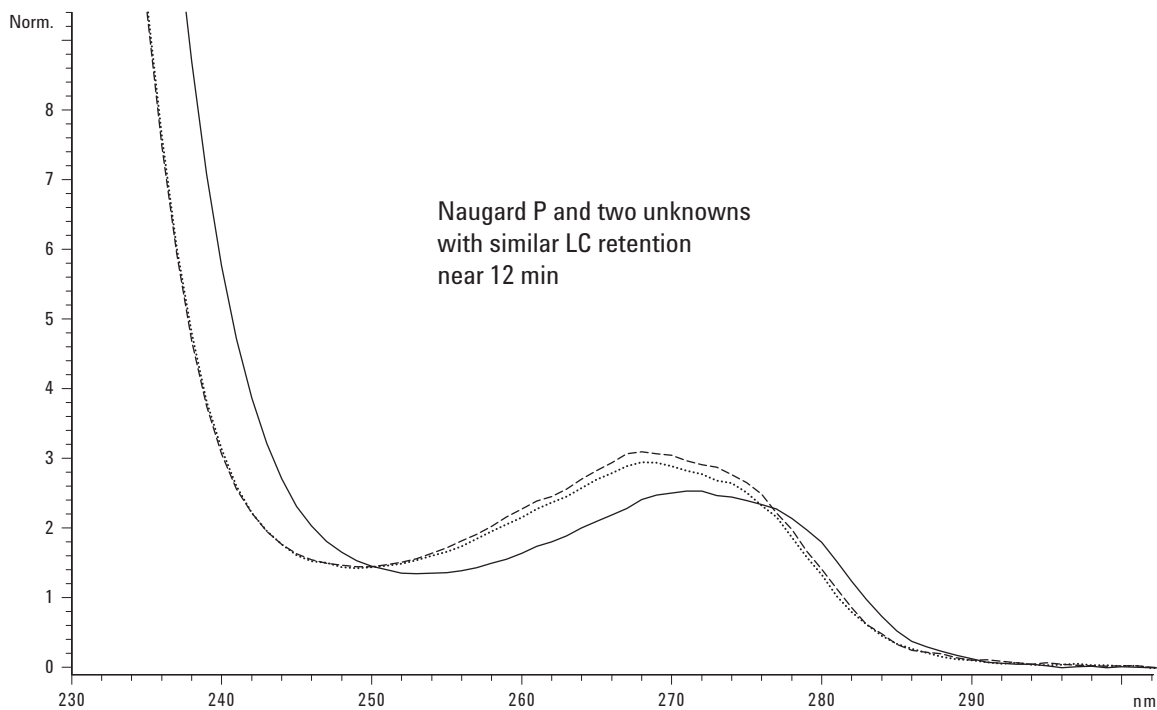


Figure 17. UV spectra of Naugard P and the two unknowns.

The positive-ion mass spectrum of Unknown 1, shown in Figure 18, is an excellent match to that of Naugard P, showing slightly more alkyl variation than the standard. This could be a different lot of Naugard P or a product from a different supplier. Unknown 2 has the primary positive-ion at m/z 647, reasonably due to a shorter alkyl chain, C_8H_{17} , compared to the C_9H_{19} alkyl chain on Naugard P.

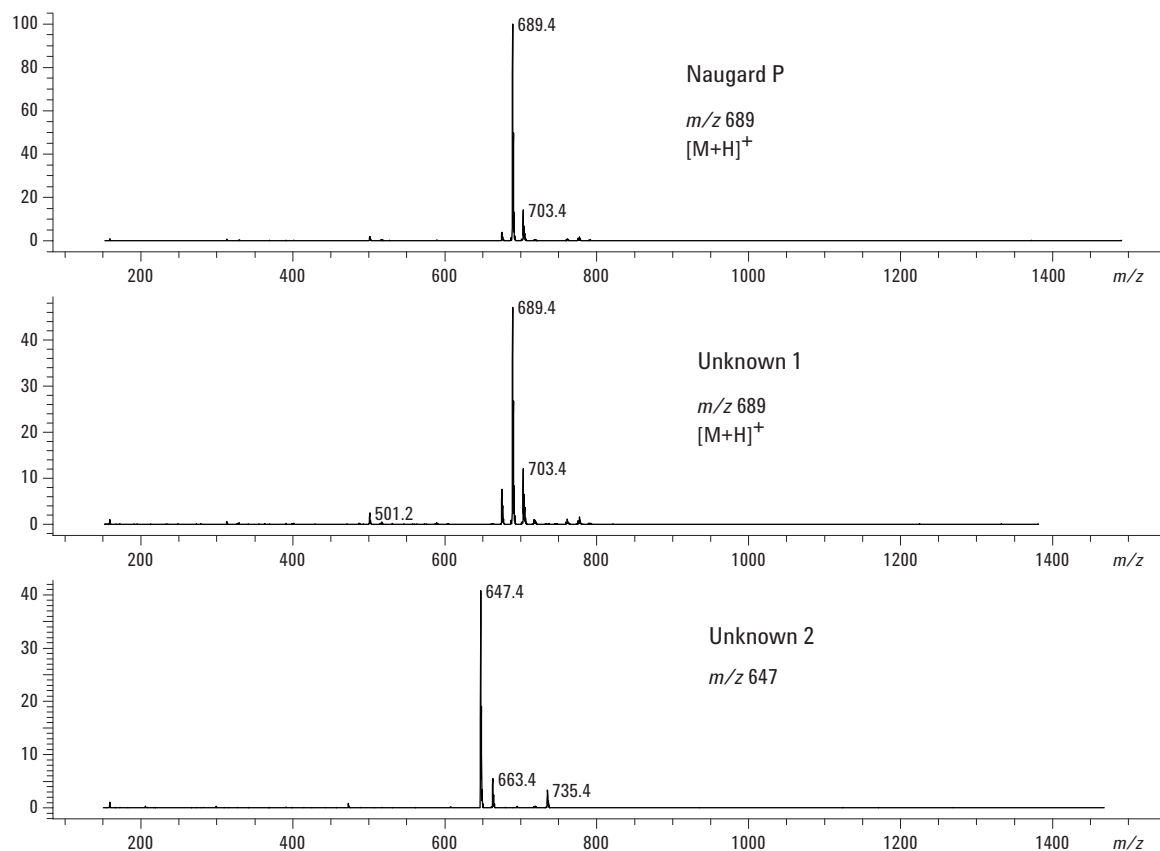


Figure 18. The positive-ion mass spectra of Naugard P and the two unknowns.

In negative-ion mass chromatograms, we see similarities to Naugard P in Unknown 1 and quite dissimilar data in Unknown 2. Recalling from earlier discussions that Naugard P is highly fragmented in negative-ion mode, the negative-ion mass spectra should be extremely helpful in supporting our initial thoughts taken from the positive-ion spectra. See Figure 19.

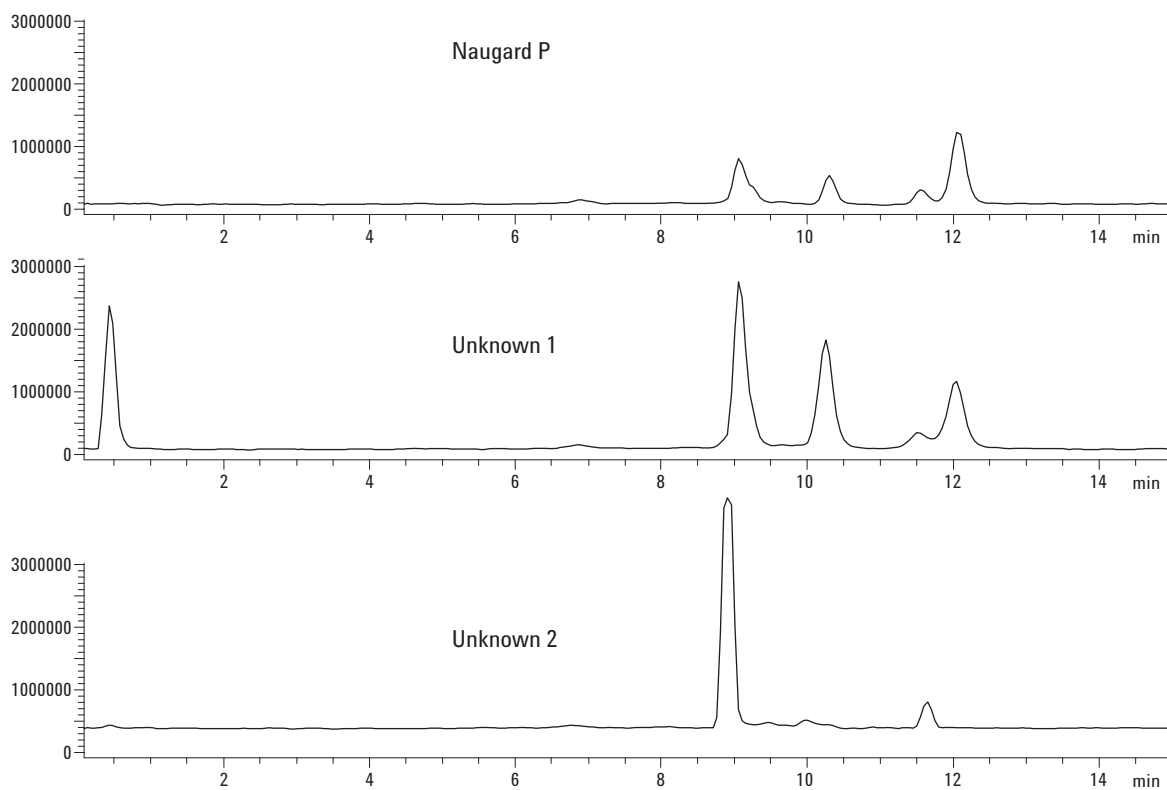


Figure 19. Total negative-ion chromatograms of Naugard P and two unknowns are compared.

The negative-ion spectra for Naugard P and Unknown 1 are an excellent match and probably offer the best support of that chemical identity and structural details. Unknown 2, however, speculatively presents two CH₂'s less in the *m/z* 501 fragment and one CH₂ less the *m/z* 219 fragment. See Figure 20. This is highly supportive of the proposed structure from the positive-ion data and allows us to conclude that, while similar to Naugard P, it is a unique product whose structure is most likely (C₆H₄-C₈H₁₇-O)₃P.

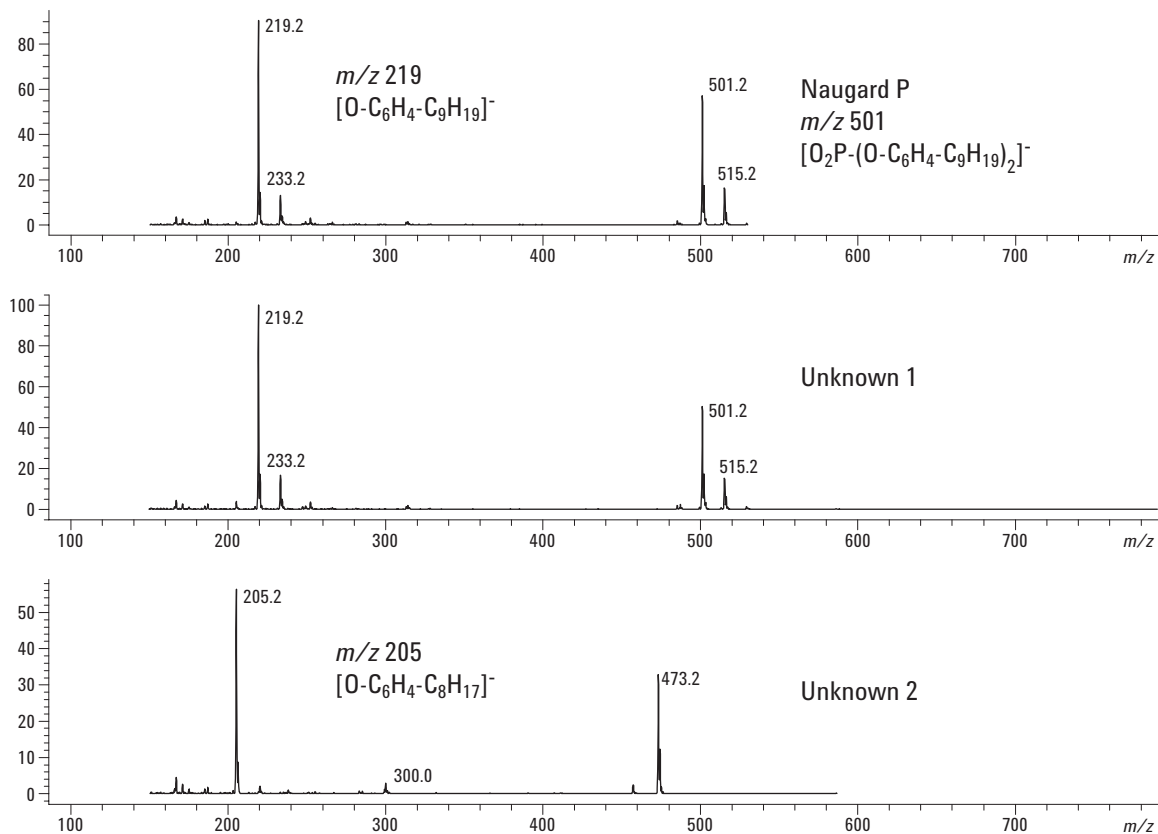


Figure 20. Negative-ion fragmentation mass spectra of Naugard P and the two unknowns.

Conclusions

- LC with UV/VIS and MSD detection is a powerful approach to compound analysis and identification.
- Mobile phase conditions affect the quality and usability of the acquired data.
- Unknown compounds can be tentatively identified with MS data.
- Additive degradation can be quickly evaluated to optimize formulations for better performance.

For More Information

For more information on our products and services, visit our web site at www.agilent.com/chem.

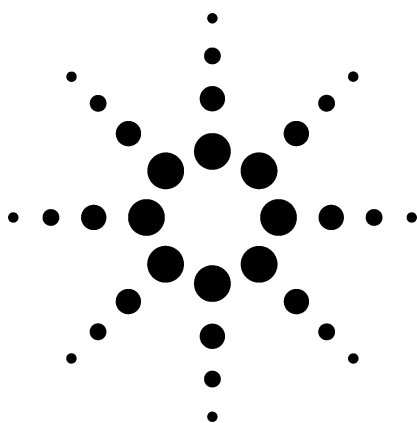
Agilent shall not be liable for errors contained herein or for incidental or consequential damages in connection with the furnishing, performance, or use of this material.

Information, descriptions, and specifications in this publication are subject to change without notice.

© Agilent Technologies, Inc. 2003

Printed in the USA
March 17, 2003
5988-8610EN

Separation of Ceftibuten Stereo Isomers with 100% Aqueous Mobile Phase Using Zorbax SB-Aq Application



Drug Development

Adebayo O. Onigbinde

Ceftibuten dihydrate is currently one of the safest antimicrobial agents available to clinicians. As a result, it is one of the most frequently prescribed antibiotics. Ceftibuten belongs to the third generation of cephalosporin antibiotics (cephems), which are used to treat many varieties of infections caused by gram-positive and negative bacteria. Ceftibuten has two stereo isomers, the (Z) and the (E) isomers.

Most HPLC solvents are considered hazardous to health and to the environment. Safe usage and disposal of large volumes of such solvents has always posed problems. Availability of columns, such as Zorbax SB-Aq, that can be used under high aqueous conditions and still retain consistent retention, resolution, selectivity, and peak shape is a great step in reducing the environmental impact of these solvents. Attempts to separate ceftibuten isomers on C18 columns with low percentages of organic modifiers (2%) did not give good resolution and peak shape (Figure 1). However, separation of ceftibuten isomers was achieved with 100% aqueous mobile phases on Zorbax SB-Aq column (Figure 2). Ceftibuten also exhibited very good linearity and a low limit of detection (LOD) (Figure 3).

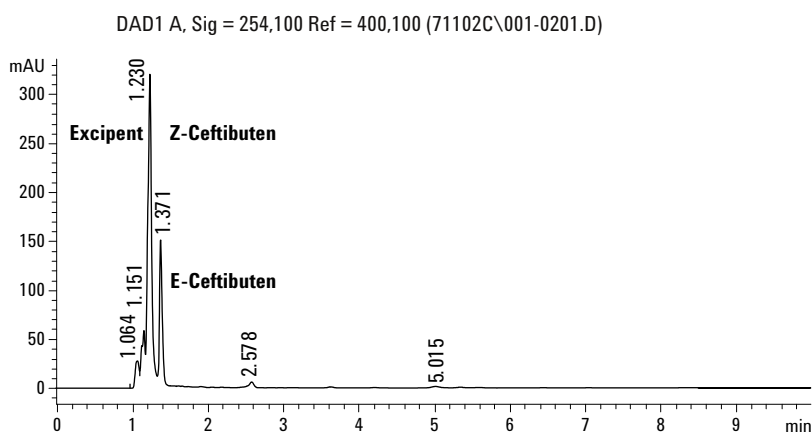


Figure 1. Separation of ceftibuten isomers on C-18 columns with low percentages of organic modifiers. Concentration of ceftibuten dihydrate: 3.0 mg/mL.

Experimental Conditions

Instrument: Agilent 1100 Series HPLC; **Temp:** ambient; **Column:** Alkyl-C18, 4.6 × 150 mm, 5 μm; **Mobile phase:** 2% ACN, 98% 10 mM ammonium acetate, pH 5.4; **Flow rate:** 1 mL/min; **Injection volume:** 5 μL; **Diode array detector:** 254 nm; **Reference:** 400 nm; **Bandwidth:** 100 nm

Highlights

- The Zorbax SB-Aq column has an alkyl bonded phase designed to eliminate phase collapse and still retain both hydrophilic and other compounds, when using highly aqueous mobile phases, including 100% water.
- Methods that require ion-pairing reagents for retention on other C8 or C18 bonded phases can often be carried out on the Zorbax SB-Aq column without ion-pairing reagents or organic modifiers.
- The Zorbax SB-Aq column separated ceftibuten stereo isomers with good peak shape and resolution in 100% aqueous phase without the use of ion-pairing agents or organic modifiers.
- The Zorbax SB-Aq column can deliver unique selectivity and resolution with very good peak shape for polar analytes that require low levels of organic modifier for adequate retention.
- The Zorbax SB-Aq column resolves compounds at a concentration commonly encountered in pharmacokinetic studies (Ceftibuten, LOD = 1.5 ng).



Agilent Technologies

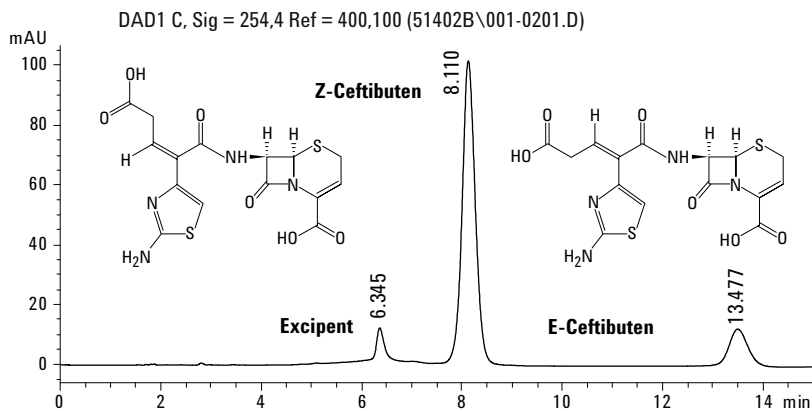


Figure 2 Separation of ceftibuten isomers with 100% aqueous phases on Zorbax SB-Aq column. Concentration of ceftibuten dihydrate: 3.0 mg/mL.

Experimental Conditions

Instrument: Agilent 1100 Series HPLC; **Temp:** ambient; **Column:** Zorbax SB-Aq, 4.6 × 150 mm, 5 μm (part number 883975-914); **Mobile phase:** 100% 10 mM ammonium acetate, pH 5.4; **Flow rate:** 1 mL/min; **Injection volume:** 5 μL; **Diode array detector:** 254 nm; **Reference:** 400 nm; **Bandwidth:** 100 nm

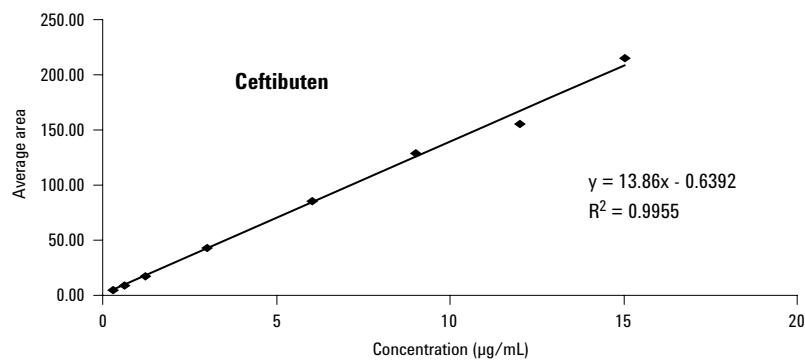


Figure 3. Good linearity and a low limit of detection for ceftibuten using a Zorbax SB-Ag column.

Adebayo Onigbinde is an applications chemist based at Agilent Technologies, Wilmington, Delaware, USA.

For More Information

For more information on our products and services, visit our Web site at www.agilent.com/chem.

Agilent shall not be liable for errors contained herein or for incidental or consequential damages in connection with the furnishing, performance, or use of this material.

Information, descriptions, and specifications in this publication are subject to change without notice.

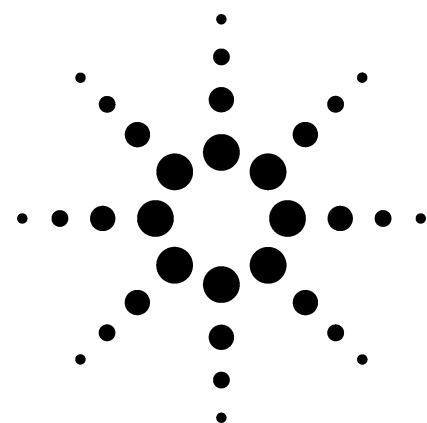
© Agilent Technologies, Inc. 2002

Printed in the USA
September 18, 2002
5988-7625EN

Extraction and HPLC Analysis of Alkaloids in Goldenseal

Application

Consumer Products and Drug Manufacturing/QA/QC



Author

Holly A. Weber
Midwest Research Institute
425 Volker Blvd
Kansas City, MO 64110
USA

Maureen Joseph
Agilent Technologies, Inc
2850 Centerville Road
Wilmington, DE 19808-1610
USA

Abstract

An ambient extraction of goldenseal root powder followed by HPLC analysis of the alkaloids on a Zorbax Rapid Resolution Eclipse XDB-C18 column provides an accurate method for the determination of key alkaloids in goldenseal, including berberine and hydrastine. The extraction and HPLC analysis can be applied to several other alkaloids, including canadine, hydrastinine, and palmatine, and may be applicable to other berberine-containing plant roots. The Rapid Resolution Eclipse XDB-C18 column is used for an isocratic separation with high resolution of all components in under 15 minutes.

Introduction

Goldenseal, *Hydrastis canadensis* L., is one of the oldest herbal medicinal plants and is of current interest as a natural medicine. There are two alkaloids present in goldenseal that are the expected active components, berberine and hydrastine. Canadine, hydrastinine, berberastine, and canadoline are minor alkaloids. Palmatine, which is closely related to berberine, is not found in *H. canadensis*, but is found in *Coptis*, another berberine-containing plant [1].

Goldenseal has been used as an anti-inflammatory and antibiotic. It has also been used to treat nasal congestion, cold, flu, and a variety of intestinal disorders. The whole root of the plant is used and is currently available in bulk (dried or powdered roots), tablets, capsules, and tinctures. Goldenseal plants have been overharvested and many are now grown on farms for use as herbal supplements. Inconsistent quantities of alkaloids are present in the products sold as herbal supplements. A simple process for extracting and analyzing the alkaloids is highly desirable to evaluate product quality. Figure 1 shows the structures of the alkaloids in goldenseal.



Agilent Technologies

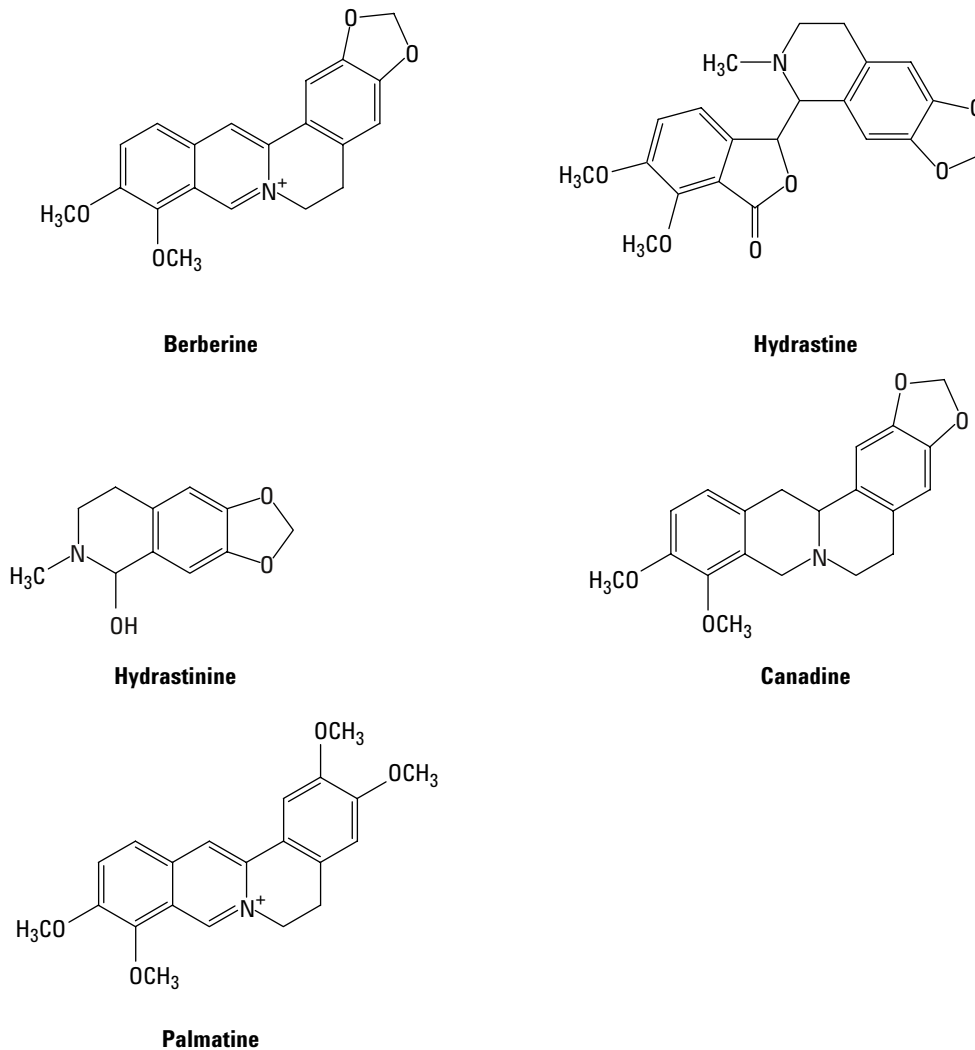


Figure 1. Structures of key alkaloids in goldenseal and related plants.

Experimental

Extraction Procedure

Literature reports by Betz and Anderson [1] and Burney [2] indicate that ambient extraction of alkaloids from *H. canadensis* is possible. This is followed by an HPLC determination for accurate quantitation of the alkaloid extracts. The optimized ambient extraction conditions used for the analysis of neat goldenseal root powder are summarized in the steps below.

1. Weigh ~ 0.5 g of root powder
2. Mix with 100 mL of acetonitrile:water:H₃PO₄ (70:30:0.1, v/v/v)
3. Sonicate 5 min, shake (wrist-action shaker) 10 min, centrifuge 5 min

4. Dilute extracts 1/5
5. Direct HPLC analysis of diluted extracts

HPLC Analysis

The HPLC analysis of alkaloids present in goldenseal needs to resolve the major alkaloids. In addition, it is desirable to resolve palmatine, because it is present in other berberine-containing plants. An HPLC method was developed to resolve all of these components. Optimum resolution and peak shape were obtained using the Zorbax Eclipse XDB-C18 column with an ammonium acetate buffer and acetonitrile. The separation is shown in Figure 2 with a complete list of the optimized conditions used. For consistent retention times, temperature control was required at 30°C [3].

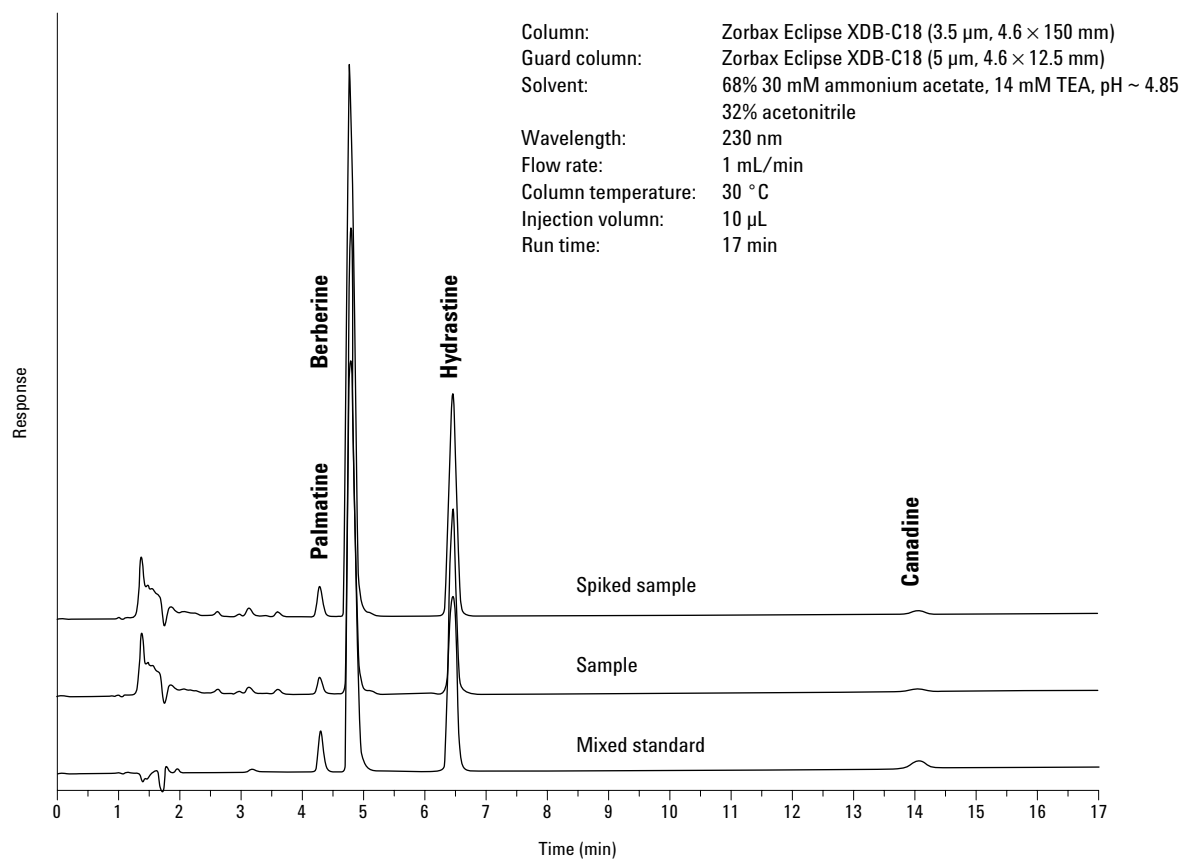


Figure 2. HPLC separation of goldenseal extract on Eclipse XDB-C18 column.

Method Validation

This HPLC method was applied in the validation of the ambient extraction method. Linearity, precision, and alkaloid recovery were investigated. Table 1 shows these results. The precision of the method is excellent, and recoveries of the different alkaloids ranged from 92%–102%, excellent for a quantitative method. The linearity was very good (Figure 3) and sensitivity was good. From the standard data, the calculated LOD (limit of detection) for berberine was 0.50 mg/mL and the LOQ (limit of quantitation) was 1.65 mg/mL, so that accurate quantitation down to low levels is possible, making it easy to test the quality of different goldenseal products.

Table 1. Validation Results of the Ambient Extraction Method

| | Palmatine | Berberine | Hydrastine | Canadine |
|--|--|--|--|---|
| Precision (n = 10) | 0.18 ±0.002(s)% | 3.06 ±0.05(s)% | 2.04 ±0.01(s)% | 0.08 ±0.001(s)% |
| Alkaloid recovery (~ 0.3–2 g of GS) (~ 0.6–1 mg/mL) (n = 12) | 0.18 ±0.003(s) | 3.10 ±0.06(s)% | 2.05 ±0.02(s)% | 0.08 ±0.001(s)% |
| Spike and recovery (n = 3) | Spike level = ~ 0.15% 92.2 ±5.5(s)% | Spike level = ~ 2.0% 101.5 ±0.2(s)% | Spike level = ~ 2.0% 101.9 ±0.2(s)% | Spike level = ~ 0.10% 101.9 ±7.9(s)% |

(s) = standard deviation

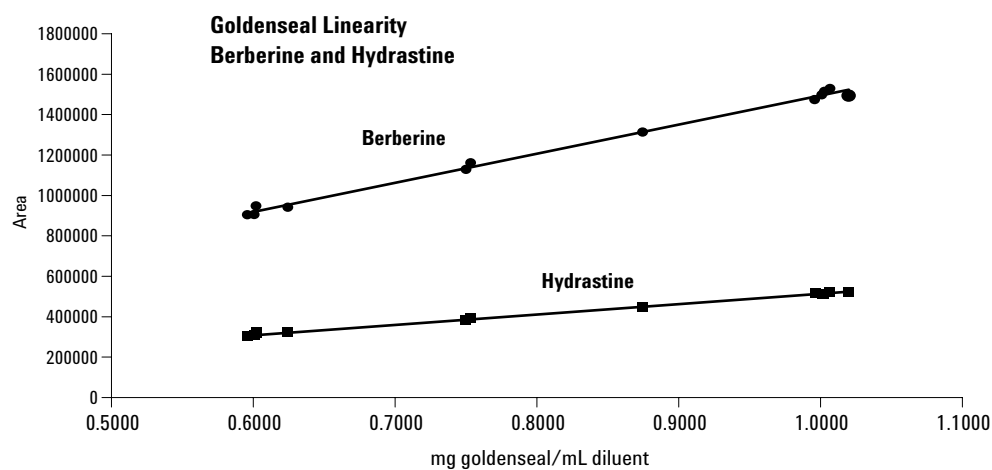
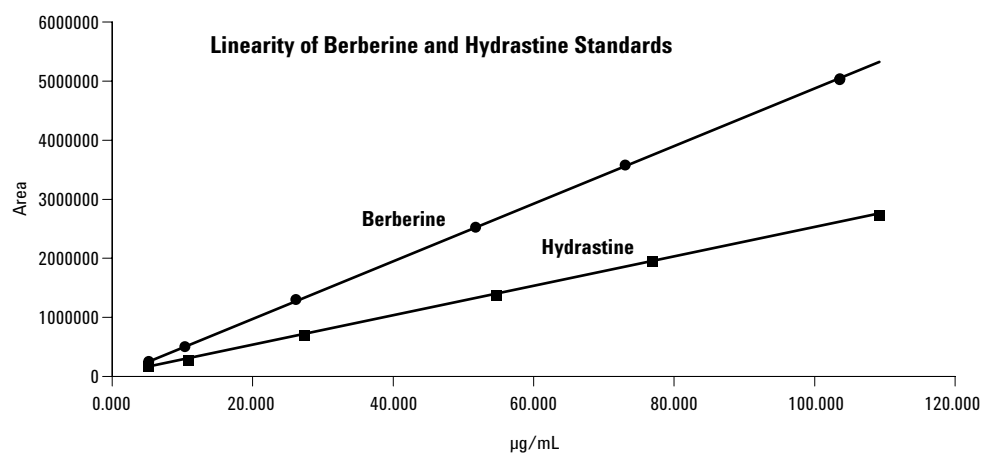


Figure 3. Linearity of berberine and hydrastine as standards and from goldenseal extracts.

Results

Goldenseal Testing

The ambient extraction and HPLC analysis method were applied to six lots of goldenseal root powder from three different vendors to determine the alkaloid content. The results are summarized in Table 2. These results demonstrate variability among vendors and the reason a good quantitative HPLC method is desirable.

Table 2. Results of Testing Goldenseal Root Powder from Multiple Lots and Multiple Vendors with the Ambient Extraction Method and HPLC

| Vendor | Lot number | % Palmatine | % Berberine | % Hydrastine | % Canadine | Total weight % of known alkaloids |
|--------|------------|-------------|-------------|--------------|------------|-----------------------------------|
| 1 | A | nd | 3.27 | 2.36 | 0.09 | 5.94 |
| | B | nd | 3.29 | 2.40 | 0.07 | 5.98 |
| 2 | C | 0.19 | 3.01 | 1.99 | 0.09 | 5.53 |
| | D | 0.18 | 3.06 | 2.04 | 0.08 | 5.36 |
| 3 | E | nd | 4.60 | 4.06 | 0.12 | 8.99 |
| | F | nd | 3.93 | 2.67 | 0.20 | 6.93 |

Conclusions

This ambient extraction method of goldenseal is simple and reliable. This is followed by an isocratic HPLC analysis with a Zorbax Rapid Resolution Eclipse XDB-C18 column, which provides high resolution and excellent peak shape of six alkaloids in 15 minutes. This analysis provides reliable quantitative results of the alkaloids in goldenseal, including berberine and hydrastine. The method was applied to goldenseal from three different vendors and may be applicable to other berberine-containing plants.

References

1. J. M. Betz, S. M. Musser, and G. M. Larkine, "Differentiation between Goldenseal (*Hydrastis canadensis* L.) and Possible Adulterants by LC/MS," presented at the 39th Annual Meeting of the American Society of Pharmacognosy, Orlando, FL, July 19–23, 1998.
2. M. L. Anderson and D. P. Burney, *J. AOAC Intern.*, 81:1005–1110 (1998).
3. H. A. Weber, et. al., *J. Liq. Chrom. and Rel. Tech.* 24(1) 87–95 (2001).

Acknowledgements

This work was performed by Holly A. Weber, Matthew K. Zart, Andrew E. Hodges, Kellie D. White, Roger K. Harris, and Alice P. Clark of Midwest Research Institute, 425 Volker Blvd, Kansas City, MO 64110.

Diane Overstreet and Cynthia Smith of the National Toxicology Program, 111 Alexander Drive, Research Triangle Park, NC 27709.

This work was funded by the National Institute of Environmental Health Sciences, Contract Nos. N01-ES-55385 and N01-ES-05457.

For More Information

For more information on our products and services, visit our Web site at www.agilent.com/chem.

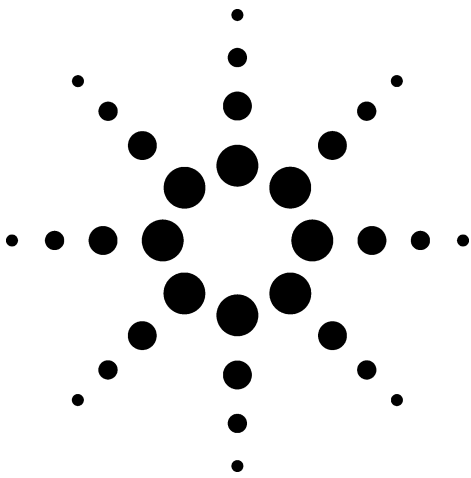
Agilent shall not be liable for errors contained herein or for incidental or consequential damages in connection with the furnishing, performance, or use of this material.

Information, descriptions, and specifications in this publication are subject to change without notice.

© Agilent Technologies, Inc. 2002

Printed in the USA
September 18, 2002
5988-7136EN

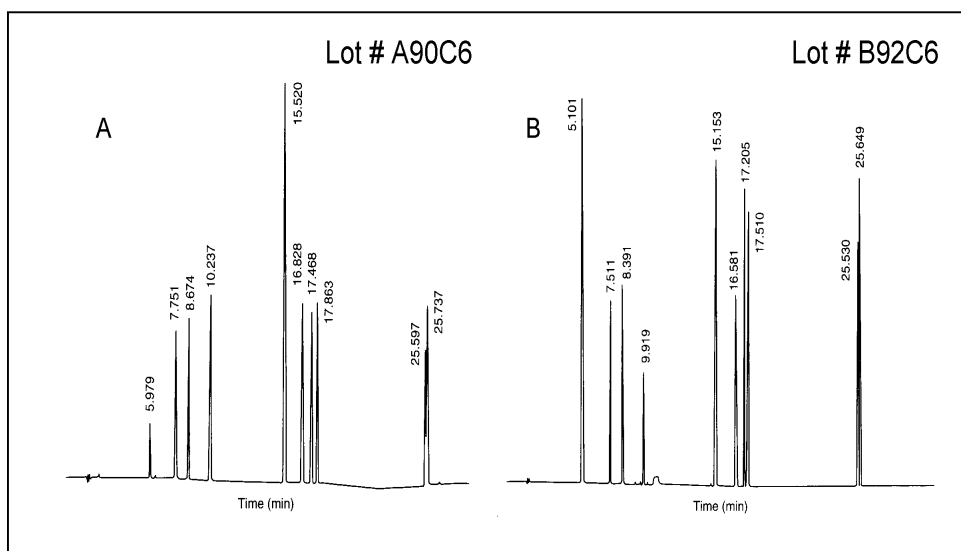




Lot-to-Lot Reproducibility Amphetamines

Application
Technical
Robert Ricker

| | |
|--------------------|--------------------|
| 1. Morphine | 6. Acetophenone |
| 2. Amphetamine | 7. Desipramine |
| 3. Methamphetamine | 8. Imipramine |
| 4. Ethylmorphine | 9. Phenylbutazone |
| 5. Salicylic Acid | 10. Mefenamic Acid |



Conditions:
ZORBAX Rx-C8 (4.6 x 250mm) Agilent (P/N: 880967-901)
Gradient: 0% B 2.2 min, then 0-100% B in 30 min.
Mobile Phase: A=1% Phosphoric Acid, 0.7% TFA
B= 80% ACN + 20% A (above)
2 mL/min; 40°C; Detect. UV(254 nm)

Highlights

- High reproducibility in elution patterns of basic drugs demonstrates the careful lot-to-lot manufacture of ZORBAX Rx and StableBond columns.
- Each step in the manufacture of ZORBAX columns must exceed stringent quality assurance specifications. Finally, each column from the lot must pass a set of quality control specifications.
- Consistent elution and good peak shape of these "silanol-sensitive" basic drugs results from the extremely homogenous silanol surface and low acidity of ZORBAX Rx-SIL.



Agilent Technologies

Robert Ricker is an application chemist based at Agilent Technologies, Wilmington, Delaware.

For more information on our products and services, visit our website at:
www.agilent.com/chem

Copyright© 2002 Agilent Technologies, Inc. All Rights Reserved. Reproduction, adaptation or translation without prior written permission is prohibited, except as allowed under the copyright laws.

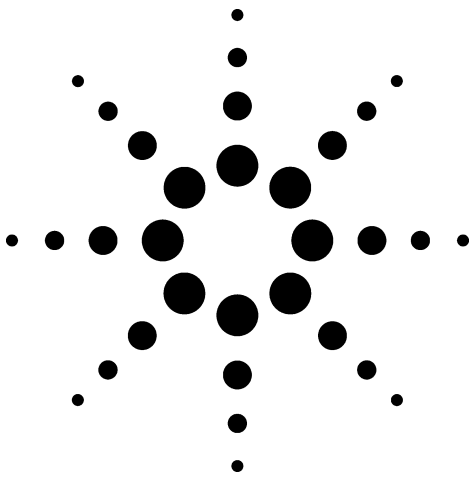
Agilent shall not be liable for errors contained herein or for incidental or consequential damages in connection with the furnishing, performance, or use of this material.

Information, descriptions, and specifications in this publication are subject to change without notice.

Printed in the USA
April 25, 2002
5988-6471EN



Agilent Technologies

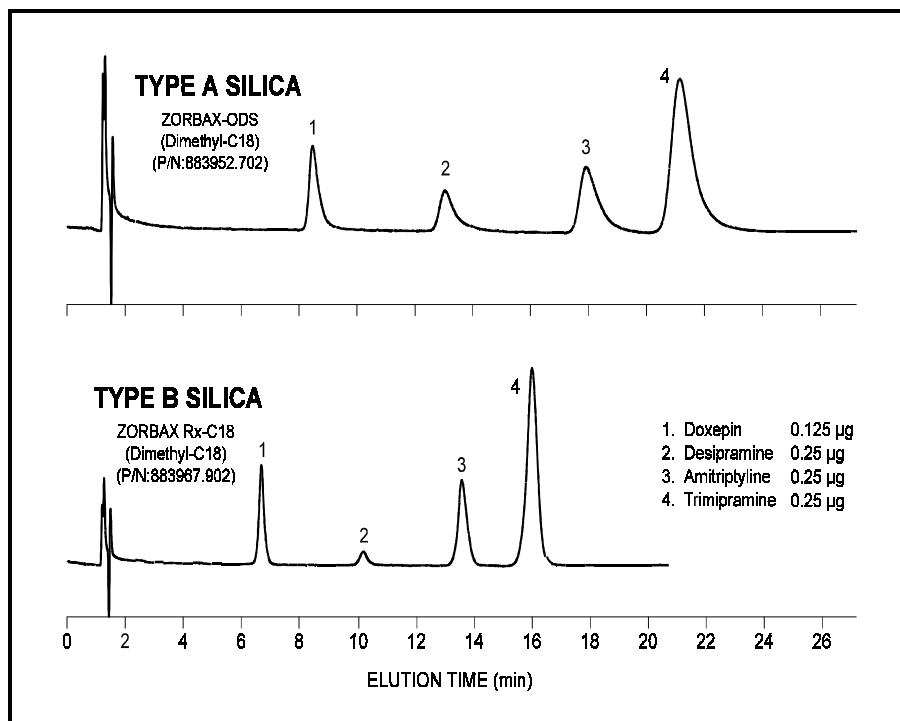


Effect of Silica-Support Type Reversed-Phase Separation of Tricyclic Antidepressants

Application

Technical

Robert Ricker



Highlights

- *Highly purified, less-acidic Type-B silica support (ZORBAX Rx-SIL) results in improved band shape and column efficiency for these basic drugs.*
- *Reduced retention for column with Type-B silica is due to lower surface area of its support.*

Conditions:

ZORBAX Columns (4.6 x 150 mm) (Agilent P/N above)
Mobile Phase: 30% ACN, 70% 25mM Sodium phosphate buffer, pH 2.5,
0.2% TEA and 0.2% TFA;
1.0 mL/min, 40°C, Detect. UV(254 nm)



Agilent Technologies

Robert Ricker is an application chemist based at Agilent Technologies, Wilmington, Delaware.

For more information on our products and services, visit our website at:
www.agilent.com/chem

Copyright© 2002 Agilent Technologies, Inc. All Rights Reserved. Reproduction, adaptation or translation without prior written permission is prohibited, except as allowed under the copyright laws.

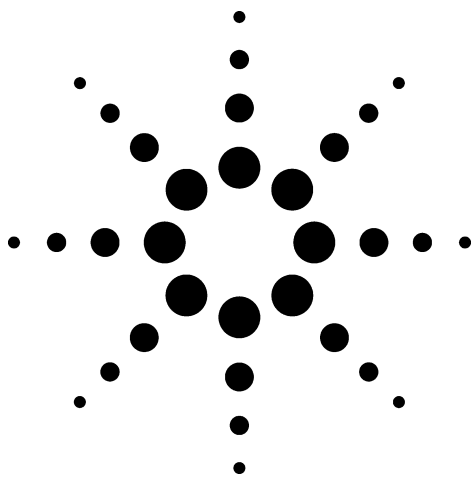
Agilent shall not be liable for errors contained herein or for incidental or consequential damages in connection with the furnishing, performance, or use of this material.

Information, descriptions, and specifications in this publication are subject to change without notice.

Printed in the USA
April 25, 2002
5988-6470EN



Agilent Technologies



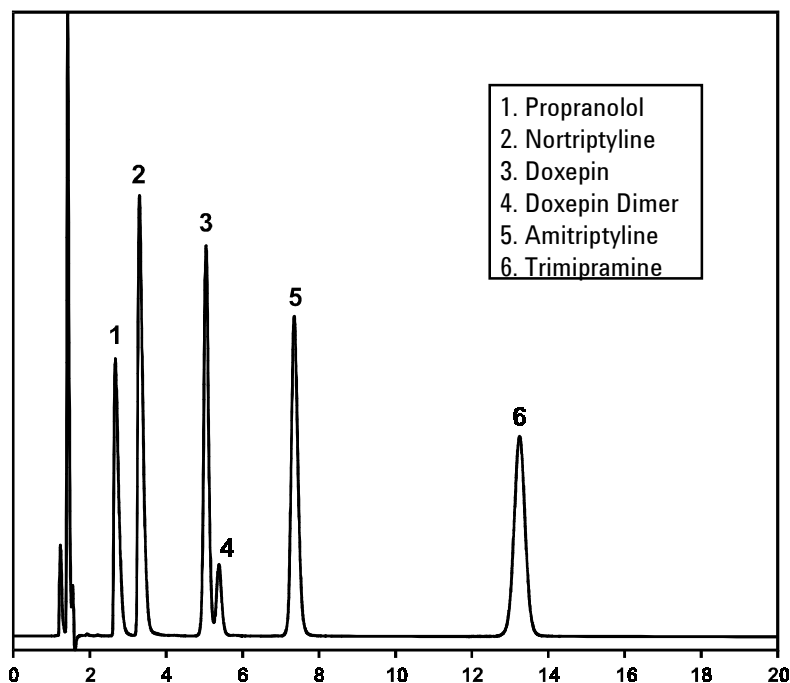
Tricyclic Antidepressants Separation with Excellent Peak Shape Using XDB-C8 and THF-Containing Mobile Phase

Application
Pharmaceutical
Robert Ricker

Tricyclic antidepressants (TCAs) are a common class of pharmaceutical compounds. Although TCAs are often separated by HPLC, older column technology limited its application in the neutral pH-range, due to broad and tailing peaks. New technologies, such as **eXtra Dense Bonding** and double end-capping allow separation of these compounds at pH 7, with dramatically improved peak shape. In comparison to other organic solvents as modifiers, THF was found to provide the best peak shape.

Highlights

- The extra densely bonded XDB-C8 provides excellent peak shape for acids, bases, and neutrals, due to more-complete coverage of the silica surface.
- The excellent peak shape demonstrated by THF in this separation, suggests that the chromatographer explore use of several solvents in developing separations.



Conditions:
ZORBAX Eclipse XDB-C8 (4.6 x 150 mm, 5 µm) (Agilent P/N: 993967-906)
Mobile Phase: 38% THF; 62% 25mM Potassium Phosphate, pH 7
Injection 10 µL, 1 mL/min, 23°C, Detect. UV (254 nm)



Agilent Technologies

Robert Ricker is an application chemist based at Agilent Technologies, Wilmington, Delaware.

For more information on our products and services, visit our website at:
www.agilent.com/chem

Copyright© 2002 Agilent Technologies, Inc. All Rights Reserved. Reproduction, adaptation or translation without prior written permission is prohibited, except as allowed under the copyright laws.

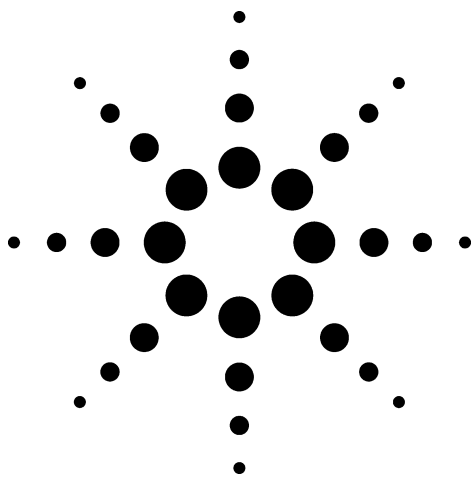
Agilent shall not be liable for errors contained herein or for incidental or consequential damages in connection with the furnishing, performance, or use of this material.

Information, descriptions, and specifications in this publication are subject to change without notice.

Printed in the USA
April 25, 2002
5988-6389EN



Agilent Technologies



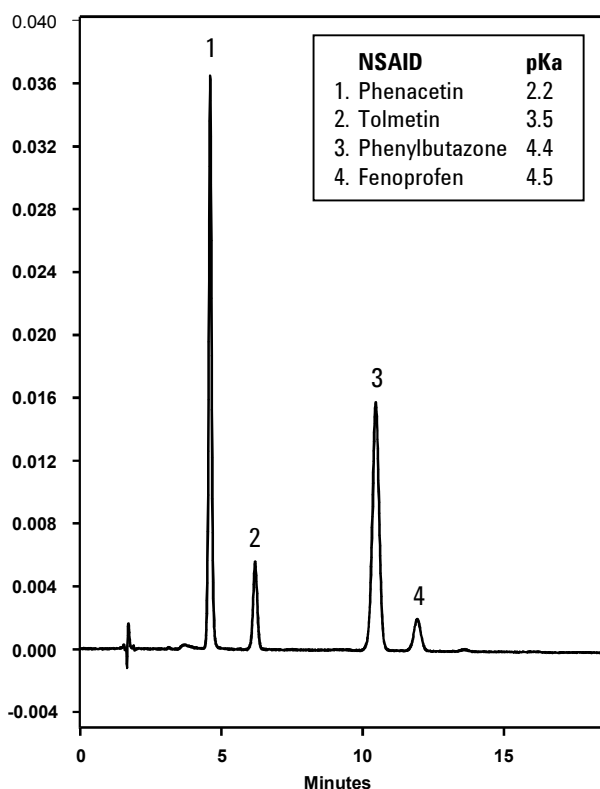
Narrow-Bore (2.1 mm) Separation of Nonsteroidal Anti-Inflammatory Drugs

Application
Pharmaceutical
Robert Ricker

Nonsteroidal anti-inflammatory drugs (NSAID) are commonly referred to as analgesics and are widely prescribed drug products used for the effective relief of mild to moderate pain and inflammation. The fast, accurate quantitation of these drugs is of considerable importance to chromatographers in pharmaceutical, health care, and research environments.

Highlights

- High-resolution separation of a mixture of analgesics is achieved with a narrow-bore column configuration which can be readily adapted to LC/MS applications.
- Eclipse XDB-C8 columns are suitable for separating acidic, basic, and neutral molecules with good peak shape. These analgesics have pKa's ranging from 2.2 to 4.5, representing more-acidic compounds.



Conditions:
ZORBAX XDB-C8 (2.1 x 150 mm) (Agilent P/N: 993700-906)
Mobile Phase: 50:50, 25mM Sodium Phosphate
(pH 7.0 with Phosphoric Acid) : MeOH
Injection: 2µL, 0.2 mL/min, 35°C, Detect. UV(254 nm)



Agilent Technologies

Robert Ricker is an application chemist based at Agilent Technologies, Wilmington, Delaware.

For more information on our products and services, visit our website at:
www.agilent.com/chem

Copyright© 2002 Agilent Technologies, Inc. All Rights Reserved. Reproduction, adaptation or translation without prior written permission is prohibited, except as allowed under the copyright laws.

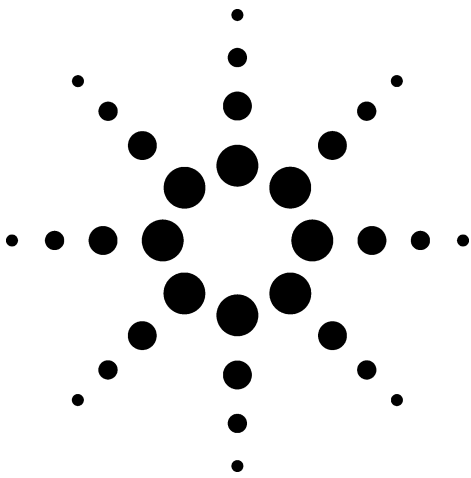
Agilent shall not be liable for errors contained herein or for incidental or consequential damages in connection with the furnishing, performance, or use of this material.

Information, descriptions, and specifications in this publication are subject to change without notice.

Printed in the USA
April 25, 2002
5988-6383EN



Agilent Technologies



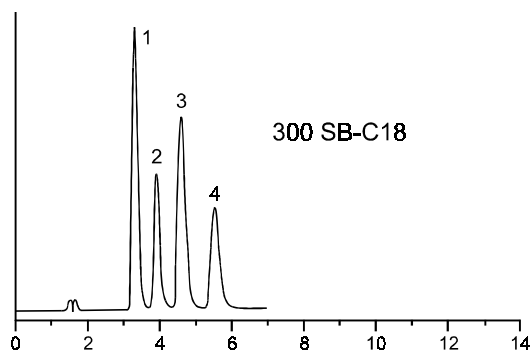
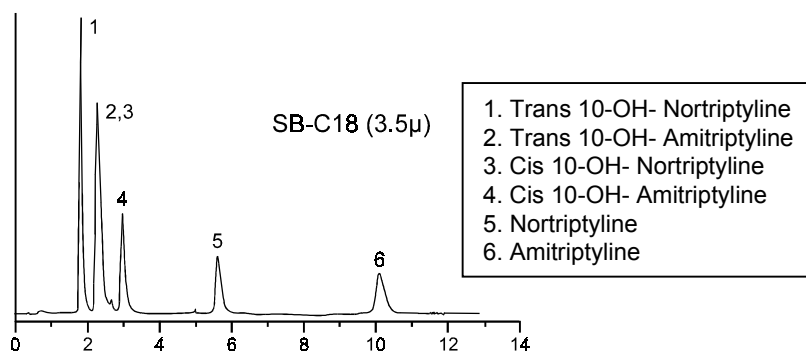
Separation of Tricyclic Antidepressants and Metabolites

Application

Pharmaceutical

Robert Ricker

Tricyclic anti-depressants (TCA) are an important class of pharmaceuticals for the treatment of depression. Analysis of TCA's and their various metabolites in a single chromatographic run can be very beneficial to research and clinical analysis of these compounds. For routine analysis, it is important that both active compounds (Amitriptyline and Nortriptyline) elute later than the 4 metabolites.



Conditions:

ZORBAX SB-C18 (3.5µm; 4.6 x 150 mm, Agilent P/N: 863953-902)

ZORBAX 300 SB-C18 (4.6 x 150 mm, Agilent P/N: 883995-902)

Mobile Phase: 40:60, 25mM Phosphate Buffer, 10mM triethylamine, pH6.2:ACN

1.2 mL/min, Detect. UV(254 nm)

Highlights

- With the addition of TEA, good peak shapes can be obtained for very basic compounds, even at pH 6.2.
- Change in the pore-size and surface area of a column packing can sometimes be helpful in obtaining the desired separation.
- Use additional caution when using silica-based columns at pH > 6 since the silica will dissolve much more quickly.



Agilent Technologies

NOTE: For Investigational / Research only. The performance characteristic for this procedure has not been established. Not for *in vitro* diagnostic procedures.

Robert Ricker is an application chemist based at Agilent Technologies, Wilmington, Delaware.

For more information on our products and services, visit our website at:
www.agilent.com/chem

Copyright© 2002 Agilent Technologies, Inc. All Rights Reserved. Reproduction, adaptation or translation without prior written permission is prohibited, except as allowed under the copyright laws.

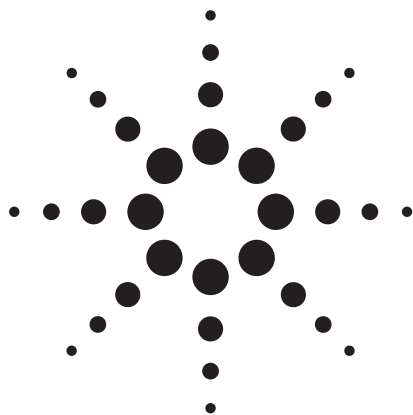
Agilent shall not be liable for errors contained herein or for incidental or consequential damages in connection with the furnishing, performance, or use of this material.

Information, descriptions, and specifications in this publication are subject to change without notice.

Printed in the USA
April 25, 2002
5988-6382EN



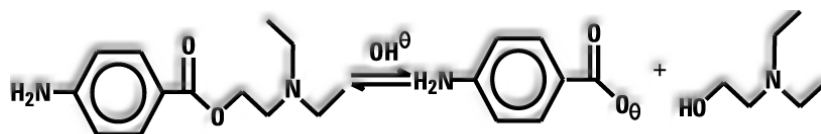
Agilent Technologies



Saponification of procaine: Kinetic measurements with the Agilent high throughput analysis system

Application Note

Udo Huber



Abstract

In this application note we describe how the cleavage of procaine, a p-aminobenzoic acid ester, can be monitored using the Agilent 220 microplate sampler (MPS) with the Agilent 1100 Series LC system. The data of the measurements is transferred to ChemStore C/S, the database module of the Agilent ChemStation Plus, for data analysis. We show that the data can then be transferred easily to a spreadsheet program, for example Microsoft[®] Excel[®], for further calculations such as determination of the rate coefficient.



Agilent Technologies

Innovating the HP Way

Introduction

Kinetic measurements play an important role in pharmaceutical chemistry. Not only for pharmacokinetics where the rate of active compound degradation has to be determined, but also for drug discovery to test the inhibition effect of a compound on an enzyme. For very fast reactions special apparatus, for example shock tubes, have to be used but slower reactions can be monitored by analyzing reaction samples at specific time intervals. This application note describes how this is achieved using the Agilent 220 MPS with the Agilent 1100 Series LC System and the Agilent ChemStation Plus software. Saponification of procaine at pH=10 was selected as a model scenario.

Procaine is a p-aminobenzoic acid ester, which can be saponificated into p-aminobenzoic acid (PABA) and an alcohol. The reaction is shown in figure 1.

Since the reaction is first order the rate of reaction can be described as:

$$v = \frac{d[\text{Ester}]}{dt} = -k \cdot [\text{Ester}]$$

with:

v (rate of reaction)

k (rate coefficient)

[Ester] (concentration of procaine)

Integration of this formula gives:

$$\ln \frac{[\text{Ester}]_t}{[\text{Ester}]_0} = -k \cdot t$$

The rate coefficient k can be determined from the slope of the straight line in the graph $\ln([\text{Ester}]_t/[\text{Ester}]_0)$ against time.

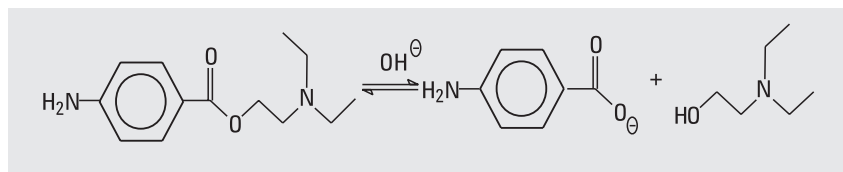


Figure 1
Saponification of procaine

Equipment

The system included an Agilent 1100 Series vacuum degasser, an Agilent 1100 Series binary pump, an Agilent 1100 Series thermostated column compartment, an Agilent 1100 Series diode array detector and an Agilent 220 micro plate sampler.

The system was controlled using the Agilent ChemStation Plus (version A.07.01) and the micro plate sampling software (version A.03.01).

System Setup Overview

1. A chromatographic method for measuring procaine and PABA was developed on the Agilent 220 MPS and the Agilent 1100 Series LC system.
2. Standards for both compounds were measured, the method was calibrated and the run time was extended to 20 minutes (figure 2).
3. Three procaine samples were dissolved in 0.025 M NaH_2PO_4 buffer adjusted to pH=10. These samples were measured with the method described before, which gives an overall run time of one hour for the three samples.
4. The measurement was repeated 24 times to give an overall study run time of 24 hours.
5. The measured data was automatically transferred to the ChemStation Plus database module where the *Charts amount against reaction time* was created.
6. To determine the rate coefficient the data was then automatically transferred to Microsoft Excel.

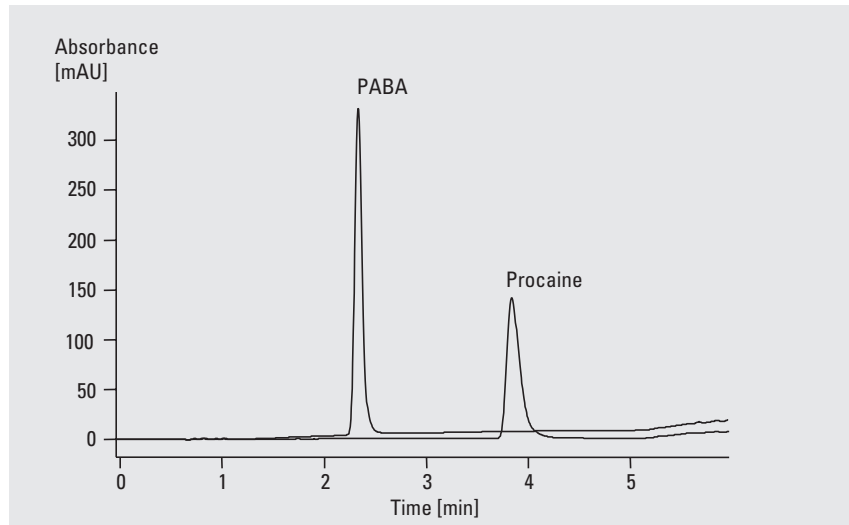


Figure 2
Measurement of standards

Mobile Phases: A= 0.025M NaH_2PO_4 in water (pH=2.5), B = ACN
Gradient: 5 % B for 3.5 min, flow 1 ml/min
5 % B to 50 % B in 1.5 min, flow 1 ml/min
50 % B for 0.5 min, flow 1 ml/min
50 % B to 5 % B in 0.5 min, flow 1 ml/min
5 % B, flow from 1 ml/min to 0.1 ml/min in 0.1 min
5 % B, flow 0.1 ml/min for 18.9 min
5 % B, flow 0.1 ml/min to 1 ml/min in 0.1 min
5 % B for 0.9 min, flow 1 ml/min
Stop time: 20 min
Column: Zorbax SB-C18, 4.6 x 75 mm, 5 μm
Column temp.: 50 °C
UV detector: DAD 204 nm/16 (reference 360 nm/100)

Results and Discussion

Method calibration

A three-level calibration was done after measuring standards for procaine and PABA using the method in figure 2.

Study setup and sample measurement

The method above was renamed four times and set up in the *Study Parameters* screen. *Injection ordered by method* was selected and three samples were set up, as shown in figure 3. Since every method runs for about 20 minutes,

each of the three samples was analyzed every hour. To measure the samples over 24 hours the study was repeated six times. This was set up in the *Start Study* window.

The study was started and the measured sample data was automatically transferred to a Chem-Station Plus database study, which was set up before.

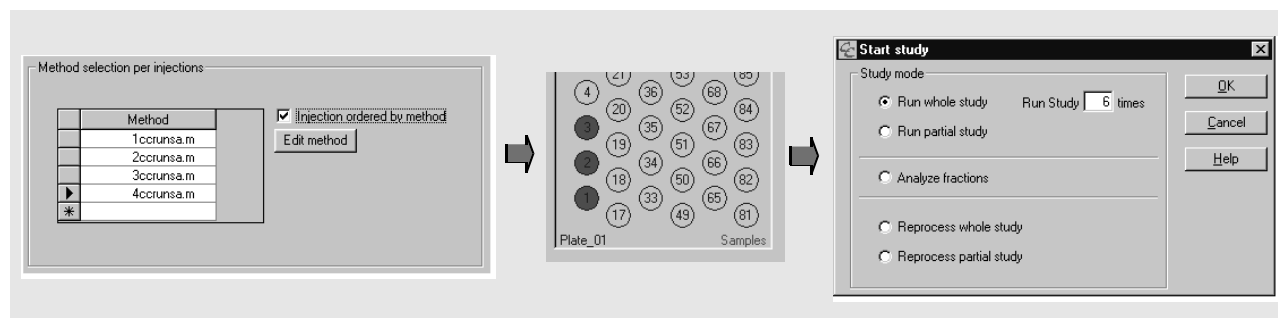


Figure 3
Study setup

ChemStation Plus database results and charts

The study results were loaded into the ChemStation Plus database module and *Sample Name*, *Injection Time* and *Amount* were displayed in *Compound* view. By selecting procaine and/or PABA in the *Compound List* the results were displayed in a comprehensible table (*Table Layout*). The

results for a specific sample were displayed using a Filter on the field *Sample Name*. The reaction is first order, as can be clearly seen in the chart shown in figure 4, which was created in the *Chart Layout* view of the ChemStation database module.

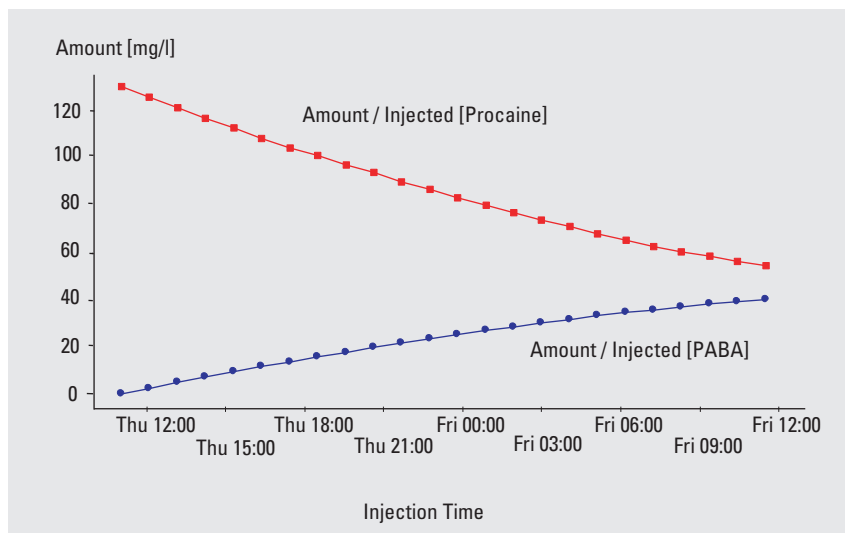


Figure 4
Saponification of procaine: Amount against reaction time

Determination of the rate coefficient by exporting the data to Microsoft Excel

The table created for procaine containing the fields *Sample Name*, *Injection Time* and *Amount* in the ChemStation Plus database module was filtered for one sample and transferred to a Microsoft Excel file. This was done using the *Export* function of the ChemStation Plus database module by selecting *Data* and *MS Excel* in the *Export* window. In Microsoft Excel the injection time difference was calculated in seconds beginning at the first injection at t_0 . The calculated value gives the x-axis of figure 5. The y-axis is calculated as $\ln([Ester]_t/[Ester]_0)$. The negative value of the rate coefficient is the slope of the resulting straight line (figure 5). The calculated results for the first seven injections are shown in table 1.

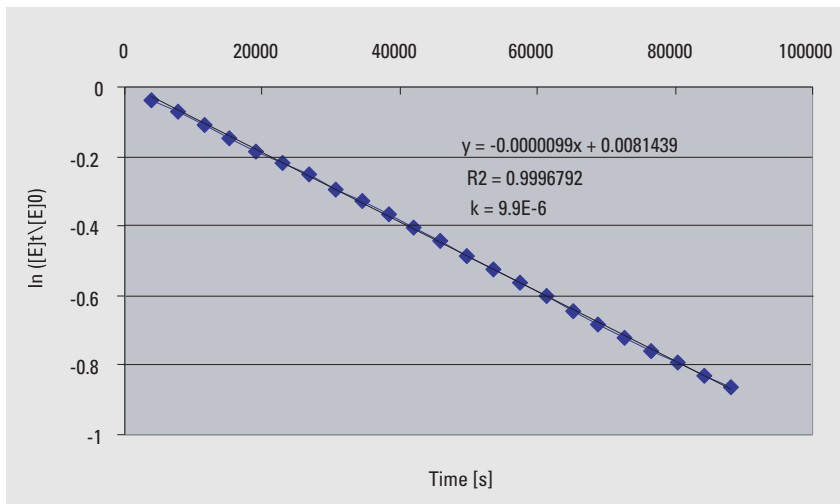


Figure 5
Determination of rate coefficient

| Sample injected (X) | Time difference [hh:mm:ss] | Time difference [s] | Procaine amount (Y) [mg/l] | $\ln \frac{[Ester]_t}{[Ester]_0}$ |
|---------------------|----------------------------|---------------------|----------------------------|-----------------------------------|
| 2/3/00 11:02:59 AM | = t_0 | | 129.838290062179 | = [Ester] ₀ |
| 2/3/00 12:06:45 PM | 1:03:46 | 3826.00 | 125.14649513062 | -0.036804741 |
| 2/3/00 1:10:30 PM | 2:07:31 | 7651.00 | 120.783350276534 | -0.072291306 |
| 2/3/00 2:14:27 PM | 3:11:28 | 11488.00 | 116.502232323668 | -0.108379319 |
| 2/3/00 3:18:14 PM | 4:15:15 | 15315.00 | 112.19641294469 | -0.146038731 |
| 2/3/00 4:22:05 PM | 5:19:06 | 19146.00 | 108.006644852136 | -0.184097002 |
| 2/3/00 5:25:56 PM | 6:22:57 | 22977.00 | 104.201332127358 | -0.21996484 |

Table 1
Calculated results

Conclusion

In this application note a kinetic measurement for the saponification of procaine at pH=10 was performed and analyzed using the Agilent 220 MPS, the Agilent 1100 Series LC system and the Agilent ChemStation Plus. The progress of the reaction was monitored in the ChemStation Plus database module and the data was transferred further to Microsoft Excel for calculation of the rate coefficient. The transfer was done automatically. It was not necessary to transfer the data manually, which would have been a slow, tedious and error-prone process.

*Udo Huber is an application
chemist based at Agilent
Technologies, Waldbronn,
Germany*

For more information on our products and services, visit our website at:
<http://www.agilent.com/chem>

Microsoft and Excel are registered trademarks of Microsoft Corporation.

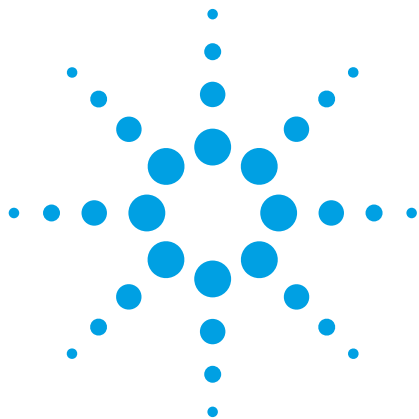
Copyright © 2000 Agilent Technologies
All Rights Reserved. Reproduction, adaptation or translation without prior written permission is prohibited, except as allowed under the copyright laws.

Printed 07/2000
Publication Number 5980-1661E



Agilent Technologies

Innovating the HP Way



Peptide Mapping of a Monoclonal Antibody using a Microfluidic-based HPLC-Chip coupled to an Agilent Accurate-Mass Q-TOF LC/MS

Application Note

Authors

Ravindra Gudihal
Agilent Technologies India Pvt. Ltd
Bangalore India

Keith Waddell
Agilent Technologies, Inc.
Santa Clara, CA USA

Abstract

The sequence characterization of a monoclonal antibody (mAb) at low nanogram levels using an Agilent HPLC-Chip system coupled to an Agilent Accurate-Mass Quadrupole Time-of-Flight (Q-TOF) LC/MS instrument is described. The exact mass measurement provided by this high performance Q-TOF LC/MS ensures confidence when determining analytes such as peptides. The superior sensitivity and mass accuracy of the HPLC-Chip LC/MS platform, combined with the powerful data processing capabilities of Agilent MassHunter and BioConfirm software, enabled complete sequence coverage of heavy and light chains and enabled mass confirmation of all identified peptides within a 4 ppm mass accuracy. The robust, reliable, and easy to use Agilent HPLC-Chip/MS System, which has significant benefits for peptide analyses, is ideally suited for the routine analysis of small quantity biopharmaceuticals.

Introduction

The sequence confirmation of therapeutic monoclonal antibodies is of prime importance before product release. Peptide mapping using LC/MS is an established analytical tool for the confirmation of amino acid sequences of monoclonal antibodies [1]. In this application note, a purified mAb was subjected to proteolytic digestion followed by peptide separation and mass determination on a HPLC-Chip coupled to an Accurate-Mass Q-TOF LC/MS. The data obtained from LC/MS were analyzed using the powerful features of the MassHunter Qualitative Analysis software package. The MS results of the trypsin digest yielded 95% sequence coverage of heavy chains and 85% of light chains, and in combination with different proteases, 100% coverage of both chains. The matched peptides were searched at a mass accuracy of 5 ppm. Furthermore, the MS/MS results obtained for peptides confirm the peptide sequence of mAb. This method of using HPLC-Chip technology in combination with True High-Definition TOF technology for antibody characterization is a valuable method in the biopharmaceutical industry for QC studies. This application note continues our studies toward complete characterization of monoclonal antibodies using advanced Agilent platforms ideal for the biopharma market [2].



Agilent Technologies

Materials

Immunoglobulin G (IgG) was obtained from ProMab Biotechnologies, Inc. DL-Dithiothreitol (DTT), iodoacetamide, Tris (hydroxymethyl)-aminomethane (Tris Base), sequence grade Glu-C, and α -chymotrypsin were purchased from Sigma Aldrich. High quality sequence grade trypsin was obtained from the Stratagene division of Agilent Technologies.

Sample pretreatment for different protease reactions:

Reduction and alkylation of an antibody under denaturation conditions

Before the digestion of the mAb with various proteases, the disulfides were reduced and alkylated under denaturation conditions. This pretreatment ensured that the monoclonal antibody was completely denatured and soluble allowing the protease to access its substrate efficiently [3, 4].

The mAb was lyophilized and reconstituted in 2 μ L of 8 M urea in 0.25 M Tris buffer, pH 7.6, containing DTT and incubated for 30 min at 37°C. 2 μ L of a solution containing iodoacetamide in 8 M urea in 0.25 M Tris buffer, pH 7.6, was added and the sample was incubated at ambient temperature in the dark for 15 min. The solution was diluted with 160 μ L of 0.25 M Tris buffer, pH 7.6, before digestion with various proteases.

Protease digestion

To the pretreated mAb solution, trypsin and α -chymotrypsin were added at a ratio of 20:1 and Glu-C at a ratio of 50:1 (protein to protease w/w). The reaction was incubated overnight for trypsin digestion, incubated 8 h for α -chymotrypsin digestion, and incubated 18 h for Glu-C digestion at 37°C before mass spectrometry analysis. The enzymatic activity was quenched by adding 1 μ L of 10% formic acid solution. The samples were either immediately analyzed by LC/MS/MS or stored at -80°C until further LC/MS/MS analysis.



Figure 1: Microfluidic-based Chip system coupled to Q-TOF mass spectrometer.

Instrumentation

The Agilent 1200 HPLC-Chip/MS Interface (PN: G4240A) was coupled with the Agilent 6520 Accurate-Mass Q-TOF LC/MS platform for LC/MS analyses (Figure 1).

LC Parameters:

HPLC-Chip: 5 μ m, ZORBAX 300SB-C18 (300Å), 40 nL enrichment column and a 75 mm x 43 mm analytical column (PN: G4240-62001).

Flow rate: 3 μ L/min from Agilent 1200 Series Capillary Pump (PN: G1382A) to the enrichment column and 600 nL/min from Agilent 1200 Series nanoflow LC pump (PN: G2226A) to the analytical column.

Solvents: 0.1% formic acid in water (A); 90% acetonitrile in water with 0.1% formic acid (B). Flush volume was set at 4 μ L.

Sample Loading: With Agilent 1200 Series Capillary Pump at 3% B.

Amount of sample injected onto the chip: 50 ng of the protein digest.

Sample analysis: Gradient with Agilent 1200 Series nanoflow LC pump as shown below.

| Time (min) | B (%) |
|------------|-------|
| Initial | 3 |
| 30 | 50 |
| 32 | 95 |
| 34 | 95 |
| 34.10 | 3 |

Stop time: 36 min

MS Parameters:

Spectra were recorded in positive ion and in centroid mode.

Vcap: 1900 V and drying gas flow of 5 L/min at 325°C was used.

Fragmentor voltage: 175 V

Data were acquired at high resolution (3,200 m/z), 4 GHz. For MS only mode, range 300–3,200 m/z . For MS/MS, spectra were acquired in auto MS/MS mode with the following parameters: MS scan, m/z 300–3,200 at 1 spectra/sec and MS/MS scan, m/z 50–3,000 at 3 spectra/sec.

Precursor selection criteria: maximum of 3 precursors above TH 1,000, active exclusion after 2 spectra for 0.5 min, preferred charges 2, 3, >3, unk (unknown). Collision Energy (CE): 3.7 V/100 Da, 2.5 V Offset. An internal mass calibration sample was infused continuously during the LC/MS runs. This internal reference mass system ensured accurate, precise, automated mass accuracy measurements during the LC/MS runs.

Data analysis: Data was processed using Agilent MassHunter Qualitative Analysis software, Agilent MassHunter BioConfirm and Agilent Spectrum Mill MS Proteomics Workbench software packages.

Molecular feature extraction: The raw data (chromatograms) were processed using the Molecular Feature Extractor (MFE) program within Agilent MassHunter Qualitative Analysis software.

Define and match sequence: Both the light and heavy chain sequences were digested using trypsin with 2 missed cleavages to generate a theoretical peptide digest list. The compounds extracted using MFE were matched against this list.

Spectrum Mill MS Proteomics Workbench: Spectrum Mill MS Proteomics Workbench was used to create a user defined database that contained the sequence information of the antibody under study. The MS/MS data was searched against this artificial database to assign the peptide sequence.

Results and discussion

Peptide mapping is routinely used for the assessment of antibody quality. **Figure 2A** shows the base peak chromatogram (BPC) of trypsin digested mAb obtained using the HPLC–Chip/MS system for nanospray

LC/MS. Inspection of the chromatogram reveals only peptide peaks with no undigested protein product. The extracted ion chromatograms (EICs) of some of the peptides for both light and heavy chains are shown in **Figure 2B**. These results show the high performance of HPLC–Chip separation, which is important in peptide mapping.

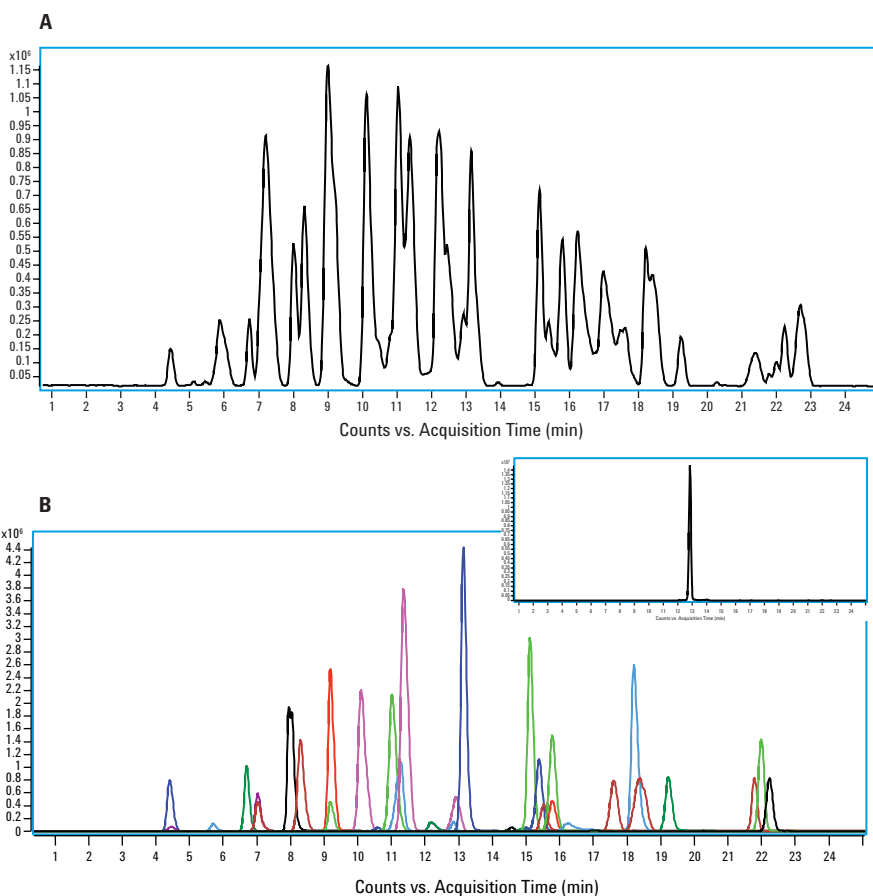


Figure 2: A. Base peak chromatogram (BPC) of trypsin digested mAb on a C18 HPLC-Chip. B. Extracted ion chromatogram (EIC) of some peptides from mAb light chains and heavy chains. The inset shows the expanded view of the peak with a narrow width of ~ 6 sec.

MFE yielded peptide masses for the LC/MS run. The peptide masses obtained for the light and heavy chains were then matched with the theoretical digest using a 5 ppm error. The theoretical digestion list of peptides for the trypsin digested mAb was generated using the BioConfirm sequence editor (define and match sequences). The list of matched peptides is shown in **Table 1**. All of the identified peptides are within a 4 ppm mass accuracy. The measured average mass deviation was found to be 1.35 ppm.

A. Light Chain

| Sequence Name | Label | Mass (Da) | Target Sequence Mass (Da) | Match Difference (ppm) |
|---------------|------------|-----------|---------------------------|------------------------|
| light chain | A(1-19) | 1996.088 | 1996.0841 | 1.98 |
| light chain | A(26-47) | 2438.1986 | 2438.1979 | 0.31 |
| light chain | A(48-56) | 992.5656 | 992.5655 | 0.15 |
| light chain | A(64-93) | 3388.5238 | 3388.5194 | 1.31 |
| light chain | A(94-107) | 1538.7191 | 1538.7154 | 2.43 |
| light chain | A(112-130) | 2101.1245 | 2101.1208 | 1.76 |
| light chain | A(113-130) | 1945.0199 | 1945.0197 | 0.09 |
| light chain | A(131-146) | 1796.8922 | 1796.888 | 2.38 |
| light chain | A(150-173) | 2676.2669 | 2676.2627 | 1.55 |
| light chain | A(150-187) | 4160.01 | 4160.0033 | 1.61 |
| light chain | A(154-173) | 2134.9657 | 2134.9615 | 1.99 |
| light chain | A(193-211) | 2140.0778 | 2140.0735 | 1.99 |
| light chain | A(195-211) | 1874.9254 | 1874.9197 | 3.06 |

B. Heavy Chain

| Sequence Name | Label | Mass (Da) | Target Sequence Mass (Da) | Match Difference (ppm) |
|---------------|------------|-----------|---------------------------|------------------------|
| heavy chain | A(1-19) | 1880.0511 | 1880.048 | 1.65 |
| heavy chain | A(20-38) | 2126.9587 | 2126.9554 | 1.56 |
| heavy chain | A(39-67) | 2927.4492 | 2927.4414 | 2.68 |
| heavy chain | A(39-65) | 2714.3216 | 2714.3188 | 1.05 |
| heavy chain | A(44-65) | 2233.0584 | 2233.0539 | 2 |
| heavy chain | A(44-67) | 2446.1802 | 2446.1765 | 1.51 |
| heavy chain | A(66-72) | 835.4663 | 835.4664 | -0.11 |
| heavy chain | A(68-72) | 622.3431 | 622.3439 | -1.28 |
| heavy chain | A(73-87) | 1768.8812 | 1768.8778 | 1.93 |
| heavy chain | A(77-87) | 1324.6816 | 1324.6809 | 0.51 |
| heavy chain | A(88-98) | 1317.5937 | 1317.5911 | 2 |
| heavy chain | A(99-105) | 714.4018 | 714.4024 | -0.94 |
| heavy chain | A(106-129) | 2531.2534 | 2531.2479 | 2.2 |
| heavy chain | A(107-129) | 2375.1509 | 2375.1468 | 1.74 |
| heavy chain | A(130-141) | 1185.6426 | 1185.6394 | 2.72 |
| heavy chain | A(142-155) | 1320.6705 | 1320.6708 | -0.21 |
| heavy chain | A(156-218) | 6712.309 | 6712.3072 | 0.27 |
| heavy chain | A(156-221) | 7054.4995 | 7054.4975 | 0.28 |
| heavy chain | A(156-222) | 7182.5962 | 7182.5925 | 0.52 |
| heavy chain | A(227-256) | 3333.643 | 3333.6349 | 2.45 |
| heavy chain | A(231-256) | 2843.4544 | 2843.4503 | 1.45 |
| heavy chain | A(257-263) | 834.4274 | 834.4269 | 0.55 |
| heavy chain | A(264-282) | 2138.0249 | 2138.0202 | 2.22 |
| heavy chain | A(283-296) | 1676.7985 | 1676.7947 | 2.25 |
| heavy chain | A(297-309) | 3115.3418 | 3115.3315 | 2.13 |
| heavy chain | A(310-325) | 1807.0038 | 1806.9992 | 2.51 |
| heavy chain | A(310-328) | 2227.2034 | 2227.2001 | 1.5 |
| heavy chain | A(335-342) | 837.496 | 837.496 | 0 |
| heavy chain | A(347-368) | 2509.3347 | 2509.3289 | 2.32 |
| heavy chain | A(349-368) | 2310.1993 | 2310.1968 | 1.08 |
| heavy chain | A(353-363) | 1285.6677 | 1285.6667 | 0.79 |
| heavy chain | A(353-368) | 1871.9648 | 1871.9629 | 1.03 |
| heavy chain | A(369-378) | 1160.6228 | 1160.6223 | 0.4 |
| heavy chain | A(379-400) | 2543.1289 | 2543.1241 | 1.9 |
| heavy chain | A(401-417) | 1872.9184 | 1872.9146 | 2.06 |
| heavy chain | A(423-447) | 3043.3964 | 3043.393 | 1.12 |
| heavy chain | A(425-447) | 2800.2679 | 2800.2598 | 2.89 |
| heavy chain | A(448-454) | 659.3488 | 659.349 | -0.35 |

Table 1: Peptide mass list after digestion of mAb with trypsin.

The matched peptides cover 95% of the heavy chains and 85% of the light chains. The BioConfirm tool enabled interpretation of the data in an easy and convenient way. In order to increase sequence coverage of the mAb, two more proteases were employed, Glu-C and α -chymotrypsin (data not shown). The results obtained from these digestions cover the sequences that were not covered earlier by trypsin digestion. This strategy of using combinations of two or more proteases helps with complete sequence characterization of the protein under study. This study (only MS) could also be achieved by using the HPLC-Chip technology coupled with a TOF analyzer such as Agilent's 6220 Accurate-Mass TOF LC/MS. However, for this study MS/MS data was also acquired as an example of further characterization of the mAb tryptic peptides under study.

The data was analyzed against the mAb sequence using Spectrum Mill MS Proteomics Workbench. The result of such an analysis is shown in **Figure 3**. **Figure 4** shows the representative MS/MS spectrum with the assigned sequence for example heavy and light chain peptides.

Agilent Spectrum Mill - Protein/Peptide Summary

Spectrum Mill Summary Settings Autovalidation Easy MS/MS MS/MS Search Spectrum Summary Build TIC Tool Belt Help

Results Shown Filtered by Validation Category: all
 Data Directory: msdataSM\promab
 hit table read - SpecFeatures read Files: 6675 Hits: 503
 beginning to assemble proteins ... proteins assembled 0.080362 sec
 proteins filtered by unique peptides 0.017179 sec
 proteins filtered by score
 calculated protein coverage maps 0.011325 sec
 beginning to roll up proteins into groups ... proteins rolled up into groups 0.002346 sec
 protein groups ready for display
 proteinGroupingMethod: oneSharedPeptide 2 Proteins listed

| Group (#) | Spectra (#) | Distinct Peptides (#) | Distinct Summed MS/MS Search Score | % AA Coverage | Mean Peptide Spectral Intensity | Database Accession # | Protein Name |
|-----------|-------------|-----------------------|------------------------------------|---------------|---------------------------------|----------------------|--------------|
| 1 | 355 | 35 | 615.91 | 94 | 1.25e+006 | 1 | Promab HClGg |
| 2 | 148 | 14 | 295.71 | 84 | 1.80e+006 | 2 | Promab LClGg |
| Totals: | | 503 | 49 | | | | |

Figure 3: Result window for Spectrum Mill based database search for the mAb trypsin digest.

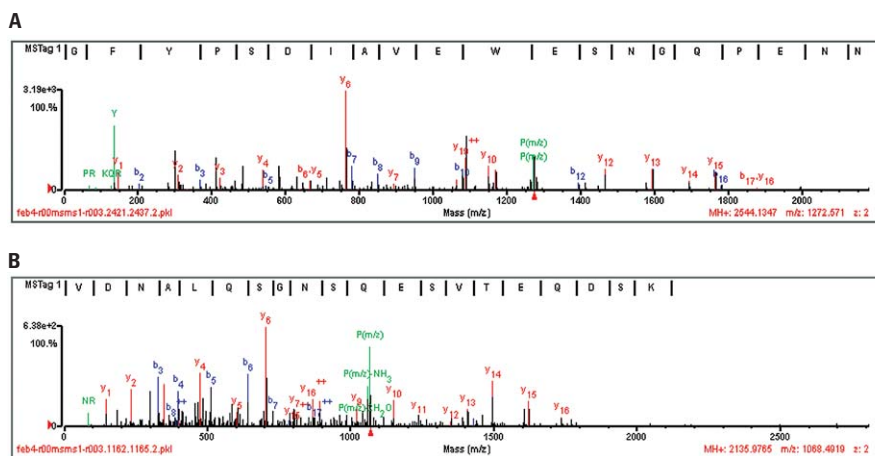


Figure 4: Representative MS/MS spectra of peptides from heavy chains (A) and light chains (B) with peptide sequences from Spectrum Mill MS Proteomics Workbench analysis.

Conclusions

The HPLC-Chip technology provides chromatographic peaks with narrow peak widths, which are important to generate high quality peptide fingerprints for large, complex proteins.

The highly accurate peptide masses determined by the Agilent 6520 Accurate-Mass Q-TOF LC/MS enables clear assignment of peptide peaks to the mAb sequence under study.

Data analysis using BioConfirm software helps with easy annotation and interpretation of the results.

The combination of HPLC-Chip technology with an Accurate-Mass Q-TOF mass spectrometer is a valuable tool for peptide mapping of small quantity biopharmaceuticals, providing analytical power that enhances peptide mapping studies.

References

1. Fiona M Greer, "MS analysis of biopharmaceutical products", *Innovation in pharmaceutical technology*, **2001**, 83-90.
2. Agilent publication 5990-3445EN: Primary Characterization of a Monoclonal Antibody Using Agilent HPLC-Chip Accurate-Mass LC/MS Technology.
3. Lihua Huang, Jirong Lu, Victor J. Wroblewski, John M. Beals, and Ralph M. Riggin, "In Vivo Deamidation Characterization of Monoclonal Antibody by LC/MS/MS", *Anal. Chem.*, **2005**, 77 (5), 1432-1439.
4. Lawrence W. Dick Jr., David Mahon, Difei Qiu, Kuang-Chuan Cheng, "Peptide mapping of therapeutic monoclonal antibodies: Improvements for increased speed and fewer artifacts", *Journal of Chromatography B*, **2009**, 877, 230-236.

www.agilent.com/chem/proteomics

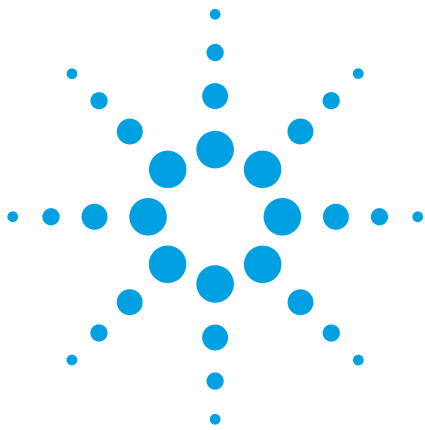
This item is intended for Research Use Only. Not for use in diagnostic procedures. Information, descriptions, and specifications in this publication are subject to change without notice.

Agilent Technologies shall not be liable for errors contained herein or for incidental or consequential damages in connection with the furnishing, performance, or use of this material.

© Agilent Technologies, Inc. 2009
Published in the U.S.A. October 12, 2009
5990-4587EN



Agilent Technologies



Tryptic digest analysis using the Agilent 1290 Infinity LC System

Application Note

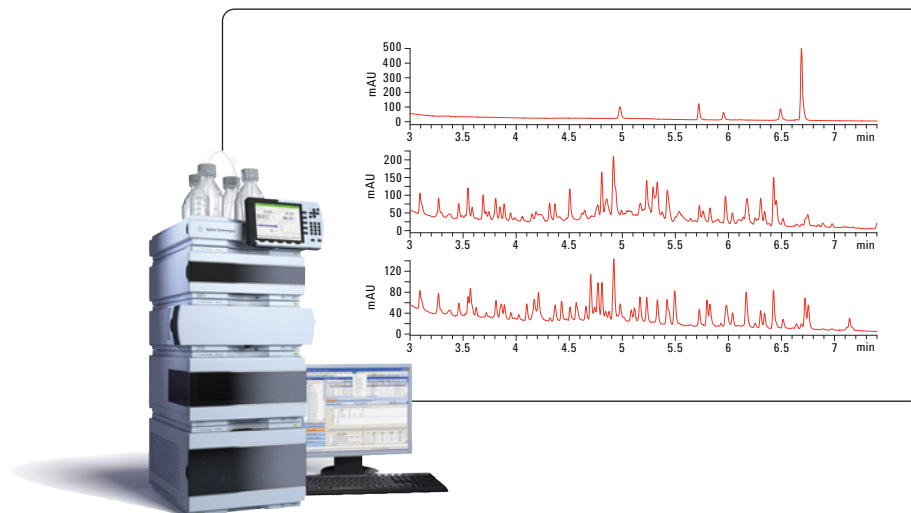
Drug Development, Production QA/QC

Authors

Gerd Vanhoenacker, Frank David,
Pat Sandra
Research Institute for Chromatography
Kennedypark 26
B-8500 Kortrijk
Belgium

Koen Sandra
Metablys
Kennedypark 26
B-8500 Kortrijk
Belgium

Bernd Glatz and Edgar Naegele
Agilent Technologies R&D and
Marketing GmbH and Co. KG
Hewlett-Packard-Str. 8
76337 Waldbronn
Germany



Abstract

This Application Note demonstrates:

- The applicability of the Agilent 1290 Infinity LC System to resolve peptide mixtures of higher complexity.
- A bovine serum albumin (BSA) tryptic digest was separated on a 250 mm × 2.1 mm id × 1.7 μm dp RP-LC column using different gradient slopes and flow rates.
- The maximum pressure applied was 900 bar. Peak capacities from 188 to 851 within total analysis times of 8 and 260 min, respectively, were obtained.



Agilent Technologies

Introduction

Peptide separations are of great importance in a variety of fields ranging from the characterization of recombinant, therapeutic proteins to proteomics-based biomarker discovery and verification. Sample complexity is enormous with typically hundreds of species encountered in biopharmaceutical preparations and many thousands of peptides in proteomics samples. Evidently, the chromatographer is confronted with an enormous separation challenge.

In this application note, the resolving power of ultra-high pressure LC (UHPLC) using the 1290 Infinity LC system is demonstrated. BSA tryptic digest was separated on a 250 mm × 2.1 mm × 1.7 μm d_p column. Peak capacity and peak capacity productivity, two powerful metrics to evaluate the separation, were determined at different gradient slopes and flow rates.

Note that an *in silico* digest of BSA generates approximately 150 peptides with one miscleavage allowed, and aspecific cleavages not taken into account.

Experimental

Instrumentation and method

An Agilent 1290 Infinity LC system with the following configuration was used:

| Part number | Description |
|-------------|---|
| G4220A | Agilent 1290 Infinity Binary Pump with integrated vacuum degasser |
| G4226A | Agilent 1290 Infinity Autosampler |
| G1316C | Agilent 1290 Infinity Thermostatted Column Compartment |
| G4212A | Agilent 1290 Infinity Diode Array Detector |

Method parameters:

| | | | |
|--------------|---|---------------|-------------------------|
| Column | C18 150 mm × 2.1 mm 1.7 μm C18 100 mm × 2.1 mm 1.7 μm | | |
| Mobile phase | A = 0.10% TFA in water/acetonitrile 98/2 v/v B = 0.08% TFA in acetonitrile | | |
| Flow rate | 0.4 mL/min or 0.2 mL/min | | |
| Gradient | 0 to 50% B | variable time | (gradient elution) |
| | 65% B | for 10 min | (column rinsing) |
| | 0% B | for 5 min | (column reconditioning) |
| Temperature | 60 °C | | |
| Injection | 10 μL | | |
| Detection | DAD, Signal 214/4 nm, Reference 400/60 nm, 40 Hz | | |

Samples

Tryptic digestion of BSA was carried out in an ammonium bicarbonate buffer at pH 8. Trypsin was added in an enzyme/substrate ratio of 1/50 and the mixture was incubated overnight at 37 °C. Another BSA sample (called BSA RA) was reduced and alkylated prior to digestion. Both samples were acidified with mobile phase A to a concentration of 3 nmol/mL prior to injection. A peptide standard mixture, used to aid in the calculation of the peak capacity, was dissolved in mobile phase A and contained bradykinin 1–5 (5 nmol/mL), angiotensin II (3 nmol/mL), neurotensin (2 nmol/mL), ACTH clip [18-39] (2.5 nmol/mL), and bovine insulin chain B (12.5 nmol/mL).

Results and Discussion

A column length of 250 mm was obtained by coupling two columns (150 and 100 mm) using a stainless steel capillary of 70 mm with an internal diameter of 0.12 mm. Performing a relatively fast gradient analysis of 8% B/min resulted in a fast analysis of the digest (Figure 1). A peak capacity of approximately 190 was generated with this short gradient time (6.25 min). This corresponded to a peak capacity production rate of over 30 peaks/min. Peak capacity was calculated by dividing the

gradient time with the average peak width at the base (4σ) determined for five standard peptides (Figure 1). The gradient applied in this note was longer than actually required to elute the last BSA fragments from the column. The reason for this is that this gradient is also applied for the analysis of other digests with more retentive peptides. When only the elution window (3 to 7.5 min) is taken into account for the calculation a peak capacity of 136 is obtained. The peak capacity productivity is not affected however; the number of peaks generated per minute remains the same.

Applying longer, more shallow gradients increases peak capacity and therefore the amount of detail visualized in the chromatogram. Evidently, the price to pay is analysis time. Figure 2 shows the result for the BSA digest analyzed with four different gradient slopes. The peak capacity tripled from 188 to 567 when the gradient time was increased from 6.25 min (8% B/min) to 50 min (1% B/min), respectively. If only the elution window of the BSA digest is taken into account for the 50-min gradient, the peak capacity is 375 in 39 min. It is clear that the chromatogram at the more shallow gradient reveals much more detail, while analysis time remains acceptable. Further increasing

the gradient time leads to a higher peak capacity, but the effect of the flatter gradient becomes less significant from a defined point and the peak capacity productivity becomes nearly fixed. This is summarized in Figure 3. Doubling the gradient time from 50 to 100 min increases the peak capacity by approximately 25% (567 to 711). However, an additional increase in the gradient time to 200 min, produces a gain in peak capacity of only approximately 15% (711 to 820). In the last situation, the analysis time is over 3 h and becomes less practical in routine operation. From Figure 3 it can be deduced that the best compromise between peak capacity and analysis time is obtained with a gradient time of 100 to 150 min.

When the flow rate and gradient slope are reduced to 0.2 mL/min and 0.5% B/min, respectively, the peak capacity increases from 567 to 645 compared to the analysis carried out at 0.4 mL/min and 1% B/min. However, the peak capacity production rate is reduced from 11.3 to 6.4 with this approach. When samples become more complex on the other hand, a moderate increase in resolution can become useful for detecting minor differences between related samples, especially when high-end qualitative detectors such as a mass spectrometer are applied.

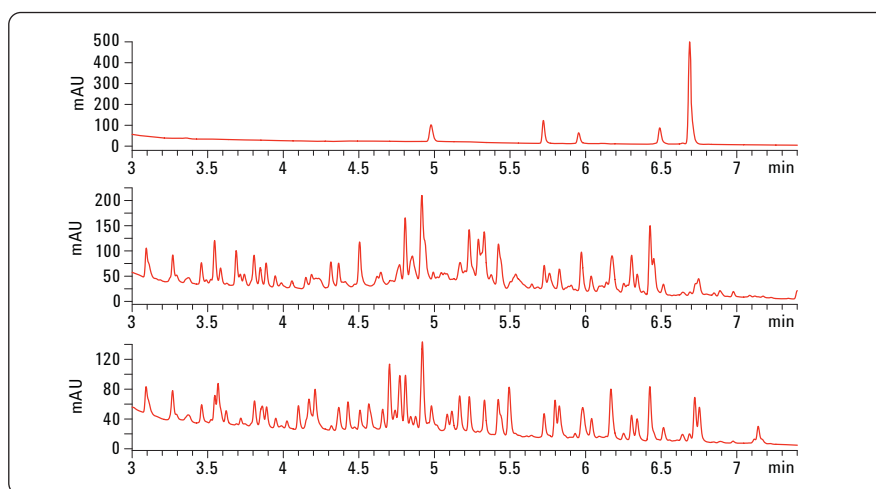


Figure 1
High speed analysis of the peptide standard mixture (upper trace), BSA digest (middle trace) and BSA RA digest (lower trace). Flow rate: 0.4 mL/min, gradient: 0–50% B in 6.25 min.

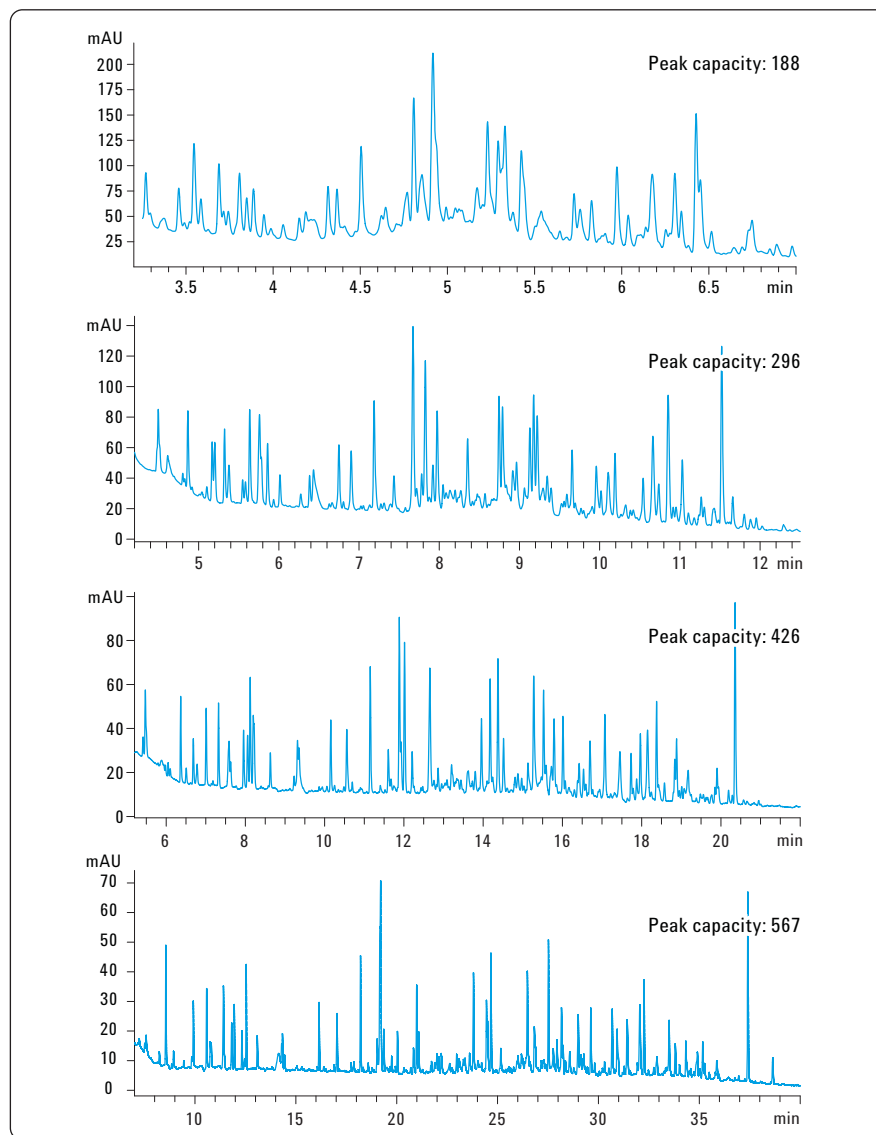
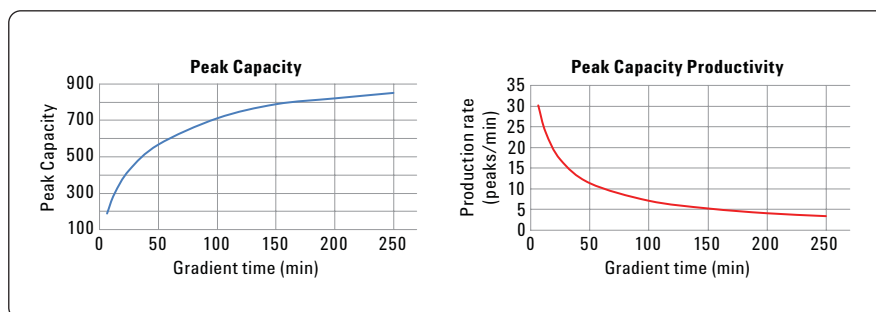


Figure 2
Analyses of the BSA digest with different gradients. Flow rate: 0.4 mL/min, gradient: 0-50%B in 6.25 min (8%/min), in 12.5 min (4%/min), in 25 min (2%/min), and in 50 min (1%/min).

Conclusion

This Application Note demonstrates the versatility of Agilent 1290 Infinity LC system for separating peptide mixtures of high complexity. Protein digests were analyzed on a 250 mm long column packed with 1.7- μm particles and operated at a pressure up to 900 bar. Depending on the need, high productivity (peak capacity of 188 in less than 10 min) or high resolution (peak capacity exceeding 800 in 3h) can be obtained.



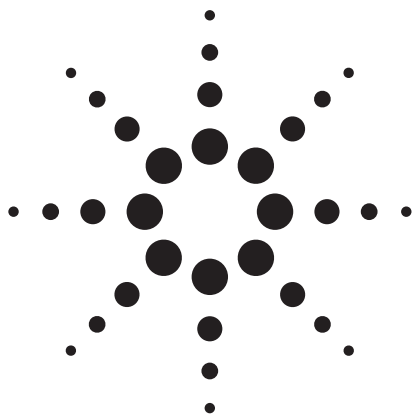
| Gradient time (min) | Gradient slope (% B/min) | Peak capacity | Peak capacity productivity (peaks/min) |
|---------------------|--------------------------|---------------|--|
| 6.25 | 8 | 188 | 30.1 |
| 12.5 | 4 | 296 | 23.7 |
| 25 | 2 | 426 | 17.0 |
| 50 | 1 | 567 | 11.3 |
| 100 | 0.5 | 711 | 7.1 |
| 150 | 0.375 | 788 | 5.3 |
| 200 | 0.25 | 820 | 4.1 |
| 250 | 0.2 | 851 | 3.4 |

Figure 3
Peak capacity and peak capacity production rate in function of gradient time.

www.agilent.com/chem/1290

© Agilent Technologies, Inc., 2009
May 1, 2009
Publication Number 5990-4031EN

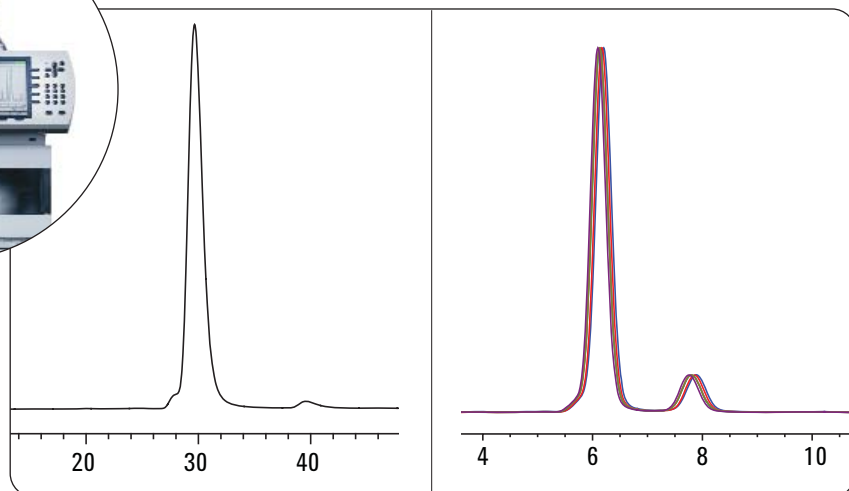




Converting the USP insulin assay method for use on the Agilent 1200 Series Rapid Resolution LC System

Application Note

Dr Courtney Milner
Dr Russell Kinghorn
BST International



Abstract

Agilent Equipment:

1200 Series Rapid Resolution LC System

Application Area:

Conversion of standard USP method to Rapid Resolution LC method

This Application Note describes conversion of the USP method for insulin from the original 77-minute analysis to a significantly shorter 16.5-minute analysis by deploying smaller, more efficient columns, without any loss of performance. The Agilent 1200 Series Rapid Resolution LC (RRLC) system was used throughout the study. This system provides the modern analytical laboratory with a highly flexible and effective tool for liquid chromatography. The Agilent 1200 Series RRLC system can be used to run existing validated or regulatory methods, achieving significant improvements in performance without the need for any hardware modifications.



Agilent Technologies

Introduction

The U.S. Pharmacopoeia (USP) is the official public standards-setting authority for all prescription and over-the-counter medicines, dietary supplements, and other healthcare products manufactured and sold in the United States. It is a non-profit organization, self-funded by the sale of products and services to a wide range of groups involved in the healthcare industry. One aspect of its services provides an extensive list of standard methods for the pharmaceutical industry to use for testing products at all stages of manufacture. An attractive aspect of these methods is the reduced necessity for in-house re-validation of the methods before use on regulated products. A potential disadvantage of the vast number of methods published by the USP, is that many have not kept pace with advances in modern equipment or the laboratories need to improve sample productivity in the global market. One of these such methods is for the testing of insulin for related substances, which has a potential run time of approximately 90 minutes.

Insulin is a naturally occurring hormone required for almost all forms of life, and in humans is widely used for the treatment of both type 1 and some cases of type 2 diabetes. It was first trialed on a human subject in 1922, and has been the compound behind no less than four Nobel prizes. Since FDA approval in 1939 insulin has been a cornerstone tool in the management of

diabetic patients.

The USP method for the assay of insulin involves a long isocratic elution, followed by a gradient to elute high molecular weight impurities. USP 29 describes a method whereby the mobile phase composition may be adjusted to ensure an insulin retention time of “about 31 minutes”¹ with the gradient not allowed to start until the elution of the degradant impurity A-21 desamido insulin. This, coupled with a long equilibration time before re-injection, can lead to an analysis time of up to 92 minutes, although this is typically 77 minutes if the gradient start time is adjusted.

Current users of this USP method will also appreciate that the method is very sensitive to minor changes in all parameters affecting the separation. The published method only eludes to this with the subtle text “Adjust the mobile phase composition and the duration of the isocratic elution to obtain a retention time of about 31 minutes”. The reality of this clause is that each time an insulin run is prepared, some minor method tweaking is required – with a 77 minute run, this is a time-consuming and unproductive process, especially as test solution should not be kept for more than 12 hours under refrigerated conditions.

The long analysis time and sensitive nature of the method highlights it as an excellent method to be evaluated with the Agilent 1200 Series RRLC system utilizing a much faster method. As with any method translation, key

criteria of the method must be maintained, such as resolution, carryover and retention time precision. Despite the obvious potential advantages to speeding up the method, a problem exists with the validity of the method without performing a full method validation. It is for this reason that many laboratories choose to continue running the published reference methods. Another significant deterrent is the fear of the process of conversion of method conditions, without the need for substantial additional method development. To alleviate this hurdle, Agilent has produced a simple to use and accurate software tool for converting from any typical column in use today (for example, from 4.6 mm ID and smaller, and 250 mm length, and shorter).

The Agilent 1200 Series RRLC system offers unique flexibility and functionality. The ability to operate the system at flow rates up to 5 mL/min and pressures up to 600 bar results in a wide choice of potential replacement columns and the speeding up of analysis. These columns include 1.8 μm particle columns, providing the same potential efficiency from a significantly shorter column. However, if this is to be done the overall system must provide the highest level of stability and performance to ensure all reproducibility data requirements can be met. The ultimate benefit of this flexibility is the removal of another barrier to change, namely, the choice of analytical system and columns to be used for both existing methods and the newly developed enhanced methods.

This Application Note describes an investigation into the reduction in analysis time of the insulin method by as much as a factor of 4.6, while at the same time meeting all criteria outlined by the USP method and using the exact same hardware with no modification or replumbing.

Equipment

The first stage of comparing an existing method to any new, improved method is the obvious proof of performance of the regulated method. In this study, the USP 29 method for related compounds was followed as written. The equipment and mobile phases used were:

Agilent 1200 Series RRLC system consisting of:

- Agilent 1200 Series binary pump SL
- Agilent 1200 Series micro vacuum degasser
- Agilent 1200 Series high performance well-plate sampler with thermostat control
- Agilent 1200 Series thermostated column compartment SL
- Agilent 1200 Series diode array detector SL with semi-micro flow cell
- Agilent Chemstation B.02.01
- Column: ZORBAX Eclipse Plus C18, 4.6 mm x 250 mm, 5 μ m (Agilent order number 959990-902)
- Column temperature: 40 °C
- Mobile phase: Prepared as described in USP method, 28.4 g of sodium sulphate dissolved in 1000 mL of water

with 2.7 mL of phosphoric acid, pH modified with ethanolamine to pH 2.3. From this the two mobile phases are prepared:

- Mobile phase A – 82:18 mixture with acetonitrile;
- Mobile phase B – 50:50 with acetonitrile.
- Gradient: The USP describes a gradient, which allows for the adjustment of the mobile phase composition to achieve an elution time of the insulin of about 31 minutes. Table 1 shows the recommended gradient and the one used for the initial method as per the USP. The flow rate is set at 1 mL/min.

Conversion of methods

The Agilent method translator software tool was used to con-

vert the gradient times to allow the use of a 100 mm x 1.8 μ m column of the same column packing (Agilent order number 959964-902). The goal was to simply translate the method to allow the use of a 1.8 μ m column providing a similar number of theoretical plates – hence just a speed enhancement. Further discussion of this conversion and the conditions used are presented in the next section.

Results and discussion

Analysis of the insulin under the USP method was undertaken to illustrate the capability of the Agilent 1200 Series RRLC system to run traditional methods, along with new higher speed methods. Figure 1 shows the chromatogram for the USP insulin method.

| USP method (modified conditions) | | | |
|----------------------------------|---------------------|---------------------|-----------------|
| Time (min) | Solution A % | Solution B % | Elution |
| 0 (0) | 81 (74.4) | 19 (25.6) | Equilibration |
| 0 – 60 (0 - 45) | 81 (74.4) | 19 (25.6) | Isocratic |
| 60 – 85 (45 - 70) | 81 – 36 (74.4 – 36) | 19 – 64 (25.6 – 64) | Linear gradient |
| 85 – 91 (70 – 76) | 36 (36) | 64 (64) | Isocratic |
| 91 – 92 (76 – 77) | 36 – 81 (36 – 74.4) | 64 – 19 (64 – 25.6) | Linear gradient |

Table 1
Comparison of USP method and final gradient for standard analysis.

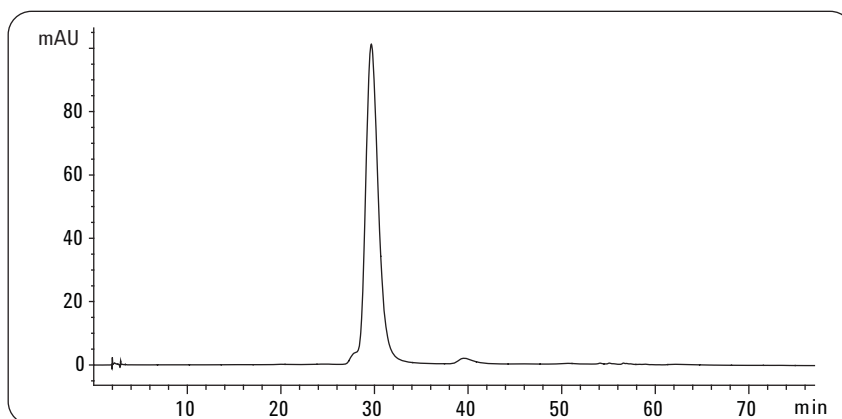


Figure 1
Chromatogram of USP insulin method.

Figure 2 shows the effect of changes of ± 0.1 mL/min on the standard flow rate of 1 mL/min.

Figure 3 illustrates the effect of temperature on the retention time while leaving all other parameters the same.

The effect of the temperature, with the lower temperature resulting in a dramatically shorter retention time (30 %), suggests the mechanism of retention is heavily dependant on the pH of the solution. As the pH of solution was measured at 20 °C and the column run at 40 °C, there could be a significant effect (up to 0.2 pH units). A further observation from this experiment was that the peak shape improved (small peak at front of major peak is removed), and as such may be in itself a superior method.

The next minor change in conditions was a 0.1 % change in the isocratic mobile phase conditions for the elution of the insulin. It was expected that this would have a significant impact on retention time also, as evidenced by the need to tailor this to each preparation of mobile phase. Figure 4 shows the effect on retention time of these changes.

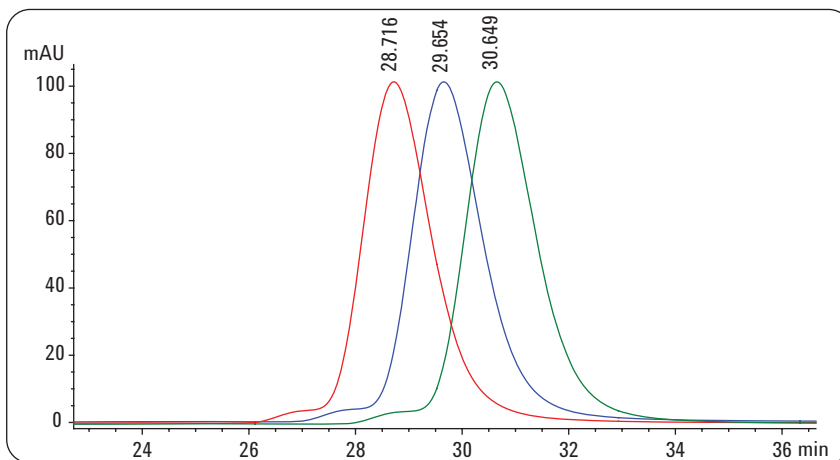


Figure 2
Effect on retention time of 0.1 mL/min change in flow rate; RT 28.7 = 1.1 mL/min, RT 29.6 = 1 mL/min, RT 30.6 = 0.9 mL/min.

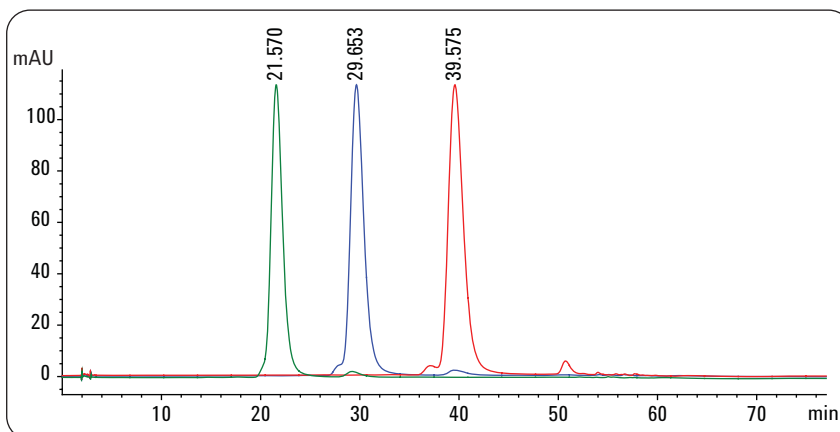


Figure 3
Effect of temperature on retention time; RT 21.57 = 35 °C, RT 29.6 = 40 °C (standard), RT 39.57 = 45 °C.

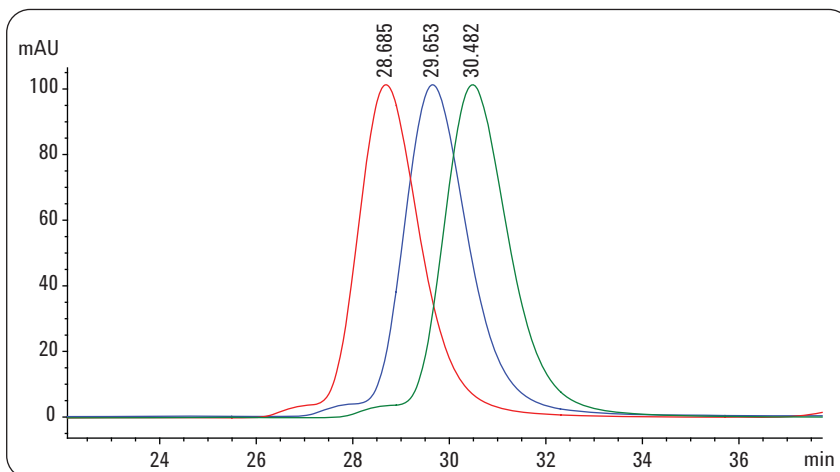


Figure 4
Effect of mobile phase composition on retention time
RT 28.68 +0.1 % mobile phase B, RT 29.65 No change. RT 30.48 -0.1% mobile phase B.

Each of these experiments highlights the sensitivity of the method to instrumental conditions. They also highlight the need to adhere to the basic structure of the USP method, as it would otherwise not be possible to validate in the laboratory. Further criteria put forward by the USP include the resolution between the insulin peak and the A-21 desamido insulin, carryover and tailing factor for the insulin.

A basic system suitability parameter for any HPLC analysis is the retention time repeatability. The experiments described highlight the requirement for precise and accurate instrument operation at all times, or basic system suitability will not be met. Table 2 shows these values as determined by these experiments, while figure 5 shows an overlay of 6 replicate injections.

Conversion to 1.8 µm columns

The conversion of the method to utilize a 1.8 µm particle column packing was performed using the Agilent method translator, using the straight conversion parameters. The column dimensions were chosen to offer the closest number of effective efficiency to that of the USP recommend column. Table 3 shows the comparison between these two columns in terms of efficiency.

Figure 6 shows the conversion program screen with parameters used for the 1.8 µm column. It can be seen from this screen that theoretically calculated time gain is a factor of 2.5, meaning a total run of 30.80 minutes. Using the time conversion, the expected retention time of the insulin

| | Experimental result | USP criteria |
|---------------------------|---------------------|--------------------------------------|
| RT insulin (min) | 29.81 | Approx. 31 |
| % RSD RT | 0.72 | < 1.6% |
| % RSD area | 0.19 | < 1% (FDA recommended ²) |
| Resolution | 3.8 | > 2.0 |
| USP tailing | 1.26 | < 1.8 |
| Symmetry | 0.75 | Not stated |
| Carryover (200% solution) | < 0.01% | Not stated |
| Total run time | 77 minutes | Up to 91 minutes |

Table 2
Summary of system performance for USP method.

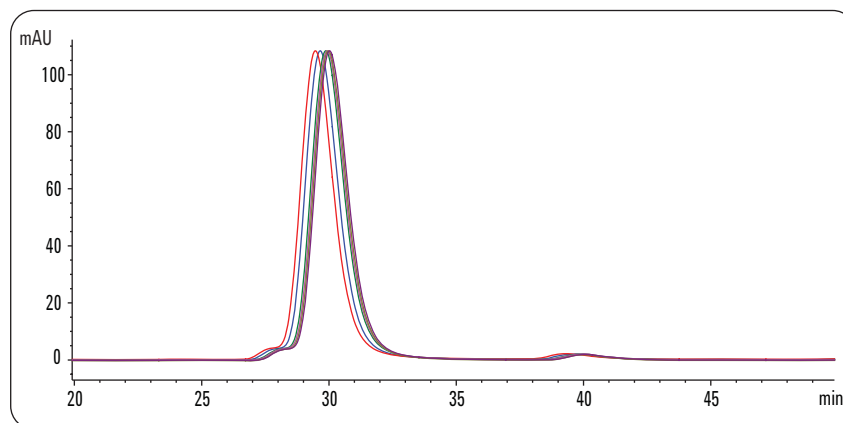


Figure 5
Retention time precision of six replicate injections of USP resolution mix.

| Column dimensions | Particle size | Theoretical efficiency | Flow rate | Effective efficiency |
|-------------------|---------------|------------------------|-----------|----------------------|
| 250 x 4.6 mm | 5 µm | 22,000 | 1 mL/min | 18,300 |
| 100 x 4.6 mm | 1.8 µm | 22,200 | 1 mL/min | 17,700 |

Table 3
Comparison of efficiency (N) between USP recommended column and rapid resolution column.



Figure 6
Conversion program screen to convert to different column dimensions.

peak was 11.9 minutes. As the same flow rate was to be used, no further changes to the Agilent 1200 Series RRLC system were required to be made, allowing for the quick swapping between methods if required.

Table 4 compares the adherence of the converted method to the required criteria. Figure 7 shows an overlay of 6 replicates at these conditions, showing that the expected efficiency for the columns was almost exactly maintained. Figure 8 shows the carryover of a blank injection after the injection of a 200 % solution.

| | Experimental result | USP criteria |
|---------------------------|---------------------|-----------------------------------|
| RT Insulin (Mins) | 11.89 | Expected RT from conversion 11.96 |
| % RSD RT | 0.21 | < 1.6% |
| %RSD area | 0.24 | < 1% (FDA recommended) |
| Resolution | 3.2 | > 2.0 |
| USP tailing | 1.15 | < 1.8 |
| Symmetry | 0.91 | Not stated |
| Carryover (200% Solution) | < 0.01% | Not stated |
| Total run time | 30.8 minutes | 2.5 time faster |

Table 4
Performance of converted method for USP insulin.

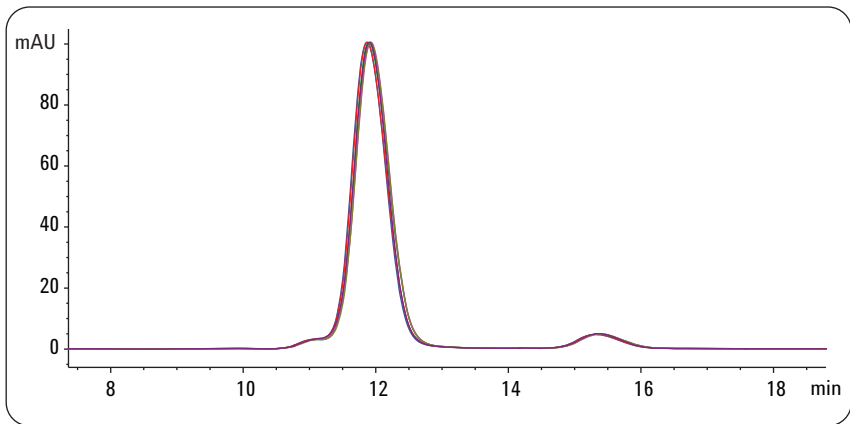


Figure 7
Overlay of 6 repeat injections using converted method.

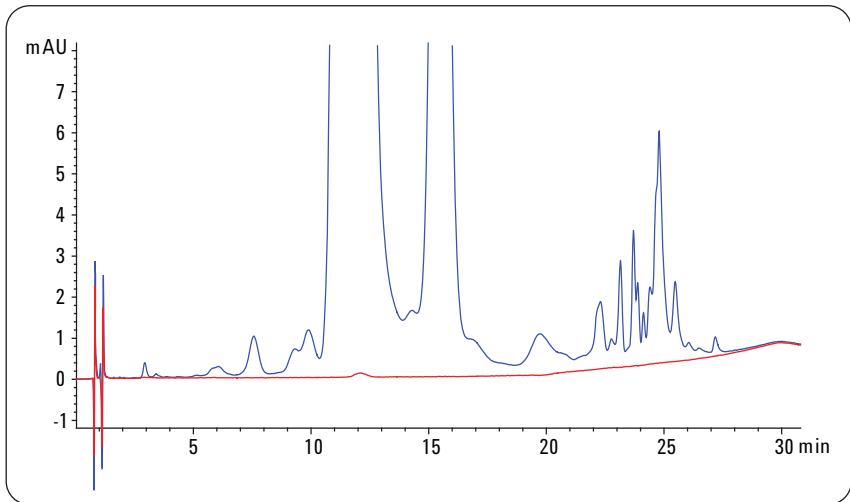


Figure 8
Chromatogram of blank injection after 200% insulin mix injection.

Further gains in analysis speed

The straight method conversion achieved a gain in speed by a factor of 2.5, however these conditions still allowed for enhancement to be made in the speed of the analysis without the loss of performance. An advantage of utilizing 1.8 μm particles is the flat van Deemter curve with linear velocity. As a result, the flow rate was increased to 1.7 mL/min and the gradient converted to provide a total analysis time of 16.5 minutes, a gain in speed by a factor of 4.6. This means that four times the analyses could be performed in a given time, enhancing the laboratories output. The same criteria were evaluated for the overall performance of the system and are shown in table 5, along with a summary of those conditions from the previous methods. Figure 9 shows the repeatability under these even faster conditions.

Conclusion

The Agilent 1200 Series Rapid Resolution LC system provides a highly flexible system that allows the user to run both conventional analytical methods, while at the same time without any changes to the hardware significantly reduce run time without loss of key system performance parameters such as repeatability, resolution or peak shape. The USP method for insulin has been used as a demonstration of the systems capability to achieve this. The sensitivity of the method to instrumental setpoints and mobile phase conditions make this a desirable method to shorten.

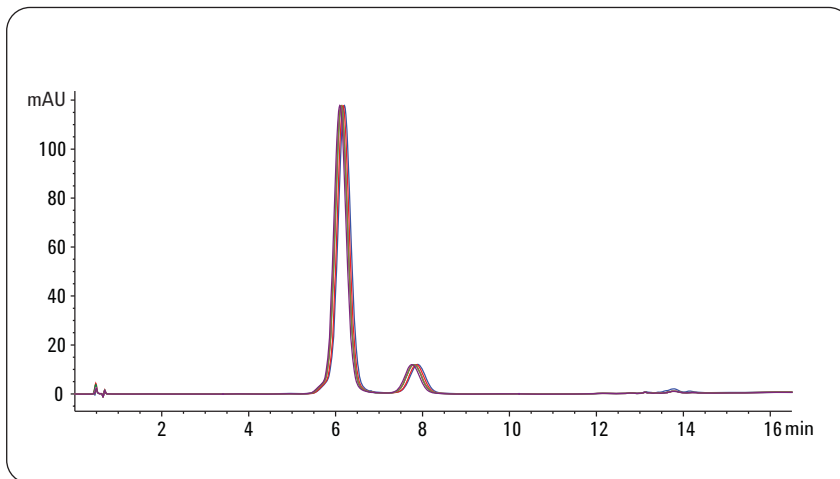


Figure 9
Very fast method for the analysis of Insulin with Agilent 1200 Series RRLC system.

| | USP method | Fast method | Very fast method |
|----------------------------|------------|--------------|------------------|
| RT insulin (min) | 29.81 | 11.89 | 6.14 |
| %RSD RT | 0.72 | 0.21 | 0.60 |
| %RSD area | 0.19 | 0.24 | 0.18 |
| Resolution | 3.8 | 3.2 | 2.8 |
| USP tailing | 1.26 | 1.15 | 1.02 |
| Symmetry | 0.75 | 0.91 | 0.95 |
| Carryover (200 % solution) | < 0.01% | < 0.01% | ND |
| Total run time | 77 minutes | 30.8 minutes | 16.5 minutes |
| Speed gain | - | 2.5 x | 4.6 x |

Table 5
Comparison of three methods for the analysis of insulin on Agilent 1200 Series RRLC system.

References

1.

The United States
Pharmacopoeia USP 29 – Insulin
pp. 1132 – 1136.

2.

Center for Drug Evaluation and
Research, U.S. Food and Drug
Administration. *Reviewer
Guidance, Validation of
Chromatographic Methods*; FDA,
Rockville, MD; Nov **1994**.

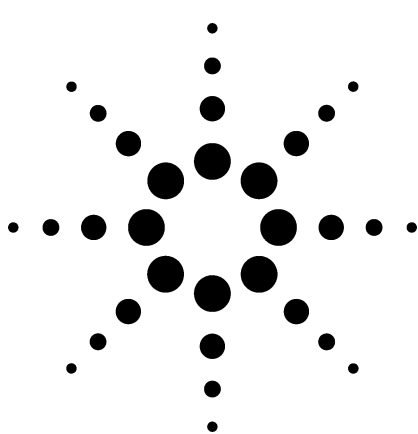
www.agilent.com/chem/1200rrht
www.bst.com.au

© 2007 Agilent Technologies Inc.

Published June 1, 2007
Publication Number 5989-6910EN



Agilent Technologies



Using the High-pH Stability of ZORBAX Poroshell 300Extend-C18 to Increase Signal-to-Noise in LC/MS

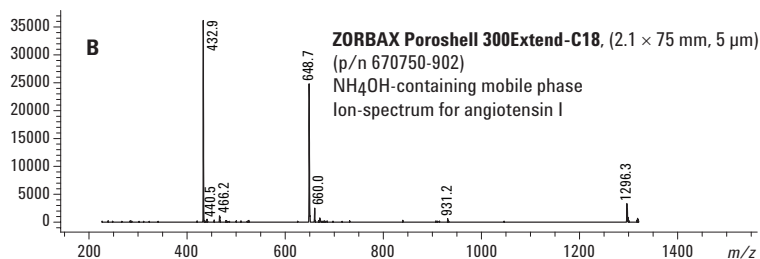
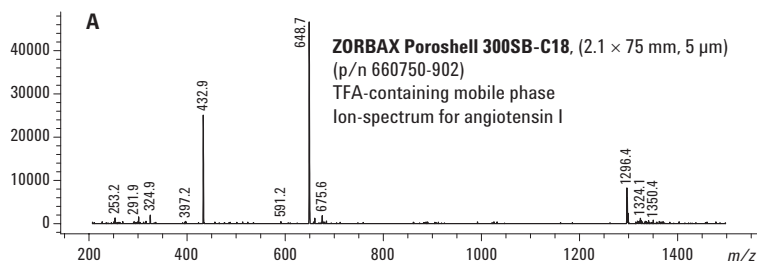
Application

Drug Manufacturing/QA/QC

Robert D. Ricker

ZORBAX Poroshell technology is designed to facilitate extremely rapid HPLC separations at high relative flow rates (high linear velocities). Poroshell particles consist of a solid silica core surrounded by a very thin (0.25 μm) porous silica crust. High linear velocities of mobile phase are tolerated because of the short diffusion distance for molecules moving into and out of this thin crust. Typical flow rates are five times that used for a comparable column packed with totally porous material.

ZORBAX Poroshell 300Extend-C18 is made using the same, reliable, Extend-C18 bonding used for ZORBAX totally porous packings; column lifetime at high pH is extended. Enhanced lifetime of the column at high pH makes the columns useful for atmospheric pressure ionization-electrospray (API-ES) mass spectrometric (MS) detection of peptides and small proteins using NH_4OH in the mobile phase. There are advantages in signal-to-noise (S/N) and in charge state distribution when using NH_4OH at high pH rather than trifluoroacetic acid (TFA) or formic acid at low pH. The following positive-mode spectra demonstrate the effect of the mobile-phase modifier on the MS signal.



Highlights

- ZORBAX Poroshell technology facilitates very rapid HPLC separations at flow rates, up to 5x that used for totally porous packing.
- ZORBAX Poroshell 300Extend-C18 allows for MS detection of peptides and small proteins using NH_4OH in the mobile phase, which can lead to reduced background noise and a higher S/N ratio.
- Reliable use of NH_4OH with ZORBAX Poroshell 300Extend-C18 provides a means of altering charge-state distribution.

Mobile phase (pH 1.8)

- A: 0.1% TFA in H_2O
- B: 0.085% TFA in ACN

Mobile phase (pH 10)

- A: 10 mM NH_4OH in H_2O
- B: 10 mM NH_4OH in ACN

Conditions

| | |
|-----------|--|
| Column | See column info in figure (operation at ambient temperature) |
| Sample | 330-ng Angiotensin I, 1- μL injection |
| Gradient | 0%–100% B in 2 min, F = 0.5 mL/min (see mobile phase at right) |
| Detection | Agilent 1100 Series MSD, API-ES Pos Scan Mode, 200–1500 m/z , 0.52 s/cycle, Capillary = 4500V, Frag = 70V, Nebulizer 35 psi, Drying gas 12 L/min @325 $^\circ\text{C}$ |



Agilent Technologies

The figure demonstrates the difference in S/N in the MS ion spectrum from angiotensin I analyzed with TFA in the mobile phase (A) or with NH₄OH in the mobile phase (B). For speed of analysis, ZORBAX Poroshell packings were used in each case - the 300SB-C18 version for stability under low-pH operation and the 300Extend-C18 version for stability under high-pH operation. Relative to the spectrum obtained using TFA, the spectrum obtained using NH₄OH shows decreased background noise, especially within the 200–400 *m/z* range. The molecular ion appears at an *m/z* of 1296, with the +2 and +3 ions appearing at 648.7 and 432.9, respectively. There is a shift from +2 being the dominant ion in TFA, to the +3 being the dominant ion in NH₄OH. Note that the abundance is similar for these ion species at low pH with TFA and at high pH with NH₄OH even though the detector is set to positive mode. While the abundance is slightly less (5000 vs. 4000) this makes use of NH₄OH with ZORBAX Poroshell 300Extend-C18 a useful technique. Not only may background noise be reduced and the charge distribution shifted, but also the column can be expected to perform reliably at high pH to produce very rapid analyses. Please refer to the following Agilent application notes for relevant information: Comparison of ZORBAX Poroshell 300Extend-C18 to totally porous packing for rapid separations at high pH, 5989-0675EN [1]. Use of low and high pH to achieve unique selectivity, 5989-0645EN and 5989-0676EN [2, 3].

The angiotensin peptides are part of a system that controls hypertension and cardiovascular structure. Angiotensin II, the principal peptide, is derived from angiotensin I by cleavage of the C-terminal dipeptide his-leu. For reference, the sequence and molecular weights of angiotensins I, II, and III are shown in Table 1.

Table 1. The Sequence and MW for Angiotensins I, II, and III

| Peptide | Peptide sequence | MW |
|-----------------|---|--------|
| Angiotensin I | asp-arg-val-tyr-ile-his-pro-phe-his-leu | 1296.5 |
| Angiotensin II | asp-arg-val-tyr-ile-his-pro-phe | 1046.2 |
| Angiotensin III | arg-val-tyr-ile-his-pro-phe | 931.1 |

References

1. R. Ricker, "Comparison of ZORBAX Poroshell 300Extend-C18 and totally porous packing in achieving very rapid, high-pH separation of peptides", Agilent Technologies, publication 5989-0675EN www.agilent.com/chem.
2. R. Ricker, "Using ZORBAX Poroshell Column Selectivity for Ultra-Fast Analysis of Angiotensin I, II, III at Low and High pH", Agilent Technologies, publication 5989-0645EN www.agilent.com/chem.
3. R. Ricker, "Using ZORBAX Poroshell 300Extend-C18 to Achieve Unique Selectivity at pH 2 and 10: Angiotensins", Agilent Technologies, publication 5989-0676EN www.agilent.com/chem.

For More Information

For more information on our products and services, visit our Web site at www.agilent.com/chem.

The author, Robert D. Ricker, Applications Expert, is based at Agilent Technologies, Inc., Wilmington, Delaware.

Agilent shall not be liable for errors contained herein or for incidental or consequential damages in connection with the furnishing, performance, or use of this material.

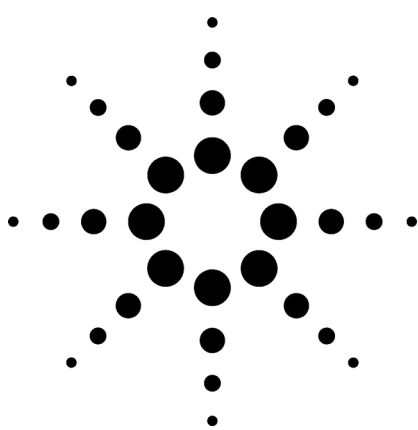
Information, descriptions, and specifications in this publication are subject to change without notice.

© Agilent Technologies, Inc. 2004

Printed in the USA
March 1, 2004
5989-0683EN



Agilent Technologies



Using ZORBAX Poroshell 300Extend-C18 to Achieve Unique Selectivity at pH 2 and 10: Angiotensins Application

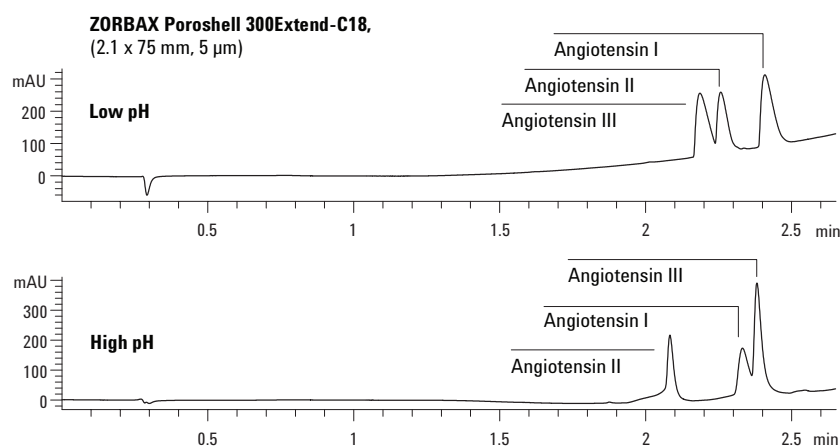
Biotechnology/QA/QC/Basic R&D

Robert D. Ricker

Selectivity (α factor) is the most powerful chromatographic parameter for obtaining resolution. In reversed-phase HPLC, change in mobile-phase pH can effectively achieve resolution where other chromatographic changes cannot. This is especially true for polar and charged analytes such as biological macromolecules. In this type of analysis, altering pH can shift the charge on the analytes as well as that on the packing surface. ZORBAX Poroshell 300Extend-C18 is made using the same, reliable, Extend-C18 bonding used for ZORBAX totally porous packings; both low-pH and high-pH mobile phases are tolerated, with extended column performance. Enhanced lifetime of the column over a broad pH range makes the material ideal for method development of peptides and small proteins. The following chromatograms demonstrate the use of mobile-phase pH to achieve selectivity differences.

Highlights

- ZORBAX Poroshell 300Extend-C18 columns provide wide range of selectivity for fast analysis of angiotensins at low and high pH.
- ZORBAX Poroshell is also available in SB-C18, SB-C8, and SB-C3 bonding for selectivity options at low pH and high temperature.
- Use of appropriate column and mobile phase permits selective isolation of angiotensin types.



Mobile phase (pH 2.4)

- A: 0.1% Formic acid in H₂O
B: 0.1% Formic acid in ACN

Mobile phase (pH 10)

- A: 10 mM NH₄OH in H₂O
B: 10 mM NH₄OH in ACN

Conditions

| | |
|-------------|---|
| Column | ZORBAX Poroshell 300Extend-C18 (2.1 x 75 mm, 5 μ m) (p/n 670750-902) |
| Sample | 330 ng each peptide |
| Gradient | 0%–100% B in 2 min (see mobile phase at right). |
| Detection | UV (215 nm) |
| Temperature | Ambient |
| Injection | 1 μ L |
| Flow rate | 0.5 mL/min |



Agilent Technologies

Angiotensins I, II, and III are part of a group of peptides that are integral to the control of hypertension. In these experiments, they also serve to show how selectivity between peptides (differing only slightly in polarity and length) may be manipulated through a change in mobile-phase pH. The three related forms of angiotensin were separated on a ZORBAX Poroshell 300Extend-C18 column at low pH (0.1% formic acid, lower chromatogram) or high pH (10-mM NH₄OH, upper chromatogram), as indicated. The flow rate, gradient time, organic percentages, temperature, and column were kept constant for the two experiments. Comparing peptide elution times from top (pH 2.4) to bottom (pH 10) chromatogram reveals a significant increase in retention for angiotensin III (from 2.2 to 2.4 min) while angiotensins II and I move toward earlier elution. From a practical standpoint, formic acid allows angiotensin I to be well resolved, while at high pH, angiotensin II is well resolved. To better understand the causes of these changes in selectivity, amino acid sequences for these angiotensin peptides are shown in Table 1. Toward lower pH, positive charges occur at the amino-terminus (NH₂-terminal) and histidine (his) residues. The carboxy-terminus (C-terminal) and aspartic acid (asp) residues will be uncharged. When pH is raised, protons will be lost, first from the C-terminal and then from the asp. Charge on the peptides will shift towards neutral and then towards overall negative charge as the NH₂-terminal and his lose a proton. Selectivity is changed with pH because of these charge changes induced in the peptides and the overall hydrophobic contribution of the amino acids making up the peptide. One other factor to consider is shift in the charge of the packing surface as any remaining silanols lose their protons and take on a negative charge. This increases retention of positively charged species, beyond that of the hydrophobic contribution to retention.

Table 1. Amino Acid Sequence and MW for Angiotensins I, II, and III

| Peptide | Peptide sequence | MW |
|-----------------|---|--------|
| Angiotensin I | asp-arg-val-tyr-ile-his-pro-phe-his-leu | 1296.5 |
| Angiotensin II | asp-arg-val-tyr-ile-his-pro-phe | 1046.2 |
| Angiotensin III | arg-val-tyr-ile-his-pro-phe | 931.1 |

For More Information

For more information on our products and services, visit our Web site at www.agilent.com/chem.

The author, Robert D. Ricker, is an Applications Scientist based at Agilent Technologies, Wilmington, Delaware.

Agilent shall not be liable for errors contained herein or for incidental or consequential damages in connection with the furnishing, performance, or use of this material.

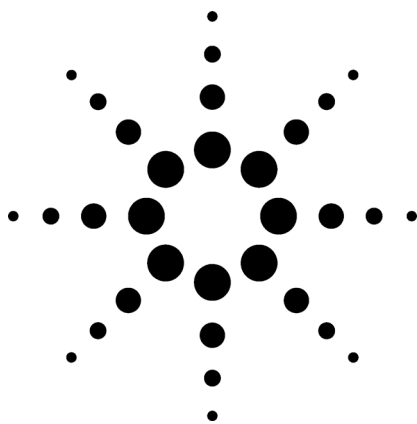
Information, descriptions, and specifications in this publication are subject to change without notice.

© Agilent Technologies, Inc. 2004

Printed in the USA
February 20, 2004
5989-0676EN



Agilent Technologies



Comparison of ZORBAX Poroshell 300Extend-C18 and Totally Porous Packing in Achieving Very Rapid, High-pH Separation of Peptides

Application

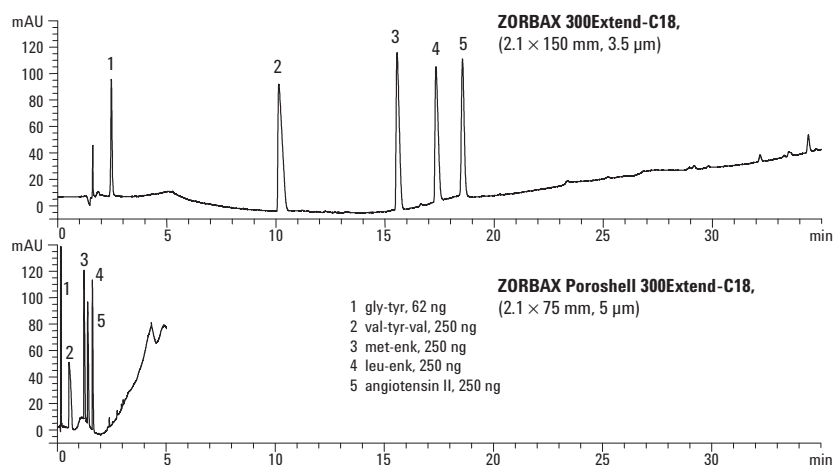
Biotechnology/QA/QC/Basic R&D

Robert Ricker

It is often desirable to reduce the time of an HPLC separation. The time saved is beneficial in basic research, as well as pharmaceutical research, product development, and product QA and QC. The superficially porous particles of ZORBAX Poroshell packings facilitate extremely rapid HPLC separations of large molecules such as proteins. These fast separations result from the very rapid rate at which biomolecules can move into and out of the thin superficially porous layer. The separation of peptides and small proteins at high pH is now possible through the use of Extend-C18-bonded Poroshell particles. The high pH may be desirable for improving selectivity, solubility, ease of downstream processing, or to change signal-to-noise and charge-state in LC/MS. The chromatograms below demonstrate the extreme savings in run time achieved using Poroshell 300Extend-C18 over a comparable, totally porous material. Alternatively, gradient times may be extended to achieve even greater resolution in typical run times of 10 to 20 min.

Highlights

- ZORBAX Poroshell columns permit up to five times faster separation of peptides/proteins over columns using totally porous silica packing.
- ZORBAX Poroshell 300Extend-C18 columns permit use of high pH separations to improve selectivity, solubility, and downstream processing.



Mobile phase

A: 10 mM NH₄OH, H₂O
B: 10 mM NH₄OH, MeOH

Gradient timetable

Upper:
0% to 100% B in 40 min
Flow: 0.2 mL/min

Lower:
0% to 100% B in 4 min
Flow: 1.0 mL/min

Conditions

| | |
|-------------|---|
| Column | ZORBAX 300Extend-C18 (2.1 × 150 mm, 3.5 μm) (p/n 763750-902) ZORBAX Poroshell 300Extend-C18 (2.1 × 75 mm, 5 μm) (p/n 670750-902) |
| Sample | Peptide standards |
| Detection | UV (215 nm) |
| Temperature | Ambient |
| Injection | 0.25 μL |



Agilent Technologies

The chromatograms were obtained using a totally porous ZORBAX 300Extend-C18, 3.5- μm packing and a superficially porous ZORBAX Poroshell 300Extend-C18, 5- μm packing. Both packings were used in 2.1-mm diameter columns; however, the totally porous material was used in a column 150 mm in length because of the common use of this size for peptide mapping. Poroshell was used in the standard 75-mm length. A typical 0.2 mL/min was used for the totally porous packing, while the Poroshell column was run at its optimum flow rate of 1 mL/min. While this is not a direct comparison, it demonstrates the common conditions for use of these two different technologies in peptide analyses. Since the structure of Poroshell packing allows Poroshell 300Extend-C18 to be run at a flow rate five times that for a standard packing, and the column is half as long, a ten-fold reduction in run time is demonstrated for Poroshell. Separation of the five peptides takes 40 min on the totally porous material and only 4 min on Poroshell, as seen in the chromatograms. Not only is the separation faster, but the re-equilibration time is also reduced five-fold, so that turn-around times are very rapid. As a result of its speed, Poroshell columns are very useful for QA, QC, basic research, and method development, as method conditions can be rapidly changed and re-assessed. ZORBAX Poroshell Extend is particularly useful because of its stability of operation at both very low and very high pH. (See Agilent publication 5989-0676EN [1].)

Reference

1. Robert Ricker, "Using ZORBAX Poroshell 300Extend-C18 to Achieve Unique Selectivity at pH 2 and 10: Angiotensins," Agilent Technologies, publication 5989-0676EN
www.agilent.com/chem

For More Information

For more information on our products and services, visit our Web site at www.agilent.com/chem. Search "Poroshell".

The author, Robert D. Ricker, is an Applications Scientist based at Agilent Technologies, Wilmington, Delaware.

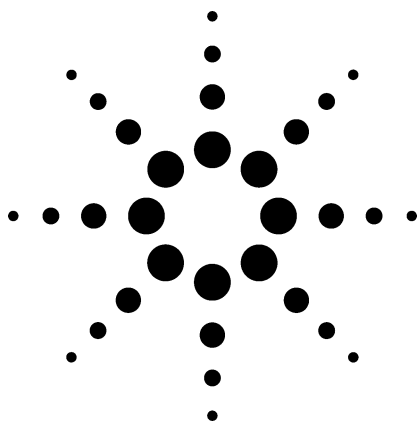
Agilent shall not be liable for errors contained herein or for incidental or consequential damages in connection with the furnishing, performance, or use of this material.

Information, descriptions, and specifications in this publication are subject to change without notice.

© Agilent Technologies, Inc. 2004

Printed in the USA
February 20, 2004
5989-0675EN

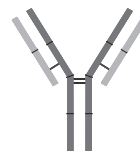




High Speed and *ultra* High Speed Peptide Mapping of Human Monoclonal IgG on ZORBAX Poroshell 300SB-C18, C8, and C3 Application

Biochemical

Cliff Woodward, Robert Ricker, Kurt Forrer, Patrik Röethlisberger



Antibodies are a group of proteins that are the key to directed immunological interaction. They can bind to an antigen (protein, glycoprotein, DNA, etc.) with extreme specificity. This property makes antibodies very valuable for use in diagnostics, general research, and for therapeutics. Treatment of intact antibodies with various chemicals and enzymes allows the specific separation of the heavy and light chains, removal of sugar moieties, and/or cleavage of the polypeptide chains. Separation of the peptide fragments (mapping) after cleavage with a proteolytic enzyme of high specificity, such as Lys-C, gives a characteristic and reproducible pattern of peaks which can be collected, sequenced, and run through a mass spectrometer (MS).

This application note demonstrates the utility of using superficially porous chromatographic media (Poroshell) to achieve substantial improvements in analysis turnaround times when running high-resolution peptide maps. Figure 1 shows comparative peptide maps of a human monoclonal antibody, Lys-C digest. Note the time scales of the separations. The Poroshell maps take one-sixth of the turnaround time and show essentially the same number of peaks. See Table 1.

Highlights

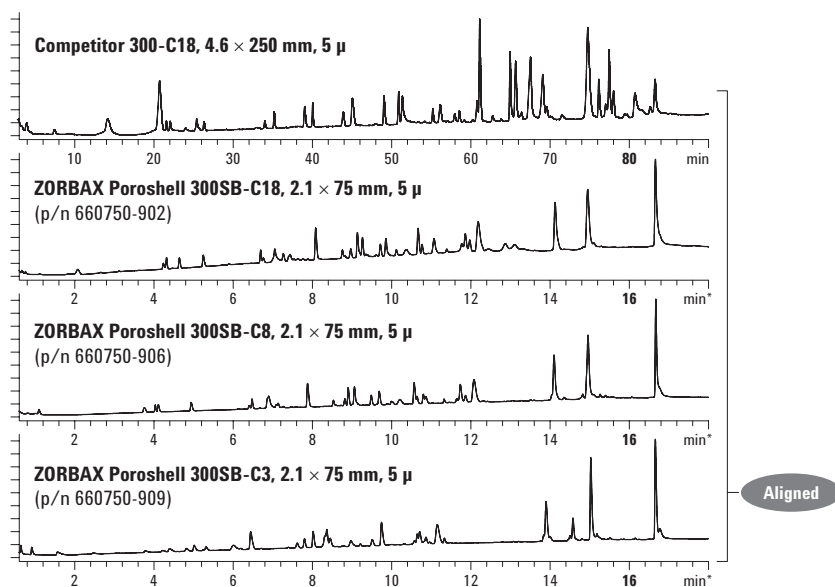
- High speed peptide separations using Poroshell technology result in high-resolution analysis in one-fifth the time.
- Method development is more rapid, since run times are shortened using Poroshell technology.
- Poroshell 300SB columns come in a variety of internal diameters and bonded phases. This gives a wide variety of choices for the optimal fast separation of proteins and peptides.



A Poroshell column is shown above with an Agilent 1100 HPLC system.



Agilent Technologies



Competitor Column Conditions

Temperature: Ambient
 Detection: UV, 210 nm
 Injection: 50 μ L
 Sample: Lys-C digest of human monoclonal antibody
 Flow: 0.3 mL/min

Poroshell Column Conditions

Temperature: 70 $^{\circ}$ C
 Detection: UV, 210 nm
 Injection: 10 μ L
 Sample: Lys-C digest of human monoclonal antibody
 Flow: 1.0 mL/min

Figure 1. High speed peptide maps of a human monoclonal antibody, Lys-C digest, using three different ZORBAX Poroshell columns and one competitive column. Note the time scales required for the separations. 16 vs 80 min respectively.

The speed and resolution of Poroshell technology require a little more explanation to fully appreciate their impact. Note that the turnaround time in Figure 1 is only 21.5 min, with all peaks eluting in less than 17 min., a reasonably fast analysis. We are also achieving the resolution observed for a typical 120 min run. This increased speed results from the high flow rate used, relative to column id. [A flow rate of 1 mL/min on a 2.1-mm id column is equivalent to 5 mL/min on a 4.6 mm id column – five-fold a typical flow rate.] Higher flow increases the volume of the gradient delivered over the same 20.5-min run time.

Simply increasing the gradient volume reduces the gradient slope, increases relative retention (k'), and results in increased resolution, that is, the resolution of a 120-min run is achieved in 20.5 min!

Competitor

Mobile phase

A = 0.1% TFA in water
 B = 0.1% TFA in ACN

Gradient timetable

| Time (min) | % Solvent B |
|------------|-------------|
| 1.00 | 00.0 |
| 10.00 | 00.0 |
| 110.00 | 50.0 |
| 120.00 | 70.0 |
| 125.00 | 00.0 |
| 135.00 | 00.0 |

Poroshell

Mobile phase

A = 0.1% TFA in water
 B = 0.1% TFA in ACN

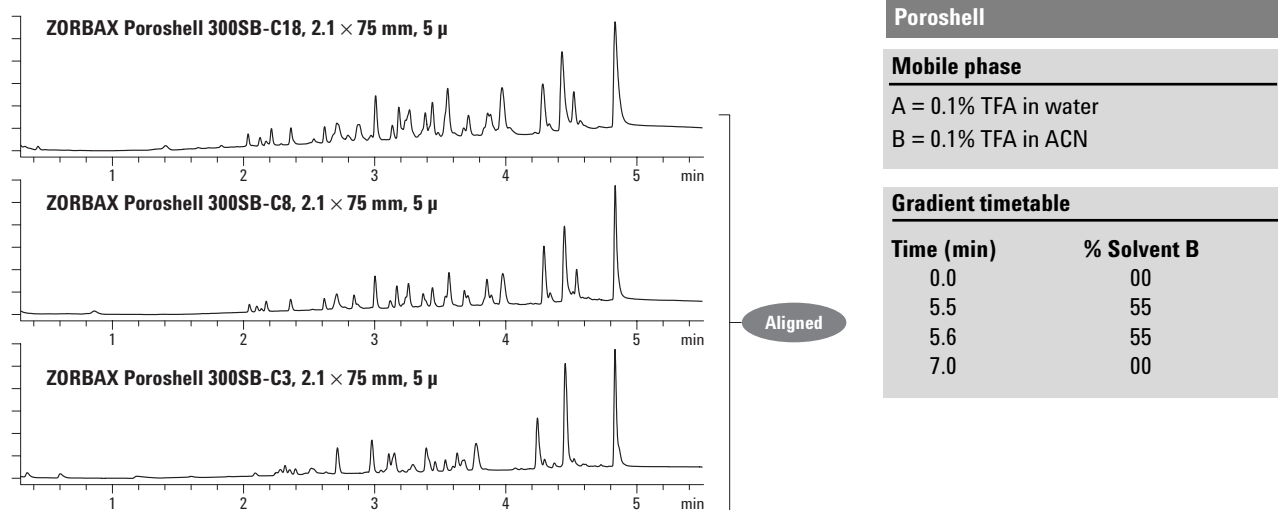
Gradient timetable

| Time (min) | % Solvent B |
|------------|-------------|
| 0.00 | 00.0 |
| 20.00 | 50.0 |
| 20.50 | 100.0 |
| 21.50 | 100.0 |

Table 1. Number of Peaks Recognized Versus Column Type

| Column | No. of peaks recognized (120 min run) | No. of peaks recognized (20.5 min runs) | No. of peaks recognized (5.6 min runs) |
|----------------|---------------------------------------|---|--|
| Competitor C18 | 57 | – | – |
| Poroshell-C18 | – | 55 | 46 |
| Poroshell-C8 | – | 58 | 48 |
| Poroshell-C3 | – | 54 | 47 |

For *ultra* high speed mapping the run time can be cut even further, to 5.6 min, as seen in Figure 2. Some resolution loss occurs (~18%–19%) which does not impact the search for tryptophan-containing peptides (Table 1). The productivity increase is simply enormous >20-fold compared, to the standard 120-min runs. For those needing really high throughput, this is the way to go. Poroshell's unique properties allow runs at *ultra* high speeds with relative impunity, particularly when using MS as the detector.

**Poroshell Column Conditions**

| | |
|--------------|---|
| Temperature: | 70 °C |
| Detection: | UV, 210 nm |
| Injection: | 10 μL |
| Sample: | Lys-C digest of human monoclonal antibody |
| Flow: | 1.0 mL/min |

Figure 2. Ultra high speed peptide maps of a human monoclonal antibody, Lys-C digest, using three different ZORBAX Poroshell columns.

For More Information

For more information on our products and services, visit our Web site at www.agilent.com/chem. Search "Poroshell".

The authors, Cliff Woodward and Robert Ricker, are Application Biochemists based at Agilent Technologies, Wilmington, Delaware.

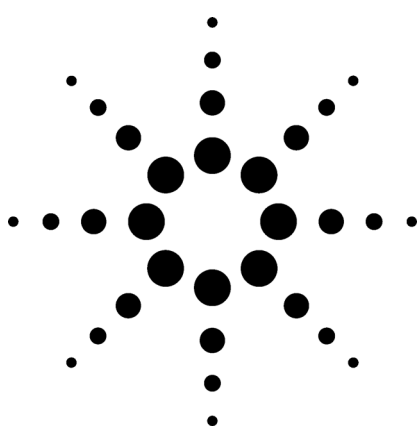
The authors, Dr. Kurt Forrer and Patrik Röethlisberger, are research scientists based at Novartis Pharma, Biotechnology, Basel.

Agilent shall not be liable for errors contained herein or for incidental or consequential damages in connection with the furnishing, performance, or use of this material.

Information, descriptions, and specifications in this publication are subject to change without notice.

© Agilent Technologies, Inc. 2004

Printed in the USA
March 1, 2004
5989-0590EN



Use of Temperature to Increase Resolution in the Ultrafast HPLC Separation of Proteins with ZORBAX Poroshell 300SB-C8 HPLC Columns

Application

Pharmaceutical

Robert D. Ricker, Jerry J. Lewis, Sr., and Erin Arenz

Introduction

For separations containing ionizable compounds, temperature is a simple tool that can effectively increase separation selectivity and, therefore, resolution. For peptides and proteins, noted peak shifts with increased or decreased temperature may be more significant than those observed with more time consuming mobile phase modifications. Since ZORBAX Poroshell 300SB columns are stable at temperatures up to 90 °C at low pH, these columns not only provide ultrafast, high resolution separations, they also offer the opportunity to use temperature to assist in optimizing resolution of these bioseparations.

Results

Figures 1 through 3 show overlaid chromatograms for eight proteins, varying in molecular weight from 3 to 45 kDa, and including insulin, glucagon, and glycosylated proteins. Separation of this diverse group of proteins is an obvious challenge. Each analyte, eluted from a ZORBAX Poroshell 300SB-C8, 2.1 × 75 mm, 5-µm column, with an impressive retention time (RT) of less than 2 min. The gradient used in each chromatographic set is linear, from 20%–70% B in 3 min; the flow rate is 1.0 mL/min, while column temperature is changed from 40 to 60 °C and then to 75 °C.

Comparing the overlaid sets of chromatograms in Figures 1 and 2, the resolution between peaks 4, 5, and 6 increased substantially, while little movement was noted between peak pairs 2/3 and 7/8 when elevating the column temperature from 40 to 60 °C. Elevating the operating temperature to 75 °C (see Figure 3) results in shifts in elution times for peaks 2, 3, 4, 5, and 6. The usefulness of temperature change in providing resolution is more obvious if one considers individual peak pairs 2 and 4, 3 and 4, and 5 and 6. Each pair shows significant improvement in resolution as temperature is elevated from 40 to 60 °C and then to 75 °C. Resolution between the peak pair 7 and 8 is best at 75 °C, further demonstrating that temperature change can induce considerable shifts in protein retention.

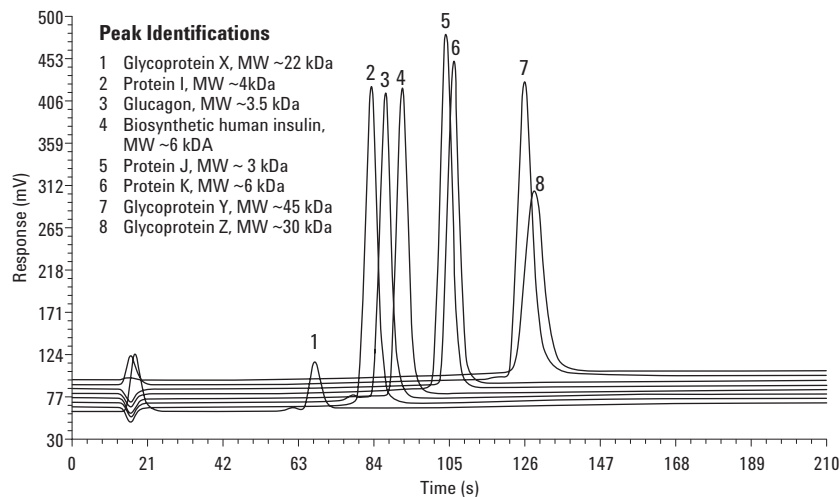
Highlights

- ZORBAX Poroshell 300SB HPLC columns are designed to provide ultrafast high resolution of peptides and proteins with excellent reproducibility – resolving complex peptide and protein samples in minutes.
- The unmatched stability of StableBond (SB) bonding at low pH enables the routine use of Poroshell 300SB columns at temperatures as high as 90 °C.
- The dynamic temperature range of the ZORBAX Poroshell 300SB columns allows the use of temperature as an effective tool to increase resolution, reduce back pressure, and shorten run times – even for the most rapid protein separations.



Agilent Technologies

In addition to its utility of operation at elevated temperatures, design of the particles comprising in Poroshell SB packings facilitates the use of higher flow rates without loss in resolution. This is possible because of Poroshell's superficially porous particles. Large molecules, which diffuse very slowly compared to small molecules, can move very quickly into and out of Poroshell's very thin (0.25 μm) outer porous layer—stopped by the solid silica core. A flow rate of 1.0 mL/min is five times that commonly used with a 2.1-mm id column and permits the use of a short gradient time of 3 min, with resulting rapid sample throughput.



Mobile phase

A = 0.1% TFA in H₂O
 B = 0.1% TFA in ACN

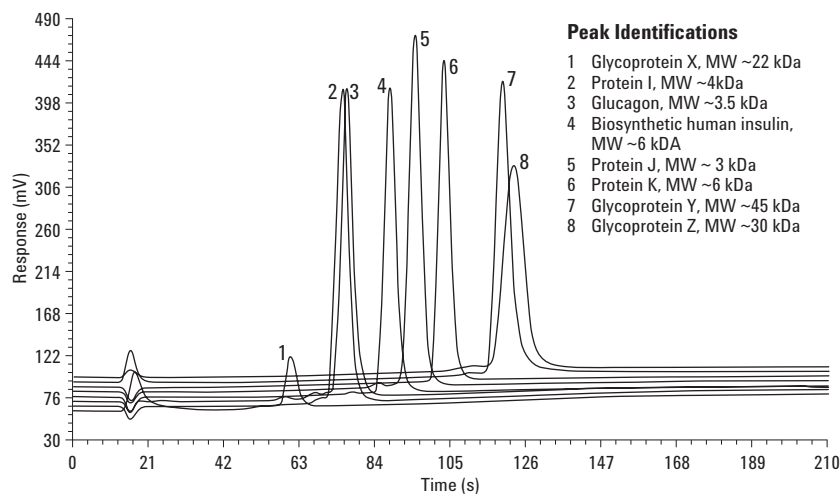
Gradient

| Time min | Solvent B |
|----------|-----------|
| 3 | 20%–70% |

Conditions

Column: **ZORBAX Poroshell 300SB-C8**, 2.1 \times 75 mm, 5 μm
 (p/n 660750-906)
 Column temperature: 40 °C
 Flow rate: 1.0 mL/min
 Detection: UV (214 nm)

Figure 1. Protein elution pattern on ZORBAX Poroshell 300SB-C8 column at 40 °C.



Mobile phase

A = 0.1% TFA in H₂O
 B = 0.1% TFA in ACN

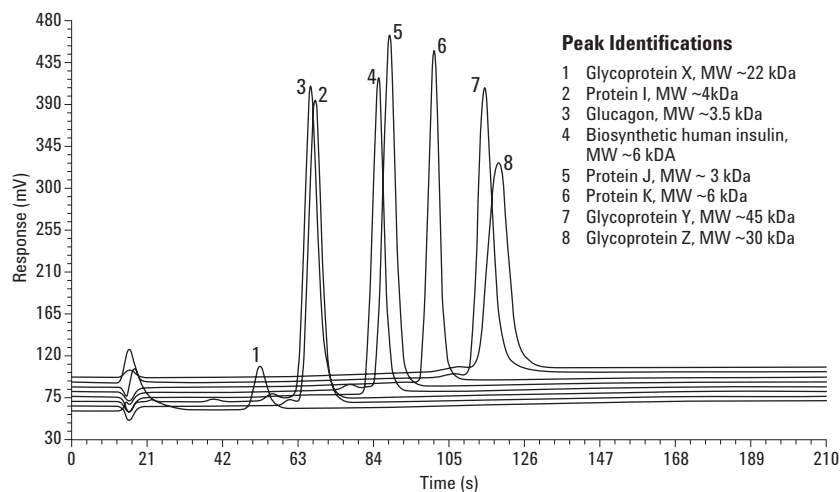
Gradient

| Time min | Solvent B |
|----------|-----------|
| 3 | 20%–70% |

Conditions

Column: **ZORBAX Poroshell 300SB-C8**, 2.1 \times 75 mm, 5 μm
 (p/n 660750-906)
 Column temperature: 60 °C
 Flow rate: 1.0 mL/min
 Detection: UV (214 nm)

Figure 2. Protein elution pattern on ZORBAX Poroshell 300SB-C8 column at 60 °C.



Mobile phase

A = 0.1% TFA in H₂O

B = 0.1% TFA in ACN

Gradient

| Time min | Solvent B |
|----------|-----------|
| 3 | 20%–70% |

Conditions

Column: **ZORBAX Poroshell 300SB-C8**, 2.1 × 75 mm, 5 μm
(p/n 660750-906)

Column temperature: 75 °C

Flow rate: 1.0 mL/min

Detection: UV (214 nm)

Figure 3. Protein elution pattern on ZORBAX Poroshell 300SB-C8 column at 75 °C.

Conclusions

ZORBAX Poroshell 300SB, 2.1 × 75 mm, 5-μm HPLC columns are an excellent choice for the rapid separation of proteins, offering high-resolution separations in minutes and the best option for using elevated temperature at low pH to increase resolution between overlapping protein peak pairs. Investigating the effects of temperature on resolution is a straightforward approach to separation optimization that can be more effective and convenient than changing other separation parameters (for example, the mobile phase composition). In this example, a mixture of very different protein molecules (insulin, glucagon, other proteins and glycoproteins) could be eluted with significantly different selectivity in less than 2 min. The actual turn-around time from injection to injection would be about 3.5 min. The power of Poroshell in method development should not be underestimated, as gradient, temperature, mobile-phase type, and detection settings can be changed, the column re-equilibrated, and the separation reassessed, all very rapidly.

Instrumentation

All work was performed using an Agilent 1100 LC equipped with a solvent degasser, binary pump, auto-sampler, heated column compartment and an ultraviolet detector.

For More Information

For more information on our products and services, visit our Web site at www.agilent.com/chem.

The authors, Robert D. Ricker (Applications Specialist) is based at Agilent Technologies, Wilmington, Delaware, Jerry J. Lewis, Sr. Research Scientist and Erin Arenz, Analytical Chemist, Biopharmaceutical R and D are located at Lilly Research Laboratories, Eli Lilly and Company, Lilly Tech Center, Indianapolis, Indiana 46221.

Agilent shall not be liable for errors contained herein or for incidental or consequential damages in connection with the furnishing, performance, or use of this material.

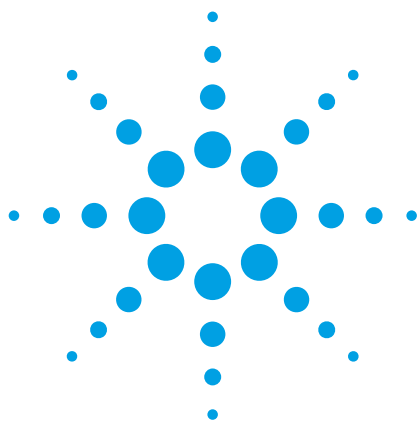
Information, descriptions, and specifications in this publication are subject to change without notice.

© Agilent Technologies, Inc. 2004

Printed in the USA
February 24, 2004
5989-0589EN



Agilent Technologies



Computer Assisted Identification of Metabolites from Pharmaceutical Drugs

Part 2: Identification of Non-expected Metabolites of Nefazodone

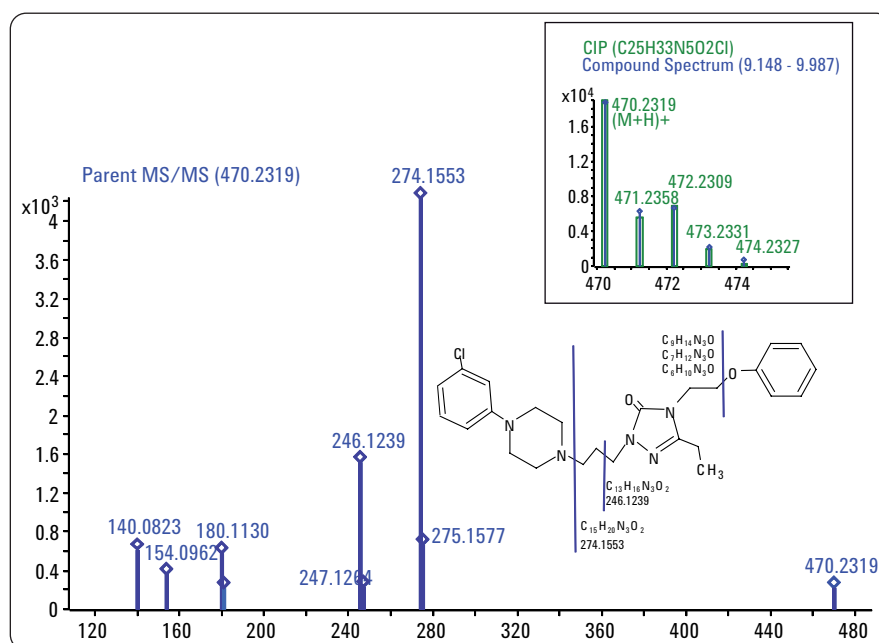
Identification of metabolites by the MassHunter Metabolite ID software from RRLC – QTOF MS data

Application Note

Metabolite identification in drug discovery and drug development

Author

Edgar Nägele
Agilent Technologies
Waldbronn, Germany



Abstract

This Application Note demonstrates:

- The use of the Agilent 1200 Rapid Resolution LC (RRLC) system for high resolution separation of metabolites from an in-vitro metabolism experiment.
- The use of the Agilent 6520 QTOF mass spectrometer for the acquisition of data for computer assisted metabolite identification.
- The use of the Agilent MassHunter Metabolite identification software for highly productive identification of expected metabolites.
- The results of the Metabolite ID data analysis for expected metabolites of the pharmaceutical drug nefazodone



Agilent Technologies

Introduction

This Application Note demonstrates the use of the Agilent 1200 RRLC system and the Agilent 6520 QTOF mass spectrometer for data acquisition from metabolism experiments and the use of the MetID software for computer assisted data analysis. The results of the data analysis will be discussed in detail for examples of non-expected metabolites from the pharmaceutical drug Nefazodone.

The identification of the expected metabolites by means of the MetID software is discussed in part I of this work¹.

Experimental and Methods

For details of the experimental conditions and methods used, see *Computer-assisted identification of the expected metabolites of Nefazodone*, publication number 5990-3606EN.

Results and discussion

For the identification of possible metabolites, the basic information

about isotope pattern, MS/MS fragmentation pattern and calculated formula of the parent drug nefazodone are taken from the control sample (Figures 1 and 2). The measured isotope pattern (blue lines, insert in figure 1) clearly shows the pattern that is

typical for a chlorinated compound, and is identical to the calculated isotope pattern (CIP, green box, insert in Figure 1) with the main ion (M+H)⁺ at m/z 470.2319 (C₂₅H₃₃N₅O₂Cl). The MS/MS spectrum shows the main fragment (M+H)⁺ at m/z 274.1553 with

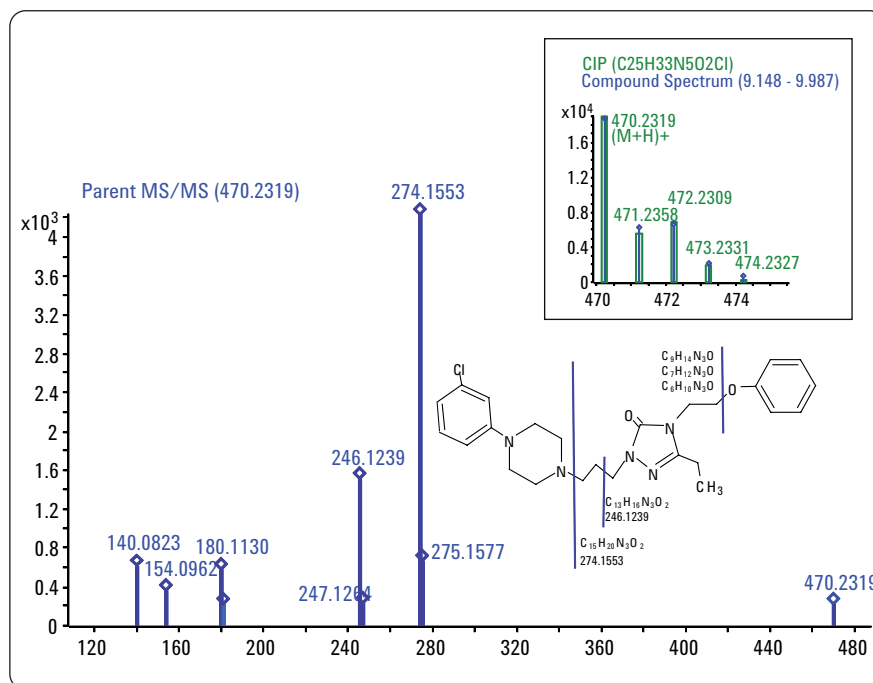


Figure 1
Mass spectrum, isotopic analysis and MS/MS spectrum for fragment assignment of the parent drug Nefazodone.

| Formula | Calc. Mass | Mass | Δ Mass [mDa] | Δ Mass [ppm] | DBE | m/z | Species | Ion Formula |
|--|------------|----------|--------------|--------------|-----|----------|--------------------|--|
| C ₂₅ H ₃₂ N ₅ O ₂ Cl | 469.2245 | 469.2246 | -0.16 | -0.35 | 12 | 470.2319 | (M+H) ⁺ | C ₂₅ H ₃₃ N ₅ O ₂ Cl |

| Isotopic pattern | | | | |
|------------------|-----------|--------------|---------|---------------|
| m/z | Calc. m/z | Δ Mass [ppm] | Abund % | Calc. Abund % |
| 470.2319 | 470.2317 | -0.35 | 100.00 | 100.00 |
| 471.2358 | 471.2347 | -2.28 | 31.86 | 29.32 |
| 472.2309 | 472.2299 | -2.24 | 33.67 | 36.56 |
| 473.2331 | 473.2322 | -1.90 | 10.14 | 9.88 |
| 474.2327 | 474.2348 | 4.50 | 2.23 | 1.50 |

Figure 2
Calculated molecular formula and mass accuracies, and isotopic analysis of Nefazodone.

| m/z | Mass | Formula | Calc. Mass | Δ Mass [mDa] | Δ Mass [ppm] | Loss Mass | Loss Formula | Neutral Loss |
|----------|----------|---|------------|--------------|--------------|-----------|--|--------------|
| 140.0823 | 139.0750 | C ₆ H ₉ N ₃ O | 139.0746 | -0.43 | -3.12 | 330.1499 | C ₁₉ H ₂₃ N ₂ OCl | 330.1482 |
| 154.0962 | 153.0890 | C ₇ H ₁₁ N ₃ O | 153.0902 | 1.25 | 8.16 | 316.1342 | C ₁₈ H ₂₁ N ₂ OCl | 316.1343 |
| 180.1130 | 179.1058 | C ₉ H ₁₃ N ₃ O | 179.1059 | 0.11 | 0.62 | 290.1186 | C ₁₆ H ₁₉ N ₂ OCl | 290.1175 |
| 246.1239 | 245.1167 | C ₁₃ H ₁₅ N ₃ O ₂ | 245.1164 | -0.23 | -0.94 | 224.1080 | C ₁₂ H ₁₇ N ₂ Cl | 224.1066 |
| 274.1553 | 273.1481 | C ₁₅ H ₁₉ N ₃ O ₂ | 273.1477 | -0.34 | -1.26 | 196.0767 | C ₁₀ H ₁₃ N ₂ Cl | 196.0751 |

Figure 3
Calculated MS/MS fragment formulas and neutral loss formulas for Nefazodone fragmentation.

the formula $C_{15}H_{20}N_3O_2$ (Figure 1). The mass of nefazodone ($C_{25}H_{32}N_5O_2Cl$), which was calculated from the measured $(M+H)^+$ ion, shows a low relative mass error of -0.35 ppm (Figure 2) and the MS/MS fragment at a mass of 273.1481 ($C_{15}H_{19}N_3O_2$) of -1.26 ppm (Figure 3). This fragment formula, together with the assigned loss formula $C_{10}H_{13}N_2Cl$ calculated for this MS/MS fragment, fits to the parent drug formula $C_{25}H_{32}N_5O_2Cl$ (Figure 3). Other MS/MS fragments are assigned to the structural formula of nefazodone (Figure 1).

In addition to the metabolites of a drug arising from known biotransformation reactions, there are also metabolic reactions that do not fit to these well-known reactions, and the metabolites are therefore unexpected. These unexpected metabolites are very often derived from the original drug molecule by cleaving off parts of the structure and applying the metabolic reaction to the remaining part of the molecule. For the drug nefazodone, there are several metabolites that follow this reaction pathway.

The first example is metabolite 7,

which elutes at about 7.8 minutes at m/z 458.1948. This metabolite clearly has the typical measured isotope pattern of a chlorinated compound (insert in Figure 4, blue lines), which fits to the calculated isotope pattern (CIP, insert in Figure 4, green boxes) for the formula $C_{23}H_{29}N_5O_3Cl$, calculated with a relative mass error of 1.03 ppm (Figure 5). The fragment pattern matching (FMP) clearly identifies the

similarities between the parent drug's MS/MS spectrum (Figure 4, blue spectrum) and the metabolized compound's MS/MS spectrum (red spectrum). The molecular ion mass is shifted by the unexpected biotransformation from the parent mass m/z 470.2319 to m/z 458.1948. This biotransformation combines the loss of an ethyl group and an additional oxidation to a keto group (Figures 4 and 6). This mass shift can

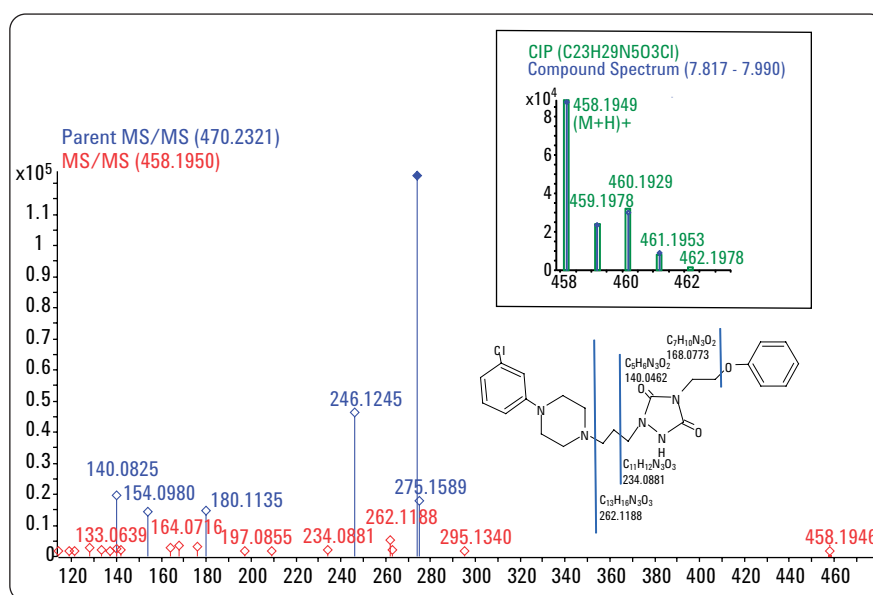


Figure 4
Mass spectrum, isotopic analysis and MS/MS spectrum with fragment assignment of the Nefazodone metabolite 7.

| Formula | Calc. Mass | Mass | Δ Mass [mDa] | Δ Mass [ppm] | DBE | m/z | Species | Ion Formula | Score |
|--------------|------------|-----------|---------------------|---------------------|-----|-----------|--------------------|--------------|-------|
| C23H28N5O3Cl | 457.18806 | 457.18759 | 0.47 | 1.03 | 12 | 458.19486 | (M+H) ⁺ | C23H29N5O3Cl | 100 |

| Isotopic pattern | | | | |
|------------------|-----------|---------------------|---------|---------------|
| m/z | Calc. m/z | Δ Mass [ppm] | Abund % | Calc. Abund % |
| 458.1949 | 458.1953 | 1.04 | 100.00 | 100.00 |
| 459.1977 | 459.1983 | 1.27 | 25.45 | 27.15 |
| 460.1929 | 460.1934 | 1.12 | 32.69 | 36.16 |
| 461.1962 | 461.1958 | -0.83 | 8.67 | 9.15 |

Figure 5
Calculated molecular formula and mass accuracies, and isotopic analysis of the Nefazodone metabolite 7.

| m/z | Mass | Formula | Calc Mass | Δ Mass [mDa] | Δ Mass [ppm] | Loss Mass | Loss Formula | Neutral Loss | FPM m/z | Shift m/z | Δ Shift [mDa] | Shift Formula |
|-----------|-----------|------------|-----------|---------------------|---------------------|-----------|--------------|--------------|-----------|-----------|----------------------|---------------|
| 121.06431 | 120.05703 | C8H8O | 120.05751 | 0.48 | 4.02 | 337.13055 | C15H20N5O2Cl | 337.13065 | | | | |
| 140.04622 | 139.03894 | C5H5N3O2 | 139.03818 | -0.76 | -5.49 | 318.14989 | C18H23N2OCl | 318.14874 | | | | |
| 168.07774 | 167.07047 | C7H10N2O | 167.06951 | -0.99 | -5.93 | 290.11866 | C16H19N2OCl | 290.11722 | 180.11347 | -12.0364 | 0.66 | -C2-H4+O |
| 234.08810 | 233.08082 | C11H11N3O3 | 233.08004 | -0.78 | -3.36 | 224.10803 | C12H17N2Cl | 224.10686 | 246.12446 | -12.0364 | 0.02 | -C2-H4+O |
| 262.11883 | 261.11156 | C13H15N3O3 | 261.11134 | -0.22 | -0.82 | 196.07673 | C10H13N2Cl | 196.07613 | 274.15579 | -12.0364 | 0.57 | -C2-H4+O |
| 458.19464 | | | | | | | | | 470.23212 | -12.0364 | 1.10 | -C2-H4+O |

Figure 6
Calculated MS/MS fragment formulas and neutral loss formulas for the Nefazodone metabolite 7 fragmentation.

also be found for some of the MS/MS fragments. One example is the fragment at m/z 262.1188 with the formula $C_{13}H_{15}N_3O_3$ calculated with -0.82 ppm. This fragment is shifted by the summarized biotransformation ($-C_2-H_4+O$) from the MS/MS fragment of nefazodone at m/z 274.1557 (Figure 6). The formulae calculated for the neutral losses fit the parent drug's formula for all MS/MS fragments. The explanation for some other MS/MS fragments is given in the formula in Figures 4 and 6.

Metabolite 8, which is another non-expected chlorine-containing metabolite, shows a measured isotope pattern that fits excellently to the calculated isotope pattern (CIP) of the chlorinated parent drug (insert in Figure 7).

The measured mass for metabolite 8 is m/z 410.1962, with the formula $C_{19}H_{28}N_5O_3Cl$ calculated with a mass deviation of -2.06 ppm (Figure 8). This formula is possible after loss of the phenyl group following hydroxylation of the parent drug. This conclusion is

supported by analysis of the MS/MS spectrum (Figure 7). The fragment at m/z 214.1182 has the formula $C_9H_{16}N_3O_3$, calculated with a mass deviation of 1.82 ppm (Figure 9). This formula is shifted from the nefazodone MS/MS fragment at m/z 180.1124 by the addition of two oxygen atoms and

two hydrogen atoms (compare to Figure 1 on page 1). The formula of the second intense MS/MS fragment of metabolite 8 at m/z 186.0873 with the formula $C_7H_{12}N_3O_3$ (-0.17 ppm) coming from a loss of an ethyl moiety gives additional support.

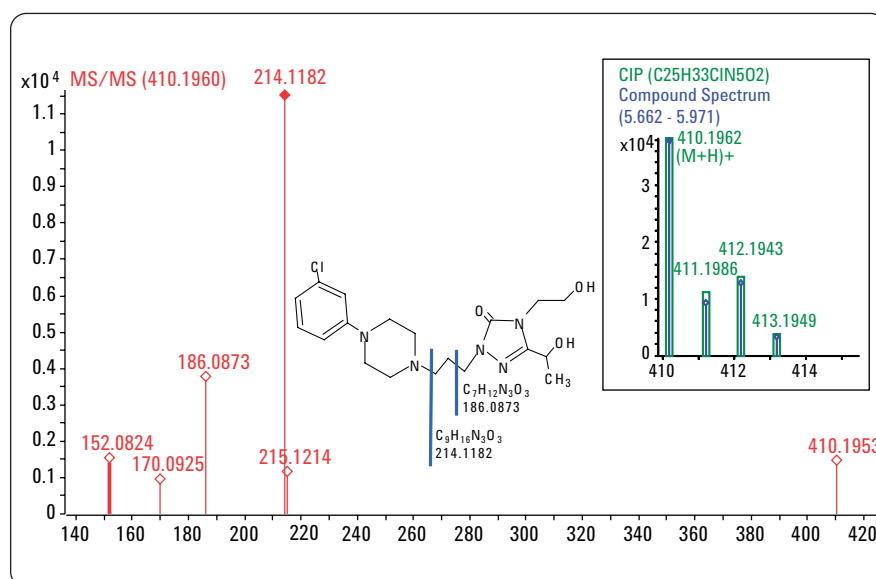


Figure 7
Mass spectrum, isotopic analysis and MS/MS spectrum with fragment assignment of the cleaved azodone metabolite 8.

| Formula | Calc. Mass | Mass | Δ Mass [mDa] | Δ Mass [ppm] | DBE | m/z | Species | Ion Formula |
|--------------|------------|----------|---------------------|---------------------|-----|----------|---------|--------------|
| C19H28ClN5O3 | 409.1881 | 409.1889 | -0.84 | -2.06 | 8 | 410.1962 | (M+H)+ | C19H29ClN5O3 |

| Isotopic pattern | | | | |
|------------------|-------------|---------------------|---------|---------------|
| m/z | Calc. m/z | Δ Mass [ppm] | Abund % | Calc. Abund % |
| 410.1962 | 410.1953 | -2.06 | 100.00 | 100.00 |
| 411.1986 | 411.1982 | -0.8 | 22.99 | 22.82 |
| 412.1943 | 412.1931 | -2.73 | 32.26 | 35.1 |
| 413.1949 | 413.1956 | 1.78 | 7.21 | 7.62 |

Figure 8
Calculated molecular formula and mass accuracies, and isotopic analysis of the cleaved Nefazodone metabolite 8.

| m/z | Ion Formula | Calc m/z | Δ m/z [mDa] | Δ m/z [ppm] | Loss Mass | Loss Formula | Neutral Loss | FPM m/z | Shift m/z | Δ Shift [mDa] | Shift Formula |
|-----------|-------------|------------|----------------------|----------------------|-----------|--------------|--------------|-----------|-------------|----------------------|---------------|
| 152.08242 | C7H10N3O | 152.08184 | -0.58 | -3.84 | 258.11351 | C12H19ClN2O2 | 258.11353 | | | | |
| 170.09245 | C7H12N3O2 | 170.09240 | -0.05 | -0.29 | 240.10294 | C12H17ClN2O | 240.10350 | | | | |
| 186.08729 | C7H12N3O3 | 186.08732 | 0.03 | 0.17 | 224.10803 | C12H17ClN2 | 224.10867 | | | | |
| 214.11823 | C9H16N3O3 | 214.11862 | 0.39 | 1.82 | 196.07673 | C10H13ClN2 | 196.07772 | 180.11243 | 34.0055 | 0.32 | +H2+O2 |

Figure 9
Calculated MS/MS fragment formulas and neutral loss formulas for the cleaved Nefazodone metabolite 8 fragmentation.

Starting from metabolite 8, additional oxidation gives the product metabolite 9. This metabolite at m/z 408.1807 shows the typical isotope pattern of a chlorinated molecule (insert in Figure 10). The formula of metabolite 9, $C_{19}H_{26}N_5O_3Cl$, was calculated with -2.43 ppm deviation (Figure 11). The MS/MS spectrum shows the most intense ion at m/z 212.1031 with the formula $C_9H_{14}N_3O_3$ (-0.51 ppm) (Figures 10 and 12). This formula can be explained by the oxidation of a hydroxyl group to a keto group in comparison to the fragment shown in the MS/SM spectrum of metabolite 8 (Figure 7 on page 4) at m/z 214.1182 ($C_9H_{16}N_3O_3$). The second intense ion at m/z 184.0715, with the formula $C_7H_{10}N_3O_3$, can be explained the same way.

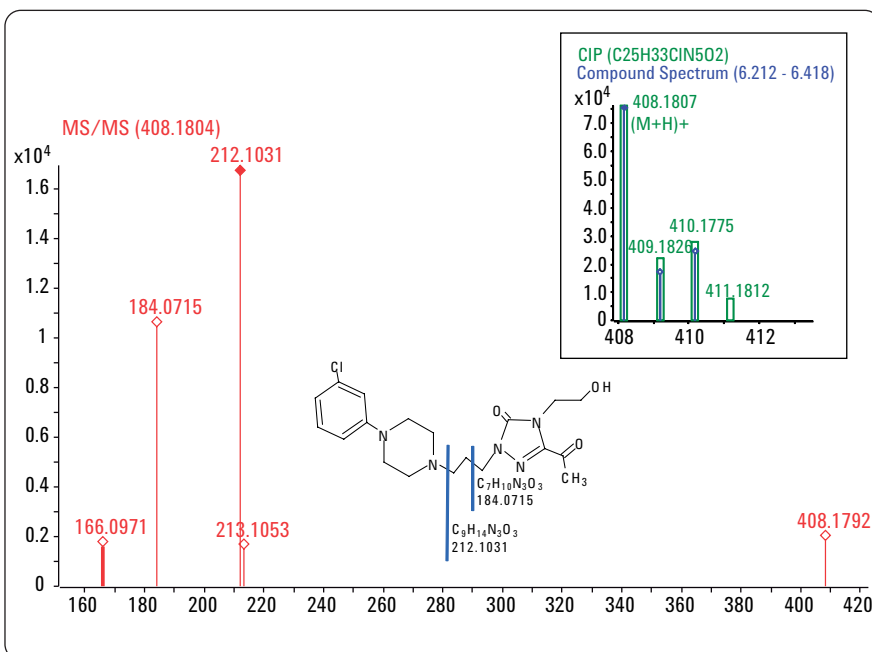


Figure 10
Mass spectrum, isotopic analysis and MS/MS spectrum with fragment assignment of the cleaved efazodone metabolite 9.

| Formula | Calc. Mass | Mass | Δ Mass [mDa] | Δ Mass [ppm] | DBE | m/z | Species | Ion Formula |
|--------------|------------|----------|---------------------|---------------------|-----|----------|--------------------|--------------|
| C19H26ClN5O3 | 407.1724 | 407.1734 | -0.99 | -2.43 | 9 | 408.1807 | (M+H) ⁺ | C19H27ClN5O3 |

| Isotopic pattern | | | | |
|------------------|-------------|---------------------|---------|---------------|
| m/z | Calc. m/z | Δ Mass [ppm] | Abund % | Calc. Abund % |
| 408.1807 | 408.1797 | -2.43 | 100.00 | 100.00 |
| 409.1826 | 409.1826 | -0.14 | 21.17 | 22.8 |
| 410.1775 | 410.1775 | 0.05 | 30.9 | 35.1 |

Figure 11
Calculated molecular formula and mass accuracies, and isotopic analysis of the cleaved Nefazodone metabolite 9.

| m/z | Ion Formula | Calc m/z | Δ m/z [mDa] | Δ m/z [ppm] | Loss Mass | Loss Formula | Neutral Loss |
|-----------|-------------|------------|----------------------|----------------------|-----------|--------------|--------------|
| 166.09707 | C8H12N3O | 166.09749 | 0.42 | 2.54 | 242.08221 | C11H15ClN2O2 | 242.08330 |
| 184.07152 | C7H10N3O3 | 184.07167 | 0.15 | 0.82 | 224.10803 | C12H17ClN2 | 224.10885 |
| 212.10308 | C9H14N3O3 | 212.10297 | -0.11 | -0.51 | 196.07673 | C10H13ClN2 | 196.07729 |

Figure 12
Calculated MS/MS fragment formulas and neutral loss formulas for the cleaved Nefazodone metabolite 9 fragmentation.

Finally, the chlorinated low-level metabolite 10, eluting at 1.88 minutes, with the low molecular mass at m/z 213.0787 and formula $C_{10}H_{13}N_2OCl$ (1.02 ppm) has been identified (Figures 13 and 14). This metabolite comes from a metabolic fragmentation of the parent drug nefazodone into the right side, which is metabolite 14, and its left chlorinated aromatic side (compare to Figure 1 on page 1 and Figure 25 on page 10). The MS/MS spectrum has two characteristic fragments at m/z 170.0362 and m/z 135.0678, which identify this metabolite (Figure 15).

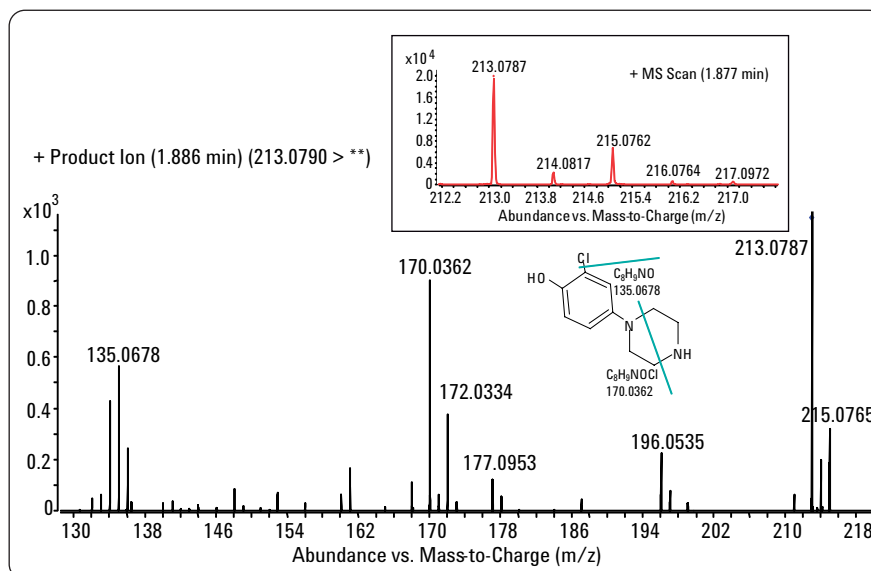


Figure 13
Mass spectrum, isotopic analysis and MS/MS spectrum with fragment assignment of the cleaved Nefazodone metabolite 10.

| Formula | Calc. Mass | Mass | Δ Mass [mDa] | Δ Mass [ppm] | DBE | m/z | Species | Ion Formula |
|----------------------|------------|----------|---------------------|---------------------|-----|----------|--------------------|----------------------|
| $C_{10}H_{13}N_2OCl$ | 212.0716 | 212.0714 | 0.22 | 1.02 | 5 | 213.0787 | (M+H) ⁺ | $C_{10}H_{14}N_2OCl$ |

| Isotopic pattern | | | | |
|------------------|-------------|---------------------|---------|---------------|
| m/z | Calc. m/z | Δ Mass [ppm] | Abund % | Calc. Abund % |
| 213.0787 | 213.0789 | 1.02 | 100.00 | 100.00 |
| 214.0817 | 214.0819 | 0.85 | 12.32 | 29.32 |
| 215.0762 | 215.0762 | -0.02 | 35.15 | 32.83 |

Figure 14
Calculated molecular formula and mass accuracies, and isotopic analysis of the cleaved Nefazodone metabolite 10.

| Measured mass | Formula | Calculated mass | Mass error [mDa] | Mass error [ppm] |
|---------------|----------------------|-----------------|------------------|------------------|
| 213.0787 | $C_{10}H_{14}N_2OCl$ | 213.0789 | 0.2 | 1.02 |
| 170.0362 | C_8H_9NOCl | 170.0367 | 0.50 | 3.05 |
| 135.0678 | C_8H_9NO | 135.0679 | 0.1 | 0.48 |

Figure 15
Calculated MS/MS fragment formulas and neutral loss formulas for the cleaved Nefazodone metabolite 10 fragmentation.

The situation becomes more complex if the initial cleavage reaction is complex and changes the isotope pattern or the MS/MS fragment pattern dramatically. For metabolite 11, the isotope pattern indicates that there is no chlorine left in the molecule (Figure 16). The molecular formula of this metabolite, $C_{19}H_{29}N_5O_2$, is calculated with -1.35 ppm relative mass error (Figure 17). Compared to the parent drug's formula, $C_{25}H_{32}N_5O_2Cl$, this indicates the cleavage of the chlorophenyl moiety (C_6H_4Cl) in the initial metabolic reaction. The MS/MS fragments of this metabolite 11 are the same as for the parent drug (Figure 16), but the neutral loss fragments are different from the parent drug's neutral loss fragments (Figure 18). For instance, for the fragment at m/z 274.1558 with the formula $C_{15}H_{19}N_3O_2$, the neutral loss formula that fits the metabolite molecule is $C_4H_{10}N_2$, which is the formula

of the cleaved piperazine moiety (Figure 18). This metabolic cleavage is the first step in a subsequent cascade

of further oxidation reactions. Metabolite 12 is derived from metabolite 11 by a hydroxylation reaction.

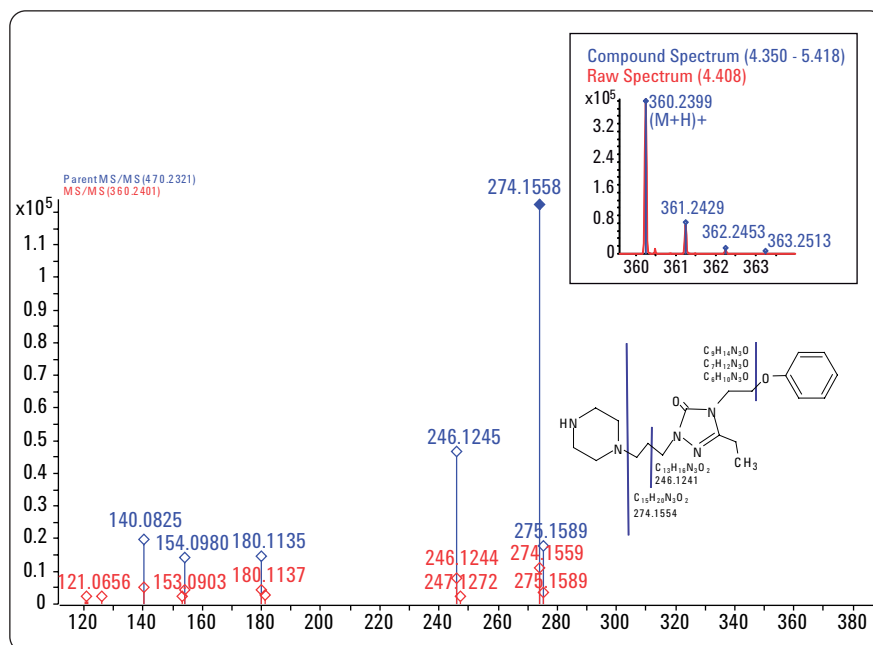


Figure 16
Mass spectrum, isotopic analysis and MS/MS spectrum with fragment assignment of the cleaved Nefazodone metabolite 11.

| Formula | Calc. Mass | Mass | Δ Mass [mDa] | Δ Mass [ppm] | DBE | m/z | Species | Ion Formula | Score |
|------------|------------|----------|---------------------|---------------------|-----|----------|---------|-------------|-------|
| C19H29N5O2 | 359.2321 | 359.2326 | -0.48 | -1.35 | 8 | 360.2398 | (M+H)+ | C19H30N5O2 | 100 |

| Isotopic pattern | | | | |
|------------------|-----------|---------------------|---------|---------------|
| m/z | Calc. m/z | Δ Mass [ppm] | Abund % | Calc. Abund % |
| 360.2399 | 360.2394 | -1.35 | 100.00 | 100.00 |
| 361.2429 | 361.2423 | -1.6 | 18.91 | 22.8 |
| 362.2453 | 362.245 | -1.04 | 2.26 | 2.9 |

Figure 17
Calculated molecular formula and mass accuracies, and isotopic analysis of the cleaved Nefazodone metabolite 11.

| m/z | Mass | Formula | Calc Mass | Δ Mass [mDa] | Δ Mass [ppm] | Loss Mass | Loss Formula | Neutral Loss |
|-----------|-----------|------------|-----------|---------------------|---------------------|-----------|--------------|--------------|
| 121.0658 | 120.05830 | C8H8O | 120.05751 | -0.79 | -6.54 | 239.17461 | C11H21N5O | 239.17453 |
| 140.08238 | 139.07511 | C6H9N3O | 139.07456 | -0.54 | -3.91 | 220.15756 | C13H20N2O | 220.15772 |
| 154.09782 | 153.09054 | C7H11N3O | 153.09021 | -0.33 | -2.16 | 206.14191 | C12H18N2O | 206.14229 |
| 180.11374 | 179.10646 | C9H13N3O | 179.10586 | -0.60 | -3.35 | 180.12626 | C10H16N2O | 180.12637 |
| 246.12437 | 245.11709 | C13H15N3O2 | 245.11643 | -0.66 | -2.70 | 114.11570 | C6H14N2 | 114.11574 |
| 274.15588 | 273.14860 | C15H19N3O2 | 273.14773 | -0.88 | -3.21 | 86.08440 | C4H10N2 | 86.08423 |

Figure 18
Calculated MS/MS fragment formulas and neutral loss formulas for the cleaved Nefazodone metabolite 11 fragmentation.

Metabolite 12 elutes at around 3.4 minutes with a mass of m/z 376.2355, and the formula $C_{19}H_{29}N_5O_3$ was calculated with -1.19 ppm relative mass error (Figures 19 and 20). The isotope pattern clearly shows a non-chlorinated compound (Figure 19). The MS/MS fragmentation pattern shows the main peak at m/z 290.1499 with the formula $C_{15}H_{19}N_3O_3$ calculated with -0.19 ppm relative mass error. This peak is shifted to higher mass than the parent's MS/MS peak at m/z 274.1553 by hydroxylation (Figure 21 and compare to metabolite 2). Metabolite 12 MS/MS fragment at m/z 156.0768 with the assigned formula $C_6H_{10}N_3O_2$ (-0.69 ppm relative mass error, Figure 21) is

derived from metabolite 11 MS/MS fragment with the formula $C_6H_{10}N_3O$ at m/z 140.0823 (-3.91 ppm relative mass error, Figure 21) by an oxidation.

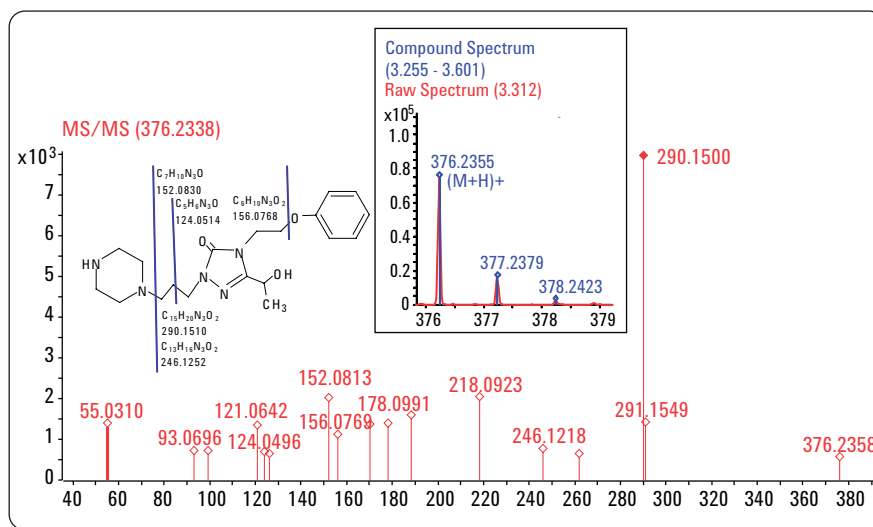


Figure 19
Mass spectrum, isotopic analysis and MS/MS spectrum with fragment assignment of the cleaved Nefazodone metabolite 12.

| Formula | Calc. Mass | Mass | Δ Mass [mDa] | Δ Mass [ppm] | DBE | m/z | Species | Ion Formula |
|------------|------------|----------|---------------------|---------------------|-----|----------|---------|-------------|
| C19H29N5O3 | 375.227 | 375.2282 | -1.19 | -3.17 | 8 | 376.2355 | (M+H)+ | C19H30N5O3 |

| Isotopic pattern | | | | |
|------------------|-------------|---------------------|---------|---------------|
| m/z | Calc. m/z | Δ Mass [ppm] | Abund % | Calc. Abund % |
| 376.2355 | 376.2343 | -3.16 | 100.00 | 100.00 |
| 377.2379 | 377.2372 | -1.94 | 18.95 | 22.84 |
| 378.2423 | 378.2398 | -6.58 | 2.19 | 3.11 |

Figure 20
Calculated molecular formula and mass accuracies, and isotopic analysis of the cleaved Nefazodone metabolite 12.

| m/z | Mass | Formula | Calc. Mass | Δ Mass [mDa] | Δ Mass [ppm] | Neutral Loss | Loss Formula | Loss Mass | FPM m/z | Shift m/z | Δ Shift [mDa] | Shift Formula |
|-----------|-----------|------------|------------|---------------------|---------------------|--------------|--------------|-----------|-----------|-------------|----------------------|---------------|
| 121.06419 | 120.05691 | C8H8O | 120.05751 | 0.61 | 5.04 | 255.16963 | C11H21N5O2 | 255.16952 | | | | |
| 124.04965 | 123.04237 | C5H5N3O | 123.04326 | 0.89 | 7.24 | 252.18417 | C14H24N2O2 | 252.18378 | | | | |
| 126.06591 | 125.05864 | C5H7N3O | 125.05891 | 0.27 | 2.19 | 250.16790 | C14H22N2O2 | 250.16813 | | | | |
| 152.08126 | 151.07398 | C7H9N3O | 151.07456 | 0.58 | 3.85 | 224.15256 | C12H20N2O2 | 224.15248 | | | | |
| 156.07686 | 155.06958 | C6H9N3O2 | 155.06948 | -0.11 | -0.69 | 220.15696 | C13H20N2O | 220.15756 | | | | |
| 170.09180 | 169.08452 | C7H11N3O2 | 169.08513 | 0.60 | 3.57 | 206.14202 | C12H18N2O | 206.14191 | | | | |
| 178.09908 | 177.09181 | C9H11N3O | 177.09021 | -1.59 | -9.00 | 198.13474 | C10H18N2O2 | 198.13683 | | | | |
| 188.10734 | 187.10007 | C12H13NO | 187.09971 | -0.35 | -1.89 | 188.12647 | C7H16N4O2 | 188.12733 | | | | |
| 218.09232 | 217.08505 | C11H11N3O2 | 217.08513 | 0.08 | 0.38 | 158.14150 | C8H18N2O | 158.14191 | | | | |
| 246.12179 | 245.11451 | C13H15N3O2 | 245.11643 | 1.92 | 7.82 | 130.11203 | C6H14N2O | 130.11061 | | | | |
| 262.11900 | 261.11173 | C13H15N3O3 | 261.11134 | -0.39 | -1.48 | 114.11481 | C6H14N2 | 114.11570 | | | | |
| 290.14997 | 289.14270 | C15H19N3O3 | 289.14264 | -0.05 | -0.19 | 86.08385 | C4H10N2 | 86.08440 | 274.1553 | 15.9949 | 0.29+0 | |
| 376.23579 | | | | | | | | | | | | |

Figure 21
Calculated MS/MS fragment formulas and neutral loss formulas for the cleaved Nefazodone metabolite 12 fragmentation.

Metabolite 13 is derived from metabolite 12 by further oxidation of the hydroxyl group to a keto group (Figures 22 and 23). Metabolite 13 shows a non-chlorinated isotope pattern with the highest abundance ion at m/z 374.2195 (insert in Figure 22). The formula of metabolite 13, C₁₉H₂₇N₅O₈, is calculated with -2.31 ppm relative mass error (Figure 23). The MS/MS fragmentation pattern shows a peak at m/z 288.1353 with the ion formula C₁₅H₁₈N₃O₃ calculated with -3.43 ppm relative mass error. This peak, coming from the cleavage of the piperazine moiety, is shifted to higher mass than the parent's MS/MS peak at m/z 274.1553 by an oxidation (Figure 24 and compare to metabolite 2). The main peak in the MS/MS spectrum of metabolite 13 occurs at m/z 168.0765 with the ion formula C₇H₁₀N₃O₃ calculated with 1.78 ppm relative mass error. This fragment can be explained by an additional loss of an ethyl group

and a benzyl group. Further fragmentation leads to the fragment peaks at m/z 154.0611 and m/z 140.0457 with the

respective formulae C₆H₈N₃O₂ (0.10 ppm) and C₅H₆N₃O₂ (-1.97 ppm) (Figure 24 and formula in Figure 22).

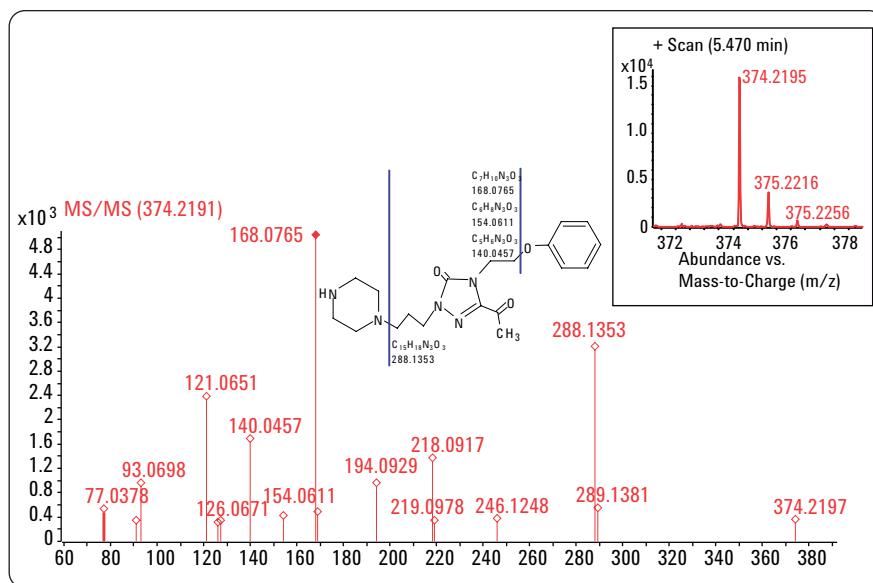


Figure 22
Mass spectrum, isotopic analysis and MS/MS spectrum with fragment assignment of the cleaved Nefazodone metabolite 13.

| Formula | Calc. Mass | Mass | Δ Mass [mDa] | Δ Mass [ppm] | DBE | m/z | Species | Ion Formula |
|---|------------|----------|--------------|--------------|-----|----------|--------------------|---|
| C ₁₉ H ₂₇ N ₅ O ₃ | 373.2114 | 373.2123 | -0.86 | -2.31 | 9 | 374.2195 | (M+H) ⁺ | C ₁₉ H ₂₈ N ₅ O ₃ |

| Isotopic pattern | | | | |
|------------------|-----------|--------------|---------|---------------|
| m/z | Calc. m/z | Δ Mass [ppm] | Abund % | Calc. Abund % |
| 374.2195 | 374.2187 | -2.31 | 100.00 | 100.00 |
| 375.2216 | 375.2216 | -0.05 | 18.49 | 22.81 |
| 376.2256 | 376.2241 | -4.01 | 2.43 | 3.1 |

Figure 23
Calculated molecular formula and mass accuracies, and isotopic analysis of the cleaved Nefazodone metabolite 13.

| m/z | Mass | Formula | Calc. Mass | Δ Mass [mDa] | Δ Mass [ppm] | Neutral Loss | Loss Formula | Loss Mass | FPM m/z | Shift m/z | Δ Shift [mDa] | Shift Formula |
|-----------|-----------|---|------------|--------------|--------------|--------------|---|-----------|----------|-----------|---------------|--------------------|
| 121.06506 | 120.05779 | C ₈ H ₈ O | 120.05751 | -0.27 | -2.27 | 253.15402 | C ₁₁ H ₁₉ N ₅ O ₂ | 253.15387 | | | | |
| 126.06707 | 125.05980 | C ₅ H ₇ N ₃ O | 125.05891 | -0.89 | -7.08 | 248.15201 | C ₁₄ H ₂₀ N ₂ O ₂ | 248.15248 | | | | |
| 127.12332 | 126.11604 | C ₇ H ₁₄ N ₂ | 126.11570 | -0.34 | -2.70 | 247.09577 | C ₁₂ H ₁₃ N ₃ O ₃ | 247.09569 | | | | |
| 140.04573 | 139.03845 | C ₅ H ₅ N ₃ O ₂ | 139.03818 | -0.27 | -1.97 | 234.17336 | C ₁₄ H ₂₂ N ₂ O | 234.17321 | | | | |
| 154.06109 | 153.05381 | C ₆ H ₇ N ₃ O ₂ | 153.05383 | 0.01 | 0.10 | 220.15800 | C ₁₃ H ₂₀ N ₂ O | 220.15756 | | | | |
| 168.07646 | 167.06918 | C ₇ H ₉ N ₃ O ₂ | 167.06948 | 0.30 | 1.78 | 206.14263 | C ₁₂ H ₁₈ N ₂ O | 206.14191 | | | | |
| 194.09287 | 193.08559 | C ₉ H ₁₁ N ₃ O ₂ | 193.08513 | -0.47 | -2.42 | 180.12622 | C ₁₀ H ₁₆ N ₂ O | 180.12626 | | | | |
| 218.09172 | 217.08444 | C ₁₁ H ₁₁ N ₃ O ₂ | 217.08513 | 0.68 | 3.14 | 156.12737 | C ₈ H ₁₆ N ₂ O | 156.12626 | | | | |
| 246.12485 | 245.11757 | C ₁₃ H ₁₅ N ₃ O ₂ | 245.11643 | -1.14 | -4.67 | 128.09424 | C ₆ H ₁₂ N ₂ O | 128.09496 | | | | |
| 288.13525 | 287.12798 | C ₁₅ H ₁₇ N ₃ O ₃ | 287.12699 | -0.99 | -3.43 | 86.08383 | C ₄ H ₁₀ N ₂ | 86.08440 | 274.1553 | 13.9793 | 0.64 | -H ₂ +O |

Figure 24
Calculated MS/MS fragment formulas and neutral loss formulas for the cleaved Nefazodone metabolite 13 fragmentation.

The non-chlorinated metabolite 14, which elutes at around 7.2 minutes with m/z 292.1666, has the formula C₁₅H₂₁N₃O₃ calculated with -3.65 ppm relative mass error (Figures 25 and 26). This formula shows a difference of -C₄H₈N₂+O to the formula C₁₉H₂₉N₅O₂ of metabolite 11 (Figures 16 and 17 on page 7) and gives evidence for the loss of the piperazine moiety followed by a hydroxylation. The MS/MS fragment pattern matching (FPM) shows the similarity of metabolite 14 to the parent drug nefazodone (Figure 25). The molecular ion of metabolite 14 can be explained by the nefazodone MS/MS fragment at m/z 274.1558 (C₁₅H₂₀N₃O₂) with a mass shift of an oxygen and two hydrogen atoms. The position of the hydroxylation can be explained by the occurrence of the new MS/MS fragment ion at m/z 198.1238 with the formula C₉H₁₆N₃O₂ (-0.67 ppm relative mass error) (Figure 27) in comparison to the

nefazodone MS/MS fragment ion at m/z 180.1135 (C₉H₁₄N₃O) (Figure 3 on page 2) by the addition of H₂O. This assumption is supported by the fact that the fragment ions at m/z 154.0986

(C₇H₁₂N₃O) and m/z 140.0819 (C₆H₁₀N₃O) are the same as in the nefazodone MS/MS spectrum (compare Figure 27 with Figure 3 on page 2).

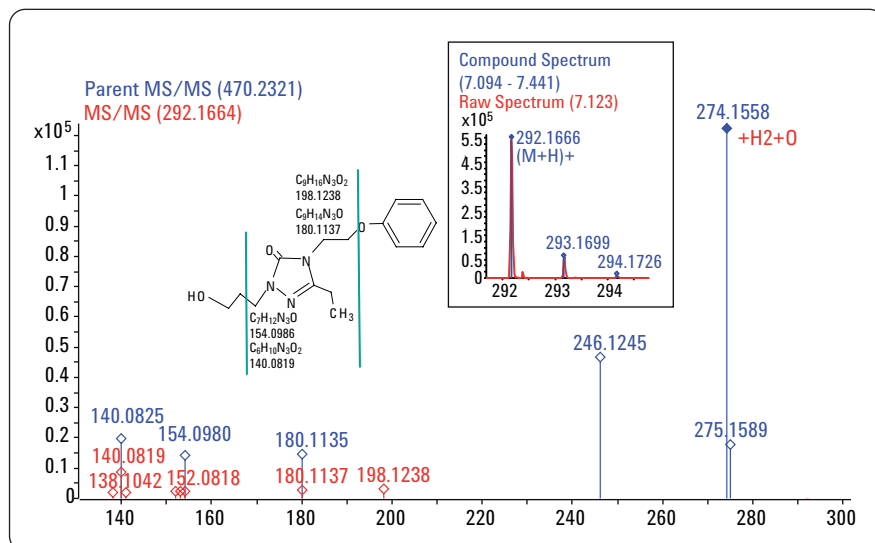


Figure 25
Mass spectrum, isotopic analysis and MS/MS spectrum with fragment assignment of the cleaved Nefazodone metabolite 14.

| Formula | Calc. Mass | Mass | Δ Mass [mDa] | Δ Mass [ppm] | DBE | m/z | Species | Ion Formula | Score |
|---|------------|-----------|--------------|--------------|-----|-----------|---------|---|-------|
| C ₁₅ H ₂₁ N ₃ O ₃ | 291.15829 | 291.15935 | -1.06 | -3.65 | 7 | 292.16663 | (M+H)+ | C ₁₅ H ₂₂ N ₃ O ₃ | 100 |

| Isotopic pattern | | | | |
|------------------|-----------|--------------|---------|---------------|
| m/z | Calc. m/z | Δ Mass [ppm] | Abund % | Calc. Abund % |
| 292.1666 | 292.1656 | -3.64 | 100.00 | 100.00 |
| 293.1699 | 293.1686 | -4.35 | 14.7 | 17.69 |
| 294.1726 | 294.171 | -5.39 | 1.69 | 2.09 |

Figure 26
Calculated molecular formula and mass accuracies, and isotopic analysis of the cleaved Nefazodone metabolite 14.

| m/z | Mass | Formula | Calc. Mass | Δ Mass [mDa] | Δ Mass [ppm] | Loss Mass | Loss Formula | Neutral Loss | FPM m/z | Shift m/z | Δ Shift [mDa] | Shift Formula |
|-----------|-----------|--|------------|--------------|--------------|-----------|---|--------------|-----------|-----------|---------------|--------------------|
| 140.08191 | 139.07464 | C ₆ H ₉ N ₃ O | 139.07456 | -0.07 | -0.53 | 152.08373 | C ₉ H ₁₂ O ₂ | 152.08450 | | | | |
| 154.09862 | 153.09134 | C ₇ H ₁₁ N ₃ O | 153.09021 | -1.13 | -7.37 | 138.06808 | C ₈ H ₁₀ O ₂ | 138.06780 | | | | |
| 180.11373 | 179.10645 | C ₉ H ₁₃ N ₃ O | 179.10586 | -0.59 | -3.30 | 112.05243 | C ₆ H ₈ O ₂ | 112.05269 | | | | |
| 198.12384 | 197.11656 | C ₉ H ₁₅ N ₃ O ₂ | 197.11643 | -0.13 | -0.67 | 94.04186 | C ₆ H ₆ O | 94.04258 | | | | |
| 292.16641 | | | | | | | | | 274.15579 | 18.01 | 0.06 | +H ₂ +O |

Figure 27
Calculated MS/MS fragment formulas and neutral loss formulas for the cleaved Nefazodone metabolite 14 fragmentation.

A subsequent oxidation of metabolite 14 leads to the two isomeric metabolites 15 and 16. Both metabolites 15 and 16 have the calculated molecular mass of 305.1375 and a typical isotope pattern for a non-chlorinated compound (Figure 28 and Figure 31 on page 12). The metabolite 15 elutes around 7.1 minutes with m/z at 306.1459 and the formula $C_{15}H_{19}N_3O_4$ calculated with -3.53 ppm relative mass error (Figures 28 and 29). The fragment pattern matching (FPM) indicates that this metabolite molecule is derived from the parent drug fragment at m/z 274.1557 by the addition of two oxygen atoms (Figure 30). The MS/MS spectrum shows a fragment at m/z 234.1239 with the formula $C_{12}H_{16}N_3O_2$ calculated with -0.68 ppm. This fragment shows the same atomic constitution as the right side of the parent drug nefazodone. The formula of the neutral loss $C_3H_4O_2$ indicates an additional metabolic oxidation reaction to a carboxylic acid in the left side of the

metabolite molecule 15 (Figures 28 and 30) compared to metabolite 14 (Figure 25 on page 10). The proposed structure of metabolite 15 is additionally supported by the fragment at m/z

140.0823 with the formula $C_6H_{10}N_3O$ (calculated with -3.38 ppm relative mass error), which is the same as for the parent drug nefazodone (Figure 1 on page 1).

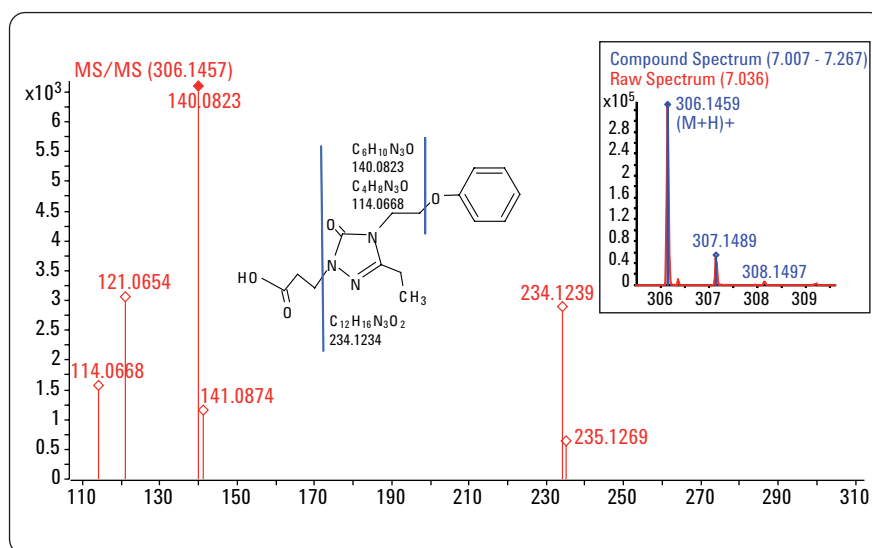


Figure 28
Mass spectrum, isotopic analysis and MS/MS spectrum with fragment assignment of the cleaved Nefazodone metabolite 15.

| Formula | Calc. Mass | Mass | Δ Mass [mDa] | Δ Mass [ppm] | DBE | m/z | Species | Ion Formula | Score |
|------------|------------|-----------|---------------------|---------------------|-----|-----------|--------------------|-------------|-------|
| C15H19N3O4 | 305.13755 | 305.13863 | -1.07 | -3.53 | 8 | 306.14591 | (M+H) ⁺ | C15H20N3O4 | 100 |

| Isotopic pattern | | | | |
|------------------|-----------|---------------------|---------|---------------|
| m/z | Calc. m/z | Δ Mass [ppm] | Abund % | Calc. Abund % |
| 306.1459 | 306.1448 | -3.52 | 100.00 | 100.00 |
| 307.1489 | 307.1478 | -3.51 | 15.22 | 17.70 |
| 308.1497 | 308.1486 | -3.52 | 1.70 | 2.10 |

Figure 29
Calculated molecular formula and mass accuracies, and isotopic analysis of the cleaved Nefazodone metabolite 15.

| m/z | Mass | Formula | Calc. Mass | Δ Mass [mDa] | Δ Mass [ppm] | Loss Mass | Loss Formula | Neutral Loss | FPM m/z | Shift m/z | Δ Shift [mDa] | Shift Formula |
|-----------|-----------|------------|------------|---------------------|---------------------|-----------|--------------|--------------|-----------|-----------|----------------------|---------------|
| 114.06681 | 113.05953 | C4H7N3O | 113.05891 | -0.62 | -5.51 | 192.07864 | C11H12O3 | 192.07890 | | | | |
| 121.06542 | 120.05815 | C8H8O | 120.05751 | -0.63 | -5.27 | 185.08004 | C7H11N3O3 | 185.08028 | | | | |
| 140.08231 | 139.07503 | C6H9N3O | 139.07456 | -0.47 | -3.38 | 166.06299 | C9H10O3 | 166.06340 | | | | |
| 234.12386 | 233.11659 | C12H15N3O2 | 233.11643 | -0.16 | -0.68 | 72.02113 | C3H4O2 | 72.02185 | | | | |
| 306.14571 | | | | | | | | | 274.15579 | 31.98983 | 0.09 | +O2 |

Figure 30
Calculated MS/MS fragment formulas and neutral loss formulas for the cleaved Nefazodone metabolite 15 fragmentation.

The isomeric metabolite 16 elutes at around 7.3 minutes and the formula was calculated with 1.77 ppm relative mass error (Figures 31 and 32). The metabolite 16 has a fragment pattern matching (FPM) that indicates that this metabolite molecule is also derived from the parent drug fragment at m/z 274.1557 by the addition of two oxygen atoms (Figure 33), but the MS/MS spectrum is different from the previous one and indicates a different structure for this metabolite. The fragment at m/z 212.1039 with the formula $C_9H_{14}N_3O_3$ indicates two additional oxygen atoms in the left part of the molecule, which is left after fragmentation of the phenyl moiety (C_6H_6O). The fragment at m/z 194.0932 with the formula $C_9H_{12}N_3O_2$ indicates the loss of a molecule of water. This leads to the conclusion that one of the oxygen atoms is in a hydroxyl group (Figures 31 and 33). The MS/MS fragment at m/z 140.0460 with the formula $C_5H_6N_3O_2$ (4.51 ppm relative mass error) indicates oxidation to a keto

group in metabolite 16 compared to the measured mass for this fragment in metabolite 15 and nefazodone at

m/z 140.0823 and m/z 140.0827 respectively, with the formula $C_6H_{10}N_3O$ (Figure 33 and Figure 3 on page 2).

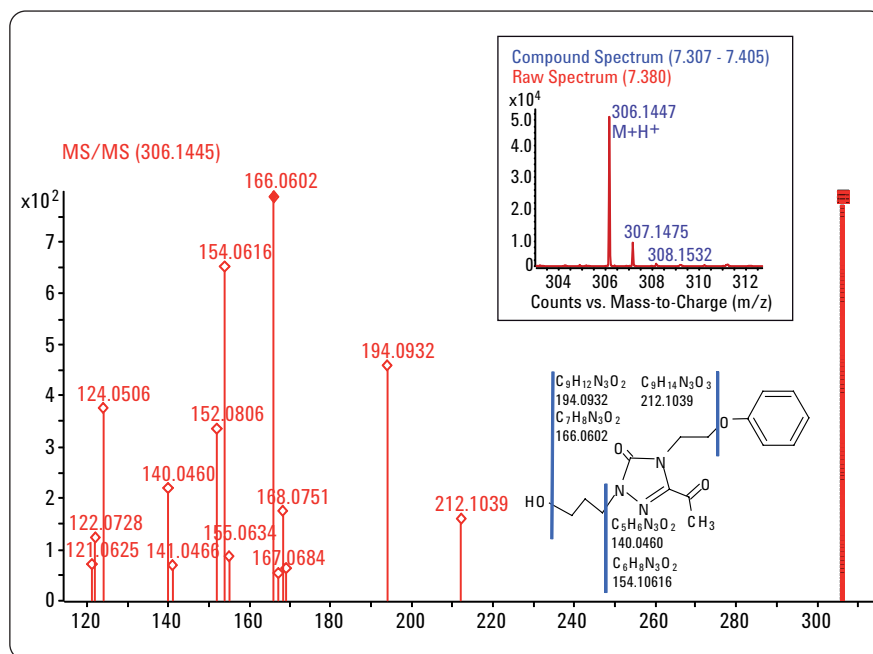


Figure 31
Mass spectrum, isotopic analysis and MS/MS spectrum with fragment assignment of the cleaved Nefazodone metabolite 16.

| Formula | Calc. Mass | Mass | Δ Mass [mDa] | Δ Mass [ppm] | DBE | m/z | Species | Ion Formula | Score |
|------------|------------|-----------|---------------------|---------------------|-----|-----------|---------|-------------|-------|
| C15H19N3O4 | 305.13755 | 305.13701 | 0.54 | 1.77 | 8 | 306.14429 | (M+H)+ | C15H20N3O4 | 100 |

| Isotopic pattern | | | | |
|------------------|-------------|---------------------|---------|---------------|
| m/z | Calc. m/z | Δ Mass [ppm] | Abund % | Calc. Abund % |
| 306.1461 | 306.1448 | -4.10 | 100.00 | 100.00 |
| 307.1494 | 307.1478 | -5.07 | 18.16 | 17.70 |
| 308.1523 | 308.1512 | -5.50 | 2.70 | 2.25 |

Figure 32
Calculated molecular formula and mass accuracies, and isotopic analysis of the cleaved Nefazodone metabolite 16.

| m/z | Mass | Formula | Calc. Mass | Δ Mass [mDa] | Δ Mass [ppm] | Loss Mass | Loss Formula | Neutral Loss | FPM m/z | Shift m/z | Δ Shift [mDa] | Shift Formula |
|-----------|-----------|-----------|------------|---------------------|---------------------|-----------|--------------|--------------|-----------|-------------|----------------------|---------------|
| 140.04608 | 139.03880 | C5H5N3O2 | 139.03818 | -0.63 | -4.51 | 166.09938 | C10H14O2 | 166.09875 | | | | |
| 154.06158 | 153.05430 | C6H7N3O2 | 153.05383 | -0.48 | -3.12 | 152.08373 | C9H12O2 | 152.08289 | | | | |
| 166.06021 | 165.05294 | C7H7N3O2 | 165.05383 | 0.89 | 5.40 | 140.08373 | C8H12O2 | 140.08426 | | | | |
| 194.09318 | 193.08590 | C9H11N3O2 | 193.08513 | -0.78 | -4.03 | 112.05243 | C6H8O2 | 112.05129 | | | | |
| 212.10394 | 211.09667 | C9H13N3O3 | 211.09569 | -0.98 | -4.62 | 94.04186 | C6H6O | 94.04053 | | | | |
| 306.14447 | | | | | | | | | 274.15501 | 31.99 | 0.37 | +02 |

Figure 33
Calculated MS/MS fragment formulas and neutral loss formulas for the cleaved Nefazodone metabolite 16 fragmentation.

Unexpected Metabolic Pathways of Nefazodone

The pharmaceutical drug nefazodone undergoes extensive metabolism in the human body and yields not only the typical expected metabolites but also several unexpected metabolites initiated by a cleavage of the original drug molecule.

The metabolites that were identified in this work as previously discussed are displayed in Figure 34 as simplified proposed metabolic pathways for the unexpected metabolites.

In the metabolic reactions that lead to the unexpected metabolites, either the skeleton of the nefazodone molecule is cleaved in a preliminary reaction

and is then modified by a further metabolic reaction, or an expected metabolite is modified by a cleavage reaction. The metabolic oxidative cleavage, which removes the ethyl group from the thiazol-3-one part of the nefazodone molecule leads directly to the unexpected metabolite 7. The cleavage of the phenyl ring from monohydroxyl metabolite 2 yields the metabolite 8. Further oxidative metabolism of the hydroxyl group, which is still present and located at the ethyl group in this molecule, leads to the oxo metabolite 9. Another metabolic pathway also starts with hydroxyl metabolite 2 but leads to the metabolite 12 by cleavage of the chlorophenyl moiety. Further oxidation yields the oxo metabolite 13. The cleavage reaction that leads from the monohydroxyl

metabolite 2 to metabolite 12 is also possible for the unchanged nefazodone molecule, which yields the cleaved metabolite 11 directly. Starting from the monohydroxyl metabolite 1, a cleavage at the piperazine ring moiety yields the hydroxy-chloro metabolite 10. This cleavage reaction could possibly also generate the hydroxy metabolite 14. A further metabolic oxidation of the unexpected metabolite 14 could lead to the oxidation product 15, which comes from an oxidation of the secondary hydroxyl group to a carboxylic acid, and also to metabolite 16, which comes from an oxidation of the ethyl side chain of the triazol-3-one ring to a methyl keto group.

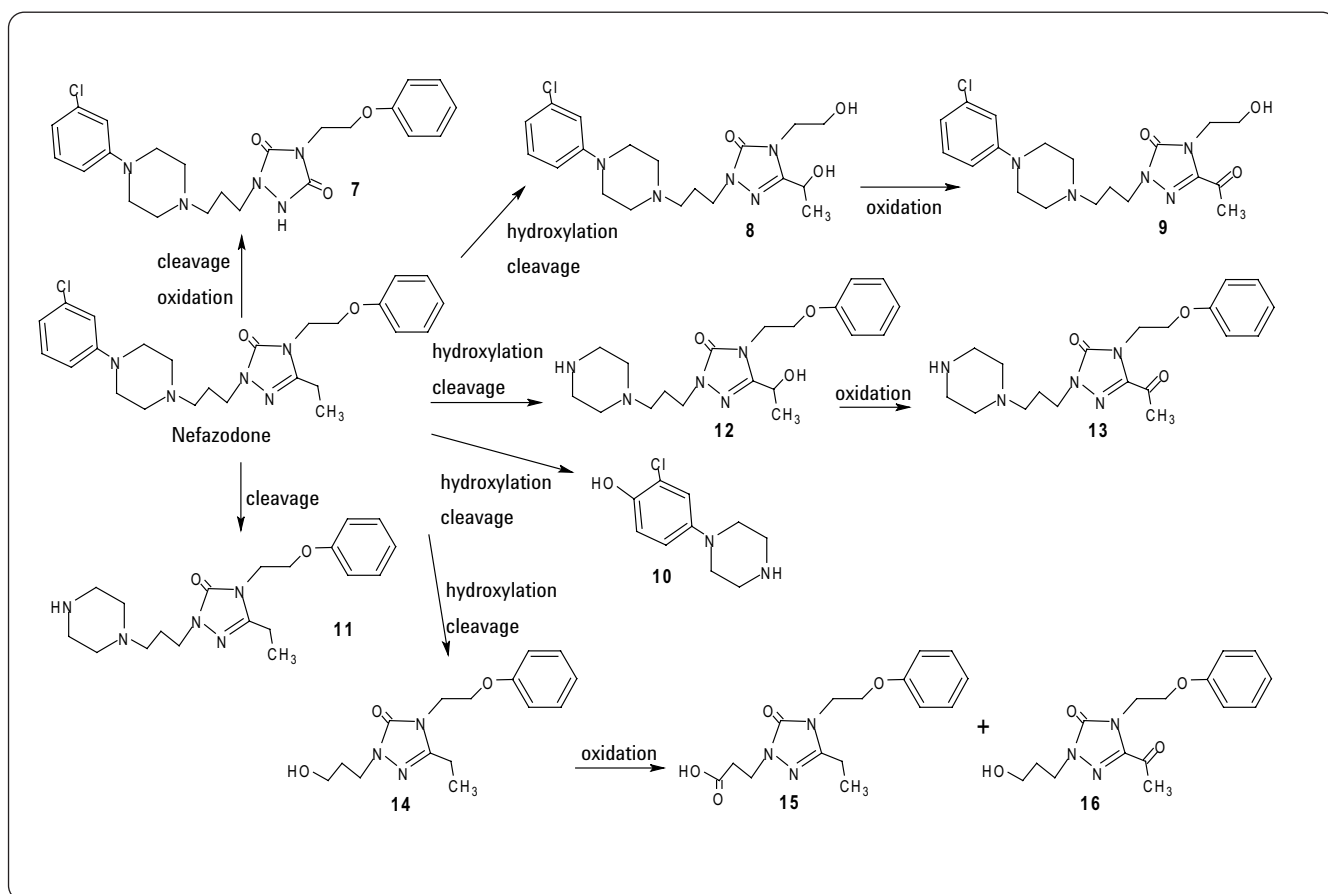


Figure 34
Proposed metabolic pathways for the unexpected metabolites of Nefazodone

Conclusion

This work demonstrates the interpretation of the results produced by the MassHunter Metabolite Identification (MetID) software for the identification of metabolites created by non-expected biotransformations. The assignment of metabolite structures by interpretation of information created from QTOF mass spectrometry data by various algorithms like isotope pattern matching, MS/MS fragment pattern matching and formula calculation based on accurate mass measurement for MS and MS/MS is demonstrated. This work is an example of the gain in productivity that can be achieved by using the MetID software for the interpretation of QTOF data from metabolite identification experiments.

References

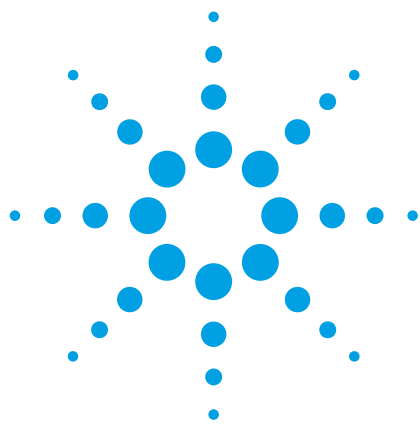
1. Edgar Naegele, Agilent Application Note "Computer assisted identification of metabolites from pharmaceutical drugs – Part I: Identification of expected metabolites of Nefazodone"
Publication number 5990-3606EN,
2009.

www.agilent.com/chem/metid

© Agilent Technologies, Inc., 2009
Published March 1, 2009
Publication Number 5990-3607EN



Agilent Technologies



Computer Assisted Identification of Metabolites from Pharmaceutical Drugs

Part 1: Identification of Expected Metabolites of Nefazodone

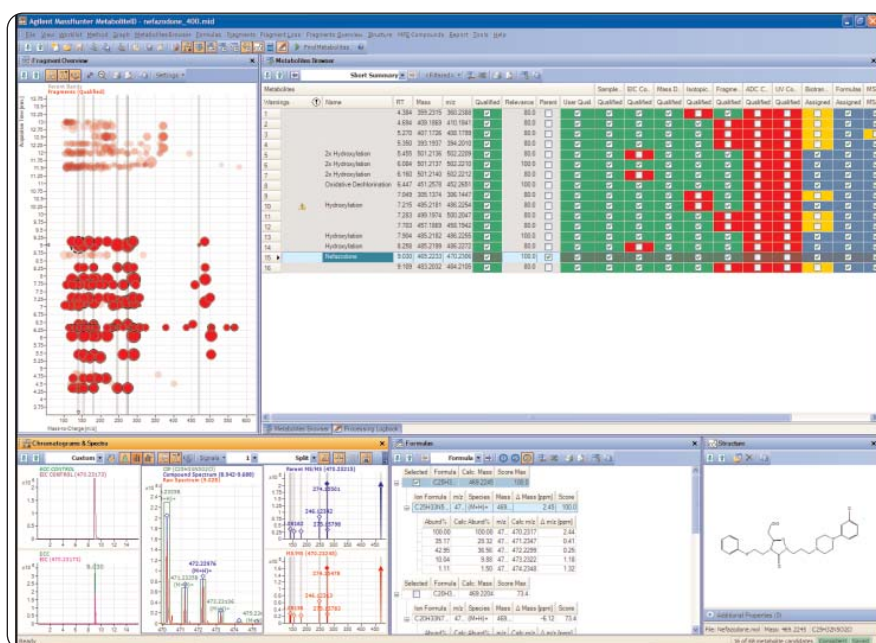
Identification of metabolites by the MassHunter Metabolite ID software from RRLC – QTOF MS data

Application Note

Metabolite identification in drug discovery and drug development

Author

Edgar Nägele
Agilent Technologies
Waldbronn, Germany



Abstract

This Application Note demonstrates:

- The use of the Agilent 1200 Rapid Resolution LC (RRLC) system for high resolution separation of metabolites from an in-vitro metabolism experiment.
- The use of the Agilent 6520 QTOF mass spectrometer for the acquisition of data for computer assisted metabolite identification.
- The use of the Agilent MassHunter Metabolite identification software for highly productive identification of expected metabolites.
- The results of the Metabolite ID data analysis for expected metabolites of the pharmaceutical drug nefazodone



Agilent Technologies

Introduction

The examination of the metabolism of new pharmaceutical drug candidates is an important step in the drug discovery and development process. For the evaluation of new technologies that improves the productivity in this important area, well known compounds are used as benchmarks. A compound that undergoes an extensive, well-documented metabolism and that can be used for this purpose is the pharmaceutical drug Nefazodone¹. To confirm the utility of the MassHunter MetID for the identification of possible metabolites, it has been tested with this particular compound. The MassHunter MetID software uses the concept of multiple cooperative algorithms for the analysis of the QTOF MS and MS/MS data as a strategy to produce a confident overall result that normalizes the influence of a single algorithm².

This Application note Demonstrates the use of the Agilent 1200 RR LC system and the Agilent 6500 Series Accurate Mass QTOF mass spectrometer for data acquisition from metabolism experiments, and the use of the MetID software for computer-assisted data analysis. The results of the data analysis are discussed in detail for examples of expected metabolites and unexpected metabolites³ from the pharmaceutical drug Nefazodone.

Experimental

Equipment

- Agilent 1200 Series Rapid Resolution LC system with binary pump SL and degasser, high performance autosampler SL (ALS SL) with thermostat, thermostated column compartment (TCC) and Agilent 6500 Series Accurate Mass QTOF mass spectrometer.

- Column: ZORBAX SB-C18, 2.1 x 150 mm, 1.8 µm particle size.

Sample preparation

Stock solutions

- Phosphate buffer 100 mM, pH 7.4 (81.8 mL 0.1 M Na₂HPO₄ + 18.2 mL 0.1 M KH₂PO₄); 5 mM MgCl₂
- Nefazodone hydrochloride 250 µM in phosphate buffer
- NADPH solution, 10 mg/mL phosphate buffer
- Microsomal S9 preparation from rat liver, 20 mg protein/mL

Metabolite sample

Dilute 25 µL of Nefazodone in 180 µL phosphate buffer in a 1.5 mL Eppendorf vial. Add 15 µL S9 preparation and 30 µL NADPH solution. Vortex and incubate for 1 h at 37°C. Stop the reaction by adding 750 µL ice cold acetonitrile and centrifuge at 14,000 rpm for 15 minutes.

Remove the supernatant into a new 1.5 mL Eppendorf vial and evaporate to dryness in a speedvac. Dissolve the remaining pellet in 250 µL HPLC solvent A.

Control sample

Dilute 25 µL of Nefazodone in 210 µL phosphate buffer in a 1.5 mL Eppendorf vial. Add 15 µL S9 preparation. Vortex and incubate for 1 h at 37 °C. Add 750 µL ice cold acetonitrile and centrifuge at 14,000 rpm for 15 minutes.

Remove the supernatant to a new 1.5 mL Eppendorf vial and evaporate to dryness in a speedvac. Dissolve the remaining pellet in 250 µL HPLC solvent A.

All chemicals and bio-reagents were purchased from Sigma-Aldrich; HPLC solvents (acetonitrile) were purchased from Merck (Germany), and HPLC water from Mallinckrodt-Baker.

Methods

High resolution RR LC method

The Agilent 1200 Series binary pump SL was operated under the following conditions:

Solvent A: Water + 0.1% formic acid (FA),
Solvent B: ACN + 0.1% FA
Flow rate: 0.5 mL/min
Gradient: 0 min 5% B, 15 min 75% B
15.1 min 95% B
16 min 95% B
Stop time: 16 min
Post time: 10 min

The Agilent 1200 autosampler SL was used to make injections of 1-10 µL sample with a 5 sec needle wash in 50% methanol and the samples were cooled to 4 °C. The TCC was operated at 60°C.

QTOF MS and MS/MS method

The Agilent 6500 Series Accurate Mass QTOF was operated in the 2GHz extended dynamic range mode with the following acquisition parameters:

Source: ESI in positive mode with dual spray for reference mass solution (m/z 121.05087 and m/z 922.00979)

Drying gas flow: 10.0 L/min
Dry gas temperature: 300 °C

Nebulizer: 45 psi
Mass range: 100-1000

Fragmentor: 200 V

Skimmer: 60 V

Capillary: 3500 V

Collision energy: 30 V

Data depended

MS/MS: 2 compounds
3 MS/MS spectra
exclusion for 0.1 min

Data analysis method in the MetID software

The first step in the analysis of the data consists of a comparison between the data file that contains the metabolite compounds (metabolite sample) and the data file that contains

only the parent drug (control sample). In this analysis, all detectable mass signals are extracted from the MS level data using the Molecular Feature Extraction (MFE) algorithm. Then, related compound isotope masses and adduct masses are grouped together into discrete molecular features, and chemical noise is removed. The compound lists of the metabolized sample and the control are then compared. All compounds that are new or increased by at least 2-fold in the metabolized sample are considered potential metabolites and are subjected to further analysis by different algorithms, which can be specified by the user. The algorithms can identify and qualify new metabolites, or can simply qualify metabolites found by another algorithm. The results of all metabolite identification algorithms are weighted and combined into a final identification relevance score. Metabolites are qualified when their final score is above a defined relevance threshold. The results from all algorithms are populated in a results table and can be inspected at a glance².

Results and discussion

For the identification of possible metabolites, the basic information about isotope pattern, MS/MS fragmentation pattern and calculated formula of the parent drug nefazodone are taken from the control sample

(Figures 1 and 2). The measured isotope pattern (blue lines, insert in Figure 1) clearly shows the pattern that is typical for a chlorinated compound, and is identical to the calculated isotope pattern (CIP, green box, insert in Figure 1) with the main ion (M+H)⁺ at m/z 470.2319 (C₂₅H₃₃N₅O₂Cl). The

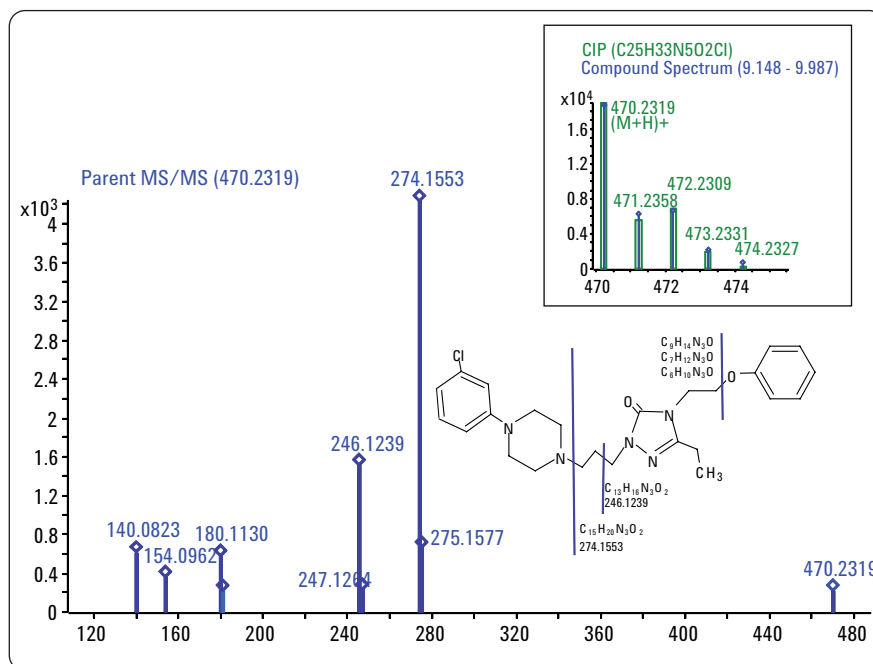


Figure 1
Mass spectrum, isotopic analysis and MS/MS spectrum for fragment assignment of the parent drug Nefazodone.

| Formula | Calc. Mass | Mass | Δ Mass [mDa] | Δ Mass [ppm] | DBE | m/z | Species | Ion Formula |
|--|------------|----------|--------------|--------------|-----|----------|--------------------|--|
| C ₂₅ H ₃₂ N ₅ O ₂ Cl | 469.2245 | 469.2246 | -0.16 | -0.35 | 12 | 470.2319 | (M+H) ⁺ | C ₂₅ H ₃₃ N ₅ O ₂ Cl |

| Isotopic pattern | | | | |
|------------------|-----------|--------------|---------|---------------|
| m/z | Calc. m/z | Δ Mass [ppm] | Abund % | Calc. Abund % |
| 470.2319 | 470.2317 | -0.35 | 100.00 | 100.00 |
| 471.2358 | 471.2347 | -2.28 | 31.86 | 29.32 |
| 472.2309 | 472.2299 | -2.24 | 33.67 | 36.56 |
| 473.2331 | 473.2322 | -1.90 | 10.14 | 9.88 |
| 474.2327 | 474.2348 | 4.50 | 2.23 | 1.50 |

Figure 2
Calculated molecular formula and mass accuracies, and isotopic analysis of Nefazodone.

| m/z | Mass | Formula | Calc. Mass | Δ Mass [mDa] | Δ Mass [ppm] | Loss Mass | Loss Formula | Neutral Loss |
|----------|----------|---|------------|--------------|--------------|-----------|--|--------------|
| 140.0823 | 139.0750 | C ₆ H ₉ N ₃ O | 139.0746 | -0.43 | -3.12 | 330.1499 | C ₁₉ H ₂₃ N ₂ OCl | 330.1482 |
| 154.0962 | 153.0890 | C ₇ H ₁₁ N ₃ O | 153.0902 | 1.25 | 8.16 | 316.1342 | C ₁₈ H ₂₁ N ₂ OCl | 316.1343 |
| 180.1130 | 179.1058 | C ₉ H ₁₃ N ₃ O | 179.1059 | 0.11 | 0.62 | 290.1186 | C ₁₆ H ₁₉ N ₂ OCl | 290.1175 |
| 246.1239 | 245.1167 | C ₁₃ H ₁₅ N ₃ O ₂ | 245.1164 | -0.23 | -0.94 | 224.1080 | C ₁₂ H ₁₇ N ₂ Cl | 224.1066 |
| 274.1553 | 273.1481 | C ₁₅ H ₁₉ N ₃ O ₂ | 273.1477 | -0.34 | -1.26 | 196.0767 | C ₁₀ H ₁₃ N ₂ Cl | 196.0751 |

Figure 3
Calculated MS/MS fragment formulas and neutral loss formulas for Nefazodone fragmentation.

MS/MS spectrum shows the main fragment (M+H)⁺ at m/z 274.1553 with the formula C₁₅H₂₀N₃O₂ (Figure 1). The mass of nefazodone (C₂₅H₃₂N₅O₂Cl), which was calculated from the measured (M+H)⁺ ion, shows a low relative mass error of -0.35 ppm (Figure 2) and the MS/MS fragment at a mass of 273.1481 (C₁₅H₁₉N₃O₂) of -1.26 ppm (Figure 3). This fragment formula, together with the assigned loss formula C₁₀H₁₃N₂Cl calculated for this MS/MS fragment, fits to the parent drug formula C₂₅H₃₂N₅O₂Cl (Figure 3). Other MS/MS fragments are assigned to the structural formula of nefazodone (Figure 1).

The following metabolites are clearly identified by several algorithms in the software such as isotope pattern matching and MS/MS fragmentation pattern matching to identify compounds whose pattern matches the patterns of the parent drug. There is also a metabolism reaction assignment for biotransformations that belong to the expected phase I metabolic reactions. The first example comes from a hydroxylation reaction. The mono-hydroxyl metabolite 1 of nefazodone,

eluting at a retention time around 7.5 minutes, with m/z 486.2267 shows the measured isotope pattern (blue lines, insert in Figure 4) of a chlorinated compound similar to the calculated isotope pattern (CIP, green box, insert in Figure 4), and shows a relative mass error of -0.68 ppm for the calculated formula (Figure 5). The MS/MS fragmentation pattern is identical to the pattern of the parent drug,

and the molecular ion is shifted by the mass of an oxygen atom (Figure 4). This indicates that the reaction takes place at the part of the molecule that is eliminated as the neutral fragment during MS/MS fragmentation (Figure 6). The fragment ion at m/z 274.1545 has the same formula as the fragment of the parent, with relative mass error of 1.70 ppm, and the neutral loss has the formula C₁₀H₁₃N₂OCl, which fits to

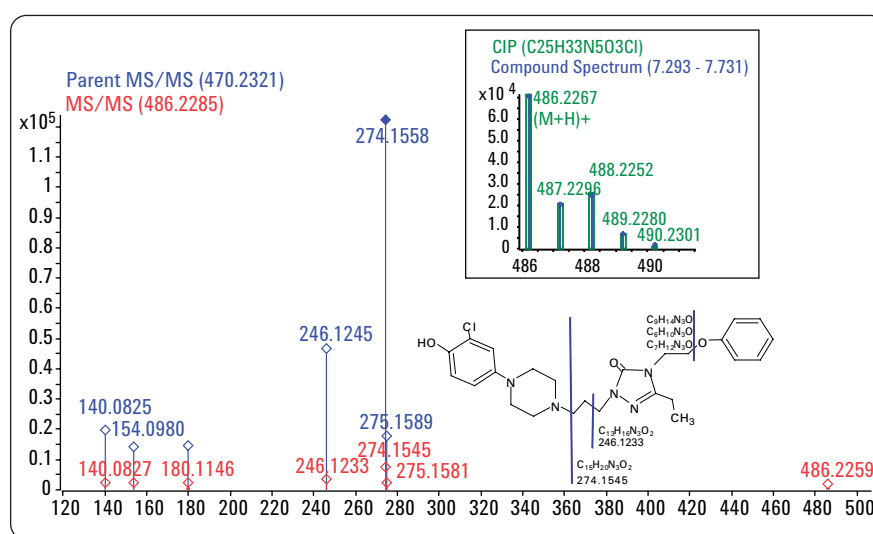


Figure 4
Mass spectrum, isotopic analysis and MS/MS spectrum with fragment assignment of the Nefazodone mono-hydroxy metabolite 1.

| Formula | Calc. Mass | Mass | Δ Mass [mDa] | Δ Mass [ppm] | DBE | m/z | Species | Ion Formula |
|--------------|------------|----------|--------------|--------------|-----|----------|--------------------|--------------|
| C25H32N5O3Cl | 485.2194 | 485.2197 | -0.33 | -0.68 | 12 | 486.2270 | (M+H) ⁺ | C25H33N5O3Cl |

| Isotopic pattern | | | | |
|------------------|-----------|--------------|--------|--------------|
| m/z | Calc. m/z | Δ Mass [ppm] | Abund% | Calc. Abund% |
| 486.2267 | 486.2266 | -0.09 | 100.00 | 100.00 |
| 487.2296 | 487.2296 | 0.01 | 26.32 | 29.36 |
| 488.2252 | 488.2248 | -0.76 | 31.76 | 36.77 |
| 489.2280 | 489.2272 | -1.64 | 8.80 | 9.95 |

Figure 5
Calculated molecular formula and mass accuracies, and isotopic analysis of the Nefazodone mono-hydroxy metabolite 1.

| m/z | Mass | Formula | Calc Mass | Δ Mass [mDa] | Δ Mass [ppm] | Loss Mass | Loss Formula | Neutral Loss | FPM m/z | Shift m/z | Δ Shift [mDa] | Shift Formula |
|----------|----------|------------|-----------|--------------|--------------|-----------|--------------|--------------|----------|-----------|---------------|---------------|
| 140.0827 | 139.0754 | C6H9N3O | 139.0746 | -0.87 | -6.27 | 346.1448 | C19H23N2O2Cl | 346.1458 | 140.0825 | | 0.26 | |
| 154.0971 | 153.0899 | C7H11N3O | 153.0902 | 0.35 | 2.32 | 332.1292 | C18H21N2O2Cl | 332.1313 | 154.0980 | | 0.82 | |
| 180.1146 | 179.1073 | C9H13N3O | 179.1077 | 0.36 | 2.00 | 306.1135 | C16H19N2O2Cl | 306.1139 | 180.1135 | | 1.14 | |
| 246.1233 | 245.1160 | C13H15N3O2 | 245.1164 | 0.44 | 1.79 | 240.1029 | C12H17N2OCl | 240.1052 | 246.1245 | | 1.20 | |
| 274.1545 | 273.1473 | C15H19N3O2 | 273.1477 | 0.46 | 1.70 | 212.0716 | C10H13N2OCl | 212.0739 | 274.1558 | | 1.25 | |
| 486.2259 | | | | | | | | | 470.2321 | 15.9949 | 1.11 | +O |

Figure 6
Calculated MS/MS fragment formulas and neutral loss formulas for the Nefazodone mono-hydroxy metabolite 1 fragmentation.

the parent formula of the mono-hydroxylated metabolite 1 (C₂₅H₃₂N₅O₃Cl). Another MS/MS fragment that gives the same result is the MS/MS fragment at m/z 246.1233 for the fragment formula C₁₃H₁₅N₃O₂ with 0.44 ppm (assigned MS/MS fragments in Figure 4 and Figure 6).

Additionally, there is a second mono-hydroxyl metabolite of nefazodone, 2, eluting at a retention time around 8.3 minutes, with the same mass and isotope pattern as 1. The difference in elution behavior indicates a different structure for 2 compared with 1. This can be seen by comparing the fragmentation pattern of the MS/MS spectrum of metabolite 2 (red spectrum) with the MS/MS fragmentation pattern of the parent drug (blue spectrum) (Figure 7). The MS/MS spectrum of 2 shows a shift from the parent drug at m/z 470.2319 by the mass of an oxygen atom to m/z 486.2279, with a deviation of -2.55 ppm for the calculated

formula (Figure 8), and a similar shift for the fragment mass at m/z 274.1582 to m/z 290.1508 with a deviation of -2.91 ppm for the calculated fragment formula (Figure 9). This fragment has the formula C₁₅H₁₉N₃O₃ and the corre-

sponding loss formula C₁₀H₁₃N₂Cl, which is identical to the parent drug's MS/MS (Figure 9). Other MS/MS fragments are assigned to the structural formula of metabolite 2, and support the proposed structure (Figure 7).

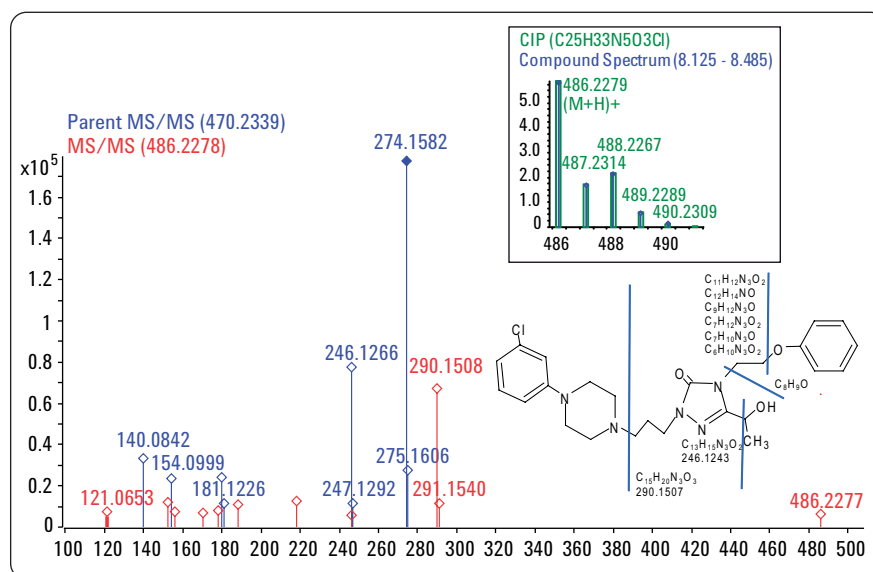


Figure 7 Mass spectrum, isotopic analysis and MS/MS spectrum with fragment assignment of the Nefazodone mono-hydroxy metabolite 2.

| Formula | Calc. Mass | Mass | Δ Mass [mDa] | Δ Mass [ppm] | DBE | m/z | Species | Ion Formula |
|--|------------|----------|--------------|--------------|-----|----------|--------------------|--|
| C ₂₅ H ₃₂ N ₅ O ₃ Cl | 485.2194 | 485.2206 | -1.24 | -2.55 | 12 | 486.2279 | (M+H) ⁺ | C ₂₅ H ₃₃ N ₅ O ₃ Cl |

| Isotopic pattern | | | | |
|------------------|-----------|--------------|--------|--------------|
| m/z | Calc. m/z | Δ Mass [ppm] | Abund% | Calc. Abund% |
| 486.2279 | 486.2266 | -2.55 | 100.00 | 100.00 |
| 487.2314 | 487.2296 | -3.66 | 27.42 | 29.36 |
| 488.2267 | 488.2248 | -3.81 | 34.81 | 36.77 |
| 489.2289 | 489.2272 | -3.52 | 7.99 | 9.95 |
| 490.2309 | 490.2297 | -2.35 | 1.24 | 1.58 |

Figure 8 Calculated molecular formula and mass accuracies, and isotopic analysis of the Nefazodone mono-hydroxy metabolite 2.

| m/z | Mass | Formula | Calc. Mass | Δ Mass [mDa] | Δ Mass [ppm] | Loss Mass | Loss Formula | Neutral Loss | FPM m/z | Shift m/z | Δ Shift [mDa] | Shift Formula |
|----------|----------|---|------------|--------------|--------------|-----------|--|--------------|----------|-----------|---------------|---------------------------------|
| 121.0653 | 120.0580 | C ₈ H ₈ O | 120.0575 | -0.48 | -3.96 | 365.1619 | C ₁₇ H ₂₄ N ₅ O ₂ Cl | 365.1625 | | | | |
| 152.0824 | 151.0751 | C ₇ H ₉ N ₃ O | 151.0746 | -0.56 | -3.70 | 334.1448 | C ₁₈ H ₂₃ N ₂ O ₂ Cl | 334.1454 | 180.1154 | -28.0313 | 1.72 | -C ₂ -H ₄ |
| 156.0776 | 155.0703 | C ₆ H ₉ N ₃ O ₂ | 155.0695 | -0.83 | -5.35 | 330.1499 | C ₁₉ H ₂₃ N ₂ O ₂ Cl | 330.1502 | 140.0842 | 15.9949 | 1.51 | +O |
| 170.0931 | 169.0859 | C ₇ H ₁₁ N ₃ O ₂ | 169.0851 | -0.73 | -4.33 | 316.1342 | C ₁₈ H ₂₁ N ₂ O ₂ Cl | 316.1347 | | | | |
| 178.0982 | 177.0909 | C ₉ H ₁₁ N ₃ O | 177.0902 | -0.68 | -3.83 | 308.1292 | C ₁₆ H ₂₁ N ₂ O ₂ Cl | 308.1296 | | | | |
| 188.1077 | 187.1004 | C ₁₂ H ₁₃ N ₃ O | 187.0997 | -0.71 | -3.78 | 298.1197 | C ₁₃ H ₁₉ N ₄ O ₂ Cl | 298.1201 | | | | |
| 218.0930 | 217.0857 | C ₁₁ H ₁₁ N ₃ O ₂ | 217.0851 | -0.61 | -2.83 | 268.1342 | C ₁₄ H ₂₁ N ₂ O ₂ Cl | 268.1348 | | | | |
| 246.1243 | 245.1170 | C ₁₃ H ₁₅ N ₃ O ₂ | 245.1164 | -0.55 | -2.24 | 240.1029 | C ₁₂ H ₁₇ N ₂ O ₂ Cl | 240.1036 | | | | |
| 290.1508 | 289.1435 | C ₁₅ H ₁₉ N ₃ O ₃ | 289.1426 | -0.84 | -2.91 | 196.0767 | C ₁₀ H ₁₃ N ₂ Cl | 196.0770 | 274.1582 | 15.9949 | 2.33 | +O |
| 486.2277 | | | | | | | | | 470.2339 | 15.9949 | 1.18 | +O |

Figure 9 Calculated MS/MS fragment formulas and neutral loss formulas for the Nefazodone mono-hydroxy metabolite 2 fragmentation.

An additional metabolic reaction oxidizes the hydroxyl metabolite 2 to the oxo metabolite 3 at m/z 484.2111 with a deviation of -0.26 ppm for the calculated formula (Figures 10 and 11). The MS/MS fragment pattern matching (FPM) indicates several fragments that are transformed by the hydroxylation followed by the oxidation (Figure 10). The main fragment at m/z 288.1350 has the formula $C_{15}H_{17}N_3O_3$ calculated with a deviation of -2.72 ppm, and some other shifted fragments are also indicated (Figure 12, formula in Figure 10).

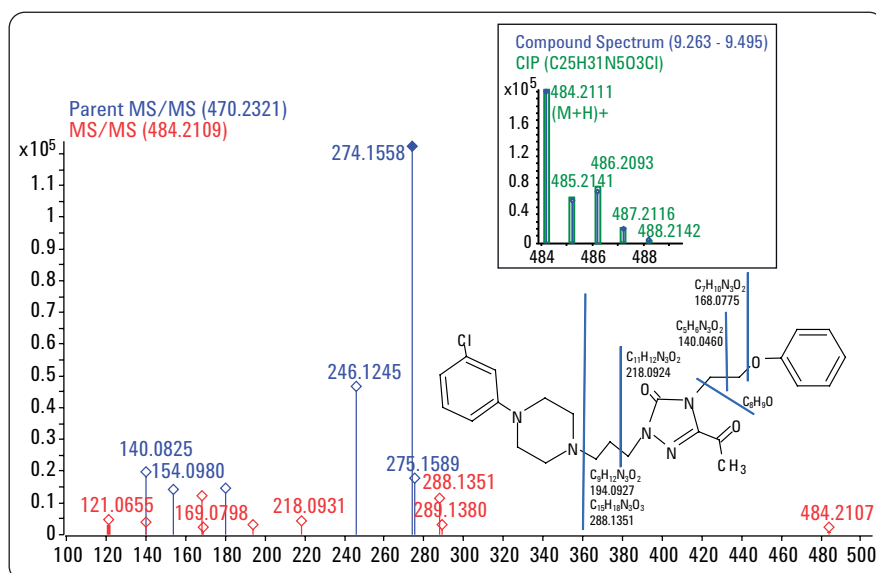


Figure 10
Mass spectrum, isotopic analysis and MS/MS spectrum with fragment assignment of the efazodone mono-oxo metabolite 3.

| Formula | Calc. Mass | Mass | Δ Mass [mDa] | Δ Mass [ppm] | DBE | m/z | Species | Ion Formula | Score |
|--------------|------------|-----------|---------------------|---------------------|-----|-----------|--------------------|--------------|-------|
| C25H30N5O3Cl | 483.20371 | 483.20384 | -0.125 | -0.26 | 13 | 484.21112 | (M+H) ⁺ | C25H31N5O3Cl | 100 |

| Isotopic pattern | | | | |
|------------------|-----------|---------------------|--------|--------------|
| m/z | Calc. m/z | Δ Mass [ppm] | Abund% | Calc. Abund% |
| 484.2111 | 484.2110 | -0.26 | 100.00 | 100.00 |
| 485.2139 | 485.2140 | 0.22 | 26.66 | 29.34 |
| 486.2092 | 486.2092 | 0.01 | 32.31 | 36.77 |
| 487.2117 | 487.2115 | -0.29 | 7.83 | 9.95 |
| 488.2169 | 488.2141 | -5.73 | 1.4 | 1.58 |

Figure 11
Calculated molecular formula and mass accuracies, and isotopic analysis of the Nefazodone mono-oxo metabolite 3.

| m/z | Mass | Formula | Calc. Mass | Δ Mass [mDa] | Δ Mass [ppm] | Loss Mass | Loss Formula | Neutral Loss | FPM m/z | Shift m/z | Δ Shift [mDa] | Shift Formula |
|-----------|-----------|------------|------------|---------------------|---------------------|-----------|--------------|--------------|-----------|-----------|----------------------|---------------|
| 121.06550 | 120.05822 | C8H8O | 120.05751 | -0.70 | -5.86 | 363.14620 | C17H22N5O2Cl | 363.14537 | | | | |
| 140.04608 | 139.03880 | C5H5N3O2 | 139.03818 | -0.63 | -4.51 | 344.16554 | C20H25N2OCl | 344.16479 | | | | |
| 168.07747 | 167.07019 | C7H9N3O2 | 167.06948 | -0.71 | -4.27 | 316.13424 | C18H21N2OCl | 316.13340 | 154.09795 | 13.97926 | 0.25 | -H2+O |
| 194.09267 | 193.08539 | C9H11N3O2 | 193.08513 | -0.27 | -1.38 | 290.11859 | C16H19N2OCl | 290.11820 | 180.11347 | 13.97926 | 0.07 | -H2+O |
| 218.09308 | 217.08580 | C11H11N3O2 | 217.08513 | -0.67 | -3.11 | 266.11859 | C14H19N2OCl | 266.11779 | | | | |
| 288.13505 | 287.12777 | C15H17N3O3 | 287.12699 | -0.78 | -2.72 | 196.07673 | C10H13N2Cl | 196.07582 | 274.15579 | 13.97926 | 0.00 | -H2+O |
| 484.21073 | | | | | | | | | 470.23212 | 13.97926 | 0.65 | -H2+O |

Figure 12
Calculated MS/MS fragment formulas and neutral loss formulas for the Nefazodone mono-oxo metabolite 3 fragmentation.

In the metabolite that elutes at a retention time around 5.5 minutes, both hydroxylations have taken place to produce the dihydroxy metabolite 4 (Figure 13). The fragment pattern matching (FPM) shows the shift of the parent drug mass by the mass of two oxygen atoms from m/z 470.2321 to m/z 502.2211, with a relative mass error of 0.88 ppm for the calculated molecular formula $C_{25}H_{32}N_5O_4Cl$ (Figure 14). One of the oxidations shifts the parent drug MS/MS fragment ion from m/z 274.1557 to m/z 290.1504, with the formula $C_{15}H_{19}N_3O_3$, which indicates the same structural modification as for the monohydroxy metabolite 2 (Figure 15 and Figure 9 on page 5). The corresponding loss formula $C_{10}H_{13}N_2OCl$ indicates the site of the second hydroxylation reaction in the molecule comparable to metabolite 1 (Figure 15 and Figure 6 on page 4). This is additionally supported by another MS/MS fragment ion at m/z 262.1188, which is

also shifted by the mass of an oxygen atom from the parent drug's MS/MS fragment at m/z 246.1244 (Figure 15 and Figure 3 on page 3). This fragment

has the formula $C_{13}H_{15}N_3O_3$ compared to $C_{13}H_{15}N_3O_2$ for the parent drug.

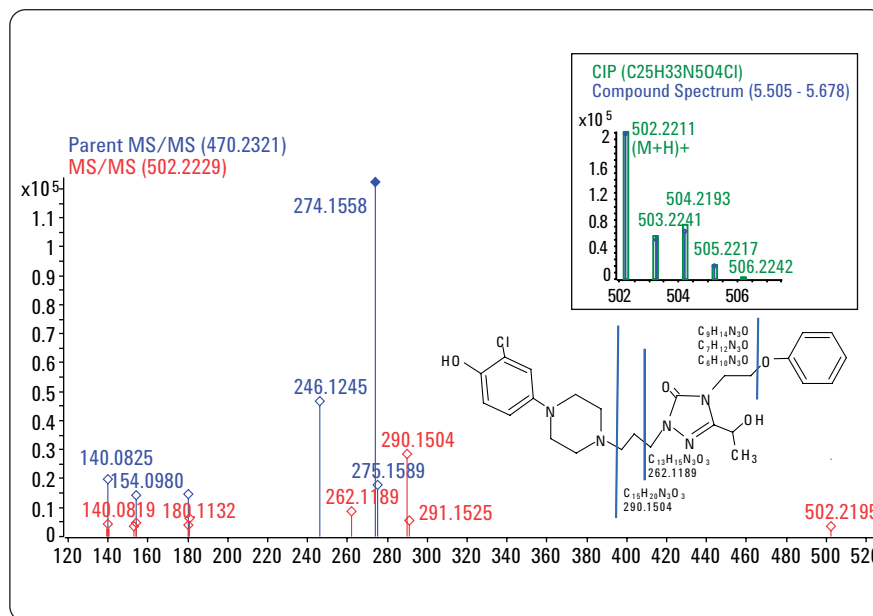


Figure 13
Mass spectrum, isotopic analysis and MS/MS spectrum with fragment assignment of the Nefazodone dihydroxy metabolite 4.

| Formula | Calc. Mass | Mass | Δ Mass [mDa] | Δ Mass [ppm] | DBE | m/z | Species | Ion Formula | Score |
|--------------|------------|-----------|---------------------|---------------------|-----|-----------|--------------------|--------------|-------|
| C25H32N5O4Cl | 501.21428 | 501.21383 | 0.44 | 0.88 | 12 | 502.22111 | (M+H) ⁺ | C25H33N5O4Cl | 100 |

| Isotopic pattern | | | | |
|------------------|-----------|---------------------|---------|--------------|
| m/z | Calc. m/z | Δ Mass [ppm] | Abund % | Calc. Abund% |
| 502.2211 | 502.2216 | 0.89 | 100.00 | 100.00 |
| 503.2240 | 503.2246 | 1.08 | 25.72 | 29.40 |
| 504.2194 | 504.2198 | 0.77 | 31.64 | 36.99 |
| 505.2222 | 505.2221 | -0.16 | 7.83 | 10.03 |

Figure 14
Calculated molecular formula and mass accuracies, and isotopic analysis of the Nefazodone dihydroxy metabolite 4.

| m/z | Mass | Formula | Calc. Mass | Δ Mass [mDa] | Δ Mass [ppm] | Loss Mass | Loss Formula | Neutral Loss | FPM m/z | Shift m/z | Δ Shift [mDa] | Shift Formula |
|-----------|-----------|------------|------------|---------------------|---------------------|-----------|--------------|--------------|-----------|-----------|----------------------|---------------|
| 140.08188 | 139.07461 | C6H9N3O | 139.07456 | -0.04 | -0.31 | 362.13972 | C19H23N2O3Cl | 362.14100 | | | | |
| 154.09701 | 153.08973 | C7H11N3O | 153.09021 | 0.48 | 3.15 | 348.12407 | C18H21N2O3Cl | 348.12588 | | | | |
| 180.11324 | 179.10596 | C9H13N3O | 179.10586 | -0.10 | -0.54 | 322.10842 | C16H19N2O3Cl | 322.10965 | | | | |
| 262.11887 | 261.11160 | C13H15N3O3 | 261.11134 | -0.26 | -0.98 | 240.10294 | C12H17N2OCl | 240.10401 | 246.12446 | 15.99 | 0.50 | +O |
| 290.15040 | 289.14312 | C15H19N3O3 | 289.14264 | -0.48 | -1.66 | 212.07164 | C10H13N2OCl | 212.07249 | 274.15579 | 15.99 | 0.31 | +O |
| 502.21955 | | | | | | | | | 470.23212 | 31.99 | 2.41 | +O2 |

Figure 15
Calculated MS/MS fragment formulas and neutral loss formulas for the Nefazodone dihydroxy metabolite 4 fragmentation.

As a following metabolism step, the dihydroxy metabolite 4 undergoes an additional oxidation to form the hydroxy-oxo metabolite 5 of nefazodone. This metabolite, with the mass at m/z 500.2058, has the formula $C_{25}H_{31}N_5O_4Cl$, calculated with a relative mass accuracy of 0.13 ppm (Figures 16 and 17).

The calculated isotope pattern (CIP) calculated for the metabolite formula $C_{25}H_{31}N_5O_4Cl$ shows an excellent fit to the measured isotope pattern (see insert in Figure 16). The fragment pattern matching (FPM) shows a similar fragmentation pattern to metabolite 3 with the exception that the original fragment at m/z 274.1557 with the formula $C_{15}H_{19}N_3O_2$ is not shifted by the mass of the oxygen only but instead by the combination of the hydroxylation reaction followed by oxidation to

m/z 288.1344, with the formula $C_{15}H_{17}N_3O_3$, calculated with -0.70 ppm relative mass accuracy (Figure 18).

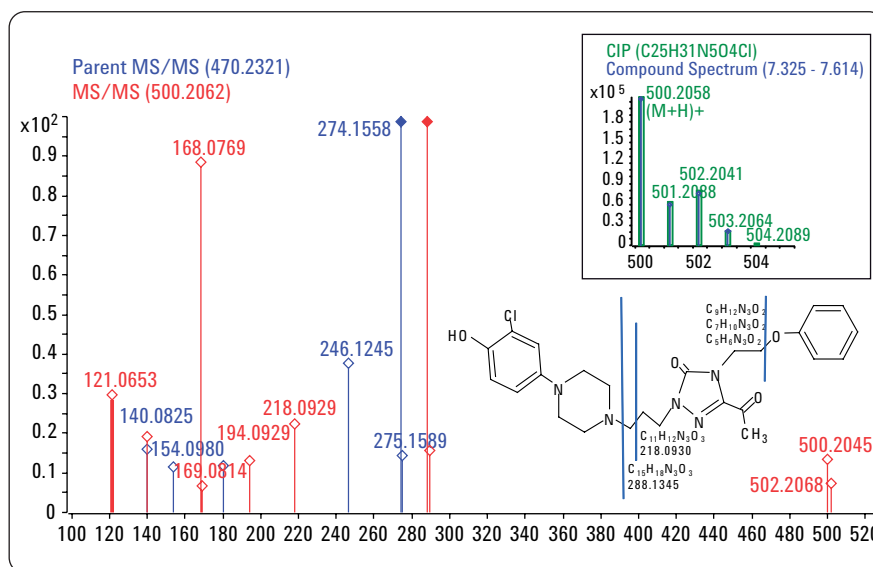


Figure 16
Mass spectrum, isotopic analysis and MS/MS spectrum with fragment assignment of the nefazodone hydroxy oxo metabolite 5.

| Formula | Calc. Mass | Mass | Δ Mass [mDa] | Δ Mass [ppm] | DBE | m/z | Species | Ion Formula | Score |
|--------------|------------|-----------|---------------------|---------------------|-----|-----------|--------------------|--------------|-------|
| C25H30N5O4Cl | 499.19863 | 499.19856 | 0.06 | 0.13 | 13 | 500.20584 | (M+H) ⁺ | C25H31N5O4Cl | 100 |

| Isotopic pattern | | | | |
|------------------|-----------|---------------------|---------|---------------|
| m/z | Calc. m/z | Δ Mass [ppm] | Abund % | Calc. Abund % |
| 502.2211 | 502.2216 | 0.89 | 100.00 | 100.00 |
| 503.2240 | 503.2246 | 1.08 | 25.72 | 29.40 |
| 504.2194 | 504.2198 | 0.77 | 31.64 | 36.99 |
| 505.2222 | 505.2221 | -0.16 | 7.83 | 10.03 |

Figure 17
Calculated molecular formula and mass accuracies, and isotopic analysis of the Nefazodone hydroxy oxo metabolite 5.

| m/z | Mass | Formula | Calc. Mass | Δ Mass [mDa] | Δ Mass [ppm] | Loss Mass | Loss Formula | Neutral Loss | FPM m/z | Shift m/z | Δ Shift [mDa] | Shift Formula |
|-----------|-----------|------------|------------|---------------------|---------------------|-----------|--------------|--------------|-----------|-----------|----------------------|---------------|
| 121.06526 | 120.05798 | C8H8O | 120.05751 | -0.46 | -3.87 | 379.14112 | C17H22N5O3Cl | 379.14091 | | | | |
| 140.04633 | 139.03906 | C5H5N3O2 | 139.03818 | -0.88 | -6.33 | 360.16046 | C20H25N2O2Cl | 360.15983 | | | | |
| 168.07685 | 167.06958 | C7H9N3O2 | 167.06948 | -0.10 | -0.60 | 332.12916 | C18H21N2O2Cl | 332.12931 | 154.09795 | 13.97926 | 0.36 | -H2+O |
| 194.09291 | 193.08564 | C9H11N3O2 | 193.08513 | -0.51 | -2.65 | 306.11351 | C16H19N2O2Cl | 306.11325 | 180.11347 | 13.97926 | 0.18 | -H2+O |
| 218.09295 | 217.08567 | C11H11N3O2 | 217.08513 | -0.55 | -2.52 | 282.11351 | C14H19N2O2Cl | 282.11321 | | | | |
| 288.13447 | 287.12719 | C15H17N3O3 | 287.12699 | -0.20 | -0.70 | 212.07164 | C10H13N2OCl | 212.07169 | 274.15579 | 13.97926 | 0.59 | -H2+O |
| 500.20445 | | | | | | | | | 470.23212 | 29.97418 | 1.85 | -H2+O2 |

Figure 18
Calculated MS/MS fragment formulas and neutral loss formulas for the Nefazodone hydroxy oxo metabolite 5 fragmentation.

The final expected metabolite 6 that was identified with assignment of a biotransformation reaction is produced by a dechlorination reaction. Here, the measured isotope pattern is changed dramatically by the dechlorination (blue lines, insert in Figure 19). But there is a clear accordance with the calculated isotope pattern (CIP) for this biotransformation (green boxes, insert in Figure 19). The formula $C_{25}H_{33}N_5O_3$ for this metabolite was calculated for the mass at m/z 452.2617 with 0.98 ppm relative mass accuracy (Figure 20). The fragment pattern matching (FPM) shows clear identity of the metabolite's fragmentation pattern compared to the parent's fragmentation pattern. The shift +O+H-Cl is assigned only to the parent (Figure 19). This means the dechlorination takes place in the part of the molecule that is lost as a neutral loss during MS/MS fragmentation. The difference formula of the neutral loss

from the fragment at m/z 274.1554 and the molecular ion at m/z 452.2651 is $C_{10}H_{14}N_2O$, which, compared to the parent drug (Figure 3 on page 5), con-

tains no chlorine but instead contains an additional oxygen and hydrogen atom (Figure 21).

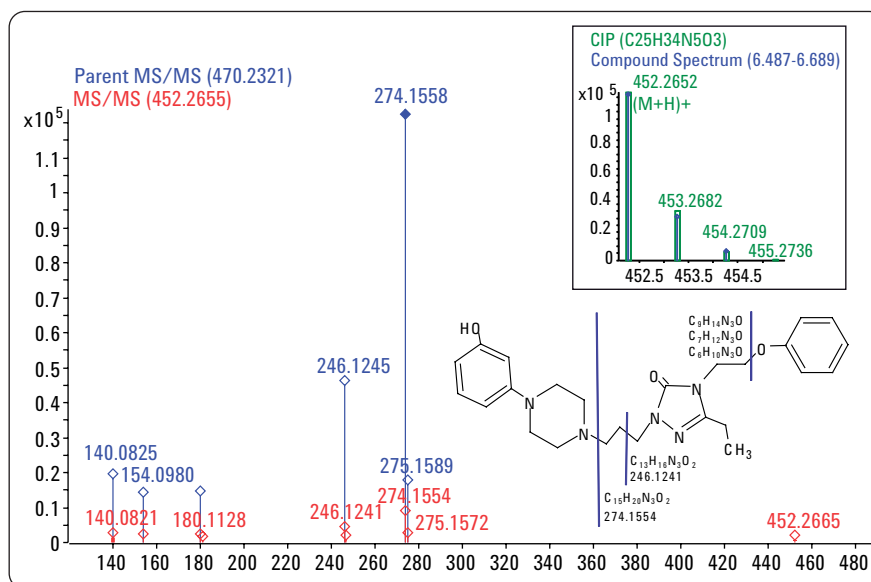


Figure 19
Mass spectrum, isotopic analysis and MS/MS spectrum with fragment assignment of the Nefazodone oxidative dechlorinated metabolite 6.

| Formula | Calc. Mass | Mass | Δ Mass [mDa] | Δ Mass [ppm] | DBE | m/z | Species | Ion Formula | Score |
|------------|------------|-----------|---------------------|---------------------|-----|-----------|--------------------|-------------|-------|
| C25H33N5O3 | 451.25833 | 451.25789 | 0.44 | 0.98 | 12 | 452.26517 | (M+H) ⁺ | C25H34N5O3 | 100 |

| Isotopic pattern | | | | |
|------------------|-----------|---------------------|---------|---------------|
| m/z | Calc. m/z | Δ Mass [ppm] | Abund % | Calc. Abund % |
| 452.2652 | 452.2656 | 0.98 | 100.00 | 100.00 |
| 453.2682 | 453.2686 | 0.93 | 24.82 | 29.37 |
| 454.2694 | 454.2714 | 4.39 | 4.16 | 4.78 |

Figure 20
Calculated molecular formula and mass accuracies, and isotopic analysis of the Nefazodone oxidative dechlorinated metabolite 6.

| m/z | Mass | Formula | Calc. Mass | Δ Mass [mDa] | Δ Mass [ppm] | Loss Mass | Loss Formula | Neutral Loss | FPM m/z | Shift m/z | Δ Shift [mDa] | Shift Formula |
|-----------|-----------|------------|------------|---------------------|---------------------|-----------|--------------|--------------|-----------|-----------|----------------------|---------------|
| 140.08205 | 139.07478 | C6H9N3O | 139.07456 | -0.22 | -1.55 | 312.18378 | C19H24N2O2 | 312.18348 | 140.08245 | 0 | 0.40 | |
| 154.09777 | 153.09049 | C7H11N3O | 153.09021 | -0.28 | -1.84 | 298.16813 | C18H22N2O2 | 298.16776 | 154.09795 | 0 | 0.18 | |
| 180.11275 | 179.10548 | C9H13N3O | 179.10586 | 0.39 | 2.15 | 272.15248 | C16H20N2O2 | 272.15278 | 180.11347 | 0 | 0.72 | |
| 246.12411 | 245.11684 | C13H15N3O2 | 245.11643 | -0.41 | -1.68 | 206.14191 | C12H18N2O | 206.14142 | 246.12446 | 0 | 0.35 | |
| 274.15542 | 273.14815 | C15H19N3O2 | 273.14773 | -0.42 | -1.54 | 178.11061 | C10H14N2O | 178.11011 | 274.15579 | 0 | 0.36 | |
| 452.26651 | | | | | | | | -0.00097 | 470.23212 | -17.9661 | 0.50 | +O+H-Cl |

Figure 21
Calculated MS/MS fragment formulas and neutral loss formulas for the Nefazodone oxidative dechlorinated metabolite 6 fragmentation.

Expected Metabolic Pathways of Nefazodone

The pharmaceutical drug nefazodone undergoes extensive metabolism in the human body and yields not only the typical expected metabolites but also several unexpected metabolites initiated by a cleavage of the original drug molecule.

The metabolites that were identified in this work as previously discussed are displayed in Figure 22 as simplified proposed metabolic pathways for the expected metabolites.

As outlined in Figure 22, there are a few metabolic reactions that do not change the skeleton of the molecule, and lead to the expected metabolites by simple modification. The monohydroxylation of nefazodone can take place either at the chlorinated phenyl ring, leading to the monohydroxyl metabolite 1, or at the ethyl group that is connected to the central triazole-3-one ring, leading to monohydroxyl metabolite 2. A further metabolic oxidation reaction, which oxidizes the hydroxyl group present in 2 into a keto group, leads to the oxo metabolite 3. The metabolic hydroxylation reaction can take place in both parts of the

molecule, leading to the dihydroxy metabolite 4. After dihydroxylation, the following metabolic oxidation leads to the oxy-hydroxyl metabolite 5. A metabolic oxidative dechlorination reaction leads to the loss of the chlorine atom from nefazodone and to the substitution of the chlorine by a hydroxyl group, yielding the dechlorinated metabolite 6. and accurate-mass-based formulae calculation. In the third step, the elucidated sample was compared with a new sample obtained from another ginseng species, and new compounds and those that increased in amount were identified.

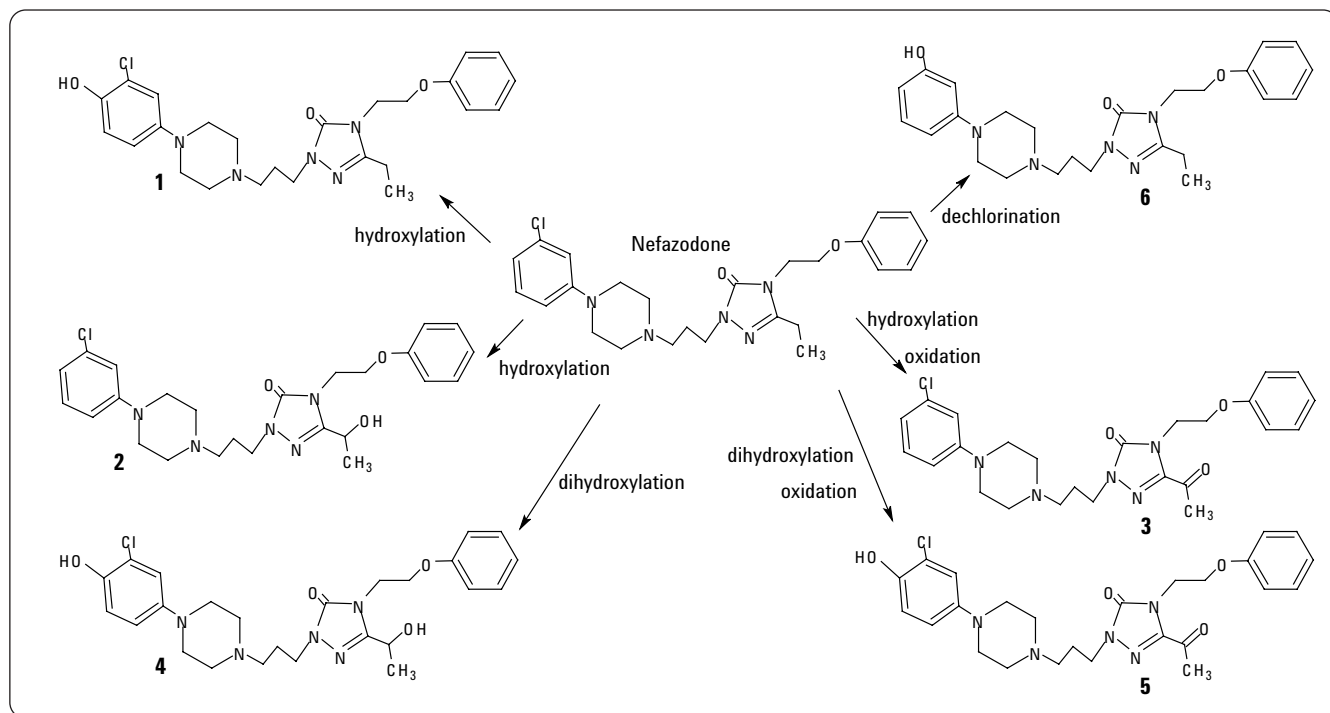


Figure 22
Proposed metabolic pathways for the expected metabolites of Nefazodone.

Conclusion

This work demonstrates the interpretation of the results produced by the MassHunter Metabolite Identification (MetID) software for the identification of metabolites created by expected biotransformations. The assignment of metabolite structures by interpretation of information created from QTOF mass spectrometry data by various algorithms like isotope pattern matching, MS/MS fragment pattern matching and formula calculation based on accurate mass measurement for MS and MS/MS is demonstrated. This work is an example of the gain in productivity that can be achieved by using the MetID software for the interpretation of QTOF data from metabolite identification experiments.

References

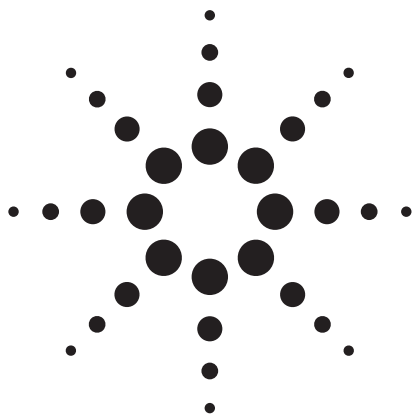
1. Amit S. Kalgutkar, Mary E. Lame, John R. Soglia, Scott M. Peterman, Nicholas Duczak, Jr., *J. Am. Soc. Mass Spectrom.*, 17, 363-375, **2006**.
2. Edgar Naegele, Agilent Application Note "An interwoven, multi-algorithm approach for computer-assisted identification of drug metabolites", *Publication number 5989-7375EN*, **2007**.
3. Edgar Naegele, "Computer assisted identification of metabolites from pharmaceutical drugs – Part II: Identification of non-expected metabolites of Nefazodone" *Publication number 5990-3607EN*, **2009**.

www.agilent.com/chem/metid

© Agilent Technologies, Inc., 2009
Published March 1, 2009
Publication Number 5990-3606EN



Agilent Technologies

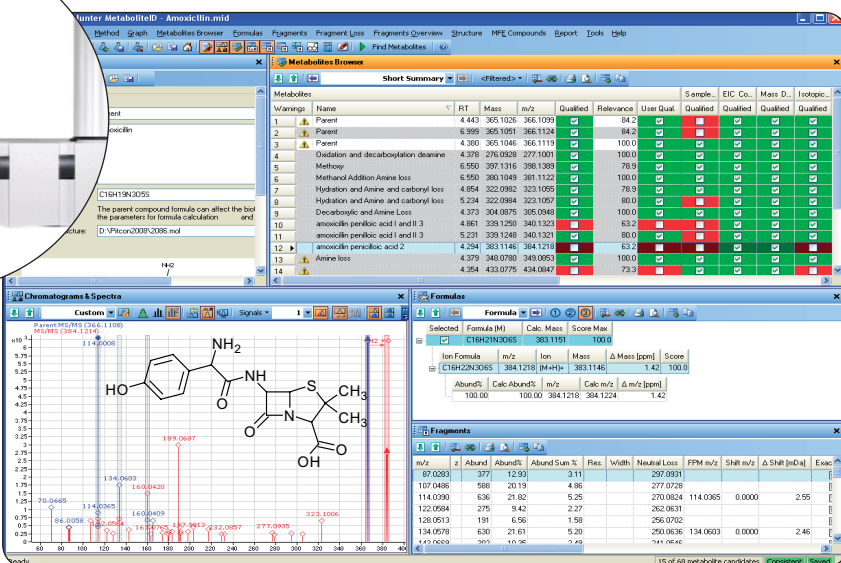
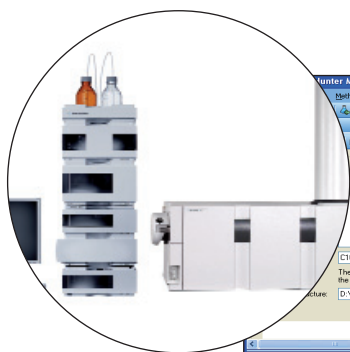


Detection and identification of impurities in pharmaceutical drugs

Computer-assisted extraction, profiling and analysis of Q-TOF data for determination of impurities using Agilent MassHunter software

Application Note

David A. Weil
Zoltan Timar
Michael Zumwalt
Edgar Naegele



Abstract

This Application Note describes:

- Extraction of high resolution, accurate mass Q-TOF data from chemical background noise using the molecular feature extractor of the Agilent MassHunter software
- Differential analysis to identify impurities in pharmaceutical drugs using the Mass Profiler algorithm of the Agilent MassHunter Profiler software.
- Generation of molecular formulas for MS and MS/MS using the molecular formula generator of the Agilent MassHunter software
- Automated analysis of a degraded pharmaceutical drug and comparison with a non-degraded standard using the Agilent MassHunterMetID software

Agilent Equipment

- 1200 Series Rapid Resolution LC
- 6520 Accurate-Mass Q-TOF
- MassHunter software

Application area

Identification of degradation products in pharmaceutical drugs during drug development and quality control



Agilent Technologies

Introduction

In the production of pharmaceutical drugs, impurities can arise due to different means such as solvents, catalysts, synthesis building blocks or degradation. Besides these causes during the production process, impurities can arise in the final purified product by slow degradation during shelf storage in the sealed package under ambient temperature conditions. To identify potential degradation impurities, degradation studies with the pure substance are performed under various conditions¹. With a basic knowledge of possible degradation products, studies with the final drug formulation under long time storage conditions are carried out. The LC/MS data obtained in such studies is often analyzed manually, which is a very time consuming process.

Modern software tools are available to improve data analysis. The first challenge is to extract the compounds of interest from the complex background that results from the matrix of the final drug formulation. This data extraction can be done with using the molecular feature extractor (MFE)² of the Agilent MassHunter software (figure 1). In the generation of the molecular features, which are the entity of molecular ions, isotopes and adducts at a certain retention time, chemical background is removed from the total ion chromatogram (TIC), and features are grouped and displayed in the processed TIC. Finally, the molecular formulas are generated for each feature, including information from isotopes and adducts generated by the molecular formula generation (MFG) algorithm of the Agilent MassHunter software. In the next step of the analysis of

the differences between two groups, the impure group and the pure (control) group are analyzed (figure 2). For this analysis the Mass Profiler algorithm³ of the Agilent MassHunter software compares a set of data of both groups and displays a plot that shows the unique features of each group. This makes it possible to find the degradation products that are unique to the impure group. The entire analysis can be performed by specialized data analysis software, comprising MFE, MFG, Mass Profiler and several other algorithms for data comparison and structure elucidation from Q-TOF MS and MS/MS information.

This Application Note describes the data analysis for detection and determination of low level impurities in final pharmaceutical drug formulations.

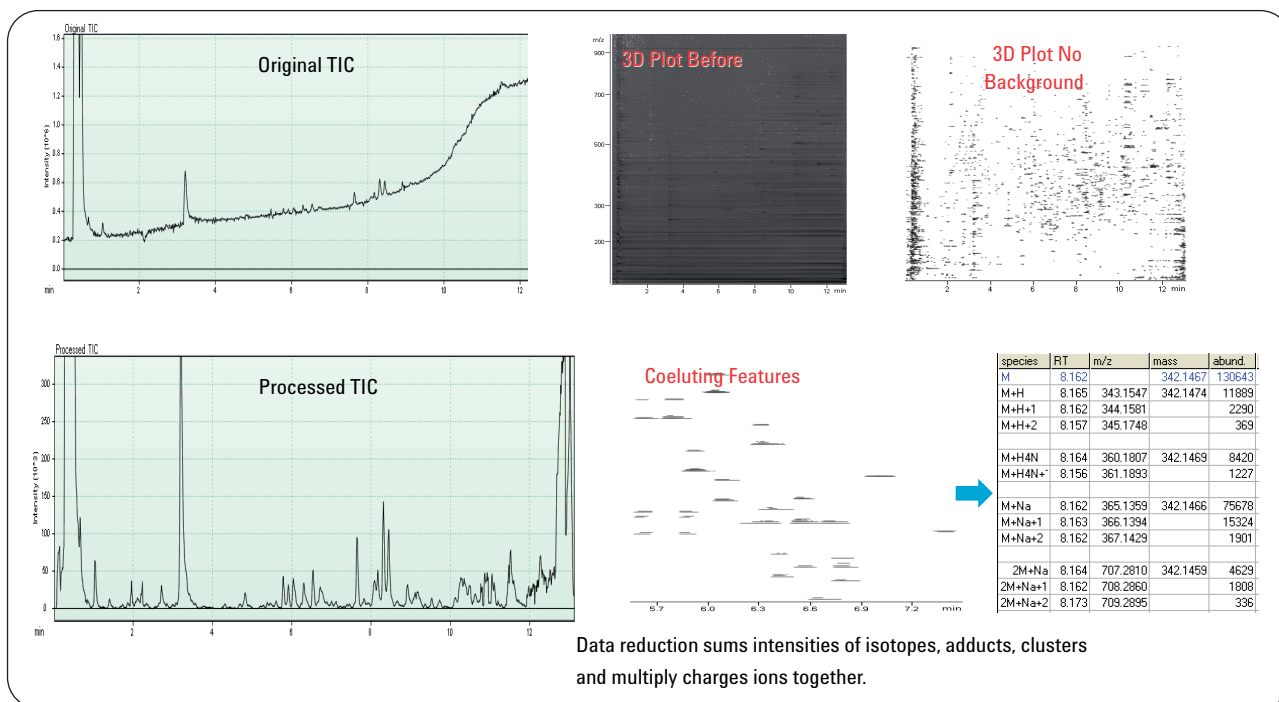


Figure 1
Automated data reduction using molecular feature extraction (MFE) of the Agilent MassHunter software.

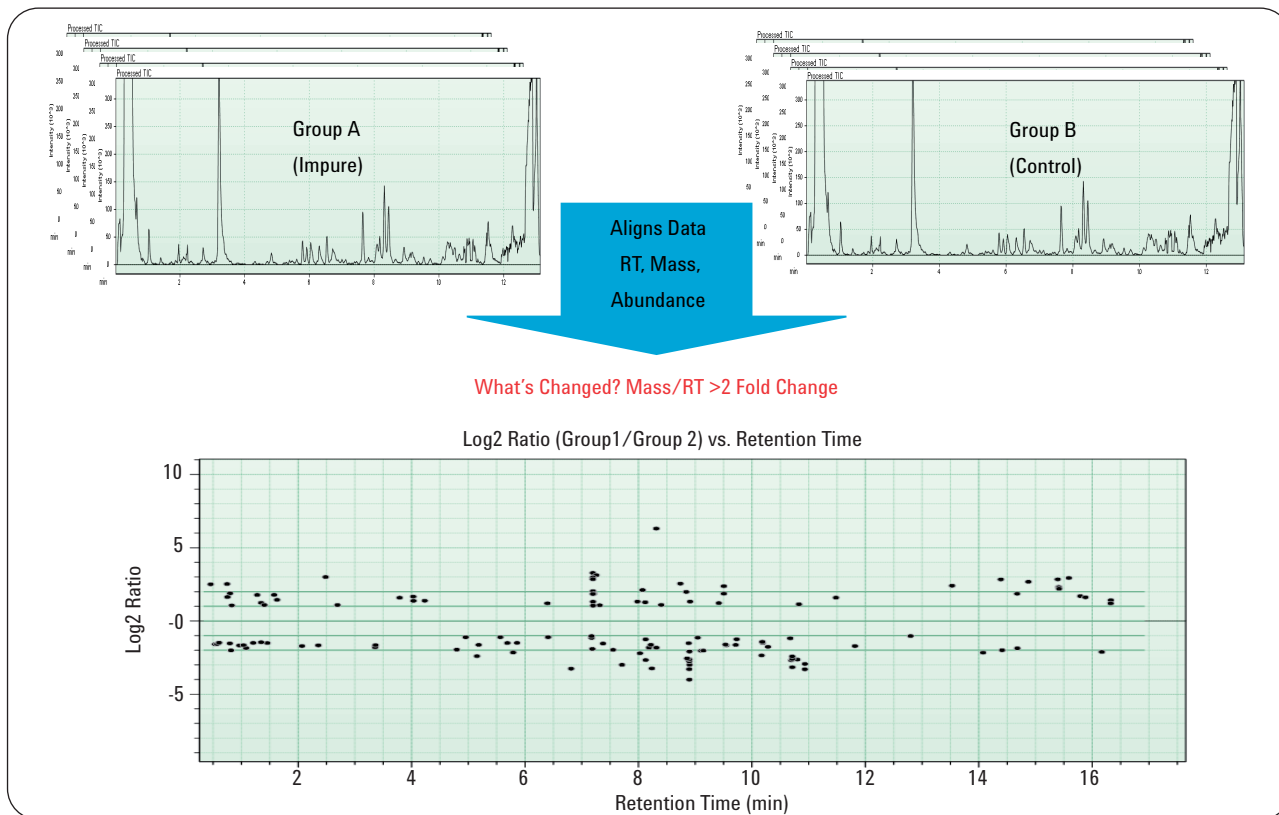


Figure 2
Impurity analysis using the Mass Profiler of the Agilent MassHunter software.

Experimental

Equipment

- Agilent 1200 Series Rapid Resolution LC system with binary pump SL and degasser, high performance autosampler SL with thermostat, and thermostated column compartment SL
- Agilent 6520 Accurate-Mass Q-TOF
- Agilent MassHunter data acquisition software, qualitative software, MFE software, Mass Profiler software and MetID software
- ZORBAX Eclipse Plus C18 column, 2.1 x 100 mm, 1.8 μ m

Sample preparation

Tablets of the antibiotic drug amoxicillin (new and stored for 6 months at ambient temperature) were dissolved in 40 mL metha-

| Use | Name | Phase | Formula | Mass | Req | Result Formula | Result Mass |
|-------------------------------------|---------------------------------------|-------|--------------|----------|-----|----------------|-------------|
| <input checked="" type="checkbox"/> | Parent | I | | 0.0000 | | C16H19N3O5S | 365.1045 |
| <input checked="" type="checkbox"/> | diketopiperazine | I | | 0.0000 | | C16H19N3O5S | 365.1045 |
| <input checked="" type="checkbox"/> | amoxicillin penicilic acid 2 | I | +H2 +O | 18.0106 | | C16H21N3O6S | 383.1151 |
| <input checked="" type="checkbox"/> | amoxicillin penicilic acid 1 and 3 | I | +H2 C=O | -25.9793 | | C15H21N3O4S | 333.1253 |
| <input checked="" type="checkbox"/> | 4-hydroxyphenylglycyl amoxicillin 4 | I | +C8H17+O2+N | 148.0477 | | C24H32N4O7S | 514.1522 |
| <input checked="" type="checkbox"/> | Methoxy | I | +C+H4+O | 32.0262 | | C17H23N3O6S | 397.1308 |
| <input checked="" type="checkbox"/> | Dimethoxy-Addition | I | +C2+O2+H4 | 60.0211 | | C18H25N3O7S | 425.1257 |
| <input checked="" type="checkbox"/> | Amine loss | I | NH3 | -17.0265 | | C16H18N2O5S | 348.0780 |
| <input checked="" type="checkbox"/> | Decarboxylic and Amine Loss | I | NH3 C=O | -61.0164 | | C15H18N3O4S | 304.0882 |
| <input checked="" type="checkbox"/> | Daidston | I | +O | 15.9949 | | C16H19N3O6S | 381.0995 |
| <input checked="" type="checkbox"/> | Oxidation | I | +O2 | 31.9898 | | C16H19N3O7S | 397.0944 |
| <input checked="" type="checkbox"/> | Hydration decarboxyl | I | +H2+O C=O | 8.9843 | | C15H21N3O6S | 355.1202 |
| <input checked="" type="checkbox"/> | Hydration and Amine and carbonyl loss | I | NH3 C=O | 43.0058 | | C15H18N2O4S | 322.0987 |
| <input checked="" type="checkbox"/> | Methoxy for Hydroxyl | I | +C+H2 | 14.0157 | | C17H21N3O5S | 379.1202 |
| <input checked="" type="checkbox"/> | Acetic Acid Addition | I | +C+H3+O2 | 47.0133 | | C17H23N3O7S | 412.1178 |
| <input checked="" type="checkbox"/> | Methanol Addition Amine loss | I | +C+H3+O NH2 | 14.9997 | | C17H23N2O6S | 380.1042 |
| <input checked="" type="checkbox"/> | Daidston and decarboxylation/daimeine | I | +O C2 O4 NH3 | -89.0113 | | C14H18N2O5S | 276.0932 |

Figure 3
Method input for MetID software.

nol/water (1/1 v/v) with 0.1 % formic acid, mixed for 20 minutes, centrifuged for 5 minutes at 14,000 rpm, and diluted 1:100 and 1:1000 with water.

High resolution LC/MS method

Solvent A: Water, 5 mM NH₄Ac
Solvent B: Methanol

Flow rate: 0.4 mL/min
Gradient: 0 min, 5 %B;
13 min, 95 %B
Stop time: 13 min
Post time: 10 min
Inj. volume: 1-10 μ L, needle wash,
samples cooled to 4 °C
Column temp.: 50 °C.

Q-TOF MS and MSMS method

Source: ESI in positive mode with dual spray for reference mass solution

Dry gas: 10.0 L/min

Dry Temp.: 250 °C

Nebulizer: 45 psi

Mass range: 100-1000

Fragmentor: 165 V

Skimmer: 60 V

Capillary: 4000 V

Collision energy: 30 V

Data-dependent MS/MS:

2 compounds, 3 MS/MS spectra, exclusion for 0.25 minutes. For data acquisition the high resolution and the enhanced dynamic range modes were used.

Data analysis with MassHunter MetID software

The first step in the analysis comprised a comparison between the data from the degradation products (sample) and the data from the pure parent drug (control).

All detectable mass signals were extracted from the MS level data using the molecular feature extraction (MFE) algorithm. Adduct masses of related compounds were grouped together into discrete molecular features and chemical noise was removed. The compound lists of the degraded sample and the control were then compared. All new compounds or those which increased in amount in the degraded sample were considered to be potential degradation products and subjected to further analysis by different user-specified algorithms. The molecular mass and structure information as well as the possible degradation reactions were introduced for the analysis (figure 3). The algorithms were able to identify and qualify

new degradants or simply qualify degradation compounds found by another algorithm. The results of all compound identification algorithms were weighted and combined to a final identification relevance score. Degradation products were qualified when their final score was above a defined relevance threshold. The results from all algorithms were collated in a results table, which could be inspected at-a-glance. The workflow in the MetID software is summarized in table 1.

| | | |
|---|----------------------------|------------------------------------|
| 1 | Parent Compound | MW, Formula and Structure |
| 2 | Transformations | List Proposed Degradation Products |
| 3 | Identification Criteria | Vary Importance of Tests |
| 4 | Find Compounds by MFE | Molecular Feature Extraction |
| 5 | Find Compounds by AutoMSMS | For MSMS data |
| 6 | Sample Comparison | Mass Profiler What is Different |
| 7 | Isotope Pattern Filtering | Best for Halogenated Species |
| 8 | Mass Defect Filtering | From Proposed Compounds |
| 9 | EIC Generation | Confirms Presence of Compounds |

Results and discussion

Following data analysis, the identified potential degradation products were then displayed in a table (figure 4). The displayed compounds were identified by various algorithms in the software, for example, the compounds were new in the degraded sample and were identified by the Mass Profiler algorithm. Other algorithms checked the fit with an isotopic pattern comparative to the

Table 1
Overview of workflow in the MetID software.

Figure 4
Proposed degradation products qualified by various algorithms.

| RT [min] | Compound name | Formula | Calculated mass | Measured mass | Mass accuracy [mDa] | Mass accuracy [ppm] |
|----------|---|---|-----------------|---------------|---------------------|---------------------|
| 3.90 | amoxicillin penicilloic acid 2 | C ₁₆ H ₂₂ N ₃ O ₆ S | 384.1224 | 384.1225 | -0.1 | -0.31 |
| 4.39 | amoxicillin 1 | C ₁₆ H ₂₀ N ₃ O ₅ S | 366.1118 | 366.1123 | -0.5 | -1.32 |
| 4.80 | amoxicillin penicilloic acid I and II 3 | C ₁₅ H ₂₂ N ₃ O ₄ S | 340.1325 | 340.1326 | -0.3 | -0.73 |
| 5.19 | amoxicillin penicilloic acid I and II 3 | C ₁₅ H ₂₂ N ₃ O ₄ S | 340.1325 | 340.1326 | -0.1 | -0.14 |
| 7.00 | diketopiperazine amoxicillin 4 | C ₁₆ H ₂₀ N ₃ O ₅ S | 366.11182 | 366.1118 | 0.02 | 0.05 |

Table 2
Measured accurate mass of amoxicillin degradation products and calculated formula (masses and accuracies are rounded).

pure parent drug and the fit in a mass defect window typical for the modifications by degradation of the parent drug. Finally, the reaction was assigned by comparison to the defined possible degradation reactions from the data analysis method.

The following known degradation products were identified in the degraded tablets:

Amoxicillin penicilloic acid (2)
at retention time
3.90 min and
 m/z 384.1225

Amoxicillin penilloic acids I and II (3)
at retention times
4.80 and 5.19 min and
isobaric masses
 m/z 340.1326 and
340.1328

Diketopiperazine amoxicillin (4)
at retention time
7.00 min and
 m/z 366.1118

The parent drug amoxicillin (1)

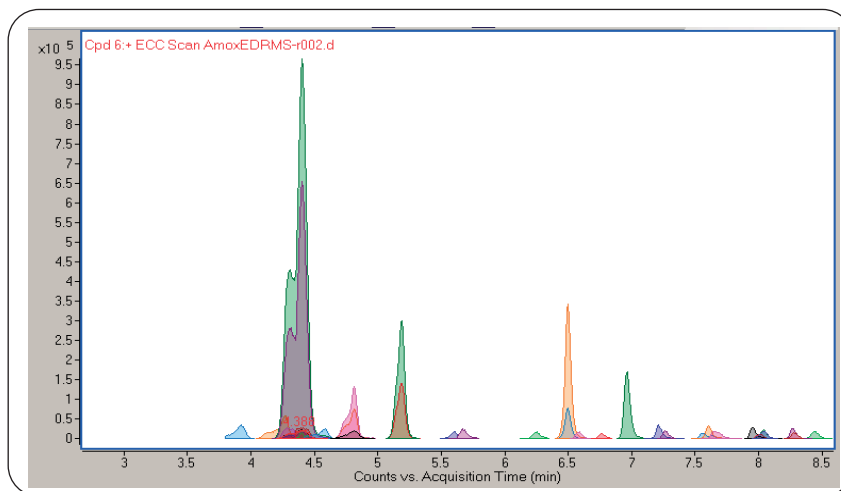


Figure 5
Extracted ion chromatograms of amoxicillin and degradation products.

was found at retention time 4.39 minutes and m/z 366.1123 (figure 5). For confirmation the software calculated the molecular formula from the measured accurate mass (table 2). The parent compound amoxicillin (1) and the impurity (4) occurred with isobaric mass. To elucidate the structure of

unknown or isomeric impure compounds, the MS/MS information was combined with the accurate mass measurements. For each MS/MS fragment a formula was calculated, which had to match with the calculated formula of the parent ion (figure 6).

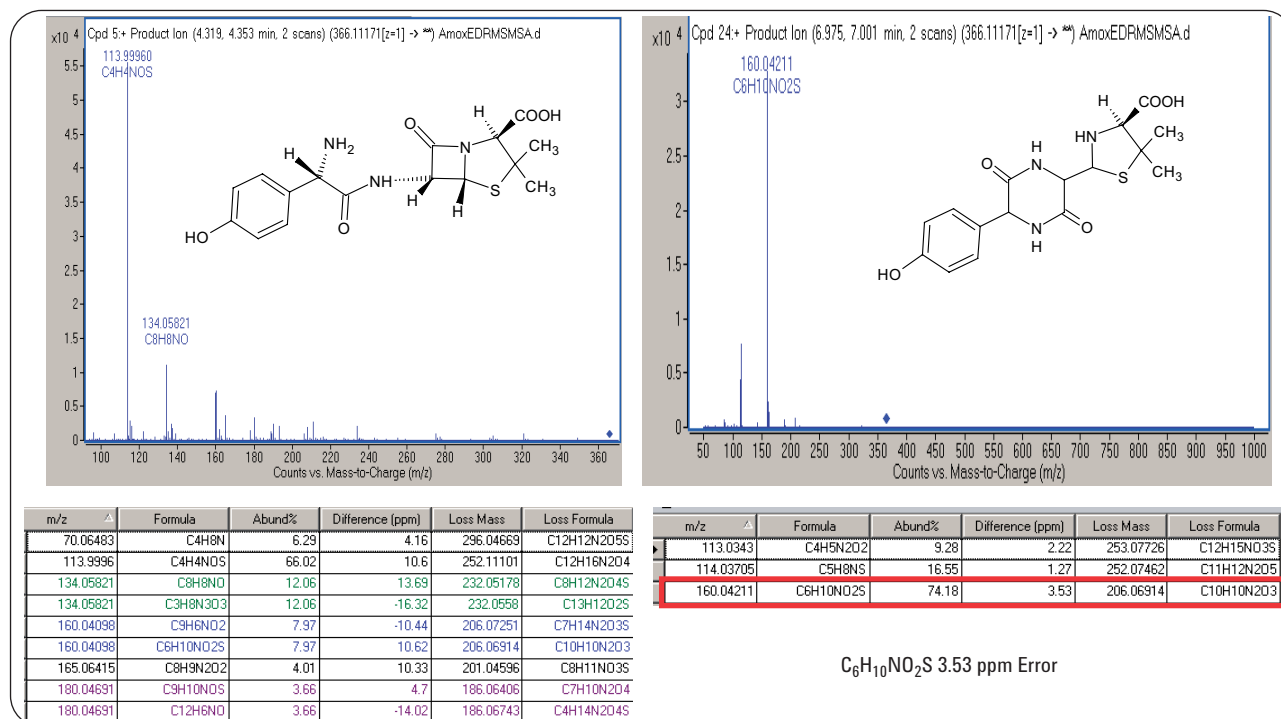


Figure 6
Structural information from MS/MS $C_{16}H_{19}N_3SO_5$.

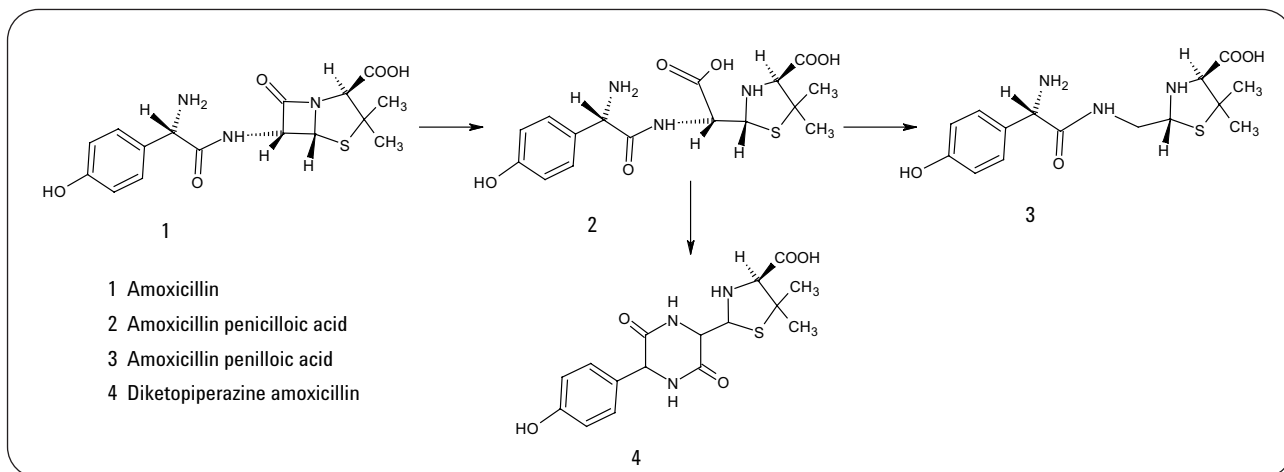


Figure 7
A possible degradation pathway.

For the isomeric compounds (1) and (4), the differences can be clearly seen from the MS/MS spectra and the calculated fragment formulas. The degradation product (4) had a main fragment at m/z 160.04211 with the formula $C_6H_{10}NO_2S$ and the remaining neutral loss had the formula $C_{10}H_{10}N_2O_3$, which fits with the parent formula $C_{16}H_{20}N_3O_5S$. The final degradation pathway for these impurities is shown in figure 7.

Conclusion

This Application Note demonstrated the use of the Agilent MassHunter MetID software for the identification of degradation products in the final formulation of the pharmaceutical drug amoxicillin. The degradation products were extracted from the Q-TOF data by the molecular feature extractor and newly emerging compounds were filtered out by the Mass Profiler algorithm. After isolation of the relevant compounds, they were classified by other algorithms such as mass defect filtering and isotopic pattern matching, and then assigned to possible degradation reactions. Finally, 17 degradation products were identified and an initial degradation pathway was assigned.

References

1.

E. Naegele, M. Moritz, *J. Am. Soc. Mass. Spectrom.*, 16, 1670–1676, **2005**.

2.

E. Naegele “Agilent MassHunter – Fast computer aided analysis of LC/ESI-TOF data from complex natural product extracts”, *Agilent Application Note, publication number 5989-5928EN*

3.

E. Naegele “Fast, computer-assisted detection of degradation products and impurities in pharmaceutical products”, *Agilent Application Note, publication number 5989-7869EN*

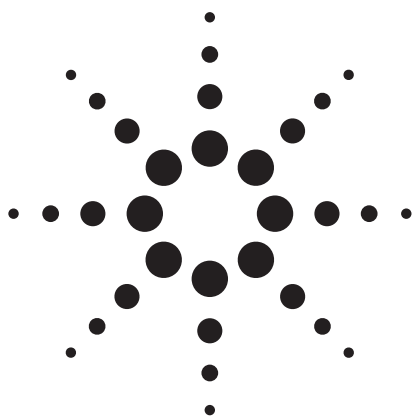
*David A. Weil, Zoltan Timar,
Michael Zumwalt, and Edgar
Naegele are Application Chemists
at Agilent Technologies,
Waldbronn, Germany.*

www.agilent.com/chem/qtof

© Agilent Technologies, Inc., 2008

Published July 1, 2008
Publication Number 5989-8529EN



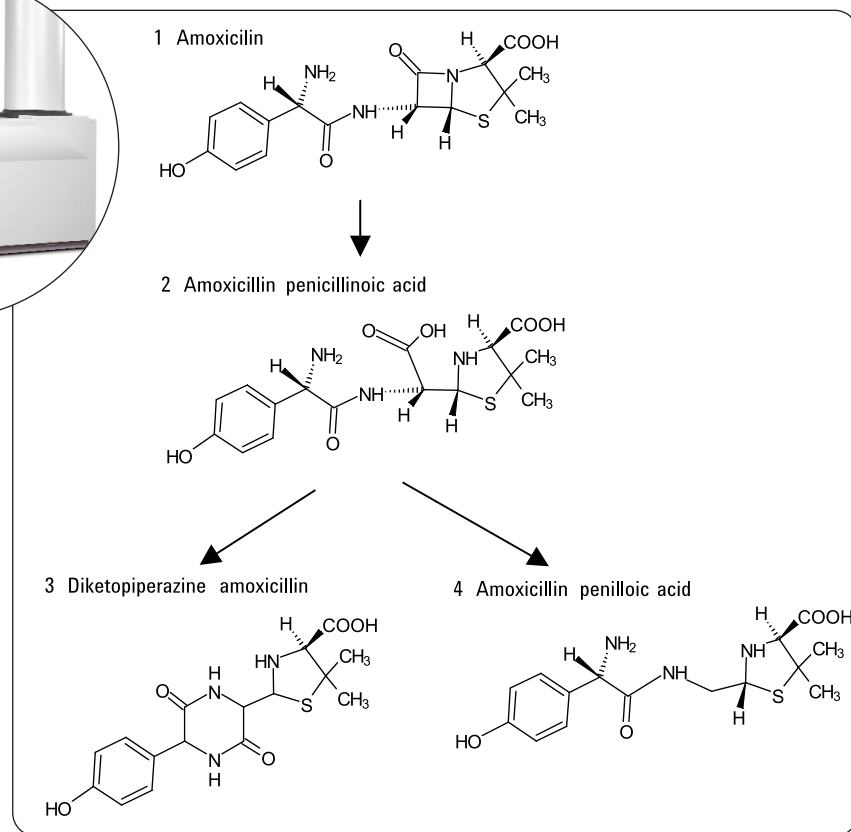


Fast, computer-assisted detection of degradation products and impurities in pharmaceutical products

Identification of minor components in drug substances using the Agilent 6210 accurate-mass, time-of-flight mass spectrometer and MassHunter Profiling software

Application Note

Edgar Naegele



Agilent Equipment

- 1200 Series RRLC system
- 6210 time-of-flight MS
- ZORBAX RRLC columns
- MassHunter Workstation software
- MassHunter Profiling software

Application Area

- Impurity and degradation product profiling in drug development

Abstract

This Application Note describes:

- Fast, high resolution separation with Agilent 1200 Series Rapid Resolution LC system
- Highly accurate mass measurement with Agilent 6210 time-of-flight MS
- Fast, computer-assisted identification of minor byproducts in pharmaceutical drugs using Agilent MassHunter Profiling software



Agilent Technologies

Introduction

In modern pharmaceutical production it is of crucial importance to identify all possible degradation products of a drug substance. These degradation products emerge under the various production and formulation conditions in very low concentration and need to be identified with highest confidence because of their potential toxicity to humans¹. The fast, computer-assisted identification of newly emerging compounds based on accurate mass measurement is the tool of choice for the identification of these degradation products and impurities. This Application Note describes the computer-assisted identification of degradation products and impurities of the antibiotic drug amoxicillin that emerge during the formulation process using accurate mass data from the Agilent time-of-flight (TOF) mass spectrometer and the Agilent MassHunter Profiling software.

Experimental

Equipment

- Agilent 1200 Series RRLC system comprising binary pump SL with degasser, high performance autosampler SL with thermostat, thermostatted column compartment and diode array detector SL.
- Agilent 6210 TOF MS, orthogonal acceleration time-of-flight mass spectrometer with dual sprayer interface for mass calibration for acquisition of molecular mass data with highest accuracy.
- MassHunter Workstation software revision A.02.00 for TOF instrument control, MassHunter Profiling software and Analyst software for data analysis.
- ZORBAX SB C18 column, 150 x 2.1 mm, 1.8 µm particle size.

RRLC method

The Agilent 1200 Series RRLC was operated under the following conditions:

- Solvent A: Water, 10 mM ammonium formate, pH 4.3;
- Solvent B: Acetonitrile
- Flow rate: 0.4 mL/min

- Gradient: 0 min, 0 %B;
0.25 min, 0 %B;
13 min, 25 %B,
23 min, 25 %B
- Stop time: 23 min
- Post time: 15 min
- Injection volume: 1 µL of sample cooled to 10 °C. The sample loop was switched to the bypass position after 0.25 min to reduce delay volume.
- Column temp.: 50 °C
- Detection: 210 nm +/-4 nm,
Ref. 360 nm +/-16 nm,
2 µL flow cell with
10 mm path.

TOF MS method

The Agilent 6210 TOF mass spectrometer was operated under the following conditions:

- Source: ESI in positive mode with dual spray for reference mass
- Dry gas: 12.0 L/min
- Dry temp.: 300 °C
- Nebulizer: 25 psi
- Scan: 50–1000
- Fragmentor: 150 V
- Skimmer: 60 V
- Capillary: 5000 V
- Sample: Various samples from a formulation trial of the antibiotic drug amoxicillin.

Results and discussion

To identify newly emerging degradation products a sample was taken from a formulation trial for reaction condition optimization and compared to a standard of the pure amoxicillin drug compound. Both samples were injected five times to acquire accurate mass TOF data to get rugged statistical data from the software-assisted data analysis. The obtained data files were grouped accordingly for the differential analysis with the MassHunter Profiling software. For the differential analysis of both groups the molecular features (grouped molecular masses of isotopes and adducts belonging to a single compound at a retention time) of each group were displayed in a \log_2 abundance plot, showing the abundance ratio of the amoxicillin sample from formulation batch A against the amoxicillin standard sample (figure 1). In the plot there are five lines for selected levels of abundance differences in the two sample groups. Molecular features lying on the line in the middle (1x) are equal in both groups, molecular features within the 2x margins were present at up to twofold abundance in one group and in the 4x margins up to four fold. Beyond these margins a feature was nearly unique or exclusively present in one group. The plot clearly shows a few molecular features with higher abundance in the degraded sample. Examination of the molecular feature data points showed molecular mass at $M=383.1150$, $M=365.1038$ and $M=339.1248$ with the respective calculated empirical formulas

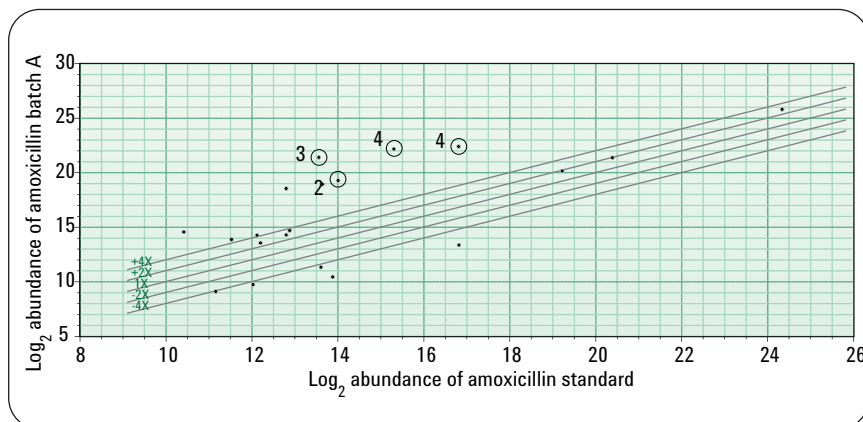


Figure 1
Comparison between a formulation batch of amoxicillin with degradation products and an amoxicillin standard using Agilent MassHunter Profiling software based on accurate ESI TOF MS data.

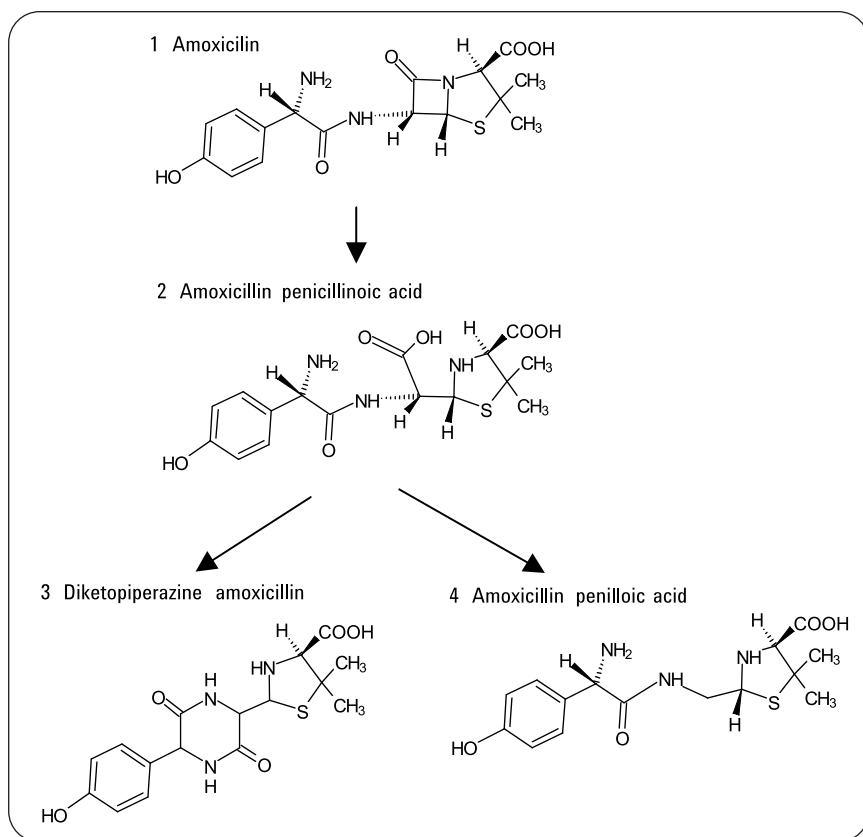


Figure 2
Degradation reactions and products from amoxicillin.

$C_{16}H_{21}N_3O_6S$, $C_{16}H_{19}N_3O_5S$ and $C_{15}H_{21}N_3O_4S$. The calculated empirical formulas were confirmed by the low relative mass errors of 0.28, 2.0 and 1.4 ppm.

The empirical formulas belong to the known amoxicillin derivatives amoxicillin penicilloic acid (2), dike-topiperazine amoxicillin (3) and amoxicillin penilloic acid (4). The degradation reaction of amoxicillin (1), which is responsible for the generation of the impurities in the final drug formulation, started with a hydrolysis reaction of the four-membered beta lactame ring to yield a carboxylic acid (2) (figure 2). Rearrangement to a six-membered ring structure leads to the dike-topiperazine derivative (3) and a decarboxylation reaction to the amoxicillin derivative (4).

The base peak chromatogram (BPC) between m/z 300–500 showed the peaks for the protonated compounds at retention times of 3.3 minutes for compound (2), 6.1 and 7.1 minutes for the diastereo isomeric compounds (4) and 8.9 minutes for compound (3). The main peak for amoxicillin was found at a retention time of 5.0 minutes (figure 3). From the MS total ion chromatogram (TIC), the extracted ion chromatograms (EIC) for compound (2), (3) and (4) were extracted (figures 4–6). The EIC for compound (2) shows the measured $[M+H]^+$ at m/z 384.1227 with a relative mass error of 0.6 ppm (figure 4).

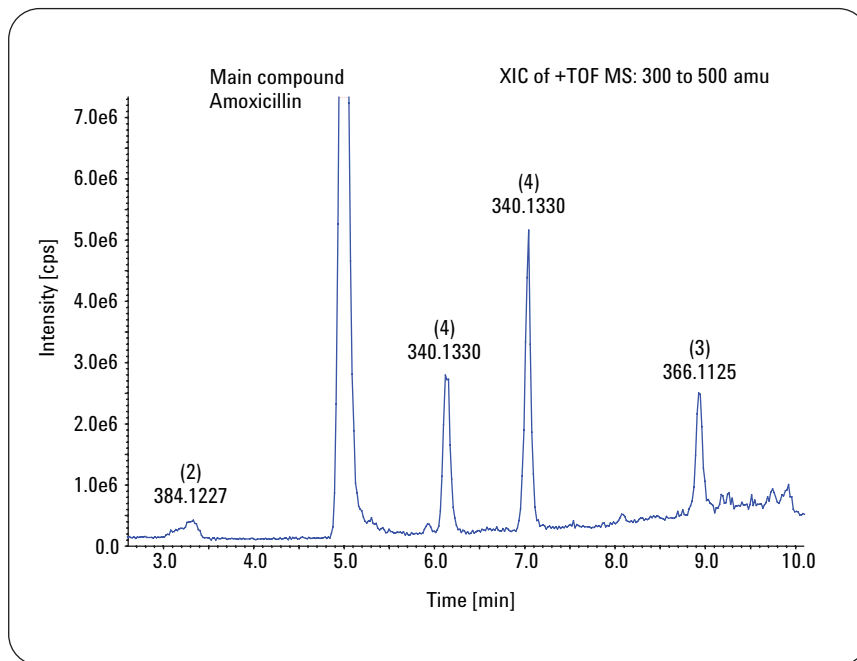


Figure 3
Base peak chromatogram (BPC) of the degraded amoxicillin sample between m/z 300–500 (see also figure 2).

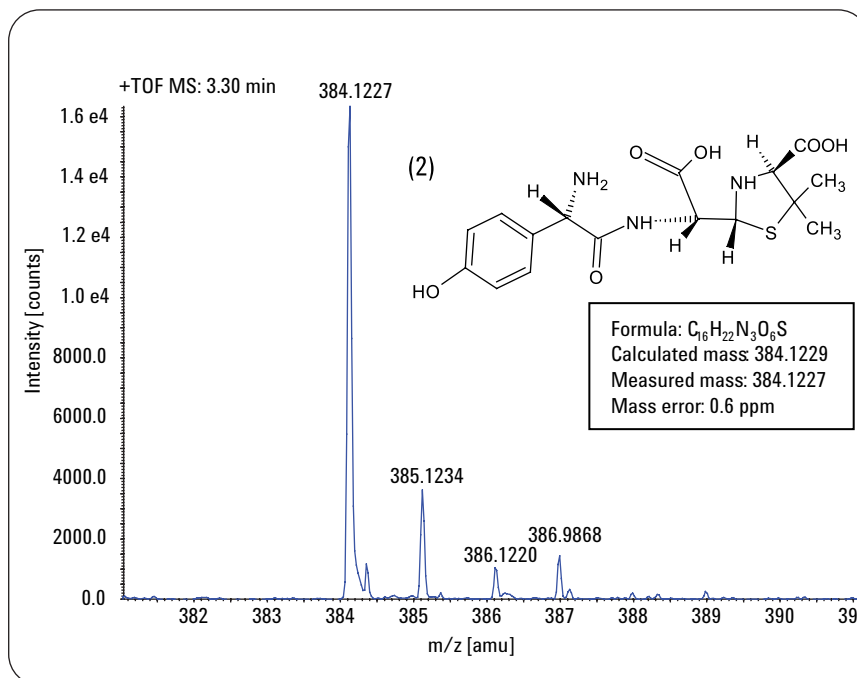


Figure 4
Mass spectrum of amoxicillin penicilloic acid (2) $[M+H]^+ = 384.1229$.

The measured $[M+H]^+$ at m/z 366.1125 for compound (3) showed a very low relative mass error of 0.36 ppm (figure 5) and the $[M+H]^+$ at m/z 340.1330 for compound (4) a relative mass error of 0.30 ppm (figure 6).

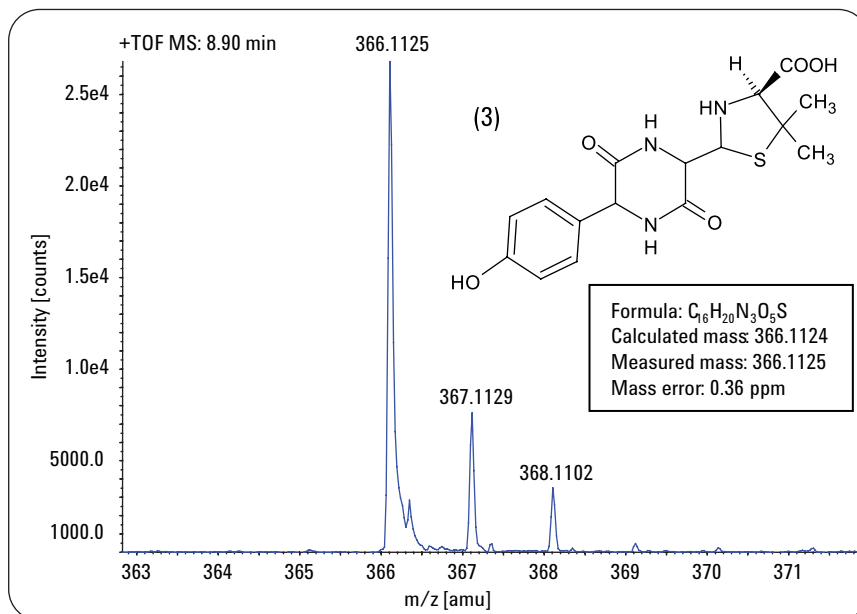


Figure 5
Mass spectrum of diketopiperazine amoxicillin (3) $[M+H]^+ = 366.1124$.

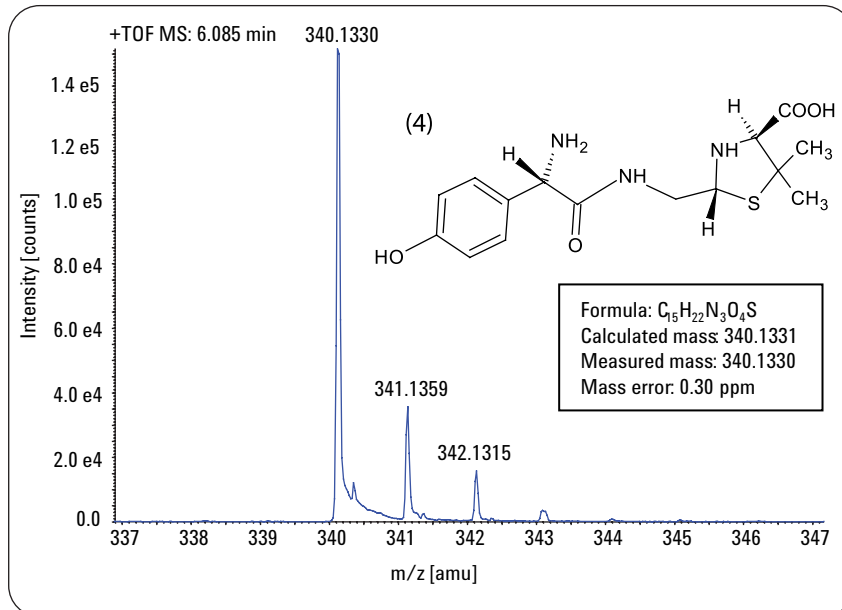


Figure 6
Mass spectrum of amoxicillin penilloic acid (4) $[M+H]^+ = 340.1331$.

Conclusion

The data presented in this Application Note showed the computer-assisted approach using the Agilent MassHunter Profiling software for the identification of degradation products in a pharmaceutical drug after a formulation trial. Newly emerging compounds were identified by the comparison to the pure standard drug compound and from the measured accurate mass ESI TOF data the empirical formulas were calculated to confirm the known identified degradation products. Finally, the mass spectra were extracted from the original MS data to confirm the identity by the measured spectra of the protonated compounds.

References

1. Görög S., "New safe medicines faster: The role of analytical Chemistry.", *Trends in Analytical Chemistry*, Vol. 22, Nos 7 + 8, **2003**.

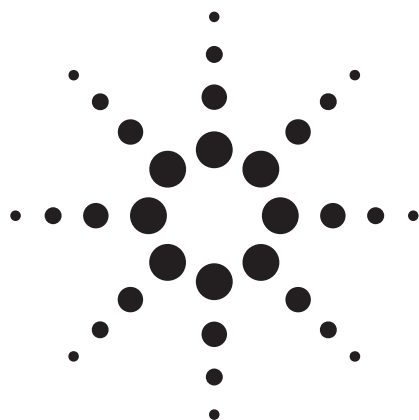
*Edgar Naegele is an Application
Chemist at Agilent Technologies,
Waldbronn, Germany.*

www.agilent.com/chem/rlc

© 2008 Agilent Technologies, Inc.

Published February 1, 2008
Publication Number 5989-7869EN



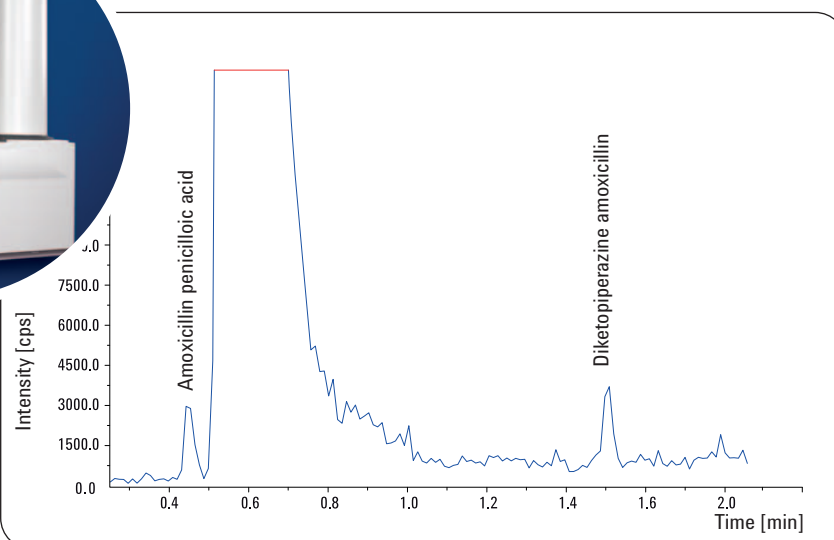


High throughput LC/MS TOF analysis of drug degradation products

Agilent 1200 Series Rapid Resolution LC and Agilent 6210 Time-of-Flight MS with alternating column regeneration

Application Note

Edgar Naegele



Abstract

This Application Note describes:

- The use of a high-throughput rapid resolution LC/MS TOF system for detection of impurities in a pharmaceutical formulation in more than 1000 samples per day.
- The instrument setup and a method for alternating column regeneration in a high-throughput LC system to reduce the overall analysis time by 50 %.
- The use of accurately measured molecular masses for formula confirmation and confident identification of impurities at levels below 0.1 %.

Agilent Equipment:

1200 Rapid Resolution LC system
6210 Time-of-Flight MS
MassHunter Workstation software

Application Area:

Pharmaceutical formulation trials
and production



Agilent Technologies

Introduction

In modern pharmaceutical production processes it is crucial to monitor drug production or formulation processes for generation of by-products. Any compounds which emerge, even at very low concentrations, as a result of production or formulation conditions must be detected and confidently identified because of their potential toxicity to humans¹.

As early as possible during drug development, it is necessary to elucidate all possible by-products which could occur during production, formulation and degradation^{2,3}. Continuous monitoring for these by-products ensures a high quality, final product.

However, monitoring of production processes and formulation trials generates a large number of samples for analysis, creating the need for a high-throughput LC/MS system, which is capable of analyzing over 1000 samples per day.

This Application Note describes the use of a high-throughput Agilent 1200 Series Rapid Resolution LC system with an Agilent 6210 Time-of-Flight mass spectrometer to monitor and identify degradation products emerging during a formulation trial of the antibiotic amoxicillin. The equipment details (figure 1), methodology and final result of the optimization with minimized by-products are described.

High throughput LC is achieved by alternating between two columns (packed with 1.8 μm particles for optimal resolution and speed^{4,5}), using overlapping injections (figure 2). The LC system is directly connected to a TOF mass spectrometer capable of scanning at a high speed compatible with the LC system and providing the necessary dynamic range of at least 3 decades. With this configuration, total analysis time for a complete set of samples was reduced by 50 %, degradation products were detected at levels below 0.1 % level and all degradation products which appeared in the formulation trial were identified by accurate mass measurement and empirical formula confirmation.

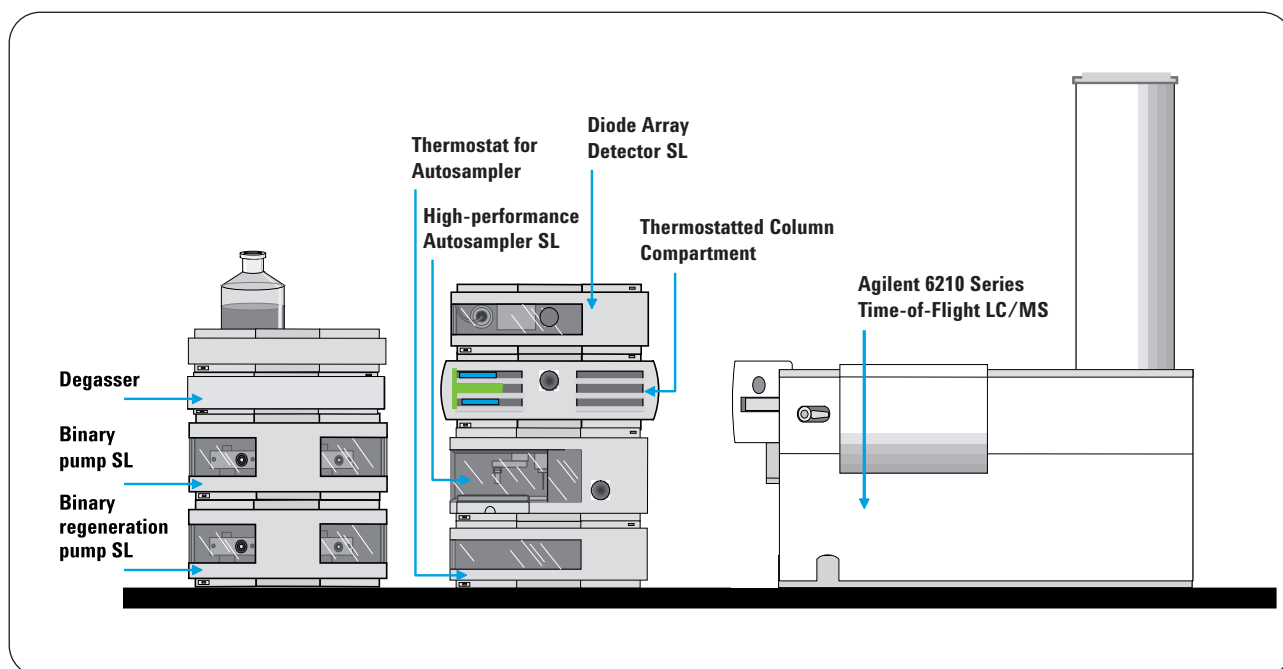


Figure 1
Instrument configuration for fast LC/TOF with alternating column regeneration.

Experimental

Equipment

- Agilent 1200 Series binary pump SL with degasser for high resolution HPLC analysis with a 1.8 μm particle size column.
- Agilent 1200 Series high performance autosampler SL with thermostat, designed to provide the lowest delay volume when used with the Agilent 1200 Series binary pump SL.
- Agilent 1200 Series thermostatted column compartment optimized for use with the Agilent 1200 Series binary pump SL and including a 2-position/10-port valve (figure 2) to enable column switching for alternating column regeneration and optional separate low dispersion heat exchangers and post column cooling for optimized delay volume conditions
- Agilent 1200 Series diode array detector SL, capable of acquiring data at a sampling rate up to 80 Hz and with built-in data storage capability.
- TOF instrument control software MassHunter

Workstation A.02.00 for data acquisition, and Analyst software for data analysis.

- Agilent 6210 TOF orthogonal acceleration time-of-flight mass spectrometer with dual sprayer interface for mass calibration to acquire molecular masses with highest accuracy. Data acquisition rate 40 Hz and positive/negative switching.
- Columns: Two ZORBAX SB C18, 2.1 x 50 mm, 1.8 μm particle size.

Method

- Solvent A: Water + 5 mM ammonium formate, pH 4.3; Solvent B: ACN
- Gradient 1: 0 min, 0 %B; 0.2 min, 0 %B; 3 min, 25 %B
Flow rate: 1 mL/min
Stop time: 3 min.
Post time: 2 min
Gradient 2: 0 min, 0 %B; 0.2 min, 0 %B; 2 min, 25 %B
Flow rate: 1 mL/min
Stop time: 2 min
Post time: 2 min.
- Column regeneration:
Solvent A: Water + 5 mM ammonium formate, pH 4.3.
Flow rate: 1 mL/min.

- Autosampler with automated delay volume reduction and overlapped injection functions; 1 μL sample injections with needle wash; samples cooled to 4 $^{\circ}\text{C}$.
- Diode array detection: 210 nm ± 4 nm, Ref. 360 ± 16 nm with 2 μL flow cell, 3 mm path length.
- Column temperature: 50 $^{\circ}\text{C}$, thermostatically controlled. At the end of a run, each column was switched into the alternate flow path for regeneration.
- MS analysis: ESI source in positive mode with dual spray for reference mass solution.
Dry gas: 12.0 L/min
Dry Temperature: 350 $^{\circ}\text{C}$
Nebulizer: 50 psi
Scan: 50-1000 at 40 Hz
Fragmentor: 200 V (300 V CID)
Skimmer: 60 V
Capillary: 5000 V

Sample:

Samples from a formulation trial of the antibiotic drug amoxicillin, collected at various time points for LC/MS analysis.

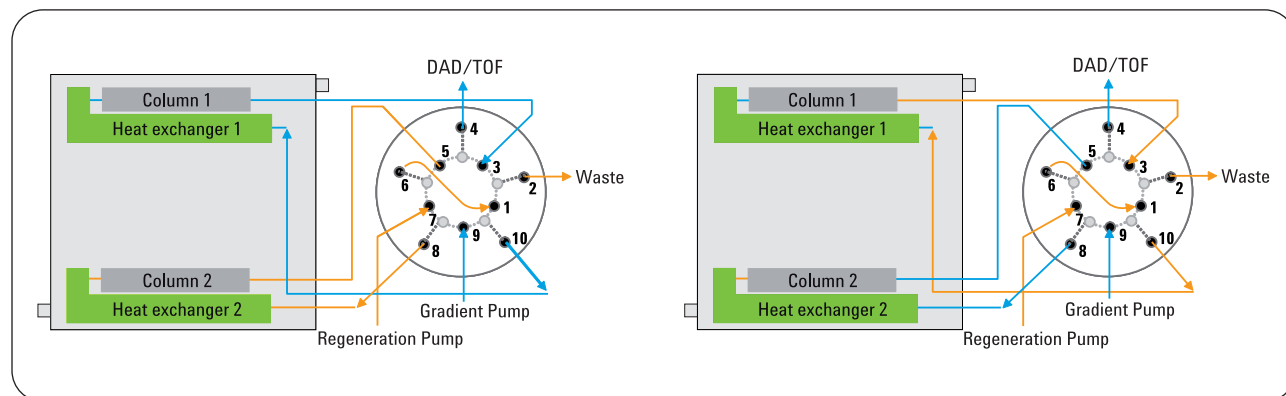


Figure 2
Column switching at the 2-position/10-port valve for fast LC/TOF with two columns (2.1 mm x 50 mm, 1.8 μL).

Results and Discussion

Reduction in total analysis time

By switching columns between alternate flow paths, so that one column was being regenerated while the other was being equilibrated, the total analysis time for a complete sample set was reduced by 50 %. Gradient and column regeneration times were 2 or 3 minutes, depending of the gradient used.

Monitoring of degradation

The emerging degradation products were identified in the MS TOF files by accurate mass measurement and empirical formula confirmation. The chromatogram obtained from the first sample shows only slight degradation (figure 3) with two degradation products at 0.95 minutes and 2.51 minutes retention time. After 30 minutes under stress conditions, significant degradation has occurred, with additional degradation products emerging at 1.92, 2.10 and 2.26 minutes (figure 4).

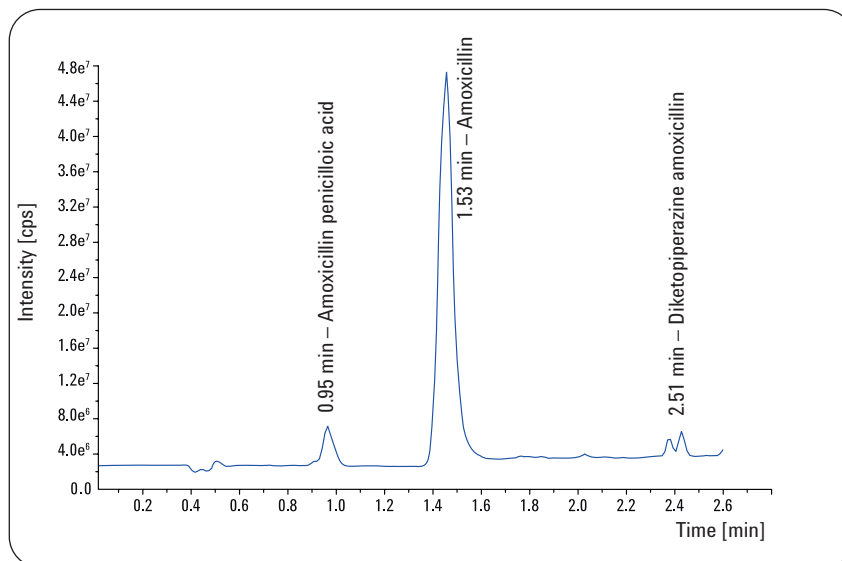


Figure 3
MS TOF TIC of the first time point in the degradation experiment of the antibiotic drug amoxicillin (gradient 1).

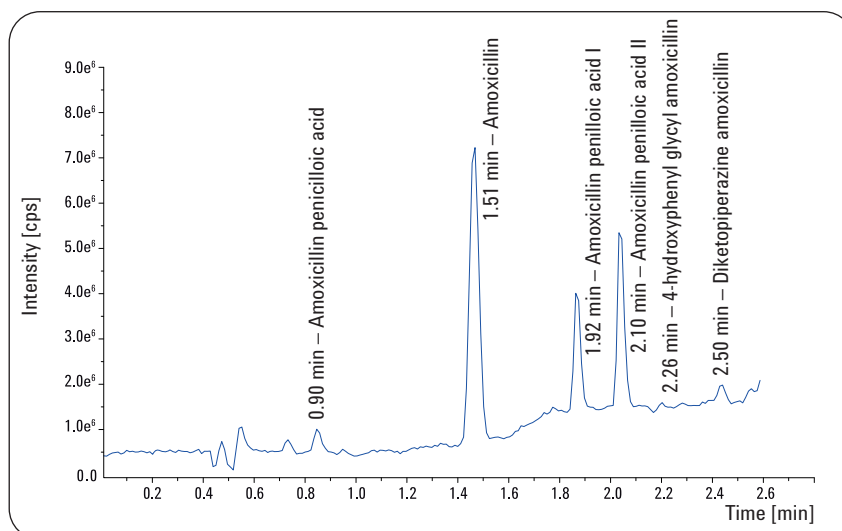


Figure 4
MS TOF TIC of the degradation experiment of the antibiotic drug amoxicillin with the identified degradation products (gradient 1).

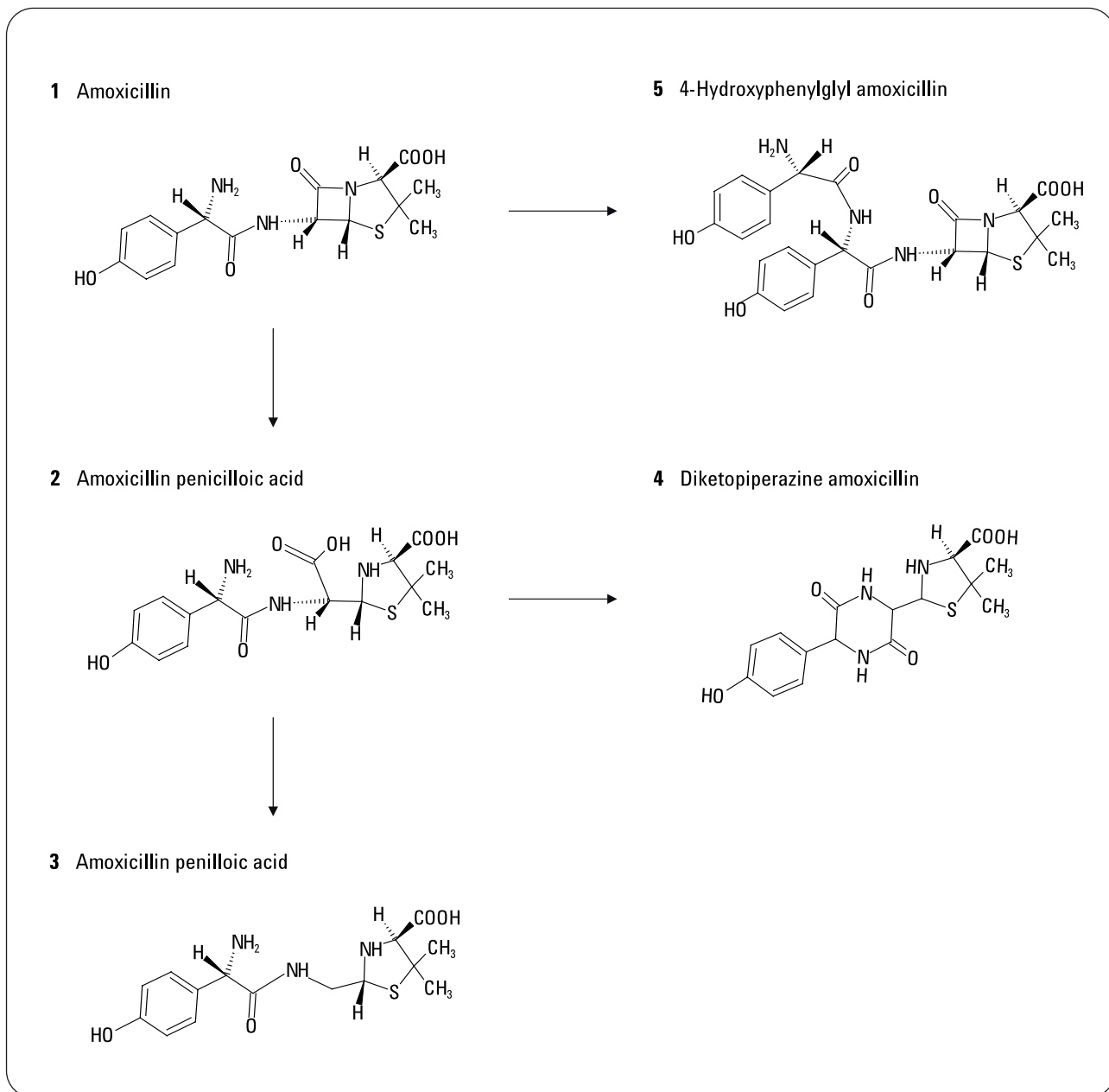


Figure 5
Degradation reactions of amoxicillin.

Identification of degradation products

The previously known degradation products were identified by empirical formula confirmation based on the highly accurate mass measurements. The degradation of amoxicillin (1) starts with an opening reaction of the four-membered beta-lactame ring and different subsequent reactions (figure 5). The first degradation product is amoxicillin penicilloic acid (2). This initial degradant undergoes further reactions.

After decarboxylation two stereoisomeric compounds amoxicillin penilloic acid (3) will be obtained or after new formation of a stable six-membered ring the stable product diketopiperazine amoxicilline (4) will be formed. The TOF mass spectrum of (2) shows the $[M+H]^+$ ion at m/z 384.1220 and the molecule fragment coming from a loss of NH_3 at m/z 367.0953 (figure 6).

Other typical CID fragments are also present, which allow identification by empirical formula confirmation (table 1).

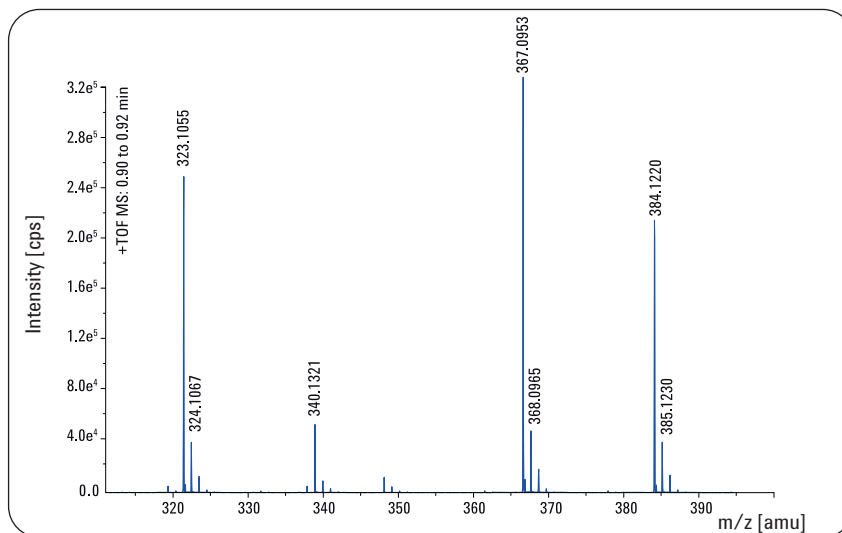


Figure 6
Extracted TOF mass spectrum of amoxicillin penicilloic acid (2).

| Measured mass | Calculated mass | Formula | Mass accuracy [mDa] | Mass accuracy [ppm] |
|---------------|-----------------|-----------------------|---------------------|---------------------|
| 384.1220 | 384.1229 | $C_{16}H_{22}N_3O_6S$ | -0.90 | 2.43 |
| 367.0953 | 367.0964 | $C_{16}H_{19}N_2O_6S$ | -1.10 | 2.95 |
| 340.1321 | 340.1331 | $C_{15}H_{22}N_3O_4S$ | -1.00 | 2.94 |
| 323.1056 | 323.1066 | $C_{15}H_{19}N_2O_4S$ | -1.00 | 2.95 |

Table 1
Achieved mass accuracies and confirmed empirical formulas of fragments from amoxicillin penicilloic acid (2) from CID experiment.

The TOF mass spectrum of degradation product (4), which has the same isobaric mass as compound (1), shows the $[M+H]^+$ ion at m/z 366.1115 and the sodium adduct at m/z 388.0931 (figure 7 and table 2). Since the degradation of amoxicillin (1) starts with the opening reaction of the four-membered beta-lactame ring giving amoxicillin penicilloic acid (2) followed by the closure to the stable six-membered diketopiperazine ring in diketopiperazine amoxicillin (4), these are the first degradants which are detectable in minor amount in a formulation of amoxicillin (figure 8).

The empirical formulas of these minor by-products were calculated with mass accuracies of 2.68 ppm for $C_{16}H_{22}N_3O_6S$ (2) and with 3.19 ppm for $C_{16}H_{20}N_3O_5S$ (4).

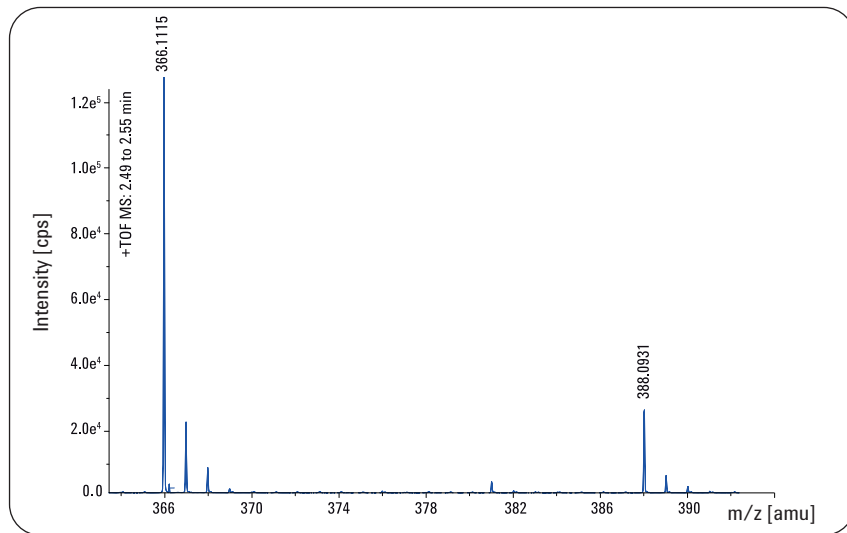


Figure 7
Extracted TOF mass spectrum of amoxicillin diketopiperazine amoxicillin (4).

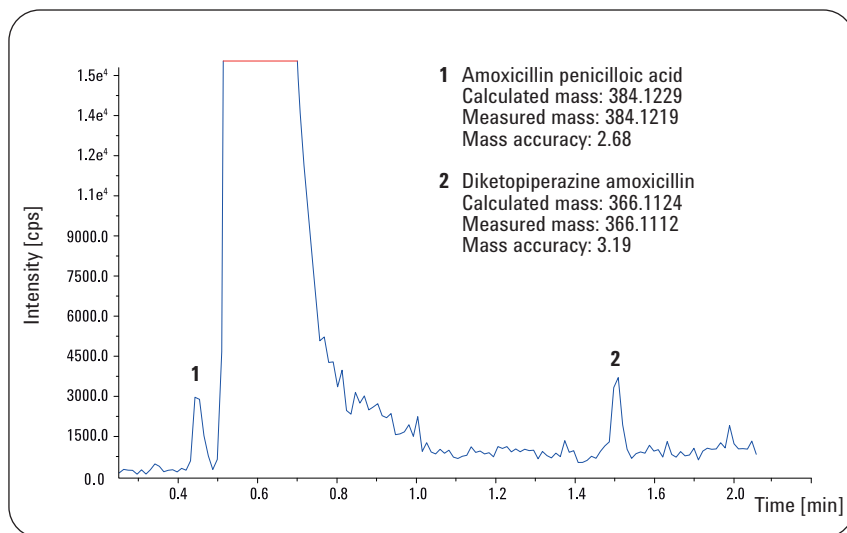


Figure 8
Detection of two 0.1 % minor impurities in a formulation of amoxicillin (gradient 2).

| Measured mass | Calculated mass | Formula | Mass error [mDa] | Mass error [ppm] |
|---------------|-----------------|-------------------------|------------------|------------------|
| 388.0931 | 388.0943 | $C_{16}H_{19}N_3O_5SNa$ | -1.2 | 3.12 |
| 366.1115 | 366.1124 | $C_{16}H_{20}N_3O_5S$ | -0.9 | 2.37 |

Table 2
Achieved mass accuracies and confirmed empirical formulas of diketopiperazine amoxicillin (4) and its sodium adduct.

Conclusion

A high throughput LC/MS TOF method for identification of degradation products in a production process or formulation trial was developed successfully using an optimized configuration of the Agilent 1200 Series RRLC system and Agilent 6210 TOF MS. The method was tested using samples from a degradation experiment of the antibiotic drug amoxicillin. A significant reduction in analysis times was achieved and degradation products were confidently identified. Identification of two degradation products with content of 0.1% confirmed that the dynamic range of the TOF MS was sufficient for this analytical task.

References

1. Görög S., "New safe medicines faster: The role of analytical Chemistry", *Trends in Analytical Chemistry*, Vol. 22, Nos 7 + 8, **2003**.
2. Edgar Naegele, "Structure elucidation of degradation products of the antibiotic drug amoxicillin – Part I: Examination of the degraded drug products by fragmentation with ion trap MSn", *Agilent Application Note, Publication Number 5989-2347EN*, **2005**.
3. Edgar Naegele, "Structure elucidation of degradation products of the antibiotic drug amoxicillin – Part II: Identification and confirmation by accurate mass measurement with ESI TOF of the compound ions and fragments after CID", *Agilent Application Note, Publication Number 5989-2348EN*, **2005**.
4. Angelika Gratzfeld-Huesgen, "Performance of the Agilent 1200 RRLC system for highest resolution", *Agilent Application Note, Publication Number 5989-4489EN*, **2006**.
5. Michael Frank, "Performance of the Agilent 1200 RRLC System for Ultra-Fast LC application with 2.1 mm i.d. columns", *Agilent Application Note, Publication Number 5989-4502EN*, **2006**.

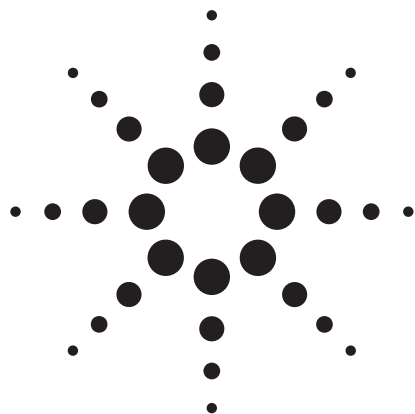
Edgar Naegele is an Application Chemist at Agilent Technologies, Waldbronn, Germany.

www.agilent.com/chem/tof

© Agilent Technologies, 2007

Published April 1, 2007
Publication Number 5989-6507EN



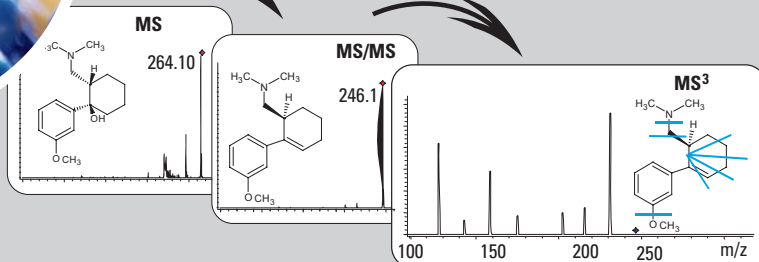
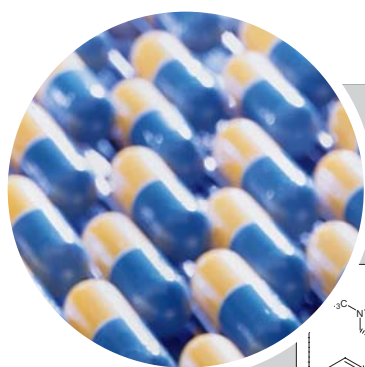


Impurity Profiling with the Agilent 1200 Series LC System

Part 1: Structure Elucidation of Impurities with LC/MS

Application Note

Edgar Nägele



Abstract

Today, it is necessary to identify and confirm the identity of all by-products appearing in the process of the development and manufacturing of a new drug substance in the pharmaceutical industry. In this Application Note the identification of by-products is demonstrated by structure elucidation by means of LC ion trap MS/MS and MS³. In addition, the identity of the synthesis by-products will be confirmed by accurate mass measurement of the molecular ions by LC/ESI TOF. Subsequent parts of this series of Application Notes will show method development and validation of a QA/QC method to detect the identified impurities in the final dosage form of the drugs³⁻⁶.



Agilent Technologies

Introduction

In modern pharmaceutical drug development and manufacturing it is crucial to identify minor impurities and by-products with the highest possible confidence because of their potential toxic effects on humans. The profiling of impurities in different phases of drug R&D is of extreme importance and a bottleneck in the entire process. Therefore, large efforts are made to develop strategies for fast impurity profiling using chromatographic, spectroscopic and hyphenated techniques¹. In combination with the resolving power of liquid chromatography, ion trap instruments are widely used mass spectrometric tools for the structure elucidation by means of their MS/MS and MSⁿ capabilities. With these instruments, it is possible to break the molecular ion of the investigated substance in fragments, which are useful for the structure elucidation. Additionally, the mass spectrometric measurement of accurate molecular mass and consequently the calculation of the empirical formula is a common method for the identification and identity confirmation of an unknown compound. ESI orthogonal acceleration time-of-flight (oaTOF) MS instruments are capable of handling this task. This Application Note will discuss the identification of synthesis by-products and residual educts derived from a synthesis of a pharmaceutical drug² (figure 1) by ion trap and ESI oaTOF mass spectrometry.

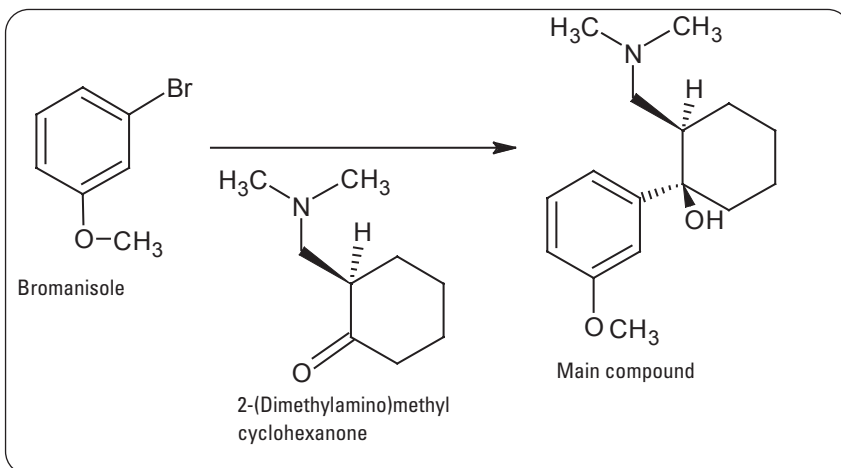


Figure 1
Synthesis of the pharmaceutical main target compound.

Experimental

Equipment

- Agilent 1200 Series Rapid Resolution LC system (RRLC): Agilent 1200 Series binary pump SL with degasser, Agilent 1200 Series high performance autosampler SL with thermostat, Agilent 1200 Series thermostated column compartment, 1200 Series diode-array detector SL
- Agilent 6000 Series mass spectrometers: Agilent 6210 Series Time-of-Flight (TOF), Agilent 6330 Series Ion Trap
- Software: ChemStation B01.01, Ion Trap software 5.2 for instrument control with Data Analysis software 4.2. TOF software A.02.01 for instrument control and Analyst software for data analysis
- Columns: ZORBAX SB C18 2.1 x 150 mm, 1.8- μ m particle size.

Method

- Solvent A: Water with 0.1% TFA
- Solvent B: AcN with 0.1 % TFA

- Flow: 0.5 mL/min
- Gradient 1: 0 min – 5 % B, 30 min 95 % B, 32 min 95 % B
- Gradient 2: 0 min – 5 % B, 30 min 50 % B, 31 min 95 % B, 32 min 95 % B. Stop time: 32 min, Post time: 10 min.
- DAD: 2- μ L cell, 10-mm path, 270 nm \pm 4 nm, ref. 360 \pm 8 nm, width 0.1 min.
- Injector: 1- μ L injection volume, needle wash 5 s with MeOH/Water 1/1
- Column oven: 60 °C
- MS – Ion Trap: source 200 °C, positive polarity, dry gas 10 L/min, nebulizer 40 psi, ICC 125000, autom. MS/MS and MS³
- MS – TOF: source 200 °C, positive polarity, dry gas 12 L/min, nebulizer 40 psi, skimmer 40 V, scan m/z 100 – 1000, reference mass solution switched on

Results and discussion

To discover all possible impurities in a pharmaceutical drug compound during the development and manufacturing process it is very important to use several orthogonal separation techniques such as liquid chromatography, gas chromatography or thin-layer chromatography in several methodologies, for example, with different columns, solvents and other instrument parameters¹. To detect all possible impurities in a technical drug sample, an LC as well as a GC separation was used as the initial analytical method.

The LC analysis, by using a gradient with a high organic content (gradient 1) for the separation, resolved five impurities in a minor concentration of about 0.1% each (figure 2A). The comparison of the educts used in the synthesis with their retention time revealed impurity F as 3-bromanisole. To confirm the identity, the UV spectra were compared because these compounds did not produce a signal in the coupled electrospray mass spectrometer. The educt impurity E was neither detectable by UV nor ESI-MS. Therefore, the sample was analyzed by GC-FID and the compound could be detected and confirmed by retention time comparison (data not shown). To achieve better separation for the remaining impurities and their analysis by time-of-flight and ion trap mass spectrometry, a shallower gradient with up to 50 % organic solvent was used (gradient 2). With this method the remaining four impurities were sufficiently resolved for their mass spectrometric analysis to gain the necessary TOF-MS as well as ion trap MS/MS and MS³ data for structure

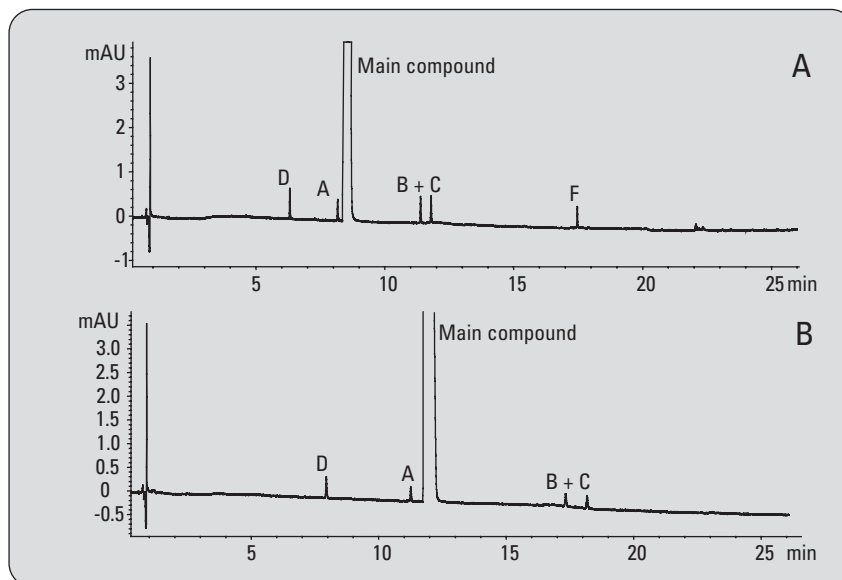


Figure 2

A) High resolution LC separation of the drug and impurities with gradient 1 and detection at UV 270 nm. B) High resolution LC separation of the drug and its impurities with gradient 2 and detection at UV 270 nm.

| Impurity | Formula | Calculated mass | Measured mass | Mass accuracy [mDa] | Mass accuracy [ppm] |
|----------|---|-----------------|---------------|---------------------|---------------------|
| A | C ₁₆ H ₂₆ NO ₂ | 264.1964 | 264.1957 | -0.7 | 2.5 |
| B | C ₁₆ H ₂₄ NO | 246.1858 | 246.1850 | -0.8 | 3.2 |
| C | C ₁₆ H ₂₄ NO | 246.1858 | 246.1851 | -0.7 | 2.9 |
| D | C ₁₅ H ₂₄ NO ₂ | 250.1807 | 250.1804 | -0.3 | 1.2 |

Table 1

Measurement of accurate masses by LC/TOF analysis of impurities and confirmation of the empirical formulas by calculating the relative mass errors.

elucidation (figure 2B).

To calculate empirical formulas for all impurities, an LC/MS-TOF analysis was performed to measure the accurate masses. It was possible to confirm all suggested formulas with sufficient mass accuracies in the single digit ppm range (table 1) with this experiment. The main compound itself has the empirical formula C₁₆H₂₆NO₂ with an accurate mass of 264.1964. The following empirical formulas for the detected impurities were calculated:

- Impurity A is an isomeric form

of the main molecule, which has the same empirical formula C₁₆H₂₆NO₂ and a measured mass at m/z 264.1957.

- Impurity B has a measured mass at m/z 246.1850 and the calculated empirical formula C₁₆H₂₄NO.
- Impurity C has the same measured mass m/z 246.1851 as impurity B and they are isomeric forms of the same molecule.
- For the remaining impurity D, the measured mass was m/z 250.1804 with the calculated empirical formula C₁₅H₂₄NO₂.

To create more dedicated

structural information about the impurities, an ion trap mass spectrometric analysis was performed. The main peak at a retention time of 12 minutes was detected with its molecular ion at m/z 264.1 in the mass spectrum. The MS/MS of this molecular ion generated the fragment ion at m/z 246.1 due to a loss of a molecule of water. An MS³ mass spectrum was not

obtained because the fragment ion at m/z 246.1 did not undergo further fragmentation (figure 3). The diastereomeric impurity (A) was detected at a retention time of 11.3 minutes at the same m/z 264.1. The molecular ion of this compound also leads to the fragment ion at m/z 246.1 due to a loss of water in the MS/MS fragmentation (figure 4B). In contrast, an MS³ spectrum could be obtained in this case (figure 4C). The fragmentation of the ion at m/z 246.1 at the MS³ level generated the main ions at m/z 215.1 due to a loss of the methoxy group; the ion at m/z 202.1 due to a loss of the dimethyl amino group; and the fragment at m/z 121.1 due to a benzylic cation. The different fragmentation behavior of the main compound and its impurity A gives evidence of their diastereoisomerism because they are following different routes of water elimination on the MS/MS level, which leads to a stereochemically different ions at m/z 246.1. Fragmentation behavior similar to the main compound was found in impurity D. The molecular ion of impurity D,

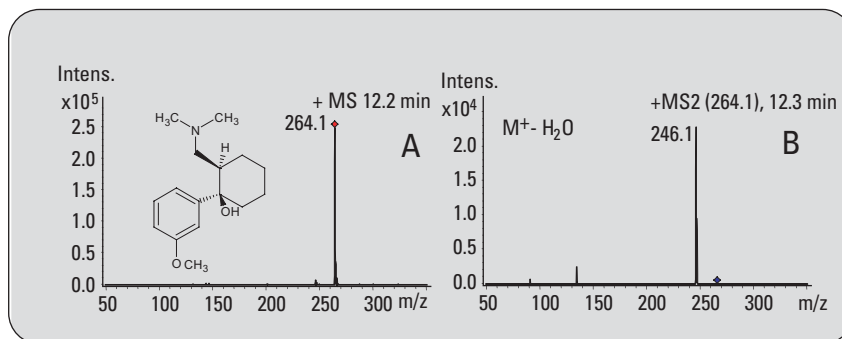


Figure 3

A) Ion Trap MS of the main compound with molecular ion at m/z 264.1 B) Ion trap MS/MS of the main compound molecular ion showing the ion at m/z 246.1.

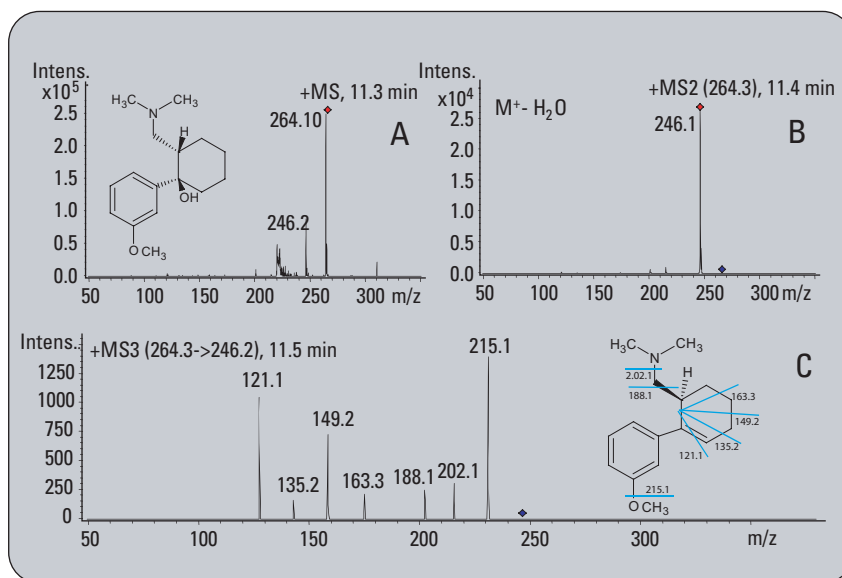


Figure 4

A) Ion Trap MS of impurity A with the molecular ion at m/z 264.1. B) MS/MS fragment ion of the impurity A at m/z 264.1. C) MS³ fragmentation of the ion at m/z 246.1.

which is generated from the drug molecule by the loss of a methyl group at m/z 250.1, generates the fragment ion at m/z 232.1 during MS/MS fragmentation by a loss of water. An MS³ fragmentation was not obtained (figure 5). Supported by similar fragmentation behavior as the main compound, it could be assumed that impurity D has the same stereochemistry as the drug molecule and therefore is the degradation product of a demethylation. The remaining impurities B and C were detected at m/z 246.2 at retention times of 17.3 and 18.2 minutes (figure 6A). The molecular ion of both impurities B and C correspond in two different ways to the molecular ion of the main compound due to a loss of water and the generation of a double bond in the molecule. The main peak in the MS/MS spectrum at m/z 202.2 is derived from a loss of the dimethyl amino group in both possible molecules (figure 6B). Further fragmentation in the MS³ experiment generated similar spectra for both impurities, resulting in fragments at m/z 173.9 and m/z 159.6 generated by a loss of the methoxy and methylene groups (figure 6C). With these results it was not possible to assign the correct location of the double bond in the molecules of the impurities B and C. Therefore, it is necessary to isolate and purify both compounds on a preparative scale for an additional NMR experiment to examine the correct stereochemistry³.

The primary products of the syn-

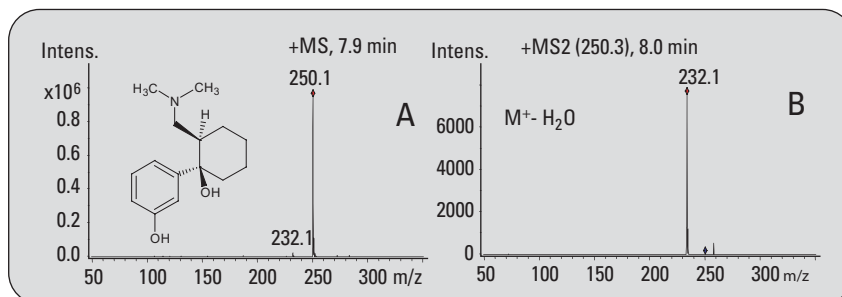


Figure 5
A) Ion trap MS of impurity D. B) Ion trap MS/MS fragmentation of m/z 250.1.

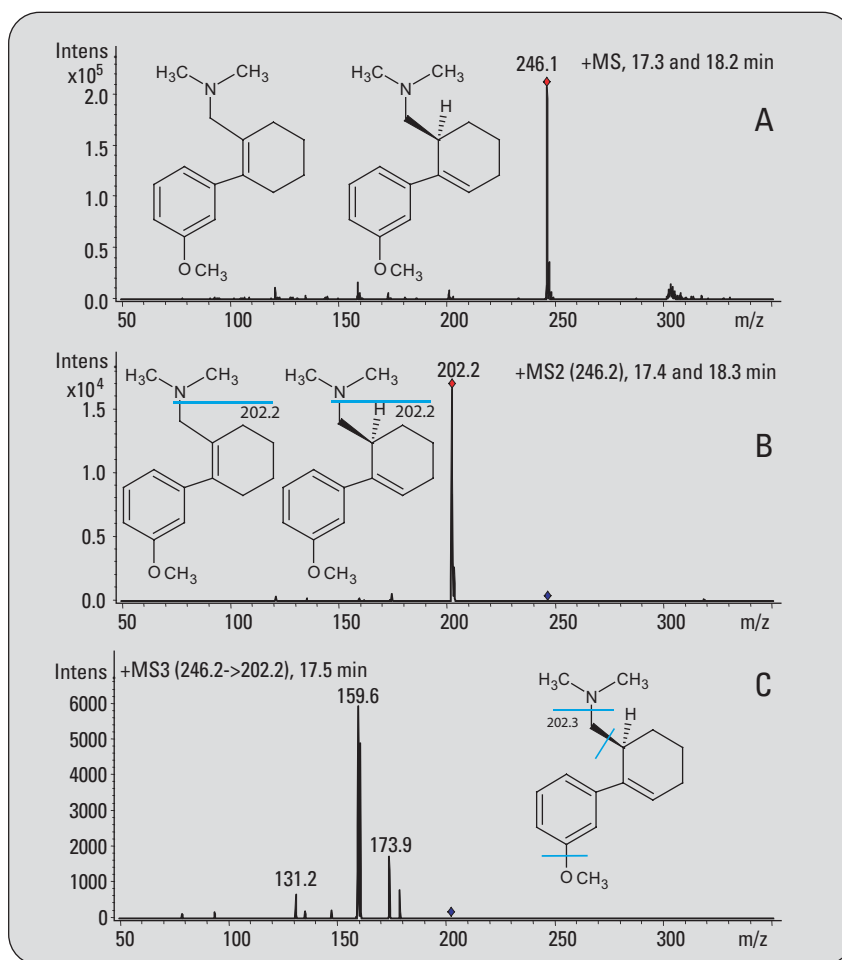


Figure 6
A) Ion Trap MS of impurities B and C at m/z 246.1. B) MS/MS fragmentation of impurity B and C to the fragments at m/z 202.2. C) Typical MS³ fragmentation spectrum of the ions at m/z 202.2 from both impurities B and C.

thesis are the drug substance and its diastereomeric counterpart, which is found after a recrystallization step in the final product as the possible minor impurity A (figure 7). Beginning with the drug molecule itself, possible impurities are the degradation products, which are formed by a loss of water (impurities B and C), and the product of an undesired demethylation reaction (impurity D). Additionally, the educts of the synthesis are also possible by-products (impurities E and F).

Conclusion

This Application Note demonstrates the use of the Agilent 1200 Series Rapid Resolution (RRLC) system with 1.8- μm RRHT columns in combination with the Agilent 6330 ion trap and the Agilent 6210 ESI TOF for the detection and structure elucidation of minor impurities in a pharmaceutical drug substance. With the 1200 Series RRLC system, the necessary resolution to detect all impurities was reached on 1.8- μm columns. The ion trap, with its MS/MS and MS^n capabilities, was used for structure elucidation and the ESI TOF for confirmation of the suggested formulas by accurate mass measurement. In this experiment all minor impurities were detected in a technical sample of a drug substance by means of orthogonal analytical methods (LC/UV, LC/MS and GC). For all impurities, structures were sug-

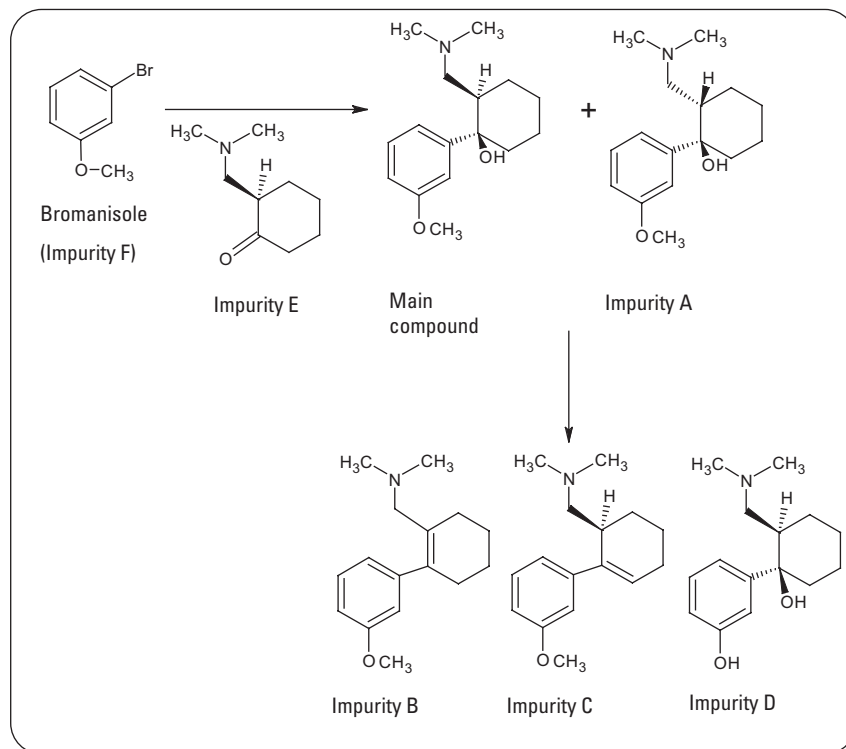


Figure 7
Identified impurities in the pharmaceutical drug synthesis of the main compound.

gested based on the MS^n analysis and their identity was confirmed by accurate mass measurement and empirical formula calculation. Subsequent steps in the impurity profiling procedure include assigning undetermined impurities, which are purified on a preparative scale, for example, NMR analysis³; and a method for QA/QC will be developed⁴, validated⁵ and applied⁶.

References

1. Sandor Görög “New Safe Medicines Faster: The Role of Analytical Chemistry.” *Trends in Analytical Chemistry* 22, 407. **2003.**
2. Victor A. Savelyev, Alexander G. Druganov, Elvira E. Shults, Genrikh A. Tolstikov, *Vorozhtsov Novosibirsk Institute of Organic Chemistry, Siberian Branch of the Russian Academy of Sciences* 9 prosp. Akad. Lavrent'eva, 630090 Novosibirsk, Russia, <http://www.nioch.nsc.ru/icnpas98/pdf/posters1/156.pdf>
3. Udo Huber “Impurity Profiling with the Agilent 1200 Series LC System – Part 2: Isolation of Impurities with Preparative HPLC” *Agilent Application Note, publication number 5989-5618EN*, 2006.
4. Michael Frank “Impurity Profiling with the Agilent 1200 Series LC System – Part 3: Rapid Condition Scouting for Method Development”, *Agilent Application Note, publication number 5989-5619EN*, **2006.**
5. Angelika Gratzfeld-Huesgen “Impurity Profiling with the Agilent 1200 Series LC System, Part 4: Method Validation of a Fast Method” *Agilent Application Note, publication number 5989-5620 EN*, **2006.**
6. Angelika Gratzfeld-Huesgen “Impurity Profiling with the Agilent 1200 Series LC System Part 5: QA/QC Application Example with Complete Sequencing” *Agilent Application Note, publication number 5989-5621EN*, **2006.**

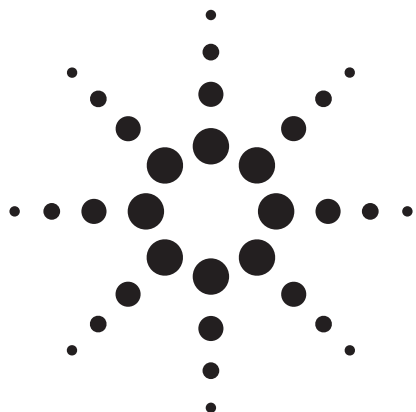
*Edgar Nägele is Application
Chemist at Agilent Technologies,
Waldbronn, Germany.*

www.agilent.com/chem/1200rr

© 2006 Agilent Technologies, Inc.

Published October 1, 2006
Publication Number 5989-5617EN



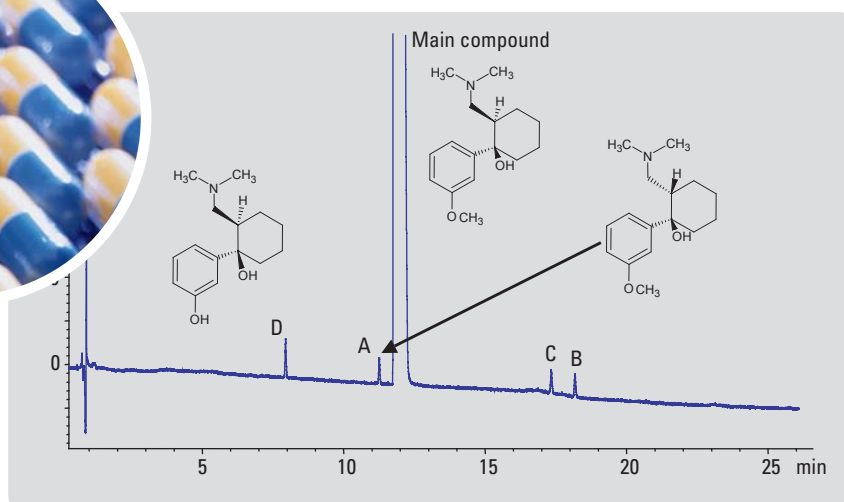


Impurity Profiling with the Agilent 1200 Series LC System

Part 2: Isolation of Impurities with Preparative HPLC

Application Note

Udo Huber



Abstract

The isolation and purification of synthesis impurities is an important task in the impurity profiling process. Ideally all impurities can be identified by hyphenated MS techniques, but usually some of them must be isolated and purified to elucidate the structure by NMR, for example. In this Application Note two impurities that could not be identified by MS are isolated from a crude sample. Starting with an analytical run using an Agilent 1200 Series Rapid Resolution LC (RRLC) system, the method was optimized regards to resolution of the critical impurity pair, and loading experiments were carried out. After scale-up to a preparative scale column, the impurities could be isolated in high purity and recovery. Sufficient amounts of each compound could be isolated after repetitive injections to elucidate the structures by NMR.



Introduction

Impurity profiling describes a group of analytical activities aimed at the detection, identification, structure elucidation and quantitative determination of organic and inorganic impurities in drugs¹. These activities are carried out across the entire drug discovery and development process, leading finally to a validated method used in QA/QC to assure the drug's safety for the patient. The first task in this process is the detection of all impurities. Various, orthogonal analytical methods such as gas chromatography, capillary electrophoresis and high-pressure liquid chromatography are used for this purpose. With the introduction of sub-2 μm particle columns for highest resolution, together with the Agilent 1200 Series RRLC system and hyphenated MS technologies such as Ion Trap and Time-of-Flight (TOF) instruments the chromatographer has at present strong tools to separate and identify the impurities in a relatively short time². However, even with the most sophisticated MS instruments, the complete structure elucidation of all compounds is often impossible. These compounds have to be isolated and purified and are then characterized by ¹H- and ¹³C-NMR. Since the impurities are present in the crude sample in low concentration, it is advantageous to use samples in which these compounds are enriched. This could be the mother liquor of a larger scale crystallization process, for example. The isolation and purification of a pair of impurities that could not be identified by MS is described in this Application Note.

Experimental

Equipment

The experiments were performed using an Agilent 1200 Series purification system containing the following modules:

- Two Agilent 1200 Series preparative pumps
- Agilent 1200 Series dual-loop autosampler PS (2000- μL loop)
- Agilent 1200 Series column organizer
- Agilent 1200 Series multi wavelength detector (flow cell: 3-mm path length)
- Agilent 1200 Series fraction collectors PS

The system was controlled using the Agilent ChemStation (rev. B.02.01. SR1).

Results and discussion

As described in a previous Application Note², the impurities A and D (chromatogram on cover page) could be identified by MS using an Ion Trap and TOF instrument. Impurities B and C, however, could not be characterized completely, and have therefore been isolated by preparative HPLC for further structure elucidation.

Method optimization

Since the sub-2 μm particle stationary phase used in the MS experiments is also available with 5- μm particle size as a preparative scale column, the method only had to be optimized for the resolution of impurities B and C and for shorter run times. The results for a sample enriched with impurities B and C are shown in figure 1.

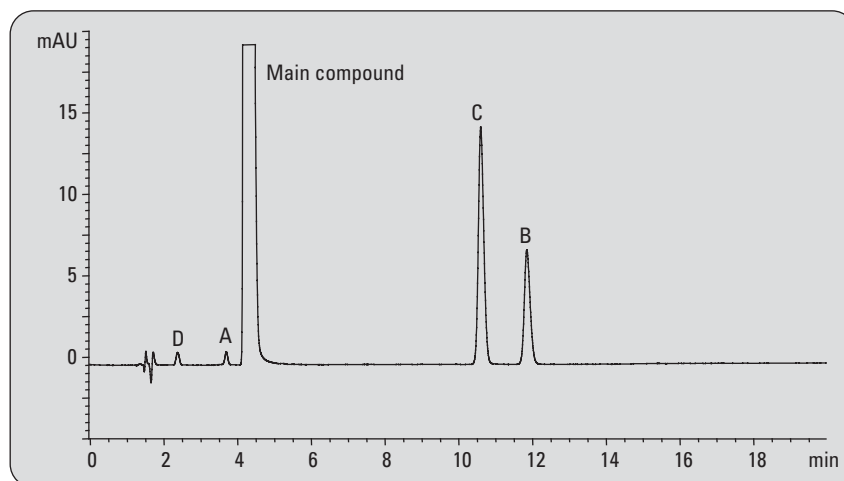


Figure 1
Optimized method for impurities C and B.

Chromatographic conditions:

| | |
|----------------|--|
| Column: | ZORBAX SB-C18 4.6 x 150 mm, 5 μm |
| Mobile phases: | Water + 0.1 % TFA = A Acetonitrile + 0.1 % TFA = B |
| Gradient: | at 0 min 25 % B at 14 min 32 % B at 16 min 50 % B |
| Stop time: | 16 min |
| Post time: | 5 min |
| Flow: | 1 mL/min |
| Injection: | 5 μL |
| Column temp.: | 30 °C |
| UV detector: | DAD 270 nm/30 (ref. 360 nm/100) Flow cell (10 mm path length) |

Loading experiments

Before scaling-up the method for a preparative-scale column loading experiments were carried out on an analytical-scale column. In addition to the original sample, some diluted solutions as well as higher volumes were injected and the chromatograms monitored for the resolution of compounds C and B. The results of the overloading experiments are shown in figures 2a and 2b. Baseline separation of the impurities C and B could still be achieved with 1.0444 mg crude sample injected onto the column.

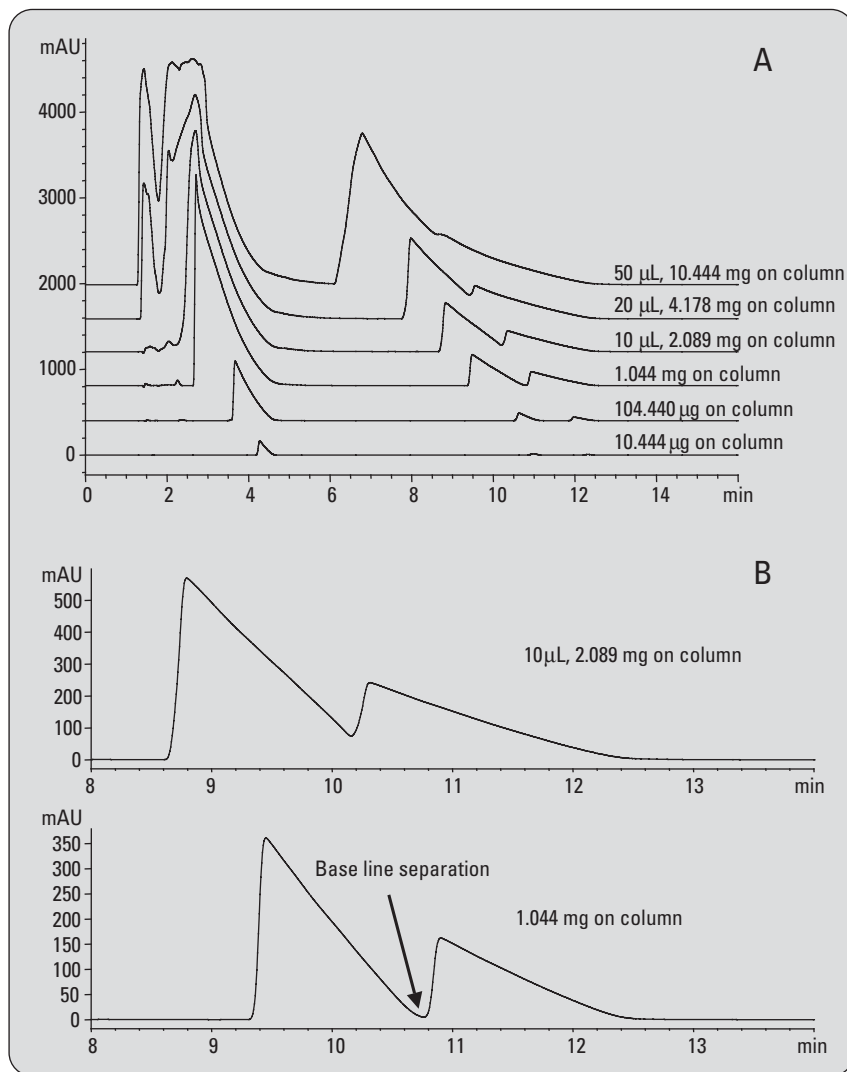


Figure 2

A) Loading experiments.

B) Baseline separation at 1.0444 mg crude sample on the column.

Scale-up calculations

The concentration of impurities C and B in the enriched sample was approximately 3 – 5 % of the main compound, which means that only about 0.03 – 0.05 mg of each impurity could have been isolated from a single injection. Therefore, the separation was scaled up to a preparative column with an inner diameter of 21.2 mm. Scale-up calculations have to be carried out for flow rate and loading as shown in figure 3. Since the stationary phase was the same as used in the first analytical run (cover page) and the loading experiments (figure 2a). The method transfer could be done without any changes in the elution order. With approximately 22 mg of crude sample applied, about 0.66 – 1.1 mg of each impurity could be isolated per injection. Therefore less than ten injections resulted in sufficient amounts for further NMR analysis.

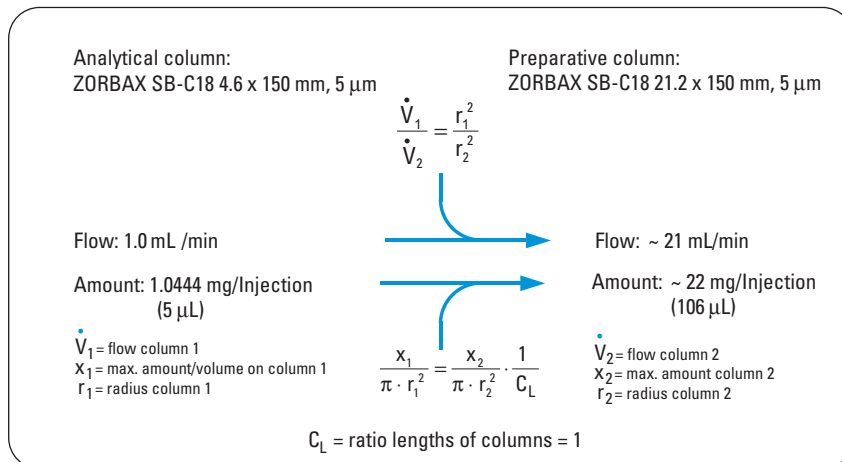


Figure 3
Scale-up calculations.

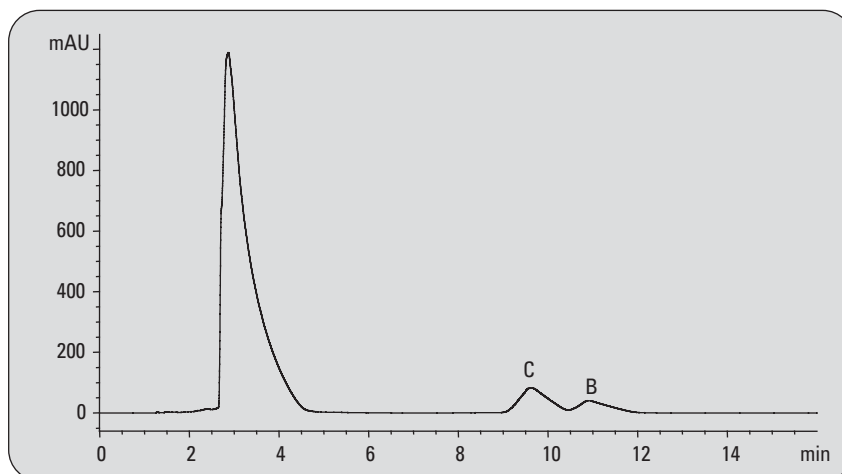


Figure 4
Run on preparative scale column according to the scale-up calculations

| | |
|------------------------------------|---|
| Chromatographic conditions: | |
| Column: | ZORBAX SB-C18 21.2 x 150 mm, 5 µm |
| Mobile phases: | Water + 0.1 % TFA = A Acetonitrile + 0.1 % TFA = B |
| Gradient: | at 0 min 25 % B at 14 min 32 % B at 16 min 50 % B |
| Stop time: | 16 min |
| Post time: | 5 min |
| Flow: | 21 mL/min |
| Injection: | 100 µL |
| Column temp.: | ambient |
| UV detector: | DAD 270 nm/30 (ref. 360 nm/100) Flow cell (3-mm path length) |

Purification parameters

To optimize the fraction collection parameters the *Fraction Preview* of the ChemStation was used.

As shown in figure 5, the chromatogram from the preparative run (figure 4) was loaded and the fraction collection parameters like threshold, up slope, down slope and upper threshold³ were adjusted until the desired fraction collection performance was achieved. In this case a simple threshold-based collection within a time window (9 – 14 minutes) gave the best result. The result of the actual fraction collection run with the parameters optimized using *Fraction Preview* is shown in figure 6.

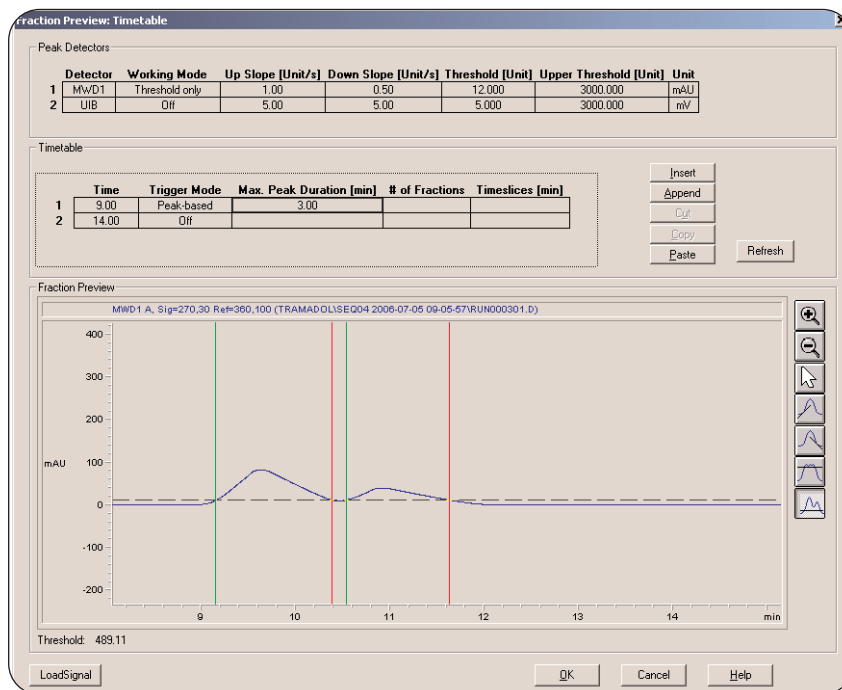


Figure 5
ChemStation *Fraction Preview*.

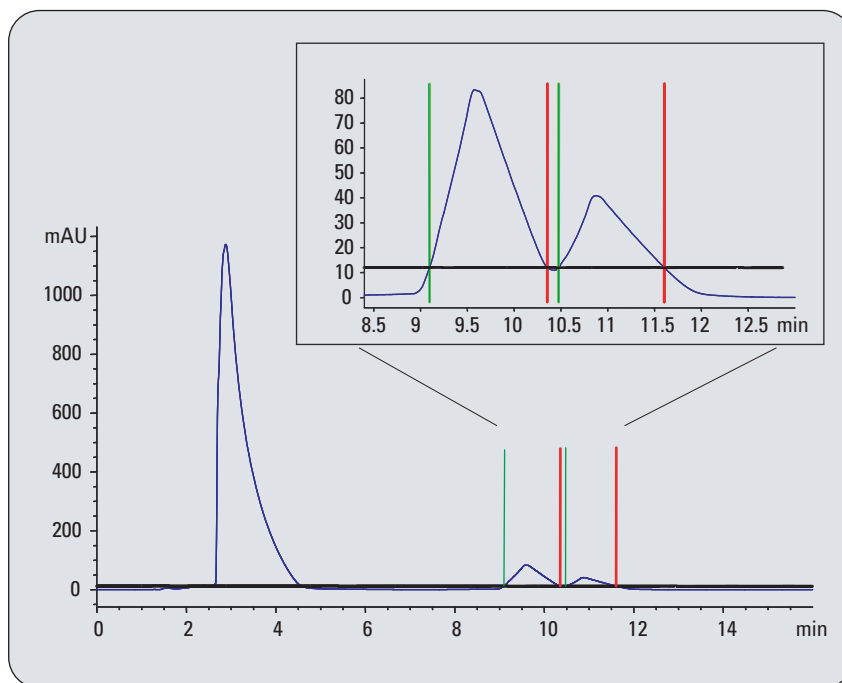


Figure 6
Result of fraction collection.

Since repetitive injections of the sample have to be done to acquire sufficient material for NMR analysis the pooling feature of the ChemStation could be used. With this feature the fractions of multiple injections are collected in the same fraction containers. In this case the volume of the fraction containers must be high enough to hold the combined volumes of all fraction collection runs. Therefore it is recommended to use the Agilent funnel tray for this application. The analysis (using the method shown in figure 1) of the combined fractions from ten consecutive purification runs is shown in figure 7. The structures as shown in figure 7 could be elucidated by NMR analysis (data not shown) after collecting sufficient pure material of impurities C and B.

Conclusion

In this Application Note the isolation and purification of two impurities was illustrated, beginning with a high-resolution analytical method that was developed on an Agilent 1200 Series RRLC system. The transfer to a standard Agilent 1200 Series and to an Agilent 1200 Series preparative system was seamless because the stationary phase was available with sub-2 μm particles in analytical column size as well as in standard 5- μm particles in preparative column sizes.

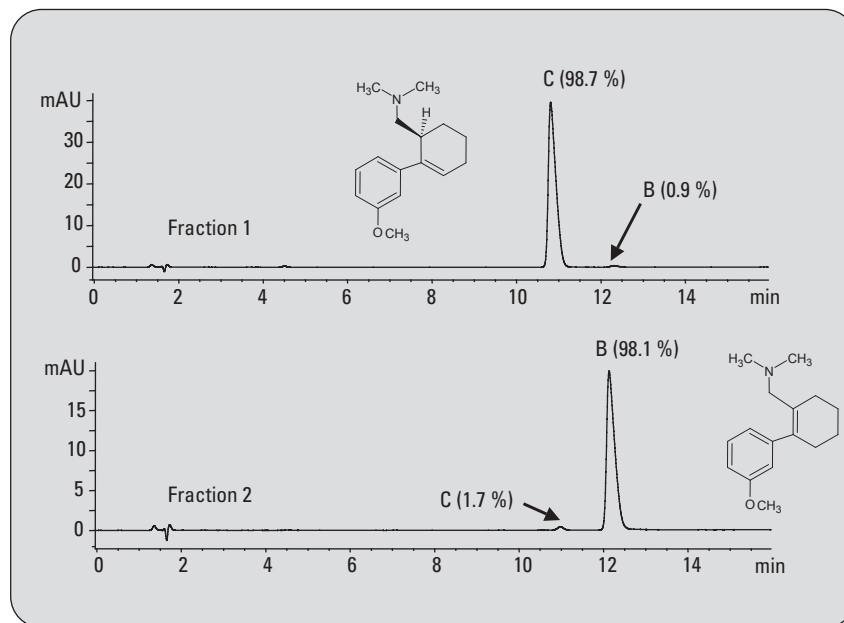


Figure 7
Identified impurities in the pharmaceutical drug synthesis of the main compound.

Therefore, the scale-up after the method optimization and loading experiments could be done directly and without any further method optimization on the preparative column. ChemStation features like the *Fraction Preview* and the automated pooling of fractions made it simple to achieve optimal purification results in a short time. The excellent purity and recovery of collected fractions made the structure elucidation of the impurities an easy task.

References

1.

Sándor Görög “New Safe Medicines Faster: The Role of Analytical Chemistry”, *Trends in Analytical Chemistry*, Vol. 22, Nos. 7+8, **2003**.

2.

Edgar Nägle “Impurity Profiling with the Agilent 1200 Series LC System: Part 1: Structure Elucidation of Impurities with LC/MS”, *Agilent Technologies Application Note*, publication number 5989-5617EN, **2006**.

3.

Udo Huber “Sophisticated Peak-based Fraction Collection – Working with Up and Down Slope”, *Agilent Technologies Application Note*, publication number 5989-0511EN, **2004**.

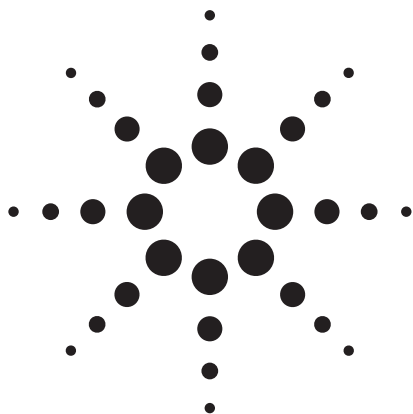
*Udo Huber is Senior Application
Chemist at Agilent Technologies,
Waldbronn, Germany.*

www.agilent.com/chem/purification

© 2006 Agilent Technologies, Inc.

Published October 1, 2006
Publication Number 5989-5618EN



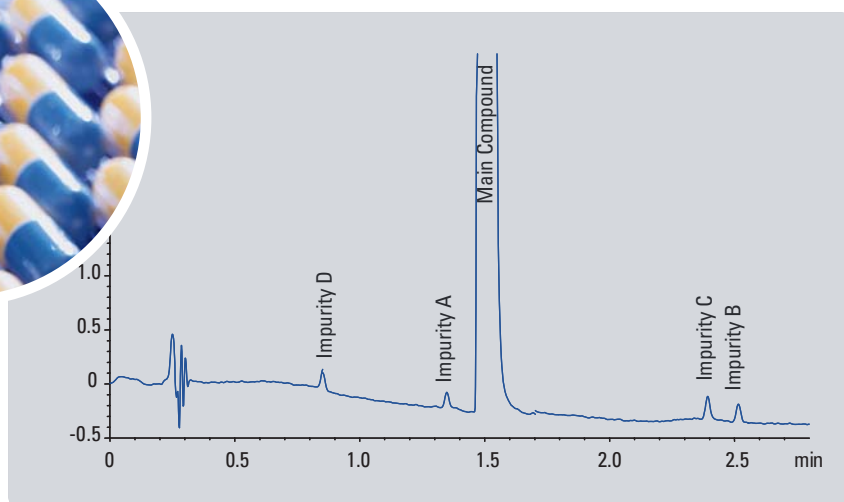
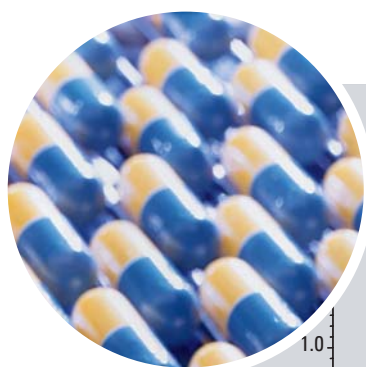


Impurity Profiling with the Agilent 1200 Series LC System

Part 3: Rapid Condition Scouting for Method Development

Application Note

Michael Frank



Abstract

Method development is one of the most time-consuming tasks in today's pharmaceutical analytical laboratories.¹ Usually, condition scouting is the first step followed by fine-tuning of the best set of parameters found. A means of speeding up the entire process by utilizing Agilent Rapid Resolution HT columns in combination with the Agilent 1200 Series Rapid Resolution LC (RRLC) system is described. How separation condition scouting and method fine-tuning resulted in a robust method for the quantization of diastereomeric and regioisomeric impurities of an active pharmaceutical ingredient within one and a half days is demonstrated. The final method not only is much faster than comparable conventional methods but also saves a significant amount of solvent.



Agilent Technologies

Introduction

Developing and validating new analytical methods is costly and time consuming. So, any means to reduce the run-time of each individual analysis is beneficial for the overall process, but no compromise in resolution, sensitivity, and especially robustness must be accepted. The availability of columns packed with sub-2 μm particles and the high quality of LC instruments required for more than 1000-fold applied methods, nowadays allows a significant acceleration in method development. At the outset often a broad scouting of separation conditions like stationary phases, mobile phase parameters (% B, buffer, pH, solvent) and operation parameters, such as gradient slope, temperature etc. are used to find the optimum starting point for fine tuning. In this Application Note we demonstrate the use of the Agilent 1200 Series Rapid Resolution LC (RRLC) system together with a variety of Agilent ZORBAX RRHT columns to search for separation conditions with run times below four minutes per analysis and yet the efficiency to get diastereomeric compounds and regioisomers separated.

Experimental

Instrumentation

- Agilent 1200 Series binary pump SL with an Agilent 1200 Series micro vacuum degasser.

- Agilent 1200 Series high performance autosampler SL with a thermostat.
 - Agilent 1200 Series thermostated column compartment SL.
 - Agilent 1200 Series diode-array detector SL. In this experiment 5 $\mu\text{L}/6\text{ mm}$ and 13 $\mu\text{L}/10\text{ mm}$ cells were used.
 - ZORBAX RRHT 1.8- μm particle columns with various stationary phases and dimensions.
- Gradient grade water from a Millipore device with different modifiers and different pH ranges was used as the mobile phase. Gradient grade acetonitrile and methanol from Merck, Darmstadt were used as the strong solvents. No additional filtering of the solvents was required. Instrument control and data acquisition were performed by the Agilent ChemStation B02.01 SR1 software.

Results and discussion

The objective of this method development was to provide a quick and robust method for quantization of production impurities of a pharmaceutical compound, which is a basic salt with a pKa of 9.4 and easily soluble in water, especially under acidic conditions. From previous experiments², it was known that the reactants (3-bromanisole and impurity E, see figure 1) could easily be detected by means other than HPLC, e.g. GC or TLC. Focus was placed on the separation of the diastereomeric impurity A and the regioisomeric dehydroxylation products B and C as well as on the demethylation product D. Structures have been elucidated by means of ion trap MS analysis, Time-of-Flight-MS analysis², and after preparative purification by NMR techniques².

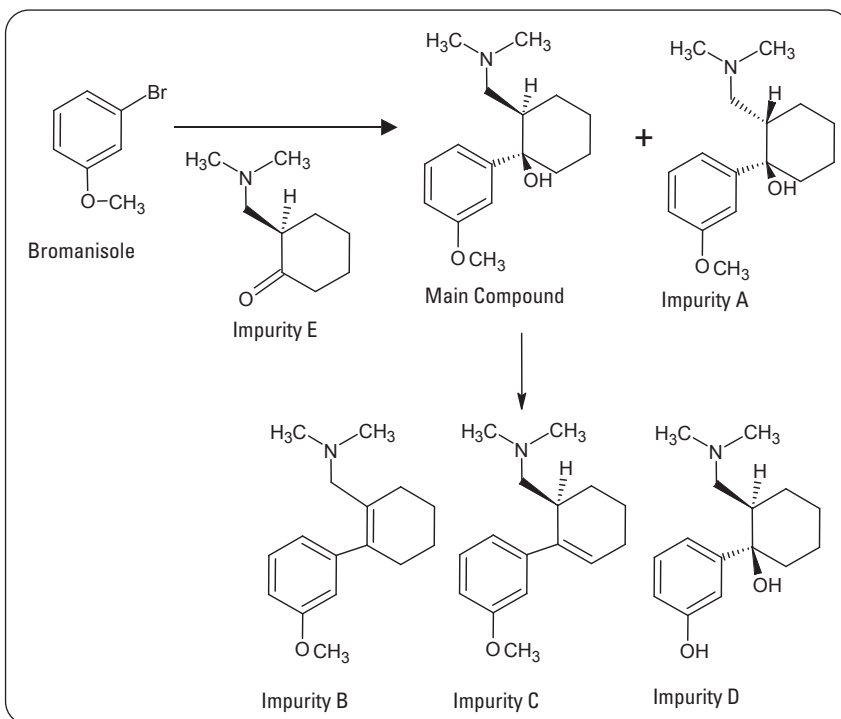


Figure 1
Structures of the by-products of the active pharmaceutical ingredient.

Comparison of the chromatograms at different wavelengths acquired by the diode-array detector led to the decision to choose 270 nm as the monitoring wavelength, because all compounds of interest had a strong absorption band at this wavelength (figure 2) and the baseline showed the fewest gradient shifts. As the main compound, as well as all impurities, had an excellent solubility in pure water, it was chosen as the solvent for dissolving the sample. Sample concentration was 0.7 mg/mL. At substantially higher concentrations, a severe tailing of the main compound could be seen due to overloading effects. During the initial condition scouting, an impurity enriched sample was used and a broad gradient of 5-95 % B was applied with a different set of stationary and mobile phases. All columns used were Agilent ZORBAX columns with a dimension of

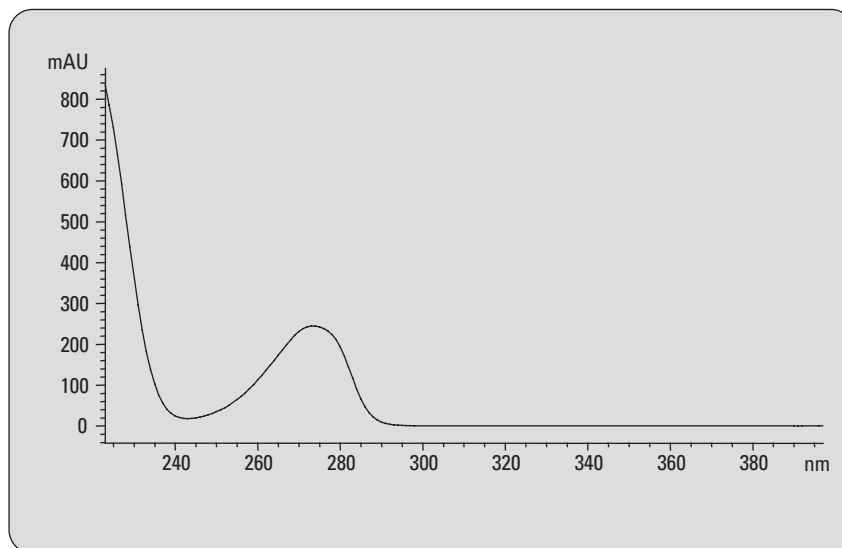


Figure 2
UV spectrum of the main compound.

50 mm x 3.0 mm ID and with a 1.8- μ m particle size. The pump was operated in the low delay volume configuration and the detector cell

was a 5 μ L/6 mm cell. Column temperature was set to 40 °C. The stationary and mobile phases used are listed in table 1 and the chro-

| Exp. Number | Stationary phase | pH | Mobile phase | Modifier | Comment |
|-------------|------------------|------|-----------------------|--------------------|--------------------------------------|
| 1 | SB CN | 1.92 | H ₂ O/ACN | TFA | 5-95 %B gradient, 40°C |
| 2 | Extend C18 | 1.92 | H ₂ O/ACN | TFA | 5-95 %B gradient, 40°C |
| 3 | XDB C18 | 1.92 | H ₂ O/ACN | TFA | 5-95 %B gradient, 40°C |
| 4 | XDB C8 | 1.92 | H ₂ O/ACN | TFA | 5-95 %B gradient, 40°C |
| 5 | SB C18 | 1.92 | H ₂ O/ACN | TFA | 5-95 %B gradient, 40°C |
| 6 | XDB C8 | 6.01 | H ₂ O/ACN | Phosphate-Buffer | 5-95 %B gradient, 40°C |
| 7 | XDB C18 | 6.01 | H ₂ O/ACN | Phosphate-Buffer | 5-95 %B gradient, 40°C |
| 8 | Extend C18 | 6.01 | H ₂ O/ACN | Phosphate-Buffer | 5-95 %B gradient, 40°C |
| 9 | SB CN | 1.92 | H ₂ O/MeOH | TFA | 5-95 %B gradient, 40°C |
| 10 | XDB C18 | 1.92 | H ₂ O/MeOH | TFA | 5-95 %B gradient, 40°C |
| 11 | Extend C18 | 1.92 | H ₂ O/MeOH | TFA | 5-95 %B gradient, 40°C |
| 12 | SB C18 | 1.92 | H ₂ O/MeOH | TFA | 5-95 %B gradient, 40°C |
| 13 | XDB C8 | 1.92 | H ₂ O/MeOH | TFA | 5-95 %B gradient, 40°C |
| 14 | SB CN | 6.01 | H ₂ O/ACN | Phosphate-Buffer | 5-95 %B gradient, 40°C |
| 15 | SB C18 | 6.01 | H ₂ O/ACN | Phosphate-Buffer | 5-95 %B gradient, 40°C |
| 16 | Extend C18 | 11.0 | H ₂ O/ACN | NH ₄ OH | 5-95 %B gradient, 40°C |
| 17 | SB C18 | 1.92 | H ₂ O/ACN | TFA | Transfer of Exp. 5 to 4.6mmID column |
| 18 | SB C18 | 1.92 | H ₂ O/ACN | TFA | 5-50 %B gradient, 40°C |
| 19 | SB C18 | 1.92 | H ₂ O/ACN | TFA | 15-50 %B gradient, 40°C |
| 20 | SB C18 | 1.92 | H ₂ O/ACN | TFA | 15-50 %B gradient, 20°C |
| 21 | SB C18 | 1.92 | H ₂ O/ACN | TFA | 15-50 %B gradient, 60°C |
| 22 | SB C18 | 1.92 | H ₂ O/ACN | TFA | 17-45%B gradient, 30°C, final method |

Table 1
Stationary and mobile phases used for the initial condition scouting and fine tuning (lower part).

matographic results (retention times and resolution of the critical pairs) are shown in figures 3 and 4. As expected, a change of selectivity by varying the mobile and/or the stationary phase had a dramatic effect on the chromatographic result. Choosing the wrong set of conditions could lead to the false impression that a rather simple mixture with just three components – one of them being the main compound – is present (for example phosphate buffer combined with the Extend C18 column). By changing the conditions, the regioisomers B and C start to separate (e.g. phosphate buffer using the ZORBAX XDB C18 column). Eventually the diastomeric impurity A and the main component also split up to reveal the actual five compounds present in this sample.

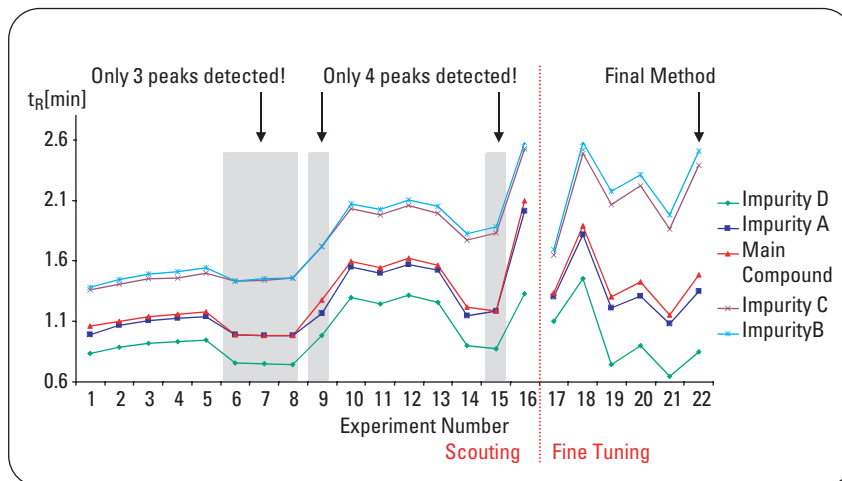


Figure 3
Retention times of the initial condition scouting and the fine tuning.

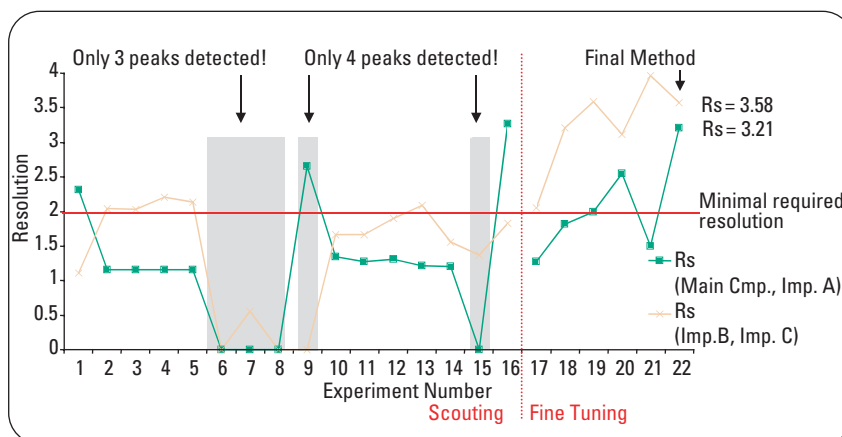


Figure 4
Resolution of the critical pairs of the initial condition scouting and the fine tuning.

Scouting method:

| | | |
|-------------------|--|---|
| Solvent: | (see table 1) | |
| Temperature: | 40 °C | |
| Flow: | 1.2 mL/min | |
| Gradient: | 0.00 min | 5 %B |
| | 3.00 min | 95 %B |
| | 3.50 min | 95 %B |
| Stop time: | 3.50 min | |
| Post time: | 1.00 min | |
| DAD: | Spectra | 190-500 nm (bandwidth 1nm), all spectra |
| | Signal A: | 270 nm (10 nm), ref. 500 nm (100 nm) |
| | Peak width: | >0.03 min (0.2 s response time) |
| | Slit: | 8 nm |
| | Balance: | pre-run |
| Injection volume: | 5 µL | |
| Injector: | Automatic delay volume reduction, Sample flush out factor = 20 Needle wash 10 s (methanol) | |

In figures 5 and 6 some examples are given to demonstrate the effect of changing the selectivity. Evaluation of the achieved retention times and resolutions from the different scouting runs demonstrates that, in general, the poorest results were obtained with weak acidic conditions (phosphate buffer). All retention times were shifted to higher values when using methanol as the strong solvent, due to its higher viscosity. In the search for the best starting point for the optimization, only conditions which did not have more than one critical pair with a resolution below 2 and none with a resolution close to zero were taken into account. Only the experiments 1-5, 13 and 16 remained. Experiment 16 yielded the best initial resolution, but also the highest retention times, and was therefore deferred (also because of the less favorable basic conditions). Experiment 13 exhibited higher retention times at comparable resolutions. Ultimately, one of a number of very similar experiments, 1 through 5, had to be selected for further optimization and fine tuning. Testing the Cyano-phase with a narrower gradient failed to significantly increase the resolution of the two regioisomeric impurities B and C. Since the differently bonded C18 stationary phases as well as the C8 stationary phase exhibited only minor differences, the StableBond C18 column was chosen for further fine tuning. Initially, the conditions of experiment 5 were transferred to a 4.6-mm ID column, which is the preferred column ID in a manufacturing QA/QC envi-

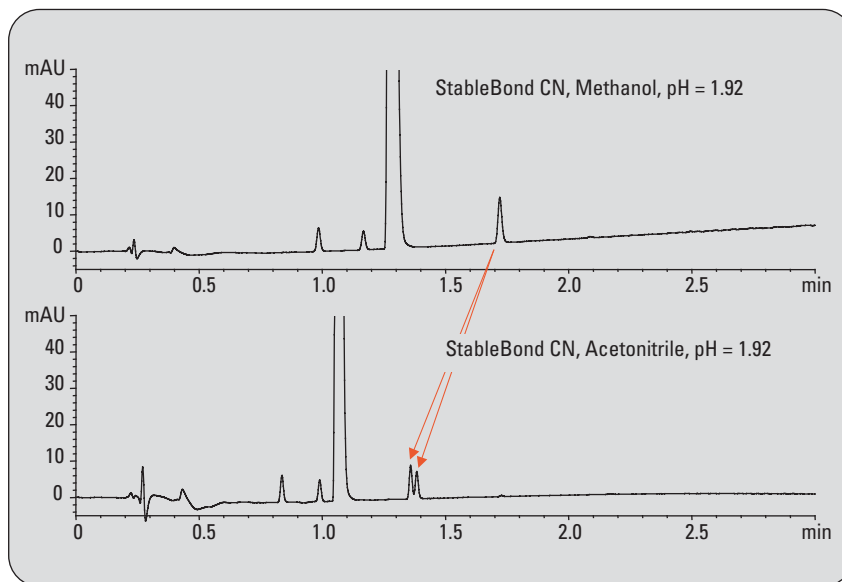


Figure 5
The regioisomers B and C appear as a single, perfect Gaussian-shaped peak using methanol as the strong solvent together with a StableBond CN column (upper trace). Just by switching to acetonitrile as the strong solvent, the two compounds split up.

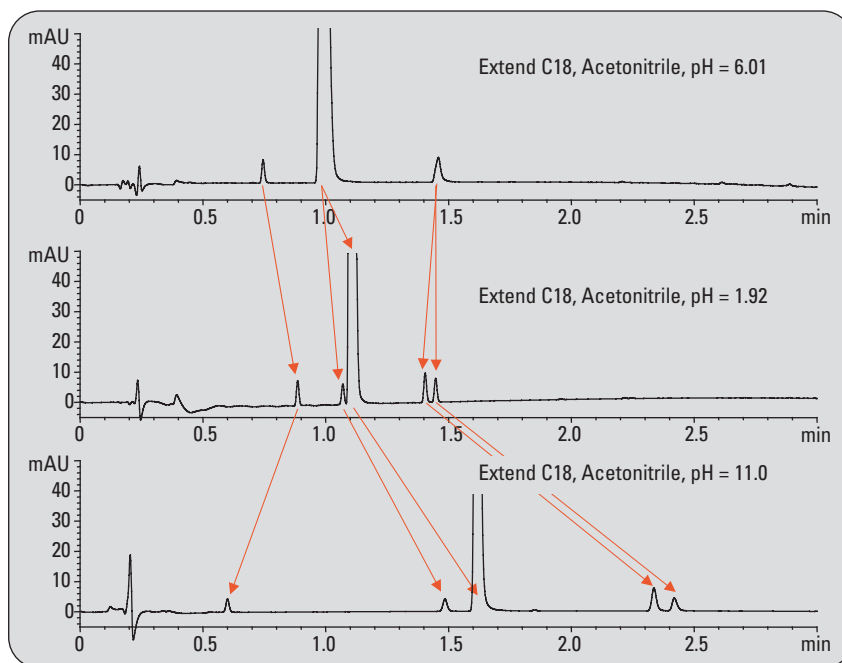


Figure 6
The effect of changing the pH is illustrated here using the ZORBAX Extend C18 column with acetonitrile as the strong solvent and phosphate buffer at pH = 6.0 in the upper trace, 0.2% TFA as acidic modifier in the middle trace (pH = 1.9) or 0.2% ammonia as the basic modifier in the bottom trace (pH = 11).

ronment. The transfer was made by geometrical scaling of the flow rate. In addition, the pump was operated in the standard delay volume configuration, the standard heat exchangers with 3 μ L internal volume were used, and a 13 μ L/10 mm cell was used in the diode-array detector. The resolutions remained practically constant, whereas a slight increase of the retention times could be detected due to the additional delay volume of the mixer and damper. The gradient range was narrowed and also the effect of different temperatures was explored to fine-tune the method (figures 3 and 4).

Unfortunately, varying the temperature achieved an opposite effect on the two critical pairs. When lowering the temperature, the resolution between impurity A and the main compound increased, however it decreased between the two regioisomers B and C. Increasing the temperature produced a better resolution for the regioisomers, but a worse resolution between impurity A and the main compound. It was decided to use 30 °C as a compromise. A resolution of more than three could be achieved for all compounds with the final method by applying a 17- 45 % acetonitrile gradient in water at pH = 1.92 (0.2 % TFA) in 2.8 min with a hold of 0.2 min at 45 % B, using a ZORBAX StableBond C18 column (50 mm x 4.6 mm ID,

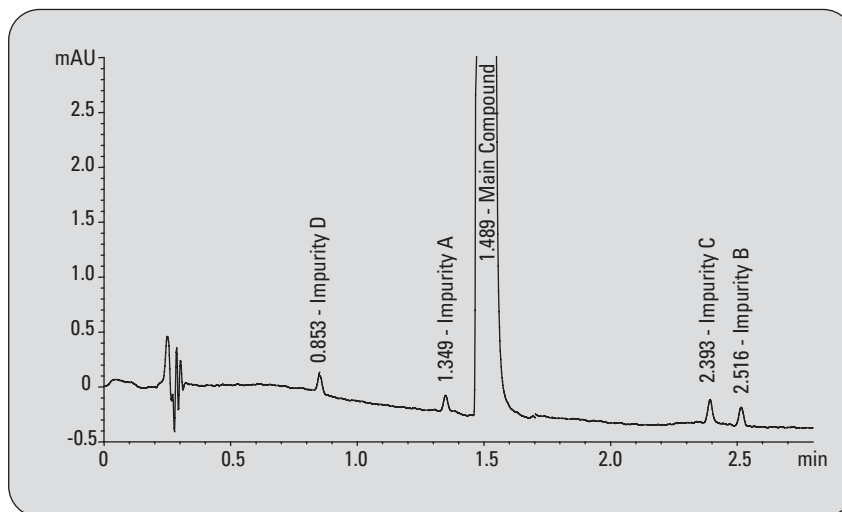


Figure 7
Applying the final method conditions to a sample containing impurities at the lower reporting level (0.05 % of main compound).

| Final method: | |
|-------------------|---|
| Solvent: | A = Water (0.2 volume.-% TFA), B = acetonitrile (0.16 volume.-% TFA) |
| Temperature: | 30 °C |
| Flow: | 2.2 mL/min |
| Gradient: | 0.00 min 17 %B 2.80 min 45 %B 3.00 min 45 %B |
| Stop time: | 3.00 min |
| Post time: | 1.00 min |
| DAD: | Spectra 190-500 nm (bandwidth 1nm), all spectra Signal A: 270 nm (8 nm), ref. 500 nm (100 nm) Peak width: >0.03 min (0.2 s response time) Slit: 8 nm Balance: pre-run |
| Injection volume: | 5 μ L |
| Injector: | no automatic delay volume reduction, Needle wash 10 s (methanol) |

1.8 μ m), at a temperature of 30 °C (figure 7). Table 2 lists some characteristic values for the separation of a sample containing impurities at the lower reporting level (0.05 % of main compound). This method

was then validated and checked for its robustness⁴ before being made available for analyzing samples in the manufacturing QA/QC environment⁵.

| Compound | Time [min] | Resolution | Area [mAU · s] | Height [mAU] | Width [s] | Area [%] | Mass [ng] |
|---------------|------------|------------|----------------|--------------|-----------|----------|-----------|
| Impurity D | 0.853 | --- | 0.25 | 0.180 | 1.30 | 0.050% | 1.76 |
| Impurity A | 1.349 | 15.96 | 0.23 | 0.150 | 1.38 | 0.046% | 1.62 |
| Main Compound | 1.489 | 3.21 | 497.10 | 222.200 | 2.11 | 99.791% | 3492.69 |
| Impurity C | 2.393 | 19.83 | 0.33 | 0.220 | 1.36 | 0.066% | 2.32 |
| Impurity B | 2.516 | 3.58 | 0.23 | 0.170 | 1.27 | 0.046% | 1.62 |

Table 2
Characteristic values of the separation of a sample containing impurities of the main compound at the lower reporting level.

Conclusion

The method development time for the demanding separation of diastereomeric and regioisomeric impurities of an active pharmaceutical ingredient could be dramatically reduced by using sub-2 μm particle columns for condition scouting and method fine-tuning. Since rather short scouting runs of 4.5 min cycle time were required, a large set of conditions could be tested merely within a day (including replicates and blanks). Additional fine-tuning lasted another half day, so after just one and a half days a method could be provided for subsequent method validation, which was also dramatically reduced in time⁴ due to the short individual run time of 4.0 min per analysis with the final method. Also keep in mind the numerous later analyses in the manufacturing QA/QC lab. During the many years of compound-production analysis time is also reduced to a fraction of old-fashioned methods, resulting in a constantly shorter release time of the product, saved storage costs of intermediates, making reactors earlier available for other production campaigns and saved solvent costs per analysis because just 8.8 mL mobile phase are consumed per analysis.

References

1. Michael W. Dong, “Modern HPLC for Practicing Scientists”, Wiley Interscience, ISBN0-471-72789-X, **2006**.
2. Edgar Nägele “Impurity Profiling with the Agilent 1200 Series LC System – Part 1: Structure Elucidation of Impurities” *Agilent Application Note, publication number 5989-5617EN*, **2006**.
3. Udo Huber “Impurity Profiling with the Agilent 1200 Series LC System – Part 2: Isolation of Impurities with Preparative HPLC” *Agilent Application Note, publication number 5989-5618EN*, **2006**.
4. Angelika Gratzfeld-Huesgen “Impurity Profiling with the Agilent 1200 Series LC System, Part 4: Method Validation of a Fast LC Method” *Agilent Application Note, publication number 5989-5620 EN*, **2006**.
5. Angelika Gratzfeld-Huesgen “Impurity Profiling with the Agilent 1200 Series LC System Part 5: QA/QC Application Example with Complete Sequencing” *Agilent Application Note, publication number 5989-5621EN*, **2006**.

*Michael Frank is Application
Chemist at Agilent Technologies,
Waldbronn, Germany.*

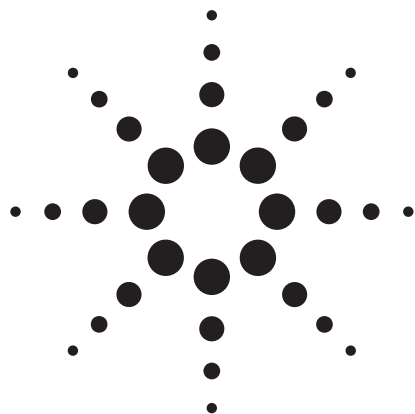
www.agilent.com/chem/1200rr

© 2006 Agilent Technologies, Inc.

Published October 1, 2006
Publication Number 5989-5619EN



Agilent Technologies

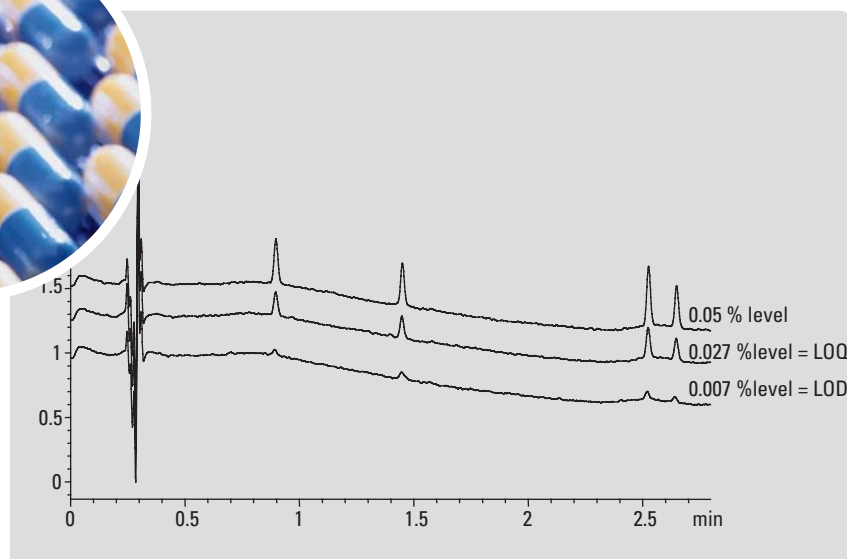
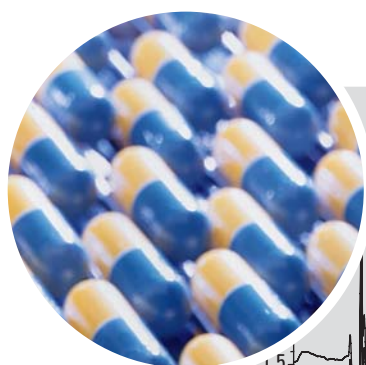


Impurity Profiling with the Agilent 1200 Series LC System

Part 4: Method Validation of a Fast LC Method

Application Note

A. G. Huesgen



Abstract

Analytical laboratories working in a regulated environment have to validate their methods, to ensure that results fulfill all regulatory requirements. The validation procedure introduced in this Application Note was based on recommendations from the U.S. Pharmacopeia (USP) and the ICH guidelines Q2B respectively. A fast LC method for one main compound and its four impurities is successfully validated.



Agilent Technologies

Introduction

Analytical laboratories working in a regulated environment must validate their methods in order to ensure that the results fulfill all regulatory requirements. In addition, the results from different users in different laboratories are comparable, even though separate equipment was used. Consequently, the method is required to be as robust as possible to compensate for variations, which might occur if different users perform the same analysis on the same or different equipment. The validation procedure introduced in this Application Note was based on recommendations from the U.S. Pharmacopeia (USP), ICH guidelines Q2B^{1,2}, as well as FDA guidelines^{4,5}, which are recognized worldwide and employed by analytical laboratories in the pharma, food, environmental and chemical industry. In the following experiment, a fast LC method for one main compound and its impurities is validated, (see figure 1 for a sample chromatogram). Method parameters were obtained from the method development group (reference 3).

Experimental

An Agilent 1200 Series Rapid Resolution LC system was used with the following modules:

- Agilent 1200 Series binary pump SL and vacuum degasser
- Agilent 1200 Series high-performance autosampler SL
- Agilent 1200 Series thermostated column compartment SL

- Agilent 1200 Series diode-array detector SL
- Data acquisition and evaluation software: Agilent ChemStation B.02.01.SR1
- ZORBAX SB C-18 RRHT columns with internal diameters of 4.6 mm and lengths of 50 mm, packed with 1.8- μ m particles
- Main compound and pure impurities were obtained using the purification procedure described in reference 6.

Validation procedure

Having done some pre-validation experiments, the following validation protocol for the above-described method³ was set up:

Validation protocol :

| | |
|---|--|
| 1. Precision of areas and RT of the main compound | 6 concentrations, 6 runs each |
| 2. Accuracy of main compound | 6 concentrations, 6 runs each |
| 3. Linearity of main compound | 6 concentrations, 6 runs each |
| 4. Carry over for main compound | 3 injections of stock solution |
| 5. Range of main compound | |
| 6. Precision of areas and RT of impurities | 7 concentrations, 6 runs each |
| 7. Accuracy of impurities | 7 concentrations, 6 runs each |
| 8. Linearity of impurities | 7 concentrations, 6 runs each |
| 9. Range of impurities | |
| 10. Limit of Detection and LOQ | |
| 11. Robustness of main compound and impurities | Different column temperatures, flow rates, injection volumes, TFA concentrations, gradient steepness, wavelength, users and instruments, no ruggedness tests |

Specificity was tested and is given, see reference 3. No further sample preparation steps were taken. The sample compounds were weighed and dissolved in water.

Results and discussion

Validation of main compound

Sample preparation:

The stock solution of the main compound contained 2.3 mg/mL. This solution was diluted to give the following desired concentrations:

Main compound:

- Stock solution: 2.3 mg/mL (used for carry over and linearity tests)

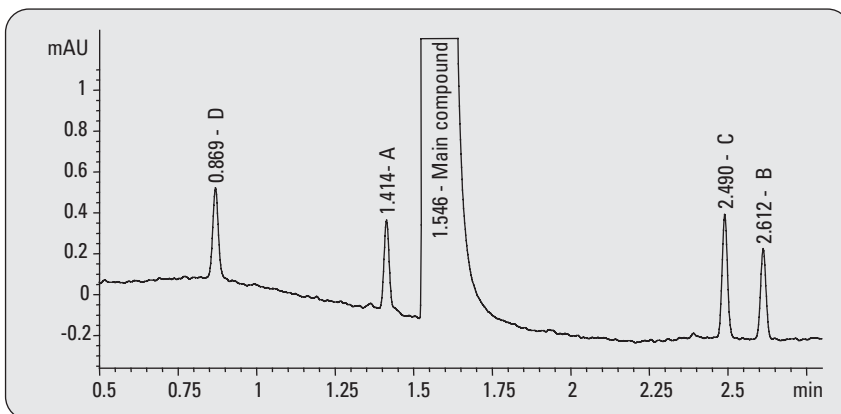


Figure 1
Analysis of the main compound and its 4 impurities. Main compound 1.15 mg/mL, impurities 0.072 % of the main compound.

- Dilution 1: 1.15 mg/mL (used for precision, accuracy, linearity and robustness tests)
- Dilution 2: 0.575 mg/mL (used for precision, accuracy, linearity test)
- Dilution 3: 0.288 mg/mL (used for precision, accuracy, linearity test)
- Dilution 4: 0.144 mg/mL (used for precision, accuracy, linearity test)
- Dilution 5: 0.072 mg/mL (used for precision, accuracy, linearity test)

1. Precision of retention times and areas

The results for retention time and area precision for all different concentration levels are summarized in figure 2. The precision limit for retention times is 0.1 % rsd. The precision limit for areas is 2 % rsd. For all concentrations the limits for retention time and area precision are fulfilled. To achieve sufficient resolution from the impurities, the concentration of the main compound should be <1.2 mg/mL.

2. Accuracy of main compound

The accuracy was tested using the above-mentioned concentrations. A maximum deviation of 2 % was set as the limit. All concentrations passed the requirement, (figure 3).

3. Linearity for main compound

The linearity was tested using all 6 concentrations. A correlation coefficient of > 0.99990 was set as the limit for this concentration range. The determined correlation coefficient was 0.99999. The response factors are within the 5 % limit from 2.3 down to 0.073 mg/mL (figure 4).

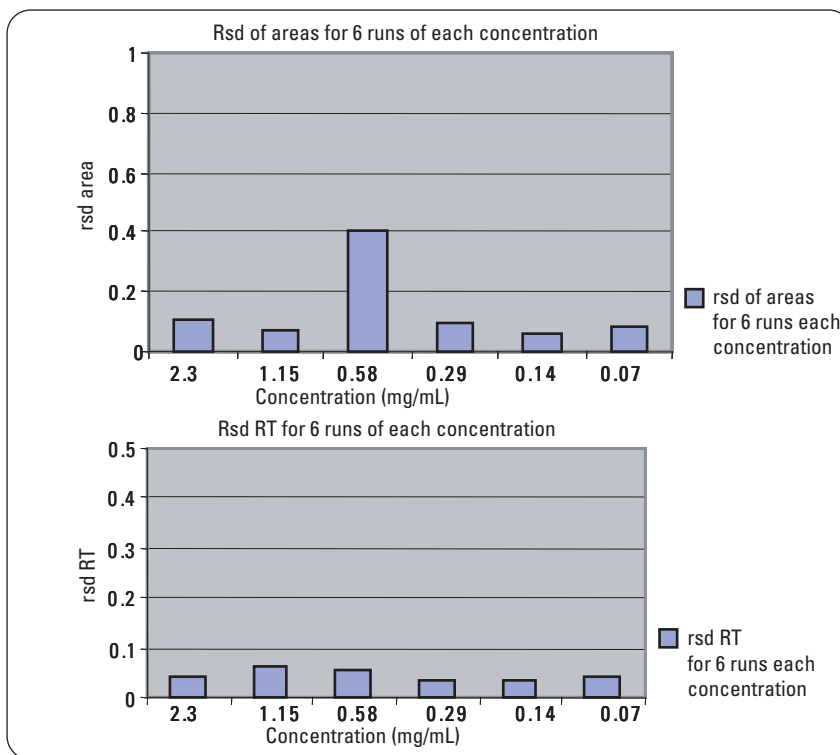


Figure 2
Precision of retention times and areas of different concentrations of the main compound; 6 runs for each concentration.

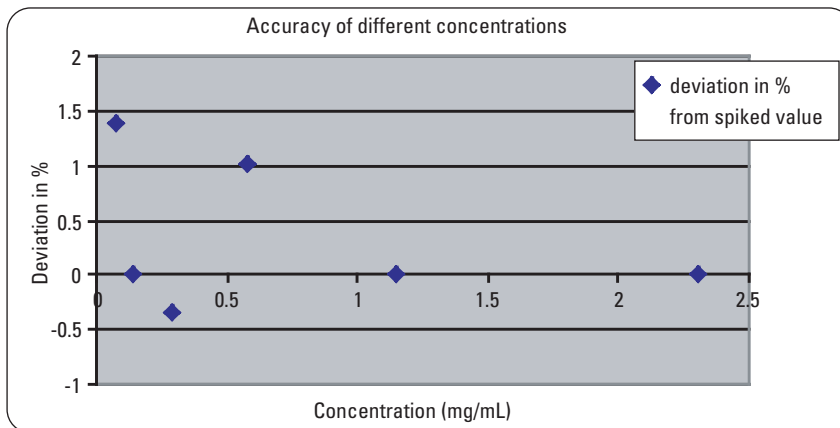


Figure 3
Accuracy for different concentrations of the main compound, 6 runs for each concentration.

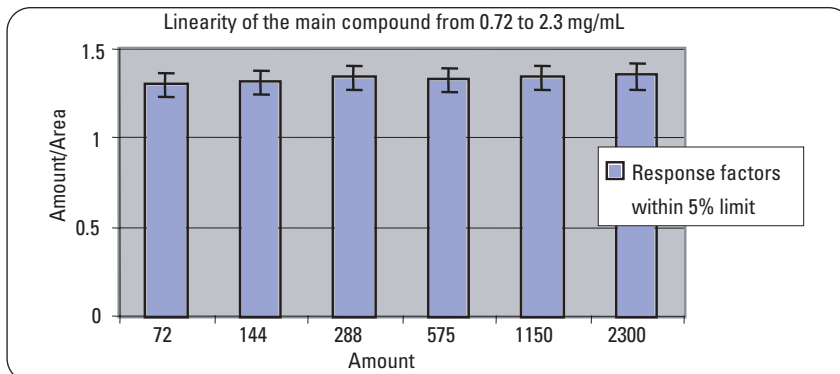


Figure 4
Linearity of the main compound.

4. Carry-over of main compound

The carry-over was evaluated by injecting the stock solution 6 times followed by the injection of 5 μL pure water. The carry-over was found to be $\sim 0.01\%$.

5. Range of main compound

The range for the main compound with good precision, accuracy and linearity lies between 2.3 down to 0.073 mg/mL.

Validation of impurities A, B, C, and D

Sample preparation

The impurities were analyzed by preparing different concentration levels using the pure impurity compounds. The stock solution contained 4.9 mg/mL for impurity A, C, and D and 4.6 mg/mL of compound B. This solution was diluted by a factor of 1:1000 to obtain a concentration in the $\mu\text{g/mL}$ range. The performance was evaluated for 7 impurity concentrations based on the diluted mixtures, see table 1.

6. Precision of retention times and areas of impurities

Precision of areas was evaluated for 6 concentrations from 0.153 up to 4.9 $\mu\text{g/mL}$ for compounds A, C and D, and from 0.144 to 4.6 $\mu\text{g/mL}$ for compound B. Precision of retention times was evaluated for all 7 concentrations. A summary of all results is shown in figure 5. The 0.05 % level fulfilled the acceptable limit of $< 5\%$ rsd for areas. The 0.027 % level showed an area precision $< 6\%$ rsd, which is within the 10 % limit. The 0.013 % level showed an area precision of $< 14\%$, which is acceptable for this low concentration. Retention time precision is below 0.5 % rsd for all

| Impurity | Dilution 6 $\mu\text{g/mL}$ (% level)* | Dilution 5 $\mu\text{g/mL}$ (% level)* | Dilution 4 $\mu\text{g/mL}$ (% level)* | Dilution 3 $\mu\text{g/mL}$ (% level)* | Dilution 2 $\mu\text{g/mL}$ (% level)* | Dilution 1 $\mu\text{g/mL}$ (% level)* | Stock solution $\mu\text{g/mL}$ (% level)* |
|----------|--|--|--|--|--|--|--|
| A | 0.077 (0.007%) | 0.153 (0.013%) | 0.306 (0.027%) | 0.613 (0.05%) | 1.225 (0.107%) | 2.45 (0.213%) | 4.9 (0.426%) |
| B | 0.072 (0.006%) | 0.144 (0.013%) | 0.287 (0.025%) | 0.575 (0.05%) | 1.150 (0.1%) | 2.30 (0.2%) | 4.6 (0.4%) |
| C | 0.077 (0.007%) | 0.153 (0.013%) | 0.306 (0.027%) | 0.613 (0.05%) | 1.225 (0.107%) | 2.45 (0.213%) | 4.9 (0.426%) |
| D | 0.077 (0.007%) | 0.153 (0.013%) | 0.306 (0.027%) | 0.613 (0.05%) | 1.225 (0.107%) | 2.45 (0.213%) | 4.9 (0.426%) |

* Percentage is based on a main compound concentration of 1.15 mg/mL

Table 1
Dilution series for impurities.

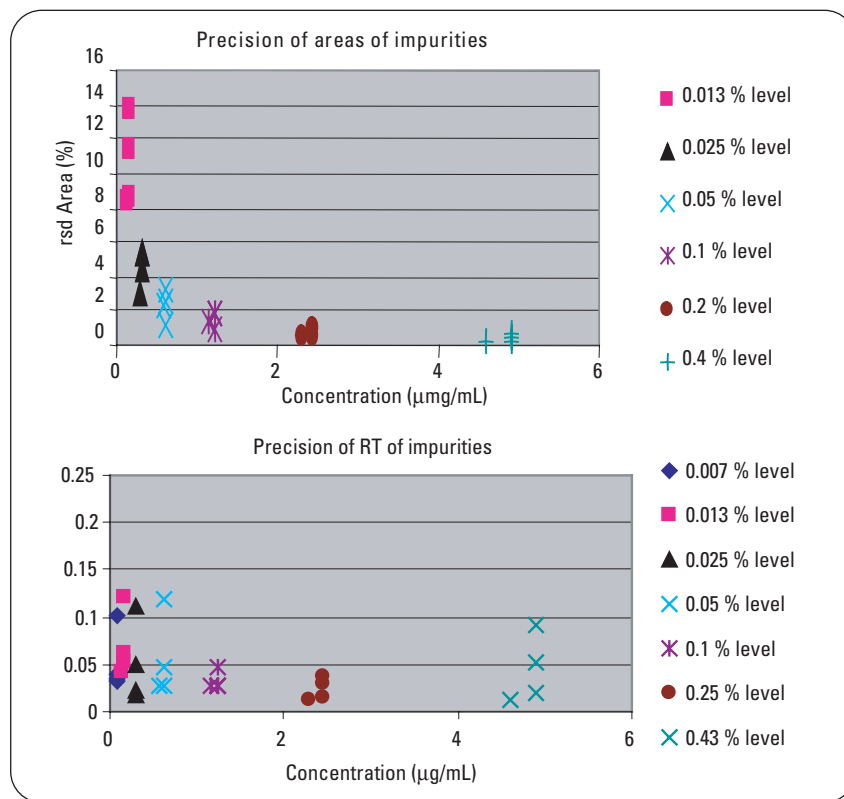


Figure 5
RSD of retention times and areas for impurities; 6 runs for each concentration .

concentrations and passed the set limit of $\text{rsd} < 0.5\%$. An example of the precision of retention times and areas is shown in figure 6. Ten chromatograms from 10 consecutive runs were superimposed and the precision of retention times is for all compounds $< 0.16\%$.

7. Accuracy of impurities

Accuracy of impurities was evaluated for the 0.027%, 0.05%, 0.107% and 0.213% level of impurities A, C and D. The 0.025%, 0.05%, 0.1% and 0.2% level of impurity B was evaluated. Spiked samples with known concentrations were analyzed and data were evaluated using auto-integration and the calibration parameters used for precision measurements. The deviation from the spiked value should not be more than $\pm 5\%$. The maximum deviation is $\pm 4.3\%$ for the determined concentration ranges (figure 7). Each concentration was injected 6 times and the average value was used as the calculated amount.

8. Linearity of impurities

The linearity of all impurities was tested using all 7 concentration levels. A correlation coefficient of > 0.9990 was set as the limit for this concentration range. The established correlation was 0.9998. Linearity based on the response factors is calculated between 4.9 $\mu\text{g/mL}$ (impurities A, C, and D), 4.6 $\mu\text{g/mL}$ (impurity B) down to 0.306 $\mu\text{g/mL}$ (impurities A, C, and D), and 0.287 $\mu\text{g/mL}$ (impurity B); an example is given in figure 8. The response is within the 5% limit for these concentration ranges.

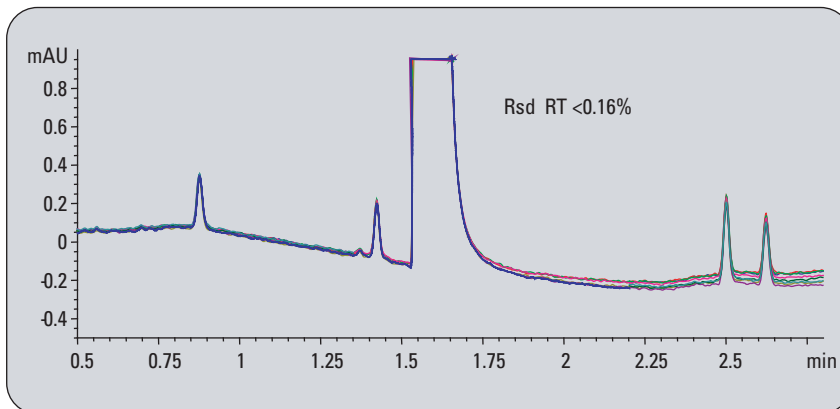


Figure 6
Overlay of 10 chromatograms within 1 sequence, RSD RT for all peaks $< 0.16\%$.

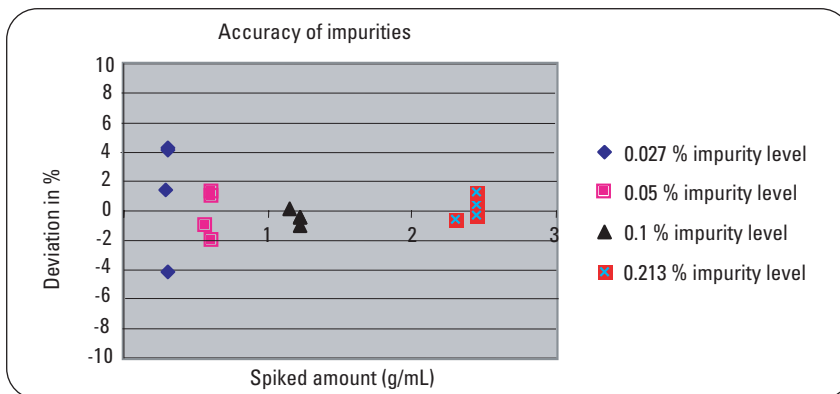


Figure 7
Determination of accuracy of impurities A, B, C, and D. 6 runs for each concentration with maximum deviation $\pm 4.5\%$ for the 0.027% level.

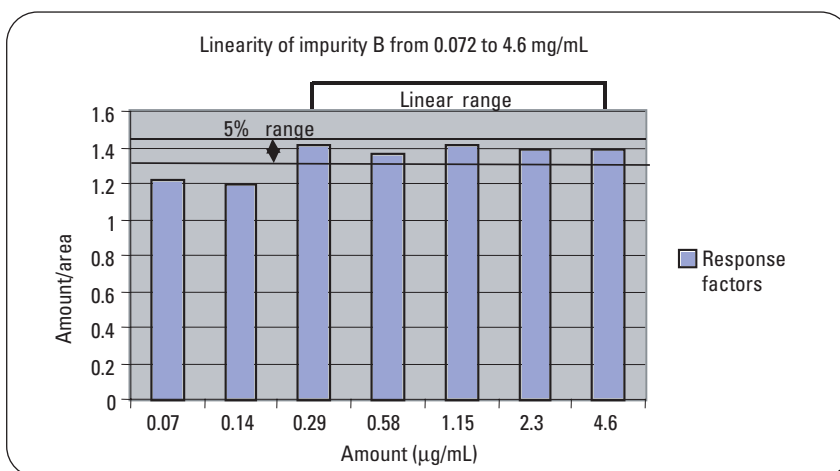


Figure 8
Linearity of impurity B across a concentration range between 0.077 to 4.9 $\mu\text{g/mL}$.

9. Range of impurities

The range of impurities with an acceptable precision, accuracy and linearity is between 0.306 µg/mL (0.287 µg/mL impurity B) and 4.9 µg/mL (4.6 µg/mL impurity B).

10. Limit of detection (LOD) and limit of quantitation (LOQ) for impurities

The limit of detection was determined using the 0.007 % level of compounds A, C and D. For compound B the 0.006% level was used. In figure 9 the resulting chromatogram, lower trace, is shown. All impurities at that concentration level have a signal to noise ratio S/N > 2 (table 2).

In figure 9 chromatograms of 2 further concentration levels for the impurities related to the main compound concentration of 1.15 mg/mL are shown. The trace in the middle shows the 0.027 % level (impurities A, C and D) and the 0.025 % level (impurity B), which is the limit of quantitation, and the upper trace shows the 0.05 % level. In table 2 the results for LOD and LOQ are summarized. The limit of quantitation was evaluated for the 0.027 and the 0.025 % concentration levels respectively. The signal to noise ratio limit for the LOQ is 10 and the values shown for the 0.027 and 0.025 % levels are proximate. The 0.05 % is clearly above the set limit. The area precision for the 0.05 % level is < 2.6 %, and for the 0.027 and 0.025 % levels the area precision is < 5.4 %.

11. Robustness of method for main compound and its impurities

To test the robustness of the method, the main compound was dissolved in water with a concen-

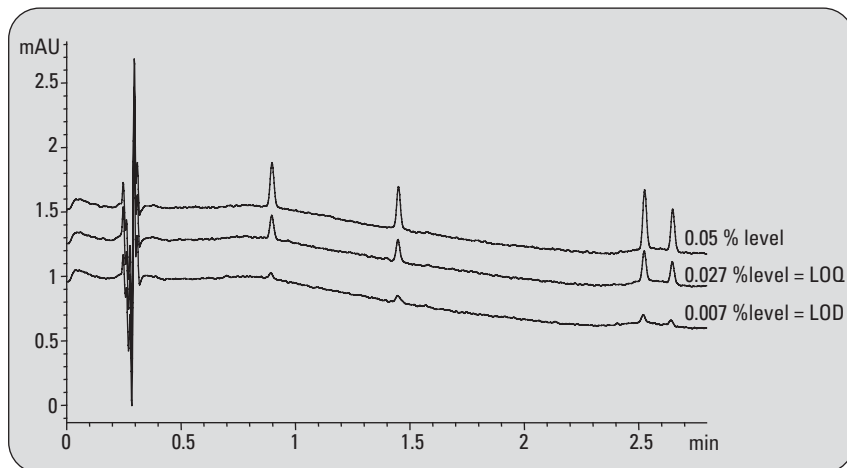


Figure 9
Chromatogram of impurities close to the limit of detection at the 0.007 % level (lower trace). The trace in the middle shows the chromatogram at the 0.027 % level, close to the limit of quantitation. The upper trace shows a chromatogram of the 0.05 % level.

| Impurity concentration | LOD | S/N | LOQ | S/N |
|------------------------|---------------|-----|---------------|------|
| A | 0.007 % level | 2.8 | 0.027 % level | 9.5 |
| B | 0.006 % level | 2.1 | 0.025 % level | 9.1 |
| C | 0.007 % level | 3.8 | 0.027 % level | 13.1 |
| D | 0.007 % level | 3.4 | 0.027 % level | 10.1 |

Table 2
LOD and LOQ for impurities.

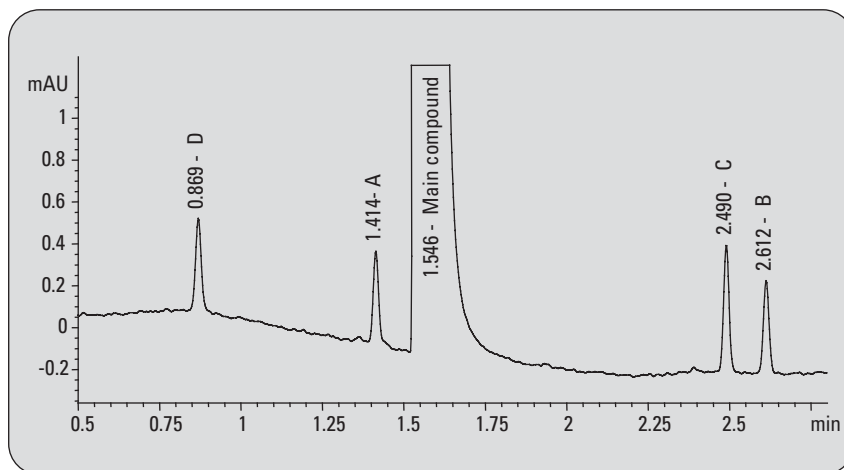


Figure 10
Chromatogram of sample used for robustness tests.

tration of 1.15 mg/mL. This solution was spiked with impurities to achieve an impurity concentration level of approximately 0.07 %

(figure 10). In table 3 the results for the main compound and impurities are summarized. The only critical parameter is the

wavelength. The wavelength should not vary more than 1 nm. All other parameter changes cause deviations for the areas of less than 2 %, which is acceptable for a main compound. The results for the impurities are also shown in table 3. All results except the wavelength change are within the 10 % limit for the areas. The wavelength should not vary more than 1 nm.

In figure 11 an example is shown for the day-to-day repeatability for retention times and areas. The results of 3 sequences are overlaid. Each sequence contained 10 runs and were analyzed on 3 consecutive days. The instrument was turned off overnight.

| Parameter changed | Deviation of amounts for the main compound (9%) | Resolution between main compound and impurity A | Deviation of amounts (%) for impurities (spiked amounts fig. 10) |
|---|---|--|--|
| Flow \pm 2 % | 1.96 % rsd | 2.56 for + 2 % change 2.55 for - 2 % change | < 9.8 % rsd for amounts |
| Column temperature \pm 5 % | 0.17 % rsd | 2.61 for 5 % change | < 5 % rsd for amounts |
| Gradient slope \pm 10 % | 0.07 % rsd | 2.59 for + 10 % change 2.51 for - 10 % change | < 3 % rsd for amounts |
| Injection volume \pm 5 % | 0.001 % from expected amount | 2.45 for + 5 % change 2.62 for - 5 % change | 6.5 % from expected amount |
| TFA concentration \pm 10 % | 0.07 % rsd | 2.49 for -10 % change 2.61 for +10 % change | < 4 % rsd for amounts \pm 18 % for area counts |
| Wavelength \pm 3 nm | \pm 10 % for area counts | 2.61 | \pm 18 % for area counts |
| Day-to-day repeatability | 0.34 % rsd for retention times | 2.60-2.63 | < 0.6 % for retention time |
| Day-to-day repeatability | 0.35 % rsd for amounts and 1.15 mg/mL weighted sample | 2.60 – 2.63 | < 4.5 % for amounts |
| 3 different instruments, \pm 0.47 % deviation different columns, intermediate precision | for 1.15 mg/mL | 2.6 -3.1 | \pm 10 % for 0.025 % level for amounts \pm 4.5 % for 0.05 % level for amounts |

Table 3
Robustness test results for main compound and impurities.

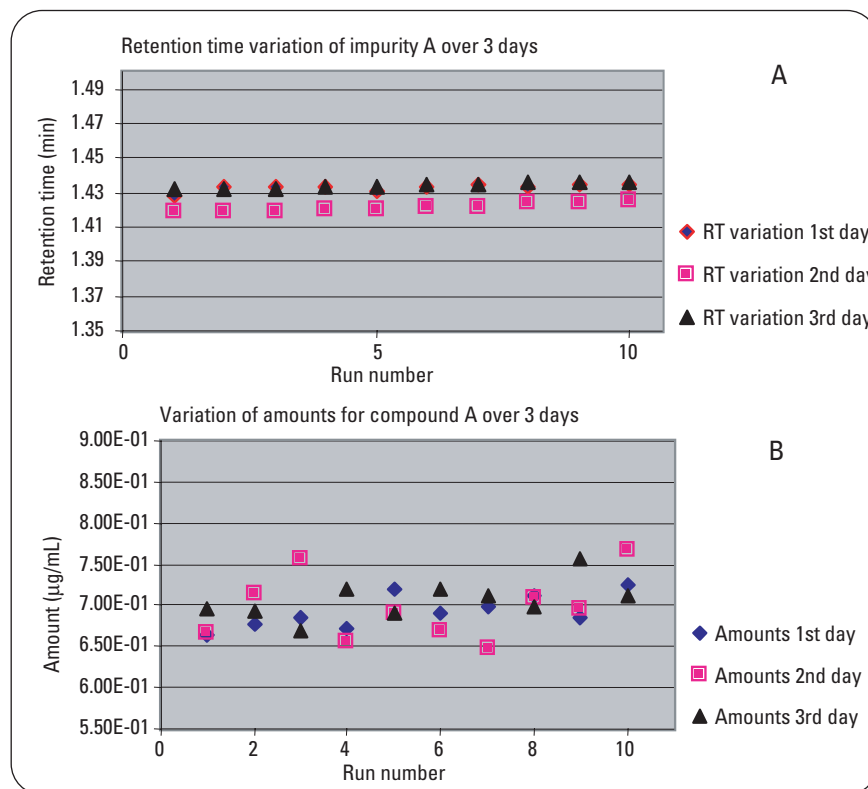


Figure 11
Day-to-day precision of retention times and areas, overlay of 3 sequences with 10 runs each. Repeatability of retention time day-to-day (figure 11a) < 0.6 %, repeatability for areas < 4.5 %, difference between highest and lowest amount < 16 % for the amounts (figure 11b).

Results of method validation

In table 4 the results of the method validation are summarized. The set limits are fulfilled. Special attention is required for the wavelength. The wavelength variation should not be more than ± 1 nm. Typically, a wavelength variation of ± 3 nm is considered acceptable. In this experiment, the limits for wavelength variations are more restrictive, based on the results.

Conclusion

A fast LC method was developed for the analysis of a main compound and four impurities. The validation of this method was successful. All requirements regarding precision, linearity, accuracy and robustness were fulfilled. This signifies that the fast LC method can be used in QA/QC labs and is compliant with USP/ICH recommendations. Faster LC methods provide the same data quality and, as an additional benefit, higher sample throughput.

References

1. International Conference on Harmonization (ICH) Q2B. Validation of Analytical Procedures: Methodology; Nov. 1996, published in the "Federal Register", Vol 62, No. 96, pages 27463-27467, May 19, 1997.
2. Internet Resources: <http://fda.gov/cder/guidance/index.htm> and <http://www.labcompliance.com>, Dr. Huber's website

| Parameters | |
|---|---------|
| Precision for areas | |
| • Main compound < 2 % for all experiments | passed |
| • Impurities < 10 % at the limit of quantitation | passed |
| Accuracy for main compound < ± 2 % | passed |
| Accuracy for impurities at LOQ ± 5 % | passed |
| Precision of Retention times < 0.5 % within 1 series | passed |
| Precision of retention time < 2 % day-to-day | passed |
| Linearity > 0.999 | passed |
| Resolution > 2 for all peaks | passed |
| LOD S/N > 2 at the ~ 0.007 % level for impurities | passed |
| LOQ S/N > 10 at the ~ 0.027 % level for impurities | passed |
| Range of the main compound: 2.3 to 0.073 mg/mL | passed |
| Range of the impurities: 4.9 (0.426 % level) to 0.287 μ g/mL (0.025 % level) | passed |
| Robustness tests for area deviation: < 2 % for main compound | passed* |
| Robustness tests for area deviation: < ± 5 % for impurities at the 0.05 % level | Passed* |

*wavelength variations of ± 1 nm are acceptable and should be carefully controlled

Table 4
Results of method validation.

3. Michael Frank "Impurity Profiling with the Agilent 1200 LC System Part 3: Rapid Condition Scouting for Method Development", *Agilent Application Note, publication number 5989-5619EN, 2006.*

4. Reviewer Guidance, Validation of Chromatographic Methods, Center for Drug Evaluation and Research, Food and Drug Administration, **1994.**

5. Guideline for Submitting Samples and Analytical Data for Methods Validation, Food and Drug Administration, **1987.**

6. Udo Huber "Impurity Profiling with the Agilent 1200 Series LC System Part 2: Isolation of Impurities with Preparative HPLC", *Agilent Application Note, publication number 5989-5618EN, 2006.*

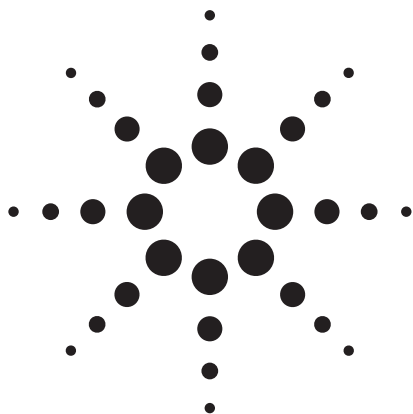
Anglika Gratzfeld-Huesgen is Application Chemist at Agilent Technologies, Waldbronn, Germany.

www.agilent.com/chem/1200

© 2006 Agilent Technologies, Inc.

Published October 1, 2006
Publication Number 5989-5620EN



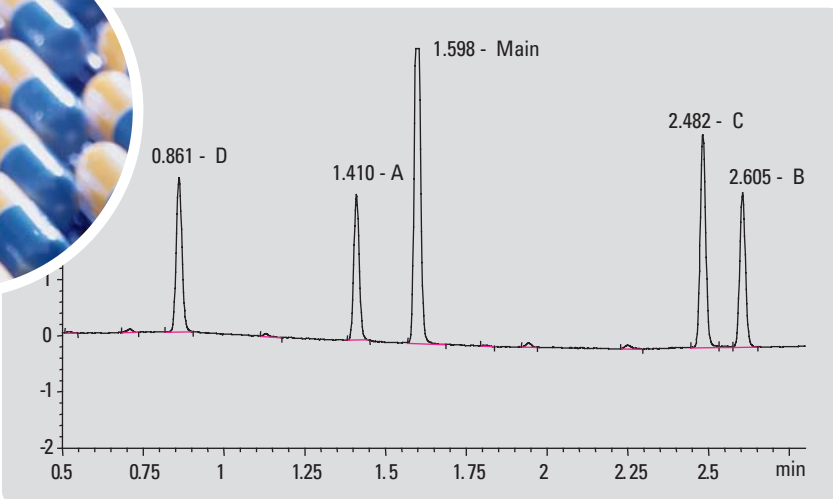


Impurity Profiling with the Agilent 1200 Series LC system

Part 5: QA/QC Application Example Using a Fast LC method for Higher Sample Throughput

Application Note

A.G. Huesgen



Abstract

Analytical QA/QC departments are faced with increasing amounts of samples and increasing demands regarding data quality and reliability. Typically, for one sample run, 10 to 15 ancillary runs have to be performed to ensure correctness of qualitative and quantitative data. Fast LC methods, which have been thoroughly validated, can help to increase sample throughput significantly without compromising data quality. This Application Note illustrates how the Agilent 1200 Series Rapid Resolution (RRLC) system in combination with sub-2- μm -particle columns and fast LC methods can assist in increasing sample throughput and decreasing costs per analysis by a factor of 3 to 4.



Introduction

Having developed a fast analytical LC method, and after validation of this fast method, the next step is to transfer this method to the QA/QC laboratory. Typically, detailed standard operation procedures (SOPs) are available to ensure that the risk for errors and misunderstandings is as small as possible. Following is an example for a standard operation procedure including a system suitability check, sequencing and pass criteria for the obtained results. The Agilent 1200 Series Rapid Resolution LC system was used to perform sequencing and reporting of system suitability checks and analysis of samples and calibration mixtures. The chromatographic conditions are based on a fast LC method developed and validated in previous notes (see references 1 and 2). Cycle times of approximately 5 minutes should allow a significant increase in sample throughput, and consequently also reduce costs. This Application Note introduces a standard operating procedure (SOP) and three samples evaluated following the SOP.

Standard operating procedure (SOP) for the determination of a main compound and four impurities, version 1.1, September 10, 2006

The standard operating procedure was developed for one main compound and its four impurities. The run time is as short as 2.8 min and the cycle time from injection to injection is approximately 5 minutes.

1.0 Instrumentation

An Agilent 1200 Series Rapid Resolution LC system is recommended with the following modules:

- 1.1 Agilent 1200 Series binary pump SL and vacuum degasser
- 1.2 Agilent 1200 Series high-performance autosampler
- 1.3 Agilent 1200 Series thermostatted column compartment SL
- 1.4 Agilent 1200 Series DAD SL for up to 80 Hz operation
- 1.5 Data acquisition and evaluation software: Agilent ChemStation B.02.01.SR1, Integration: autointegration and the advanced integration mode should be used for better integration results.
- 1.6 ZORBAX SB C-18 columns with internal diameters of 4.6 mm and lengths of 50 mm, packed with 1.8- μ m particles should be used.

2.0 Preparation of samples

- 2.1 **Sample preparation:** 1 mg/mL of the sample (main compound and four impurities (A,B,C,D)) is dissolved in water and 5 μ L of this solution are injected.
- 2.2 **System suitability sample:** A stock solution is prepared with the following concentrations: main compound: 10 μ g/mL, impurities A, B, C and D: 5 μ g/mL each.
- 2.3 **Calibration mixture:** Two calibration mixtures are prepared. Each calibration mixture should contain: main compound: approximately 1 mg/mL, impurity A, B, C, and D: 0.1 % level.
- 2.4 **Control sample:** The same concentration of impurities as the system suitability sample, but main compound concentration should be 1 mg/mL.

3.0 Chromatographic conditions

- 3.1 **Column**
50 x 4.6 mm ZORBAX SB C-18, 1.8 μ m for 600 bar operation
- 3.2 **Pump**
Solvent A: Water + 0.2 % TFA and Solvent B: ACN + 0.16 % TFA
Gradient: 17 to 45 % B in 2.8 min, holdover 0.2 min,
Stop time: 3 min
Post time: 1 min
Flow rate: 2.2 mL/min
- 3.3 **Autosampler**
Injection volume: 5 μ L, wash 10 s for exterior of needle
- 3.4 **Thermostatted column compartment**
Temperature: 30 $^{\circ}$ C
- 3.5 **Detector**
13- μ L cell, Peak width = > 0.03 min, Slit width: 8 nm, sSignal: 270/10 nm, ref. 500/100 nm

Page 1 of 6

4.0 Performance tests

Several tests are needed to qualify a sample as passed or failed. Calibration mixtures and control samples have to be used as well as blank samples containing a solvent which is also used for sample dilution. Table 1 is a compendium of requirements to determine precision, sensitivity, resolution and other method performance parameters for the samples.

| | Sample | Purpose | Number of injections |
|-----|--------------------------------------|---|----------------------|
| 4.1 | Blank solution (pure sample solvent) | Verify baseline stability and identify artifacts | 2 to 3 |
| 4.2 | Control sample | Verify sensitivity and resolution | 1 |
| 4.3 | Calibration mixture 1 | Verify stability of response | 3 |
| 4.4 | Calibration mixtures 2 | Verify stability of response and correctness of calibration mixture 1 | 3 |
| 4.5 | System suitability sample | Verify precision of areas and retention times, resolution, peak width, k' and signal to noise ratio | 6 |
| 4.6 | Sample | Quantitation of impurities and main compound and determination of precision of areas and RT | 3 |

Table 1

Tests required to qualify samples as passed or failed.

Page 2 of 6

Based on the requirements defined in the table in section 4.0 Performance tests, the following sequence table was set up in the Agilent ChemStation software. Figure 1 shows an example chromatogram for system suitability testing.

| Line | Location | Sample name | Method name | Inj/ location | Sample type | Data file | Injection vol. |
|------|----------|-------------|-------------|---------------|-------------|-----------|----------------|
| 1 | P1-E-01 | water | IMPURITIES1 | 3 | Sample | Water1_1 | 5 |
| 2 | P1-C-03 | Suitability | IMPURITIES1 | 6 | sample | Suita_1 | 5 |
| 3 | P1-E-01 | water | IMPURITIES1 | 2 | Sample | Water1_2 | 5 |
| 4 | P1-C-04 | Calib1 | IMPURITIES1 | 3 | Calibration | Calib1_1 | 5 |
| 5 | P1-E-02 | water | IMPURITIES1 | 2 | Sample | Water2_1 | 5 |
| 6 | P1-C-05 | Calib2 | IMPURITIES1 | 3 | Calibration | Calib2_1 | 5 |
| 7 | P1-E-02 | water | IMPURITIES1 | 2 | Sample | Water2_2 | 5 |
| 8 | P1-E-08 | control | IMPURITIES1 | 1 | sample | Control_1 | 5 |
| 9 | P1-E-03 | water | IMPURITIES1 | 2 | Sample | Water3_1 | 5 |
| 10 | P1-D-03 | Sample1 | IMPURITIES1 | 3 | Sample | Sample1_1 | 5 |
| 11 | P1-E-03 | water | IMPURITIES1 | 2 | Sample | Water3_2 | 5 |
| 12 | P1-D-04 | Sample2 | IMPURITIES1 | 3 | Sample | Sample2_1 | 5 |
| 13 | P1-E-04 | water | IMPURITIES1 | 2 | Sample | Water4_1 | 5 |
| 14 | P1-D-05 | Sample3 | IMPURITIES1 | 3 | Sample | Sample3_1 | 5 |
| 15 | P1-E-04 | water | IMPURITIES1 | 2 | Sample | Water4_2 | 5 |
| 16 | P1-C-04 | Calib1 | IMPURITIES1 | 3 | Calibration | Calib1_2 | 5 |
| 17 | P1-E-05 | water | IMPURITIES1 | 2 | Sample | Water5_1 | 5 |
| 18 | P1-C-04 | Calib2 | IMPURITIES1 | 3 | Calibration | Calib2_2 | 5 |

Table 2
Examples of sequences with system suitability test samples at the beginning and calibration and further samples in the following lines. In between the sample and calibration runs, pure water must be injected.

5.0 Test limits

5.1 System suitability test

To test whether the system is still fulfilling the method requirements, a solution between 4 and 10 µg/mL of the main compound and impurities A, B, C and D is prepared. This solution is injected every day prior to the first analysis.

The following parameters must be tested. The following limit settings have to be fulfilled:

- 5.1.1 Precision of areas must be < 2 % rsd.
- 5.1.2 Precision of retention times must be < 0.5 % rsd.
- 5.1.3 Resolution must be > 2 for all peaks.
- 5.1.4 Maximum peak width must be < 0.08 min at half height.
- 5.1.5 k' must be 5 < k' < 25.
- 5.1.6 Signal-to-noise ratio must be > 50 for all peaks.

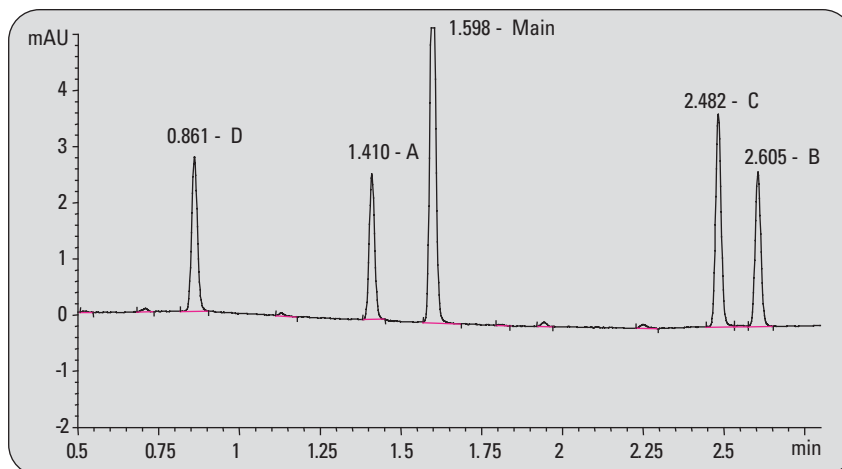


Figure 1
Analysis of sample used for suitability tests.

The results of the system suitability sample shown in figure 1 are summarized in table 3. All limit criteria are fulfilled.

The calibration run results are summarized in table 4. All limit criteria are fulfilled.

The control sample results are summarized in table 5. All limit criteria are fulfilled.

| Compound | Amount | RSD RT | RSD Area | Resolution | PW | K' | S/N |
|---------------|------------|--------|----------|------------|-----------|-------|-------|
| A | 4.9 µg/mL | 0.142 | 0.155 | 9.48 | 0.018 min | 11.43 | 75.3 |
| B | 4.5 µg/mL | 0.062 | 0.483 | 3.88 | 0.019 min | 21.95 | 79.3 |
| C | 5.1 µg/mL | 0.069 | 0.399 | 6.76 | 0.019 min | 20.88 | 109.7 |
| D | 4.4 µg/mL | 0.246 | 0.201 | - | 0.019 min | 6.61 | 79.8 |
| Main compound | 9.99 µg/mL | 0.107 | 0.160 | 6.13 | 0.018 min | 13.09 | 109.7 |

Table 3
System suitability test results.

5.2 Calibration runs

Evaluation of the calibration runs ensures that the obtained sample run results are reliable.

The precision of retention times and areas of the calibration runs must be evaluated.

- 5.2.1 The precision of area must be < 5 % rsd above the 0.03 % level for all impurities.
- 5.2.2 Precision of area must be < 20 % rsd below the 0.03 % level for all impurities.
- 5.2.3 The precision of area must be < 1 %rsd for the main compound.
- 5.2.4 The precision for retention times should be < 0.5% rsd.

Page 4 of 6

| Compound | Amount | % level | RSD RT | RSD Area |
|---------------|-------------|---------|--------|----------|
| A | 1.016 µg/mL | 0.102 % | 0.142 | 0.155 |
| B | 0.976 µg/mL | 0.098 % | 0.062 | 0.790 |
| C | 1.026 µg/mL | 0.103 % | 0.069 | 0.804 |
| D | 0.927 µg/mL | 0.093 % | 0.246 | 0.201 |
| Main compound | 1 mg/mL | 100 % | 0.107 | 0.166 |

Table 4
Calibration run results.

5.3 Control sample

The control sample is used to check the method performance with respect to resolution and limit of detection.

- 5.3.1 Resolution for all peaks must be > 2.
- 5.3.2 Limit of detection must be <0.01 % level for all impurities.

Page 5 of 6

| Compound | Amount | Resolution | S/N | % Level of LOD |
|---------------|-----------|------------|------|----------------|
| A | 4.9 µg/mL | 17.5 | 22 | 0.008 % |
| B | 4.5 µg/mL | 3.81 | 23.6 | 0.008 % |
| C | 5.1 µg/mL | 17.88 | 31.5 | 0.0078 % |
| D | 4.4 µg/mL | - | 22 | 0.008 % |
| Main compound | 1 mg/mL | 2.6 | - | - |

Table 5
Control sample results.

Table 6 shows the area and retention time precision results of the main compound and the impurities of the analyzed samples.

In table 7 the amounts found are summarized. The amounts of impurities do not exceed the limit of 0.5 % for all 3 samples.

5.4 Sample run precision and determination of amounts

Samples must be injected 3 times and precision for areas and retention times must be determined for the main compound and the impurities.

- 5.4.1 Area precision of the main compound must be < 1 % rsd.
- 5.4.2 Retention time precision must be < 0.5 % rsd.
- 5.4.3 Precision for areas of impurities in the 0.05 up to the 0.4 % level must be < 10 % rsd, below the 0.05 % level down to the 0.02% level area precision should be < 20 % rsd
- 5.4.4 Retention time precision for impurities must be < 0.5 % rsd
- 5.4.5 Determination of the amount of the main compound in ng/mL.
- 5.4.6 Determination of the impurity level in %.
- 5.4.7 Percentage of allowed total impurity amount must be < 0.5 %.

Page 6 of 6

| | Sample 1 | Sample 2 | Sample 3 |
|----------------------|-------------|------------|-------------|
| Main compound | | | |
| RSD area | 0.145 | 0.233 | 0.093 |
| RSD retention time | 0.104 | 0.045 | 0.037 |
| Impurities | | | |
| RSD area | 1.33-10.54 | 0.563-3.98 | 5.50-8.49 |
| RSD retention time | 0.039-0.106 | 0.058-0.24 | 0.013-0.050 |

Table 6

Results obtained from the main compound of the 3 analyzed samples, 3 injections each.

| | Sample 1, total 0.071 % impurities (passed) | Sample 2, total 0.257 % impurities (passed) | Sample 3, total 0.11 % impurities (passed) |
|-------------------------|---|---|--|
| Amount of main compound | 999.58 ng/mL | 1001.51 ng/mL | 998.93 ng/mL |
| Impurity A, % level | 0.02 % | 0.066 % | 0.028 % |
| Impurity B, % level | 0.019 % | 0.066 % | 0.03 % |
| Impurity C, % level | 0.017 % | 0.07 % | 0.03 % |
| Impurity D, % level | 0.015 % | 0.055 % | 0.022 % |

Table 7

Amounts of main compound and impurities found in the analyzed samples.

Conclusion

Analytical QA/QC departments are faced with increasing amounts of samples and increasing demands regarding data quality and reliability. Typically, for one sample run, 10 to 15 ancillary runs have to be performed to ensure correctness of qualitative and quantitative data. Fast LC methods, which have been thoroughly validated, can help to increase sample throughput significantly without compromising data quality. The sequence used included 47 runs, which took about 3.9 hours including 30 minutes for system suitability testing. A sequence using a conventional method of about a 20-min cycle time would take approximately 15.7 hours. This represents a significant increase in sample throughput for the fast LC method. Solvent savings are also significant. With a 20-min cycle time, 47 runs and a flow rate of 2.2 mL/min, 2068 mL of solvent are required. Using the fast method described here a 5-min cycle time requires only 517 mL solvent for 47 runs. The cost per analysis will therefore drop significantly by approximately a factor of 3 to 4. See table 8 for an example. Revalidation of a method can take up to 2 weeks and cost about \$4,000. In our example, after the analysis of about 500 runs updating a method to a fast analysis is cost effective.

| Cycle time | 20 min cycle time | 5 min cycle time |
|--------------------------|-------------------|------------------|
| Runs/year* | 26208 | 104832 |
| Approx. costs/analysis | \$11.35 | \$2.85 |
| Approx. cost/1000 runs** | \$11,350 | \$2,850 |
| Cost savings /1000 runs | - | \$8,500 |
| Increase in throughput | - | 4 times |

Table 8
Increase in sample throughput and cost savings using fast LC methods

*24 hour/day, 7 days/week, 52 weeks/year

**Solvents and disposal = \$31/l, labor/h = \$30.

References

1. Michael Frank "Impurity Profiling with the Agilent 1200 Series LC System- Part 3: Rapid Condition Scouting for Method Development", *Agilent Application Note, publication number 5989-5619EN, 2006.*
2. Angelika Gratzfeld-Huesgen "Impurity Profiling with the Agilent 1200 Series LC system- Part 4: Method Validation of a Fast LC Method", *Agilent Application Note, publication number 5989-5620EN, 2006.*

*Anglika Gratzfeld-Huesgen is
Application Chemist at Agilent
Technologies, Waldbronn,
Germany.*

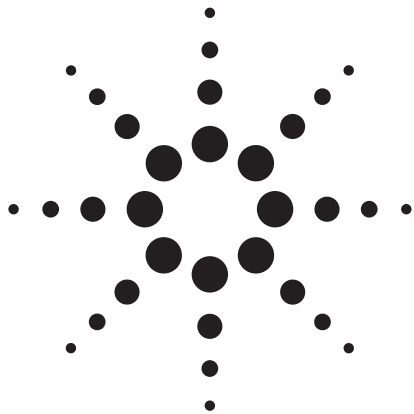
www.agilent.com/chem/1200

© 2006 Agilent Technologies, Inc.

Published October 1, 2006
Publication Number 5989-5621EN



Agilent Technologies



Analysis of a complex natural product extract from ginseng – Part I: Structure elucidation of ginsenosides by rapid resolution LC–ESI TOF with accurate mass measurement

Application Note

Edgar Nägele

Abstract

Since prehistoric times extracts from herbs have been used for medical treatment of disease. Their activity and effects on humans were found by trial and error over generations. A good example of achieved efficiency is traditional Chinese medicine (TCM). In Western medicine drugs derived from natural origin are gaining importance due to their potential. However, Western pharmaceutical quality standards require a deep knowledge about the ingredients in medicine based on natural products.

This Application Note will demonstrate the use of the rapid resolution LC with rapid resolution high throughput (RRHT) columns for the separation of the ingredients found in a complex ginseng root extract and the measurement of accurate masses by an ESI orthogonal acceleration time-of-flight MS (oaTOF) for the structure elucidation. The use of a rapid resolution LC system together with an ion trap MS for structure elucidation will be discussed in part two of this work⁸.



Agilent Technologies

Introduction

Crude extracts of herbal and animal origin have been used for medical treatment of disease in all ancient cultures around the globe since prehistoric time. Their activity for treatment of different diseases and other effects on humans were found by trial and error over hundreds of years and the knowledge about this medicine was inherited from generation to generation. A good example of the efficiency achieved during this process of optimization is the herbal based traditional Chinese medicine (TCM). Since these drugs are often complex mixtures containing hundreds of chemically varied substances with different effects or synergisms a quality control and quality assurance of medical potency is very difficult. A widely used and accepted method by the U.S. Food and Drug Administration (FDA) and World Health Organization (WHO) is chromatographic fingerprinting^{1,2}.

In addition to the importance of the chromatographic fingerprint, which is capable of identifying a particular herb and distinguishing between closely related species in a qualitative manner, the quantitative analysis of medical plant extracts is also gaining importance. For traditional medicines a quantitative analysis is crucial to their quality control and to determine the absolute content of pharmaceutical effective substances as well as potentially toxic undesirable natural substances³. In Western medicine drugs derived from natural origins are gaining importance due to their potential. However Western pharmaceutical quality standards require a deep knowledge about the ingredients

in medicine based on natural products. Since traditional herbal medicines often contain hundreds of substances with only a few bioactive compounds it is necessary to develop new strategies to screen these plant extracts for biologically active compounds and for their pharmacological effectiveness on animal or cellular models as well as receptor and enzyme based tests⁴. A famous Asian herb, which has been used in herbal medicine for more than 5000 years is the ginseng (*Panax* species) root. Pharmacological effects of ginseng which have been reported are, for example, stimulatory and inhibitory effects on the central nervous system (CNS), antistress, antihyperglycemic, antineoplastic and immunomodulatory effects⁵. The main active compounds of the ginsenosides are triterpene saponins from which more than 80 have been isolated and characterized during the past years. An enormous amount of work has been done during the last 30 years to develop analytical methods for the analysis of ginseng extracts and medical formulations. The method of choice for the analysis of complex natural product extracts, like those derived from the ginseng root, is high performance liquid chromatography (HPLC)⁶. LC/MS equipment such as LC/ESI oaTOF for accurate mass measurement and LC/ion trap or LC/triple quadrupole instruments for structure elucidation by MS/MS and MSⁿ are currently being used to determine the complex and similar structures of ginsenosides⁷. This Application Note will demonstrate the use of the Agilent 1200 Series Rapid Resolution LC system with

RRHT columns for separating the ingredients found in a complex ginseng root extract and the measurement of accurate masses by an ESI oaTOF MS. For the structure elucidation CID fragmentation was carried out and the measured accurate masses were used to calculate empirical formulas of the fragments. The use of the high resolution LC system together with an ion trap MS for structure elucidation by MSⁿ will be discussed in part two of this work⁸.

Experimental

Equipment

- Agilent 1200 Series binary pump SL with degasser. This pump has the capability to deliver a pressure of up to 600 bar, which is necessary to perform high resolving HPLC analysis on a 1.8- μ m particle size RRHT column to get the best resolution performance.
- Agilent 1200 Series high performance autosampler SL with thermostat. This autosampler is especially designed to work together with the 1200 Series binary pump SL at the lowest delay volume.
- Agilent 1200 Series thermostated column compartment (TCC). This TCC is ready for use together with the high pressure binary pump with optional separate heat exchangers and post column cooling under optimized delay volume conditions and alternating column regeneration with an optional 2-position/10-port valve.
- Agilent 1200 Series diode-array detector SL (DAD). This DAD is capable of acquiring data at a sampling rate up to 80 Hz. This device has a built-in data storage capability.

- Agilent 6200 Series MSD TOF. Orthogonal acceleration time-of-flight mass spectrometer with dual sprayer interface for mass calibration to acquire molecular masses with highest accuracy. This time-of-flight mass spectrometer is capable of acquiring data at 40 Hz and pos/neg switching.
- Picard TOF software A02.00. Software used for data acquisition with the TOF LC/MS system.
- Analyst Software. Software for TOF and UV data analysis.
- Column. ZORBAX SB C18, 2.1 x 150 mm, 1.8 μm

Sample

Powdered freeze-dried Asian ginseng root (1g) (Panax ginseng) was treated ultrasonically for 30 minutes in 10 mL methanol, filtered and directly used for analysis.

The set-up of the Agilent 6200 Series MSD TOF system is shown in figure 1. In this set-up the Agilent 1200 Series binary pump SL is connected to the Agilent 1200 Series high performance autosampler SL with a 0.17-mm i.d. stainless steel capillary. To reduce delay volume, the seat capillary in the Agilent 1200 Series high performance autosampler SL has an 0.12-mm i.d., which is the same kind of capillary that connects the low delay volume (1.4 μL) heat exchanger in the Agilent 1200 Series thermostatted column compartment to the column. A 2- μL cell is built into the Agilent 1200 Series diode-array detector SL for UV detection. The outgoing capillary is connected directly to the sprayer of the electrospray source at the time-of-flight mass spec-

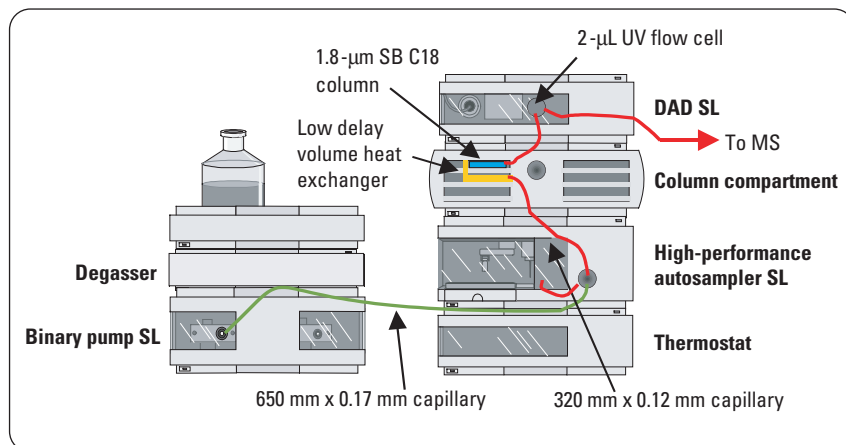


Figure 1
Agilent 1200 Series binary LC system for MS using a low delay volume configuration.

trometer, which is capable of acquiring spectra at 40 Hz. This instrument set-up is optimized to achieve the highest possible resolution, which is demonstrated by the UV analysis of a complex natural product extract obtained from Asian ginseng root (Panax ginseng) (see below). The full performance of the Agilent 1200 Series binary system in the high resolution configuration is demonstrated in another publication⁹. It is also possible to use this system in a high throughput environment by making minor changes¹⁰.

Methods:

- The Agilent 1200 Series binary pump SL was operated under the following conditions:
Solvent A: water + 0.1 % TFA
Solvent B: AcN + 0.1 % TFA
Flow: 0.5 mL/min
Gradient: 0 min 5 % B, 1 min 5 % B, 60 min 85 % B, 61 min 95 % B, 70 min 95 % B
Stop time: 70 min
Post time: 15 min
- The Agilent 1200 Series high performance autosampler SL was used to make injections of

10 μL sample and the samples were cooled to 10 °C. The sample loop was switched to bypass after 1 minute to reduce delay volume.

- The Agilent 1200 Series thermostatted column compartment, equipped with the 1.4- μL low delay volume heat exchanger, was set at 50° C.
- The Agilent 1200 Series diode-array detector SL was operated at 80 Hz for data acquisition at a wavelength of 220 nm/4, ref. 360/100 with a 2- μL flow cell, 30-mm path length.
- Agilent 6200 Series MSD TOF was operated under the following conditions:
Source: ESI in positive mode with dual spray for reference mass
Dry gas: 12 L/min
Dry Temp.: 200 °C
Nebulizer: 35 psi
Scan: 200-1300
Fragmentor: 150 V or 300 V for CID
Skimmer: 60 V
Capillary: 3000 V

Conditions for both experiments:

Pumps

Solvent A: H₂O + 0.1 % TFA
Solvent B: ACN + 0.1 % TFA
Gradient: 10 % to 95 % ACN in 40 min,
hold for 1 min
Flow rate: 0.4 mL/min

Autosamplers

Injection volume: 3 μ L

Thermostatted column compartments

Temperature: 50° C

Detectors

DAD 2- μ L cell and 20 Hz, 220 nm

Results and discussion

To compare the resolution performance of the Agilent 1200 Series Rapid Resolution LC system to an Agilent 1100 Series standard LC system, the analysis of a complex natural product extract was performed on an Agilent 1100 Series system with its maximum pressure at 400 bar equipped with a 5- μ m particle size column and in comparison on an Agilent 1200 Series system with its maximum pressure at 600 bar equipped with a RRHT column with a 1.8- μ m particle size. The system backpressure was about 520 bar using the 2.1 x 150 mm, 1.8- μ m column. The resulting UV chromatograms acquired at 220 nm clearly demonstrate the better resolution of the peaks on the Agilent 1200 Series system (figure 2). The peak width (FWHM) of the majority of the peaks in the UV chromatogram is below 0.1 min with baseline separation. This excellent resolution, which can be achieved with the Agilent 1200 Series pump in combination with the RRHT column results in significantly more MS information useful for compound identification.

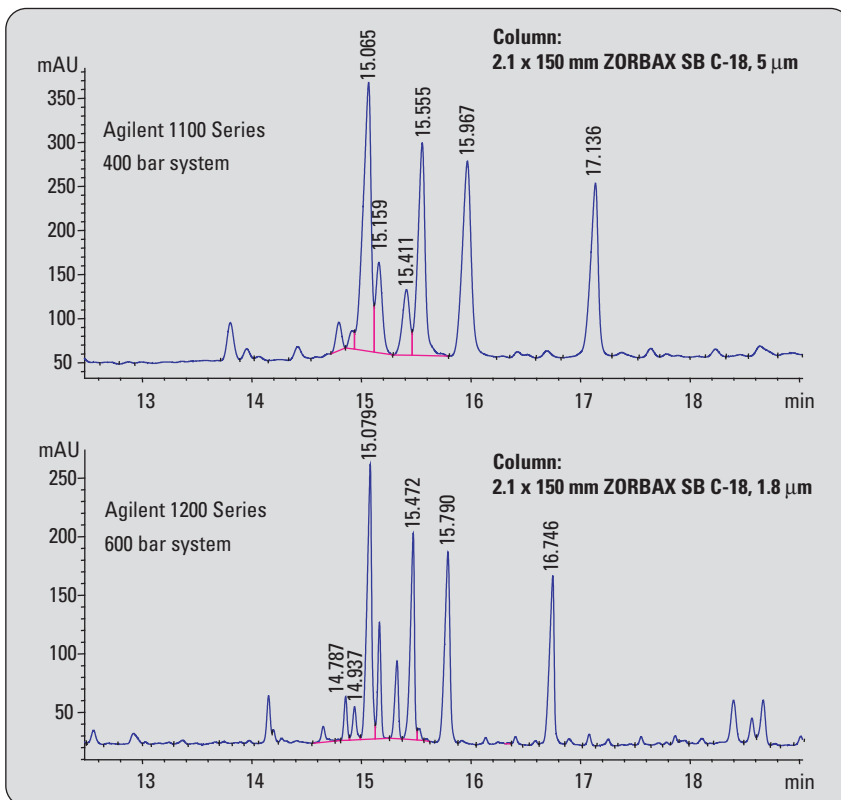


Figure 2
Ginseng extract using a 400 bar system with a 5- μ m particle column and using a 600-bar system with a 1.8- μ m particle column.

After separation of the individual compounds, which are components of the crude complex extract from the ginseng root, by means of rapid resolution HPLC on a 1.8- μ m particle size RRHT column, they are subjected to accurate mass measurement by means of an ESI oaTOF. The main constituents elute between 20 and 33 minutes and are marked as ginsenosides Re, Rf, F₁₁, Rb₁, Rc, Rb₂ and Rd in the base peak chromatogram (figure 3). The ESI oaTOF data of the ginsenosides Rb₁, Rc and Re were analyzed in more detail for structure elucidation

while the species dependent ginsenosides Rf and F₁₁ are discussed in another publication¹¹.

The ginsenoside Rb₁ eluting at 27.7 min was identified by its protonated molecular ion at m/z 1109.6129 and calculation of the corresponding empirical formula with a mass accuracy of -1.90 ppm relative to 2.10 mDa. A loss of one molecule of water leads to the ion at m/z 1091.6012 with -0.91 ppm mass accuracy. A CID experiment was performed for structure elucidation at an elevated skimmer voltage, which presented addition-

al information in the TOF spectrum (figure 4). The loss of one of the glucose chains resulted in the ions at m/z 785.5047 and m/z 325.1136 with mass accuracies of 0.53 ppm and -0.39 ppm, respectively. A series of ions resulting from a consecutive loss of water from the ion m/z 785.5047 was also identified with high mass accuracy. Further loss of the second glucose chain from the molecule resulted in the ion at m/z 425.3784 with -0.14 ppm mass accuracy. This ion is derived from the triterpenoid core structure common to all ginsenosides. A loss of one molecule of water resulted in the ion at m/z 407.3679 with 0.10 mDa and -0.30 ppm mass accuracy. This set of CID fragments together with the molecular ion and the set of calculated empirical formulas confirm the structure of the ginsenoside Rb₁. The fragmentation pattern is shown in figure 4 and the mass accuracies and empirical formulas are summarized in table 1. The ginsenoside Rc with 29.3 min retention time was identified after empirical formula calculation by

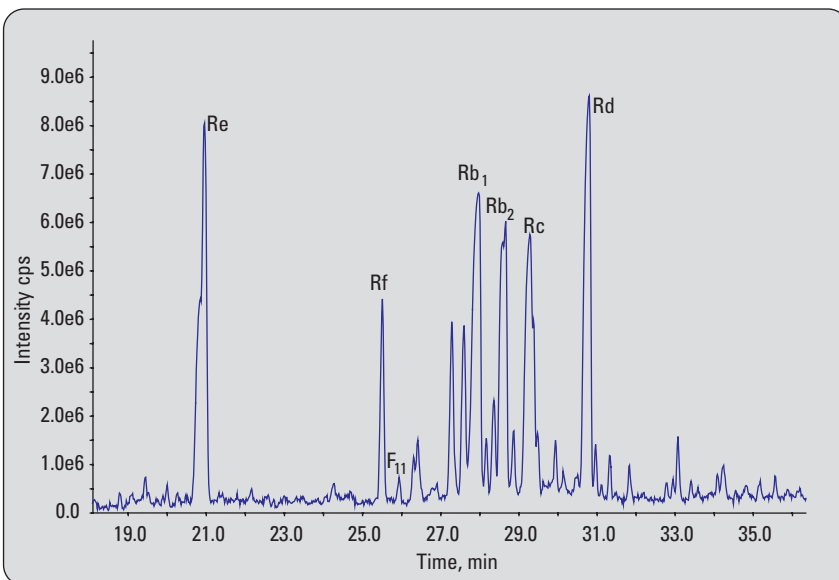


Figure 3
RR-LC-TOF basepeak chromatogram of the area containing the main components of the Asian ginseng root extract.

| Measured mass | Calculated mass | Formula | Mass accuracy [mDa] | Mass accuracy [ppm] |
|---------------|-----------------|---|---------------------|---------------------|
| 1109.6129 | 1109.6108 | C ₅₄ H ₉₃ O ₂₃ | 2.10 | -1.90 |
| 1091.6012 | 1091.6002 | C ₅₄ H ₉₁ O ₂₂ | 1.00 | -0.91 |
| 785.5047 | 785.5051 | C ₄₂ H ₇₃ O ₁₃ | -0.40 | 0.53 |
| 767.4950 | 767.4946 | C ₄₂ H ₇₁ O ₁₂ | 0.40 | -0.58 |
| 749.4854 | 749.4840 | C ₄₂ H ₆₉ O ₁₁ | -1.40 | 1.88 |
| 425.3784 | 425.3783 | C ₃₀ H ₄₉ O | 0.10 | -0.14 |
| 407.3679 | 407.3678 | C ₃₀ H ₄₇ | 0.10 | -0.30 |
| 343.1248 | 343.1240 | C ₁₂ H ₂₃ O ₁₁ | 0.80 | 2.23 |
| 325.1136 | 325.1135 | C ₁₂ H ₂₁ O ₁₀ | 0.10 | -0.39 |

Table 1
Empirical formulas and achieved mass accuracies for the structure elucidation of ginsenoside Rb₁ by ESI oaTOF.

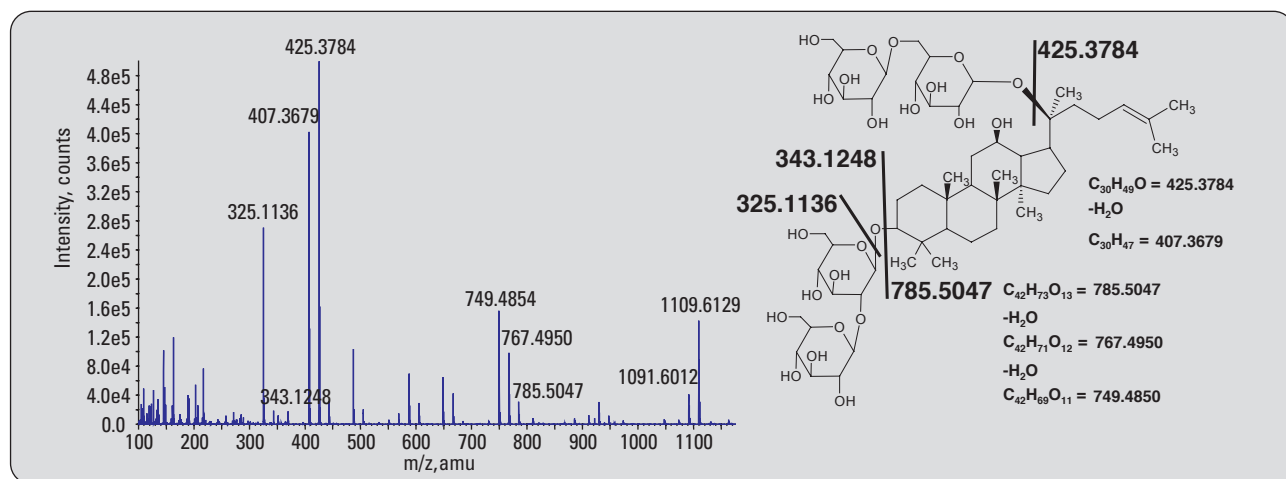


Figure 4
Accurate mass measurement of ginsenoside Rb₁ and its CID fragments by ESI oaTOF.

its molecular ion at m/z 1079.5991 and a product obtained by the loss of a molecule of water at m/z 1061.5888 with mass accuracies of 1.02 ppm and 0.78 ppm, respectively. The fragmentation obtained at a higher skimmer voltage starts with a loss of the sugar residues arabinose and glucose followed by a loss of water from the remaining molecule fragment (figure 5). The fragmentation of the sugar moieties resulted in the initial ions at m/z 785.5060 and at m/z 755.4936 with mass accuracies of -1.12 ppm and 1.26 ppm, respectively. After complete loss of all saccharide moieties the triterpenoide core structure was detected at m/z 425.3785 with high mass accuracy -0.37 ppm for the calculated empirical formula. The cleaved glucose chain was detected at m/z 325.1134 with 0.22 pmm mass accuracy. The fragmentation pattern is shown in figure 5 and the achieved mass accuracies for all fragments are summarized in table 2. The ginsenosides Rc and Rb₂, which elute at 28.7 min retention

time are structure isomers with the same empirical formula and molecular mass. In the ginsenoside Rc the sugar arabinose is in the furanose form and in the ginsenoside Rb₂ the arabinose is in its pyranose form.

The last of the main ingredients, which was classified in the examined ginseng root extract is ginsenoide Re. This compound, which elutes at 20.8 min, was identified by empirical formula calculation from the mass at m/z 947.5585 with a high mass accuracy

of 0.60 mDa or -0.59 ppm (figure 6). The CID fragmentation gave further evidence for the identity of this substance. After cleavage of the saccharide moieties there are two remaining main fragments. The fragment obtained after a loss of a molecule of glucose with m/z 767.4957 was measured with a mass accuracy of -1.50 ppm. A consecutive loss of water yields the ion at m/z 749.4855. After a further loss of the glucose disaccharide the fragment of the triterpenoide core structure at m/z 441.3739 with a mass accuracy of

| Measured mass | Calculated mass | Formula | Mass accuracy [mDa] | Mass accuracy [ppm] |
|---------------|-----------------|---|---------------------|---------------------|
| 1079.5991 | 1079.6002 | C ₅₃ H ₉₁ O ₂₂ | -1.10 | -1.02 |
| 1061.5888 | 1061.5896 | C ₅₃ H ₈₉ O ₂₁ | -0.88 | 0.78 |
| 785.5060 | 785.5051 | C ₄₂ H ₇₃ O ₁₃ | 0.90 | -1.12 |
| 767.4939 | 767.4946 | C ₄₂ H ₇₁ O ₁₂ | -0.70 | 0.85 |
| 749.4846 | 749.4840 | C ₄₂ H ₆₉ O ₁₁ | 0.60 | -0.81 |
| 755.4936 | 755.4946 | C ₄₁ H ₇₁ O ₁₂ | -1.00 | 1.26 |
| 737.4830 | 737.4840 | C ₄₁ H ₆₉ O ₁₁ | -1.00 | 1.34 |
| 719.4723 | 719.4734 | C ₄₁ H ₆₇ O ₁₀ | -1.10 | 1.56 |
| 425.3785 | 425.3783 | C ₃₀ H ₄₉ O | 0.20 | -0.37 |
| 407.3679 | 407.3678 | C ₃₀ H ₄₇ O | 0.10 | -0.30 |
| 325.1134 | 325.1135 | C ₁₂ H ₂₁ O ₁₀ | -0.10 | 0.22 |

Table 2
Empirical formulas and achieved mass accuracies for the structure elucidation of ginsenoside Rc by ESI oaTOF.

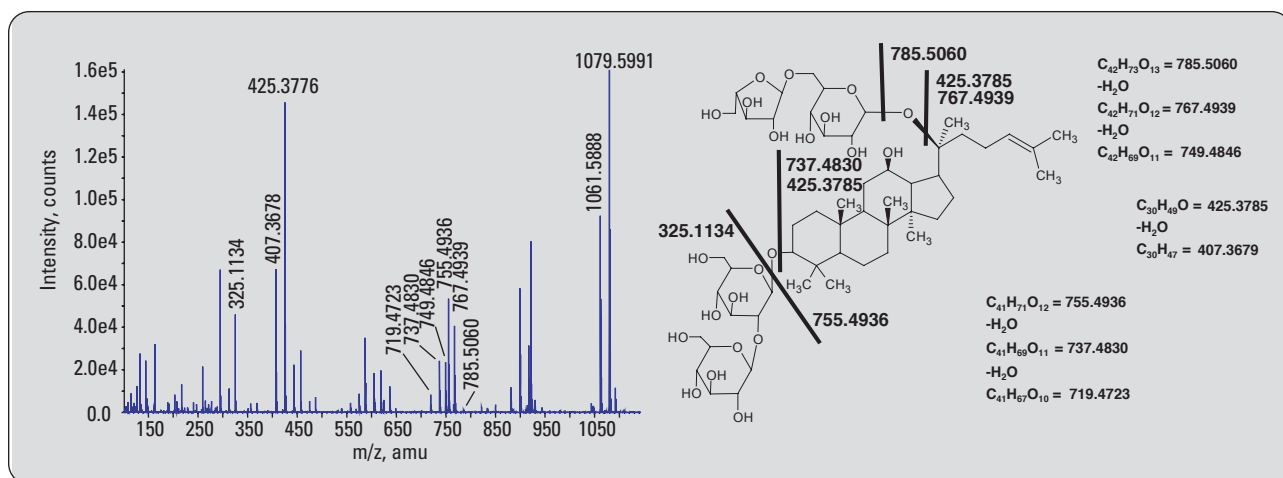


Figure 5
Accurate mass measurement of ginsenoside Rc and its CID fragments by ESI oaTOF.

0.35 ppm occurred. After a further successive loss of water, this fragment yields to the ions at m/z 423.3625 and m/z 405.3519 with 0.45 ppm and 0.55 ppm respectively. The calculated empirical formulas and mass accuracies of the measured fragments are summarized in table 3.

| Measured mass | Calculated mass | Formula | Mass accuracy [mDa] | Mass accuracy [ppm] |
|---------------|-----------------|----------------------|---------------------|---------------------|
| 947.5585 | 947.5579 | $C_{48}H_{83}O_{18}$ | 0.60 | -0.59 |
| 767.4957 | 767.4946 | $C_{42}H_{71}O_{12}$ | 1.10 | -1.50 |
| 749.4855 | 749.4840 | $C_{42}H_{49}O_{11}$ | 1.50 | -2.01 |
| 441.3731 | 441.3733 | $C_{30}H_{49}O_2$ | -0.20 | 0.35 |
| 423.3625 | 423.3627 | $C_{30}H_{47}O$ | -0.20 | 0.45 |
| 405.3519 | 405.3521 | $C_{30}H_{45}$ | -0.20 | 0.55 |

Table 3
Empirical formulas and achieved mass accuracies for the structure elucidation of ginsenoside Re by ESI oaTOF.

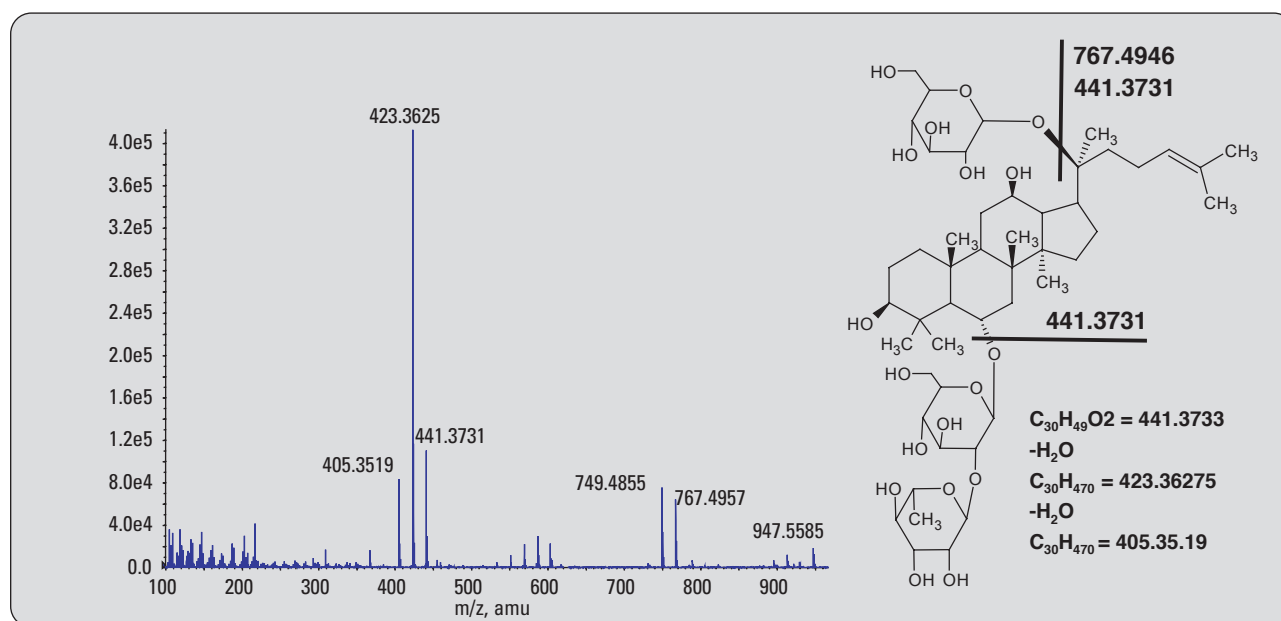


Figure 6
Accurate mass measurement of ginsenoside Re and its CID fragments by ESI oaTOF.

Conclusion

The featured application with the Agilent 1200 Series Rapid Resolution LC system together with the Agilent 6200 Series MSD TOF proves its capability for use in structure elucidation of natural products in highly complex extracts from plant origins. In this application a highly complex extract from ginseng root was analyzed with the Agilent 1200 Rapid Resolution LC/TOF system. A comparison to the predecessor Agilent 1100 Series system clearly

demonstrated the higher resolution that is achieved by the new system equipped with a 1,8- μ m particle size column. Complex structures of three ginsenosides, which are the main compounds of the extract, could be elucidated by the interpretation of the obtained TOF spectra. The proposed structures were confirmed by empirical formula calculation of the molecular ions as well as for the fragments of the molecules obtained by CID. All measured masses have accuracies in the lower single digit range and

therefore confirm the structures with highest confidence. With this detailed knowledge about the ingredients of the natural plant extract it is possible to use the high resolution LC/TOF technology to monitor the content of an extract before usage in a pharmaceutical formulation. This is achieved in a fully automated manner and confirms the compound's identity by measuring its mass with highest accuracy and empirical formula confirmation.

References

1. U.S. Food and Drug Administration, "Guidance for Industry botanical Drug Products", **2000**.
2. World Health Organization, "General Guidelines for Methodologies on Research and Evaluation of Traditional Medicine", **2000**.
3. Drasar P, Moravcova J. "Recent advances in analysis of Chinese medical plants and traditional medicines.", *J. Chrom. B 1-2*, *812*, 3-21,
4. Huang X., Kong L., Li X., Chen X., Guo M., Zou H. „Strategy for analysis and screening of bioactive compounds in traditional Chinese medicines.”, *J. Chrom. B 1-2*, *812*, 71-84, **2004**.
5. Attele A.S., Wu J.A., Yuan C.S. *Biochem. Pharmacol.* *58*, 1685-1693, **1999**.
6. Fuzzati N. "Analysis methods of ginsenosides.", *J. Chrom B1-2*, *812*, 114-133, **2004**.
7. Wang X., Sakuma T., Asafu-Adjaye E., Shiu G. K. „Determination of ginsenosides in plant extracts from *Panax ginseng* and *Panax quinquefolius* L. by LC/MS/MS.”, *Anal. Chem.* *71*, 1579-1584, **1999**.
8. Naegele, E., "Examination of a complex natural product extract from ginseng - Part II: Structure elucidation of ginsenosides by high resolution LC-ion trap by MSⁿ" *Agilent Application Note*, publication number 5989-4705EN, **2006**.
9. "Performance of Agilent 1200 SL LC system for highest resolution." *Agilent Application Note*, publication number 5989-4489EN, **2006**.
10. "Performance of the Agilent 1200 SL HPLC System for Ultra-Fast LC Applications with 2.1-mm i.d. columns." *Agilent Application Note*, publication number 5989-4502EN, **2006**.
11. Naegele, E, "Examination of a complex natural product extract from ginseng - Part III: Species differentiation of ginseng and authentication of ginseng products by LC/MS", *Agilent Application Note*, publication number 5989-4706EN, **2006**.

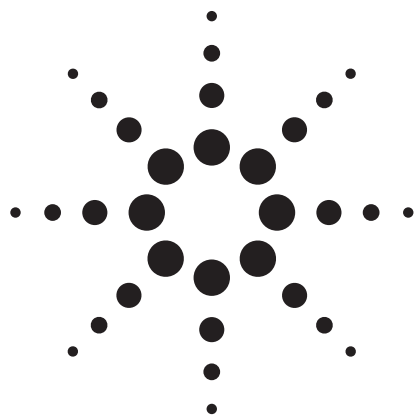
Edgar Nägele is Application Chemist at Agilent Technologies, Waldbronn, Germany.

www.agilent.com/chem/1200

Copyright © 2006 Agilent Technologies
All Rights Reserved. Reproduction, adaptation or translation without prior written permission is prohibited except as allowed under the copyright laws.

Published February 1, 2006
Publication Number 5989-4506EN





Analysis of a complex natural product extract from ginseng – Part II: Structure elucidation of ginsenosides by high resolution ion trap LC/MS

Application Note

Edgar Nägele

Abstract

Since prehistoric time extracts from herbs have been used for medical treatment of disease. Their activity and effects on humans were found by trial and error over generations. A good example of achieved efficiency is traditional Chinese medicine (TCM). In Western medicine drugs derived from natural origins are gaining importance due to their potential. However, Western pharmaceutical quality standards require a deep knowledge about the ingredients in medication based on natural products. This Application Note will demonstrate the use of the Agilent 1200 Series Rapid Resolution LC system with Rapid Resolution High Throughput (RRHT) columns for the separation of the ingredients found in a complex ginseng root extract. The information obtained with an ion trap MSⁿ and MRM is used to determine the structure of the ingredients and for quality control purposes.



Agilent Technologies

Introduction

Crude extracts of herbal and animal origin have been used for medical treatment of disease in all ancient cultures around the world since prehistoric time. Their activity for treatment of different diseases and other effects on humans were found by trial and error over hundreds of years and the knowledge about this medicine was passed on from generation to generation. A good example of the efficiency achieved during this process of optimization is the herbal based traditional Chinese medicine (TCM). A famous Asian herb, which has been used in herbal medicine for more than 5000 years is the ginseng root (*Panax ginseng*). The main active compounds of the ginsenosides are triterpene saponins of which more than 80 have been isolated and characterized during the past years. A lot of work was done during the last 30 years to develop analytical methods for the analysis of ginseng extracts and medical formulations. The method of choice for the analysis of complex natural product extracts such as those derived from the ginseng root is high performance liquid chromatography (HPLC)¹. LC/MS equipment, e.g LC/ESI oaTOF for accurate mass measurement and ion trap LC/MS or triple quadrupole LC/MS instruments for structure elucidation by MS/MS and MSⁿ are currently used to determine the complex and similar structures of ginsenosides². In particular, it is possible to confirm the authenticity of the pharmaceutical ginseng products and differentiate between their active ingredients using the ion trap MSⁿ fragmentation patterns³.

This Application Note will demonstrate the Agilent 1200 Series Rapid Resolution LC system with 1.8- μ m columns for the separation of the ingredients found in a complex ginseng root extract. The information obtained with an ion trap MSⁿ and MRM is used to determine the structure of the ingredients and for quality control purposes. The use of a high resolution LC system together with an ESI oaTOF for accurate mass measurement is described in Part I in this series of Application Notes⁴.

Experimental

Equipment

- Agilent 1200 Series binary pump SL with a degasser. This pump has the capability to perform high resolution HPLC analysis on a 1.8- μ m particle size RRHT column and achieve the best performance.
- Agilent 1200 Series high performance autosampler SL with a thermostat. This autosampler is especially designed to work with the Agilent 1200 Series binary pump SL to ensure lowest delay volumes.
- Agilent 1200 Series thermostatted column compartment (TCC). The TCC is ready for use with the Agilent 1200 Series binary pump SL and optional separate heat exchangers, as well as post column cooling, under optimized delay volume conditions, together with alternating column regeneration with an optional 2-position/10-port valve.
- Agilent 1200 Series diode array detector SL (DAD). This DAD is capable of acquiring data with a sampling rate of up to 80 Hz. In case of network problems, this

device has a built-in data storage capability.

- Agilent 6330 Ion Trap LC/MS. The ion trap is operated with a standard ESI source and able to scan with 26,000 m/z/sec. The MSⁿ spectra are acquired data dependent and fully automated.
- The software used for instrument control was ChemStation B01.03, ion trap software 5.3, and for data analysis the ion trap data analysis software 3.3.
- Column: ZORBAX SB C18, 2.1 x 150 mm, 1.8 μ m

Sample

Powdered freeze-dried Asian ginseng root (1g) (*Panax ginseng*) was treated ultrasonically for 30 minutes in 10 mL methanol, filtered and directly used for analysis.

The set-up of the Agilent 6330 Ion Trap LC/MS system is shown in figure 1. The Agilent 1200 Series binary pump SL is connected to the Agilent 1200 Series high performance autosampler SL (ALS SL) with a 0.17-mm i.d. stainless steel capillary. To reduce delay volume, the seat capillary in the ALS SL has an i.d. of 0.12 mm. The same kind of capillary connects to the low delay volume (1.6 μ L) heat exchanger in the Agilent 1200 Series thermostatted column compartment, which is connected to the column. A 2- μ L cell is built into the Agilent 1200 Series diode array detector SL for UV detection. The outgoing capillary is directly connected to the sprayer of the electrospray source of the 6330 Ion Trap LC/MS, which is capable of acquiring data with a scan speed of 26,000 m/z/sec. This instrument set-up is optimized to achieve the highest possible resolution, which is demonstrated

by the UV analysis of a complex natural product extract obtained from Asian ginseng root (*Panax ginseng*). To illustrate the performance, a comparative analysis on an Agilent 1100 Series LC system (5- μm particle size column) and on an Agilent 1200 Series Rapid Resolution LC system (1.8- μm particle size column) is presented⁴. The resulting UV chromatograms acquired at 220 nm clearly demonstrate the better resolution of the peaks on the Agilent 1200 Series Rapid Resolution LC system. The peak width (FWHM) of the majority of the peaks in the UV chromatogram is below 0.1 min with baseline separation. The full performance of the Agilent 1200 Series Rapid Resolution LC system in the high resolution configuration is documented in a separate Application Note⁵. It is also possible to use this system, with minor changes, in a high throughput environment, which is described in another Application Note⁶.

Methods

- The Agilent 1200 Series binary pump SL was operated under the following conditions:
 - Solvent A: water + 0.1 % TFA
 - Solvent B: AcN + 0.1 % TFA
 - Flow: 0.5 mL/min
 - Gradient: 0 min 5 % B,
1 min 5 % B,
60 min 85 % B,
61 min 95 % B,
70 min 95 % B
 - Stop time: 70 min
 - Post time: 15 min

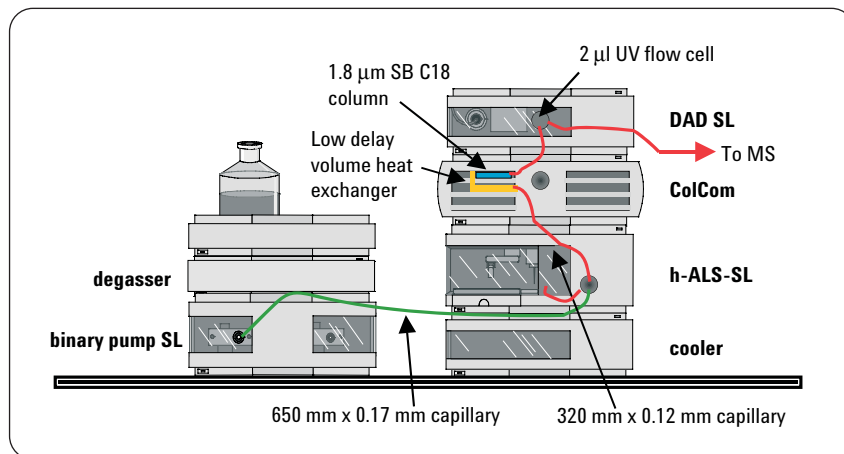


Figure 1
Agilent 1200 Series Rapid Resolution LC system for MS in low delay volume configuration.

- The Agilent 1200 Series high performance autosampler SL was used for injections of 10 μL sample and the samples were cooled to 10 $^{\circ}\text{C}$. The sample loop was switched to bypass after 1 minute to reduce delay volume.
- The Agilent 1200 Series thermostatted column compartment SL was adjusted to 50 $^{\circ}\text{C}$ equipped with the low delay volume heat exchanger.
- The Agilent 1200 Series diode-array detector SL was operated at 80 Hz for data acquisition at a wavelength of 220 nm/4, ref. 360/100 with the 2- μL flow cell, 30-mm path length.
- The 6330 Ion Trap LC/MS was operated under the following conditions:
 - Source: ESI in positive mode.
 - Dry gas: 5.0 L/min
 - Dry temp.: 300 $^{\circ}\text{C}$
 - Nebulizer: 15 psi
 - Target: 125,000
 - Max. accum. time: 100 ms
 - Scan: 200-1300
 - Averages: 2
 - MSⁿ: Automated MS/MS and MS³

Results and discussion

After separation of the individual compounds, which are components of the crude extract, from the ginseng root by means of high resolution HPLC on a 1.8- μm particle size column, they are subjected to fragmentation for MSⁿ. The major ingredients elute between 20 and 33 minutes and are recorded as ginsenosides Re, Rf, F₁₁, Rb₁, Rb₂, Rc, Rd in the base peak chromatogram (figure 2). The high resolution of the column used resolves a large amount of minor compounds from the ginseng extract, which may also be analyzed because the high scan rate of 26,000 m/z/sec allow sufficient ion trap MS/MS and MSⁿ data to be acquired. The ion trap MS/MS and MS³ data of the ginsenosides Re, Rb₁ and Rc were investigated in more detail for structure elucidation while the species-dependent ginsenosides Rf and F₁₁ is discussed in another part of this study⁷.

The simple MS scan delivers the mass of the molecular ion in its protonated and sodiated form (figure 3). The ratio of protonated and sodiated ions depends on the electrospray source temperature because the sodiated complexes are more stable at higher temperatures than the protonated ions, which decompose due to a loss of water and other fragmentations. The MS scan delivers the ions at m/z 928.9 $[M+H-H_2O]^+$, 946.9 $[M+H]^+$, 969.1 $[M+Na]^+$ for ginsenoside Re; at m/z 1090.1 $[M+H-H_2O]^+$, 1108.5 $[M+H]^+$, 1131.1 $[M+Na]^+$ for ginsenoside Rb₁ and at m/z 1059.71 $[M+H-H_2O]^+$, 1077.75 $[M+H]^+$, 1101.1 $[M+Na]^+$ for ginsenoside Rc.

The conditions for the MS/MS and MS³ fragmentation in the 6330 Ion Trap LC/MS were essentially chosen to produce sodiated ions. The fragmentation of these ions gave much clearer fragmentation and additional structural information compared to the protonated ions, whose fragments were similar to the CID fragments discussed in part 1 of this study⁴.

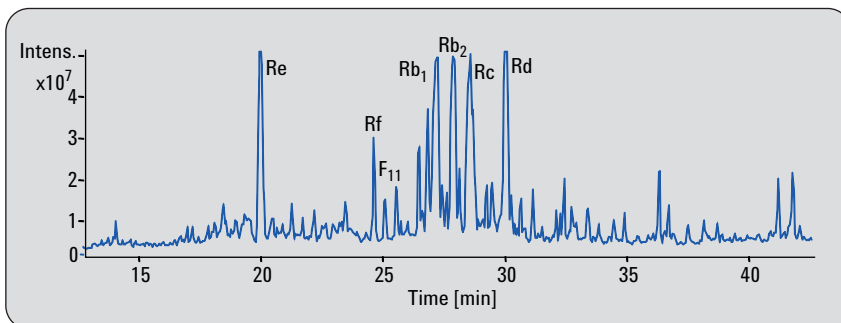


Figure 2
Base peak chromatogram of ginseng extract by high resolution LC ion trap on a 1.8 μ m particle column.

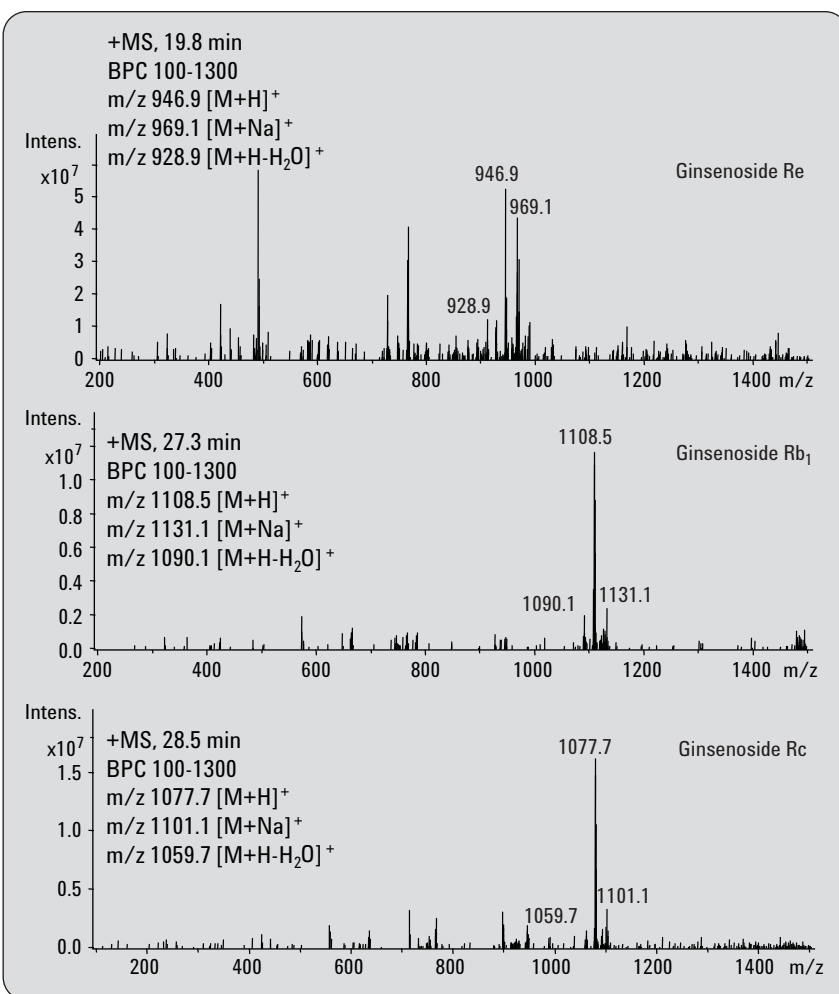


Figure 3
Mass spectra of ginsenosides Re, Rc and Rb₁.

Only one fragment is produced in MS/MS for the ginsenoside Re at m/z 789.9 by a loss of a molecule of glucose from the sodiated molecular ion (figure 4). In MS^3 this sodiated fragment is cleaved into two parts, whereas the detected ion at m/z 349.2 comes from the cleaved disaccharide moiety. In comparison, for the ginsenoside Rc there are two fragments obtained by MS/MS. There is also one at m/z 789.5 and another one at m/z 335.1 for the arabinose saccharide (figure 5). The disaccharide at m/z 365.1 is cleaved off from the ion at m/z 789.5 in the MS^3 stage. The ginsenoside Rb₁ has another different fragmentation pattern where the molecular ion is cleaved to the ions at m/z 789.5 and m/z 365.1 by a loss of the glucose chain in the MS/MS stage. In the MS^3 stage the fragment obtained at m/z 789.5 also loses the same disaccharide at m/z 356.1 (figure 6).

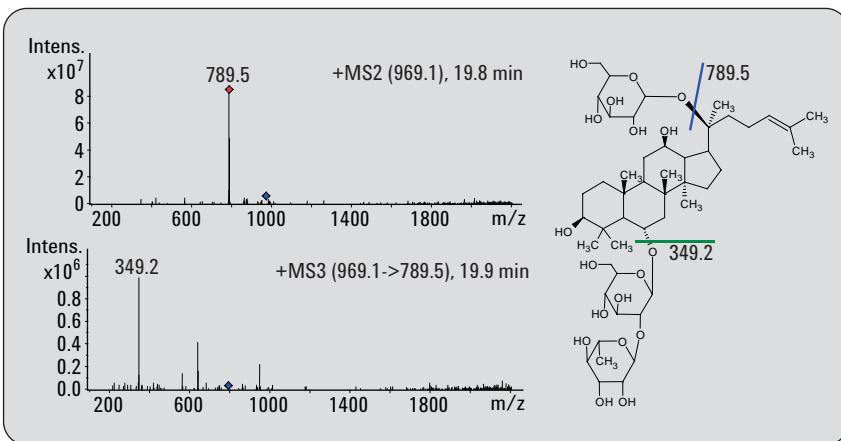


Figure 4
MS/MS and MS^3 fragmentation for structure elucidation of ginsenoside Re with ion trap LC/MS.

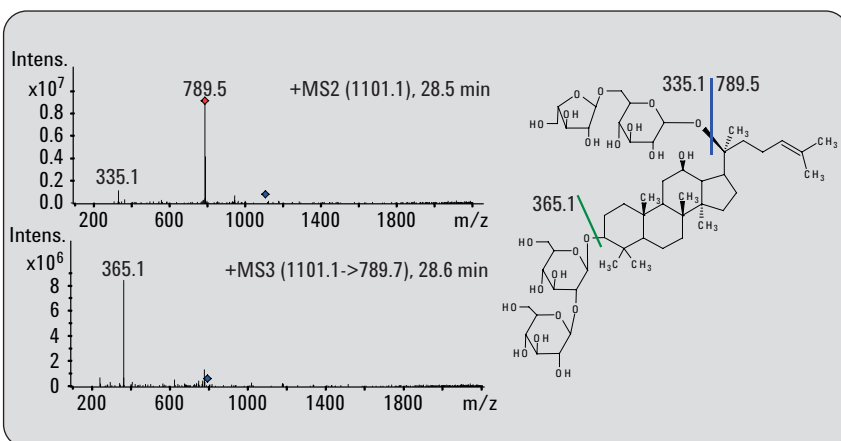


Figure 5
MS/MS and MS^3 fragmentation for structure elucidation of ginsenoside Rc with ion trap LC/MS.

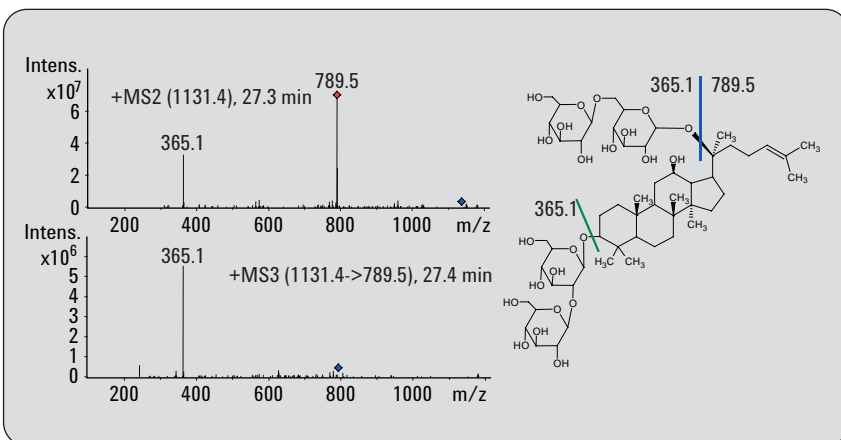


Figure 6
MS/MS and MS^3 fragmentation for structure elucidation of ginsenoside Rb₁ with ion trap LC/MS.

It is possible to distinguish between the different ginsenosides contained in the ginseng root extract with these MS/MS and MS³ fragmentation patterns because the different saccharide molecules connected to the triterpenoid core structure will be cleaved off in a different but characteristic way. If the specific fragmentation pattern in MS/MS and MS³ mode of the various ginsenosides is known, it helps to detect the presence of a special compound in the plant extract in a very specific manner with the ion trap MRM. MS/MS-MRM on the sodiated molecular ions of the ginsenosides Re, Rb₁ and Rc shows exactly their presence in the crude ginseng root extract (figure 7). The obtained MS/MS spectra are in accordance with the spectra obtained in the experiments described above (figures 4-6). In addition, the isomeric ginsenosides Rb₂ and Rd are also detected.

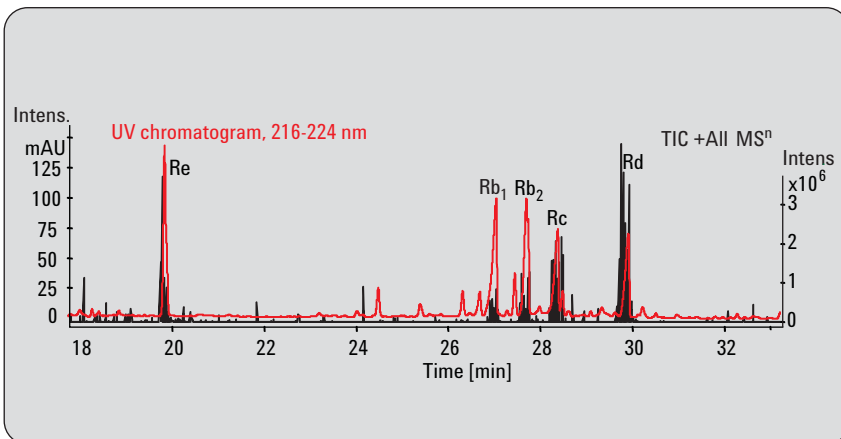


Figure 7
MS/MS-MRM of the sodiated molecular ions of ginsenosides Re, Rb₁ and Rc together with the UV chromatogram obtained from a crude ginseng root.

Conclusion

The Agilent 1200 Series Rapid Resolution LC system in combination with the Agilent 6330 Ion Trap LC/MS proves its capability in structure elucidation of natural products in highly complex extracts from plant origin. In this study a highly complex extract from ginseng root was analyzed by with the Agilent 1200 Series Rapid Resolution LC system and the Agilent 6330 Ion Trap LC/MS system. Complex structures of three ginsenosides, which are the main compounds of the extract, could be elucidated by the interpretation of the MS/MS and MS³ ion trap data obtained. The detailed knowledge of the different fragmentation data can be used to control the quality of natural extracts or pharmaceutical products by ion trap MRM when applied to special ingredients.

References

1. Fuzzati N. "Analysis methods of ginsenosides.", *J. Chrom B1-2*, 812, 2004, 114-133.
2. Wang X., Sakuma T., Asafu-Adjaye E., Shiu G. K. „Determination of ginsenosides in plant extracts from Panax ginseng and Panax quinquefolius L. by LC/MS/MS.", *Anal. Chem.* 71, 1579-1584, **1999**.
3. Chan T.W.D., But P.P.H., Cheng S.W., Kwok I.M.Y., Lau F.W., Xu H.X. "Differentiation and authentication of Panax ginseng, Panax quinquefolius, and ginseng products by using HPLC/MS." *Anal. Chem.* 72, 1281-1287. **2000**.
4. "Examination of a complex natural product extract from Ginseng – Part I: Structure elucidation of Ginsenosides by high resolution LC – ESI oaTOF with accurate mass measurement", *Agilent Application Note, Publication number 5989-4506*, **2006**.
5. "Performance of the Agilent 1200 SL HPLC System for Ultra-Fast LC Applications with 2.1-mm i.d. columns." *Agilent Application Note, publication number 5989-4502EN*, **2006**.
6. "Performance of Agilent 1200 SL LC system for highest resolution." *Agilent Application Note, publication number 5989-4489EN*, **2006**.
7. "Examination of a complex natural product extract from Ginseng - Part III: Species differentiation ginseng and authentication of ginseng products by LC/MS", *Agilent Application Note, Publication Number 5989-4706EN*, **2006**.

*Edgar Nägele is Application
Chemist at Agilent Technologies,
Waldbronn, Germany.*

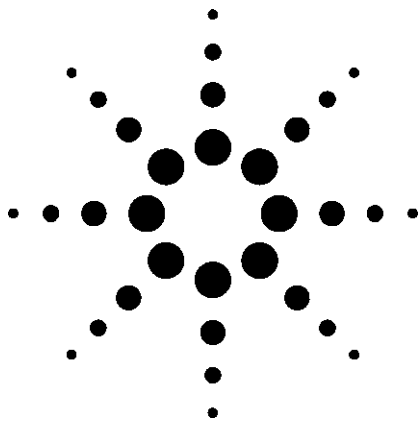
www.agilent.com/chem/1200

Copyright © 2006 Agilent Technologies
All Rights Reserved. Reproduction, adaptation
or translation without prior written permission
is prohibited except as allowed under the
copyright laws.

Published February 1, 2006
Publication Number 5989-4705EN



Agilent Technologies



Hydrophilic Interaction Chromatography (HILIC) Separation of Basic Drugs using MS/MS Detection

Application

Drug Analysis

Authors

Tatsunari Yoshida, Kazuo Yamanaka, and Hiroki Kumagai
Yokogawa Analytical Systems, Inc.
9-1 Takakura-Cho, Hachioji-Shi, Tokyo 192-0033
Japan

Ronald E. Majors
Agilent Technologies, Inc.
2850 Centerville Road
Wilmington, DE 19808-1610
USA

Abstract

The basic drugs, ranitidine and paroxetine were successfully separated using hydrophilic interaction liquid chromatography (HILIC). The elution order was reversed compared to reversed-phase liquid chromatography (RPLC). Good linearity was shown over the 0.5–100 ppb levels. A spiked serum was cleaned up by protein precipitation and an aliquot was directly injected into the HILIC/ESI-MS system. Recovery was found to be 98% for ranitidine and 79% for paroxetine at the 100 ppb level.

Introduction

Because of its versatility, RPLC is the most widely used technique in all of HPLC. It separates molecules based on the hydrophobic interactions between the nonpolar stationary phase and the

organic portions of typical analytes. However, the retention of polar analytes often requires a highly aqueous mobile phase to achieve retention. Highly aqueous systems sometimes lead to problems such as phase collapse (dewetting) [1], decreased sensitivity in mass spectroscopic detection due to poor mobile phase desolvation and ion suppression, and still may not allow retention of very polar analytes. Some specialized packings were developed to allow the use of highly aqueous systems such as polar embedded phases, hydrophilically endcapped reversed phase bonded silicas, wide-pore low-density bonded silicas, short-chain phases, and other special designs [2].

An alternative technique for the separation of highly polar analytes that gets around some of the problems associated with RPLC is HILIC. HILIC requires a high percentage of a nonpolar mobile phase and a polar stationary phase, similar to the requirements in normal phase chromatography (NPC). However, unlike NPC, which uses nonpolar solvents such as hexane and methylene chloride and tries to exclude water from the mobile phase, HILIC requires some water in the mobile phase to maintain a stagnant enriched water layer on the surface into which analytes may selectively partition. In addition, water-miscible organic solvents are used instead of the water-immiscible solvents used in NPC. With HILIC, sorbents such as bare silica, bonded diol, and polyhydroxyethylaspartamide are used. Polar analytes are well retained



Agilent Technologies

and elute in order of increasing hydrophilicity, just the inverse of RPLC. Sometimes, under HILIC conditions, polar analytes will show a very different selectivity compared to RPLC. It was demonstrated recently that the mechanism of HILIC involves various combinations of hydrophilic interaction, ion exchange, and reversed-phase retention by the siloxane on the silica surface [3].

Basic drugs with amine functionality are often separated by RPLC, and under acidic conditions when protonated may show decreased retention. In the present study, we investigated the separation of basic drugs in serum using RPLC on a C18 column and HILIC on bare silica gel employing electrospray ionization (ESI) and MS/MS detection.

Basic Drugs Studied

The structures of the basic drugs studied are depicted in Figure 1. Paroxetine (Figure 1a) is a psychotropic drug that is administered orally. It has a water solubility of 5.4 mg/mL and in its free base form its molecular weight (MW) is 329.36. Ranitidine (Figure 1b) is an antiulcerative and works by decreasing the amount of acid that the stomach produces. It is freely soluble in water and methanol but sparingly soluble in ethanol. Its MW is 314.41 in its free base form.

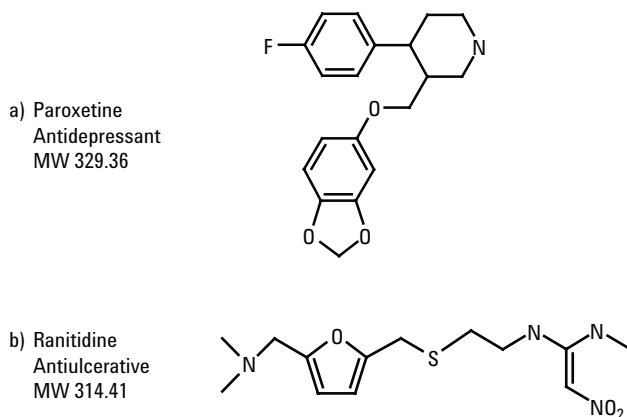


Figure 1. Structures of drug compounds studied.

Chromatographic System

Since mass spectrometry (MS) using ESI was employed for detection, we elected to use 2.1-mm internal diameter (id) columns where the normal flow rate was more compatible.

RPLC

| | |
|---------------------|--|
| Instrument: | Agilent Series 1100LC |
| Column: | ZORBAX Eclipse XDB-C18, 2.1 mm × 150 mm, 5 μm) |
| Mobile phase: | A: 8-mM HCOONH ₄ in water B: 8-mM HCOONH ₄ in 95% acetonitrile (MeCN)/5% water |
| Gradient: | 5% B to 90% B in 10 min |
| Column temperature: | 40 °C |
| Sample volume: | 5 μL |
| Flow rate: | 0.3 mL/min |

HILIC

Everything same as for RPLC except for column and gradient conditions:

| | |
|-----------|---|
| Column: | ZORBAX RX-SIL, 2.1 mm × 150 mm, 5 μm |
| Gradient: | 100% B to 50% B in 10 min |

Mass Spectrometry

| | |
|---------------------|-------------------------|
| Instrument: | Series 1100 LC/MSD Trap |
| Ionization: | Positive ESI |
| Scan range: | 100–500 <i>m/z</i> |
| SIM ions: | <i>m/z</i> = 315, 330 |
| Drying gas: | 10 L/min at 350 °C |
| Nebulizer gas: | 45 psi |
| Fragmentor voltage: | 0.25 V |

Results and Discussion

In order to select the best SIM for online monitoring, the MS spectra of the drug standards were run. Figure 2 shows that an M+1 ion was observed but ions at m/z of 192.0 and 175.9 were used for paroxetine and ranitidine, respectively, since they showed stronger signals. These ions were monitored in subsequent runs.

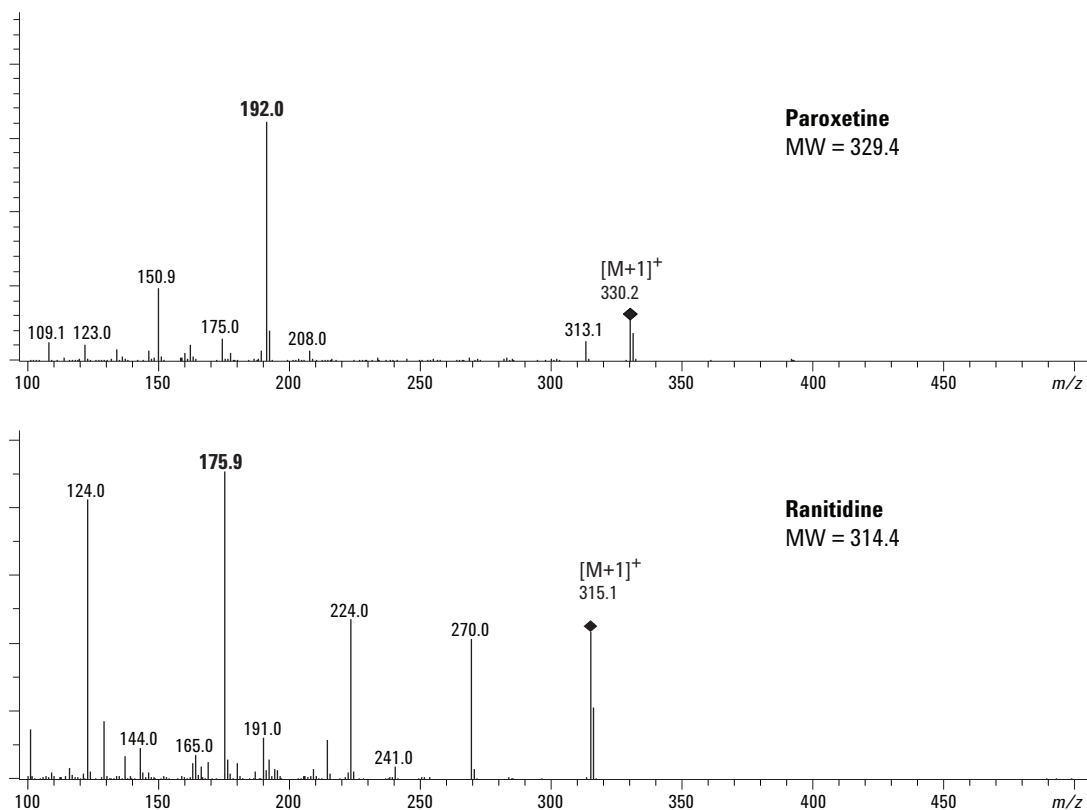


Figure 2. MS/MS spectra of drug standards showing ions selected for subsequent fragmentation.

The RPLC gradient elution total ion chromatogram of standards, shown in Figure 3, gave an excellent and relatively fast separation of the two drugs. However, with ranitidine there was some tailing at the 100 ppb (parts per billion) level. Since we were interested in the measurement of lower levels in serum, this separation was deemed unacceptable so we switched our attention to the HILIC conditions.

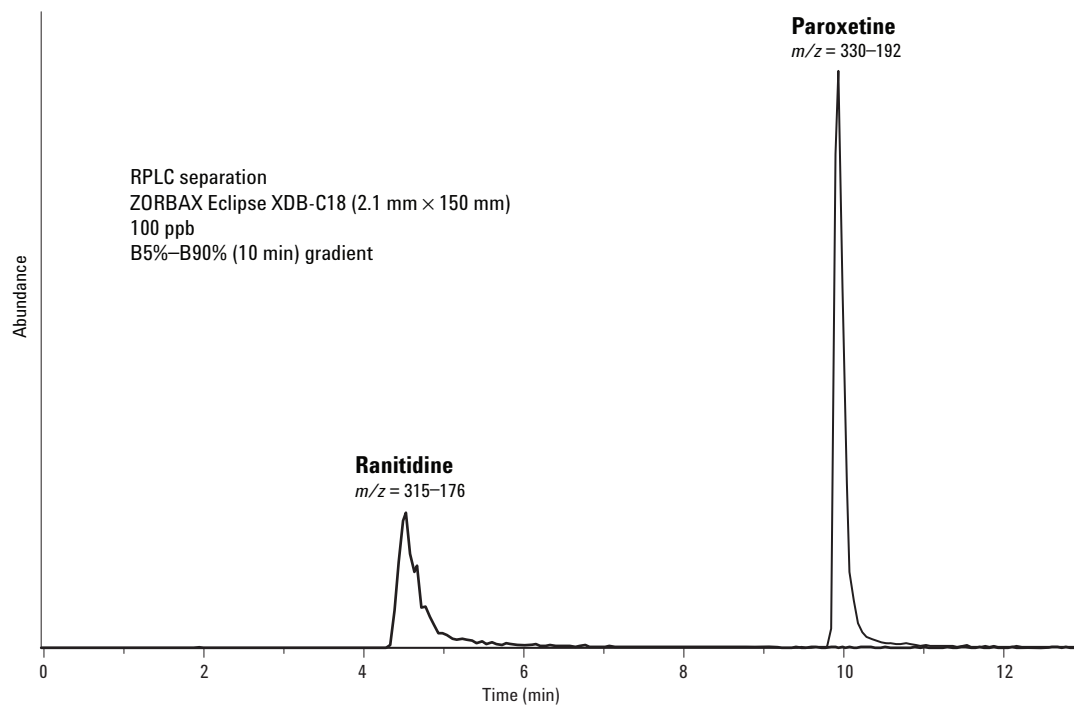


Figure 3. LC/MS/MS separation of paroxetine and ranitidine on ZORBAX Eclipse XDB-C18 column (RPLC mode).

Figure 4 depicts the separation of the two drug standards using HILIC on a silica gel column. Note that the elution order was reversed as might be expected but the peak shape for ranitidine was improved over the RPLC separation. The selectivity was not as good as with RPLC; nevertheless excellent baseline resolution was achieved. In addition, under the conditions employed, the separation was faster than with RPLC.

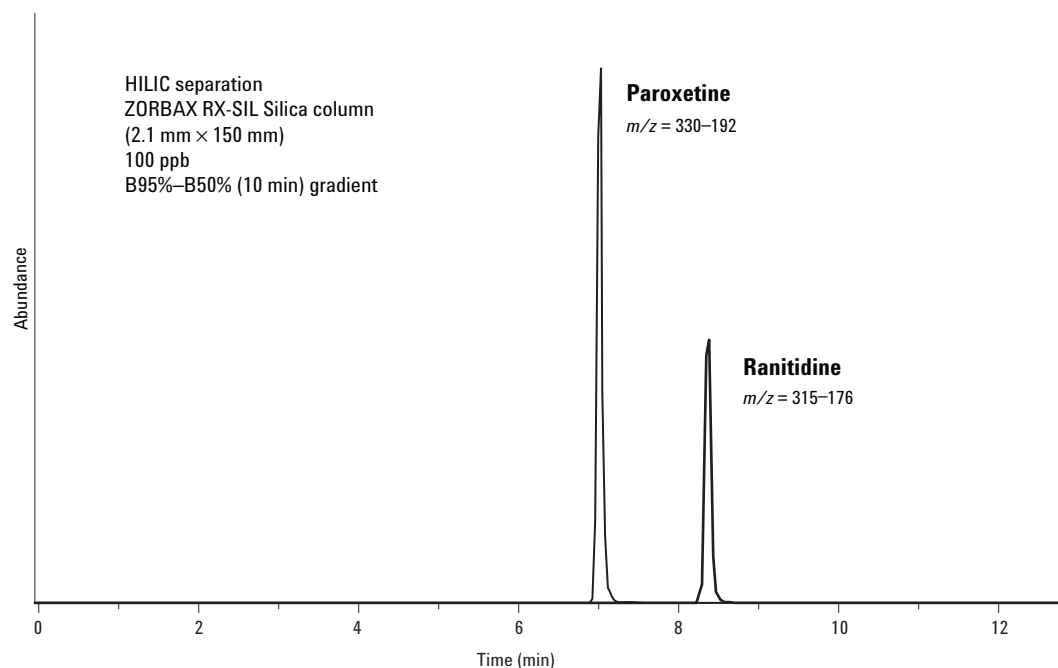


Figure 4. LC/MS/MS Separation of paroxetine and ranitidine on ZORBAX RX-SIL column (HILIC mode) – 100 ppb level.

Figure 5 shows the same separation but now at the 0.5-ppb level. Good sensitivity was noted for both drugs.

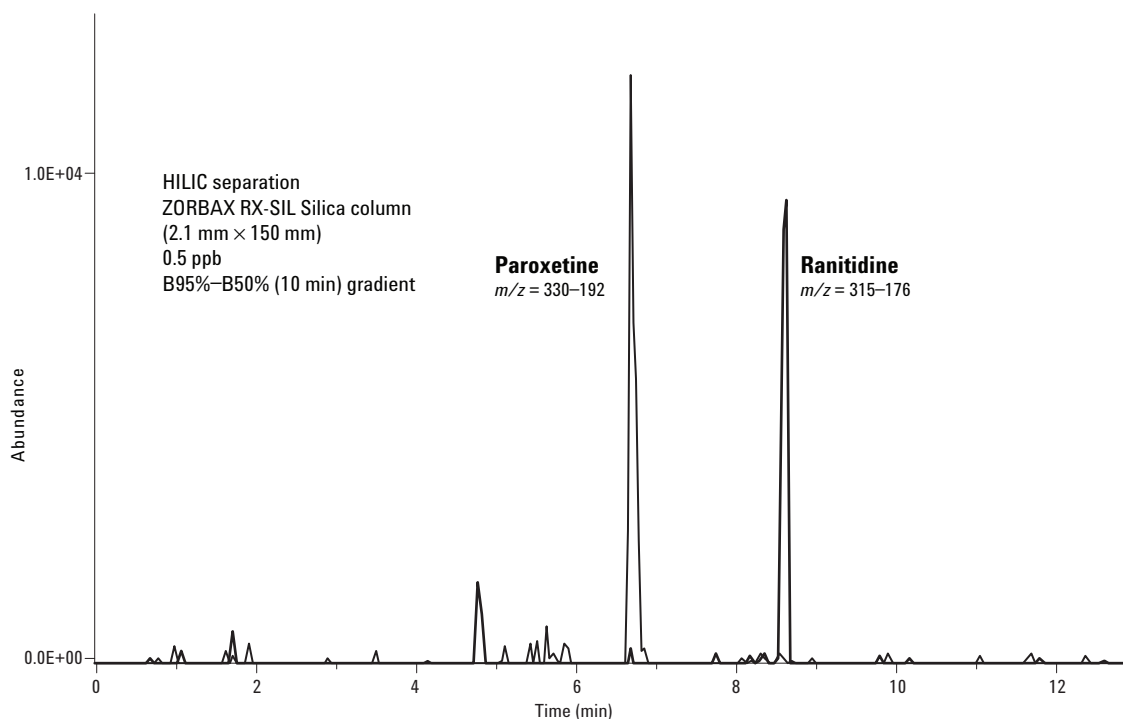


Figure 5. LC/MS/MS Separation of paroxetine and ranitidine on ZORBAX RX-SIL column (HILIC mode) – 0.5 ppb level.

We constructed a calibration curve as shown in Figure 6 and both drug compounds gave good linearity with an acceptable correlation coefficient over the expected concentration range.

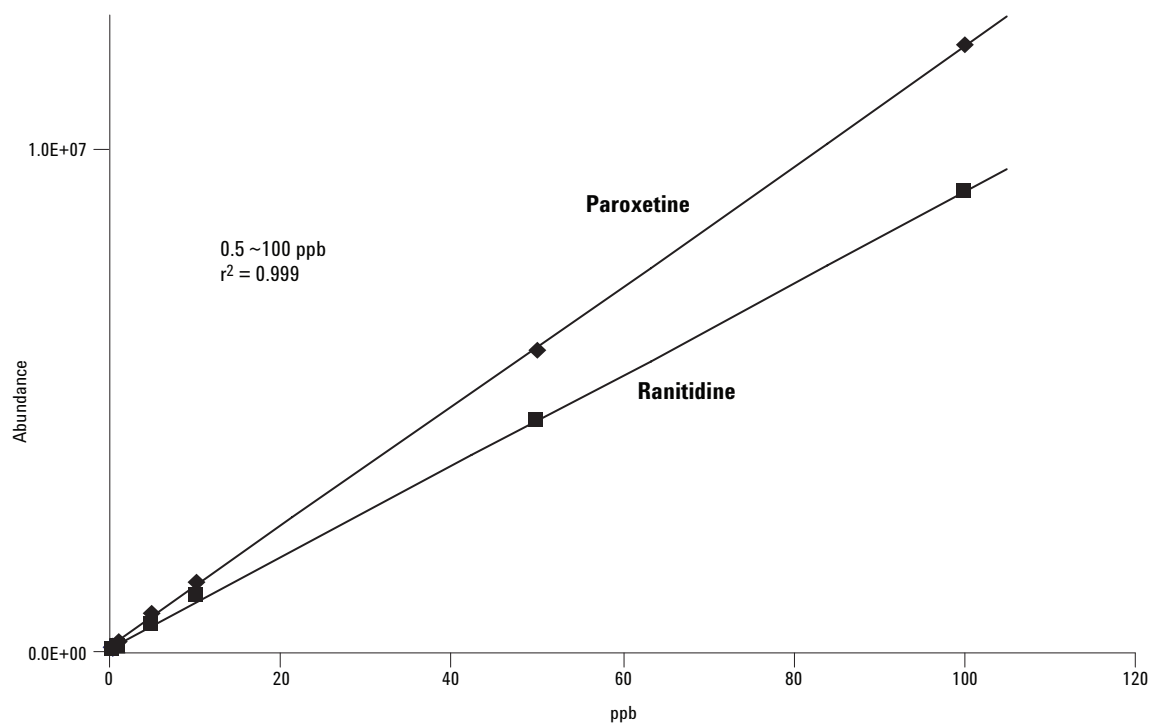


Figure 6. Linearity of paroxetine and ranitidine on ZORBAX RX-SIL Column (HILIC Mode).

Next, a human serum sample was spiked with a 5- μ L aliquot of each drug compound (20 ppm) and the sample was prepared according to the sample preparation protocol outlined in Figure 7.

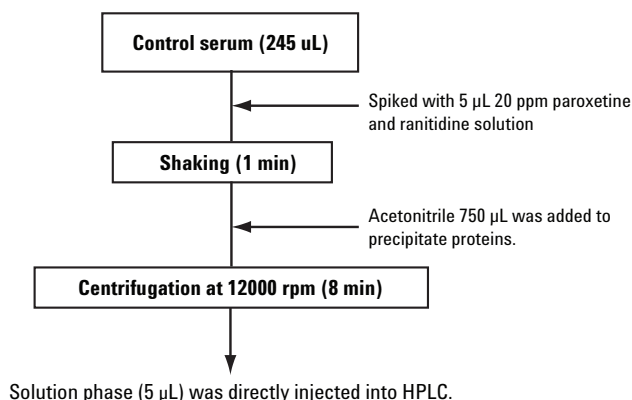


Figure 7. Sample preparation procedure of spiked serum.

A 5- μ L aliquot of the cleaned-up serum sample containing the drugs was injected into the HILIC column. The resulting ion chromatograms of Figure 8 (upper trace LC/MS and lower trace LC/MS-MS) show that both compounds were able to be measured at the 100 ppb level serum. Recovery was 79% for paroxetine and 98% for ranitidine, both acceptable at these levels.

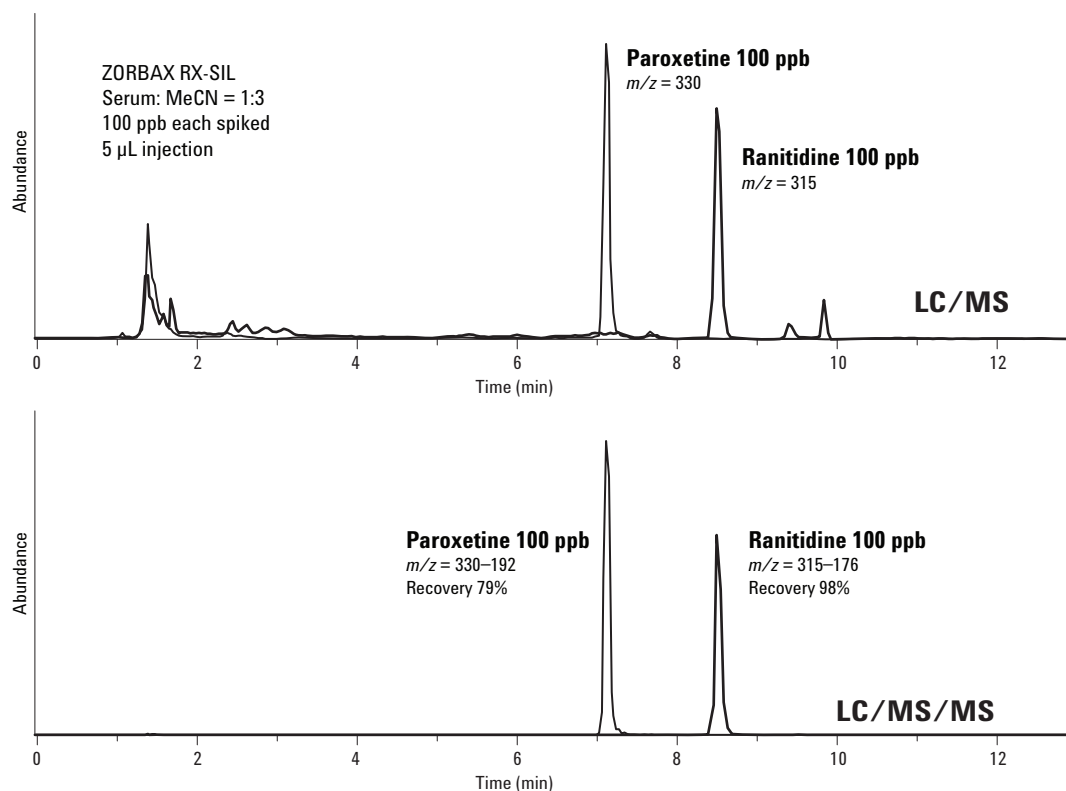


Figure 8. LC/MS and LC/MS/MS analysis of paroxetine and ranitidine spiked into human serum with ZORBAX RX-SIL Column.

Conclusion

Ranitidine and paroxetine were successfully separated using the HILIC mode. The elution order was reversed compared to the RPLC mode. Good linearity was shown over the 0.5–100 ppb levels. A spiked serum was cleaned up by protein precipitation and an aliquot was directly injected into the HILIC/ESI-MS system. Recovery was found to be 98% for ranitidine and 79% for paroxetine at the 100-ppb level.

References

1. M. Przybyciel and R. E. Majors, (2002), *LCGC No. America*, **20** (6), 516–523.
2. R. E. Majors and M. Przybyciel, (2002), *LCGC No. America*, **20** (7), 584–593.
3. W. Naidong, (2003), *J. Chromatogr. B*, **796**, 209–224.

For More Information

For more information on our products and services, visit our Web site at www.agilent.com/chem.

Agilent shall not be liable for errors contained herein or for incidental or consequential damages in connection with the furnishing, performance, or use of this material.

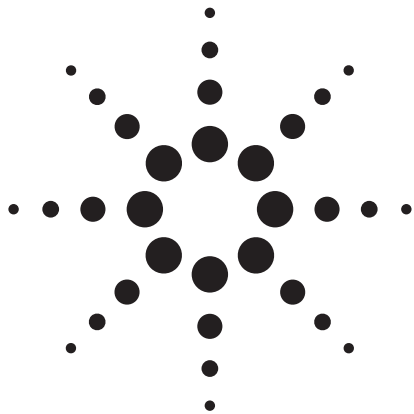
Information, descriptions, and specifications in this publication are subject to change without notice.

© Agilent Technologies, Inc. 2005

Printed in the USA
September 8, 2005
5989-3761EN



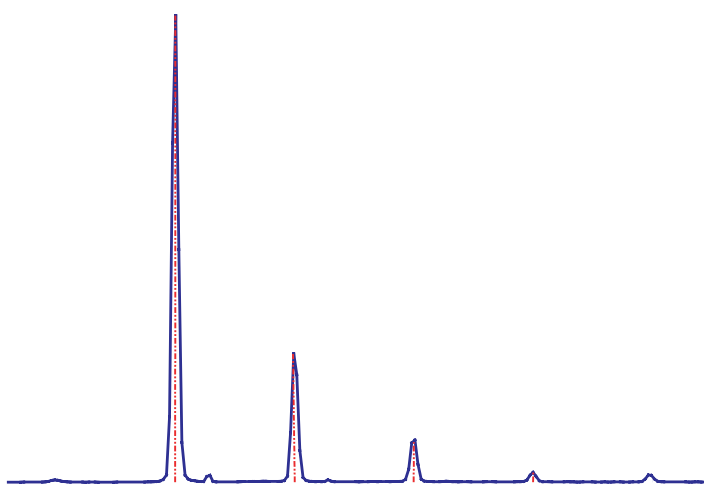
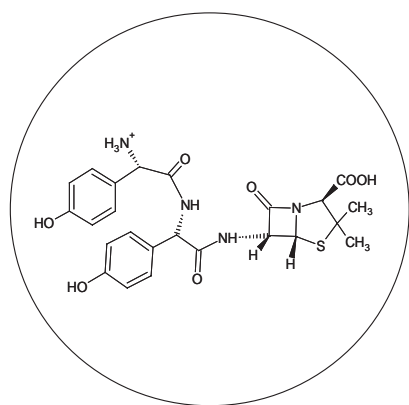
Agilent Technologies



Statistic evaluation of mass accuracy measurements by ESI TOF with a sample of degradation products from the antibiotic drug amoxicillin

Application Note

Edgar Nägele



Abstract

The measurement of accurate molecular mass by mass spectrometry and calculation of the corresponding empirical formula is an important step in the identification process of small molecules in a range of application fields. In order to rely on the measured values it is important to know the performance of the mass spectrometer for accurate mass measurement. In this Application Note the mean and standard deviation of repeatedly measured mass accuracies from a real-life pharmaceutical sample will be presented.



Agilent Technologies

Introduction

For a reliable empirical formula confirmation it is necessary to set a mass accuracy limit which takes the acceptable uncertainty of the accurate molecular mass measurement into consideration. For instance, for a mass measurement of m/z 118 (where C₀₋₁₀₀, H₃₋₇₄, O₀₋₄ and N₀₋₁₅) there must be no alternative formulas within 34 ppm before such a claim is made.

Increasing the mass measurement to m/z 750 (where C₀₋₁₀₀, H₂₅₋₁₁₀, O₀₋₁₅ and N₀₋₁₅) there are 626 alternative formulas within 5 ppm. The error measurement acceptable at m/z 750 must be 0.018 ppm to eliminate all alternative formulas¹. Therefore, it is necessary to know the instrument performance for the determination of accurate molecular mass and the empirical formula. Knowing mean and the standard deviation of measured accurate masses over a certain mass range is of crucial interest to exclude possible empirical formulas, which are outside of the statistic confidence interval². For that purpose there are some methods for the statistical evaluation of accurate mass measurement quality by a mass spectrometer instrument described in applicable literature³. Several years ago only operation intensive magnetic sector field and FT mass spectrometers were able to perform these measurements with sufficient mass accuracy. Nowadays, comparably easy-to-use and inexpensive ESI orthogonal acceleration TOF (oaTOF) instruments are also capable of handling this task. This is clearly demonstrated by a comparison study of different types of mass spectrometer instruments for the determination of accurate

mass of small molecules⁴. This was made possible by some technical innovations in TOF technology introduced during the past years. One of the main technical innovations is the development of orthogonal acceleration TOF technology, which decouples the ion beam velocity spread from the TOF axis, which provides better resolution of the TOF mass spectrometers⁵. In this environment the coupling of continuous ionization sources such as the electrospray ionization (ESI) source with orthogonal acceleration TOF mass analyzers is of special importance for LC-ESI TOF applications. A high mass accuracy is only achieved when a reference compound, a reference mass, is simultaneously introduced into the mass spectrometer with the analyte itself. Mixing the LC column effluent with a stream of reference material can result in ion suppression, discrimination or adduct formation. To prevent mixing the analyte and the reference compound prior to spray ionization, an innovation which applies a dual ESI sprayer interface is used^{6,7}. This instrument is capable of achieving resolutions above 15,000 and mass accuracies in the single digit ppm range for small molecules⁴. In this Application Note the mean and standard deviation of repeatedly measured mass accuracies from a real life pharmaceutical sample of degraded antibiotic amoxicillin will be presented.

Experimental

Equipment

- The ESI TOF MS analysis was performed with the Agilent LC/MSD TOF equipped with a dual sprayer source for the

simultaneous infusion of the reference mass solution.

- The LC system used was an Agilent 1100 Series capillary LC system containing a capillary pump with a micro vacuum degasser, a micro well-plate autosampler with a thermostat and a column compartment.
- The column used was a ZORBAX SB Aq, 0.3 mm x 150 mm, 3.5 μ m.
- The software used for instrument control was TOF software A01.01 and for data analysis Analyst QS software.

Methods

- The Agilent 1100 Series capillary pump was operated under the following conditions:
Solvent A: water, 10 mM ammonium formate, pH 4.1;
Solvent B: ACN
Column flow: 8 μ L/min,
Primary flow: 500-800 μ L/min
Gradient: 0 min 0 % B, 1 min 0 % B, 13 min 25 % B, 23 min 25 % B
Stop time: 23 min
Post time: 15 min.
- The Agilent 1100 Series autosampler was used to make injections of 1 μ L sample and the samples were cooled. The sample loop was switched to bypass after 1 minute to reduce delay volume.
- The mass spectrometer was operated under the following conditions:
Source: ESI in positive mode with dual spray for reference mass.
Dry gas: 7.0 L/min
Dry Temp.: 300 °C
Nebulizer: 15 psi
Scan: 50-1000
Fragmentor: 300 V for CID
Skimmer: 60 V
Capillary: 5000 V
- Sample preparation: The antibi-

otic amoxicillin was stressed under acidic conditions. Approximately 1 mL of amoxicillin solution (25 mg/mL in DMSO) was added to 1 mL 0.1 M HCl solution. The sample was stirred for 1 hour at room temperature (RT = 25 °C) and then diluted (1:10 with DMSO).

Results and discussion

The complex real life pharmaceutical sample, which was used for this instrument performance evaluation under real application conditions, is a mixture of degradation products of the antibiotic drug amoxicillin obtained by acid treatment of the pharmaceutical drug substance. Five compounds, which were identified in an earlier examination of this sample^{8,9}, were used for the performance evaluation of accurate mass measurement by the ESI oaTOF (figure 1). In this earlier work the structure elucidation of the degradation products was done by ion trap mass spectrometry⁸ and the final identity confirmation was performed by accurate mass measurement and empirical formula calculation using the ESI oaTOF⁹. Herein, the sample was measured once and the mass accuracy of each compound was determined. To also confirm the molecular identity of the fragments obtained earlier in the ion trap experiment, the ESI oaTOF experiment was repeated at a higher capillary voltage to induce CID fragmentation. With the obtained data of high mass accuracy the compounds could be identified with sufficient confidence (figure 2A - E). The obtained set of data, consisting of the accurate mass of the molecular ions and the corresponding fragments for each com-

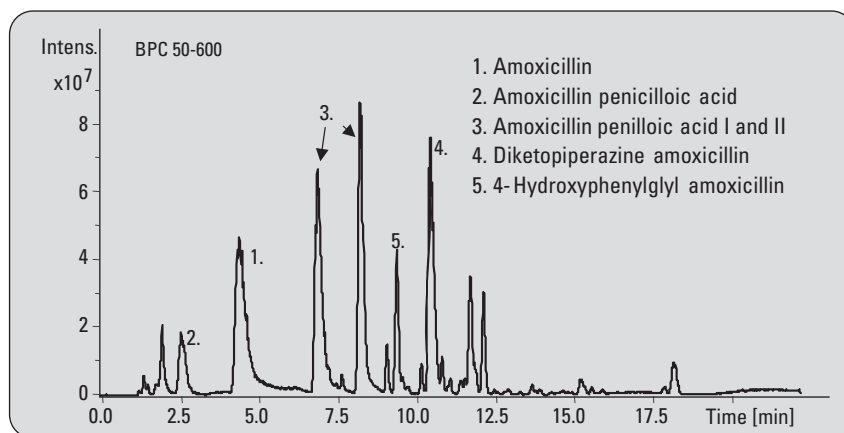


Figure 1
BPC of amoxicillin (1) and its degradation products after acid exposure..

pound, was not enough to make a reliable statistical analysis. Therefore, the measurement was repeated five times to obtain enough data points to make a legitimate statistical statement. Altogether, the five experiments provided 135 data points between m/z 114 and m/z 515 comprising the molecular ions and the fragments of the compounds (table 2A – E). The tables show the individually measured masses of the molecular ions and their fragments as well as the individual mean mass and standard deviation thereof. For each measured mass the mass accuracy was calculated in mDa and ppm. The calculated mean and its standard deviation of the mDa and ppm values are shown in table 2A – E. To obtain the value and the confidence interval of the accuracy performance over the used mass range the mean and the standard deviation of all mDa and ppm accuracy data was calculated. The overall mass accuracy was calculated as 1.73 ppm with a standard deviation of 0.97 respective to 0.39 mDa with a standard deviation of 0.21. The standard deviation (s) gives the confidence

interval with a probability to find the measured value around the mean. The confidence interval of $3s$ contains the value with 99.7 % probability. Therefore, for one of the measured masses of 4-hydroxy-phenylglycyl amoxicillin **5** all possible empirical formulas within a window of 3 ppm around the measured mass at m/z 515.1596 were calculated. Within this mass accuracy window and a possible formula in the range of $C_{0-100}H_{0-200}N_{0-10}O_{0-10}S_{0-5}$ there are 12 possible empirical formulas. To find the right empirical formula out of this set of possible formulas an isotopic intensity analysis of the mass spectrum by comparison to a calculated isotopic ratio was done (figure 3). The isotopic ratio analysis showed clearly that only the calculated empirical formula for 4-hydroxyphenylglycyl amoxicillin **5**, which contains one sulfur atom, exactly matches the measured isotopic ratios. All other empirical formulas in the 3 ppm mass accuracy window contained none or more than one sulfur atom, which resulted in an isotopic ratio easily distinguished from the measured isotopic ratio.

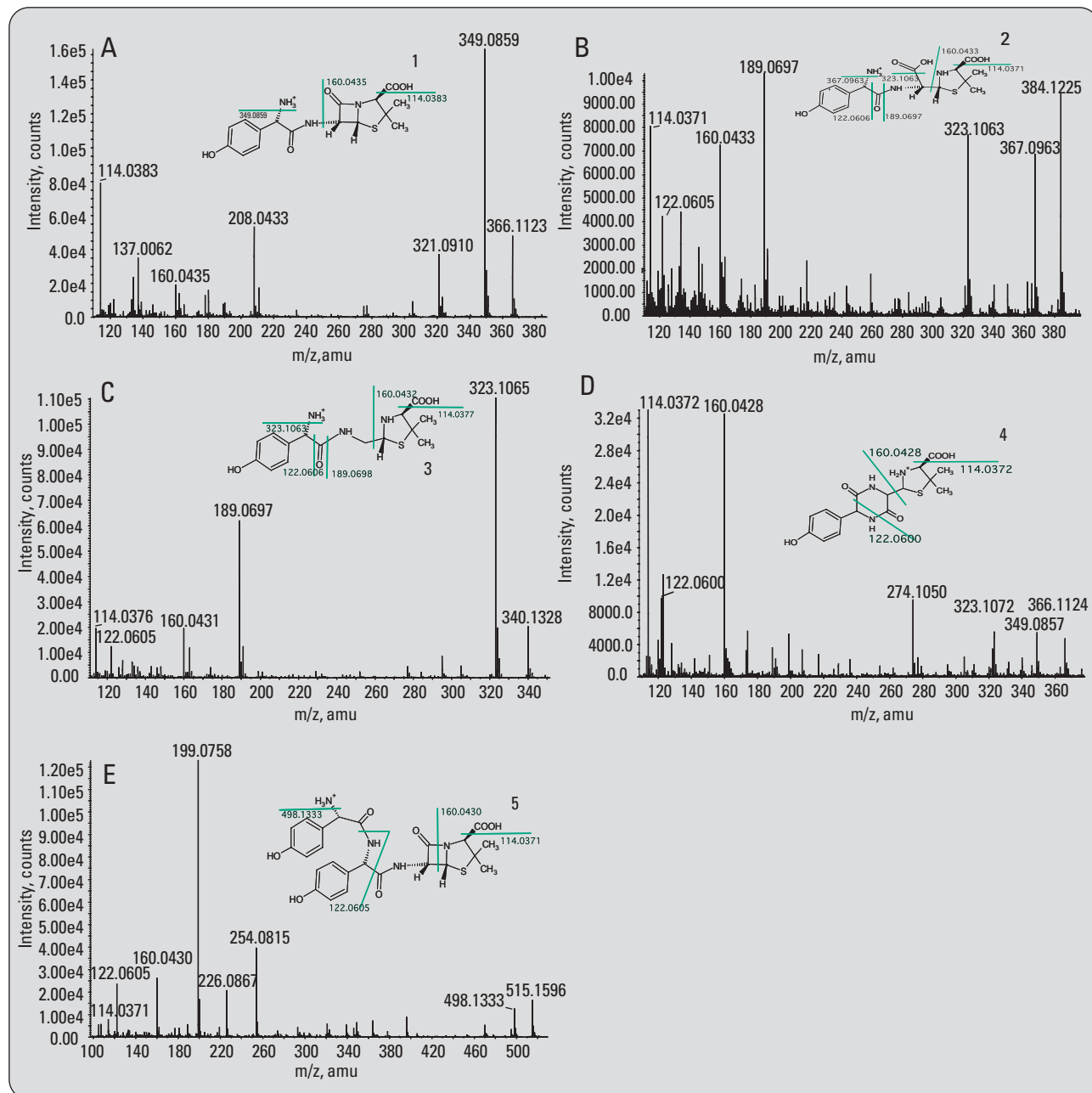


Figure 2

ESI oaTOF analysis of amoxicillin (1) and its degradation products after acidic exposure for accurate mass measurement and compound confirmation

A) amoxicillin (1) (C₁₆H₁₉N₃O₅S), [M+H]⁺ = m/z 366.1124

B) amoxicillin penilloic acid (2) (C₁₆H₂₁N₃O₆S), [M+H]⁺ = m/z 384.1229

C) amoxicillin penilloic acid I and II (3) (C₁₅H₂₁N₃O₄S), [M+H]⁺ = m/z 340.1331

D) diketopiperazine amoxicillin (4) (C₁₆H₁₉N₃O₅S), [M+H]⁺ = m/z 366.1124

E) 4-hydroxyphenylglycyl amoxicillin (5) (C₂₄H₂₆N₄O₇S), [M+H]⁺ = m/z 515.1600

| Measured mass | Mean SD [$\times 10^{-4}$] | Calculated mass | Formula | Mass accuracy [mDa] | Mean [mDa] SD [mDa] | Mass accuracy [ppm] | Mean [ppm] SD [ppm] |
|---------------|------------------------------|-----------------|-----------------------|---------------------|---------------------|---------------------|---------------------|
| 366.1123 | 366.1125 1.80 | 366.1124 | $C_{16}H_{20}N_3O_5S$ | -0.10 | 0.14 | 0.27 | 0.41 |
| 366.1125 | | | | 0.10 | | -0.27 | |
| 366.1127 | | | | 0.30 | | -0.82 | |
| 366.1126 | | | | 0.20 | | -0.55 | |
| 366.1123 | | | | -0.10 | | 0.27 | |
| 349.0859 | 349.0859 2.50 | 349.0858 | $C_{16}H_{17}N_2O_5S$ | 0.10 | 0.30 | -0.28 | 0.86 |
| 349.0862 | | | | 0.40 | | -1.14 | |
| 349.0865 | | | | 0.70 | | -2.00 | |
| 349.0861 | | | | 0.30 | | -0.86 | |
| 349.0859 | | | | 0.10 | | -0.28 | |
| 160.0435 | 160.0435 0.50 | 160.0432 | $C_6H_{10}NO_2S$ | 0.30 | 0.26 | -1.87 | 1.46 |
| 160.0434 | | | | 0.20 | | -1.25 | |
| 160.0434 | | | | 0.20 | | -1.25 | |
| 160.0435 | | | | 0.30 | | -1.87 | |
| 160.0435 | | | | 0.30 | | -1.87 | |
| 114.0383 | 114.0378 4.80 | 114.0377 | C_5H_8NS | 0.60 | 0.42 | -5.26 | 3.60 |
| 114.0372 | | | | -0.50 | | 4.38 | |
| 114.0374 | | | | -0.30 | | 2.63 | |
| 114.0382 | | | | 0.50 | | -4.38 | |
| 114.0379 | | | | 0.20 | | -1.75 | |

Table 1A

Summary of the mass accuracy and precession data measurement for the Amoxicillin (1) and its degradation products and their CID fragments measured with the ESI TOF (mean and standard deviation SD of the ppm values)

A) amoxicillin (1) ($C_{16}H_{19}N_3O_5S$), $[M+H]^+ = m/z$ 366.1124

| Measured mass | Mean SD [$\times 10^{-4}$] | Calculated mass | Formula | Mass accuracy [mDa] | Mean [mDa] SD [mDa] | Mass accuracy [ppm] | Mean [ppm] SD [ppm] |
|---------------|------------------------------|-----------------|-----------------------|---------------------|---------------------|---------------------|---------------------|
| 384.1225 | 384.1226 4.10 | 384.1229 | $C_{16}H_{22}N_3O_6S$ | -0.40 | 0.38 | 1.04 | 0.98 |
| 384.1225 | | | | -0.40 | | 1.04 | |
| 384.1230 | | | | 0.10 | | -0.26 | |
| 384.1221 | | | | 0.80 | | -2.08 | |
| 384.1231 | | | | 0.20 | | -0.52 | |
| 367.0963 | 367.0965 4.61 | 367.0964 | $C_{16}H_{19}N_2O_6S$ | -0.10 | 0.38 | 0.27 | 1.03 |
| 367.0961 | | | | -0.30 | | 0.82 | |
| 367.0969 | | | | 0.50 | | -1.36 | |
| 367.0960 | | | | -0.40 | | 1.09 | |
| 367.0970 | | | | 0.60 | | -1.63 | |
| 323.1063 | 323.1068 3.63 | 323.1066 | $C_{15}H_{19}N_2O_2S$ | -0.30 | 0.34 | 0.93 | 1.05 |
| 323.1069 | | | | 0.30 | | -0.93 | |
| 323.1071 | | | | 0.50 | | -1.55 | |
| 323.1065 | | | | -0.10 | | 0.31 | |
| 323.1071 | | | | 0.50 | | -1.55 | |
| 189.0697 | 189.0700 1.81 | 189.0698 | $C_7H_{13}N_2O_2S$ | -0.10 | 0.18 | 0.53 | 0.95 |
| 189.0699 | | | | 0.10 | | -0.53 | |
| 189.0699 | | | | 0.10 | | -0.53 | |
| 189.0700 | | | | 0.20 | | 1.05 | |
| 189.0702 | | | | 0.40 | | 2.11 | |
| 160.0433 | 160.0435 1.95 | 160.0432 | $C_6H_{10}NO_2S$ | 0.10 | 0.26 | -0.62 | 1.62 |
| 160.0434 | | | | 0.20 | | -1.25 | |
| 160.0434 | | | | 0.20 | | -1.25 | |
| 160.0438 | | | | 0.60 | | -3.75 | |
| 160.0434 | | | | 0.20 | | -1.25 | |
| 122.0605 | 122.0605 2.60 | 122.0606 | C_7H_8NO | -0.10 | 0.20 | 0.82 | 1.36 |
| 122.0605 | | | | -0.10 | | 0.82 | |
| 122.0605 | | | | -0.10 | | 0.82 | |
| 122.0610 | | | | 0.40 | | -2.50 | |
| 122.0603 | | | | -0.30 | | 1.87 | |
| 114.0371 | 114.0375 3.19 | 114.0377 | C_5H_8NS | -0.60 | 0.30 | 5.26 | 1.57 |
| 114.0375 | | | | -0.20 | | 1.75 | |
| 114.0380 | | | | 0.30 | | -2.63 | |
| 114.0375 | | | | -0.20 | | 1.75 | |
| 114.0375 | | | | -0.20 | | 1.75 | |

Table 1B

Summary of the mass accuracy and precession data measurement for the Amoxicillin (1) and its degradation products and their CID fragments measured with the ESI TOF (mean and standard deviation SD of the ppm values)

B) amoxicillin penicilloic acid (2) ($C_{16}H_{21}N_3O_6S$), $[M+H]^+ = m/z$ 384.1229

| Measured mass | Mean SD [$\times 10^{-4}$] | Calculated mass | Formula | Mass accuracy [mDa] | Mean [mDa] SD [mDa] | Mass accuracy [ppm] | Mean [ppm] SD [ppm] |
|--|------------------------------|-----------------|-----------------------|--|---------------------|--|---------------------|
| 340.1328 340.1334 340.1332 340.1338 340.1335 | 340.1333 3.71 | 340.1331 | $C_{16}H_{22}N_3O_4S$ | -0.30 0.30 0.10 0.70 0.40 | 0.36 0.22 | 0.88 -0.88 -0.29 -2.06 -1.17 | 1.05 0.44 |
| 323.1065 323.1065 323.1062 323.1062 323.1070 | 232.1065 3.27 | 323.1066 | $C_{15}H_{19}N_2O_4S$ | -0.10 -0.10 -0.40 -0.40 0.40 | 0.28 0.16 | 0.31 0.31 1.24 1.24 -1.24 | 0.86 0.50 |
| 189.0697 189.0699 189.0696 189.0703 189.0699 | 189.0699 2.68 | 189.0698 | $C_7H_{13}N_2O_2S$ | -0.10 0.10 -0.20 0.50 0.10 | 0.20 0.17 | 0.53 -0.53 1.05 -2.64 -0.53 | 1.06 0.91 |
| 160.0431 160.0433 160.0429 160.0438 160.0432 | 160.0433 3.36 | 160.0432 | $C_6H_{10}NO_2S$ | -0.10 0.10 -0.30 0.60 -0.10 | 0.24 0.22 | 0.62 -0.62 1.87 -3.75 0.62 | 1.49 1.37 |
| 122.0605 122.0605 122.0598 122.0613 122.0602 | 122.0605 5.50 | 122.0606 | C_7H_8NO | -0.10 -0.10 -0.80 0.70 -0.40 | 0.42 0.32 | 0.82 0.82 6.55 -5.73 3.27 | 3.43 2.67 |
| 114.0376 114.0373 114.0372 114.0378 114.0373 | 114.0374 2.51 | 114.0377 | C_5H_8NS | -0.10 -0.40 -0.50 0.10 -0.40 | 0.30 0.18 | 0.87 3.50 4.38 -0.87 3.50 | 2.62 1.64 |

Table 1C

Summary of the mass accuracy and precession data measurement for the amoxicillin (1) and its degradation products and their CID fragments measured with the ESI TOF (mean and standard deviation SD of the ppm values)

C) amoxicillin penilloic acid I and II (3) ($C_{15}H_{21}N_3O_4S$), $[M+H]^+ = m/z$ 340.1331

| Measured mass | Mean SD [$\times 10^{-4}$] | Calculated mass | Formula | Mass accuracy [mDa] | Mean [mDa] SD [mDa] | Mass accuracy [ppm] | Mean [ppm] SD [ppm] |
|--|------------------------------|-----------------|-----------------------|---|---------------------|--|---------------------|
| 366.1124 366.1127 366.1126 366.1127 366.1127 | 366.1126 1.30 | 366.1125 | $C_{16}H_{20}N_3O_5S$ | -0.10 0.20 0.10 0.20 0.20 | 0.16 0.05 | 0.27 -0.54 -0.27 -0.54 -0.54 | 0.42 0.14 |
| 349.0857 349.0870 349.0848 349.0868 349.0859 | 349.0860 8.90 | 349.0858 | $C_{16}H_{17}N_2O_5S$ | -0.10 1.20 -1.00 1.00 0.10 | 0.68 0.53 | 0.22 -3.44 2.86 -2.86 -0.22 | 1.92 1.56 |
| 160.0428 160.0434 160.0431 160.0434 160.0439 | 160.0433 4.08 | 160.0432 | $C_6H_{10}NO_2S$ | -0.40 0.20 -0.10 0.20 0.70 | 0.32 0.24 | 2.50 -1.25 0.62 -1.25 -4.37 | 1.99 1.49 |
| 122.0600 122.0605 122.0604 122.0605 122.0604 | 122.0604 2.10 | 122.0606 | C_7H_8NO | -0.60 -0.10 -0.20 -0.10 -0.20 | 0.24 0.20 | 4.92 0.82 1.64 0.82 1.64 | 1.96 1.70 |
| 114.0372 114.0372 114.0372 114.0372 114.0372 | 114.0376 2.45 | 114.0377 | C_5H_8NS | -0.50 -0.10 -0.10 0.10 0.10 | 0.18 0.17 | 4.38 0.88 0.88 -0.88 -0.88 | 1.58 1.56 |

Table 1D

Summary of the mass accuracy and precession data measurement for the amoxicillin (1) and its degradation products and their CID fragments measured with the ESI TOF (mean and standard deviation SD of the ppm values)

D) diketopiperazine amoxicillin (4) ($C_{16}H_{19}N_3O_5S$), $[M+H]^+ = m/z$ 366.1124

| Measured mass | Mean SD [$\times 10^{-4}$] | Calculated mass | Formula | Mass accuracy [mDa] | Mean [mDa] SD [mDa] | Mass accuracy [ppm] | Mean [ppm] SD [ppm] |
|---------------|------------------------------|-----------------|-----------------------|---------------------|---------------------|---------------------|---------------------|
| 515.1596 | 515.1607 6.83 | 515.1600 | $C_{24}H_{27}N_4O_7S$ | -0.40 | 0.84 | 0.76 | 1.63 |
| 515.1605 | | | | 0.50 | | -0.97 | |
| 515.1608 | | | | 0.80 | | -1.55 | |
| 515.1613 | | | | 1.30 | | -2.52 | |
| 515.1612 | | | | 1.20 | | -2.39 | |
| 498.1333 | 498.1343 8.09 | 498.1335 | $C_{24}H_{24}N_3O_7S$ | -0.20 | 0.88 | 0.40 | 1.76 |
| 498.1342 | | | | 0.70 | | -1.40 | |
| 498.1338 | | | | 0.30 | | -0.60 | |
| 498.1349 | | | | 1.40 | | -2.81 | |
| 498.1353 | | | | 1.80 | | -3.61 | |
| 160.0430 | 160.0436 5.55 | 160.0432 | $C_6H_{10}NO_2S$ | -0.20 | 0.50 | 1.25 | 3.25 |
| 160.0434 | | | | 0.20 | | -1.25 | |
| 160.0434 | | | | 0.20 | | -1.25 | |
| 160.0440 | | | | 0.80 | | -4.99 | |
| 160.0444 | | | | 1.12 | | -7.50 | |
| 122.0605 | 122.0608 4.60 | 122.0606 | C_7H_8NO | -0.10 | 0.34 | 0.82 | 2.79 |
| 122.0605 | | | | -0.10 | | 0.82 | |
| 122.0605 | | | | -0.10 | | 0.82 | |
| 122.0611 | | | | 0.50 | | -4.10 | |
| 122.0615 | | | | 0.90 | | -7.40 | |
| 114.0371 | 114.0372 2.77 | 114.0377 | C_5H_8NS | -0.60 | 0.48 | 5.46 | 4.03 |
| 114.0369 | | | | -0.80 | | 7.01 | |
| 114.0374 | | | | -0.30 | | 2.63 | |
| 114.0371 | | | | -0.60 | | 5.26 | |
| 114.0376 | | | | -0.10 | | 0.87 | |

Table 1E

Summary of the mass accuracy and precession data measurement for the amoxicillin (1) and its degradation products and their CID fragments measured with the ESI TOF (mean and standard deviation SD of the ppm values)

E) 4-hydroxyphenylglycyl amoxicillin (5) ($C_{24}H_{26}N_4O_7S$), $[M+H]^+ = m/z$ 515.1600

Conclusion

For the determination of an empirical formula it is of crucial importance to work with a mass spectrometer, which can measure accurate molecular masses with the highest possible accuracy to minimize the number of possible formulas in a given mass accuracy window around the measured mass value. This Application Note evaluates the mean mass accuracy and its standard deviation achievable by means of the ESI oaTOF instrument under real life conditions with a pharmaceutical sample of the degraded antibiotic drug amoxicillin. The statistic evaluation of the obtained data showed that an empirical formula of an unknown compound could be expected in a mass accuracy window of 3 ppm around the measured mass value with a reliability of 99.7% (3s). It is common for

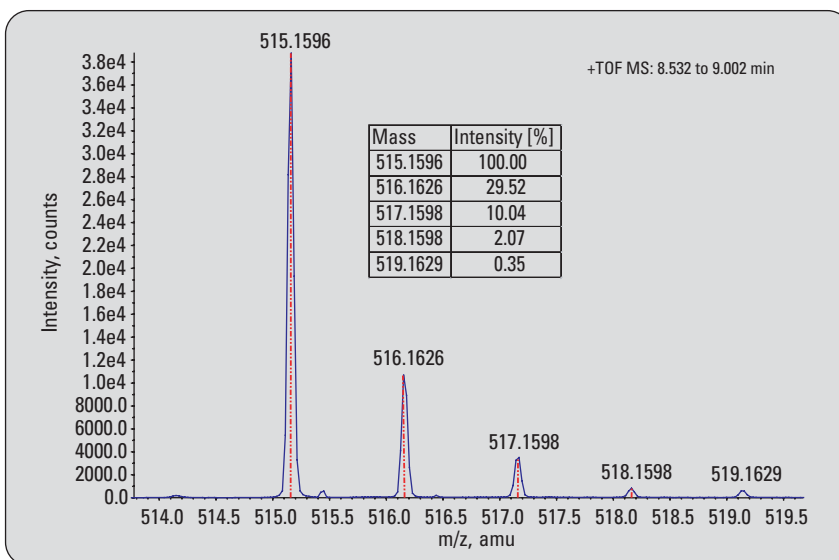


Figure 3

Measured isotopic ratio of 4-hydroxyphenylglycyl amoxicillin overlaid by the calculated isotopic ratio (red line) and calculated intensities for the isotopic mass peaks.

higher molecular weight compounds to have more than one possible empirical formula within this mass accuracy window. To determine the right formula an

additional analysis of the measured isotopic ratio of the molecular ion by comparing it to a calculated isotopic ratio is outlined.

References

1. "Instructions for Authors," *J. Am. Soc. Mass spectrom.* 14(12), **2003**.
2. M. P. Balogh "Debating resolution and mass accuracy in mass spectrometry", *spectroscopy* 19(10), Oct., 34-40, **2004**.
3. T. M. Sack, R. L. Lapp, M. L. Gross, B. J. Kimble "A method for the statistical evaluation of accurate mass measurement quality", *Int. J. Mass Spectrom. Ion Process.* 61, 191-213, **1984**.
4. Bristow A.W. T., Webb K. S. "Inter-comparison study on accurate mass measurement of small molecules in mass spectrometry." *J. Am. Mass Spectrom.* 14: 1086-1098, **2003**.
5. Guilhaus M., Mlynski V., Selby D. "Perfect Timing: Time-of-flight Mass Spectrometry." *Rapid Commun. Mass Spectrom.* 11: 951-962, **1997**.
6. Andrien B.A., Whitehouse C., Sansone M.A. "Proceedings of the 46th ASMS Conference on Mass Spectrometry and Allied Topics", *May 31 – June 4, Orlando, FL, pp 889-890, 1998*.
7. Dresch T., Keefe T., Park M., "Proceedings of the 47th ASMS Conference on Mass Spectrometry and Allied Topics", *June 13 – 18, Dallas, TX, pp 1865-1866, 1999*.
8. Naegele, E., Moritz, R., "Structure elucidation of degradation products of the antibiotic drug amoxicillin – Part I: Examination of the degraded drug products by fragmentation with ion trap MSⁿ.", *Agilent Publication Number 5989-2347EN, 2005*.
9. Naegele, E., Moritz, R., "Structure elucidation of degradation products of the antibiotic drug amoxicillin – Part II: Identification and confirmation by accurate mass measurement with ESI TOF of the compound ions and the fragments after CID." *Agilent Publication Number 5989-2348EN, 2005*.

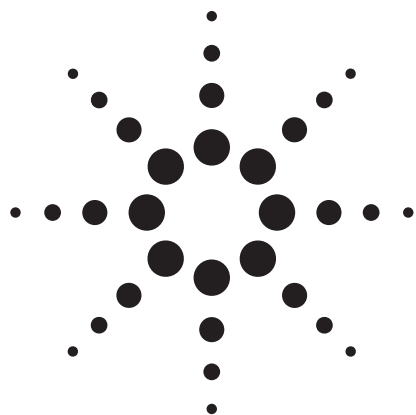
Edgar Nägele is Application Chemist at Agilent Technologies, Waldbronn, Germany.

www.agilent.com/chem/tof

Copyright © 2005 Agilent Technologies
All Rights Reserved. Reproduction, adaptation or translation without prior written permission is prohibited except as allowed under the copyright laws.

Published August 1, 2005
Publication Number 5989-3561EN



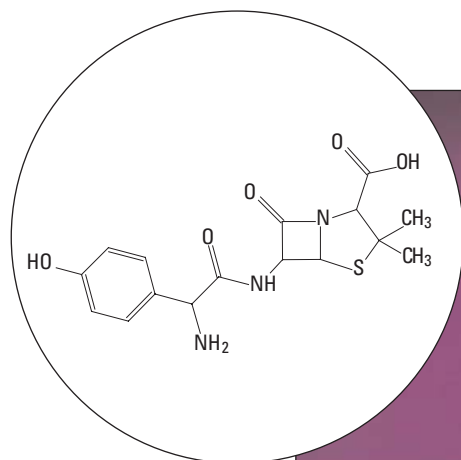


Structure elucidation of degradation products of the antibiotic drug amoxicillin

Part I: Examination of the degraded drug products by fragmentation with ion trap MSⁿ

Application Note

Edgar Nägele
Ralf Moritz



Abstract

Today, it is necessary to identify and confirm the identity of all compounds appearing in the process of the discovery and the development of a new drug substance in the pharmaceutical industry.

In this Application Note the identification and confirmation of degradation products from a final dosage of the antibiotic drug amoxicillin obtained under stress conditions will be demonstrated by structure elucidation with LC ion trap MS/MS and MS³. The identity confirmation of the degradation products by accurate mass measurement of the molecular ions and of the CID fragments by LC/ESI oaTOF will be discussed in Part II of this work¹.



Agilent Technologies

Introduction

In modern pharmaceutical drug discovery and development it is of crucial importance to identify an unknown compound with the highest possible confidence because of its potential toxic effects on humans. Such a compound could be, for instance, the pharmaceutical active substance itself, a minor byproduct out of the production process, a secondary substance in a drug isolated from a natural source, a metabolite created in the human body or a degradation product of the pharmaceutical agent created under harsh storage conditions.

Widely used mass spectrometric tools for the structure elucidation are ion trap instruments with MS/MS and MSⁿ capabilities. With these instruments it is possible to break the molecular ion of the investigated substance in fragments, which are useful for the structure elucidation. It is possible to do this under full control by a repeatable isolation and fragmentation of the fragments derived from the original substance. Recently, the use of an ion trap for MSⁿ fragmentation and structure elucidation together with an ESI oaTOF instrument to measure accurate molecular mass and calculate of the empirical formula, and consequently the identity confirmation of an unknown compound was impressively demonstrated in several published applications. For instance, MS/MS and MS³ experiments were performed to gain structural information for the identification of a photooxygenation product of a broadspectrum antibiotic used for live stock² and for the identification of highly

complex polyene macrolides isolated from *Streptomyces noursei* by means of an ion trap monitored purification process³.

In this Application Note the identification of degradation products from the antibiotic drug amoxicillin obtained under harsh conditions will be demonstrated by means of structure elucidation with an LC ion trap MS/MS and MS³. The obtained and interpreted data are used to build up a degradation pathway of amoxicillin.

Experimental

Equipment

- The ESI ion trap (Part I of this work) and the ESI TOF MS analysis (Part II of this work) was performed with the Agilent 1100 Series LC/MSD ion trap XCT plus and with the Agilent LC/MSD TOF equipped with a dual sprayer source for the simultaneous infusion of the reference mass solution.
- The LC system used was an Agilent 1100 Series capillary LC system containing a capillary pump with a micro vacuum degasser, a micro well-plate autosampler with a thermostat and a column compartment.
- The column used was a ZORBAX SB-Aq, 0.3 mm x 150 mm, 3.5 µm.
- The software used for instrument control was ChemStation A10.02, ion trap software 4.2, TOF software A.01 and for data analysis the ion trap data analysis software 3.2 and Analyst QS software.

Methods

- The Agilent 1100 Series capillary pump was operated under the following conditions: Sol-

vent A: Water, 10 mM ammonium formate, pH 4.1; Solvent B: ACN. Column flow: 8 µL/min, Primary flow: 500-800 µL/min. Gradient: 0 min 0 % B, 1 min 0 % B, 13 min 25 % B, 23 min 25 % B. Stop time: 23 min. Post time: 15 min.

- The Agilent 1100 Series autosampler was used to make injections of 1 µL. The sample loop was switched to bypass after 1 minute to reduce delay volume.
- The mass spectrometers were operated under the following conditions:

Part I – Ion Trap MS:

Source: ESI in positive mode
Dry gas: 5.0 L/min
Dry temp.: 300 °
Nebulizer: 15psi
Target: 150,000
Max. accum. time: 50 ms
Scan: 200-60
Averages: 2
Automated MS/MS and MS³

Part II – ESI TOF MS:

Source: ESI in positive mode with dual spray for reference mass
Dry gas: 7.0 L/min
Dry temp.: 300 °C
Nebulizer: 15 psi
Scan: 50-1000
Fragmentor: 150 V or 300 V for CID
Skimmer: 60 V
Capillary: 5000 V

- Sample preparation: The antibiotic amoxicillin was stressed under acidic conditions. Approximately 1 mL of amoxicillin solution (25 mg/mL in DMSO) was added to 1 mL 0.1 M HCl solution. The sample was stirred for 1 hour at room temperature (RT = 25 °C) and

then diluted (1:10 with DMSO).
Results and discussion

The degradation of amoxicillin (1) was induced by subjecting the pure drug substance to harsh conditions, as described in the experimental section. Aliquots of this solution were collected at various timeframes and subjected to capillary chromatography to separate the accumulated degradation products. The base peak chromatogram (BPC) obtained clearly shows the degradation of amoxicillin into various products (figure 1). The chromatogram also assigns the degradation products, which were identified by structure elucidation with ion trap MS/MS and MS³ experiments and confirmed by accurate mass determination with ESI TOF MS and empirical formula calculation for the molecular

ions and the CID fragments in Part II of this work¹. The mass of the protonated amoxicillin (1) at m/z 366.1 was extracted at a retention time of 4.0 minutes from the base peak chromatogram

together with the peak for the isomeric compound (4) at 10.5 min (figure 2A). The amoxicillin peak also contains a potassium adduct at m/z 404.0 and a product generated under the conditions of mass

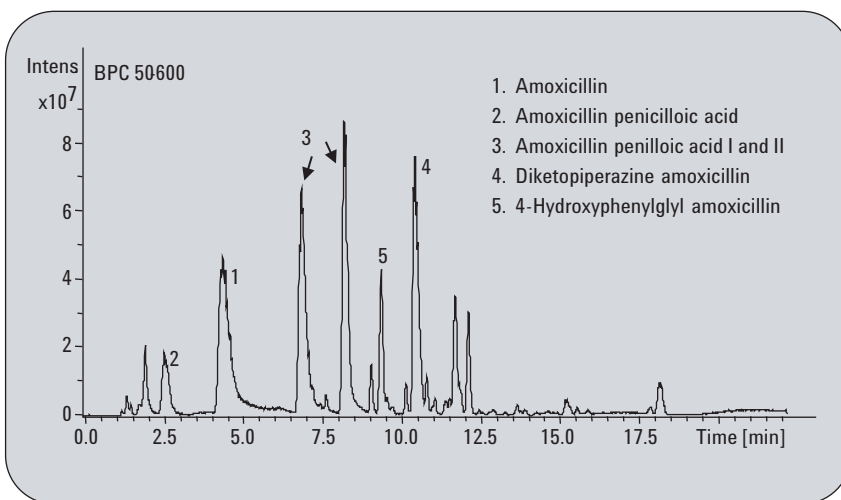


Figure 1
 BPC of amoxicillin (1) and its degradation products

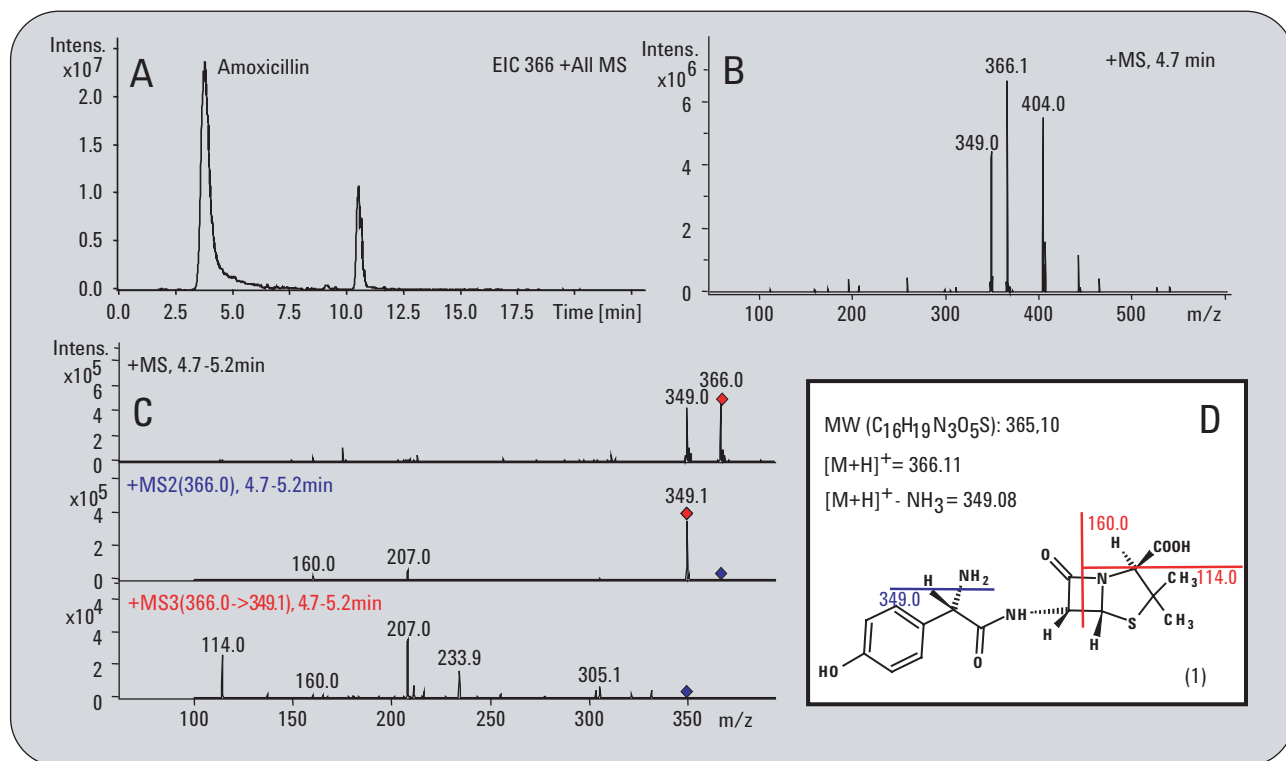


Figure 2
 Amoxicillin (1) (C₁₆H₁₉N₃O₅S), [M+H]⁺ = 366.11 m/z
 A) EIC of amoxicillin. B) MS of amoxicillin at 4.7 min.
 C) MS, MS/MS and MS³ between 4.7 and 5.2 min of amoxicillin. D) Fragmentation of amoxicillin according to the MS/MS and MS³.

spectrometry analysis by the loss of ammonium at m/z 349.0 (figure 2B). The product ion of ammonium loss is also generated under MS/MS conditions in the ion trap as a major product at this stage (figure 2C). The MS³ analysis starting with this ion results in two new ions at m/z at 114.0 and at m/z 160.0, which could be easily assigned to the corresponding fragmentation (figures 2C and 2D). The degradation of amoxicillin (1) in an acidic medium starts with

the opening of the four membered beta lactam ring and yields the product amoxicillin penicilloic acid (2) containing a free carboxylic acid group, which gives a higher polarity to this molecule. This leads to a shift towards an earlier retention time in the RP LC separation, which is shown in the EIC of protonated amoxicillin penicilloic acid (2) at m/z 384.0 at 2.6 minutes (figure 3A). The mass spectrum shows the protonated molecular ion of (2) and also its

potassium adduct at m/z 422.0 (figure 3B). The fragmentation of the molecular ion of (2) resulted in two product ions. The ion resulting from a loss of ammonia at m/z 376.1 and the product ion from additional decarboxylation resulting from the loss of the free carboxylic acid group at m/z 323.1 (figure 3C). This ion is the precursor of the following MS³ fragmentation leading to the fragment ions with m/z 189.0 and the fragment ion of the thiazolidine ring at

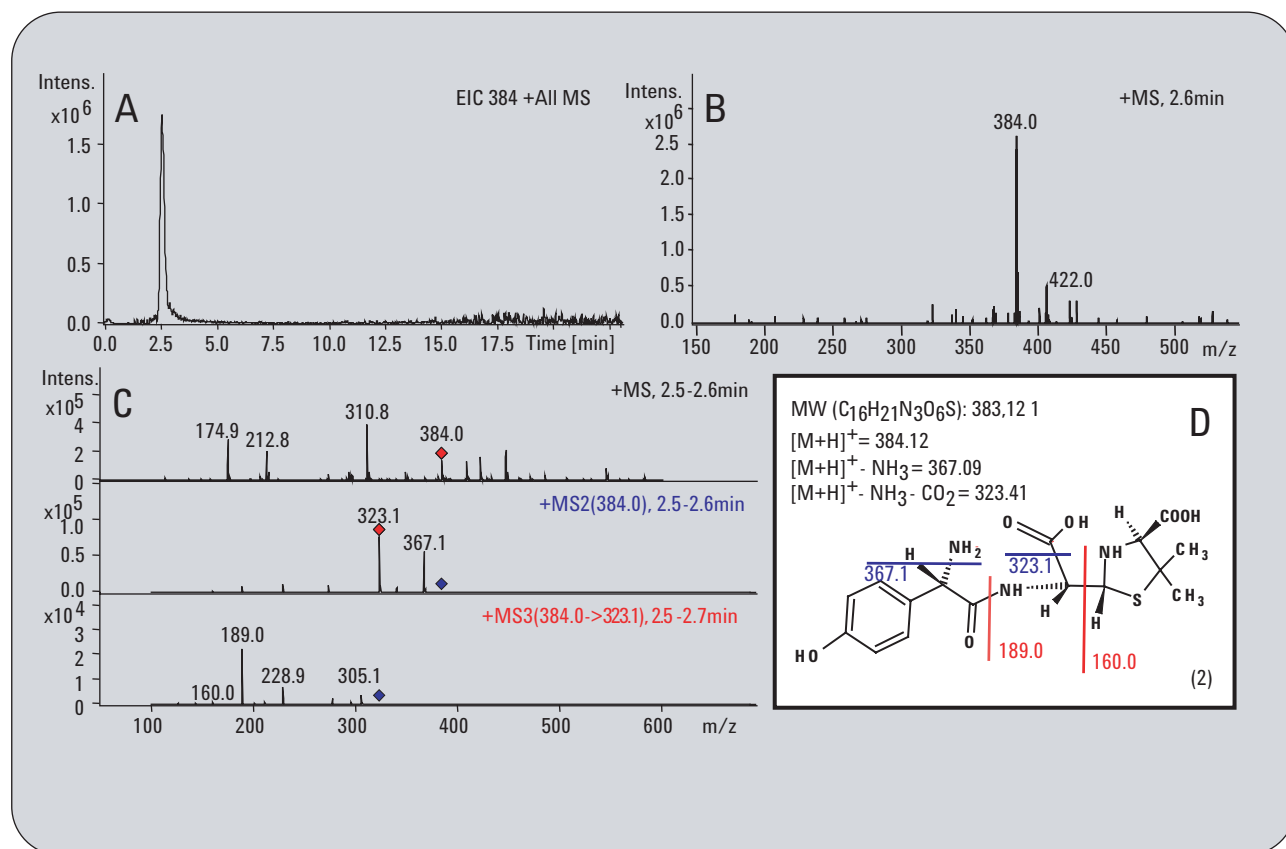


Figure 3
A Amoxicillin penicilloic acid (2) (C₁₆H₂₁N₃O₆S), [M+H]⁺ = 384.12 m/z
A) EIC of amoxicillin penicilloic acid.
B) MS of amoxicillin penicilloic acid at 2.5 min.
C) MS, MS/MS and MS³ between 2.5 and 2.6 min of amoxicillin penicilloic acid.
D) Fragmentation of amoxicillin penicilloic acid according to the MS/MS and MS³.

m/z 160.0 (figure 3D).

Starting with compound (2) there are two possible ways of further degradation. The first one is based on the decarboxylation of the free carboxylic acid and leads to the stereoisomeric compounds amoxicillin penilloic acid I and II (3).

The second possible degradation reaction of intermediate (2) is the closure of a new stable six mem-

bered ring to Diketopiperazine amoxicillin (4). Both reaction products were identified in the amoxicillin solution stored under harsh conditions. The protonated stereo isomeric amoxicillin penilloic acids I and II (3) both at m/z 340.2 were extracted from the BPC at 6.7-7.3 and 8.5-9.0 minutes (figure 4A). They were found as the protonated species as well as

in the form accompanied by potassium at m/z 378.0 (figure 4B).

From the MS/MS analysis the product of a loss of ammonium (figure 4C) and from the MS³ fragmentation the molecule fragment with m/z 188.9 were assigned (figure 4D). Identical mass spectra and fragmentation patterns were obtained for both stereo isomers

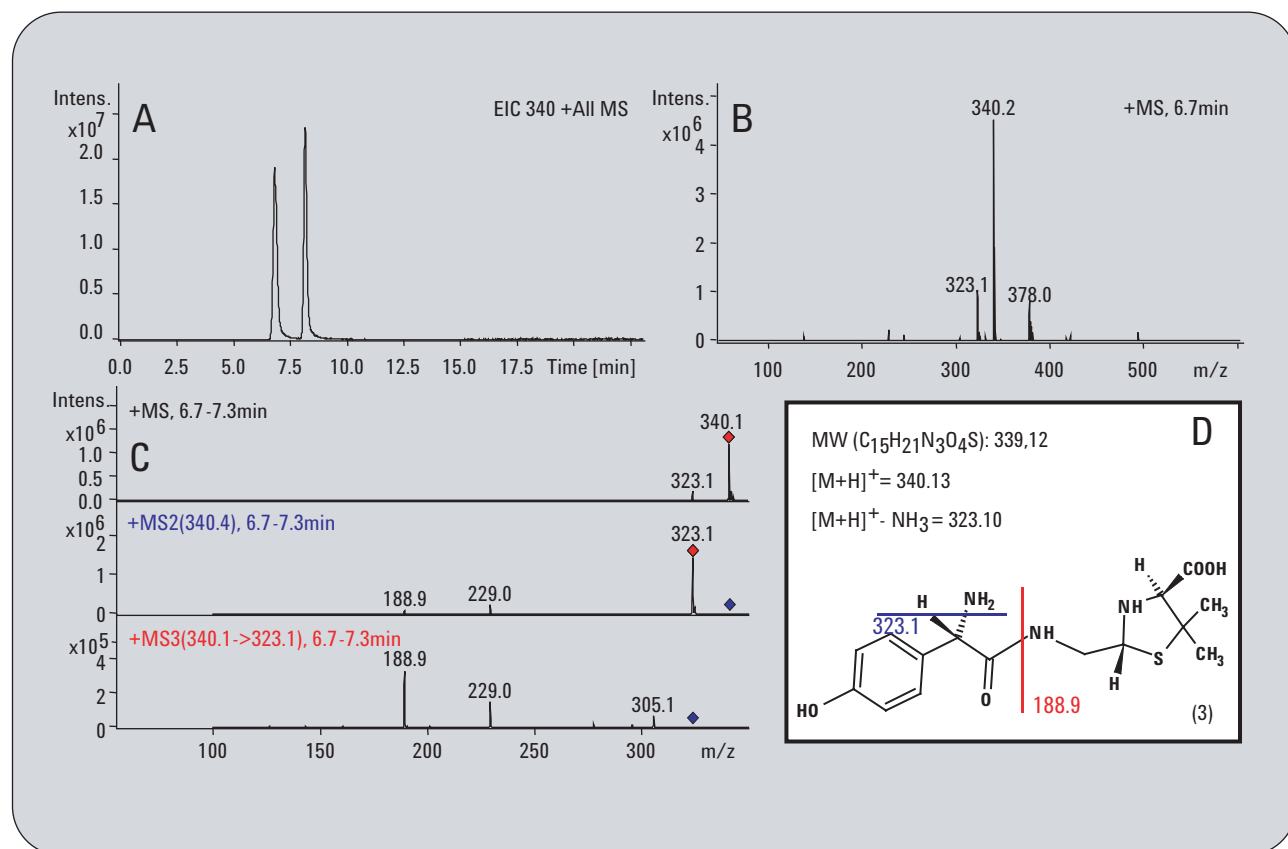


Figure 4

Amoxicillin penilloic acid I and II (3) ($C_{15}H_{21}N_3O_4S$), $[M+H]^+ = 340.13$ m/z

A) EIC of amoxicillin penilloic acid I and II.

B) MS of amoxicillin penilloic acid at 6.7 min.

C) MS, MS/MS and MS³ between 6.7 and 7.3 min of amoxicillin penilloic acid.

D) Fragmentation of amoxicillin penilloic acid according to the MS/MS and MS³.

under both peaks.

The second reaction product derived from compound (2) the protonated diketopiperazine amoxicillin (4) at m/z 366.0 was extracted from the BPC and the corresponding peak is shown in the EIC at a retention time of 10.4 minutes (figure 5A). In addition,

the protonated form of the compound is also accompanied by potassium giving the positive charge as indicated at m/z 404.0 in the mass spectrum (figure 5B). In the MS/MS experiment the molecule undergoes fragmentation by cleavage of the bond between the six membered diketopiperazine

ring and the five membered thiazolidine ring yielding a fragment at m/z 206.2 and a fragment at m/z 160.0 (figure 5C). Further MS³ fragmentation yields the product ion at m/z 114.1 obtained by the cleavage of a carboxylic acid group from the thiazolidine ring

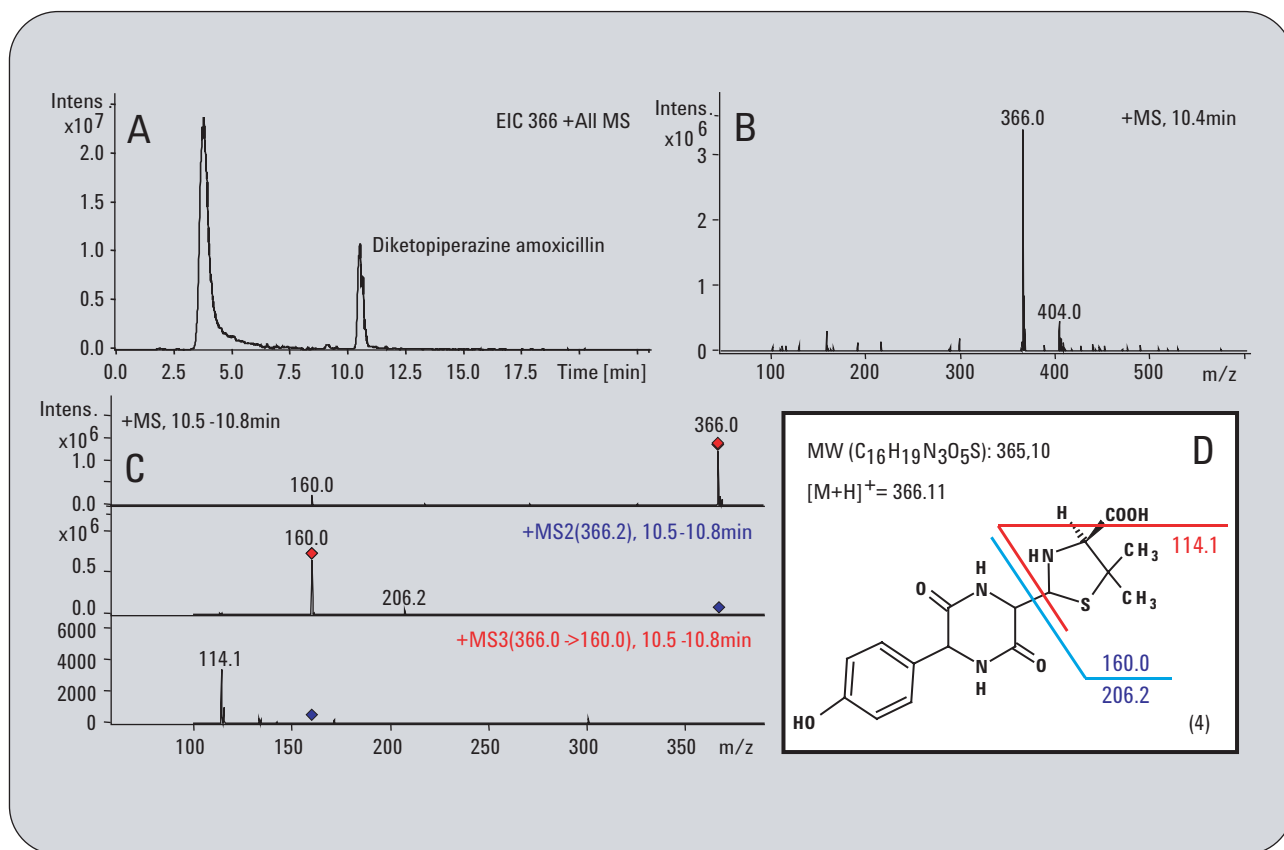


Figure 5
Diketopiperazine amoxicillin (4) (C₁₆H₁₉N₃O₅S), [M+H]⁺ = 366.11 m/z
A) EIC of diketopiperazine amoxicillin.
B) MS of diketopiperazine amoxicillin 10.4 min.
C) MS, MS/MS and MS³ between 10.4 and 10.7 min of diketopiperazine amoxicillin.
D) Fragmentation of diketopiperazine amoxicillin according to the MS/MS and MS³.

moiety (figures 5C and 5D). In another reaction pathway amoxicillin (1) reacts in a nucleophilic attack on itself whereas the benzylic carbonyl group is attacked by the free amino group and undergoes condensation to 4-Hydroxyphenylglyl amoxicillin (5). The protonated molecular ion at

m/z 515.0 was extracted from the BPC at 9.3 minutes (figure 6A) and found together with the potassium adduct (figure 6B). The MS/MS measurement reveals a product at m/z 498.0 from a separation of ammonium and also a product at m/z 339.1 from degradation of the five membered thia-

zolidine ring. The MS³ step unraveled the structure with a loss of a carbonyl group and finally yielded a benzylic amino fragment at m/z 122.1 (figure 6C and 6D). The final degradation pathway of amoxicillin (1) with the identified

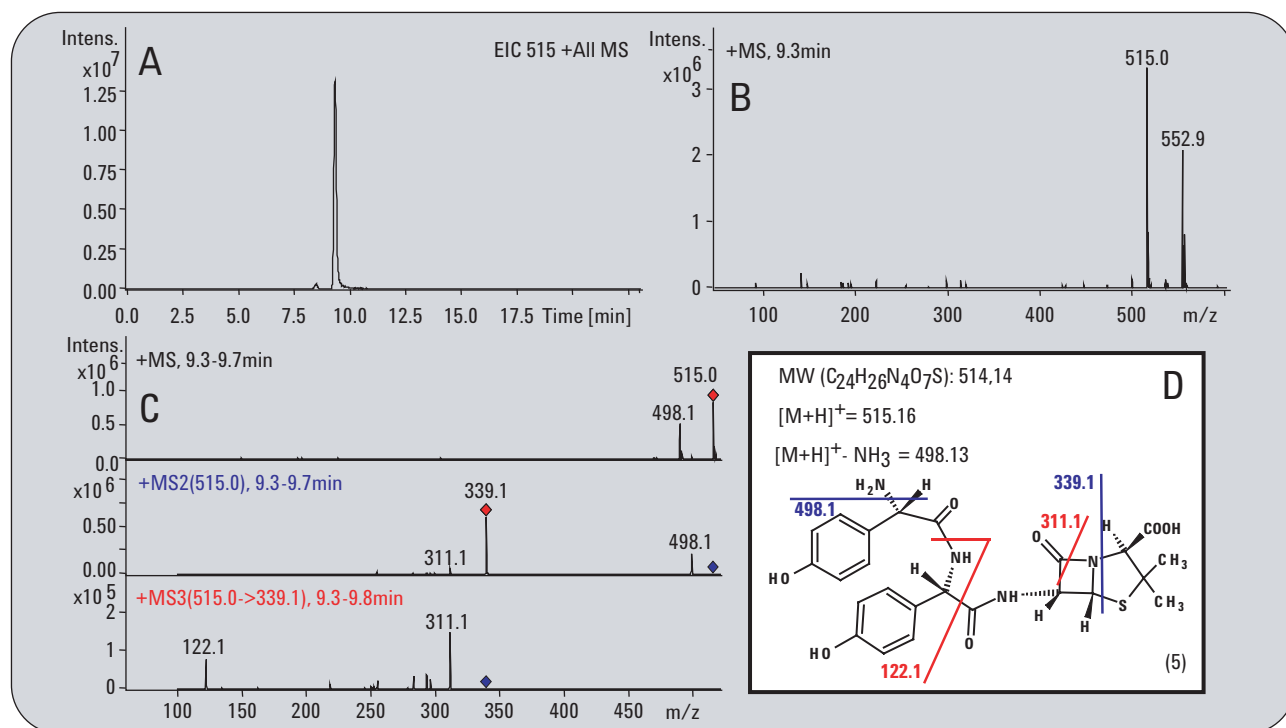


Figure 6
4-Hydroxyphenylglyl amoxicillin (5) (C₂₄H₂₆N₄O₇S) [M+H]⁺ = 515.16 m/z
A) EIC of 4-Hydroxyphenylglyl amoxicillin. B) MS of 4-Hydroxyphenylglyl amoxicillin 10.4 min. C) MS, MS/MS and MS³ between 9.3 and 9.7 min of 4-Hydroxyphenylglyl amoxicillin. D) Fragmentation of 4-Hydroxyphenylglyl amoxicillin according to the MS/MS and MS³.

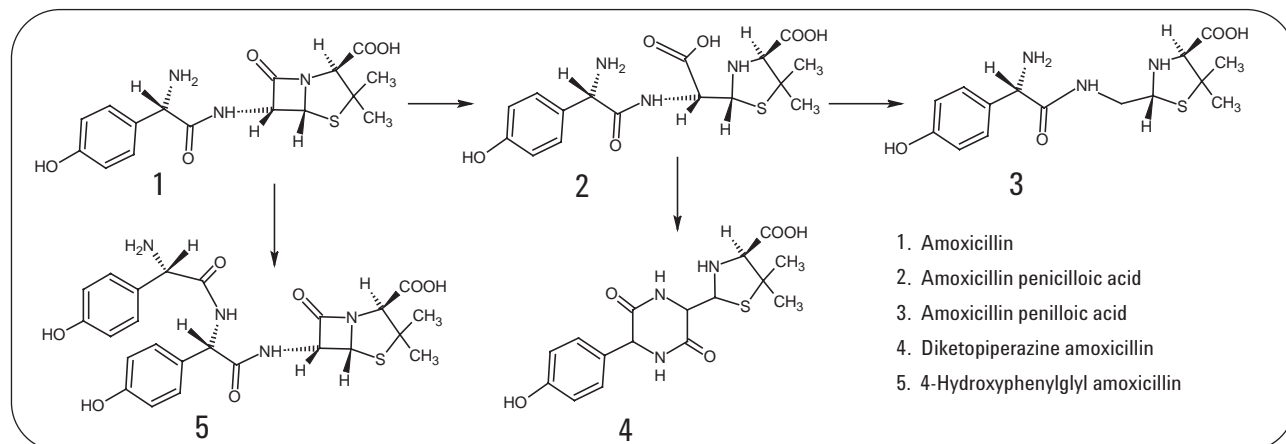


Figure 7
Degradation pathway of amoxicillin.

degradation products is summarized in figure 7.

Conclusion

The presented work describes the elucidation of the degradation pathway of the pharmaceutical substance amoxicillin, a commonly used antibiotic drug. The creation of degradation products, which may possibly be formed under harsh storage or production conditions was artificially induced. The degradation products created from amoxicillin were separated by capillary LC and analyzed by an MS ion trap in MS/MS and MS³ mode. The fragments obtained were used for the structure elucidation of the possible degradation products and for the creation of a degradation pathway. Further results of this work will be described in Part II¹, which presents the confirmation of the obtained ion trap results by the measurement of accurate mass and empirical formula confirmation of the degradation products by LC/ESI oaTOF. In Part III⁴ the obtained knowledge about the degradation of amoxicillin will be applied for the identification of minor byproducts in a drug development formulation trial by accurate mass determination with LC/ESI oaTOF.

References

1. Naegele, E., Moritz, R., "Structure elucidation of degradation products of the antibiotic drug Amoxicillin – Part II: Identification and confirmation by accurate mass measurement with ESI TOF of the compound ions and the fragments after CID." *Agilent Publication Number 5989-2348EN*, **2005**.
2. Eichhorn P., Aga D.S., "Identification of a photooxygenation product of chlorotetracycline in hog lagoons using LC/ESI-ion-trap-MS and LC/ESI-time-of-flight-MS." *Anal. Chem.* **76**: 6002-6011, **2004**.
3. Bruheim P., Borgos S.E.F., Tsan P., Sellta H., Ellingsen T.E., Lancelin J.-M., Zotchev S.B., "Chemical diversity of polyene macrolides produced by *Streptomyces noursei* ATCC11455 and recombinant strain ERD44 with genetically altered polyketide synthase NysC." *Antimicrob. Agents Chemother.* **48**: 4120-4129, **2004**.
4. Nägele, E., Moritz, R., "Structure elucidation of degradation products of the antibiotic drug amoxicillin – Part III: Identification of minor byproducts in a formulation trial with accurate mass measurement by ESI TOF and ion trap MRM" *Agilent Publication Number 5989-2470EN*, **2005**.

*Edgar Nägele is Application Chemist at Agilent Technologie, Waldbronn, Germany.
Ralf Moritz is Analytical Chemist at Sandoz GmbH, Kundl, Austria.*

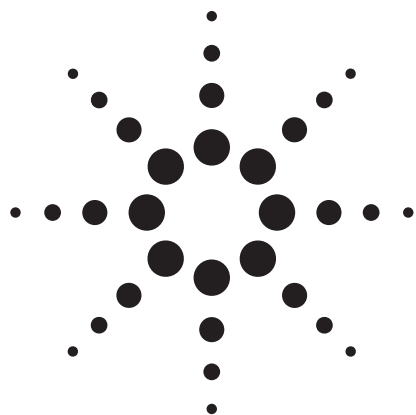
www.agilent.com/chem/1100

Copyright © 2005 Agilent Technologies
All Rights Reserved. Reproduction, adaptation or translation without prior written permission is prohibited, except as allowed under the copyright laws.

Published June 1, 2005
Publication Number 5989-2347EN



Agilent Technologies

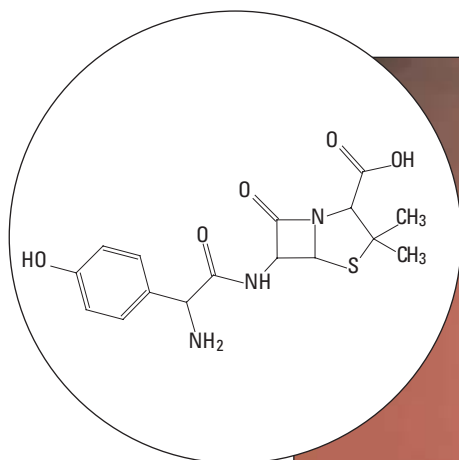


Structure elucidation of degradation products of the antibiotic drug amoxicillin

Part II: Identification and confirmation by accurate mass measurement with ESI TOF of the compound ions and the fragments after CID

Application Note

Edgar Nägele
Ralf Moritz



Abstract

Today, it is necessary to identify and confirm the identity of all compounds appearing in the process of the discovery and the development of a new drug substance in the pharmaceutical industry.

In this Application Note the confirmation of degradation products from a final dosage of the antibiotic drug amoxicillin obtained under stress conditions, whose structures were elucidated by ion trap MS/MS and MS³ in a former work (Part I¹), will be demonstrated by accurate mass measurement and empirical formula confirmation for the molecular ions and for the CID fragments by LC/ESI oaTOF.



Agilent Technologies

Introduction

In modern pharmaceutical drug discovery and development it is of crucial importance to identify an unknown compound with the highest possible confidence because of its potential toxic effects on humans. Such a compound could be, for instance, the pharmaceutical active substance itself, a minor byproduct out of the production process, a secondary substance in a drug isolated from a natural source, a metabolite created in the human body or a degradation product of the pharmaceutical agent created under storage conditions. In addition to the repertoire of analytical methods for structure elucidation, the mass spectrometric measurement of accurate molecular mass and consequently the calculation of the empirical formula is a common method for the identification and identity confirmation of an unknown compound. Several years ago only operation intensive magnetic sector field and FT mass spectrometers were able to perform these measurements with sufficient accuracy. Nowadays, comparably easy to use and inexpensive ESI orthogonal acceleration TOF (oaTOF) instruments are also capable of handling this task. This is clearly demonstrated by a comparison study of different types of mass spectrometer instruments for the determination of accurate mass of small molecules². This was made possible by some technical innovations in TOF technology introduced during the past years. One of the main technical innovations is the development of orthogonal acceleration TOF technology, which decouples the ion beam velocity spread from the

TOF axis, which provides better resolution of the TOF mass spectrometers³. In this environment the possibility of coupling continuous ionization sources like the electrospray ionization (ESI) source with orthogonal acceleration TOF mass analyzers is of special importance for LC-ESI TOF applications. A high mass accuracy is only achieved when a reference mass is simultaneously introduced into the mass spectrometer with the analyte itself. Mixing the LC column effluent with a stream of reference material can result in ion suppression, discrimination or adduct formation. To prevent mixing the analyte and the reference compound prior to spray ionization, a innovation which applies a dual ESI sprayer interface is used^{4,5}. This instrument is capable of achieving resolutions above 15,000 and mass accuracies below 1 ppm for small molecules². Recently, the implementation of oaTOF instruments for the measurements of accurate molecular mass and the calculation of the total formula and consequently the identity confirmation of an unknown compound was impressively demonstrated in a considerably high number of published applications⁶⁻¹¹. For instance, LC-ESI oaTOF was used for the characterization of in vitro drug metabolites by accurate mass determination of the molecular ion and CID fragments^{6,7}, for the quantization and accurate mass measurement of pharmaceutical drugs in plasma⁸, for the characterization of trace level impurities in a drug substance⁹, with an additional ion trap instrument for MS/MS and MS³ experiments to gain structural information for the identifica-

tion of a photooxygenation product of a broadspectrum antigotic used for live stock¹⁰ and for the identification of highly complex polyene macrolides isolated from *Streptomyces noursei* by means of an ion trap monitored purification process¹¹. In this Application Note the confirmation of formerly identified degradation products from the antibiotic drug amoxicillin obtained under harsh conditions will be demonstrated by means of accurate mass measurement of the molecular ions and CID fragments using an LC/ESI oaTOF for the confirmation of the molecular formula and the fragment formulas. The structure elucidation with an LC ion trap MS/MS and MS³ is discussed in Part I of this work¹. Both sets of data are combined and used to build up a degradation pathway of amoxicillin.

Experimental

Equipment

- The ESI ion trap (Part I of this work) and the ESI TOF MS analysis (Part II of this work) was performed with the Agilent 1100 Series LC/MSD ion trap XCT plus and with the Agilent LC/MSD TOF equipped with a dual sprayer source for the simultaneous infusion of the reference mass solution.
- The LC system used was an Agilent 1100 Series capillary LC system containing a capillary pump with a micro vacuum degasser, a micro well-plate autosampler with a thermostat and a column compartment.
- The column used was a ZORBAX SB-Aq, 0.3 mm x 150 mm, 3.5 μ m.

- The software used for instrument control was ChemStation A10.02, ion trap software 4.2, TOF software A.01 and for data analysis the ion trap data analysis software 3.2 and Analyst QS software.

Methods

- The Agilent 1100 Series capillary pump was operated under the following conditions: Solvent A: Water, 10 mM ammonium formate, pH 4.1; Solvent B: ACN. Column flow: 8 μ L/min, Primary flow: 500-800 μ L/min. Gradient: 0 min 0 % B, 1 min 0 % B, 13 min 25 % B, 23 min 25 % B. Stop time: 23 min. Post time: 15 min.
- The Agilent 1100 Series autosampler was used to make injections of 1 μ L sample. The sample loop was switched to bypass after 1 minute to reduce delay volume.
- The mass spectrometers were operated under the following conditions:
 - Part I – Ion Trap MS:
 - Source: ESI in positive mode.
 - Dry gas: 5.0 L/min
 - Dry temp.: 300 °C
 - Nebulizer: 15 psi
 - Target: 150,000
 - Max. accum. time: 50 ms

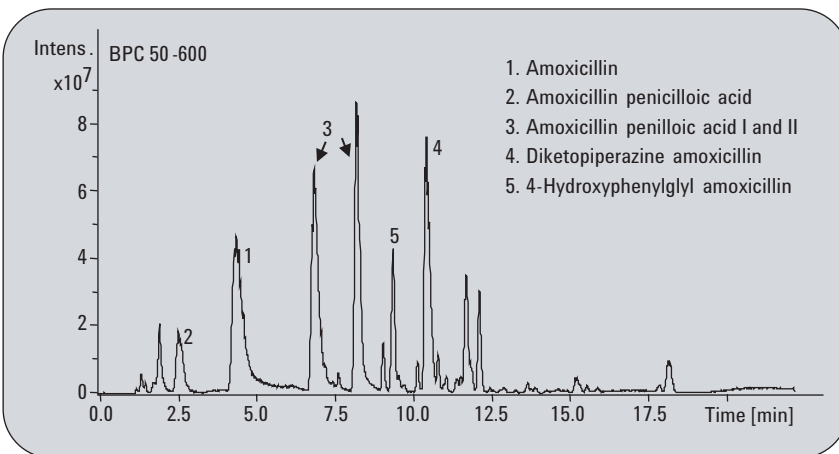


Figure 1
BPC of amoxicillin (1) and its degradation products

Scan: 200-600
Averages: 2
Automated MS/MS and MS³

Part II – ESI TOF MS:
Source: ESI in positive mode with dual spray for reference mass.

Dry gas: 7.0 L/min
Dry temp.: 300 °C
Nebulizer: 15 psi
Scan: 50-1000.
Fragmentor: 150 V or 300 V for CID
Skimmer: 60 V
Capillary: 5000 V

- Sample preparation: The antibiotic amoxicillin was stressed under acidic conditions. Approximately 1 mL of amoxicillin solution (25 mg/mL in DMSO) was added to 1 mL 0.1 M HCl solution. The sample was stirred for 1 hour at room temperature (RT = 25 °C) and then diluted (1:10 with DMSO).

Results and discussion

The degradation of amoxicillin (1) was induced by subjecting the pure drug substance to harsh conditions, as described in the

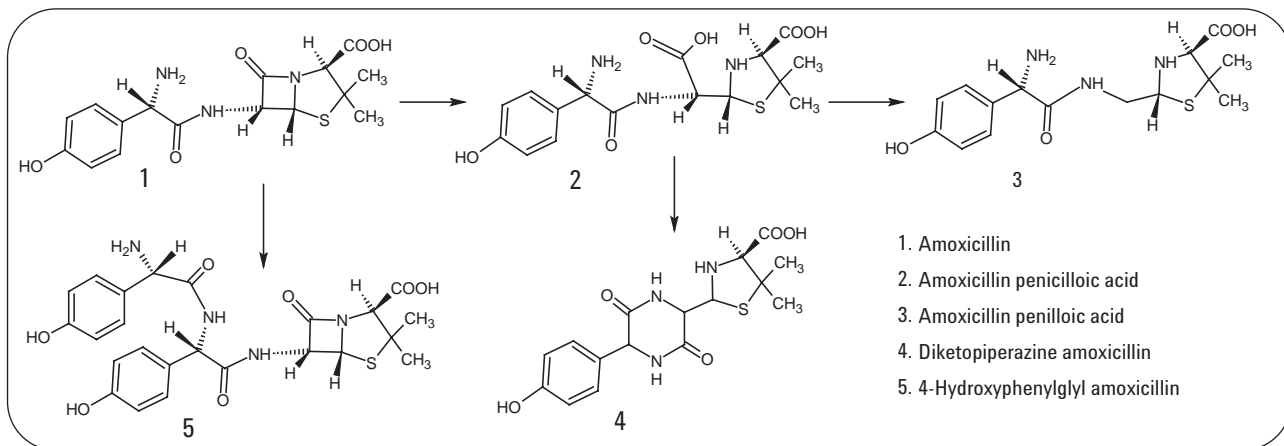


Figure 2
Degradation pathway of amoxicillin

experimental section. Aliquots of this solution were collected at various timeframes and subjected to capillary chromatography to separate the accumulated degradation products. The base peak chromatogram (BPC) obtained clearly shows the degradation of amoxicillin into various products (figure 1). The chromatogram assigns the degradation products, which were identified by structure elucidation with ion trap MS/MS and MS³ experiments (see Part I of this work¹). The final degradation pathway of amoxicillin (1)

created from the results obtained in Part I with the identified degradation products is summarized in figure 2. For the identity confirmation by accurate mass measurement and formula calculation of the proposed intermediates (figure 2), which are involved in the degradation pathway of amoxicillin (1) the analysis was performed on an ESI oaTOF instrument connected to a capillary LC for separation of the amoxicillin degradation products. The experiment was performed twice using different fragmentor voltages of

150 V and 300 V in the TOF MS. At a fragmentor voltage of 150 V there is no collision induced dissociation (CID) observed whereas a good fragmentation for the molecular ion from the separated degradation products are observed at a voltage of 300 V. The measured molecular mass for amoxicillin (1) at m/z 366.1116 has a deviance of 0.08 mDa or 2.18 ppm to the calculated molecular mono isotopic mass (figure 3A). For structural confirmation a useful fragmentation for amoxicillin (1) besides the molecular

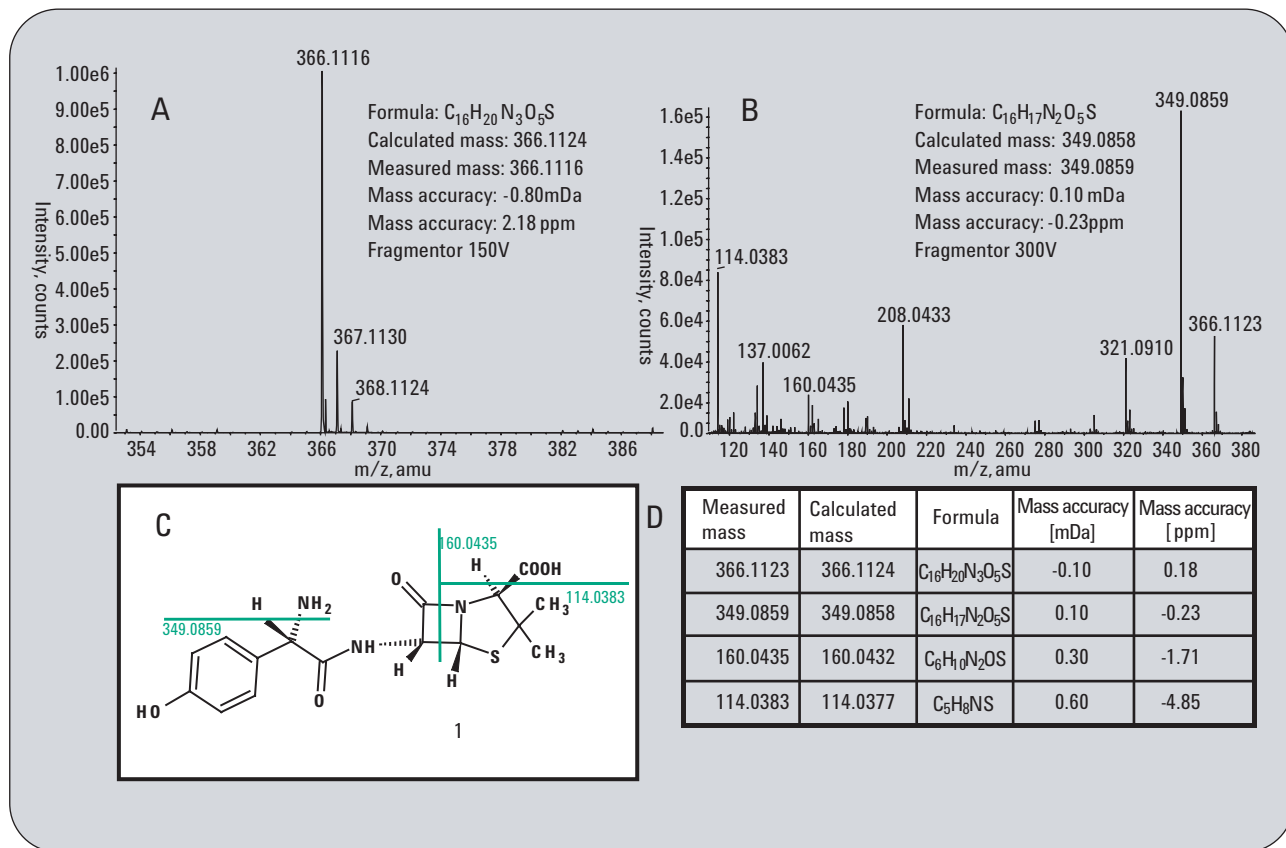


Figure 3

Amoxicillin (1), (C₁₆H₁₉N₃O₅S), [M+H]⁺ = 366.1124 m/z

A) Accurate mass measurement of the molecular ion of amoxicillin.

B) Accurate mass measurement of the CID fragment ions of amoxicillin.

C) CID fragmentation pattern of amoxicillin.

D) Mass accuracy of all CID fragments of amoxicillin.

ion is obtained by the application of an increased fragmentor voltage up to 300 V (figure 3B). The main fragment shown in the mass spectrum is the product of a loss of ammonium at m/z 349.0859, which has a deviance to the calculated mass of 0.1 mDa and 0.23 ppm. The formula $C_6H_{10}NO_2S$ of the fragment at m/z 160.0435 obtained by the cleavage of the five membered thiazolidine ring from the molecule ion is calculated with a mass accuracy of 0.3 mDa and 1.71 ppm. This is the

only elemental formula calculated given the measured mass and a 5 ppm mass accuracy window. This gives undoubted evidence of the chemical structure. The complete fragmentation is shown in figure 3C and the mass accuracy of each fragment is outlined in table 3D.

The first degradation product of amoxicillin (1) obtained after breaking the four membered beta lactam ring amoxicillin penicilloic acid (2) was confirmed by

accurate mass measured at m/z 384.1212, with 4.50 ppm mass accuracy and empirical formula calculation with the ESI TOF at a fragmentor voltage of 150 V (figure 4A). The structure of this degradation product was confirmed by the appearance of the special fragment at m/z 323.1063 with 0.78 ppm mass accuracy, which is the product of a decarboxylation reaction (figure 4B). The complete fragmentation pattern of amoxicillin penicilloic acid (2) also reveals fragments at

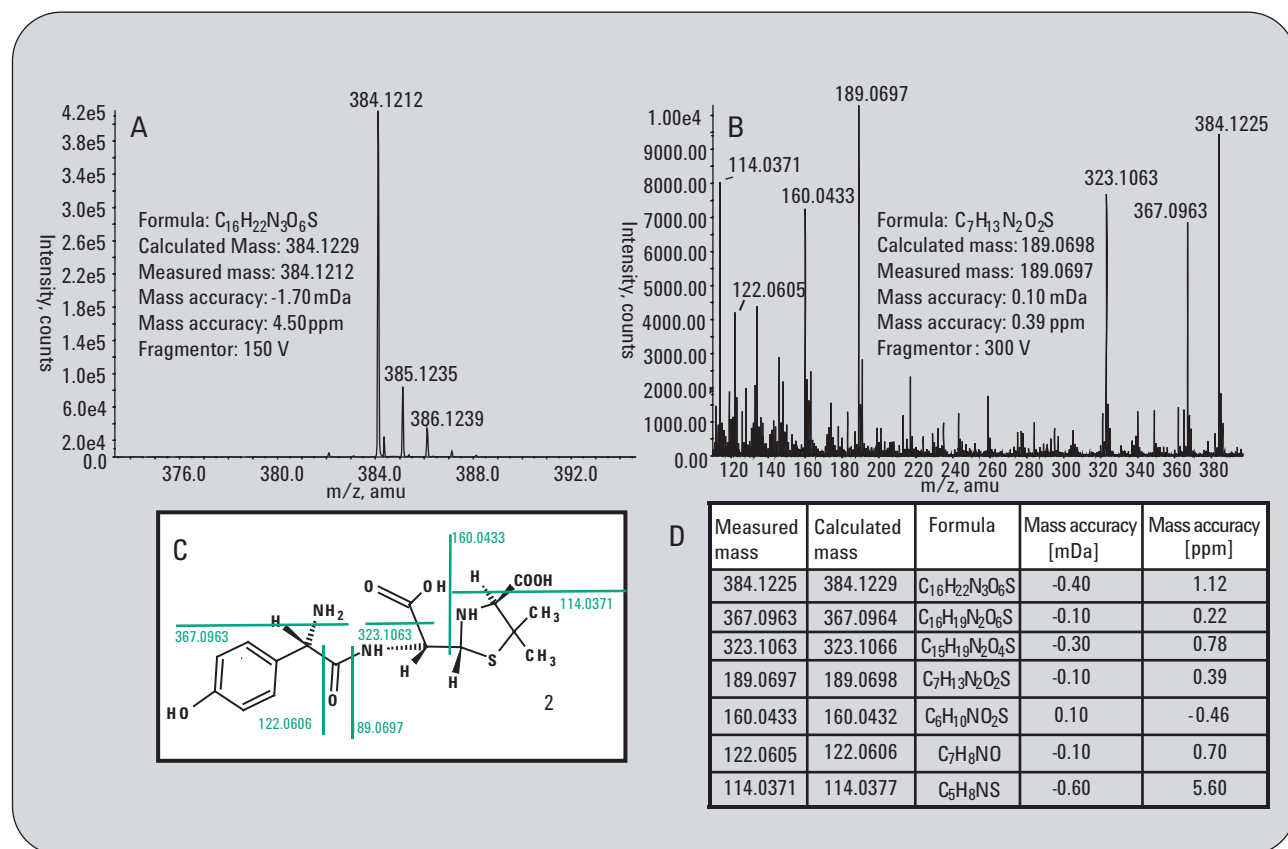


Figure 4
A) Amoxicillin penicilloic acid (2), ($C_{16}H_{21}N_3O_6S$), $[M+H]^+ = 384.1229 m/z$
A) Accurate mass measurement of the molecular ion of amoxicillin penicilloic acid.
B) Accurate mass measurement of the CID fragment ions of amoxicillin penicilloic acid.
C) CID fragmentation pattern of amoxicillin penicilloic acid.
D) Mass accuracy of all CID fragments of amoxicillin penicilloic acid.

m/z 122.0606 and at m/z 189.0697 with high mass accuracy, which are important for the structure confirmation (figures 4B and 4C). The complete information obtained from the CID fragments of amoxicillin penicilloic acid (2) is summarized in table 4D with their empirical formula and the measured mass accuracies. The subsequent degradation products obtained from amoxicillin

penicilloic acid (2) by a decarboxylation of the free carboxylic acid group are the stereoisomeric amoxicillin penilloic acids I and II (3). Their identity was confirmed by accurate mass measurement and formula confirmation at m/z 340.1333 with a deviation of 0.20 mDa, 0.57 ppm from the theoretical mass ($C_{15}H_{22}N_3O_4S$) (figure 5A). The main fragment ion obtained in the CID spectrum is

the product from a loss of ammonium at m/z 323.1065 (figure 5B). The same fragment ion was obtained as a product after the loss of ammonia followed by a decarboxylation from amoxicillin penicilloic acid (2) (figure 4B) and therefore confirms the identity of the degradation products amoxicillin penilloic acid I and II (3). The identified fragmentations and fragment ions are outlined in fig-

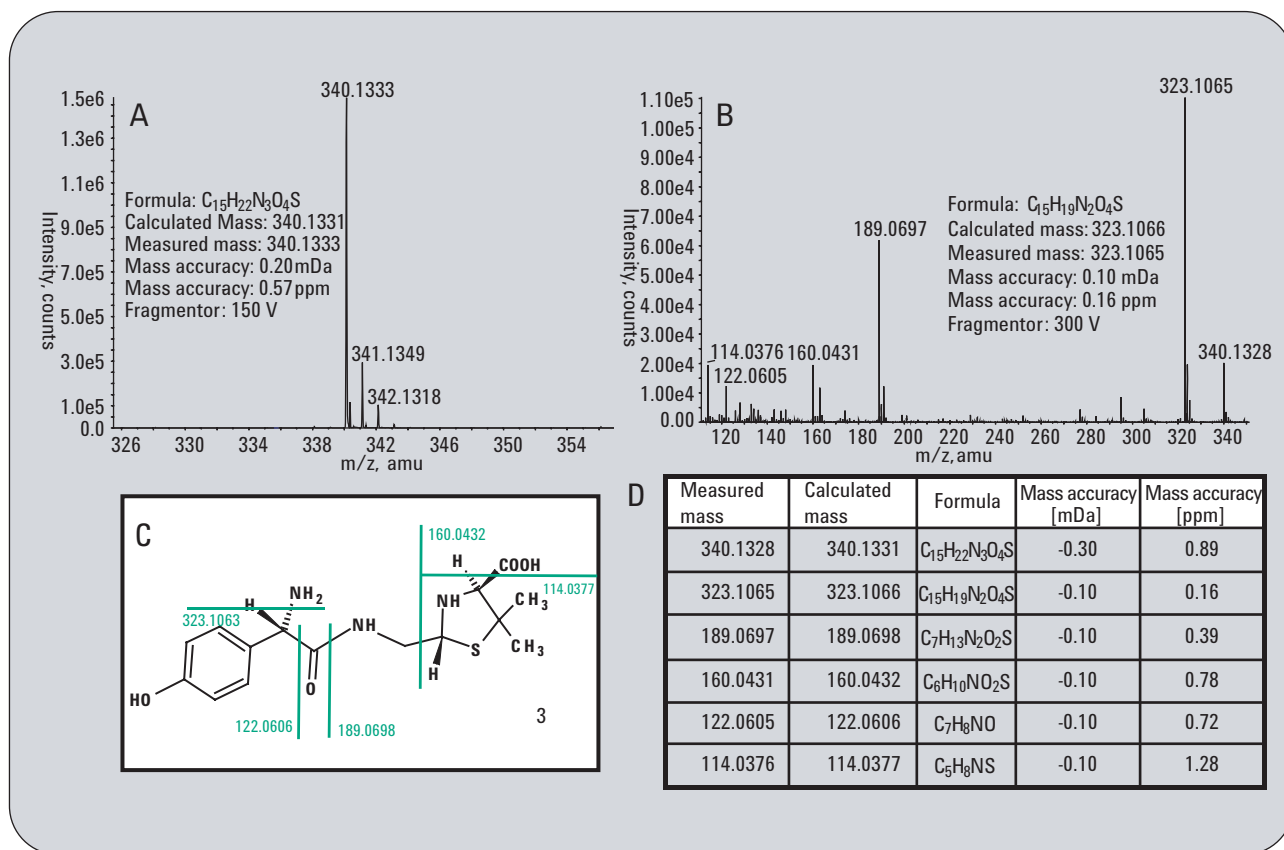


Figure 5
 Amoxicillin penilloic acid I and II (3), ($C_{15}H_{21}N_3O_4S$), $[M+H]^+ = 340.1331$
 A) Accurate mass measurement of the molecular ion of amoxicillin penilloic acid I and II.
 B) Accurate mass measurement of the CID fragment ions of amoxicillin penilloic acid I and II.
 C) CID fragmentation pattern of amoxicillin penilloic acid I and II.
 D) Mass accuracy of all CID fragments of amoxicillin penilloic acid I and II.

ure 5C and summarized in table 5D. The stereo isomeric forms of (3) resolved in the peaks at 6.7-7.3 min and 8.5-9.0 min gave the same mass accuracies and the same CID fragments. Beginning with amoxicillin penicilloic acid (2), the degradation pathway also leads to diketopiperazine amoxicillin (4) by a formation of a six

membered ring structure (figure 6). The molecular identity of the protonated molecular ion given by the formula $C_{16}H_{19}N_3O_5S$ was confirmed by accurate mass measurement with the ESI TOF at m/z 366.1137 with 3.63 ppm accuracy (figure 6A). The main CID fragment accrues from a cleavage of the molecule at the bond

between the six and the five membered ring and belongs to the five membered thiazolidine ring at m/z 160.0428 with a mass accuracy of 2.65 ppm (figure 6B). The confirmed fragmentation is shown in figure 6C and the fragments are summarized in table 6D.

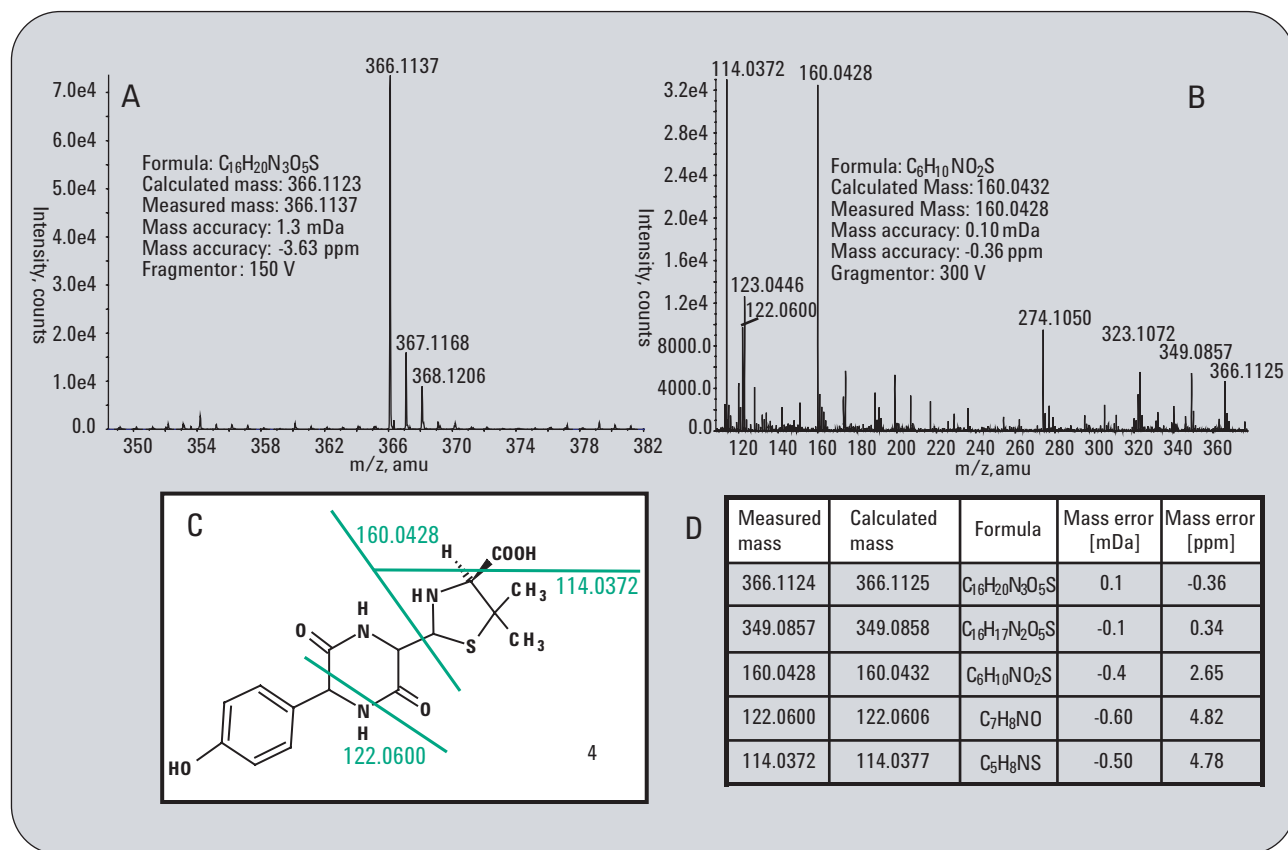


Figure 6
 Diketopiperazine amoxicillin (4) ($C_{16}H_{19}N_3O_5S$) [$M+H$]⁺ = 366.1125 m/z
 A) Accurate mass measurement of the molecular ion of diketopiperazine amoxicillin.
 B) Accurate mass measurement of the CID fragment ions of diketopiperazine amoxicillin.
 C) CID fragmentation pattern of diketopiperazine amoxicillin.
 D) Mass accuracy of all CID fragments of diketopiperazine amoxicillin.

Finally, the chemical identity of the product obtained from a self-condensation reaction of Amoxicillin (1) to 4-Hydroxyphenylglyly amoxicillin (5) was confirmed by means of the ESI TOF instrument. The molecular ion at m/z 515.1601 with the calculated formula

$C_{24}H_{27}N_4O_7S$ was confirmed with a mass accuracy of 0.19 ppm (figure 7A). The CID fragments useful for the identification come from a loss of ammonium, a loss of the five membered thiazolidine ring from the parent molecule and from a residual benzyl imminium

ion (figures 7B and 7C). The fragment ions are measured with sufficient accuracy for unambiguous identification of the fragments and consequently the molecule (table 7D).

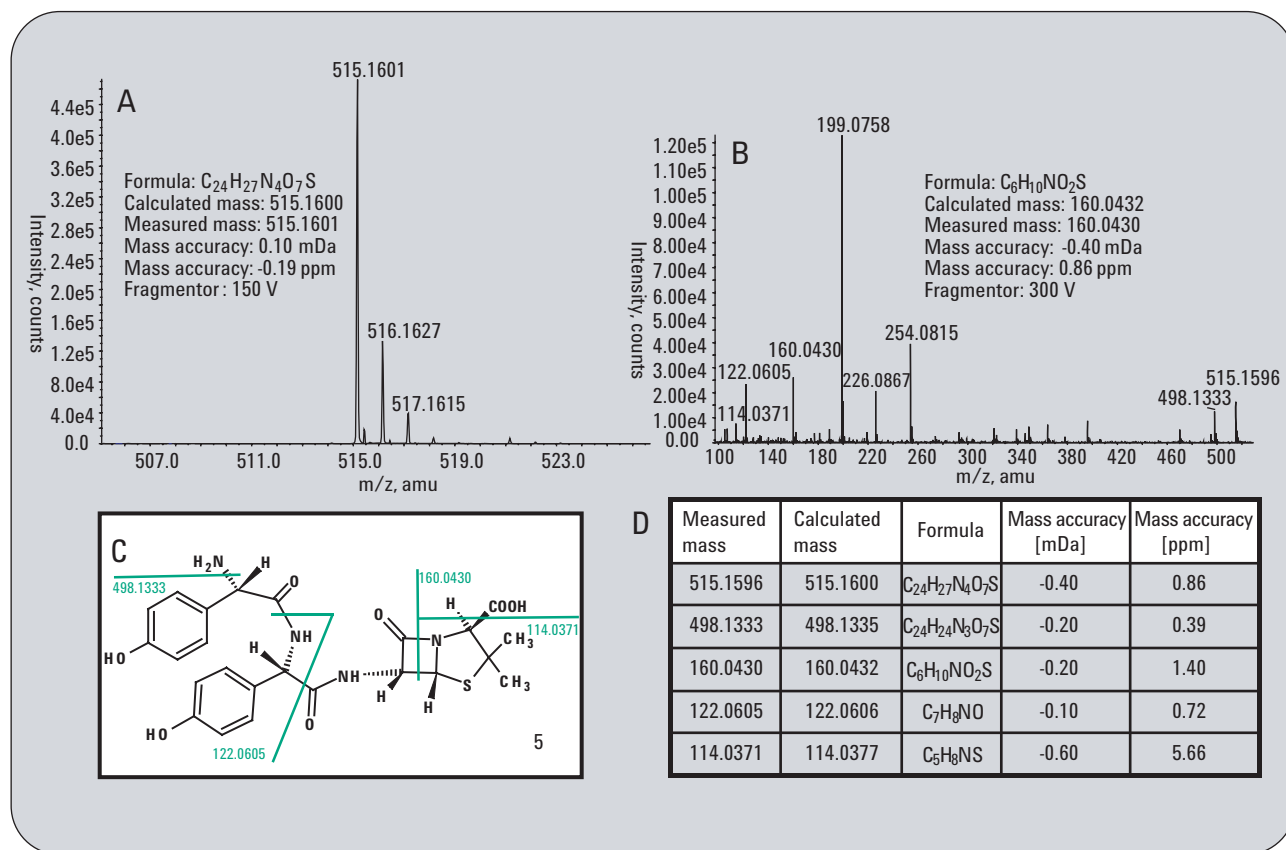


Figure 7

4-hydroxyphenylglyly amoxicillin (5) ($C_{24}H_{26}N_4O_7S$), $[M+H]^+$ = 515.1600

A) Accurate mass measurement of the molecular ion of 4-hydroxyphenylglyly amoxicillin.

B) Accurate mass measurement of the CID fragment ions of 4-hydroxyphenylglyly amoxicillin.

C) CID fragmentation pattern of 4-hydroxyphenylglyly amoxicillin.

D) Mass accuracy of all CID fragments of 4-hydroxyphenylglyly amoxicillin.

Conclusion

The presented work describes the confirmation of the degradation pathway of the pharmaceutical substance amoxicillin, a commonly used antibiotic drug, which was unraveled in Part I of this work¹. The creation of the degradation products, which may possibly be formed under harsh storage conditions was induced artificially. The identity of the proposed degradation products were confirmed by accurate mass measurement with ESI TOF and empirical formula calculation for the molecular ions of the degradation products. Additionally, a CID experiment was carried out with the ESI TOF instrument by increasing the fragmentor voltage. In this experiment the molecular identity of the fragments, which are derived from the degradation products of amoxicillin, were confirmed. The same fragments were generated in a controlled manner in the ion trap experiments, which are described in detailed in Part I¹. The molecular mass obtained from the molecular ions of the degradation products and the molecular masses of their CID fragments, which were measured with highest mass accuracy of less than 1 ppm by ESI TOF, confirm the proposed amoxicillin degradation pathway.

In Part III¹² the obtained knowledge obtained about the degradation of amoxicillin will be applied for the measurement of minor byproducts in a drug development formulation trial by accurate mass measurement with LC/ESI oaTOF and byproduct monitoring with ion trap MRM mode.

References

1. Naegele, E., Moritz, R., "Structure elucidation of degradation products of the antibiotic drug amoxicillin – Part I: Examination of the degraded drug products by fragmentation with ion trap MSⁿ.", *Agilent Publication Number 5989-2347EN*, **2005**.
2. Bristow A.W.T., Webb K.S. "Inter-comparison study on accurate mass measurement of small molecules in mass spectrometry." *J. Am. Mass Spectrom.* **14**: 1086-1098, **2003**.
3. Guilhaus M., Mlynski V., Selby D. "Perfect Timing: Time-of-flight Mass Spectrometry." *Rapid Commun. Mass Spectrom.* **11**: 951-962, **1997**.
4. Andrien B.A., Whitehouse C., Sansone M.A. "Proceedings of the 46th ASMS Conference on Mass Spectrometry and Allied Topics", *May 31 – June 4, Orlando, FL, pp 889-890*, **1998**.
5. Dresch T., Keefe T., Park M. "Proceedings of the 47th ASMS Conference on Mass Spectrometry and Allied Topics", *June 13 – 18, Dallas, TX, pp 1865-1866*, **1999**.
- 6.

Zhang H., Henion J. "Application of Atmospheric pressure ionization time-of-flight mass spectrometry coupled with liquid chromatography for the characterization of in vitro drug metabolites", *Anal. Chem.* 72: 3342-3348, **2000**.

7. Michelsen P., Karlsson A.A. "Accurate mass determination of a metabolite of a potential diagnostic drug candidate by high performance liquid chromatography with time-of-flight mass spectrometry." *Rapid Commun. Mass Spectrom.* 13: 2146-2150, **1999**.

8. Zhang H., Heinig K., Henion J. "Atmospheric pressure ionization time-of-flight mass spectrometry coupled with fast liquid chromatography for quantization and accurate mass measurements of five pharmaceutical drugs in human plasma." *J. Mass Spectrom.* 35: 423-431, **2000**.

9. Eckers C., Haskins N., Langridge J. "The use of liquid chromatography combined with a quadrupole time-of flight analyzer for the identification of trace impurities in drug substance." *Rapid Commun. Mass Spectrom.* 11: 1916-1922, **1997**.

10.

Eichhorn P., Aga D.S. "Identification of a photooxygenation product of chlorotetracycline in hog lagoons using LC/ESI-ion trap-MS and LC/ESI-time-of-flight-MS." *Anal. Chem.* 76: 6002-6011, **2004**.

11. Bruheim P., Borgos S.E.F., Tsan P., Sellta H., Ellingsen T.E., Lancelin J.-M., Zotchev S.B. "Chemical diversity of polyene macrolides produced by *Streptomyces noursei* ATCC11455 and recombinant strain ERD44 with genetically altered polyketide synthase NysC." *Antimicrob. Agents Chemother.* 48: 4120-4129, **2004**.

12. Naegele, E., Moritz, R., "Structure elucidation of degradation products of the antibiotic drug amoxicillin – Part III: Identification of minor byproducts in a formulation trial with accurate mass measurement by ESI TOF and ion trap MRM", *Agilent Publication Number 5989-2470EN*, **2005**.

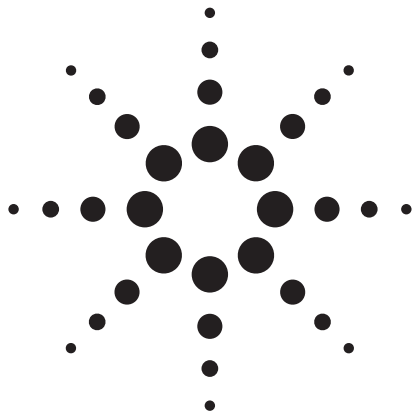
*Edgar Nägele is Application
Chemist at Agilent Technologies,
Waldbronn, Germany.
Ralf Mortiz is Analytical Chemist
at Sandoz GmbH, Kundl, Austria.*

www.agilent.com/chem/1100

Copyright © 2005 Agilent Technologies
All Rights Reserved. Reproduction, adaptation
or translation without prior written permission
is prohibited, except as allowed under the
copyright laws.

Published June 1, 2005
Publication Number 5989-2348EN



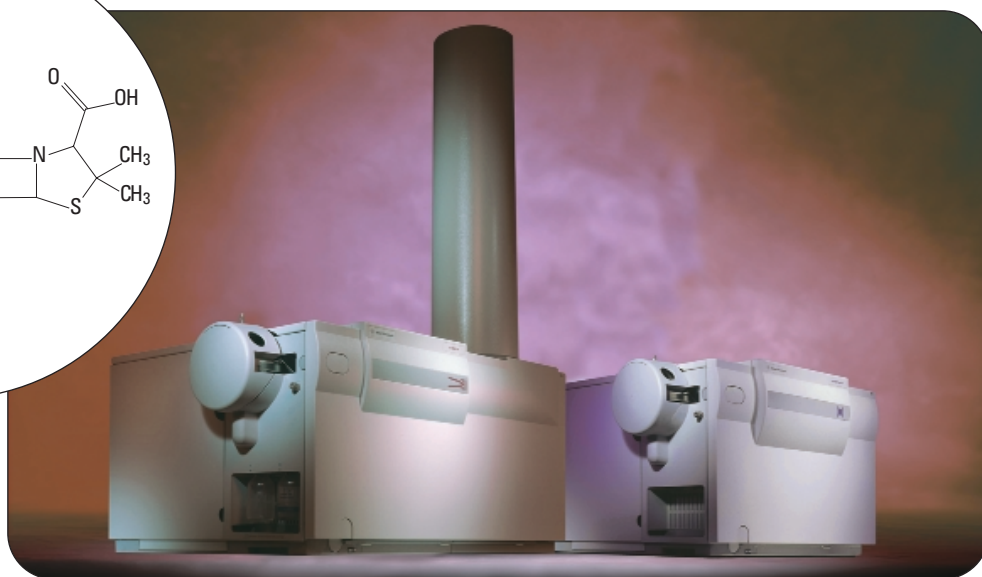
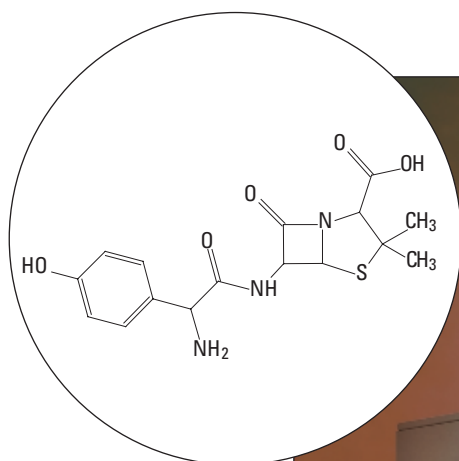


Structure elucidation of degradation products of the antibiotic drug amoxicillin

Part III: Identification of minor byproducts in a formulation trial with accurate mass measurement using ESI TOF and ion trap MRM

Application Note

Edgar Nägele
Ralf Moritz



Abstract

In this Application Note the identification and confirmation of degradation products, which have emerged in a formulation trial of the antibiotic drug amoxicillin under nonoptimal conditions will be demonstrated. The tools used were an LC ion trap MRM for confirmation and an LC/ESI oaTOF for identity confirmation by means of accurate mass measurement of the molecular ions. The required knowledge about the structure of the possible degradation products was obtained in a degradation study of amoxicillin, which is described in two earlier Application Notes^{1,2}.



Agilent Technologies

Introduction

In modern pharmaceutical drug manufacturing it is of crucial importance to identify a minor byproducts with the highest possible confidence because of their potential toxic effects on humans. Widely used mass spectrometric tools for structure elucidation are ion trap instruments with their MS/MS and MSⁿ capabilities. With these instruments it is possible to break the molecular ion of the investigated substance into fragments, which are useful for structure elucidation. It is possible to do this under full control by a controlled repeatable isolation and fragmentation of the fragments derived from the original substance. If the structure and its fragmentations are known it is possible to monitor special fragmentation patterns of different compounds with the “Multi Reaction Mode” (MRM) of the ion trap. Therefore, the ion trap can work under very specific conditions to monitor selected compounds emerging in a production process. In addition to the repertoire of analytical methods for structure elucidation, the mass spectrometric measurement of accurate molecular mass, and consequently the calculation of the empirical formula is a common method for the identification and identity confirmation of an unknown compound. Several years ago only operation-intensive magnetic sector field and FT mass spectrometers were able to perform these measurements with sufficient accuracy. Nowadays, comparably easy to use and inexpensive ESI orthogonal acceleration TOF (oaTOF) instruments are also capable of

handling this task. This is clearly demonstrated by a comparison study of different types of mass spectrometer instruments for the determination of accurate mass of small molecules³. This is possible due to technical innovations in TOF technology introduced during the past years. One of the main technical innovations is the development of orthogonal acceleration TOF technology, which decouples the ion beam velocity spread from the TOF axis. As a result the TOF mass spectrometers⁴ provide better resolution. In this environment the possibility of coupling continuous ionization sources like the electrospray ionization (ESI) source with orthogonal acceleration TOF mass analyzers is of special importance for LC-ESI TOF applications. A high mass accuracy is only achieved when a reference compound, e.g. a reference mass, is simultaneously introduced into the mass spectrometer with the analyte itself. Mixing the LC column effluent with a stream of reference material can result in ion suppression, discrimination or adduct formation. To prevent mixing the analyte and the reference compound prior to spray ionization, an innovation which applies a dual ESI sprayer interface is used^{5,6}. This instrument is capable of achieving resolutions above 15,000 and mass accuracies in the single digit ppm range for small molecules³. For the measurement of trace level impurities in pharmaceutical drug substances it is necessary that the TOF instrument possesses a high dynamic range. This is achieved by the introduction of the analog-to-digital converter (ADC), which digitizes the

detector signal by sampling the amplified detector output at a fixed interval as a data recorder⁷ regardless if it is from a small or large ion current. Recently, the implementation of oaTOF instruments for the measurement of accurate molecular mass and the calculation of the empirical formula and consequently the identity confirmation was impressively demonstrated for the characterization of trace level impurities in a drug substance⁸. In this Application Note the identification and confirmation of degradation products, which have emerged in a formulation trial of the antibiotic drug amoxicillin under no optimum conditions will be demonstrated by means of ion trap MRM and accurate mass measurement using ESI oaTOF.

Experimental

Equipment

- The ESI ion trap analysis (part I of this application)¹ and the ESI TOF MS analysis (part II of this application)² were performed with the Agilent 1100 Series LC/MSD ion trap XCT plus and with the Agilent LC/MSD TOF, equipped with a dual sprayer source for the simultaneous infusion of the reference mass solution.
- The LC system used was an Agilent 1100 Series capillary LC system containing a capillary pump with a micro vacuum degasser, a micro well-plate autosampler with a thermostat and a column compartment.
- The column used was a ZORBAX SB Aq, 0.3 mm x 150 mm, 3.5 μm.

- The software used for instrument control was ChemStation A10.02, ion trap software 4.2, TOF software A01. For data analysis the ion trap data analysis software 4.2 and Analyst QS software was used.

Methods

- The Agilent 1100 Series capillary pump was operated under the following conditions:
 - Solvent A: Water, 10 mM ammonium formate, pH 4.1
 - Solvent B: ACN
 - Column flow: 8 μ L/min,
 - Primary flow: 500-800 μ L/min.
 - Gradient: 0 min 0 % B, 1 min 0 % B, 13 min 25 % B, 23 min 25 % B
 - Stop time: 23 min
 - Post time: 15 min
- The Agilent 1100 Series autosampler was used to make injections of 1 μ L sample. The sample loop was switched to bypass after 1 minute to reduce delay volume.
- The mass spectrometers were operated under the following conditions:
 - Ion Trap MS:
 - Source: ESI in positive mode
 - Dry gas: 5.0 L/min
 - Dry Temp.: 300 °C
 - Nebulizer: 15 psi
 - Target: 150,000
 - Max. accum. time: 50 ms
 - Scan: 200-600

- Averages: 2
- Automated MS/MS and MS³
- ESI TOF MS:
 - Source: ESI in positive mode with dual spray for reference mass
 - Dry gas: 7.0 L/min
 - Dry temp.: 300 °C
 - Nebulizer: 15 psi
 - Scan: 50-1000
 - Fragmentor: 150 V
 - Skimmer: 60 V
 - Capillary: 5000 V
- Samples: Dried powder from formulation trials of amoxicillin dissolved in buffer A, 1 mg/mL.

Results and discussion

All degradation products, which emerged under nonoptimal

process conditions in a formulation trial of the antibiotic drug amoxicillin are clearly detected in the extracted ion chromatogram (EIC) by means of ion trap mass spectrometry (figure 1). The compound amoxicillin penicilloic acid I and II **3** and the compound 4-hydroxyphenylglycyl amoxicillin **4** occur in minor abundance and the degradation products amoxicillin penicilloic acid **2** and diketopiperazine amoxicillin **5** are the main byproducts. After integration of the peaks they were placed in relation to amoxicillin **1** and their ratio in the mixture was calculated (table 1). Since the byproducts, which may occur in a production process are well known from previous stability studies, it is possible to monitor only the appear-

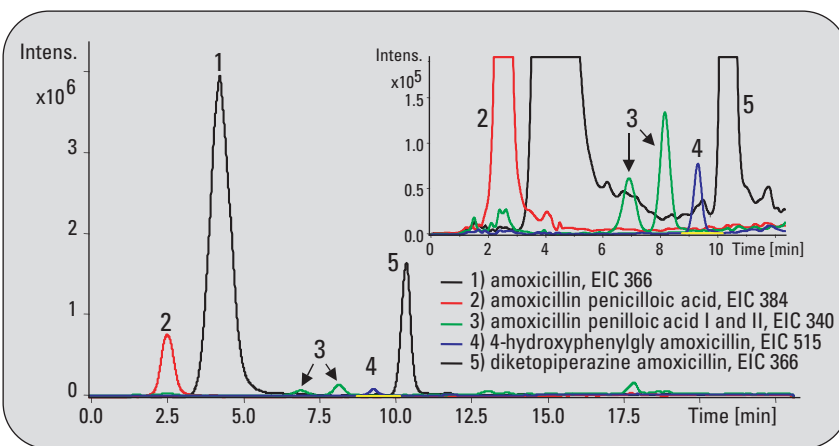


Figure 1
Degradation products of amoxicillin in a formulation trial batch detected by ion trap MS in MRM mode.

| RT [min] | Area [x 10 ⁶] | Height [x 10 ⁵] | Compound | Ratio compared to amoxicillin [%] |
|----------|---------------------------|-----------------------------|--------------------------------------|-----------------------------------|
| 2.5 | 24.24 | 7.59 | amoxicillin penicilloic acid | 12.81 |
| 4.3 | 189.19 | 39.35 | amoxicillin | 100.00 |
| 6.9 | 1.93 | 0.59 | amoxicillin penicilloic acid I or II | 1.02 |
| 8.1 | 3.35 | 1.31 | amoxicillin penicilloic acid I or II | 1.77 |
| 9.3 | 1.58 | 0.76 | 4-hydroxyphenylglycyl amoxicillin | 0.83 |
| 10.4 | 36.66 | 1.63 | diketopiperazin amoxicillin | 19.37 |

Table 1
Ratio of degradation products compared to amoxicillin in percent.

ance of those undesired products by using the MRM with the ion trap mass spectrometer. This was

done with the sample obtained from the formulation trial (figure 2). The isolated mass m/z 384.0 for

amoxicillin penicilloic acid with the characteristic MS and MS/MS fragmentation obtained in the

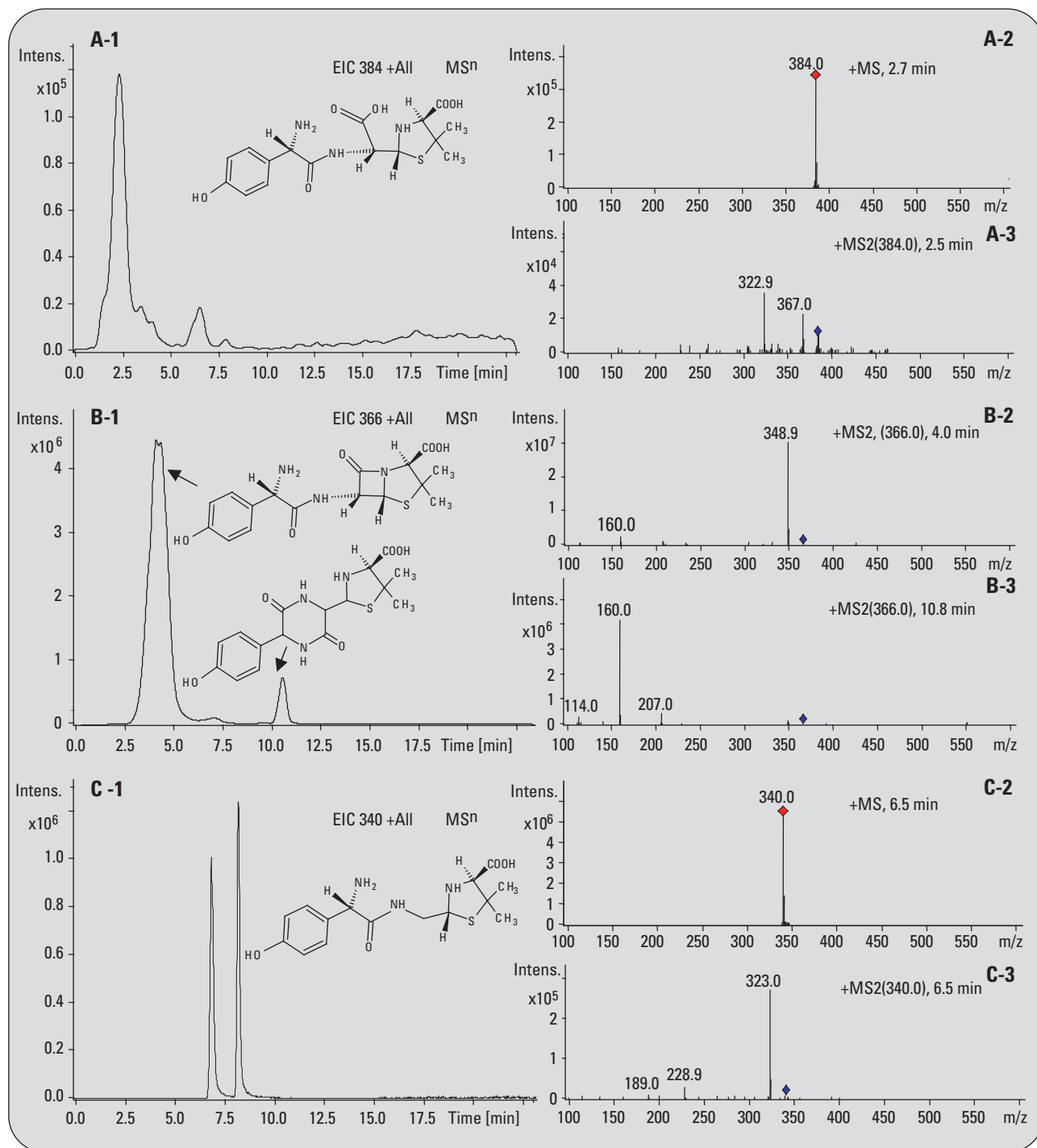


Figure 2-1
Extracted ion chromatograms of amoxicillin degradation products and identification by MS/MS in MRM mode
A) amoxicillin penicilloic acid 2 B) amoxicillin 1 and diketopiperazine amoxicillin 5 C) amoxicillin penicilloic acids I and II 3.

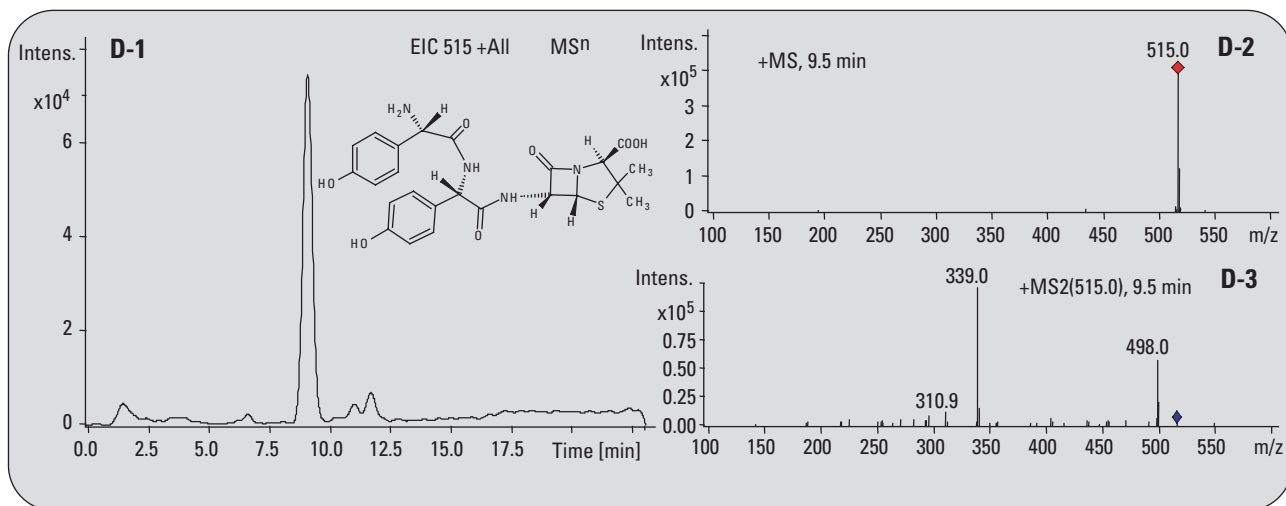


Figure 2-2
 Extracted ion chromatograms of amoxicillin degradation products and identification by MS/MS in MRM mode
 D) 4-hydroxyphenylglycyl amoxicillin 4.

MRM mode is shown in figure 2A. Figure 2A-1 depicts the EIC of the isolated molecular mass, figure 2A-2 the corresponding mass spectrum and figure 2A-3 the MS/MS chart. The fragmentation shows the characteristic ion representing a loss of ammonium and a subsequent decarboxylation. Figure 2B-1 shows the chromatogram of the isolated ions with m/z 366.0. It clearly shows both isomers, amoxicillin **1** itself and the rearranged diketopiperazine amoxicillin **5**. It is easy to distinguish between them by looking at the MS/MS spectra (figures 2B-2 and 2B-3). Amoxicillin **1** shows the ion with a loss of ammonium at m/z 348.9 and diketopiperazin **5** shows the ions characteristic with a break between the five and six membered rings at

m/z 207 and at m/z 160.0 in the MRM. The isolated compounds at m/z 340.0 amoxicillin penilloic acid I and II **3** are shown in figure 2C-1. The MS and MS/MS with the typical fragmentation is shown in figures 2 C-2 and 2 C-3. The ion at m/z 323.0 comes from a loss of ammonium and the ion at m/z 189.0 from a fragmentation of the amid bond. Finally, figures D-1 and D-2 show the EIC and the MS of the isolated compound 4 with m/z 515.1. The MS/MS chart shows the characteristic fragments of a loss of ammonium at m/z 498.1, and the ions resulting from the fragmentation of the thiazole ring at m/z 339.0 and m/z 310.9. The results of these experiments have determined that the ion trap in MRM is a valuable tool for identification of known impurities in e.g.

a production trial.

To confirm the identity of the compounds in the amoxicillin sample from the formulation trial by accurate mass measurement and empirical formula calculation the sample was analyzed by ESI or TOF. The empirical formula report for all compounds in the sample was automatically generated. The mass spectra for all compounds are shown in figure 3 and the calculated mass accuracies and corresponding empirical formulas are listed in table 1.

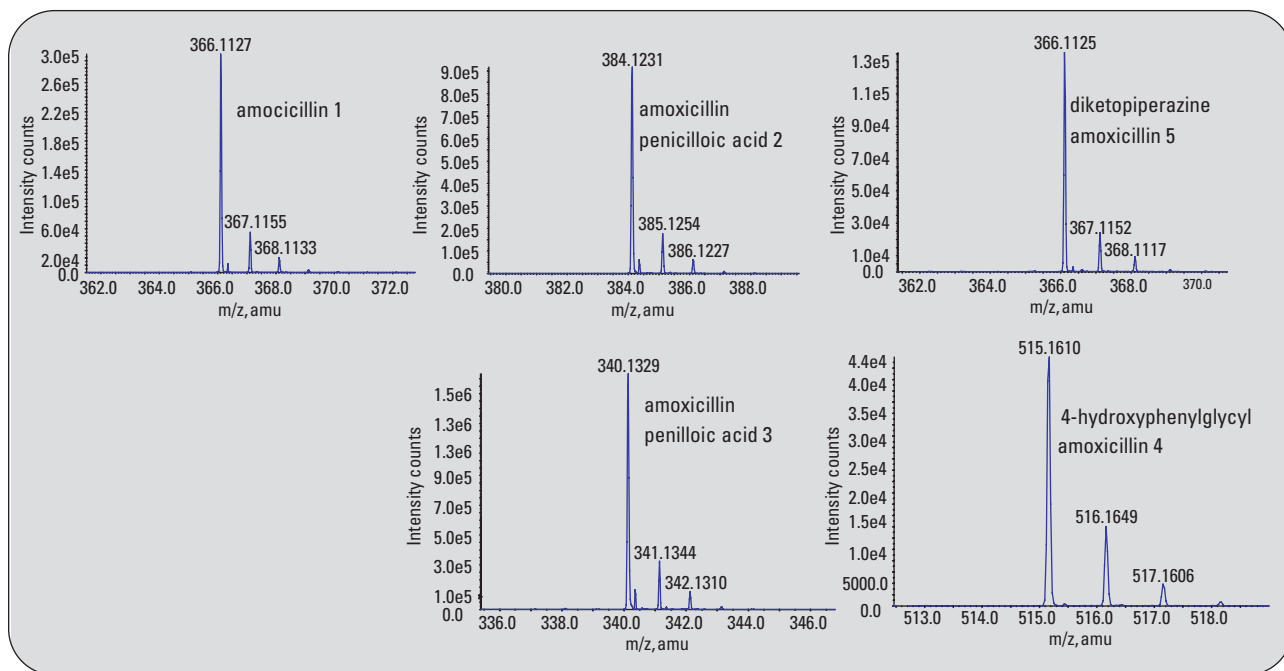


Figure 3
Identity confirmation of amoxicillin degradation products from a formulation trial batch by accurate mass measurement with ESI TOF .

| RT [min] | Compound name | Formula | Calculated mass | Measured Mass | Mass accuracy [mDa] | Mass accuracy [ppm] |
|----------|---------------------------------------|---|-----------------|---------------|---------------------|---------------------|
| 2.7 | amoxicillin penilloic acid 2 | C ₁₆ H ₂₂ N ₃ O ₆ S | 384.1229 | 384.1231 | 0.2 | -0.43 |
| 4.0 | amoxicillin 1 | C ₁₆ H ₂₀ N ₃ O ₅ S | 366.1124 | 366.1127 | 0.3 | -0.90 |
| 6.5 | amoxicillin penilloic acid I and II 3 | C ₁₅ H ₂₂ N ₃ O ₄ S | 340.1331 | 340.1329 | -0.2 | 0.6 |
| 9.5 | 4-hydroxyphenylglycyl amoxicillin 4 | C ₂₄ H ₂₇ N ₃ O ₇ S | 515.1600 | 515.1610 | 1.0 | -1.8 |
| 10.8 | diketopiperazine amoxicillin 5 | C ₁₆ H ₂₀ N ₃ O ₅ S | 366.1124 | 366.1125 | 0.1 | -0.40 |

Table 2
Measured masses of amoxicillin and its degradation products by ESI oaTOF, calculated mass accurcies and empirical fomulas.

The identity of all degradation products including the minor compounds amoxicillin penilloic acid I and II 3 as well as 4-hydroxyphenylglycyl amoxicillin 4 could be identified with high mass accuracies below 1 ppm and 2 ppm, respectively. With these data the identity of all compounds is confirmed with high mass accuracy and the capability to use the ESI TOF in a production environment

for pharmaceutical substances is demonstrated. Due to regulatory guidelines it is not permitted to have more than 0.1 % of a minor byproduct in a final formulation of a pharmaceutical drug. Therefore, it is a basic requirement of each analytical instrument, used in a production environment, to be able measure over a dynamic range for more than three decades and to detect minor impurities

amid a content of 0.1 % besides a major compound. This task could be fulfilled by the ion trap in MRM as well as ESI TOF with automated empirical formula confirmation. The EIC of the isolated *m/z* 366.0 in MRM clearly shows the minor impurity of diketopiperazine amoxicillin 5 with a content of 0.15 % along with the major compound amoxicillin 1 in a highly optimized process

(figure 4). It is easy to distinguish between both products by their mass spectrum and the ion m/z 348.9, which comes from a loss of ammonium only obtained from amoxicillin **1**. It is also possible to identify this compound using accurate mass measurement by means of the ESI TOF and automated empirical formula confirmation (figure 5). The minor byproduct is identified by its empirical formula and a mass accuracy of 0.7 mDa and 1.99 ppm.

Conclusion

This Application Note demonstrates the possibility of using the ion trap as well as the ESI TOF for the identification of byproducts occurring in the production process of pharmaceutical drugs and minor impurities in final drug substances. The ion trap can be used in MRM for the selective detection of impurities, which are known from previous stability and degradation trails. This is achieved with a specific isolation of the molecular ion and subsequent generation of an MS/MS. With the ESI TOF it is possible to detect minor impurities by an automatically generated empirical formula and identity confirmation of the compound by high mass accuracy measurement in the single digit ppm range. These methods combined complement each other as the ion trap MRM delivers structural information and the ESI TOF analysis confirms these results by accurate mass measurement.

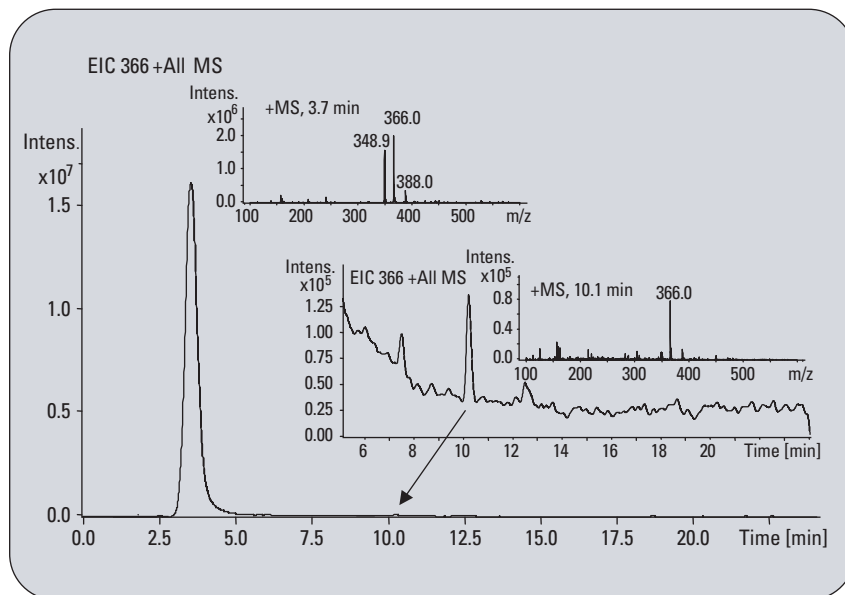


Figure 4
Detection of 0.15 % of a minor impurity diketopiperazine amoxicillin in amoxicillin by ion trap MRM at m/z 366.

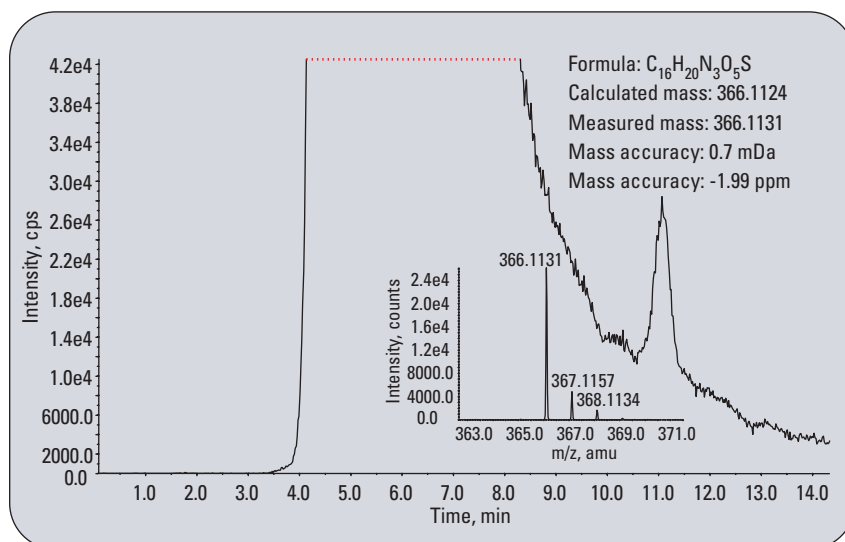


Figure 5
ESI TOF and accurate mass measurement for the identification of the minor impurity diketopiperazine amoxicillin **5** in the major compound amoxicillin **1**.

References

1. "Structure elucidation of degradation products of the antibiotic drug amoxicillin – Part I: Examination of the degraded drug products by fragmentation with ion trap MSⁿ." *Agilent Technologies Application Note, Agilent Publication Number 5989-2347EN, 2005.*
2. "Structure elucidation of degradation products of the antibiotic drug amoxicillin – Part II: Identification and confirmation by accurate mass measurement with ESI TOF of the compound ions and the fragments after CID." *Agilent Technologies Application Note, Agilent Publication Number 5989-2348EN, 2005.*
3. Bristow A.W.T., Webb K.S. "Inter-comparison study on accurate mass measurement of small molecules in mass spectrometry." *J. Am. Mass Spectrom. 14: 1086-1098, 2003.*
4. Guilhaus M., Mlynski V., Selby D. "Perfect Timing: Time-of-flight Mass Spectrometry." *Rapid Commun. Mass Spectrom. 11: 951-962, 1997.*
5. Andrien B.A., Whitehouse C., Sansone M.A. "Proceedings of the 46th ASMS Conference on Mass Spectrometry and Allied Topics", *May 31 – June 4, Orlando, FL, pp 889-890, 1998.*
6. Dresch T., Keefe T., Park M. "Proceedings of the 47th ASMS Conference on Mass Spectrometry and Allied Topics", *June 13 – 18, Dallas, TX, pp 1865-1866, 1999.*
7. "Time-of-Flight Mass Spectrometry", *Agilent Technologies Technical Overview, Publication number 5989-0373EN, 2003.*
8. Eckers C., Haskins N., Langridge J. "The use of liquid chromatography combined with a quadrupole time-of flight analyzer for the identification of trace impurities in drug substance." *Rapid Commun. Mass Spectrom. 11: 1916-1922, 1997.*

*Edgar Nägele is Application Chemist at Agilent Technologies, Waldbronn, Germany.
Ralf Moritz is Analytical Chemist at Sandoz GmbH, Kundl, Austria.*

www.agilent.com/chem/tof

Copyright © 2005 Agilent Technologies
All Rights Reserved. Reproduction, adaptation or translation without prior written permission is prohibited, except as allowed under the copyright laws.

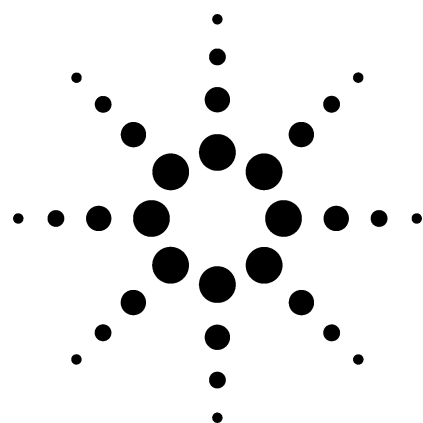
Published June 1, 2005
Publication Number 5989-3071EN



Therapeutic Drug Monitoring by LC/MSD - Clozapine, an Example

Application

Pharmacology



Author

Kolbjørn Zahlsten and Trond Aamo
Department of Clinical Pharmacology
St. Olav Hospital
University Hospital of Trondheim, Trondheim
Norway

Jerry Zweigenbaum
Agilent Technologies, Inc.
2850 Centerville Road
Wilmington, DE 19808-1610
USA

Abstract

Therapeutic drug monitoring is performed by LC/MS on a routine basis at St. Olav Hospital. Over 200 drugs are analyzed for both identification and quantification using this technique. This is made practical by high-throughput analysis and the use of carefully applied methodology. The method for clozapine and its metabolite, desmethyl-clozapine is given as an example. The advantages over immunoassay are briefly discussed.

Introduction

Therapeutic drug monitoring (TDM) has been available for many years for drugs with a narrow therapeutic index (for example, digoxin, theophylline, and lithium). Analyses for most of these drugs have been performed with immunological techniques. For many years clinicians believed that

there was no need to perform TDM on a routine basis for the majority of other drugs. However, during the past few years there has been increased focus on, and a growing awareness of, the interindividual variability in response to drug exposure. This variability may be due to pharmacodynamic, pharmacokinetic, environmental (food, tobacco smoke, ethanol), psychological (insight into the disease), and compliance factors. The lack of ways to correct for many aspects of this variability, other than pure clinical judgement, has evoked a renaissance for TDM. Initially the focus of the “new” TDM was directed towards treatment of psychiatric and neurological disorders, but TDM is now expanding into other medical areas.

TDM at St. Olav Hospital

The Department of Clinical Pharmacology at St. Olav Hospital, Trondheim, routinely monitors more than 200 different drugs, almost exclusively by liquid chromatography/mass spectrometry (LC/MS). For example, there are methods available for more than 20 drugs used for treatment of schizophrenia and other psychoses. One of the drugs in this group that is routinely monitored is clozapine, which is analyzed in about 200 samples per month. Other drugs in the same group include, but are not limited to, olanzapine, quetiapine, ziprasidone, risperidone, sertindole, amisulpiride, haloperidol, perphenazine, zuclopentixol, fluphenazine, chlorpromazine, thioridazine, and chlorpromazine. Similar repertoires are also available for other groups such as antidepressants and mood stabilizers.



Agilent Technologies

Clozapine

Clozapine is mainly used against therapy resistant schizophrenia. Clozapine's mechanism of action is not completely understood, but it is assumed that a combination of a weak dopamine antagonism together with combined serotonin agonism and antagonism are the most important mechanisms. Clozapine is metabolized to numerous metabolites, mainly by the cytochrome P450 (CYP1A2) enzymes, and the half-life in blood usually is within the range of 6–36 hours. Some data indicate that individuals with a high level of desmethylclozapine are more susceptible to develop agranulocytosis; that is a potentially lethal adverse event.

Experimental

In the TDM-service, clozapine and one of its metabolites, desmethylclozapine, are measured in serum by the Agilent Technologies 1100 LC/MSD. The LC/MS with a single quadrupole provides both the selectivity and sensitivity needed for this analysis. Both the ruggedness of the methodology and the instrumentation make it a cost effective process for continuous operation. The use of in-house instrument engineers and meticulous documentation of maintenance operations along with the records obtained from operation 24 hours a day, 7 days a week provide “up-time” of greater than 95%.

All analytical results are transferred to a database. The actual concentration in the serum is interpreted by a MD (specialist in clinical pharmacology). The interpretations usually consist of an

evaluation of the concentration/dose relationship in the actual sample together with evaluation of age, possible drug-drug interactions, possible adverse events if focused by the clinician, etc. versus therapy success or lack of success. New measurements are always compared with previous results in the database. The overall impression is that TDM is an extremely valuable tool for the clinician in the decision making process.

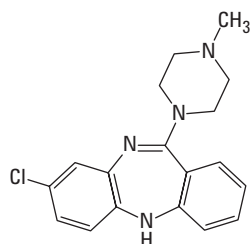
Table 1 gives the extraction procedure for the preparation of blood serum for the analysis of clozapine and its metabolite.

Table 1. Procedure to Extract Clozapine and its Metabolite from Blood Serum

| Step | Action |
|------|---|
| 1. | Take 0.5-mL serum (standard, QC or sample). |
| 2. | Add 50 µL of 10-nM flurazepam [internal standard (ISTD) for clozapine]. |
| 3. | Add 50 µL of 10-nM periciazin (ISTD for desmethylclozapine). |
| 4. | Mix (short). |
| 5. | Add 4 mL of hexane: n-butanol: acetonitrile (93:5:2). |
| 6. | Mix 5-min on rotary mixer. |
| 7. | Centifuge 3000 rpm 5 min. |
| 8. | Transfer organic phase. |
| 9. | Evaporate under stream of air at 40 °C. |
| 10. | Reconstitute in 50-µL methanol. |
| 11. | Transfer to vial with 150 µL insert and cap with crimp-on cap. |

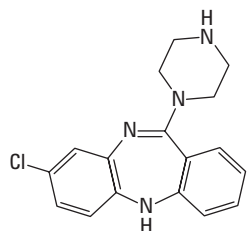
Two internal standards (ISTDs) are used, flurazepam and periciazin. The structures of each are shown in Figure 1.

Targets



Molecular formula = $C_{18}H_{19}ClN_4$
 Monoisotopic mass = 326.129824 Da

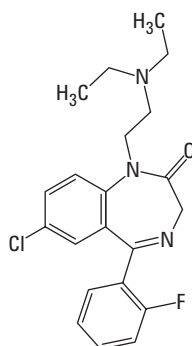
Clozapine



Molecular formula = $C_{17}H_{17}ClN_4$
 Monoisotopic mass = 312.114174 Da

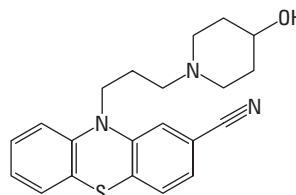
Desmethylclozapine

ISTDs



Molecular formula = $C_{21}H_{23}ClFN_3O$
 Monoisotopic mass = 387.151368 Da

Flurazepam



Molecular formula = $C_{21}H_{23}N_3OS$
 Monoisotopic mass = 365.156183 Da

Periciazin

Figure 1. Structures of clozapine, desmethylclozapine and their ISTDs (shown to their right).

Instrument conditions for the analysis are shown in Table 2.

Table 2. Instrumental Conditions for the Analysis

LC/MS Analysis

LC Conditions

| | |
|--|---|
| Instrument | Agilent 1100 LC/MSD with Quaternary pump and electrospray |
| Column | ZORBAX SB-C18, 4.6 mm × 30 mm × 3.5 μm, p/n 833975-902 |
| Mobile phase | Methanol: 50-mM ammonium acetate in water (60:40) |
| Flow rate | 1 mL/min |
| Standard automatic liquid sampler (ALS) with needle wash | |

MS Conditions

| | |
|------------------|------------------|
| Injection Volume | 2.5 μL |
| Nebulizer | 25 psi at 350 °C |
| Drying gas | 9 L/min |

| | RT (min) | Target | Qualifier |
|--------------------|----------|------------------|-------------------|
| Clozapine | 3.0 | 327.0/frag 100 V | 270.0/frag 150 V |
| Desmethylclozapine | 1.3 | 313.0/frag 100 V | 270.0/ frag 150 V |
| Flurazepam | 2.2 | 388.1/frag 100 V | |
| Periciazin | 1.9 | 365.5/frag 100 V | |

Calibration is done with zero serum using spiked concentrations of calibration standards (clozapine and desmethylclozapine): 0, 25, 100, 500, 1000, 2000, 3000, and 4000 nM. The calibration curves use a quadratic fit (because of the wide range of concentration) with $r^2 > 0.999$. Quality control samples are prepared with zero serum using spiked concentrations of QCs (clozapine and desmethylclozapine): 500, 500, 1000, 1000, 3000 and 3000 nM.

The QCs are run randomly distributed among the samples.

Results

Figure 2 shows the selected ion chromatograms of the target compounds with qualifying ions and their ISTDs for the 25 nM standard.

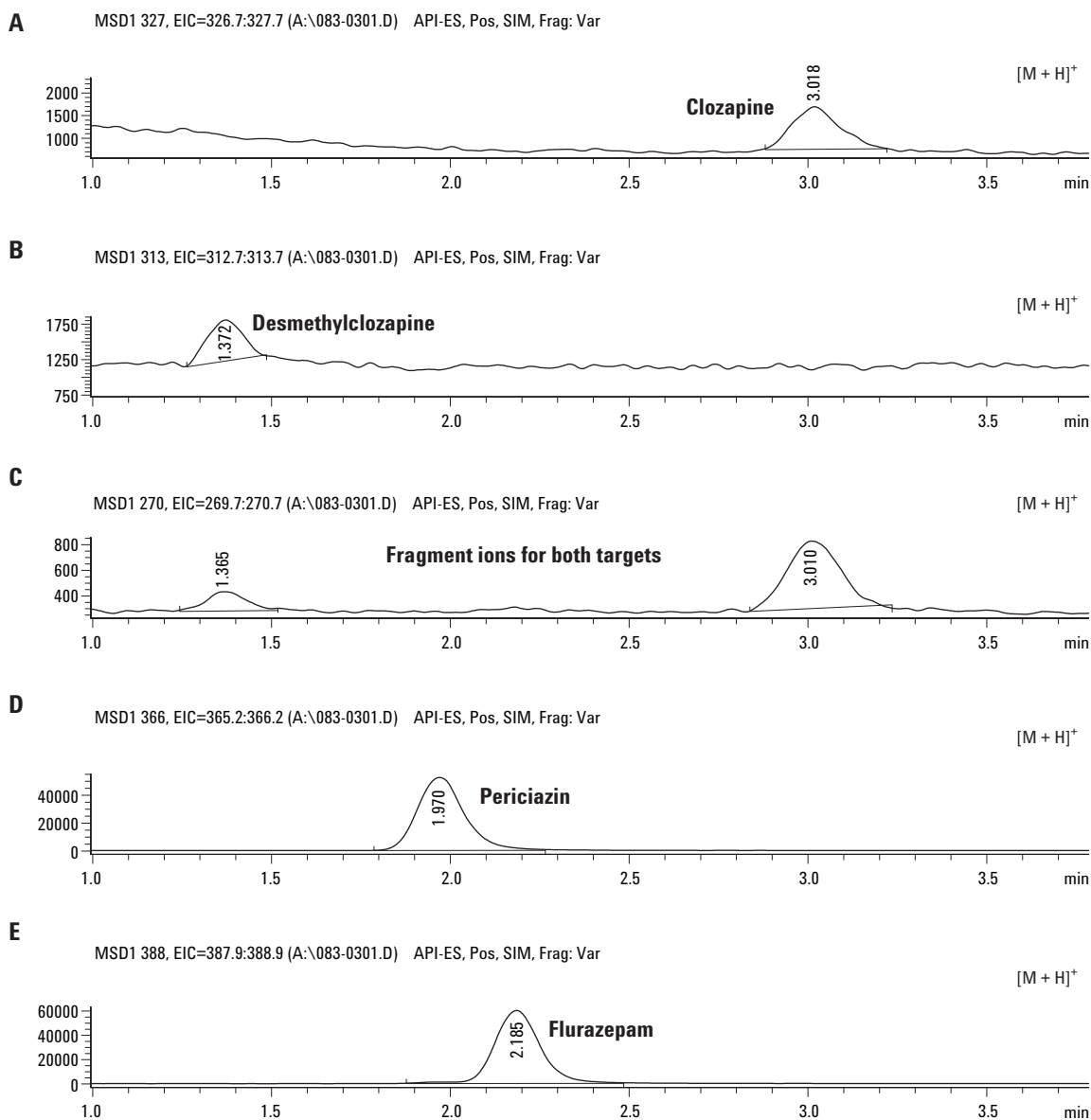


Figure 2. Selected ion chromatograms for 25 nM clozapine, desmethylclozapine, and their ISTDs. All chromatograms show the $[M+H]^+$ ions. Figure 2A is derived from clozapine, 2B from desmethylclozapine, 2C from fragments from both target compounds (after neutral loss of 1-N-methylaziridine), 2D from periciazin, and 2E from flurazepam.

Up-front collision-induced-dissociation (CID) is sufficient to produce a qualifier ion to increase the specificity of the analysis. This is the lowest standard in serum and represents a concentration typically below normal therapeutic monitoring levels. There is variation of the serum matrix from one sample to another but that variation is not sufficient to have any impact on the analysis.

Figure 3 shows a blank containing the ISTDs and Figure 4 presents the results of a patient sample at a typical lower level (for true patient samples). In this patient sample, the clozapine was measured at 366 nM, and the metabolite at 365 nM. Note how clean the signals are with no interference. The methods demonstrated were robust for a period of 5 years.

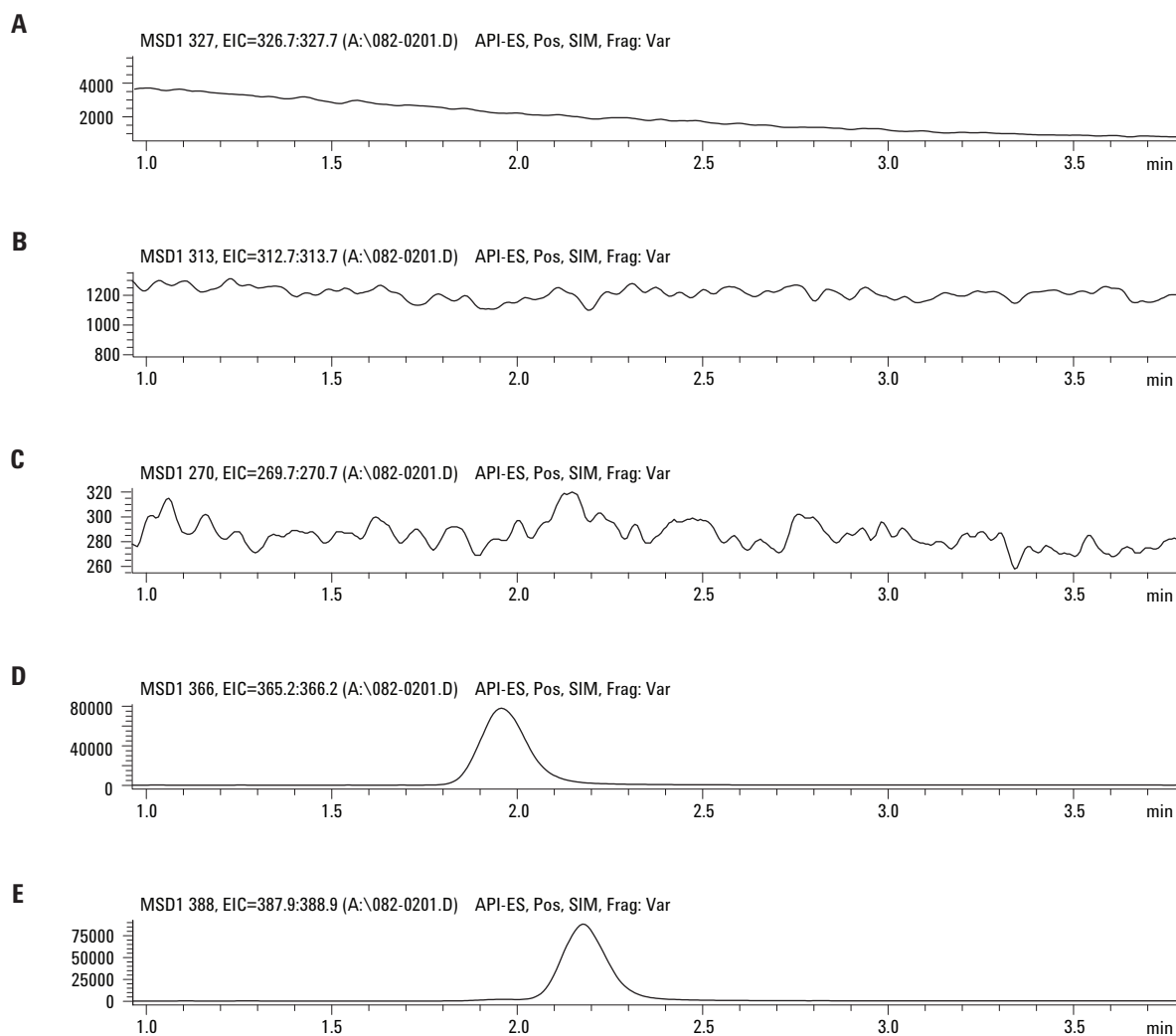


Figure 3. Extracted ion chromatograms (EIC) of blank clozapine in blood serum with ISTDs.

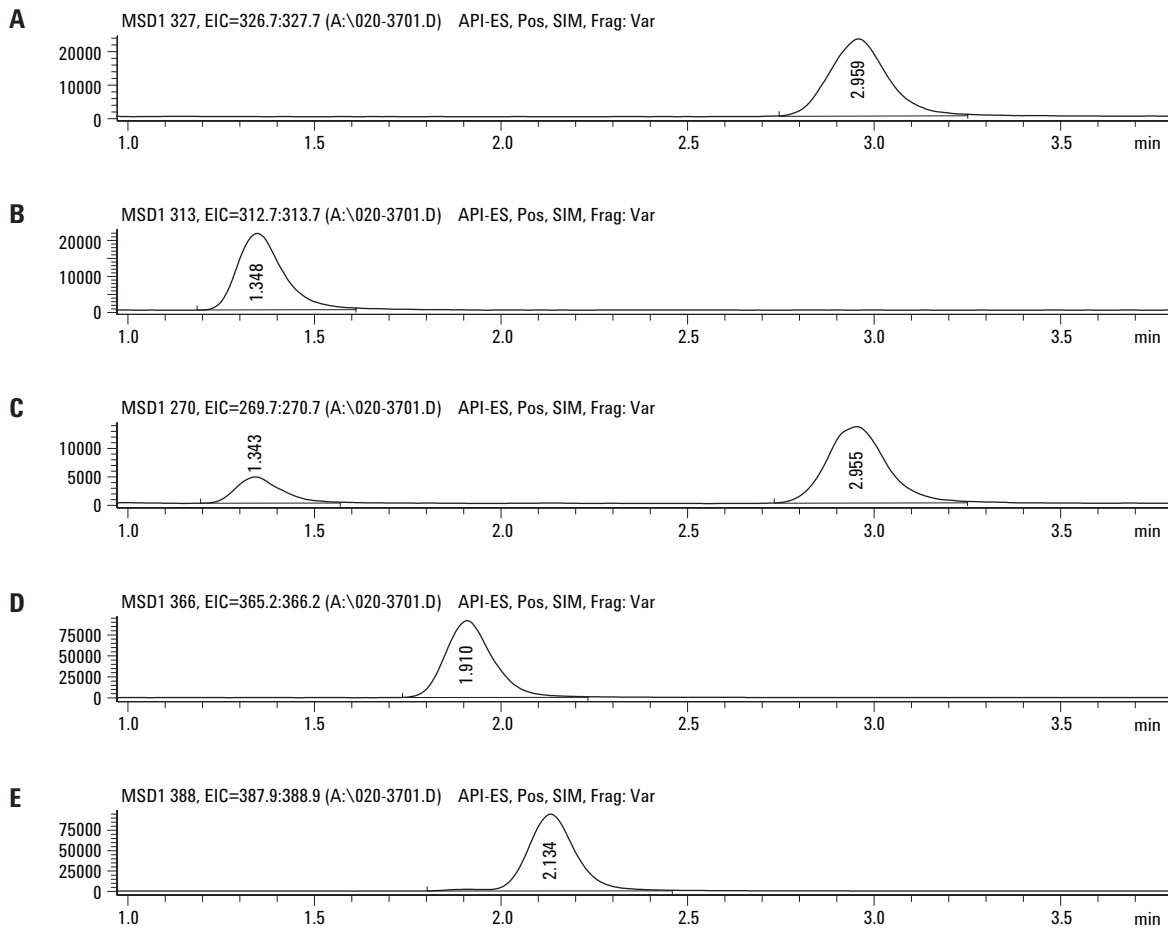


Figure 4. EIC of patient sample at a typical low level.

Reproducibility

True day-to-day reproducibility with different instruments and different operators is obtained through the evaluation of the QC samples. These are shown in Table 3, as a 3-month rolling average.

Table 3. True Reproducibility of Analysis (3-month rolling average)

| | 25 nM | 500 nM | 3000 nM |
|--------------------|-------|--------|---------|
| Clozapine | 6.1% | 6.1% | 7.8% |
| Desmethylclozapine | 9.1% | 8.0% | 7.6% |

Table 4 shows a 1 day example of the QC results at the different levels.

Table 4. True Reproducibility of Analysis (1 day example)

| | 500 | 1000 | 3000 |
|--------------------|-----|------|------|
| Clozapine | 596 | 1068 | 3361 |
| | 543 | 1068 | 2935 |
| Desmethylclozapine | 462 | 1026 | 3345 |
| | 534 | 992 | 2904 |

Once per month QC samples from Heatcontrol/ Cardiff Bioanalytical Services Ltd. are analyzed and a report generated. A 12-month control chart of the Bias Index Score (BIS) is shown in Figure 5. The BIS is defined as the difference of the laboratory's measurement from the consensus mean scaled in terms of a chosen common coefficient of variation for all participants. If the exact coefficient of variation is used, a BIS value of 300 corresponds to 3 standard deviations (SDs). External quality control samples are used for any TDM analyte that is available.

For More Information

For more information on our products and services, visit our Web site at www.agilent.com/chem.

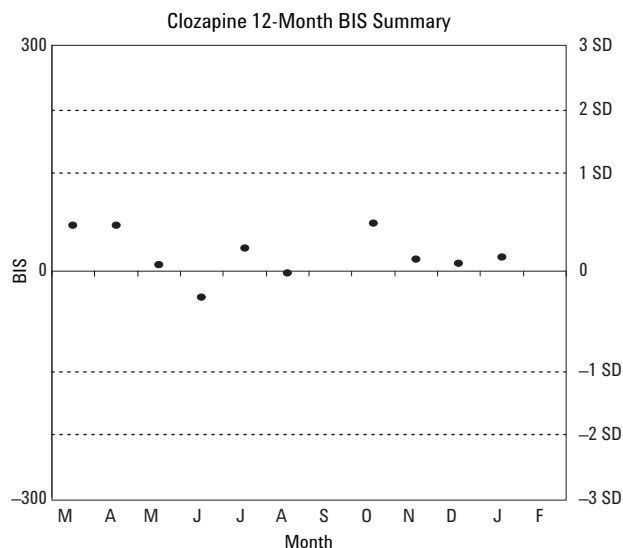


Figure 5. Control chart for external quality sample.

Conclusion

Through the use of well developed and validated methodology, carefully documented procedures followed by highly skilled and trained operators (technicians or engineers), and rigorous QC incorporated into good laboratory practices, this lab routinely performs therapeutic drug monitoring, clozapine as an example, with LC/MS running 24 hours a day, 7 days a week. For clozapine, typical serum levels for patients range from 450 nM to 3000 nM.

Jerry Zweigenbaum, 302-633-8661
e-mail: J_Zweigenbaum@Agilent.com
Kolbjørn Zahlsen, e-mail: zahlsen@online.no

Agilent shall not be liable for errors contained herein or for incidental or consequential damages in connection with the furnishing, performance, or use of this material.

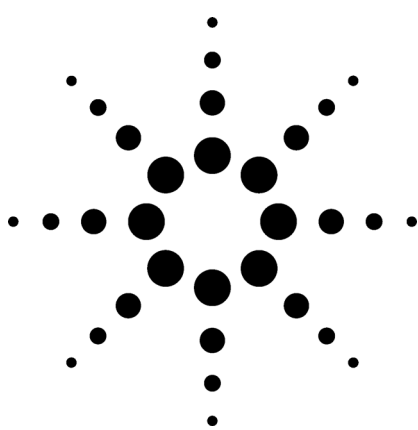
Information, descriptions, and specifications in this publication are subject to change without notice.

© Agilent Technologies, Inc. 2004

Printed in the USA
August 18, 2004
5989-1267EN



Agilent Technologies



High Efficiency, High Throughput LC and LC/MS Applications Using ZORBAX Rapid Resolution HT Columns

Application

Drug Manufacturing/QA/QC

William E. Barber and Maureen Joseph

Introduction

Short chromatographic run times increase productivity because more samples can be run in less time when the analysis time is reduced. Short run times are achieved by using shorter HPLC columns. To truly maintain productivity, resolution and efficiency need to be maintained with short columns. This is done effectively by using short columns with smaller particle sizes. For the greatest efficiency in the shortest column lengths (50 mm and shorter), new 1.8- μm particles can be used for a wide range of high throughput liquid chromatography (LC) and liquid chromatography/mass spectrometry (LC/MS) applications.

Experimental

To demonstrate the potential of the 1.8- μm particle size columns, we converted a standard USP assay method into a high throughput analysis by using a Rapid Resolution High Throughput (RRHT) column. In this first example, we converted the USP analysis of triamcinolone into a high throughput method without changing the resolution required. The traditional USP method calls for a 3.9×300 mm, 10- μm L1 column and suggests a retention time of 10 minutes while requiring $R_s > 3$ for triamcinolone and the internal standard hydrocortisone. This is easily achieved, as shown in Figure 1A.

To convert this to a high throughput application, a 4.6×30 mm, 1.8- μm Eclipse XDB-C18 was substituted using the same analysis conditions. The result (Figure 1B) is a 2-minute retention time, increasing sample throughput 5 \times . The resolution and efficiency of this 2-minute analysis exceed that of the original method using a column with 1/10 the length. The original USP method also suggested starting with a mobile phase composition of 60% methanol: 40% water. When this mobile phase was used a run time of 0.7 minutes was achieved (Figure 1C) while the resolution was more than double what is required. The end result is a method with 10 \times the sample throughput of the original method with no compromise in resolution.

Highlights

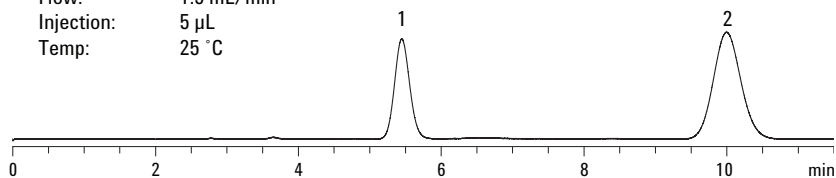
- Standard USP assay methods for triamcinolone and guaifenesin were converted into high throughput methods using Agilent RRHT columns with 1.8- μm particles, while still exceeding minimum resolution requirements.
- Throughput increases of 8 to 10 \times were demonstrated.



Agilent Technologies

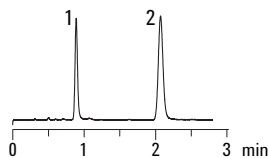
1A

USP L1 Column: 3.9 × 300 mm, 10 μm
 Eluent: 47% Methanol: 53% Water
 Flow: 1.5 mL/min
 Injection: 5 μL
 Temp: 25 °C



| Peak | RT | N | Rs |
|------|------|------|-----|
| 1 | 5.45 | 3199 | 0 |
| 2 | 9.99 | 3212 | 8.1 |

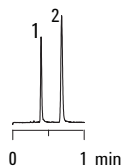
1B



RRHT Column (L1)
ZORBAX Eclipse XDB-C18: 4.6 × 30 mm, 1.8 μm
 Part number 923975-902
 Eluent: 47% Methanol: 53% Water
 Flow: 1.5 mL/min
 Injection: 1 μL
 Temp: 25 °C

| Peak | RT | N | Rs |
|------|------|------|------|
| 1 | 0.89 | 3256 | 0 |
| 2 | 2.07 | 4851 | 11.8 |

1C



RRHT Column (L1)
ZORBAX Eclipse XDB-C18: 4.6 × 30 mm, 1.8 μm
 Part number 923975-902
 Eluent: 60% Methanol: 40% Water
 Flow: 1.5 mL/min
 Injection: 1 μL
 Temp: 25 °C

| Peak | RT | N | Rs |
|------|------|------|-----|
| 1 | 0.40 | 2991 | 0 |
| 2 | 0.69 | 4025 | 6.9 |

Figure 1. Throughput comparisons for triamcinolone using different column and gradient conditions. Peak 1: triamcinolone, 0.2 μg/μL, Peak 2: hydrocortisone, 0.3 μg/μL. Minimum required resolution: 3.0.

Figure 2 shows a dramatic increase in throughput for the USP assay of guaifenesin. This calls for a 4.6×250 -mm L1 column and a $R_s > 3$ for the guaifenesin and benzoic acid internal standard (Figure 2A). Both 4.6×50 mm and 4.6×30 -mm RRHT columns were substituted to evaluate different choices in column lengths for high throughput applications. The 50-mm column length (Figure 2B) improves throughput 5 \times while maintaining 70% of efficiency and 78% of the resolution of the 250 mm, 5- μ m column. The 30 mm, 1.8 μ m provides 8 \times the sample throughput and R_s of 8.6, nearly 3 \times the method requirements (Figure 2C).

2A

USP L1 Column

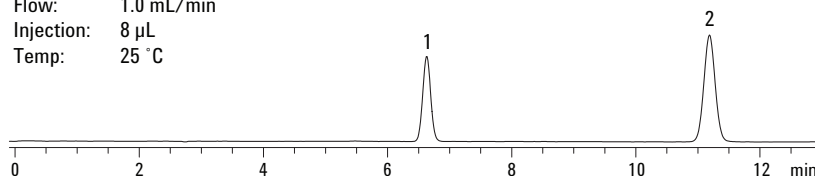
ZORBAX Eclipse XDB-C18: 4.6×250 mm, 5 μ m

Eluent: 40% Methanol: 60% Water: 1.5% Glacial Acetic Acid

Flow: 1.0 mL/min

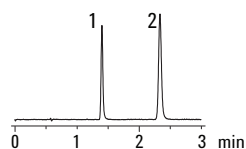
Injection: 8 μ L

Temp: 25 $^{\circ}$ C



| Peak | RT | N | R_s |
|------|-------|--------|-------|
| 1 | 6.63 | 12,737 | 0 |
| 2 | 11.19 | 18,552 | 15.8 |

2B



RRHT Column (L1)

ZORBAX Eclipse XDB-C18: 4.6×50 mm, 1.8 μ m

Eluent: 40% Methanol: 60% Water: 1.5% Glacial Acetic Acid

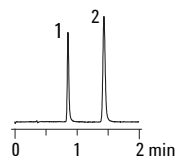
Flow: 1.0 mL/min

Injection: 2 μ L

Temp: 25 $^{\circ}$ C

| Peak | RT | N | R_s |
|------|------|--------|-------|
| 1 | 1.40 | 11,421 | 0 |
| 2 | 2.33 | 12,909 | 12.3 |

2C



RRHT Column (L1)

ZORBAX Eclipse XDB-C18: 4.6×30 mm, 1.8 μ m

Eluent: 40% Methanol: 60% Water: 1.5% Glacial Acetic Acid

Flow: 1.0 mL/min

Injection: 2 μ L

Temp: 25 $^{\circ}$ C

| Peak | RT | N | R_s |
|------|------|-------|-------|
| 1 | 0.85 | 5,855 | 0 |
| 2 | 1.43 | 7,300 | 8.6 |

Figure 2. Throughput comparisons for guaifenesin using different column and gradient conditions. Peak 1: guaifenesin, 0.04 μ g/ μ L, Peak 2: benzoic acid, 0.10 μ g/ μ L. Minimum required resolution: 3.0.

Conclusion

These two examples show that RRHT columns with 1.8- μ m particles can be used to increase productivity and sample throughput for LC analyses. These columns are also available with a 2.1-mm internal diameter to achieve the same throughput increases for LC/MS analyses. Time savings with these columns can be dramatic while still achieving high resolution.

For More Information

For more information on our products and services, visit our Web site at www.agilent.com/chem.

Authors William E. Barber (Applications Specialist) and Maureen Joseph (LC Columns Product Manager) are based at Agilent Technologies, Wilmington, Delaware.

Agilent shall not be liable for errors contained herein or for incidental or consequential damages in connection with the furnishing, performance, or use of this material.

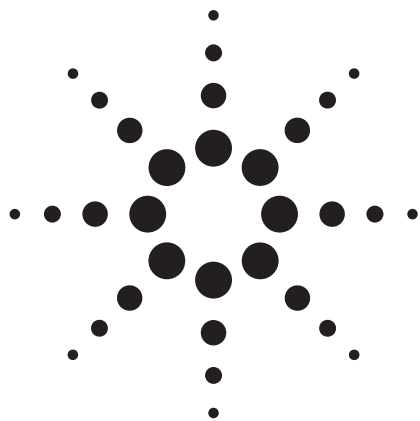
Information, descriptions, and specifications in this publication are subject to change without notice.

© Agilent Technologies, Inc. 2004

Printed in the USA
January 20, 2004
5989-0540EN



Agilent Technologies



Analysis of Ephedrine Isomers using the LC/MSD Quadrupole System

Application Note

Patrick Perkins
Agilent Technologies

Introduction

Various isomers of ephedrine are naturally occurring active components in the herbal remedies *ma huang* and *ephedra*, used since ancient times as a treatment for bronchial distress. These alkaloids also cause stimulant effects and increased metabolic rates when ingested, and preparations containing them are often mixed with stimulants, e.g., caffeine, for increased effect. The herbal extract, which has numerous pseudonyms, is a common ingredient in many over-the-counter dietary supplements (so-called “fat burners”) sold as aids for weight loss. Unfortunately, there appear to be significant health risks associated with the use of ephedra and other preparations containing ephedrine. In September 1994, the US FDA expressed concern over the safety, effectiveness, and use of herbal products and dietary supplements containing ephedra. Supplements

containing ephedra have been implicated in the deaths of at least two professional athletes, and ephedra in any form is a banned substance by many athletic governing organizations, including the International Olympic Committee, the US Olympic Committee, and the National Collegiate Athletic Association. Sales of products containing ephedra currently are banned in many US states. Interestingly, the ephedrine isomer pseudoephedrine is a common ingredient in over-the-counter nasal decongestants and cold remedies.

The Agilent 1100 Series LC/MSD quadrupole mass spectrometer was used to detect the presence of ephedrine and pseudoephedrine in an herbal remedy. Its ease of use, excellent sensitivity at low mass, and robust operation make this system a good choice for routine analysis of these substances.



Agilent Technologies

Experimental

All experiments were performed using an Agilent 1100 Series LC/MSD quadrupole mass spectrometer system comprised of Agilent 1100 Series LC modules: binary pump, vacuum degasser, and autosampler; and an Agilent 1100 Series LC/MSD model SL. An Agilent ZORBAX SB-Aq column was used for the analytical separation.

Calibration standards were prepared from ephedrine and pseudoephedrine standards (1 mg/mL in methanol, Cambridge Isotope Laboratories, Andover, MA) by dilution in the mobile phase. The herbal remedy of *Ephedra sinica* was purchased as an over-the-counter acidic extract in alcoholic solution, centrifuged (14,000 rpm, ten minutes) to sediment any solids, and then diluted 10,000-fold in the mobile phase prior to injection. The MSD was tuned in positive electrospray mode using the Autotune program with default parameters. Data reduction was performed using the Analyst accessory software package available from Agilent Technologies under license from PE SCIEX.

Results and Discussion

Figure 1 shows the results of replicate injections of a blank solution followed by injections of 1 pg each ephedrine and pseudoephedrine. In spite of the fact that the mobile phase was 100% aqueous, the SB-Aq column had more than enough separation power to efficiently resolve these isomers in a short period of time.

EXPERIMENTAL CONDITIONS

Chromatographic Conditions

| | |
|---------------------|--|
| Column: | 2.1 mm x 50 mm ZORBAX SB-Aq 3.5 μ m (p/n 871700-914) |
| Mobile phase: | A = 0.1% formic acid in water, isocratic |
| Flow rate: | 0.4 mL/min |
| Column temperature: | 35 °C |
| Injection volume: | 1 μ L |

MS Conditions

| | |
|-----------------------------|------------------------------------|
| Source: | ESI, positive mode |
| Drying gas flow: | 13 L/min |
| Nebulizer: | 60 psig |
| Drying gas temperature: | 350 °C |
| Capillary voltage: | -900 V |
| Chromatographic peak width: | 0.10 min |
| Time filter: | Yes |
| SIM: | 166.10 <i>m/z</i> , 580 msec dwell |
| Fragmentor: | +60 V |
| EM gain: | 0.2 |

Figure 2 shows the calibration curves for ephedrine and pseudoephedrine over the range of 1–1000 pg injected. The calibration curve for each analyte is linear ($r^2 = 1.0000$ for both analyte curves) for three orders of magnitude concentration range.

Analysis of the herbal remedy indicated both ephedrine and pseudoephedrine were present at a concentration of 1.2 and 0.6 mg/mL, respectively, for a total of 1.8 mg/mL ephedrines. This agrees well with the concentration of 1.6–2.2 mg/mL specified on the label of the product.

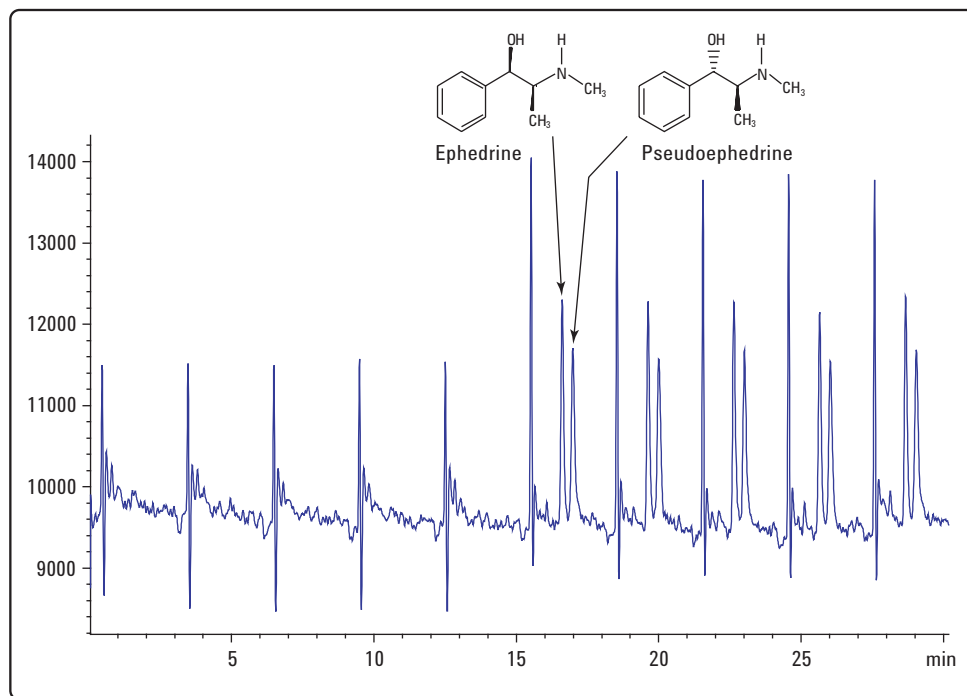
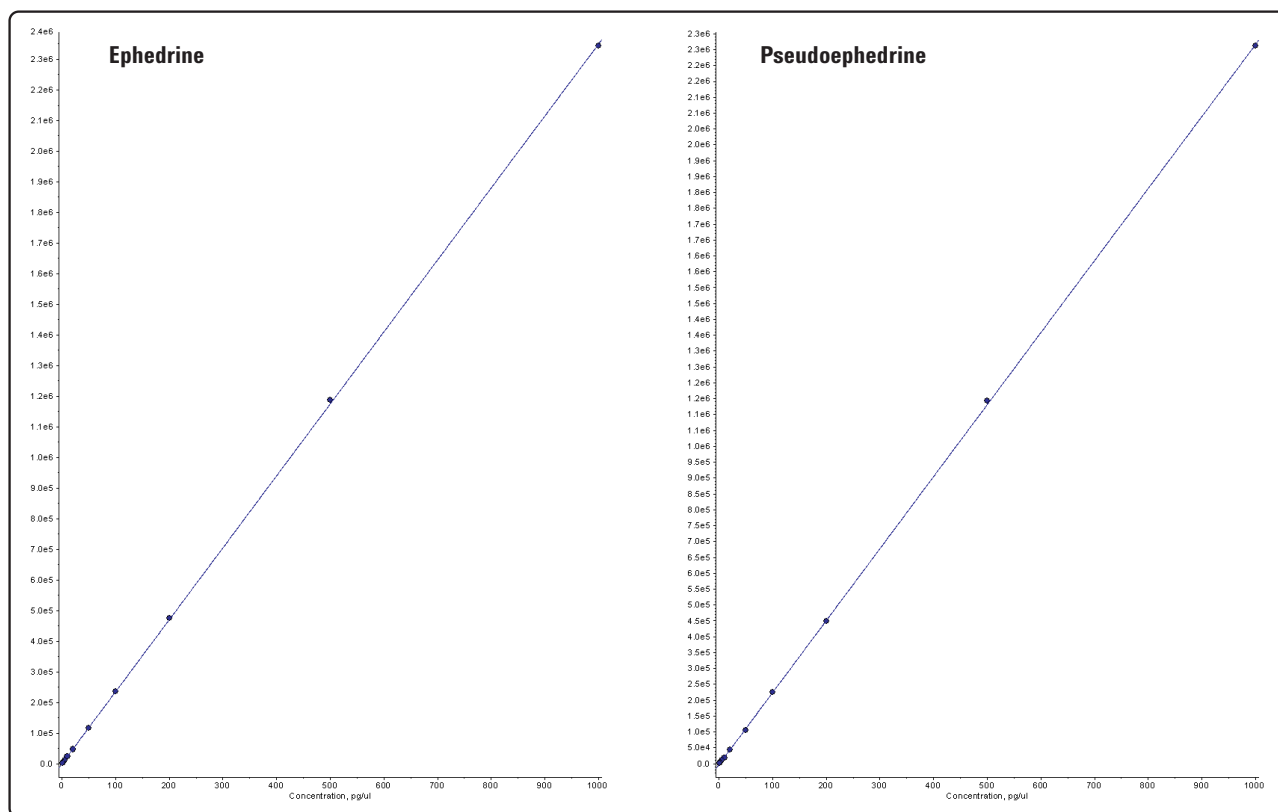


Figure 1. Replicate injections of blank solvent and a calibration standard containing 1 pg each ephedrine and pseudoephedrine

Figure 2. Calibration curves for ephedrine (left) and pseudoephedrine (right), 1–1000 pg injected



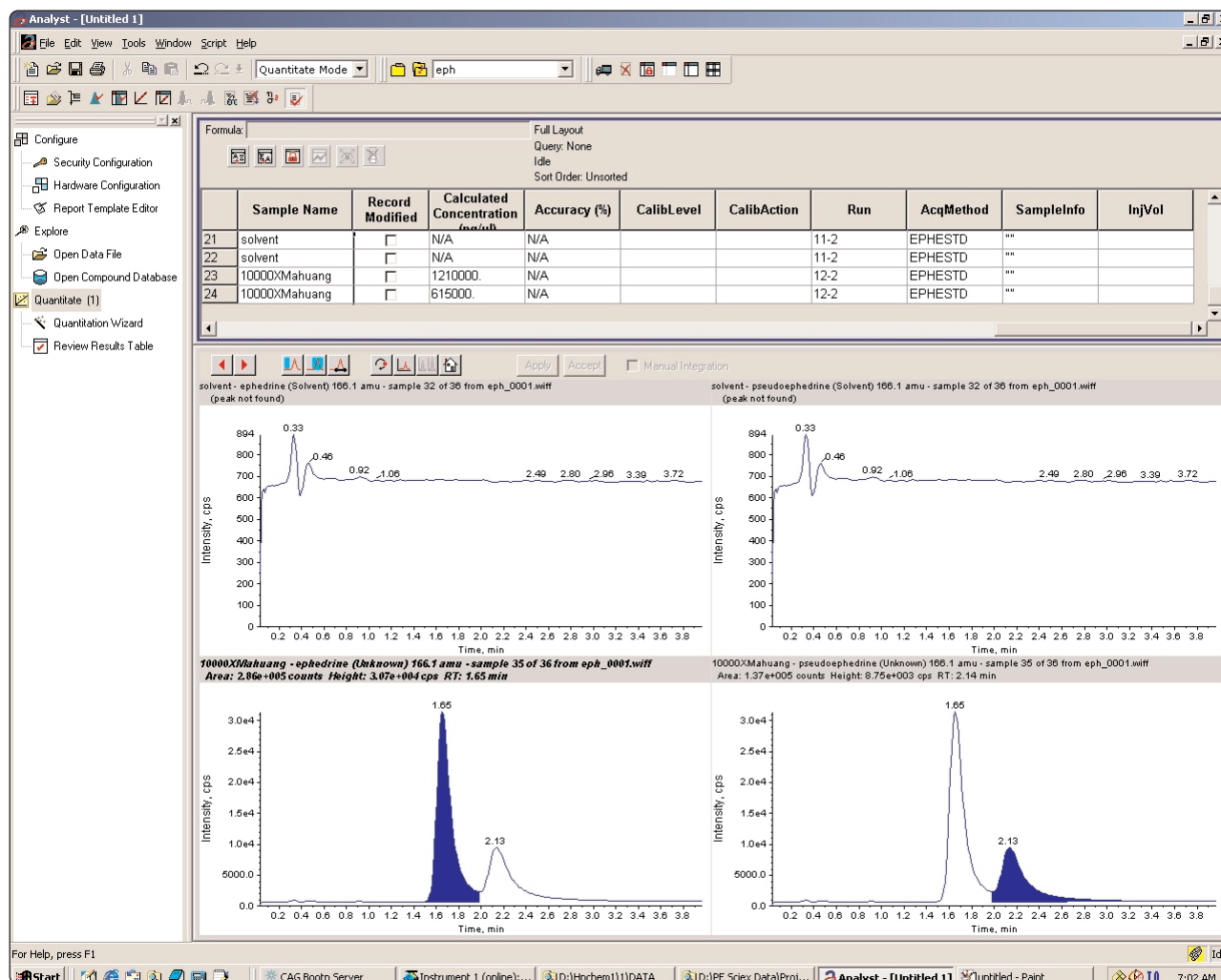


Figure 3. Analysis of an over-the-counter herbal extract of *Ephedra sinica* diluted 10,000-fold. The response of a blank solvent injection is shown in the top two traces, and the bottom two traces show the response of ephedrine (left) and pseudoephedrine (right) analyzed immediately after the blank. Quantitated amounts are 1.2 mg/mL ephedrine and 0.6 mg/mL pseudoephedrine, respectively.

Conclusions

Ephedrine isomers, active components of the banned substance ephedra, are found in many dietary supplements, energy supplements, and cold remedies. The Agilent Series 1100 LC/MSD quadrupole system has the sensitivity and linearity to successfully analyze for these compounds, assuming appropriate sample preparation.

Author

Patrick D. Perkins is a senior application chemist at Agilent Technologies in Santa Clara, California U.S.A.

www.agilent.com/chem

© Agilent Technologies, Inc. 2003

Information, descriptions and specifications in this publication are subject to change without notice. Agilent Technologies shall not be liable for errors contained herein or for incidental or consequential damages in connection with the furnishing, performance or use of this material.

Printed in the U.S.A. November 21, 2003
5989-0389EN



Agilent Technologies



Structural Determination of Ginsenosides Using MSⁿ Analysis

Linda L. Lopez

Introduction

Ginseng root, a traditional Chinese herbal remedy, contains more than a dozen biologically active saponins called ginsenosides. This class of natural products is believed to play an important role in the treatment and prevention of a number of diseases including atherosclerosis, arthritis, asthma, diabetes, stroke, multiple sclerosis, and endotoxin liver injury.^{1–3} Ginsenosides are among a growing class of herbal and vitamin products known as nutraceuticals, that is, food products that have pharmacological benefits to human health because of their therapeutic properties. With an estimated 15 million patients at risk of potentially adverse drug-herb interactions,⁴ there is renewed interest in the isolation and characterization of these compounds.

Ginsenosides are structurally described as glycosides consisting of an aglycone moiety, which is typically a triterpenoid or steroid, and one or more covalently linked sugar monomers. Since most ginsenosides contain multiple oligosaccharide chains at different positions in the molecule, structural elucidation of these compounds can be quite complicated. Tandem mass spectrometric methods have been developed for the characterization of ginsenosides contained in ginseng extracts.⁵ However, MS/MS experiments carried out on a triple quadrupole mass spectrometer using a collision cell typically generate complex product ion spectra that are often difficult to interpret. This is because first-stage product ions tend to undergo further collisions with the background gas to yield second and third generation fragments that cannot be easily distinguished from first-stage MS/MS product ions.

MSⁿ analysis in an ion trap mass spectrometer permits multiple isolation and fragmentation stages, ensuring that product ions in each stage are specifically related to the precursor ion from that particular stage. This type of stepwise fragmentation can be quite advantageous because it allows product ion origins to be unambiguously assigned, making MS/MS spectra simpler to interpret and permitting individual fragmentation pathways to be followed.

This note demonstrates the power of MSⁿ analysis for the structural determination of ginsenosides from a ginseng root extract.

Experimental

All experiments were done using an Agilent 1100 Series LC/MSD Trap system composed of a binary pump, vacuum degasser, autosampler, and thermostatted column compartment with column-switching valve. The system was operated with the electrospray ionization (ESI) source in the positive ion mode.

Reagent grade chemicals and HPLC grade solvents were used in preparing mobile phases and standards.

Results and Discussion

Figures 1a–c show the full scan MS, MS/MS and MS³ spectra from direct infusion of the Rb1 ginsenoside standard, along with proposed origins of the observed product ions. The mass spectrum of Rb1 (Figure 1a) shows predominantly the intact [M+Na]⁺ pseudomolecular ion at *m/z* 1131.7, with little or no decomposition of the labile ginsenoside adduct under typical ESI interface conditions using a drying gas temperature of 350°C. This is in contrast to previous studies in which a room temperature API interface was required to observe an intact molecular ion,⁵ and emphasizes the gentle nature of the orthogonal spray ion source on the LC/MSD Trap.

Structural Determination of Ginsenosides Using MSⁿ Analysis

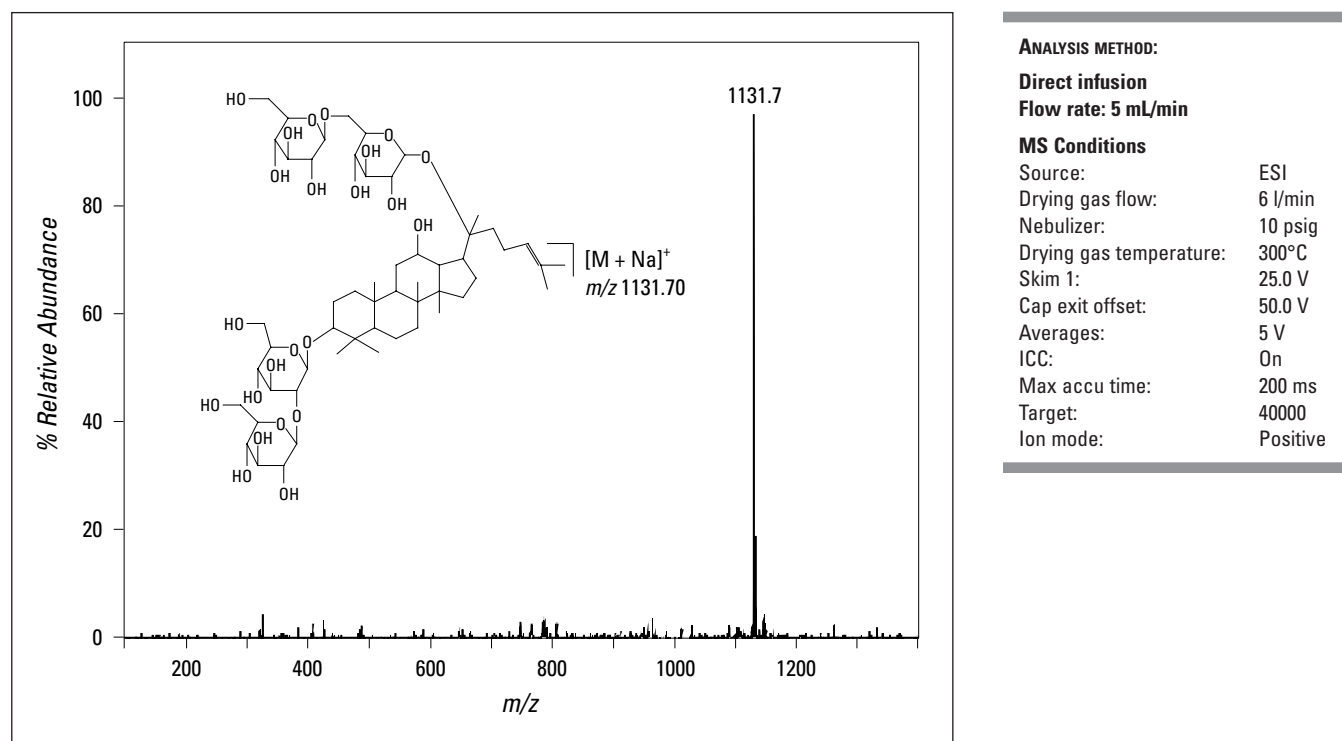


Figure 1a. Full scan mass spectrum of ginsenoside Rb1 standard.

MS/MS of the m/z 1131.7 sodium adduct shown in Figure 1b yields a product ion at m/z 789.6 corresponding to cleavage of a single glycosidic bond. For the case of the ginsenoside Rb1, which contains two isomeric oligosaccharide chains, cleavage at either glycosidic linkage would result in isobaric fragment ions at m/z 789.6. Subsequent isolation and fragmentation of m/z 789.6 (Figure 1c) yields two products: (1) a more abundant ion corresponding to loss of the oligosaccharide chain ($-\text{Glc}^2-\text{Glc}$) at m/z 365.1 and (2) loss of a deoxyhexose sugar at m/z 627.5. The stepwise fragmentation observed in the ion trap provides specific information on molecular structure; however, in this case it is not possible to establish the initial site of glycosidic bond cleavage in the molecule.

For use as a reference in the interpretation of ginsenoside Rb1 fragmentation spectra, several analogs of ginsenoside Rb1 were analyzed by ion trap LC/MSⁿ. In this manner an MS/MS comparative method was devised based on the premise that ginsenoside Rb1 would be expected to retain substructures of the related ginsenosides. For example, Figure 2 shows the

total ion chromatogram generated from online LC/MS³ analysis, as well as extracted ion chromatograms of the pseudomolecular ions of each chromatographic peak generated from a water extract of American ginseng root. Figures 3a and 3b show the online product ion spectra of the ginsenoside Rb2 which contains two different oligosaccharide chains. Isolation and fragmentation of the pseudomolecular ion at m/z 1101.6 yields a single ion at m/z 789.7 resulting from cleavage of the $-\text{Glc}^6-\text{Ara}(\text{p})$ disaccharide linkage. Comparison of the product ion spectra of ginsenosides Rb1 with Rb2 shows isobaric product ions (m/z 789.7), thus supporting the proposed fragmentation pattern for ginsenoside Rb1 shown in Figure 1. Furthermore, m/z 789.7 was a major fragment ion observed in the product ion spectra of all the ginsenosides analyzed, providing a substructural template that supports the fragmentation patterns proposed for Rb1 and Rb2.

Subsequent isolation of the m/z 789.7 precursor generates a full scan MS³ spectrum, which is shown in Figure 3b along with proposed origins of the observed product ions.

Structural Determination of Ginsenosides Using MSⁿ Analysis

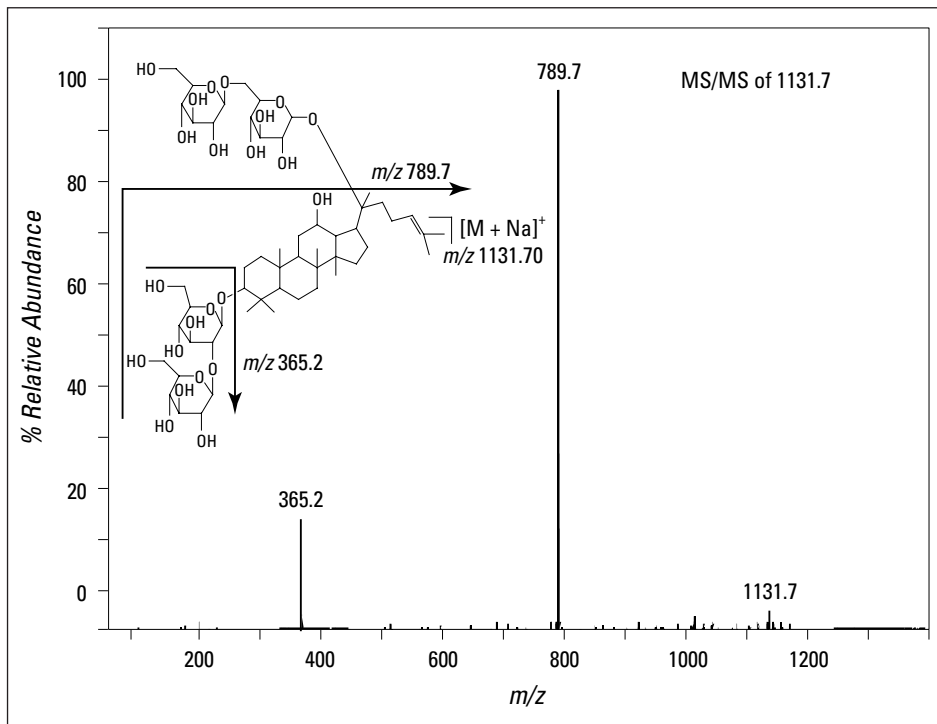


Figure 1b. Product ion spectrum generated from infusion of ginsenoside Rb1 standard by MS/MS analysis of m/z 1131.7 ($[M+Na]^+$).

ANALYSIS METHOD:

Direct infusion
Flow rate: 5 mL/min

MS Conditions

| | |
|-------------------------|----------|
| Source: | ESI |
| Drying gas flow: | 6 l/min |
| Nebulizer: | 10 psig |
| Drying gas temperature: | 300°C |
| Skim 1: | 25.0 V |
| Cap exit offset: | 50.0 V |
| Averages: | 5 V |
| ICC: | On |
| Max accu time: | 200 ms |
| Target: | 40000 |
| Ion mode: | Positive |

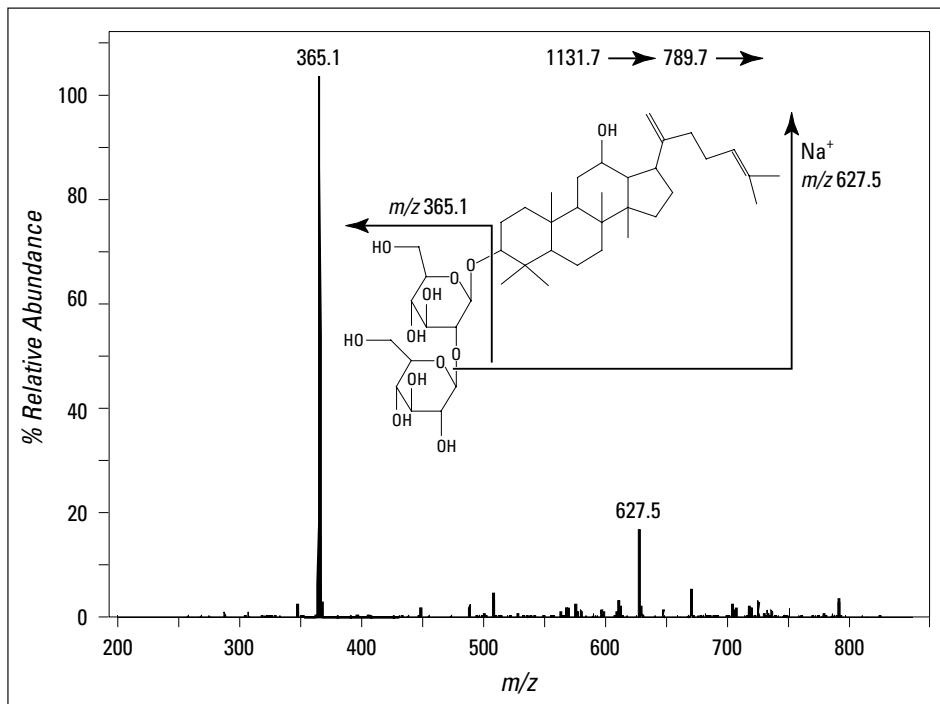


Figure 1c. Product ion spectrum generated from infusion of ginsenoside Rb1 standard by MS³ analysis of m/z 789.7 (from m/z 1131.7).

ANALYSIS METHOD:

Direct infusion
Flow rate: 5 mL/min

MS Conditions

| | |
|-------------------------|----------|
| Source: | ESI |
| Drying gas flow: | 6 l/min |
| Nebulizer: | 10 psig |
| Drying gas temperature: | 300°C |
| Skim 1: | 25.0 V |
| Cap exit offset: | 50.0 V |
| Averages: | 5 V |
| ICC: | On |
| Max accu time: | 200 ms |
| Target: | 40000 |
| Ion mode: | Positive |

Structural Determination of Ginsenosides Using MSⁿ Analysis

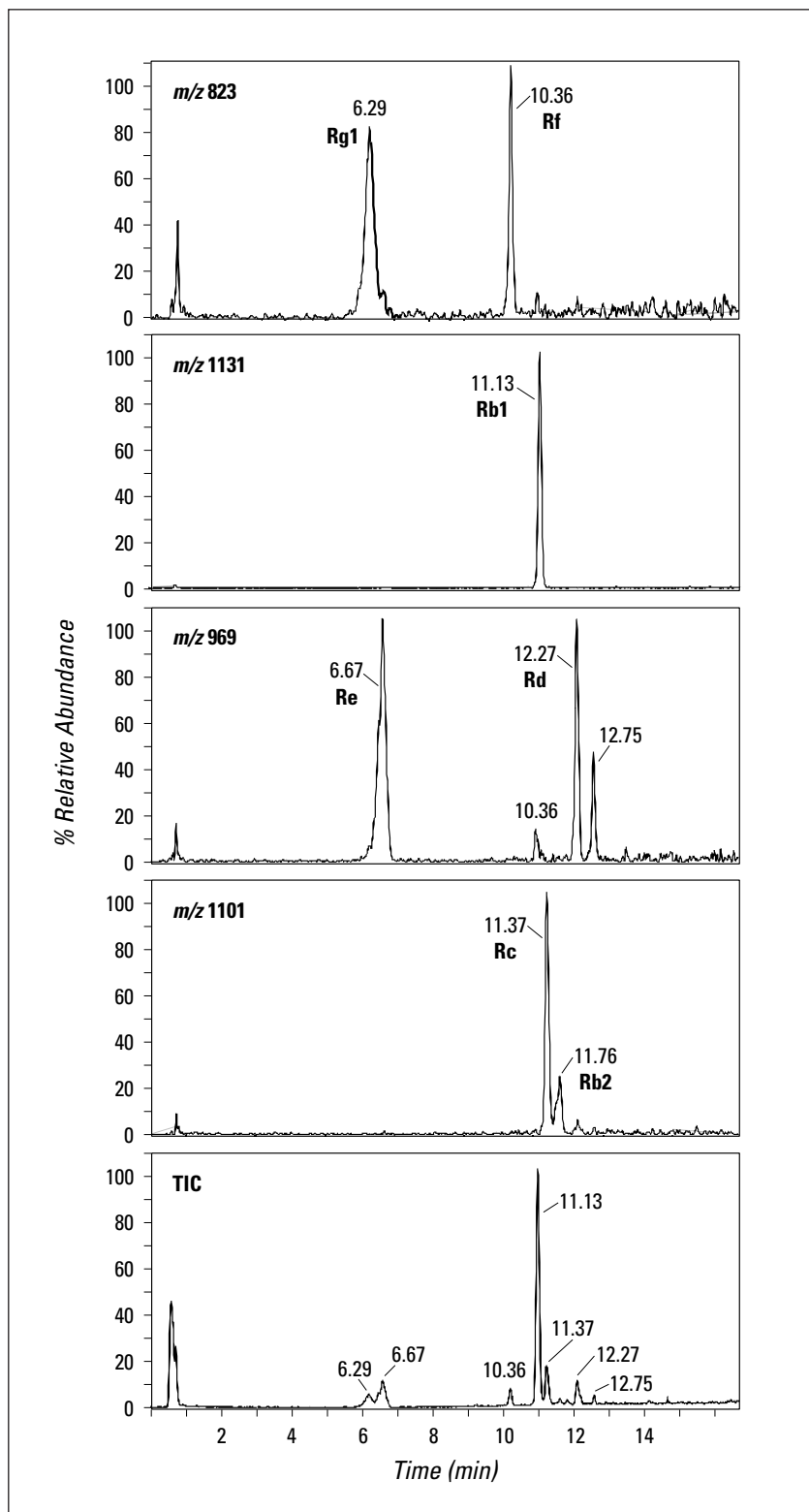


Figure 2. Total ion chromatogram (TIC) and extracted ginsenoside pseudomolecular ion chromatograms generated from LC/MSⁿ analysis of ginseng root extract.

Structural Determination of Ginsenosides Using MSⁿ Analysis

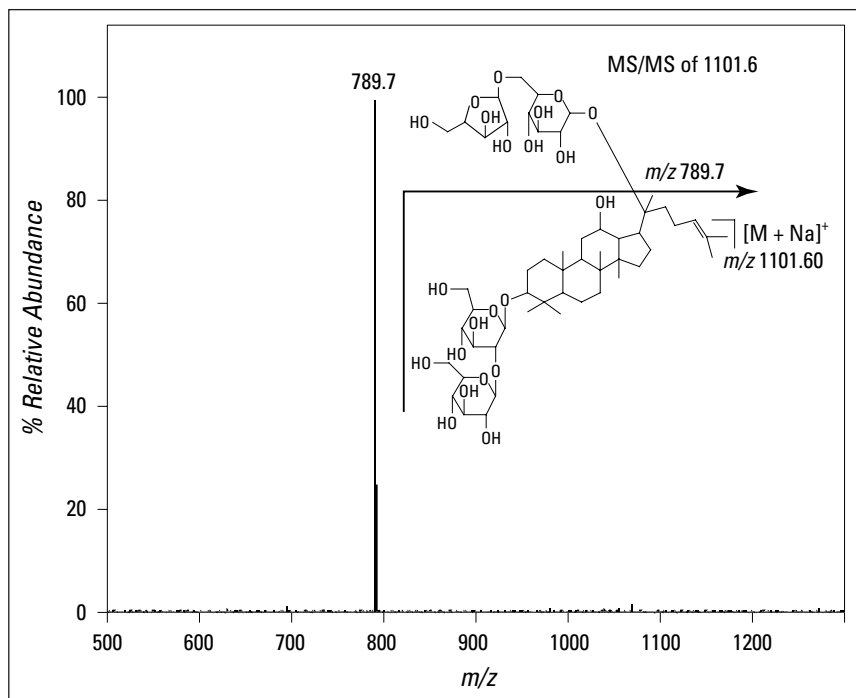


Figure 3a. Product ion spectrum generated from ginseng root extract by LC/MSⁿ analysis of m/z 1101.6 ($[M+Na]^+$).

ANALYSIS METHOD:

Chromatographic Conditions

Column: 2 × 50 mm Zorbax[®] SB-C18,
3.5 μm (p/n 863954-302)

Mobile phase: A = 0.01% acetic acid
in water;
B = acetonitrile

Gradient: start with 20% B
at 1 min 20% B
at 11 min 95% B

Flow rate: 0.3 ml/min
Injection volume: 10 μl

MS Conditions

Source: ESI
Drying gas flow: 7 l/min
Nebulizer: 30 psig
Drying gas
temperature: 300°C
Skim 1: 25.0 V
Cap exit offset: 50.0 V
Averages: 5 V
ICC: On
Max accu time: 200 ms
Target: 40000
Ion mode: Positive

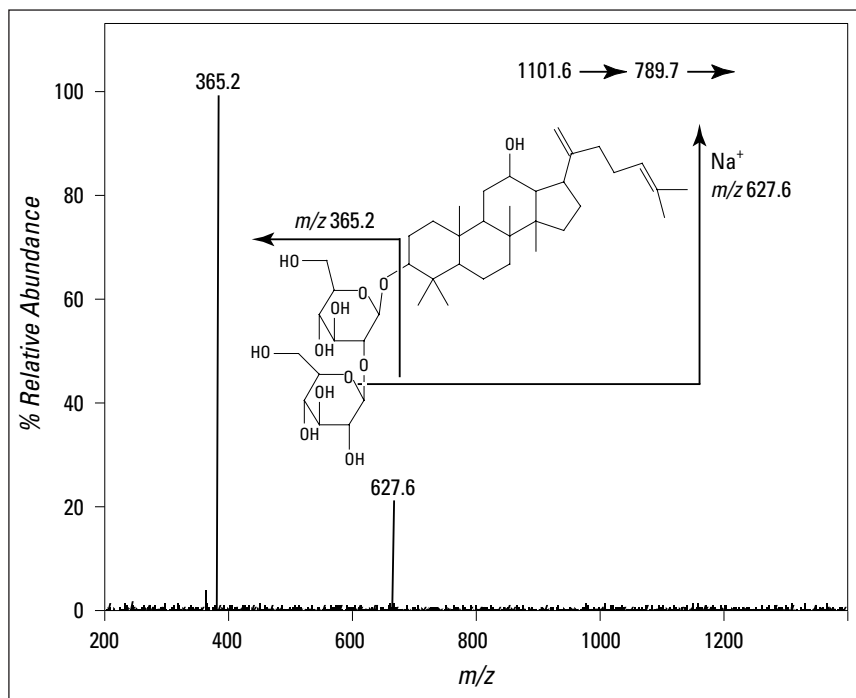


Figure 3b. Product ion spectrum generated from ginseng root extract by LC/MSⁿ analysis of m/z 789.7 (from m/z 1101.6).

ANALYSIS METHOD:

Chromatographic Conditions

Column: 2 × 50 mm Zorbax[®] SB-C18,
3.5 μm (p/n 863954-302)

Mobile phase: A = 0.01% acetic acid
in water;
B = acetonitrile

Gradient: start with 20% B
at 1 min 20% B
at 11 min 95% B

Flow rate: 0.3 ml/min
Injection volume: 10 μl

MS Conditions

Source: ESI
Drying gas flow: 7 l/min
Nebulizer: 30 psig
Drying gas
temperature: 300°C
Skim 1: 25.0 V
Cap exit offset: 50.0 V
Averages: 5 V
ICC: On
Max accu time: 200 ms
Target: 40000
Ion mode: Positive



Structural Determination of Ginsenosides Using MSⁿ Analysis

Conclusions

MSⁿ analysis using an ion trap mass spectrometer specifically selects the desired precursor ion and dissociates it to produce a specific fragmentation pattern in individual stages. As a result, it is a powerful analytical tool for deducing molecular structure. Electrospray ionization provides a soft ionization technique for generating predominantly intact molecular or pseudomolecular ions with little or no structurally relevant fragment ions in the mass spectra. MS/MS fragmentation in an ion trap mass spectrometer is useful because the product ions generated are derived only from the original molecular ion and are not the result of any additional fragmentation, as can be the case with collision induced dissociation (CID) in a collision cell. Additional MS stages tend to show stepwise fragmentations in which all or most of the ion current is localized in a single product ion, greatly facilitating interpretation of the spectra.

References

1. Kim Y. C., Kim S. R., Markelonis G. J., Oh T. H., *J. Neurosci. Res.* **53**, 1998, 426–32.
2. Kim H. S., Hong Y. T., Jang C. G., *J. Pharm. Pharmacol.* **50**, 1998, 555–60.
3. Yokozawa T.; Liu Z. W.; Dong E., *Nephron.* **78**, 1998, 201–6.
4. Smolinske S. C., *J. Am. Med. Womens Assoc.* **54**, 1999, 191–2.
5. Wang X., Sakuma, T., Asafu-Adjaye, E., Shiu, G.K., *Anal. Chem.* **71**, 1999, 1579–84.

Author

Linda L. Lopez is an applications chemist at Agilent Technologies in Palo Alto, CA.

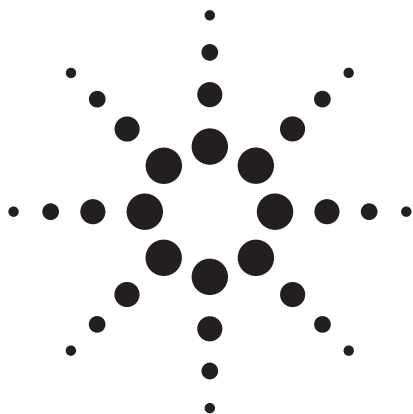
Agilent Technologies shall not be liable for errors contained herein or for incidental or consequential damages in connection with the furnishing, performance or use of this material.

Information, descriptions and specifications in this publication are subject to change without notice.

Copyright © 2000
Agilent Technologies
All rights reserved.

Reproduction and adaptation is prohibited.

Printed in the U.S.A. January 2000
(23) 5968-8869E



Simultaneous dual capillary column headspace GC with flame ionization confirmation and quantification according to USP <467>

Application Note

Joseph M. Levy
Michael Kraft



Abstract

The Application Note describes the implications for laboratories of the latest revision of the United States Pharmacopoeia (USP) residual solvents analysis method that will take effect on July 1, 2008. Laboratories will eventually face the task of performing confirmation analysis with their gas chromatography (GC) systems for the various target compounds. In this note a GC method based on headspace sampling is presented, which meets the requirements of the latest USP revision and provides the high precision and sensitivity necessary for quantitative confirmation analysis of residual solvents in pharmaceutical products. The method uses an Agilent 7890A GC system with the following components:

- Agilent headspace sampler (G1888)
- Dual matched capillary columns (DB-WAX and DB-624) of different polarities in a single split/splitless inlet
- Dual flame ionization detector

Agilent Equipment

- 7890A GC system
- G1888 headspace sampler

Application Area

- Pharmaceutical quality control
- Pharmaceutical development
- Residual solvents analysis



Agilent Technologies

Introduction

In 1988, the United States Pharmacopoeia (USP) provided control limits and testing criteria for several organic volatile impurities (OVIs) under the official General Chapter <467>. The compounds were chosen based on relative toxicity and only applied to drug substances and some excipients. In an effort to harmonize with the International Conference for Harmonization (ICH), the USP has proposed the adoption of a slightly modified version of Quality-3C (Q3C) methodology, which has been scheduled for implementation on July 1, 2008. The methodology provides an approach to residual solvent analysis that considers a patient's exposure to a solvent residue in the drug product. Solvents have been classified based on their potential health risks into three main classes:

- Class 1: Solvents should not be used because of the unacceptable toxicities or deleterious environmental effects.
- Class 2: Solvents should be limited because of inherent toxicities.
- Class 3: Solvents that may be regarded as less toxic and of lower risk to human health.

Testing is only required for those solvents used in the manufacturing or purification process of drug substances, excipients, or products.

The new <467> General Chapter provides an optional method to determine when residual solvent testing is required for Class 2 solvents. Each Class 2 solvent is assigned a permitted daily exposure (PDE) limit, which is the

pharmaceutically acceptable intake level of a residual solvent. When the solvent level in drug substances, excipients, and drug product are below the PDE limit for a given solvent, testing is not required when the daily dose is less than 10 grams. When the level of solvent is expected to be above the PDE limit, testing would be required to determine whether the solvent was removed during the formulation process.

The USP has provided a method for the identification, control, and quantification of Class 1 and 2 residual solvents for either water soluble or insoluble compounds. The method calls for a gas chromatographic analysis with flame ionization detection (FID) and headspace sampling from either water or organic diluents. The monograph has suggested two procedures: Procedure A G43 (DB-624) phase and Procedure B G16 (DB-WAX) phase. Procedure A is used first. If a compound is determined to be above the specified concentration limit, then Procedure B should be used to confirm its identity. Since there are known co-elutions on both phases, the orthogonal selectivity ensures that co-elutions on one phase will be resolved on the

other. Neither procedure is quantitative, so to determine the concentration the monograph specifies Procedure C, which utilizes whichever phase will give the fewest co-elutions.

In this study all of the three procedures were combined. This was achieved by the use of simultaneous dual capillary column GC. Instead of injecting onto two independent capillary columns of differing polarities, which is required for component confirmation, a single injection was made by headspace sample introduction onto two columns simultaneously. Each column was connected to its own FID. This simultaneous GC injection can be accomplished in several ways:

- Splitter (analogous to a glass tee or a capillary flow splitter)
- Press-fit connector (where the capillary column is seated by pressing into a y-shaped glass connector).
- Two-holed ferrule with a single two-holed column nut (this is the approach highlighted in this application note).

Experimental

A two-holed ferrule (figure 1) and a single two-holed column nut

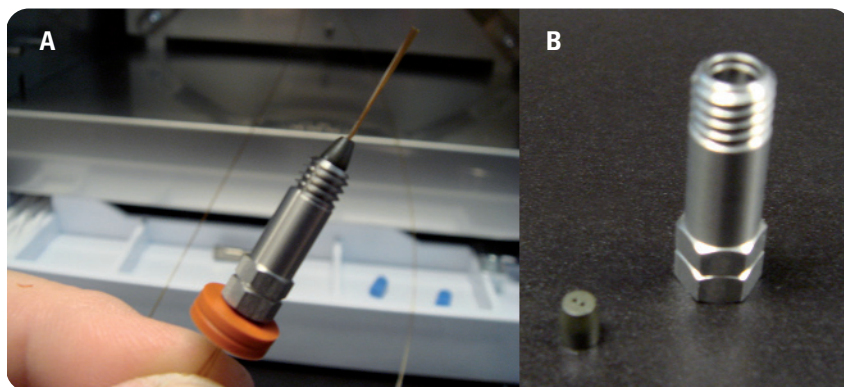


Figure 1
Two-holed ferrule/column nut for the installation of simultaneous dual capillary column into a single inlet with two FIDs.

were used for both capillary columns, resulting in just as many connections as there are when using a single capillary column. The traditional approaches that utilize splitters and press-fit connectors are plagued with multiple connections and therefore multiple leak possibilities. There is also the ability to use the new multidimensional capillary flow device technology (such as Deans switching) that can be configured into an Agilent 7890A GC. However, the 7890A GC used for this study was not configured with that capability. Using the two-holed ferrule approach was very convenient because it did not require the purchase of any extensive parts. Any split/splitless inlet in a 7890A GC could be easily adapted to this approach. The only requirement to ensure proper precision and quantification for simultaneous two-holed dual column GC is to use two matched columns (each with identical lengths and internal diameters). After careful installation of both columns into the single inlet, each capillary column was connected to two identical flame ionization detectors. The signals from both detectors were simultaneously acquired using Agilent ChemStation software (version B.03.01). Table 1 lists the optimized GC and headspace operational variables.

Figure 2 represents a schematic block diagram of the 7890A and headspace configuration for the experiments. Standard solutions (appropriate standards were purchased from Sigma-Aldrich) were all prepared quantitatively in dimethyl sulfoxide (DMSO). Multilevel standards were prepared in 100 mL volumetric flasks

| | GC inlet mode | Split |
|--|---------------------------|---|
| 7890A GC | GC inlet mode | Split |
| | Inlet temperature | 175 °C |
| | Inlet pressure | 30.0 psi |
| | Split ratio | 15:1 |
| | Split flow | 154.78 mL/min |
| | Carrier gas | Helium |
| | Column 1 carrier flow | 10.3 mL/min |
| | Column 2 carrier flow | 9.92 mL/min |
| | Initial oven temperature | 35.0 °C |
| | Initial time | 20.0 min |
| | Temperature ramp rate | 30.0 °C/min |
| | Final temperature | 240 °C |
| | Final hold time | 0.500 min |
| | Column mode | Constant flow |
| | FID temperature | 250 °C |
| | FID hydrogen air flow | 40.0 mL/min |
| | FID air flow | 400 mL/min |
| FID air flow constant column + makeup | Σ of 30.0 mL/min | |
| Total run time | 27.3 min | |
| Headspace sampler | Loop size | 1.00 mL |
| | Vial pressure | 15.4 psi |
| | Headspace oven | 85.0 °C |
| | Loop temperature | 100 °C |
| | Transfer line temperature | 150 °C |
| | Equilibration time | 30.0 min (high shake) |
| | GC cycle time | 39.0 min |
| | Pressurization | 0.200 min |
| | Vent (loop fill) | 0.100 min |
| | Loop equilibration time | 0.0500 min |
| | Inject time | 1.00 min |
| | GC columns | Column 1: DB-WAX, 30 m, 0.32 mm ID, 0.25 μm (1237032) |
| Column 2: DB-624, 30 m, 0.32 mm ID, 1.80 μm (123-1334) | | (Back FID) |
| | | |

Table 1
Optimized GC and headspace operational variables.

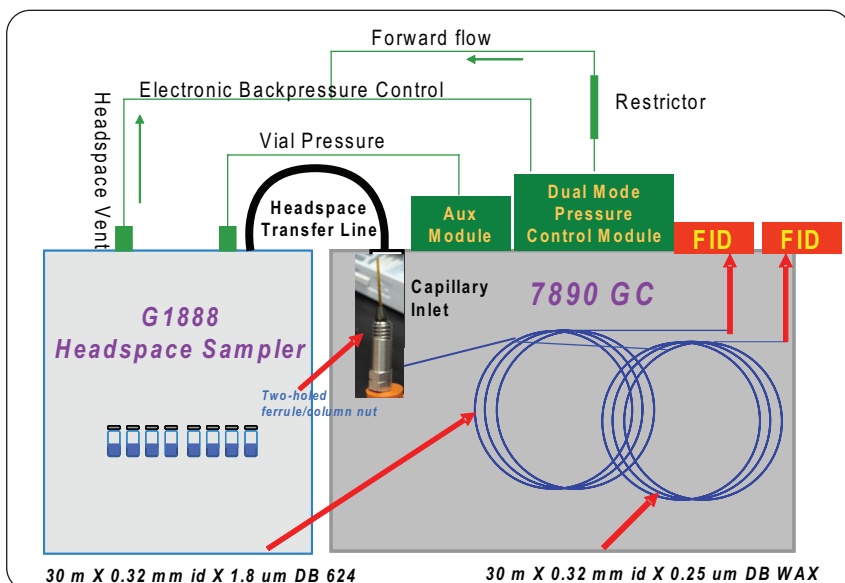


Figure 2
Instrument schematic.

using organic-free water. These aqueous dilutions were then transferred with electronic pipettes as 1 mL and 5 mL aliquots into 10 mL and 20 mL screw-cap headspace vials. The screw caps included Teflon-faced septa. All of the standard solutions were analyzed as multiple replicates using the following sequence of sample types:

- DMSO blank
- Water blank
- Calibration standard mixes (between 3 to 12 replicates)
- Blanks were prepared with 1 mL of the water or DMSO diluents, respectively.

Results and discussion

Table 2 lists the elution patterns for the various targets on the highly polar DB-WAX column and the intermediately polar DB-624 column.

Figures 3 and 4 show representative chromatograms for the various calibration standard analyses that were obtained. These results represent culminations of several experiments where both the HS and GC parameters were optimized.

| Retention time (minutes) | Signal | Target analyte |
|--------------------------|--------|---|
| 0.605 | 1 | Hexane |
| 0.693 | 1 | Cyclohexane |
| 0.699 | 1 | 1,1-dichloroethane |
| 0.758 | 1 | Methyl cyclohexane |
| 0.935 | 2 | Methanol |
| 0.939 | 2 | Hexane |
| 0.978 | 1 | trans 1, 2 dichloroethene/Tetrahydrofuran* |
| 1.062 | 1 | 1,1,1-trichloroethane/carbon tetrachloride* |
| 1.156 | 1 | Methanol |
| 1.278 | 1 | 1,2-dimethoxyethane |
| 1.311 | 1 | Methylene chloride |
| 1.364 | 1 | Benzene |
| 1.501 | 2 | 1,1-dichloroethane |
| 1.734 | 2 | Acetonitrile |
| 1.788 | 1 | cis 1,2-dichloroethene |
| 1.803 | 1 | Trichloroethylene |
| 1.852 | 2 | Methylene chloride |
| 1.874 | 1 | Acetonitrile |
| 2.074 | 2 | trans 1,2-dichloroethene |
| 2.139 | 1 | Chloroform |
| 2.316 | 1 | Toluene |
| 2.339 | 2 | Nitromethane |
| 2.653 | 1 | 1,4-dioxane |
| 2.817 | 1 | 1,2-dichloroethane |
| 3.046 | 1 | 2-hexanone |
| 3.069 | 2 | Chloroform |
| 3.124 | 2 | cis 1,2-dichloroethene |
| 3.487 | 2 | Tetrahydrofuran |
| 3.601 | 2 | 1,2-dimethoxyethane |
| 3.821 | 2 | 1,1,1-trichloroethane |
| 3.871 | 2 | Cyclohexane |
| 4.031 | 1 | Ethyl benzene |
| 4.072 | 2 | Carbontetrachloride |
| 4.227 | 1 | p-xylene |
| 4.454 | 1 | m-xylene |
| 4.455 | 2 | Benzene/1,2-dichloroethane** |
| 4.611 | 2 | Trichloroethylene |
| 4.994 | 1 | Nitromethane |
| 5.870 | 1 | o-xylene |
| 5.918 | 2 | Pyridine |
| 5.966 | 1 | Pyridine |
| 6.343 | 2 | Methyl cyclohexane |
| 7.070 | 2 | 1,4-dioxane |
| 7.272 | 1 | Chlorobenzene |
| 10.193 | 2 | 2-hexanone |
| 10.803 | 2 | Toluene |
| 16.530 | 1 | DMF |
| 16.611 | 2 | Tetralin |
| 20.699 | 2 | DMF |
| 21.044 | 2 | Chlorobenzene |
| 21.541 | 2 | Ethyl benzene |
| 21.810 | 2 | m-xylene/p-xylene** |
| 21.874 | 1 | DMA |
| 22.363 | 2 | o-xylene |
| 22.924 | 1 | Tetralin |
| 22.939 | 2 | DMA |
| 23.266 | 2 | DMSO |
| 23.638 | 1 | DMSO |

Table 2
Dual column headspace-GC/FID target analyte elution order (signal 1: FID1, DB-WAX; signal 2: FID2, DB-624).

*coelute on the DB-WAX column only **coelute on the DB-624 column only

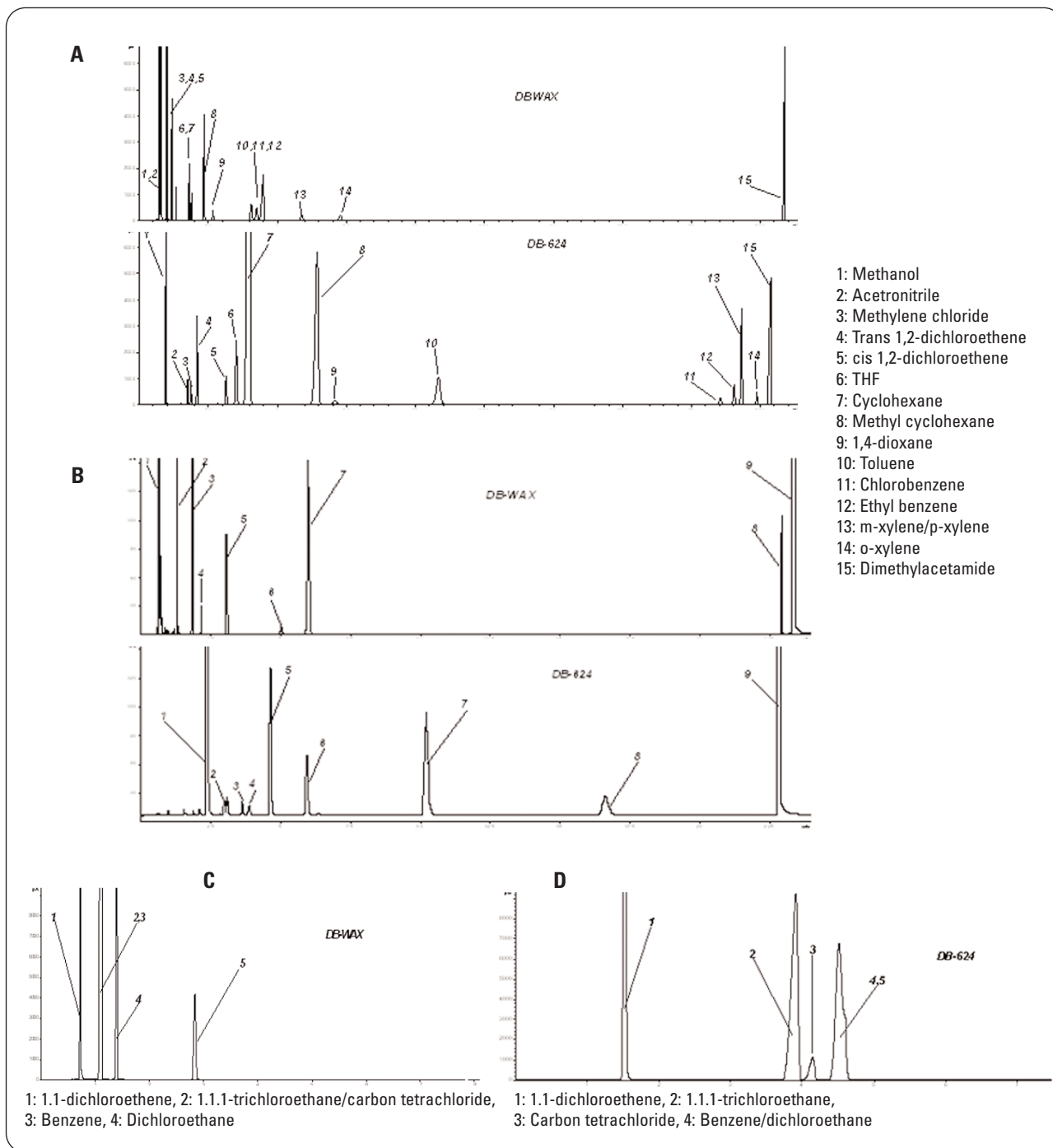


Figure 3
 Selected dual column headspace-GC/FID calibration standard analysis.
 A) Dual Column Headspace GC/FID, Matched columns (30 M x 0.32 mm ID), Target Mix 1
 B) Dual Column Headspace GC/FID, Matched Columns (30 M x 0.32 mm ID), Target Mix 2
 C) Dual Column Headspace GC/FID, DB-WAX (30 M x 0.32 mm ID, 0.25 μ m), Target Mix 3
 D) Dual Column Headspace GC/FID, DB-WAX (30 M x 0.32 mm ID, 1.8 μ m), Target Mix 3.1

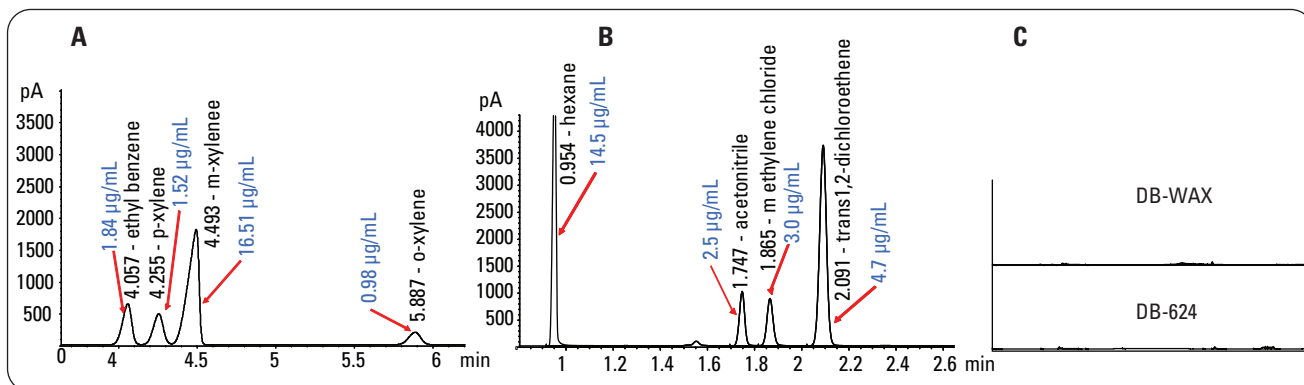


Figure 4
Representative low level standard calibrations and headspace-GC system blank (using 1 mL of diluent water in a 10 mL headspace vial).
A) Dual Column Headspace GC/FID, DB-WAX (30 M x 0.32 mm ID, 0.25 µm), Zoomed in snapshot at low concentration levels
B) Dual Column Headspace GC/FID, DB-624 (30 M x 0.32 mm ID, 1.8 µm), Zoomed in snapshot at low concentration levels
C) Dual Column Headspace GC/FID, Water Blank, Zoomed in snapshot

Table 3 summarizes the compositions of the various standard mixtures. These mixtures were all custom made.

Several method modifications were made to ensure the required sensitivities and precision of the respective target analytes, while at the same time trying to minimize total analysis times without compromising peak separations. Headspace sampling precision, sensitivity and turnaround were all improved by the following:

- Setting the vial-shake setting to “high”
- Pressurizing the headspace vials to 15 psi
- Pressurizing the headspace sampling loop to 9 psi (with back pressure regulation)
- Setting the carrier gas pressure to 35 psi
- Setting the headspace venting time (which essentially fills the sample loop) to 0.1 minutes or less

With the evolution of the electronic pneumatics to the newest generation in the 7890A GC, the gas

| Target mix 1 | DB-624 | DB-WAX |
|--------------|--------------------------|--|
| | Methanol | Cyclohexane |
| | Acetonitrile | Methyl cyclohexane |
| | Methylene chloride | trans 1,2-dichloroethene/Tetrahydrofuran |
| | trans 1,2-dichloroethene | Methanol |
| | cis 1,2-dichloroethene | Methylene chloride |
| | Tetrahydrofuran | cis 1,2-dichloroethene |
| | Cyclohexane | Acetonitrile |
| | Methyl cyclohexane | Toluene |
| | 1,4--dioxane | 1,4-diosane |
| | Toluene | Ethyl benzene |
| | Chlorobenzene | p-xylene |
| | Ethyl benzene | m-xylene |
| | m-xylene/p-xylene | o-xylene |
| | o-xylene | Chlorobenzene |
| | DMA | DMA |
| Target mix 2 | DB-624 | DB-WAX |
| | Hexane | Hexane |
| | Nitromethane | 1,2-dimethoxyethane |
| | Chloroform | Trichloroethylene |
| | 1,2-dimethoxyethane | Chloroform |
| | Trichloroethylene | 2-hexanone |
| | Pyridine | Nitromethane |
| | 2-hexanone | Pyridine |
| | Tetralin | Tetralin |
| | DMSO | DMSO |
| Target mix 3 | DB-624 | DB-WAX |
| | 1,1-dichloroethene | 1,1-dichloroethene |
| | 1,1,1-trichloroethane | 1,1,1-trichloroethane/carbon tetrachloride |
| | Carbon tetrachloride | Benzene |
| | Benzene | 1,2-dichloroethane |

Table 3
Composition and elution orders of target analyte standards.

sampling loop in the headspace sampler can now be controlled to 0.001 psi. It can also be efficiently pressurized throughout the duration of the timed headspace events cycle with back pressure control. The elevation of the column pressures for the GC runs allowed column flows near 10 mL/min for both of the 0.32 mm id columns and not only enhanced precision and sensitivity but also the resolution of the peaks. In short, the capillary columns functioned better at elevated flow (pressure). Elevating the column flows too high could result in loss of separation.

This is why it would even be more beneficial to reduce column diameters further to 0.18 mm. Column pressure can be increased even more with lower flows that would help maintain the same linear velocities. The resulting narrow peaks in this study (peak widths as small as 0.001 seconds) provided improved separations which worked well with the control of column pressures with the 7890A GC. Table 4 lists the reproducibility of the various selected targets for the dual GC column separations.

In term of instrumentation, the results were also significantly impacted by the following capillary inlet parts:

- Inlet liner, low pressure drop (Agilent part number 5183-4647)
- New polished gold-plated inlet seal (Agilent part number 5788-5367)

To maintain excellent precision and peak shapes, these inlet parts needed to be replaced on a regular basis and were to be treated as ultra-clean parts. Typically, the

| Target analyte | ICH class | Excipient limit concentration (µg/mL) | Retention time repeatability (%RSD) | Area repeatability (%RSD) | Excipient MDL# (ppm) |
|----------------------|-----------|---------------------------------------|-------------------------------------|---------------------------|----------------------|
| Benzene | 1 | 2 | 0.011 | 1.43 | 0.1 |
| 1,2-dichloroethane | 1 | 5 | 0.015 | 2.47 | 0.3 |
| 1,1-dichloroethene | 1 | 8 | 0.010 | 2.24 | 0.4 |
| Carbon tetrachloride | 1 | 5 | 0.010 | 2.11 | 0.4 |
| Methylene chloride | 2 | 600 | 0.010 | 2.15 | 40.1 |
| Hexane | 2 | 290 | 0.014 | 3.18 | 12.9 |
| Cyclohexane | 2 | 3880 | 0.040 | 2.59 | 46.1 |
| Trichloroethylene | 2 | 80 | 0.010 | 1.49 | 2.1 |
| Toluene | 2 | 890 | 0.015 | 2.02 | 11.8 |
| Ethylbenzene | 2 | 369 | 0.004 | 2.11 | 20.2 |
| o-xylene | 2 | 195 | 0.001 | 1.33 | 7.1 |
| 1,4-dioxane | 2 | 80 | 0.010 | 1.7 | 9.6 |

Table 4
Retention time and peak area precision, and calculated method detection limits of representative target analytes for the dual column method (note that benzene and 1,2-dichloroethane are completely resolved by almost 1.5 minutes on the DB-WAX column – this is a dramatic improvement over the traditional co-elution on the DB-624 column for the low level detection of benzene and 1,2-dichloroethane).

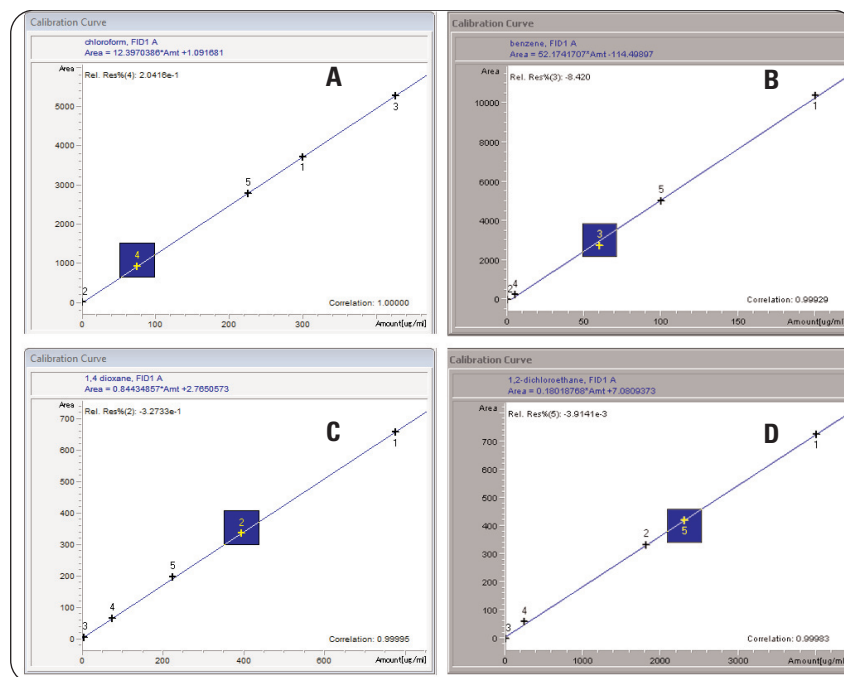


Figure 5
Calibration curves for some of the target analytes on the DB-WAX column.
A) Chloroform, Linearity: 1.0000
B) Benzene, Linearity: 0.99929
C) 1,4-Dioxane, Linearity: 1.0000
D) 1,2-Dichloroethane, Linearity: 0.99983

two-holed column nuts (Agilent part number 05921-21170) were used to coincide with the short style graphite/vespel two-holed ferrules (0.5 mm for 0.32 mm ID columns, Agilent order number 5062-3581; 0.4 mm for 0.25 mm ID and smaller, Agilent order number 5062-3580). Five dilutions of standard solutions were prepared ranging from one tenth to two times the limit concentration to determine the linearity of the calibration curves. These linearity plots of the calibration curves are shown in figures 5 and 6 for the DB-WAX and DB-624 capillary columns. The linearity results for methylene chloride, 1,2 dichloroethane, 1,4-dioxane, chloroform and trichloroethylene are shown for these target analytes for each of the columns.

Conclusion

Using the on-line combination of a sample preparation device (Agilent headspace sampler) and the most advanced GC in the world (Agilent 7890A), a viable, precise and quantitative method was developed for the revised USP <467> regulations for residual solvents with the following benefits:

- Simultaneous dual capillary column confirmation of targets using DB-WAX and DB-624 columns with dual flame ionization detection.
- Optimized GC and headspace sampler operational variables.
- Direct dual column inlet connection without any instrumental modifications.

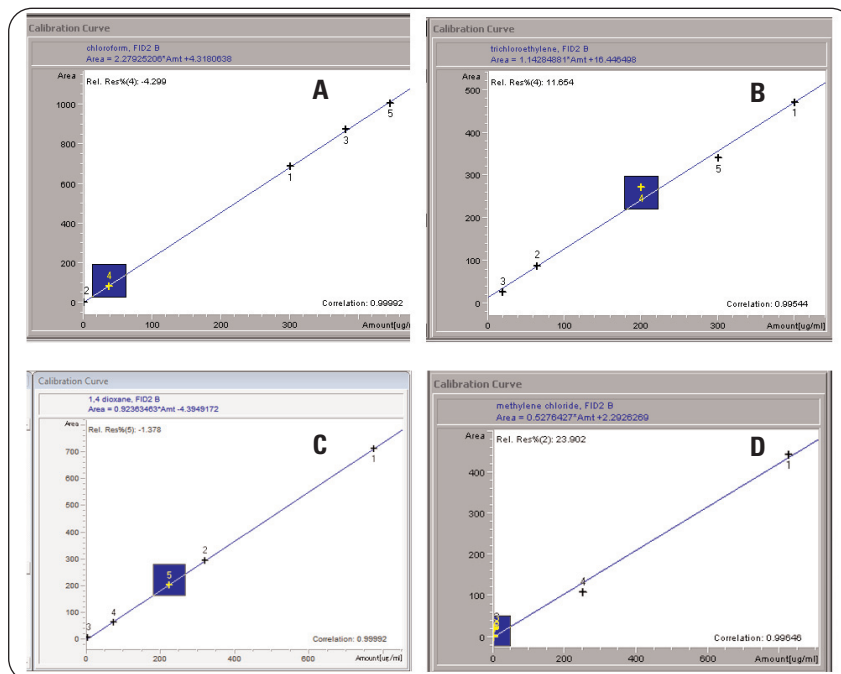


Figure 6
DB-624 calibration curves for selected target analytes on the DB-624 column.
A) Chloroform, Linearity: 0.99992
B) Trichloroethylene, Linearity: 0.99544
C) 1,4-Dioxane, Linearity: 1.0000
D) Methylene Chloride, Linearity: 0.99646

- Use of electronic pneumatic control to enhance the operational characteristics of the headspace sampler (G1888) and the GC 7890A.
- High precision and sensitivity coupled with an automated headspace sampler and a GC cycle time in less than one hour per sample.

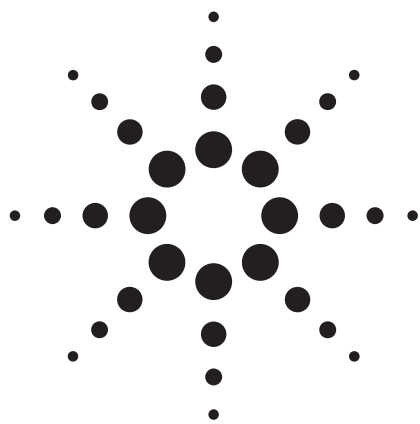
*Joseph M. Levy is a freelance application chemist.
Michael Kraft is Industry Marketing Manager for Pharma/Biopharma Solutions and Process Development & Manufacturing QA/QC.*

www.agilent.com/chem/pharmaqaqc

© 2008 Agilent Technologies Inc.

Published April 1, 2008
Publication Number 5989-8085EN





Fast Analysis of USP 467 Residual Solvents using the Agilent 7890A GC and Low Thermal Mass (LTM) System

Application Note

Pharmaceutical

Author

Roger L Firor
Agilent Technologies, Inc.
2850 Centerville Road
Wilmington, DE 19808
USA

Abstract

A dual column residual solvent analysis according to USP 467 (2008-09 revision) was performed using the Low Thermal Mass (LTM) system installed on an Agilent 7890A GC system. The G1888 Automated Headspace sampler connected to the volatiles interface was used for sample introduction. A Capillary Flow Technology (CFT) two way splitter was used to split the sample equally to a 5 inch 7 M x 0.25 mm x 1.4 μm Agilent J&W DB-624 column and a 5 inch 7 M x 0.25 mm x 0.25 μm Agilent J&W HP-INNOWax column. Each column module was connected to its own FID by retention gaps. Aqueous solutions of Class 1, Class 2A, and Class 2B solvents were analyzed. Sensitivity, linearity, and resolution met the requirements of USP 467. Overall cycle times for the analysis of all specified Class 1 and Class 2A and 2B solvents were reduced to 10 min.



Agilent Technologies

Introduction

Residual solvents in pharmaceuticals may remain from the manufacturing process of the active pharmaceutical ingredients (API) or final product. The level of residual solvents are monitored and controlled for a number of reasons that include safety, effect on crystalline form, solubility, bioavailability, and stability. All drug substances, excipients, and products are included under USP 467.

The LTM (Low Thermal Mass) chromatographic system is combined with static headspace sampling for the analysis of residual solvents in pharmaceuticals according to USP 467 revised general chapter 2008. [1] This chapter follows guidelines set by the International Conference for Harmonization (ICH) Q3C. [2] Residual solvents are divided into three classes based on possible toxicity. Class 1 solvents are considered the most toxic and should be avoided in manufacture. These solvents may also pose an environmental risk. Class 2 solvents (2A, 2B, and 2C) are less toxic with limited use. Class 2C solvents have higher boiling points and some of them require analysis by non-headspace methods. Class 3 are least toxic and should be used as solvents where practical. Headspace GC is used for determination of Class 1 and Class 2 solvents, while most Class 3 solvents are analyzed by a nonspecific method such as loss on drying. Each Class 2 solvent has a "permitted daily exposure" (PDE) limit. If a given solvent tests below the PDE limit then further testing is not required (daily dose below 10 grams). Option 2 of the general chapter, which looks at the total solvent added for all components of the drug product, is used for daily amounts above 10 g.

This work follows the guidelines of the method with the exception of column dimensions and GC oven programs. Column dimensions and program rates were optimized to gain a significant reduction in analysis time and overall cycle time.

Alternate methodologies such as those described here can be used, however, validation and comparison to the original USP monograph may be required. The FDA also requires that any new ANDA provide the data necessary to prove control of residual solvents prior to a generic drug approval.

USP 467 specifies three procedures as follows for Class 1 and Class 2 residual solvents:

1. Procedure A: Identification and limit test
2. Procedure B: Confirmatory test
3. Procedure C: Quantitative test

Procedure A uses a G43 phase (Agilent J&W DB-624 column in this work) and Procedure B uses a G16 phase (Agilent J&W HP-INNOWax column in this work). In general a particular co-elution that occurs on one of these phases will not occur on the other.

Experimental

The water soluble procedures were used for standard sample preparation to demonstrate system performance. Insoluble articles require use of DMSO, DMF, or other suitable non-aqueous solvent. The methodology used is very similar for both solvent systems.

A diagram of the dual column system used is shown in Figure 1. The setup splits the effluent from the headspace equally to the J&W DB-624 and J&W HP-INNOWax columns for a simultaneous dual channel analysis. Previous work has been described using conventional oven heating and two-hole ferrules with the split/splitless inlet for dual column residual solvents. [3] Configuration and parameter settings for the LTM system are given in Table 1.

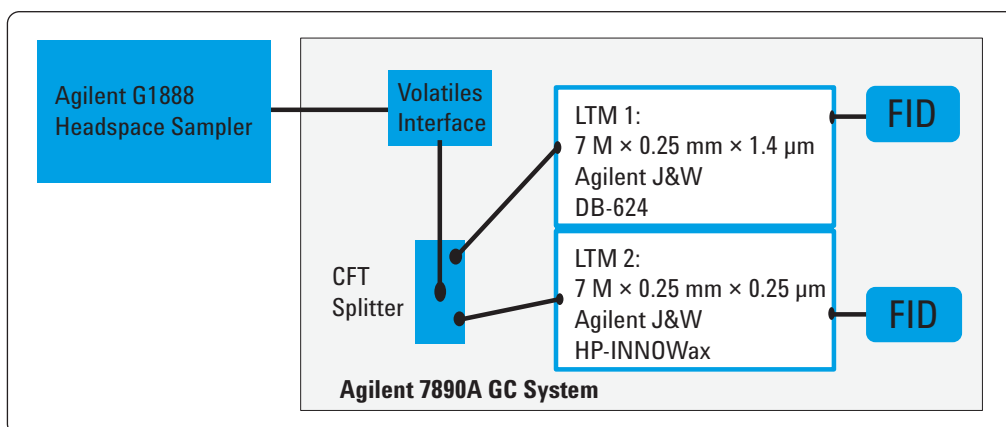


Figure 1. System diagram showing CFT splitter use in dual LTM column configuration.

Table 1. Residual Solvent System Parameters

| Standards | |
|-----------|---|
| Class 1: | p/n 5190-1566, equivalent to USP Mixture RS |
| Class 2A: | p/n 5190-0491, equivalent to USP Mixture A RS |
| Class 2B: | p/n 5190-0492, equivalent to USP Mixture B RS |

Software

| | |
|--------------|------------------|
| ChemStation: | B.04.02 |
| Headspace: | G2923AA, A.01.06 |
| LTM: | G6586AA |

7890A Configuration and Method Parameters

| | |
|---|---|
| Inlet: | Volatiles Interface, 120 °C |
| Pressure program: | 12 psig (4 min) to 22 psig (2 min) at 2.0 psi/min |
| Split ratio: | 14:1, He carrier |
| Detectors: | Dual FID |
| CFT: | Two-way splitter, G3181B |
| 7890A oven: | Isothermal at 220 °C |
| LTM Module 1: | 7 M × 0.25 mm × 1.4 µm J&W DB-624 |
| LTM Module 2: | 7 M × 0.25 mm × 0.25 µm J&W HP-INNOWax |
| Module connections to CFT splitter and FID's: | 0.5 M × 0.25 mm deactivated retention gap |
| LTM module programs: | See Table 3. |

G1888A Headspace Parameters

| | |
|--------------------------|---------------------------------|
| Oven: | 80 °C |
| Loop: | 90 °C |
| Transfer line: | 110 °C |
| Cycle time: | LTM program dependent |
| Vial Equilibration time: | 60 min |
| Pressurize time: | 0.15 min |
| Loop fill: | 0.15 min |
| Loop equilibration: | 0 min |
| Inject: | 0.50 min |
| Vials: | 10 mL, high shake |
| Vial pressure: | 16.0 psig for 7890A Aux channel |

Standard solutions of the Class 1, Class 2A, and Class 2B solvents were prepared in pure water according to the USP 467 procedures shown in Table 2. These stock solutions can be stored for 1 to 2 months at room temperature in a well sealed volumetric. Two grams of sodium sulfate was added to each headspace vial to assist with headspace extraction.

Table 2. Standard Preparation

Class 1 solvents

1. 1.0 mL stock solution vial plus 9 mL DMSO diluted to 100 mL
2. 1.0 mL from step 1 diluted to 100 mL with water
3. 10 mL from step 2 diluted to 100 mL with water
4. 1.0 mL step 3 and 5 mL water in 10 mL HS vial

Class 2A solvents

1. 1.0 mL stock solution vial, diluted to 100 mL
2. 1.0 mL from step 1 in 5 mL water in 10 mL HS vial

Class 2B solvents

1. 1.0 mL stock solution vial, diluted to 100 mL
2. 1.0 mL step 1 in 5 mL water in 10 mL HS vial

Headspace samples were also prepared for the Class 2A solvents at other concentrations ranging from about 10 times below USP limit values to 6 times above to demonstrate linearity. Results are shown in Figure 2. For example, according to USP Procedure A, the limit concentration (in prepared headspace vials) for 1,4 dioxane is 3.17 µg/mL. The concentrations used (µg/mL) for linearity were 0.190, 0.317, 1.90, 3.17, and 19.0 in water.

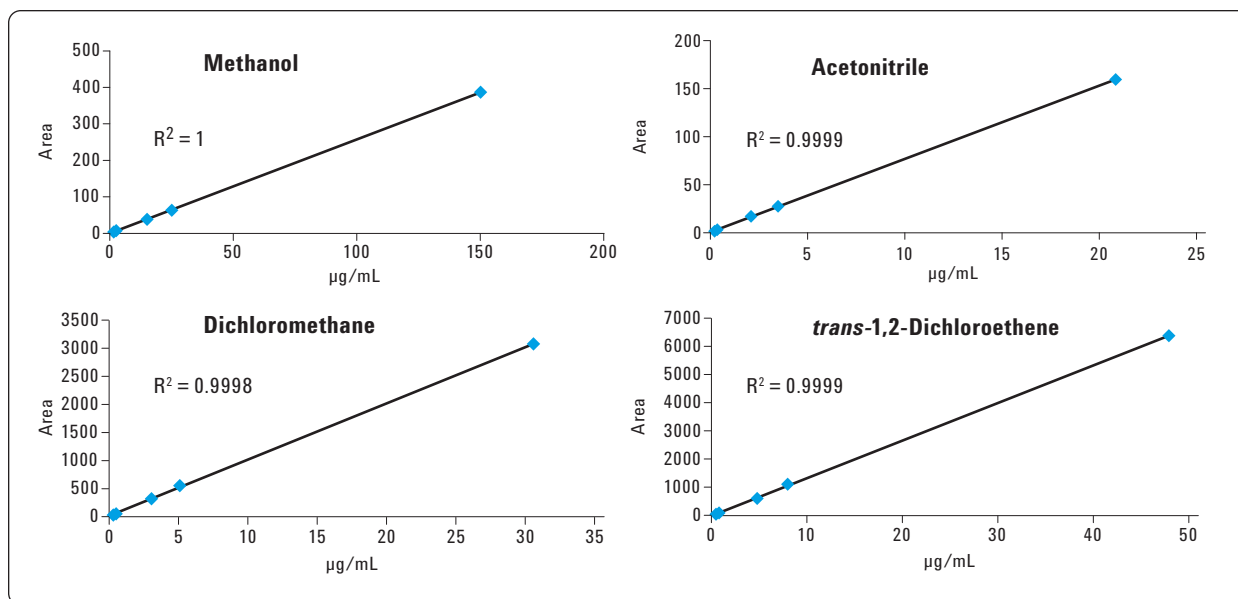


Figure 2. Calibration curves for Class 2A solvents from approximately 10 times below limit values to 6 times above. (Continued)

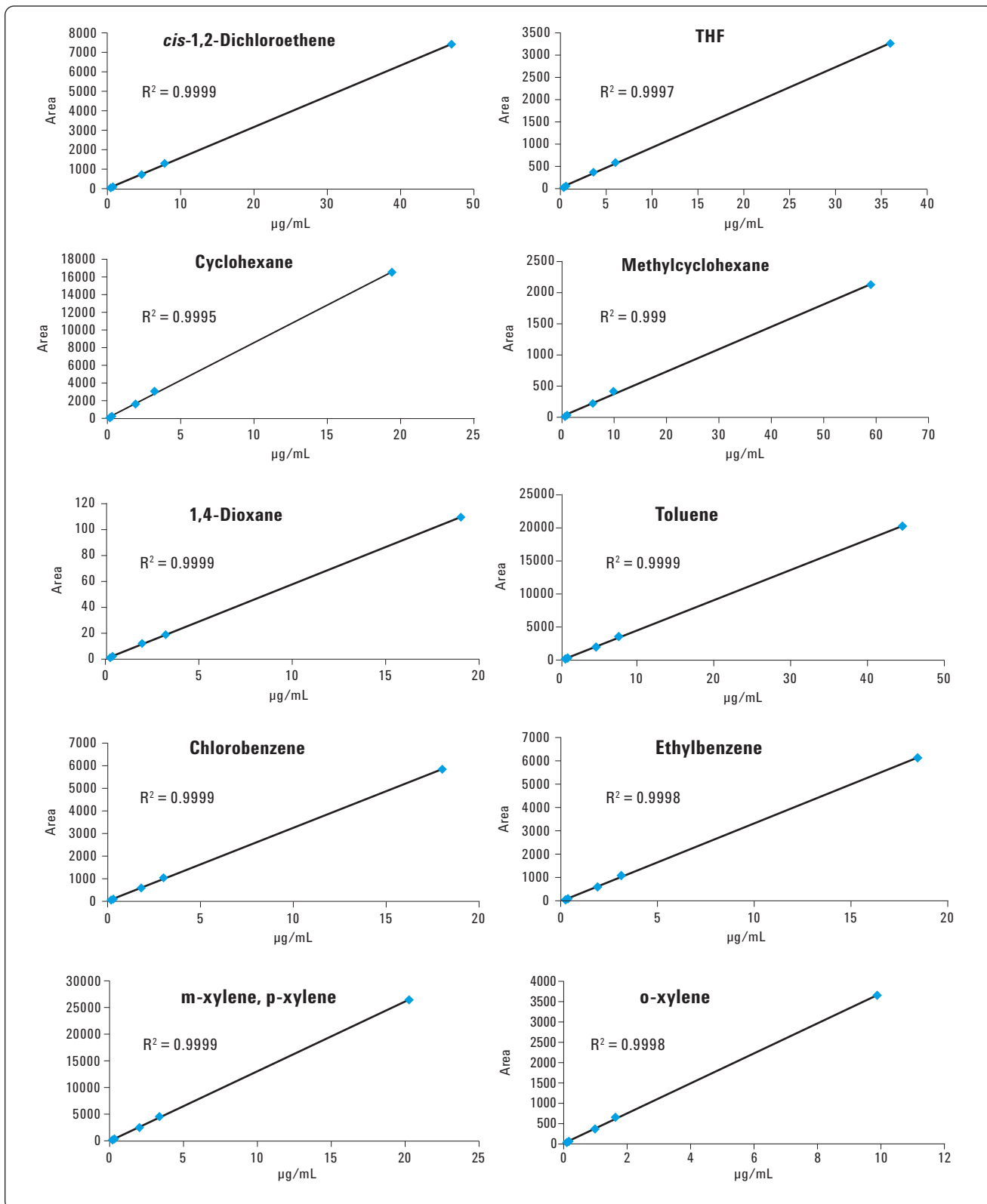


Figure 2. Calibration curves for Class 2A solvents from approximately 10X below limit values to 6X above.

Discussion

In temperature-programmed gas chromatography, which is required for residual solvent analysis, oven cool down time has a major impact on overall cycle time. LTM column modules cool down at considerably faster rates compared to air bath ovens due to their very low thermal mass and cooling fan configuration directly below the column assembly. LTM columns are also capable of much higher temperature programmed ramp rates, which shorten cycle time further. Maximum practical program rates will depend on a number of factors including column dimensions, phase ratio, carrier gas, and the separation required. When translating a conventional air bath method to the LTM format, Agilent Method Translation software can be used to calculate starting conditions. An example is shown in Figure 3 for translating from a standard 30 M column to a 7 M LTM module. LTM program rates ranging from 60 °C/min to 120 °C/min gave acceptable results in terms of meeting required resolution of specific sol-

vent pairs. Previous work describing the use of LTM technology for a generic set of residual solvents employed a 20 m × 0.18 mm, 1.0 µm J&W DB-624 column. [5]

A comparison of various column dimensions and program rates are shown in Table 3. Air bath and LTM methods are included. The table includes entries for the same column (7 M) dimension in air bath and LTM configurations, which allows a valid comparison of overall cycle time. Note that the maximum air oven program rates possible for the 7890A 120V and 220V GC systems, over the range needed for this application (35 °C to 240 °C), are 30 °C/min and 45 °C/min, respectively. When comparing against a 220V 7890A GC, the LTM still achieves a 50% reduction in cycle time. Throughout this work, both LTM columns were controlled from the LTM ChemStation Software add-on module and operated with identical oven programs. However, the LTM columns can each have unique programs that assist with optimization. The only restraint is that both column programs start at the same time. Ending times may be different

| GC Method Translation | | Criterion: <input checked="" type="radio"/> Translate Only <input type="radio"/> Best Efficiency <input type="radio"/> Fast Analysis <input type="radio"/> None | | Speed gain: 6.60729 | |
|--|---------|---|----------------------------------|---------------------|--|
| | | Original Method | Translated Method | | |
| Column | | | | | |
| Length, | m | 30 | <input type="checkbox"/> | 7 | |
| Internal Diameter, | µm | 320 | <input type="checkbox"/> | 250 | |
| Film | | | <input type="radio"/> Unlock | | |
| Thickness, | µm | 1.80 | <input type="radio"/> | 1.41 | |
| Phase Ratio | | 44.44 | <input checked="" type="radio"/> | 44.44 | |
| Carrier Gas | | | <input type="checkbox"/> | | |
| Enter one Setpoint | | Helium | <input type="checkbox"/> | Helium | |
| Head Pressure, | psi | 16.305 | | 9.399 | |
| Flow Rate, | mLn/min | 4.0000 | | 3.1250 | |
| Outlet Velocity, | cm/sec | 89.06 | | 113.99 | |
| Average Velocity, | cm/sec | 54.95 | | 84.71 | |
| Hold-up Time, | min | 0.909952 | | 0.137719 | |
| Outlet Pressure (absolute), | psi | 14.696 | <input type="checkbox"/> | 14.696 | |
| Ambient Pressure (absolute), | psi | 14.696 | <input type="checkbox"/> | 14.696 | |
| Oven Temperature 1-ramp Program | | | | | |
| | | Ramp Rate | Final Temp. | Final Time | |
| | | °C/min | °C | min | |
| | Initial | | | | |
| | Ramp 1 | 10.000 | 40 | 20 | |
| | | | | | |
| | | 66.073 | 250 | 3.027 | |
| Sample Information None | | | | | |

Figure 3. Method translation from standard 30 M column to an Agilent J&W DB-624 7 M LTM column. See www.agilent.com/chem/methodtranslator to download this tool.

Table 3. Cycle Times for Various Column and Oven Type Configurations

| Heating | Column | Program | Cool down | Cycle time |
|---------------|---|---|--|------------------|
| 7890A (120V) | 30 M × 0.53 mm × 3.0 μm Agilent J&W DB-624 | 40 °C (20 min) to 240 °C (20 min) at 10 °C/min | 6 min 50 sec with 3 min oven equil. | 67 min |
| 7890A (120) | 7 M × 0.25 mm × 1.4 μm Agilent J&W DB-624 | 35 °C (5 min) to 240 °C (5 min) at 30 °C/min* | 8 min 25 sec with 3 min oven equil. | 25 min 15 sec |
| 7890A (220) | 7 M × 0.25 mm × 1.4 μm Agilent J&W DB-624 | 35 °C (5 min) to 240 °C (5 min) at 30 °C/min** | 8 min 25 sec with 3 min oven equil. | 22 min 30.sec |
| LTM (Fast) | 7 M × 0.25 mm × 1.4 μm Agilent J&W DB-624 | 35 °C (5 min) to 240 °C (5 min) at 30 °C/min | 1 min 45 sec (one module system) | 15 min 10 sec |
| LTM (Faster) | 7 M × 0.25 mm × 1.4 μm Agilent J&W DB-624 | 35 °C (5 min) to 240 °C (3 min) at 100 °C/min | 1 min 45 sec (one module system) | 11 min 45 sec |
| LTM (Fastest) | 7 M × 0.25 mm × 1.4 μm Agilent J&W DB-624 | 35 °C (4 min) to 240 °C (3 min) at 120 °C/min | 1 min 45 sec (one module system) | 10 min 30 sec |

LTM chromatograms of Class 1 solvents are shown in Figures 4A and 4B on Agilent J&W DB-624 and J&W HP-INNOWax modules, respectively. Resolution between two Class 2A solvents (acetonitrile and methylene chloride on J&W DB-624 columns) meets method requirements as shown in Figure 5. Signal-to-noise ratio's for all Class 1 solvents are greater than 3 at specified limit concentrations.

Chromatograms for Class 2A and 2B solvents on both J&W DB-624 and J&W HP-INNOWax phases are shown in Figures 6 and 7. All Class 1, 2A, and 2B solvents combined at limit

concentrations are shown in Figure 8. Peak identifications and limit concentrations in prepared headspace vials are shown in Table 4. Note that operating at 120 °C/min yields a cycle time of 10.5 minutes.

Headspace vial equilibration times were kept at 60 min in this work, following USP 467. However, it should be noted that equivalent results can be obtained with 30 min heating times [3]. Additional benefits in sensitivity and repeatability are possible using electronic back pressure control of the headspace vial venting (loop fill) process. This is discussed at length in Application Note 5989-6079EN [6].

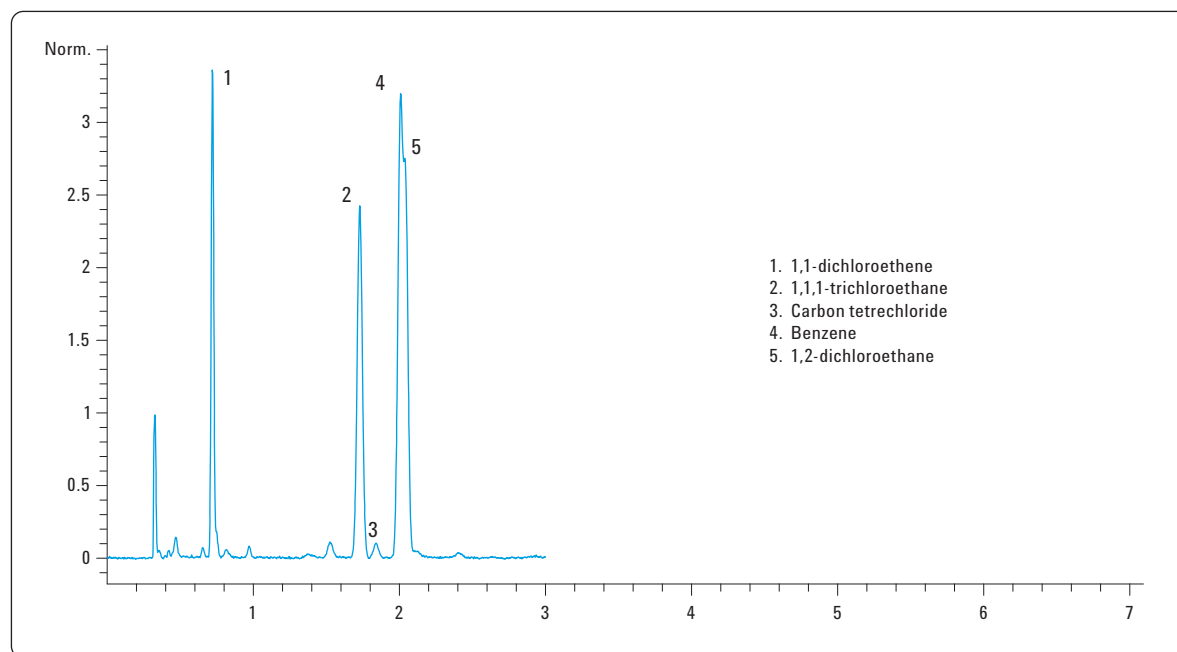


Figure 4A. Class 1 residual solvents at limit concentration on an Agilent J&W DB-624 column at 60 °C/min program rate.

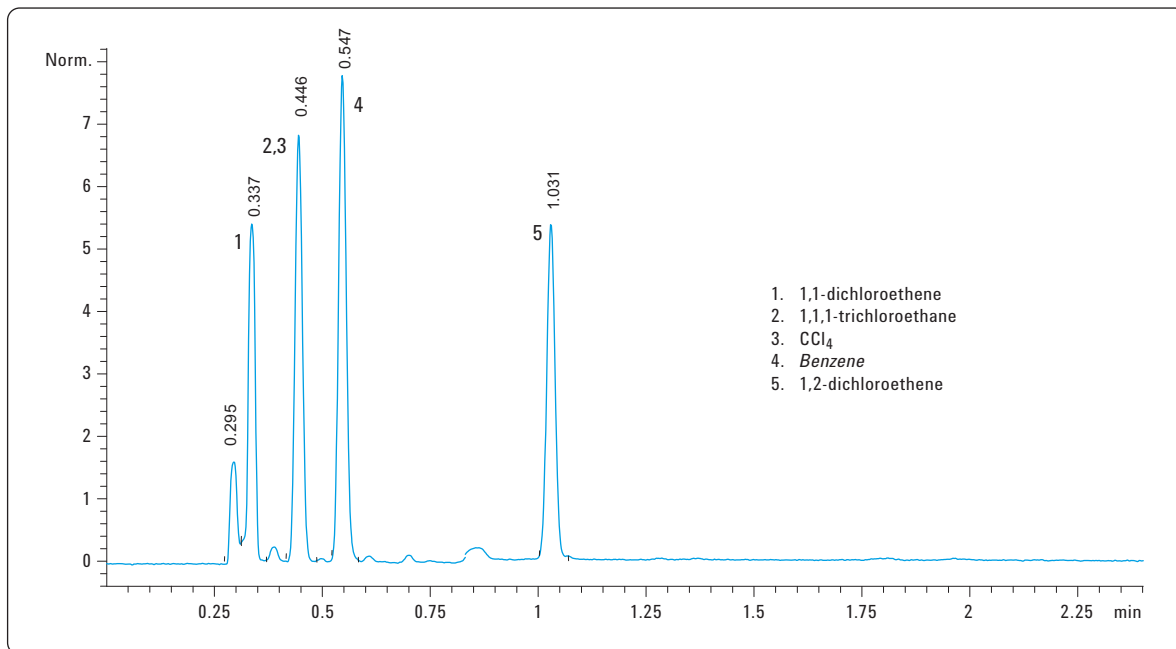


Figure 4B. Class 1 residual solvents at limit concentration on an Agilent J&W HP-INNOWax column at 60 °C/min.

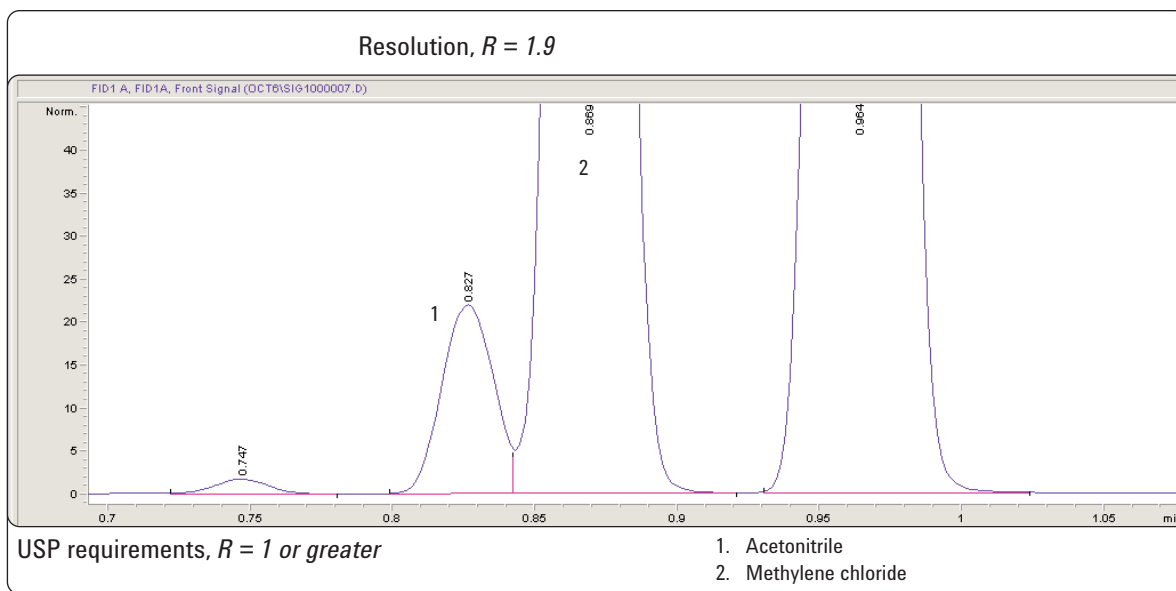


Figure 5. Acetonitrile/methylene chloride resolution.

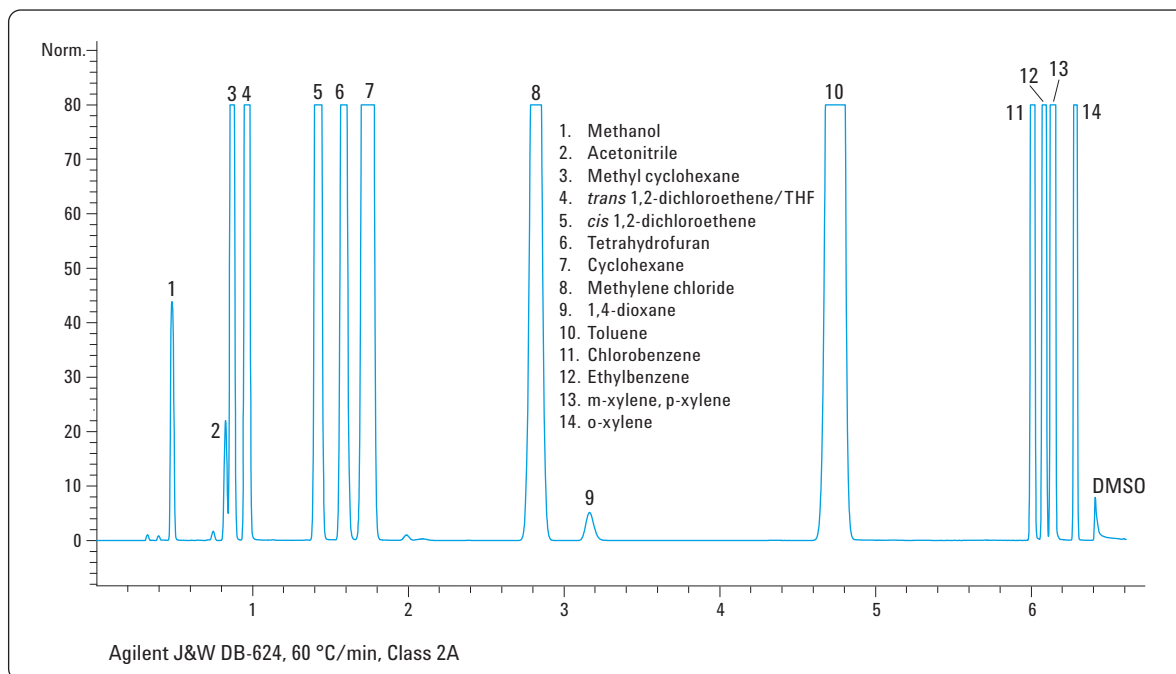


Figure 6A. Class 2A solvents at limit concentration on an Agilent J&W DB-624 column, 60 °C/min.

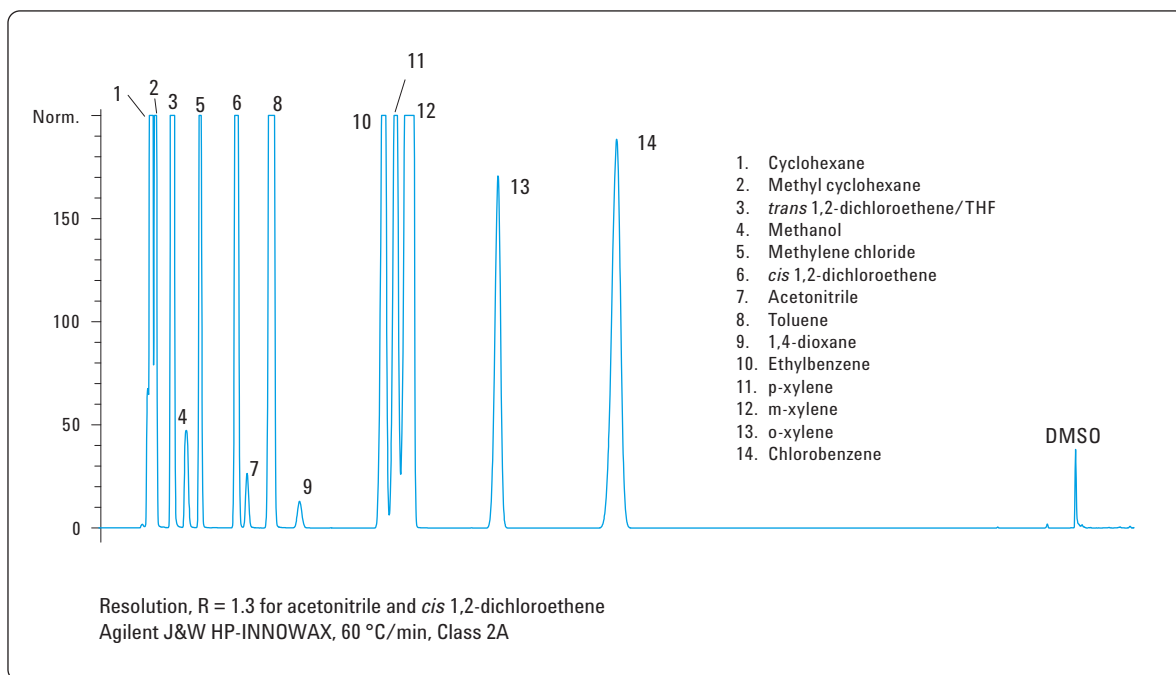


Figure 6B. Class 2A solvents at limit concentration on an Agilent J&W HP-INNOWax column, 60 °C/min.

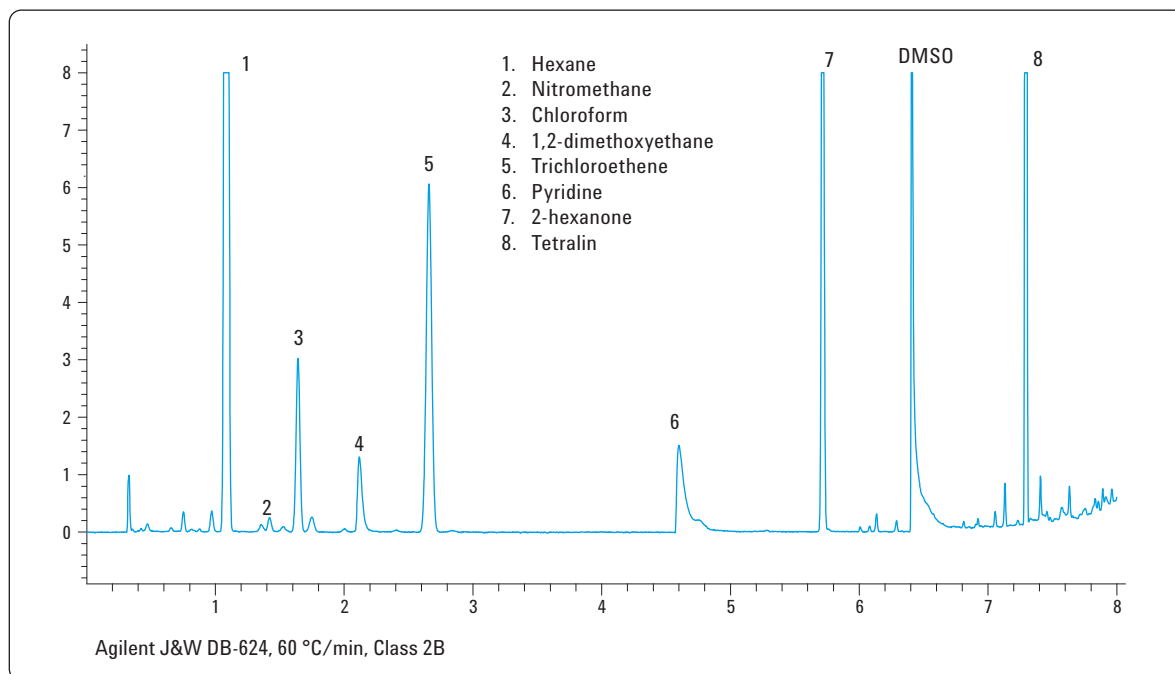


Figure 7A. Class 2B solvents at limit concentration on Agilent J&W DB-624 column, 60 °C/min

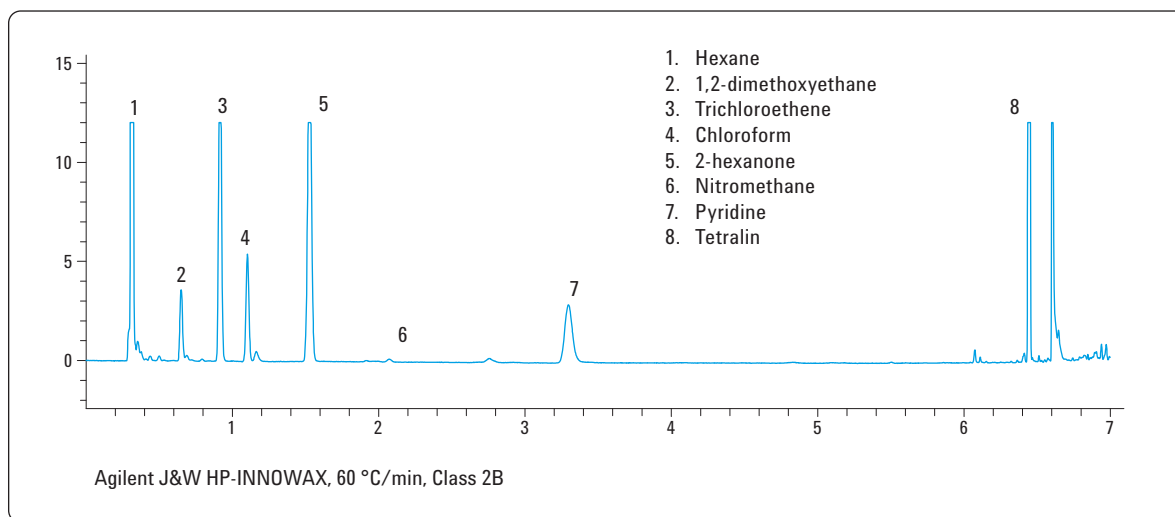


Figure 7B. Class 2B solvents at limit concentration on Agilent J&W HP-INNOWax column, 60 °C/min.

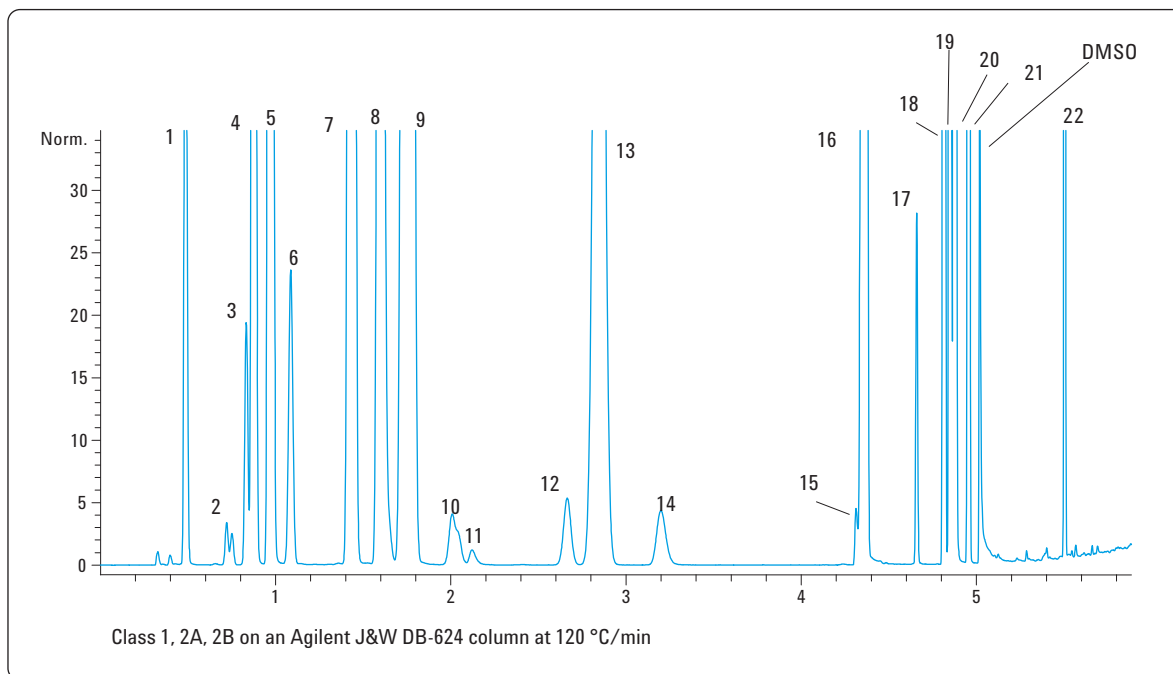


Figure 8. Class 1, 2A, and 2B solvents at limit concentration on Agilent J&W DB-624 column, 120 °C/min. Peak IDs in Table 4.

Table 4. Peak Numbering for Figure 8 and Actual Headspace Vial Concentrations

| Class 1 | Conc (µg/mL) | Class 2A | Conc (µg/mL) | Class B | Conc (µg/mL) |
|--------------------------|--------------|-------------------------------------|--------------|-------------------------|--------------|
| 2. 1,1-dichloroethene | 66.7 | 1. Methanol | 25.0 | 6. Hexane | 0.483 |
| 9. 1,1,1-trichloroethane | 83.3 | 3. Acetonitrile | 3.41 | 7. Nitromethane | 0.083 |
| 9. Carbon tetrachloride | 33.3 | 4. Methylene chloride | 5.00 | 8. Chloroform | 0.100 |
| 10. 1,2-dichloroethane | 41.7 | 5. <i>trans</i> -1,2-dichloroethene | 7.83 | 11. 1,2-dimethoxyethane | 0.167 |
| 10. Benzene | 16.7 | 7. <i>cis</i> -1,2-dichloroethene | 7.83 | 12. Trichloroethene | 0.133 |
| | | 8. Tetrahydrofuran | 6.00 | 15. Pyridine | 0.333 |
| | | 9. Cyclohexane | 3.23 | 17. 2-hexanone | 0.083 |
| | | 13. Methylcyclohexane | 9.83 | 22. Tetralin | 0.167 |
| | | 14. 1,4-dioxane | 3.17 | | |
| | | 16. Toluene | 7.42 | | |
| | | 18. Chlorobenzene | 3.00 | | |
| | | 19. Ethylbenzene | 3.07 | | |
| | | 20. <i>m, p</i> -xylene | 3.38 | | |
| | | 21. <i>o</i> -xylene | 1.63 | | |

Coelutions on DB-624

- *cis*-1,2-dichloroethene, nitromethane
- THF, chloroform
- Cyclohexane, CCl₄, 1,1,1-trichloroethane
- Benzene, 1,2-dichloroethane

Conclusions

A 6X overall reduction in cycle time is possible when converting from the standard methodology to a LTM based system for residual solvent analysis. Capillary flow technology can be employed to conveniently analyze on two column phases (Agilent J&W DB-624 and Agilent J&W HP-INNOWax columns) simultaneously from a single headspace injection. LTM column dimensions of 7M x 0.25 mm provide a good compromise among speed, ease-of-use, and capacity while meeting the resolution requirements of USP 467. This general methodology using LTM technology should be particularly attractive to new drug development where variations to the USP procedures are appropriate and fast method optimization is desired.

The Chemstation method integrates Agilent 7890A GC/Agilent G1888A Headspace, and LTM control through add-on software modules for ease of setup, operation, method integration, and compliance.

References

1. USP 32-NF 27, General Chapter USP <467> Organic Volatile Impurities, United States Pharmacopeia. Pharmacopoeia Convention Inc., Rockville, MD, 8/2009.
2. International Conference on Harmonization (ICH) of Technical Requirements for the Registration of Pharmaceuticals for Human Use, Q3C (R4): Impurities guideline for residual solvents, Step 4, July 1997.
3. Joseph M. Levy and Michael Kraft, "Simultaneous Dual Capillary Column Headspace GC With Flame Ionization Confirmation and Quantification According to <USP467>," Agilent Technologies publication 5989-8085EN, 2008.
4. Frank David, Roman Szucs, Jay Makwans, and Pat Sandra, "Fast Capillary GC using a Low Thermal Mass Column Oven for the Determination of Residual Solvents in Pharmaceuticals," Pfizer Analytical Research Centre, Ghent University, Krijgslann, Ghent, Belgium, J. Sep. Sci. 2006, 29, 695-698, 2006.
5. Roger L. Firor, "The Determination of Residual Solvents in Pharmaceuticals Using the Agilent G1888 Network Headspace Sampler," Agilent Technologies publication 5989-1263EN, 2004.
6. Albert E. Gudat and Roger L. Firor, "Improved Retention Time, Area Repeatability, and Sensitivity for Analysis of Residual Solvents," Agilent Technologies publication 5989-6079EN, 2007.

For More Information

For more information on our products and services, visit our Web site at www.agilent.com/chem.

www.agilent.com/chem

Agilent shall not be liable for errors contained herein or for incidental or consequential damages in connection with the furnishing, performance, or use of this material.

Information, descriptions, and specifications in this publication are subject to change without notice.

© Agilent Technologies, Inc., 2010
Printed in the USA
January 26, 2010
5990-5094EN



Agilent Technologies

Improved Retention Time, Area Repeatability, and Sensitivity for Analysis of Residual Solvents

Application Brief

Albert E. Gudat and Roger L. Firor

Because many solvents pose a major risk to human health, national and international regulatory bodies such as the U.S. FDA, the United States Pharmacopoeia (USP), and the International Conference on Harmonization (ICH) require analysis for residual solvents in pharmaceutical products. Solvents are divided into three classes on the basis of possible risk. Class 1 solvents should be avoided. Class 2 solvents should be limited. Class 3 solvents are considered to have low toxic risk. The ongoing trend toward lower contaminant levels designated as safe requires more and more sensitive and accurate methods of analysis.

The system used in this study consists of an Agilent 7890A GC and an Agilent G1888 automated headspace sampler (HS). Both an EPC Aux module (HS vial pressure control) and dual mode PCM module (backpressure control of the HS vent) available on the 7890A are employed for improved headspace sampling.

Experimental

| | |
|----------------|---------------------|
| Injection port | Volatiles interface |
| Temperature | 160 °C |
| Split ratio | 2:1 to 4:1 typical |
| Carrier gas | Helium |
| Carrier flow | 9 mL/min |

7890A GC conditions

| | |
|---------------------|--|
| Initial temperature | 35 °C |
| Initial time | 0 min |
| Rate | 25 °C/min |
| Final temperature | 250 °C |
| Final time | 15 min |
| Column | 30 m x 0.45 mm x 2.55 µm DB-624, Part # 124-1334 |
| BPR set point | 5.000 psig |

G1888 headspace sampler

| | |
|---------------------------|--------------------|
| Loop size | 1 mL |
| Vial pressure | 14 psig to 20 psig |
| Headspace oven | 85 °C |
| Loop temperature | 100 °C |
| Transfer line temperature | 120 °C |
| GC cycle time | 50 min |
| Pressurization | 0.2 min |
| Vent (loop fill) | 0.5 min |
| Inject | 0.5 min |

Highlights

Use of the advanced electronic pneumatics available on the 7890A result in more reliable and repeatable analysis of residual solvents by headspace-GC.

- Increased Precision: 7890A with BPR of 5.000 psi on the HS sampling loop decreased %RSD in area to 3% from 5%¹ on an HS/6890GC system. Retention time improved to +/- 0.001 min.
- Increased Sensitivity: Pressurization of the HS loop by BPR can double the peak area vs. loop sampling at atmospheric pressure.
- Decreased Cycle Time: Backflushing of high-boiling-point solvents and late-eluting background peaks decreased sample turnaround time for Class 1 residual solvents by 50%.
- DB-624 Column: The Agilent DB-624 column in the 0.45 mm id provides superior resolution, low bleed, and high capacity for the complex mixture and wide concentration range encountered for Class 1 and Class 2 solvents.

¹HS vent at atmospheric pressure. Experiment performed on a day with significant changes in barometric pressure.



Agilent Technologies

Discussion

Low-level residual solvents are typically determined by gas chromatography (GC) coupled with a flame ionization detector (FID) and a static headspace sampling device. Figure 1 shows a chromatogram of a standard solution of Class 1 and Class 2 residual solvents at the allowed limit concentrations as defined by the ICH (between 2 and 5,000 ppm). Pharmaceutical quality control laboratories currently face a number of instrument-related issues:

- The area precision in HS analysis can be compromised primarily due to atmospheric pressure variations influencing the amount of analytes injected from the loop in a gas sampling valve (GSV).
- The sensitivity is low for some low-concentration analytes (for example, benzene).
- Sample turnaround time/analysis time is excessive and caused by late-eluting impurities and high-boiling solvents/diluents (such as 1,3-dimethyl-2-imidazolidinone [DMI] with a boiling point of 225 °C).

New capillary flow technology and state-of-the-art pneumatic electronics implemented in the 7890A GC addresses these issues and significantly improves the analysis of residual solvents. Figure 2 shows a block diagram of the HS/VI/GC/FID system. The HS transfer line is interfaced to the GC by a volatiles interface (VI), which is operated at 2:1 split ratio for improved sensitivity. The sample pressure in the gas sampling valve loop of the HS sampler is controlled to within 0.001 psi by an electronic backpressure regulator (BPR) to significantly improve area precision. This function is part of the dual mode Programmable Control Module (PCM) on the 7890A GC. Sensitivity is also improved by pressurizing the sample in the loop of the GSV. Finally, implementation of a column backflush facilitated by a capillary-flow-technology splitter and aided by fast oven cool-down time decreases the sample turnaround time; this is shown in Figure 3. Figure 4 shows typical repeatability in peak area and retention time and the Method Detection Limit (MDL) for o-xylene as a representative example. [1]

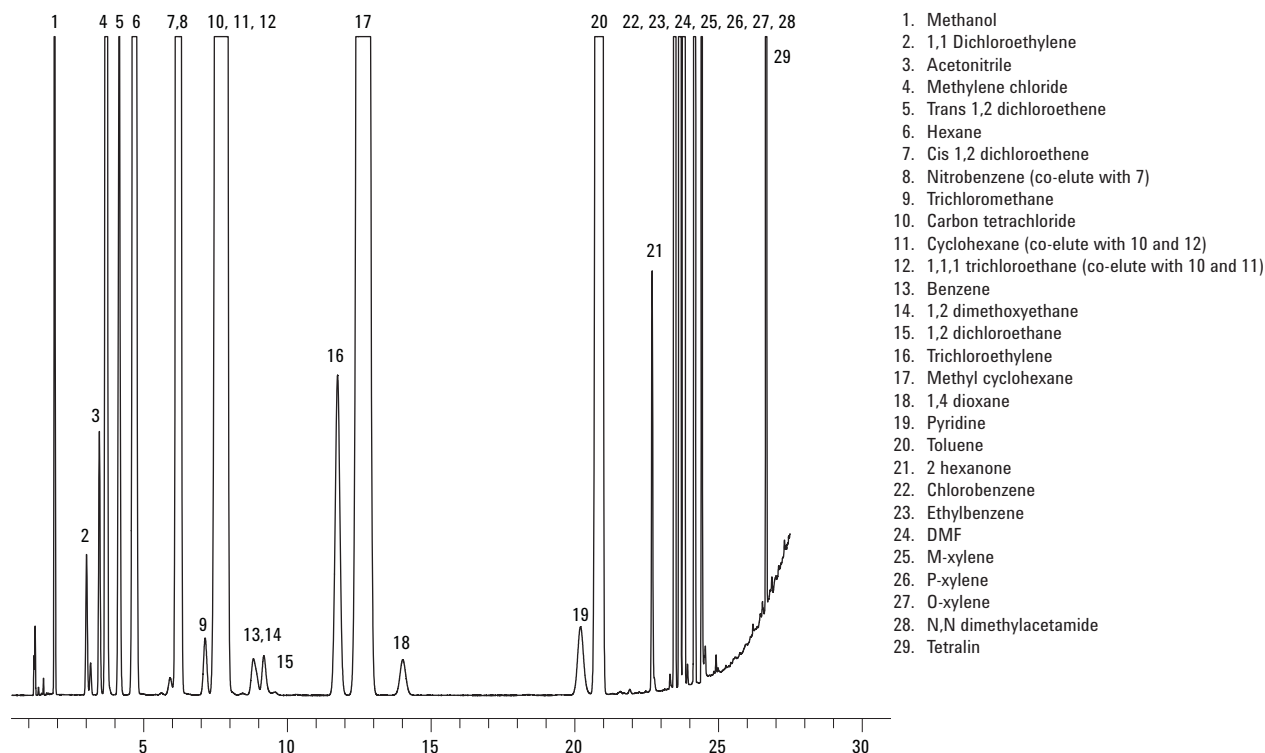


Figure 1. Class 1 and Class 2 residual solvents.

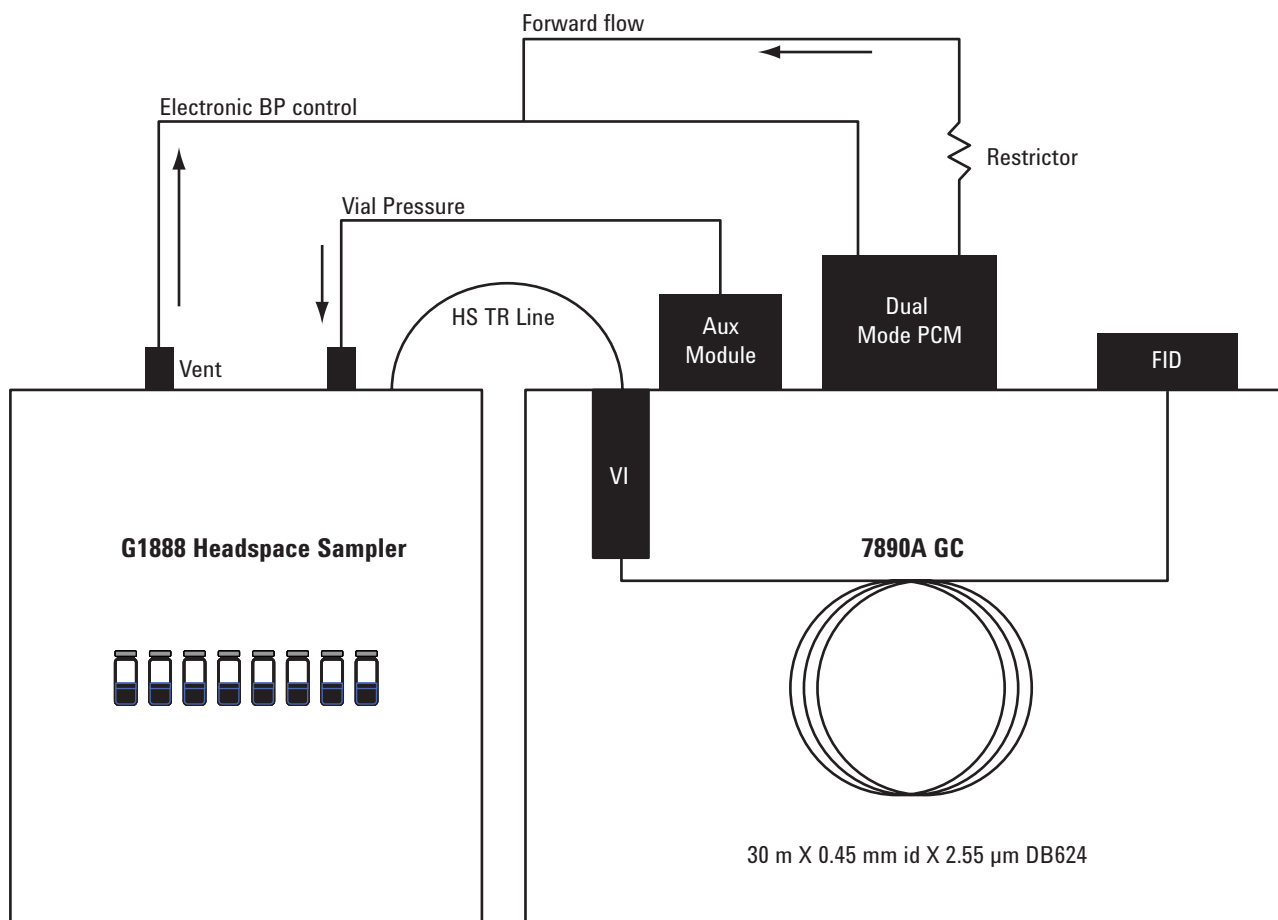


Figure 2. Block diagram of residual solvents configuration without backflush.

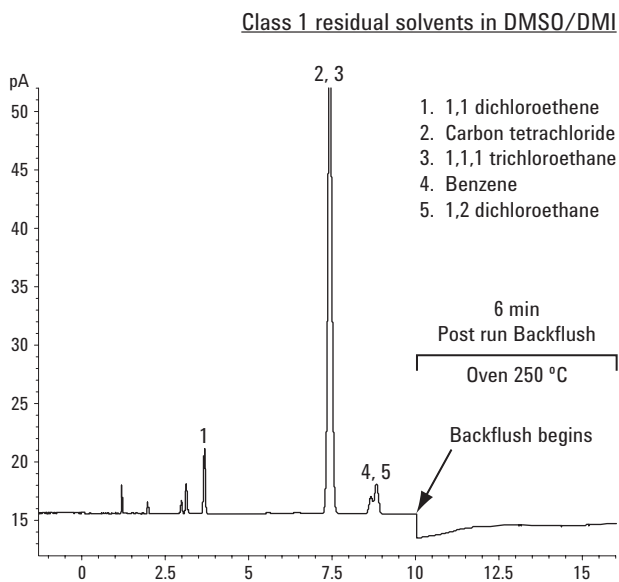


Figure 3. Backflush of Class 1 residual solvents in DMSO/DMI.

$t_R = 23.251 \pm 0.001$ min
 @ 99 % Confidence level
 $RSD_{Area} = 2 \%$
 Method detection limit = 9.8 ppm [1]

ICH Class 2 solvent

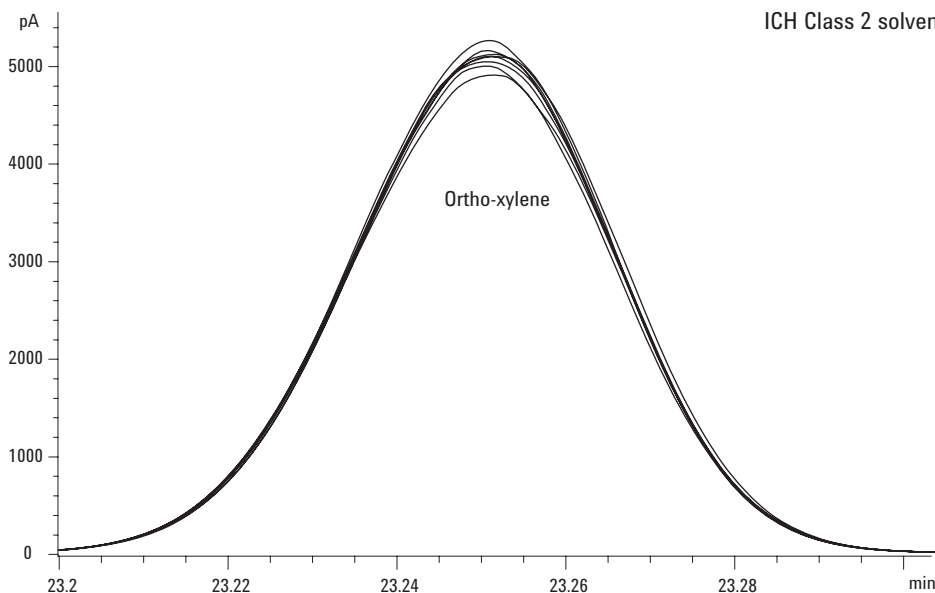


Figure 4. O-xylene (195 ppm), overlay N = 8 (BPR of HS loop @ 5 psi, HS vial pressurized to 20 psi).

References

1. $MDL = s * t(n-1, 1-\alpha = 99) = s * 3.143$, where $(n-1, 1-\alpha)$ = Student's t value for the 99% confidence level with $n-1$ degrees of freedom. N = number of trials, s = standard deviation of the 7 trials. US EPA Method 524.2, Revision 4, 1992.

For More Information

For more information on our products and services, visit our Web site at www.agilent.com/chem.

Agilent shall not be liable for errors contained herein or for incidental or consequential damages in connection with the furnishing, performance, or use of this material.

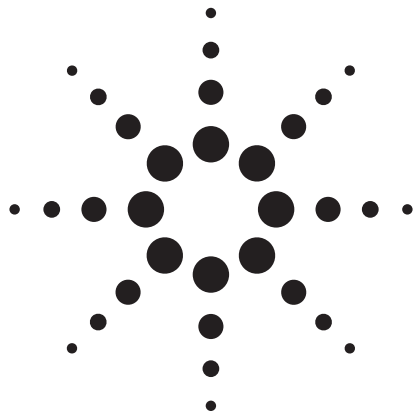
Information, descriptions, and specifications in this publication are subject to change without notice.

© Agilent Technologies, Inc. 2007

Printed in the USA
 January 10, 2007
 5989-6079EN



Agilent Technologies

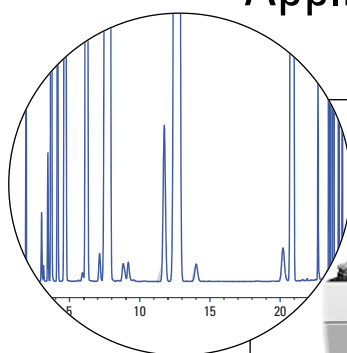


Better precision, sensitivity, and higher sample throughput for the analysis of residual solvents in pharmaceuticals

Using the Agilent 7890A GC system with G1888 headspace sampler in drug quality control

Application Note

Albert E. Gudat
Roger L. Firor
Ute Bober



Abstract

Laboratories using headspace GC for the analysis of pharmaceutical impurities face a number of instrument-related issues:

- Area precision is negatively impacted by atmospheric pressure changes.
- Sensitivity is poor for some low-concentration analytes.
- Presence of high-boiling impurities noticeably extends the analysis time per sample and may even damage the analytical column.

In this Application Note an established Agilent 6890 GC method for residual solvents is transferred to the Agilent 7890A GC without any major changes. The results on both systems are compared.

Overall, the Agilent 7890A GC system delivers at least the same or better performance than the Agilent 6890N GC system:

- The new technology of the Agilent 7890A GC can significantly improve area and retention time repeatability and sensitivity.
- It can drastically reduce the overall analysis time, hence increasing sample throughput and productivity.

Agilent Equipment
7890A GC system,
G1888 headspace sampler

Application Area
Pharmaceutical quality control
Impurity analysis



Agilent Technologies

Introduction

Because many solvents pose a major risk to human health, national and international regulatory bodies such as the United States Food and Drug Administration (U.S. FDA), the United States Pharmacopoeia (USP), the European Pharmacopoeia (EP), and the International Conference on Harmonization (ICH) require analysis for residual solvents in pharmaceutical drug substances, excipients and final products. Solvents are divided into three classes on the basis of possible risk. Class 1 solvents should be avoided. Class 2 solvents should be limited. Class 3 solvents are considered to have low toxic risk. The ongoing trend toward lower contaminant levels designated as safe requires more sensitive and accurate methods of analysis. New USP <467> regulations for residual solvents begin in July 2007. The goal of this initiative is the final alignment with the ICH Q3C(R3) guideline, which has also been adopted by the EP.

The analysis for residual solvents in pharmaceutical products and for solvents considered extractables/leachables in pharmaceutical packaging materials is typically done using headspace (HS) GC with a flame-ionization detector (FID) or, for identification and confirmation, with mass-selective detection (MSD). This has been covered in references 1-3. Residual solvents is the most common application for headspace GC in pharmaceutical quality control. Laboratories using HS GC currently face a number of issues related to the analysis of volatiles and semi-volatiles:

- The area precision in HS analysis can be compromised primarily due to atmospheric pressure variations influencing the amount of analytes injected from the sampling loop in the HS gas sampling valve (GSV).
- The sensitivity is poor for some low-concentration analytes, e.g., benzene.
- Sample turn-around time can be excessive, caused by late-eluting impurities and high-boiling solvents/diluents, e.g., 1,3-dimethyl-2-imidazolidinone (DMI) with boiling point of 225 °C.

Further, when the need for new analytical equipment arises, the first question is whether an established validated method can be easily transferred to the next generation of instruments without any additional method development and resulting in no or minimal revalidation effort. The purpose of this study was to at the least demonstrate equivalence of the HS/7890A GC/FID and HS/6890N GC/FID systems when both are operated without pressure regulation of the sampling loop content of the HS GSV. But more importantly, to also show how new capillary flow technology, fifth generation pneumatics, and state-of-art electronics implemented in the 7890A GC have effectively addressed the above issues with significant improvements in area and retention time precision, sensitivity and productivity with increased sample throughput for residual solvent analysis.

Note: A list of acronyms and short-hand terms used in the text, figures and descriptions of experiments and calculation formulas are included in the appendix on page 8.

Experimental

Both 6890N and 7890A GC were equipped with an Agilent headspace sampler, volatiles interface (VI) and FID. Table 1 gives the experimental conditions used with the HS/VI/6890N/FID and HS/VI/7890A/FID systems. The 7890A system is operated with and without backpressure regulation on the HS sampling loop, whereas the 6890N does not have backpressure regulation. To calculate the repeatability expressed as %RSD values in area and retention time and to determine statistical Method Detection Limit (MDL) for each analyte, 20 identical samples were prepared. A standard solution in water was first prepared in a 100 mL volumetric flask by adding Restek class 1 and class 2 standards with an Eppendorf pipette. 5 mL of the aqueous standard was subsequently transferred quickly to 10 mL headspace vials containing 3 g sodium sulfate and immediately sealed with Teflon-seal caps. Each vial was then vortex mixed for half a minute. Ten of these samples were subsequently used with the 6890N system and ten with the 7890A system – both systems were operated without pressure control on the HS sampling loop. At the end of the HS equilibration, the HS vials were pressurized to 14.000 psi by an auxiliary (AUX) Electronic Pneumatic Control (EPC) module and injected in either the 6890N GC or the 7890A GC system. The same DB 624 column was used in the two GCs for the sequence of injections in order to eliminate the influence of batch-to-batch variations in column quality.

Another set of 20 samples was prepared in the same way as described before for use with the 7890A system, but now implementing backpressure regulation on the HS sampling loop. Figures 1, 2 and 3 show diagrams of the 7890A system where new pneumatic features of pressure regulation of the HS sampling loop, HS vial pressurization and backflush can be applied. At the end of the HS equilibration, the HS vials were pressurized to 20.000 psi by an AUX EPC channel and the loop was regulated at 5.000 psi with the backpressure regulator channel of the Pneumatic Control Module (PCM).

| 6890N or 7890A GC | | G1888A Headspace Sampler | |
|------------------------|---|--------------------------|-------------------|
| Injection port | Volatiles interface | Loop size | 1 mL |
| Temperature | 160 °C | Vial pressure | 14.0 psig |
| Split ratio | 2 : 1 | Headspace oven | 85 °C |
| Carrier gas | Helium | Loop temp | 100 °C |
| Carrier flow | 9 mL/min | Transfer line temp | 120 °C |
| GC oven program | | Equilibration time | 30 min, low shake |
| Initial temperature | 35 °C | GC cycle time | 50 min |
| Initial time | 20 min | Pressurization | 0.15 min |
| Rate | 25 °C/min | Vent (loop fill) | 0.5 min |
| Final temp | 250 °C | Inject | 0.5 min |
| Final time | 15 min | | |
| Column: | 30 m x 0.45 mm x 2.55 µm DB-624 Agilent part number 124-1334 | | |
| Standards | | | |
| ICH class 1 and 2 | Restek #36228 (Class 1) #36229 (class 2A) #36230 (class 2B) | | |

Table 1
Instrument conditions for residual solvents analysis.

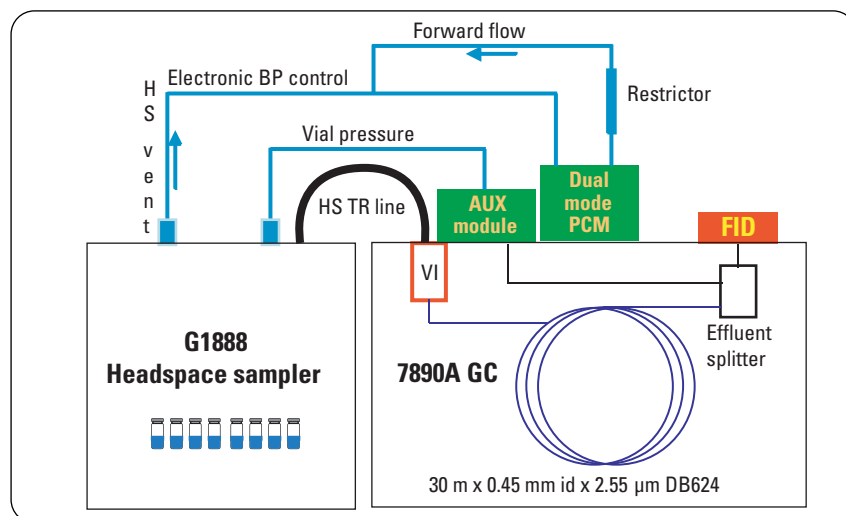


Figure 1
Block diagram of the 7890A GC configuration with backflush capability used in the backflush experiments.

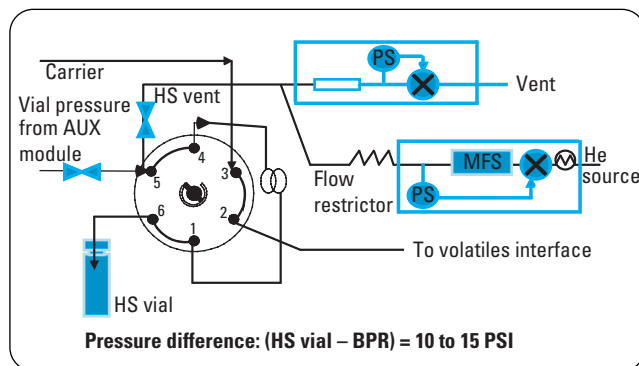


Figure 2
Headspace (HS) sampling scheme with backpressure regulation (BPR).

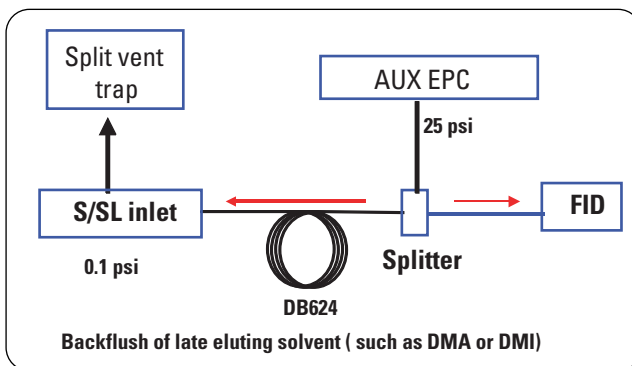


Figure 3
Schematic diagram of the reversed column flow used for backflushing of late eluting solvents.

| Residual solvents | ICH Class | Excipient limit concentration [ppm] | 7890A GC with BPR* | | 7890A GC at Atm P (no BPR) | | 6890N GC at Atm P (HS valve) | | | | |
|--------------------------------|-----------|-------------------------------------|--------------------------|-------------|----------------------------|--------------------------|------------------------------|----------------------|--------------------------|-------------|-------|
| | | | Repeatability [%RSD] N=8 | | Excipient MDL# [ppm] | Repeatability [%RSD] N=8 | | Excipient MDL# [ppm] | Repeatability [%RSD] N=8 | | |
| | | | t _R | Area | | t _R | Area | | t _R | Area | |
| benzene | 1 | 2 | 0.014 | 2.43 | 0.1 | 0.012 | 5.62 | 0.2 | 0.010 | 9.52 | 0.2 |
| 1,2-dichloroethane | 1 | 5 | 0.005 | 4.47 | 0.7 | 0.02 | 8.03 | 0.5 | 0.016 | 8.63 | 0.5 |
| 1,1-dichloroethene | 1 | 8 | 0.013 | 3.24 | 0.8 | 0.011 | 16.63 | 3.3 | 0.022 | 9.82 | 1.1 |
| methylene chloride | 2 | 600 | 0.009 | 2.85 | 54.9 | 0.016 | 7.15 | 61.4 | 0.018 | 8.20 | 62.7 |
| hexane | 2 | 290 | 0.014 | 4.18 | 23.1 | 0.027 | 7.15 | 33.2 | 0.020 | 10.61 | 39.1 |
| cyclohexane | 2 | 3880 | 0.042 | 3.59 | 341.0 | 0.012 | 4.29 | 299.9 | 0.018 | 9.79 | 501.1 |
| trichloroethylene | 2 | 80 | 0.012 | 2.69 | 5.8 | 0.016 | 5.29 | 7.9 | 0.013 | 7.91 | 7.9 |
| toluene | 2 | 890 | 0.025 | 2.11 | 46.3 | 0.024 | 5.41 | 85.9 | 0.031 | 7.90 | 90.3 |
| ethylbenzene | 2 | 369 | 0.002 | 2.27 | 24.4 | 0.002 | 4.90 | 35.3 | 0.003 | 7.40 | 35.5 |
| ortho xylene | 2 | 195 | 0.001 | 1.86 | 9.8 | 0.001 | 5.12 | 19.0 | 0.002 | 7.00 | 18.4 |
| Average for 29 solvents | | | 0.013 | 2.83 | | 0.017 | 8.77 | | 0.021 | 9.34 | |

* Backpressure regulation (HS-valve outlet pressure is regulated) # Method detection limit

Table 2

Retention time and area repeatability and calculated MDLs of representative residual solvents for the 7890A and 6890N HS/VI/GC/FID systems.

Results from the experiments are summarized in table 2. From the 29 solvents some representative class 1 and 2 solvents were selected and the results summarized in this table. Further, the average values for all 29 solvents are shown. A series of experiments was also performed to demonstrate potential sensitivity gains realized from pressurizing the HS loop. This time, however, instead of preparing 5 mL aqueous standards in HS vials containing the 3 g of sodium sulfate, a Restek class 2B standard was used as is. A 5 µL capillary tube was filled by capillary flow action with the standard. The outside of the tube was carefully wiped with tissue paper, quickly transferred to an empty 10 mL headspace vial and immediately capped. This procedure ensured accurate and reproducible sample preparation by eliminating user bias to the extent possible in preparing identical samples. Results from this series of experiments are shown in figure 7. The error bars in the figure represent a 95 % confidence level (± 2 times standard deviation or sigma).

Finally, the system was reconfigured to facilitate a column backflush to quickly remove late eluting impurities or high boiling solvent or diluents. This configuration is shown in figure 3. Instead

of using the GC volatiles inlet (VI), a split/splitless (S/SL) inlet was interfaced to the headspace transfer line. The VI configuration is anticipated to have a limited backflush flow rate with the 0.45 mm diameter column, a limitation not

observed with the S/SL inlet. The VI configuration was not tested for backflush operation.

Results and discussion

A typical chromatogram of residual solvents is shown in figure 4

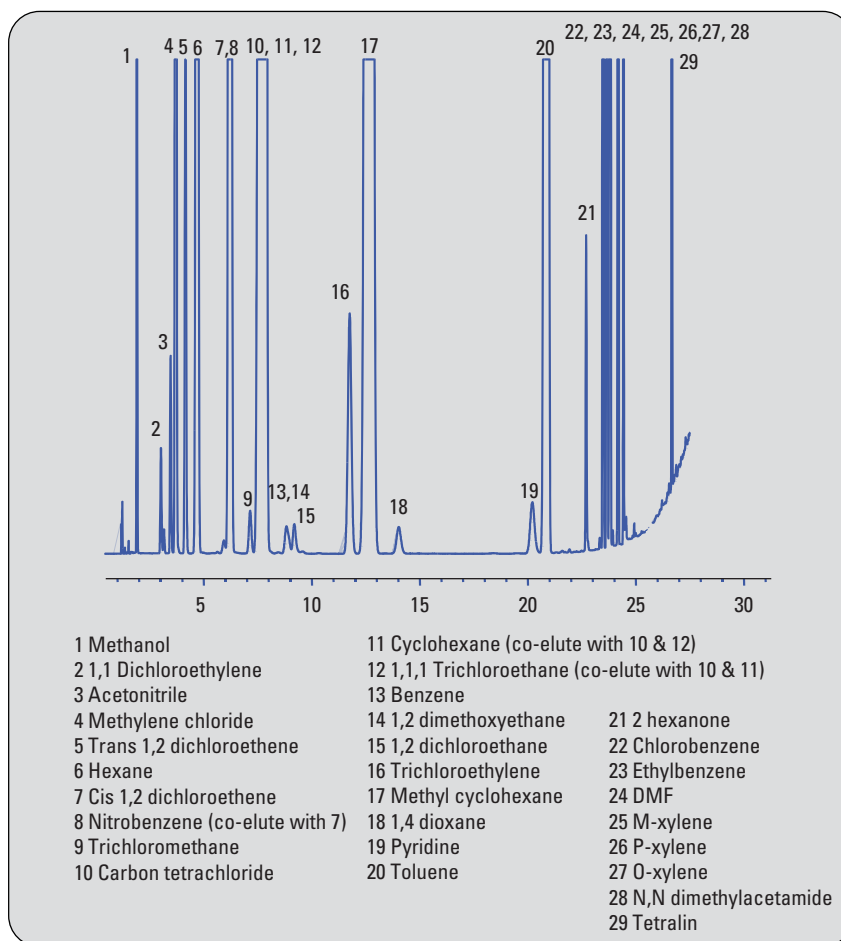


Figure 4
Gas chromatogram of class 1 and 2 residual solvents.

and repeatability data for area and retention time of an early- and late-eluting peak are shown in figure 5. An improvement in area precision by a factor of 3 was typically observed, as in this example for 1,1-dichloroethylene. However, in some cases up to a factor of 4 was determined, for example, for o-xylene. Overall, the performance of the 7890A system is better than the 6890N system. A summary of performance characteristics for some representative class 1 and 2 analytes is given in table 2.

Improving peak area precision

From the results presented in table 2 and figure 6 the following conclusions can be drawn:

- Overall, the 7890A and 6890N show the same area repeatability when no backpressure regulation of the HS sampling loop is applied. Under the same conditions the results don't exhibit significant differences. The average area precision [%RSD] for 29 residual solvents (shown on the bottom line of table 2) for both systems is 9 %.
- The 7890A GC with backpressure regulation of the HS sampling loop, is at least 3 times better than the 7890A GC (or 6890N GC) operated without pressure regulation of the HS sampling loop. For individual analytes an improvement by a factor of 4 was observed in some cases, as shown in figure 5 for o-xylene.
- The observed differences are even more apparent when considering a very turbulent day with large variations in atmospheric pressure. This is when a series of measurement are performed. The data presented in figure 6 was obtained on such a stormy day. Under extreme weather conditions the averaged area repeatability can increase to 16 % when no backpressure regulation is applied. However, a method with optimized backpressure regulation fully com-

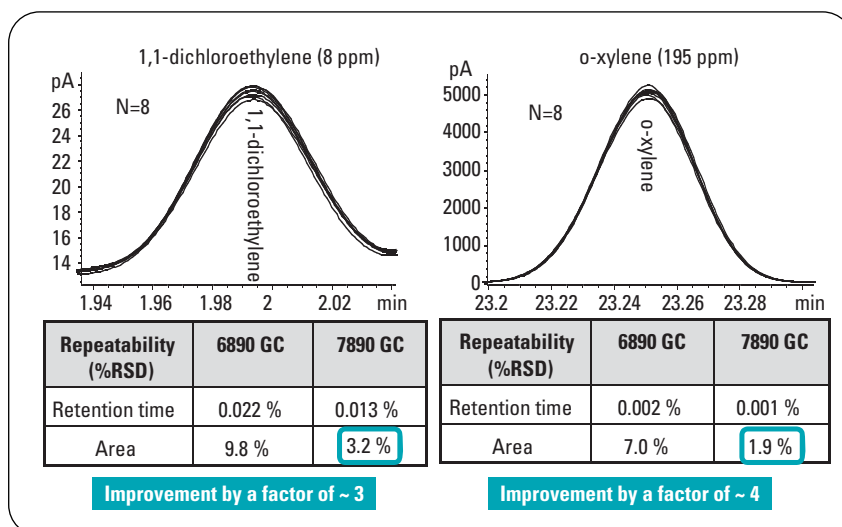


Figure 5
Examples of improved area and retention time precision by applying backpressure regulation (backpressure regulation: 5.000 PSI, headspace vial pressure: 20.000 PSI).

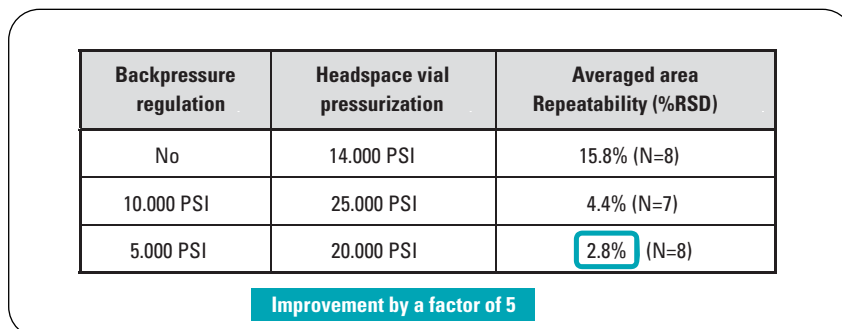


Figure 6
Backpressure regulation – Effect of reducing atmospheric pressure variation at vent. Variability in loading the gas sampling valve can occur based on atmospheric pressure differences.

pensates for the atmospheric pressure instabilities and the measured averaged repeatability returns to the same value of 3 % that was obtained under stable weather conditions in the previous experiments. The reason is that variability in loading the gas sampling valve can occur based on atmospheric pressure differences. This can happen when running the same method in different geographic locations at different altitudes or, as shown here, during a turbulent stormy day with large variations in atmospheric pressure. With backpressure regulation the gas sampling valve can operate under a constant set of conditions and precision and sensitivity improve.

Improving retention time precision

Similar to the results obtained for peak area precision a positive impact on the repeatability of retention time was observed:

- In comparison to the 6890N GC the averaged retention time repeatability for all 29 residual solvents measured on the 7890A GC was generally better, no matter whether backpressure regulation was applied or not.
- With backpressure regulation of the HS sampling loop the averaged retention time repeatability measured on the 7890A GC was best. It improved by a factor of two relative to the 6890N GC without any pressure regulation.

Optimizing sensitivity with backpressure regulation

Overall sensitivity could be doubled by applying backpressure regulation compared to the 6890N or the 7890A GC without backpressure regulation. Figure 7 shows the area changes for 1,4-dioxane with HS-vial pressurization and HS sampling loop pressurization. The more we pressurize the vial, the more we dilute the HS sample. This is clearly shown when the x-axis is zero (where the backpressure regulator is not used and the loop is exposed to atmospheric pressure). Pressurizing the HS vial to 14, 35 and 60 psi gives the highest peak area at 14 psi.

When regulating the pressure in the loop with the BPR, we see an increasing area count that reaches a maximum and then decreases and eventually would give zero area counts. Once the top of the curve is reached, the depressurization of the HS vial through the HS loop (the venting cycle) is opposed by the excessive high backpressure and the sample flow through loop will diminish and may even reverse. After we reach the top of the curve, we no longer trap a representative sample in the loop. The pressure difference ($P_{\text{HS-Vial}} - \text{BPR}$) should be 10 to 15 psi in order to collect and inject a proper HS sample.

Increase efficiency with backflush

The backflush capability of the 7890A GC allows to remove late eluting compounds by reversing the flow. The benefits are:

- Shorter analysis time
- Extended capillary column life time.

Because this system has EPC, as soon as the last analyte of interest has eluted from the column, the AUX module can be pressure-programmed to a higher pressure (25 psi in this example) at the same time that the split/splitless

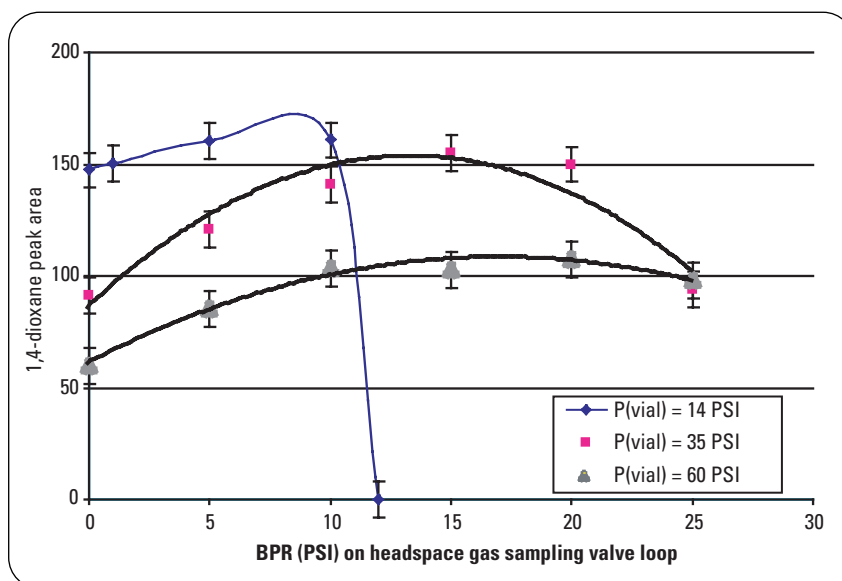


Figure 7
Improving sensitivity with the 7890A GC. Variation in peak area with headspace vial and sampling loop pressure.

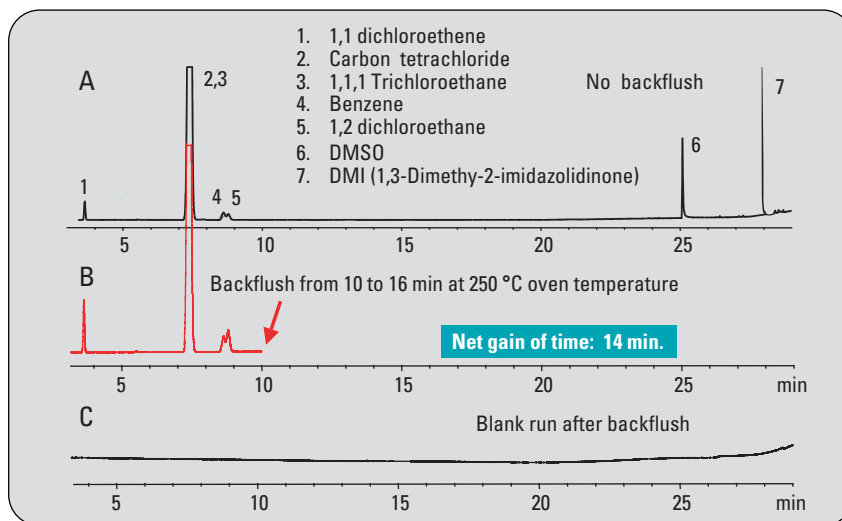


Figure 8
Example of how backflushing helps to decrease analysis time and increase workload efficiency (chromatogram of a sample containing all ICH class 1 residual solvents): A. Initial situation (no backflush) B. Reduced analysis time using backflush C. Blank run after backflush.

inlet is programmed to a lower pressure (0.1 psi in this example). Now the flow in the column is reversed, backflushing the remaining eluents out through the split vent of the inlet. Figure 3 shows a schematic overview of the functionality. For the backflush experiment samples containing only class 1 residual solvents were prepared in DMSO and DMI, both high boiling diluents (figure 8). A

typical chromatogram of such a sample lasting more than 30 minutes is shown in figure 8A. Since all the class 1 solvents elute in 10 minutes at 35 °C isothermal, a backflush was initiated from 10 to 16 minutes with an elevated column temperature of 250 °C. As a result the net gain of time per run was 14 minutes (figure 8B). The high-boiling compounds were successfully removed as can be

seen from the chromatogram of the blank run that was executed afterwards (figure 8C). In this example backflush improves efficiency by almost doubling sample throughput. The fast oven cool-down of the 7890A GC further contributes to those time savings.

Equal in linearity

To measure linearity five dilutions were prepared ranging from 1/10th to two times the limit concentration. Based on the USP <467> method where 100 mg of the excipient/drug product is dissolved in 5 mL of water with 3 grams of Na₂SO₄, the solution concentration in 5 mL of water was converted to the concentration of the residual solvent in the 100 mg of excipient with the formula: $c_e \text{ [ppm]} = 50 \cdot c_v$. In the following text this concentration is described as excipient equivalent concentration c_e while c_v is the vial solution concentration. The linearity results for some representative residual solvents for the 7890A GC are compared to similar experiments for the 6890N GC¹ system in figures 9 and 10, respectively. The corresponding calculated values for linearity, slope and intercept are summarized in tables 3a and 3b.

Overall, the 7890A and 6890N GC systems compare well. All calibration curves are linear over a range from 1/10th to 2 times the limit concentration. The signal-to-noise (S/N) data, limit of detection (LOD) and limit of quantitation (LOQ) indicate that the systems are similar in performance (LOD and LOQ data are only shown for the 7890A in table 3a). Results from the MDL calculations (see table 2 and the appendix for the MDL equation) and a comparison of S/N ratios calculated for samples at the limit concentration indicate that the 7890A GC system is at least two times better in sensitivity than the 6890N GC system.

| | Methylene Chloride | Benzene | 1,4-Dioxane | Chloroform | Trichloroethylene |
|-----------|--------------------|---------|-------------|------------|-------------------|
| Linearity | 0.99945 | 0.99859 | 0.99606 | 0.99362 | 0.99967 |
| Slope | 6.0935 | 50.2950 | 0.4214 | 2.7160 | 14.3362 |
| Intercept | 228.3704 | 4.6045 | 11.4008 | 5.2606 | 106.9926 |
| LOD | 10.2 | 0.02 | 2.5 | 0.25 | 0.07 |
| LOQ | 10.4 | 0.06 | 8.4 | 0.82 | 0.23 |

Table 3a
Linearity, LOD and LOQ results for the 7890A Headspace GC/FID system.

| | Methylene Chloride | Benzene | 1,4-Dioxane | Chloroform | Trichloroethylene |
|-----------|--------------------|---------|-------------|------------|-------------------|
| Linearity | 0.9988 | 0.9995 | 0.9996 | 0.9991 | 0.9991 |
| Slope | 252.82 | 2106.2 | 15.268 | 192.41 | 535.39 |
| Intercept | 19.987 | 0.0015 | 0.3239 | 0.1851 | 3.7229 |

Table 3b
Linearity results for the 6890N Headspace GC/FID system.

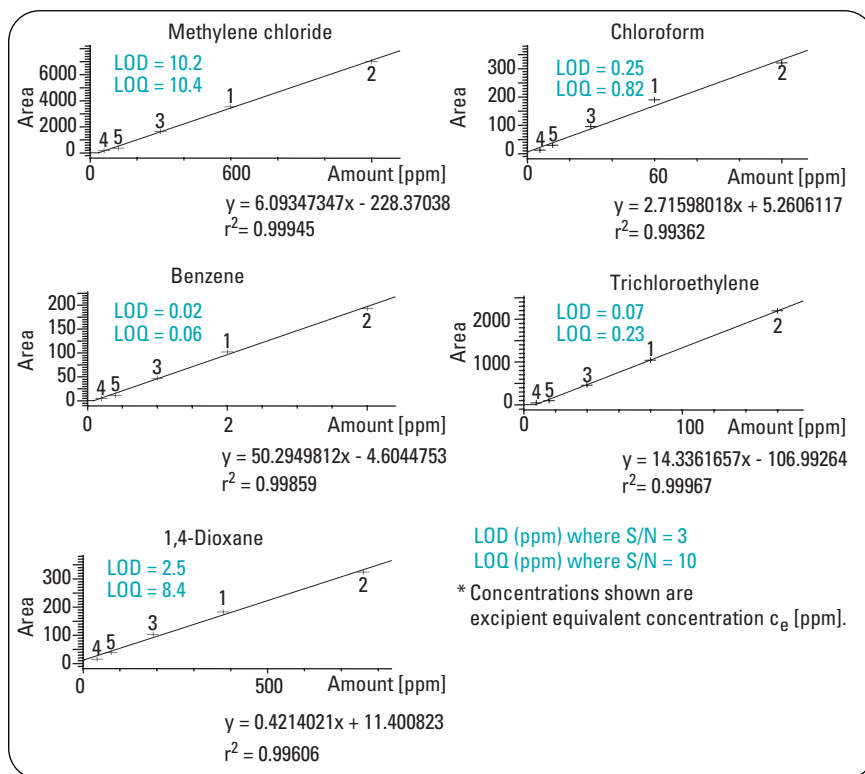


Figure 9
Linearity plots for some residual solvents determined for the 7890A Headspace GC/FID system*.

Conclusion

It was demonstrated that the 7890A GC delivers better results than the 6890 GC. In summary:

- It was possible to directly transfer an established method from the 6890 to the 7890A GC without any method development or altering the performance.
- Without backpressure regulation the 7890A GC shows the same or better performance.

- The backpressure regulation from the 7890A GC eliminates the influence of atmospheric pressure variations.
- With optimized backpressure regulation of the headspace sampling loop from the 7890A GC area precision (%RSD) could be improved by a factor of 3 to 5
- Under the same conditions retention time stability increased to ±0.001 min. (improved by a factor of 2)

- Sensitivity was doubled by pressurizing the headspace sampling loop of the 7890A GC.
- The backflush capability of the 7890A GC significantly reduces overall analysis time (in the example by 50 %).
- Both systems are equal in performance when evaluating linearity data.

The experimental setup in this application is suitable for routine analysis of residual solvents. However, it does not provide any further information when unknowns are present. The solution is to couple the GC to the Agilent 5975C Series MSD, where you can achieve superior results for both identification of unknowns and quantitation of target compounds.

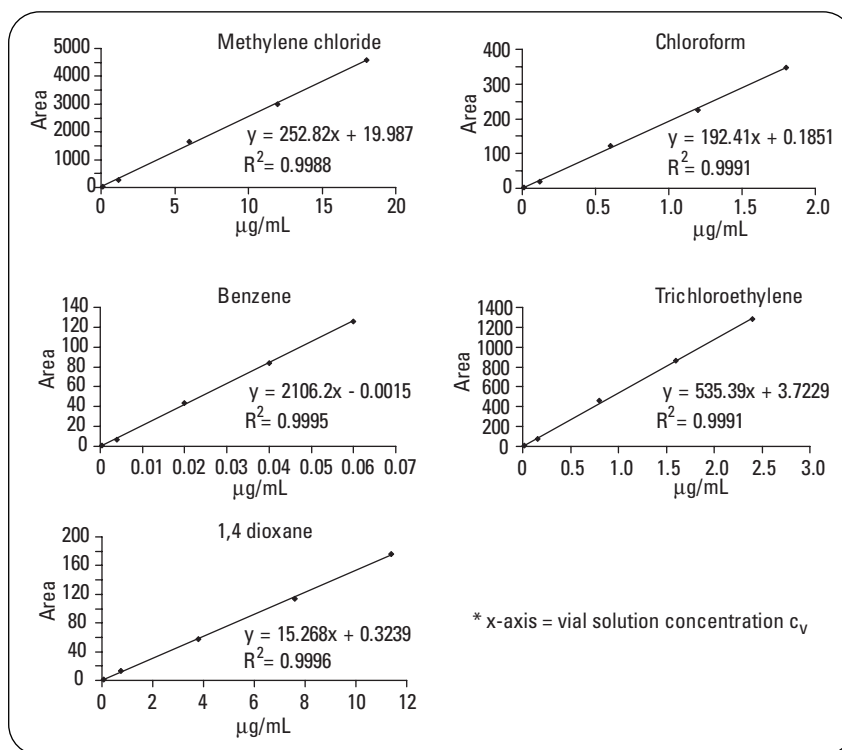


Figure 10
Linearity plots for some residual solvents determined for the 6890N Headspace GC/FID system*.

References

1. Roger L. Firor, "The Determination of Residual Solvents in Pharmaceuticals Using the Agilent G1888 Network Headspace Sampler," *Agilent Application Note, Publication Number 5989-1263EN, 2004.*
2. Roger L. Firor and Albert E. Gudat, "The Determination of Residual Solvents in Pharmaceuticals using the Agilent G1888 HS/6890N GC/5975 inert MSD System," *Agilent Application Note, Publication Number 5989-3196EN, 2005.*
3. Albert E. Gudat and Roger L. Firor, "The Determination of Extractables and Leachables in Pharmaceutical Packaging Materials using Headspace/GC/MS," *Agilent Application Note, Publication Number 5989-5494EN, 2006.*

Appendix

List of acronyms

| | |
|---|---|
| %RSD – percent relative standard deviation | LOD – limit of detection (S/N = 3) |
| [limit] – limit concentration | LOQ – limit of quantitation (S/N = 10) |
| Atm P – atmospheric pressure | MDL – method detection limit (statistical) |
| AUX – auxiliary | MFS – mass flow sensor |
| BP – back pressure | min – minutes |
| BPR – backpressure regulation | MSD – mass selective detector |
| C_v – vial solution concentration | P(Vial) – headspace vial pressure |
| C_e – excipient equivalent concentration | PCM – pneumatic control module |
| Cal – calibration | PS – pressure sensor |
| DMA – dimethyl acetamide | PSI – pounds per square inch |
| DMI – 1,2-dimethyl-2-imidazolidinone | RT – retention time |
| DMSO – dimethyl sulfoxide | S/N – signal-to-noise ratio |
| EP – European Pharmacopoeia | S/SL – capillary split/splitless inlet |
| EPC – electronic pneumatic control | TR – transfer |
| FID – flame ionization detector | U.S. FDA – United States Food and Drug Administration |
| GC – gas chromatograph | USP – United States Pharmacopoeia |
| GSV – gas sampling valve | VI – volatiles inlet |
| HS – headspace | X – proportional valve |
| ICH – International Conference on Harmonization | |

Statistical Method Detection Limit (MDL)

$$MDL = s \cdot t_{(n-1, 1-\alpha=99)} = s \cdot 3.143$$

Where

$t_{(n-1, 1-\alpha)}$ = Student's t value for the 99% confidence level with n-1 degrees of freedom

n = number of trials

s = standard deviation of the 7 trials

USEPA Method 524.2 (Revision 4, August 1992)

Roger L. Firor and Albert E. Gudat are Application Chemists at Agilent Technologies, Inc., USA.

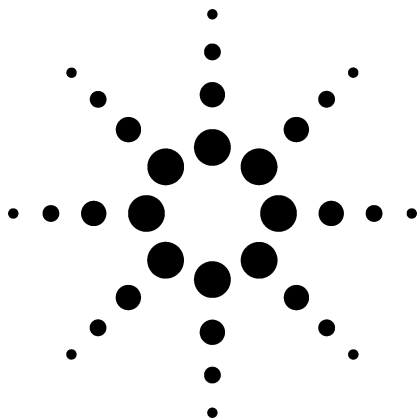
Ute Bober is Program Manager at Agilent Technologies, Waldbronn, Germany.

www.agilent.com/chem/pharmaqaqc

© 2007 Agilent Technologies, Inc.
Published February 15, 2007
Publication Number 5989-6023EN



Agilent Technologies



Headspace Analysis of Organic Volatile Impurities by USP <467> Using the DB-624 and the HP-Fast GC Residual Solvent Column

Application

Drug Manufacturing/QA/QC, Drug Testing, and Production-QA/QC

Authors

A. D. Broske, D. DiUbaldo, D. R. Gere
Agilent Technologies, Inc.
2850 Centerville Road
Wilmington, DE 19808-1610
USA

Abstract

The United States Pharmacopeia (USP) <467> specifies the gas chromatographic conditions, injection technique, and column type and dimensions for the analysis of organic volatile impurities (OVIs) in bulk pharmaceuticals and excipients. This USP method also specifies the maximum permissible levels of five solvents in pharmaceutical products. In this application, experimental conditions are described detailing the headspace analysis of these solvents using the Agilent 6890 GC and the standard dimension 3.0 μm DB-624 (G-43 equivalent phase) column. The work was extended to include the same analysis using the HP-Fast GC Residual Solvent column to reduce the separation time by almost a factor of three without loss of component resolution. Good linearity and precision are obtained over the concentration range of interest for both columns.

Introduction

USP <467> [1, 2] documents the methodologies for evaluating organic volatile impurities (OVI) present in pharmaceutical formulations and excipients.

This USP method details the use of three sample introduction techniques including direct (splitless) injection, described in Method components I and V; dynamic headspace (purge and trap) injection, described in Method components II and III; and static headspace, described in Method component IV. The USP Method specifies the analysis of five solvents and the maximum allowable concentrations. The solvents of interest include:

| | |
|--------------------|---------|
| Methylene chloride | 100 ppm |
| Benzene | 100 ppm |
| Trichloroethylene | 100 ppm |
| 1,4-Dioxane | 100 ppm |
| Chloroform | 50 ppm |

In the Gudat and Sievert [3] evaluation of static headspace and direct sample introduction techniques for these solvents, the authors concluded that even though both methods were acceptable for the analysis, the static headspace method was preferred because of increased sensitivity for chloroform. In addition, with the static headspace method, the GC system was not as easily contaminated, which reduced the need for routine maintenance [4].

Firor, et al. [5], showed that good precision and linearity were obtained for the five solvents when using short headspace heating times and vigorous agitation. Chang, et al. [6], and Brillante, et al. [7], showed that the optimized headspace conditions worked well for the efficient transfer of the solvents but selected the HP-INNOWax capillary



Agilent Technologies

column to do the separation. Although the stationary phase was not equivalent to the G-43 phase specified in the method (DB-624 column), the analysis time was short and the data demonstrated good precision and linearity.

Experimental

A standard stock solution of the five solvents was prepared as previously described [6]. One half gram (0.5 grams) of chloroform and one gram each of the other solvents was dissolved in 100 mL of methanol. The stock solution was stored in a refrigerator until needed. A series of working standards was prepared daily by diluting the equivalent of 2 µL to 200 µL of stock solution to 100 mL with organic-free 18 megohm water. For the GC analysis, 5 mL of each working standard was placed in a headspace vial containing 1.0 ±0.1 gram of anhydrous sodium sulfate and sealed immediately. The samples were mixed with a vortex mixer to dissolve any insolubles.

The Agilent 7694 headspace sampler equipped with a Silcosteel® transfer line was used as the injection device. The GC analysis was done using an Agilent 6890 GC. All headspace and GC operating conditions are listed in Table 1. Both the standard DB-624 column and a new HP-Fast GC Residual Solvent column designed for rapid solvent analysis were evaluated for this analysis.

Results and Discussion

The objectives of this work were to first verify the suitability of the standard DB-624 column that is equivalent to the G-43 phase for the analysis of the five solvents at the concentrations specified by USP <467>. Second, we wanted to evaluate the suitability of an HP-Fast GC Residual Solvent column for the analysis of these solvents to reduce the GC analysis time to less than 10 minutes.

Figure 1 shows a typical chromatogram of the OVI components obtained using the chromatographic

conditions and the standard G-43 column specified in the USP method. The sample analysis time including the headspace, GC analysis, and oven cooldown is complete in about 45 minutes. The oven ramp is slow at the beginning when the solvent peaks are eluting from the column then is ramped up quickly to remove less volatile components and clean the column before the next injection.

Table 1. Headspace and GC Operating Conditions

| Headspace conditions | |
|---|--|
| Carrier gas pressure: | 3.5 psi |
| Oven temp: | 85 °C |
| Loop temp: | 95 °C |
| Transfer line temp: | 110 °C |
| Vial pressure: | 10 psi |
| Vial equilibration time: | 10 min |
| Pressurization time: | 0.2 min |
| Loop fill time: | 0.15 min |
| Loop equilibration time: | 0.05 min |
| Injection time: | 1.00 min |
| GC Conditions using the standard G-43 (DB-624) column | |
| GC: | 6890 |
| Column: | DB-624, 30 m × 0.53 mm × 3.0 µm (part no. 125-1334) |
| Carrier: | Helium, 35 cm/min, constant flow |
| Oven: | 40 °C (5 min) to 90 °C at 2 °C/min 90 °C to 250 °C at 30 °C/min |
| Injection: | Headspace, 180 °C, split 7/1 |
| Detector: | FID, 260 °C |
| GC Conditions using the Fast G-43 (HP-Fast GC Residual Solvent) column | |
| GC: | 6890 |
| Column: | HP-Fast GC Residual Solvent Column (HP part no. 19095V-420) |
| Carrier: | Helium, 30 cm/min, constant flow |
| Oven: | 40 °C (1.7 min) to 90 °C at 6 °C/min 90 °C to 250 °C at 30 °C/min |
| Injection: | Headspace, 180 °C, split 7/1 |
| Detector: | FID, 260 °C |

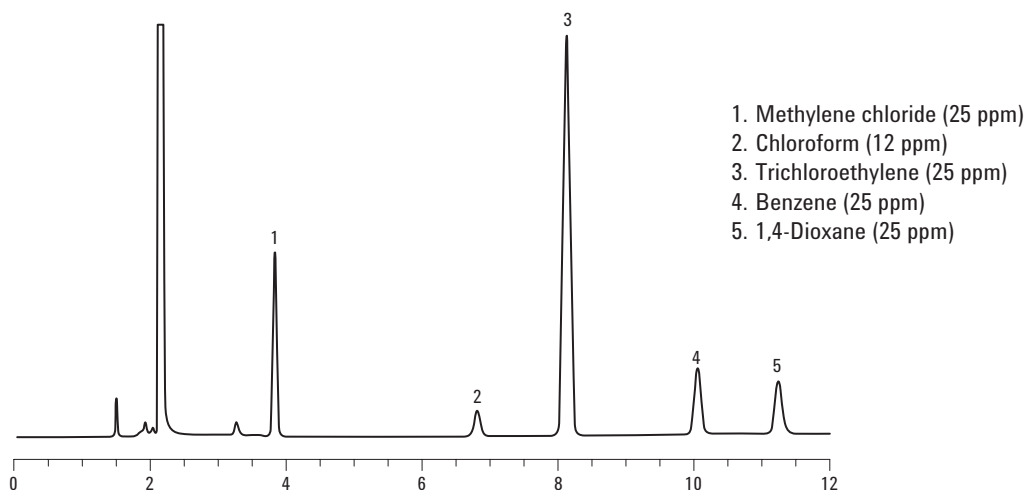


Figure 1. Headspace analysis of five organic volatile impurities using standard DB-624 column.

Table 2 shows a summary of the average area response and average %RSD calculated from the five replicate runs of each working standard for the concentration range shown. The average area responses for all the solvents were well below the range of 15% established by the USP method.

Table 2. Average Area Responses and Relative Standard Deviations

| | 2 ppm | 10 ppm | 25 ppm | 50 ppm | 100 ppm | 200 ppm | Avg. % RSD |
|--------------------|-------|--------|--------|--------|---------|---------|------------|
| Methylene chloride | 2.6 | 8.0 | 22.0 | 46.7 | 89.8 | 175.9 | 6.7 |
| Chloroform | 0.6 | 1.7 | 5.1 | 11.2 | 20.0 | 43.2 | 7.8 |
| Benzene | 8.8 | 30.0 | 88.9 | 201.9 | 392.1 | 805.4 | 5.4 |
| Trichloroethylene | 1.6 | 5.0 | 15.5 | 36.8 | 70.5 | 147.8 | 6.5 |
| 1,4-Dioxane | 1.8 | 5.8 | 15.2 | 31.6 | 66.3 | 129.9 | 8.0 |

Figure 2 shows the calibration curve for chloroform. Linear response over the specified range was evidenced by the good correlation coefficient.

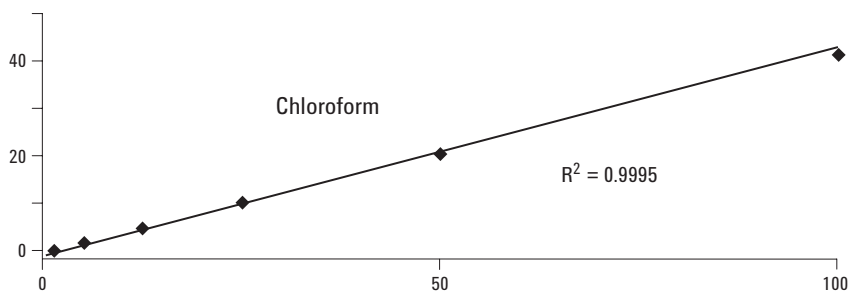


Figure 2. Calibration curve for chloroform.

Table 3 summarizes the calculated correlation coefficients and the estimated detection limits for the five solvents. The DB-624 column gave results within the allowable range set by the method.

Table 3. Correlation Coefficients and Calculated Minimum Detection Limits (S/N>3)

| | Concentration range, ppm | Correlation coefficient | MDL ppm |
|--------------------|--------------------------|-------------------------|---------|
| Methylene chloride | 2–200 | 0.9998 | 0.10 |
| Chloroform | 1–100 | 0.9995 | 0.70 |
| Benzene | 2–200 | 0.999 | 0.06 |
| Trichloroethylene | 2–200 | 0.9998 | 0.31 |
| 1,4-Dioxane | 2–200 | 0.9990 | 0.32 |

To demonstrate the utility of the DB-624 column, a sample containing 22 different common solvents was prepared. In the resulting chromatogram (Figure 3), most of the solvents are resolved from one another and all solvents elute from the column within approximately 15 minutes. The second goal of this analysis was to reduce the analysis time by a factor of two so the GC separation could be completed in approximately the same time as the head-space introduction. To this end, a capillary column was designed specifically to complete the separation in less time while maintaining the desired resolution but with a stationary phase equivalent to the G-43 phase described in USP <467>.

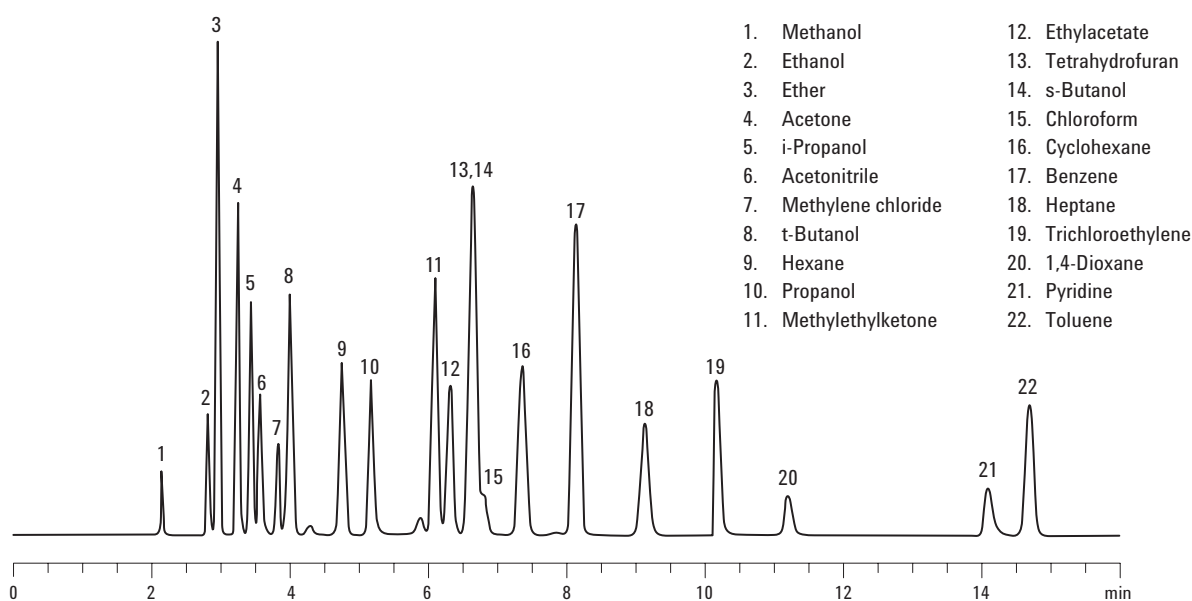


Figure 3. Solvent mixture on standard DB-624 column.

Figure 4 shows the analysis of the standard five solvents on the HP-Fast GC Residual Solvent column. The total analysis time including headspace, GC analysis, and oven cool-down is about 25 minutes. This is less than half the time required to complete the analysis on the standard (3.0 μm) DB-624 column. The reasons for the speed gain are the use of a faster temperature profile and a thinner stationary phase film thickness.

The performance of the HP-Fast GC Residual Solvent column was evaluated by correlation coefficients for the solvent calibration curves and peak area reproducibility. Calibration curves for each solvent were constructed using the same standard stock solutions and the same headspace conditions. The GC analysis was completed using the faster oven ramp detailed in Table 1.

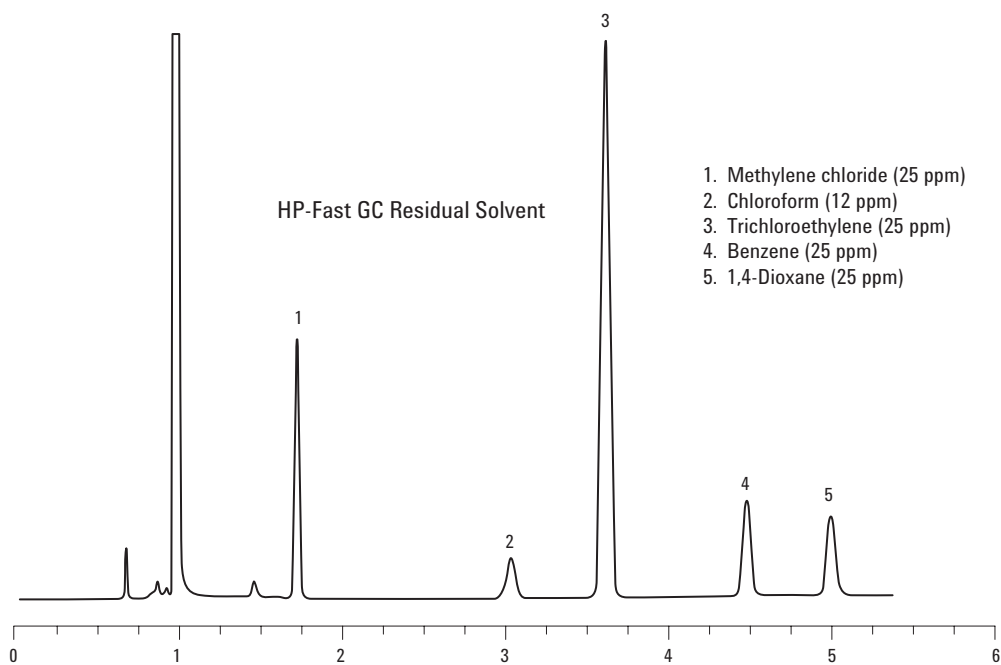


Figure 4. Headspace analysis of five organic volatile impurities using HP-Fast GC Residual Solvent column.

Table 4 shows a summary of the average area response %RSD calculated from the five replicate runs of each working standard for the concentration range shown on the HP-Fast GC Residual Solvent column. The average area responses for all five solvents on the HP-Fast GC Residual Solvent column were well below the range of 15% established by the USP method. In fact, the calculated values show slightly better reproducibility than the thicker film column.

Table 4 Average Area Responses and Relative Standard Deviations

| | 2 ppm | 10 ppm | 25 ppm | 50 ppm | 100 ppm | 200 ppm | Avg. % RSD |
|--------------------|-------|--------|--------|--------|---------|---------|------------|
| Methylene chloride | 5.4 | 19.8 | 54.0 | 106.3 | 201.4 | 387.1 | 3.2 |
| Chloroform | 1.4 | 4.3 | 10.9 | 20.9 | 39.1 | 77.4 | 4.1 |
| Benzene | 17.8 | 64.8 | 174.0 | 339.4 | 650.5 | 1295.2 | 4.6 |
| Trichloroethylene | 4.3 | 11.4 | 28.3 | 55.8 | 109.1 | 220.9 | 6.8 |
| 1,4-Dioxane | 1.1 | 5.5 | 14.8 | 31.5 | 64.4 | 127.9 | 2.9 |

Figure 5 shows the calibration curve for chloroform as an example. Linear response over the specified range was evidenced by the good correlation coefficient. Here again the fast column gave slightly better linearity (higher correlation coefficients and estimated detection limits) than the standard column.

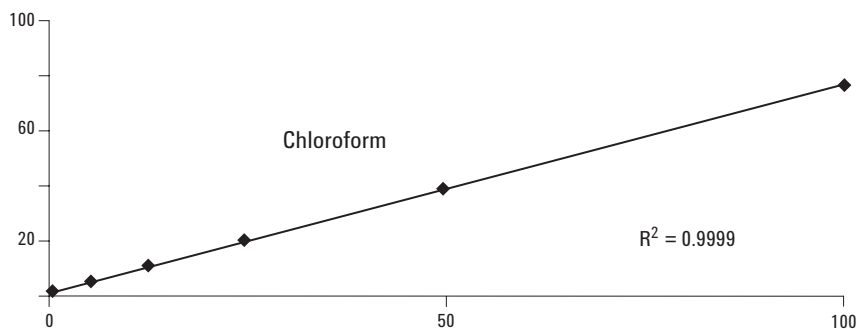


Figure 5. Calibration curve for chloroform on the HP-Fast GC Residual Solvent column.

Table 5 summarizes calculated correlation coefficients and an estimate of the detection limits for the solvents of interest.

Table 5. Correlation Coefficients and Calculated Minimum Detection Limits (S/N>3)

| | Concentration range, ppm | Correlation coefficient | MDL ppm |
|--------------------|--------------------------|-------------------------|---------|
| Methylene chloride | 2–200 | 0.9996 | 0.05 |
| Chloroform | 1–100 | 0.9999 | 0.28 |
| Benzene | 2–200 | 0.9999 | 0.04 |
| Trichloroethylene | 2–200 | 0.9999 | 0.18 |
| 1,4-Dioxane | 2–200 | 0.9999 | 0.17 |

Another benefit of using the HP-Fast GC Residual Solvent column is that the peak widths are about one third of the peak width of the same component on the standard column. The reduced peak width resulted in the reduction of the minimum detectable amount of each one of the five solvents when the HP-Fast GC Residual Solvent column was used.

Figure 6 shows an example of a mixture of 22 different solvents on the HP-Fast GC Residual Solvent column. All separations were completed in approximately 6 minutes without loss of component resolution.

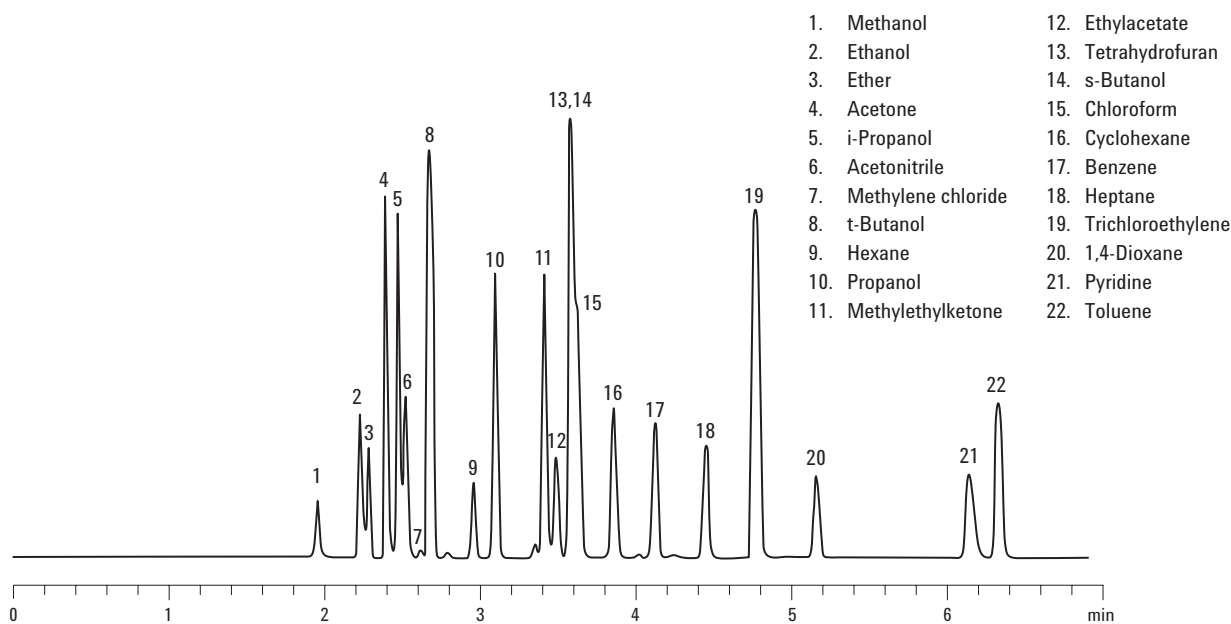


Figure 6. Solvent mixture on the HP-Fast GC Residual Solvent column.

Conclusion

The use of the standard DB-624 column with the Agilent 7694 headspace sampler and the Agilent 6890 GC resulted in the accurate and precise determination of the solvents specified in USP <467>. To reduce analysis times, the HP-Fast GC Residual Solvent column was developed. Using this column reduced analysis times by one half and actually provided better quantitation and lower detection limits.

References

1. Organic Volatile Impurities <467>, USP 32-NF 18, pp. 1746-1748, 1995.
2. Organic Volatile Impurities <467>, USP 32-NF 18, Sixth Supplement, pp. 3766-3768.
3. A. E. Gudat and H. J. P. Sievert, "Analysis of Volatile Compounds in Excipient Materials," Hewlett-Packard Company, Application Note 228-208, Publication No. 5091-5610E, October 1992.
4. K. J. Dennis, P. A. Josephs, and J. Dokladalova, "Proposed Automated Headspace Method for Organic Volatile Impurities <467> and Other Solvents," Pharmacopeial Forum, 18, 2962 (1992).
5. R. L. Firor, P. L. Wylie, L. Cobelli, and M. Bergna, "Performing USP Method <467> Using the HP 7694 Headspace Sampler," Hewlett-Packard Company, Application Note 228-237, Publication No. 5091-7757E, May 1993.

6. I. L. Chang, D. DiUbaldo and W. J. Sanders, "Headspace Analysis of Organic Volatile Impurities in Bulk Pharmaceutical Chemicals," Hewlett-Packard Company, Application Note 228-255, Publication No. 5091-9661E, January 1994.
7. S. M. Brillante, R. L. Firor, P. L. Wylie, I. L. Chang and D. DiUbaldo, "USP Headspace Analysis of Organic Volatile Impurities in Bulk Pharmaceutical Chemicals," Hewlett-Packard Company, Application Note 228-309, Publication No. 5963-7109E, July 1995.

For More Information

For more information on our products and services, visit our web site at www.agilent.com/chem.

Agilent shall not be liable for errors contained herein or for incidental or consequential damages in connection with the furnishing, performance, or use of this material.

Information, descriptions, and specifications in this publication are subject to change without notice.

Silcosteel® is a registered trademark of the Restek Corporation.

© Agilent Technologies, Inc. 2002

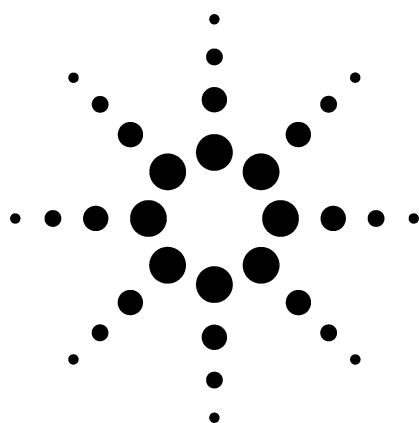
Printed in the USA
January 8, 2003
5988-8387EN



Agilent Technologies

A Unified Gas Chromatography Method for Aromatic Solvent Analysis

Application



Gas Chromatography

Author

James D. McCurry
Agilent Technologies, Inc.
2850 Centerville Rd.
Wilmington DE 19808
USA

Abstract

A single, easy-to-use GC method for aromatic solvent purity analysis is described that meets the chromatographic requirements of ten separate ASTM methods. This method can be used to obtain identical results on both the Agilent 6890 and 6850 Series Gas Chromatographs designed for the method development lab and the routine production lab respectively. Reproducibility of results between instruments, between labs, and over time are further improved by applying the technique of retention time locking to this unified method.

Introduction

The producers and users of many aromatic hydrocarbons evaluate the product quality by measuring the purity of the material along with specific contaminants. For these types of measurements the most commonly used analysis technique is gas chromatography (GC). In an effort to standardize analysis procedures, the American Society of Testing and Materials (ASTM) has developed and

published a number of GC methods specific to an aromatic compound or class of compounds.¹ These methods have evolved over time to meet the requirements of new materials specifications or to incorporate new GC technologies (i.e. capillary columns replacing packed columns). The result of this evolution is a large number of methods that are remarkably alike. In practice, many QA laboratories that support a variety of chemical processes typically devote one GC instrument to each ASTM method they must run.

Recently, there has been a move by many chemical companies to consolidate lab facilities, simplify measurements, and reduce the costs that chemical measurements add to production. Laboratory space is expensive and is becoming limited. Where three or four GCs were operating in the past, there is now only space and budget for one or two. Another part of this trend is to have non-traditional personnel such as plant operators; technicians and engineers perform chemical analyses. Since these personnel are not trained as analytical chemists, simpler methods are needed to perform the analyses without losing measurement performance.

Accommodating these changes in the lab environment makes it necessary to explore alternative approaches to performing GC analyses. One approach is to develop a method that combines the elements of several separate ASTM methods.



Agilent Technologies

A single method has a number of advantages over multiple methods. Fewer GCs could be used in place of a larger number of instruments previously dedicated to individual methods; thus reducing required lab space. By running one method, any GC could also serve as a backup for instruments that are undergoing maintenance or repair. This would result in shorter down times and better utilization of lab space. A single method would also eliminate the need to stock multiple columns and supplies. Plant operators would also find it easier to use since they would only need to be trained once on a single procedure.

Another important advantage to a single aromatics method lies in the use of retention time locking (RTL). RTL is a technique that allows any Agilent 6890 or 6850 GC systems running the same method to obtain nearly identical retention times. Comparing data between instruments, between laboratories, or over time can be difficult due to variations in retention times. This is further complicated when using multiple methods since the

different columns and operating conditions result in different retention times for the same compound. For instance, there are eight ASTM methods that measure p-xylene; however, p-xylene retention times range from 6 to 16 minutes depending on the method's operating conditions (column, flow, temperature). By using one method for all aromatic samples, retention time variations can be reduced to less than 0.5 minutes. Then by applying RTL to this method, system-to-system retention time variations can be further reduced to less than 0.03 minutes. Retention time precision on this order greatly simplifies comparison of data between systems, between laboratories, and over time.

This application note describes a GC method that is chromatographically suitable for a wide range of samples typically analyzed by ten different ASTM methods. Table 1 lists these ten methods along with the ASTM recommended columns and reporting specifications.

Table 1. Ten ASTM Methods for the GC Analysis of Aromatic Solvents

| ASTM Method | Title | Liquid phase | Column type | Report specifications |
|--------------------|---|-----------------------------|-----------------------------|--|
| D2306 | Std Test for C8 Aromatic Hydrocarbons | 0.25 µm Carbowax | Capillary 50 m × 0.25 mm | wt% of individual C8 HC |
| D2360 | Std Test for Trace Impurities in Monocyclic Hydrocarbons | 0.32 µm Carbowax | Capillary 60 m × 0.32 mm | wt% of individual aromatic impurities, total impurities, purity |
| D3760 | Std Test for Cumene | 0.25 µm Carbowax | Capillary 50 m × 0.32 mm | wt% of individual impurities, cumene purity (wt%) |
| D3797 | Std Test for o-Xylene | 0.5 µm Carbowax | Capillary 60 m × 0.32 mm | wt% of individual impurities, o-xylene purity (wt%) |
| D3798 | Std Test for p-Xylene | 0.25 µm Carbowax | Capillary 50 m × 0.32 mm | wt% of individual impurities, total impurities, p-xylene purity (wt%) |
| D4492 | Std Test for Benzene | 0.25 µm Carbowax | Capillary 50 m × 0.32 mm | wt% of individual impurities, benzene purity(wt%) |
| D4534 | Std Test for Benzene in Cyclic Products | 10%TCEPE on Chromasorb P | Packed 3.7 m × 3.175 mm | wt% of benzene |
| D5060 | Std Test for Impurities in Ethylbenzene | 0.5 µm Carbowax | Capillary 60 m × 0.32 mm | wt% of individual impurities, ethylbenzene purity |
| D5135 | Std Test for Styrene | 0.5 µm Carbowax | Capillary 60 m × 0.32 mm | wt% of individual impurities, styrene purity |
| D5917 | Std Test for Trace Impurities in Monocyclic Hydrocarbons (ESTD Cal) | 0.25 µm Carbowax | Capillary 60 m × 0.32 mm | wt% individual impurities, wt% total non-aromatics, wt% total C9 aromatics, purity of main component |

Experimental

Two Agilent 6890 Plus Series gas chromatographs and four Agilent 6850 gas chromatographs were used for this work. Each GC was equipped with a split/splitless capillary inlet, a flame ionization detector (FID) and an Agilent 7683 Automatic Liquid Sampler (ALS). The split/splitless inlets were fitted with high-pressure Merlin Microseal Septa (Agilent Part no. 5182-3442) and spilt-optimized liners (Agilent Part no. 5183-4647). Injections were made using 10 μ L gas-tight syringes (Agilent Part no. 5181-8809) designed for use with the Merlin Microseal. Table 2 lists the instrument conditions used for this method. An Agilent Chemstation was used for all instrument control, data acquisition and data analysis.

Table 2. Conditions for Unified Aromatic Solvents Method

| | |
|-------------------|---|
| Column | HP-Innowax, 60 m \times 0.32 mm \times 0.5 μ m Agilent Part no.19091N-216 |
| Carrier Gas Inlet | Helium @ 20.00 psi constant pressure mode Split/Splitless @ 250 $^{\circ}$ C 100:1 to 400:1 split ratio |
| Oven Temp | 75 $^{\circ}$ C (10 min); 3 $^{\circ}$ C/min to 100 $^{\circ}$ C (0 min) 10 $^{\circ}$ C/min to 145 $^{\circ}$ C (0 min) |
| Detector | FID @ 250 $^{\circ}$ C Data acquisition rate @ 20 Hz |
| Injection Size | 0.1 to 1.0 μ L |

An n-hexane solution was prepared containing 0.1 wt% of all the aromatic solvents and impurities specified for analysis by the ten ASTM methods listed in Table 1. This standard was used to develop the RTL calibration and to assess the separation of each compound. Final evaluation of this unified method was done by running the recommended standards specified in each of the ten ASTM methods.

Results and Discussion

Figure 1 shows a chromatogram of the hexane solution containing an aggregate of aromatic solvents and impurities. For most compounds, baseline resolution was achieved. There are two pairs that are only partially resolved. The first pair, p-ethyltoluene and m-ethyltoluene, are also not resolved in the original ASTM method (D-5060 Impurities in ethylbenzene) and, along with o-ethyltoluene, are reported as total ethyltoluene. Therefore, the results presented here represent the same result obtained with the original ASTM method. A second pair, diethylbenzene and n-butylbenzene are also only partially resolved. Again, this does not present a problem since these two components are not typically found together in the same material. Diethylbenzene is sometimes found as a contaminant in ethylbenzene (ASTM D-5060) while n-butylbenzene is used as the internal standard for cumene analysis (ASTM D3760).

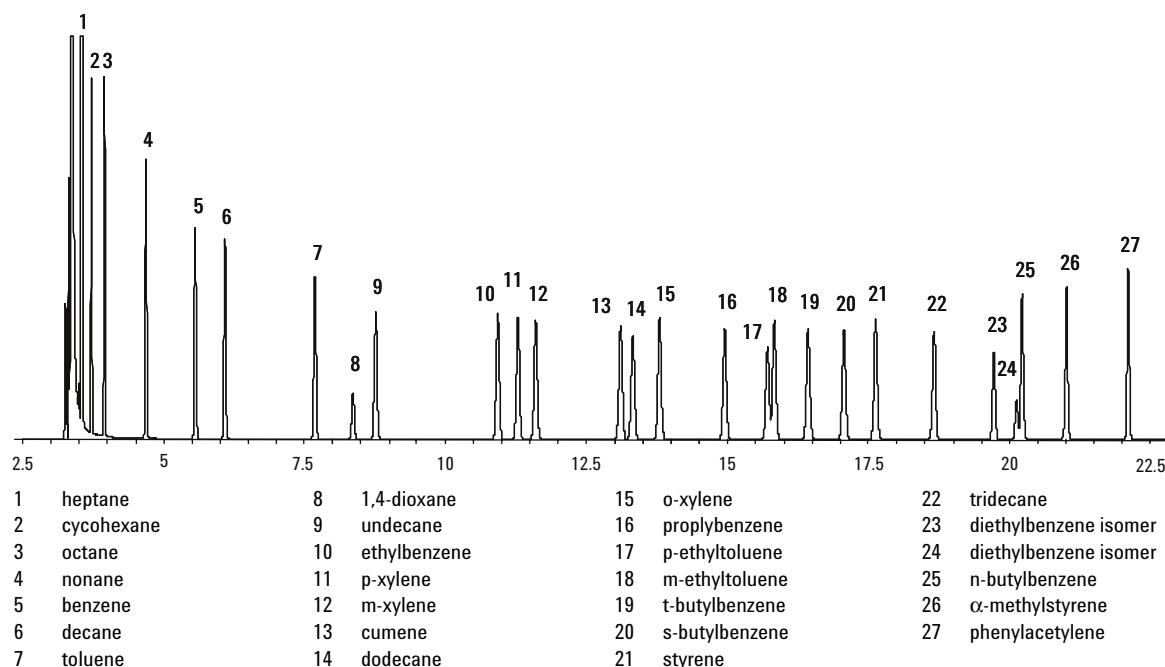


Figure 1. Separation of the 27 compounds analyzed by the ten ASTM aromatics methods listed in Table 1.

Retention Time Locking (RTL)

Retention time locking calibration was performed using t-butylbenzene as the target peak. Figure 2 shows the five RTL calibration runs with the retention times of t-butylbenzene indicated and Figure 3 shows the RTL calibration. These calibration runs do not have to be repeated by anyone wishing to lock this method on their Agilent 6890 or 6850 GC

systems. To use this RTL calibration, simply create a new method with conditions outlined in Table 2, then use the Chemstation RTL software to create a new RTL calibration and enter the data shown in Figure 3. The GC can then be locked by running a sample containing t-butylbenzene and using the RTL software to re-lock the method. The general theory and use of RTL is detailed in previous publications.²

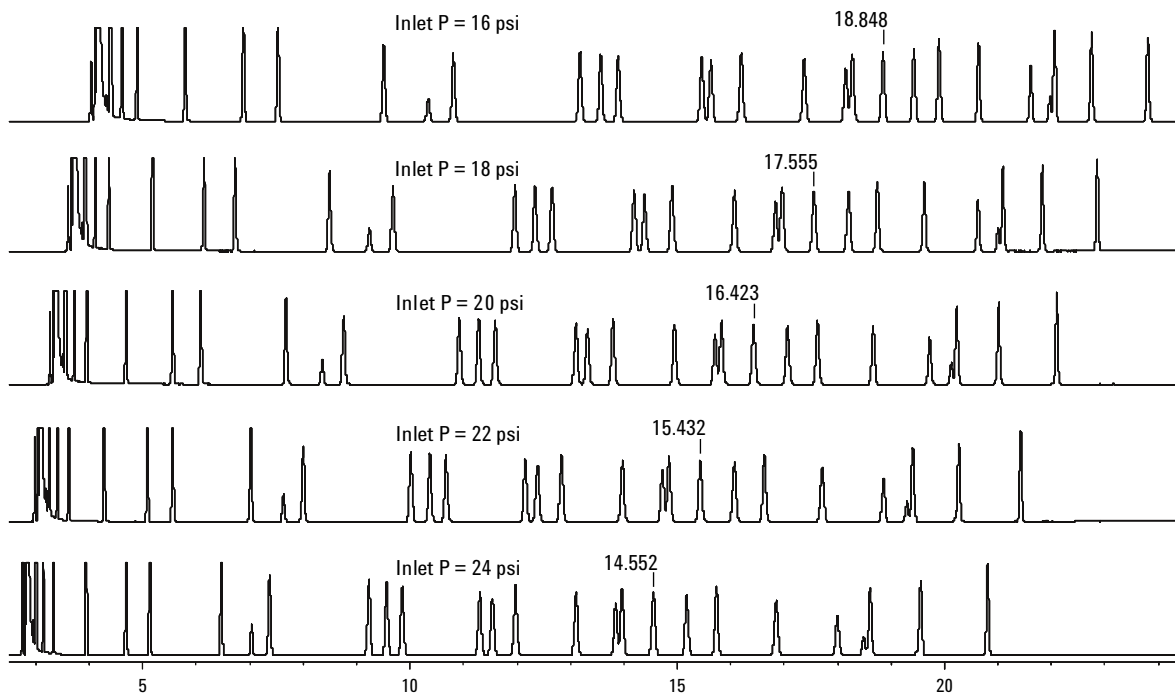


Figure 2. Retention time locking calibration runs using t-butylbenzene as the RTL target peak.

| Run | Pressure | Ret Time |
|-------|----------|----------|
| Run 1 | 16 | 18.849 |
| Run 2 | 18 | 17.555 |
| Run 3 | 20 | 16.423 |
| Run 4 | 22 | 15.432 |
| Run 5 | 24 | 14.552 |

Pressure Units: psi

Desired Ret Time: 16.423

Min relock pressure: 15

Max relock pressure: 25

Compound Name: t-Butylbenzene

Figure 3. Retention time locking calibration using t-butylbenzene as the RTL target peak.

A total of six GC systems, two 6890s and four 6850s, were configured to run this unified method. Each GC was retention time locked using a t-butylbenzene target retention time of 16.423 minutes. Figure 4 shows an overlay of the locked chromatograms from each of the six GCs. Table 3 lists the retention times and precision of each compound in the standard mix. Excellent retention time precision was observed for the 6890 and 6850 instruments across the entire time range of the chromatographic run. Peaks falling within the initial 10-minute isothermal time had a standard deviation of about 0.02 minutes. Those peaks eluting during the 3 °C/min program ramp had a standard deviation of 0.01 minutes and those eluting in the 10 °C/min ramp showed a standard deviation of 0.03 minutes

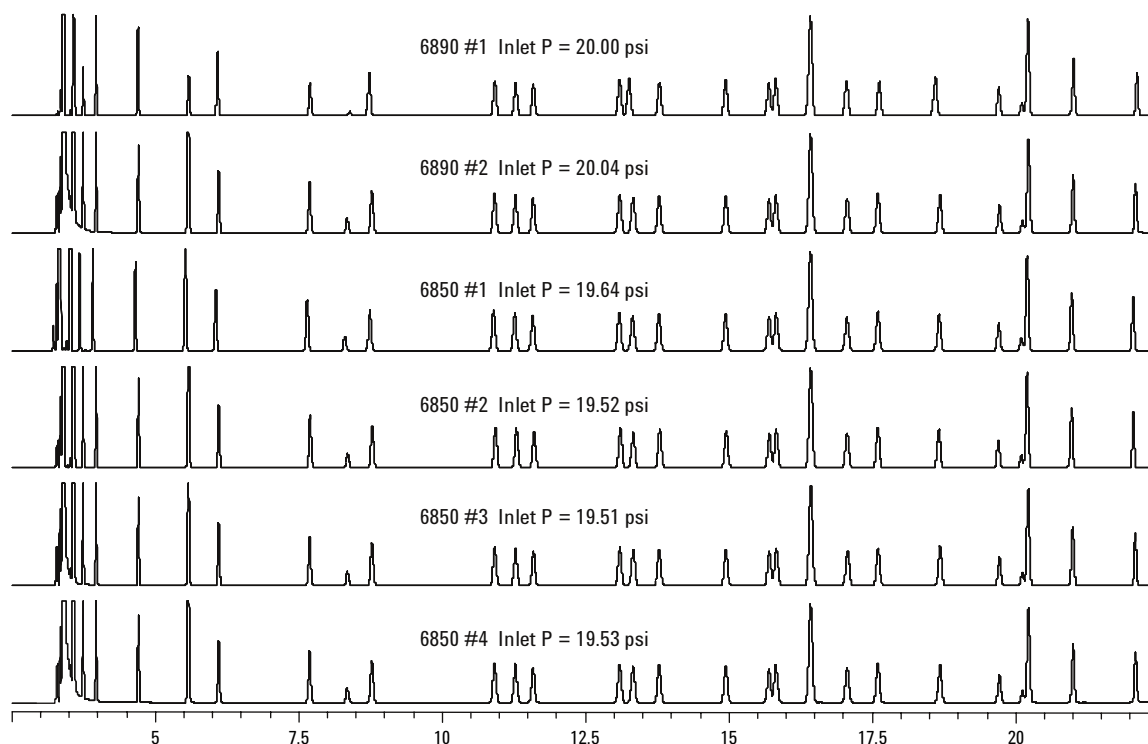


Figure 4. Using RTL, excellent retention time precision was observed for all 27 compounds analyzed using the unified aromatics method. Details of retention time precision are listed in Table 3.

Table 3. Retention Time Precision for Each Compound Analyzed by the Unified Method

| Compound | Retention time (min) | | | | | | Std Dev | Range |
|-------------------------|----------------------|---------|---------|---------|---------|------------|--------------|--------------|
| | 6890 #1 | 6890 #2 | 6850 #1 | 6850 #2 | 6850 #3 | 6850 #4 | | |
| heptane | 3.572 | 3.568 | 3.508 | 3.569 | 3.566 | 3.568 | 0.025 | 0.064 |
| cyclohexane | 3.745 | 3.742 | 3.682 | 3.743 | 3.741 | 3.742 | 0.025 | 0.063 |
| octane | 3.969 | 3.971 | 3.911 | 3.972 | 3.970 | 3.971 | 0.024 | 0.061 |
| nonane | 4.696 | 4.704 | 4.646 | 4.705 | 4.703 | 4.704 | 0.023 | 0.059 |
| benzene | 5.581 | 5.572 | 5.518 | 5.576 | 5.572 | 5.572 | 0.023 | 0.063 |
| decane | 6.084 | 6.105 | 6.053 | 6.106 | 6.104 | 6.105 | 0.021 | 0.053 |
| toluene | 7.694 | 7.686 | 7.646 | 7.695 | 7.687 | 7.686 | 0.018 | 0.049 |
| 1,4-dioxane | 8.386 | 8.342 | 8.306 | 8.350 | 8.346 | 8.342 | 0.025 | 0.080 |
| undecane | 8.732 | 8.776 | 8.741 | 8.782 | 8.777 | 8.776 | 0.022 | 0.050 |
| ethylbenzene | 10.922 | 10.915 | 10.899 | 10.932 | 10.918 | 10.915 | 0.011 | 0.033 |
| p-xylene | 11.282 | 11.278 | 11.267 | 11.295 | 11.280 | 11.278 | 0.009 | 0.028 |
| m-xylene | 11.592 | 11.587 | 11.577 | 11.604 | 11.589 | 11.587 | 0.009 | 0.027 |
| cumene | 13.097 | 13.097 | 13.089 | 13.110 | 13.098 | 13.097 | 0.007 | 0.021 |
| dodecane | 13.264 | 13.334 | 13.323 | 13.337 | 13.333 | 13.334 | 0.028 | 0.073 |
| o-xylene | 13.790 | 13.781 | 13.778 | 13.795 | 13.782 | 13.781 | 0.007 | 0.017 |
| propylbenzene | 14.940 | 14.943 | 14.939 | 14.951 | 14.945 | 14.943 | 0.004 | 0.012 |
| p-ethyltoluene | 15.696 | 15.699 | 15.699 | 15.706 | 15.702 | 15.699 | 0.003 | 0.010 |
| m-ethyltoluene | 15.819 | 15.820 | 15.820 | 15.827 | 15.823 | 15.820 | 0.003 | 0.008 |
| t-butylbenzene | 16.423 | 16.424 | 16.420 | 16.426 | 16.426 | 16.424 | 0.002 | 0.006 |
| s-butylbenzene | 17.049 | 17.060 | 17.053 | 17.059 | 17.063 | 17.060 | 0.005 | 0.014 |
| styrene | 17.623 | 17.600 | 17.600 | 17.600 | 17.603 | 17.600 | 0.009 | 0.023 |
| tridecane | 18.602 | 18.683 | 18.665 | 18.661 | 18.681 | 18.683 | 0.031 | 0.081 |
| diethylbenzene | 19.707 | 19.718 | 19.701 | 19.700 | 19.713 | 19.718 | 0.008 | 0.018 |
| diethylbenzene | 20.111 | 20.123 | 20.101 | 20.101 | 20.116 | 20.123 | 0.010 | 0.022 |
| n-butylbenzene | 20.217 | 20.225 | 20.201 | 20.203 | 20.219 | 20.225 | 0.011 | 0.024 |
| α -methylstyrene | 21.011 | 21.003 | 20.976 | 20.975 | 20.994 | 21.003 | 0.015 | 0.036 |
| phenylacetylene | 22.115 | 22.090 | 22.050 | 22.050 | 22.081 | 22.090 | 0.025 | 0.065 |
| | | | | | | Avg | 0.015 | 0.039 |

For this method it is not always necessary to use t-butylbenzene to perform retention time locking. Analysts who want to use this method for samples not containing t-butylbenzene can select another compound as the RTL target peak. Compounds that do not elute near temperature program transitions can serve as RTL target peaks. Table 4 lists the other suitable RTL target compounds along with the retention time data for constructing alternate RTL calibrations for this method. For instance, if one were preparing the benzene standard prescribed by ASTM method D4492, the toluene in that standard could serve as the RTL target compound. It is not necessary to perform the five RTL calibration runs. Simply create a new RTL calibration using the inlet pressures and toluene retention times from Table 4. This example of an RTL calibration using toluene is shown in Figure 5.

Table 4. Retention Time Locking Calibration Data for Unified Aromatics Method

| Compound | Retention time (min) at each inlet pressure | | | | |
|-----------------|---|-----------|-----------|-----------|-----------|
| | 16.00 psi | 18.00 psi | 20.00 psi | 22.00 psi | 24.00 psi |
| nonane | 5.794 | 5.174 | 4.682 | 4.279 | 3.943 |
| benzene | 6.880 | 6.143 | 5.558 | 5.080 | 4.681 |
| toluene | 9.507 | 8.489 | 7.680 | 7.018 | 6.468 |
| cumene | 15.460 | 14.188 | 13.100 | 12.148 | 11.305 |
| o-xylene | 16.189 | 14.897 | 13.791 | 12.825 | 11.969 |
| propylbenzene | 17.370 | 16.064 | 14.646 | 13.968 | 13.100 |
| t-butylbenzene* | 18.849 | 17.555 | 16.423 | 15.432 | 14.552 |
| s-butylbenzene | 19.424 | 18.201 | 17.061 | 16.063 | 15.176 |
| n-butylbenzene | 22.054 | 21.090 | 20.220 | 19.404 | 18.607 |
| styrene | 19.891 | 18.743 | 17.620 | 16.621 | 15.733 |
| α-methylstyrene | 22.745 | 21.824 | 21.010 | 20.261 | 19.552 |
| phenylacetylene | 23.795 | 22.852 | 22.097 | 21.421 | 20.800 |

*t-butylbenzene used as RTL target peak for this publication (target RT = 16.423 min).

Figure 5. Alternate retention time locking calibration for the unified aromatics method that uses toluene as the locking target compound.

Evaluation of Calibration Standards

The calibration standards specified by each of the ten ASTM methods were prepared and run using this unified method. Each standard was run with Agilent 6890 and Agilent 6850 series gas chromatographs that were retention time locked using t-butylbenzene as the target peak (RT = 16.423 min.).

D2306 - Standard Test for C8 Aromatic Hydrocarbons

Figure 6 shows the chromatograms of the D2306 calibration standard run on Agilent 6890 and 6850 gas chromatographs. The injection size for both runs was 0.1 µL and the split ratio was 400:1.

D2360 - Standard Test for Trace Impurities in Monocyclic Hydrocarbons

The standard calibration mix specified by D2360 was prepared in p-xylene. Figure 7 shows the chromatograms of the D2360 calibration standard. Injection size was 1.0 µL and the split ratio was 100:1. The ethylbenzene peak (RT = 10.98 min) elutes just before p-xylene and was much broader than the other contaminants. This peak shape was due to a reverse solvent effect caused by the overloaded p-xylene along with an oven starting temperature (75 °C) that was much lower than the p-xylene boiling point (138 °C). A broad ethylbenzene peak was also observed in the original ASTM D2360 method.³

D3760 - Standard Test for Analysis of Isopropylbenzene (Cumene)

Figure 8 shows the chromatograms of the D3760 calibration standard. The injection size for both runs was 1.0 µL and the split ratio was 100:1. The xylene isomers' concentrations were not listed because they were not added to the standard, but were present as trace contaminants in the cumene used to prepare the standard. Since both GCs are retention time locked, the identification of each xylene isomer could be easily made.

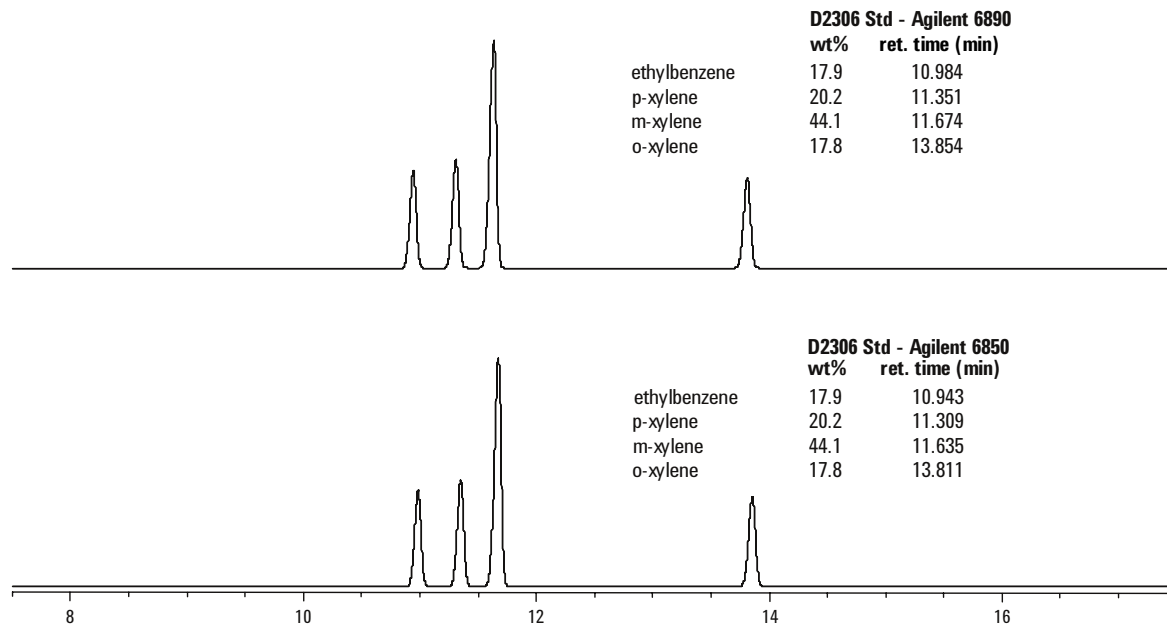


Figure 6. ASTM D2306 C8 aromatic hydrocarbon quantitative calibration standard run on Agilent 6890 (top) and 6850 (bottom) using the retention time locked unified aromatics method.

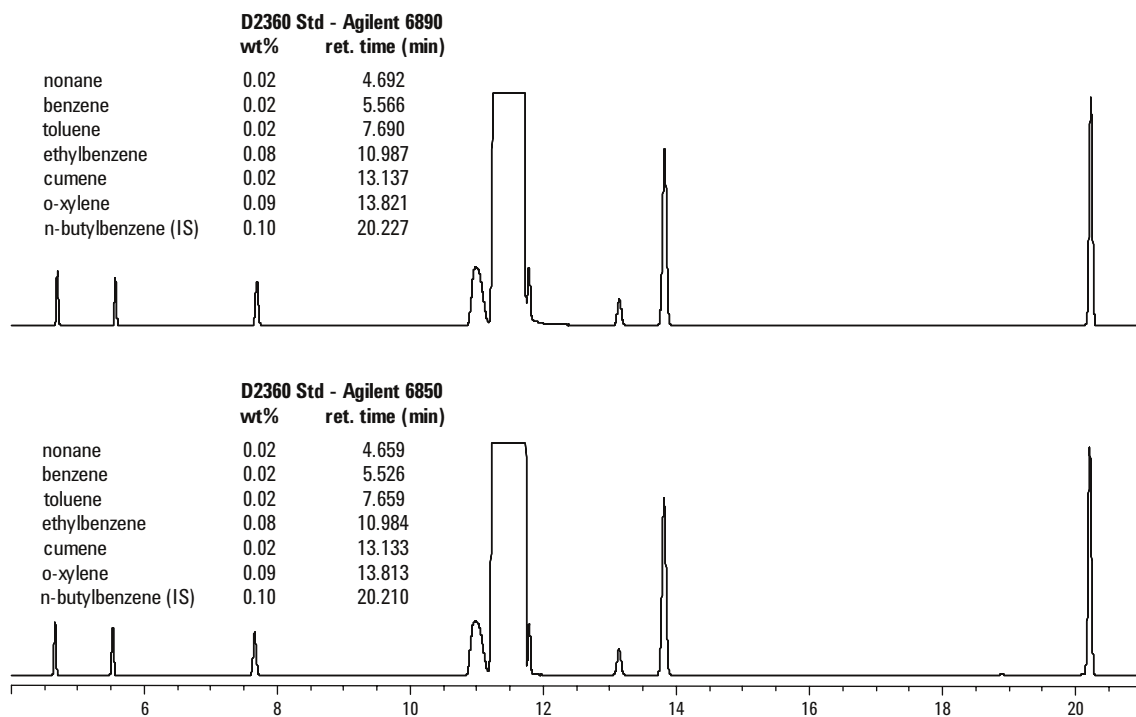


Figure 7. ASTM D2360 monocyclic hydrocarbon quantitative calibration standard run on Agilent 6890 (top) and 6850 (bottom) using the retention time locked unified aromatics method.

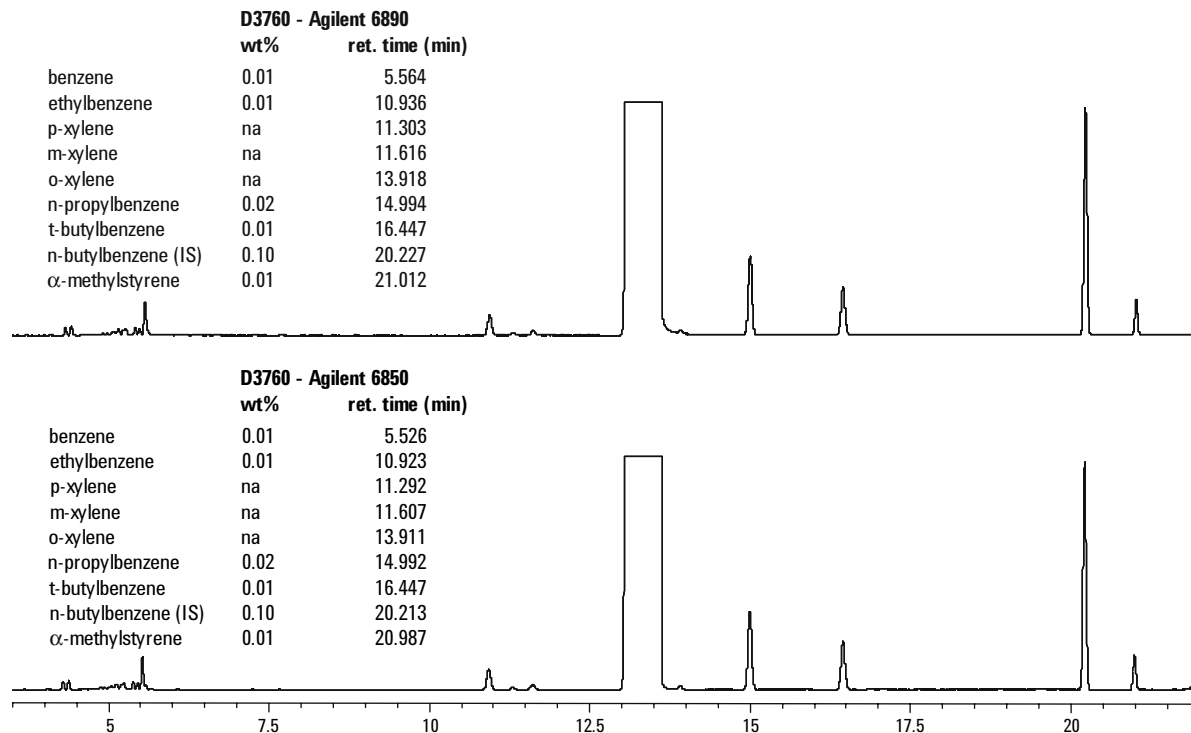


Figure 8. ASTM D3760 isopropylbenzene (cumene) quantitative calibration standard run on Agilent 6890 (top) and 6850 (bottom) using the retention time locked unified aromatics method.

D3797 - Standard Test Method for Analysis of o-Xylene

Figure 9 shows the chromatograms of the D3797 calibration standard. The injection size was 1.0 μ L and the split ratio was 100:1. The broadening of the cumene peak (RT = 13.28 min) was due to the reverse solvent effect of the overloaded o-xylene peak. This was also observed in the original ASTM D3797 method.

D3798 - Standard Test Method for Analysis of p-Xylene

Figure 10 shows the chromatograms of the D3798 calibration standard. The injection size was 1.0 μ L and the split ratio was 100:1. The ethylbenzene

peak shows the same broadening observed in the D2360 standard. The original ASTM D3798 method specifies that the valley points between the large p-xylene peak and the ethylbenzene and m-xylene contaminants should be less than 50% of the contaminants' peak height. Figure 11 shows the details of this separation using the unified method. For each GC this requirement was met for both the ethylbenzene and the m-xylene.

D4492 - Standard Test for Analysis of Benzene

Figure 12 shows the chromatograms of the D4492 calibration standard. The injection size was 1.0 μ L and the split ratio was 100:1.

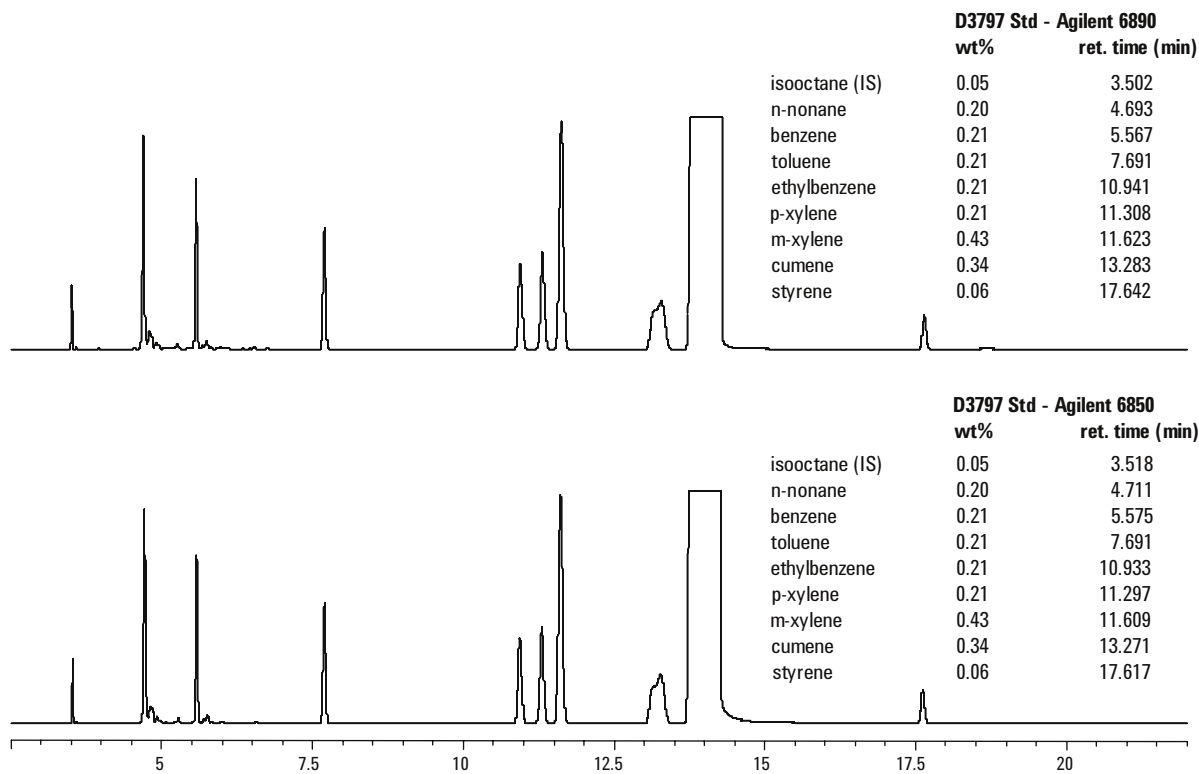


Figure 9. ASTM D3797 o-xylene quantitative calibration standard run on Agilent 6890 (top) and 6850 (bottom) using the retention time locked unified aromatics method.

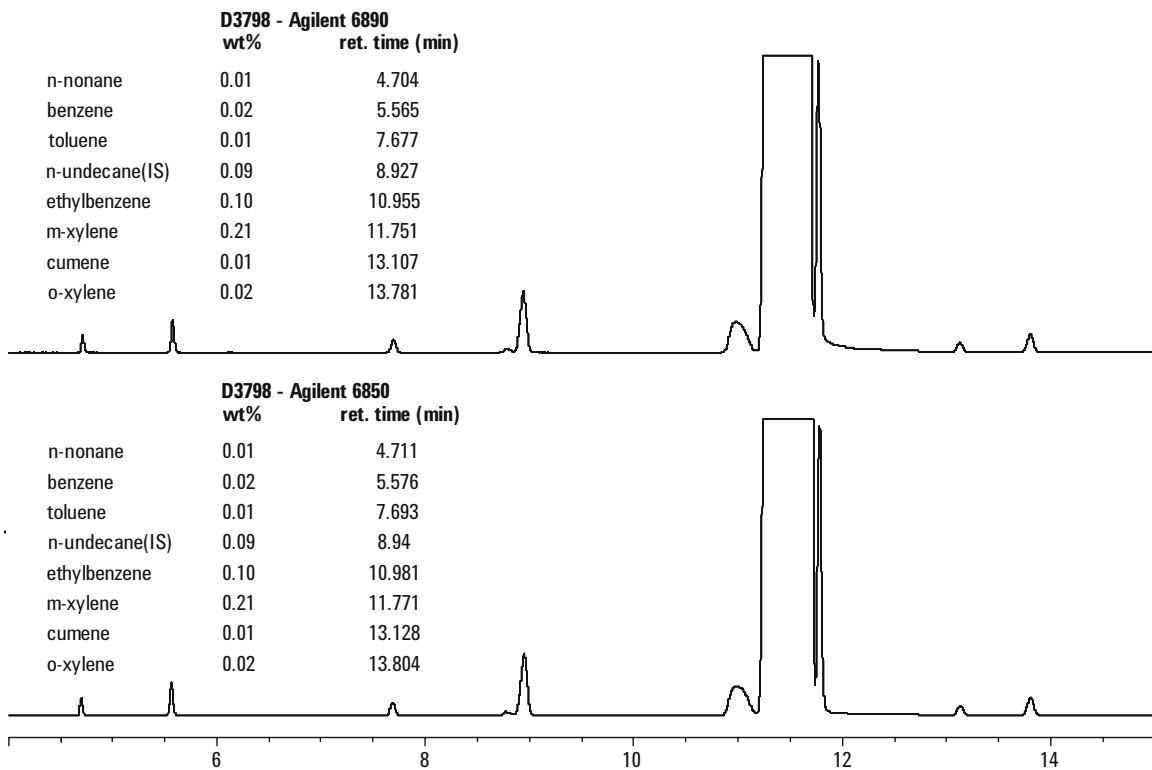


Figure 10. ASTM D3798 p-xylene quantitative calibration standard run on Agilent 6890 (top) and 6850 (bottom) using the retention time locked unified aromatics method.

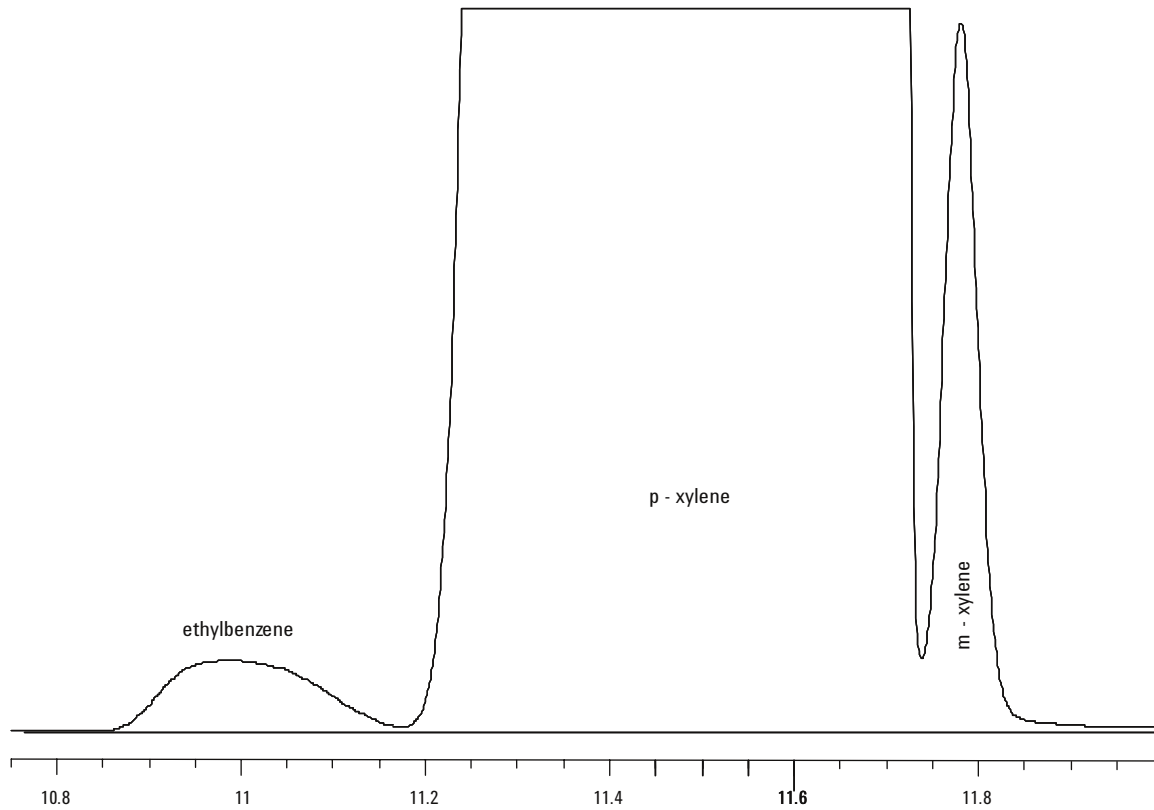


Figure 11. Expanded view from Figure 10 shows excellent separation of m-xylene from p-xylene peak using the unified aromatics method.

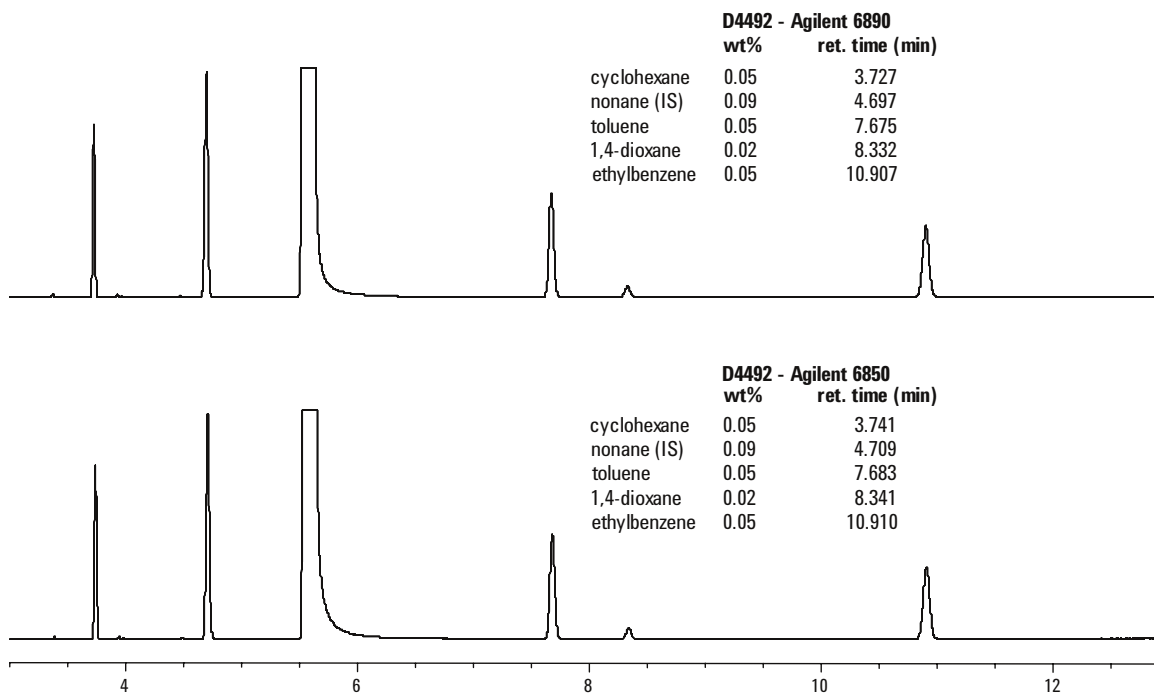


Figure 12. ASTM D4492 benzene quantitative calibration standard run on Agilent 6890 (top) and 6850 (bottom) using the retention time locked unified aromatics method.

D4534 Standard Test Method of Benzene Content of Cyclic Products - Cyclohexane

Figure 13 shows the chromatograms of the D4534 calibration standard containing 8 mg/kg (ppm) benzene in cyclohexane. The injection size was 1.0 μ L and the split ratio was 100:1.

D4534 Standard Test Method of Benzene Content of Cyclic Products - Toluene

Figure 14 shows the chromatograms of the D4534 calibration standard containing 9 mg/kg (ppm) benzene in toluene. The injection size was 1.0 μ L and the split ratio was 100:1. Several contaminants were found in the toluene used to prepare this standard. Most of these contaminants were identified, but the peak at 15.3 minutes did not correspond to the retention times of those listed in Table 3. If the GC systems were not retention time

locked, one might assume that this contaminant could be n-propylbenzene or p-ethyltoluene. However, given the retention time precision expected with RTL, it is clear that this contaminant is an unknown.

GC/MS is the best approach to identify this unknown, but under the same GC conditions, GC/MS retention times are often considerably faster than those obtained using atmospheric detectors. However, by combining retention time locking with a technique called method translation, one can obtain GC/MS retention times nearly identical to those found with conventional GC.⁴ This makes identifying unknown peaks much easier. Figure 15 shows the D4534 toluene standard run on both the Agilent 6850 and the Agilent 5973 GC/MS. A mass spectral library search of the unknown peak at 15.320 minutes identifies this compound as chlorobenzene. The source of the chlorobenzene was found to be the toluene used to prepare the standard.

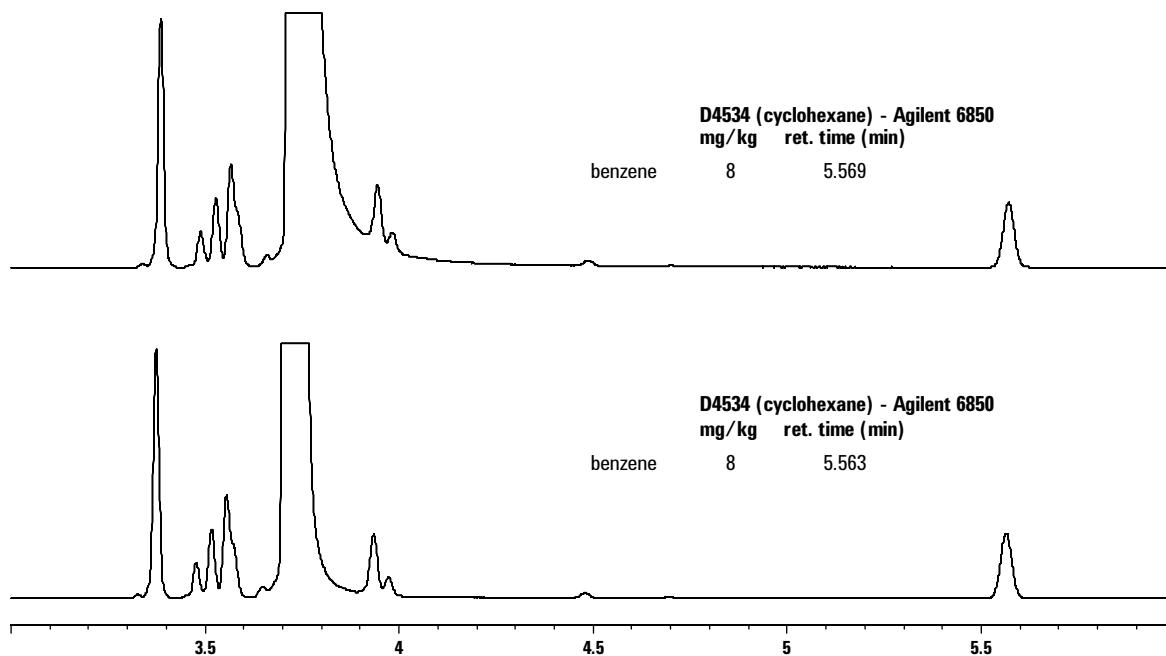


Figure 13. ASTM 4534 cyclohexane quantitative calibration standard run on Agilent 6890 (top) and 6850 (bottom) using the retention time locked unified aromatics method.

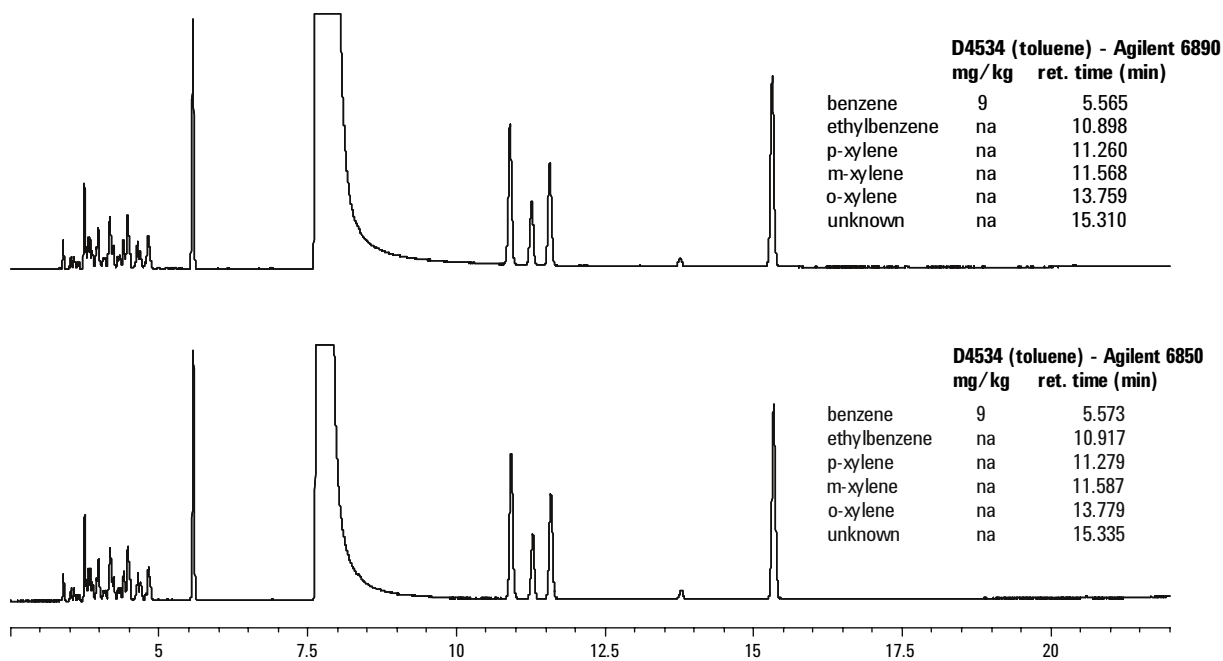


Figure 14. ASTM D4534 toluene quantitative calibration standard run on Agilent 6890 (top) and 6850 (bottom) using the retention time locked unified aromatics method.

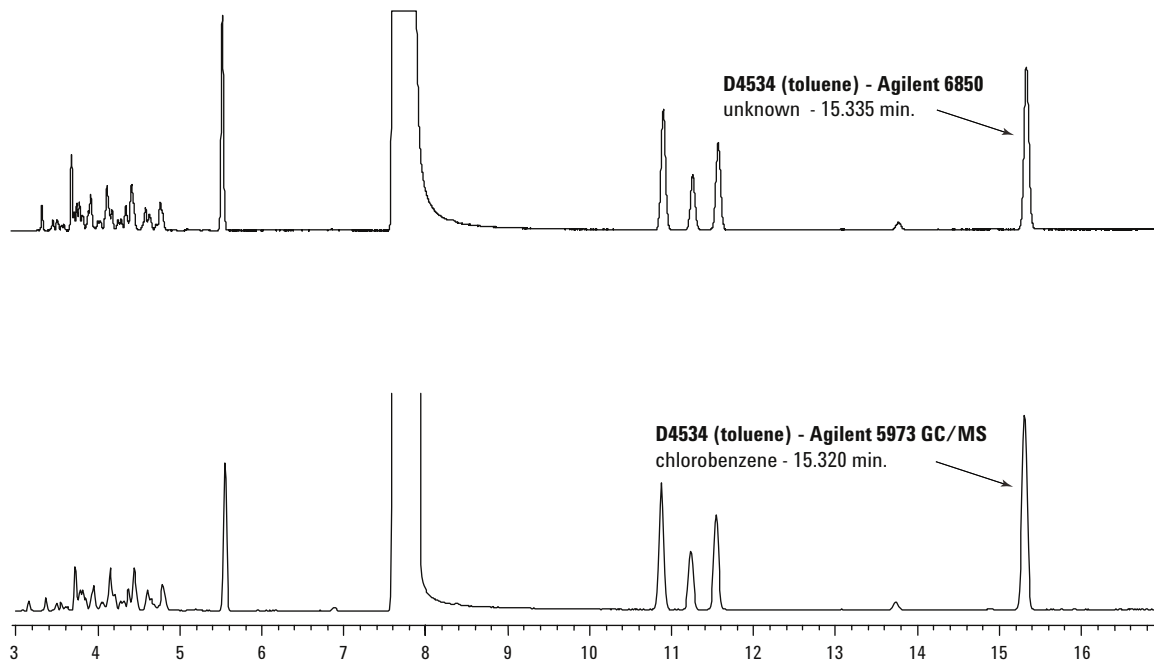


Figure 15. Unknown contaminant found in D4534 toluene standard (top) was identified as chlorobenzene using the retention time locked unified aromatics method run on the Agilent 5973 GC/MS (bottom).

D4534 Standard Test Method of Benzene Content of Cyclic Products - Cumene

Figure 16 shows the chromatograms of the D4534 calibration standard containing 5 mg/kg (ppm) of benzene in cumene. The injection size was 1.0 μ L and the split ratio was 100:1. Details of these

chromatograms are shown in Figure 17. Although benzene is well resolved, there are still some C9 hydrocarbons that elute near benzene. These compounds represent a potential source of interference when measuring small amounts of benzene (less than 5 mg/kg) in cumene.

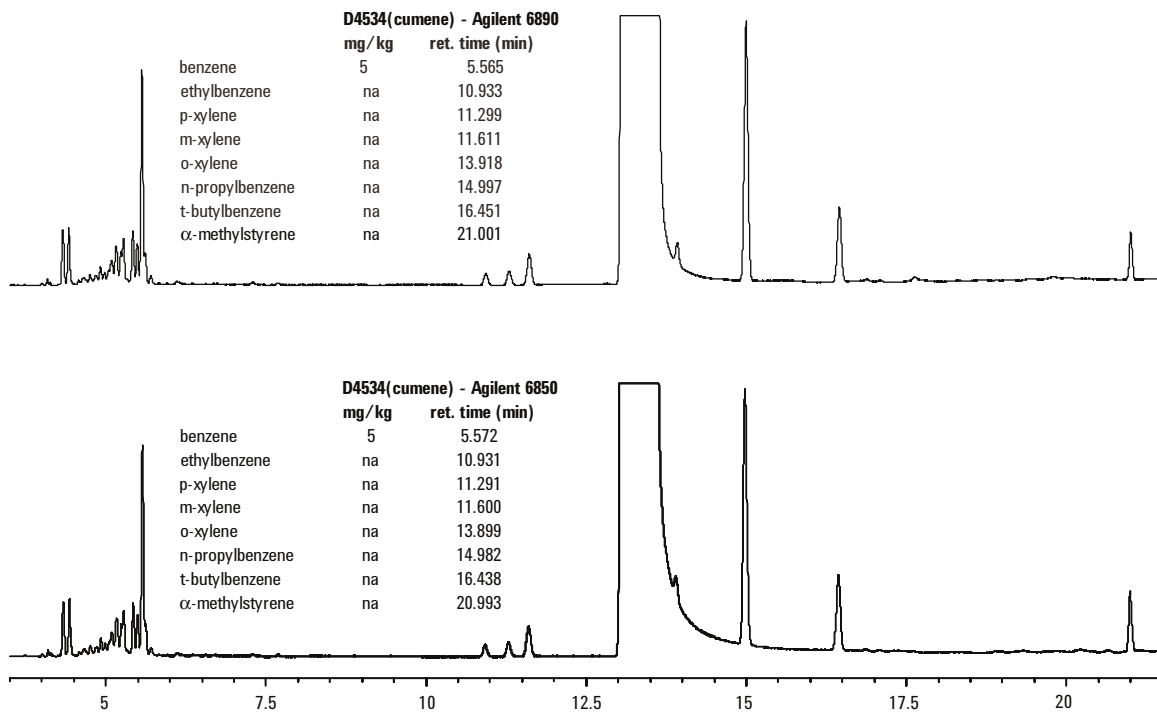


Figure 16. ASTM D4534 cumene quantitative calibration standard run on Agilent 6890 (top) and 6850 (bottom) using the retention time locked unified aromatics method.

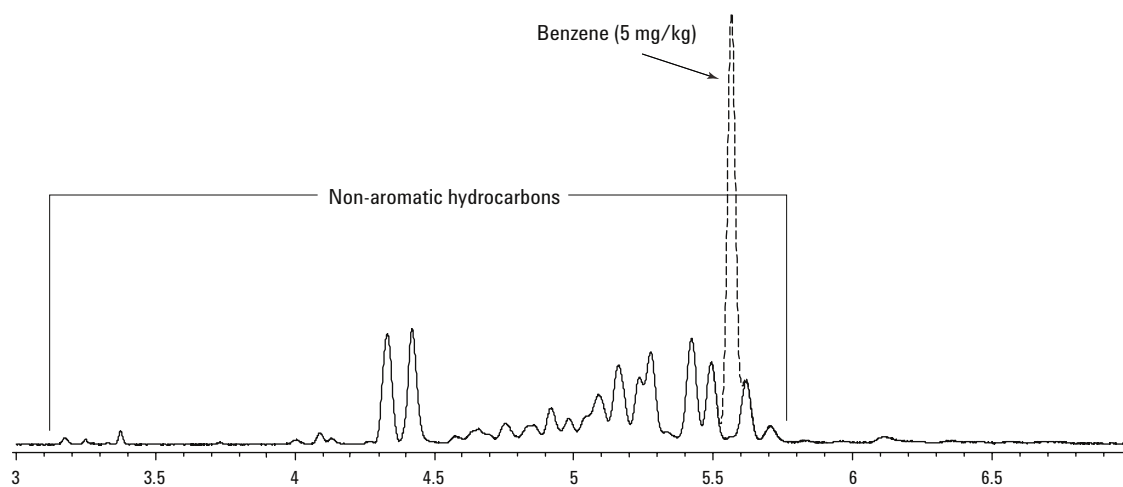


Figure 17. Details of the D4534 cumene standard showing the separation of 5 mg/kg of benzene from non-aromatic hydrocarbons typically found in cumene.

D5060 Standard Test Method for Determining Impurities in High-Purity Ethylbenzene

Figure 18 shows the chromatograms of the D5060 calibration standard. The injection size was 1.0 μ L and the split ratio was 100:1.

D5135 Standard Test Method for Analysis of Styrene by Capillary Gas Chromatography

Figure 19 shows the chromatograms of the D5135 calibration standard. The injection size was 1.0 μ L and the split ratio was 100:1.

D5917 Standard Test for Trace Impurities in Monocyclic Hydrocarbons (ESTD Cal)

This method is identical to D2360 without the addition of the internal standard, n-butylbenzene, so that the chromatogram shown in Figure 7 is a good representation of an expected result. However, since n-butylbenzene is not included in the standard or samples for D5917, the run time of the unified method can be reduced to approximately 15 minutes.

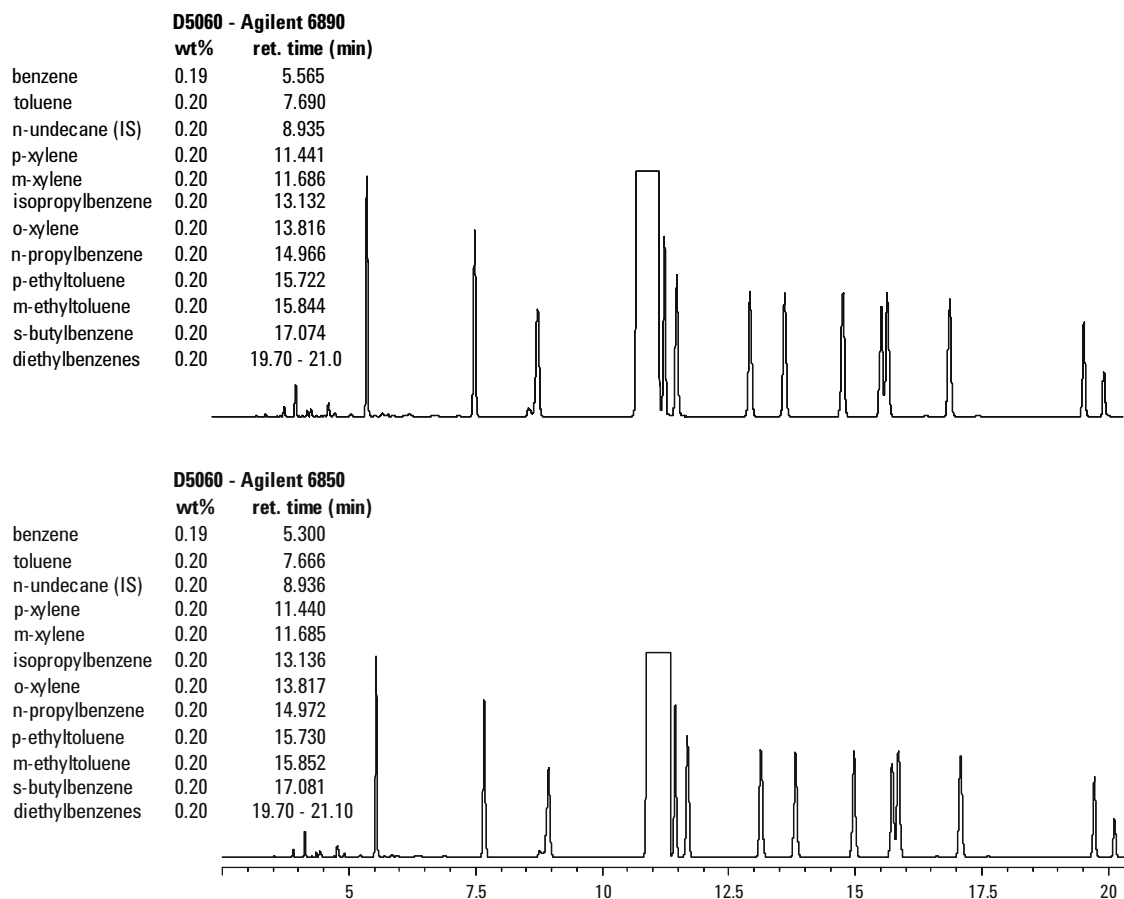


Figure 18. ASTM D5060 ethylbenzene quantitative calibration standard run on Agilent 6890 (top) and 6850 (bottom) using the retention time locked unified aromatics method.

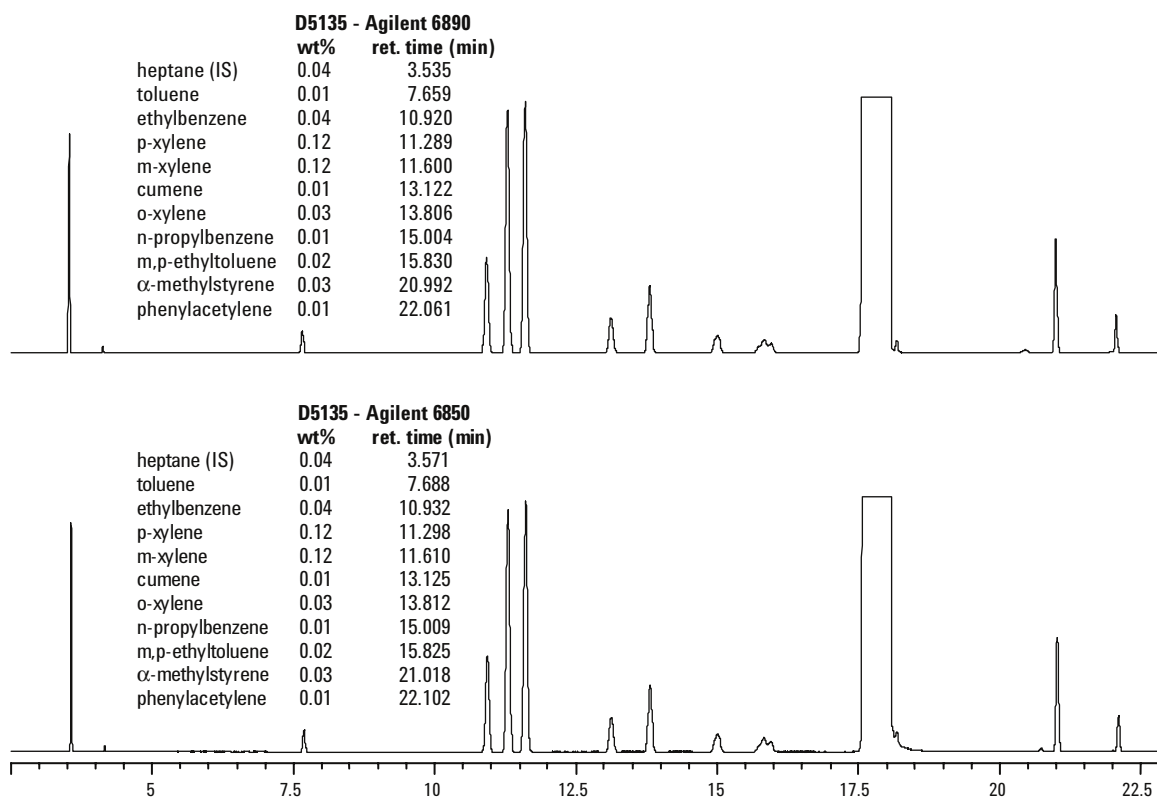


Figure 19. ASTM D5135 quantitative calibration standard run on Agilent 6890 (top) and 6850 (bottom) using the retention time locked unified aromatics method.

Conclusions

The analysis of many different bulk aromatic solvents in the QA/QC laboratory presents the analyst with an array of ASTM methods specific to each material. In an effort to simplify these measurements for today's laboratory environment, the chromatographies of ten ASTM methods were consolidated into one method. This unified method can resolve the 27 compounds found in aromatic materials and can successfully run the calibration standards used by each ASTM method to determine solvent purity. This versatile method can be run on both the Agilent 6890 and 6850 GC to yield consistent results between the method development lab and the plant production lab. To further improve performance, retention time locking (RTL) was applied to the unified method so that retention time standard deviation for each compound in any sample is less than 0.03 minutes. This allows easy comparison of results between instruments, laboratories and over time. The retention time locked unified method meets the need for a fast, simple method that can be run in today's production laboratories.

References

1. Annual Book of ASTM Standards, Vol. 6.04 *Paint - Solvents; Aromatic Hydrocarbons*, ASTM, 100 Bar Harbor Drive, West Conshohocken, PA 19428 USA.
2. V. Giarrocco, B.D. Quimby, and M.S. Klee, *Retention Time Locking: Concepts and Applications*, Agilent Technologies, Application Note 228-392, Publication number 5966-2469E, December 1997.
3. ASTM Method D2360, *Standard Test for Trace Impurities in Monocyclic Hydrocarbons*, Annual Book of ASTM Standards, Vol. 6.04, ASTM, 100 Bar Harbor Drive, West Conshohocken, PA 19428 USA.
4. B.D. Quimby, L.M. Blumberg, M.S. Klee, and P.L. Wylie, *Precise Time-scaling of Gas Chromatographic Methods Using Method Translation and Retention Time Locking*, Agilent Technologies, Publication number 5967-5820E, May 1998.

Agilent shall not be liable for errors contained herein or for incidental or consequential damages in connection with the furnishing, performance, or use of this material.

Information, descriptions, and specifications in this publication are subject to change without notice.

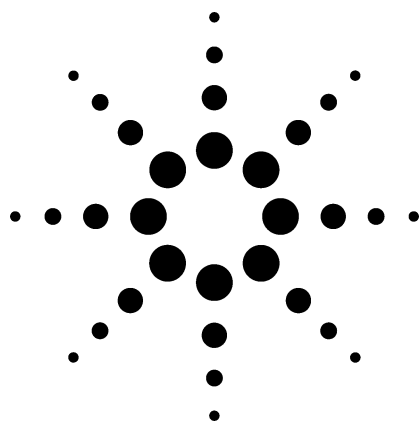
Copyright© 2001
© Agilent Technologies, Inc.

Printed in the USA
August 6, 2001
5988-3741EN



Agilent Technologies

Retention Time Locking Using USP 467 Standard Sample and Automated Headspace Sampling



Application

Gas Chromatography

August 1999

Authors

C. Kai Meng and
Matthew S. Klee
Agilent Technologies, Inc.
2850 Centerville Road
Wilmington, DE 19808-1610
USA

Abstract

Agilent Technologies' retention time locking (RTL) software gives chromatographers the ability to match retention times precisely from any Agilent 6890 Series or Agilent 6850 gas chromatograph (GC) system to any other, as long as the systems are equipped with electronic pneumatics control. Results from different systems are virtually identical, independent of inlet, detector, operator, or location. This application note explains the successful implementation of RTL for an automated headspace GC system.

Key Words

Retention time locking, RTL,
USP 467, residual solvents, headspace, gas chromatography,
6890 Plus, Agilent 7694A

Introduction

Retention time is the primary tool for identifying peaks in gas chromatography. Peak identification is usually done by comparing the retention time of an unknown peak to peaks in a standard sample. It is critical, therefore, to minimize variation in the retention times of peaks to ensure proper peak identification and method validation.

Variation in retention time is common with gas chromatographs, even within a single GC system. Routine column trimming or a difference in column length from the nominal length changes peak retention time. For systems running duplicate methods, the resulting differences in retention times make it difficult to compare results. In these cases, reviewing or comparing data among systems is complicated and a new calibration table, integration events table, and timed events table may be needed.

Retention time locking enables chromatographers using the same nominal

column to *match retention times within thousandths of a minute* in any 6890 Series GC or 6850 GC system equipped with electronic pneumatics control (EPC). EPC offers unwavering pressure and flow control. When combined with other factors such as stable and reproducible oven temperatures and highly consistent capillary columns, RTL becomes a very valuable tool for GC analysis.

With precise results from system to system, RTL can also be used as a system suitability assessment tool. If, for example, should system locking not be achieved for polar compounds, even though other compounds do lock, it becomes clear that there is some added system activity (such as inlet or column contamination).

It is common today to keep response calibration records and to update the integration timetable periodically for each column and each GC system. This is tedious and time-consuming. RTL presents a new option to match



Agilent Technologies

Innovating the HP Way

all retention times from day to day and instrument to instrument in a manner analogous to re-zeroing a balance or re-calibrating a pH meter to the correct value.

Retention time locking is achieved by adjusting the column head pressure according to an RTL calibration table specific for each method. The USP 467 protocol suggests that carrier gas linear velocity should be “about” 35 cm/s. Therefore, the typical USP 467 SOP specifies a range for the inlet pressure (for example, 4.7 ± 0.5 psi) to accommodate inter-system and inter-column differences. The SOP can easily go one step further by specifying the retention time of a compound to simplify the calibration

task and minimize timetable changes. For instance, ASTM method D 5134-92 requires the operator to “set carrier gas flow rate such that the retention time of toluene at 35 °C is 29.6 ± 0.2 min.” If the target peak can be locked within the inlet pressure range, the system meets the system suitability criterion and is ready for analysis.

The RTL Process

The RTL calibration process involves correlating inlet pressure with the retention time of any selected target compound—the locking compound^{1,2}. This target compound, usually found in the normal method

calibration standard, is then used to lock other GC systems. Agilent’s RTL software (G2080AA) integrates into the Agilent ChemStation (version A.05.02 or later), providing the tool required to determine the proper inlet pressure for locking the retention time quickly and easily. The locking compound should be easily identifiable, symmetrical, and should elute in the most critical part of the chromatogram. Polar and labile compounds should be avoided as locking compounds.

Once the target compound is chosen, the next step is to perform five calibration runs with different inlet pressures. The runs are made at identical conditions except for inlet pressure

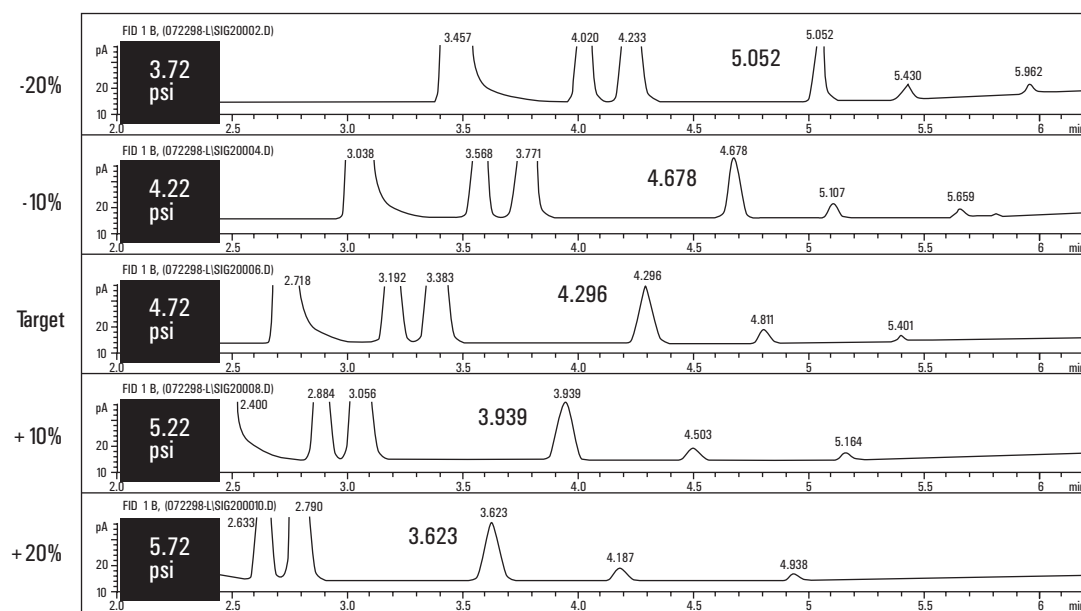


Figure 1. Five calibration runs to generate the five pairs of inlet pressures and corresponding retention times of the target compound.

(as shown in figure 1). The pressures used are typically:

- Target pressure – 20%
- Target pressure – 10%
- Target pressure (nominal method pressure)
- Target pressure + 10%
- Target pressure + 20%

After the five runs are complete, the retention times and corresponding inlet pressures of the target compound from all five runs are entered into the ChemStation RTL software (G2080AA) to generate an RTL calibration file. Figure 2 shows the dialog box used to enter the calibration data. After the data are entered, the software program reveals the maximum retention time deviation determined from the fitted data curve, as shown in figure 3.

| Run | Pressure | Ret Time |
|-------|----------|----------|
| Run 1 | 3.72 | 5.052 |
| Run 2 | 4.22 | 4.678 |
| Run 3 | 4.72 | 4.296 |
| Run 4 | 5.22 | 3.939 |
| Run 5 | 5.72 | 3.623 |

Pressure Units: psi

Desired Ret Time: 4.296

Min relock pressure: 2

Max relock pressure: 15

Column: 1

Compound Name (optional): peak @ ca. 4.3 min.

Figure 2. Dialog box used for entering retention time locking calibration data.

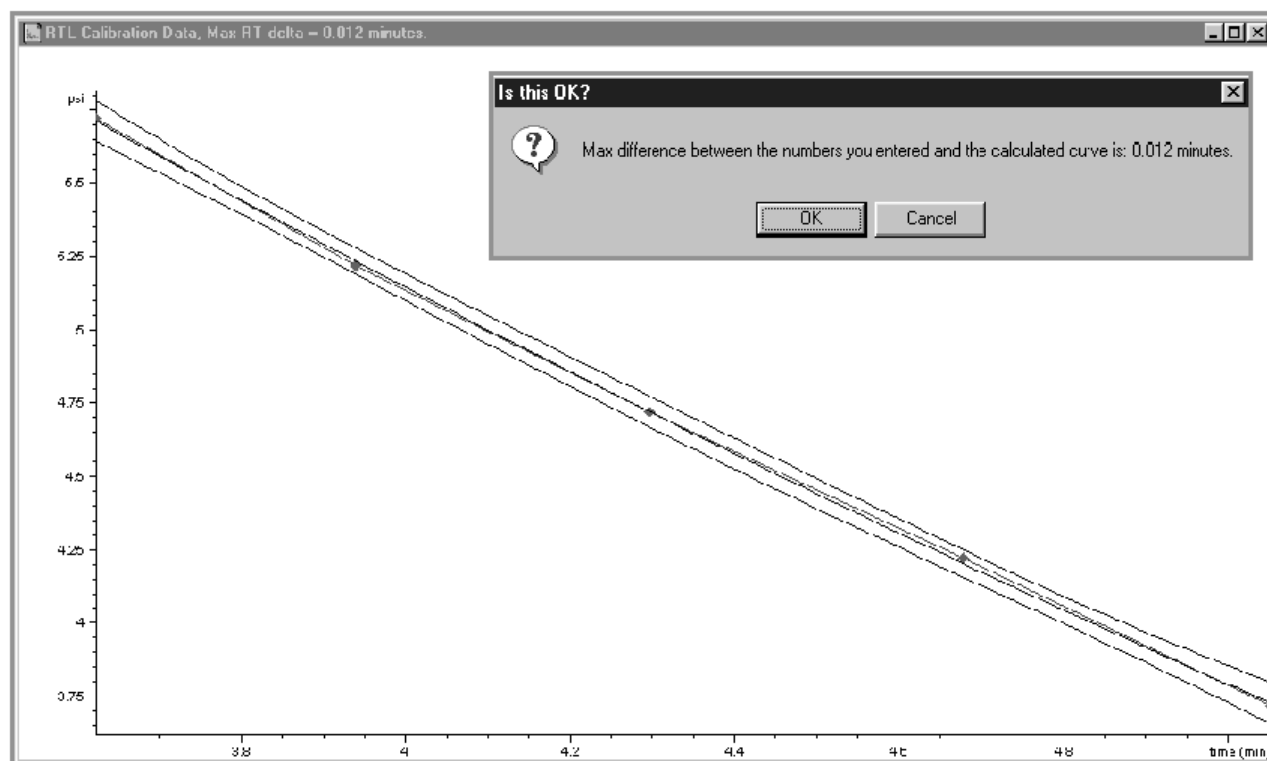


Figure 3. Plot of calibration data displayed by the RTL software.

The four calibration lines in figure 3 are as follows:

1. A point-to-point fit
2. The best curve fit of the five points
3. + 1 standard deviation from the best curve fit
4. - 1 standard deviation from the best curve fit

If the fit is acceptable, the retention time versus pressure calibration is stored and becomes part of the GC method. This calibration needs to be generated only once, is stored within the method, and can then be used on a duplicate instrument, regardless of location.

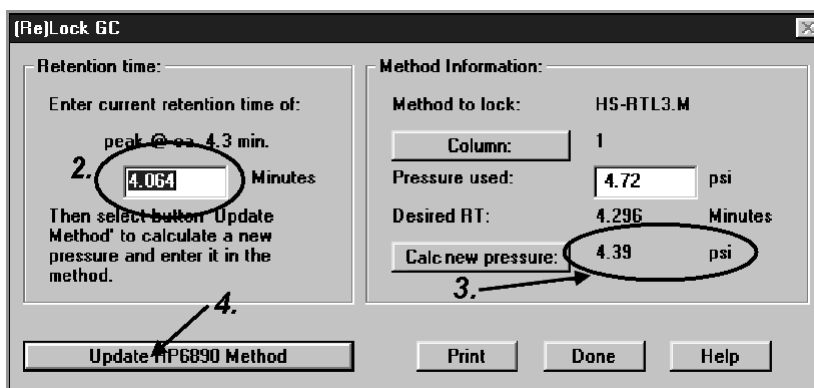


Figure 4. Dialog box used to calculate locking pressure and update the 6890 GC method (first lock). The numbers 2, 3, and 4 refer to the steps on the left.

Relocking a System or Locking Another GC

With the calibration stored in the GC method, the procedure for relocking a system or locking another 6890 or 6850 GC is easy:

1. Set up the method parameters, with nominal head pressure (for example 4.72 psi) and run a standard containing the target compound.
2. Enter the actual retention time of the target compound into the “(Re)Lock GC” dialog box (see figure 4).
3. Press the “Calc. new pressure:” button to obtain the proper inlet pressure for locking.
4. Update the GC method with the new calculated pressure, and save the method.
5. Run the standard again at the new pressure, and compare the retention time obtained to the desired retention time.
6. Repeat steps 2 to 5, if necessary.

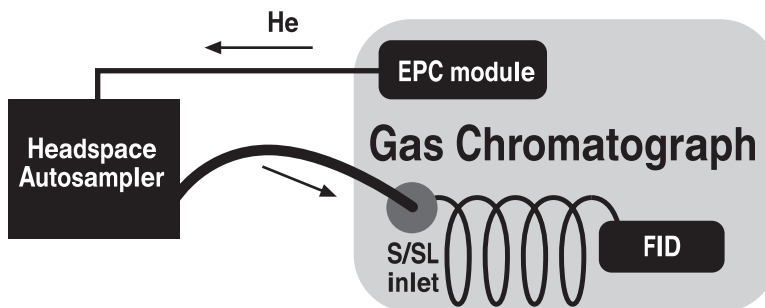


Figure 5. The flow configuration for this study.

Experimental

A 6890 Plus GC with a 7694A headspace autosampler was used to verify retention time precision and reproducibility with RTL. The headspace autosampler transfer line was connected to the split/splitless (S/SL) inlet carrier line using a zero dead volume (ZDV) union (see figure 5). The standard sample was a USP 467

calibration mixture (USPM-4670, Ultra Scientific, North Kingston, RI) diluted 500:1 with water. The components and the final concentrations were: methylene chloride (10 ppm), chloroform (1 ppm), benzene (2 ppm), trichloroethylene (2 ppm), and 1,4-dioxane (2 ppm).

Results and Discussion

The target retention time for the locking compound was 4.296 min, as seen in figure 1. The inlet pressure was 4.72 psi (established now as the nominal method and pressure). Relocking the target peak was required after cutting off one meter of column (a common procedure). After cutting, the new retention time at 4.72 psi was 4.064 min. The 4.064 value was entered into the RTL software (see figure 4), which then calculated the new pressure to be 4.39 psi. At 4.39 psi, the retention time of the target peak improved to 4.314 min (versus the target 4.296 min). In this example, a second lock was needed to match retention times to within 0.001 min. Figure 6 shows the process of entering the current retention time (4.314 min) to get the desired new pressure (4.42 psi). Indeed, by using the inlet pressure of 4.42 psi, the retention time of the target peak was locked at 4.297 min, which was within 0.001 min of the target retention time of 4.296 min.

| | |
|-----------------------------|--|
| Inlet | Split/splitless (5:1 split), 200 °C, constant pressure, helium carrier gas |
| Column | HP-INNOWax polyethylene glycol, part no. 19095N-123, 30 m x 530 µm x 1 µm |
| Oven | 50 °C (3.5 min), 10 °C/min to 60 °C (0 min), 40 °C/min to 190 °C (1 min) |
| Detector | FID, 300 °C, H ₂ = 40 mL/min, air = 450 mL/min, nitrogen makeup = 45 mL/min |
| Sample | 5 mL in 10-mL headspace vial |
| Headspace zone temperatures | Oven = 85 °C, loop = 95 °C, transfer line = 100 °C |
| Headspace event times | Vial equilibration time = 15.0 min, pressure time = 0.30, loop fill = 0.15, loop equilibration time = 0.02, Injection = 0.50 |
| Headspace vial pressure | 15 psi |
| ChemStation | Version A.06.01, RTL software G2080AA |

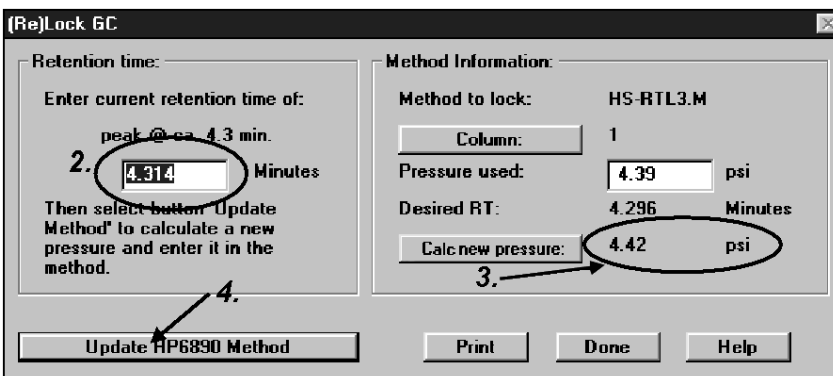


Figure 6. Dialog box used to calculate locking pressure and update the 6890 GC method (second lock). The numbers 2, 3, and 4 refer to the steps on page 4.

Figure 7 overlays the four GC runs discussed above.

Retention time locking is applicable even for regulated environments, for cases when columns are not changed or trimmed for extended periods of time, or when results are not compared from system to system. Besides providing the capability to match retention times within thousandths of a minute, RTL helps confirm system suitability quickly and easily:

1. *When locking a new system*, if the locking for some or all of the peaks gives a poor fit (a large delta RT), the system is not working properly.
2. *When using a locked method*, any shift in retention time (caused by leaks or flow restrictions) signals a system problem.
3. *After changing or trimming a column*, if relocking cannot be achieved after two attempts, the system should be carefully examined for problems.

The SOP can specify that the retention time of a reference peak should be $xx.xx \text{ minutes} \pm 0.2 \text{ minute}$, for example. The ability of a system to maintain a fixed retention time for the reference peak provides high confidence in peak identifications and affirms good system performance. Moreover, when the retention time is locked, anomalies with peak shape, peak width and peak resolution are recognized more easily as immediate signs of system problems.

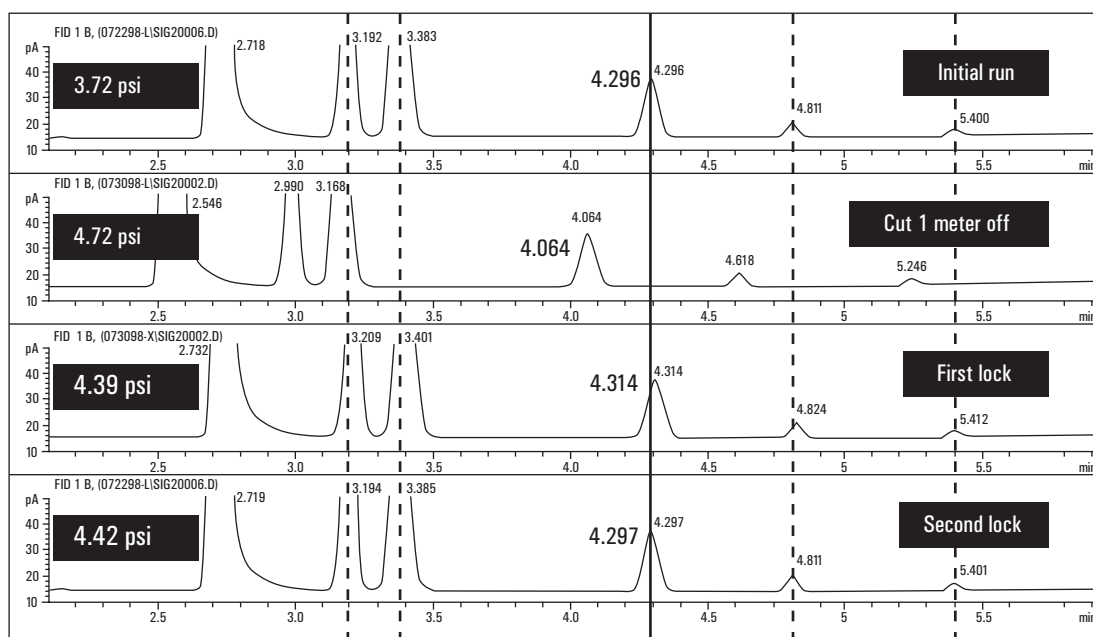


Figure 7. Comparison with the original chromatogram after one meter of column was cut off, and after two RTL operations.

Conclusions

In chromatography, most peak identification is performed by comparing the retention time of an unknown to that of a standard. It is much easier to identify peaks and validate methods if there is no variation in the retention time of each compound after column installation or trimming. Retention time locking can also help to ensure system suitability before samples are run.

This study demonstrates that RTL can be applied to a headspace-GC system.

References

1. V. Giarrocco, B. Quimby, and M. Klee, "Retention Time Locking: Concepts and Applications," Agilent Technologies, Application Note 228-392, Publication 5966-2469E, December 1997.
2. B. Quimby et al., "Precise Time-Scaling of Gas Chromatographic Methods Using Method Translation and Retention Time Locking," Agilent Technologies, Application Note 228-401, Publication 5967-5820E, May 1998.

Agilent shall not be liable for errors contained herein or for incidental or consequential damages in connection with the furnishing, performance, or use of this material.

Information, descriptions, and specifications in this publication are subject to change without notice.

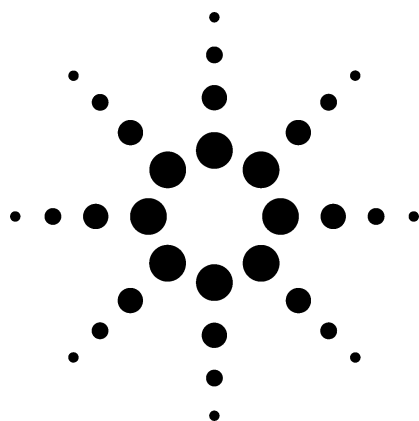
Copyright ©2000
Agilent Technologies, Inc.

Printed in the USA 3/2000
5968-3760E



Agilent Technologies
Innovating the HP Way

Headspace Analysis of Residual Ethylene Oxide in Sterilized Medical Devices



Application

Gas Chromatography

May 1998

Authors

Chin-Kai Meng
Agilent Technologies, Inc.
2850 Centerville Road
Wilmington, DE 19808-1610
USA

Richard A. Borders
Kimberly-Clark Corporation
1400 Holcomb Bridge Road
Roswell, GA 30076
USA

Jennifer V. Smith
Agilent Technologies, Inc.
Analytical Marketing Center
2850 Centerville Road
Wilmington, DE 19808-1610
USA

Abstract

The analysis of residual ethylene oxide in medical devices using automatic headspace sampling with gas chromatography is described. Ethylene oxide, a known carcinogen, was analyzed in the range of 1 to 300 ppm in polyvinyl chloride (PVC) resin beads and high-density polyethylene (PE) resin beads.

Key Words

Ethylene oxide, medical devices, sterilization, automatic headspace sampler, round robin, Agilent 7694A, Agilent 6890

Introduction

Ethylene oxide (EO), a known carcinogen, is used to sterilize medical devices. For many years, quantitating the amount of residual EO present after sterilization has been a challenge. Numerous round robins have studied various extraction and chromatographic methods to determine the best analytical approach. Agilent Technologies, along with 11 other laboratories, studied the efficacy of using automatic headspace sampling and capillary column gas chromatography with flame ionization detection (GC/FID) analysis in quantitating residual traces of EO.

This study used EO residues in the range of 1 to 300 ppm in polyvinyl chloride (PVC) resin beads and high-density polyethylene (PE) resin beads. The headspace method of the Association for the Advancement of Medical Instrumentation recommends using a packed column. This round robin study used a polyethylene glycol capillary column.



Agilent Technologies

Innovating the HP Way

Experimental

Instrumentation and Analytical Conditions

Table 1 lists the instrumentation and conditions used in this study for the headspace analysis of EO in PVC and PE resin beads. To test for instrument-to-instrument variation, two identically configured GC systems were used.

Reagents

Methanol, pesticide residue analysis grade (from Burdick & Jackson, Cat. 230-4), was used in preparing standards. Ethylene oxide standards (50 mg/mL) in methanol (Supelco, 4-8838) were used in preparing the standard curve.

Solutions and Standards

The authors used the following procedure in preparing the standards:

1. Primary standard (50 mg/mL): Score ampoule and transfer contents to a 2-mL vial and seal. This produced a 50- μ g/ μ L primary standard.
2. Add about 4 mL of methanol to each of two 5-mL volumetric flasks and about 0.5 mL to a 1-mL volumetric flask.
3. Transfer 200 μ L of the primary standard to the 1-mL volumetric flask. Dilute to the mark with methanol and cap. Mix by repeatedly inverting the flask. This produced a 10-mg/mL standard.
4. Transfer 100 μ L of primary standard to the first of the 5-mL volumetric flasks. Dilute to the mark with methanol and cap. Mix by repeatedly inverting the flask. This produced a 1-mg/mL standard.

Table 1. System Configuration and Conditions

| Instrumentation | |
|----------------------------|--|
| Gas chromatograph | 6890 Series |
| Headspace sampler | 7694A |
| Column | HP-Wax (polyethylene glycol) 30 m \times 0.32 mm \times 0.50 μ m |
| Inlet | Split/splitless @ 105 °C, Split ratio = 50:1 |
| Detector | Flame ionization @ 200 °C |
| GC Conditions | |
| Oven temperature | 30 °C |
| Carrier gas | Helium at 7.0 psi |
| Headspace Conditions | |
| Oven temperature | 100 °C |
| Valve and loop temperature | 105 °C |
| Transfer line temperature | 105 °C |
| Sample equilibration time | 60 minutes |
| Vial pressurization time | 0.50 minutes |
| Loop fill time | 0.15 minutes |
| Loop equilibration time | 0.05 minutes |
| Injection time | 5.30 minutes |
| GC cycle time | 20 minutes |
| Loop size | 1 mL |
| Vial pressure | 10 psi |
| Shaking | None |

5. Transfer 10 μ L of primary standard to the second 5-mL volumetric flask. Dilute to the mark with methanol and cap. Mix by repeatedly inverting the flask. This produced a 0.1-mg/mL standard.
6. Transfer each standard to 2-mL vials and seal. Fill each vial fully to minimize the amount of headspace, but do not overfill. The liquid should not touch the septa.
7. Store standards in a freezer until used.

The external calibration curve was made by introducing micro-liter quantities of each standard into a 20-mL headspace vial and then injecting the headspace into a gas chromatograph (GC). Table 2 shows the standard curve preparation.

Table 2. Standard Curve Preparation

| Standard Concentration (mg/mL) | Injection into 20-mL Vial (μ L) | Sample Amount (μ g) |
|--------------------------------|--------------------------------------|--------------------------|
| 0.1 | 1 | 0.1 |
| 0.1 | 2 | 0.2 |
| 0.1 | 5 | 0.5 |
| 0.1 | 10 | 1 |
| 1.0 | 2 | 2 |
| 1.0 | 5 | 5 |
| 1.0 | 10 | 10 |
| 10 | 2 | 20 |
| 10 | 5 | 50 |
| 10 | 10 | 100 |
| 50 | 6 | 300 |
| 50 | 15 | 750 |

Sample Analysis

The analytical system was calibrated using the series of 12 standards listed in table 2. The standards were placed into the automatic headspace sampler, and the temperature was allowed to equilibrate for at least 15 minutes before the analysis.

Two empty sealed headspace vials were used as blanks to check for carryover. A base polymer that had not been exposed to EO was used to check for matrix interference.

One gram (± 0.02 g) of each sample was weighed and placed into a headspace sample vial. The samples were spiked with different concentrations of standards to create control as well as low-, medium-, and high-concentration samples. The samples were analyzed immediately for EO content using the method of standard addition shown in table 3.

The sequence of analysis was maintained over 2 days, the first day using PVC resin beads and the second day using PE resin beads. These analyses produced two sets of data over a range of concentrations from 1 to 400 μg .

Results and Discussion

The analyses were carried out on two separate headspace and GC systems to examine the robustness of the method and the sample preparation.

The correlation coefficients are 0.9998 for each GC system. The precision data (percent relative standard deviation) are 2.14 and 5.76 for the two systems. The response factor of each concentration is within ± 5 percent of the average response factor of all concentrations for each system. This confirms good linearity for the headspace samples. A typical chromatogram is shown in figure 1.

Table 3. Method of Standard Addition

| Vial | Sample | Standard Added |
|------|---|--|
| 1 | PEM | |
| 2 | Blank | |
| 3 | PEC | |
| 4 | PEC spiked with 1 μg of EO | 10 μL of 0.1 mg/mL standard |
| 5 | PEC spiked with 2 μg of EO | 2 μL of 1.0 mg/mL standard |
| 6 | PEC spiked with 3 μg of EO | 3 μL of 1.0 mg/mL standard |
| 7 | PEC spiked with 4 μg of EO | 4 μL of 1.0 mg/mL standard |
| 8 | PEM | |
| 9 | Participant lab, 10- μg standard | 10 μL of 1.0 mg/mL standard |
| 10 | PEL | |
| 11 | PEL spiked with 1 μg of EO | 10 μL of 0.1 mg/mL standard |
| 12 | PEL spiked with 2 μg of EO | 2 μL of 1.0 mg/mL standard |
| 13 | PEL spiked with 3 μg of EO | 3 μL of 1.0 mg/mL standard |
| 14 | PEL spiked with 4 μg of EO | 4 μL of 1.0 mg/mL standard |
| 15 | Participant lab, 10- μg standard | 10 μL of 1.0 mg/mL standard |
| 16 | PEM | |
| 17 | PEM spiked with 10 μg of EO | 10 μL of 1.0 mg/mL standard |
| 18 | PEM spiked with 20 μg of EO | 2 μL of 10 mg/mL standard |
| 19 | PEM spiked with 30 μg of EO | 3 μL of 10 mg/mL standard |
| 20 | PEM spiked with 40 μg of EO | 4 μL of 10 mg/mL standard |
| 21 | Participant lab, 10- μg standard | 10 μL of 1.0 mg/mL standard |
| 22 | PEM | |
| 23 | PEH | |
| 24 | PEH spiked with 100 μg of EO | 2 μL of 50 mg/mL standard |
| 25 | PEH spiked with 200 μg of EO | 4 μL of 50 mg/mL standard |
| 26 | PEH spiked with 300 μg of EO | 6 μL of 50 mg/mL standard |
| 27 | PEH spiked with 400 μg of EO | 8 μL of 50 mg/mL standard |
| 28 | Blank | |
| 29 | Participant lab, 10- μg standard | 10 μL of 1.0 mg/mL standard |
| 30 | PEM | |

Note: PEC, PEL, PEM, and PEH are received round robin samples at controlled (PEC), low (PEL), medium (PEM), and high (PEH) concentrations of PE resin beads.

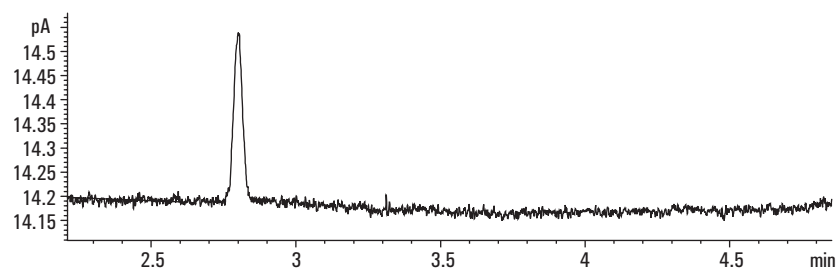


Figure 1. Ethylene oxide standard at 0.1 μg .

The external calibration curve results for both systems are shown in table 4.

Table 5 shows the results of EO concentrations from spiked PVC and PE in two systems using standard addition quantitation. The results are similar between the two systems, which implies that both the method and the sample preparation are repeatable. However, the responses between spiked PVC and PE are quite different. This might be due to matrix effect. It is suggested that the analysts determine the levels of EO present experimentally with each matrix.

Figure 2 presents a typical standard addition plot. The negative of the x-axis intercept is the determined sample concentration (0.75 ppm).

Conclusions

The results of this study indicate that the headspace method combined with capillary columns is accurate and reliable for detecting any EO residue in sterilized medical instruments. A possible matrix effect may require analysts to determine the levels of EO present experimentally with each matrix.

The method showed good precision that is not matrix-dependent. The data demonstrate that the range of analysis for standards can be determined for quantities from 1 to 750 ppm (μg).

Table 4. External Calibration Curve

| Standard Concentration (μg) | System 1 Area | System 1 Response Factor | System 2 Area | System 2 Response Factor |
|--|---------------|--------------------------|---------------|--------------------------|
| 0.1 | 0.75 | 7.48 | 0.87 | 8.74 |
| 0.2 | 1.39 | 6.94 | 1.80 | 8.99 |
| 0.5 | 3.61 | 7.22 | 4.45 | 8.89 |
| 1 | 7.04 | 7.04 | 9.04 | 9.04 |
| 2 | 14.83 | 7.42 | 17.88 | 8.94 |
| 3 | 36.72 | 7.34 | 45.36 | 9.07 |
| 10 | 70.28 | 7.03 | 89.05 | 8.91 |
| 20 | 145.88 | 7.29 | 183.14 | 9.16 |
| 50 | 359.12 | 7.18 | 450.25 | 9.01 |
| 100 | 706.85 | 7.07 | 910.81 | 9.11 |
| 300 | 2,125.24 | 7.08 | 2,608.12 | 8.69 |
| 750 | 5,144.66 | 6.86 | 6,425.34 | 8.57 |
| Blank | None Detected | | | |

Table 5. Ethylene oxide results from spiked PVC and PE in two instruments using standard addition quantitation.

| Material and Spiked EO Concentration | Instrument 1, ppm | Instrument 2, ppm |
|--------------------------------------|-------------------|-------------------|
| PVC, 0 ppm | 0.00 | 0.00 |
| PVCL, 1 ppm | 0.99 | 0.93 |
| PVCM, 20 ppm | 15.98 | 16.91 |
| PVCH, 300 ppm | 239.00 | 225.00 |
| PE, 0 ppm | 0.00 | 0.00 |
| PEL, 1 ppm | 0.75 | 0.73 |
| PEM, 20 ppm | 4.70 | 5.75 |
| PEH, 300 ppm | 142.00 | 134.00 |

Note: PVCL, PVCM, PVCH, PEL, PEM, and PEH are received round robin samples at low (PVCL and PEL), medium (PVCM and PEM), and high (PVCH and PEH) of PVC and PE resin beads.

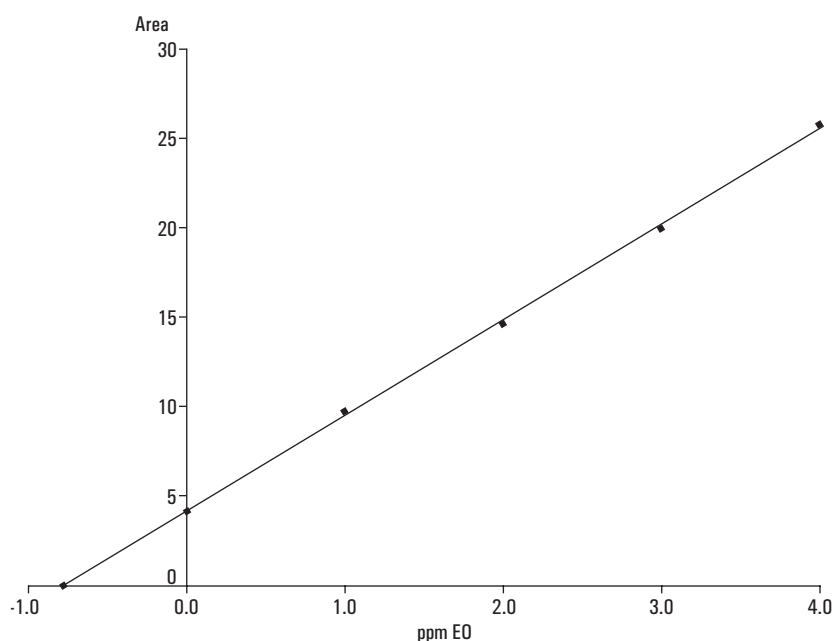


Figure 2. Standard addition plot for the low-concentration PE sample.

References

1. Lao, N. T., et al., "Interlaboratory Comparison of Analytical Methods for Residual Ethylene Oxide at Low Concentration Levels in Medical Device Materials," *Journal of Pharmaceutical Sciences*, 84 (5), 647-655, May 1995.
2. AAMI Reference Method, "Recommended Practice for Determining Residual Ethylene Oxide in Medical Devices," Arlington, VA, AAMI EOR-1986, October 1986.
3. "Biological Evaluation of Medical Devices—Part 7: Ethylene Oxide Residuals," ANSI/AAMI/ISO 10993-7, 1995.
4. Miller, J. C., Miller, J. N., and Horwood, E., *Statistics for Analytical Chemistry*, 3rd edition, Prentice Hall (New York), 1993.

Agilent shall not be liable for errors contained herein or for incidental or consequential damages in connection with the furnishing, performance, or use of this material.

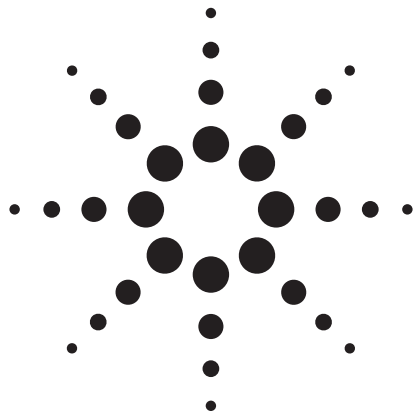
Information, descriptions, and specifications in this publication are subject to change without notice.

Copyright © 2000
Agilent Technologies, Inc.

Printed in the USA 4/2000
5966-4034E



Agilent Technologies
Innovating the HP Way



The determination of residual solvents in pharmaceuticals using the Agilent G1888 headspace/6890N GC/5975 inert MSD system

Application Note

Roger L. Firor
Albert E. Gudat

Abstract

The Agilent G1888 network headspace sampler (HS) interfaced to an Agilent 6890N gas chromatograph (GC) and configured with an Agilent 5975 inert mass-selective detector (MSD) were used for the determination of regulated residual solvents. Standard mixtures in water were used at various concentrations including levels at or below published acceptance guidelines to demonstrate system performance. Solvents in class 1 and class 2 according to ICH guidelines (including those listed in USP 467) were included. The MSD was operated in synchronous SIM/scan mode to collect both selected ion monitoring (SIM) and scan data for compound quantitation and identification, respectively. Method detection limits (MDLs) for 27 solvents were determined.



Agilent Technologies

Introduction

Organic volatile impurities (OVIs) can result from the manufacture of active pharmaceuticals, excipients, or other drug products. Many can be used to enhance yields, improve crystallization or increase solubility¹. Other factors such as packaging, transportation, and storage can also impact the level of residual solvents. Gas chromatography coupled with static headspace sampling is acknowledged as an easy-to-use high-throughput analytical tool for the determination of low level solvent impurities in drugs and can be found in nearly all QC laboratories in pharmaceutical manufacturing. Sample prep is relatively simple, and the methodology is easily validated as per specific monographs.

General guidelines established by the International Conference on Harmonization (ICH) divide solvents into three classes². Class 1 solvents should not be used in manufacture because of toxicity or environmental impact while class 2 solvent use should be limited due to potential toxicity. Solvents regarded as posing a lower risk to human health are class 3. Solvents listed in USP 467 include a subset of specific class 1 and class 2 solvents. This work will demonstrate the analysis and quantitation of class 1 and 2 solvents. See table 1A-C for a listing of residual solvents.

Residual solvent and other contaminant levels designated as safe have trended downward in recent years as information about potential harmful effects of long-term and/or low-level exposures accumulate and as the detection sensitivity of analytical instrumentation

| Solvent | Concentration limit (ppm) | Concern |
|-----------------------|---------------------------|--------------------------------|
| Benzene | 2 | Carcinogen |
| Carbon tetrachloride | 4 | Toxic and environmental hazard |
| 1,2-dichloroethane | 5 | Toxic |
| 1,1-dichloroethene | 8 | Toxic |
| 1,1,1-trichloroethane | 1,500 (revised 10 ppm) | Environmental hazard |

Table 1A
Class 1 solvents in pharmaceutical products (solvents that should be avoided)².

| Solvent | PDE (mg/day) | Concentration limit (ppm) |
|------------------------|--------------|---------------------------|
| Acetonitrile | 4.1 | 410 |
| Chlorobenzene | 3.6 | 360 |
| Chloroform | 0.6 | 60 |
| Cyclohexane | 38.8 | 3,880 |
| Cis 1,2-dichloroethene | 18.7 | 1,870 |
| Dichloromethane | 6.0 | 600 |
| 1,2-dimethoxyethane | 1.0 | 100 |
| N,N-dimethylacetamide | 10.9 | 1,090 |
| N,N-dimethylformamide | 8.8 | 880 |
| 1,4-dioxane | 3.8 | 380 |
| 2-ethoxyethanol | 1.6 | 160 |
| Ethyleneglycol | 6.2 | 620 |
| Formamide | 2.2 | 220 |
| Hexane | 2.9 | 290 |
| Methanol | 30.0 | 3,000 |
| 2-methoxyethanol | 0.5 | 50 |
| Methylbutyl ketone | 0.5 | 50 |
| Methylcyclohexane | 11.8 | 1,180 |
| N-methylpyrrolidone | 48.4 | 4,840 |
| Nitromethane | 0.5 | 50 |
| Pyridine | 2.0 | 200 |
| Sulfolane | 1.6 | 160 |
| Tetralin | 1.0 | 100 |
| Toluene | 8.9 | 890 |
| 1,1,2-trichloroethene | 0.8 | 80 |
| Xylene ¹ | 21.7 | 2,170 |

¹Usually 60% m-xylene, 14% p-xylene, 9% o-xylene with 17% ethyl benzene

Table 1B
Class 2 solvents in pharmaceutical products² (PDE = personal daily exposure).

| Solvent | Concentration limit (ppm) |
|--------------------|---------------------------|
| Methylene chloride | 600 |
| Chloroform | 60 |
| Benzene | 2 |
| Trichloroethylene | 80 |
| 1,4-dioxane | 380 |

Table 1C
Solvents in pharmaceutical products according to USP 467 Method IV.

improves. For example, based on new toxicity data, a 2003 change in the regulations for residual solvents stipulate a ten-fold reduc-

tion of the 1997 PDE (personal daily exposure) and residual concentration limits for the solvent N-methylpyrrolidone³. It also reclass-

sifies tetrahydrofuran from a class 3 to a class 2 category solvent with PDE and concentration limitations more restrictive than toluene. Table 1A-B lists current PDE and concentration limits for class 1 and class 2 residual solvents in pharmaceutical products⁴.

Experimental

The HS/GC/MSD system described in this work provided for compound identification, confirmation and quantitation of resolved or coeluting peaks. 10-mL headspace vials with teflon seal caps were used containing 5 mL water as the matrix with 3 grams sodium sulfate added. The headspace sampler was equipped with a 1-mL sample loop. Sufficient flow must be maintained through the system to avoid excessive peak broadening, therefore split injection is used. At the chosen split ration of 5:1, the headspace sample loop is swept fast enough to produce good peak shapes.

A mass spectral quantitation database was set up manually by identifying unique ions for each solvent and selecting quantitation by target ions. The AutoSIM setup program in the data analysis software (version D.02.00) was applied, resulting in 16 SIM groups for the 27 analytes in the sample.⁷ This automated setup processes full scan data into SIM acquisition parameters. A new SIM/Scan method was then saved with the automatically generated SIM timetable incorporated. These groups are shown in figure 1.

| Start Time (min) | Default Dwell (ms) | Group Label | Calc Cycles/Sec | Ion 1 | Ion 2 | Ion 3 | Ion 4 | Ion 5 | Ion 6 |
|------------------|--------------------|-------------|-----------------|-------|-------|-------|-------|-------|-------|
| 1 | 0.000 | 50 Auto_1 | 8.3 | 31.1 | 32.1 | | | | |
| 2 | 2.890 | 50 Auto_2 | 5.8 | 61.1 | 96 | 98 | | | |
| 3 | 3.690 | 50 Auto_3 | 2.1 | 39.1 | 40.1 | 41.1 | 49.1 | 61.1 | 84 |
| 4 | 5.020 | 50 Auto_4 | 5.8 | 41.1 | 57.2 | 86.2 | | | |
| 5 | 6.170 | 50 Auto_5 | 5.8 | 61.1 | 96.1 | 98.1 | | | |
| 6 | 7.470 | 50 Auto_6 | 1.6 | 56.2 | 61.1 | 69.2 | 83 | 84.2 | 85 |
| 7 | 9.510 | 50 Auto_7 | 2.1 | 45.1 | 49 | 51.1 | 60.1 | 62.1 | 64 |
| 8 | 11.660 | 50 Auto_8 | 5.8 | 95 | 130 | 132 | | | |
| 9 | 13.610 | 50 Auto_9 | 5.8 | 69.2 | 83.2 | 96.2 | | | |
| 10 | 15.010 | 10 Auto_10 | 19.2 | 43.1 | 58.1 | 88.1 | | | |
| 11 | 18.570 | 50 Auto_11 | 3.1 | 51.1 | 52.1 | 65.2 | 79.1 | 91.2 | 92.2 |
| 12 | 22.710 | 50 Auto_12 | 5.8 | 43.1 | 58.1 | 100.2 | | | |
| 13 | 23.990 | 30 Auto_13 | 3.1 | 42.1 | 44.1 | 65.2 | 73.1 | 77.2 | 91.2 |
| 14 | 25.100 | 50 Auto_14 | 5.8 | 91.2 | 105.2 | 106.2 | | | |
| 15 | 25.590 | 50 Auto_15 | 5.8 | 44 | 72.1 | 87.1 | | | |
| 16 | 27.160 | 50 Auto_16 | 5.8 | 91.2 | 104.2 | 132.2 | | | |

Figure 1
Output from the AutoSIM setup used to generate the time-programmed SIM groups and dwell times of the ions to be monitored.

6890N GC

Injection port Volatiles interface
 Temperature 160 °C
 Split ratio 5 : 1
 Carrier gas Helium
 Carrier flow 1.5 mL/min

GC oven program

Initial temperature 35 °C
 Initial time 20 min.
 Rate 25 °C/min.
 Final temperature 250 °C
 Final time 10 min
 Columns 30 m x 0.25 mm x 1.4 µm DB-624, part# 122-1334

G1888A headspace sampler

Loop size 1 mL
 Vial pressure 12.0 psig
 Headspace oven 85 °C
 Loop temperature 100 °C
 Transfer line temperature 120 °C
 Equilibration time 30 min., high shake
 GC cycle time 50 min.
 Pressurization 0.15 min.
 Vent (loop fill) 0.2 min.
 Inject 0.5 min.

5975 inert MSD

Synchronous SIM/scan mode on
 SIM 16 groups for 27 analytes
 Scan 30 to 200 amu, samples 2¹
 Threshold 75
 Source temperature 230 °C
 Quad temperature 150 °C
 Tune atune.u
 ChemStation software G1701DA D.02.00

Standards

USP 467 Restek #36007
 ICH class 1 and 2 Restek #36261 (class 1 revised)
 #36229 (class 2A)
 #36230 (class 2B)

Results and discussion

Most quality control labs in pharmaceutical manufacturing employ gas chromatography for the determination of residual solvents that are included in either USP 467 or the more extensive list covered in ICH guidelines. Capillary gas chromatography based on the 624 phase (USP G43) is widely used for separation. A different stationary phase such as DB-1701 or DB-5 can be utilized in specific methods when coelution has been identified. However, coelution is usually not a problem with mass spectrometric detection when the coeluting compounds each have unique ions.

Headspace sampling has many advantages over direct liquid injection including the avoidance of large water injections that can result in column degradation and coelution. Headspace equilibration time is normally set at 60 minutes as specified in USP 467, however, in most cases 30 minutes is sufficient when operating at 85 °C equilibration temperature.⁵ Instead of adding the USP specified 1 gram of sodium sulfate to the 10-mL headspace vial containing 5 mL of water, 3 grams of sodium sulfate was added to ensure super saturation at 85 °C and to force the maximum analyte concentration into the headspace.

Table 2 lists concentrations and identifications of class 1 and class 2 solvents used to produce the sim/scan chromatograms shown in figure 3. These concentrations equal the guideline limits based on a 100 mg sample of the pharmaceutical or excipient dissolved in 5 mL

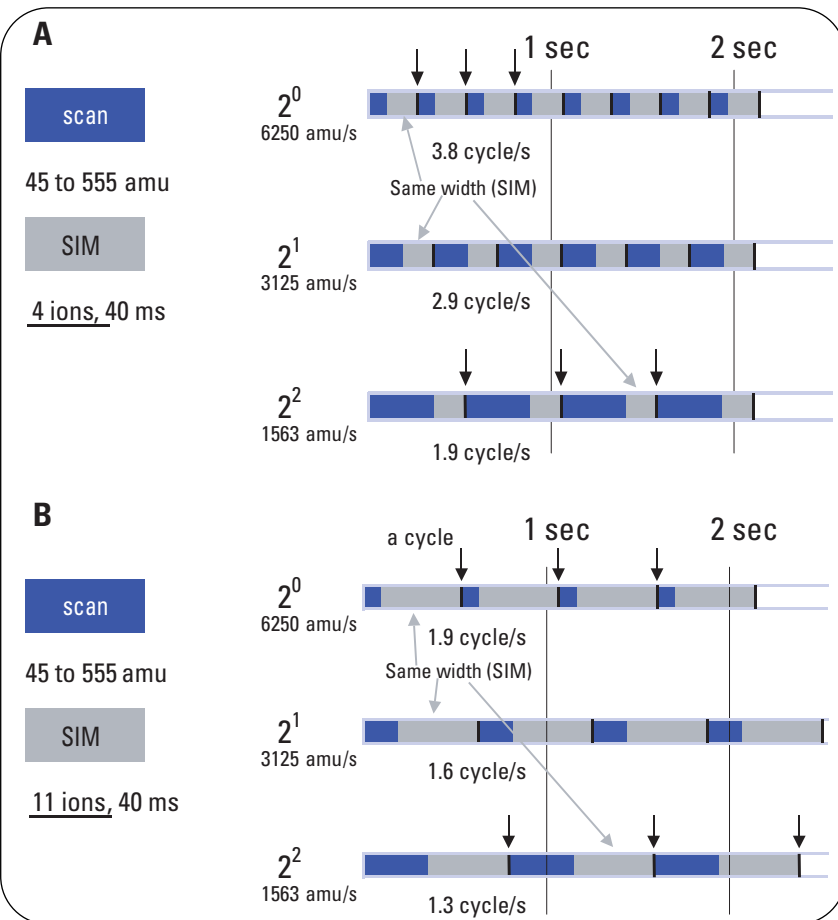


Figure 2
A) SIM/Scan operation with selected sampling rates for 4-ion group, 40 ms dwell.
B) SIM/Scan operation with selected sampling rates for 11-ion group, 40 ms dwell.

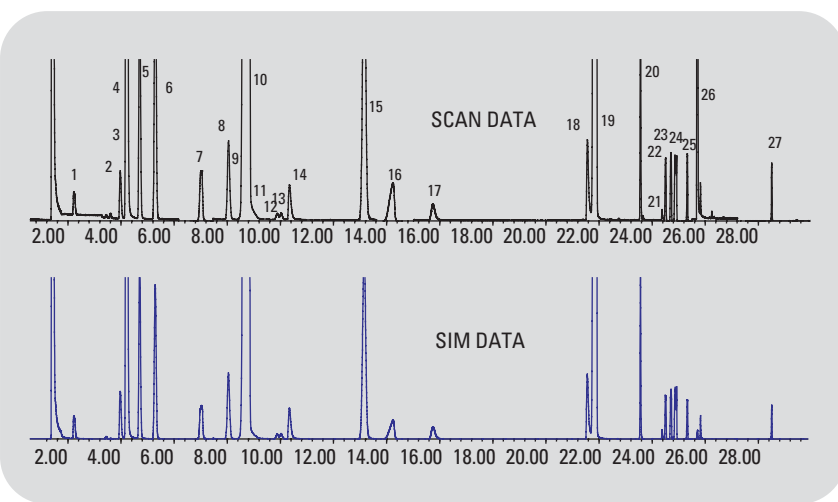


Figure 3
Class 1 and Class 2 residual solvents acquired in synchronous SIM/scan mode for concentration given in tables 1A-B.

water. Concentrations used throughout this work are defined as the equivalent concentration of a solvent in the excipient (ppm) placed into the headspace vial. Figure 4 gives the chromatograms for the USP 467 solvents at 1/10th the limit concentration. Figure 5 illustrates the resolution and SIM sensitivity realized for benzene and 1,2-dichloroethane at low concentrations. Calibration curves for SIM data of a few solvents including those from the USP 467 method are shown in figure 6. Linear results are seen over a concentration range that extends well below recommended maximum concentrations. The curves for methylene chloride and o-xylene are included to illustrate the effect of detector saturation during the elution of giant-size peaks even though big electron multiplier voltage de-creases were scheduled (figure 7). The effect of such a voltage reduction can be seen in figure 4 as the signal appears to drop to near zero at around 7 and 14 minutes.

The synchronous SIM/Scan mode of acquisition provides for collection of both SIM data and full scan data in a single run. See figures 2a and 2b for an example graphical representation of the SIM/Scan data acquisition approach used for 4 and 11 ion groups, respectively.⁸ Note the time spent on SIM is the same regardless of sampling rate. The time spent on scan will vary depending on sampling rate setting. Chromatograms from a synchronous SIM/Scan acquisition of class 1 and class 2 solvents at the

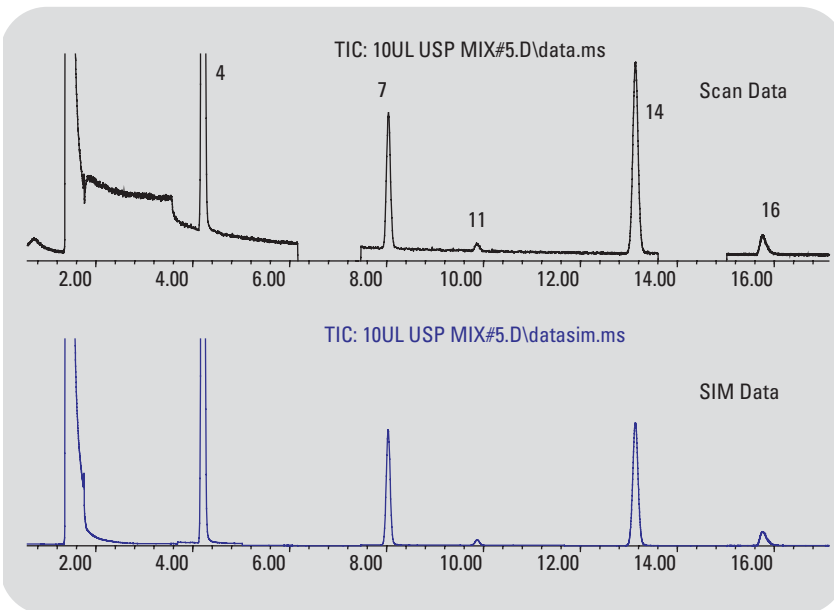


Figure 4
 USP 467 residual solvents at 1/10th the limit concentrations: 1. Methylene chloride 60 ppm, 2. Chloroform 6 ppm, 3. Benzene 0.2 ppm, 4. Trichloroethylene 8 ppm, 5. 1,4-dioxane 38 ppm.

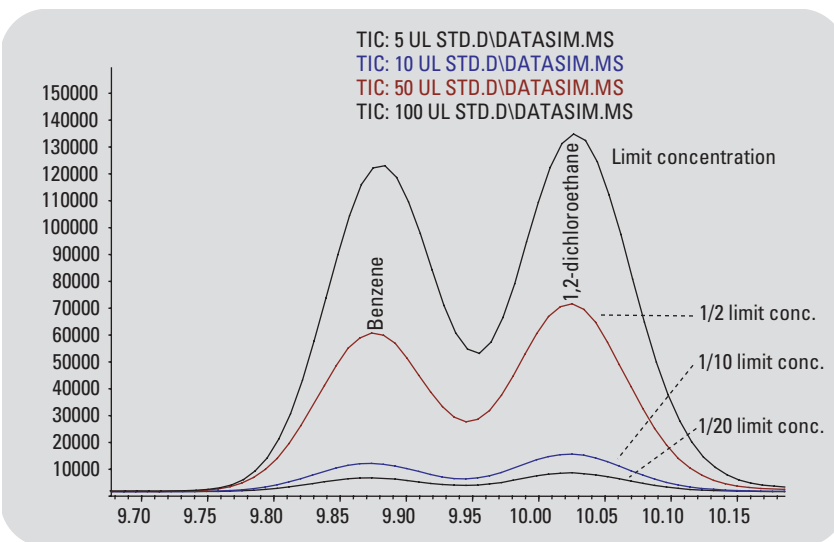


Figure 5
 Resolution and sensitivity for benzene and 1,2-dichloroethane.

limit excipient concentrations from table 2 are shown in figure 3. Method detection limits (MDLs) for SIM data are given in table 2. MDLs were calculated as specified in the US EPA Method 524.2⁶. Seven headspace vials containing class 1 and 2 solvents at 1/10th the limit excipient concentration (table 3) were prepared and analyzed. The formula in table 3 was then used to calculate the MDLs for all target compounds. Given the somewhat limited dynamic range of the MSD and the large range of limit concentrations for the analytes (from a low of 2 ppm for benzene to a high of 4840 ppm for N-methylpyrrolidone), time programmed changes to the electron multiplier voltage (EM) were necessary to keep the very large peaks from saturating the electronics and still achieve meaningful areas for the smaller peaks.

Since chromatograms usually show additional peaks from sources other than those coming from the target compounds, spectra obtained from the scan data can very effectively be used for unknown identification by library searches or manual interpretation. Such was the case also with the standard analyzed in this work. One large peak at 25.71 minutes did not belong to the list of targets. Library search of the spectrum identified the peak as Dimethylsulfoxide (DMSO). This was not surprising since DMSO was the solvent used for the preparation of the standards. However, other extraneous peaks could just as easily be identified from the full spectrum. This is one of the great advantages of doing synchronous SIM/Scan data acquisition where the SIM data is used for sensitive and reproducible quantitation while the scan data is

| Solvent | (#), t _R (min) | MDL(ppm) | Solvent | (#), t _R (min) | MDL (ppm) |
|------------------------|---------------------------|----------|--------------------------------|---------------------------|-----------|
| Methanol | (1) 2.23 | 54 | Trichloroethylene | (14) 13.13 | 2 |
| 1,1-dichloroethene | (2) 3.44 | 0.2 | Methyl cyclohexane | (15) 14.09 | 43 |
| Acetonitrile | (3) 3.98 | 9 | 1,4-dioxane | (16) 15.77 | 8 |
| Methylene chloride | (4) 4.21 | 24 | Pyridine | (17) 21.57 | 7 |
| Hexane | (5) 5.28 | 7 | Toluene | (18) 21.81 | 151 |
| Cis 1,2-dichloroethene | (6) 7.00 | 117 | 2-hexanone | (19) 23.56 | 1 |
| Chloroform | (7) 8.04 | 2 | Chlorobenzene | (20) 24.49 | 38 |
| Carbon tetrachloride | (8) 9.07 | 0.1 | Ethylbenzene | (21) 24.69 | 43 |
| Cyclohexane | (9) 8.65 | 334 | N,N-dimethylformamide | (22) 24.43 | 36 |
| 1,1,1-trichloroethane | (10) 8.50 | 0.2 | m-xylene* | (23) 24.86 | 195 |
| Benzene | (11) 9.88 | 0.1 | p-xylene* | (24) 24.86 | 195 |
| 1,2-dichloroethane | (12) 10.02 | 0.2 | o-xylene | (25) 25.31 | 19 |
| 1,2-dimethoxyethane | (13) 10.38 | 2 | N,N-dimethyl-acetamide | (26) 25.83 | 50 |
| | | | 1,2,3,4-tetrahydro-naphthalene | (27) 28.50 | 5 |

*Coeluting peaks on DB 624 column with no unique and differentiating ms ions.

Table 2
Class 1 and class 2 residual solvent method detection limits (MDL) and retention times (t_R).

$$MDL = s \cdot t_{(n-1, 1-\alpha=99)} = s \cdot 3.143$$

Where:

t_(n-1, 1-alpha=99) = Student's t value for the 99 % confidence level with n-1 degrees of freedom

n = number of trials

Table 3
Formula for MDL calculations from EPA Method 524.2.

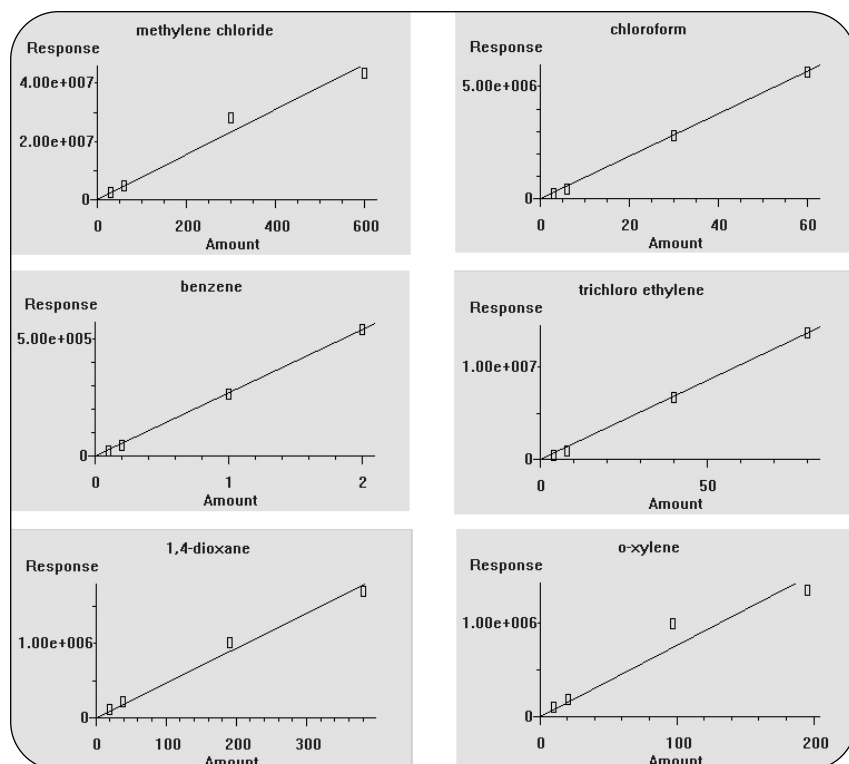


Figure 6
Calibration plots for USP 467 solvents and ortho-xylene.

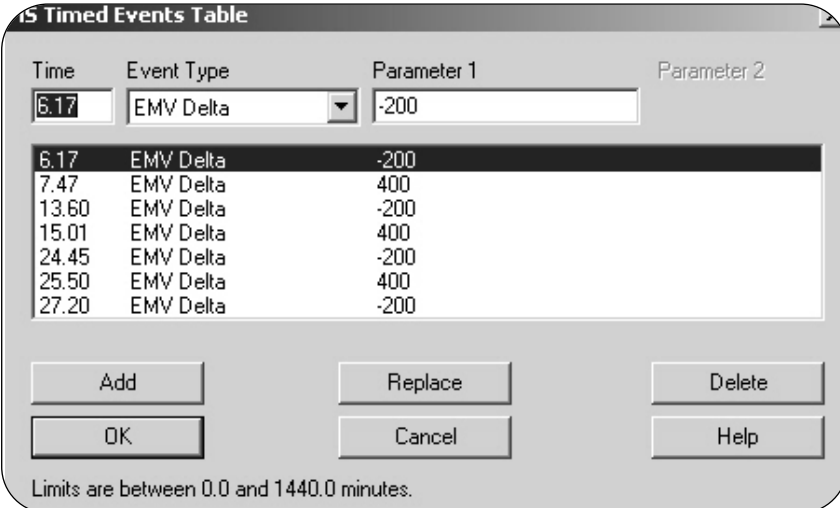
used for unknown identification. The Agilent implementation allows collection of both SIM and scan data in a very narrow cycle time.⁸ The SIM masses used for identification and quantitation of the solvents in the work are listed in table 4.

Conclusions

Manufacturers of pharmaceuticals must ensure that residual solvents (organic volatile impurities or OVIs) and related contaminants are not present in their products or are present below levels stipulated as safe by regulation. One of the impediments to accurate determination of impurities at very low levels is the proclivity for analyte interaction and/or reaction with the internal surfaces of the instrument sample path. To eliminate this problem, a new inert G1888 headspace sampler was developed. Carryover, a common concern in older headspace samplers is also greatly reduced.⁵ The whole system has a non-reactive, non-adsorptive sample flow path from the point of injection through detection. When coupled to the 5975 inert MSD which utilizes a solid inert source superior results are obtained when the need for unknown identification, confirmation, and quantitation is required. Analytical results obtained from the inert HS/GC/5975 MSD provides excellent sensitivity when utilizing SIM/Scan data acquisition. This feature of the 5975 MSD allows for very low level detection and quantitation of target ions while also searching for unknowns using scan. Confirmation is still possible since library searchable full scan data is collected along with SIM data for best sensitivity. This feature is made possible in

| Quant | Q1 | Q2 | Name |
|-------|-------|-------|-------------------------------|
| 31.1 | 32.1 | | Methanol |
| 61.1 | 96 | 98 | 1,1-dichloroethene |
| 41.1 | 40.1 | 39.1 | Acetonitrile |
| 86 | 49.1 | | Methylene chloride |
| 98 | 61.1 | | 1,2-dichloroethene |
| 57.2 | 41.1 | 86.2 | Hexane |
| 96.1 | 61.1 | 98.1 | Cis 1,2-dichloroethene |
| 83 | 85 | 87 | Chloroform |
| 97 | 99 | 61.1 | 1,1,1-trichloroethane |
| 84.2 | 56.2 | 69.2 | Cyclohexane |
| 116.9 | 119 | 120.9 | Carbon tetrachloride |
| 78.1 | 77.1 | 51.1 | Benzene |
| 62.1 | 64 | 49 | 1,2-dichloroethane |
| 45.1 | 60.1 | 90.1 | 1,2-dimethoxyethane |
| 130 | 132 | 95 | Trichloroethylene |
| 83.2 | 98.2 | 69.2 | Methylcyclohexane |
| 88.1 | 58.1 | 43.1 | 1,4-dioxane |
| 79.1 | 52.1 | 51.1 | Pyridine |
| 91.2 | 92.2 | 65.2 | Toluene |
| 58.1 | 43.1 | 100.2 | Hexanone |
| 73.1 | 44.1 | 42.1 | N,N-dimethylformamide |
| 112.1 | 77.2 | 114.1 | Chlorobenzene |
| 91.2 | 106.2 | 65.2 | Ethylbenzene |
| 91.2 | 106.2 | 105.2 | m- & p-xylene |
| 91.2 | 106.2 | 105.2 | o-xylene |
| 87.1 | 72.1 | 44 | N,N-dimethylacetamide |
| 104.2 | 132.2 | 91.2 | 1,2,3,4-tetrahydronaphthalene |

Table 4
SIM masses used for quantitation of the analyzed solvents. Quant target = ion used for identification and quantitation, Q1, Q2 = qualifier ions used for identification.



| Time | Event Type | Parameter 1 | Parameter 2 |
|-------|------------|-------------|-------------|
| 6.17 | EMV Delta | -200 | |
| 6.17 | EMV Delta | -200 | |
| 7.47 | EMV Delta | 400 | |
| 13.60 | EMV Delta | -200 | |
| 15.01 | EMV Delta | 400 | |
| 24.45 | EMV Delta | -200 | |
| 25.50 | EMV Delta | 400 | |
| 27.20 | EMV Delta | -200 | |

Limits are between 0.0 and 1440.0 minutes.

Figure 7
Run time table for changes to the electron multiplier voltage.

the Agilent 5975 without a compromise in performance by use of “performance” or fast electronics.⁸ The methods and procedures outlined in this work illustrate new potential approaches to the analysis of residual solvents. The ChemStation software used is the

G1701DA MSD Productivity ChemStation (version D.02.00). For regulated laboratories the MSD Security ChemStation (G1732AA) provides the ability to work in full compliance with 21 CFR Part 11⁹. Before transferring methods into routine use laborato-

ries should validate their methods according to the respective guidelines published by industrial committees and regulatory agencies, such as the ICH (International Conference on Harmonization), USP (United States Pharmacopeia) or EP (European Pharmacopeia). Methods developed and validated with the system described in this Application Note can then be used in quality control with the MSD Security ChemStation.

References

1. Anil M. Dwivedi, "Residual Solvent Analysis in Pharmaceuticals", *Pharmaceutical Technology*, 42-46, Nov. 2002.
2. "Guidance for Industry, Q3C Impurities: Residual Solvents", U.S. Department of Health and Human Services, FDA, Center for Drug Evaluation and Research (CDER), Center for Biologics Evaluation and Research (CBER), ICH, Dec. 1997.
3. "Revised PDEs for NMP and THF", *Federal Register*, 68, (219), Notices, 64353, Nov. 2003.
4. "Limits of Residual Solvents", *Federal Register*, 62, (247), Notices 67380-67381, Dec. 1997.
5. Roger L. Firor, "The Determination of Residual Solvents in Pharmaceuticals Using the Agilent G1888 Network Headspace Sampler", *Agilent Technologies Application Note*, publication number 5989-1263EN, June 2004.
6. "US EPA Method 524.2, Measurement of Purgeable Organic Compounds in Water by Capillary Column Gas Chromatography/Mass Spectrometry", Revision 4, Aug. 1992.
7. Harry Prest and David W. Peterson, "New Approaches to the Development of GC/MS Selected Ion Monitoring Acquisition and Quantitation Methods", *Agilent Technologies Application Note*, publication number 5988-4188EN, Nov. 2001.
8. Chin-Kai Meng, "Improving Productivity with Synchronous SIM/Scan", *Agilent Technologies Application Note*, publication number 5989-3108EN, May 2005.
9. "Agilent MSD Security ChemStation for GC/MS Systems", *Specifications*, publication number 5989-2015EN, Jan. 2005.

Roger L. Firor and Albert E. Gudat are Application Chemists at Agilent Technologies, Inc. Paramus, NJ, USA.

www.agilent.com/chem

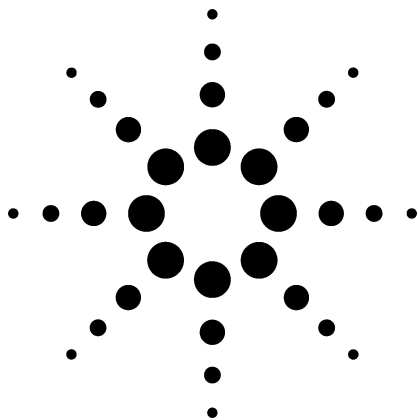
© Copyright 2005 Agilent Technologies

All Rights Reserved. Reproduction, adaptation or translation without prior written permission is prohibited, except as allowed under the copyright laws.

Published June 1, 2005
Publication Number 5989-3196EN



Agilent Technologies



The Determination of Residual Solvents in Pharmaceuticals Using the Agilent G1888 Network Headspace Sampler

Application

Pharmaceuticals

Author

Roger L. Firor
Agilent Technologies, Inc.
2850 Centerville Road
Wilmington, DE 19808-1610
USA

Abstract

The G1888 Network Headspace Sampler interfaced to 6890N gas chromatographs configured with either an FID or 5973 inert MSD were used for the determination of regulated residual solvents. Standard mixtures in water were used at various concentrations including levels below published acceptance guidelines to demonstrate system performance. Included were Class 1 and Class 2 solvents, according to the International Conference on Harmonization, and those listed in USP 467. Repeatability, inertness, and carryover reduction are improved compared to previous generation samplers, using the automated 70-sample G1888 with Siltek flow path. Integrated control and sequencing of the sampler is incorporated into the Agilent GC ChemStation through an add-on software module.

Introduction

Organic volatile impurities (OVIs) can result from the manufacture of active pharmaceuticals or other drug products. Many are used to enhance yields, improve crystallization, or increase solubility [1]. Other factors such as packaging, transportation, and storage can also impact the level of residual solvents. Gas chromatography (GC) coupled with static headspace sampling, acknowledged as an easy-to-use high-throughput analytical tool for the determination of low-level solvent impurities in drugs, can be found in nearly all Quality Control (QC) laboratories in pharmaceutical manufacturing facilities. Sample prep is relatively simple and the methodology is easily validated as per specific monographs.

General guidelines established by the International Conference on Harmonization (ICH) divide solvents into three classes [2]. The Class 1 solvents should not be used in pharmaceutical manufacture because of toxicity or environmental impact, while use of Class 2 solvents should be limited due to potential toxicity. Class 3 solvents are regarded as posing a lower risk to human health. Solvents listed in USP 467 include a subset of specific Class 1 and Class 2 solvents.

This application note will demonstrate the analysis and quantitation of Class 1 and Class 2 solvents. See Table 1 for a listing of residual solvents.



Agilent Technologies

Table 1A. Class 1 Solvents in Pharmaceutical Products - To Be Avoided [2]

| Solvent | Concentration limit (ppm) | Concern |
|-----------------------|----------------------------------|--------------------------------|
| Benzene | 2 | Carcinogen |
| Carbon tetrachloride | 4 | Toxic and environmental hazard |
| 1,2-Dichloroethane | 5 | Toxic |
| 1,1-Dichloroethene | 8 | Toxic |
| 1,1,1-Trichloroethane | 1500 | Environmental hazard |

Table 1B. Class 2 Solvents in Pharmaceutical Products [2]

| Solvent | Permissible daily exposure (ppm) (mg/day) | Concentration limit (ppm) |
|-----------------------|--|----------------------------------|
| Acetonitrile | 4.1 | 410 |
| Chlorobenzene | 3.6 | 360 |
| Chloroform | 0.6 | 60 |
| Cyclohexane | 38.8 | 3880 |
| 1,2-Dichloroethene | 18.7 | 1870 |
| Dichloromethane | 6.0 | 600 |
| 1,2-Dimethoxyethane | 1.0 | 100 |
| N,N-Dimethylacetamide | 10.9 | 1090 |
| N,N-Dimethylformamide | 8.8 | 880 |
| 1,4-Dioxane | 3.8 | 380 |
| 2-Ethoxyethanol | 1.6 | 160 |
| Ethyleneglycol | 6.2 | 620 |
| Formamide | 2.2 | 220 |
| Hexane | 2.9 | 290 |
| Methanol | 30.0 | 3000 |
| 2-Methoxyethanol | 0.5 | 50 |
| Methylbutyl ketone | 0.5 | 50 |
| Methylcyclohexane | 11.8 | 1180 |
| N-Methylpyrrolidone | 48.4 | 4840 |
| Nitromethane | 0.5 | 50 |
| Pyridine | 2.0 | 200 |
| Sulfolane | 1.6 | 160 |
| Tetralin | 1.0 | 100 |
| Toluene | 8.9 | 890 |
| 1,1,2-Trichloroethene | 0.8 | 80 |
| Xylene* | 21.7 | 2170 |

* Usually 60% m-xylene, 14% p-xylene, 9% o-xylene with 17% ethyl benzene.

Table 1C. Solvents in Pharmaceutical Products, According to USP 467

| Solvent | Concentration limit (ppm) |
|--------------------|----------------------------------|
| Methylene chloride | 600 |
| Chloroform | 60 |
| Benzene | 2 |
| Trichloroethylene | 80 |
| 1,4-dioxane | 380 |

Residual solvent and other contaminant levels, designated as safe, have trended downward in recent years as information about potential harmful effects of long-term and/or low-level exposures accumulate and as the detection sensitivity of analytical instrumentation improves. For example, based on new toxicity data, a 2003 change in the regulations for residual solvents stipulate a 10-fold reduction of the 1997 PDE (permitted daily exposure) and residual concentration limits for the solvent N-methylpyrrolidone [3]. It also reclassifies tetrahydrofuran from a Class 3 to a Class 2 category solvent with PDE and concentration limitations more restrictive than toluene [3]. Table 1B also lists PDE and concentration limits for Class 1 and Class 2 residual solvents in pharmaceutical products [4].

Experimental

Two systems are described in this work. The first, based on flame ionization detection is considered the system of choice for routine QC work, while the second system with mass selective detection provides unknown determination, possible quantitation of near-coeluting peaks, and solvent confirmation. Ten-milliliter headspace vials were used for all experiments containing 5 mL water as the matrix, with 1-g sodium sulfate added to assist with analyte extraction. The headspace sampler was equipped with a 1-mL sample loop. Since a sufficient flow must be maintained through the system to avoid excessive peak broadening, a split injection is used. A 2:1 split ratio is the lowest recommended with typical 0.53-mm id column flows.

Table 2. Instrument Conditions

| FID system | | 5973 inert system | |
|---------------------------------|---|---------------------------------|---|
| 6890N GC | | 6890N GC | |
| Injection port | Volatiles interface | Injection port | Volatiles interface |
| Temperature | 160 °C | Temperature | 160 °C |
| Split ratio | 2:1 to 5:1 | Split ratio | 2:1 to 5:1 |
| Carrier gas | Helium | Carrier gas | Helium |
| Carrier flow | 9 mL/min | Inlet pressure | 2.7 psi |
| Detector | FID, 250 °C | Column flow | 1.7 mL/min |
| GC oven program | | GC oven program | |
| Initial temperature | 35 °C | Initial temperature | 35 °C |
| Initial time | 20 min | Initial time | 20 min |
| Rate | 25 °C/min | Rate | 20 °C/min |
| Final temperature | 250 °C | Final temperature | 250 °C |
| Final time | 15 min | Final time | 15 min |
| Columns | 30 m × 0.53 mm × 3 µm DB-624 30 m × 0.45 mm × 2.55 µm DB-624 | Column | 30 m × 0.32 mm × 1.8 µm DB-624 |
| G1888A Headspace Sampler | | G1888A Headspace Sampler | |
| Loop size | 1 mL | Same settings as FID system | |
| Vial pressure | 14.0 psig | 5973 inert | |
| Headspace oven | 85 °C | Scan | 30 to 200 amu, samples 2 |
| Loop temp | 100 °C | SIM | 100 ms dwell |
| Transfer line temp | 120 °C | Source temperature | 230 °C |
| Equilibration time | 30 min, low shake | Quad temperature | 150 °C |
| GC Cycle time | 50 min | Tune | BFB.u |
| Pressurization | 0.15 min | Standards | |
| Vent (loop fill) | 0.15 min | USP 467 | Restek #36228 AccuStandard NF-467-R |
| Inject | 0.5 min | ICH Class 1 and 2 | Restek #36228 (Class 1) #36229 (Class 2A) #36230 (Class 2B) |

Discussion

GC System

Most quality control labs in pharmaceutical manufacturing employ gas chromatography (GC) for the determination of residual solvents that are included in either USP 467 or in the more extensive list covered in ICH guidelines. Capillary GC based on the 624 phase (USP G43) is widely used for solvent separation. A different stationary phase such as DB-1701, DB-5, or DB-WAX (USP G16) can be used in specific methods when coelution is identified. Headspace sampling has many advantages over direct liquid injection including the avoidance of large water injections that can result in column degradation.

Table 3 lists concentrations and identifications of Class 1 and Class 2 solvents used to produce the chromatogram shown in Figure 1.

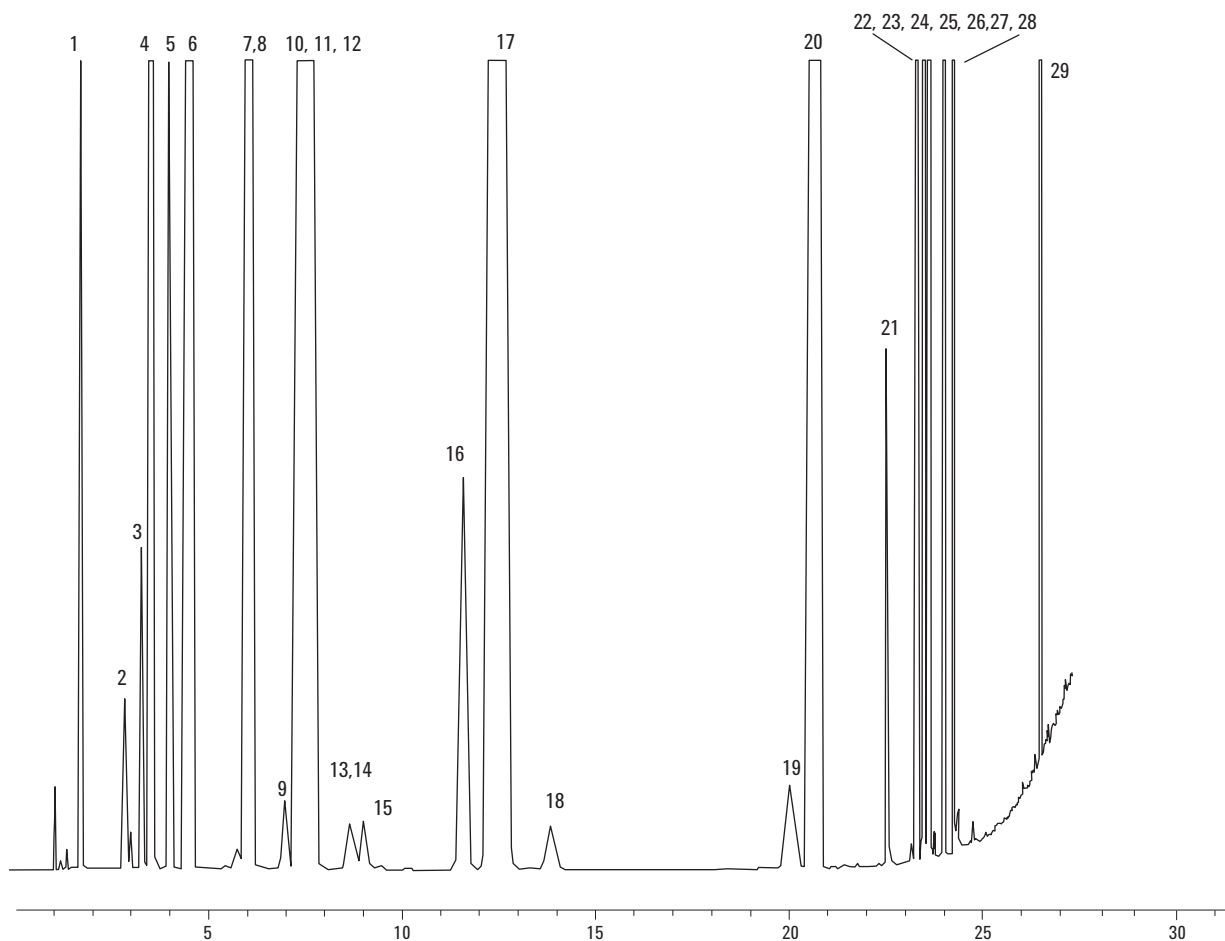


Figure 1. Class 1 and Class 2 residual solvents. G1888, 6890N with FID and volatiles interface.

These concentrations equal the guideline limits based on a 100-mg sample of the pharmaceutical dissolved in 5 mL. USP 467 solvents are shown in Figure 2 at concentrations below the required levels (10 μ L Restek std. #36228). Excellent signal-to-noise ratio is still achieved. Concentrations used throughout this work are defined as the analyte concentration present in the headspace vial prior to sampling.

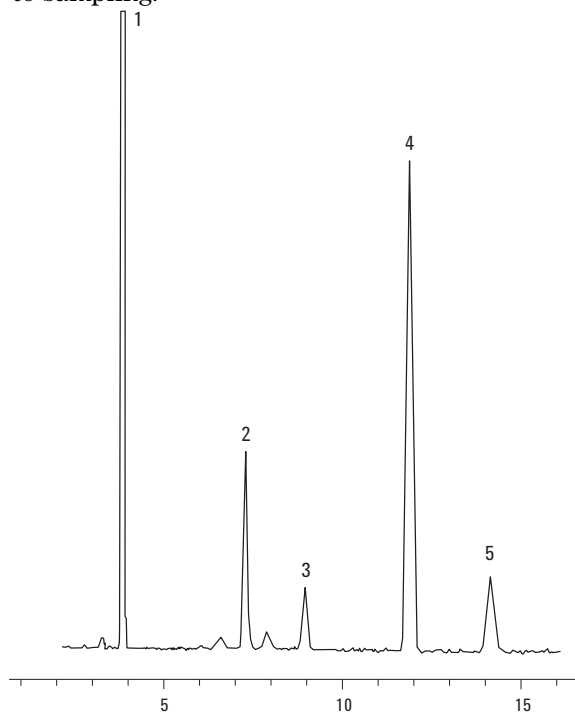


Figure 2. Identifications and concentrations: 1. Methylene chloride 1.2 μ g/mL, 2. Chloroform 0.12 μ g/mL, 3. Benzene 0.004 μ g/mL, 4. Trichloroethylene 0.16 μ g/mL, 5. 1,4-dioxane 0.76 μ g/mL.

Coelutions that occur on the DB-624 column under the chromatographic conditions and concentrations employed are listed in Table 4. Using the 30 m \times 0.45 mm \times 2.55 μ m DB-624 column, benzene and 1,2-dichloro-ethane can be resolved at a 35 $^{\circ}$ C oven temperature, as seen in Figure 3.

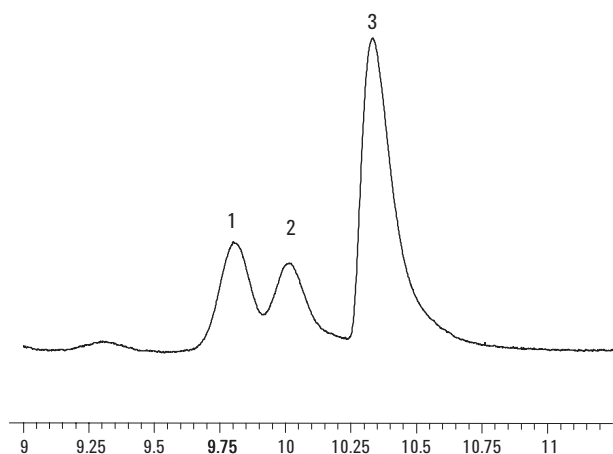


Figure 3. Resolution of benzene and 1,2 dichloroethane. Peak identifications: 1. benzene, 2. 1,2-dichloroethane, 3. 1,2-dimethoxyethane.

Calibration curves for selected solvents included in USP 467 are shown in Figure 4. Linear results are seen over a concentration range that extends well below recommended maximum concentrations. The concentration range is well within the linear dynamic range of the thick film 0.53 mm and 0.45-mm id columns.

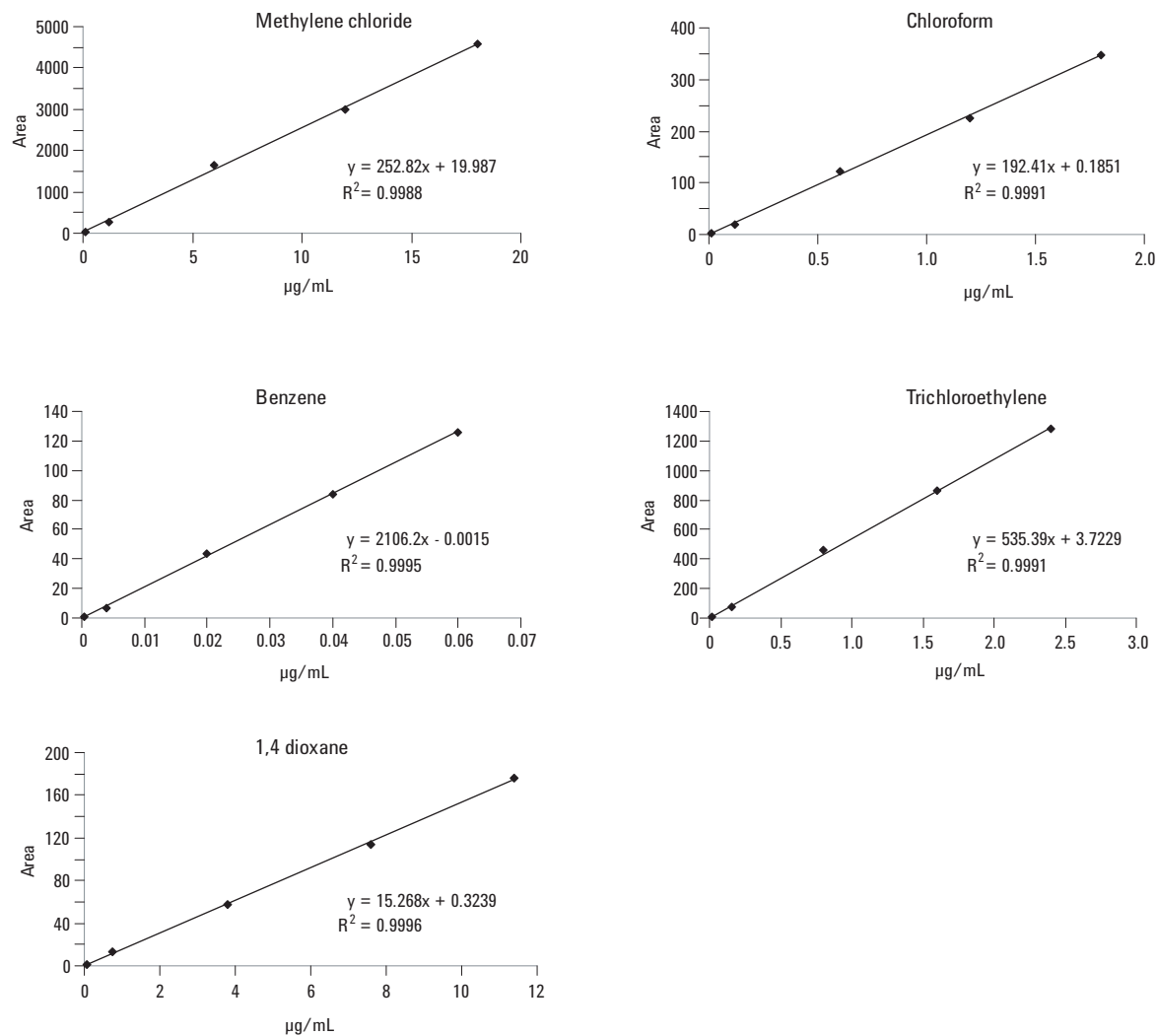


Figure 4. Calibration plots for selected solvents.

Headspace equilibration time is normally set at 60 min; however, in most cases 30 min is sufficient. Figure 5 illustrates an overlay of a 30- and 60-min headspace equilibration for a selected portion of the chromatogram (Class 1 and 2 solvents). Little overall difference is seen in the peak areas; although for some compounds 30-min equilibration produces marginally larger areas.

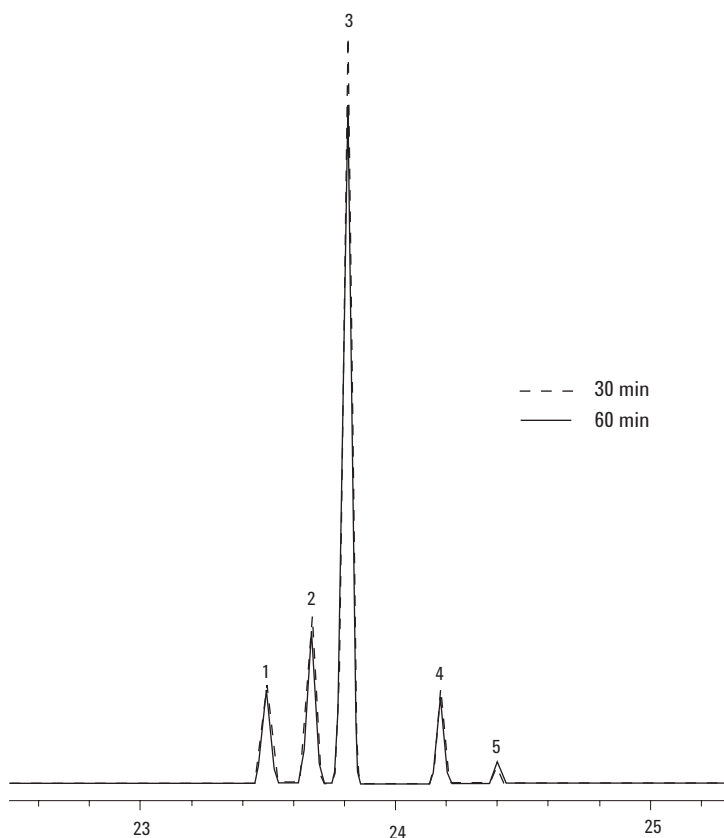


Figure 5. Overlay of selected compounds after 30- and 60-min headspace equilibration times. 1. Chlorobenzene, 2. Ethylbenzene and DMF, 3. m-xylene, p-xylene, 4. o-xylene, 5. N,N-dimethylacetamide.

Table 3. Class 1 and Class 2 Residual Solvent Concentrations*. Table ID Column Corresponds to Chromatogram Numbering

| Solvent | ID | Conc. ($\mu\text{g/mL}$) | Solvent | ID | Conc. ($\mu\text{g/mL}$) |
|--------------------------------|----|----------------------------|-----------------------|----|----------------------------|
| Methanol | 1 | 60 | Trichloroethylene | 16 | 1.6 |
| 1,1-Dichloroethane | 2 | 0.16 | Methyl cyclohexane | 17 | 236 |
| Acetonitrile | 3 | 8.2 | 1,4-Dioxane | 18 | 7.6 |
| Methylene chloride | 4 | 12 | Pyridine | 19 | 4 |
| Hexane | 6 | 5.1 | Toluene | 20 | 17.8 |
| <i>cis</i> -1,2-dichloroethane | 7 | 37.4 | 2-Hexanone | 21 | 1 |
| Nitrobenzene | 8 | 1 | Chlorobenzene | 22 | 7.6 |
| Chloroform | 9 | 1.2 | Ethylbenzene | 23 | 7.38 |
| Carbon tetrachloride | 10 | 0.08 | N,N-dimethylformamide | 24 | 17.6 |
| Cyclohexane | 11 | 77.6 | m-xylene | 25 | 26.04 |
| 1,1,1-Trichloroethane | 12 | 30 | p-xylene | 26 | 6.08 |
| Benzene | 13 | 0.04 | o-xylene | 27 | 3.9 |
| 1,2-Dichloroethane | 14 | 0.1 | N,N-dimethylacetamide | 28 | 21.8 |
| 1,2-Dimethoxyethane | 15 | 2 | Tetraline | 29 | 2 |

*Concentrations shown are headspace vial solution concentrations prior to sampling. Peak 5 (*trans* 1,2 dichloroethane) is not listed in the table as a Class 1 or Class 2 solvent.

Table 4. Coelutions on 0.53-mm id DB-624

| Coelution group | Solvents |
|-----------------|---|
| 1 (partial) | Benzene, 1,2 dichloroethane |
| 2 | Nitrobenzene, <i>cis</i> -1,2 dichloroethene |
| 3 | Carbon tetrachloride, Cyclohexane, 1,1,1- trichloroethane** |
| 4 | Ethylbenzene, DMF |
| 5 | m-xylene, p-xylene |

* Trichloroethane will separate from CCl₄ in absence of cyclohexane

+ Figure 6 shows separation on a 30 m x 0.45 mm x 2.55 μm DB-624 Agilent part no.124-1334.

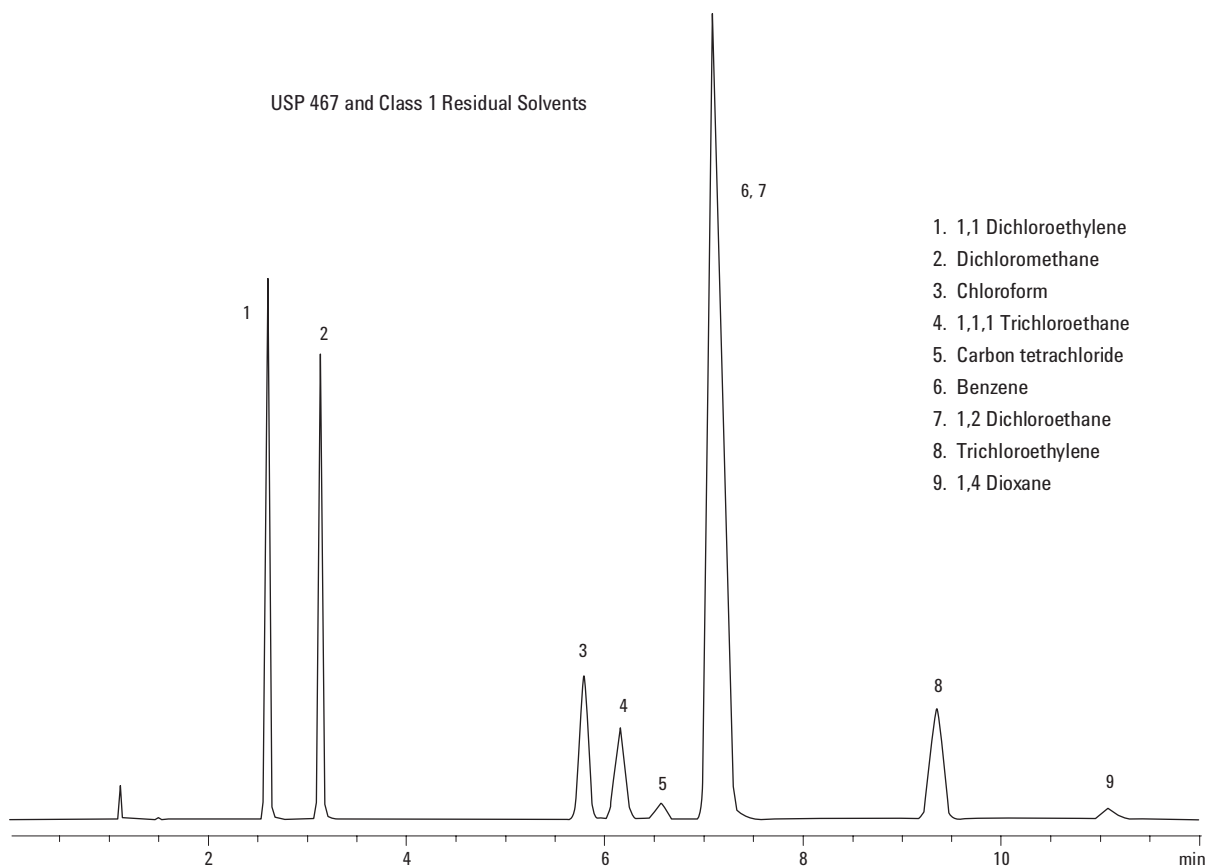


Figure 6. USP 467 and Class 1 solvents at 1 ppm each on the 30 m x 0.45 mm x 2.55 μm DB-624 column. Starting GC oven temperature was 40 °C.

MSD System

A TIC of Class 1 and Class 2 solvents produced with a G1888/6890N/5973 inert system is shown in Figure 7.

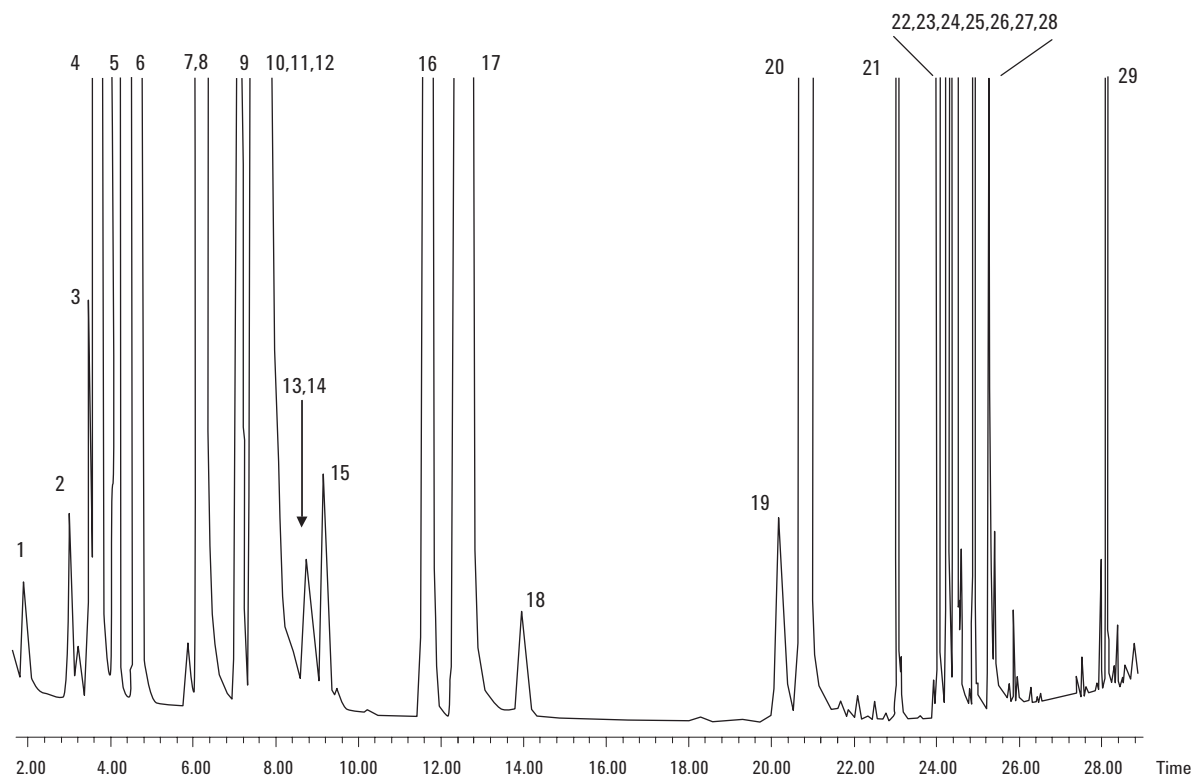


Figure 7. TIC of Class 1 and Class 2 solvents. See Table 3 for compound identifications.

Analyte solution concentrations and peak identifications are as indicated in Table 3. Gas chromatography/mass spectrometry (GC/MS) offers an alternative methodology to flame ionization detection (FID) that can be useful to solve coelution problems or identify unknowns. Also, excellent sensitivity and selectivity can be achieved in Selected Ion Monitoring (SIM) mode, which may be useful for drug manufacturing process development to identify and quantify trace impurities.

Carryover

In practice, nonaqueous solvents are commonly used in testing since extraction of many common solvents used in pharmaceutical manufacturing are not water soluble. Some common solvents include DMA (N,N-dimethylacetamide), DMSO, pyridine, and DMI (1,3-Dimethyl-2-imidazolidinone). Because many of the solvents used are high boiling, the possibility of headspace carryover exists. Improvements in the thermal zone temperature uniformity in the G1888 reduce the condensation of high-boiling materials in various flow path lines and vent valve.

The G1888 incorporates a new feature that allows users to program the vent purge time, labeled “Sequence Vent Purge” in the advanced functions menu. This represents the time interval when the vent line is purged as a post injection event. The default time of 30 seconds can be increased up to an approximate maximum of the cycle time. For the carryover experiments in this work, a vent purge time of 20 min was used to further reduce the possibility of solvent carryover.

One hundred microliters of pure solvent was introduced into 10-mL vials. Larger amounts of solvent will not result in an increase in the amount injected. A 10-vial sequence was set up with alternating solvent and water blank vials using the chromatographic program shown in the experimental section. This test was performed for pyridine, DMSO, and DMA. For all three solvents, carryover ($[\text{amount solvent area from blank vial}/\text{solvent area from solvent vial}] \times 100$) was under 0.006%. In addition, the solvent areas for all blanks had $\pm 3\%$ RSDs, indicating an absence of trending. As an additional carryover check, 10 consecutive vials of DMA (100 μL per 10-mL vial) were run at a Headspace oven temperature of 100 °C. These were followed by two water blanks. The first blank showed carryover of 0.004% and the second 0.001%.

One of the most effective solvent systems used today by pharmaceutical companies is DMI with a boiling point of 225 °C. Table 5 lists the system set points used in a carryover test with this solvent. Alternating vials of DMI and water blank were run in a headspace sequence. Results are shown in Figure 8.

The large concentration of DMI overloads the column and leads to some inconsistency in areas, however, it is not a concern given the purpose of this test. Measured carryover is under 0.003%.

Table 5. Setting Used for DMI Carryover Test

| | |
|---------------------|---|
| Headspace oven | 220 °C |
| Loop | 250 °C |
| Transfer line | 250 °C |
| Vial eq. time | 30 min |
| Sequence vent purge | 20 min |
| Sample | 100- μL DMI in 10-mL vial |
| Blanks | 5- μL water in 10-mL vial |
| Volatiles interface | 250 °C |
| Split ratio | 10:1 |
| Oven program | 35 °C (0 min) to 260 °C (15 min) at 25 °C/min |

To check for carryover of the actual analytes, a test scheme similar to that used for the pure solvents was chosen. One hundred microliters of the USP 467 standard (Restek # 36007) was placed in 5-mL water/1 g Na_2SO_4 . These vials were alternated with pure water blanks in a 10-vial sequence at 85 °C equilibration temperature. No measurable area for the analytes could be integrated in any of the runs.

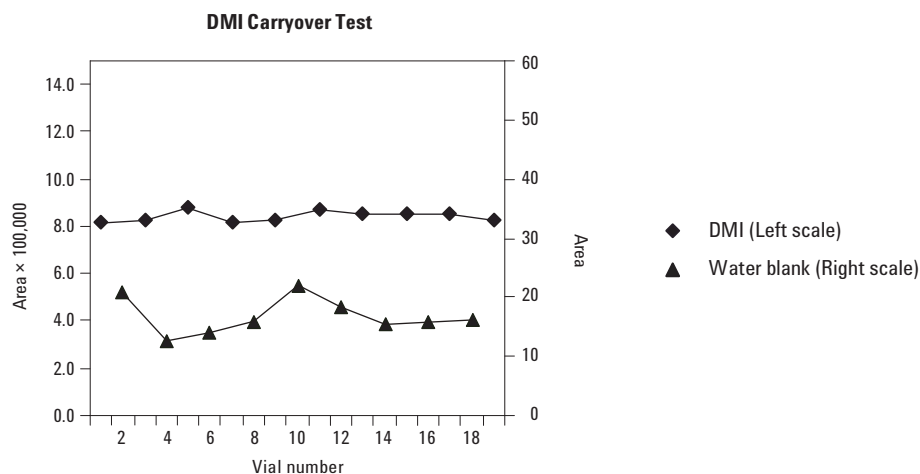


Figure 8. DMI carryover results.

Conclusions

Manufacturers of pharmaceuticals must ensure that residual solvents, OVIs, and related contaminants are not present in their products, or are present below levels stipulated as safe by regulation. One of the impediments to accurate determination of impurities at very low levels is the tendency for analyte interaction and/or reaction with the internal surfaces of the instrument sample path. To eliminate this problem, a new inert headspace sampler, the G1888 system was developed. This instrument possesses a nonreactive, nonadsorptive sample flow path from the point of injection through detection. This significantly reduces carry-over, a common problem with older instrumentation. High temperature heated zones extend the choice of solvent systems that can be used. When coupled to the 5973 inert MSD, which uses a solid inert source, superior results are obtained when the need for unknown identification or confirmation is required. Analytical results obtained for broad classes of solvents, used in medicinal products by the G1888 Headspace Sampler systems, described in this application show reduced carry-over, excellent detection sensitivity, and good linear response over the ppm to ppb range.

The methods and procedures outlined in this work illustrate potential approaches to the analysis of residual solvents. Laboratories should perform system suitability studies and validate their methods according to ICH or USP guidelines.

References

1. Anil M. Dwivedi, Residual Solvent Analysis in Pharmaceuticals, (Nov., 2002) *Pharmaceutical Technology*, 42-46.
2. Guidance for Industry, Q3C Impurities: Residual Solvents, U.S. Department of Health and Human Services, FDA, Center for Drug Evaluation and Research (CDER), Center for Biologics Evaluation and Research (CBER) Dec. 1997, ICH.
3. Revised PDEs for NMP and THF, Federal Register, 68, (219), Nov. 2003, Notices, 64353.
4. Limits of Residual Solvents, Federal Register, 62, (247), Dec. 1997, Notices 67380-67381.

For More Information

For more information on our products and services, visit our Web site at www.agilent.com/chem.

Agilent shall not be liable for errors contained herein or for incidental or consequential damages in connection with the furnishing, performance, or use of this material.

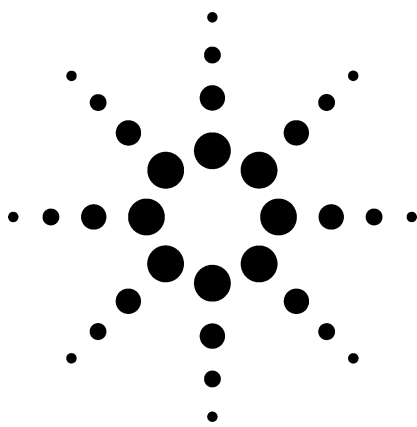
Information, descriptions, and specifications in this publication are subject to change without notice.

© Agilent Technologies, Inc. 2004

Printed in the USA
June 21, 2004
5989-1263EN



Agilent Technologies



A New Approach to the Analysis of Phthalate Esters by GC/MS

Application

Gas Chromatography/Mass Spectrometry

March 2001

Authors

Cameron George
Agilent Technologies, Inc.
91 Blue Ravine Road
Folsom, California 95630-4714
USA

Harry Prest
Agilent Technologies, Inc.
1601 California Avenue
Palo Alto, California 94304-1111
USA

Abstract

A new instrumental method for the determination of 29 phthalate esters, including six recently banned from baby toys by the European Union, using positive chemical ionization and retention-time locking is described. Positive chemical ionization provides a high degree of selective ionization for the phthalates, primarily producing spectra in which the protonated molecule ($M+1$) is the base peak. This provides easy discrimination among the phthalates on the basis of their molecular weight, while retention-time locking increases confidence in the identification of the various isomers.

In this approach, both pure compounds and technical mixtures are considered. Although this work focuses on the more commonly used 1,2-substituted esters, the 1,3-isomers and 1,4-isomers are also characterized.

The combination of positive chemical ionization and retention-time locking makes the method rugged, durable and applicable to a wide variety of matrices.

Introduction

The widespread use and manufacture of plastics have made the phthalate esters one of the most ubiquitous classes of compounds in our everyday environment. These “plasticizers” increase polymer flexibility due to their function as intermolecular “lubricants”. Because they are additives and not reagents, they are not chemically bound in the polymer and are available to leach from the matrix. Phthalates are also components of cosmetics, detergents, building products (flooring, sheeting, films), lubricating oils, PCB substitutes, carriers in pesticide formulations and solvents. Consequently, the potential for human exposure is very high. Toxicological studies have linked some of these compounds to liver and kidney damage, and to possible testicular or reproductive-tract birth defect problems, characterizing them as endocrine disruptors. Scientists at the U.S. Centers for Disease Control have, for the first time, documented human exposure to phthalates by determinations of the monoester metabolites in human urine [1]. Their work leads to the conclusion that “phthalate exposure is both higher and more common than previously suspected.”

Of particular concern were the significantly higher concentrations of the dibutyl phthalate metabolite in urine of women of childbearing age (20-40 years) than in other portions of the population.

The presence of phthalate esters in polyvinyl chloride (PVC) toys has generated the most



Agilent Technologies

controversy. While regulators in Greece have completely banned soft PVC toys, Austria, Denmark, Finland, France, Germany, Norway and Sweden have unilaterally banned phthalates in PVC toys for children under three years old. In December of 1999, the European Union (EU), concerned with a “serious and immediate risk” to children, placed an emergency ban on six of the phthalate esters in soft PVC toys and childcare products meant to be placed in the mouths of children under the age of three [2]. None of the six banned phthalates may exceed 0.1% by weight.

These heightened concerns suggest the need for an improved method of detecting and characterizing phthalate esters which is applicable to a wide variety of matrices. This application note describes such an analytical method.

Phthalate Structure and Mass Spectra

The three primary structures of phthalates are shown in Figure 1. Although there are three possible positions for the ester linkages, the most commonly used phthalates are based on the 1,2-benzenedicarboxylic acid structure (top). There are an infinite number of possible alkyl side chains, (R) and an infinite number of combinations of the side groups (R and R'). For example, the diisononyl phthalate consists of an array of compounds due to the isomeric branched-chain alkyl groups on both side chains.

For phthalate esters with saturated alkyl side chains (without oxygen), the most intense peak in the electron impact (EI) ionization mass spectrum at 70 eV is always at m/z 149 due to the rapid formation and stability of the ion shown in Figure 2. (The only exception is $R=R'=CH_3$ where the base peak is at m/z 163).

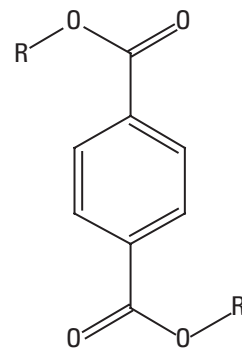
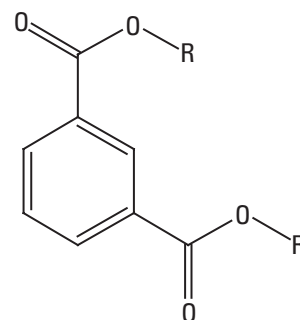
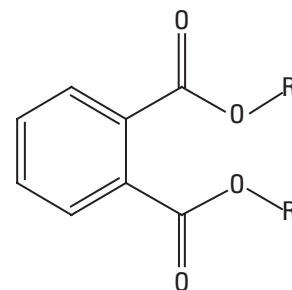


Figure 1. Phthalic ester (top) or the 1,2-benzenedicarboxylic acid ester, isophthalic ester (middle) or the 1,3-benzenedicarboxylic acid ester, and terephthalic ester (bottom) or the 1,4-benzenedicarboxylic acid ester. R and R' represent alkyl side chains which may be branched and contain oxygen.

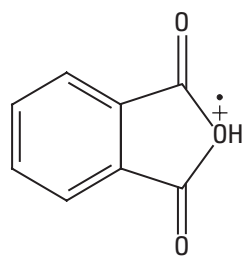


Figure 2. The most abundant ion in the mass spectra of the phthalate esters with saturated alkyl side chains; m/z 149. The exception is for dimethyl phthalate where both R and R' are CH_3 and so the H on the oxygen is replaced by CH_3 and consequently m/z 163 becomes the base peak.

Invariably, the molecular ion is very weak or altogether absent; other fragments that provide information on the phthalate identity are also of very low abundance. As an example, consider the EI mass spectrum of dibutyl phthalate, one of the six banned by the EU, and bis(4-methyl-2-pentyl) phthalate in Figure 3. Identifying fragments have relative intensities of less than 10%. Gas chromatography provides some separation of the phthalates, but with the array of possible isomers and essentially a single identifying ion (i.e., m/z 149), distinguishing the individual phthalates of concern is difficult. More confident identification of the phthalates is possible using chemical ionization mass spectrometry in conjunction with retention-time locking (RTL).

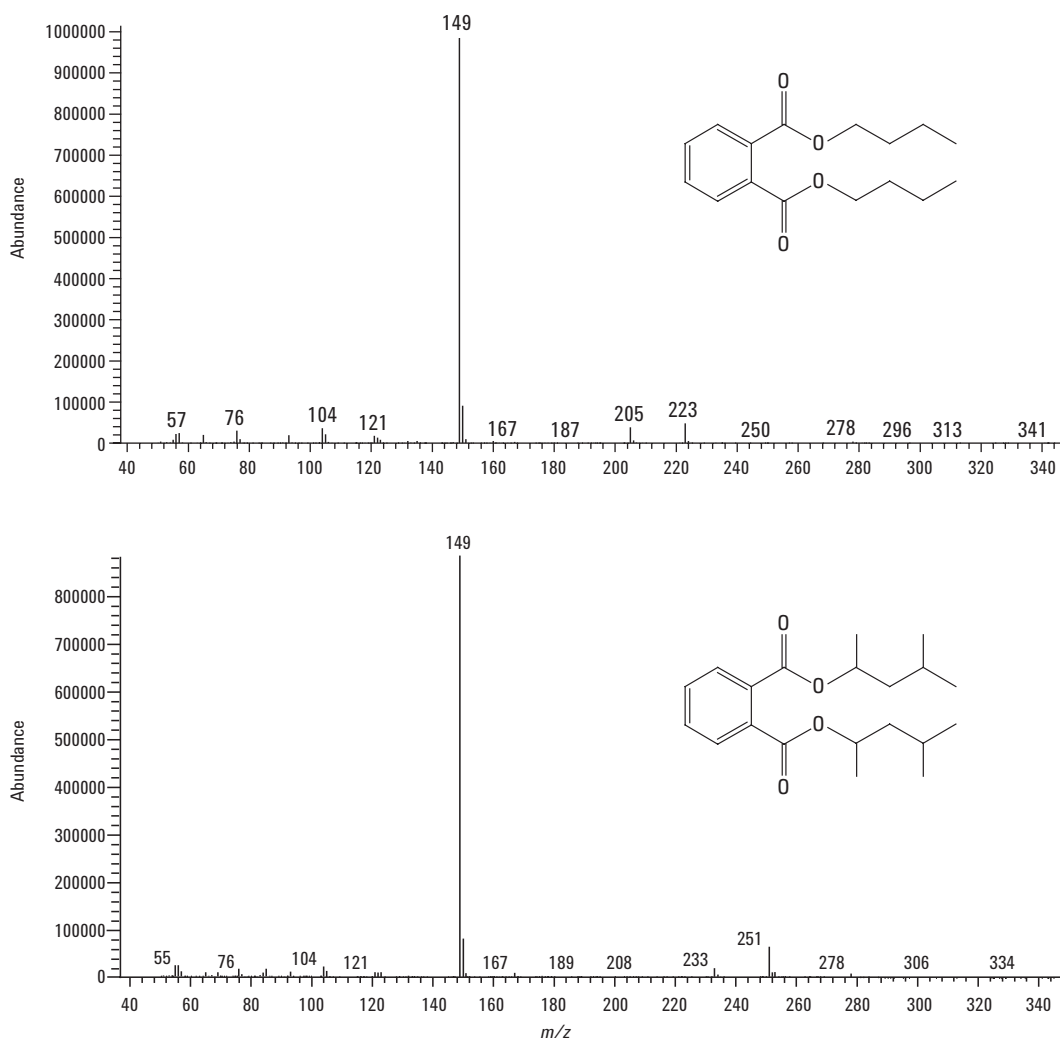


Figure 3. Electron impact ionization mass spectra of di-n-butyl phthalate (upper panel) and bis(4-methyl-2-pentyl) phthalate (lower panel) from m/z 50 to 350 at 70 eV. Notice the lack of intense fragments and molecular ions. The molecular weights are 278 and 334 g/mole, respectively.

Retention-time locking allows compound retention times achieved on any one Agilent 6890 gas chromatograph (GC) to be replicated to within a few seconds on any other Agilent 6890 gas chromatograph (GC) applying the same GC method [3-5]. RTL is a powerful approach to compound identification. RTL allows the creation of compound acquisition methods and quantitation databases that can be reproduced in any laboratory, anywhere, because a compound can have a universally fixed and reproducible retention time. It is important that RTL be applied in conjunction with the appropriate detection scheme and sample preparation methods.

Chemical ionization provides a more selective form of ionization than electron impact [6]. By judicious choice of the reagent gases, the degree of compound fragmentation can be controlled to a certain extent. In positive chemical ionization, methane reagent gas usually provides more fragmentation than gases of higher proton affinity such as ammonia. Less fragmentation would be helpful in identifying the phthalates. Instead of all phthalates generating a single, similar ion, positive ionization can provide phthalate ester molecular weights.

Experimental

Phthalate esters were obtained from Ultra Scientific (North Kingstown, RI), AccuStandard (New Haven, CT), and ChemServices (West Chester, PA) as neat compounds and mixtures. Dilutions were made in isooctane (Burdick and Jackson Grade, VWR Scientific).

The configuration and operating parameters of the Agilent 6890Plus GC (standard 120V or “faster ramping” 220V), 7683 Automatic Liquid Sampler and 5973N MSD with CI option used for acquiring the data are given in the following tables. PCI reagent gas purities were 99.99% or higher.

Injection Parameters

| | | |
|----------------------------|------------------|----------|
| Injection Mode | Pulsed Splitless | |
| Injection Port Temperature | 300°C | |
| Pulse Pressure & Time | 25.0 psi | 1.00 min |
| Purge Flow & Time | 20.0 mL/min | 3.00 min |
| Gas Saver Flow & Time | 20.0 mL/min | 3.00 min |

Oven Parameters

| | | |
|------------------------|----------|----------|
| Temperature Program | 80°C | 1.00 min |
| 50.00°C/min | 200°C | 0.00 min |
| 15.00°C/min | 350°C | 2.00 min |
| Oven Equilibrium Time | 0.25 min | |
| MSD Transfer Line Temp | 325°C | |

Column Parameters

| | | |
|----------------------------|--|---------------|
| GC column (122-5532) | DB-5MS 30 m; 0.25 mm i.d.; 0.25 µm film | |
| Initial Flow & Mode | 1.2 mL/min | Constant Flow |
| Detector & Outlet Pressure | MSD | Vacuum |

Mass Spectrometer Parameters

| | | |
|--------------------------------|---------------------------------|--|
| Tune Parameters | PCI Autotune (NH ₃) | |
| Electron Multiplier Voltage | Autotune + 400V | |
| Solvent Delay | 4.00 min | |
| Scan Parameters | 194 - 550 m/z | |
| Quadrupole Temperature | 150°C | |
| Source Temperature | 250°C | |
| Ammonia Gas Flow (MFC setting) | 0.5 mL/min (10%) | |

Miscellaneous Parts

| | | |
|-----------------------|-----------|------------------------------------|
| Septa | 5182-0739 | BTO septa (400°C) |
| Liner | 5062-3587 | Deactivated 4 mm i.d. single taper |
| GC column ferrule | 5181-3323 | 250 µm Vespel |
| MSD interface ferrule | 5082-3508 | 0.4 mm i.d. graphitized Vespel |

Results and Discussion

As expected using methane as the reagent gas, the PCI mass spectra of the phthalates show ions corresponding to the protonated molecule $[M+H]^+$ and adducts $[M+C_2H_5]^+$ and $[M+C_3H_5]^+$. Because of the relatively vigorous fragmentation produced by methane, the spectra of the dialkyl phthalate esters still resemble that produced in EI. In most cases, the fragment at m/z 149 is the base peak, however ions at m/z $M+1$, $M+29$ and $M+41$ are relatively intense with $[M+H]^+$ from 10% to 30% (Figure 5). The dialkyl phthalate spectra also show a fragment corresponding to loss of one of the alkyloxy side chains to produce an ion shown in Figure 4. This is the most intense fragment for the dimethyl and diethyl phthalates and for the dibutyl and dipentyl (diamyl) phthalates, about 75% of the 149 base peak. As the length of ester alkyl chain increases, the intensity of this fragment decreases. (Apparently, in the dialkyl isophthalates, loss of the alkyl side chain not accompanied by the oxygen may be a preferred route.)

Although positive chemical ionization with methane provides more information than EI on phthalate identity, the methane reagent is still rather unselective in ionization and will produce more chemical noise in the background, complicating identification in complex matrices.

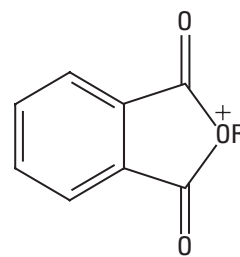


Figure 4. One of the most intense fragments in the methane PCI spectra of the phthalate esters is formed by loss of one of the alkyloxy side groups.

Applying ammonia as the reagent gas in PCI to reduce chemical noise and enhance identification of the phthalates is a more useful approach. The relatively gentle ionization produces protonation of the dialkyl phthalates, with m/z $M+1$ the base peak in their spectra. When combined with retention-time locking, identification of phthalates becomes further simplified. Compare the spectra of the di-*n*-butyl phthalate acquired using methane versus ammonia as the reagent gas (Figure 5). The protonated molecule is the single dominant peak in the ammonia PCI mass spectrum of the di-*n*-butyl phthalate, and the adduct at m/z 296 ($[M+NH_4]^+$) is relatively small.

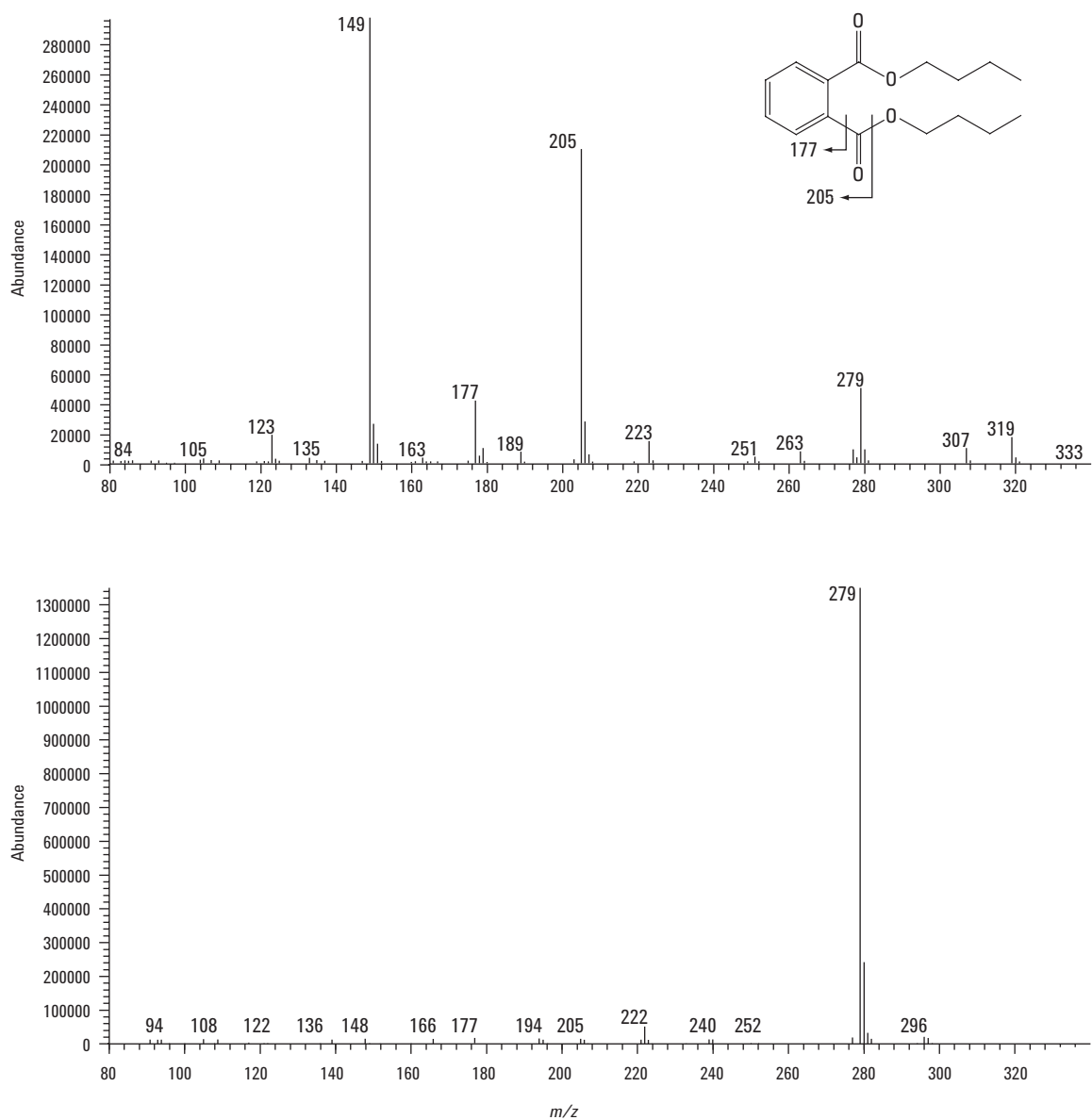
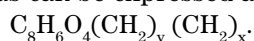


Figure 5. PCI methane (upper panel) and ammonia (lower panel) mass spectra of di-n-butyl phthalate. The PCI methane mass spectrum shows substantial fragmentation but relative to the EI spectrum in Figure 3, high abundance for the higher m/z ions such as the protonated molecule at m/z 279. The ion at m/z 205 is generated by loss of an oxybutyl fragment; a process described in Figure 4. The PCI-ammonia mass spectrum consists almost completely of the protonated molecule.

This implies an easy method for identification. Whereas the EI spectra of the phthalates most frequently result in a base peak at m/z 149, the dialkyl phthalate PCI-ammonia spectra have base peaks at $m/z = M+1$. All dialkyl phthalates molecular formulas can be expressed as



These phthalates have (nominal) molecular masses given by

$$M = 166 + (x + y) \cdot 14, \text{ or}$$

$$M = 166 + (w) \cdot 28,$$

where x and y are the side chain lengths, and the second formula applies to symmetrical side chains (i.e., $x = y = w$). For example, di-*n*-butyl phthalate has $x = y = 4$, and therefore a (nominal) molecular mass of 278 which produces m/z 279 as the base

peak. Interestingly, the PCI-ammonia spectra of the dialkyl isophthalates and terephthalates appear to have base peaks at m/z $M+18$ due to $[M+NH_4]^+$. Because of the greater steric access to the ester linkages, adduct formation may be preferred.

Table 1 gives the phthalate names, CAS numbers, molecular formula, nominal molecular mass, base peak in the PCI-ammonia spectrum and the RTL elution times. These retention times are "locked" relative to diphenyl phthalate, which has been chosen as the RTL locking compound and locked to elute at 9.450 min. Notice that the branched chain isomers elute prior to their straight chain forms on this column phase.

Table 1. Phthalate compound names, Chemical Abstracts Services numbers (CAS), molecular weights (M. Wt.), molecular formulas, nominal base peak in the PCI-ammonia spectrum and retention time (RT) in minutes. Retention times are locked relative to diphenyl phthalate (9.450 min). Retention time ranges are given for the isoalkyl phthalate technical mixtures. Phthalates banned by the EU are indicated by an asterisk*. Benzyl benzoate is included since it is used as a surrogate in U.S. Environmental Protection Agency Method 8061.

| Name | CAS | M. Wt. | Molecular Formula | Base Peak | RT (min) |
|---|------------|--------|---|-----------|---------------|
| dimethyl phthalate | 131-11-3 | 194 | $C_8H_4O_4(CH_3)_2$ | 195 | 4.32 |
| dimethyl isophthalate | 1459-93-4 | 194 | $C_8H_4O_4(CH_3)_2$ | 212 | 4.54 |
| diethyl phthalate | 84-66-2 | 222 | $C_8H_4O_4(C_2H_5)_2$ | 223 | 4.81 |
| diethyl terephthalate | 636-09-9 | 222 | $C_8H_4O_4(C_2H_5)_2$ | 240 | 5.06 |
| benzyl benzoate | 120-51-4 | 212 | $C_{14}H_{12}O_2$ | 230 | 5.62 |
| diisobutyl phthalate | 84-69-5 | 278 | $C_8H_4O_4(C_4H_9)_2$ | 279 | 5.95 |
| di- <i>n</i> -butyl phthalate* | 84-74-2 | 278 | $C_8H_4O_4(C_4H_9)_2$ | 279 | 6.40 |
| bis(2-methoxyethyl) phthalate | 117-82-8 | 282 | $C_8H_4O_4(C_2H_4OCH_3)_2$ | 283 | 6.57 |
| diamyl phthalate | 131-18-0 | 306 | $C_8H_4O_4(C_5H_{11})_2$ | 307 | 6.94 |
| bis(2-ethoxyethyl) phthalate | 605-54-9 | 310 | $C_8H_4O_4(C_2H_4OC_2H_5)_2$ | 311 | 7.13 |
| butyl benzyl phthalate* | 85-68-7 | 312 | $C_8H_4O_4(C_4H_9)(CH_2C_6H_5)$ | 313 | 8.42 |
| diphenyl phthalate | 84-62-8 | 318 | $C_8H_4O_4(C_6H_5)_2$ | 319 | 9.45 |
| diphenyl isophthalate | 744-45-6 | 318 | $C_8H_4O_4(C_6H_5)_2$ | 319 | 10.30 |
| dicyclohexyl phthalate | 84-61-7 | 330 | $C_8H_4O_4(C_6H_{11})_2$ | 331 | 9.32 |
| bis(4-methyl-2-pentyl) phthalate | 146-50-9 | 334 | $C_8H_4O_4(CH_3C_5H_{10})_2$ | 335 | 6.93 |
| diisohexyl phthalates | 146-50-9 | 334 | $C_8H_4O_4(C_6H_{13})_2$ | 335 | 7.55 - 8.28 |
| dihexyl phthalate | 84-75-3 | 334 | $C_8H_4O_4(C_6H_{13})_2$ | 335 | 8.34 |
| dibenzyl phthalate | 523-31-9 | 346 | $C_8H_4O_4(CH_2C_6H_5)_2$ | 347 | 10.51 |
| hexyl-2-ethylhexyl phthalate | 75673-16-4 | 362 | $C_8H_4O_4(C_2H_5C_6H_{12})(C_6H_{13})$ | 363 | 8.84 |
| bis(2- <i>n</i> -butoxyethyl) phthalate | 117-83-9 | 366 | $C_8H_4O_4(C_2H_4OC_4H_9)_2$ | 367 | 8.98 |
| bis(2-ethylhexyl) phthalate* | 117-81-7 | 390 | $C_8H_4O_4(C_2H_5C_6H_{12})_2$ | 391 | 9.32 |
| di- <i>n</i> -octyl phthalate* | 117-84-0 | 390 | $C_8H_4O_4(C_8H_{17})_2$ | 391 | 10.28 |
| dioctyl isophthalate | 137-89-3 | 390 | $C_8H_4O_4(C_8H_{17})_2$ | 408 | 10.84 |
| diisononyl phthalates* | 28553-12-0 | 418 | $C_8H_4O_4(CH_3C_8H_{17})_2$ | 419 | 9.40 - 11.10 |
| dinonyl phthalate | 84-76-4 | 418 | $C_8H_4O_4(C_9H_{19})_2$ | 419 | 11.19 |
| diisodecyl phthalates* | 26761-40-0 | 446 | $C_8H_4O_4(CH_3C_9H_{18})_2$ | 447 | 10.16 - 11.86 |
| didecyl phthalate | 84-77-5 | 446 | $C_8H_4O_4(C_{10}H_{21})_2$ | 447 | 12.05 |
| diundecyl phthalate | 3648-20-2 | 474 | $C_8H_4O_4(C_{11}H_{23})_2$ | 475 | 12.87 |
| didodecyl phthalate | 2432-90-8 | 502 | $C_8H_4O_4(C_{12}H_{25})_2$ | 503 | 13.65 |
| ditridecyl phthalate | 119-06-2 | 530 | $C_8H_4O_4(C_{13}H_{27})_2$ | 531 | 12.01 - 13.81 |

Technical formulations of the isoalkyl phthalates tended to contain substantial amounts of the straight chain isomer, which may convolute quantitation as well as peaks that may be construed as originating from nonequivalent side chains i.e., $x \neq y$ in equation 1). These impurities can be detected as $M \pm 14$ around the mass of the nominal isomer. For example, technical grade diisononyl phthalate contains compounds that generate ions at m/z 391 (minor), 405, 433, and 447 in addition to the nominal diisononyl phthalate compound at m/z 419. The “gentle” ionization of ammonia reagent gas, the elution times and the study of the

spectra of other pure isomers, such as the dinonyl phthalate, suggest that these fragments are not formed by the PCI process but are due to these different alkyl side chain impurities (Figure 6). To demonstrate the utility of the PCI-ammonia compared to conventional EI analysis, consider the chromatograms presented in Figure 7. The EI spectra of the phthalates produce m/z 149 as the base peak for all the phthalates present; distinguishing ions are minor constituents (<10% relative intensity), making identification complicated. However, by examining the appropriate PCI-ammonia ions, the various phthalates are easily distinguished.

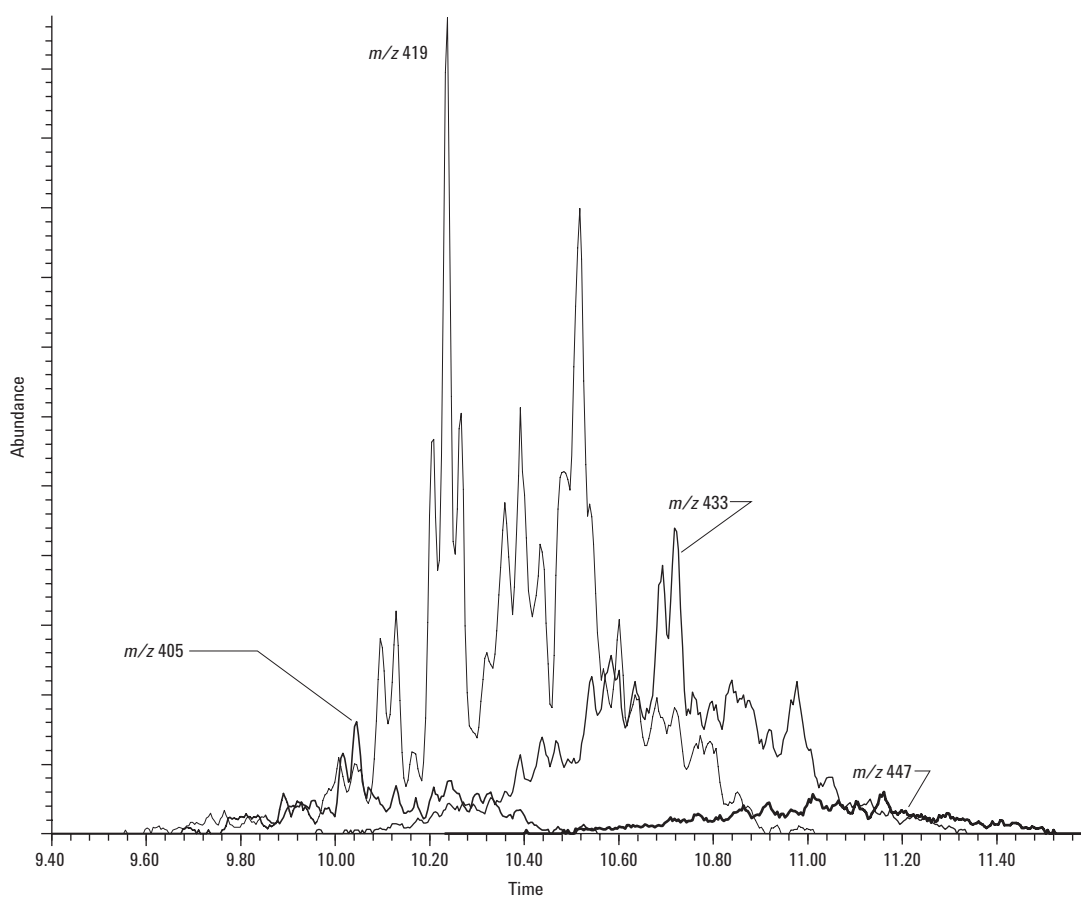


Figure 6. PCI-Ammonia extracted ion chromatogram of technical diisononyl phthalate. The diisononyl appears as the major component at m/z 419 while ions at m/z 405, 433, and 447 indicate alkyl chains shorter by one CH_2 unit and longer by one and two CH_2 units respectively.

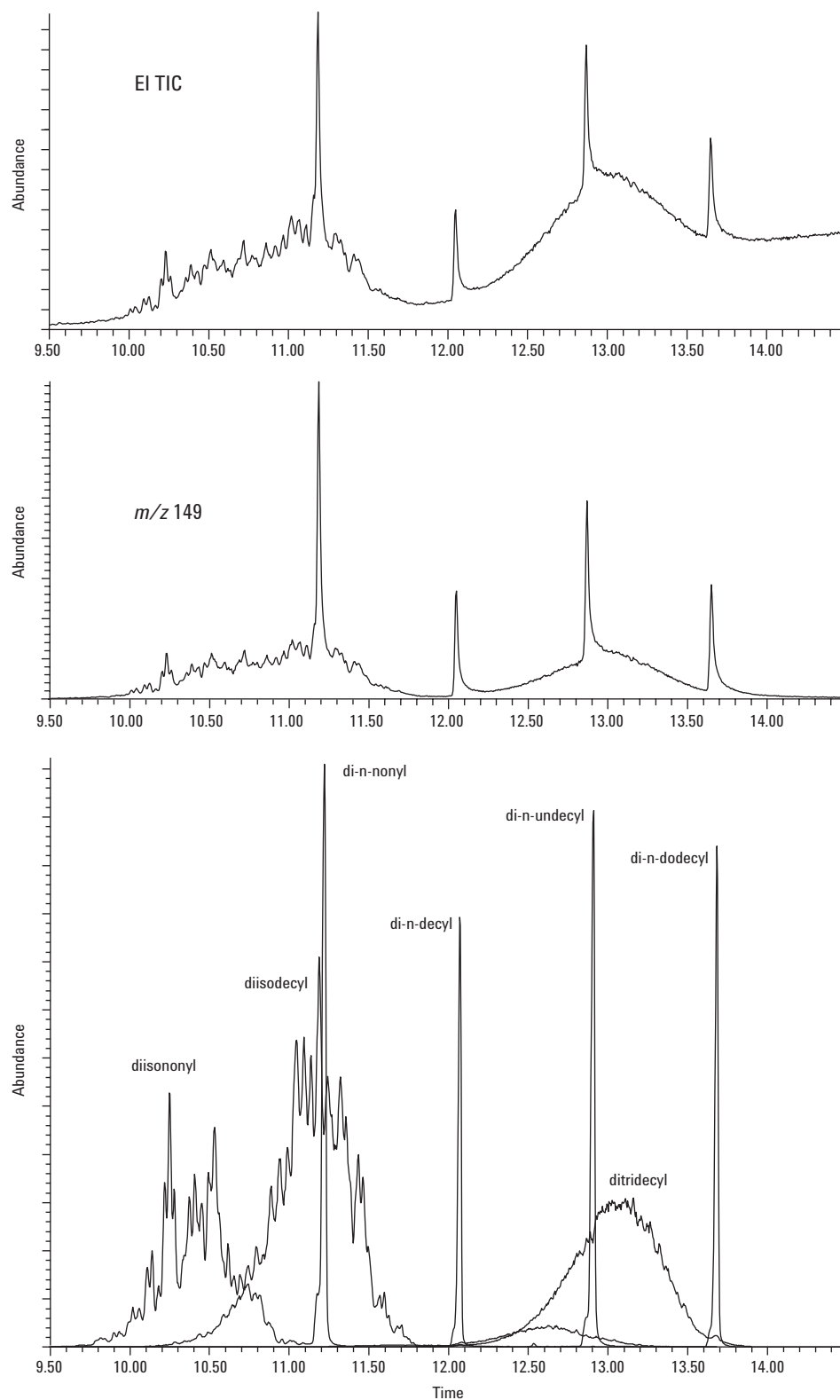


Figure 7. Chromatograms of dinonyl, diisononyl, didecyl, diisodecyl, diundecyl, didodecyl, ditridecyl phthalate esters in EI (upper panel), EI as an extracted ion chromatogram at m/z 149 (middle panel), and PCI-extracted ion chromatogram with ions selected for the individual phthalate classes as given in Table 1. The EI information is insufficient to identify coeluting phthalates. For example, the dinonyl and diundecyl phthalates are "buried under" the signals from the isodecyl and ditridecyl phthalates.

Conclusions

Applying GC - electron impact (EI) mass spectrometry to the determination of phthalates requires full chromatographic separation. The EI spectra of the phthalates are distinguished only by ions of very low intensity. In EI, the phthalates produce a single common ion (m/z 149) as the most intense spectral peak, regardless of the alkyl side chain substitution. Applying tandem mass spectrometry (i.e., EI/MS/MS) gains nothing, because there is a common parent ion, and therefore any daughter ions would also be non-unique. However, the combination of positive chemical ionization with retention-time locking allows even complex mixtures of phthalates to be characterized. Ammonia reagent gas produces the protonated molecule as the base peak, which immediately allows the phthalates to be distinguished on the basis of their substitution. PCI is also an advantage in complex matrices, where the non selective ionization of EI produces a high chemical background. This method should therefore be suitable for use in phthalate determinations in environmental media, plastics, cosmetics and many other matrices.

“Locking” the retention time enhances confidence in the characterization of the various phthalate isomers on the basis of their definitive retention time. This is especially helpful for determinations using selected ion monitoring (SIM), since SIM groups need not be edited after column maintenance [4]. The data in Table 1 facilitate the development of a SIM method. The extension of the method to phthalates which elute at higher temperatures ($>350^{\circ}\text{C}$) is also easily accomplished.

References

1. Blount, B.C., et al., Levels of seven urinary metabolites in a human reference population. *Environmental Health Perspectives*, 2000. 108 (10): p. 979-982.
2. *Official Journal of the European Communities, Decision 198/815/EC*. 1999, European Commission; European Union Scientific Committee on Toxicology, Ecotoxicology, and the Environment.
3. Giarrocco, V., B. Quimby, and M. Klee, *Retention Time Locking: Concepts and Applications*. 1998, Publication number (23) 5966-2469E, Agilent Technologies.
4. Prest, H. and P. Cormia, *Retention Time Locking: Advantages in GC/MS SIM Analysis*. 1999, Publication number (23) 5967-3797E, Agilent Technologies.
5. Prest, H. and K. Weiner, *Retention Time Locking: Creating Custom Retention Time Locked Screener Libraries*. 1999, Publication number (23) 5968-8657E, Agilent Technologies.
6. Harrison, A.G., *Chemical Ionization Mass Spectrometry*. Second ed. 1992: CRC Press.

For more information

For more information on our products and services, you can visit our site on the World Wide Web at: <http://www.agilent.com/chem>.

Agilent Technologies shall not be liable for errors contained herein or for incidental or consequential damages in connection with the furnishing, performance, or use of this material.

Information, descriptions, and specifications in this publication are subject to change without notice.

Copyright © 2001
Agilent Technologies
All rights reserved. Reproduction and adaptation are prohibited.

Printed in the U.S.A.
March 7, 2001
5988-2244EN



Agilent Technologies



Determination of the Vasodilator Isosorbide-5-Mononitrate in Human Plasma using GC/MS with Electron Capture Negative Ion Chemical Ionization

Application Note

Drug Testing

A. Khan-Raja and P. R. Robinson

Simbec Research Limited, Merthyr Tydfil, United Kingdom, CF48 4DR

Chris Sandy

Agilent Technologies, United Kingdom

Introduction

The 1998 Nobel Prize in Physiology and Medicine was awarded for work demonstrating “Signal transmission by a gas that is produced by one cell, penetrates through membranes and regulates the function of another cell...” This work, which elucidated the role of nitric oxide (NO) in the dilation of blood vessels, has led to the development of a series of vasodilatory drugs for use as anti-anginal and anti-impotence medications (e.g., Viagra®). It is perhaps ironic that the best known of the anti-anginal medications, nitroglycerin, apparently had been prescribed to no lesser a patient than the founder of the Prize, Alfred Nobel.

An example of a more recent vasodilator typical of the organic nitrate agents is the anti-anginal agent 1,4:3,6-dianhydro-D-glucitol 5-nitrate, or isosorbide-5-mononitrate (Figure 1). Isosorbide-5-mononitrate and the other organic nitrate anti-angina medications require different dosing approaches than most other chronically used drugs. Usually, drug dosage

is designed to maintain plasma concentrations in excess of that ensuring minimum efficacy. However this approach appears inappropriate for organic nitrate drugs, because the patient develops nitrate tolerance.

One of the difficulties in designing an optimal dosing interval is sensitive detection of the organic nitrate. This Application Note demonstrates a successful approach to sensitive detection and accurate quantitation of one member of this class of drugs, the isosorbide-5-mononitrate (IS5MN), using electron capture negative ion chemical ionization (ECNI). It also demonstrates an important advantage of ECNI: greater selectivity. IS5MN contains electrophilic oxygen atoms which provide a high cross section for electron capture relative to the biogenic interferences present in the plasma. This selectivity, combined with high sensitivity, allows detection and quantitation of electrophilic compounds in complex matrices such as biological samples.



Agilent Technologies

Innovating the HP Way

Experimental

A 1-ml aliquot of the plasma sample is spiked with *p*-nitrobenzyl alcohol, which serves as an internal standard (IS), at 250 ng/ml. One milliliter of deionized water is added and the sample thoroughly mixed before liquid-liquid extraction with ethyl acetate (solvent:aqueous, 10:2 v/v). The sample is then centrifuged, the upper layer removed and transferred and then evaporated to dryness. The residue is immediately derivatized by adding BSTFA+1% TMCS in dry pyridine (1:1 v/v). The trimethyl-silyl derivatives of the IS5MN and IS are shown in Figure 1. The excess agent is evaporated and the sample reconstituted in 200 μ l of dry hexane.

GC-MS-ECNI analysis of the sample is made according to the instrumental parameters given in Table 1.

Table 1. GC and MSD Instrumental Parameters

| GC Injection Parameters | |
|------------------------------|---|
| Autosampler | 7683 ALS |
| Injection | 1- μ l |
| Mode | Pulsed Splitless |
| Injector temperature | 250°C |
| GC Oven Parameters | |
| GC column | J&W DB1701 15m, 0.25 mm i.d., 0.25 μ m film |
| Carrier gas | Helium |
| Column flow | 1.2 ml/min, constant flow |
| Initial temperature | 60°C |
| Ramp rate | 30°C/min |
| Final temperature | 260°C |
| Transfer line | 280°C |
| MSD Parameters | |
| Mode | NCI |
| Buffer gas | Ammonia |
| Mass Flow Controller setting | 20% |
| Source temperature | 150°C |
| Quadrupole temperature | 103°C |
| Tune parameters | NCI autotune |

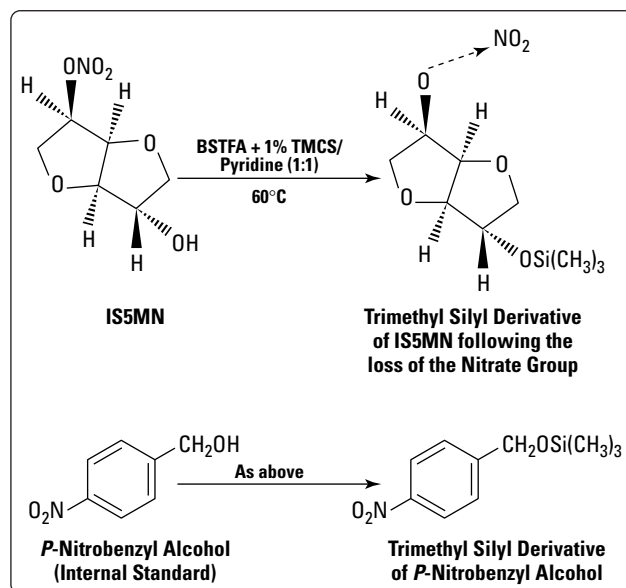


Figure 1. Chemical structures of the Isosorbide-5-mononitrate (IS5MN) and *p*-nitrobenzyl alcohol (IS) and the derivatization scheme.

Results

The mass spectra of the trimethyl-silyl derivatives of the IS5MN and IS show very little fragmentation (Figures 2 and 3) as expected in electron capture negative chemical ionization (ECNI). Quantitative analysis used selected ion monitoring ions of 217 m/z and 225 m/z , respectively. A calibration curve, constructed using standards of nominally 10, 50, 100, 200, 500, 750, 1000 ng/ml concentrations, was linear over the entire range with an r^2 value of 0.996 (Figure 4).

To test the accuracy and precision of the method, intraday and interday batches were analyzed. These results, shown in Tables 2 and 3, demonstrate that the accuracy achieved was better than $\pm 6\%$ of the true value and the reproducibility better than 6.4% for IS5MN concentrations from 20 to 800 ng/ml. The quantitation limit for IS5MN is nominally 10 ng/ml (Figure 5). This method has proved extremely useful in evaluating the pharmacokinetics and bioequivalence of a number of IS5MN preparations in human subjects.

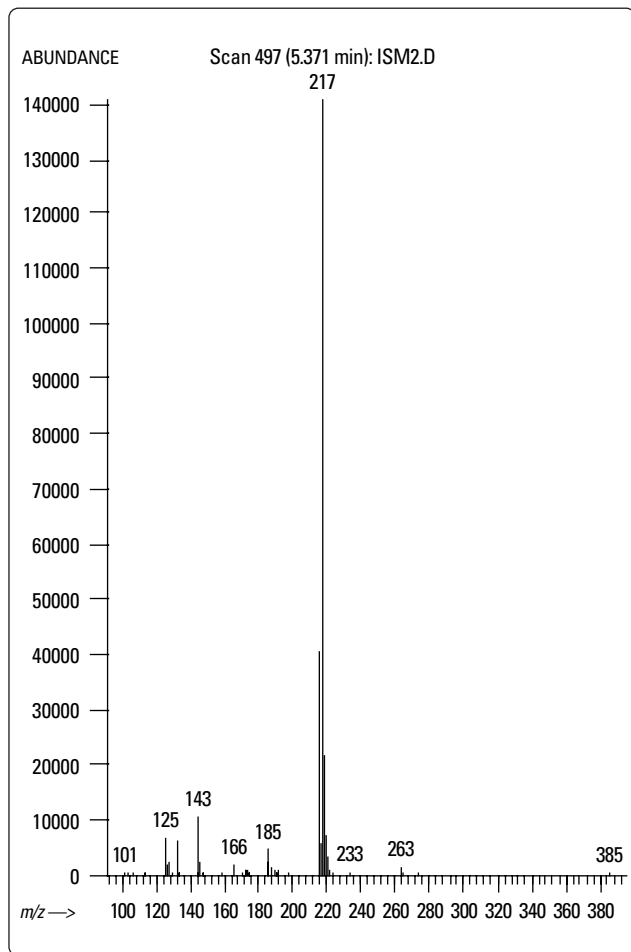


Figure 2. Electron capture negative ion chemical ionization mass spectrum of the trimethyl-silyl derivative of isosorbide-5-mononitrate from 100 to 400 amu using ammonia buffer gas.

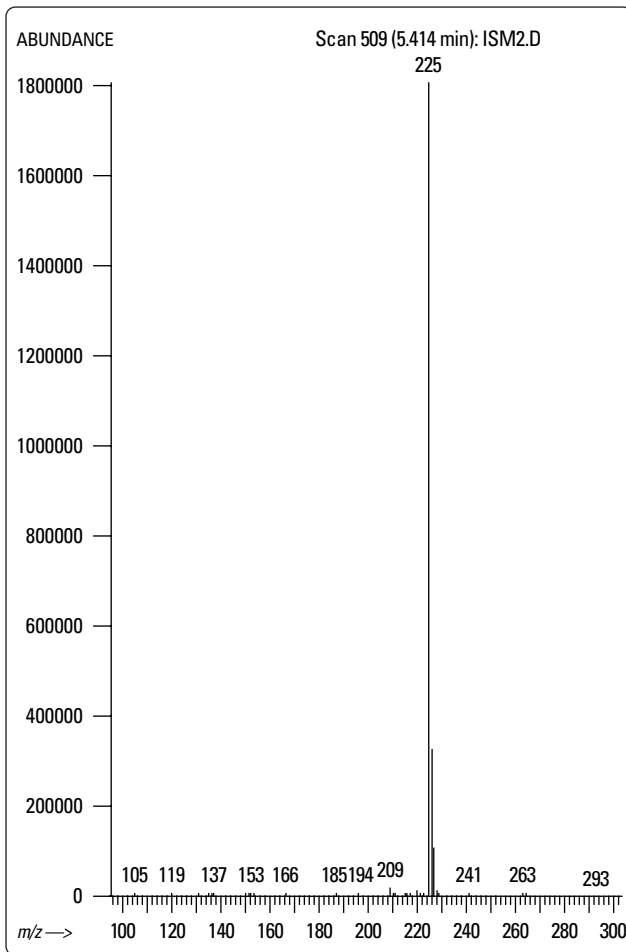


Figure 3. Electron capture negative ion chemical ionization mass spectrum of the trimethyl-silyl derivative of *p*-nitrobenzyl alcohol internal standard from 100 to 400 amu using ammonia buffer gas.

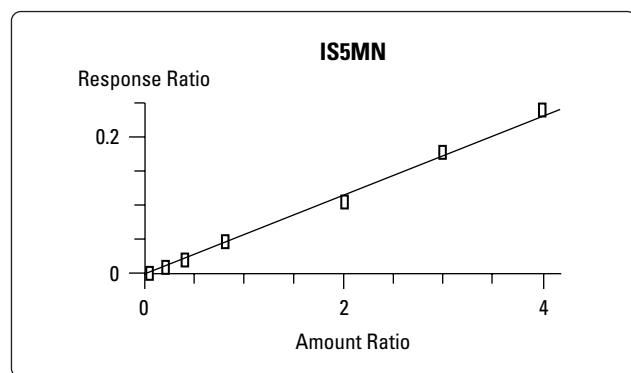


Figure 4. Calibration curve for IS5MN from 10 ng/ml to 1000 ng/ml, $r^2 = 0.996$.

Table 2. Summary of intra-batch quality control data (n=6)

| Control Concentration (ng ml ⁻¹) | Mean Determined Value (ng ml ⁻¹) | Imprecision | | Accuracy (Mean as % of Actual Concentration) |
|--|--|--------------------|------------------------------|--|
| | | Standard Deviation | Coefficient of Variation (%) | |
| 20.00 | 20.90 | 1.33 | 6.38 | 104.50 |
| 150.09 | 142.14 | 0.95 | 0.67 | 94.70 |
| 399.24 | 396.28 | 15.06 | 3.80 | 99.26 |
| 795.32 | 807.77 | 31.49 | 3.90 | 101.57 |

Table 3. Summary of inter-batch quality control data (n=6)

| Control Concentration (ng ml ⁻¹) | Mean Determined Value (ng ml ⁻¹) | Imprecision | | Accuracy (Mean as % of Actual Concentration) |
|--|--|--------------------|------------------------------|--|
| | | Standard Deviation | Coefficient of Variation (%) | |
| 20.00 | 20.94 | 0.95 | 4.54 | 104.70 |
| 150.09 | 146.86 | 8.27 | 5.63 | 97.85 |
| 399.24 | 421.16 | 16.25 | 3.86 | 105.49 |
| 795.32 | 824.00 | 28.37 | 3.44 | 103.61 |

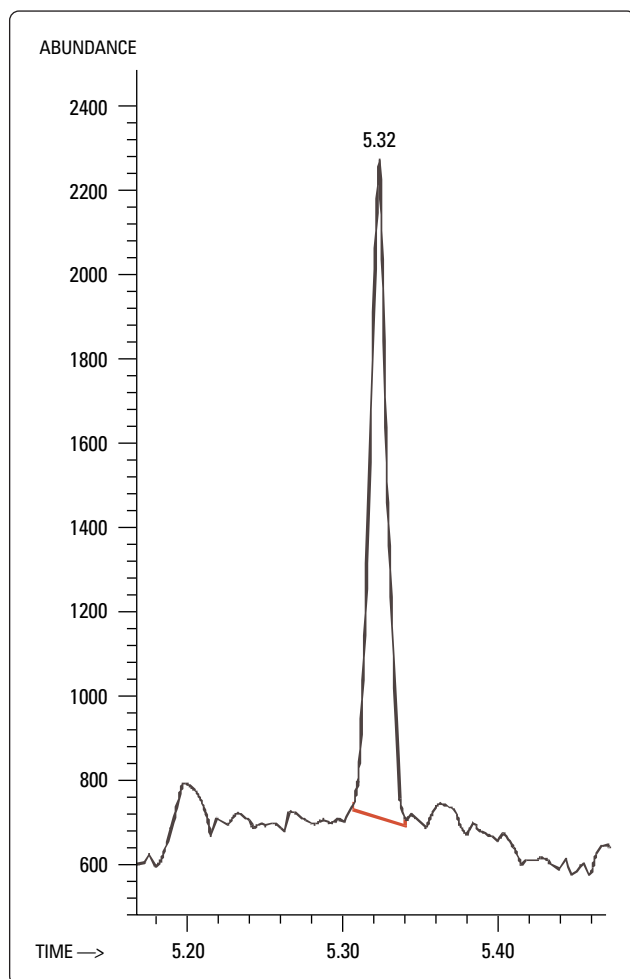


Figure 5. Extracted ion chromatogram for ECNI-SIM acquisition of a 10 ng/ml IS5MN plasma standard. Displayed is the 217 amu ion and ± 0.15 min of the expected retention time for the analyte. The analyte shows an RMS signal-to-noise greater than 100 even at a concentration near the quantitation limit.

Acknowledgments

The authors acknowledge the assistance of Harry Prest in generating this application note.

Authors

A. Khan-Raja is a principal scientist and **P. R. Robinson** is a manager in the Bioanalytical Unit at Simbec Research Limited, Merthyr Tydfil, United Kingdom, CF48 4DR.

Chris Sandy is an Mass Spectrometry Product Specialist at Agilent Technologies, United Kingdom.

For more information on our products and services, you can visit our site on the World Wide Web at: <http://www.agilent.com/chem>

Agilent Technologies shall not be liable for errors contained herein or for incidental or consequential damages in connection with the furnishing, performance or use of this material.

Information, descriptions and specifications in this publication are subject to change without notice.

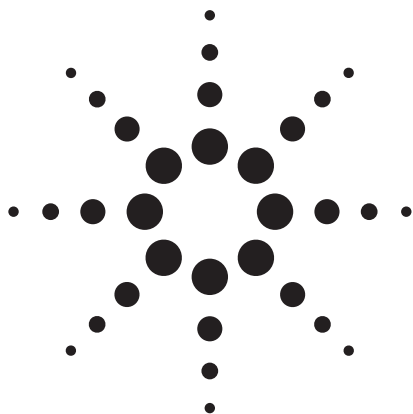
Copyright © 2000
Agilent Technologies
All rights reserved.
Reproduction and adaptation is prohibited.

Printed in the USA July 2000
(23) 5980-2080E



Agilent Technologies

Innovating the HP Way



Fast determination of five toxic elements in Traditional Chinese Medicine (TCM) by ICP-MS

Application Note

Binfeng Xia
Zhuqing Lu
XinMei Wang
Ke Wang
Shen Ji



Abstract

Five toxic elements in 10 different types of Traditional Chinese Medicines (TCM) were analyzed by Inductively Coupled Plasma Mass Spectrometry (ICP-MS). To do this, a sample digestion method and standard operation procedures were developed. Reproducibility and recovery were tested for method validation. The Agilent ICP-MS method is proven to be highly sensitive, and its fast acquisition time makes it highly suitable to analyze trace toxic elements in TCMs.

Agilent Equipment

Agilent 7500 ICP-MS

Application Areas

Pharmaceutical



Agilent Technologies

Introduction

Traditional Chinese Medicine (TCM) herbs and their manufactured products have been used for thousands of years for prevention and treatment of disease in China. TCM materials are made up of plants, animals and minerals with the majority being various parts of medical plants. The contents of heavy metals in TCMs have been commonly studied from the viewpoints of toxicity and bio-availability. The roots or leaves of the plant can absorb heavy metals such as Pb, Cd, Hg and As from the atmosphere, water and soil, and these can finally accumulate at a particular position in the plant through the cytosol.

Different regulations propose to limit the content of heavy metals in herbs (table 1). The most stringent of these regulations is that from the Food and Drug Administration (FDA). Therefore, it is important to determine these elements as accurately and as unambiguously as possible.

Inductively coupled plasma mass spectrometry (ICP-MS) has quickly become the technique of choice for the determination of elements in a wide range of samples. It has been used widely for measurement of trace and ultra-trace elements in the environmental and biological materials. The advantages of choosing ICP-MS for measurement include rapid and simultaneous multi-elemental determinations, low spectral interferences, excellent detection limits and the ability to analyze isotopic ratios.

In this study, the ICP-MS technique was applied to measure five toxic elements in TCM samples from different areas in China.

Experimental

Instrumentation and reagents

In this study a 7500c ICP-MS instrument was used, which uses an Octopole Reaction System. Sample digestion was done by microwave digestion.

Concentrated HNO₃ (68% w/v, GR, Merck) was used for sample digestion and cleaning of the digestion tubes. Deionized water was used throughout.

Operation parameters

The ICP-MS operation parameters are listed in table 2.

Sample digestion and calibration curves

The TCMs were dried at 60 °C for four hours, and ground into powder. 0.5 g powder were weighed precisely into a microwave digestion tube (50 mL, PFA), and then 10 mL 65 % HNO₃ was added. The powdered TCM and HNO₃ were placed in a microwave digestion system and subjected to a standard program of heating. Following digestion the solubilized TCM samples were transferred into a PTFE volumetric flask and the digestion tube was washed three times using pure water.

| Regulations (µg/kg) | Pb | Cd | Hg | As |
|--|-------|-----|-----|------|
| Proposed regulation on "TCM Quality Standard" | | | | |
| Chinese Pharmacopeia | 5000 | 500 | 200 | 200 |
| Chinese regulations on imported herb supplements | 5000 | 300 | 200 | 2000 |
| French regulations on imported herb supplements | 5000 | 200 | 100 | 5000 |
| US FDA regulations on the medicines and functional food | 1000 | 300 | 26 | 20 |
| South-East Asia regulations on imported herb supplements | 20000 | N/A | 500 | 5000 |

Table 1
Regulations on heavy metals in TCM or herb supplements.

Working parameters

| | |
|------------------------|--|
| RF power | 1350 W |
| Nebulizer | PFA 200 µL/min nebulizer |
| Spray Chamber | Scott double pass 2±0.1 °C |
| Data Acquisition Mode | Spectrum Analysis Mode and Full Quant Mode |
| Sampling depth | 7.0 mm |
| Carrier gas flow rate | 1.18 L/min |
| Total Acquisition Time | 90 s |

Table 2
Instrumental parameters of Agilent ICP-MS.

| STD | As | Pb | Cd | Cu | Hg |
|-------|------|------|-----|-----|-----|
| Blank | 0 | 0 | 0 | 0 | 0 |
| 1 | 1.0 | 1.0 | 0.5 | 50 | 0.2 |
| 2 | 5.0 | 5.0 | 2.5 | 100 | 0.5 |
| 3 | 10.0 | 10.0 | 5 | 200 | 1 |
| 4 | 20.0 | 20.0 | 10 | 500 | 2 |
| 5 | | | | | 5 |

Table 3
Calibration curve range (µg/L).

200 µL of a 1 µg/mL Au solution was also added into the digested sample to stabilize Hg. The solution was finally made up to 50 mL. The system blank solution was made by the same procedure except that no TCM was added. The calibration curve standards were also prepared from 10% HNO₃.

The internal standard (1:10 diluted Agilent Internal Standard Mix, part number 5183-4680) was automatically added on-line to samples during analysis. Ge (72) was used as internal standard reference element of Cu and As. In (115) was used as internal standard reference element of Cd (114). Bi (209) was used as internal standard reference element of Pb and Hg.

The samples were run according to a modified method based on USEPA 200.8

Results and discussion

Calibration linear range

All five element's calibration curves show good linearity, R² values are between 0.9990 and 0.9999.

Reproducibility of the sample preparation

Ten TCMs were investigated: Xiyangshen, Danshen, Huangqi, Ganchao, Huangbo, Baishao, Chenpi, Lingzhi, Jinyinhua, and Huanxieye drugs. All samples were ground into powder and five repeated samples (0.5 g powder for every sampling) were taken from 10 batches. Powders were digested by microwave digestion. Reproducibility was good for all samples. The Xiyangshen medicine is taken here as an example.

The results prove that the ICP-MS method and the sampling and digestion method are very good for trace toxic elements analysis, even at low concentration levels.

Blank spike recoveries

Cd, As, Pb, Cu, Hg were spiked into the digestion tube, followed by microwave digestion and then made up to a blank spike recovery solution with concentrations similar to TCM samples. The spike recoveries test results are shown in table 5. A total of eight blank spike recoveries solutions were made for statistical purposes. The results again illustrate that microwave digestion is a very good method for sample digestion without loss of target elements during digestion.

Sample spike recoveries

0.25 g powder was taken from each of the ten TCMs, six times parallel sampling was done for each material. Using the measured concentrations of the metals in the TCM guidelines, six undigested samples were spiked using standard stock solutions. All spikes were done in pairs and the levels chosen for spiking were 40 %, 50 % and 60 % of the levels found in the originally analysed TCMs. Then the samples were digested and measured by ICP-MS. The results for the Xiyangshen drug are summarised in Table 6. Even though the spike levels were low (with respect to the elements in the sample itself) the recoveries are excellent and highlight that the digestion method is effective, without loss of material.

| No | Cu | As | Cd | Hg | Pb |
|--------|------|------|-------|------|------|
| 1 | 5962 | 33.8 | 94.9 | 127 | 68.5 |
| 2 | 6394 | 29.7 | 91.4 | 141 | 66 |
| 3 | 6577 | 30.7 | 93.6 | 157 | 68.8 |
| 4 | 6312 | 32.1 | 92.2 | 137 | 66.9 |
| 5 | 7000 | 28 | 100.9 | 169 | 76.8 |
| AVG | 6449 | 30.9 | 94.6 | 146 | 69.4 |
| RSD(%) | 5.9 | 7.2 | 4.0 | 11.4 | 6.2 |

Table 4
Reproducibilities for Xiyangshen samples (µg/kg).

| Element | Cu | As | Cd | Hg | Pb |
|---------|------|-------|-------|-------|-------|
| Avg(%) | 98.8 | 106.0 | 102.2 | 110.0 | 100.7 |
| RSD | 1.8 | 1.0 | 1.1 | 1.3 | 1.9 |

Table 5
Blank spike recoveries.

| No | Cu | As | Cd | Hg | Pb |
|-----|-------|-------|-------|-------|-------|
| 1 | 112.3 | 111.0 | 97.3 | 88.3 | 130.6 |
| 2 | 120.8 | 90.6 | 110.9 | 101.2 | 122.7 |
| 3 | 89.6 | 94.7 | 111.0 | 78.4 | 120.7 |
| 4 | 110.3 | 88.5 | 108.1 | 93.2 | 134.4 |
| 5 | 91.6 | 107.8 | 111.7 | 80.7 | 108.4 |
| 6 | 117.4 | 89.2 | 101.8 | 97.6 | 111.3 |
| Avg | 107.0 | 97.0 | 106.8 | 89.9 | 121.4 |
| RSD | 12.4 | 10.2 | 5.5 | 10.2 | 8.5 |

Table 6
Spike recoveries for Xiyangshen after microwave digestion and ICP-MS analysis.

Results and discussion

Average

Ten types of TCMs were selected as targets, and ten samples were collected from different local areas for each type. The samples were analyzed by ICP-MS, the average results are listed in table 7. While the data in table 7 suggests that all measurements were below the regulated levels for heavy metals, please note that these are averages; some samples were above the regulated limits. Interestingly, even for the same TCM type, the toxic element concentrations varied from very low trace levels to highly contaminated, when the samples are taken from different sources. For example, Hg concentrations in 10 Baishao samples varied from 5 µg/kg to 14 µg/g, with almost 3000 times difference.

Statistical results for 100 TCM samples, summarized in tables 8 to 10

These results show how many samples out of 100 have been detected to show high toxic elements content.

Conclusion

All samples contained toxic elements below proposed limits, but element analysis by ICP-MS of ten different Traditional Chinese Medicines (see table 1) from different geographical locations showed that variability for the amount of each element was very high. This might correlate with the differing contamination level and different contamination types due to soil and water contamination in different areas. Taking good care when growing plants, such as in Good Agriculture Practice (GAP) of TCMs will be crucial in the future to maintain consistent quality. The Agilent ICP-MS has been proven to be an ideal analytical method for determination of toxic

| TCMs | Cu | As | Cd | Hg | Pb |
|------------|-------|------|-----|------|------|
| Baishao | 5403 | 376 | 72 | 1775 | 280 |
| Huangqi | 7692 | 313 | 27 | 4805 | 383 |
| Lingzhi | 8162 | 224 | 65 | 247 | 154 |
| Jinyinhua | 11698 | 3105 | 113 | 127 | 1885 |
| Ganchao | 8968 | 536 | 12 | 89 | 278 |
| Danshen | 10404 | 594 | 69 | 22 | 948 |
| Xiyangshen | 5281 | 82 | 104 | 25 | 131 |
| Huanxieye | 5198 | 276 | 12 | 159 | 249 |
| Huangbo | 2457 | 323 | 14 | 77 | 769 |
| Chenpi | 2842 | 328 | 32 | 166 | 1298 |

Table 7
Average results (µg /kg).

| Elem | Range (µg/kg) | ≥2000 | ≥3000 | ≥5000 | ≥10000 | ≥20000 |
|------|---------------|-------|-------|-------|--------|--------|
| Cu | 1289-19038 | 97 | 83 | 68 | 20 | 0 |

Table 8
Cu in 100 TCMs (sample amounts).

| Elem | Range (µg/kg) | ≥100 | ≥500 | ≥1000 | ≥2000 | ≥5000 |
|------|---------------|------|------|-------|-------|-------|
| Pb | 69-3909 | 92 | 34 | 24 | 6 | 0 |

Table 9
Pb in 100 TCMs (sample amounts).

| Elem | Range (µg/kg) | ≥100 | ≥200 | ≥300 | ≥500 | ≥1000 |
|------|---------------|------|------|------|------|-------|
| As | 12-10348 | 81 | 62 | 38 | 23 | 14 |
| Cd | 2.4-212 | 21 | 2 | 0 | 0 | 0 |
| Hg | 0.4-36009 | 34 | 18 | 17 | 11 | 5 |

Table 10
As, Cd, Hg in 100 TCMs (sample amounts).

elements in TCMs, since this system can determine trace level impurities very efficiently. In combination with optimized microwave digestion, this has reduced the matrix interferences significantly. Additionally, ICP-MS enables very fast measurement of a full set of elements, saving time for other laboratories tasks.

References

1. "Determination of Toxic Elements in Traditional Chinese Medicine Using Inductively Coupled Plasma Mass Spectrometry"; *Agilent Publication Number 5989-5591EN*, 2006.

2. This Paper is an extract of a Chinese publication: *Modern Instrumentation, first edition, 2004.*

Binfeng Xia, Zhuqing Lu, XinMei Wang, Ke Wang, Shen Ji, Shanghai Institute for Food and Drug Control (China).

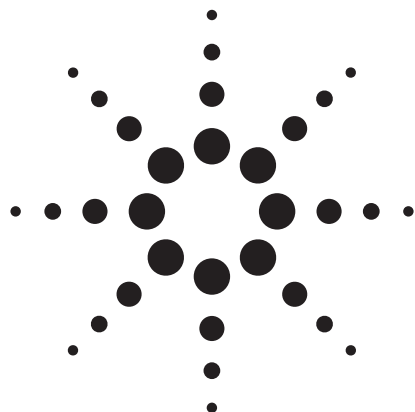
www.agilent.com/chem

© 2007 Agilent Technologies, Inc.

Published December 1, 2007,
Publication Number 5989-7590EN



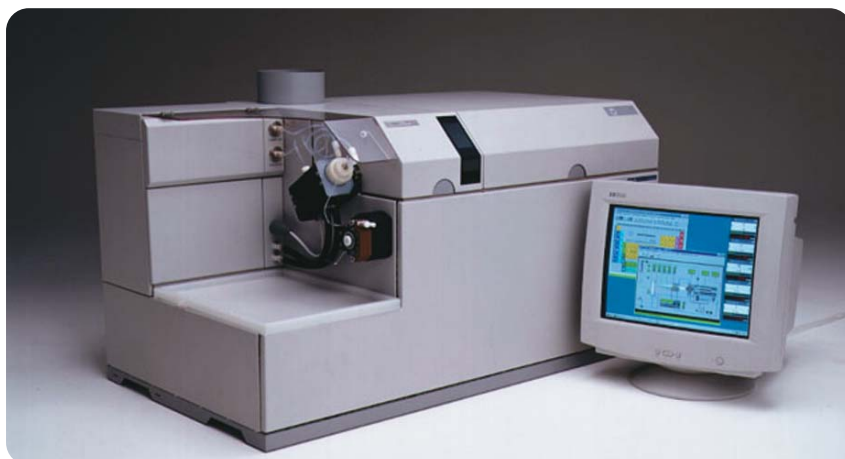
Agilent Technologies



Determination of Toxic Elements in Traditional Chinese Medicine Using Inductively Coupled Plasma Mass Spectrometry

Application Note

Hua Zhang
Yan-zhi Shi
Yu-hong Chen
Ying-feng Wang



Abstract

This Application Note describes a method for the analysis of Be, Cr, Mn, Ni, Cu, Zn, As, Ag, Cd, Ba, Hg, Tl and Pb in Traditional Chinese Medicines using Inductively Coupled Plasma Mass Spectrometry (ICP-MS). The samples were dissolved by microwave digestion. To validate the method, two certified reference materials were digested and measured. The method detection limits for all target elements were between 0.1-7.2 ng·g⁻¹.



Agilent Technologies

Introduction

Traditional Chinese Medicines (TCMs) and their related products have been widely used in China for centuries. The Chinese government as well as academic research scientists are paying greater attention to the safety issues of TCM in clinical use. This is a key issue which needs to be resolved to improve the development of TCM to meet international standards and advance its worldwide acceptance. With the recent developments in science and technology, people are becoming more aware of the risks associated with heavy metals such as mercury (Hg), arsenic (As), lead (Pb) and cadmium (Cd), which are present in some TCMs. After these elements enter the human body, they will severely damage the hemopoietic, immune, nervous and reproductive systems. Because these substances cannot be completely excreted from the body, they will accumulate and finally have an impact on health. Therefore the analysis of toxic heavy metals is crucial in quality control of TCMs and regulations have been implemented to restrict their levels¹. The export of TCMs is under intense pressure due to strict regulations, and the high content of heavy metals in traditional Chinese medicine has resulted in international response.

Limiting other toxic or harmful elements, such as beryllium (Be), chromium (Cr), nickel (Ni), silver (Ag), barium (Ba) and thallium (Tl), have not been clearly specified in current hygiene rules and

regulations yet. However, with the improvement of living standards and a desire for good health, people now care more about whether these elements offer advantages or disadvantages for their wellbeing. Therefore, strict control of the content of these elements in TCM is required.

In addition, manganese (Mn) is good for the human endocrine, nervous, and enzyme systems and is the key element of most enzymes as well as supporting normal myocardial metabolism. Zinc is good for the immune system. Lack of zinc (Zn) will harm normal cell metabolism and lack of copper (Cu) is one of the reasons for coronary heart disease². However, if the level of these elements is too high, they will place human health at risk.

By nature TCM is very complex and contains many elements which have different concentration levels – high and low. In the past, they have been analyzed by a combination of ASS, AFS and AES technology. These procedures are time-consuming and costly³. ICP-MS is fast becoming the technique of choice for the determination of elements in a wide range of samples. Additionally, it has the widest linear range (nine orders of magnitude, from 1 ng·mL⁻¹ to 1000 µg·mL⁻¹), the highest sensitivity and lowest detection limit for metals, as well as the ability to rapidly and accurately measure multiple elements simultaneously. The latest revision of the Pharmacopoeia of the People's Republic of China (Chinese

Pharmacopoeia 2005) now includes ICP-MS as one of the standard methods for the determination of heavy metals in herbal medicines⁴.

In this study, microwave digestion is used for sample preparation. High temperature and a closed system assure fast and complete digestion and avoid the loss of those elements which can easily evaporate, such as arsenic and mercury. Thirteen toxic elements including Be, Cr, Mn, Ni, Cu, Zn, As, Ag, Cd, Ba, Hg, Tl and Pb were analyzed using the microwave digestion-ICP-MS method. The method is validated by using two certified reference materials: shrub leaves and tea leaves. The results obtained agree with the certified values. The recovery experiment of standard addition was applied in the study to evaluate the proposed method. The recovery percentages are between 90.3 -109.7 %.

Experimental

Instrumentation

An Agilent 7500 Series c ICP-MS was used in this study (table 1). The samples were prepared by microwave digestion with a CEM

| | |
|----------------|--|
| Nebulizer: | Babington nebulizer |
| Spray chamber: | Quartz scott-type, Peltier-thermostatted to 2 ± 0.1 °C |
| Torch: | Quartz, 2.5 mm ID |
| Interface: | Ni cone |

Table 1
Agilent 7500c ICP-MS instrument details.

MARS5 microwave digestion system (CEM Co. Ltd, USA), including microwave oven, PTFE-TFE high pressure vessel and fixed tray. Deionized water (Milli-Q ultrapure water system) was used.

Reagents

Nitric acid (HNO₃), trace metal grade (Merck); hydrogen peroxide (H₂O₂), MOS grade; standard stock solution: 10 µg·mL⁻¹ mixed standard solution including Be, Cr, Mn, Ni, Cu, Zn, As, Ag, Cd, Ba, Hg, Tl and Pb. Calibration standards were prepared by using applicable dilutions of standard stock solution with 5 % HNO₃; Hg stock solution: 1000 µg·mL⁻¹ (National Analytical Center for Iron & Steel, China). Calibration standards were prepared by using applicable dilutions of standard stock solution with 5 % HNO₃, internal standard solution: 1.0 µg·mL⁻¹. Diluted from 10 µg·mL⁻¹ Li, Sc, Ge, Y, Tb and Bi mixed standard solution. (Agilent part number 5183-4680) with 5 % HNO₃, Tune solution: 10 ng·mL⁻¹ ⁷Li, ⁵⁹Co, ⁸⁹Y, ¹⁴⁰Ce and ²⁰⁵Tl mixed standard solution (2 % HNO₃) (Agilent part number. 5184-3566). Deionized water (18.2 MΩ) produced with the Milli-Q®

ultrapure water purification system (Millipore Corp.) was used in all standard solution and sample preparations. Certified reference materials: GBW07602 (shrub leaves) and GBW08513 (tea leaves).

Sample pretreatment

Exactly 0.5000 g of sample were weighed and placed into the PTFE vessel. 6 mL HNO₃ and 1 mL H₂O₂ were added. Because of the large organic content of TCM and the large amount of sample, pre-digestion is recommended. To prevent sample loss due to an explosion caused by gas and pressure build-up produced in the digestion process, the sample was dissolved in the solution and placed in the microwave oven. First, the temperature was raised and set at 120 °C for approximately 5 minutes, then the sample was cooled completely and the pressure was allowed to drop to normal. Subsequently, the digestion program specified in table 2 was followed. After digestion the vessel was cooled to room temperature and the contents poured into a 50-mL PET bottle. The vessel and cap were washed with a small amount of distilled water several times and this mixture was added

to the PET bottle. Water was added to bring the exact weight to 50.00 g. The procedure for reagent blanks is identical to that for test samples and is carried out concurrently without a sample.

ICP-MS parameters and target element isotopes

The sample solution was analyzed under the optimized condition. The target element isotopes are summarized in table 3. ⁷²Ge was selected as the internal standard element for Be, Cr, Mn, Ni, Cu, Zn and As. ¹¹⁵In was selected as the internal standard element for Ag, Cd and Ba and ²⁰⁹Bi was selected as the internal standard element for Hg, Tl and Pb. ICP-MS parameters were automatically optimized by the instrument. All of the specifications meet the installation requirements including sensitivity, background, oxide, doubly charge, stability, etc. The parameters are listed in table 4.

| Stage | Power | | Ramp (min) | T (°C) | Hold (min) |
|-------|---------|-----|------------|--------|------------|
| | Max (W) | % | | | |
| 1 | 1200 | 100 | 5:00 | 120 | 5:00 |
| 2 | 1200 | 100 | 6:00 | 180 | 20:00 |

Table 2
Microwave digestion program.

| Parameter | Set value |
|----------------------------|--------------------------|
| Power | 1350 W |
| Flow rate of plasma gas | 15.0 L·min ⁻¹ |
| Flow rate of auxiliary gas | 1.0 L·min ⁻¹ |
| Flow rate of carrier gas | 1.12 L·min ⁻¹ |
| Sampling rate | 0.4 mL·min ⁻¹ |
| Sampling depth | 7 mm |
| Orifice of sampling cone | 1.0 mm |
| Orifice of skimmer cone | 0.4 mm |
| Data acquisition mode | Quantitative analysis |
| Integration time | 0.3 s /isotope |
| Cerium oxide/Cerium | <0.5 % |
| Doubly charge | <2 % |

Table 4
ICP-MS operating parameters.

| Element | Be | Cr | Mn | Ni | Cu | Zn | As | Ag | Cd | Ba | Hg | Tl | Pb |
|---------|----|----|----|----|----|----|----|-----|-----|-----|-----|-----|-----|
| Isotope | 9 | 52 | 55 | 60 | 63 | 66 | 75 | 107 | 114 | 137 | 202 | 205 | 208 |

Table 3
Target element isotopes.

Calibration curves

The mixed stock solution and Hg stock solution were diluted to 0.1, 0.5, 2, 10 ng·mL⁻¹ using 5 % HNO₃ respectively. The blank solution is 5 % HNO₃. The blank and calibration solutions were measured under optimized conditions. The calibration curve was automatically plotted by the instrument. Linear correlation coefficients (r) in all calibration curves were better than 0.9999.

Results and discussion

Method detection limit

The blank sample was analyzed 11 times under optimized conditions. The method detection limits (MDL) for each element were calculated (table 5).

| Element | MDL (ng·g ⁻¹) |
|---------|---------------------------|
| Be | 0.1 |
| Cr | 7.2 |
| Mn | 1.1 |
| Ni | 1.9 |
| Cu | 2.5 |
| Zn | 3.4 |
| As | 3.5 |
| Ag | 0.6 |
| Cd | 0.8 |
| Ba | 2.4 |
| Hg | 1.1 |
| Tl | 0.1 |
| Pb | 0.9 |

Table 5
Method detection limits (MDL).

Determination of standard materials

To evaluate reliability and accuracy, the microwave digestion ICP-MS method was applied to the determination of two certified reference materials: GBW07602 (shrub leaves) and GBW08513 (tea leaves). The results are in strong agreement with the certified values, a comparison is shown in table 6.

Recovery

The percent recovery for each element was determined using the standard addition method to evaluate the reliability and accuracy of the method. Percent recoveries of all elements were between 90.3 % and 109.7 %. The results were considered satisfactory (table 7).

Sample analysis

This study analyzed 13 toxic

elements in seven TCMs purchased on the market. Each sample was analyzed eight times and the accuracy (RSD %) varied between 0.3 % and 6.8 % (table 8). According to the results in Table 8, not all TCMs meet the minimum legal requirements. The concentrations of some elements highly exceed the limit allowed. However, in most TCMs the amount of all toxic elements is low.

| Element | GBW07602 (shrub leaves) | | GBW08513 (tea leaves) | |
|---------|---------------------------------------|-----------------------------------|---------------------------------------|-----------------------------------|
| | Certified value μg·g ⁻¹ | Found value μg·g ⁻¹ | Certified value μg·g ⁻¹ | Found value μg·g ⁻¹ |
| Be | 0.056 ± 0.014 | 0.046 | / | 0.088 |
| Cr | 2.3 ± 0.3 | 2.000 | / | 2.200 |
| Mn | 58 ± 6 | 54.000 | 2170 ± 110 | 2074.000 |
| Ni | 1.7 ± 0.4 | 1.700 | 5.09 ± 0.76 | 4.940 |
| Cu | 5.2 ± 0.5 | 4.600 | 8.96 ± 0.59 | 8.230 |
| Zn | 20.6 ± 2.2 | 19.800 | 22.6 ± 1.5 | 22.400 |
| As | 0.95 ± 0.12 | 0.790 | 0.180 ± 0.049 | 0.134 |
| Ag | 0.027 ± 0.006 | 0.024 | / | 0.022 |
| Cd | 0.14 ± 0.06 | 0.180 | 0.023 ± 0.004 | 0.022 |
| Ba | 19 ± 3 | 17.000 | 120 ± 10 | 112.000 |
| Hg | / | 42.500 | 0.017 | 0.018 |
| Tl | / | 0.015 | / | 0.016 |
| Pb | 7.1 ± 1.1 | 6.100 | 1.00 ± 0.05 | 0.910 |

Table 6
Comparison of found value and certified value.

| Element | Spiked value (ng·mL ⁻¹) | Found value (ng·mL ⁻¹) | Recovery percentage (%) |
|---------|--|---------------------------------------|----------------------------|
| Be | 10 | 9.37 | 93.7 |
| Cr | 10 | 10.63 | 106.3 |
| Mn | 10 | 10.97 | 109.7 |
| Ni | 10 | 10.24 | 102.4 |
| Cu | 10 | 10.68 | 106.8 |
| Zn | 10 | 10.36 | 103.6 |
| As | 10 | 10.89 | 108.9 |
| Ag | 10 | 9.20 | 92.0 |
| Cd | 10 | 9.25 | 92.5 |
| Ba | 10 | 9.16 | 91.6 |
| Hg | 5 | 4.87 | 97.3 |
| Tl | 10 | 9.58 | 95.8 |
| Pb | 10 | 9.03 | 90.3 |

Table 7
Results of the recovery experiments.

| Name of sample Element | | Gegen Soup | Zhike San | Guifudihuang Pill | Huanglianshangqing Pill | Jinsangsanjie Pill | Naodesheng Pill | Shugan Pill |
|------------------------|-------------|------------|-----------|-------------------|-------------------------|--------------------|-----------------|-------------|
| Be | Found value | 0.020 | 0.009 | 0.032 | 0.034 | 0.060 | 0.037 | 0.013 |
| | RSD% | 5.2 | 2.6 | 1.0 | 5.1 | 2.0 | 1.4 | 5.2 |
| Cr | Found value | 0.34 | 0.46 | 1.40 | 1.58 | 4.89 | 1.74 | 4.76 |
| | RSD% | 2.0 | 2.0 | 1.9 | 2.6 | 2.3 | 2.5 | 0.8 |
| Mn | Found value | 34.77 | 17.80 | 54.78 | 30.37 | 87.23 | 23.96 | 124.4 |
| | RSD% | 0.7 | 2.4 | 1.1 | 2.20 | 1.21 | 2.62 | 3.10 |
| Ni | Found value | 1.09 | 1.17 | 1.24 | 1.64 | 3.09 | 1.50 | 3.15 |
| | RSD% | 0.6 | 0.9 | 1.4 | 0.8 | 2.2 | 1.8 | 1.8 |
| Cu | Found value | 1.49 | 1.68 | 4.08 | 8.85 | 15.23 | 3.56 | 5.38 |
| | RSD% | 0.6 | 0.6 | 0.6 | 2.5 | 2.3 | 2.38 | 0.46 |
| Zn | Found value | 5.66 | 4.82 | 21.27 | 18.57 | 37.07 | 15.33 | 22.59 |
| | RSD% | 0.6 | 1.1 | 2.4 | 1.3 | 1.5 | 1.7 | 1.7 |
| As | Found value | N.D. | 0.26 | 0.46 | 0.79 | 0.89 | 0.56 | 29.14 |
| | RSD% | 1.6 | 1.4 | 3.9 | 3.5 | 5.7 | 3.3 | 1.5 |
| Ag | Found value | 0.0009 | 0.0008 | 0.005 | 0.007 | 0.079 | 0.006 | 0.007 |
| | RSD% | 5.3 | 6.3 | 2.1 | 5.8 | 3.5 | 5.6 | 4.3 |
| Cd | Found value | 0.022 | 0.042 | 0.10 | 0.11 | 0.15 | 0.077 | 0.082 |
| | RSD% | 5.5 | 1.5 | 1.2 | 2.7 | 1.9 | 3.6 | 2.0 |
| Ba | Found value | 5.86 | 8.94 | 15.32 | 44.76 | 167.8 | 136.7 | 12.98 |
| | RSD% | 1.1 | 1.7 | 1.4 | 2.1 | 2.8 | 0.3 | 0.9 |
| Hg | Found value | 0.003 | 0.002 | 0.85 | 0.088 | 0.027 | 0.076 | 5.05 |
| | RSD% | 6.8 | 5.8 | 3.3 | 5.5 | 5.0 | 3.5 | 0.6 |
| Tl | Found value | 0.008 | 0.027 | 0.025 | 0.020 | 0.033 | 0.036 | 0.014 |
| | RSD% | 1.3 | 2.4 | 2.7 | 3.6 | 3.2 | 1.1 | 4.1 |
| Pb | Found value | 0.15 | 0.16 | 0.93 | 1.54 | 2.14 | 0.68 | 1.69 |
| | RSD% | 0.7 | 1.1 | 2.6 | 2.1 | 1.7 | 1.5 | 1.3 |

Table 8
Analytical results of TCMs (n = 8). Unit: $\mu\text{g g}^{-1}$.

Conclusion

The evidence suggests that the current TCM market is complex and strict management and quality controls are needed to ensure that the maximum allowable limits of toxic elements set by regulations are not exceeded. National and local drug administrations also require regulations to manage and control the production and sale of TCMs. The study uses microwave digestion for sample preparation, With optimized working parameters all elements in different medicines are analyzed simultaneously with an Agilent 7500 Series c ICP-MS. This method is validated with certified reference materials by conducting recovery experiments using known standard additions. It offers many advantages over other alternative techniques, such as precision and accuracy, simplicity, rapidity, low limits of detection and multiple element determination.

References

1. Wang Xiao-ru, "Application of Inductively Coupled Plasma Mass Spectrometry." *Chemical Industry Press. Bei Jing.*, 102, **2005**.
2. Dong Hong-bo, Han Li-qing, Dong Shun-fu, "Instrumentation & Analysis Monitoring" (3): 29~30, **2002**.
3. Yu Zi-li, Guang Lei, "Analytical Technique of Metal Ion". *Chemical Industry Press. Bei Jing*, 225~226, **2004**.
4. Determination of Lead (Pb), Cadmium (Cd), Arsenic (As), Mercury (Hg) and Copper (Cu), Ch. P 2005 (English version), Appendix IX B, p. 54-56.

Hua Zhang is a postgraduate student in the chemistry department of the Capital Normal University, Yan-zhi Shi and Ying-feng Wang are professors at the Analytical Center of the Capital Normal University, Beijing, China. Yu-hong Chen is Application Engineer at Agilent Technologies Co. Ltd, China.

www.agilent.com/chem

© Agilent Technologies, 2006

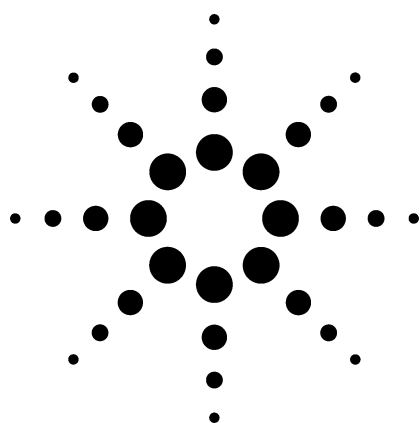
Published August 1, 2006
Publication Number 5989-5591EN



Agilent Technologies

The Use of Collision/Reaction Cell ICP-MS for the Simultaneous Determination of 18 Elements in Blood and Serum Samples

Application



Clinical

Authors

R. Wahlen, L. Evans, J. Turner, and R. Hearn
LGC Limited, Queens Road
Teddington, Middlesex, TW11 0LY
UK

Abstract

This study describes the development of a robust high-throughput analytical method for the determination of 18 elements (15 trace elements and 3 electrolytes) in blood and serum samples using an Agilent Technologies 7500ce collision/reaction cell ICP-MS system. The only sample preparation necessary was dilution using an alkaline diluent containing ammonia, EDTA Triton X-100, and butan-1-ol. Instrument calibration was performed using external calibration with internal standardization. The performance of the method exceeded a previously-used magnetic sector HR-ICP-MS method by at least a factor of three in terms of sample throughput and matched the precision and detection limits of that method.

Introduction

The analysis of metals in clinical fluids such as whole blood, serum, and urine has been used for many years to provide information on toxicity, work-place exposure, and nutrient availability, and as a diagnostic tool for a number of ailments. The fact that many trace metals are present at variable and often low concentrations (sub ng/mL range) in different clinical sample types has presented clinical analysts with a variety of challenges. In addition, matrix components, such as organic compounds, proteins, or electrolyte salts that may interfere with the analysis of trace elements, are

often present at elevated levels (mg/mL or above). The matrix to be analyzed, the amount of sample that can be taken and the means of sampling may also impose restrictions. Sufficient volumes of urine can normally be obtained from patients with noninvasive techniques, whereas the collection of whole blood or serum samples usually involves use of needle and syringe and generally yields smaller sample volumes (often only μL or mL) for analysis. The analysis technique employed should therefore provide the following capabilities: sufficiently low detection limits (DLs), ability to overcome matrix related interferences, sufficient linearity to measure a wide concentration range in unknown samples, simultaneous multi-elemental determinations, and ability to cope with small sample volumes.

Analysis of clinical matrices by inductively coupled plasma mass spectrometry (ICP-MS) is becoming more widespread since ICP-MS meets a number of the above requirements, namely very low DLs for many trace metals (sub ng/mL), relative freedom from interferences, simultaneous multi-elemental determination, and suitability for small sample volumes, as well as providing isotopic information and the possibility of employing isotope dilution mass spectrometry (IDMS) as a high-caliber reference calibration technique. When analyzed by ICP-MS, many of the elements of interest suffer from mass spectral interferences derived from the sample matrix. Before the development of sufficiently sensitive collision/reaction cell (CRC) quadrupole ICP-MS instruments, matrix-based spectral interferences were overcome by the use of sector field or high-resolution ICP-MS (HR-ICP-MS) [1] or by non-mass spectroscopic techniques such as atomic fluorescence (AF) [2] or atomic



Agilent Technologies

absorption spectroscopy (AAS) [3]. Another way of overcoming matrix-effects is the use of sample digestion using concentrated acids or ashing techniques [4]. These techniques can be expensive, time-consuming, and/or less suitable for high sample throughput.

In our laboratory, magnetic sector HR-ICP-MS (Element 1, ThermoFinnigan) was used [1, 5] for monitoring post- and pre-operation samples from patients with metal-on-metal hip replacements. After 1:20 dilutions of blood and serum samples with approximately 0.7-mM ammonia, 0.01-mM EDTA, and 0.07% (v/v) Triton X-100 or 1:15 dilutions of urine samples with 1% HNO₃, the elements such as Al, V, Co, Cr, Mo, Ni, and Ti were analyzed. The main drawbacks of this technique were cost, practicality, and duration of instrument set-up, as well as instrument down-time and matrix tolerance during analytical runs containing more than ~30 blood or serum samples.

Objectives

The aim of this work was to develop a robust ICP-MS methodology based on CRC quadrupole ICP-MS (CRC-ICP-MS), capable of measuring a wide range of elements in a single analysis after only a simple dilution of the samples.

A simple dilution of the samples was selected as the preferred sample preparation method, as acid digestion techniques can increase the sample turnaround time, cost, and the potential for contamination.

In order to achieve the required sample throughput of up to 100 samples per batch, the quantitation method had to be based on external calibration. Minimal instrument drift was therefore paramount in order to reduce the need for frequent recalibration or drift correction.

The target elements included the trace metals Al, As, Cd, Co, Cr, Cu, Fe, Mn, Mo, Ni, Pb, Sb, Se, V, and Zn as well as the electrolytes K, Mg, and Na.

The sensitivity achieved needed to match previously obtained DLs using HR-ICP-MS in our laboratory of 0.2 ng/mL (for example, Co, Mo) and 1.0 ng/mL (Ni) in the undiluted samples.

Sample Preparation

All samples, standards, and quality control (QC) materials were diluted 20-fold using a solution containing approx. 0.7-mM ammonia, 0.01-mM EDTA, and 0.07% (v/v) Triton X-100. Butan-1-ol

was added to the diluent as a carbon source at 1.5% (v/v) in order to improve matrix matching between standards and samples and thereby increase the accuracy for analytes such as As and Se, whose ionization behaviors in the plasma are affected by the carbon content [6]. In order to keep the chemistry of the sample introduction system stable throughout the run, the diluent was also used for pre- and post-analysis rinse functions. Commonly used rinse acids such as HNO₃, even at dilute levels of 1%, can lead to coagulation or precipitation of clinical matrix components and result in tubing or nebulizer blockages.

The selection of internal standard (IS) elements and the IS concentration is very important. The choice of elements is often restricted in clinical analysis due to the presence of many of the elements that are usually used in environmental applications at ng/mL levels in clinical samples. Blood and serum samples were analyzed in semi-quantitative mode to determine the most suitable IS elements, that is, those which were not present or present at the lowest levels in relative terms. For elements that were present in the samples, such as Sc, the concentration of the IS was added at such a level that the contribution from Sc in the sample to the total ⁴⁵Sc signal would be negligible. The chosen IS elements (Sc, Ge, Rh, In, and Tl) were added to the diluent at a concentration of 20 ng/mL. Addition of the IS in this way negated possible mixing problems if online addition of the IS via a T-piece was used.

Instrumentation

An Agilent 7500ce Octopole Reaction System (ORS) ICP-MS was used in three different gas modes: hydrogen, helium, and standard or no-gas mode. The ICP-MS conditions and the isotopes, integration times and gas modes for the multi-elemental determination are given in Tables 1 and 2. Quantitation on all isotopes was performed using the three central points of the spectral peaks.

A 100-μL/min PFA microflow nebulizer was used and sample uptake and washout times were reduced using the larger diameter peristaltic pumps of the Integrated Sample Introduction System (ISIS). The pump speed was set at 0.1 rps during the analysis and washout in order to minimize overloading of the sample introduction system and the plasma with matrix components. The torch was equipped with a 2.5-mm diameter injector and the Shield Torch system was used. Nickel (Ni) cones were used at all times.

The total acquisition time per sample was 208 s. This included the sequential loading of the H₂, He, and Std tune files and a 40 s equilibration and stabilization time between the different gas modes. Each sample/standard solution was analyzed sequentially in all gas modes before the autosampler probe moved to the next sample. After each sample, the autosampler probe was rinsed for 5 s using 5% HNO₃ and the sample introduction system was then rinsed using the diluent for 30 s.

Table 1. ICP-MS Parameters Used in the Different Gas Modes

| | H ₂ | He | Std |
|-------------------------|----------------|------|----------|
| Rf Power (W) | 1500 | 1500 | 1500 |
| Carrier gas (L/min) | 0.87 | 0.87 | 0.87 |
| Make up gas (L/min) | 0.17 | 0.17 | 0.17 |
| Spray chamber temp (°C) | 2 | 2 | 2 |
| Gas flow (mL/min) | 4 | 4 | Not used |

Table 2. Analysis Parameters for the Analytes of Interest

| Analyte | Isotope monitored (m/z) | Integration time per mass (s) | Internal standard used (m/z) | Gas mode used |
|---------|-------------------------|-------------------------------|------------------------------|----------------|
| Na | 23 | 0.3 | 45 | He |
| Mg | 24 | 0.3 | 45 | He |
| Al | 27 | 3.0 | 45 | He |
| K | 39 | 0.3 | 45 | He |
| V | 51 | 1.5 | 45 | He |
| Cr | 53 | 3.0 | 45 | He |
| Mn | 55 | 0.9 | 45 | Std |
| Fe | 56 | 0.3 | 45 | H ₂ |
| Co | 59 | 1.5 | 45 | He |
| Ni | 60 | 1.5 | 45 | He |
| Cu | 65 | 0.9 | 72 | He |
| Zn | 66 | 0.3 | 72 | He |
| As | 75 | 1.5 | 72 | He |
| Se | 78 | 1.5 | 72 | H ₂ |
| Mo | 95 | 1.5 | 103 | Std |
| Cd | 111 | 1.5 | 115 | Std |
| Sb | 121 | 0.9 | 115 | Std |
| Pb | Sum of 206, 207 and 208 | 0.9 | 205 | Std |

Method Performance and Robustness

The stability of the proposed methodology was tested by running blood and serum samples in a sequence over a 10-hour period (a total of 90 samples, including calibration standards and QC checks) and monitoring the behavior of IS elements, calibration slopes, and check standards.

Instrument Stability - Signal Variation for IS Elements

Typical signal variation for the IS elements of choice (Sc, Ge, Rh, In, Tl) was 4.8%–9.3% in hydrogen mode, 5.5%–8.2% in helium mode, and 6.7%–10.0% in standard mode. This was assessed during a 90-sample sequence of blood and serum samples. Figure 1 shows the variation for the IS elements throughout the 10-hour run. Sc is present in some clinical sample types at ng/mL levels, which can be seen here after sample 8.

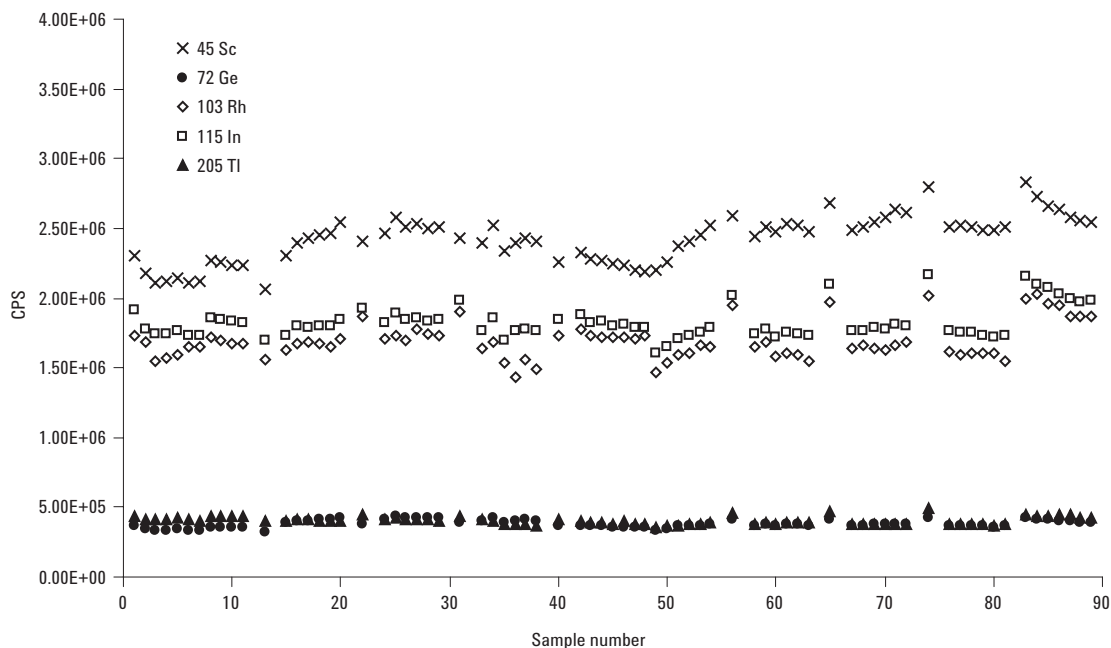


Figure 1. Variation of the IS signals in standard mode throughout the 10-hour run.

Calibration Repeatability and Linearity

Overlaying calibration curves from the beginning, middle, and end of the 10-hour run assessed the robustness of the calibration technique. The correlation coefficients for the mean slope of three calibrations for V, Se, and Pb (Figure 2) during a 10-hour sequence ranged from 0.9997 to 1.0000 and indicate the robustness of the method with these matrices. The calibration coefficients for all elements measured were generally better than $r^2 > 0.9900$.

Check Standards

Check standards at 1 ng/mL level were analyzed throughout the run after every nine samples for

the trace metals and were within 10% of the expected value for the elements tested.

Effects of Sample Matrix on the Sample Introduction System

Using dilution factors of 20-fold or less for analysis of these matrices by HR-ICP-MS lead to frequent problems with the sample introduction system, especially blocking of the torch injector. When using quadrupole ICP-MS as described above, dilution factors of 15- and 10-fold could be used without detrimental effects on the sample introduction system (Figure 3) or instrument performance. Reagent blanks were monitored after the analytical run, and no significant deterioration in the DLs or increase in the background levels was observed.

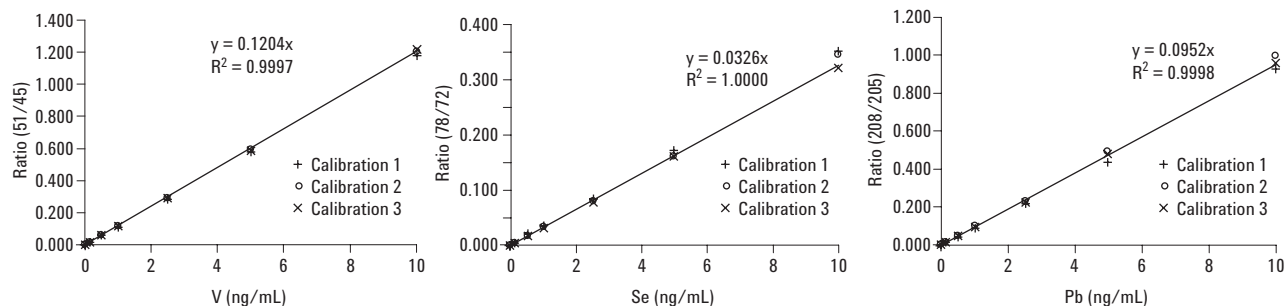


Figure 2. Linearity of overlaid calibration curves for V, Se, and Pb, showing stability of the external calibration approach throughout a 90-sample sequence.

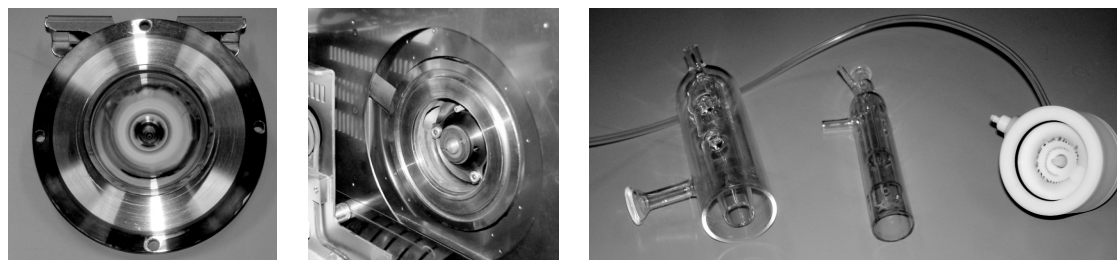


Figure 3. Photos of the interface and sample introduction system after a 90-sample run. Both the sampler and skimmer cones show minor matrix deposits. The 2.5-mm injector torch used was relatively deposit-free. The blood deposits on the spray chamber and the nebulizer block were removed using a sodium hypochlorite solution.

Analysis of Certified Reference Materials (CRMs)

Multiple sub-samples (n=4) of the certified reference material NIST SRM 1598 Bovine serum and the reference material Seronorm MR9067 (whole human blood, level 2) were diluted 20-fold as described above and analyzed using the conditions described in Tables 1 and 2. These materials were chosen because they represented different clinical matrices and contained a wide range of analytes of interest ranging in concentration levels from sub ng/mL to mg/mL. Levels for the same analytes often varied by more than an order of magnitude between the two materials. Certificate data for both materials as well as method DLs (calculated back to the undiluted sample and based on 3 s of the blank concentration) for the method proposed here are shown in Table 3.

The analytical data for both materials were converted to percent recovery data relative to the certified or indicative values and are shown in Figure 4a) and b). The combination of the reference materials chosen for this study provided certified values with uncertainty estimates for all of the elements determined except for Na, where only an indicative value was available. The recovery for Na compared to the indicative value was 99.0%, and the data for the remaining elements measured fell within the uncertainty range for either one or both of the reference materials. Where the certificate values were not achieved (for example, V, Cr, and Cd), the certified concentrations in SRM 1598 were below the DL for the method. Na, As, Ni, and Pb are quoted as indicative values only in SRM 1598 (Table 3.).

Table 3. Certified Concentrations for the Analytes of Interest in the SRM NIST 1598 and the Reference Material Seronorm MR9067. Method DLs Calculated Back to the Undiluted Sample are Given for Comparative Purposes.

| Trace elements | NIST SRM 1598 Bovine serum (ng/g) | Seronorm MR9067 human blood level 2 (ng/mL) | DL (ng/mL) |
|-----------------------|-----------------------------------|---|----------------|
| Al | 3.7±0.9 | 39–71 | 0.8 |
| As | 0.2* | 10.6–11.8 | 0.1 |
| Cd | 0.089±0.016 | 4.8–6.0 | 0.1 |
| Co | 1.24±0.016 | 4.6–5.8 | 0.1 |
| Cr | 0.14±0.08 | 5.1–6.3 | 1.0 |
| Cu | 720±40 | NA | 0.4 |
| Fe | 2550±100 | NA | 19 |
| Mn | 3.78±0.32 | 10.1–13.3 | 0.1 |
| Mo | 11.5±1.1 | 5.3–6.7 | 0.1 |
| Ni | 0.7* | 5.1–8.6 | 0.2 |
| Pb | 0.6* | 373–417 | 0.1 |
| Sb | NA | 25–28 | 0.5 |
| Se | 42.4±3.5 | 114–130 | 0.2 |
| V | 0.06* | 3.1–4.2 | 0.1 |
| Zn | 890±60 | NA | 3.0 |
| Major elements | (µg/g) | | (ng/mL) |
| K | 196±5 | NA | 100 |
| Mg | 20.0±0.4 | NA | 1.5 |
| Na | 3000* | NA | 5.0 |

*Is indicative value only

NA Not applicable

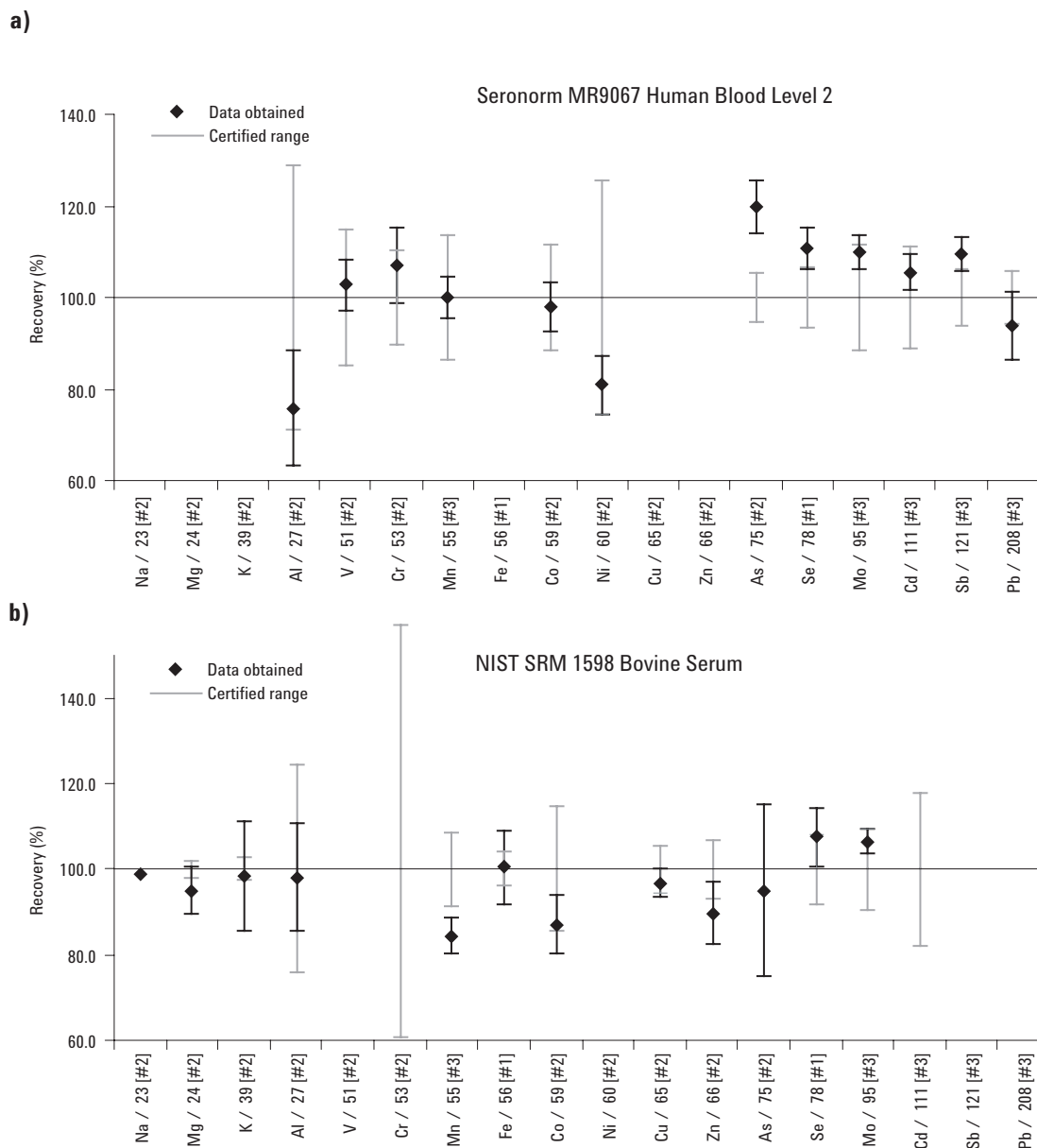


Figure 4. Data obtained expressed relative to the certified data for a) Human blood Seronorm MR9067 and b) Bovine serum SRM NIST 1598. Errors bars represent expanded uncertainties for data obtained and certified ranges for the reference materials. The numbers after the isotopes indicate the tune step used (#1 = H₂, #2 = He, #3 = Std).

Importance of Matrix-Matching and Choice of IS Elements

The data for As and Se in MR 9067 are slightly high compared to the certified mean value, and this could be due to a higher carbon content in this matrix. When increasing the level of butan-1-ol in the diluent from 0% to 3% v/v, recoveries for these analytes decreased and approached 100% (Figure 5). When no butan-1-ol was added to the diluent, recoveries for As and Se were significantly higher than the mean certified values (by 94% and

72% respectively) in comparison to recoveries obtained with butan-1-ol addition at 1.5% (v/v). A complete matrix match was achieved for both samples by using the standard addition technique for As and Se in both reference materials. Recoveries for Se were 95.8% and 99.9% in NIST SRM 1598 and Seronorm MR9067 respectively, and 102.6% for As in Seronorm MR9067. Figure 5 also indicates that the effect of the carbon addition on both elements is slightly different.

Seronorm whole blood - MR9067

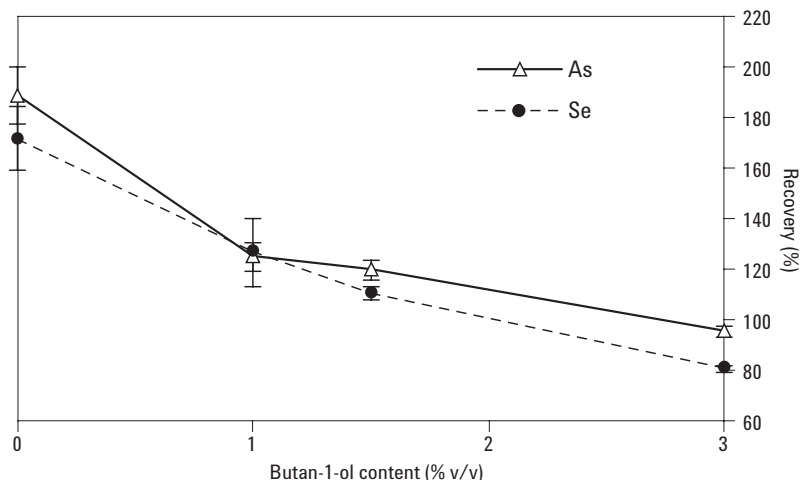


Figure 5. Recovery data for As and Se in Seronorm whole blood (Level 2) with varying levels of butan-1-ol addition to the diluent.

According to the data obtained here, an addition of 3% would be best for As (mean recovery of 95.4 ±2.3%), whereas the ideal volume of butan-1-ol addition for this sample and dilution level for Se is closer to 2%.

For such elements where the ionization is affected by matrix components in the plasma, it is therefore imperative to obtain a good level of matrix matching for the greatest accuracy. If this is not possible, for example if the carbon levels in different samples vary significantly, it may be better to use a different sample preparation procedure such as closed-vessel microwave digestion in order to destroy the organic carbon matrix. However, this can significantly increase the sample turn-around time for large sample batches.

only exception to this spiking regime was Fe in MR9067, for which no certificate or indicative value was available before the analysis and where the spike concentration added (20 ng/mL) was not sufficiently high above the determined sample concentration (400 ±5 µg/mL) to give meaningful recovery data. The mean data for all spike levels for the trace metal analytes are shown in Table 4.

Spike recoveries for all elements fell within 100 ±20%, and all except Fe, Se and Mo were within 100 ±10%. The high Se recoveries are thought to be due to the fact that the matrix matching for carbon content consisted of only 1.5% butan-1-ol. High recoveries for Mo were also observed when the samples were analyzed by HR-ICP-MS, and this effect is currently under closer investigation.

Spike Recovery Data

Spike recovery experiments were performed on both materials for the trace metal analytes at 2–4 different levels with concentrations ranging from 2–5 times of the original analyte concentrations. The

Table 4. Mean Spike Recovery Data Obtained for Both Reference Materials

| | NIST SRM 1598 bovine serum | Seronorm MR9067 human blood level 2 |
|-----------|-----------------------------------|-------------------------------------|
| 100% ±5% | Al, V, Cr, Mn, Cu, Zn, Cd, Sb, Pb | Al, V, Cr, Mn, Co, Ni, Cu, Cd |
| 100% ±10% | Co, Ni, As | Zn, As, Sb, Pb |
| 100% ±15% | Fe, Se | Se |
| 100% ±20% | Mo | Mo |

Conclusions

A robust CRC-ICP-MS method was developed that is capable of high sample throughput (up to 100 samples per batch) for a large suite of elements in difficult clinical matrices after simple dilution. The method robustness was demonstrated by minimal signal drift during analytical sequences of 10-hour duration, negating the need for frequent recalibration. The method DLs achieved matched those of a previously used HR-ICP-MS method. Further improvements in method DLs can be achieved by reducing the dilution levels of the clinical matrices, which is possible due to the robustness of the sample introduction system. Good agreement within the uncertainty of certificate values was achieved for all of the target analytes in both reference materials where certified data were available across concentration levels ranging from ng/mL–mg/mL level. Spike recoveries for all elements fell within 100 ±20%, and all except Fe, Se, and Mo were within 100 ±10%.

Acknowledgements

The work described was supported under contract with the Department of Trade and Industry, UK as part of the National Measurement System Valid Analytical Measurement (VAM) program.

Agilent Technologies are gratefully acknowledged for provision of the ce lens system upgrade on the 7500 ICP-MS for the work described here.

References

1. C.P. Case, L. Ellis, J.C. Turner, and B. Fairman (2001) *Clinical Chemistry*, **47**, 2, 275–280.
2. J.A. Holcombe and T.M. Rettberg (1986) *Anal. Chem.*, **58**, 124R.
3. A. Taylor, and P. Green (1988) *JAAS*, **3**, 115–118.
4. L. Dunemann (1991) *Nachr. Chem. Tech. Lab.*, **39**, 10, M3.
5. D. Ladon, A. Doherty, R. Newson, J. Turner, M. Bhamra, and C.P. Case (2004) *The Journal of Arthroplasty*, **19**, 8, 78–83.
6. E.H. Larsen, and S. Stürup (1994) *JAAS*, **9**, 1099–1105.

For More Information

For more information on our products and services, visit our Web site at www.agilent.com/chem.

raimund.wahlen@lgc.co.uk

Agilent shall not be liable for errors contained herein or for incidental or consequential damages in connection with the furnishing, performance, or use of this material.

Information, descriptions, and specifications in this publication are subject to change without notice.

© Agilent Technologies, Inc. 2005

Printed in the USA
June 10, 2005
5989-2885EN



Agilent Technologies

Evaluation of Conventional ICP-MS and ORS-ICP-MS for Analysis of Traditional Chinese Medicines

Application

Pharmaceuticals

Authors

Dengyun Chen

Agilent Technologies Co., Ltd. (China)

XinMei Wang, Shen Ji

The Medical Testing Center of Shang-Hai (China)

Miao Jing, Xiaoru Wang

The First Institute of Oceanography, S.O.A

Qingdao, 266061

China

Abstract

Traditional medicines based on herbal products and extracts play an ever increasing role around the world. This work describes the development of a method to fully characterize the inorganic content of Traditional Chinese Medicines (TCM) using Inductively Coupled Plasma Mass Spectrometry (ICP-MS).

Using an Agilent 7500a ICP-MS instrument, the reliability of both the ICP-MS hardware and USEPA Method 200.8 were evaluated for the determination of a range of elements in TCM. Several Certified Reference Materials (CRM), including both key trace elements such as As, Pb, Hg, Cd, and major components such as P, Ca, Fe, K, and Na, were digested and measured using the Agilent ICP-MS instrument during method evaluation.

In an extension to the work, an Agilent 7500c ICP-MS with Octopole Reaction System (ORS) was used to determine As and Se in a Peach Leaf CRM. The ORS results, acquired without the use of interference correction equations, compared more favorably with the reference values than results obtained from the non-cell ICP-MS results using interference correction equations.

Introduction

Herbs and herbal products play an important role in the healthcare of nearly 80% of the world population, particularly in developing countries. For example, TCM herbs and their manufactured products have been used for thousands of years for the prevention and treatment of disease in China and, since the late 1800's, in some synthetic pharmaceuticals used in orthodox medical practice. TCM materials are made up mainly of medicinal botanicals, but can contain extracts taken from other types of plants, animals, and minerals. While whole plants are sometimes suitable as crude herbs, most often processed roots, rhizomes, fruits, seeds, flowers, leaves, wood, bark, and vine stems are incorporated. The raw materials are processed according to specified procedures and made into "Ying Pian" for supply as components of prescribed composite formulae or "Fu Fang" for patient use. All medicinal products for human and animal use must meet proven quality, safety, and efficacy. However, the quality assurance of herbal medicinal products can be problematic because of the many unidentified chemical entities in the finished products. The determination of the elemental composition of these sample types plays a very important part in the quality assurance of TCM, as is specified in programs such as Good Agriculture Practice (GAP), Good Sourcing Practice (GSP), Good Laboratory Practice (GLP), Good Manufacturing Practice (GMP), and Good Clinical Trial Practice (GCTP).



Agilent Technologies

The heavy metal content of TCM herbs is commonly studied from the viewpoint of toxicity and bio-availability. Heavy metals such as Pb, Cd, Hg, and As may be introduced into herbs in a variety of ways, including contamination during cultivation, processing, and storage. Plant roots or leaves may absorb heavy metals from the atmosphere, water, and soil. These heavy metals can accumulate at a particular position in the plant. The distribution of heavy metals varies greatly within different parts of the plants. Other elements present in herbs may have a curative or nutritional effect. Many nutritional elements, such as Mg, Zn, Mn, Ni, Cu, and Se, are essential for human health.

ICP-MS is fast becoming the technique of choice for the determination of elements in a wide range of samples. It is used widely for the measurement of trace and ultratrace elements in environmental and biological materials. It allows rapid and simultaneous multi-elemental determination of samples and offers a number of advantages compared to ICP-OES (optical emission spectroscopy), including fewer spectral interferences, low detection limits (DLs), and the ability to measure isotopic ratios. In this study, ICP-MS was applied to the determination of trace and major elements in TCM samples in the same run. The accuracy, precision, and DLs of the method, as well as the analytical results of several certified reference materials (CRM), are presented. Results obtained using a non-cell ICP-MS and the interference correction equations specified in EPA 200.8 method are compared to results for As and Se obtained using ORS cell-technology.

Experimental

Instrumentation and Reagents

An Agilent 7500a and a 7500c ORS ICP-MS were used in this study; see Table 1 for the operating parameters. The samples were prepared by microwave digestion (CEM MARS, CEM Co. Ltd, USA) or in a sealed PTFE high pressure vessel (100 mL) developed in the laboratory. Concentrated nitric acid (68% w/v, GR, Merck) was used for sample digestion and the cleaning of the digestion tubes. Deionized water (Milli-Q ultrapure water system) was used throughout.

Table 1. 7500a/7500c ICP-MS Operating Parameters

| | |
|-----------------------|--|
| RF power | 1350W (7500a), 1500W (7500c) |
| Nebulizer | Babington nebulizer |
| Spray chamber | Scott double pass, 2±0.1 °C |
| Torch | Fassel |
| Data acquisition mode | Spectrum Analysis Mode and Full Quant Mode |
| Sampling depth | 7.0 mm |
| Carrier gas flow rate | 1.08 L/min |
| Make-up gas flow rate | 0.0 L/min |

The microwave digestion procedures followed the Standard Operating Procedure (SOP) of the instrument manual for plant samples. The CRM results indicated no significant difference between the two digestion methods.

Results and Discussion

Method DLs of TCM by 7500a ICP-MS (non-cell)

Several CRMs (National Research Centre for Certified Reference Materials, Beijing, China) were selected to test the accuracy, precision, and DLs of the method: Tea (GBW 07605), Tea Leaf (GBW 08513), Peach Leaf (GBW 08501), Wheat Powder (GBW 08503), Rice Powder (GBW 08502), and Pig Liver (GBW 08551). The 7500a measured values and the certified values are listed in Table 2.

Table 2. The Certified Values of the CRMs and the Measured Values by 7500a ICP-MS (Non-Cell)

| Element (Units) | Tea | | Tea leaf | | Wheat | | Rice | | Pig liver | |
|--------------------|-----------|----------|-----------|----------|-----------|----------|-----------|----------|-----------|----------|
| | Certified | Measured | Certified | Measured | Certified | Measured | Certified | Measured | Certified | Measured |
| 23 Na (µg/g) | * | † | * | † | * | † | 8.4±0.6 | 8.47 | 2330±40 | 2162 |
| 24 Mg (µg/g) | 1700±100 | 1847 | 2760±240 | 2747 | 551±21 | 594 | 120±5 | 125.7 | 747±26 | 643 |
| 27 Al (ng/g) | (3000) | 2652 | * | 6748 | * | 25.1 | * | † | * | 81993 |
| 31 P (µg/g) | 2840±60 | 2991 | 1480±80 | 1504 | (1500) | 1607 | - | 739.2 | (13000) | 12820 |
| 39 K (µg/g) | 16600±600 | 17440 | 8630±620 | 8363 | 1980±140 | 2001 | 656±15 | 663.8 | 11500±200 | 10724 |
| 43 Ca (µg/g) | 4300±200 | 4333 | 8000±660 | 7459 | 441±22 | 431.8 | * | † | 197±7 | 203 |
| 52 Cr (ng/g) | 800±20 | 819.4 | (2000) | 1897 | * | 88.7 | * | 20.14 | * | 1341 |
| 55 Mn (µg/g) | 1240±40 | 1265 | 2170±120 | 2008 | 19.6±1 | 20.1 | 9.8±0.2 | 9.7 | 8.32±0.19 | 8.75 |
| 57 Fe (µg/g) | 264±10 | 266.9 | 347±12 | 353.7 | 39.8±2.6 | 37.1 | 5.1±0.2 | 4.1 | 1050±40 | 1055 |
| 59 Co (ng/g) | 180±20 | 201 | (180) | 186.9 | * | 15.7 | * | 4.9 | (100) | 94 |
| 60 Ni (ng/g) | 4600±300 | 4813 | 5090±760 | 4953 | * | 123.4 | * | 50.5 | * | 227 |
| 65 Cu (µg/g) | 17.3±1 | 18.3 | 8.96±0.58 | 7.77 | 4.4±0.3 | 4.6 | 2.6±0.2 | 2.92 | 17.2±0.5 | 17.5 |
| 66 Zn (µg/g) | 26.3±0.9 | 27.9 | 22.6±1.5 | 21.5 | 22.7±2 | 23.7 | 14.1±0.5 | 15.1 | 172±4 | 171 |
| 75 As (ng/g) | 280±30 | 279.6 | 180±48 | 152.2 | 220±20 | 166 | 51±3 | 56.8 | 44±4 | 48 |
| 82 Se (ng/g) | (72) | 112.1 | 40±6 | 90.6 | (100) | 57.8 | 45±8 | 13.6 | 940±30 | 1054 |
| 114 Cd (ng/g) | 57±8 | 65.6 | 23±4 | 26.5 | 31±2 | 25.9 | 20±2 | 18.2 | 67±2 | 83 |
| 137 Ba (µg/g) | 58±3 | 56.2 | 120±10 | 103.8 | * | 1.85 | * | 104.6 | * | 494 |
| 202 Hg (ng/g) | (13) | 9.9 | (17) | 25.9 | * | 1.7 | * | 191.9 | * | 327 |
| 208 Pb (ng/g) | 4400±200 | 4409 | 1000±40 | 853.7 | 350±80 | 359.5 | 750±100 | 756.6 | 540±20 | 549 |
| 232 Th (ng/g) | 61±8 | 53.4 | 104±14 | 93.5 | * | 3.8 | * | 0.455 | * | 2.2 |
| 238 U (ng/g) | * | 15.34 | * | 36.8 | * | 1.3 | * | * | * | 3 |

* Not certified

† Not measured

The 7500a ICP-MS-measured values are in good agreement with the certified values, with errors less than 10% for all except a few elements (Table 2). All elements were measured in the same analytical run and all the samples were digested using the same method. The results illustrate good agreement with certified values of tea and tea leaf (useful analogs of leaf based TCM), wheat and rice powder (representative of seed type TCM), and pig liver (typical of animal derived TCM), and illustrate that the method is applicable to the analysis of herbal medicines. Key elements, such as As, Pb, Hg, and Cd, were determined at trace levels along with the major components, such as P, Ca, Fe, K, and Na, over a concentration range of about eight orders. The wide dynamic range (nine orders) of the 7500a ICP-MS contributes to the good recoveries. The results illustrate that the method is applicable for elemental analysis of TCM.

Method detection limits (MDL) were determined using the pig liver sample. Pig liver was selected because the high levels of NaCl and organic material present in the digest make it suitable to evaluate the matrix interference removal effect of the EPA 200.8 interference correction equations. Seven measurements of the sample were carried out at different times over a period of approximately 10 days (Table 3) to obtain a measurement of external precision and MDL.

Table 3. MDL of the Pig Liver Sample

| Element (unit) | LIVER | LIVER01 | LIVER02 | LIVER03 | LIVER04 | LIVER05 | LIVER06 | LIVER07 | Average | %RSD | MDL in solid sample |
|----------------|--------|---------|---------|---------|---------|---------|---------|---------|---------|------|---------------------|
| 23 Na (µg/g) | 2244 | 2200 | 2192 | 2144 | 2104 | 2088 | 2135 | 2189 | 2162 | 2.5 | 0.14 |
| 24 Mg (µg/g) | 667.8 | 653.8 | 654.5 | 644 | 628.3 | 629.3 | 630.8 | 637.1 | 643 | 2.2 | 0.01 |
| 31 P (µg/g) | 12980 | 12700 | 12860 | 12750 | 12910 | 12790 | 12800 | 12770 | 12820 | 1 | 0.3 |
| 39 K (µg/g) | 10810 | 10780 | 10710 | 10660 | 10530 | 10640 | 10810 | 10850 | 10724 | 1.0 | 0.5 |
| 43 Ca (µg/g) | 204.6 | 204.6 | 203.5 | 202.4 | 200.7 | 201.7 | 203.5 | 205 | 203 | 1 | 3.9 |
| 57 Fe (µg/g) | 1059 | 1036 | 1069 | 1066 | 1050 | 1059 | 1051 | 1053 | 1055 | 1.0 | 0.4 |
| 27 Al (ng/g) | 80990 | 86520 | 86980 | 76130 | 77650 | 79040 | 75690 | * | 81993 | 5.8 | 6.9 |
| 52 Cr (ng/g) | 1411 | 1393 | 1377 | 1330 | 1308 | 1300 | 1302 | 1310 | 1341 | 3.4 | 16 |
| 55 Mn (ng/g) | 8937 | 8820 | 8792 | 9063 | 8387 | 8792 | 8655 | 8580 | 8753 | 2.4 | 11 |
| 59 Co (ng/g) | 95.13 | 95.35 | 92.57 | 94.81 | 92.69 | 93.02 | 92.9 | 93.5 | 94 | 1 | 1.4 |
| 60 Ni (ng/g) | 233.2 | 229.1 | 227.9 | 223.5 | 225.9 | 226.2 | 227.2 | 225.9 | 227 | 1.3 | 6.0 |
| 65 Cu (ng/g) | 17630 | 17540 | 17380 | 17450 | 17450 | 17500 | 17540 | 17390 | 17485 | 0.5 | 2.3 |
| 66 Zn (ng/g) | 173900 | 169600 | 169000 | 167900 | 171500 | 168400 | 173100 | 175700 | 171138 | 1.7 | 11 |
| 75 As (ng/g) | 40.35 | 63.33 | 33.69 | 34.72 | 43.33 | 58.25 | 56.42 | 50.17 | 48 | 24 | 25 |
| 82 Se (ng/g) | 1085 | 1081 | 1052 | 1036 | 1033 | 1058 | 1046 | 1037 | 1054 | 1.9 | 34 |
| 114 Cd (ng/g) | 84.69 | 83.16 | 80.76 | 83.33 | 84.77 | 83.1 | 82.35 | 84.72 | 83 | 1.7 | 0.8 |
| 137 Ba (ng/g) | 496 | 492.7 | 497.4 | 495.9 | 491 | 488.9 | 493.2 | 498.5 | 494 | 0.7 | 1.4 |
| 202 Hg (ng/g) | 329.3 | 327.2 | 328.5 | 329.3 | 325 | 327.7 | 320.6 | 331 | 327 | 1.0 | 1.6 |
| 208 Pb (ng/g) | 547.9 | 545.3 | 548.7 | 548.3 | 548.6 | 550.2 | 548.3 | 554.1 | 549 | 0.5 | 0.6 |
| 232 Th (ng/g) | 2.21 | 2.03 | 2.14 | 2.23 | 2.29 | 2.24 | 2.14 | 2.08 | 2.2 | 4.0 | 0.08 |
| 238 U (ng/g) | 3.49 | 3.33 | 3.63 | 3.29 | 3.47 | 3.15 | 3.4 | 3.38 | 3 | 4.2 | 0.08 |

* Not tested

The MDL data summarized in Table 3 illustrates that the sensitivity of the method is sufficient to apply to actual TCM samples for most elements, with the exception of As and Se (MDL of 25 ng/g and 34 ng/g, respectively). In this case, in order to achieve the regulatory values specified by the World Health Organization (WHO) and the U.S. Food and Drug Administration (FDA) (Table 4), Collision Reaction Cell (CRC) technology was applied in the form of the Agilent 7500c with ORS. The 7500c was evaluated for its ability to remove the interference from ArCl on ⁷⁵As and ArAr on ⁷⁸Se.

Table 4. Regulations Governing Heavy Metals in TCM or Herb Supplements [1]

| Regulations (µg/g) | Pb | Cd | Hg | As |
|--|----|-----|-------|------|
| Recommended regulation on "TCM Quality Standard" | 5 | 0.5 | 0.2 | 0.2 |
| Green Trade Standards of Importing and Exporting Medicinal plants and Preparations | 5 | 0.3 | 0.2 | 2 |
| French regulations on imported herb supplements | 5 | 0.2 | 0.1 | 5 |
| US FDA regulations on medicines and functional food | 1 | 0.3 | 0.026 | 0.02 |
| South-East Asia regulations on imported herb supplements | 20 | N/A | 0.5 | 5 |

Interference Equations or ORS Reaction Gas

The Peach Leaf CRM was digested using the sealed pressure vessel procedure. The sample was analyzed in two modes: using the 7500c ORS in normal (no-gas) mode and in gas mode using hydrogen as a reaction gas. The results shown in Table 5 were acquired in no-gas mode and without the use of EPA 200.8 interference correction equations.

Table 5. Peach Leaf (CRM 08501) Results by ICP-MS - no ORS Cell Gas and No Interference Correction Equations

| Element (unit) | Reference value | Determined value |
|----------------|-----------------|------------------|
| 52 Cr (ng/g) | 940±140 | 949 |
| 59 Co (ng/g) | (250) | 229 |
| 63 Cu (µg/g) | 10.4±1.6 | 9.1 |
| 66 Zn (µg/g) | 22.8±2.5 | 20.7 |
| 75 As (ng/g) | 340±60 | 425 |
| 82 Se (ng/g) | (40) | 95.4 |
| 114 Cd (ng/g) | 18±8 | 14.7 |
| 137 Ba (µg/g) | 18.4±1.8 | 17.7 |
| 202 Hg (ng/g) | 46±12 | 58 |
| 208 Pb (ng/g) | 990±80 | 922 |

As expected from the previous results obtained using the 7500a and the 7500c in non-gas mode, results show good agreement with the reference values for all elements except As and Se. The higher recoveries for As and Se were possibly caused by the high Cl in the sample and Kr in the Ar gas.

In order to test the reliability of the EPA 200.8 interference correction equations to account for the interference on As and Se, these elements were determined using two tuning methods. In the first mode (#1), no gas was added to the ORS and the interference correction equations were applied. In the second mode (#2), 4.5-mL H₂ was added to the ORS and no correction equations were used. The results can be compared in Table 6.

Table 6. Comparing Two Approaches to Management of Interferences on As and Se in Peach Leaf CRM

| Element (unit) | Tune | Reference value | Determined value | Element (unit) | Tune | Reference value | Determined value |
|----------------|--------------------------|-----------------|------------------|----------------|------|-----------------|------------------|
| 75 As (ng/g) | #1 Standard non-gas mode | 340±60 | 386 | 78 Se (ng/g) | #1* | (40) | 73 |
| 75 As (ng/g) | #2 H ₂ mode | 340±60 | 350 | 82 Se (ng/g) | #2** | (40) | 44 |

*Interference equations applied but no ORS cell gas.

**4.5 mL H₂ added to ORS gas and no interference equations.

The data highlights the effectiveness of the H₂/ORS combination in removing the ArCl (75) and ArAr (78) interferences on As and Se. In contrast, relying only on the USEPA 200.8 interference correction equations provides less reliable results. The As measurement value was in the reference value range, but the RSD was high and Se can only be measured at mass 82. The elevated result at mass 82 is the result of interference from Kr.

Conclusions

The study demonstrates the suitability of ICP-MS for the determination of trace and major elements in various digested CRMs and its applicability to the analysis of TCM. However, for full coverage of all key elements in TCM, ORS-ICP-MS is necessary to remove molecular overlaps on As and Se. While applying interference correction equations summarized in USEPA 200.8 to “normal” ICP-MS results did not provide reliable results for As and Se; in the peach leaf CRM, operating the 7500c ORS in hydrogen gas mode provides a simple and accurate method for the determination of these elements. Although not emphasized in this application report, the 7500 ORS instruments can be used to provide reliable results for all elements in a single analysis, without the need for interference equations.

References

1. BinFeng XIA et al., (2004) *Modern Instruments*, **10 (1)**, 17–19.
2. Department of International Trade, PRC, Green Trade Standards of Importing & Exporting Medicinal Plants & Preparations, Industry Regulations of Department of International Trade, PRC, wm2-2001, 2001,4, 25.

For More Information

For more information on our products and services, visit our Web site at www.agilent.com/chem.

Agilent shall not be liable for errors contained herein or for incidental or consequential damages in connection with the furnishing, performance, or use of this material.

Information, descriptions, and specifications in this publication are subject to change without notice.

© Agilent Technologies, Inc. 2005

Printed in the USA
March 21, 2005
5989-2570EN

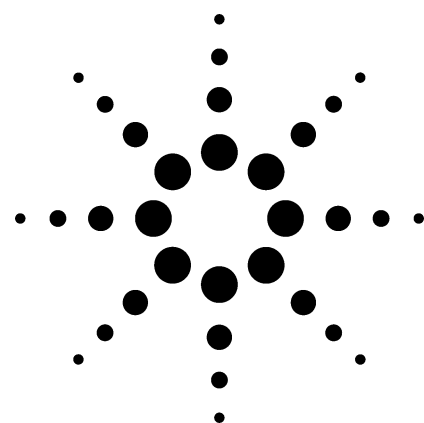


Agilent Technologies

Rapid and Reliable Routine Analysis of Urine by Octopole Reaction Cell ICP-MS

Application

Clinical



Authors

Peter Heitland
Medical Laboratory Bremen, Haferwende 12
D-28357 Bremen
Germany

Ed McCurdy
Agilent Technologies
Lakeside, Cheadle Royal Business Park
Stockport
United Kingdom

Abstract

The Agilent 7500c Inductively Coupled Plasma Mass Spectrometer (ICP-MS) was used for the fast, routine, and reliable analysis of 23 trace elements in urine. The complete method validation for all elements is described, including the evaluation of short-term and long-term stability, the analysis of different reference materials and the discussion of precision and accuracy in internal and external quality assurance. The urine samples were analyzed directly after a low dilution of 1/5 (v/v) with 1% (v/v) nitric acid. Using this simple sample preparation method, one operator can prepare more than 100 samples in less than 1 hour. An ICP-MS fitted with an octopole-based collision/reaction cell enables the simultaneous determination of all 23 elements either in the normal concentration range for the essential elements or at concentration levels relevant for occupational and environmental health.

Introduction

Assessment of the concentration of bioactive elements present in patients is typically achieved by analyzing easily extractable fluids (urine, blood, serum, and plasma). The concentrations of essential (for example, Se, Mo, Co, Cu, and Zn) and nonessential elements including toxic or carcinogenic substances (for example, Be, Pb, Pt, Cd, U) can provide valuable information regarding exposure and can suggest possible treatments for many complaints.

Many laboratories involved in trace metal analysis of these sample types are replacing single-element techniques such as Graphite Furnace Atomic Absorption Spectroscopy (GFAAS) with multi-element techniques, such as collision/reaction cell Inductively Coupled Plasma Mass Spectrometry (ICP-MS). While ICP-MS was previously used for the analysis of clinical samples, new octopole reaction cell technology has significantly improved the measurement of some clinically important analytes that suffer overlaps from matrix-based interferences.

Instrumentation

Method development and routine analysis was carried out using an Agilent 7500c ICP-MS, which features an Octopole Reaction System (ORS) collision/reaction cell. The cell is pressurized with a gas, such as helium or hydrogen, to remove the plasma and matrix-based interferences that inhibit the trace analysis of elements such as Cr, As, and Se by conventional ICP-MS. The design of the ORS



Agilent Technologies

enables the routine, high throughput, multi-element determination of trace level analytes in complex and varying matrices.

The 7500c was used with a Babington nebulizer and standard quartz Scott-type double-pass spray chamber. The instrument was optimized using a solution containing ^7Li , ^{59}Co , ^{89}Y , and ^{205}Tl (10 $\mu\text{g/L}$) for sensitivity (high signal/background ratio) across the mass range and low interference levels ($\text{CeO}^+/\text{Ce}^+ < 1\%$ and $\text{Ce}^{2+}/\text{Ce}^+ < 3\%$). The collision/reaction gases were optimized using the in-built software routines.

All instrumental conditions (see Table 1) are controlled from the 7500 system's ChemStation PC, including all gases (four plasma gases, plus helium and hydrogen reaction gases), torch position and sample introduction parameters such as sample flow rate and plasma power. A major benefit of fully automated and autotuneable system optimization is that "target-tuning" conditions can be selected, which are then achieved independently of operator expertise. This greatly simplifies the validation of the system performance, for both internal and external audit purposes, as well as ensuring consistent operation in laboratories where multiple users may operate the instrument on a routine basis.

Further details of the instrument have been described in previous publications [1, 2, 3].

Table 1. ICP-MS Operating Conditions

| | |
|-----------------------------------|------|
| Power/W | 1500 |
| Outer gas flow (L/min) | 14 |
| Intermediate gas flow (L/min) | 1.0 |
| Nebulizer gas flow (L/min) | 1.14 |
| Torch injector tube diameter (mm) | 2.5 |
| Hydrogen cell gas flow (mL/min) | 3.4 |
| Helium cell gas flow (mL/min) | 3.2 |
| Sample uptake rate (mL/min) | 0.4 |
| Integration time per mass (s) | 1.0 |
| Extract lens voltage (V) | 2 |
| Lens 1, 3 voltage (V) | -160 |
| Lens 2 voltage (V) | 40 |
| Cell entrance voltage (V) | -36 |
| Cell exit voltage (V) | -27 |
| Plate bias voltage (V) | -43 |

Sample Preparation and Calibration

Urine samples were collected in polyethylene containers over a period of 24 hours. Prior to collection the containers were cleaned with 5% (v/v) ultrapure HNO_3 . The samples were acidified with 100 μL of 65 % (v/v) HNO_3 per 20 mL and stored in a refrigerator at 5 $^\circ\text{C}$. The instrument was calibrated using the method of standard additions (MSA). The dilution factor was 1 mL of urine in 5 mL of total volume. In seven calibration solutions the concentrations of the elements Ba, Be, Co, Cd, Cr, In, Li, Mn, Mo, Pb, Pt, Rh, Sb, Sn, Tl, U, V, and W were 0, 0.01, 0.05, 0.1, 0.2, 0.5, and 2 $\mu\text{g/L}$, respectively. The concentrations for the elements As, Se, Li, Cu, and Zn were 0, 0.1, 0.5, 1, 2, 5, and 20 $\mu\text{g/L}$ respectively, and two higher concentration Zn standards were included at 100 and 200 $\mu\text{g/L}$. The concentration of the internal standard was 5 $\mu\text{g/L}$ Tb in all sample and calibration solutions. Tb was chosen because it is monoisotopic and shows no relevant interferences from oxide or doubly ionized species.

Following vigorous shaking of the actual urine samples, 1 mL of the sample was acidified with 100 μL of concentrated HNO_3 in a 10-mL autosampler polypropylene tube and 500 μL of the internal standard solution was added. This solution was made up to 5 mL with deionized water using a 5-mL bottle-top dispenser and the samples were homogenized using a magnetic stirrer. This is a simple and accurate procedure that enables the preparation of more than 100 samples in less than 1 hour by a single analyst.

Control samples were used for internal quality assurance purposes. One mL of the freshly prepared control material was made up with nitric acid, internal standard solution and deionized water in the same way as described for the actual samples.

Results and Discussion

It was found that the urine samples could be analyzed directly in a 1/5 (v/v) dilution with deionized water and nitric acid. No clogging of the nebulizer and no particle deposition in the injector tube was observed during 12 hours of analyses. It should be noted that the standard torch of the 7500c has an injector internal diameter of 2.5 mm, which is wider and therefore more matrix tolerant than the "high matrix" torches available as an option on other ICP-MS instruments.

LODs (limits of detection) were determined from $LOD=3 RSD_b c/SBR$ as proposed by Boumans [4], where RSD_b is the relative standard deviation of the background intensity of 10 measurements, c is the concentration of the element in solution, and SBR is the signal-to-background ratio.

The LODs in the undiluted urine are in the range 0.4 ng/L (for ^{238}U) to 143 ng/L (for ^{78}Se). See Table 2. The LODs of the essential trace elements Co, Cu, Zn, Se, and Mo are two orders of magnitude below the normal range of these elements in the urine of healthy humans. For many elements, the LODs are mainly limited by contamination. Therefore, careful control of impurities in all reagents is important.

Table 2. Analytical Figures of Merit: LODs and RSDs of Measured Intensities for the Evaluation of Repeatability, Short-Term Stability and Long-Term Stability

| Isotope | LOD (ng/L) | % RSD | | |
|------------|-----------------|-------------|--------------|---------------|
| | Undiluted urine | 2 min, n=10 | 20 min, n=20 | 5 hours, n=60 |
| 7Li | 6 | 0.8 | 2.7 | 4.5 |
| 9Be | 4 | 1.5 | 4.2 | 3.9 |
| ^{52}Cr | 16 | 1.7 | 3.1 | 4.6 |
| ^{51}V | 16 | 2.4 | 3.4 | 4.1 |
| ^{55}Mn | 21 | 3.0 | 3.1 | 3.6 |
| ^{59}Co | 5 | 1.8 | 2.6 | 4.9 |
| ^{60}Ni | 9 | 2.9 | 3.4 | 5.1 |
| ^{63}Cu | 121 | 0.9 | 3.1 | 4.4 |
| ^{66}Zn | 92 | 0.8 | 3.0 | 5.1 |
| ^{75}As | 73 | 2.1 | 2.8 | 5.6 |
| ^{78}Se | 143 | 2.4 | 3.7 | 6.2 |
| ^{98}Mo | 27 | 1.8 | 2.8 | 5.4 |
| ^{103}Rh | 0.6 | 1.2 | 3.3 | 4.8 |
| ^{111}Cd | 8 | 2.4 | 3.2 | 3.9 |
| ^{115}In | 4 | 0.5 | 3.0 | 3.7 |
| ^{118}Sn | 19 | 1.6 | 3.2 | 5.8 |
| ^{121}Sb | 6 | 1.1 | 2.6 | 5.3 |
| ^{138}Ba | 8 | 1.5 | 2.8 | 4.1 |
| ^{184}W | 7 | 0.9 | 2.2 | 4.6 |
| ^{195}Pt | 3 | 0.7 | 1.9 | 3.8 |
| ^{205}Tl | 3 | 0.6 | 2.1 | 2.3 |
| ^{208}Pb | 2 | 0.7 | 2.3 | 2.5 |
| ^{238}U | 0.4 | 1.2 | 2.2 | 3.2 |

Repeatability and short-term stability were investigated by measuring the RSDs of the mass intensities for all elements ($c=5 \mu\text{g/L}$) in two periods of 2 min (with 10 measurements) and 20 min (with 20 measurements), respectively. The RSDs are in the range 0.6%–3.0% for reproducibility and 1.9%–4.2% for short-term stability (Table 2), which are completely satisfactory figures of merit for urine analysis. Long-term stability was investigated by measurement of the intensities every 5 minutes over a period of 5 hours (60 measurements). RSDs are in the range 2.5%–6.2% with some excellent values, for example, for ^{208}Pb and ^{205}Tl (Table 2). All results for long-term stability investigations were obtained without internal standardization.

Interference Removal

In order to avoid the possible interferences described in Table 3, the elements As, Ba, Co, Cd, Cu, V, Cr, Mn, Mo, Rh, and Zn were determined using helium as a collision gas. Se was determined using hydrogen as a reaction gas. Hydrogen was found to be better in overcoming interferences from argon molecular ions $^{40}Ar^{40}Ar^+$ or $^{38}Ar^{40}Ar^+$. Hydrogen (3.4 mL/min) was added to achieve the best compromise for the lowest background equivalent concentration (BEC) and reduced background intensity for ^{80}Se and ^{78}Se . A benefit of the ORS system is its simple optimization. After initial optimization, cell gas flow rates do not need to be adjusted, and the same He flow rate was used for all analytes measured in this mode. The same cell voltages were used for all analytes. In addition, the ORS eliminates the need for interference correction equations, which improves accuracy in variable matrices such as urine.

Table 3. Some Common Spectral Interferences for Urine Analysis by ICP-MS

| Ion | Interfering ions |
|--------------|---|
| $^{51}V^+$ | $^{35}Cl^{16}O^+$ |
| $^{52}Cr^+$ | $^{40}Ar^{12}C^+$, $^{35}Cl^{16}OH^+$ |
| $^{53}Cr^+$ | $^{37}Cl^{16}O^+$ |
| $^{59}Co^+$ | $^{43}Ca^{16}O^+$ |
| $^{60}Ni^+$ | $^{44}Ca^{16}O^+$, $^{23}Na^{37}Cl^+$ |
| $^{63}Cu^+$ | $^{40}Ar^{23}Na^+$ |
| $^{66}Zn^+$ | $^{32}S^{16}O^{18}O^+$ |
| $^{75}As^+$ | $^{40}Ar^{35}Cl^+$, $^{40}Ca^{35}Cl^+$ |
| $^{78}Se^+$ | $^{38}Ar^{40}Ar^+$ |
| $^{80}Se^+$ | $^{40}Ar^{40}Ar^+$, $^{79}BrH^+$ |
| $^{82}Se^+$ | $^{32}S^{16}O_3^+$ |
| $^{95}Mo^+$ | $^{79}Br^{16}O^+$ |
| $^{98}Mo^+$ | $^{81}Br^{16}OH^+$ |
| $^{103}Rh^+$ | $^{40}Ar^{63}Cu^+$ |
| $^{111}Cd^+$ | $^{95}Mo^{16}O^+$ |

Quality Assurance

Several control materials from different suppliers and pooled urines were analyzed to investigate the precision and accuracy of our method for internal quality assurance purposes. The variation coefficients (VCs) for the analyses of two control samples for each element were measured. Intra-day VCs (one sample preparation, 10 measurements of the same sample) are in the range 2.2%–5.4%, whereas inter-day VCs (10 different sample preparations, 10 measurements at different days by different analysts) are in the range 6.0%–14.2%. All of these values are normally acceptable for essential trace element and toxic metal analysis of clinical samples.

The data in Tables 4, 5, 6 are the measured concentrations compared with the certified concentrations of the control materials. The measured concentrations are the average values of 10 acquisitions of the control sample by different analysts taken on different days. Plus/Minus values are calculated from the standard deviation of the 10 measurements. The limits of the target values were set by the supplier of each control material. The comparison of the target values with the measured values shows sufficient agreement for most of the elements, without significant outliers for samples with lower concentrations. We found some disagreement for a few elements, for example, the measured Sb concentration is low in Lyphocheck® level 1 and the Cr concentration is high in the same control sample. The As value for Clincheck® level 2 was found to be low. Because good recoveries for those elements were achieved in the other control materials, it is possible that the recommended values are not accurate, possibly as a result of contamination.

The analysis results for 63 urine samples of the general population are listed in Table 7. These results are very helpful to demonstrate the performance and applicability of the method. The concentrations in Table 7 are not creatinine-adjusted, but creatinine was measured in the range 0.6–1.7 g/L urine for all subjects with a geometric mean of 1.1 g/L which is typical for the general population. The geometric mean values of Pb, Co, Ba, and Tl are in good agreement with results published in the American Second National Report on Human Exposure to Environmental Chemicals published in 2003 [5]. Essential trace element concentrations of Cu, Zn, and Se are in the typical concentration ranges described for healthy humans in the European Community [6]. Our mean value for Mo of 45 µg/L is close to 43 µg/L determined for the Danish population [7]. The geometric mean value for Li (18 µg/L) is in good agreement with a study in Japan [8]. Table 7 provides additional information about the elemental concentration range in urine for other elements including Be, Cr, Ni, and Cd.

Table 4. Comparison of Measured and Certified Concentrations in the Urine Reference Material Lyphocheck®

| Element | Concentration (µg/L) | | | |
|---------|----------------------|-----------|---------------------|-----------|
| | Lyphocheck, level 1 | | Lyphocheck, level 2 | |
| | Measured | Certified | Measured | Certified |
| Cr | 1.7±0.2 | 1.2±0.2 | 18.6±2.6 | 20.2±4.1 |
| Co | 6.6±0.7 | 6.9±1.4 | 18.9±1.4 | 19.1±4.2 |
| Cu | 24±2.1 | 26.7±5.4 | 45±5.5 | 50±10 |
| Se | 56±5.3 | 49±10 | 192±17 | 187±37 |
| As | 65±6 | 67±14 | 162±15 | 163±33 |
| Cd | 8.4±1.1 | 8.6±1.7 | 14.9±1.9 | 15.6±3.1 |
| Sb | 6.9±1.1 | 9±1.8 | 34.8±4.4 | 36.9±7 |
| Tl | 9.6±0.8 | 9.7±2.0 | 185±17 | 198±40 |
| Pb | 13.5±1.1 | 14.3±2.9 | 68±5 | 69±14 |

Table 5. Comparison of Measured and Certified Concentrations in the Urine Control Materials Clinchek® and Medisafe™

| Element | Concentration (µg/L) | | | | | | | |
|---------|----------------------|-----------|-------------------|-----------|-------------------|-----------|-------------------|-----------|
| | Clinchek, level 1 | | Clinchek, level 2 | | Medisafe, level 1 | | Medisafe, level 2 | |
| | Measured | Certified | Measured | Certified | Measured | Certified | Measured | Certified |
| Be | 0.02±0.01 | 0.03±0.01 | 0.12±0.02 | 0.13±0.04 | | | | |
| V | 17.2±1.5 | 17±5 | 41±3.6 | 45±9 | | | | |
| Cr | 9.3±0.9 | 10±1.8 | 31±2.9 | 33±5 | 10±1.1 | 10±3 | 1.8±0.3 | 2±0.6 |
| Mn | 5.8±0.6 | 5.6±1.4 | 16±1.7 | 17±4 | | | | |
| Ni | 10.2±1 | 9.8±2 | 45.7±3.2 | 44±8 | | | | |
| Co | 5.0±0.3 | 5.4±1.1 | 33±2.1 | 33±6 | | | | |
| Cu | 56±5 | 62±10 | 121±9 | 120±20 | | | | |
| Zn | 225±31 | 250±40 | 567±65 | 620±75 | | | | |
| Se | | | | | 23±3 | 20±6 | 205±28 | 200±50 |
| As | 30±3.3 | 31±8 | 61±7 | 72±16 | 57±7 | 50±11 | 248±30 | 250±60 |
| Cd | 8.3±1.2 | 8.4±1.4 | 15.1±1.2 | 15±3 | 11.6±1.4 | 13±3 | 7.2±0.9 | 8±1.8 |
| Sn | | | | | 4.5±0.6 | 5±1.2 | 45±6 | 50±12 |
| Ba | | | | | 5.4±0.6 | 5±1.7 | 56±7 | 50±18 |
| Pb | 29±2.5 | 28±6 | 72±9 | 64±11 | 133±11 | 130±32 | 85±7 | 80±18 |
| Tl | 3.1±0.3 | 3.2±0.9 | 15.9±1.3 | 17±5 | | | | |

Table 6. Comparison of Measured and Certified Concentrations in Pooled Urine Control Samples

| Element | Concentration (µg/L) | | | |
|---------|----------------------|-----------|---------------------|-----------|
| | Urine pool, level 1 | | Urine pool, level 2 | |
| | Measured | Certified | Measured | Certified |
| Li | 5.4±0.7 | 5±0.8 | 11±0.9 | 10±1.2 |
| Be | 0.5±0.07 | 0.5±0.08 | 0.9±0.1 | 1±0.1 |
| In | 0.5±0.1 | 0.5±0.07 | 1.1±0.13 | 1±0.07 |
| Mo | 1.1±0.13 | 1±0.13 | 5.3±0.4 | 5±0.26 |
| Rh | 0.5±0.11 | 0.5±0.1 | 0.9±0.08 | 1±0.08 |
| W | 0.6±0.1 | 0.5±0.12 | 0.9±0.14 | 1±0.1 |
| Pt | 0.4±0.11 | 0.5±0.1 | 0.9±0.1 | 1±0.08 |
| U | 0.5±0.1 | 0.5±0.07 | 1.1±0.06 | 1±0.05 |

Table 7. Analytical Results for 63 Human Subjects

| Element | Range (µg/L) | *Geometric mean (µg/L) | 95 % Percentile (µg/L) |
|---------|-----------------|---------------------------|---------------------------|
| Li | 3–86 | 14 | 47 |
| Be | LOQ–0.028 | 0.007 | 0.02 |
| V | LOQ–0.19 | 0.037 | 0.13 |
| Cr | LOQ–0.47 | 0.11 | 0.44 |
| Mn | LOQ–0.52 | 0.049 | 0.14 |
| Co | 0.03–2.1 | 0.11 | 0.98 |
| Ni | LOQ–3.5 | 0.37 | 1.5 |
| Cu | 1.3–10.8 | 4.7 | 8.3 |
| Zn | 19–665 | 139 | 305 |
| As | 0.5–197 | 14 | 149 |
| Se | 1–140 | 15 | 90 |
| Mo | 10–174 | 38 | 91 |
| Rh | LOQ–0.004 | 0.002 | 0.003 |
| Cd | LOQ–0.35 | 0.075 | 0.43 |
| In | LOQ–0.8 | 0.039 | 0.43 |
| Sn | 0.06–12.6 | 0.8 | 5.5 |
| Sb | LOQ–1.3 | 0.037 | 0.18 |
| Ba | 0.4–5.1 | 1.3 | 3.3 |
| W | LOQ–0.19 | 0.012 | 0.08 |
| Pt | LOQ–0.026 | 0.005 | 0.008 |
| Tl | 0.005–0.11 | 0.1 | 0.19 |
| Pb | 0.1–0.24 | 0.52 | 0.76 |
| U | LOQ–0.024 | 0.0014 | 0.01 |

* Concentrations below the LOQ were calculated as LOQ/2

Conclusions

Methodology based on the Agilent 7500c ORS ICP-MS was used successfully for the routine analysis of urine. The system is especially applicable to laboratories with high sample throughput requirements for multi-element determinations and elemental screening. Because spectral interferences are removed with the ORS and LODs are completely satisfactory, the instrumental long-term stability becomes one of the most important criteria for reliable routine analysis. Long-term stability is determined by the robustness of the ICP-MS and its tolerance to continuous exposure to high matrix samples. A combination of system design (low flow nebulizer, exceptionally wide diameter torch injector and high plasma temperature) and optimization (tuning for minimal matrix oxides) provides the 7500c with the required matrix tolerance. In combination with a fast and simple sample preparation method, this is the key to fast and accurate analysis of urine samples in a routine clinical laboratory.

References

1. E. McCurdy and G. Woods, (2004) *J. Anal. At. Spectrom.*, **19**, 607-615.
2. P. Leonhard, R. Pepelnik, A. Prange, N. Yamada and T. Yamada, (2002) *J. Anal. At. Spectrom.*, **17**, 189-196.
3. R. R. de la Flor St. Remy, M. L. Fernández Sánchez, J. B. López Sastre and A. Sanz-Medel, (2004) *J. Anal. At. Spectrom.*, **19**, 616-622.
4. P. W. J. M. Boumans, (1991) *Spectrochim. Acta*, **46B**, 641-665.
5. Second National Report on Human Exposure to Environmental Chemicals, National Center for Environmental Health Division of Laboratory Sciences, Atlanta, Georgia, 2003.
6. C. Minoia, E. Sabbioni, P. Apostoli, R. Pietra, L. Pozzoli, M. Gallorini, et al (1990) *Sci. Total Environ.*, **95**, 89-105.
7. B. S. Iversen, C. Menne, M. A. White, J. Kristiansen, J. Molin Christensen and E. Sabbioni, (1998) *Analyst*, **123**, 81-85.
8. K. Iguchi, K. Usuda, K. Kono, T. Dote, H. Nishura, M. Shimahara, et al (1999) *J. Anal. Tox.*, **23**, 17-23.

For More Information

For more information on our products and services, visit our Web site at www.agilent.com/chem.

Author e-mail: Peter.Heitland@mlhb.de

Acknowledgements

Lymphocheck® is a registered trademark of Bio-Rad Laboratories.

Clinchek® is a registered trademark of IRIS Technologies.

Medisafe™ is a trademark of FUTUREMED Health Products, Inc.

Agilent shall not be liable for errors contained herein or for incidental or consequential damages in connection with the furnishing, performance, or use of this material.

Information, descriptions, and specifications in this publication are subject to change without notice.

© Agilent Technologies, Inc. 2005

Printed in the USA

March 21, 2005

5989-2482EN



Ion Chromatography (IC) ICP-MS for Chromium Speciation in Natural Samples

Application

Environmental

Authors

Tetsushi Sakai
Agilent Technologies
Musashino Center Building
1-19-18 Naka-cho Musashino-shi
Tokyo 180-0006
Japan

Ed McCurdy
Agilent Technologies
Lakeside, Cheadle Royal Business Park
Stockport
United Kingdom

Steve Wilbur
Agilent Technologies, Inc.
3380 146th PI SE Suite 300
Bellevue, WA 98007
USA

Abstract

Trace measurements of the element chromium (Cr) are of interest in a wide range of applications and matrices. In the environment, Cr exists in two different oxidation states, the trivalent Cr(III) cation and hexavalent Cr(VI) anion. In mammals, Cr(III) is an essential element involved in the regulation of glucose; however, the element in its hexavalent form demonstrates mutagenic and carcinogenic effects at relatively low levels. Because of this duality, total Cr measurements do not provide sufficient information to establish potential toxicity. In order to assess the potential toxicity of the Cr level in a sample, it is the Cr(VI) concentration that must be measured, rather than the total Cr concentration. A new method was developed to couple Ion Chromatography to Octopole Reaction Cell ICP-MS (inductively coupled plasma mass

spectrometry), to give a simple and reliable method for the separation and measurement of Cr(III) and Cr(VI), and so provide an accurate indication of the toxicity of the Cr level in a sample. This method has the merit of being applicable to high matrix samples, such as hard drinking water, due to the optimization of the sample preparation method and the chromatography. Also, the ICP-MS method provides excellent signal to noise, as a result of the removal of potentially interfering background species in the reaction cell, allowing the accurate determination of toxicologically useful levels of Cr(VI), at concentrations below 0.1 µg/L.

Introduction

The measurement of chromium toxicity is a requirement across a wide range of sample types, including drinking water, foodstuffs, and clinical samples (the latter used primarily to assess occupational exposure). However, it is the hexavalent form of Cr - Cr(VI) that is the toxic form, while the trivalent form - Cr(III) is an essential element for human nutrition. Methods to establish the potential toxicity of Cr must therefore determine the concentration of Cr(VI), rather than simply total Cr.

Two common approaches are used to address the issue: First, if the total Cr level measured is below the toxic level for Cr(VI), then it is reasonable to state that the Cr level will not be toxic, even if all of the Cr is present as Cr(VI). However, this approach can lead to a large number of false positives if samples contain a high concentration of Cr(III), so a more accurate approach is to separate and measure the Cr(VI) itself or, ideally, separate and measure both forms of Cr, giving an indication of the level of total Cr AND the level of toxic



Agilent Technologies

Cr(VI), from a single analysis.

Separating and detecting individual forms or species of elements is usually a straightforward analytical challenge, but Cr is an unusual case in this respect. This is because the common forms of Cr in natural samples such as water are chromate (CrO_4^{2-}) for Cr(VI) and chromic ion (Cr^{3+}) for Cr(III). Chromate is an anion and the chromic ion is cationic, so a single ion exchange method will not work for both forms under the same conditions. A further problem is that Cr(III) is the most stable oxidation state in samples such as water, whereas Cr(VI) ions are strong oxidizing agents and are readily reduced to Cr(III) in the presence of acid or organic matter. Consequently great care must be taken during sample collection, storage and preparation, to ensure that the Cr species distribution present in the original sample is maintained up to the point of analysis.

Experimental

The method described in this application note used an optimized sample stabilization method, in which the samples were incubated at 40 °C with EDTA, which forms a complex with the Cr(III), allowing a single chromatographic method to be used to separate the Cr(III)EDTA complex and the Cr(VI). The reaction to form the Cr(III)EDTA complex is dependent on the incubation time and temperature, with complete conversion occurring after less than 1 hour at 60 °C or 3 hours at 40 °C. Complete conversion did not occur even after 7 hours incubation

at room temperature.

Note that a relatively high concentration of EDTA is required for this method to be applicable to natural water samples, since other ions, such as Ca and Mg, which are commonly present at 10's or 100's mg/L in hard drinking water for example, would compete with the Cr(III) to form EDTA complexes, leading to low and matrix dependent Cr(III) recovery.

The combination of the separation of the Cr species using ion chromatography (IC), together with analysis of the separated species using ICP-MS, offers an ideal analytical method, as it permits the individual Cr species to be separated using a simple, low cost IC configuration. ICP-MS detection also allows the separated Cr species to be measured at extremely low concentrations, providing accurate assessment of exposure levels, even for natural or background Cr concentrations.

ICP-MS has excellent sensitivity and so is a good detector for many trace elements. The introduction of collision/reaction cells (CRC's) for ICP-MS allows Cr to be measured even more accurately and with better sensitivity, using the main isotope at mass 52, with removal of the primary matrix-based interferences ArC and ClOH. The sample preparation method, column type and chromatographic conditions used for Cr speciation are shown in Table 1. Note that, in addition to the stabilization of the samples with Na EDTA, EDTA was also added to the mobile phase, to stabilize the Cr(III) complex during separation. In addition, it was found that the use of pH 7 was essential for species stabilization and

Table 1. Chromatographic Conditions for Cr Speciation

| | |
|---------------------------|---|
| Cr column | Agilent part number G3268A, 30 mm × 4.6-mm id |
| Mobile phase | 5 mM EDTA (2Na), pH 7 adjust by NaOH |
| Flow rate | 1.2 mL/min |
| Column temperature | Ambient |
| Injection volume | 50–500 µL |
| Sample preparation | |
| Reaction temperature | 40 °C |
| Incubation time | 3 h |
| EDTA concentration | 5–15 mM pH 7 adjust by NaOH |

optimum chromatographic separation.

The IC configuration used for the work presented in this note is illustrated in Figure 1. Note that the nonmetal IC pump (Metrohm 818 IC Pump was used to deliver the mobile phase, but the sample loop was filled and switched using the optional Integrated Sample Introduction System (ISIS) of the Agilent 7500ce ICP-MS. While this configuration maintains the high precision and relatively high pressure of the IC pump, it provides a much simpler and lower-cost alternative to a complete IC or HPLC system,

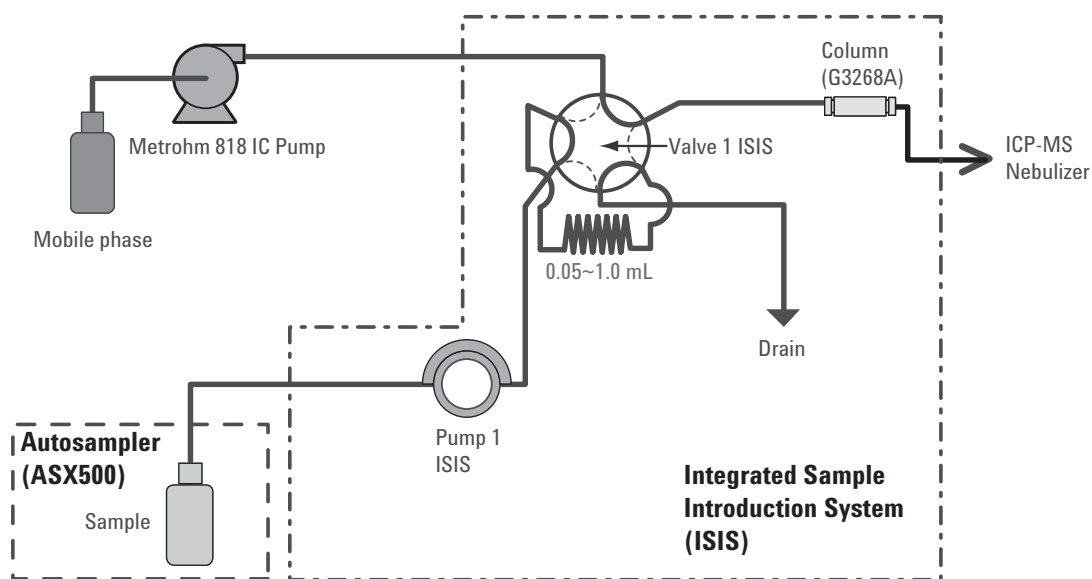


Figure 1. IC-ICP-MS configuration used for Cr speciation.

since only the IC pump module is required in addition to the ICP-MS system.

Results and Discussion

Under the conditions described above, with ICP-MS detection using the Agilent 7500ce in H₂ cell gas mode to remove the ArC and ClOH interferences on Cr at mass 52, detection limits (DLs) of <20 ng/L were obtained for the individual Cr species, as shown in Table 2. Many international regulations for hexavalent Cr specify a maximum allowable concentration of 1 µg/L, with a required DL of one-tenth of this level (100 ng/L), and even the small sample volume injection of 100 µL easily meets these

Table 2. DLs for Cr Species by IC-ICP-MS

| Inject/ μ L | RT/min | | Peak height/counts | | Peak area/counts | | DL (ng/L)* | |
|-----------------|---------|--------|--------------------|--------|------------------|---------|------------|--------|
| | Cr(III) | Cr(VI) | Cr(III) | Cr(VI) | Cr(III) | Cr(VI) | Cr(III) | Cr(VI) |
| 50 | 0.79 | 2.09 | 8548 | 4261 | 1082295 | 914804 | 69.5 | 139.4 |
| 100 | 0.79 | 2.09 | 13688 | 7173 | 1704312 | 1525147 | 43.4 | 82.8 |
| 250 | 0.85 | 2.21 | 33967 | 20830 | 4939876 | 4546219 | 17.5 | 28.5 |
| 500 | 0.97 | 2.39 | 44870 | 37502 | 10268086 | 9398651 | 13.2 | 15.8 |

*Detection limits calculated as three times the peak-to-peak signal-to-noise as measured on standard chromatograms.

requirements. However, increasing the injection volume to 500 μ L allowed the DLs to be reduced to 13.2 ng/L for Cr(III) and 15.8 ng/L for Cr(VI).

For a simple standard solution, these conditions give an excellent signal to noise for both Cr species, as illustrated in Figure 2. This chromatogram shows the separation of the two Cr species each at a concentration of 0.1 μ g/L (ppb), using an injection

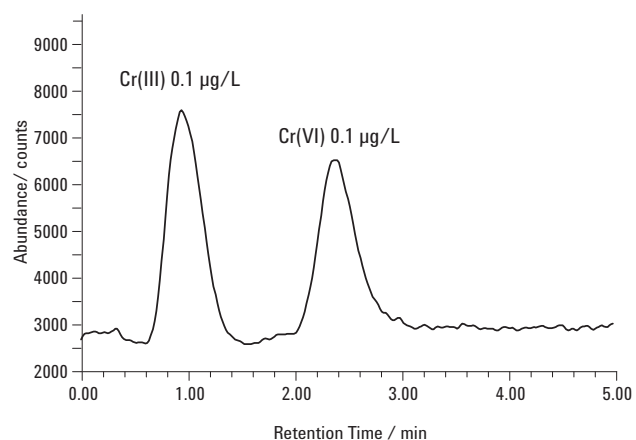


Figure 2. Separation and detection of Cr(III) and Cr(VI) at a concentration of 0.1 μ g/L each species.

volume of 500 μ L. Clearly the peaks are easily detected above the background and the baseline separation of the two species in a total time of about 3 minutes is also illustrated.

Using a series of synthetic standard solutions at low concentrations, a calibration was created for each of the two Cr species. Quantification was based on

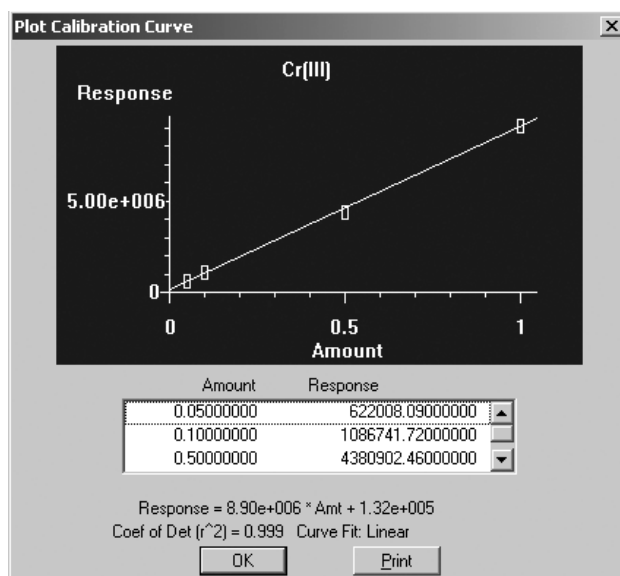


Figure 3. Calibration for Cr(III) - Standard concentrations 0.05, 0.1, 0.5 and 1.0 μ g/L.

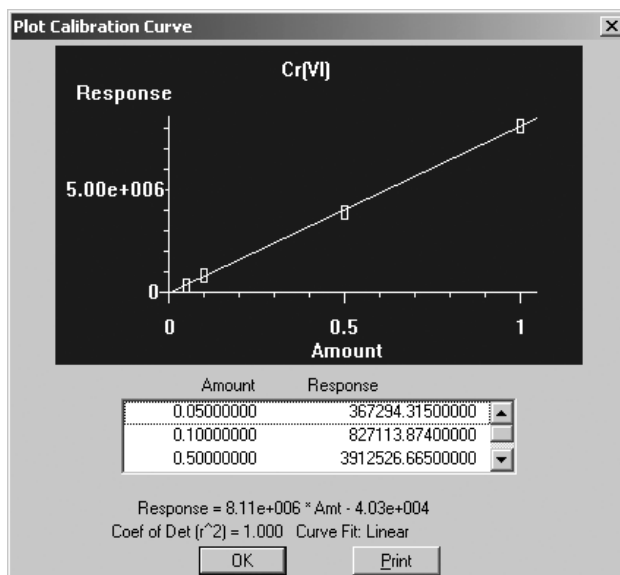


Figure 4. Calibration for Cr(VI) - Standard concentrations 0.05, 0.1, 0.5 and 1.0 μ g/L.

peak area. The calibrations obtained for Cr(III) and Cr(VI) are illustrated in Figures 3 and 4, respectively, each showing excellent sensitivity and linearity.

In addition to sensitivity, species stability, chromatographic separation and calibration linearity, for the method to be suitable for routine analysis, it is essential that it provides acceptable long-term stability. In chromatographic analysis, stability is governed by two factors, RT stability and peak area stability. The data in Table 3 illustrates both of these parameters and indicates that the stability of the method is certainly acceptable for routine operation.

Routine Analysis

Of more interest for the routine analysis of chromium species (or specifically hexavalent Cr) in natural water samples is the maintenance of this excellent sensitivity, stability and chromatographic separation in samples that contain a high concentration of other ions. In order to test the suitability of the method for these real-world sample types, the method was applied to the determination of both Cr species in both spiked and unspiked mineral water samples.

The first sample evaluated was a leading French mineral water referred to in this study as mineral water A. Figure 5 shows the chromatogram of the two Cr species in the unspiked and spiked samples of mineral water A. The major element composition of the water is also shown in the table inset in Figure 5, indicating the typical drinking water com-

Table 3. Stability of RT and Peak Area for Multiple 500 μ L Injections of 0.5 μ g/L Each Cr Species

| Number | RT/min | | Peak height/counts | | Peak area/counts | |
|--------|--------------|-------------|--------------------|-------------|------------------|-------------|
| | Cr(III)-EDTA | Cr(VI) | Cr(III)-EDTA | Cr(VI) | Cr(III)-EDTA | Cr(VI) |
| 1 | 0.969 | 2.338 | 23514 | 18437 | 5331427 | 4621752 |
| 2 | 0.969 | 2.338 | 22642 | 18784 | 5280683 | 4758462 |
| 3 | 0.969 | 2.338 | 22832 | 18615 | 5220349 | 4742259 |
| 4 | 0.952 | 2.338 | 24104 | 19944 | 5470760 | 4800723 |
| 5 | 0.969 | 2.372 | 22797 | 19203 | 5287094 | 4726640 |
| 6 | 0.969 | 2.405 | 23830 | 19328 | 5498172 | 4760285 |
| 7 | 0.985 | 2.338 | 23971 | 19479 | 5481984 | 4824934 |
| 8 | 0.969 | 2.338 | 23393 | 19675 | 5474510 | 4883193 |
| 9 | 0.969 | 2.355 | 23070 | 20097 | 5355106 | 4892160 |
| 10 | 0.969 | 2.372 | 23826 | 19896 | 5428247 | 4886400 |
| Avg | 0.97 | 2.38 | 23398 | 19346 | 5382833 | 4789681 |
| STD | 0.008 | 0.014 | 534.45 | 581.88 | 100413.18 | 85782.42 |
| RSD% | 0.80 | 0.57 | 2.28 | 3.01 | 1.87 | 1.79 |

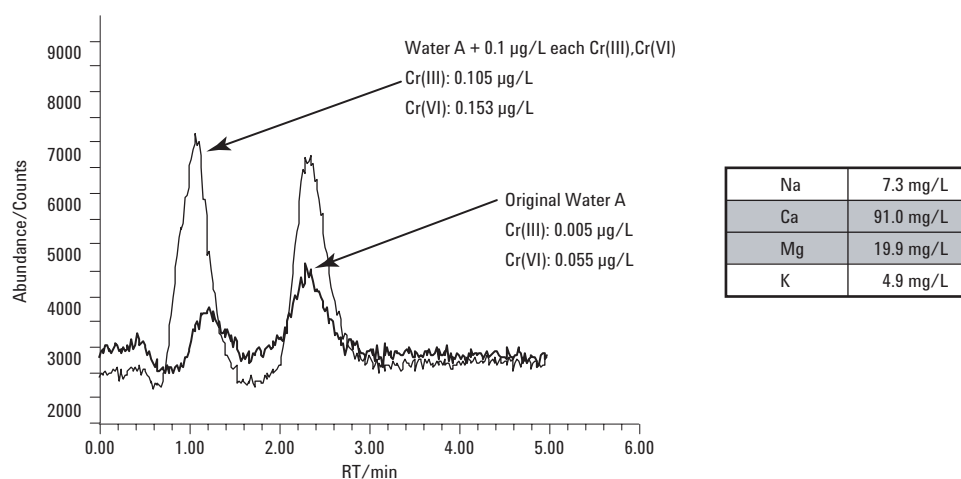


Figure 5. Major element composition (mg/L) and chromatogram for spiked and unspiked mineral water A.

position of about 100 mg/L Ca and between 5 mg/L and 20 mg/L of the other major elements K, Mg and Na.

The spike recovery data for mineral water A is shown in Table 4, indicating the very low level at which the Cr species were quantified (0.005 µg/L

Table 4. Spike Recovery Data for 0.1 µg/L Spikes of Cr(III) and Cr(VI) in Mineral Water A

| Element | Original mineral water A | Found (µg/L) | | Recovery (%) |
|---------|--------------------------|--------------|-------------|--------------|
| | | Spike added | Spike found | |
| Cr(III) | 0.005 | 0.10 | 0.105 | 100.0 |
| Cr(VI) | 0.055 | 0.10 | 0.150 | 95.0 |

and 0.055 µg/L for Cr(III) and Cr(VI), respectively), and the excellent spike recovery accuracy for the low concentration spikes in this sample - better than 5% error in both cases.

The second mineral water sample analyzed was another French mineral water, referred to as mineral water B, which has among the highest levels of calcium and sulfates of any commonly available mineral water (over 450 mg/L Ca and more than 1000 mg/L sulfates). As for the mineral water A sample, mineral water B was analyzed with and

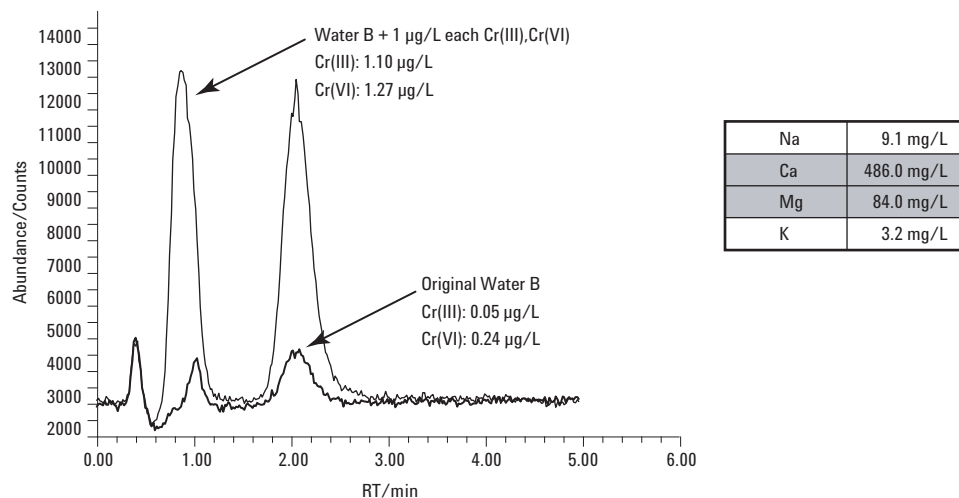


Figure 6. Major element composition (mg/L) and chromatogram for spiked and unspiked mineral water B.

without a spike of the two Cr species and the spike recovery was assessed. The results for the measured chromatograms are shown in Figure 6, while the spike recovery data are shown in Table 5.

As shown for the mineral sample A, the major element composition of the mineral water is shown as an inset in the chromatogram, illustrating the very high mineral levels in mineral water B. Despite these high major element levels, the optimized sample preparation and chromatographic method gave good chromatographic separation and excellent spike recovery results for both Cr species. A higher spike level was used for mineral water B, due to the higher baseline (unspiked) concentration for the Cr species in this sample.

The ability to recover low concentration spikes for both Cr species in such a high matrix sample indicates the effectiveness of the optimized method for sample stabilization, which ensures that a high enough concentration of EDTA is available for complete complexation of the Cr(III) species, even in the presence of a high level of competing ions.

Furthermore the accurate recovery of low concentration spikes of both species indicates that potential problems of species interconversion (reduction of Cr(VI) to Cr(III)) was avoided through the selection of an appropriate pH for the samples and the

mobile phase, together with the use of EDTA in the mobile phase as well as for sample stabilization. See Table 5.

Conclusions

A new method for the stabilization and analysis of Cr(III) and Cr(IV) in natural, high matrix water samples was developed and optimized with DLs in the region of 0.05 µg/L for 100-µL injections, or 0.015 µg/L for larger, 500-µL injections.

Reliable and stable separation of the Cr(III) and Cr(VI) species was achieved in a method taking approximately 3 minutes per sample and the separation and accurate quantification of the two species could be maintained even in the presence of a high concentration of competing ions, such as >500 mg/L mineral elements in the highly mineralized water.

Accurate and interference-free determination of Cr at the low concentrations (0.1 µg/L) required by international regulations was made possible by the simple and consistent operation of the Agilent 7500ce in reaction mode, using H₂ as a cell gas. This mode of operation does not preclude the simultaneous analysis of other analytes of interest, such as As, in contrast to the use of highly reactive cell gases such as CH₄ or NH₃.

Table 5. Spike Recovery Data for 1.0 µg/L Spikes of Cr(III) and Cr(VI) in a Highly Mineralized Water (B)

| Element | Original mineral water B | Found (µg/L) | | |
|---------|--------------------------|--------------|-------------|--------------|
| | | Spike added | Spike found | Recovery (%) |
| Cr(III) | 0.05 | 1.0 | 1.10 | 105 |
| Cr(VI) | 0.24 | 1.0 | 1.27 | 102 |

For More Information

For more information on our products and services, visit our Web site at www.agilent.com/chem.

Agilent shall not be liable for errors contained herein or for incidental or consequential damages in connection with the furnishing, performance, or use of this material.

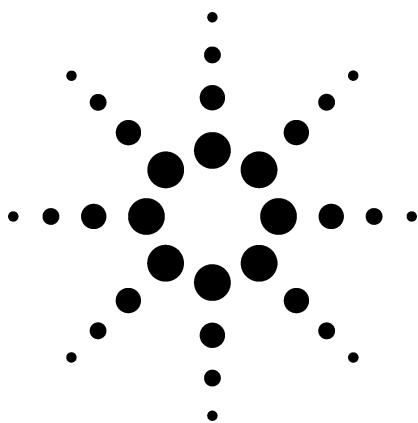
Information, descriptions, and specifications in this publication are subject to change without notice.

© Agilent Technologies, Inc. 2005

Printed in the USA
April 27, 2005
5989-2481EN



Agilent Technologies



A Comparison of the Relative Cost and Productivity of Traditional Metals Analysis Techniques Versus ICP-MS in High Throughput Commercial Laboratories

Application

Author

Steve Wilbur
Agilent Technologies, Inc.
3380 146th Pl SE Suite 300
Bellevue, WA 98007 USA

Abstract

A financial model was developed to help the metals laboratory using graphite furnace atomic absorption and inductively coupled plasma optical emission spectroscopy calculate the potential savings by switching to inductively coupled plasma mass spectrometry. Results based on several typical laboratory examples are presented.

Introduction

The past 5 years have seen significant growth in the use of inductively coupled plasma mass spectrometry (ICP-MS) for the analysis of trace metals in many applications in the environmental, semiconductor, geological, and health sciences industries. This growth is driven by three factors. First is the need for increasingly lower limits of detection for many metals in many applications. Second is the significantly improved performance, reliability, and ease of use of modern ICP-MS instruments. And third is economics.

Traditionally, most elemental analysis has been performed by either atomic absorption (AA) or optical emission spectroscopy (OES). Generally, the ultratrace (sub-ppb) elements were measured by graphite furnace atomic absorption (GFAA), a highly sensitive single-element technique. The trace and minor (ppb to ppm) elements were measured

by inductively coupled plasma optical emission spectroscopy (ICP-OES), which is less sensitive but capable of simultaneous multi-element analysis.

As the need for sub-ppb detection limits extends to more elements in more samples, ICP-OES becomes less useful and the reliance on GFAA increases. However, GFAA, while sensitive, is slow, expensive to operate, and has limited dynamic range. Because GFAA is much slower than ICP-OES, many routine labs have a dedicated GFAA instrument for each analyte that is required to be measured by GFAA - multiple GFAAs working with one ICP-OES. Furthermore, the analysis of mercury will add the need for a third technique, either cold vapor AA or atomic fluorescence. However, in the interest of simplicity, a separate mercury analyzer was not considered in the examples used. Each of these techniques may require separate sample handling and preparation, as well as separate analysis, data processing and archival, significantly increasing the cost per sample.

The subject of this application note is to evaluate the productivity and cost effectiveness of ICP-MS as a routine, highly sensitive, multi-element technique where a single ICP-MS instrument has the potential to replace an ICP-OES, multiple GFAAs, and a mercury analyzer for most routine elemental analyses. The analytical applicability of ICP-MS to many types of samples is already well established. More recently, the introduction of the Octopole Reaction System on the 7500 Series ICP-MS instruments from Agilent has removed the final performance barriers that have prevented ICP-MS being proposed as a complete replacement for GFAA and ICP-OES.



Agilent Technologies

Methods

To facilitate this study, a spreadsheet-based sample cost comparison model was developed in Excel. This tool allows the user to provide detailed parameters related to numbers and types of samples, as well as associated costs of sample preparation, instrumentation, and analysis. Output is simply cost of analysis per sample. Also reported are the total time required for sample analysis per month, the number of analysts required, and the number of instruments. The model compares the results for GFAA, ICP-OES, and ICP-MS. While it will allow almost any values to be entered for most parameters, the results presented here are based on values obtained from several commercial laboratories doing these analyses. No model can exactly predict the results for all situations and still be simple enough to be useful. Therefore, in the interest of simplicity, a number of assumptions were made in the design of the model and in the example data entered. We feel that the assumptions are realistic and do not impart significant bias on the results. The tool is easy to use and can allow a laboratory to quickly and simply evaluate the cost effectiveness of the three techniques based on laboratory-specific information.

Assumptions

- GFAA system costs US\$30K
- ICP-OES system costs US\$100K
- ICP-MS system costs US\$180K
- Cost of funds (finance) is 6%
- General facilities costs, such as laboratory space, utilities etc., are ignored since they are difficult to estimate and do not significantly affect the results in most cases.

- An instrument operator can keep a modern, automated GFAA, ICP-OES, or ICP-MS running for two shifts (16 hours) per day. When analysis times exceed 16 hours per day for any technique, additional instrumentation and operators will be required. Instruments are added in increments of one; operators are added in fractions since it is assumed that they can be shared with other tasks in the laboratory and cost calculations are based only on the portion of time the operator spends on the specific analysis.
- GFAA is a single element technique. Instruments with multiple lamps still perform a single analysis at a time. Typical analysis time is 90 seconds per element and each element requires two replicate analyses (burns).
- ICP-OES and ICP-MS are multi-element techniques and the number of elements does not significantly effect the analysis time. This is not strictly true, but the assumption is reasonable for the sake of simplicity.
- GFAA will use pressurized argon and the consumption is 40 hours of use per cylinder (\$100).
- GFAA graphite tubes and platforms cost \$50 per set and last for 100 burns.
- ICP-MS and ICP-OES will use liquid argon and the typical consumption is 3 weeks of use per dewar (\$250).
- ICP-MS detectors last typically for 3 years and the cost per year is amortized based on 3-year lifetime.

Results

Several typical laboratory scenarios were evaluated by varying the current instrument complement of the laboratory, and by varying the current and anticipated number of samples to be analyzed per month. Also examined was the effect of the number of elements that must be analyzed by GFAA (in the case of laboratories without ICP-MS) to meet required DLs.

Scenario 1

Laboratory currently has one GFAA plus one ICP-OES, which are paid for. ICP-MS must be purchased and amortized over 3 years. See Table 1.

Table 1. Scenario 1

| Samples/ month | GFAA elements | # GFAA required | Cost/sample GFAA + ICP-OES | # ICP-MS required | Cost/ sample ICP-MS | Savings/ month |
|---------------------------|--------------------------|----------------------------|---|------------------------------|------------------------------------|---------------------------|
| 400 | 8 | 1 | \$41 | 1 | \$30 | \$4,536 |
| 1000 | 8 | 2 | \$33 | 1 | \$15 | \$18,196 |
| 5000 | 8 | 9 | \$31 | 2 | \$9 | \$112,968 |

Scenario 2

Laboratory currently has two GFAA plus one ICP-OES, which are paid for. ICP-MS must be purchased and amortized over 3 years. See Table 2.

Table 2. Scenario 2

| Samples/ month | GFAA elements | # GFAA required | Cost/sample GFAA + ICP-OES | # ICP-MS required | Cost/ sample ICP-MS | Savings/ month |
|---------------------------|--------------------------|----------------------------|---|------------------------------|------------------------------------|---------------------------|
| 400 | 8 | 1 | \$41 | 1 | \$30 | \$4,536 |
| 1000 | 8 | 2 | \$32 | 1 | \$15 | \$17,283 |
| 5000 | 8 | 9 | \$31 | 2 | \$9 | \$112,055 |

Scenario 3

Laboratory currently has no instrumentation and must decide on purchasing GFAA plus ICP-OES versus ICP-MS. See Table 3.

Table 3. Scenario 3

| Samples/ month | GFAA elements | # GFAA required | Cost/sample GFAA + ICP-OES | # ICP-MS required | Cost/ sample ICP-MS | Savings/ month |
|---------------------------|--------------------------|----------------------------|---|------------------------------|------------------------------------|---------------------------|
| 400 | 8 | 1 | \$51 | 1 | \$30 | \$8,491 |
| 1000 | 8 | 2 | \$37 | 1 | \$15 | \$22,151 |
| 5000 | 8 | 9 | \$32 | 2 | \$9 | \$116,923 |

Scenario 4

Comparison of costs per sample as a function of number of GFAA elements. (All instruments must be purchased.) See Table 4.

Table 4. Scenario 4

| Samples/ month | GFAA elements | # GFAA required | Cost/sample GFAA + ICP-OES | # ICP-MS required | Cost/ sample ICP-MS | Savings/ month |
|-------------------|------------------|--------------------|----------------------------------|----------------------|---------------------------|-------------------|
| 1000 | 2 | 1 | \$24 | 1 | \$14 | \$9,601 |
| 1000 | 4 | 1 | \$28 | 1 | \$14 | \$12,751 |
| 1000 | 8 | 2 | \$38 | 1 | \$14 | \$22,151 |
| 1000 | 10 | 3 | \$42 | 1 | \$14 | \$27,490 |

Discussion

In all cases, even when the laboratory already owns two graphite furnaces and one ICP-OES (a common configuration) and must purchase the ICP-MS, the cost per sample is lower for ICP-MS. This is mainly due to the high cost of consumables for GFAA plus the fact that GFAA and ICP-OES requires two separate sample prep steps. Additionally, as the number of samples increases from a conservative number of 400 per month to 1000 and 5000 per month, the differential becomes much greater. This is caused by rapidly increasing labor costs for GFAA, as well as the much higher sample capacity of ICP-MS, lower consumables costs, and requirements for only a single sample prep.

Return on Investment for ICP-MS

A simple return on investment (ROI) can be calculated from the above tables. In this case, the cost per month of the new ICP-MS system is approximately US \$5500.00 (assuming purchase price of US\$180K financed for 3 years at 6%). Figure 1 shows the payback times for a laboratory that already owns two GFAAs and one ICP-OES as a function of the sample load. The y-axis represents the accumulated monthly savings of using ICP-MS versus GFAA + ICP-OES for three different sample loads compared to the unpaid balance on the ICP-MS instrument. As can be seen, the accumulated savings of ICP-MS is equal to the payoff amount after just 4 months when analyzing 2000 samples per month. Even when analyzing as few as 400 samples per month, the accumulated savings is sufficient to pay off the ICP-MS instrument in around 20 months. In this case, eight furnace elements are assumed. Other assumptions are as above.

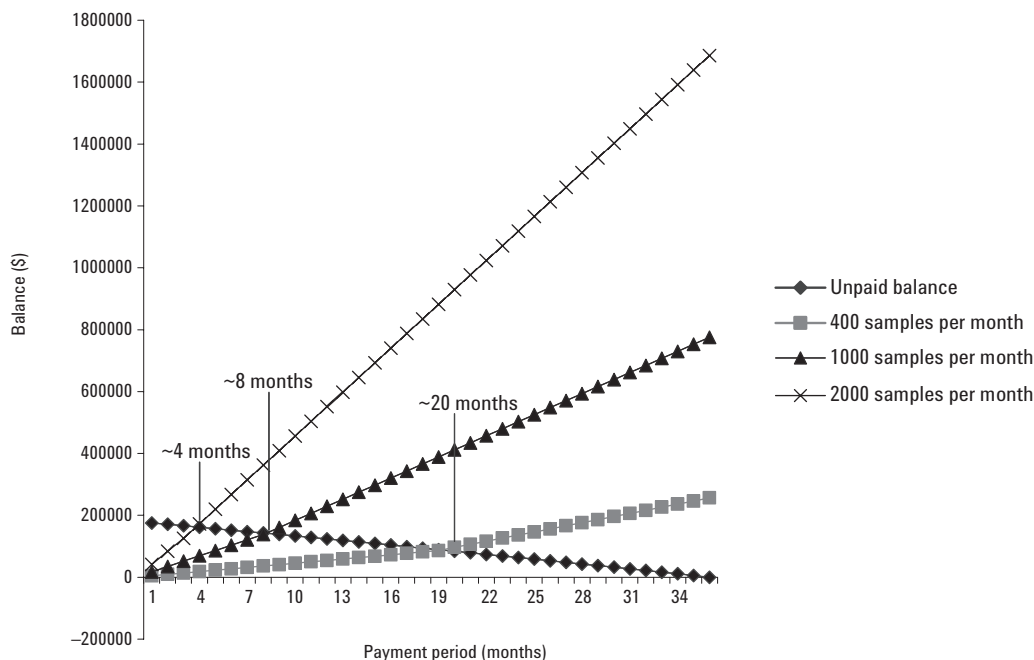


Figure 1. Cumulative return on investment of ICP-MS purchase for three sample levels plotted against the monthly unpaid balance on the ICP-MS. In this case, it is assumed that the accumulated revenue will be used to pay off the loan when the balance equals the residual loan amount. At that point, the net monthly revenue is increased by the loan amount. In this example, laboratories running 2000 samples per month will be able to pay off the ICP-MS in about 4 months, 1000 sample laboratories in about 8 months, and 400 sample laboratories in about 20 months. At the end of 36 months (the original loan period), net revenue exceeds \$200K for the 400 sample lab, \$750K for the 1000 sample lab, and \$1.7 million for the 2000 sample lab.

Conclusions

For almost any metals laboratory, analyzing at least 100 samples per week (400 per month) and using a combination of GFAA and ICP-OES for the analysis, converting to ICP-MS will save money. Depending on the number of samples, the payback for the ICP-MS can be as short as a few months. The cost advantages are not reduced significantly, even if the laboratory already owns its GFAA and ICP-OES instruments. They are also not significantly affected by the number of GFAA elements. As Scenario 4 shows, for the laboratory analyzing at least 1000 samples per month with only two elements by GFAA, the cost savings of switching to ICP-MS is approximately \$10,000 per month. Add to this the increased confidence in results obtained by ICP-MS, the ability to analyze all analyte elements at GFAA (or better) DLs, and the robustness and simplicity of operation of modern ICP-MS instruments, and the choice becomes simple. The productivity of ICP-MS in a high-volume laboratory can quickly pay off the purchase price and increase laboratory profitability significantly.

For More Information

For more information on our products and services, visit our Web site at www.agilent.com/chem.

Agilent shall not be liable for errors contained herein or for incidental or consequential damages in connection with the furnishing, performance, or use of this material.

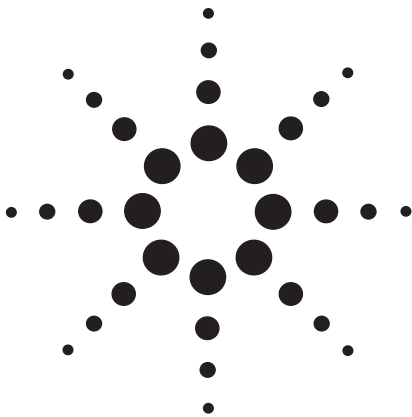
Information, descriptions, and specifications in this publication are subject to change without notice.

© Agilent Technologies, Inc. 2005

Printed in the USA
January 17, 2005
5989-1585EN



Agilent Technologies



Determination of Platinum Compounds by LC-ICP-MS

Application Note Pharmaceutical



Abstract

Platinum compounds such as cisplatin were analyzed using the combination of a high performance liquid chromatograph and an 4500 ICP-MS. Good separation of two types of Pt compounds, cis - amminedichloro - (cyclohexylamine) platinum (II) and bis (acetato) ammine - dichloro (cyclohexylamine) platinum (IV), can be clearly demonstrated.

The detection limit as Pt was 2 ug/L(ppb), corresponding to the amount of 0.1 ng Pt.



Agilent Technologies

Innovating the HP Way

Introduction

Cisplatin is an antineoplastic drug with proven effectiveness against numerous animal and human tumors. With its broad spectrum of antitumor activity, cisplatin is one of the most important drugs in clinical oncology developed in the second half of this century.

However, cisplatin has some side effects such as nephrotoxicity and nausea, which brought on a search for second generation platinum compounds with less nephrotoxicity and greater anti-tumor activity. In order to investigate the behavior of platinum compounds, a selective and sensitive analytical method is required. Until now, high performance liquid chromatography (HPLC) using either off-line AAS detection or on-line UV detection is widely used for platinum compounds determination. However, it is time consuming and there is a lack of sensitivity or/and specificity. ICP-MS is now a mature technique to analyze trace level of elements with high throughput.

This application note describes the determination of platinum compounds by the 4500 ICP-MS with liquid chromatography.

Experimental

Instrumentation

The high performance liquid chromatography used in this work consisted of Agilent 1050 LC system with 50 μ L loop and a ODS C_{18} column (150 mm x 4.6 mm I.D., 5 μ m particle size). The column temperature was set at 30 $^{\circ}$ C, and the sample flow rate was 1 mL/min. The eluent from the HPLC column was directly connected to the nebulizer of 4500 ICP-MS using ETFE tubing

| | |
|-------------------------------|---|
| Plasma gas flow rate | 16.0 L/min |
| Aux. gas flow rate | 1.0 L/min |
| Carrier gas flow rate | 0.84 L/min |
| RF Power | 1250 W |
| Nebulizer | Concentric - type |
| Spray chamber | Glass, double pass |
| Spray chamber temp | 1 $^{\circ}$ C |
| ICP torch injector | Quartz, 2.5 mm |
| Sampler cone | Nickel |
| Skimmer cone | Nickel |
| Sampling depth | 7 mm |
| Points/mass | 1 |
| Acquired mass | 5 mass: ^{194}Pt , ^{195}Pt , ^{196}Pt , ^{115}In and ^{205}Tl |
| Integration time/mass | 0.2 sec |
| Total acquisition time/sample | 2500 sec |

Table 1.
4500 ICP-MS Operating Parameters

(80 cm x 0.3 mm I.D.). Parameters for 4500 ICP-MS are given in Table 1.

Sample Preparation

Eluent used was the mixture of 1 mM heptanesulphonic acid, 0.1% acetic acid, and 20% methanol. Platinum compounds analyzed were cis - amminedichloro - (cyclohexylamine) platinum (II) (*JM118*) and bis (acetato) ammine - dichloro (cyclohexylamine) platinum (IV) (*JM216*) purchased from Johnson Matthey Electronics (Ward Hill, MA, USA).

Each compound was diluted by 0.1% Triton X - 100 and 0.1% HNO_3 .

In and Tl were used as the internal standard elements. A 500 μ g/L of mixed internal standard solution was added on-line at the time of analysis using a peristaltic pump. The flow rate of internal standard solution was 20 μ L/min, which makes approximately 10 μ g/L of In and Tl in a final solution.

This solution was also used for tuning of the 4500 ICP-MS.

Results

The chromatogram for 3.73 mg/L of JM118, which corresponds to 1.95 mg/L Pt is shown in Fig. 1. The sharp peak at around 500 seconds is the signal due to cis - aminedichloro - (cyclohexylamine) platinum (II). The ratios of signals on $m/z=194$, 195 and 196 fit the Pt isotope ratio, which identifies the peaks. Some other peaks are also shown, which might be derivative of Pt compounds.

JM216 was also analyzed to check the level of cis - aminedichloro - (cyclohexylamine) platinum (II). The chromatogram for 2.29 mg/L of JM216 is shown in Fig. 2. The peaks for bis (acetato) ammine - dichloro (cyclohexylamine) platinum (IV) is shown at about 2300 sec. Among the several impurity peaks, the peak for cis - aminedichloro - (cyclohexylamine) platinum (II) can be detected, and its concentration was about 165 μ g/L, which corresponds to 72 mg/g in solid.

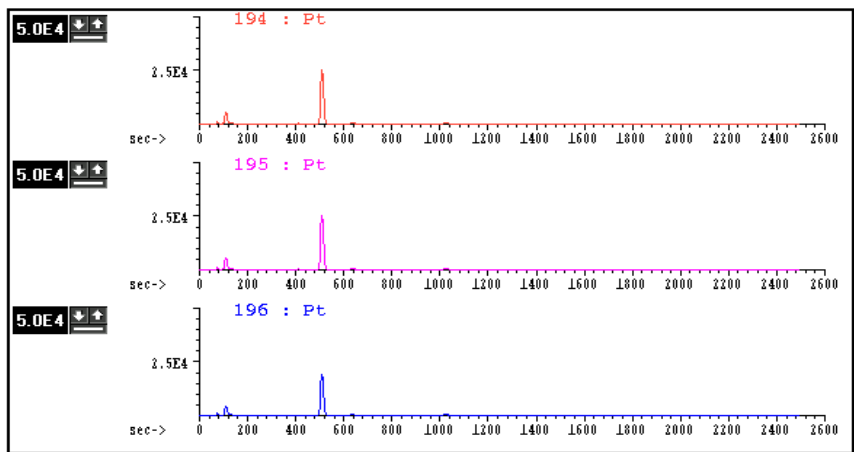


Fig. 1
Chromatogram of platinum in JM118

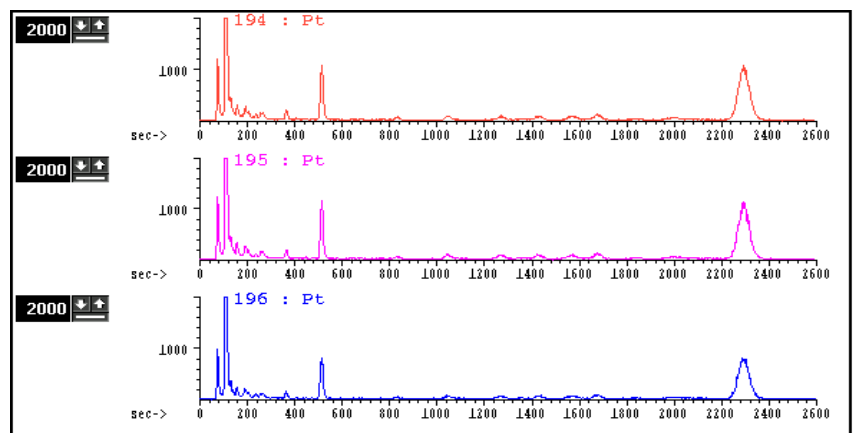


Fig.2
Chromatogram of platinum in JM216

The detection limit defined as the amount producing a signal three times the standard deviation of the noise was 2 ug/L of Pt, corresponding to the amount of 0.1 ng Pt. The detection limit could be increased if only one mass was analyzed or a larger sample loop used.

Although the internal standard elements were not used this time, it would be useful for the correction of signal drift when analyzing samples for a long time.

Conclusion

Platinum compounds can be detected with simple treatment (just dissolution) by 4500 ICP-MS with HPLC.

The combination of HPLC separation capabilities and the 4500 ICP-MS high sensitivity and selectivity enable the determination of platinum compounds down to ng levels.

Agilent Technologies shall not be liable for errors contained herein or for incidental or consequential damages in connection with the furnishing, performance or use of this material.

Information, descriptions and specifications in this publication are subject to change without notice.

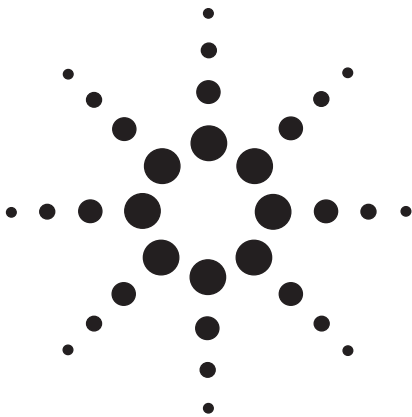
Visit our website at
<http://www.agilent.com/chem/icpms>

Copyright © 2000
Agilent Technologies, Inc.
Printed 4/2000
Publication number 5968-8185E



Agilent Technologies

Innovating the HP Way



Speciation of Arsenic Compounds in Urine of Dimethylarsinic Acid Orally Exposed Rat by Using IC-ICP-MS

Submitted to : Applied Organometallic Chemistry, vol. 10, 707-711 (1996)

Application Note

Clinical



Abstract

A combined system of ion chromatography (IC) with inductively coupled plasma mass spectrometry (ICP-MS) as an element selective detector has been used for the determination of arsenic compounds. Seven arsenic compounds were separated by cation exchange chromatography. Subsequently, the separated arsenic compounds were directly introduced into ICP-MS and were detected at m/z 75. Detection limits for the seven arsenic compounds ranged from 0.8 to 3.8 $\mu\text{g As/l}$. The IC-ICP-MS system was applied to the determination of arsenic compounds in the urine of dimethylarsinic acid (DMAA) exposed rats. DMAA was the most abundant arsenic compound detected. Arsenous acid, monomethylarsonic acid, and trimethylarsine oxide were also detected.



Agilent Technologies

Innovating the HP Way

Introduction

Inorganoarsenic compounds have been documented as carcinogens of the skin and lungs.¹ Most mammals, including humans, are able to methylate inorganoarsenic compounds to monomethylarsonic acid (MMAA) and dimethylarsinic acid (DMAA).^{2,3} It is well known that the biological availability and toxicological effects of arsenic compounds depend upon the chemical forms. The methylated arsenic compounds have a lower toxicity and a lower affinity for tissue constituents than inorganoarsenic compounds. However, recent *in vitro* studies indicate that DMAA may be a potent clastogenic agent and induce chromosome aberrations, such as tetraploid formation.^{4,5}

A combined system of inductively coupled plasma mass spectrometry (ICP-MS) and ion chromatography (IC) is a sensitive and precise tool for speciation study on trace metallic compounds.⁶⁻¹⁰ The authors have reported that anionic and nonionic arsenic compounds in the urine were determined by the combined system of IC-ICP-MS with anion exchange mode.^{11,12} Five arsenic compounds were separated by anion exchange mode within 8 minutes. The proposed IC-ICP-MS method was applied to the

determination of arsenic compounds in the urine of DMAA chronically exposed rats in studies on cancer induction by DMAA.^{13,14} Arsenous acid (As(III)), MMAA, DMAA and trimethylarsine oxide (TMAO) were detected in the urine of DMAA exposed rats.

However, change of retention time of arsenic compounds by a large amount of chloride in the urine was observed during the measurements because *chloride* was very strongly retained in the anion exchange mode. Furthermore, TMAO was often overlapped with an unknown peak eluted at the void volume, because TMAO was weakly retained on the anion column. Qualitative analysis using only one separation mode is not sufficient for other applications, because many forms of arsenic compounds are metabolized into urine. A more accurate toxicological evaluation of arsenic exposure, therefore, should be based on data obtained by several separation modes.

In this study, cation exchange chromatography was used instead of anion exchange chromatography as separation device. An effectiveness of the IC-ICP-MS system with cation exchange mode on the determination of arsenic compounds was evaluated. The

IC-ICP-MS system was applied to the determination of arsenic compounds in the urine of DMAA exposed rats.

Materials and Methods

Reagents

Arsenic compounds used in this experiment are listed in Table 1. TMAO was prepared by oxidation of trimethylarsine (TMA) with 30 % hydrogen peroxide. Stock solutions (100 mg As/l) were prepared by dissolving in pure water. Analytical solutions were prepared by diluting the stock solutions to the required concentration. Other reagents were purchased from Wako Pure Chemical Industries (Osaka, Japan).

Instruments

The ion chromatograph used in this experiment was Model IC7000 from Yokogawa Analytical Systems Inc. (Tokyo, Japan). For the separation of arsenic compounds, three separation modes: ion exclusion chromatography (IEC), size exclusion chromatography (SEC) and cation exchange chromatography (CEC) were used. All columns were purchased from Yokogawa Analytical Systems Inc.. Excelpak CHA-E11 (300 mm x 7.8 mm i.d.) which is packed with sulfonated polystyrene resin with 3.5 mequiv./g dry was chosen as IEC column. Excelpak SEC-W12 (300 mm x 7.8 mm i.d.) which is packed with non-ionic hydrophilic polymer resin was chosen as SEC column. Excelpak ICS-C45 (150 mm x 4.6 mm i.d.) packed with polymer based hydrophilic cation exchange resin with 2.3 mequiv./g of dry was chosen as CEC column. Nitric acid was chosen as a mobile phase.

| Compounds | Manufacturer |
|-----------------------------------|--|
| Arsenous acid [As(III)] Na salt | Wako Pure Chemical Industries (Osaka, Japan) |
| Arsenic acid [As(V)] 2Na salt | Wako Pure Chemical Industries |
| Monomethylarsonic acid [MMAA] | Tri Chemical Laboratory (Yamanashi, Japan) |
| Dimethylarsinic acid [DMAA] | Sigma (MO, USA) |
| Trimethylarsine [TMA] | Strem Chemicals (MA, USA) |
| Arsenobetaine [AsBe] | Tri Chemical Laboratory |
| Arsenocholine [AsC] | Tri Chemical Laboratory |
| Tetramethylarsonium iodide [TMAI] | Tri Chemical Laboratory |

Table 1
Arsenic compounds used in this study

The ICP-MS used in this experiment was Model 4500 from Agilent Technologies, Inc. (DE, USA). ICP-MS operational conditions are described in Table 2. A 500 mm x 0.3 mm i.d. of poly[ethylenetetrafluoroethylene] tube was used to connect the IC column and the nebulizer of the ICP-MS.

Results and Discussion

Selection of separation column

First of all, separation of arsenic compounds by three separation mode was examined. Nitric acid was used as a mobile phase, and the concentrations of nitric acid for IEC, SEC, and CEC modes

were chosen 0.002 mol/l, 0.005 mol/l and 0.01 mol/l, respectively. The ion chromatograph was operated following conditions; flow rate of the mobile phase is 1.0 ml/min, column temperature is 40 °C, and injection volume is 50 µl.

On IEC separation, inorganoarsenic compounds, such as As(III) and arsenic acid (As(V)), were completely separated, but organoarsenic compounds except MMAA and DMAA were not eluted. On SEC separation, five arsenic compounds, viz. As(III), As(V), MMAA, DMAA and TMAO, were separated, but cationic arsenic compounds were overlapped with these arsenic compounds.

SEC mode will be used for the determination of arsenic compounds in the urine, because these five arsenic compounds are main metabolic arsenic compounds in urine. However, it was decided that SEC mode was not suited to the determination of arsenic compounds in urine of DMAA administered rats, that is the purpose of this study, because of lack of the resolution of MMAA and DMAA. On the other hand, seven arsenic compounds except for As(V) were completely separated by CEC mode with optimizing for the mobile phase concentration. According to these results of this preliminary experiments, Excelpak ICS-45 was chosen as the separation column.

| | |
|--------------------|---|
| RF power | 1300 W |
| RF reflected power | < 1 W |
| Plasma gas | 16.0 L/min |
| Auxiliary gas | 1.00 L/min |
| Carrier gas flow | 1.06 L/min |
| Sampling depth | 6 mm |
| Mass | 75 (⁷⁵ As) ,77 (⁴⁰ Ar ³⁷ Cl) |
| Integration time | 0.5 sec (m/z 75) 0.05 sec (m/z 77) |
| Number of scans | 1 |

Table 2
ICP-MS operational conditions

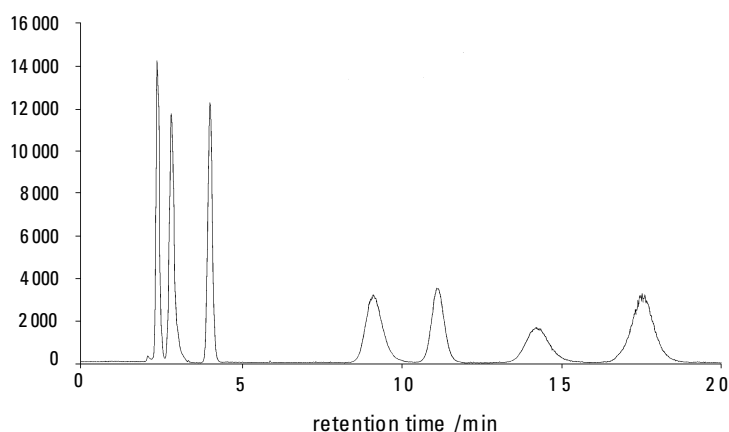


Fig. 1
Chromatograms of seven standard arsenic compounds. Separation conditions : mobile phase is 0.008 mol/l nitric acid, flow rate is 1.0 ml/min, and column temperature is 50 °C. ICP-MS operational conditions are the same as those given in Table 2. Sample, 0.1 mg As/l each; injection volume 50 µl. As(V) was not added to the sample solution.

Separation of arsenic compounds on cation exchange mode

Several parameters, such as concentration of mobile phase, mobile phase flow rate and column temperature, were examined in order to produce the optimal conditions on CEC mode. The optimized IC operational conditions were determined as follows; mobile phase is 0.008 mol/l nitric acid, flow rate is 1.0 ml/min, and column temperature is 50 °C.

A chromatogram of the seven standard arsenic compounds is shown in Fig. 1. The concentrations of the seven standards were 0.1 mg As/l each. Arsenobetaine (AsBe), arsenocholine (AsC) and tetramethylarsonium iodide (TMAI) were separated based on cation exchange mechanism. TMAO was also clearly retained. It is speculated that the cationic character of TMAO is due to protonation of the As=O bond under the acidic conditions.¹⁰ On the other hand, As(III) and MMAA showed poor retention due to ion exclusion interaction based on the

charge of the packing materials. Although As(V) was not added to the sample solution, a small peak of As(V) which might be produced by oxidation of As(III), was observed immediately before the peak of MMAA.

Method statistics

The detection limits and the reproducibility (RSD) for the seven arsenic compounds were calculated using 0.1 mg As/l standard solutions by injecting a 50 µl sample. The detection limits were calculated from 3 times the base line noise. The reproducibility for each standard was obtained from five replicates of the peak area. Table 3 gives the detection limits and the reproducibility for arsenic compounds.

Interference from chloride

In ICP-MS with the current introduction method, interference of the polyatomic ion $^{40}\text{Ar}^{37}\text{Cl}^+$ at m/z 75 due to high chloride content in the sample solution has been observed.^{9, 15, 16} In order to check the ArCl^+ ion interference at m/z 75, a 1000 mg/l chloride solution was analyzed and was detected at m/z 75 and 37.

An ArCl^+ ion was observed immediately before the peak of MMAA. The peak area of ArCl^+ ion produced from 1000 mg/l chloride corresponded to that of 1.3 µg As/l.

Application to the determination of arsenic compounds in rat urine

The IC-ICP-MS system was applied to the determination of metabolic arsenic compounds in

the urine of rats to which DMAA was administered. Rats were given 50 mg/kg b.w. of DMAA by single oral administration. The urine samples were collected by forced urination at 0 and 4 hours after the dosage. The urine was diluted 20 times by pure water and 50 µl of the diluted urine was injected into the IC-ICP-MS system.

As(III), MMAA, DMAA, TMAO and AsBe were clearly detected in the urine at 4 hours after the dosage, while trace DMAA and AsBe was detected in the urine at 0 hours, that is the blank urine. Chromatogram of the diluted urine at 4 hours after the dosage are shown in Fig. 2. DMAA was the most abundant arsenic compound in the urine. Relatively high proportions of TMAO were observed in the chromatogram. Lesser amounts of MMAA and As (III) were also detected. Furthermore, two unknown peaks were detected in chromatogram. It is estimated that former and latter unknown peaks are anionic and cationic arsenic compound, respectively, due to their retention. Even though it has been reported that AB was not produced in mammals¹⁷, AsBe was detected in the urine of DMAA exposed rats. It is concluded that AsBe came from the feed, because the concentration of AsBe in the urine at 4 hours was equivalent to that in the blank urine.

| Arsenic compounds | Detection limits [µg As/l] | RSD [%] (n = 5) |
|-------------------|----------------------------|-----------------|
| As(III) | 0.83 | 0.74 |
| MMAA | 0.73 | 1.25 |
| DMAA | 0.81 | 0.32 |
| TMAO | 2.20 | 1.62 |
| AsBe | 2.09 | 1.03 |
| AsC | 3.88 | 1.07 |
| TMAI | 3.27 | 2.75 |

Table 3
Comparison of detection limits and reproducibility

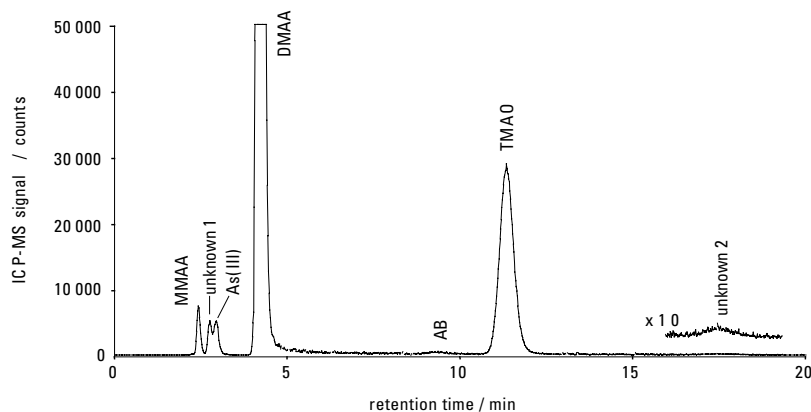


Fig. 2
Chromatogram of arsenic compounds in the diluted urine of DMAA exposed rats at 4 hours after the dosage. Conditions are the same as those given in Fig. 1.

In conclusion, the IC-ICP-MS system with cation exchange chromatography as the separation device was found to be a sensitive speciation method for metabolic arsenic compounds in the urine of DMAA exposed rats. The presented method demonstrated not only good detection limits, but also facilitated the sample preparation process. The IC-ICP-MS system will be useful for biological monitoring and toxicological evaluation of arsenic compounds.

References

1. IARC (International Agency for Research on Cancer), Monographs on the Evaluation of the Carcinogenic Risk of Chemicals to Man: Some Metals and Metallic Compounds, Vol. 23, pp. 39, 1980. International Agency for Research on Cancer, Lyon.
2. H. Yamauchi and Y. Yamamura, *Ind. Health*, **17**, 79 (1979).
3. M. Vahter, L. Friberg, B. Rahnster, A. Nygren and P. Nolinder, *Int. Arch. Occup. Environ. Health*, **57**, 79 (1986).
4. G. Endo, K. Kuroda, A. Okamoto and S. Horiguchi, *Bull. Environ. Contam. Toxicol.*, **48**, 131 (1992).
5. J. T. Dong and X. M. Luo, *Mutat. Res.*, **302**, 97 (1993).
6. N. P. Vela, L. K. Olson and J. A. Caruso, *Anal. Chem.*, **65**, 585A (1993).
7. J. Thompson and R. Houk, *Anal. Chem.*, **58**, 2541 (1986).
8. Y. Shibata and M. Morita, *Anal. Chem.*, **61**, 2116 (1989).
9. B. S. Sheppard, J. A. Caruso, D. T. Heitkemper and K. A. Wolnik, *Analyst*, **117**, 971 (1992).
10. E. H. Larsen, G. Pritzl and S. H. Hansen, *Anal. At. Spectrom.*, **8**, 557 (1993).
11. K. Kawabata, Y. Inoue, H. Takahashi and G. Endo, *Appl. Organomet. Chem.*, **8**, 245 (1994).
12. Y. Inoue, K. Kawabata, H. Takahashi and G. Endo, *J. Chromatogr. A*, **675**, 149 (1994).
13. S. Yamamoto, Y. Konishi, T. Murai, M. Shibata, T. Mastuda, K. Kuroda, G. Endo and S. Fukushima, *Appl. Organomet. Chem.*, **8**, 197 (1994).
14. S. Yamamoto, Y. Konishi, T. Matuda, T. Murai, M. Shibata, I. Matsui-Yuasa, S. Otani, K. Kuroda, G. Endo and S. Fukushima, *Cancer Res.*, **15**, 1271 (1995).
15. M. Vaughan and G. Horlick, *Appl. Spectrosc.*, **40**, 434 (1986).
16. S. Branch, L. Ebdon, M. Ford, M. Foulkes and P. O'Neill, *Anal. At. Spectrom.*, **6**, 151 (1991).
17. M. Vahter, E. Marafante and L. Dencker, *Sci. Total Environ.*, **30**, 197 (1983).

Agilent Technologies shall not be liable for errors contained herein or for incidental or consequential damages in connection with the furnishing, performance or use of this material.

Information, descriptions and specifications in this publication are subject to change without notice.

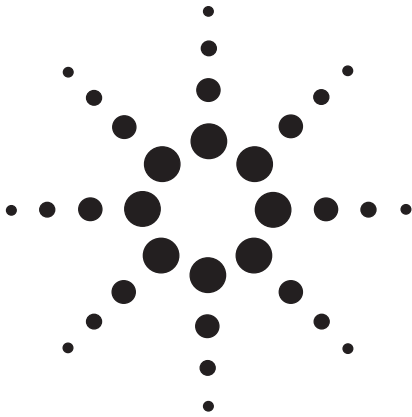
Visit our website at
<http://www.agilent.com/chem/icpms>

Copyright © 2000
Agilent Technologies, Inc.
Printed 4/2000
Publication number 5968-3050E



Agilent Technologies

Innovating the HP Way



Practical Benefits of Abundance Sensitivity in ICP-MS

Application Note

Don Potter



Abstract

In ICP-MS, good abundance sensitivity is necessary in that it enables the measurement of a trace peak at an adjacent mass to a major peak. In the analysis of high matrix samples, for example in environmental testing, a system possessing good abundance sensitivity gives the analyst confidence that values reported will reflect the true concentration of analytes present, rather than spectral overlap from matrix elements. This application note describes how mass spectrometer and vacuum system design influences abundance sensitivity, using the 4500 ICP-MS as an example.



Agilent Technologies
Innovating the HP Way

Introduction

Abundance sensitivity is often confused with resolution. In fact a mass spectrometer can possess good resolving power yet have relatively poor abundance sensitivity. This application note will consider quadrupole analyzers, where, high resolution would be typically 0.5 amu at 10% valley. Abundance sensitivity is a measure of the spectrometer's ability to completely separate a trace peak from a major peak at an adjacent mass, and while resolution is generally measured at 10% of the peak height, abundance sensitivity, by definition, depends on peak width at the baseline. Therefore, any significant peak broadening at the baseline, or any noise, or 'structure' on the edges of the peak, such as precursors, would adversely affect the system's abundance sensitivity.

Design Factors Affecting Abundance Sensitivity

There are two main design factors affecting abundance sensitivity: the design and performance of the analyzer, and the operating vacuum pressure within the analyzer stage. The 4500 ICP-MS benchtop inductively coupled plasma mass spectrometer (ICP-MS) will be used as an example of how careful system design can optimize performance. The quadrupole used in the 4500 ICP-MS is the same unit used in the Agilent 5989 MS Engine research grade mass spectrometer and is manufactured by Agilent Technologies. The quadrupole rods are machined from solid molybdenum. Mo is used because it has an extremely low coefficient of expansion, ensuring the precise alignment of the rods is not affected

by temperature changes. The use of solid Mo also eliminates any of the potential distortion problems associated with plated rods, due to different rates of expansion within the rod. The cross-sectional shape of the rods is also critical for optimum performance - a hyperbolic cross-section is the theoretically correct shape ⁽¹⁾. Most quadrupoles employ rods with a circular cross-section which approximate a hyperbolic

field, since they are cheaper to manufacture and easier to assemble. The quadrupole used in the 4500 ICP-MS features true hyperbolic rods for optimum performance. The principal advantage of a hyperbolic quadrupole is better transmission at higher resolution. Typically, changing from 0.9 to 0.5 resolution results in a decrease in transmission of only 20%, compared to ~50% with round rods. The practical benefit

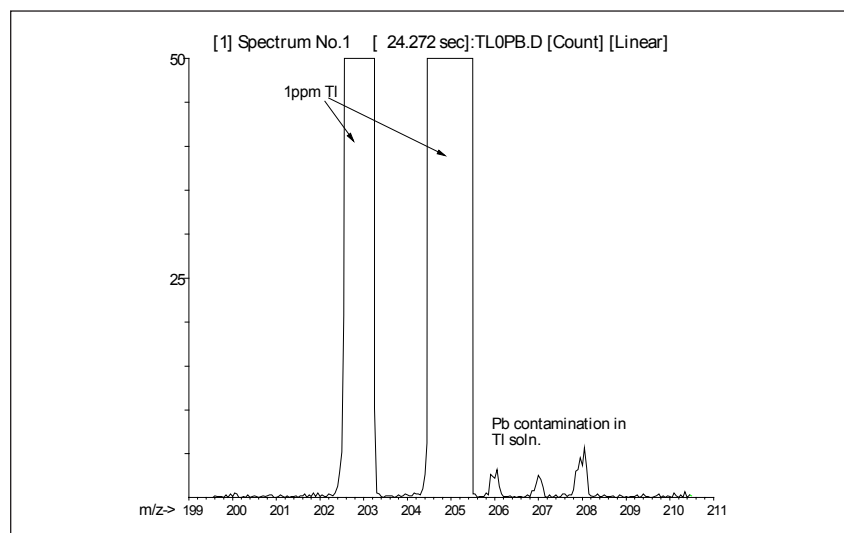


Fig. 1. Spectra obtained from 1ppm Tl solution

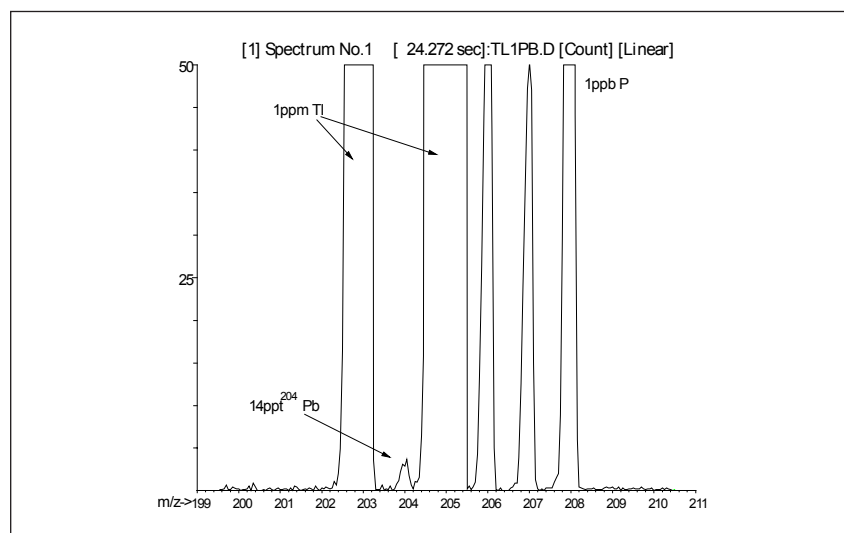


Fig. 2. Spectra obtained from 1ppm Tl/1ppb Pb solution

to the analyst is that the 4500 ICP-MS can be operated at the same resolution setting (0.75) for all applications, even for ultratrace analysis. Unlike other systems, the analyst is not forced to choose between good resolution and sensitivity, thereby removing another variable from day to day operation.

In addition to quadrupole design, the frequency at which

the quadrupole operates also has a fundamental effect on abundance sensitivity. The higher the frequency, the better the abundance sensitivity. This is because the ions are subjected to more oscillations in the RF field as they pass through the quadrupole. This increases the chance that only ions of the correct m/z value remain stable as they pass through the quadrupole, and results in 'cleaner' peaks with

little tailing. The 4500 ICP-MS uses a custom designed solid state quadrupole RF generator, built by Agilent. Operating at 3.0MHz rather than the more typical 2.2-2.5MHz, it is the highest frequency generator available in ICP-MS, and a major contributing factor to the 4500 ICP-MS's excellent abundance sensitivity. To drive a quadrupole above 2.5Mhz requires a specialized power supply due to the high voltages necessary to operate at high frequencies. The 4500 ICP-MS quadrupole power supply was designed in house and the result of a major design initiative.

Aside from quadrupole performance, the vacuum at which the analyzer operates also has an effect on abundance sensitivity. The higher the vacuum, the better the abundance sensitivity. This is because there are less residual gas molecules in the vacuum chamber, resulting in fewer ion/gas collisions. This in turn results in an ion beam with a tighter kinetic energy spread, which minimizes tailing on the leading edge (low mass side) of the peak. The vacuum design of the 4500 ICP-MS incorporates the turbomolecular pump directly coupled to the main chamber, via large diameter flanges. This ensures that pumping capacity is optimized, resulting in a very low operating pressure in the analyzer chamber of $\sim 5 \times 10^{-6}$ Torr. A low operating pressure helps minimize any peak tailing, which is an important contributor to good abundance sensitivity performance. Finally, the analyzer stage turbo-pump is mounted directly beneath the detector entrance aperture ensuring the detector is maintained at the highest possible vacuum which prolongs detector lifetime and helps reduce random background levels.

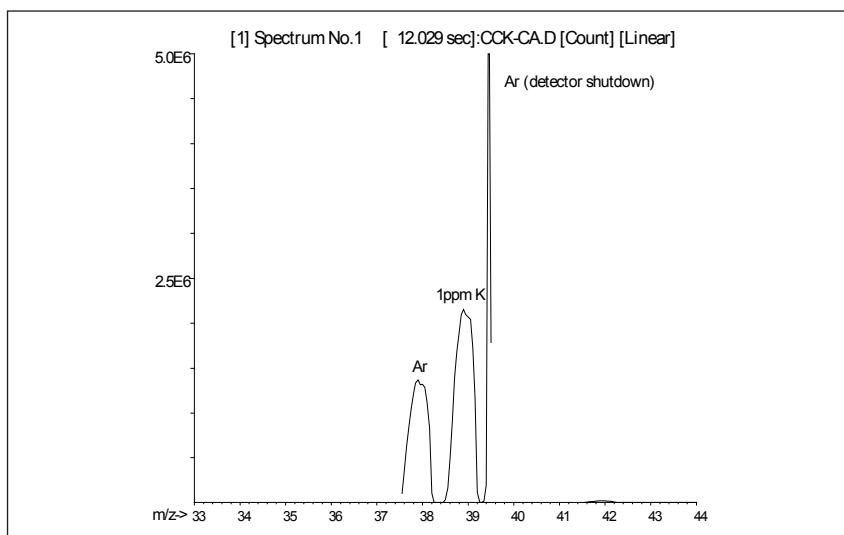


Fig. 3.
Spectra showing separation of Ar isotopes from 1ppm K

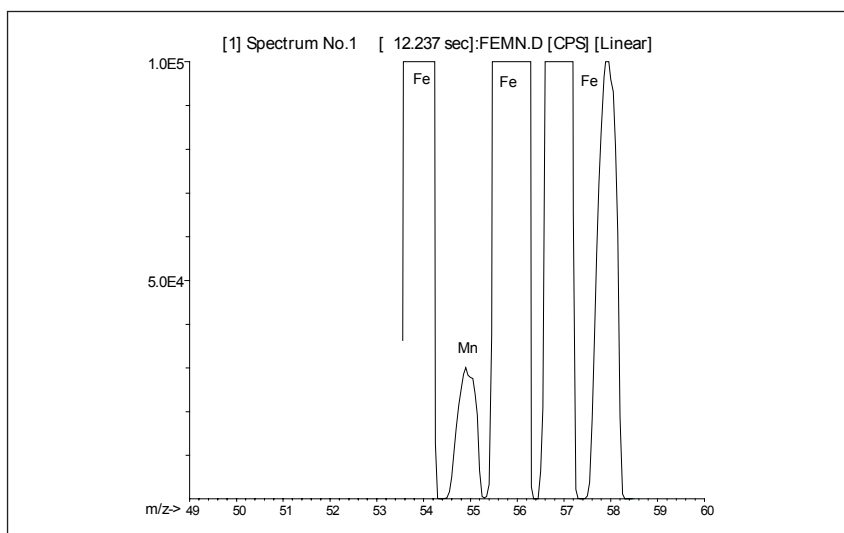


Fig. 4.
1ppm Fe / 1ppb Mn - linear scale

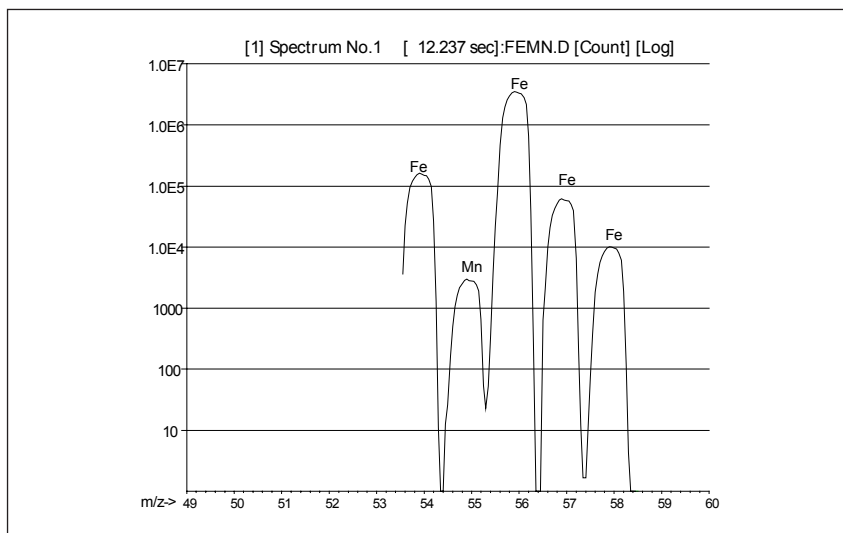


Fig. 5.
1ppm Fe/1ppb Mn - log scale

Abundance Sensitivity Performance

To check the abundance sensitivity of the 4500 ICP-MS a solution of 1ppm Tl was aspirated and the quadrupole scanned across the mass range 200-210 amu. This was repeated with 1ppb Pb added to the solution, and the spectra obtained compared (Figs. 1 & 2).

All measurements in this work were made at the standard at resolution setting - 0.75amu at 10% valley. Tl has 2 isotopes, at 203 and 205 amu. In between is the minor Pb isotope at 204 amu. If abundance sensitivity is poor the ^{204}Pb peak would be obscured by the leading edge of the ^{205}Tl peak. Fig. 1 shows the spectra obtained from the Tl solution; the Tl peaks are straight sided, reaching the baseline without any significant tailing on the low mass side. Pb is present as an impurity in the Tl standard, and the major Pb isotopes can be clearly seen. Fig. 2 shows the same Tl peaks, but with Pb present at 1ppb, giving a ^{204}Pb concentration of 14ppt, assuming natural abundance.

The ^{204}Pb peak is completely separated from the ^{205}Tl peak, at a concentration of 705ppb, demonstrating excellent abundance sensitivity.

The practical benefit of good abundance sensitivity is the assurance that erroneously high analyte concentration values are not caused by peak overlap. A good example is shown in Fig. 3, which shows the scanning spectra obtained from a solution of 1ppm K.

Normally, K is measured only by peak hopping, to avoid overlap of the ^{39}K peak by the adjacent ^{40}Ar peak. Fig. 3 shows complete separation of the whole ^{39}K peak, enabling K measurement in scanning mode, which is often preferable in research work, or when using laser ablation.

In environmental analysis, high levels of Fe are often found in site remediation samples. The measurement of Mn in the presence of high levels of Fe requires good abundance sensitivity to avoid overlap from the ^{56}Fe peak.

Figs. 4 & 5 show the spectra obtained from a solution containing 1ppb Mn and 1ppm Fe, both in linear and log scale. Mn is completely separated from the Fe peaks. The sensitivity of the system in this case was 25MHz/ppm at Mn, demonstrating that sensitivity was not compromised by any increase in resolution to achieve peak separation. Fig 5., the log scale spectra, clearly shows the symmetry of the peaks obtained from the 4500 ICP-MS, and peak widths of <1amu wide, even at the background levels.

Conclusion

Careful design of not only the analyzer and quadrupole RF generator, but also of the vacuum system is necessary to achieve good abundance sensitivity. This gives the analyst confidence that data reported is not compromised by peak overlap. Another important advantage is the analyst is not forced to choose between sensitivity and peak separation (increased resolution). By leaving the resolution fixed at one setting for all applications, a variable is removed from day to day operation, improving routine ease of use.

References

1. Miller, P.E. and Denton, M.B. (1986) The Quadrupole Mass Filter: basic operating concepts. J. Chem. Ed. 63, 617-622

Don Potter is a Business Development
Manager at Agilent Technologies, Inc.,
Manchester, UK

Agilent Technologies shall not be liable for
errors contained herein or for incidental or
consequential damages in connection with the
furnishing, performance or use of this material.

Information, descriptions and specifications in
this publication are subject to change without
notice.

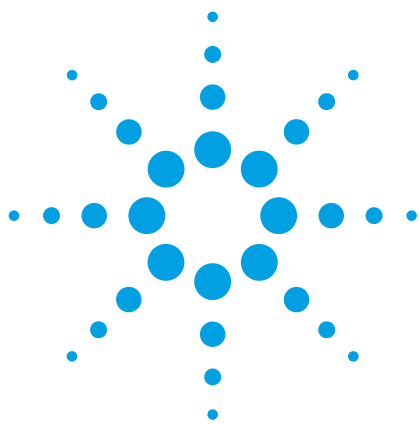
Visit our website at
<http://www.agilent.com/chem/icpms>

Copyright © 2000
Agilent Technologies, Inc.
Printed 4/2000
Publication number 5964-9024E



Agilent Technologies

Innovating the HP Way



Ultra-low level impurity analysis by capillary zone electrophoresis

Application Note

Pharmaceutical

Author

Gordon Ross
Agilent Technologies,
Waldbronn, Germany

Abstract

Capillary zone electrophoresis (CZE) is an inherently high efficiency liquid phase separation technique. This makes it very suitable for the separation of closely related compounds and can be of particular use in the analysis of drug impurities. Regulatory requirements demand the demonstration of the purity of any drug substance and the acceptable criteria for presence of impurities are around 0.1 %. This means that the analysis not only has to have an adequate sensitivity, but also that the linear range is such that the minor component may be quantitatively reported as a corrected (area/area) percent of the main component. By using the Agilent CE high sensitivity detection cell, sensitivity can be increased by an order of magnitude, with linearity increased over 3-fold compared to conventional capillaries. This enables the determination of impurities in drug substances below the 0.1 % area/area level. Figure 1 shows the linear range achievable using the high-sensitivity cell, illustrating its linearity over 2.2 AU.

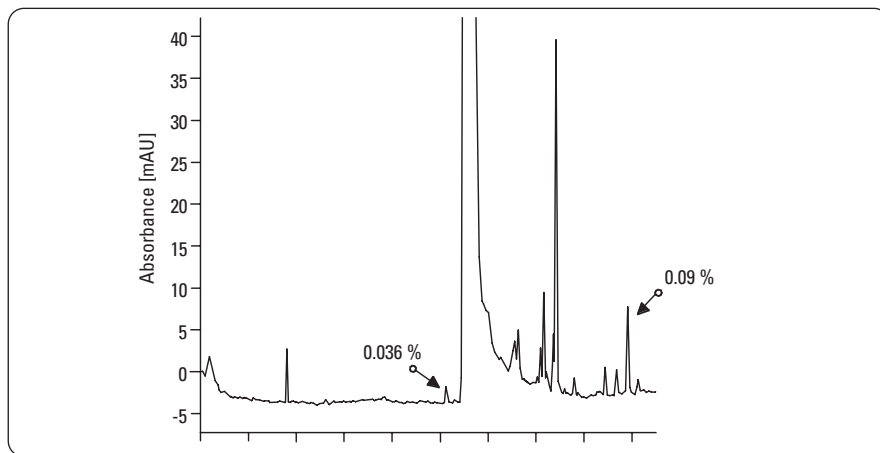


Figure 1
Linear range of high sensitivity cell.



Agilent Technologies

Experimental

All experiments were performed on the Agilent Capillary Electrophoresis system which is computer controlled via Agilent ChemStation software. High sensitivity detection was achieved using the Agilent High-Sensitivity Detection Cell (part number G1600-68713) and capillaries.

During a shelf life study of ranitidine, the anti-ulcer drug was analyzed for the presence of impurities after 12 months exposure to light and room temperature. Figure 2 shows the analysis of the main peak indicating that this is at the upper levels of the linear range of detection. An expanded view of the base of the peak shows the number of impurities present at very low levels. Given the linear range of the detection cell, it is possible to calculate the impurity level of these peaks at less than 0.1 % area/area of the main peak.

Conclusion

CZE in conjunction with the high-sensitivity detection cell, may be used to determine impurity levels in drugs at less than 0.1 % area/area. This level is appropriate to that required for regulatory submissions.

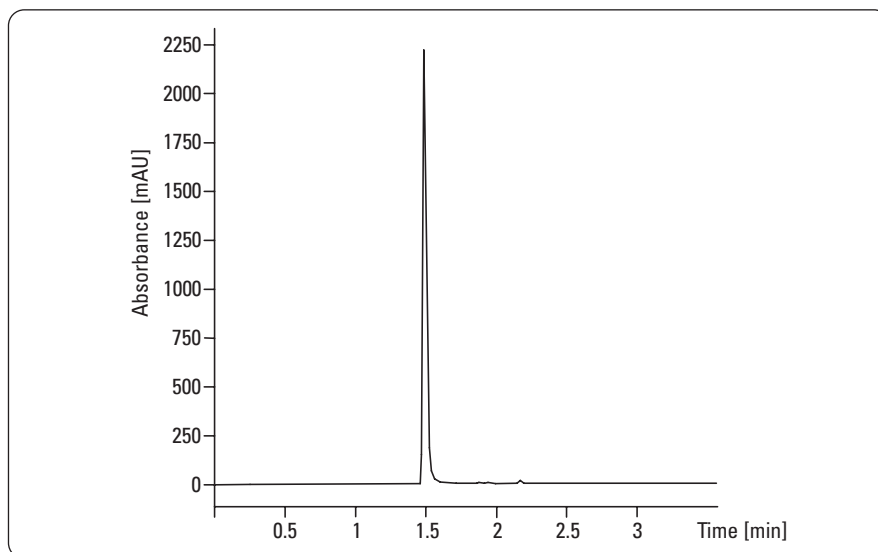


Figure 2
CZE analysis of ranitidine.

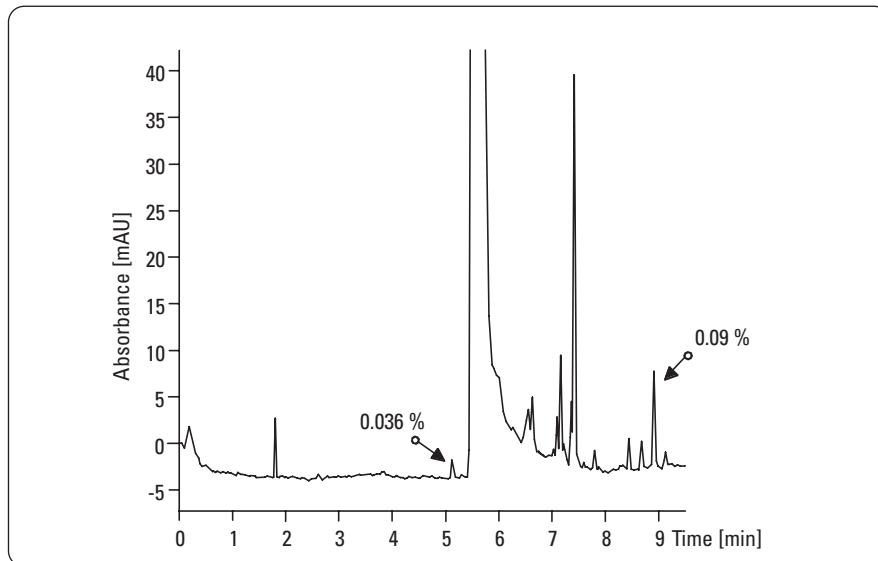


Figure 3
Low level determination of ranitidine impurities.

Chromatographic conditions (figures 2, 3)

Buffer: 20 mM borate pH 9.3
Capillary: 56 cm eff (64.5) x 75 μ m id
Injection: 200 mbars
Run: 20 °C, 30 kV
Detection: 225/20 nm (high sensitivity cell)

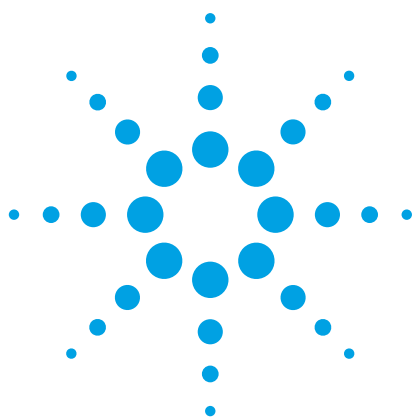
www.agilent.com/chem/ce

© Agilent Technologies Inc., 1997-2009

Published March 1, 2009
Publication Number 5990-3381EN



Agilent Technologies



Analysis of chlorogenic acid in traditional Chinese medicines by capillary electrophoresis

Carsten Buhlmann and
Gordon Ross

Pharmaceutical

Abstract

Chlorogenic acid (CA) (figure 1) is an ester of caffeic acid and quinic acid. All three of these substances naturally occur in many plants. CA which is present in the surface skin of peaches, inhibits the cutin-digesting enzyme of the brown rot fungus, *Monilinia fructicola*, demonstrating its antifungal activity. It has also shown antioxidant activity. CA is an active constituent of *Flor. Lonicerae*. CZE has been used for its analysis in the plant and in some traditional medicines which contain this plant as a constituent¹. Although HPLC has been used for the analysis of traditional Chinese medicines (TCM), the “dirty” matrix of the prepared sample can prove problematic for the LC column. Since CE operates using small bore unpacked tubing, it is much more tolerant of complex matrices and more robust when used for their analysis. Here we describe how CA can be identified and quantified in some Chinese traditional medicines using capillary electrophoresis.

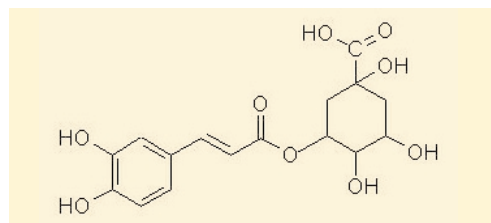


Figure 1
Structure of chlorogenic acid

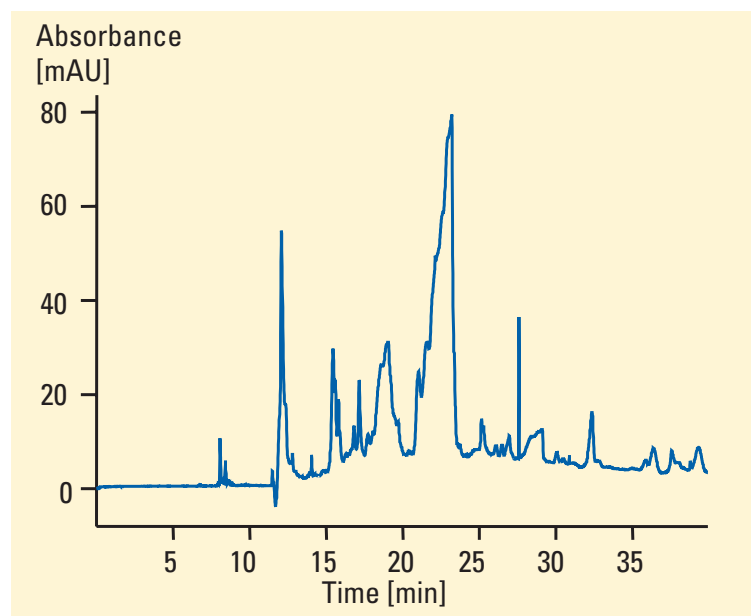


Figure 2
Extract of zhi zi jin hua wan TCM

Conditions

Injection

10 sec @ 50 mbar

Capillary

L= 64.5 cm, l= 56 cm, 50 µm id

Buffer

40 mM phosphate

80 mM boric acid containing 5 %

ethanol with apparent pH adjusted to 7.0

Voltage

20 kV

Temperature

20°C

Detection

254 nm



Agilent Technologies

Innovating the HP Way

Experimental

All analyses were performed using an Agilent CE system equipped with diode array detection and controlled via a PC running the Agilent Chemstation software. Traditional medicine samples and standards were the kind gift of Professor H. Liu, Peking University, Beijing, PR China. Other reagents were supplied by Sigma.

Extraction

The indicated amounts of pulverized samples were soaked with 7 ml 50 % ethanol/water overnight and extracted by stirring for 30 minutes. After centrifugation (4000 rpm, 10 minutes) the extraction was repeated two more times. The combined extraction volume was made up to 25 ml and filtered through 0.45 µm. Liquid samples were simply diluted and filtered before measurement. The analysis of extracts using the above method gives a complex electropherogram (figure 2). Identification of CA is more problematic. When injected individually as a standard it migrates in an area occupied in the sample injection by three peaks, all of which have similar spectra. By spiking samples with pure CA it can be unequivocally identified in the prepared TCM extract (figure 3). The table below shows the calculated amounts of CA in *Flor Lonicerae*, in some TCMs and in a coffee extract.

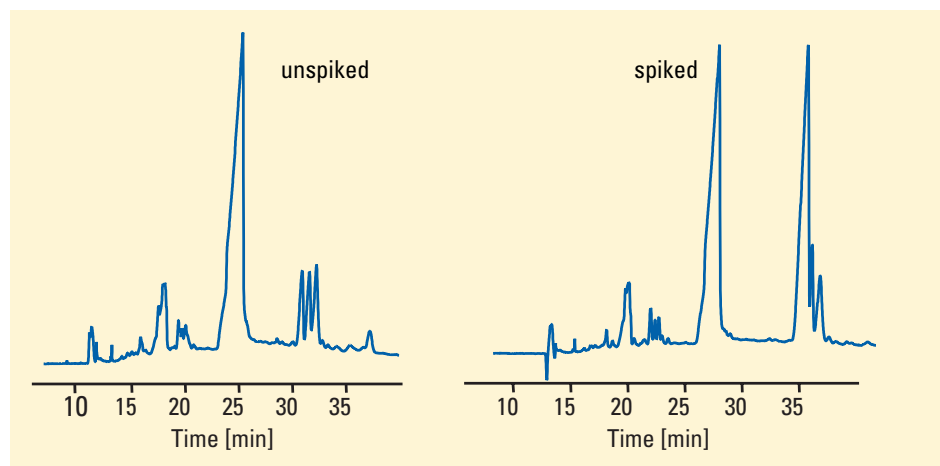
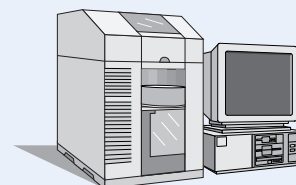


Figure 3
Identification of chlorogenic acid in shung huang lian by spiking

| Medicine | Chlorogenic acid [mg/l] | Powder weight [g] | Content [mg/g] or [mg/ml] |
|----------------------------------|-------------------------|-------------------|---------------------------|
| <i>Flos Lonicerae</i> | 670 | 0.946 | 17.83 |
| Zhi zi jin hua wan | 61.18 | 3.34 | 0.49 |
| Vc yin qiao pain | 104.1 | 2.83 | 0.85 |
| Yin qiao jie du pain | 542.9 | 2.9 | 3.50 |
| Xiao er qing re jie du kou fu ye | 31.14 | liquid | 0.39 |
| Shung huang lian | 187.8 | liquid | 2.10 |
| Cafe (hot water extract) | 197.23 | liquid | 0.20 |

Equipment

- Agilent Capillary Electrophoresis system
- Agilent ChemStation



References

- 1 Long, H, Yang, J, Liu, H, Wang, T, Huang, A and Sun, Y, Journal of Chinese Pharmaceutical Sciences, 8 (1999) 152-157.

Carsten Buhlmann and Gordon Ross are application chemists at Agilent Technologies, Waldbronn, Germany

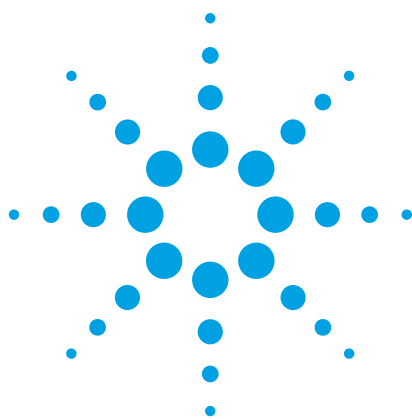
For more information on our products and services, visit our website at <http://www.agilent.com/chem>

© Copyright 2000 Agilent Technologies
Released 03/2000
Publication Number 5980-0457E



Agilent Technologies

Innovating the HP Way



Analysis of fangchinoline and tetrandrine in Chinese traditional medicine by capillary electrophoresis

Carsten Buhlmann
and Gordon Ross

Pharmaceutical

Abstract

The analysis of plant extracts is problematic due to the very complex nature of the sample matrix which makes identification of individual constituents a challenge. The task is made even more difficult since some separation techniques, for example, HPLC, cannot easily deal with such matrices and injection can lead to column fouling. CE on the other hand is capable of high resolution analysis of such samples and indeed can be characterized by its ability to handle complex and crude samples with a minimum of sample preparation. CE is therefore ideal for the analysis of these natural products. Fangchinoline and tetrandrine are two alkaloids which are present in *Radix Stephaniae tetradrae* S. Moore. These compounds have pain-relieving effects, can reduce blood pressure and also have antineoplastic and antibiotic activity. Therefore, they are of pharmaceutical interest. The plant is often used in various Chinese herbal preparations. Here we describe application of a CE method¹ to quantitative analysis of these alkaloids in some Chinese traditional medicines.

Experimental

All analyses were performed using an Agilent CE system equipped with diode array detection and controlled via a PC running the Agilent Chemstation software. Traditional medicine samples and standards were the kind gift of Professor H. Liu, Peking University, Beijing, PR China. Other reagents were supplied by Sigma.

Figure 2
Structure of fangchinoline and tetrandrine

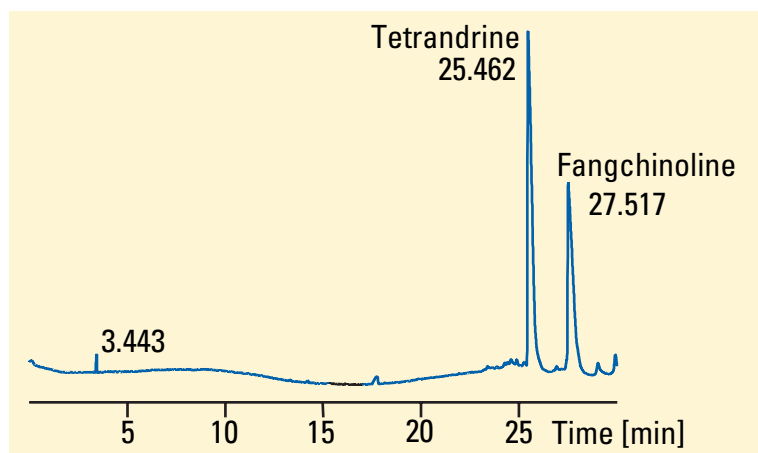
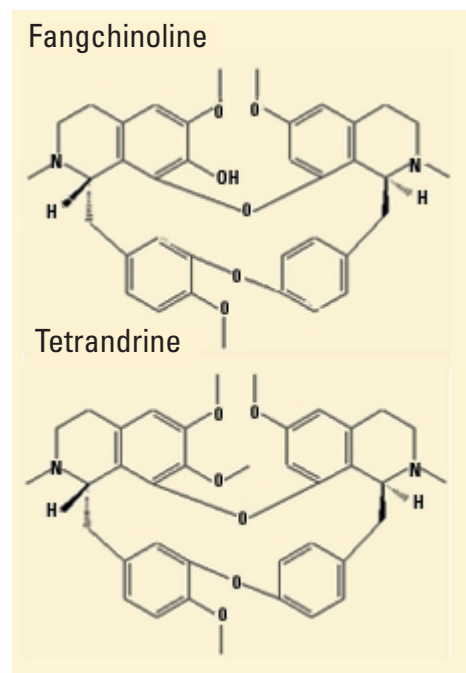


Figure 1
Separation of fangchinoline and tetrandrine in a traditional medicine



Agilent Technologies

Innovating the HP Way

Extraction: 2 g of each pulverised herbal drug were extracted with 7 ml 50% ethanol by stirring for 30 minutes, followed by centrifugation (4000 rpm, 10 minutes). The extraction was repeated two more times and the combined extracts were filtered through 0.45- μ m pore. For electrokinetic injection, a volume of 200 mM NaCl solution, equivalent to one fifth of the sample volume was added to the sample to equalize the sample conductivity. The analytical conditions were: buffer: 60mM phosphoric acid\TAE, 50 mM Tween-20, 20 % methanol, pH 2,5; capillary: 64,5cm (56cm) \times 50 μ m; detection: 214,10; injection: 4 kV \cdot 23 s; voltage: 20.2 kV; temperature: 19° C.

Results

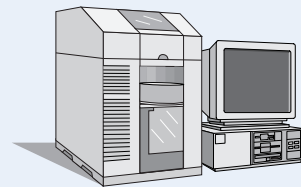
The medicines were separated using a MEKC system with Tween-20 as the surfactant. This resulted in a very clean electropherogram where two peaks could easily be seen (figure 1). Due to their similar structure (figure 2) tetrandrine and fangchinoline have very similar spectra and therefore were identified by spiking experiments with pure standards. After identification (figure 1) the two alkaloids were quantified in a number of traditional Chinese medicines. Linearity was determined for both compounds over the range of 5 to 250 μ g /ml. Linearity was greater than 0.9999 for both analytes. Reproducibility of migration times was very good (<0.4%). For quantitation, the reproducibility of peak areas was acceptable (<4%) but depended on the medicine and therefore the sample matrix (table1).

Conclusions

CE is very well suited to the analysis of components of traditional Chinese medicines due to its robust capability of handling complex sample matrices. Two endogenous alkaloids, tetrandrine and fangchinoline could be identified and quantified in a number of different traditional medicines.

Equipment

- Agilent Capillary Electrophoresis system software
- Agilent ChemStation



References

- 1 Yang, J., Long, H., Liu H and Sun, Y. J. Chromatogr A. 811, **1998**, 274-279.

Carsten Buhlmann and Gordon Ross are application chemists at Agilent Technologies, Waldbronn, Germany

© Copyright 2000 Agilent Technologies
Released 03/2000
Publication Number 5980-0456E

| Name of medicine | Tetrandrine | | | | Fanchinoline | | | |
|------------------------------------|-------------|-----------|-----------|--------|--------------|-----------|-----------|--------|
| | [mg/L] | %RSD area | %RSD time | [mg/g] | [mg/L] | %RSD area | %RSD time | [mg/g] |
| Fang ji guan jie wan | 28.41 | 2.44 | 0.32 | 0.41 | 17.03 | 3.45 | 0.36 | 0.25 |
| Qu feng gu tong lu | 6.96 | 1.89 | 0.08 | 0.07 | 3.88 | 2.15 | 0.07 | 0.04 |
| Ling long gan mao jiao nang | 16.52 | 1.08 | 0.23 | 0.17 | 9.79 | 1.16 | 0.22 | 0.10 |
| Xi xian feng shi wan | 7.47 | 5.58 | 0.28 | 0.07 | 3.54 | 2.11 | 0.29 | 0.04 |
| Feng shi zhi ton gao | 7.14 | 0.05 | 0.15 | 0.08 | 3.93 | 1.16 | 0.15 | 0.04 |
| Shen jin dan jiao nang | 10.94 | 3.33 | 0.21 | 0.12 | 5.81 | 3.97 | 0.25 | 0.07 |
| Radix <i>Stephaniae tetrandrae</i> | 233.26 | 1.09 | 0.21 | 5.52 | 185.04 | 1.06 | 0.22 | 4.38 |

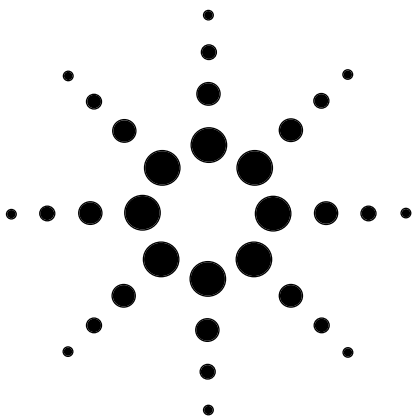
Table 1

Migration time and peak area reproducibility (n=3) and quantitation of tetrandrine and fangchinoline in various traditional Chinese medicines



Agilent Technologies

Innovating the HP Way

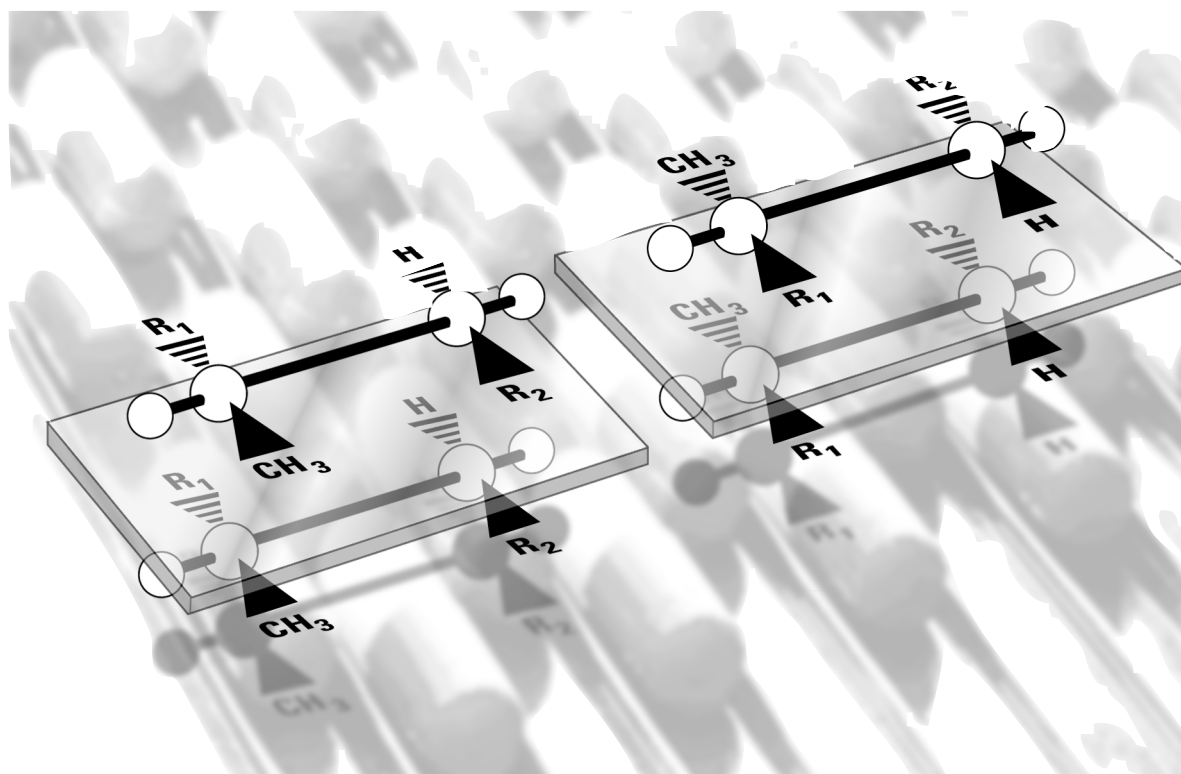


Development of a method for separation of the four stereoisomers of troglitazone using capillary electrophoresis

Application Note

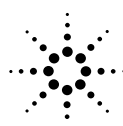
Pharmaceutical

Herbert Godel and Gordon Ross



Abstract

This application note describes the development of a method using capillary electrophoresis (CE) to separate the four stereoisomers of troglitazone. Excellent resolution between the stereoisomers was achieved by using a borate buffer with SDS and Heptakis (2,3,6-tri-O-methyl)- β -cyclodextrin and by optimizing the capillary temperature. Other factors such as the reproducibility of migration times and peak areas were also investigated.



Agilent Technologies
Innovating the HP Way

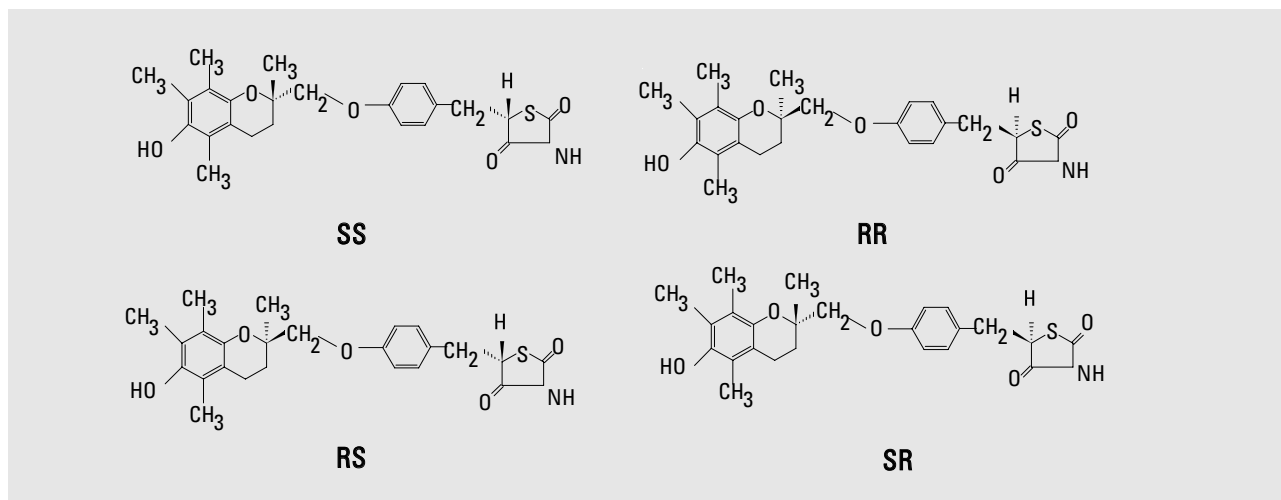


Figure 1
Structures of the four stereoisomers of troglitazone

Introduction

Troglitazone, an enhancer of the action of insulin and inhibitor of hepatic gluconeogenesis, was discovered in the research laboratories of Sankyo Co. Ltd., Tokyo, Japan,^{1,2} and has been shown to be orally effective in both non-insulin dependent and insulin-dependent diabetes mellitus.^{3,6} Troglitazone is an equal mixture of four stereoisomers involving two asymmetric centers at the 2 position of the chroman ring and the 5 position of the thiazolidine ring (figure 1).

In one of the racemates the two enantiomers have the R,R and S,S configuration, respectively, and the enantiomers of the other racemate are the R,S and S,R configuration, respectively. Two of the four stereoisomers that are not mirror images of each other (i.e. S,S and S,R) are diastereoisomers.

The chemical name for troglitazone is (\pm)-5-[4-(6-hydroxy-2,5,7,8-tetramethylchroman-2-ylmethoxy)benzyl]-2,4-thiazolidinedione.

As the pharmacodynamic activities of enantiomers of a drug may differ drastically there is a need to study the pharmacological and toxicological properties of optically active compounds. A reliable and accurate assay is therefore necessary to isolate the stereoisomer of interest.

Chromatography is well suited for the stereospecific analysis of free drugs and drugs in biological fluids and is widely used for this purpose.

Chromatographic techniques including thin-layer chromatography (TLC), gas chromatography (GC), high-performance liquid

chromatography (HPLC), and supercritical fluid chromatography (SFC) have all been employed for chiral recognition. In recent years, capillary electrophoresis has become a powerful technique for the separation of a variety of complex mixtures. The main advantages of CE are its high separation efficiency and low consumption of sample and solvents. Therefore the technique is a very attractive separation tool.

Micellar electrokinetic chromatography (MEKC), an important mode of CE is widely used for the separation of non-polar molecules. This technique uses buffers containing micelles which form a non-polar phase into which molecules can partition. This type of partitioning is equivalent to that in reversed-phase HPLC.

Sodium dodecyl sulfate (SDS), the most widely used anionic surfactant, is an attractive choice because it gives excellent selectivity for a wide range of compounds. It is available in high purity, and is inexpensive.

The separation of diastereoisomers can be successfully achieved by MEKC with achiral micellar solution alone. However, for the separation of enantiomers by MEKC with achiral micelles, a chiral selector is added to the separation buffer. The chiral selectors most used in this method are cyclodextrins (CD). This technique has been called “cyclodextrin modified micellar electrokinetic chromatography” (CD-MEKC). Chiral separation occurs due to the formation of transient non-covalent structures of CD and the diastereoisomers which differ in their energy of formation. In CD-MEKC, the solutes are distributed among three phases: an aqueous phase, the micelle and the CD.

Literature research has shown that of the numerous reports on chiral resolution by CE, about 80 % use one of the cyclodextrins as the optically active reagent. CDs are relatively inexpensive, easy to use, and readily available. CE with its two major modes, capillary zone electrophoresis (CZE) and micellar electrokinetic capillary chromatography is gaining acceptance in the pharmaceutical field for the separation of drugs.

The CE approaches mentioned, are relatively simple when compared with HPLC in which expensive chiral stationary phases are frequently used.

Experimental

All experiments were performed using an Agilent Capillary Electrophoresis system equipped with a diode array detector. An Agilent ChemStation was used for system control, data acquisition and data analysis. Buffer components were of the highest available purity.

The fused-silica capillaries, 50 μm i.d., with effective lengths of either 56 or 72 cm, as noted, were from Agilent Technologies. The capillary was cooled with the Peltier cooling unit built into the CE system. The applied voltage in all cases was 30 kV. Separation conditions for the final method were as follows:

- inlet buffer = 2.5 mM sodium borate pH 9.4, 20 mM SDS, 56 mM Heptakis (2,3,6-tri-O-methyl)- β -cyclodextrin;
- outlet buffer = 2.5 mM sodium borate pH 9.4, 20 mM SDS;
- injection by pressure = 50 mbar for 3 seconds
- capillary length = 72 cm effective, 50 μm i.d.;
- operating temperature = 10 $^{\circ}\text{C}$
- detection by UV at 200 nm.

New capillaries were conditioned by rinsing with 1 N sodium hydroxide, 0.1 N sodium hydroxide, and inlet buffer. The CE instrument was programmed to rinse with inlet buffer for 5 minutes prior to each injection. In order to maintain satisfactory reproducibilities of peak response and migration time, new inlet and outlet vials were used after every five injections.

All buffer solutions and samples were filtered through 0.2 μm filters before use.

The samples used were prepared by dissolution in ethanol, and either injected directly or further diluted with water.

Experimental conditions are given in the individual figure captions.

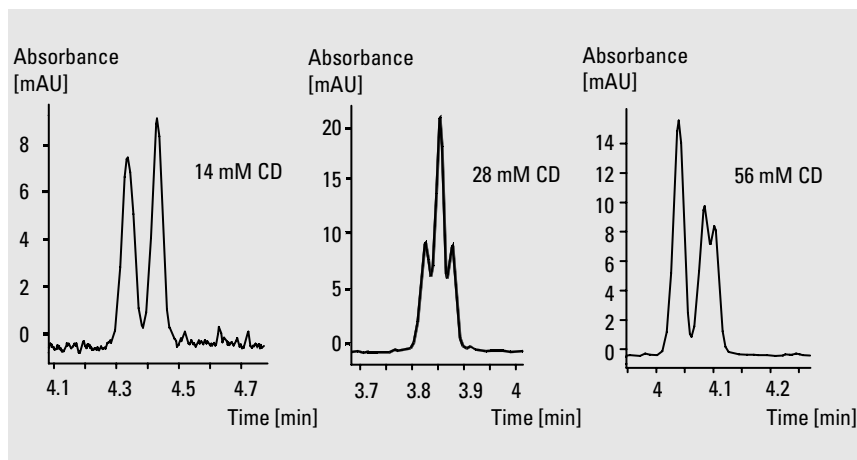


Figure 2
The impact of cyclodextrin concentration on the resolution of Troglitazone stereoisomers

Conditions

Buffer: 2.5 mM borate pH 9.4, 20 mM SDS, Heptakis (2,3,6-tri-O-methyl)- β -cyclodextrin
 Voltage: 30 kV
 Capillary: l = 56 cm, 50 μ m id
 Temperature: 25 $^{\circ}$ C
 Detection: 200 nm, 10 nm Bw

Results and discussion

Initially an HPLC method was used which gave a resolution of about 1 between the first two eluting stereoisomers. It also had a fairly long run time (35 min). Therefore, it was decided to try to develop a method using cyclodextrin-modified MEKC in order to improve the resolution and shorten the run time.

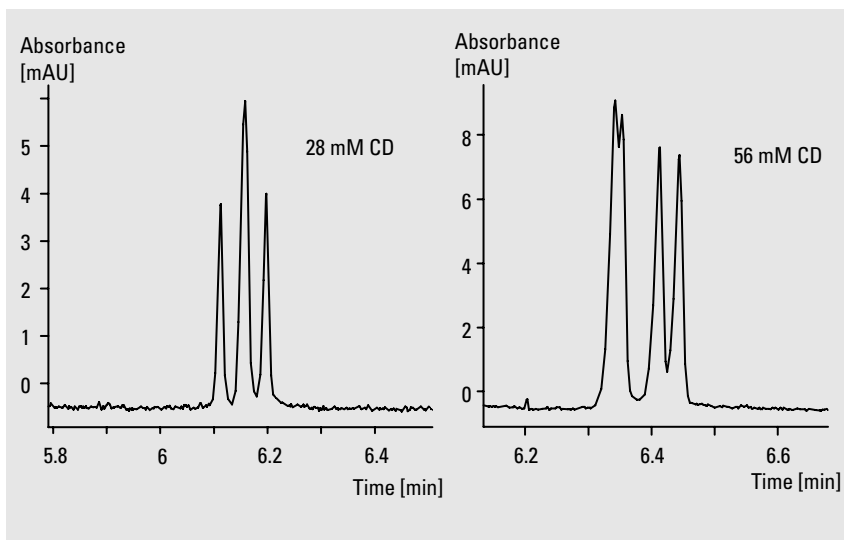
In MEKC the minimum surfactant concentration is defined by the critical micelle concentration (CMC) which is 8 mM for SDS. The optimum concentration is best determined experimentally because the actual CMC is affected by pH and ionic strength of the buffer.

One of the first steps in method development for chiral drugs with cyclodextrins is the selection of the appropriate cyclodextrin. The size of the CD cavity in conjunction with its chemical modifications determines the degree of solute interaction. Chiral recognition is dependent on both the size of the cavity and the lipophilicity of the rim substituents on the CD.

Using γ -cyclodextrin and Heptakis (2,6-di-O-methyl)- β -cyclodextrin no resolution was obtained. Use of Heptakis (2,3,6-tri-O-methyl)- β -cyclodextrin showed clear advantages and a partial resolution of the diastereoisomers was achieved. Figure 2 shows the impact of cyclodextrin concentration on the resolution of troglitazone stereoisomers.

The higher cyclodextrin concentration naturally favors complex formation so the drug spends more time in complexed form. The charge to mass ratio is reduced and likewise its mobility. If the cyclodextrin concentration is too high, valuable separation time may be wasted without meaningful gain in resolution. In some cases there can be an optimum cyclodextrin concentration, below and above which resolution decreases.

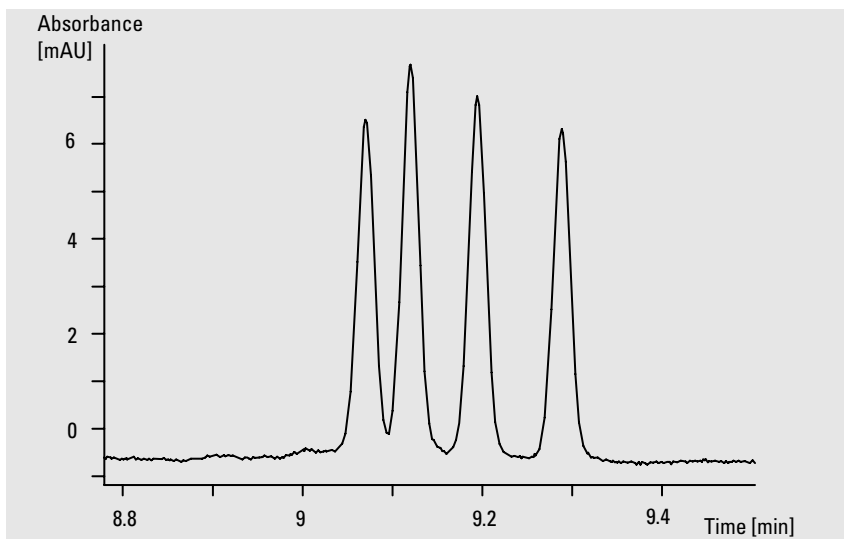
The influence of the capillary length is shown by comparing the rightmost panel in figure 2 and figure 3. The longer the solutes remain in the capillary, the better the differentiation based on the difference of the mobility of the enantiomers.



Conditions

Buffer: 2.5 mM borate pH 9.4, 20 mM SDS, Heptakis (2,3,6-tri-O-methyl)- β -cyclodextrin
 Voltage: 30 kV
 Capillary: l = 72 cm, 50 μ m id
 Temperature: 25 $^{\circ}$ C
 Detection: 200 nm, 10 nm Bw

Figure 3
 Effects of increasing capillary effective length (compare with figure 2)



Conditions

Buffer: 2.5 mM borate pH 9.4, 20 mM SDS, 56 mM Heptakis(2,3,6-tri-O-methyl)- β -cyclodextrin
 Voltage: 30 kV
 Capillary: l = 72 cm, 50 μ m id
 Temperature: 10 $^{\circ}$ C
 Detection: 200 nm, 10 nm Bw

Figure 4
 Optimized separation of the four stereoisomers of troglitazone

By lowering the temperature to 10 $^{\circ}$ C, but using the same concentrations of sodium borate buffer, SDS and cyclodextrin, the separation of all four stereoisomers was achieved with baseline resolution of all peaks (figure 4).

Lowering the capillary temperature increases the migration times since mobility always decreases as viscosity increases. A secondary effect might be an increase in the equilibrium constant since complex stability may be enhanced at low temperatures.

Numerous parameters such as the viscosity of the buffer solution, the pK_a of the solute and the complexation constant with cyclodextrin are directly affected by variations in the temperature. Therefore, it is not surprising that the temperature exerts a great influence on the separation. In some cases, separation can only be obtained at sub-ambient temperatures.

The resolution between the enantiomers was 1.3 for peaks 1 and 2 and 2.5 for peaks 3 and 4.

The corrected peak area reproducibilities for eight injections for each peak were < 2 % RSD, and the migration times < 0.5 % RSD. The percentage of each isomer was calculated using corrected peak areas and were comparable to the label claim. See table 1.

Conclusions

Troglitazone was best resolved into its four stereoisomers by using CD-MEKC with SDS and Heptakis (2,3,6-tri-O-methyl)- β -cyclodextrin dissolved in borate buffer pH 9.4. The advantages of this method over HPLC are that the analysis is less expensive, there is less organic waste, improved resolution and a shorter run time.

| | % isomer corrected peak area | label claim |
|--------|------------------------------|-------------|
| Peak 1 | 23.8 | 21.9 |
| Peak 2 | 27.2 | 28.3 |
| Peak 3 | 25.7 | 26.3 |
| Peak 4 | 23.4 | 23.6 |

Table 1
The percentage isomer using corrected peak area compared to label claim

The best conditions for good separation as well as ruggedness and reproducibility of the method were found to be 2.5 mM sodium borate buffer, 20 mM SDS, and 56 mM Heptakis (2,3,6-tri-O-methyl)- β -cyclodextrin at a capillary temperature of 10 °C. Resolution of the four stereoisomers was dependent on the type of CD used, the CD concentration and the capillary temperature. The precision and day-to-day reproducibility of the method was good. This method can be used to determine the relative amounts of the four stereoisomers in troglitazone tablets.

Acknowledgements

The authors wish to thank Nina Cauchon, Lou Welebob, Roy McCune and Robert Giuffre for their contributions and helpful suggestions.

References

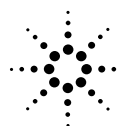
1. T. Yoshioka, T. Fujita, T. Kanai, Y. Aizawa, T. Kurumada, K. Hasegawa, and H. Horikoshi, *J. Med. Chem.* **1989**, 32, 421–428.
2. T. Yoshioka, Y. Aizawa, T. Fujita, K. Nakamura, K. Sasahara, H. Kuwana, T. Kinoshita, and H. Horikoshi, *Chem. Pharm. Bull.*, **1991**, 39(8), 2124–2125.
3. T. Fujiwara, S. Yoshioka, T. Yoshioka, I. Ushiyama, and H. Horikoshi, *Diabetes*, **1988**, 37, 1549–1558.
4. T. Kuzuya, Y. Iwamoto, K. Kosaka, K. Takebe, T. Yamanouchi, M. Kasuga, H. Kajinuma, Y. Akanuma, S. Yoshida, Y. Shigeta, and S. Baba, *Diabetes Res. Clin. Pract.*, **1991**, 11, 147–154.
5. S. Suter, J. Nolan, P. Wallace, B. Gumbiner, J. Olefsky, *Diabetes Care*, **1992**, 15, 193–203.
6. M. Tominaga, M. Igarashi, M. Daimon, H. Eguchi, M. Matsumoto, A. Sekikawa, K. Yamatani, and H. Sasaki, *Endocr. J.*, **1993**, 40 (3), 343–349.
7. S. Terabe, *Trends Anal. Chem.*, **1989**, 8, 129–134.

The authors are application chemists at Agilent Technologies, Waldbronn, Germany

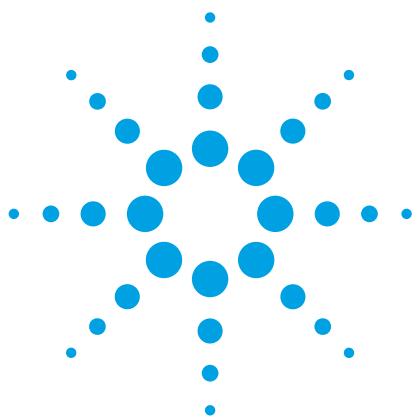
For the latest information and services visit our world wide web site:
<http://www.agilent.com/chem>

Copyright © 1997 Agilent Technologies
All Rights Reserved. Reproduction, adaptation or translation without prior written permission is prohibited, except as allowed under the copyright laws.

Publication Number 5966-3111E



Agilent Technologies
Innovating the HP Way



Oligonucleotide Analysis by Capillary Gel Electrophoresis

Gordon Ross and
Ulrike Jegle

Biopharmaceutical

Abstract

Oligonucleotides cannot be successfully separated according to size using conventional capillary zone electrophoresis (CZE) because they have similar mobilities independent of their chain length. This is due to the addition of equivalent unit charge for every additional nucleotide, and nucleotides themselves have similar masses. This means that their charge to mass ratio remains very similar. Such analytes can be separated according to their chain length by using a sieving matrix. In order to perform this separation the capillary must be filled with a sieving matrix so that smaller oligonucleotides move faster through the capillary than larger, slower moving analytes. By using the Agilent Oligonucleotide Kit, combined with the Agilent Capillary Electrophoresis system, oligonucleotides can be separated. The kit comprises a choice of sieving polymers which can be tailored to the sample under study. In order to correctly identify analytes by their size, a high degree of reproducibility is also necessary between standards and samples. This is achieved by using a PVA coated capillary and the Oligonucleotide Kit. The kit may be used to analyze single and double stranded DNA oligonucleotides, single stranded RNA oligonucleotides and antisense oligonucleotides. The sieving polymer solutions have been optimized for separating oligonucleotides with a chain length 5 to 80 nucleotides.

Experimental

All experiments were performed using the Agilent Capillary Electrophoresis system equipped with diode array detection and computer controlled via Agilent ChemStation software. Oligonucleotides were separated using the Oligonucleotide Kit (order number 5063-6530).

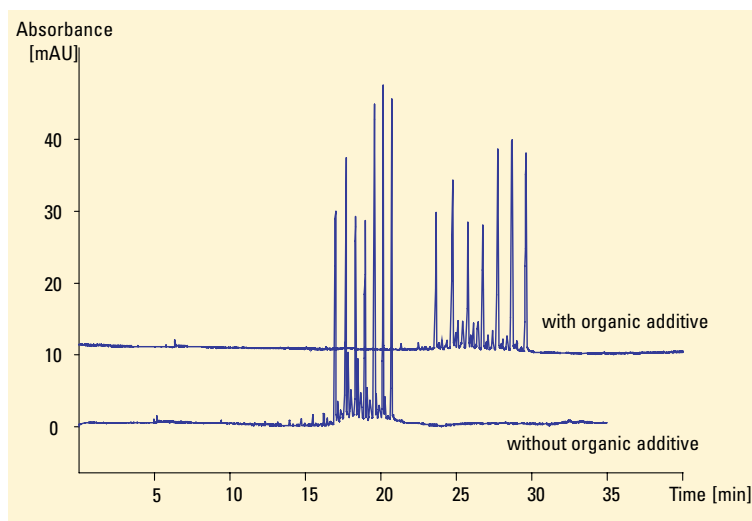


Figure 1
Separation of oligonucleotide standard pd(A) 12–18 using polymer solution A and polymer solution B

Conditions

Buffer Oligonucleotide kit neutral buffer (order number 8500-6886)
Sieving Solution Polymer solution A (order number 8500-6887) or B (8500-6889)
Capillary PVA coated 24.5 cm eff × 100 μm i.d. (order number G1600-60419)
Flush Regimen High pressure flush from outlet -7.5 bar for 3 minutes
Injection 7 s at -10 kV
Run -25 kV, 30 °C
Detection 260 nm/8 nm DNA filter (order number G1600-62700)
Sample Oligonucleotide pd(A) 12–18



Agilent Technologies
Innovating the HP Way

Figure 1 shows the separation of an oligonucleotide standard pd(A) 12–18 using polymer solution A and polymer solution B. In this case the organic additive in polymer solution B enhances the resolution of the separation. Reproducibility and robustness are demonstrated in figure 2 by the highly reproducible migration times taken from an exemplary 6 runs at 0.35 % RSD over 73 runs. The kit can be used for checking the purity of oligonucleotide preparations (figure 3) with the benefit of being able to tailor the polymer solution to the needs of the analysis. In this case using solution A—without organic—provides a better resolution of the 15–mer failure sequence in this 16–mer oligonucleotide.

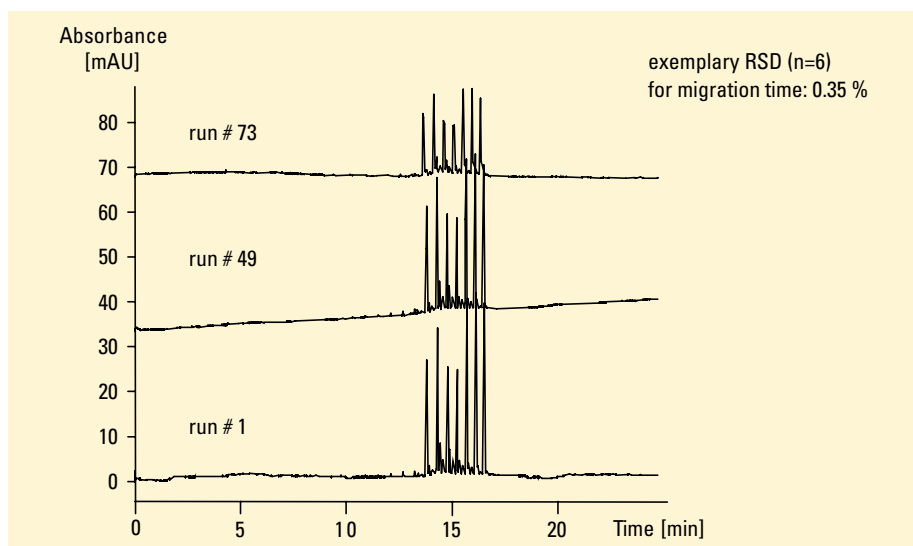


Figure 2
Reproducibility of migration time—polymer solution

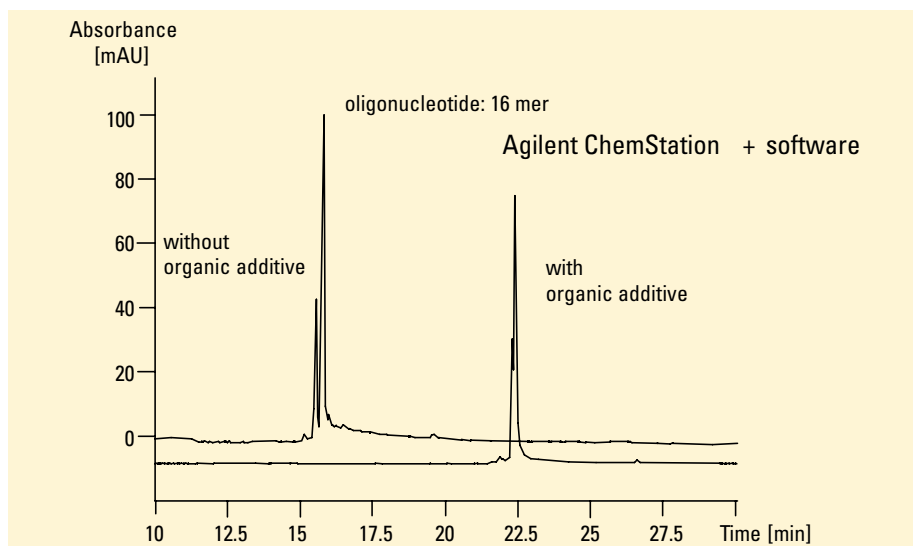


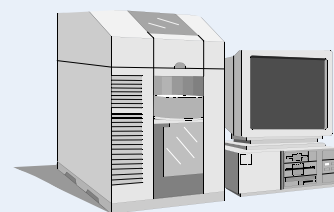
Figure 3
Optimal polymer solution for purity check

Conclusions

The Agilent Oligonucleotide Kit is suitable for the analysis of oligonucleotides in the range 5 to 80–mers. Migration time reproducibility can be achieved at less than 1 % RSD for both the polymer A and polymer B.

Equipment

- Agilent Capillary Electrophoresis system
- Agilent CE high-sensitivity detection cell
- Agilent ChemStation + software



The authors are application chemists at Agilent Technologies, Waldbronn, Germany.

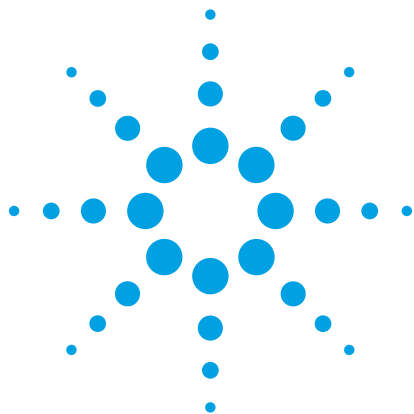
For more information on our products and services, visit our worldwide website at <http://www.agilent.com/chem>

© Copyright 1997 Agilent Technologies
Released 06/97
Publication Number 5965-9037E



Agilent Technologies

Innovating the HP Way



High Sensitivity SDS-protein Separations by Capillary Electrophoresis

Gordon Ross

Biopharmaceutical

Abstract

Conventional electrophoresis (CE) of SDS-protein complexes is performed on a 2-dimensional slab, gel manufactured from polyacrylamide. This allows the on-gel staining of the separated protein complexes using such techniques as silver staining which although offering the highest sensitivity is, however, not quantitative. At best this technique is semi-quantitative due to the staining and detection (densitometry) techniques used to quantitate the separated bands. Capillary electrophoresis is inherently a quantitative instrumental method of analysis. CE may be used in conjunction with replaceable gel matrices in order to separate SDS-protein complexes with high resolution.

Experimental

All experiments were performed using the Agilent Capillary Electrophoresis system equipped with diode array detection and computer controlled via Agilent ChemStation software. The instrument was fitted with the Agilent CE high sensitivity detection cell offering an increased pathlength of 1.2 mm and increased linear range to approximately 1300 mAU with less than 1 % deviation from linearity.

The capillary was filled with the sieving gel using the internal 1 bar pressure of the Agilent CE system. The time taken to fill and replace the capillary contents was approximately 10 minutes.

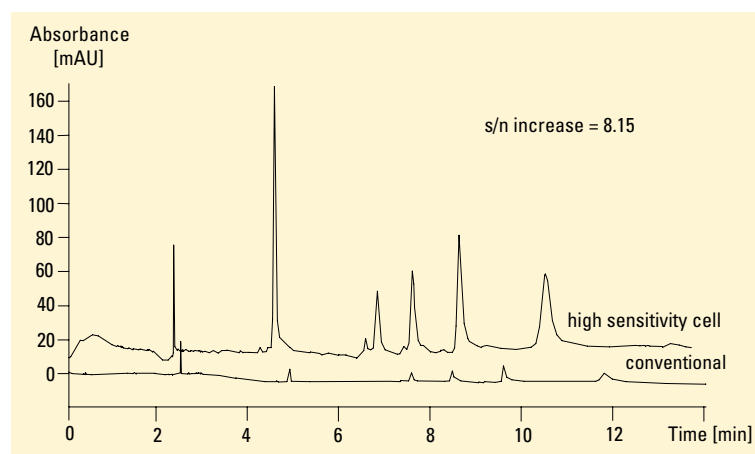


Figure 1
SDS-protein capillary gel electrophoresis

Figure 1 illustrates the increases in sensitivity obtained over the supplied BioRad SDS-protein kit

Conditions

Capillary 400 mm (485) × 75 μm i.d.

Buffer

BioRad SDS-protein sieving buffer

Injection 5 s at -10 kV

Run -15 kV

Temperature 40 °C

Detection 220 nm/30 nm high sensitivity detection cell



Agilent Technologies

Innovating the HP Way

using the Agilent CE high sensitivity detection cell. In comparison to the results obtained from the 50 μm i.d. capillary used in the BioRad kit the signal to noise was increased by a factor of approximately 8.5 for each peak. A graph of log MW versus migration time relative to that of the reference peak (benzoic acid) provides a linear relationship with $r^2 = 0.9988$ (figure 2).

Conclusions

The Agilent CE high sensitivity cell can be used in for capillary gel electrophoresis experiments. In conjunction with bare fused silica capillaries, increases in sensitivity of over 8-fold can be achieved for SDS-protein determinations.

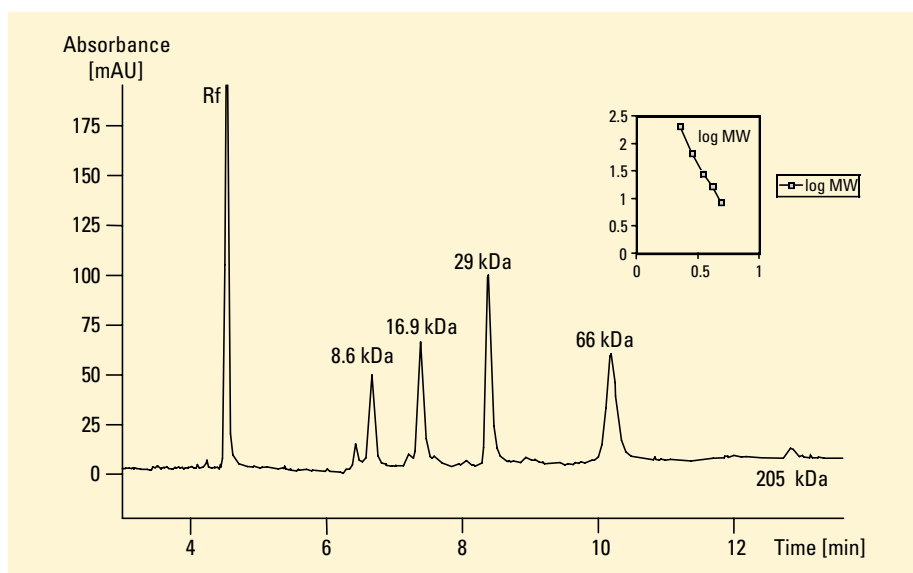
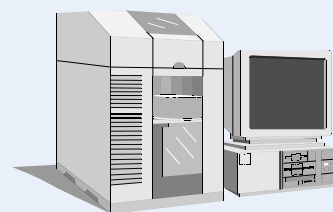


Figure 2
SDS-protein capillary gel electrophoresis with high sensitivity cell

Equipment

- Agilent Capillary Electrophoresis System
- Agilent CE high-sensitivity detection cell
- Agilent ChemStation + software



Gordon Ross is application chemist at Agilent Technologies, Waldbronn, Germany.

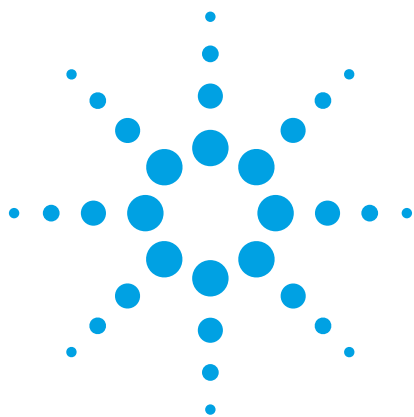
For more information on our products and services, visit our worldwide website at <http://www.agilent.com/chem>

© Copyright 1997 Agilent Technologies
Released 06/97
Publication Number 5965-9035E



Agilent Technologies

Innovating the HP Way



Ultra-Low Level Impurity Analysis by Capillary Zone Electrophoresis

Gordon Ross

Pharmaceutical/
chemical

Abstract

Capillary zone electrophoresis (CZE) is an inherently high efficiency liquid phase separation technique. This makes it very suitable for the separation of closely related compounds and can be of particular use in the analysis of drug impurities. Regulatory requirements demand the demonstration of the purity of any drug substance and the acceptable criteria for presence of impurities are around 0.1 %. This means that the analysis not only has to have an adequate sensitivity, but also that the linear range is such that the minor component may be quantitatively reported as a corrected (area/area) percent of the main component. By using the Agilent CE high sensitivity detection cell, sensitivity can be increased by an order of magnitude, with linearity increased over 3-fold compared to conventional capillaries. This enables the determination of impurities in drug substances below the 0.1 % area/area level. Figure 1 shows the linear range achievable using the high-sensitivity cell, illustrating its linearity over 2.2 AU.

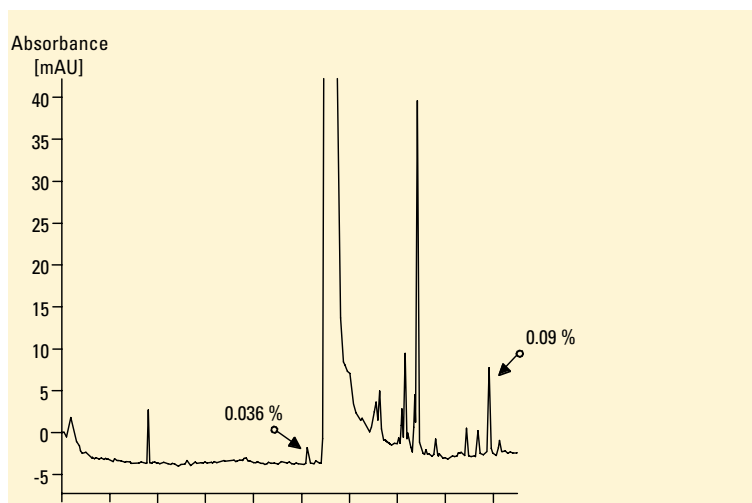


Figure 1
Linear range of high sensitivity cell

Experimental

All experiments were performed on the Agilent Capillary Electrophoresis system which is computer controlled via Agilent ChemStation software. High sensitivity detection was achieved using the Agilent CE high-sensitivity detection cell (order number G1600-68713) and capillaries.



Agilent Technologies
Innovating the HP Way

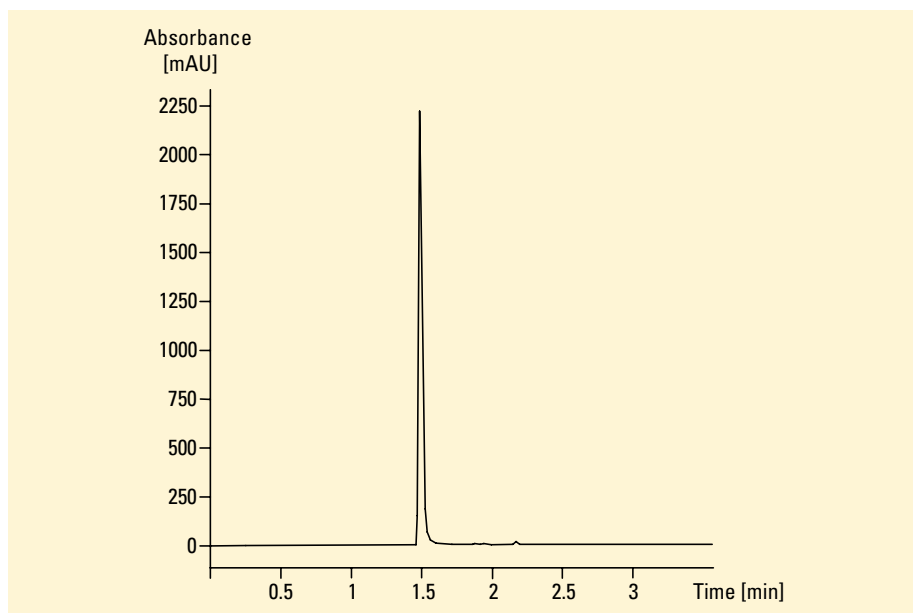


Figure 2
CZE analysis of ranitidine

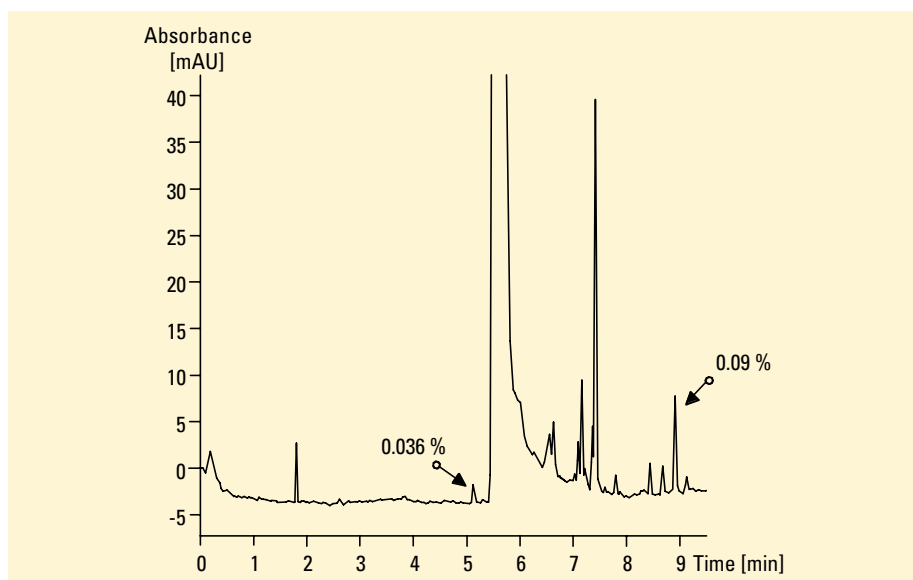


Figure 3
Low level determination of ranitidine impurities

During a shelf life study of ranitidine, the anti-ulcer drug was analyzed for the presence of impurities after 12 months exposure to light and room temperature. Figure 2 shows the analysis of the main peak indicating that this is at the upper levels of the linear range of detection. An expanded view of the base of the peak shows the number of impurities present at very low levels. Given the linear range of the detection cell, it is possible to calculate the impurity level of these peaks at less than 0.1 % area/area of the main peak.

Conditions (figures 2, 3)

Buffer 20 mM borate pH 9.3
Capillary 56 cm eff (64.5) × 75 μm i.d.
Injection 200 mbars
Run 20 °C, 30 kV
Detection 225/20 nm (high sensitivity cell)

Conclusions

CZE in conjunction with the high-sensitivity detection cell, may be used to determine impurity levels in drugs at less than 0.1 % area/area. This level is appropriate to that required for regulatory submissions.

Equipment

- Agilent Capillary Electrophoresis system
- Agilent CE high-sensitivity detection cell
- Agilent ChemStation + software

Gordon Ross is application chemist at Agilent Technologies, Waldbronn, Germany.

For more information on our products and services, visit our worldwide website at <http://www.agilent.com/chem>

© Copyright 1997 Agilent Technologies
 Released 06/97
 Publication Number 5965-9034E



Analysis of Steroid Isomers by Capillary Electrochromatography

Gordon Ross and
Rainer Schuster

Pharmaceutical

Abstract

Capillary electrochromatography (CEC) is a fusion of capillary electrophoresis and liquid chromatography which preserves and exploits the best aspects of both techniques. The separation is achieved for neutral molecules essentially through chromatographic selectivity mechanisms, while the mobile phase is propelled through the packed capillary by electromotive forces. Efficiencies can be increased by as much as ten-fold, compared with conventional LC systems. Such increases in efficiency can allow faster method development times and also separations of very closely related compounds. This application brief contrasts the first-pass separation of α and β isomers of 17-hydroxyoestradiol using HPLC and CEC. These isomers differ only by the position of the 17-OH group (figure 1).

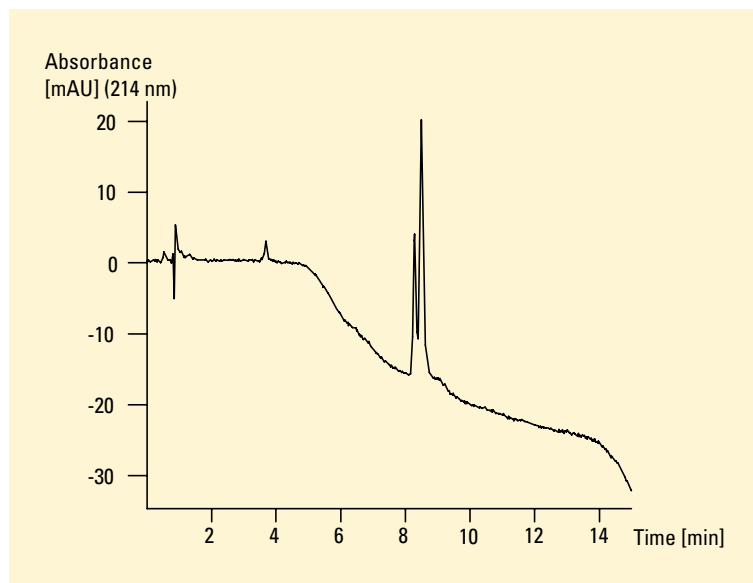


Figure 2
Separation of alpha and beta 17-OH estradiol by HPLC

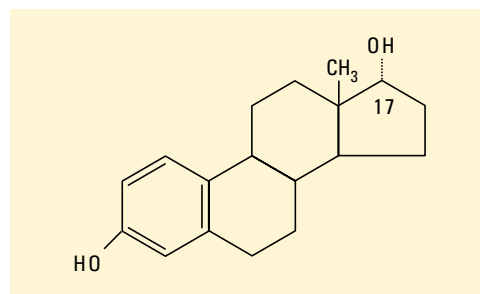


Figure 1
Structure of 17-OH estradiol

Conditions

Column 3 μ m ODS 125 mm \times 2 mm i.d.

Mobile Phase

NH₄Ac pH 7.0/acetonitrile (50/50)

Flow 0.26 ml/min

Temp 38 $^{\circ}$ C



Agilent Technologies

Innovating the HP Way

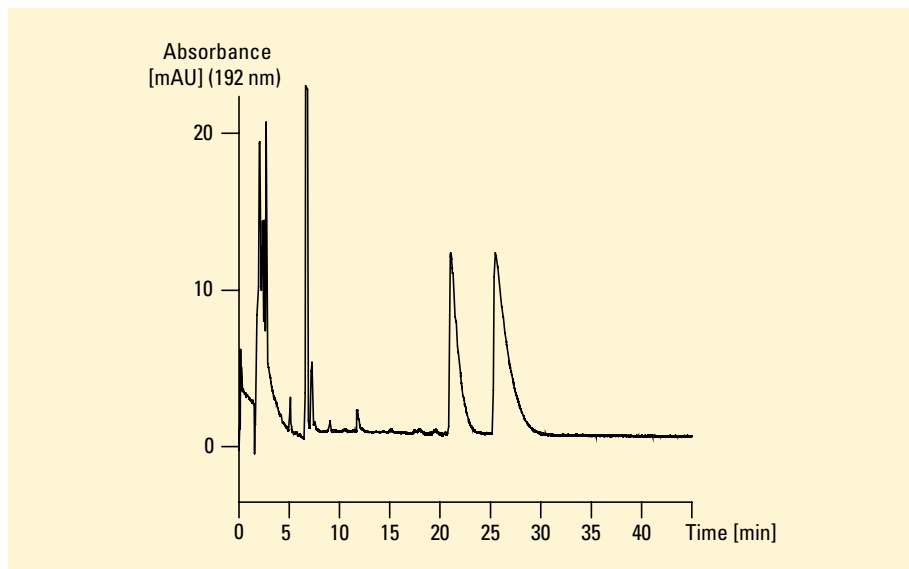


Figure 3
Separation of alpha and beta 17-OH estradiol isomers by CEC

Experimental

The CEC separation was performed using the Agilent Capillary Electrophoresis system equipped with diode array detector and computer controlled via Agilent ChemStation software. CEC capillary columns were Agilent CEC C18. The Agilent CE system is uniquely designed for operating CEC in that it can apply up to 12 bar pressure simultaneously to both vials in order to suppress bubble formation and maximize reliability.

HPLC of the isomers was carried out using a HP 1090 Series II liquid chromatograph equipped with diode-array detection and computer controlled via Agilent ChemStation software.

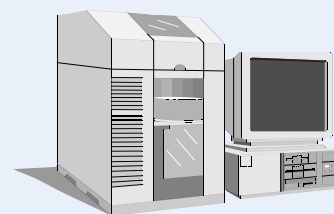
Figure 2 shows the separation obtained from HPLC analysis of these compounds. However in obtaining a rapid analysis the compounds are only partially resolved. When using CEC (figure 3) for separation, it should be noted that the retention time is markedly increased. This is due to the difference in stationary phase since the CEC phase has been specifically designed to meet the requirements of CEC. The two isomers are however well resolved and fully capable of quantitation.

Conditions

Column Agilent 3 μ m CEC C18, 250 mm (335 mm) \times 0.1 mm id
Mobile Phase 25 mM TRIS/acetonitrile (5/95)
Voltage 25 kV
Temperature 30 $^{\circ}$ C
Injection 10 s at 10 kV
Pressure 10 bar both sides

Equipment

- Agilent Capillary Electrophoresis System
- Agilent 1090 Series II LC
- Agilent ChemStation + software



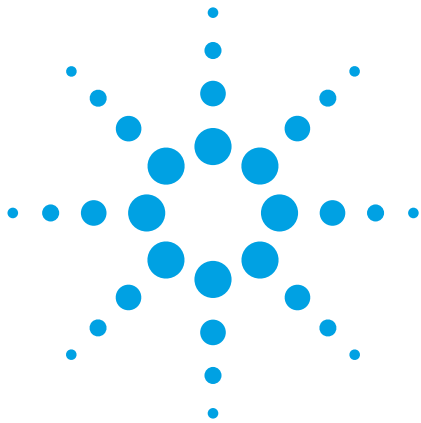
Gordon Ross and Rainer Schuster are application chemists at Agilent Technologies, Waldbronn, Germany.

For more information on our products and services, visit our worldwide website at <http://www.agilent.com/chem>

© Copyright 1997 Agilent Technologies
Released 06/97
Publication Number 5965-9030E



Agilent Technologies
Innovating the HP Way



Integrated Biology Solutions

The Agilent 2100 Bioanalyzer System - A Compliant Tool in Life Sciences

IQ OQ/PV 21CFR part 11

Technical Overview

The Agilent 2100 Bioanalyzer is an integrated, inexpensive, compliant solution for the analysis of nucleic acids, proteins, or cells. The new Agilent 2100 expert software (G2946CA) enables users to run the Agilent 2100 Bioanalyzer in regulated lab environments. With IQ (Installation Qualification), OQ/PV (Operational Qualification /Performance Verification) compliant services, and 21CFR part 11 compliance, the system can easily be used for the quality control and analysis of antibodies, protein pharmaceuticals, and other biomolecules such as RNA and DNA.

The Agilent 2100 Bioanalyzer Solution

Since the introduction of the Agilent 2100 Bioanalyzer in 1999, the application portfolio of the 2100 Bioanalyzer has increased steadily. This multi-purpose system is able to analyze DNA, RNA, proteins, and cells on one platform. The Agilent 2100 solution comprises the bioanalyzer instrument, software, as well as application-specific consumables (chip kits). Using the lab-on-a-chip technology, the 2100 Bioanalyzer integrates sample handling, separation, detection, and data analysis on a microfluidic chip. This approach greatly reduces analysis time and sample amount. Depending on the application, up to 12 samples can be automatically analyzed in less than 30 minutes. Data is acquired and archived in digital format. With the introduction of the Agilent 2100 Bioanalyzer expert software (G2946CA) and Agilent 2100 security pack software (G2949CA), the operational area of the 2100 Bioanalyzer is extended further. The software now supports IQ, OQ/PV, and

with security pack loaded, 21CFR part 11 compliance, (electronic signatures, and records regulations). This is a prerequisite for use of the Agilent 2100 Bioanalyzer in regulated environments, for example, in pharmaceutical QA/QC labs. A tight quality control of the consumables combined with a lot-specific declaration of conformity to manufacturing specifications ensures the high quality of the LabChip kits and reagents [1]. Agilent Technologies' declaration of conformity for the 2100 Bioanalyzer instrument and the declaration of system validation for the Agilent 2100 expert and security pack software complete the design qualification (DQ) documentation. (See Figure 1.)

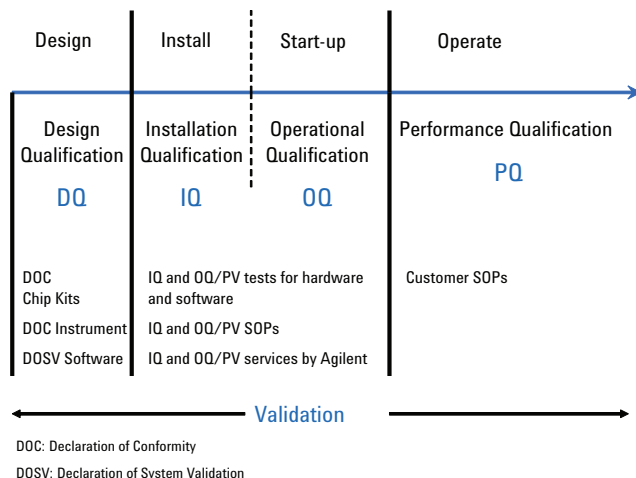


Figure 1. The four 'Q's of compliance, Design Qualification (DQ), Installation Qualification (IQ), Operational Qualification (OQ) and Performance Qualification (PQ). Agilent provides services for DQ, IQ and OQ. Standard Operating Procedures (SOPs) are developed by the customer for PQ.

The Agilent 2100 Expert Software

The Agilent 2100 expert software (G2946CA) has been upgraded to include a new functionality that will objectively assess the quality of an RNA sample. The proprietary algorithm will independently and automatically provide a RIN score (RNA Integrity Number), determining the integrity of the sample. The RIN algorithm has been “trained” using a neural network to assess the overall quality of the sample by comparing six key areas of the sample’s electropherogram. The RIN score provides a valuable tool for all researchers working in the RNA QC field. With the added functionality of 21CFR part 11 compliance and electronic signatures, the bioanalyzer is positioned to be the instrument used for the validation of biomolecules whether the sample is RNA, DNA, cells, or proteins.

The hardware and software requirements for the 2100 expert software are listed below:

PC hardware (minimum requirements):

- CPU: Pentium IV
- RAM: 512 Mbyte
- Ports: 1–2 serial ports
- VGA: Resolution of 1024 × 768
- Hard Disk: 60 Gbyte

The software can control two instruments from one PC using the two RS232 comports to connect to the individual instruments. To operate the instrument, a valid license key for instrument control is required. In addition, separate licenses are required to activate the different modules in the software. There are three modules available in the 2100 expert bioanalyzer software: electrophoresis (G2947CA), cell fluorescence (G2948CA), and security pack (G2949CA). Cell fluorescence and electrophoresis license keys provide access to their respective assays, such as antibody staining, apoptosis, etc. for cell fluorescence, and the electrophoresis license is used for the associated molecular assays, DNA, RNA, and protein. The security pack module allows for operation in a fully secure environment, meaning that no one can acquire or access data without a proper user account and identification. All actions performed within the secured environment are tracked and documented with a clear, traceable audit trail. If no license keys are provided, software functionality is limited to data review and evaluation mode only.

A dedicated ‘Declaration of System Validation’ ensures that the 2100 expert software was developed according to the quality process and life cycle followed by the ‘Life Sciences and Chemical Analysis’ division of Agilent Technologies. Life cycle checkpoint details were reviewed and approved by management. The product was found to meet its functional and performance specifications, and release criteria on the release to shipment date.

Compliance Products and Services for the Agilent 2100 Bioanalyzer System

With the 2100 expert software, Agilent offers compliance services for the 2100 Bioanalyzer system. Compliance services can be purchased any time. A certified customer engineer will test and verify the functionality of the hardware and software, thereby qualifying the system. Table 1 summarizes the options that are available for B- and C- Type bioanalyzer instruments (with serial numbers above DE 13701001). For A-type instruments (with serial numbers lower than DE 13701000), the 2100 expert software supports running OQ/PVs based on a SOP developed by the customer.

Table 1. List of Compliant Services Available

| Description Option | Service | Product number | |
|--------------------------|---------|----------------|-----|
| 2100 Bioanalyzer system* | IQ | R1015A | – |
| 2100 Bioanalyzer system* | OQ/PV | R1016A | – |
| 2nd cartridge | OQ/PV | R1016A | 001 |
| 2nd 2100 Bioanalyzer | OQ/PV | R1016A | 002 |
| Security pack | OQ/PV | R1016A | 003 |

* System comprises 2100 Bioanalyzer instrument, 2100 expert software, and one cartridge of choice.

Instrument Qualification

IQ ensures upon delivery that the Agilent 2100 Bioanalyzer instrument and the 2100 expert software are installed correctly from the moment the components are unpacked to the point the system is ready for operation – documenting the completeness of shipping, the operating environment, and the components of the system. The IQ includes tests to verify that the software and hardware are installed properly and that all electrical connections are correct. The correct installation of computer software is checked by the verification part (in the verification context) of the 2100 expert software.

IQ should be performed after installation of hardware or software.

The IQ services for the Agilent 2100 Bioanalyzer system include:

Hardware IQ

- Shipment checklist
- Installation according to checklist
- Documentation of instrument details
- System checkout using the autofocus chip to generate a signal
- Certification (document and sign) – audit-ready documentation confirming correct installation of the bioanalyzer

Software IQ

- Software check – IQ tool checks the integrity and revision of the program components
- Certification (document and sign) – audit-ready documentation confirming correct installation of the 2100 expert software

Operational Qualification

The OQ is the process of demonstrating that an instrument will function according to its operational specifications in the selected environment [2]. The OQ does not test to ensure the instrument meets the manufacturer's performance specifications. The Operational Qualification ensures basic accuracy of the system and its ability to function properly. OQ is performed after IQ, to verify and document an Agilent instrument's ability to meet specified performance criteria after it is installed. The OQ involves a comprehensive test of the complete system using established conditions. A key benefit to this procedure is to ensure the basic accuracy and precision of the 2100 Bioanalyzer system and to uncover any potential problems before they occur. (See Figure 2). Agilent recommends that preventive maintenance be performed on the instrument prior to an OQ.

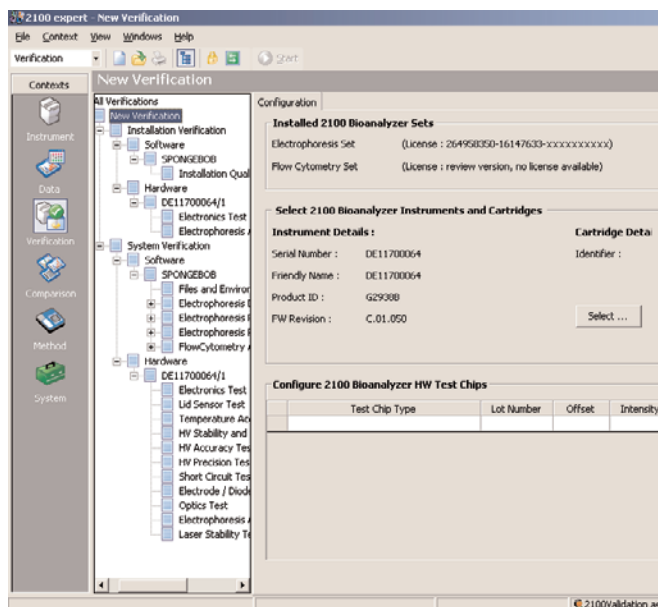


Figure 2. The verification context of the 2100 expert software.

OQ should be performed:

- After installation of hardware or software (after the initial installation)
- After major events, such as repair, upgrades, or relocation
- After any software change that affects system security, data integrity, or administrative controls
- At regular intervals during routine use

The OQ/PV services for the Agilent 2100 bioanalyzer system include:

Hardware OQ/PV

- Instrument validation tests - for example, short circuit test, High Voltage (HV) stability test, HV accuracy test, temperature test, autofocus test, electrode/diode test, laser stability test, etc. using the diagnostic chips provided with the system
- Audit-ready documented evidence confirming that the Agilent 2100 Bioanalyzer is performing according to its operational specifications in the user's lab

Software OQ/PV

- Data calculation engine and software algorithm test
- Test of data files compared with master files
- Audit-ready documented evidence confirming that the Agilent 2100 expert software is performing according to its operational specifications in the user's lab

21CFR part 11 Compliance

Full FDA compliance requires that the software fulfills all rules defined under 21CFR part 11. 21CFR part 11 specifies the requirements of electronic recording, such as data security, data integrity, and audit traceability. With the addition of the security pack module, the 2100 expert software (G2949CA) is now fully compatible with 21CFR part 11. Users are clearly identifiable with distinct user names and passwords. Users are first defined in the operating system and then are set-up with specified roles and functions for use in the 2100 Expert software by the administrator. The different roles available are:

| Operator | Permission |
|----------------------|--------------------------------|
| Standard Operator | Run Methods |
| Advanced Operator | Develop and modify methods |
| 2100 Administrator | Setup of users |
| Backup Operator | Archiving/De-archiving files |
| Validation Operator | Validation of system |
| 2100 Unlock Operator | Unlock system after timing out |
| 2100 Guest | Review of data (read only) |

The expert software limits the functionality of the user as defined by their role, that is, a standard operator cannot act as a validation operator or vice versa. A customer-defined method is developed detailing the instrument and assay type used for the measurement. The method further details the functions of the user for the particular method, that is the number of peer review cycles the data must go through before final approval or rejection of the sample. All adjustments or manipulation of the data is tracked in the secure area and is accompanied by an electronic signature.

Conclusion

With the introduction of the 2100 Expert software (G2946CA), Agilent Technologies addresses the needs of customers in pharmaceutical QA/QC labs and manufacturing departments. By offering IQ and OQ/PV support services, the usage of lab-on-a-chip technology is extended to customers working in regulated environments. The added functionality of the security pack (G2949CA) enables the Agilent 2100 Bioanalyzer to be a fully compliant solution for the analysis of nucleic acids, proteins, or cells.

References

1. T. Preckel, M. Valer, and M. Kratzmeier, "Quality Control for the Agilent 2100 Bioanalyzer Protein 200 Plus LabChip Kits", Agilent Technologies, publication 5989-3336EN
2. P. Bedson, and M. Sargent, (1996), "The development and application of guidance on equipment qualification of analytical instruments", *Accreditation and Quality Assurance*, **1 (6)**, 265–274.

Agilent Online Resources at your Fingertips

- Ask the Experts - Learn how to get the most out of your Agilent products.
- Special offers - Benefit from savings on Agilent products and services.
- Events calendar - See Agilent at leading industry conferences and trade shows.
- Web links - Go directly to detailed information on the Web.

About Agilent's Integrated Biology Solutions

Agilent Technologies is a leading supplier of life science research systems that enable scientists to understand complex biological processes, determine disease mechanisms and speed drug discovery. Engineered for sensitivity, reproducibility and workflow productivity, Agilent's integrated biology solutions include instrumentation, microfluidics, software, microarrays, consumables and services for genomics, proteomics and metabolomics applications.

For More Information

Learn more:

www.agilent.com/chem/labonachip

Buy online:

www.agilent.com/chem/store

Find an Agilent customer center in your country:

www.agilent.com/chem/contactus

U.S. and Canada

1-800-227-9770

agilent_inquiries@agilent.com

Europe

info_agilent@agilent.com

Asia Pacific

adinquiry_aplsca@agilent.com

Agilent shall not be liable for errors contained herein or for incidental or consequential damages in connection with the furnishing, performance, or use of this material.

Information, descriptions, and specifications in this publication are subject to change without notice.

© Agilent Technologies, Inc. 2005

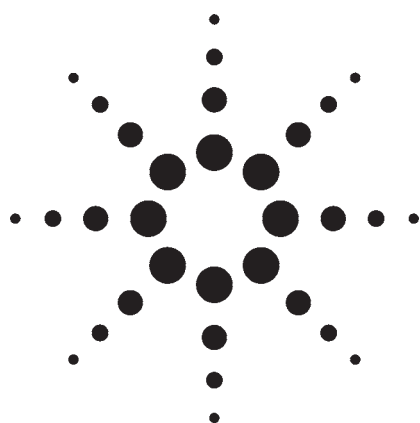
Printed in the USA
December 27, 2005
5989-4278EN



Agilent Technologies

Quality Control for the Agilent 2100 Bioanalyzer Protein 200 Plus LabChip Kits

Technical Overview



Proteomics

Authors

Tobias Preckel, Marc Valer, and Martin Kratzmeier
Agilent Technologies, Inc.
Waldbronn, Germany

Introduction

Lab-on-a-Chip (LoaC) technology has had a major impact on the automation of protein analysis. Traditionally, SDS-PAGE gels are run for sizing and quantitation of proteins. Microfluidic protein analysis is now beginning to replace this traditional method. In August 2002, the Food and Drug Administration (FDA) announced a significant new initiative, pharmaceutical-current Good Manufacturing Practices (GMPs) for the 21st Century, to enhance and modernize the regulation of pharmaceutical manufacturing and product quality. With the increasing focus on proteins as pharmaceutical drugs and diagnostic tools, there is a strong demand for standardized and reproducible protein analysis methods that comply with GLP (good laboratory practices), GMP, and 21CFR Part 11 requirements. Here, LoaC technology can offer a benefit. For protein analysis, it integrates sample handling,

separation, staining, destaining, detection, and digital data processing. In addition, due to the integration of several individual procedures, an increase in throughput and reproducibility can be achieved. However, the quality of the reagents and consumables is crucial to obtain high quality and reliable data. This technical note describes some of the typical quality control tests and specifications that apply to the Protein 200 Plus LabChip kits.

Protein 200 Plus Assay Specifications

The specifications of the bioanalyzer Protein 200 Plus assay are shown in Table 1. These were conservatively set, and compliance of the assay with these specifications was demonstrated across a large number of instruments and sample conditions (such as salt content and individual users). With regard to the accuracy of sizing protein samples, the results are typically within 20% C.V. of the expected value. However, it is important to keep in mind that specific proteins or modified proteins (such as glycosylated proteins) can migrate differently than would be expected from their molecular weight (MW) depending on their structure and modification [1].



Agilent Technologies

Table 1. Protein 200 Plus Assay Specifications

| | |
|------------------------------------|--|
| Sizing range | 14–200 kDa |
| Typical sizing accuracy | 20% C.V.* |
| Sizing reproducibility | 10% C.V.* |
| Sizing resolution | 10% difference in MW |
| Minute detectable concentration | |
| PBS | 20 µg/mL (BSA) |
| 0.5 M NaCl | 40 µg/mL (BSA) |
| Max. protein concentration | 4 mg/mL |
| Linear dynamic range | 20–2000 µg/mL |
| Quantitation reproducibility | 20% C.V. |
| Sample buffer myosin calibration | HSA standard curve slope: 0.8–1.2 |
| Ladder quality | No major impurities, minor impurities at 18 and 25 kDa |
| Ladder quantity | Mean peak height >100 FU |
| Physical specifications | |
| Samples per chip: | 10 + ladder |
| Time to first result: | 5 min |
| Time to last result: | 25 min |
| Minimum volume of sample required: | 4 µL |

*C.V. (coefficient of variation) is defined as standard deviation × 100/average of measured values.

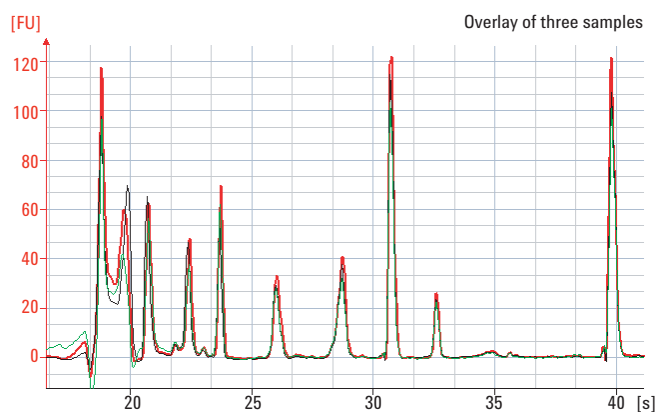
Sizing Accuracy and Reproducibility

Figure 1A highlights the resolution of individual protein bands. The overlay of 3 individual runs (one chip) indicates excellent measurement reproducibility. The table below Figure 1A shows the accuracy and reproducibility of the sizing data obtained with the Protein 200 Plus assay for the individual protein bands in the standard. In this

case, sizing accuracy was within 90% or better of the expected size. In Figure 1B, accuracy and reproducibility of sizing was investigated for carbonic anhydrase on four instruments and two different buffer conditions. The average size of 28.6 kDa compares well with the mass-spectrometry-determined size of the protein [2]. The graph shows that sizing does not depend on the salt concentration.

A) Sizing accuracy and reproducibility

(Bio-Rad CE-SDS protein size standard, Order no. 148-2015, non-catalog item)



| Expected | 14 | 21 | 31 | 45 | 66 | 97 | 116 | kDa |
|----------|------|------|------|------|------|------|-------|-----|
| Average | 13.3 | 20.5 | 28.5 | 44.5 | 67.8 | 94.2 | 118.5 | kDa |
| SD | 0.5 | 0.5 | 0.5 | 0.5 | 1.3 | 0.8 | 0.5 | |
| CV | 3.9 | 2.7 | 1.9 | 1.2 | 2.0 | 0.8 | 0.5 | |

B) Sizing reproducibility

Carbonic anhydrase, Sigma order no. C-2273, 100 µg/mL in PBS or 0.5 M NaCl

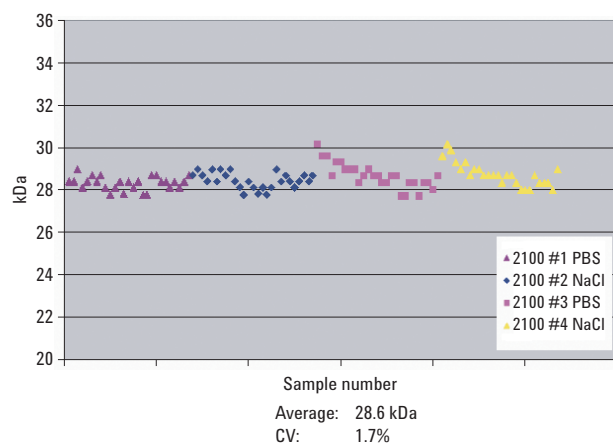


Figure 1. A) Sizing Resolution. A protein standard (BioRad CE-SDS Protein Standard, order no. 148-2015) was diluted 1:10 in phosphate buffered saline (PBS). Two µL were mixed with 4 µL of sample buffer (supplied in kit) and were run on a Protein 200 Plus LabChip (27 samples on three different instruments). A representative overlay of individual samples of one chip is shown. **B) Sizing Reproducibility.** One hundred µg/mL carbonic anhydrase (Sigma order no. C-2273) in either PBS or in 0.5 M NaCl were run on several chips on four instruments. The experimentally determined size of the protein is plotted against the sample number, and each dot represents an individual measurement. The MS determined size is 29.000 Da [2]. Twenty-seven samples were run on a total of 18 chips by two independent users. Two reagent batches and two chip batches were used.

Sizing Resolution

Figure 2 shows the quality of sizing resolution of a self-mixed protein standard for two independent runs from two different validation tests.

β -lactoglobulin (18.7 kDa) and trypsin inhibitor (20.8 kDa), which differ in molecular weight (MW) by 10%, were well separated in both runs. Also, carbonic anhydrase I was separated from carbonic anhydrase II (28.3 versus 31.0 kDa; 8.7% difference in MW). With the exception of trypsinogen (MW 26.7 kDa), which could not be completely separated from carbonic anhydrase II (MW 28.3 kDa; 5.6% difference in MW), all other proteins could be separated with baseline separation.

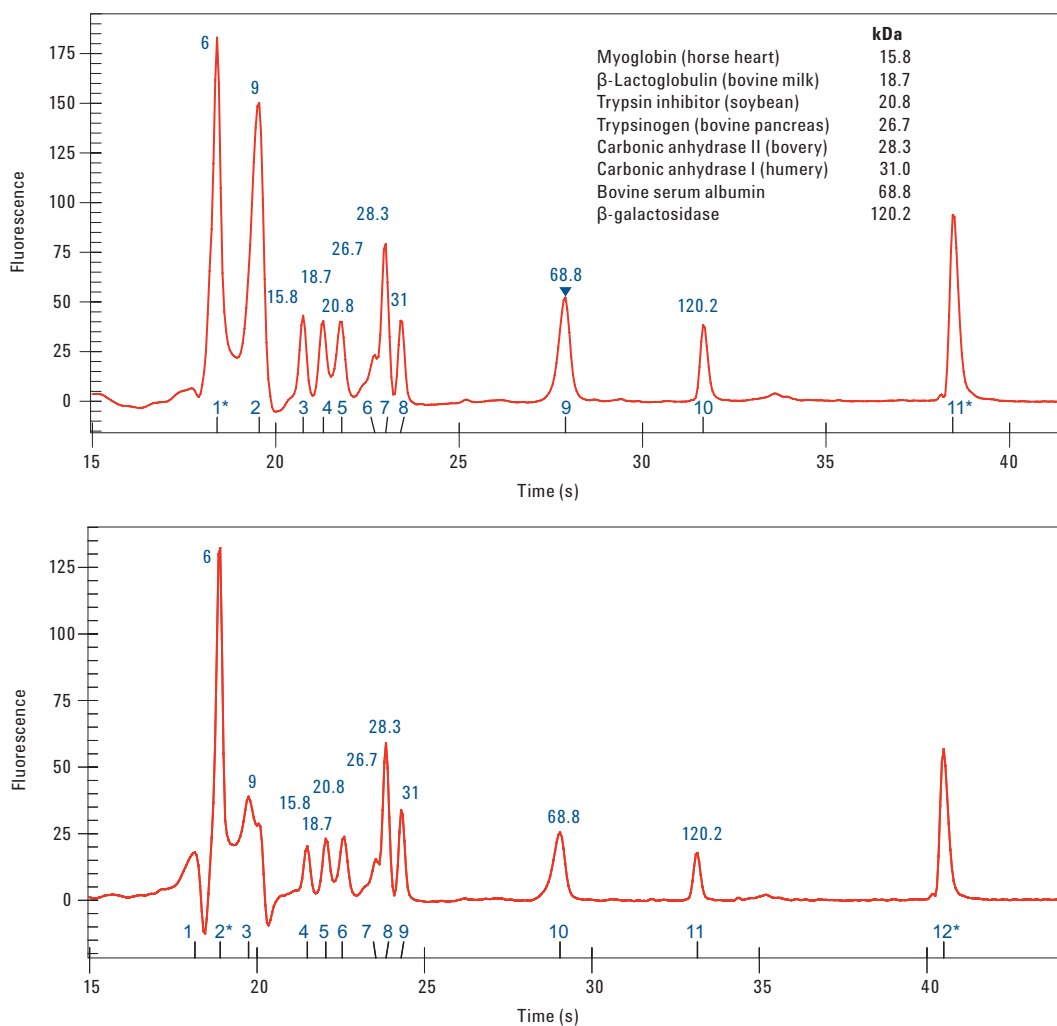


Figure 2. Sizing resolution. A self-made protein mixture of eight different proteins in a concentration of approximately 65 μ g/mL each in PBS was prepared and analyzed with the Protein 200 Plus LabChip kit.

Detection Limit

To assess the minimal detectable protein concentration of the assay bovine serum albumin (BSA), samples in PBS (Figure 3A) and in 0.5 M NaCl (Figure 3B) were tested. Samples were run in triplicate on each chip ($n = 45$, 15 individual chips). Three representative electropherograms are overlaid. BSA ($20 \mu\text{g/mL}$) in PBS (upper panel) was detected with a good signal/noise ratio (S/N) of 6, whereas $40 \mu\text{g/mL}$ BSA in 0.5 M NaCl (lower panel) could be detected with a high S/N ratio of 8. The data demonstrates that the specified detection limit of 20 and $40 \mu\text{g/mL}$ BSA, respectively, is easily reached by the assay.

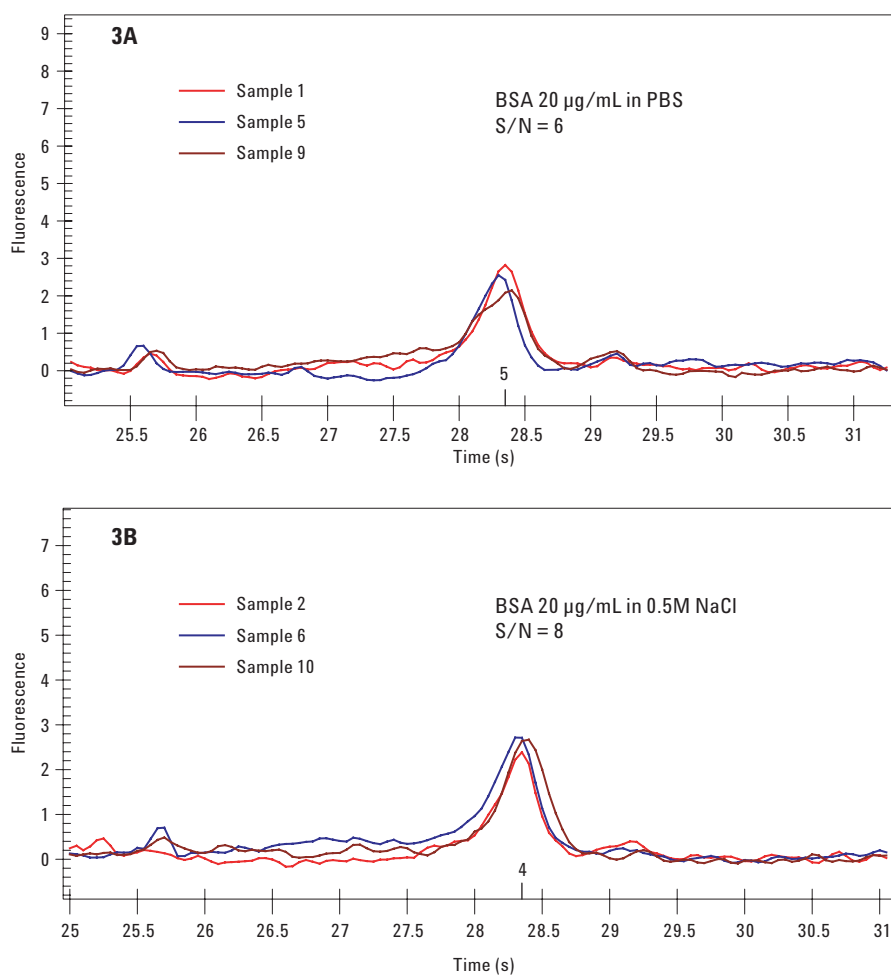


Figure 3. Sensitivity (minimal detectable concentration). BSA ($20 \mu\text{g/mL}$) in PBS (upper panel) and $40 \mu\text{g/mL}$ BSA in 0.5 M NaCl (lower panel) were run in triplicate on a single protein chip. Individual runs were overlaid.

Linear Dynamic Range

The linear dynamic range of the Protein 200 assay is specified for 0.02–2 mg/mL of protein. Using a human serum albumin (HSA) standard (Figure 4), the quality of quantitation across the specified dynamic range was assessed. Each of the five concentrations was measured 16 times with a mean C.V. of 10.5%. The slope of the curve indicates the batch-to-batch reproducibility, with 1 and no uncertainty being perfect reproducibility, of the

upper marker concentration calibration procedure within the sample buffer. The external HSA standards used have a highly reproducible protein concentration. Thus, the slope of the HSA curve is a critical quality parameter. Expected for this calibration curve is a slope between 1.0 ± 0.2 . This means that the relative concentration that is calculated (for example HSA 1000) should always be between 800 and 1200 $\mu\text{g/mL}$. In this representative measurement it is 0.995, and it is well inside the specified value of 0.8–1.0.

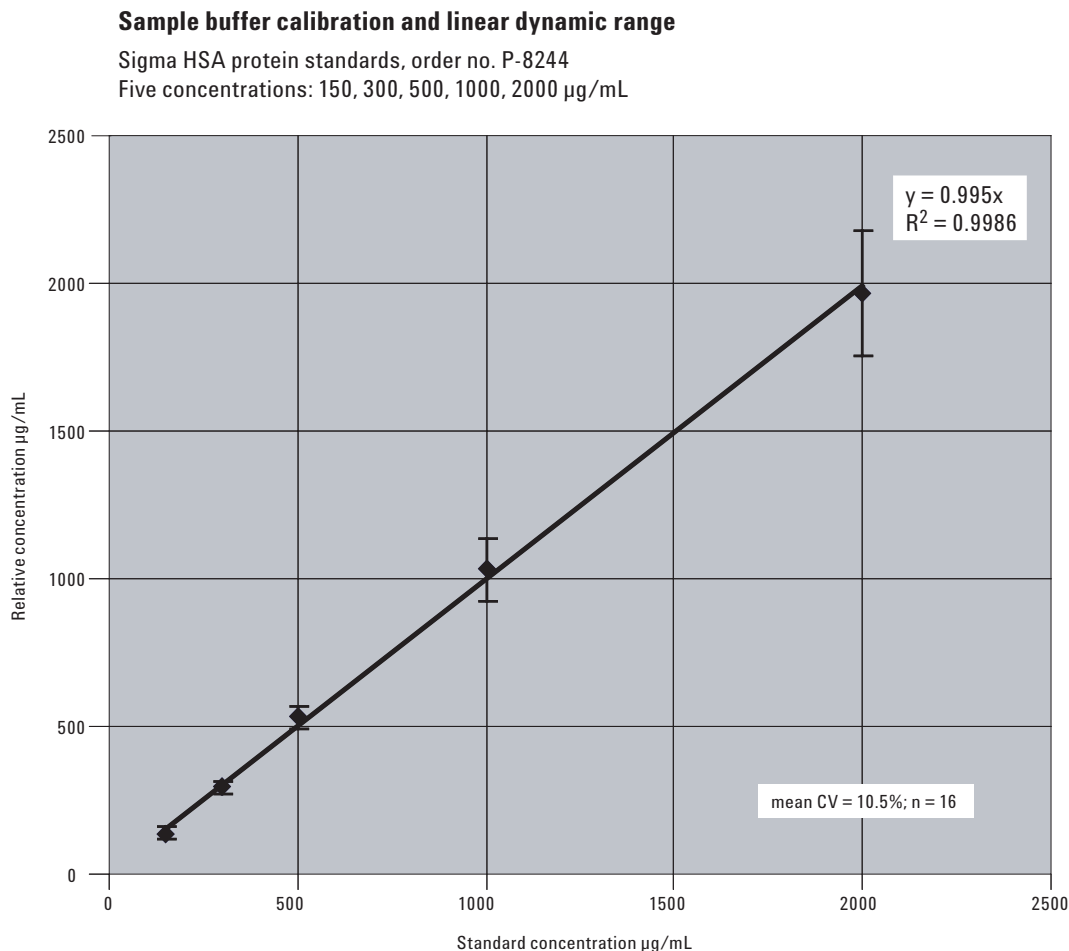


Figure 4. Sample buffer calibration and linear dynamic range. An HSA protein standard (Sigma order no. P-8244) was run at five different concentrations (0.15, 0.3, 0.5, 1, 2 mg/mL). For each concentration, 16 individual runs were performed.

Area Reproducibility

Agilent specifies an area reproducibility of 20% C.V. relative to the upper marker. Figure 5 shows data obtained with 100 µg/mL BSA in 10-mM Tris/75-mM NaCl, which was run as a sample across several chips and 11 instruments. Whereas there is some area variability between instruments and chip runs due to either slightly different optical setups or differences in electrokinetic sample injection, the average area reproducibility for an individual instrument is 15.1%. For determination of concentration, the area of each protein peak is correlated to the area of the upper marker in each individual sample. Therefore, area differences between instruments or individual chip runs are accounted for and do not affect quantitation.

Area variance in low ionic strength samples

BSA 100 µg/mL in 10-mM Tris, 75-mM NaCl

Mean CV per instrument: 15.1%

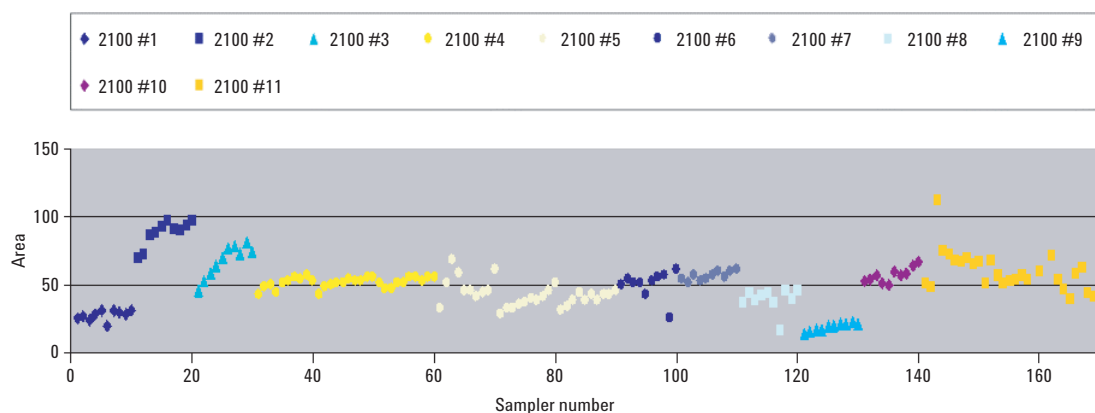


Figure 5. Area variance in low ionic strength samples. BSA (100 µg/mL) in 10-mM Tris/75-mM NaCl was run as a sample across several chips and instruments. Each dot represents an individual measurement. Area is in arbitrary units. Overall 170 samples (17 chips with 10 samples each) were measured across 11 instruments by six independent users.

Conclusion

Here we show representative tests to assess compliance of the Protein 200 Plus LabChip kit with the factory specifications. Specifications such as resolution and minimal detectable concentration were analyzed by different individual users on a variety of bioanalyzer instruments. Typical and representative data was well within or exceeded specifications in all cases.

References

1. L. Kelly and P. Barthmaier, Glycoprotein Sizing on the 2100 Agilent Bioanalyzer, Agilent Technologies, publication 5989-0332EN, www.agilent.com/chem
2. Puschett et al. (2003) Molecular effects of Volume Expansion on the renal sodium Phosphate cotransporter, *Am. J. Med. Sci.* **326:1**.

For More Information

For more information on our products and services, visit our Web site at www.agilent.com/chem.

Agilent shall not be liable for errors contained herein or for incidental or consequential damages in connection with the furnishing, performance, or use of this material.

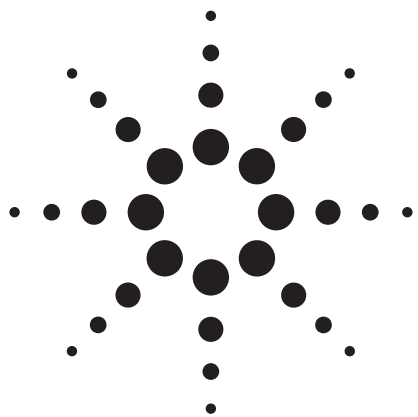
Information, descriptions, and specifications in this publication are subject to change without notice.

© Agilent Technologies, Inc. 2005

Printed in the USA
July 29, 2005
5989-3336EN



Agilent Technologies



Using the Agilent 2100 bioanalyzer for quality control of protein samples prior to MS-analysis

Application

Barbara Fischer
Frank Siedler

Introduction

Whereas in the past mass spectrometers (MS) were confined to the realm of small molecules, the development of soft ionization methods such as matrix-assisted laser desorption/ionization (MALDI) and electrospray ionization (ESI) revolutionized the analysis of large biomolecules^{1, 2}. Today, the analysis of proteins up to 300 kDa using MS has become a routine method to gain molecular weight information with high accuracy and structural information. However, sample purity greatly influences the results of MS analysis. In MS service facilities, scientists have to rely on the information provided by the customers and the quality of the sample preparation they have done. Bad results are often the consequence of customers being too optimistic about their own samples. Especially concentration and purity are often overestimated. To avoid unproductive MS runs, a fast and simple precheck is valuable. In this Application Note we show that the Agilent 2100 bioanalyzer can be used for quality control of protein samples prior to MS analysis. A corresponding data set analyzed with LC/MS and with the Agilent 2100 bioanalyzer using the Protein 200 Plus LabChip[®] kit is shown.

Experiments

All samples were adjusted to a concentration of 1 mg/mL by dilution with the appropriate buffer prior to the analysis (based on information given by the customer).

LC-MS analysis

The experimental setup comprised:

- Micro-HPLC-Pump (ABI 140C)
- Autosampler (PE200)
- HPLC column (Nucleosil C8 125 x 2 mm, 5 μ , 120 Å from Macherey & Nagel)
- UV detector (ABI 785A) set to 214 nm, in row with
- Single quadrupole mass spectrometer (API165 from Applied Biosystems) with a 1:10 flow splitter

The analysis was performed as follows:

10 μ L sample was injected and the proteins were separated with a flow of 250 μ L/min. A linear gradient was applied using eluent A (0.1 % TFA in water) and eluent B (0.1 % TFA in acetonitrile) from 5 % eluent B within 15 minutes to 95 % eluent B. The gradient was started with 20 % eluent B when analyzing samples with low salt or very hydrophobic proteins. For MS detection an ESI-spray source was used in positive ion mode with an ionization voltage of 5000 V and an orifice potential of 40 V. The analysis was carried out with a full scan between 600 and 1800 m/z (2.7 s/scan). For deconvolution the “Biotoolbox” software was used.

Agilent 2100 bioanalyzer and the Protein 200 Plus assay

Samples and chips were prepared according to the protocol provided

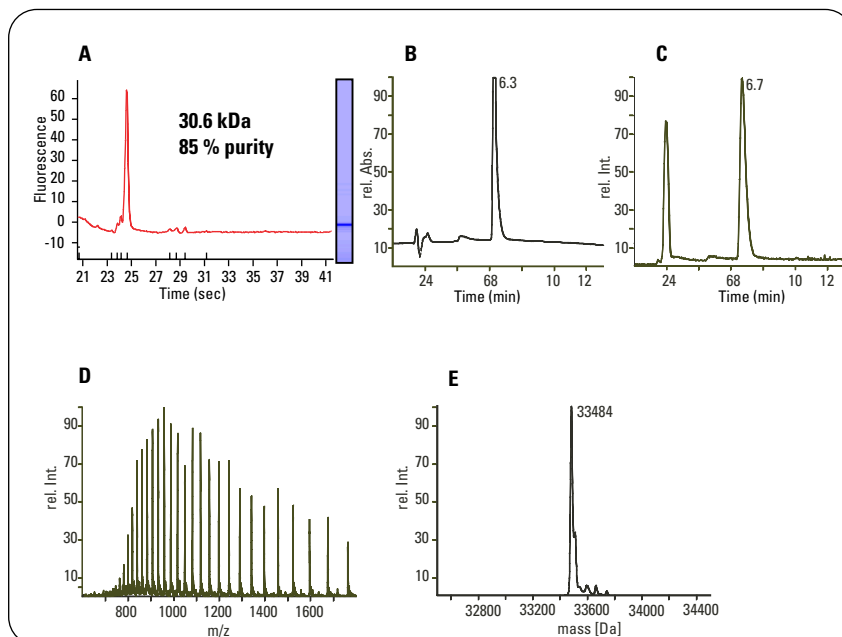


Figure 1
Results of the analysis of protein 9-15 with the Agilent 2100 bioanalyzer and the LC/MS method, expected molecular weight (MW) 33484 Da. A. Agilent 2100 bioanalyzer electropherogram B. UV-signal at 214 nm C. Total ion current (TIC) D. Raw mass spectrum E. Deconvoluted mass spectrum

| | Expected MW [Da] (provided by customer) | MW by MS [Da] | MW by bioanalyzer [kDa] |
|-------------|--|-----------------------------|--|
| Sample 2-11 | 26111 | 26237 (additional Glu) | 24.5 |
| Sample 3-12 | 26392 | 26405 | 24.5 |
| Sample 9-15 | 33484 | 33484 | 30.6 |
| Sample 16 | ~30000 | ~30000 is present | 2 main peaks at 65.9/131.9, small peak at 30 |
| Sample 21 | ~47880 + multiple Label (n x 180Da) | 47889 + n x 180Da (n=0,1,2) | 43.7 + multimers |
| Sample 22 | ~70000 | 71471 | main peak at 60.9, smaller peak at 48.5 |
| Sample 23 | 33484 | 33483 | 30.6 |

Table 1
Comparison between the expected molecular weight (MW), MW determined with MS-analysis and Agilent 2100 bioanalyzer.

with the Protein 200 Plus LabChip kit. The kit includes 25 chips, spin filters and all reagents needed for the experiments including the Agilent Protein 200 Plus ladder and the upper and lower marker premixed in the sample buffer. The chip-based separations were performed on the Agilent 2100

bioanalyzer using the dedicated Protein 200 Plus software assay. The software automatically determines the size of each protein in kDa, its relative concentration to the upper marker and the percent total of the protein. Latter gives direct information on the purity of a particular protein.

Results and discussion

Several protein samples were analyzed both with the LC/MS method (optimized for robust online desalting and rough separation of impurities) as well as the Agilent 2100 bioanalyzer and the Protein 200 Plus assay. A summary of the results is shown in table 1.

The protein sample 9-15 for example did not cause any problem during MS analysis (figure 1). It was purified by the customer using a gel-column and was provided in a low salt buffer (50 mM Tris/HCl, 1 mM EDTA). A molecular weight of 33484 Da was expected. The UV-chromatogram showed a single peak at 6.3 minutes (figure 1B), which corresponds to the peak at 6.7 min in the TIC (figure 1C). After deconvolution of the correlated mass spectrum (figure 1D) the protein mass was found to be exactly as expected (figure 1E). Also, the 2100 bioanalyzer electropherogram (figure 1A) showed a main peak at 30.6 kDa with a purity of 85.0 %, which corresponds nicely to the MS results. For protein sample 16 the results were already more difficult to interpret (figure 2). The protein was purified with a Ni-NTA-column and was provided in a buffer with relatively high ionic strength compared to the protein sample 9-15 (50 mM NaH₂PO₄, 250 mM imidazole, 300 mM NaCl). A molecular weight of approximately 30 kDa was expected. The UV chromatogram showed a main peak at 4.7 minutes and some minor peaks at 7.4 minutes and 11.2 minutes. However, the TIC showed two prominent signals (figure 2C) – one at 5.1 minutes, which corresponds to the 4.7 minutes signal

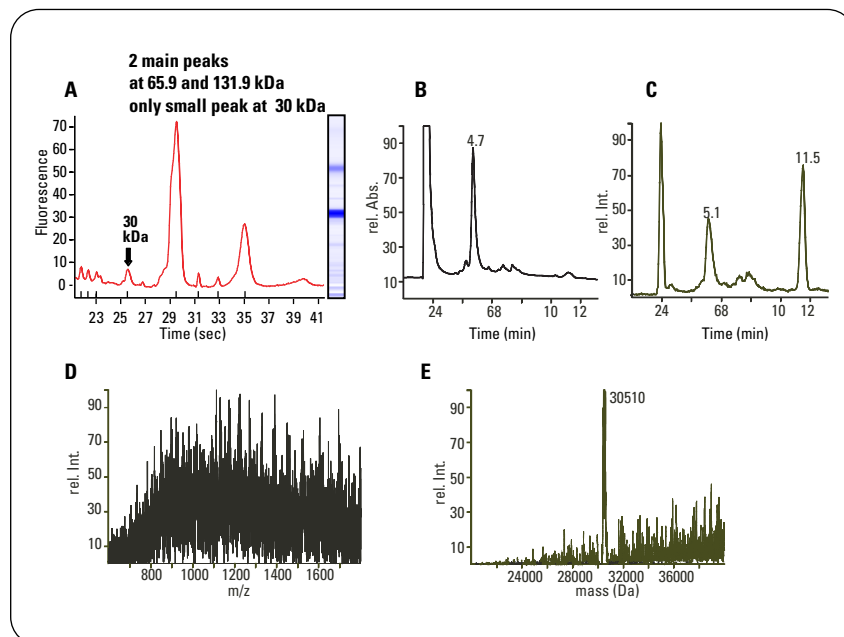


Figure 2
Results of the analysis of protein 16 with the Agilent 2100 bioanalyzer and the LC/MS method, expected molecular weight (MW) 30 kDa. **A.** Agilent 2100 bioanalyzer electropherogram **B.** UV-signal at 214 nm **C.** Total ion current **D.** Mass spectrum (5.1 min) **E.** Deconvoluted mass spectrum (5.1 min)

in the UV, and a second peak at 11.5 minutes, which seemed to be only a minor impurity in the UV but was obviously easy to ionize. Both TIC signals were analyzed, where the first mass spectrum turned out to be very noisy (figure 2D), which is usually an indication for inhomogeneous samples and/or a high tendency for aggregation. As expected, the deconvolution yielded several mass peaks of which the most intense around 30 kDa could only be considered as a hint that the expected protein is present. The second mass spectrum showed a polymer pattern between 600 and 900 m/z (data not shown). However, the data from the analysis with the Agilent 2100 bioanalyzer already showed that only a small peak of the expected

30 kDa protein is visible in the electropherogram (figure 2A). Instead, the analysis revealed two main peaks at 65.9 kDa and 131.9 kDa.

30 kDa protein is visible in the electropherogram (figure 2A). Instead, the analysis revealed two main peaks at 65.9 kDa and 131.9 kDa.

Conclusion

The presented data showed that there is a good correlation between the results determined with the Agilent 2100 bioanalyzer and MS-analysis. Since the Agilent 2100 bioanalyzer provides a fast, standardized method for protein analysis with automated and detailed data analysis, it is an ideal tool for quality control prior to MS analysis. In this case, the LC/MS method lasted approximately 20 minutes and additional 10 minutes are needed for column equilibra-

tion and sample preparation. By comparison, the Agilent 2100 bioanalyzer can analyze 10 samples within 45 minutes including sample preparation. Depending on the kit, proteins from 5-200 kDa can be analyzed with a resolution of 10 %, or better, throughout the size range^{3, 4}. However, sizing accuracy is strongly dependent on the protein characteristics, which is also the case for other methods such as traditional gel-electrophoreses (SDS-PAGE) or size exclusion chromatography. Sizing reproducibility is in the range of 0.5–5 %. In contrast, excellent mass accuracy of 0.01 % and very high sensitivity can be obtained by mass spectrometry if the protein sample fulfills the purity criteria needed for the analysis. Comparing the sizing results from the Agilent 2100 bioanalyzer with those obtained by MS, the absolute error of size determination with the Agilent 2100 bioanalyzer ranges from 6–14 % for the proteins analyzed in this study. With the help of the Agilent 2100 bioanalyzer “dirty” samples can be identified and only “clean” samples with the right concentration will be subjected to MS analysis. This pre-screening reduces costs and significantly saves time. Furthermore, the Agilent 2100 bioanalyzer can reveal additional information, such as concentration determination or the formation of multimers, which was not possible with the LC/MS method described.

References

1. *M. Karas, F. Hillenkamp, Anal. Chem. 60, 2299, 1998.*
2. *J. B. Fenn, M. Mann, C. K. Meng, S. F. Wong and C. M. Whitehouse, Science 64, 246, 1989.*
3. “Differences and similarities between the Protein 200 assay and SDS-Page” *Agilent Application Note, Publication number 5988-3160EN, 2001.*
4. “Fast analysis of proteins between 5-50 kDa” *Agilent Application Note, Publication number 5988-8322EN, 2002.*

We thank Elisabeth Weyher for the LC/MS analyses.

Barbara Fischer (Technical Assistant) and Frank Siedler (Group Leader) are responsible for the mass spectrometry service at the Max-Planck-Institute, Martinsried, Germany.

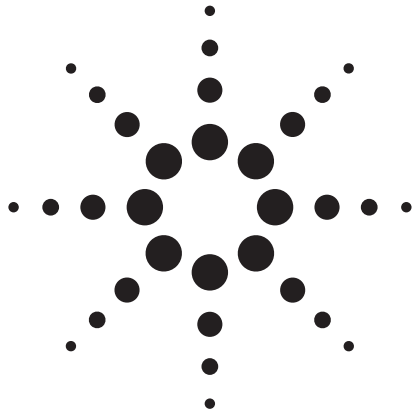
www.agilent.com/chem/labonachip



Caliper®, LabChip®, and the LabChip logo® are US registered trademarks of Caliper Technologies Corp.

Copyright © 2004 Agilent Technologies
All Rights Reserved. Reproduction, adaptation or translation without prior written permission is prohibited, except as allowed under the copyright laws.

Published March 1, 2004
Publication Number 5989-0771EN



Glycoprotein sizing on the Agilent 2100 bioanalyzer

Application

Lenore Kelly
Peter Barthmaier

Abstract

Glycoproteins analyzed either by traditional SDS-PAGE or on the Agilent 2100 bioanalyzer frequently migrate at a different size than anticipated from the known molecular weight. Because the glycan attachment can keep the protein from assuming a rod shape, and will also change the charge-to-mass ratio from the bound detergent, migration is often slowed down, making the glycoprotein appear too large. After enzymatic deglycosylation, the resulting proteins now migrate at the expected sizes.



Agilent Technologies



Introduction

In eukaryotic cells, glycosylation of proteins is a common post-translational modification. Many proteins appear as glycoforms with different isoelectric points (pI) and/or molecular mass. Glycan attachments to proteins, which may comprise multiple sites and contain highly branched moieties, make the molecule bulky and hydrophilic. When denaturing glycoproteins in a detergent solution for SDS-PAGE, the hydrophilic nature of the attachment will alter the stoichiometry of the detergent association, changing the charge density of the complex. Secondly, the bulky glycan portion will not permit the formation of a rod shaped protein-detergent complex. Because the shapes and the charge-to-mass ratios are not comparable to the proteins used in the ladder, migration times and hence molecular weight estimations of glycoproteins from electrophoretic techniques can be very different from the predicted size based on the molecular composition or mass spectrometry measurements. Analysis of such samples, performed on the Agilent 2100 bioanalyzer or with SDS-PAGE, is susceptible to these sizing anomalies. In order to accurately size the proteins, the glycan portion must be removed. Either hydrazinolysis or enzymatic methods can be used to cleave all common classes of oligosaccharides from glycoproteins. After the complete removal of the glycans, the Agilent 2100 bioanalyzer will provide accurate measurement of the molecular weight and concentration of the sample.

Experimental

An N-Glycosidase F Deglycosylation Kit was purchased from Roche Diagnostics GmbH (Mannheim, Germany). All proteins and 2-mercaptoethanol were purchased from Sigma Aldrich, (St. Louis, MO, USA). PBS and purified water were purchased from Amresco, (Solon OH, USA). Novex Pre-Cast gels and Tris-Glycine SDS 2X sample buffer were purchased from Invitrogen (Carlsbad, CA, USA). GelCode® Blue Staining Reagent was purchased from Pierce Biotechnology (Rockford, IL, USA). The Agilent 2100 bioanalyzer and the Protein 200 Plus LabChip kit were obtained from Agilent Technologies Deutschland GmbH (Waldbronn, Germany).

Deglycosylation reactions

Proteins were dissolved to 10 mg/mL in deionized water; 5 µL aliquots were reduced and denatured with the kit denaturation buffer for 3 minutes at 98 °C. Then enzymatic deglycosylation was performed in the kit reaction buffer for 1 hour at 37 °C as directed in the Working Procedure for Complete Deglycosylation included in the Roche kit. Control protein (non-deglycosylated reactions) had additional reaction buffer added in lieu of enzyme solution. The control glycoprotein mixture included in the kit was reacted in a similar fashion.

SDS-PAGE

Samples were prepared in Tris-Glycine SDS 2X sample buffer, 2-mercaptoethanol was added to the sample. Samples were run on a Novex 12% Tris-Glycine Pre-Cast gel at 120 V. Following electrophoresis, the gel

was washed with water and stained with GelCode® Blue Staining Reagent for one hour. The gel was then destained by washing with water, and scanned using an Alpha Imager (Alpha Innotech Corporation, San Leandro, CA, USA)

Protein 200 Plus Assay

The chip-based protein analysis was performed on the Agilent 2100 bioanalyzer using the Protein 200 Plus LabChip kit and dedicated Protein 200 Plus software assay. Samples containing 0.5 – 1.67 mg/mL of each protein were denatured as specified in the Reagent Kit Guide using the Protein 200 Plus Sample Buffer with added 2-mercaptoethanol. All chips were prepared according to the Reagent Kit Guide. The Protein 200 Plus LabChip kit includes 25 chips, a syringe, 4 spin filters and all required reagents except for reducing agent.

Results and discussion

The 2100 bioanalyzer separates samples through a viscous linear polymer in the microfluidic chip through the careful control of currents and voltages. In order for the sample to move in an electrical field, a charge must be associated with the proteins. According to the Protein 200 Plus protocol, samples are first heat denatured in a lithium dodecylsulfate (LDS) solution to give the proteins a uniform charge to mass ratio. Denatured proteins are assumed to bind dodecylsulfate with a fairly constant stoichiometry and to assume a rod shape. A noncovalently bound fluorophore, present in the gel/dye mix, becomes more

intensely fluorescent upon association with the detergent-protein complex. Samples are separated through the sieving gel matrix and detected by laser-induced fluorescence. Comparison of migration times of the sample proteins relative to the Protein 200 Plus ladder and the alignment to internal standards allows for the accurate sizing of the unknown samples. The implicit assumptions are that all detergent-protein complexes assume a completely unfolded cigar-like shape and that the charge-to-mass ratio of this complex is constant. This holds true for most reduced proteins. The shapes and the charge-to-mass ratios of glycoproteins are not comparable to the proteins used in the ladder and are therefore effecting the size determination.

To determine the effect of glycosylation, several proteins were analyzed on the Agilent 2100 bioanalyzer before and after deglycosylation. Glycans can either be removed by hydrazinolysis or enzymatic methods. However, hydrazinolysis destroys the protein chain, so to analyze the intact protein, enzymatic procedures must be used. A number of endoglycosidases have been characterized that can remove various oligosaccharide chains, but many

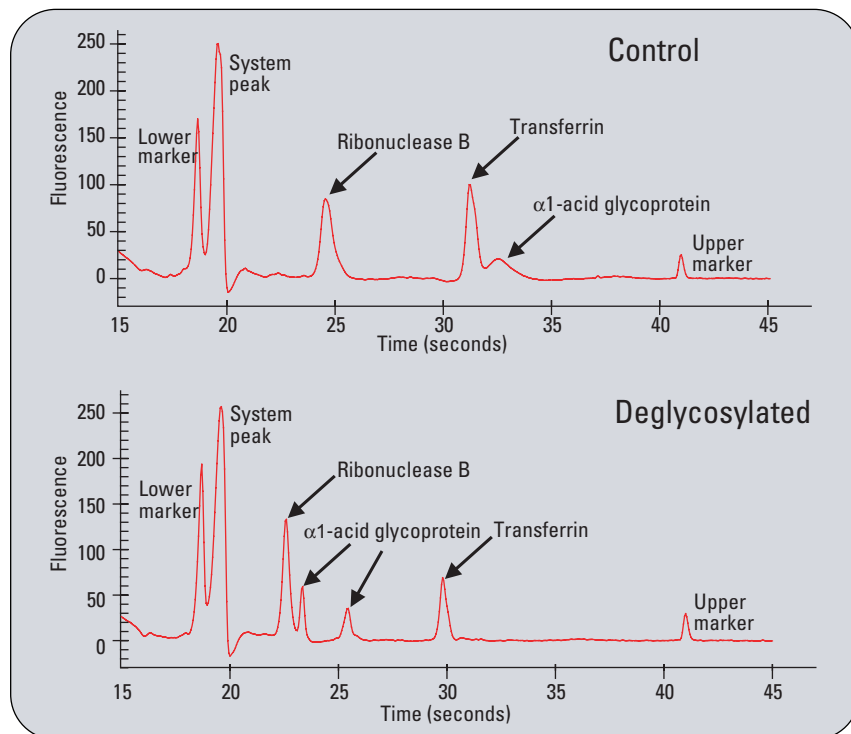


Figure 1
The glycoprotein test mixture provided with the N-Glycosidase F Deglycosylation kit showing α 1-acid glycoprotein, transferrin and ribonuclease B was run as a positive control on a Protein 200 Plus kit. Also visible are the lower marker, system peak, and upper marker that are characteristic of Agilent 2100 bioanalyzer runs. The analysis of the proteins before and after reaction with N-glycosidase F is shown.

of them are fairly specific and thus of limited utility. One class of enzymes reacts with asparagine-linked glycan chains. N-glycosidase F is able to release all common classes of N-glycans from the protein backbone. A glycoprotein test mixture was provided with

the N-Glycosidase F Deglycosylation kit. The test mixture, containing α 1-acid glycoprotein, transferrin and ribonuclease B, was used as a positive control. After treatment with the glycosidase, all three proteins migrated faster at a smaller molecular weight (figure 1 and

| Glycoprotein | Protein 200 Plus | | SDS-PAGE | | Theoretical Mw |
|------------------------------|------------------|-------------|----------|--------|----------------|
| | Mw (+) | Mw (-) | Mw (+) | Mw (-) | |
| Ovalbumin | 43,3 | 37.2 & 39.6 | 45,0 | 44,0 | 41,9 |
| Ovomucoid | 86,0 | 28,4 | 26,0 | 18,0 | 20,5 |
| IgG Heavy Chain | 57,9 | 51,3 | 50,0 | 49,0 | 50,0 |
| IgG Light Chain | 27,9 | 27,9 | 22,0 | 22,0 | 27,0 |
| Transferrin | 92,1 | 72,0 | 70,0 | 69,0 | 60,0 |
| α 1-acid glycoprotein | 110,0 | 22.7 & 36.5 | 40,0 | 26,0 | 22,0 |
| Ribonuclease B | 30,4 | 18,4 | 17,0 | 15,0 | 14,7 |

Table 1
Sizing comparison between the Agilent 2100 bioanalyzer and SDS-PAGE, before (+) and after deglycosylation (-), all sizes are shown in kDa.

table 1). Initially $\alpha 1$ -acid glycoprotein was a very broad peak (2 seconds wide). After treatment with N-glycosidase F, 2 peaks separated, the larger peak at 36.5 kDa probably represents incomplete reacted isoform(s). Unreacted ribonuclease showed 2 peaks at 18.8 and 30.4 kDa. After deglycosylation the larger peak moved to 18.8 kDa. Two glycosylated forms of ribonuclease exist in addition to ribonuclease A, the nonglycosylated form which was observed at 18.8 in both runs. Transferrin initially ran at 92.0 kDa and shifted to 72.0 kDa after treatment.

The proteins selected for analysis were observed to run at a larger molecular weight relative to the size anticipated from sequence information. The protein set contained several kinds of oligosaccharides. Before glycosidase treatment the ovalbumin peak ran at 43.3 kDa on the bioanalyzer. After treatment ovalbumin (figure 2a) exhibited a main peak with a leading shoulder. Both peaks (37.2 kDa and 39.6 kDa) migrated faster than the untreated protein. Ovalbumin from hen egg whites contains a mono-N-glycosylated form with a glycan chain on Asn-292. It is recognized to be microheterogeneous with respect to the glycan. This heterogeneity manifested as an asymmetrical peak with a leading edge in the starting material. The ovalbumin species did not react at the same rate with the enzyme during the 1-hour incubation, resulting in a large peak with a definitive shoulder.

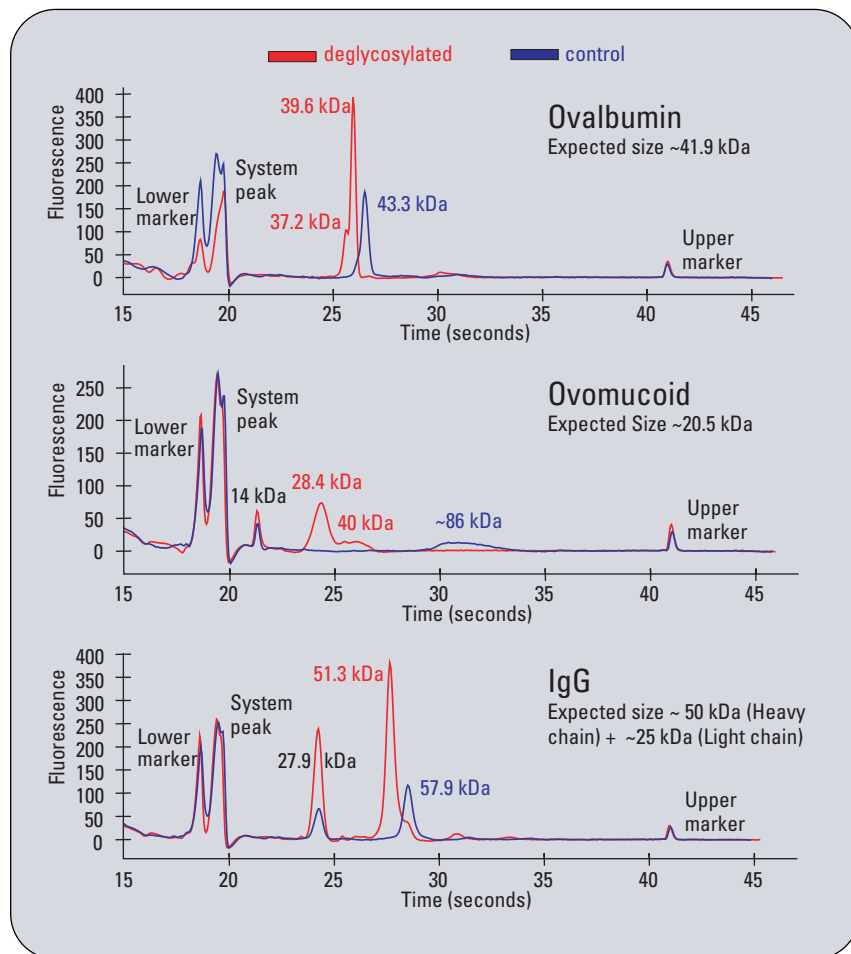


Figure 2
Ovalbumin, Ovomuroid and IgG were analyzed with the 200 Plus LabChip assay before (blue) and after (red) reaction with N-glycosidase F. After removal of the glycan attachments, proteins clearly shift to smaller sizes.

Ovomuroid was also a very broad peak at approximately 86 kDa before exposure to N-glycosidase F. After deglycosylation the peak migrated twice as fast at 28.4 kDa, with a trailing shoulder of incompletely deglycosylated material at approximately 40 kDa. Ovomuroid contains both sulfated oligosaccharides and sialyloligo-saccharides

and is frequently problematic on SDS-PAGE gels and the Agilent 2100 bioanalyzer. An impurity of approximately 14 kDa was also found to be present in the sample. This impurity, however, did not change size after treatment indicating it had no glycan attachments. The immuno γ -globulin is separated into heavy and light chains after

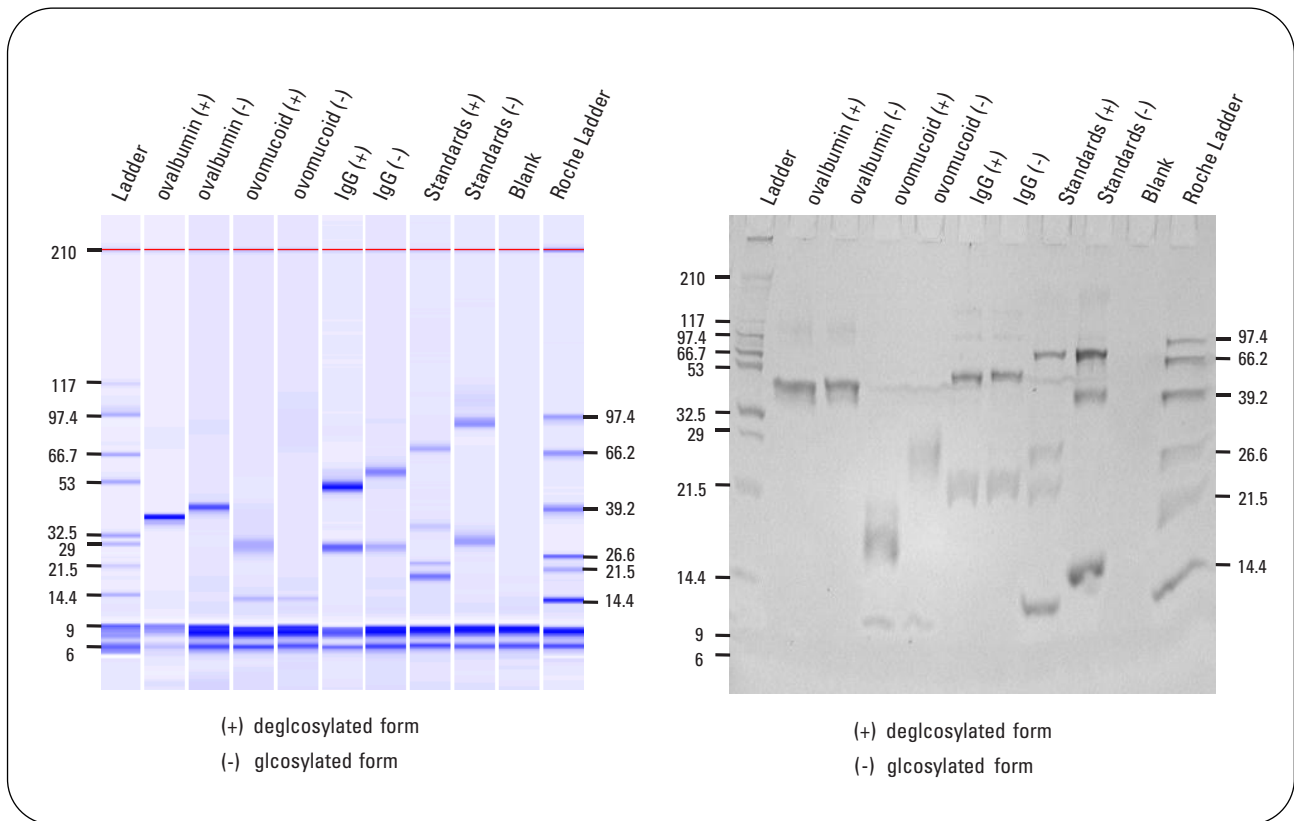


Figure 3
Comparison of the gel-like image generated by the Agilent 2100 bioanalyzer software and a SDS-PAGE slab gel. Both techniques show similar banding patterns. For some proteins, such as ovalbumin and IgG heavy chain, the shift in size after deglycosylation is more evident on the Agilent 2100 bioanalyzer.

reduction. When deglycosylated, the light chain migrated in the same position as before, whereas the heavy chain now moved faster. A small shoulder of heavy chain migrated at the original time, indicating the incomplete removal of the carbohydrate, similar to the observations of ovalbumin and ovomucoid. Even monoclonal antibodies are recognized to have isoforms that can be separated by capillary isoelectric focusing.

All proteins were also run on an SDS-PAGE slab gel. Comparison between the slab gel and the Agilent 2100 bioanalyzer is shown in figure 3. Clear and definitive sizing was determined by the Agilent 2100 bioanalyzer, where results are displayed in a tabular format, an electropherogram and a gel-like image. All samples contain an upper and lower marker. The upper and lower markers are used to align the samples with the ladder.

This helps to reduce the “smiling” effect that is commonly seen on slab gels.

Conclusion

The Agilent 2100 bioanalyzer is designed to size and quantitate a wide range of proteins. Occasionally, as with SDS-PAGE, sizing anomalies will occur. Proteins that are heavily glycosylated can be

problematic because of the large carbohydrate attachments.

Removal of the glycan components of these glycoproteins allow for the resulting protein to migrate more rapidly on the protein

LabChips. Because most glycoproteins have heterogeneous carbohydrate attachments, it is reasonable that the reaction rates with the N-glycosidase F may vary. One major peak for each deglycosylated protein was present. Other peaks probably representing unreacted glycoprotein isoforms were also found. All of the different species, glycosylated, deglycosylated and various isoforms were clearly visualized using the Agilent 2100 bioanalyzer.

References

1. Proteomics, S.R. Pennington and M. J. Dunn, eds., *BIOS Scientific Publishers, Oxford. P 257, 2001.*
2. Handbook of Capillary Electrophoresis, J.P. Landers, ed., *CRC Press, Ann Arbor. P. 257., 1993.*
3. Tarentino, A.L. & Plummer, T.H. *Methods in Enzymology* 138, 770, **1987.**
4. Grossman, P.D. et al., *Anal. Chem.* 61;1186,. **1989.**
5. Suzuki, T. et al., *Proc. Natl. Acad. Sci. USA.* 1997 June 10; 94(12):6244, **1997.**
6. Landers, op. cit., p 38, 108.
7. Yamashita K. et. al, *Carbohydr Res.*, Jul 15; 130;271, **1984.**
8. Landers, op. cit., p 108.

Lenore Kelly is Senior Applications Engineer and Peter Barthmaier is Assay Support Biochemist at Agilent Technologies, Palo Alto, CA, USA.

www.agilent.com/chem/labonachip



Caliper®, LabChip®, and the LabChip logo® are US registered trademarks of Caliper Technologies Corp.

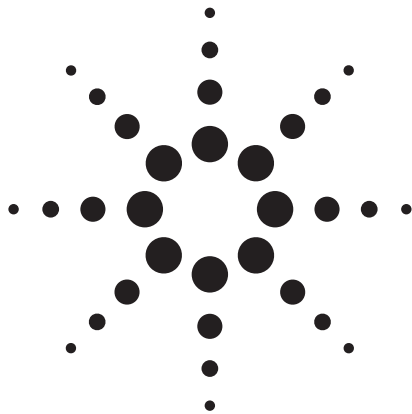
The information in this publication is subject to change without notice.

Copyright © 2003 Agilent Technologies
All Rights Reserved. Reproduction, adaptation or translation without prior written permission is prohibited, except as allowed under the copyright laws.

Published December 8, 2003
5989-0332EN



Agilent Technologies



Analysis of bispecific antibodies using the Agilent 2100 bioanalyzer and the Protein 200 Plus assay

Application

Tanja Neumann

Introduction

The discovery of hybridoma technology by Kohler and Milstein in 1975 induced a new era in antibody research and clinical development. Nowadays large antibody libraries exist and many new methods have evolved in order to specifically isolate and design antibodies with desired characteristics for unique applications. Engineered antibodies now represent over 30 % of biopharmaceuticals in clinical trials¹.

Bispecific antibodies contain two different binding specificities fused together and can be used as powerful therapeutic reagents. In cancer therapy, for example, half of the bispecific antibody is engineered to effectively target tumor-associated antigens. The other half of the bispecific antibody can then deliver a cytotoxic payload, such as radionuclides, toxins or immune effector cells (figure 1) to the tumor. The analysis of such antibodies during development, production and purification in terms of quantitation, purity and integrity is more than crucial.

In this study we show that the Agilent 2100 bioanalyzer together with the Protein 200 Plus LabChip[®] kit is an ideal tool to substitute for the traditional and labor-intensive SDS-PAGE analysis. The disposable Protein 200 Plus chip can analyze 10 protein samples in less than 30 minutes. In addition, the bioanalyzer can perform antibody analysis under both reducing and non-reducing conditions in a single chip run.

Experiments and Results

Bispecific antibody samples were kindly provided from a biopharmaceutical company. Reduced and

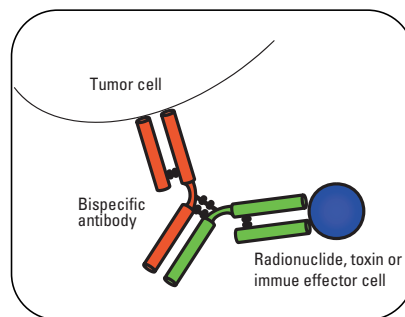


Figure 1
Schematic illustration of the strategic use of bispecific antibodies in cancer therapy

non-reduced antibodies were analyzed side by side using the 2100 bioanalyzer. The chip-based separations were performed with the Protein 200 Plus LabChip[®] kit and dedicated Protein 200 Plus assay software. All chips were prepared according to the protocol provided with the kit. The kit includes 25 chips, spin filters and all the reagents necessary for an experiment, including the Protein 200 Plus ladder, as well as the upper and lower marker pre-mixed in the sample buffer.

Figure 2 exemplifies the results obtained. In this case the bispecific antibody consists of two different heavy and light chains stemming from diverse organisms. The gel-like image of the analysis under reduced conditions (figure 2A) shows a clear separation between the sets of two different light and heavy chains. This level of resolution was not achieved using a 4–12 % gradient SDS-PAGE gel (figure 2A). Although the light chains were separated on the SDS-PAGE gel, the two heavy chains were not—they merged into one band.



Agilent Technologies



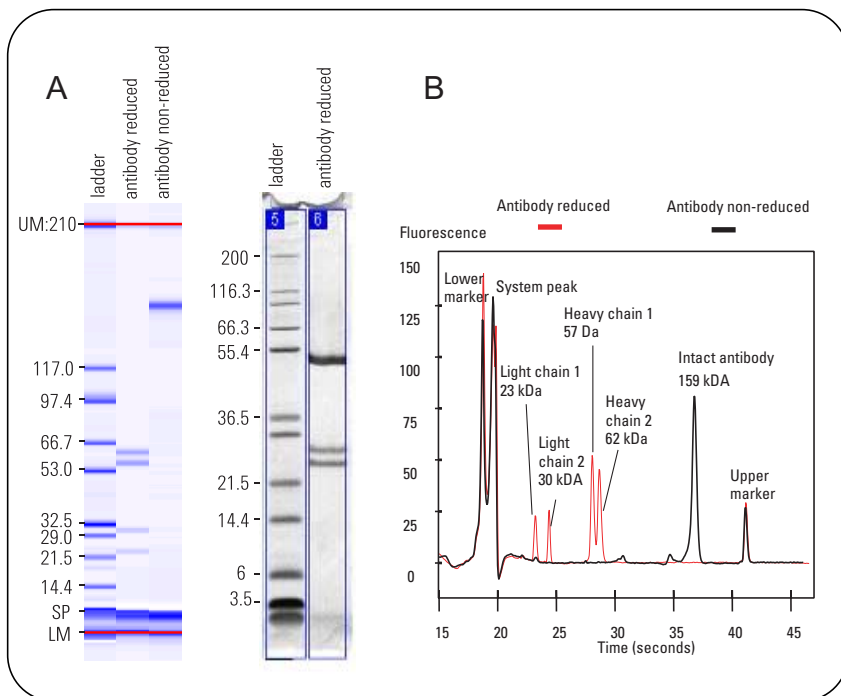


Figure 2
Example of the performed analysis on the Agilent 2100 bioanalyzer using the Protein 200 Plus assay (A) Comparison of the gel-like image (left) and a scanned, Coomassie stained 4-12 % SDS-PAGE gel (right) The numbers indicate the molecular weight in kDa. (B). Overlay of the 2100 bioanalyzer electropherograms of reduced and non-reduced antibody sample is shown.

Figure 2B shows the overlay of the electropherograms of the analysis under reduced and non-reduced conditions. The automated data analysis assigned a size of 159 kDa to the intact antibody. In addition, two minor peaks at 87 kDa and 134 kDa were detected, which represent 5 % of the total sample amount. The reduced antibody analysis revealed two light chain peaks at 23 kDa and 30 kDa and two heavy chain peaks at 57 kDa and 62 kDa. The absence of the larger peaks indicates that they may consist of associated heavy and light chains, which fall apart under reducing conditions.

Conclusion

Traditional SDS-PAGE serves as a standard method for protein analysis, however, SDS-PAGE is very labor-intensive, time-consuming and difficult to standardize. In contrast the Agilent 2100 bioanalyzer provides a fast, standardized method with automated and detailed data analysis. Depending on the kit chosen, proteins from 5–200 kDa can be analyzed with a resolution of 10 %, or better, throughout the size range^{2,3}. These attributes of speed, automation and resolution make the Agilent 2100 bioanalyzer the perfect tool for analysis of bispecific antibodies.

References

1. Peter J. Hudson and Christelle Souriau, “Engineered antibodies”. *Nature Medicine* (2003); 9: 129-134
2. “Differences and similarities between the Protein 200 assay and SDS-Page”, Agilent Technical Note, (2001) Publication Number 5988-3160EN
3. “Fast analysis of proteins between 5-50 kDa” Agilent Application Note (2002) Publication Number 5988-8322EN

Tanja Neumann is an Assay Support Biochemist at Agilent Technologies, Waldbronn, Germany.

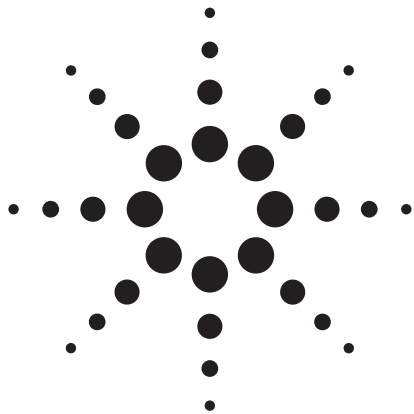
www.agilent.com/chem/labonachip



LabChip® and the LabChip Logo are registered trademarks of Caliper Technologies Corp. in the U.S. and other countries.

Copyright © 2003 Agilent Technologies
 All Rights Reserved. Reproduction, adaptation or translation without prior written permission is prohibited, except as allowed under the copyright laws.

Published June 1, 2003
 Publication Number 5988-9651EN



Quality control of antibodies using the 2100 bioanalyzer and the Protein 200 Plus assay

Application

Tanja Neumann
Andrea Zenker

Abstract

Antibodies are commonly used in diagnostics, as research tools (for example protein arrays) or as biopharmaceutical therapeutics. In all cases the successful production of antibodies requires precise testing and quality control. The key quality criteria include: protein identification, quantitation and the monitoring of purity and stability. Agilent's 2100 bioanalyzer, the first commercial lab-on-a-chip analysis tool, developed in collaboration with Caliper Technologies Corporation, was used to verify the suitability of this technology for antibody quality control. The system allows sizing and analysis proteins of 5 to 200 kDa, depending on the application. In addition, it determines the relative quantitation based on internal standards for each sample, or absolute quantitation based on user-defined calibration standards. The micro-fabricated chips with distinct microfluidic channels allows antibody analysis under both reducing and non-reducing conditions in a single run. In this Application Note we demonstrate the use of the system for the evaluation of a stress stability test of two different antibodies.



Agilent Technologies



Experiments and Results

Antibody samples were kindly provided from a customer in the pharmaceutical industry. For the first sample a stress stability test was performed for one month at 40 °C, for the second sample the stress test was done for 12 weeks at 40 °C. The standard samples and the stress test samples were

analyzed under reducing conditions on the Agilent 2100 bioanalyzer using a Protein 200 Plus LabChip® kit and the dedicated Protein 200 Plus software assay. All chips were prepared according to the protocol provided with the Protein 200 Plus LabChip kit. The kit includes 25 chips, spin filters and all the reagents needed for the experiments including the Protein

200 Plus ladder as well as the upper and lower marker premixed in the sample buffer.

To validate the performance of the instrument three individual users measured the samples on two separate instruments using two lots of reagents on different days. Thus a total number of twelve chips were run. The samples were

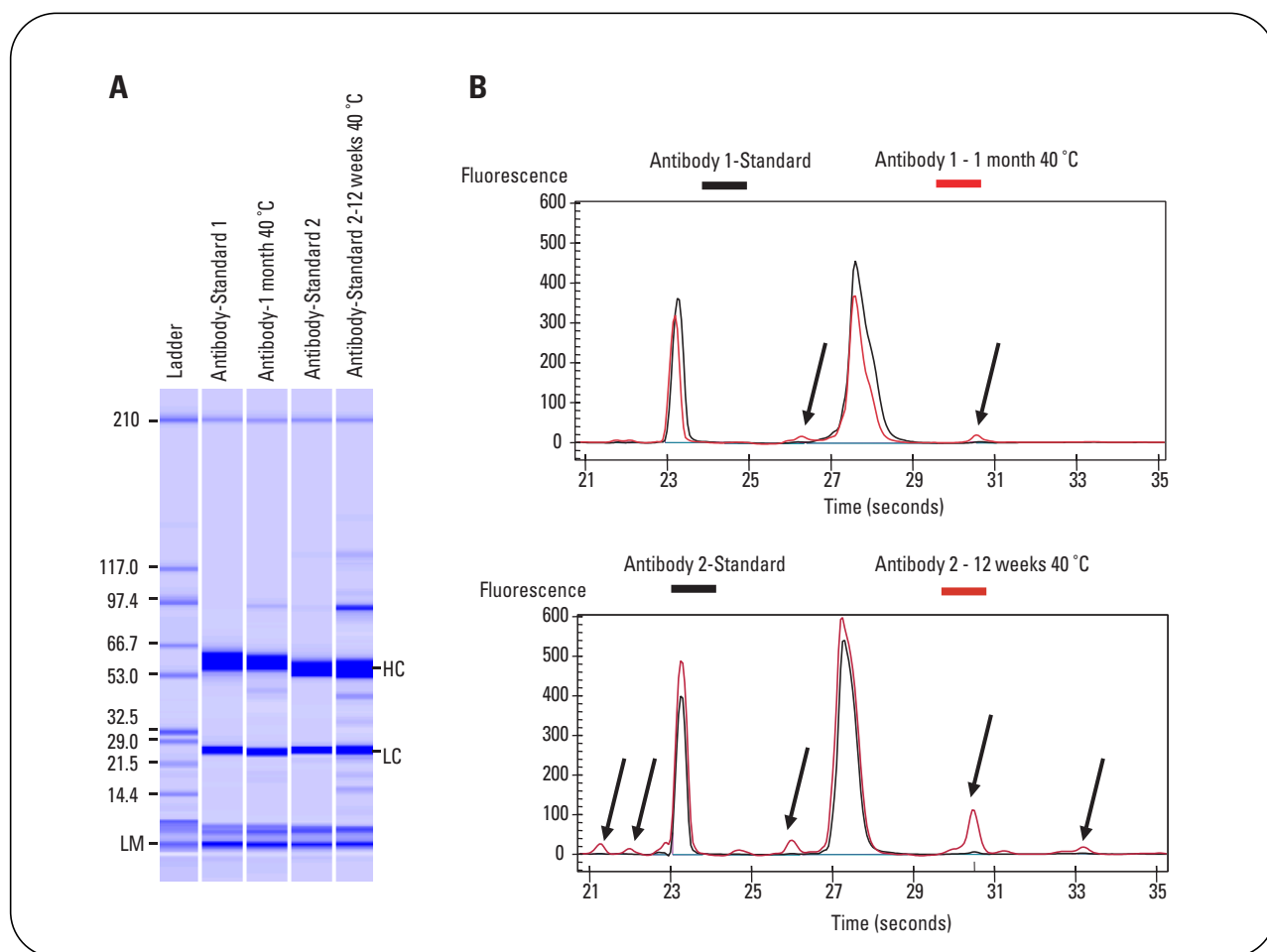


Figure 1 Representative example of the performed validation on the Agilent 2100 bioanalyzer using the Protein 200 Plus assay under reduced conditions. The gel-like image (A) and overlay of the corresponding electropherograms (B) are shown. Incubation of the antibodies at elevated temperature lead to the formation of additional peaks.

diluted 1:3 in PBS buffer (Life Technologies GmbH, Karlsruhe, Germany) in order to adjust the concentration of the samples to approximately 5 mg/ml total protein concentration. Sample preparation was performed individually for each chip. All samples were loaded twice on each chip. Therefore, 24 analyses per sample were evaluated using the following Protein 200 Plus assay settings for peak integration: minimum peak height of 0.1, minimum peak width of 0.1 and slope threshold of 4.0.

An example of the performed analysis is depicted in figure 1. Figure 1A shows the gel-like image of the four different antibody samples (2 standards, 2 test samples) aligned to the ladder sample. The ladder includes proteins of known sizes, was analyzed on each chip and was used for size determination. Figure 1B displays the overlay of the corresponding electropherograms. Both standard samples show almost only two peaks corresponding to the light (LC) and heavy chain (HC) of the antibody respectively. After incubation of the antibodies at elevated temperatures additional peaks appear in the electropherograms (marked with an arrow) due to degradation of the antibody or the formation of aggregates, larger products. Table 1 shows the results of the validation study. On average 98.76 % of standard antibody sample 1 corresponds to the light and heavy chain of the antibody. After incubation for one month at 40°C the two chains represent only 93.78% of the whole protein

| | Average | StDev | CV [%] |
|------------------------------|---------|-------|--------|
| Sample 1 - Standard | 98.76 | 0.61 | 0.62 |
| Sample 1 - 1 month at 40 °C | 93.78 | 0.93 | 0.99 |
| Sample 2 - Standard | 98.38 | 0.66 | 0.67 |
| Sample 2 - 12 weeks at 40 °C | 85.34 | 1.48 | 1.73 |

Table 1
Results of the validation study. The proportion of the sum of the light and heavy chain from the total protein concentration of the sample was calculated. Average, StDev and relative StDev are displayed (n = 24).

amount detected. Antibody 2 was incubated for 12 weeks at 40°C and the proportion of light and heavy chain decreases from an average of 98.38 % to 85.34 %. An excellent reproducibility below 2 % CV was achieved

Conclusion

In this study we show that the Agilent 2100 bioanalyzer can be used as an ideal tool to study the stability of antibodies in stress tests with excellent reproducibility. This application is commonly used as a quality control step in QA/QC departments in order to trigger typical degradation and aggregation patterns for a specific antibody. Those patterns will be used in the down stream processes of antibody production and formulations.

Traditional denaturing sodium dodecylsulfate-polyacrylamide gel electrophoreses (SDS-PAGE) still serves as one of the standard methods for the QC of antibodies. SDS-PAGE is labor-intensive, time-consuming and difficult to stan-

dardize (1-3). In contrast the Agilent 2100 bioanalyzer provides a fast, standardized method with automated and detailed data analysis.

References

1. "Comparison of different protein quantitation methods", Agilent Application Note, (2002) Publication Number 5988-6576EN
2. "Differences and similarities between the Protein 200 assay and SDS-Page", Agilent Technical Note, (2001) Publication Number 5988-3160EN
3. Ryo Ohashi, José Manuel Otero, Adam Chwistek, Jean-François P. Hamel, "Determination of monoclonal antibody production in cell culture using novel microfluidic and traditional assays" *Electrophoresis* (2002); 23: 3623-3629

*Tanja Neumann is an Assay Support Biochemist at Agilent Technologies, Waldbronn, Germany
Andrea Zenker is a Field Engineer at Agilent Technologies, Waldbronn, Germany.*

www.agilent.com/chem/labonachip



LabChip® and the LabChip Logo are registered trademarks of Caliper Technologies Corp. in the U.S. and other countries.

Copyright © 2003 Agilent Technologies
All Rights Reserved. Reproduction, adaptation or translation without prior written permission is prohibited, except as allowed under the copyright laws.

Published June 1, 2003
Publication Number 5988-9648EN



www.agilent.com/chem

© Agilent Technologies, Inc., 2010
April 1, 2010
Publication Number 5990-5819EN



Agilent Technologies